UNCLASSIFIED

AD NUMBER

AD907109

NEW LIMITATION CHANGE

TO

Approved for public release, distribution unlimited

FROM

Distribution authorized to U.S. Gov't. agencies only; Administrative/Operational Use; DEC 1972. Other requests shall be referred to Federal Aviation Administration, Washington, DC 20590.

AUTHORITY

FAA ltr, 26 Apr 1977

THIS PAGE IS UNCLASSIFIED

THIS REPORT HAS BEEN DELIMITED
AND CLEARED FOR PUBLIC RELEASE
UNDER DOD DIRECTIVE 5200.20 AND
NO RESTRICTIONS ARE IMPOSED UPON
ITS USE AND DISCLOSURE.

DISTRIBUTION STATEMENT A

APPROVED FOR PUBLIC RELEASE;
DISTRIBUTION UNLIMITED.

AD907109

Report No. FAA-SS-72-42

SUPERSONIC TRANSPORT NOISE REDUCTION TECHNOLOGY SUMMARY

PHASE I

SUMMARY OF GE4/SST ACOUSTIC SUPPRESSION RESEARCH

VOLUME 1

J.F. Brausch
V.L. Doyle

Group Engineering Division
Aircraft Engine Group
General Electric Company
Cincinnati, Ohio 45215

DDC
RECEIVED
FEB 7 1973

December 1972

FINAL REPORT

Approved for U.S. Government only. Transmittal of this document outside the U.S. Government must have prior approval of the Supersonic Transport Office.

Prepared for

DEPARTMENT OF TRANSPORTATION
FEDERAL AVIATION ADMINISTRATION
Supersonic Transport Office
Washington, D.C. 20590

Best
Available
Copy

The contents of this report reflect the views of the General Electric Company, which is responsible for the facts and the accuracy of the data presented herein. The contents do not necessarily reflect the official views or policy of the Department of Transportation. This report does not constitute a standard, specification, or regulation.

1. Report No.	2. Government Accession No.	3. Recipient's Catalog No.
FAA-SS-72-42 Vol. I of II		

4. Title and Subtitle	5. Report Date
SUMMARY OF GE4/SST ACOUSTIC SUPPRESSION RESEARCH	DECEMBER 1972
	6. Performing Organization Code
7. Author(s)	8. Performing Organization Report No.
J. F. BRAUSCH and V. L. DOYLE	R72-AEG-342 Vol. I of II
	10. Work Unit No.
9. Performing Organization Name and Address	11. Contract or Grant No.
Group Engineering Division Aircraft Engine Group General Electric Company Cincinnati, Ohio 45215	FA-SS-71-13
	13. Type of Report and Period Covered
12. Sponsoring Agency Name and Address	FINAL
Department of Transportation Federal Aviation Administration Supersonic Transport Office, Washington, D.C. 20590	14. Sponsoring Agency Code

15. Supplementary Notes

16. Abstract

A development program for a commercial supersonic aircraft and engines was sponsored by the Federal Aviation Administration during a five-year period from 1966 through 1971. The unique propulsion system, an afterburning turbojet, required acoustic suppression techniques to reduce its noise levels to those federally regulated for subsonic aircraft. An acoustic suppression research program was conducted by the General Electric Company to develop technology applicable to prototype and commercial supersonic engines. Primary emphasis was on jet noise suppressor development through model and engine testing. Various systems were studied including ejector pumping, simple mechanical primary and secondary suppressors, fluid injectants, multi-element tube nozzles, acoustically treated ejectors, highly segmented annular plug nozzles, etc. A research study on fundamental jet noise generation and reduction mechanisms was conducted at the General Electric Corporate Research and Development Center. In addition, investigatory tests were conducted for identification of total system noise. Application of a choked inlet and an open A_8 exhaust cycle were studied for noise reduction. Source turbomachinery noise generation and suppression through treatment application were investigated. This report summarizes the acoustic and aerodynamic technology with emphasis toward development of guidelines for future applications.

17. Key Words (Suggested by Author(s))		18. Distribution Statement
Supersonic Transport Jet Noise Suppressors Supersonic Jet Noise Fundamental Jet Mechanisms Two-Stage Ejector Nozzles Simple Mechanical Suppressors	Multi-Tube Suppressors Acoustic Ejectors Segmented Jet Plug Nozzles Engine System Noise Turbomachinery Noise	Approved for U. S. Government only. Transmittal of this document outside the U. S. Government must have prior approval of the Supersonic Transport Office.

19. Security Classif. (of this report)	20. Security Classif. (of this page)	21. No. of Pages	22. Price
Unclassified	Unclassified	799	

TABLE OF CONTENTS

Section		Page
	VOLUME I	
	ABSTRACT	i
	TABLE OF CONTENTS	iii
	LIST OF TABLES	vii
	LIST OF ILLUSTRATIONS	xiii
	SUMMARY	1
I.	INTRODUCTION	3
II.	JET NOISE TEST FACILITIES	7
	II.A AERO/ACOUSTIC TEST FACILITIES	9
	II.B JENOTS SCALE MODEL ACOUSTIC TEST FACILITY	13
	II.C PEEBLES SITE 4D FULL SCALE ENGINE TEST FACILITY	31
	II.D CORPORATE RESEARCH AND DEVELOPMENT CENTER'S SCALE MODEL AERO/ACOUSTIC TEST FACILITIES	39
	II.E FLUIDYNE ENGINEERING SCALE MODEL WIND TUNNEL TEST FACILITIES	45
III.	DATA ACQUISITION AND REDUCTION METHODS	49
	III.A JENOTS DATA ACQUISITION AND REDUCTION	53
	III.B PEEBLES SITE 4D DATA ACQUISITION AND REDUCTION	67
IV.	DATA PRESENTATION, FORM AND PURPOSE	75
V.	JET NOISE SUPPRESSOR CONFIGURATIONS AND PARAMETRIC STUDIES	81
	V.A MODEL AND ENGINE SUPPRESSOR CATEGORIES	83
	V.B TWO-STAGE EJECTOR NOZZLE TESTS ON SUPPRESSOR MODELS AND FULL SCALE ENGINE	89
	V.C PRIMARY SUPPRESSOR MODELS WITH CONICAL EJECTORS	137
	V.C.1 PRIMARY RADIAL RODS WITHIN TSEN 3	141

PRECEDING PAGE BLANK-NOT FILMED

TABLE OF CONTENTS (Continued)

Section		Page
	VOLUME I (Continued)	
V.C.2	PRIMARY THRUST REVERSER TAB VARIATIONS FOR MODEL AND ENGINE TESTS	181
V.C.3	PRIMARY VENTED CHUTE SUPPRESSORS	231
V.D	FLUID INJECTANT SUPPRESSORS	245
V.D.1	HOLLOW RADIAL SPOKES WITH AMBIENT PUMPING AND AXIAL INJECTING SIMULATED COMPRESSOR DISCHARGE BLEED	249
V.D.2	HOLLOW RADIAL SPOKES WITH RADIAL AND AXIAL AIR AND WATER INJECTION	271
V.D.3	AIR AND WATER INJECTION OVER PRIMARY THRUST REVERSER TABS	281
V.E	SECONDARY REVERSER-SUPPRESSOR FLAPS	289
V.F	MULTI-TUBE/HOLE SUPPRESSOR MODEL STUDIES	305
V.F.1	COMPARISON OF TUBE LENGTH, AREA RATIO, SECONDARY EJECTOR AND SECONDARY EJECTOR AIR FLOW EFFECTS ON 72 TUBE/HOLE NOZZLES	309
V.F.2	BASEPLATE AND TUBE EXIT PLANE STAGGER ANGLE VARIATIONS ON 72 TUBE MODEL SUPPRESSORS	329
V.F.3	VARIATIONS OF A 37 TUBE NOZZLE	375
V.F.4	TUBE END VARIATIONS ON 37 STRAIGHT, CONVERGENT, GREATREX AND CANTED END TUBES	419
V.F.5	TUBE INTERNAL AND EXTERNAL LENGTH TO DIAMETER STUDIES ON AN 85 TUBE NOZZLE	475
V.F.6	HOLE SHAPE, EQUAL AND UNEQUAL HOLE SIZE AND SPACING STUDIES ON 97 HOLE PLATES	523
V.F.7	VARIATIONS OF 97 TUBE PRIMARY NOZZLE WITH LARGE AND SMALL CENTER HOLE; COMPARISONS WITH HARDWALL AND 7.5% OPEN LINED EJECTORS	555

TABLE OF CONTENTS (Continued)

Section		Page
	VOLUME I (Concluded)	
V.F.8	GEOMETRIC VARIATIONS OF CENTER HOLE SHAPE ON 97 HOLE NOZZLE; HARDWALL AND ACOUSTICALLY LINED EJECTOR COMPARISONS; D_S/D_{Td} VARIATIONS	581
V.F.9	MULTI-HOLE NOZZLE PARAMETRIC VARIATIONS OF AREA RATIO, HOLE NUMBER, SHROUD D_S/D_{Td}, AND SHROUD AXIAL SPACING, X_S	633
V.F.10	MULTI-TUBE PRELIMINARY DESIGN NUMBER 3 (PD-3)	747
APPENDIX A	NOMENCLATURE	
	VOLUME II	
V.	JET NOISE SUPPRESSOR CONFIGURATIONS AND PARAMETRIC STUDIES (Concluded)	1
V.G	ACOUSTIC EJECTORS ON TUBE AND CONICAL NOZZLES	7
V.H	ANNULAR PLUG NOZZLE SUPPRESSOR MODEL STUDIES	69
V.H.1	PODS, TUBES, CHUTES, C.D.B. AND PRIMARY FLAPS ON ANNULAR PLUG NOZZLES	73
V.H.2	MULTI-ELEMENT SPOKE/CHUTE MODEL SUPPRESSOR PARAMETRIC INVESTIGATIONS ON ANNULAR PLUG NOZZLES	131
VI.	SYSTEM STUDIES	221
VI.A	CHOKED INLET - GE4 ENGINE	223
VI.B	EXHAUST NOZZLE OPEN AREA SCHEDULE - GE4 ENGINE	259
VI.C	TURBOMACHINERY NOISE ON GE4 ENGINE	267
VI.C.1	COMPRESSOR SOURCE NOISE IDENTIFICATION WITH ACOUSTIC PROBES	271
VI.C.2	COMPRESSOR TIP SHROUD TREATMENT STUDY	285
VI.C.3	NOISE SOURCE IDENTIFICATION WITH DIRECTIONAL MICROPHONE ARRAY	299

TABLE OF CONTENTS (Concluded)

Section			Page
		VOLUME II (Concluded)	
	VI.C.4	J79 TURBOMACHINERY NOISE TEST	307
	VI.C.5	GE4 ENGINE 435-007 NEAR AND FAR FIELD ACOUSTIC MEASUREMENTS	321
VII.		GENERAL ELECTRIC CORPORATE RESEARCH AND DEVELOPMENT CENTER'S FUNDAMENTAL JET NOISE WORK	345
	VII.A	SUPERSONIC JET NOISE SUPPRESSION RESULTS AND PREDICTION METHODS	349
	VII.A.1	INTRODUCTION	351
	VII.A.2	CHARACTERISTICS OF SUBSONIC AND SUPERSONIC JETS	353
	VII.A.3	ACOUSTICS OF SHOCK WAVES IN SUPERSONIC JETS	358
	VII.A.4	PARALLEL FLOW AND CONVERGENT NOZZLES WITH RODS, SHROUD, AND INDUCED FLOW	367
	VII.A.5	REVERSE SLOTTED CONE SUPPRESSORS	380
	VII.A.6	MULTITUBES AND MULTISHROUDS SUPPRESSORS	384
	VII.A.7	SUPERSONIC JET NOISE SUPPRESSOR MODEL	396
	VII.A.8	CONCLUSIONS	405
APPENDIX A		NOMENCLATURE	484

LIST OF TABLES

Table		Page
II.A.1	Facility Capabilities and Limitations.	12
III.A-1	Octave Band Atmospheric Absorption Values.	61
III.A-2	GE/Boeing Agreed Atmospheric Absorption Values.	61
V.A-1	Jet Suppressor Categories.	87
V.B-1	Test Summary (Model 5.1 STAR).	100
V.B-2	Test Summary (Model 4.32", 4.82", and 5.14" I.D. Cones).	101
V.B-3	Test Summary (Model 4.32-3B, 4.82-3B and 5.14-3B).	103
V.B-4	Test Summary (Model 5.1S-3B, 5.1S-3B-1 and 5.1S-3B-2).	106
V.B-5	Test Summary (Model 5.1S-3B-4 and 5.1S-3B-5).	109
V.B-6	Test Summary (Model 5.6-56-7).	115
V.B-7	Test Summary (Model 5.6-56-1).	116
V.B-8	Test Summary (Model 5.6-26-2).	117
V.B-9	Test Summary (Model 5.6-56-3).	118
V.B-10	Test Summary (Model 5.6-56B-7, -8, -10, -11, and -12).	127
V.C.1-1	Test Summary (Model 5.1S-3B-6, -7, -8, -9 and -10).	150
V.C.1-2	Test Summary (Model 4.9B-161-3B and -3B-1).	157
V.C.1-3	Test Summary (Model 4.9B-162-3B and -3B-1).	158
V.C.1-4	Test Summary (Model 4.9B-163-3B and -3B-1).	159
V.C.1-5	Test Summary (Model 4.9B-164-3B and -3B-1).	160
V.C.1-6	Test Summary (Model 4.9B-165-3B and -3B-1).	161
V.C.1-7	Test Summary (Model 4.9B-166-3B).	162
V.C.1-8	Test Summary (Model 4.9-3B-1 and -3B-2).	171

LIST OF TABLES (Continued)

Table		Page
V.C.1-9	Test Summary (Model 4.9-3B-3 and -3B-4).	172
V.C.2-1	Test Summary (Model 4.32" Cone).	190
V.C.2-2	Test Summary (Model 4.82" Cone).	191
V.C.2-3	Test Summary (Model 5.14" Cone).	194
V.C.2-4	Test Summary (Model 4.9-4B-R7).	196
V.C.2-5	Test Summary (Model 4.9-4B-R7-1).	200
V.C.2-6	Test Summary (Model 4.9-4B-R7-2).	202
V.C.2-7	Test Summary (Model 5.1-4B-R2).	204
V.C.2-8	Test Summary (Model 4.3-4B-R6).	206
V.C.2-9	Test Summary (Model 4.9-4B-R8).	207
V.C.2-10	Test Summary (Model 4.9-4B-R8-1).	214
V.C.2-11	Test Summary (Model 5.637" Cone).	216
V.C.2-12	Test Summary (Model 5.6-56B-14).	217
V.C-2-13	Test Summary (Model 5.6-56B-15).	218
V.C-2-14	Test Summary (Model 5.6-56B-16).	238
V.C.3-1	Test Summary (Model III-14).	239
V.C.3-2	Test Summary (Model III-15).	317
V.F.1-1	Test Summary (Model 4.0H72).	320
V.F.1-2	Test Summary (Model 4.88H-121-72).	337
V.F.2-1	Test Summary (Model 4.3" Cone).	342
V.F.2-2	Test Summary (Model 4.0T72-4).	345
V.F.2-3	Test Summary (Model 4.0T72-5).	350
V.F.2-4	Test Summary (Model 4.0T72-30-1).	

LIST OF TABLES (Continued)

Table		Page
V.F.2-5	Test Summary (Model 4.0T72-60-1).	353
V.F.2-6	Test Summary (Model 4.0T72-30).	356
V.F.2-7	Test Summary (Model 4.0T72-60).	359
V.F.3-1	Test Summary (Model 4.1-T37-10CS).	383
V.F.3-2	Test Summary (Model 4.1-T37-10CSEL).	388
V.F.3-3	Test Summary (Model 4.1-T37-3.5).	396
V.F.3-4	Test Summary (Model 4.1-T37-4.1).	400
V.F.3-5	Test Summary (Model 4.1-T37-5.3).	404
V.F.4-1	Test Configuration Summary.	433
V.F.4-2	Test Summary (Model 4.1" Cone).	435
V.F.4-3	Test Summary (Model 4.1T37-23).	440
V.F.4-4	Test Summary (Model 4.1T37-27).	443
V.F.4-5	Test Summary (Model 4.1T37-31).	446
V.F.4-6	Test Summary (Model 4.1T37-29).	449
V.F.4-7	Test Summary (Model 4.1T37-21).	452
V.F.4-8	Test Summary (Model 4.1T37-25).	455
V.F.5-1	Test Summary (Model 4.3" Cone).	482
V.F.5-2	Test Summary (Model 3.4T85).	486
V.F.5-3	Test Summary (Model 3.4T85-1).	489
V.F.5-4	Test Summary (Model 3.4T85-2).	492
V.F.5-5	Test Summary (Model 3.4T85-3).	495
V.F.5-6	Test Summary (Model 3.4T85-4).	498
V.F.5-7	Test Summary (Model 3.4T85-5).	501
V.F.5-8	Test Summary (Model 3.4T85-6).	504

LIST OF TABLES (Continued)

Table		Page
V.F.6-1	Test Summary (Model 4.2SH97).	529
V.F.6-2	Test Summary (Model 4.2H97-1).	532
V.F.6-3	Test Summary (Model 4.88H121-97).	541
V.F.6-4	Test Summary (Model 4.2H97).	545
V.F.6-5	Test Summary (Model 4.39H97).	549
V.F.7-1	Test Summary (Model 4.2T97).	563
V.F.7-2	Test Summary (Model 4.2T97-1).	567
V.F.7-3	Test Summary (Model 4.2T97-7.7CS).	571
V.F.7-4	Test Summary (Model 4.2T97-7.7CS-1).	575
V.F.8-1	Test Summary (Model 4.3" Cone).	587
V.F.8-2	Test Summary (Mode . 4.2H97N-1).	592
V.F.8-3	Test Summary (Model 4.2H97N-2).	596
V.F.8-4	Test Summary (Model 4.2H97N-CS-2).	600
V.F.8-5	Test Summary (Model 4.2H97N-CS-3).	604
V.F.8-6	Test Summary (Model 4.2H97N-CS).	608
V.F.8-7	Test Summary (Model 4.2H97N-CS-4).	612
V.F.8-8	Test Summary (Model 4.2H97N-CS-1).	616
V.F.8-9	Test Summary (Model 4.2H97N-CS-5).	620
V.F.8-10	Test Summary (Model 4.2H97N-CS-6).	624
V.F.9-1	Test Summary (Model 5.7" I.D. Cone).	646
V.F.9-2	Test Summary (Model 6.0H85-2.0).	657
V.F.9-3	Test Summary (Model 6.0H85-2.0).	660
V.F.9-4	Test Summary (Model 6.0H85-2.3).	663

LIST OF TABLES (Concluded)

Table		Page
V.F.9-5	Test Summary (Model 6.0H85-2.7).	666
V.F.9-6	Test Summary (Model 6.0H85-3.1).	669
V.F.9-7	Test Summary (Model 6.0H85-4.0).	672
V.F.9-8	Test Summary (Model 6.0H85-4.0).	675
V.F.9-9	Test Summary (Model 6.0H55-2.7).	691
V.F.9-10	Test Summary (Model 6.0H55-2.7).	694
V.F.9-11	Test Summary (Model 6.0H121-2.7).	697
V.F.9-12	Test Summary (Model 6.0H85-2.7-CS1-1).	713
V.F.9-13	Test Summary (Model 6.0H85-2.7-CS2-1).	716
V.F.9-14	Test Summary (Model 6.0H85-2.7-CS3).	719
V.F.9-15	Test Summary (Model 6.0H85-2.7-CS2-3).	735
V.F.9-16	Test Summary (Model 6.0H85-2.7-CS2).	738
V.F.10-1	Test Summary (Model 1).	763
V.F.10-2	Test Summary (Model 3).	766
V.F.10-3	Test Summary (Model 4).	769
V.F.10-4	Test Summary (Model 5).	772

LIST OF ILLUSTRATIONS

Figure		Page
II.B-1	JENOTS Noise Facility.	24
II.B-2	Central Air Supply System, Building 401.	25
II.B-3	Schematic of JENOTS Main Air Pipe and Burner System.	26
II.B-4	JENOTS Control Panel.	27
II.B-5	Schematic of JENOTS Sound Data Microphone System.	28
II.B-6	JENOTS Ground Run-Up Silencer.	29
II.C-1	Peebles Acoustic Test Site.	37
II.C-2	Typical Engine Installation on Acoustic Stand at Peebles.	38
II.D-1	Research and Development Center 2 Inch and 6 Inch Diameter Aero/Acoustic Facilities.	44
III.A-1	Schematic of JENOTS Pre-Late 1969 Acoustic Data Acquisition/Reduction System.	62
III.A-2	JENOTS Acoustic Monitoring and Digital Recording Systems.	63
III.A-3	Schematic of JENOTS Post-Late 1969 Acoustic Data Acquisition System.	64
III.A-4	Schematic of JENOTS Post-Late 1969 Acoustic Data Reduction System.	65
III.B-1	Schematic of Peebles Site 4D Acoustic Data Acquisition System.	70
III.B-2	Schematic of Peebles Site 4D/Instrumentation Data Room Acoustic Data Reduction System.	71
III.B-3	Instrumentation Data Room, Acoustic Data Reduction Equipment.	72
III.B-4	Instrumentation Data Room, Acoustic Data Reduction Equipment.	73
V.B-1	TSEN-3 Hardware used for Investigation of Geometric Variations.	98

PRECEDING PAGE BLANK-NOT FILME

LIST OF ILLUSTRATIONS (Continued)

Figure		Page
V.B-2	Schematic of TSEN=3 used for Investigation of Geometric Variations.	99
V.B-3	Comparison of 300 Ft. Sideline Jet Noise Levels for Cone and Star Primaries.	102
V.B-4	Effect of D_S/D_8 Variations within TSEN-3 on 300 Ft. Sideline Jet Noise Levels.	104
V.B-5	Effect of D_S/D_8 Variations within TSEN-3 on Spectra and Directivity.	105
V.B-6	Effect of D_S Positioning with TSEN=3 on 300 Ft. Sideline Jet Noise Levels.	107
V.B-7	Effect of D_S Positioning within TSEN=3 on Spectra and Directivity.	108
V.B-8	Effect of Blow-In-Door Flow Area Variation within TSEN-3 on 300 Ft. Sideline Jet Noise Levels.	110
V.B-9	Effect on Blow-In-Door Flow Area Variation within TSEN=3 on Spectra and Directivity.	111
V.B-10	TSEN=56 Hardware for Investigation of D_9/D_S Variation.	112
V.B-11	TSEN=56 Hardware Installation for D_9/D_S Investigation.	113
V.B-12	Schematic of TSEN=56 used for Investigation of D_9/D_S Variations.	114
V.B-13	Effect of D_9/D_S Variation within TSEN=56 on 300 Ft. Sideline Jet Noise Levels.	119
V.B-14	Effect of D_9/D_S Variation within TSEN=56 on Jet Noise Levels and Suppression Characteristics.	120
V.B-15A-D	Effect of D_9/D_S Variation within TSEN=56 on Spectra and Directivity.	121-124
V.B-16	TSEN=56 Air Handling Characteristics.	125
V.B-17	Schematic of TSEN=56 Plus Shroud Configurations.	126
V.B-18A,B	300 Ft. Sideline Jet Noise Levels for TSEN=56 Plus Shroud Configurations.	129,130

LIST OF ILLUSTRATIONS (Continued)

Figure		Page
V.B-19	Effect of Shroud on TSEN-56 PNL Suppressions.	131
V.B-20A,B	Effect of Shroud on TSEN-56 Spectra and Directivity.	132,133
V.B-21	GE4/SST Engine 432-002 Mounted on Peebles Site IV Acoustic Facility.	134
V.B-22	GE4 Engine Noise Measurements - Conical Primary and Conical Primary Plus TSEN.	135
V.B-23	GE4 Engine Noise Measurements - Star Primary Plus TSEN.	136
V.C.1-1	Schematic of TSEN 3 with (8) Radial Rods Aft of Star Primary Plane 8.	149
V.C.1-2	Effect of Radial Rod Penetration within TSEN 3 on 300 Ft. Sideline Jet Noise Levels.	152
V.C.1-3	Effect of Radial Rod Penetration within TSEN 3 on 300 Ft. Sideline PNL Suppression.	153
V.C.1-4A,B	Effect of Radial Rod Penetration within TSEN 3 on Spectra and Directivity.	154,155
V.C.1-5	Schematic of (16) Radial Rod Primary Nozzle Plus TSEN 3.	156
V.C.1-6A-D	Effect of Radial Rod Penetration and Axial Spacing, X_S, of TSEN 3 on 300 Ft. Sideline Jet Noise Levels.	163-166
V.C.1-7A,B	Effect of Radial Rod Angularity and Axial Spacing, X_S, of TSEN-3 on 300 Ft. Sideline Jet Noise Levels.	167,168
V.C.1-8	Effect of Radial Rod Penetration and Angularity on 300 Ft. Sideline PNL Suppression.	169
V.C.1-9	Schematic of TSEN-3 with (8) Radial Rods at Two Axial Locations.	170
V.C.1-10	Effect of Radial Rod Penetration at Different Axial Positions Within TSEN 3 on 300 Ft. Sideline Jet Noise Levels.	173
V.C.1-11	Effect of Radial Rod Penetration and Axial Location on 300 Ft. Sideline PNL Suppression.	174

LIST OF ILLUSTRATIONS (Continued)

Figure		Page
V.C.1-12	Two Stage Ejector Nozzle Aerodynamic Model Hardware.	175
V.C.1-13	Aerodynamic Performance of TSEN with Conical Primary and (8) Radial Rods.	176
V.C.1-14	Secondary Nozzle Contour Static Pressure Distribution of TSEN with and without Radial Rods.	177
V.C.1-15	Exhaust Nozzle of GE4 Block I Engine with (8) Radial Rods at 65% Penetration.	178
V.C.1-16	Effect of (8) Radial Rods on 300 Ft. Sideline Jet Noise Levels and PNL Suppression of GE4 Block I Engine.	179
V.C.2-1	Primary Thrust Reverser Tabs Installed in TSEN 4.	188
V.C.2-2	Schematic and List of Test Configurations of TSEN 4 with Primary Thrust Reverser Tabs.	189
V.C.2-3	300 Ft. Sideline Jet Noise Levels for Average Conical Baseline.	195
V.C.2-4	300 Ft. Sideline Jet Noise Levels for TSEN 4 with 4.82" Cone and Primary Thrust Reverser Tabs, α=11 1/2°.	197
V.C.2-5	300 Ft. Sideline Jet Noise Levels for TSEN 4 with 4.82" Cone Primary Thrust Reverser Tabs, α=18°.	199
V.C.2-6	300 Ft. Sideline Jet Noise Levels for TSEN 4 with 4.82" Cone Primary Thrust Reverser Tabs, α=24°.	201
V.C.2-7	300 Ft. Sideline Jet Noise Levels for TSEN 4 with 5.14" Cone and Primary Thrust Reverser Tabs, D_S/D_8 = 1.18.	203
V.C.2-8	300 Ft. Sideline Jet Noise Levels for TSEN 4 with 4.32" Cone and Primary Thrust Reverser Tabs, D_S/D_8 = 1.41.	205
V.C.2-9	300 Ft. Sideline Jet Noise Levels for 8 and 4 Primary Tabs within TSEN 4.	208
V.C.2-10	Effect of Primary Thrust Reverser Tab Angle on 300 Ft. Sideline PNL Suppression.	209

LIST OF ILLUSTRATIONS (Continued)

Figure		Page
V.C.2-11	Effect of Primary Thrust Reverser Tabs and D_S/D_8 Variation within TSEN 4 on 300 Ft. Sideline PNL Suppression.	210
V.C.2-12	Effect of Primary Thrust Reverser Tab Number on 300 Ft. Sideline PNL Suppression.	211
V.C.2-13	Primary Thrust Reverser Tabs Installed on 5.367" I.D. Primary Nozzle without Two-Stage Ejector, TSEN-56.	212
V.C.2-14	Schematic and Test Configuration Summary of Conical Primary Plus TSEN 56 with (16) Primary Thrust Reverser Tabs.	213
V.C.2-15	Effect of Primary Thrust Reverser Tabs and D_9/D_S Variation within TSEN 56 on 300 Ft. Sideline Jet Noise Levels.	219
V.C.2-16	Effect of Primary Thrust Reverser Tabs and D_9/D_S Variation within TSEN 56 on 300 Ft. Sideline PNL Suppression.	220
V.C.2-17	Primary Thrust Reverser Tab System Hardware for Aerodynamic Models.	221
V.C.2-18	Static Performance of the Primary Reverser Tab Suppressor System.	222
V.C.2-19	Engine Hardware for Primary Thrust Reverser Tab Suppressor Tests.	223
V.C.2-20	Effect of Primary Thrust Reverser Tabs within GE4 Block I Engine on 300 Ft. Sideline Jet Noise Levels.	224
V.C.2-21	Comparison of Model and Engine Peak 300 Ft. Sideline PNL Suppression with Primary Thrust Reverser Tabs.	225
V.C.2-22A-E	Comparison of Model and Engine Spectra and Directivity with Primary Thrust Reverser Tabs.	226-230
V.C.3-1	Primary Vented Chute Nozzle Hardware.	236
V.C.3-2	Schematic of Primary Vented Chute Suppressor Configurations.	237
V.C.3-3	300 Ft. Sideline Jet Noise Levels and PNL Suppression as a Function of P_{T8}/P_o for Primary Chuted Suppressors at High Ideal Jet Velocities.	240

LIST OF ILLUSTRATIONS (Continued)

Figure		Page
V.C.3-4	300 Ft. Sideline Spectra and Directivity for Primary Chuted Suppressors at High Ideal Jet Velocities.	241
V.C.3-5	300 Ft. Sideline Jet Noise Levels and PNL Suppression for Primary Chuted Suppressors at Low Ideal Jet Velocities.	242
V.C.3-6	300 Ft. Sideline Spectra and Directivity for Primary Chuted Suppressors at Low Ideal Jet Velocities.	243
V.D.1-1	Schematic of Test Hardware for Vented and Simulated C.D.B. Injectant Study.	255
V.D.1-2	Hollow Spoke Design for Injectant Study.	256
V.D.1-3	Hollow Radial Spoke-Design T1.	257
V.D.1-4	Hollow Radial Spoke-Design T3.	258
V.D.1-5	Hollow Radial Spoke C.D.B. Flow Calibration.	259
V.D.1-6	300 Ft. Sideline Peak Jet Noise Levels using T1 Hollow Spokes.	260
V.D.1-7	300 Ft. Sideline Peak Jet Noise Levels using T3 Hollow Spokes.	261
V.D.1-8	300 Ft. Sideline Peak PNL Suppression of Vented and Pressurized Spoke Systems.	262
V.D.1-9	300 Ft. Sideline Suppression Effect of Simulated Compressor Discharge Bleed.	263
V.D.1-10A-C	Effect of Simulated C.D.B. on Spectra Suppression with T1 Hollow Spokes.	264-266
V.D.1-11A-C	Effect of Simulated C.D.B. on Spectra Suppression with T3 Hollow Spokes.	267-269
V.D.2-1	Schematic of Primary Spoke/Fluid Injection Suppressor System.	275
V.D.2-2	Effect of Air Injection on 300 and 1500 Ft. Sideline PNL Suppression Characteristics of Primary Spoke System.	276
V.D.2-3	Effect of Air Injection on 300 Ft. Sideline Spectral Characteristics of Primary Spoke System.	277

LIST OF ILLUSTRATIONS (Continued)

Figure		Page
V.D.2-4	Effect of Water Injection on 300 and 1500 Ft. Sideline PNL Suppression Characteristics of Primary Spoke System.	278
V.D.2-5	Effect of Water Injection on 300 Ft. Sideline Spectral Characteristics of Primary Spoke System.	279
V.D.3-1	Schematic of Primary Tab/Fluid Injection Suppressor System.	285
V.D.3-2	Effect of Air and Water Injection on 300 Ft. Sideline PNL Suppression Characteristics of Primary Thrust Reverser Tab System.	286
V.D.3-3	Effect of Air and Water Injection on 1500 Ft. Sideline PNL Suppression Characteristics of Primary Thrust Reverser Tab System.	287
V.E-1	Scale Model Secondary Reverser - Suppressor Flap Configurations.	294
V.E-2	300 Ft. Sideline Peak PNL Levels for F1 Flaps with D_S/D_8 = 1.41, 1.26 and 1.18.	295
V.E-3	300 Ft. Sideline Peak PNL Levels for F7 Flaps with D_S/D_8 = 1.41, 1.26 and 1.18.	296
V.E-4	300 Ft. Sideline Peak PNL Levels for F15 Flaps with D_S/D_8 = 1.41, 1.26 and 1.18.	297
V.E-5	300 Ft. Sideline Peak PNL Levels for 4.32", 4.82" and 5.14" D_8 Cones.	298
V.E-6	Effect of D_S/D_8 on PNL Suppression for F1, F7 and F15 Reverser - Suppressor Flaps.	299
V.E-7	Effect of T_{T8} on PNL Suppression for F1, F7 and F15 Reverser - Suppressor Flaps.	300
V.E-8	Effect of Flap Planform on 300 Ft. Sideline Peak PNL Spectra at D_S/D_8 = 1.41, 1.26 and 1.18.	301
V.E-9	Effect of D_S/D_8 on 300 Ft. Sideline Peak PNdB Angle Spectra for F1, F7 and F15 Flaps.	302
V.E-10	Effect of Flap Planform on 300 Ft. Sideline 60° Spectra at D_S/D_8 = 1.41, 1.26 and 1.18.	303

LIST OF ILLUSTRATIONS (Continued)

Figure		Page
V.E-11	Effect of D_s/D_8 on 300 Ft. Sideline 60° Spectra for F1, F7 and F15 Flaps.	304
V.F.1-1	72 Hole Plate Hardware, Description and Test Summary.	317
V.F.1-2	300 Ft. Sideline Jet Noise Levels for a 72 Hole Plate, AR_d = 2.65.	318
V.F.1-3	1500 Ft. Sideline Jet Noise Levels for a 72 Hole Plate, AR_d = 2.65.	319
V.F.1-4	Schematic of 72 Hole Plate and Test Summary.	320
V.F.1-5	300 Ft. Sideline Jet Noise Levels for a 72 Hole Plate, AR_d = 2.0.	321
V.F.1-6	1500 Ft. Sideline Jet Noise Levels for a 72 Hole Plate, AR_d = 2.0.	322
V.F.1-7	Effect of External Tube Length to Tube Internal Diameter on 300 Ft. and 1500 Ft. Sideline PNL Suppressions for 72 Tube/Hole Nozzles.	323
V.F.1-8	Effect of Area Ratio on 300 Ft. and 1500 Ft. Sideline PNL Suppressions for 72 Hole Plates.	324
V.F.1-9	Effect of Area Ratio and Tube Length on Aerodynamic Performance for 72 Tube/Hole Nozzles.	325
V.F.1-10	Schematic of 72 Tube Primary Nozzle Plus Cylindrical Ejector (Shroud) Configurations used with and without Secondary Flow.	326
V.F.1-11	Effect of Open and Blocked Secondary Air Passages on 300 Ft. and 1500 Ft. Sideline PNL Suppressions for a 72 Tube Primary Nozzle with Cylindrical Ejector.	327
V.F.1-12	Effect of Secondary Cylindrical Ejector on Aerodynamic Performance for a 72 Tube Nozzle.	328
V.F.2-1	72 Tube Nozzle Hardware for Baseplate and Tube Exit Plane Stagger Configurations.	335
V.F.2-2	Schematic of 72 Tube Nozzle Configurations for Baseplate and Tube Exit Plane Stagger Variations.	336
V.F.2-3	300 Ft. Sideline Jet Noise Levels for Average Baseline Conical Nozzle.	340

LIST OF ILLUSTRATIONS (Continued)

Figure		Page
V.F.2-4	1500 Ft Sideline Jet Noise Levels for Average Baseline Conical Nozzle.	341
V.F.2-5	300 Ft. Sideline Jet Noise Levels for a 72 Tube Nozzle with Flat Baseplate and Coplanar Tube Exit.	343
V.F.2-6	1500 Ft. Sideline Jet Noise Levels for a 72 Tube Nozzle with Flat Baseplate and Coplanar Tube Exit.	344
V.F.2-7	300 Ft. Sideline Jet Noise Levels for a 72 Tube Nozzle with Flat Baseplate and Coplanar Tube Exit.	346
V.F.2-8	1500 Ft. Sideline Jet Noise Levels for a 72 Tube Nozzle with Flat Baseplate and Coplanar Tube Exit.	347
V.F.2-9	300 Ft. Sideline PNL Suppression Comparisons for 72 Tube Nozzles with Flat Baseplates and Coplanar Exits.	348
V.F.2-10	1500 Ft. Sideline PNL Suppression Comparisons for 72 Tube Nozzles with Flat Baseplates and Coplanar Exits.	349
V.F.2-11	300 Ft. Sideline Jet Noise Levels for a 72 Tube Nozzle with 30° Baseplate Stagger and Coplanar Tube Exit.	351
V.F.2-12	1500 Ft. Sideline Jet Noise Levels for a 72 Tube Nozzle with 30° Baseplate Stagger and Coplanar Tube Exit.	352
V.F.2-13	300 Ft. Sideline Jet Noise Levels for a 72 Tube Nozzle with 60° Baseplate Stagger and Coplanar Tube Exit.	354
V.F.2-14	1500 Ft. Sideline Jet Noise Levels for a 72 Tube Nozzle with 60° Baseplate Stagger and Coplanar Tube Exit.	355
V.F.2-15	300 Ft. Sideline Jet Noise Levels for a 72 Tube Nozzle with 30° Baseplate and Tube Exit Stagger.	357
V.F.2-16	1500 Ft. Sideline Jet Noise Levels for a 72 Tube Nozzle with 30° Baseplate and Tube Exit Stagger.	358
V.F.2-17	300 Ft. Sideline Jet Noise Levels for a 72 Tube Nozzle with 60° Baseplate and Tube Exit Stagger.	360

LIST OF ILLUSTRATIONS (Continued)

Figure		Page
V.F.2-18	1500 Ft. Sideline Jet Noise Levels for a 72 Tube Nozzle with 60° Baseplate and Tube Exit Stagger.	361
V.F.2-19	Effect of Baseplate and Tube Exit Plane Stagger on 300 Ft. Sideline PNL Suppressions for a 72 Tube Nozzle.	362
V.F.2-20	Effect of Baseplate and Tube Exit Plane Stagger on 1500 Ft. Sideline PNL Suppressions for a 72 Tube Nozzle.	363
V.F.2-21A-G	Effect of Baseplate and Tube Exit Plane Stagger on 300 Ft. Sideline Spectra and Directivity.	364-370
V.F.2-22	Effect of Baseplate and Tube Exit Plane Stagger on Mean Baseplate Pressure Ratio.	371
V.F.2-23	Effect of Baseplate and Tube Exit Plane Stagger on Nozzle Exit to Mean Baseplate Pressure Ratio.	372
V.F.2-24	Effect of Baseplate and Tube Exit Plane Stagger on Baseplate Drag Coefficient.	373
V.F.3-1	Schematic of 37 Greatrex Tube Nozzle with Fiberglass Lined Ejector.	382
V.F.3-2	300 Ft. Sideline Jet Noise Levels for 37 Greatrex Tube + Fiberglass Ejector.	384
V.F.3-3	1500 Ft. Sideline Jet Noise Levels for 37 Greatrex Tube + Fiberglass Ejector.	385
V.F.3-4	300 and 1500 Ft. Sideline PNL Suppression Levels for 37 Greatrex Tube + Fiberglass Ejector.	386
V.F.3-5	Schematic of 37 Greatrex Tube Nozzle with Rigimesh Lined Ejector.	387
V.F.3-6	300 Ft. Sideline Jet Noise Levels for 37 Greatrex Tubes + Rigimesh Ejector.	389
V.F.3-7	1500 Ft. Sideline Jet Noise Levels for 37 Greatrex Tubes + Rigimesh Ejector.	390
V.F.3-8	300 and 1500 Ft. Sideline PNL Suppression for 37 Greatrex Tube + Rigimesh Ejector.	391

LIST OF ILLUSTRATIONS (Continued)

Figure		Page
V.F.3-9	Hardware for 37 Tube High Temperature Models.	392
V.F.3-10	Schematic of Hardware for 37 Tube High Temperature Models.	393
V.F.3-11	300 Ft. Sideline Jet Noise Levels for the 4.32" I.D. Baseline Conical Nozzle.	394
V.F.3-12	1500 Ft. Sideline Jet Noise Levels for the 4.32" I.D. Baseline Conical Nozzle.	395
V.F.3-13	300 Ft. Sideline Jet Noise Levels for 37 Tube High Temperature Model, AR_d = 3.5.	397
V.F.3-14	1500 Ft. Sideline Jet Noise Levels for 37 Tube High Temperature Model, AR_d = 3.5.	398
V.F.3-15	300 and 1500 Ft. Sideline PNL Suppressions for 37 Tube High Temperature Model, AR_d = 3.5.	399
V.F.3-16	300 Ft. Sideline Jet Noise Levels for 37 Tube High Temperature Model, AR_d = 4.1.	401
V.F.3-17	1500 Ft. Sideline Jet Noise Levels for 37 Tube High Temperature Model, AR_d = 4.1.	402
V.F.3-18	300 and 1500 Ft. Sideline PNL Suppressions for 37 Tube High Temperature Model, AR_d = 4.1.	403
V.F.3-19	300 Ft. Sideline Jet Noise Levels for 37 Tube High Temperature Model, AR_d = 5.3.	405
V.F.3-20	1500 Ft. Sideline Jet Noise Levels for 37 Tube High Temperature Model, AR_d = 5.3.	406
V.F.3-21	300 and 1500 Ft. Sideline PNL Suppressions for 37 Tube High Temperature Model, AR_d = 5.3.	407
V.F.3-22	300 Ft. Sideline PNL Suppression Comparison for 37 Tube High Temperature Models, AR_d = 3.5, 4.1 and 5.3.	408
V.F.3-23	1500 Ft. Sideline PNL Suppression Comparison for 37 Tube High Temperature Models, AR_d = 3.5, 4.1 and 5.3.	409
V.F.3-24A-H	300 Ft. Sideline Spectra and Directivity Comparison for 37 Tube High Temperature Models.	410-417

LIST OF ILLUSTRATIONS (Continued)

Figure		Page
V.F.4-1	Schematic of Tube Nozzle Hardware Specifics for Tube End Study.	429
V.F.4-2	Schematic of 37 Tube Nozzle Configuration with Straight End Tubes.	430
V.F.4-3	Typical Tube Hardware for End Variation Study.	431
V.F.4-4	37 Greatrex End Tubes in AR_d = 4 Baseplate.	432
V.F.4-5	Schematic of 37 Tube Nozzle Configuration with Canted End Tubes.	434
V.F.4-6	300 Ft. Sideline Jet Noise Levels for 4.148" Cone.	438
V.F.4-7	1500 Ft. Sideline Jet Noise Levels for 4.148" Cone.	439
V.F.4-8	300 Ft. Sideline Jet Noise Levels for 37 Straight End Tube Nozzle, AR_d = 4.0.	441
V.F.4-9	1500 Ft. Sideline Jet Noise Levels for 37 Straight End Tube Nozzle, AR_d = 4.0.	442
V.F.4-10	300 Ft. Sideline Jet Noise Levels for 37 Straight End Tube Nozzle, AR_d = 3.0.	444
V.F.4-11	1500 Ft. Sideline Jet Noise Levels for 37 Straight End Tube Nozzle, AR_d = 3.0.	445
V.F.4-12	300 Ft. Sideline Jet Noise Levels for 37 Canted End Tube Nozzle, AR_d = 4.0.	447
V.F.4-13	1500 Ft. Sideline Jet Noise Levels for 37 Canted End Tube Nozzle, AR_d = 4.0.	448
V.F.4-14	300 Ft. Sideline Jet Noise Levels for 37 Canted End Tube Nozzle, AR_d = 3.0.	450
V.F.4-15	1500 Ft. Sideline Jet Noise Levels for 37 Canted End Tube Nozzle, AR_d = 3.0.	451
V.F.4-16	300 Ft. Sideline Jet Noise Levels for 37 Greatrex End Tube Nozzle, AR_d = 4.0.	453
V.F.4-17	1500 Ft. Sideline Jet Noise Levels for 37 Greatrex End Tube Nozzle, AR_d = 4.0.	454

LIST OF ILLUSTRATIONS (Continued)

Figure		Page
V.F.4-18	300 Ft. Sideline Jet Noise Levels for 37 Greatrex End Tube Nozzle, AR_d = 3.0.	456
V.F.4-19	1500 Ft. Sideline Jet Noise Levels for 37 Greatrex End Tube Nozzle, AR_d = 3.0.	457
V.F.4-20	Comparison of 300 Ft. Sideline PNL Suppression for Straight, Greatrex, and Canted End Tubes.	458
V.F.4-21	Comparison of 1500 Ft. Sideline PNL Suppression for Straight, Greatrex, and Canted End Tubes.	459
V.F.4-22	Change in PNL Suppression Due to Area Ratio Variation.	460
V.F.4-23	Change in PNL Suppression Due to Tube Exit Cant.	461
V.F.4-24	Gain in PNL Suppression Due to Greatrex End Tubes.	462
V.F.4-25	Comparison of PNL Suppression for 1968 and 1969 Test Results on 37 Greatrex End Tubes.	463
V.F.4-26A-F	Effect of Straight, Greatrex and Canted End Tubes on Spectra and Directivity.	464-469
V.F.4-27	Octave Band Spectral Suppression Attributable to Addition of Greatrex Tube Ends.	470
V.F.4-28	Effect of Tube End Variations on Mean Base Pressure Ratio.	471
V.F.4-29	Effect of Tube End Variations on Nozzle Exit to Mean Base Pressure Ratio.	472
V.F.4-30	Effect of Tube End Variations on Baseplate Drag Coefficient.	473
V.F.5-1	Basic 85 Tube Hardware Configuration used in the External/Internal Tube Length Variation Study.	480
V.F.5-2	Schematic of 85 Tube Nozzle used in External/Internal Tube Length Study.	481
V.F.5-3	300 Ft. Sideline Jet Noise Levels for Average Conical Baseline.	484
V.F.5-4	1500 Ft. Sideline Jet Noise Levels for Average Conical Baseline.	485

LIST OF ILLUSTRATIONS (Continued)

Figure		Page
V.F.5-5	300 Ft. Sideline Jet Noise Levels for an 85 Tube Nozzle, L_{ti}/D_t = 10.47.	487
V.F.5-6	1500 Ft. Sideline Jet Noise Levels for an 85 Tube Nozzle, L_{ti}/D_t = 10.47.	488
V.F.5-7	300 Ft. Sideline Jet Noise Levels for an 85 Tube Nozzle, L_{ti}/D_t = 8.14.	490
V.F.5-8	1500 Ft. Sideline Jet Noise Levels for an 85 Tube Nozzle, L_{ti}/D_t = 8.14.	491
V.F.5-9	300 Ft. Sideline Jet Noise Levels for an 85 Tube Nozzle, L_{ti}/D_t = 6.98.	493
V.F.5-10	1500 Ft. Sideline Jet Noise Levels for an 85 Tube Nozzle, L_{ti}/D_t = 6.98.	494
V.F.5-11	300 Ft. Sideline Jet Noise Levels for an 85 Tube Nozzle, L_{ti}/D_t = 5.81.	496
V.F.5-12	1500 Ft. Sideline Jet Noise Levels for an 85 Tube Nozzle, L_{ti}/D_t = 5.81.	497
V.F.5-13	300 Ft. Sideline Jet Noise Levels for an 85 Tube Nozzle, L_{ti}/D_t = 4.65.	499
V.F.5-14	1500 Ft. Sideline Jet Noise Levels for an 85 Tube Nozzle, L_{ti}/D_t = 4.65.	500
V.F.5-15	300 Ft. Sideline Jet Noise Levels for an 85 Tube Nozzle, L_{ti}/D_t = 3.49.	502
V.F.5-16	1500 Ft. Sideline Jet Noise Levels for an 85 Tube Nozzle, L_{ti}/D_t = 3.49.	503
V.F.5-17	300 Ft. Sideline Jet Noise Levels for an 85 Tube Nozzle, L_{ti}/D_t = 1.74.	505
V.F.5-18	1500 Ft. Sideline Jet Noise Levels for an 85 Tube Nozzle, L_{ti}/D_t = 1.74.	506
V.F.5-19	Effect of Internal/External Tube Length to Tube Internal Diameter Ratio on PNL Suppression.	507
V.F.5-20A,B	Effect of Tube Internal Length to Tube Internal Diameter, L_{ti}/D_t, on PNL Suppressions for Different Jet Velocities.	508,509

LIST OF ILLUSTRATIONS (Continued)

Figure		Page
V.F.5-21A-H	Effect of Tube Length to Tube Diameter Ratio on 300 Ft. Sideline Spectra and Directivity.	510-517
V.F.5-22	Effect of Tube Length to Tube Diameter Ratio on Mean Baseplate Pressure Ratio.	518
V.F.5-23	Effect of Tube Length to Tube Diameter Ratio on Nozzle Exit to Mean Baseplate Pressure Ratio.	519
V.F.5-24	Effect of Tube Length to Tube Diameter Ratio on Baseplate Drag Coefficient.	520
V.F.5-25	Baseplate Drag Coefficient as a Function of Tube Internal Length to Tube Internal Diameter Ratio.	521
V.F.6-1	Hardware and Schematic of 97 Hole Baseplates with Trapezoidal and Circular Hole Patterns.	528
V.F.6-2	300 Ft. Sideline Jet Noise Levels for a 97 Trapezoidal Hole Plate with Greatrex Center.	530
V.F.6-3	1500 Ft. Sideline Jet Noise Levels for a 97 Trapezoidal Hole Pate with Greatrex Center.	531
V.F.6-4	300 Ft. Sideline Jet Noise Levels for a 97 Hole Plate with 96 Circular Holes Plus Greatrex Center.	533
V.F.6-5	1500 Ft. Sideline Jet Noise Levels for a 97 Hole Plate with 96 Circular Holes Plus Greatrex Center.	534
V.F.6-6	Effect of Trapezoidal and Circular Hole Shapes on 300 Ft. and 1500 Ft. Sideline PNL Suppressions for 97 Hole Plate Nozzles.	535
V.F.6-7A-D	Effect of Trapezoidal and Circular Hole Shapes on 300 Ft. Sideline Spectra and Directivity.	536-539
V.F.6-8	Schematic of 97 Hole Baseplate Composite Showing Equal and Unequal Circular Hole Sizes and Spacing Patterns.	540
V.F.6-9	300 Ft. Sideline Jet Noise Levels for a 97 Hole Plate with Equal Hole Sizes and Spacing.	542
V.F.6-10	1500 Ft. Sideline Jet Noise Levels for a 97 Hole Plate with Equal Hole Sizes and Spacing.	543

LIST OF ILLUSTRATIONS (Continued)

Figure		Page
V.F.6-11	Comparison of 300 Ft. and 1500 Ft. Sideline PNL Suppressions for a 97 Hole Plate with Equal Hole Sizes and Spacing.	544
V.F.6-12	300 Ft. Sideline Jet Noise Levels for a 97 Hole Plate with Unequal Hole Sizes and Spacings.	546
V.F.6-13	1500 Ft. Sideline Jet Noise Levels for a 97 Hole Plate with Unequal Hole Sizes and Spacing.	547
V.F.6-14	Comparison of 300 Ft. and 1500 Ft. Sideline PNL Suppressions for a 97 Hole Plate with Unequal Hole Sizes and Spacing.	548
V.F.6-15	300 Ft. Sideline Jet Noise Levels for a 97 Hole Plate with Unequal Hole Sizes and Spacing.	550
V.F.6-16	1500 Ft. Sideline Jet Noise Levels for a 97 Hole Plate with Unequal Hole Sizes and Spacing.	551
V.F.6-17	Comparison of 300 Ft. and 1500 Ft. Sideline PNL Suppressions for a 97 Hole Plate with Unequal Hole Sizes and Spacing.	552
V.F.6-18	Effect of Hole Size and Spacing on 300 Ft. and 1500 Ft. Sideline PNL Suppressions for 97 Hole Plate Nozzles.	553
V.F.7-1	97 Tube Primary Nozzle Hardware, AR_d = 2.0.	560
V.F.7-2	97 Tube Primary Nozzle with Hardwall Ejector.	561
V.F.7-3	Schematic of 97 Tube Nozzle with Hardwall and Acoustically Treated Ejector.	562
V.F.7-4	300 Ft. Sideline Jet Noise Levels for a 97 Tube Nozzle with Large Center Hole.	564
V.F.7-5	1500 Ft. Sideline Jet Noise Levels for a 97 Tube Nozzle with Large Center Hole.	565
V.F.7-6	300 Ft. and 1500 Ft. Sideline PNL Suppressions for a 97 Tube Nozzle with Large Center Hole.	566
V.F.7-7	300 Ft. Sideline Jet Noise Levels for a 97 Tube Nozzle with Small Center Hole.	568

LIST OF ILLUSTRATIONS (Continued)

Figure		Page
V.F.7-8	1500 Ft. Sideline Jet Noise Levels for a 97 Tube Nozzle with Small Center Hole.	569
V.F.7-9	300 Ft. and 1500 Ft. Sideline PNL Suppressions for a 97 Tube Nozzle with Small Center Hole.	570
V.F.7-10	300 Ft. Sideline Jet Noise Levels for a 97 Tube Nozzle with Large Center Hole Plus Hardwall Ejector.	572
V.F.7-11	1500 Ft. Sideline Jet Noise Levels for a 97 Tube Nozzle with Large Center Hole Plus Hardwall Ejector.	573
V.F.7-12	300 Ft. and 1500 Ft. Sideline PNL Suppressions for a 97 Tube Nozzle with Large Center Hole Plus Hardwall Ejector.	574
V.F.7-13	300 Ft. Sideline Jet Noise Levels for a 97 Tube Nozzle with Large Center Hole Plus Lined Ejector.	576
V.F.7-14	1500 Ft. Sideline Jet Noise Levels for a 97 Tube Nozzle with Large Center Hole Plus Lined Ejector.	577
V.F.7-15	300 Ft. and 1500 Ft. Sideline PNL Suppressions for a 97 Tube Nozzle with Large Center Hole Plus Lined Ejector.	578
V.F.7-16	Comparison of PNL Suppressions for Variations of 97 Tube Nozzle.	579
V.F.7-17	Aerodynamic Static Performance of 97 Tube Nozzle with Large Center Hole Plus Hardwall Ejector.	580
V.F.8-1	Schematic of 97 Hole Nozzle with Hardwall and Acoustically Treated Ejector.	586
V.F.8-2	300 Ft. Sideline Jet Noise Levels for the 4.32" I.D. Baseline Conical Nozzle.	590
V.F.8-3	1500 Ft. Sideline Jet Noise Levels for the 4.32" I.D. Baseline Conical Nozzle.	591
V.F.8-4	300 Ft. Sideline Jet Noise Levels for a 97 Hole Nozzle with Small Round Center Hole.	593

LIST OF ILLUSTRATIONS (Continued)

Figure		Page
V.F.8-5	1500 Ft. Sideline Jet Noise Levels for a 97 Hole Nozzle with Small Round Center Hole.	594
V.F.8-6	300 Ft. and 1500 Ft. Sideline PNL Suppressions for a 97 Hole Nozzle with Small and Round Center Hole.	595
V.F.8-7	300 Ft. Sideline Jet Noise Levels for a 97 Hole Nozzle with Greatrex Center.	597
V.F.8-8	1500 Ft. Sideline Jet Noise Levels for a 97 Hole Nozzle with Greatrex Center.	598
V.F.8-9	300 Ft. and 1500 Ft. Sideline PNL Suppressions for a 97 Hole Nozzle with Greatrex Center.	599
V.F.8-10	300 Ft. Sideline Jet Noise Levels for a 97 Hole Nozzle with Greatrex Center Plus Hardwall Ejector, $D_S/D_{Td} = 1.125$.	601
V.F.8-11	1500 Ft. Sideline Jet Noise Levels for a 97 Hole Nozzle with Greatrex Center Plus Hardwall Ejector, $D_D/D_{Td} = 1.125$.	602
V.F.8-12	300 Ft. and 1500 Ft. Sideline PNL Suppressions for a 97 hole Nozzle with Greatrex Center Plus Hardwall Ejector, $D_S/D_{Td} = 1.125$	603
V.F.8-13	300 Ft. Sideline Jet Noise Levels for a 97 Hole Nozzle with Greatrex Center Plus Hardwall Ejector, $D_S/D_{Td} = 1.155$.	605
V.F.8-14	1500 Ft. Sideline Jet Noise Levels for a 97 Hole Nozzle with Greatrex Center Plus Hardwall Ejector, $D_S/D_{Td} = 1.155$.	606
V.F.8-15	300 Ft. and 1500 Ft. Sideline PNL Suppressions for a 97 Hole Nozzle with Greatrex Center Plus Hardwall Ejector, $D_S/D_{Td} = 1.155$.	607
V.F.8-16	300 Ft. Sideline Jet Noise Levels for a 97 Hole Nozzle with Greatrex Center Plus Hardwall Ejector, $D_S/D_{Td} = 1.185$.	609
V.F.8-17	1500 Ft. Sideline Jet Noise Levels for a 97 Hole Nozzle with Greatrex Center Plus Hardwall Ejector, $D_S/D_{Td} = 1.185$.	610

LIST OF ILLUSTRATIONS (Continued)

Figure		Page
V.F.8-18	300 Ft. and 1500 Ft. Sideline PNL Suppressions for a 97 Hole Nozzle with Greatrex Center Plus Hardwall Ejector, D_S/D_{Td} = 1.185	611
V.F.8-19	300 Ft. Sideline Jet Noise Levels for a 97 Hole Nozzle with Greatrex Center Plus 4% Open Lined Ejector, D_S/D_{Td} = 1.185.	613
V.F.8-20	1500 Ft. Sideline Jet Noise Levels for a 97 Hole Nozzle with Greatrex Center Plus 4% Open Lined Ejector, D_S/D_{Td} = 1.185.	614
V.F.8-21	300 Ft. and 1500 Ft. Sideline PNL Suppressions for a 97 Hole Nozzle with Greatrex Center Plus 4% Open Lined Ejector, D_S/D_{Td} = 1.185.	615
V.F.8-22	300 Ft. Sideline Jet Noise Levels for a 97 Hole Nozzle with Greatrex Center Plus 7.5% Open Lined Ejector, D_S/D_{Td} = 1.185.	617
V.F.8-23	1500 Ft. Sideline Jet Noise Levels for a 97 Hole Nozzle with Greatrex Center Plus 7.5% Open Lined Ejector, D_D/D_{Td} = 1.185.	618
V.F.8-24	300 Ft. and 1500 Ft. Sideline PNL Suppressions for a 97 Hole Nozzle with Greatrex Center Plus 7.5% Open Lined Ejector, D_S/D_{Td} = 1.185.	619
V.F.8-25	300 Ft. Sideline Jet Noise Levels for a 97 Hole Nozzle with Greatrex Center Plus 15% Open Lined Ejector, D_S/D_{Td} = 1.185.	621
V.F.8-26	1500 Ft. Sideline Jet Noise Levels for a 97 Hole Nozzle with Greatrex Center Plus 15% Open Lined Ejector, D_S/D_{Td} = 1.185.	622
V.F.8-27	300 Ft. and 1500 Ft. Sideline PNL Suppressions for a 97 Hole Nozzle with Greatrex Center Plus 15% Open Lined Ejector, D_S/D_{Td} = 1.185.	623
V.F.8-28	300 Ft. Sideline Jet Noise Levels for a 97 Hole Nozzle with Greatrex Center Plus 22.5% Open Lined, Cerafelt Packed, Ejector, D_S/D_{Td} = 1.185.	625
V.F.8-29	1500 Ft. Sideline Jet Noise Levels for a 97 Hole Nozzle with Greatrex Center Plus 22.5% Open Lined, Cerafelt Packed, Ejector, D_S/D_{Td} = 1.185.	626

LIST OF ILLUSTRATIONS (Continued)

Figure		Page
V.F.8-30	300 Ft. and 1500 Ft. Sideline PNL Suppressions for a 97 Hole Nozzle with Greatrex Center Plus 22.5% Open Lined, Cerafelt Packed, Ejector, D_S/D_{Td} = 1.185.	627
V.F.8-31	Comparison of 300 Ft. and 1500 Ft. Sideline PNL Suppressions for a 97 Hole Nozzle with and without a Central Greatrex.	628
V.F.8-32	Effect of Secondary Hardwall Ejector D_S/D_{Td} Variation on 300 Ft. Sideline PNL Suppressions for 97 hole Nozzles with Greatrex Center.	629
V.F.8-33	Effect of Secondary Hardwall Ejector D_S/D_{Td} Variation on 1500 Ft. Sideline PNL Suppressions for 97 Hole Nozzles with Greatrex Center.	630
V.F.8-34	Effect of Acoustically Lined Ejector Variations on 300 Ft. Sideline PNL Suppressions for 97 Hole Nozzles with Greatrex Center.	631
V.F.8-35	Effect of Acoustically Lined Ejector Variations on 1500 Ft. Sideline PNL Suppressions for 97 Hole Nozzles with Greatrex Center.	632
V.F.9-1	Schematic of 5.7" I.D. Conical Nozzle Used in Baseline Comparisons.	645
V.F.9-2	300 Ft. Sideline Jet Noise Levels for Average Baseline Conical Nozzle.	653
V.F.9-3	1500 Ft. Sideline Jet Noise Levels for Average Baseline Conical Nozzle.	654
V.F.9-4	Multi-Hole Nozzle Hardware Used in Parametric Investigations of Area Ratio and Hole Number.	655
V.F.9-5	Schematic of 85 Hole Nozzle Used in Parametric Investigation of Area Ratio.	656
V.F.9-6	300 Ft. Sideline Jet Noise Levels for an 85 Hole Nozzle, AR_d = 2.0.	658
V.F.9-7	1500 Ft. Sideline Jet Noise Levels for an 85 Hole Nozzle, AR_d = 2.0.	659
V.F.9-8	300 Ft. Sideline Jet Noise Levels for an 85 Hole Nozzle, AR_d = 2.0.	661

LIST OF ILLUSTRATIONS (Continued)

Figure		Page
V.F.9-9	1500 Ft. Sideline Jet Noise Levels for an 85 Hole Nozzle, AR_d = 2.0.	662
V.F.9-10	300 Ft. Sideline Jet Noise Levels for an 85 Hole Nozzle, AR_d = 2.3.	664
V.F.9-11	1500 Ft. Sideline Jet Noise Levels for an 85 Hole Nozzle, AR_d = 2.3.	665
V.F.9-12	300 Ft. Sideline Jet Noise Levels for an 85 Hole Nozzle, AR_d = 2.7.	667
V.F.9-13	1500 Ft. Sideline Jet Noise Levels for an 85 Hole Nozzle, AR_d = 2.7.	668
V.F.9-14	300 Ft. Sideline Jet Noise Levels for an 85 Hole Nozzle, AR_d = 3.1.	670
V.F.9-15	1500 Ft. Sideline Jet Noise Levels for an 85 Hole Nozzle, AR_d = 3.1.	671
V.F.9-16	300 Ft. Sideline Jet Noise Levels for an 85 Hole Nozzle, AR_d = 4.0.	673
V.F.9-17	1500 Ft. Sideline Jet Noise Levels for an 85 Hole Nozzle, AR_d = 4.0.	674
V.F.9-18	300 Ft. Sideline Jet Noise Levels for an 85 Hole Nozzle, AR_d = 4.0.	676
V.F.9-19	1500 Ft. Sideline Jet Noise Levels for an 85 Hole Nozzle, AR_d = 4.0.	677
V.F.9-20	Effect of Area Ratio on 300 Ft. Sideline PNL Suppressions for 85 Hole Nozzles.	678
V.F.9-21	Effect of Area Ratio on 1500 Ft. Sideline PNL Suppressions for 85 Hole Nozzles.	679
V.F.9-22A-C	Effect of Area Ratio on 1500 Ft. Sideline Spectra for 85 Hole Nozzles.	680-682
V.F.9-23A-C	Effect of Area Ratio on 1500 Ft. Sideline Directivity for 85 Hole Nozzles.	683-685
V.F.9-24	Effect of Area Ratio on Mean Baseplate Pressure for 85 Hole Nozzles.	686

LIST OF ILLUSTRATIONS (Continued)

Figure		Page
V.F.9-25	Effect of Area Ratio on Nozzle Exit to Mean Baseplate Pressure Ratio for 85 Hole Nozzles.	687
V.F.9-26	Effect of Area Ratio on Baseplate Drag Coefficient for 85 Hole Nozzles.	688
V.F.9-27	Multi-Hole Nozzle Hardware Used in Parametric Investigation of Hole Number.	689
V.F.9-28	Schematic of 55, 85, and 121 Hole Nozzles for Parametric Investigation of Hole Number at Constant Area Ratio, AR_d = 2.7.	690
V.F.9-29	300 Ft. Sideline Jet Noise Levels for 55 Hole Nozzle.	692
V.F.9-30	1500 Ft. Sideline Jet Noise Levels for 55 Hole Nozzle.	693
V.F.9-31	300 Ft. Sideline Jet Noise Levels for 55 Hole Nozzle.	695
V.F.9-32	1500 Ft. Sideline Jet Noise Levels for 55 Hole Nozzle.	696
V.F.9-33	300 Ft. Sideline Jet Noise Levels for 121 Hole Nozzle.	698
V.F.9-34	1500 Ft. Sideline Jet Noise Levels for 121 Hole Nozzle.	699
V.F.9-35	Effect of Hole Number on 300 Ft. Sideline PNL Suppressions for Multi-Hole Nozzles.	700
V.F.9-36	Effect of Hole Number on 1500 Ft. Sideline PNL Suppressions for Multi-Hole Nozzles.	701
V.F.9-37A-C	Effect of Hole Number on 1500 Ft. Sideline Spectra with 55, 85 and 121 Hole Nozzles.	702-704
V.F.9-38A-C	Effect of Hole Number on 1500 Ft. Sideline Directivity with 55, 85 and 121 Hole Nozzles.	705-707
V.F.9-39	Effect of Hole Number on Mean Baseplate Pressure Ratio.	708
V.F.9-40	Effect of Hole Number on Nozzle Exit to Mean Baseplate Pressure Ratio.	709

LIST OF ILLUSTRATIONS (Continued)

Figure		Page
V.F.9-41	Effect of Hole Number on Baseplate Drag Coefficient.	710
V.F.9-42	Secondary Shroud Hardware Used with an 85 Hole Nozzle for Parametric Investigation of D_S/D_{Td} Ratio.	711
V.F.9-43	Schematic of Shrouded 85 Hole Nozzle for Parametric Investigation of D_S/D_{Td} Ratio.	712
V.F.9-44	300 Ft. Sideline Jet Noise Levels for Shrouded 85 Hole Nozzle, D_S/D_{Td} = 1.05.	714
V.F.9-45	1500 Ft. Sideline Jet Noise Levels for Shrouded 85 Hole Nozzle, D_S/D_{Td} = 1.05.	715
V.F.9-46	300 Ft. Sideline Jet Noise Levels for Shrouded 85 Hole Nozzle, D_S/D_{Td} = 1.10.	717
V.F.9-47	1500 Ft. Sideline Jet Noise Levels for Shrouded 85 Hole Nozzle, D_S/D_{Td} = 1.10.	718
V.F.9-48	300 Ft. Sideline Jet Noise Levels for Shrouded 85 Hole Nozzle, D_S/D_{Td} = 1.15.	720
V.F.9-49	1500 Ft. Sideline Jet Noise Levels for Shrouded 85 Hole Nozzle, D_S/D_{Td} = 1.15.	721
V.F.9-50	Effect of D_S/D_{Td} Ratio on 300 Ft. Sideline PNL Suppressions for Shrouded 85 Hole Nozzle.	722
V.F.9-51	Effect of D_S/D_{Td} Ratio on 1500 Ft. Sideline PNL Suppressions for Shrouded 85 Hole Nozzle.	723
V.F.9-52A-C	Effect of D_S/D_{Td} Ratio on 1500 Ft. Sideline Spectra for Shrouded 85 Hole Nozzle.	724-726
V.F.9-53A-C	Effect of D_S/D_{Td} Ratio on 1500 Ft. Sideline Directivity for Shrouded 85 Hole Nozzle.	727-729
V.F.9-54	Effect of D_S/D_{Td} Ratio on Mean Baseplate Pressure Ratio.	730
V.F.9-55	Effect of D_S/D_{Td} Ratio on Nozzle Exit to Mean Baseplate Pressure Ratio.	731
V.F.9-56	Effect of D_S/D_{Td} Ratio on Baseplate Drag Coefficient.	732

LIST OF ILLUSTRATIONS (Continued)

Figure		Page
V.F.9-57	Shroud Hardware Configuration Used in Shroud Axial Spacing Variations with an 85 Hole Nozzle.	733
V.F.9-58	Schematic of Shrouded 85 Hole Nozzle for Parametric Investiation of Shroud Axial Spacing.	734
V.F.9-59	300 Ft. Sideline Jet Noise Levels for Shrouded 85 hole Nozzle with Shroud Axial Spacing, X_S = 4.73".	736
V.F.9-60	1500 Ft. Sideline Jet Noise Levels for Shrouded 85 Hole Nozzle with Shroud Axial Spacing, X_S = 4.73".	737
V.F.9-61	300 Ft. Sideline Jet Noise Levels for Shrouded 85 Hole Nozzle with Shroud Axial Spacing, X_S = 7.47".	739
V.F.9-62	1500 Ft. Sideline Jet Noise Levels for Shrouded 85 Hole Nozzle with Shroud Axial Spacing, X_S = 7.47".	740
V.F.9-63	Effect of Shroud Axial Spacing on 300 Ft. Sideline PNL Suppressions for Shrouded 85 Hole Nozzle.	741
V.F.9-64	Effect of Shroud Axial Spacing on 1500 Ft. Sideline PNL Suppressions for Shrouded 85 Hole Nozzle.	742
V.F.9-65	Effect of Shroud Axial Spacing on Mean Baseplate Pressure Ratio.	743
V.F.9-66	Effect of Shroud Axial Spacing on Nozzle Exit to mean Baseplate Pressure Ratio.	744
V.F.9-67	Effect of Shroud Axial Spacing on Baseplate Drag Coefficient.	745
V.F.10-1	Schematic of PD-3 Aerodynamic Cold Flow Nozzles.	756
V.F.10-2	Schematic of PD-3 Acoustic Hot Flow Nozzles.	757
V.F.10-3	PD-3 Plain and Greatrex Tube Designs for Cold Flow Aerodynamic and Hot Flow Acoustic Models.	758
V.F.10-4	PD-3 Acoustic and Aerodynamic Hardware - Models 1 and 3.	759

LIST OF ILLUSTRATIONS (Continued)

Figure		Page
V.F.10-5	PD-3 Aerodynamic Hardware - Models 4 and 5.	760
V.F.10-6	PD-3 Acoustic and Aerodynamic Hardware - Models 5 and 6.	761
V.F.10-7	PD-3 Aerodynamic Hardware - Models 7 and 8.	762
V.F.10-8	300 Ft. Sideline Jet Noise Levels for PD-3 Model 1.	764
V.F.10-9	1500 Ft. Sideline Jet Noise Levels for PD-3 Model 1.	765
V.F.10-10	300 Ft. Sideline Jet Noise Levels for PD-3 Model 3.	767
V.F.10-11	1500 Ft. Sideline Jet Noise Levels for PD-3 Model 3.	768
V.F.10-12	300 Ft. Sideline Jet Noise Levels for PD-3 Model 4.	770
V.F.10-13	1500 Ft. Sideline Jet Noise Levels for PD-3 Model 4.	771
V.F.10-14	300 Ft. Sideline Jet Noise Levels for PD-3 Model 5.	773
V.F.10-15	1500 Ft. Sideline Jet Noise Levels for PD-3 Model 5.	774
V.F.10-16	Comparison of 300 Ft. Sideline Peak PNL Suppression for PD-3 Models 1, 3, 4 and 5.	775
V.F.10-17	Comparison of 1500 Ft. Sideline Peak PNL Suppression for PD-3 Models 1, 3, 4 and 5.	776
V.F.10-18A-E	Effect of PD-3 Tube End Variations on 300 Ft. Sideline Spectra.	777-781
V.F.10-19A-E	Effect of PD-3 Tube End Variations on 300 Ft. Sideline Directivity.	782-786
V.F.10-20A-C	Octave Band Spectral Suppression Attributable to Addition of PD-3 Greatrex Tube Ends.	787-789
V.F.10-21	OASPL and PNL Suppression Attributable to Addition of PD-3 Greatrex Tube Ends.	790
V.F.10-22	Summary of Octave Band Spectral Suppression Attributable to Addition of PD-3 Greatrex Tube Ends.	791

LIST OF ILLUSTRATIONS (Concluded)

Figure		Page
V.F.10-23	Comparison of Greatrex Tube End Designs for PD-3 and 37 Tube Models.	792
V.F.10-24	Comparison of Octave Band Spectral Suppression Attributable to Greatrex Tube Ends on PD-3 and 37 Tube Models.	793
V.F.10-25	Aerodynamic Performance (C_{D8} and C_{fg}) for PD-3 Models 1, 3, 5 and 7 Without Ejector, Comparing Greatrex and Plain Tubes, Staggered and Coplanar Exits.	794
V.F.10-26	Aerodynamic Performance (C_{D8} and C_{fg}) for PD-3 Models 2, 4, 6 and 8 With Ejector, Comparing Greatrex and Plain Tubes, Staggered and Coplanar Exits.	795
V.F.10-27	Thrust Loss Breakdown for PD-3 Plain and Greatrex Tube Cold Flow Aerodynamic Models.	796

SUMMARY

This two volume document presents the results of five years of intensive study by the General Electric Company in the development of acoustic suppressor technology related to the GE4 engine for the Boeing Supersonic Transport. The work was sponsored under contract by the Federal Aviation Agency.

The report documents the jet noise suppressor configurations and parametric studies investigated on scale model nozzles and full scale engines. Results of system studies investigating turbomachinery noise and jet noise on GE4 and J79 engines are presented.

The results of individual studies conducted on series of model suppressor configurations are presented as full scale results. Scale model acoustic measurements taken on a 40 ft. arc were scaled by frequency, size, and measuring arc to full scale application using an 8:1 scale factor. All data presented in this report are of simulated or actual engine size and engine frequency range, except for the data from the Corporate Research and Development Center's supersonic jet noise suppression results and prediction methods, all of which are presented as scale model results (Section VII.A).

Volume I of this summary report contains major Sections I through IV and part of Section V (through V.F.10). Volume II contains the remainder of Section V (i.e. V.G, V.H.1 and V.H.2) and the last two sections of the report, Sections VI and VII. Appendix A - Nomenclature, is included in both Volumes I and II.

I. INTRODUCTION

I. INTRODUCTION

In 1964 General Electric entered the competition to provide the powerplant for the United States Supersonic Transport and, ultimately, was awarded the Federal Aviation Agency contract in late 1966 to develop the engines for the prototype aircraft.

At the initial conception of the program, noise (especially as it affects the community around airports) was a matter of concern but did not dominate in the engine selection and design. The initial approach was one of establishing the most economically attractive engine/airframe combination and then identifying the operational procedures which provided the minimum community noise intrusion. As the program progressed, the impact of noise became more pronounced. For Phase III of the program, noise goals both at takeoff and approach were set as requirements.

The original engine proposed for Phase III by General Electric in 1966 was a 475 pps, fully augmented turbojet with a two-stage ejector nozzle (TSEN). Based upon analysis and a vast background of engine, component, and model scale testing, it could be shown that the limiting noise source at the sideline monitoring point was the jet; the turbomachinery was the major noise contributor at approach. At the community monitoring point, both jet and turbomachinery noise were important, the dominance depending upon engine size and exact power setting. To meet the quoted noise goals at the community and approach locations, the exhaust nozzle was operated on an open area schedule with the inlet choked. The basic Two Stage Ejector Nozzle was studied in depth to optimize the geometry for best pumping techniques to attain minimum jet noise. In addition jet suppressor programs developed simple primary nozzle mechanical suppressors such as primary rods, tabs, and ventilated chutes. These were employed within the conical primary - TSEN system and provided nominal low jet noise suppression. Other systems employing part of the secondary reverser mechanism were investigated as secondary flap suppressors.

During the course of the program, although the engine cycle remained relatively constant, the engine increased in size. The power settings at takeoff and approach were also raised to be consistent with increases in aircraft weight and modified design. Concurrent with these changes, the engine/aircraft noise

PRECEDING PAGE BLANK-NOT FILMED

goals were reduced in several steps as a result of community reaction to noise and in light of impending federal regulations. To meet the reduced goals a major noise program was conducted, developing technology to control the supersonic jet noise and turbomachinery noise. Primary emphasis during this period was on high jet noise suppression techniques, particularly multi-element tube nozzles. A substantial research effort systematically developed multi-tube technology and established guidelines for tube nozzle design.

In 1969 the Federal Aviation Agency issued "Noise Standards: Aircraft Type Certification" referred to as FAR36. These noise standards became the goal for the production SST. Engine designs and suppression technology development were realigned to that goal. At takeoff, the perceived noise level at the 0.35-nmi sideline was not to exceed 108 EPNdB, cutback noise underneath the aircraft 3.5-nmi from the start of the takeoff roll was not to exceed 108 EPNdB, and approach noise at a point 1-nmi from the threshold was not to exceed 108 EPNdB.

It became evident that the state of the art jet noise suppression technology could not develop the fully augmented turbojet engine capable of meeting the new noise goals. Meeting these goals required a substantial engine modification and advanced suppression techniques. Thorough design studies of high-airflow engines and noise suppression systems were conducted. These studies were supported by scale model acoustic and aerodynamic test programs. The recommended engine configuration at the conclusion of the program was a high-flow turbojet engine operating without augmentation at takeoff. The most promising jet noise suppressor was in the form of a multi-element spoke/chute annular plug system. Primary emphasis was then directed toward development of this jet noise suppressor system, in addition to continued turbomachinery noise studies, until program termination in March, 1971.

II. JET NOISE TEST FACILITIES

II.A AERO/ACOUSTIC TEST FACILITIES

PRECEDING PAGE BLANK-NOT FILMED

II.A AERO/ACOUSTIC TEST FACILITIES

The aero/acoustic tests conducted during the investigation of jet noise suppression for the GE4/SST program were performed on several different acoustic and aerodynamic test facilities, located both in General Electric plants and at outside vendor locations.

The majority of the jet suppressor acoustic tests were conducted on scale-model facilities such as the JENOTS hot-jet facility at the General Electric plant in Evendale, Ohio (discussed in Section II.B), and the hot and cold jet stands at the General Electric Corporate Research and Development Center in Schenectady, New York, (discussed in Section II.D). Full-scale engine testing was performed at Peebles Proving Ground, Peebles, Ohio on the GE4 acoustic facility, Site 4D (discussed in Section II.C).

Aerodynamic static and installed gross thrust measurements obtained for suppressor systems were made on scale model nozzles at the FluiDyne Engineering Corporation's Medicine Lake Laboratories (Section II.E), located at Medicine Lake, Wisconsin.

These facilities, mentioned briefly here, are discussed individually and more fully in the following sections. A description of the test facility with capabilities and limitations is included in each section. Table II.A-1 briefly summarizes the capabilities and limitations of the major jet acoustic facilities used on this program.

PRECEDING PAGE BLANK-NOT FILMED

TABLE II.A-1 FACILITY CAPABILITIES AND LIMITATIONS

	SCALE FACTOR	P_{T8}/P_o	T_{T8}	FREQUENCY RANGE	ACOUSTIC ARENA & DATA ACQUISITION
Peebles/GE4	1	Engine Cycle		To 10 KHz	Multi Mic - Stationary Field 0° - 160° From Inlet Other Mics as Required Simultaneous Recording
JENOTS/Model	6-10	4.0	3000°F	To 40 KHz (B&K) To 80 KHz (Direct Record)	Multi Mic - Stationary Field 20° - 160° From Inlet Other Mics as Required Individual Recording
R & DC/Model	20 7 to 10	5.0	Amb. to 1260°R	To 16 KHz Or 80 KHz	Single Mic Traverse System

II.B JENOTS SCALE MODEL ACOUSTIC TEST FACILITY

II.B JENOTS SCALE MODEL ACOUSTIC TEST FACILITY

The JENOTS (Jet Engine Noise Outdoor Test Stand) facility, located at the north end of the General Electric plant at Evendale, Ohio, is the prime jet noise facility. It consists of a hot-jet test stand, capable of operating up to 6" I.D. nozzles at pressure ratios up to 4:1 at temperatures of 3000° F. A control room is housed in an adjacent building.

JENOTS Test Stand and Acoustic Arena

The test stand was designed to be relatively free from sound reflections due to nearby structures. Its location also minimizes the high intensity noise interference with the operation of the other test facilities in the area.

The basic test rig consists of a primary 10" air pipe, a J-47 "pre-burner", and a 12" water jacketed after-burning section ending in a flange for mounting test nozzles. A 4" secondary air line is located above the primary.

The acoustic arena is exposed to ambient conditions. The ground plane is composed of concrete to approximately a 20 ft. radius from the nozzle exit. The remainder of the acoustic arena is composed of crushed rock from 20 to 40 ft. radius. A grassy field exists beyond the acoustic arena with no structures present that resulted in acoustic reflection interference at the microphone positions. The nozzle centerline and microphone heights above the ground are about 55 inches.

An array of permanent microphone stations are located on a 40 ft. polar arc. Prior to 1969, acoustic data was normally recorded at 10° intervals from 30° to 90° relative to the jet exhaust axis. During facility modifications in 1969, additional microphones were installed on the 40 ft. arc at 20° and 100° to 160°, thereby increasing the number of permanent sampling positions to 15 (20° to 160° on a 40 ft. arc). A photograph of the test rig and permanent arc of microphones is shown in Figure II.B-1.

Air Supply Systems

Three types of air are available for the JENOTS facility. They are as follows:

PRECEDING PAGE BLANK-NOT FILMED

Central Air Supply (401 Test Air)	300 psi	100 pps
Shop Air	100 psi	10 pps
Instrument Air (filtered)	100 psi	-

Compressor Boost (C/B) air is used to augment required air flows.

o Central Air Supply System

The Central Air Supply System, Figure II.B-2, is the basic air supply system for the Evendale component test complex. It continuously provides up to 100 pps of airflow at pressures up to 300 psig. The Central Air Supply System consists of an arrangement of five multistage centrifugal compressors driven by synchronous motors through speed-increasing gears. Flexibility of operation is obtained by the ability to stage the compressors in series or in parallel, in various combinations for a wide range of pressures and flows or for use as exhausters.

Test air is supplied to the JENOTS test stand through a 10" air line which connects to the central air supply 14" air line. The shutoff valve for the JENOTS facility is a remotely controlled 250 lbs., 10" Kennedy gate valve located opposite Building 315. The air flow in the 10" line is controlled and adjusted by two pairs of valves, each pair connected in parallel. In each case a 4" plug valve is in parallel with an 8" butterfly valve. The 4" valves serve as the fine adjustment while the coarse adjustment is set with the 8" valves. The pair of valves upstream of the main air orifice is used for setting orifice pressure and orifice ΔP. The 4" plug valve features a regulator for automatic pressure control. The pair of valves downstream of the orifice are used for flow rate control.

The main airflow is measured by a Daniels square edge orifice 5.000" in diameter with $\beta = .499$. The orifice is mounted in a quick change, orifice plate holder. The inside diameter of main air line is 10.020".

The 10" air line has a blow-down leg prior to the burners. A manually operated 6" gate valve is mounted on the 6" blowdown pipe. The air pressure limitation in this section is 300 psig at ambient temperature.

o Shop Air

A 4" shop air line crossover provides for use of shop air through the 10" air line. It features a 4" regulator controlled pneumatic operated gate valve mounted on the crossover. A rupture disk assembly is mounted on the crossover to prevent high pressure 401 air leaking upstream in the shop air line. Pressure is limited to 125 psi by the rupture disk.

Shop air may also be conducted through the 14" line directly into the 10" line by valving at the 401 Air Supply.

o Secondary Air

A 4" secondary air line is connected to the primary 10" line between the orifice and the upstream control valves. It contains 4", 300# Daniels pressure-tapped mounting flanges, with Meriam square edge orifice plates of different sizes available. The secondary air line terminates above the 12" burner section and has four 2" pipe fittings to which secondary air systems can be connected. This system has been used to inject air into the second stage of two stage ejector nozzles.

o C/B Air

C/B air may be used in any of the systems previously described. It is usually used in conjunction with shop air in the 10" line to augment pressure and airflow in meeting test requirements without resorting to use of 401 test air.

o Instrument Air

The instrument air system consists of 3/4" line connecting to the instrument air supply. The instrument air line runs to the test stand where it is used for operating air and fuel control valves and shutoff solenoids for JP-4, H_2 and N_2. Instrument air is also conducted to the control room through a 1/2" line for operating panel loaders, temperature controllers and pressure transducers used with the digital data acquisition system.

Fuel System

The fuel system provides JP-4 from a fuel supply up to a maximum of 500 pph @ 1000 psi. Hydrogen is available from a 12-bottle rack and is used pri-

marily for burner ignitors. Nitrogen obtained from a 9275 ft.^{3} capacity nitrogen trailer is used for purging the hydrogen and JP-4 lines.

JP-4 fuel is drawn from a 4000 gallon fuel supply. A 1-1/2" pipe connects to the fuel line and runs to the JENOTS Facility fuel pad just opposite the northeast corner of Building 315.

At the fuel pad, a pumping, cooling, filtering and bypass function operation is performed. The pumping unit is designed to bypass fuel during low fuel demand, yet provides up to a maximum of 5000 pph at 1000 psi to the test pad when required.

From the fuel pad, fuel arrives at the test stand where it goes through an automatic cut-off valve that is controlled by the flame tunnel water pressure. The valve remains open while the flame tunnel outlet water pressure is above 12 psig. After the shutoff valve, the fuel line is reduced to a 3/4" SS pipe and connects to two filters connected in parallel followed by two C A T/C's for fuel temperature measurement at the test pad. After the T/C's, a flow-meter is mounted in the line to measure total flow. From this point, the fuel line divides into four units. These units consist of the preburner, afterburner "pilot", afterburner "local" and afterburner "fill" fuel systems. Mounted on each unit in order are a manual shutoff valve,a flowmeter, and a fuel control valve. In the case of the preburner, the fuel line is divided into the small and large slot subsystems with each branch having its own control valve. Figure II.B-3 is a schematic of the burner systems on the JENOTS stand.

Using combinations of these units, a wide range of temperatures and airflows can be obtained while keeping relatively stable and uniform burner condition. The control valves can be fitted with several available inner bodies (trim size) depending on the required range of operation. In addition to the automatic fuel shutoff valve, operating on cooling water pressure, the system has other safety features.

The fuel pad contains a relief valve set for 1000 psig, and a thermoswitch that stops the fuel pump if fuel temperatures exceeds 140° F. The fuel control valve for the preburner is equipped with an API over and under temperature shutoff. The afterburner "local" fuel control valve is connected to API overtemperature shutoff.

Burner System

The burner system consists of a preburner (P/B) and afterburner (A/B) mounted in the main air pipe as shown in Figure II.B-3.

o Preburner

A J-73 large and small slot fuel nozzle and J-47 burner "can" is used for the JENOTS preburner. A large and small slot fuel supply line, each with its own control valve, is available to the preburner. An ignitor torch is used for lighting the preburner. A spark plug ignitor and hydrogen are supplied to the torch tube. The tube is perforated to allow air to mix with the hydrogen.

o Afterburner

The afterburner consists of the A/B ignitor torch, A/B pilot, and two sets of A/B spray bars. The ignitor torch is a 1/2" stainless tube housing, an A. C. spark plug ignitor, and inlets for the H_2, N_2 purge and air supply line using instrument air. The A/B pilot is made up of a simplex fuel nozzle, a swirl cup, and a "V" gutter flame holder. The 8 A/B spray bars are mounted between the pilot and ignitor torch and use both "local" and "fill" fuel systems. The dual spray bars are used when high air flows (above 11 pps) are required.

Domestic Water System

The water system is supplied by domestic water and is available up to 60 psi @ 300 gpm. A drain for the water is supplied at the test pad.

o Cooling Water

Domestic water is used for cooling of the 12" flame tunnel, the plane 7, IR probes, water-cooled adapter sections, and various test configurations. In addition, the heat exchanger at the fuel pad utilizes the domestic water supply.

Water is supplied by a 6" underground water line that connects to an 8" water main. A 6" manual gate valve serves as a water supply shutoff. The water supply line terminates at the south edge of the test pad where a second 4" pipe section rises vertically above the ground. At this terminal point, three 2" pipe fittings are welded. Water is conducted to the flame tunnel water

jacket, IR, T/C water jacket manifold and adapter water jackets through 2" 150# gate valves and 2" AN hose.

A 1-1/2" water pipe is diverted to the fuel pad heat exchanger connecting to the 4" water supply line just downstream of the primary shutoff valve.

Facility Instrumentation and Data

o Airflow

For each test run, a set of data is taken that is not specifically obtained from the test model. This data is know as facility data and consists of air flow, fuel flow, tunnel temperatures and pressures, cooling water temperatures and pressures, and meteorological data. The control panel for facility operation is shown in Figure II.B-4.

Primary air flow is obtained with a Daniels 316SS, square edge orifice 5.000" in diameter on a pipe diameter of 10.020" with $\beta = 0.499$. Data taken are main air orifice (MAO) temperatures, MAO upstream pressure P_1, and MAO ΔP (P_1-P_2). Airflow is tabulated on the log sheets and recorded on digital punch tape to be computed using the JENOTS quick look, time sharing program and a GE-635 computer program.

Secondary air flow (when specific tests require it) is measured with a square edge Meriam 316SS orifice 1.250" in diameter on a 4.026" pipe with β = 0.310. Pressures are obtained by 4" Daniels orifice flange static taps. Data used to calculate air flow are upstream pressure, ΔP and secondary air line temperature.

o Fuel Flow

Fuel flow is obtained using Fisher Porter flowmeters. Flow readings are taken of the preburner, A/B pilot, A/B local, A/B fill and total flow. Data is recorded on the log sheet and digital punch tape. In addition, the log sheet records fuel specific gravity (from sample taken at fuel pad measured with a hydrometer) fuel temperature, and fuel pump discharge pressure.

o Tunnel Temperature

In addition to the temperature readings taken to calculate primary and secondary air flow, 8 CA T/C probes are used to measure A/B inlet (P/B discharge)

Plane 5 temperatures. One of these T/C's is used for input to the Plane 5 auto temperature controller that regulates fuel flow to the preburner. Another T/C is used as an input to the API undertemperature and one for the overtemperature trip-out.

The temperature readout is taken on the Brown potentiometer and recorded on the log sheet. Another set of eight water cooled IR T/C's is used to measure flame tunnel (A/B discharge) temperature at Plane 7. Two of these T/C's are used as inputs for the T_7 auto temperature controller, which is used to maintain a preset temperature by adjusting A/B local fuel flow. The controller is used on test runs requiring the same T_7 temperature for a number of readings as a means of cutting down time for setting test points. One T/C is used as an input for the T_7 API overtemperature trip-out. T_7 temperatures in mV are measured on the Brown potentiometer and recorded on the log sheet.

o Tunnel Pressures

Static pressure measurements are made at the P/B inlet (Plane 3), A/B inlet (Plane 5) and A/B discharge (Plane 7). These measurements are made on a Wallace and Tiernan pressure gage in psia for recording on the log sheets.

o Cooling Water

Cooling water pressure at the inlet and outlet is measured with a pressure transmitter and read in the cell on a remote pressure gauge. Temperatures are measured using CA T/C's and read out on the Brown potentiometer.

o Meteorological Data

Readings are taken of the outside air temperature and pressure and recorded both on the log sheet and digital punch tape. In addition, wet and dry bulb temperatures for relative humidity, wind speed in mph, and wind direction are recorded on the log sheets. These data are used in correlating sound data.

Sound Data Recording System

The sound data system is made up of an array of microphones mounted in protective stands and positioned around the test model on a 40 ft. radius as shown in Figure II.B-5. A more complete description of the sound data recording

system is discussed in the data acquisition and recording section of this report (Section III).

Ground Runup Silencer

A modified J85 portable ground run-up suppressor is mounted on tracks in line aft of the test section. (See Figure II.B-6). The track is a double length of 6" X 6" X 1/2" angle iron 120 feet long, mounted on 10" X 3" X 8' wocden ties.

The silencer is chain driven by a 7.5 HP 1750 RPM electric motor. The power from the motor is transmitted to two sets of drive wheels through a 15 to 1 gearbox by means of sprockets and ASA #100 cotter pin roller chain. The two sets of drive wheels are mounted on the aft dolly that also serves as the aft support of the silencer. Two sets of wheels and the forward dolly serve as the forward support.

A spring operated electric cable reel pays out cable as the silencer is moved forward in position, and automatically rewinds as it is moved back.

The silencer is controlled remotely from the JENOTS control room by a forward and backward switch and a start and stop button. Automatic stop switches are mounted on either end of the track. They are tripped by the silencer as it arrives at either position. At the forward end of the track, a pair of pneumatic buffers utilizing instrument air are mounted on the tracks. The buffers serve to stop the silencer from damaging the test stand in the event the trip switch or manual stop switch failed. The drive motor features a brake which is engaged whenever a stop switch is activated.

Digital Data Acquisition System

A digital data acquisition system is used to obtain both a duplicate set of facility data, limited to those inputs required for calculating air flow and fuel flow and additional pressure and temperatures lines for various test model instrumentation requirements.

A total of 125 pressure lines, 96 CA T/C circuits and 21 IR T/C circuits are available for use with the digital system.

One hundred pressure lines out of the 125 connect to a bank of 8 scanner valves containing 25 psia transducers. Each scanner valve can measure eleven pressures per transducer for a total of 88 pressures in the 0 - 25 psia range that can be measured at one time. Twenty-five pressure lines are routed to a cabinet containing five individual transducers that handle pressures 0-50, 100, and 500 psia but can be changed to meet specific requirements. The 8 scanners are used for measuring model pressures, while the individual transducers measure facility air flow data.

The CA T/C's are used to measure main air flow temperature and various skin temperatures on the models. The IR T/C's are used to measure flame tunnel temperature. These signals are then fed into an automatic switching unit in an ordered manner and conducted through digital amplifiers to a digital printer and a digital punch. The printer stamps respective digital position numbers and parameters in "counts" on a ribbon paper that can be correlated, with the aid of a "hook-up" sheet, to readings in engineering units. The punch unit perforates digital punch tape which is used for inputing the time-sharing teletype system for processing to engineering units and calculations. The punched digital tape is also submitted to the data reduction section, to be transferred to computer cards for the GE-635 JENOTS Wake Analysis data reduction program.

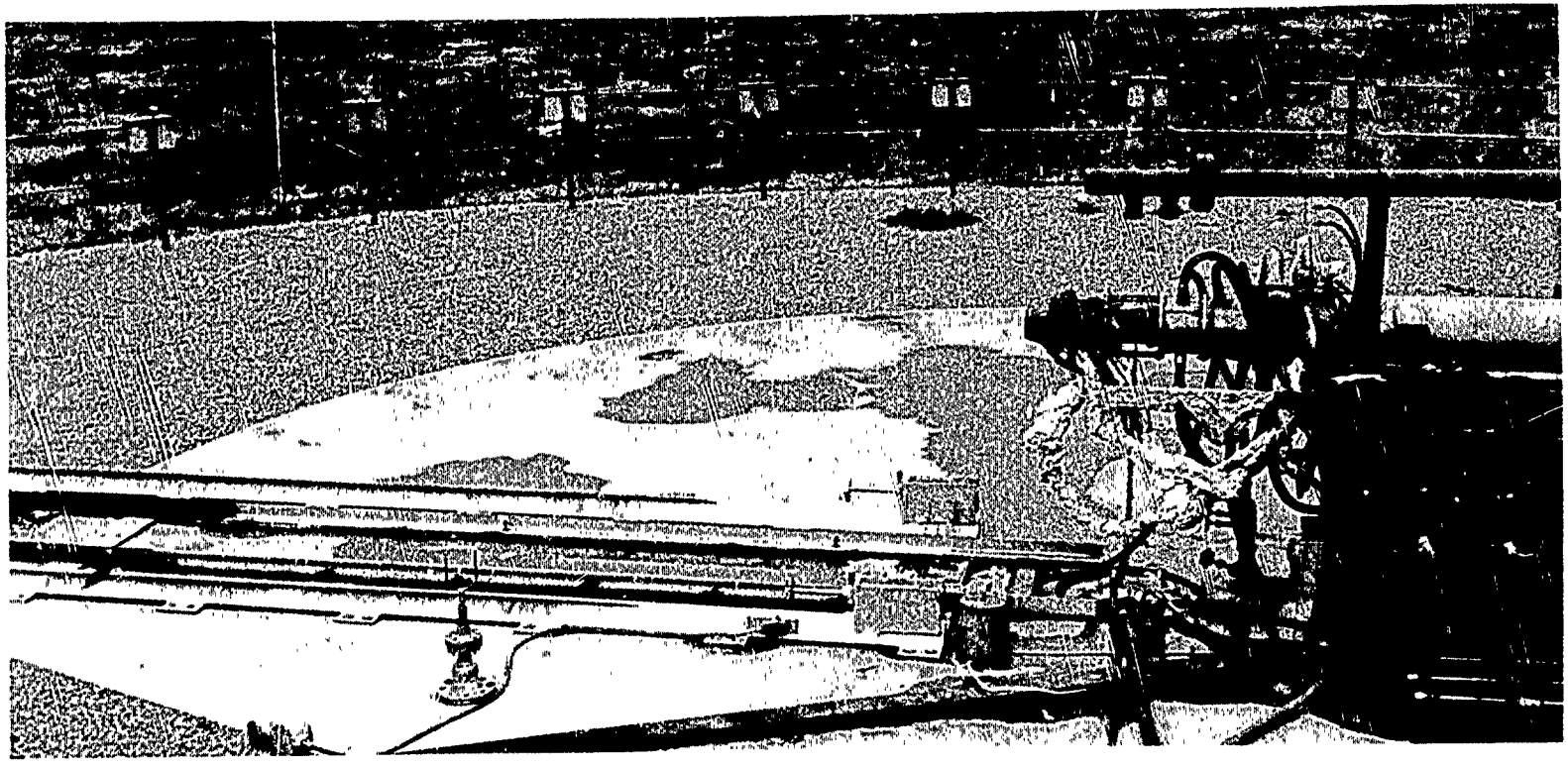

FIGURE II.B-1 JENOTS NOISE FACILITY

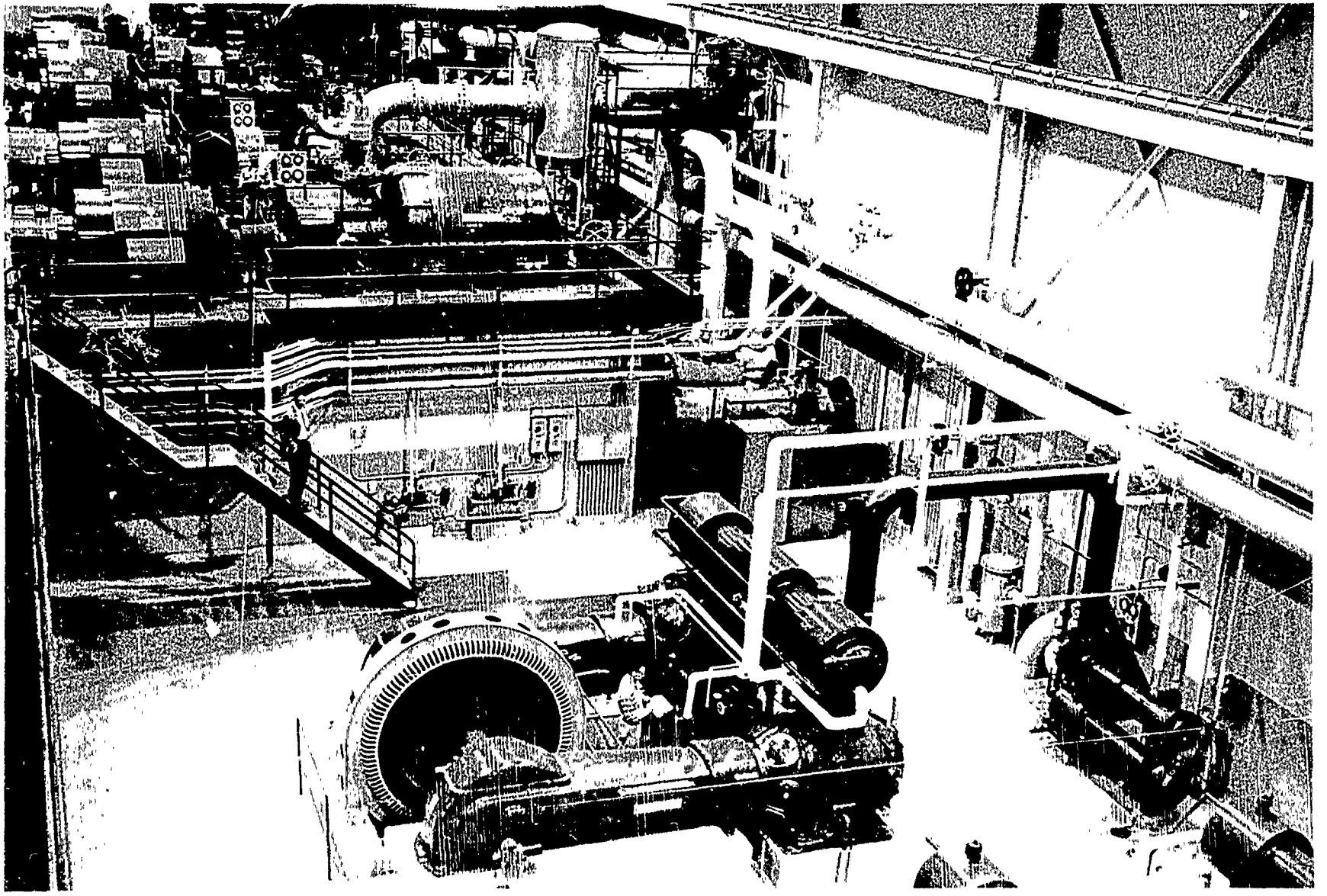

FIGURE II.B-2 CENTRAL AIR SUPPLY SYSTEM, BUILDING 401

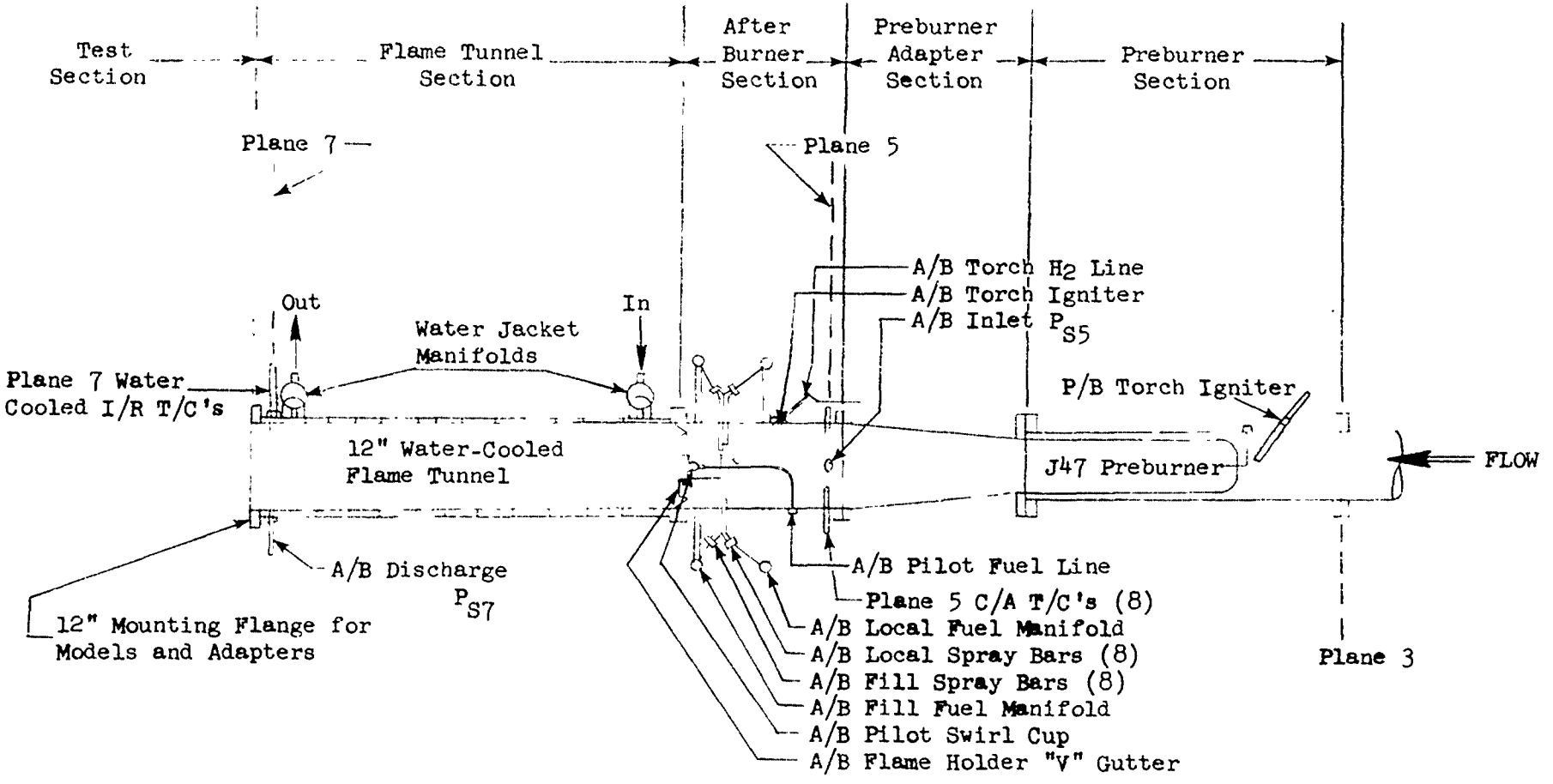

FIGURE II.B-3 SCHEMATIC OF JENOTS MAIN AIR PIPE AND BURNER SYSTEM

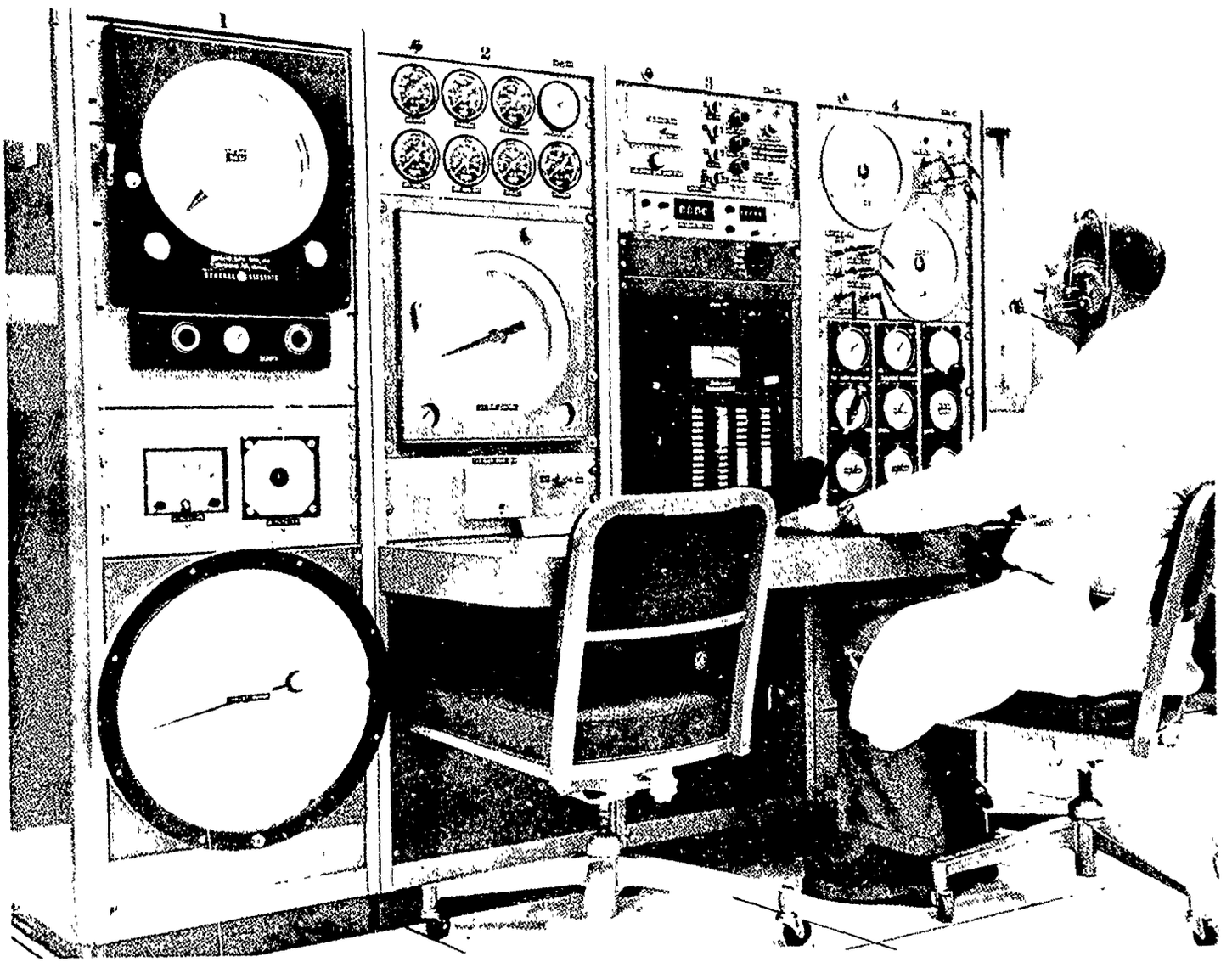

FIGURE II.B-4 JENOTS CONTROL PANEL

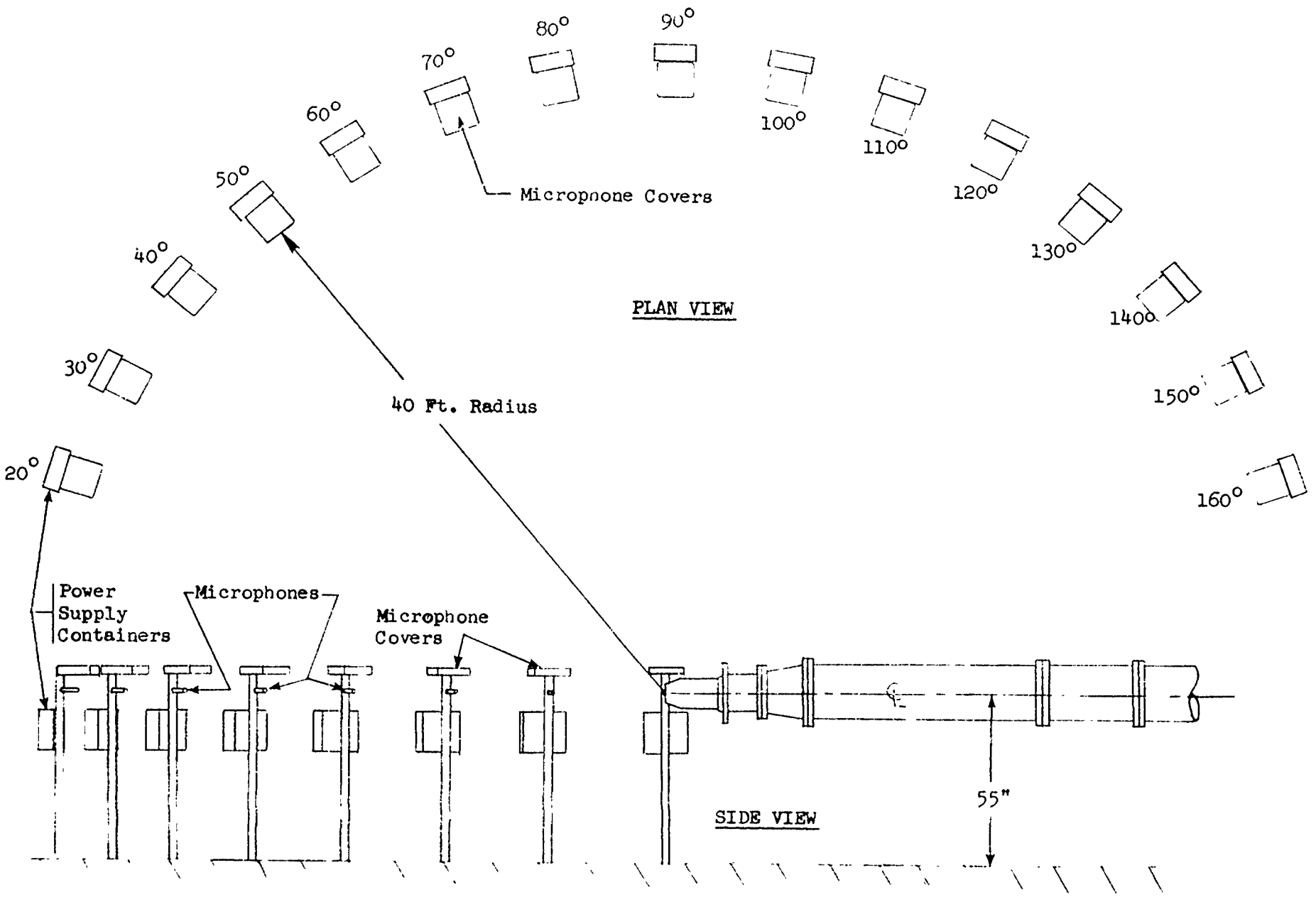

FIGURE II.B-5 SCHEMATIC OF JENOTS SOUND DATA MICROPHONE SYSTEM

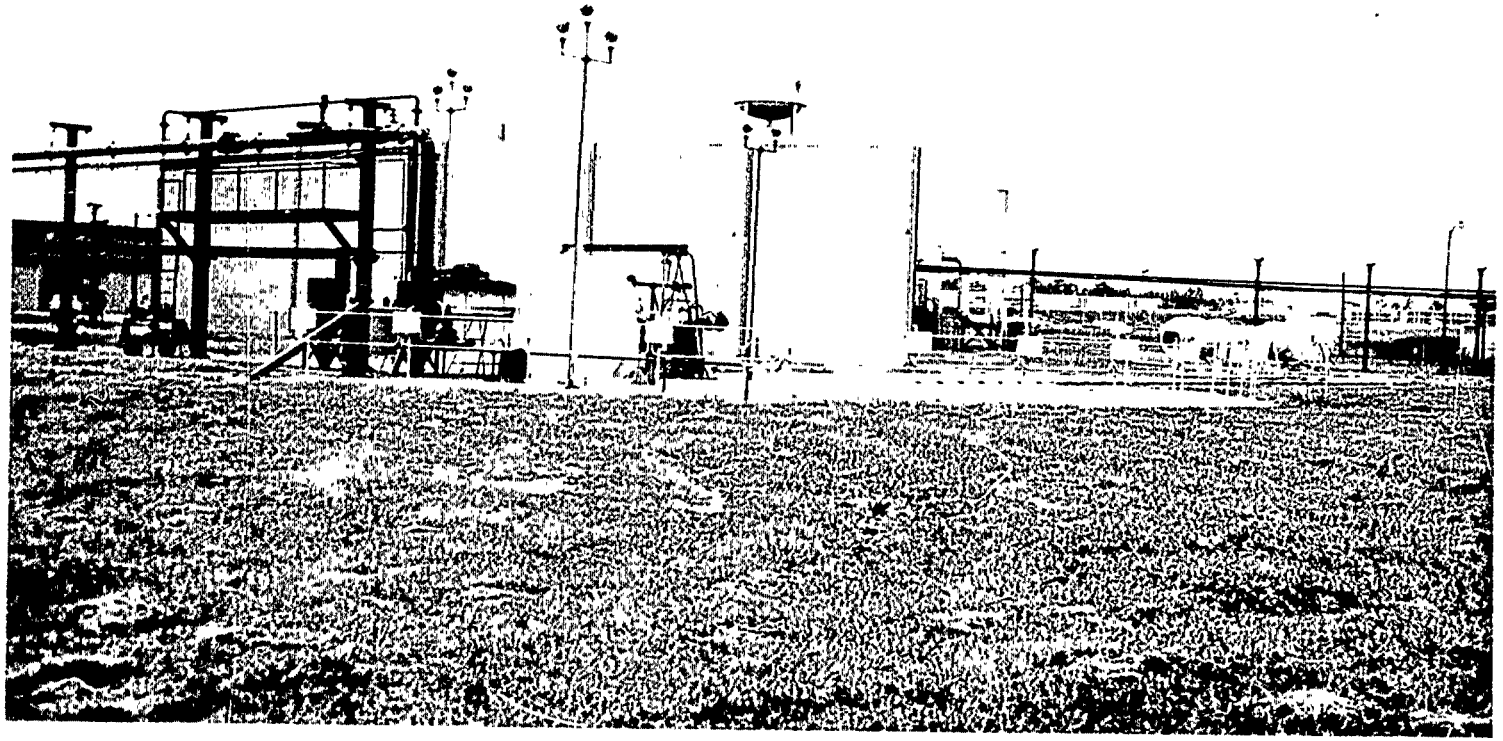

FIGURE II.B-6 JENOTS GROUND RUN-UP SILENCER

II.C PEEBLES SITE 4D FULL SCALE ENGINE TEST FACILITY

PRECEDING PAGE BLANK-NOT FILMED

II.C PEEBLES SITE 4D FULL SCALE ENGINE TEST FACILITY

The Peebles Proving Ground occupies 5,000 acres of land near Peebles, Ohio, 83 miles east of Cincinnati. First opened in 1955 as an outdoor testing area for jet and rocket engines, the proving ground has since broadened its services and facilities to encompass an almost unlimited variety of tests.

Peebles Pad 4D Acoustic Facility

This major Peebles noise facility consists of an engine thrust frame capable of accepting engines and recording thrust up to 100,000 pounds. Figure II.C-1 is an aerial view of the facility showing the Site 4D acoustic arena in the lower left of the photo. The engines are supported from above with the engine centerline approximately 13 feet above the ground. Figure II.C-2 shows a typical engine installation on the Acoustic Facility.

The sound field consists of level, crushed rock over a 250-foot arc centered about the engine. Normal far field measurements for an engine such as the GE4 were taken on a 250-foot radius over this crushed rock sound field. Permanent microphones are located at 10° increments from 0° to 160° to the inlet on the 250-foot arc, and are wired directly to the control/data acquistion room. The microphones generally are set to match the engine centerline height.

In addition to the fixed far field microphone locations, engine acoustic probes and near field microphone systems can be accommodated.

Steady-state and fluctuating plume measurements also have been taken on this facility.

Control Room Capabilities

The test facility at Peebles is a complete modern complex with all instrumentation necessary to evaluate propulsion performance. The control room has the following capabilities:

- Fully automatic data center, no manual readings required
- Display of any instrumentation for monitoring purposes at the main operating panel.
- The data is recorded on paper punch tape for the IBM program.

PRECEDING PAGE BLANK-NOT FILMED

- The facility can record the following instrumentation, which is presently available, in 60 seconds:

  a. 400 temperatures
  b. 400 pressures
  c. 52 channels of dynamic tape
  d. 30 channels of static stress
  e. any number of speeds and fuel flows
  f. 12 channels of vibration

Instrumentation

The facility is designed for full automatic recording of all data. The utilization of a master program board permits rapid changeover and continuous display of any instrumentation parameter to the control console or engineering area for monitoring or calculations, while maitaining continuous recording of data at all times.

Instrumentation capabilities consist of 3 basic types of data recording.

- Tape
- Direct Writing
- Digital

- The tape system permits the recording of 52 channels of transient or dynamic data at various recording speeds, with a supply reel of 5000 feet of tape. There are 30 channels of static stress and 12 channels of vibration available. Twenty-six oscilloscopes provide direct monitoring of the parameters being recorded. Any parameter that can be converted into an electrical signal can be recorded on tape. Pressures are not normally read on tape. Accessories to the basic system include built-in power supplies transducer switching panels, individual monitor scope and oscillators for beat frequency measurements, panoramic analyzers for 'quick look' at a parameter for its basic frequency and harmonics, electronic counters, high-speed, 2-channel oscillograph for visual indication and record of a rapidly changing variable, and a 2-channel playback system to permit playing back any previously recorded channel of tape.

- The direct-writing (analog recording) system consists of 24 basic amplifiers each driving its own electrically heated stylus to provide 24 channels of

direct-writing oscillograph recording. Each basic amplifier makes use of a preamplifier which, when properly selected for the particular type of measurement to be made, can be calibrated to record any type of variable that can be converted into an electrical signal. This system is ideal for transient type monitoring where a permanent record is desired.

- The digital recorder is a medium speed, automatic digital system which provides a printout, paper tape punch or combination of both, of 5 characters of data at a rate of 5 per second, with printer operation of 10 per second with paper tape recording only. It has the capabilities of recording 900 channels of data consisting of 400 temperatures and 400 pressures with crossover capability. However, only a limited number of the channels are applicable to hot flows. CA & CC thermocouples plus speed, fuel flow, thrust, etc. can also be recorded. Fixed data such as date, barometer readings, etc. can also be dialed-in for a permanent record. The resultant perforated paper tape is converted to IBM cards via tape-to-card converter. The cards are then fed into the computer program. It requires 168 seconds to process the discharged perforated tape. A teletype link with the computer facility in Cleveland, Ohio takes between 20 minutes to one hour to process. This system eliminates the need for manual logging of any data that is necessary for the test program.

Instrumentation Readout Accuracies

Temperature:	0.02 percent of full scale, or ± 3 microvolts, whichever is greater
Pressures:	± 0.2 percent of full-scale calibration
Speeds:	± 0.1 percent of calibrated range
Thrust:	± 0.2 percent of calibrated range
Fuel Flow:	± 0.1 percent of calibrated range
Transient:	± 3 percent of calibrated range
Barometer:	± 0.0008 inch (Hg) abs.
Vibration:	± 5 percent of calibrated range
Dynamic Stress	± 15 percent of calibrated range
Static Stress:	± 10 percent of calibrated range

Hydrocarbon Fuel Supply System

The supply system consist of two 150,000 gallon-ground floating roof storage tanks, a 15-horsepower centrifugal fuel pump, rated at 500 gpm at 65 psig, tank isolation valves for each of the storage tanks, a high-capacity, 10-micron filter in the tank fill line, a similar filter on the test pad just ahead of the engine fuel pumps, and a fast operating electrically operated ball valve at the test pad termination for rapid fuel shut-off when required. All test engines are presently using JP5 fuel.

Air Compressor Starting System

The system consists of two 450 HP electric motor driven air compressors, capable of producing 5 pps non-vitiated air flow at a minimum of 90 psig. In mid 1969 an added 12 pps at 120 psig was installed. Eight-inch piping and control valves are used throughout the system to keep pressure losses low. In 1969 ten inch piping was installed.

Thrust Systems

Three test stands are available at site 4 as seen in Figure II.C-1. Thrust measuring ability ranges from 0-100,000 lbs. in the forward direction, and 0-50,000 lbs. in the thrust reverser directions. Several types of load measuring devices are utilized; strain gage load cells, etc. The measurement accuracies of systems conform to MIL Spec E5009B.

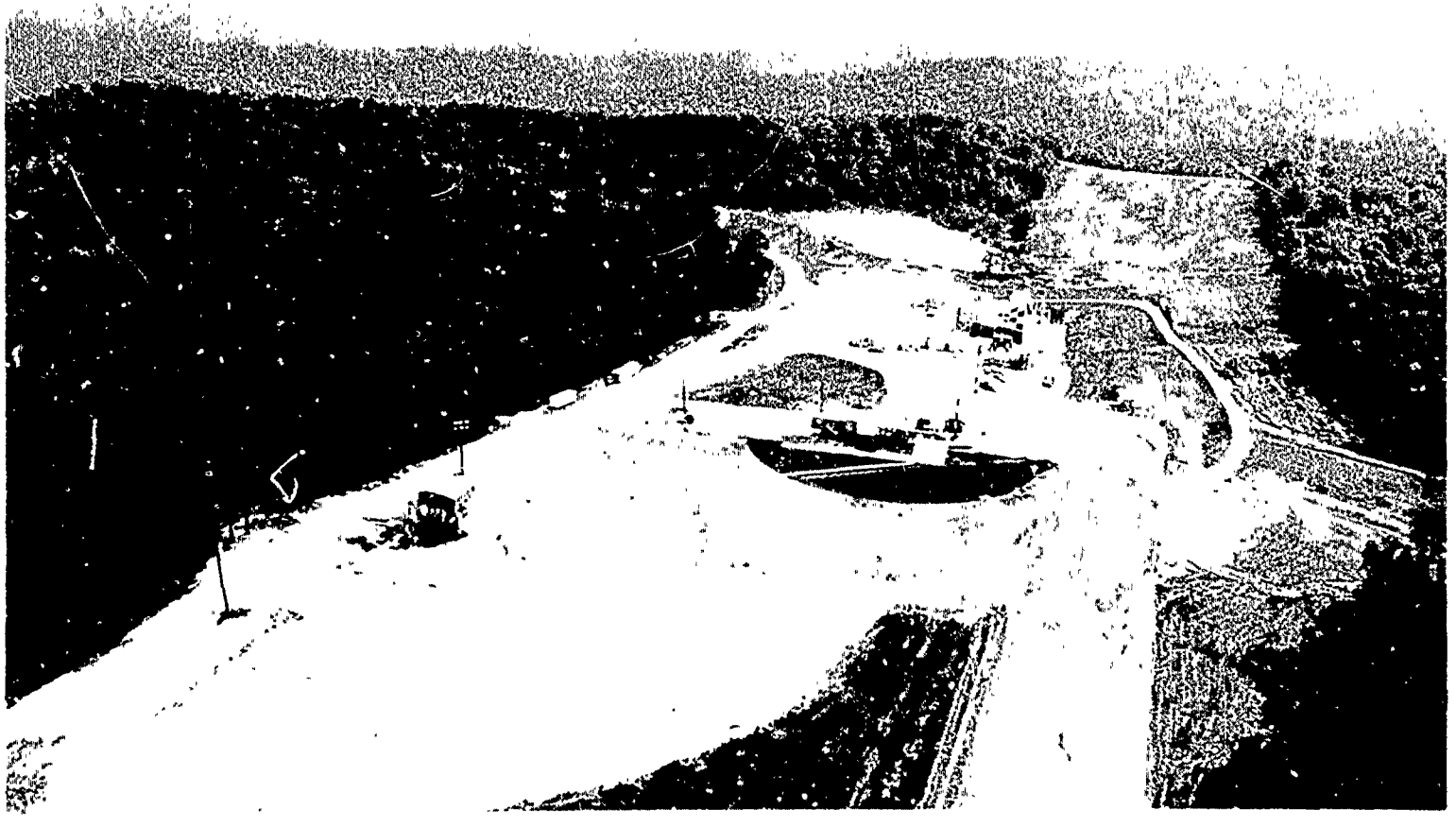

FIGURE II.C-1 PEEBLES ACOUSTIC TEST SITE

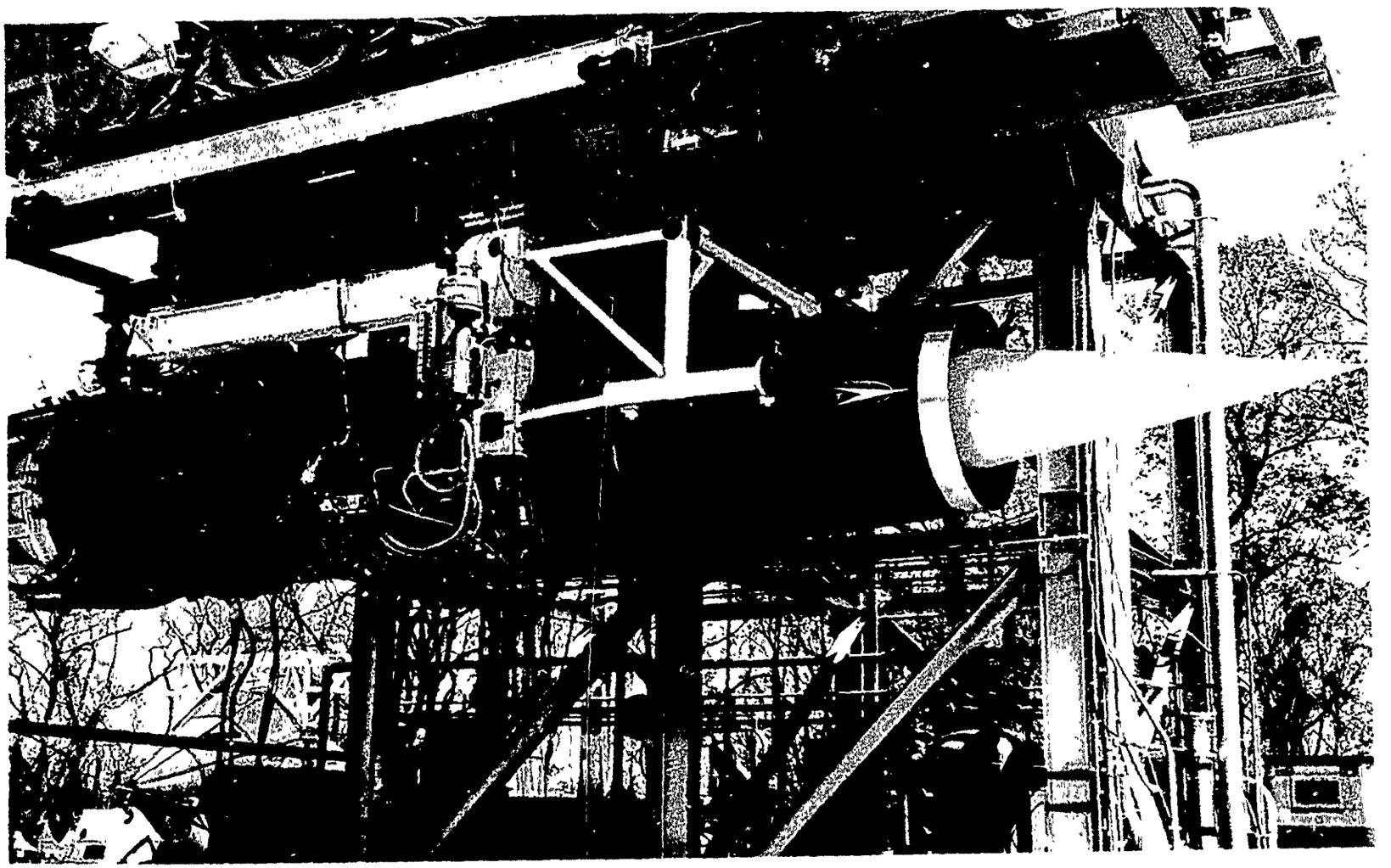

FIGURE II.C-2 TYPICAL ENGINE INSTALLATION ON ACOUSTIC STAND AT PEEBLES

II.D CORPORATE RESEARCH AND DEVELOPMENT CENTER'S SCALE MODEL AERO/ACOUSTIC TEST FACILITIES

II.D CORPORATE RESEARCH AND DEVELOPMENT CENTER SCALE MODEL AERO/ACOUSTIC TEST FACILITIES

At the General Electric Corporate Research and Development Center (R&DC) in Schenectady, New York, three scale model jet facilities were available for acoustic and aerodynamic flow measurements. These facilities ranged from a small one-inch, indoor cold jet to two outdoor facilities, capable of running heated jets supersonically on 2 in. and subsonically on 6 in. nominal diameter nozzles and recording acoustic as well as aerodynamic data.

Considerable supersonic jet noise basic research, plus suppression technology related to the supersonic transport, have been conducted on these facilities.

Air Supply Systems and Gas Fired Heater

Two compressor systems are used to supply air to the test facilities. A large gas fired air heater is available to heat the air to 1260° R at 500 psig for hot jet experiments. Various combinations of the air systems are used to obtain specific flow conditions for investigating the flow and acoustic characteristics of subsonic and supersonic jets.

The first compressor system consists of a) two reciprocating 4-stage compressors each driven by an 800 HP motor, and b) a smaller 4-stage compressor driven by a 200 HP motor. To obtain supersonic Mach numbers greater than 1.4 with a nominal 2 in. diameter nozzle, both 800 HP, 4-stage compressors are required. With this system, heated air can be supplied up to 800° F at a flow rate of 5 lbs/sec. With all three compressors (2 - 800 HP and 1 - 200 HP) in parallel, it is possible to operate nominal 6 in. diameter nozzles at 850 ft/sec at a flow rate of approximately 10 lbs/sec. The second system consists of two banks of fuller centrifugal compressors with each bank powered by a 350 HP motor. It is possible to operate a 6 in. diameter nozzle over a Mach number range of 0.10 to 0.9 at flow rates up to 11 lbs/sec. By combining these two compressor systems (2 - 800 HP, 1 - 200 HP and 2 - 350 HP compressors) it is possible to supply approximately 20 lbs/sec of air at a pressure of 30 psia.

The compressed air is passed through after-coolers, large oil separators and settling tanks. From the settling tanks the compressed air flows through

PRECEDING PAGE BLANK-NOT FILMED

an 8 inch diameter insulated pipe so that heated air can be used to investigate the effect of jet temperature on the flow and acoustic characteristics of subsonic and supersonic jets.

From the main 8 in. pipe the flow is diverted through the two 4 in. diameter lines. A Fisher pressure control system was installed on one 4 in. pipe for regulating the nozzle plenum pressure. With this automatic air flow control system it is possible to maintain the pressure at a preselected constant operating value. The 4 in. lines are rejoined to the 8 in. pipe which supplies air to the test facilities.

Outdoor Test Facilities

Two outdoor facilities are available, one capable of running hot flow up to 800° F with 2 in. diameter nozzles and the other up to 800° F with nominal 6 in. diameter nozzles.

Figure II.D-1 shows the outdoor hot jet aero/acoustic facilities used to test nominal 2 in. and 6 in. diameter nozzles. The air supplied to these facilities flows through the 8 in. diameter insulated pipe shown in Figure II.D-1 where a valve system distributes the air either directly to the 6 in. test nozzle facility, o to the 2 in. test nozzle facility through a 4 in. branch supply line off the 8 in. main.

The facility air supply lines (4 in. and 8 in. diameter) terminate in plenum chambers located 6 ft. above ground and 60 ft. away from the building housing the compressors. The plenum chambers are provided with flow straightening screens that break up large eddies into smaller ones. Test nozzle sections are attached to the ends of the plenum chambers. Both facilities are located at a sufficient distance from other structures to provide an effectively free field environment for a full 180° arc.

o 2-Inch Facility

The 2-inch facility is equipped with an acoustic field at a 10-foot radius with eight microphone positions set at centers of equal area, assuming uniform radiation through slices of a hemisphere. Acoustic data are recorded on tape up to 80 KHz, using a B&K single microphone traversing system and a Norelco recorder. A wake rake system, which can traverse the jet plume axially and

radially, also is available and is used to support steady-state or fluctuating aerodynamic probe instrumentation. The facility is capable of running 2-inch jets up to a pressure ratio of 10:1. The air can also be heated indirectly using a gas-fired heat exchanger and, thus, supply air up to 800°F at the nozzle exit. However, most tests conducted on this facility were done at ambient temperature. A 12 in. diameter plenum chamber is located upstream of the test nozzle. A scale factor of 20:1 was used on this facility. Considerable testing has been conducted on this facility to understand the basic mechanisms for shock-free and underexpanded supersonic jet noise. The rig also has relative thrust measurement capability.

o 6-Inch Facility

The 6-inch outdoor jet facility is aimed primarily at the understanding and reduction of low-velocity jet noise (although the rig can be run up to a pressure ratio of 3:1 and 800° F). The facility can accommodate nozzles 4 in. to 6 in. diameter. Microphones are located at a 30-foot arc, and again data up to 80 KHz are tape recorded. The plenum chamber for this facility is 24 in. diameter. The scale factor for this facility was from 7 to 10:1.

Indoor Cold Jet Facility

A 1-inch diameter convergent nozzle attached to a 6 in. diameter plenum chamber was used inside the Fuller compressor room to obtain the mean velocity and piezoelectric impact pressure probe fluctuation distributions for jet Mach numbers of 0.6 and 1.4. Compressed air at 125 psig and 1.25 lbs/sec is supplied to this nozzle by the 200 HP compressor. With this indoor test nozzle facility it is possible to make detailed radial surveys of the impact pressure and piezoelectric pressure probe fluctuations over a large distance from the nozzle exit. These radial surveys at various distances from the nozzle exit are difficult to conduct outdoors with the 2 inch and 6 inch nozzles shown in Figure II.D-1, because of the wind conditions. Also, with the indoor nozzle it is easier to obtain optical photographs of the jet flow field with a short duration spark source.

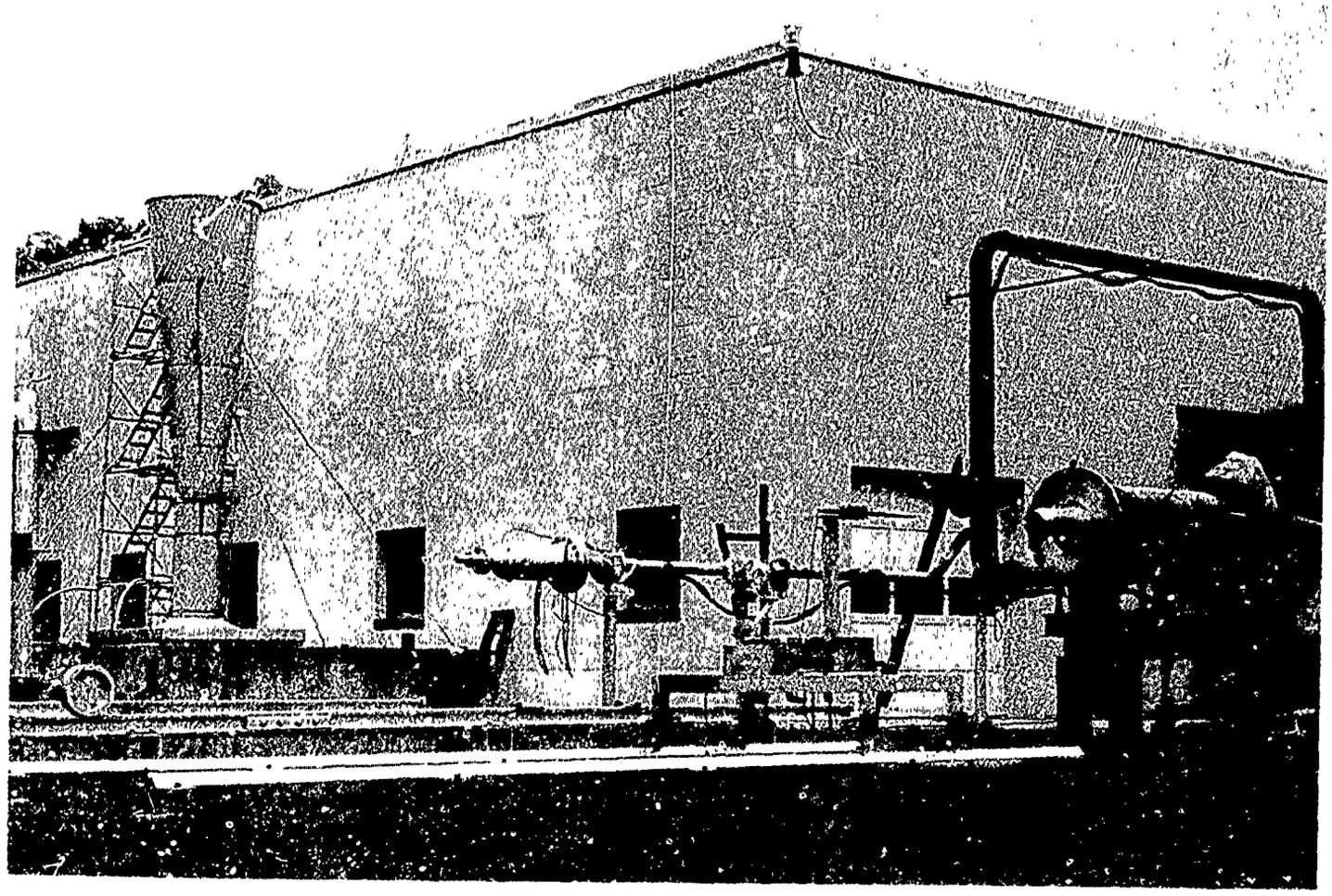

FIGURE II.D-1 RESEARCH AND DEVELOPMENT CENTER 2 INCH AND 6 INCH DIAMETER AERO/ACOUSTIC FACILITIES

II.E FLUIDYNE ENGINEERING SCALE MODEL WIND TUNNEL TEST FACILITIES

II.E FLUIDYNE ENGINEERING AERODYNAMIC TEST FACILITIES

Aerodynamic testing performed during the GE4 jet noise suppression program, was conducted on several groups of scale model suppressors at FluiDyne Engineering Corporation's Medicine Lake Aerodynamics Laboratory, Medicine Lake, Wisconsin. Testing was performed in three separate facilities. Early static thrust measurements were taken on multi-tube suppressor models (PD-3 Series, Section V.F.10) in the Channel 12 Static Thrust Stand. Later tests involving the multi-element spoke/chute suppressors on annular plug nozzles (Section V.H.2) were conducted in the Channel 10 Transonic Wind Tunnel, and the Channel 7 Static Thrust Stand.

Thrust data for all three facilities were obtained by direct force measurement using a strain gage force balance system.

66-Inch Transonic Tunnel: Channel 10

Channel 10 is a transonic wind tunnel having a 66 x 66-inch slotted wall test section. In the multi-element spoke/chute test series (Section V.H.2) it was used for achieving external flow Mach numbers of 0, .35, .5, .9, and 1.1. This is an induction-type tunnel in which atmospheric air is drawn through the test section using air ejectors to reduce the downstream pressure. The required test section Mach number is obtained by controlling the mass flow to the ejectors. Water condensation in the test section is avoided by burning propane upstream of the inlet.

Static nozzle tests (M = 0) were conducted in this facility with the ejectors off by adding a windscreen to shield the model from local induced flow effects.

The Channel 10 thrust data were obtained by direct force measurement using a strain gage force balance system. This balance permits the measurement of net installed nozzle thrust during tests with external flow around the model. The balance was located just upstream of the test nozzle in the support tube. (In the case of the static thrust stands, the model and force balance assembly were mounted downstream of the facility stagnation chamber). The test nozzle was structually isolated from the upstream (grounded) portion of the balance system by a thin elastic membrane. The force on the model assembly downstream of the seal was transmitted via the balance strain gage elements to a digital readout system. The force balance system used in the channel 10 testing was the same as that used for the static thrust stands, Channels 7 & 12.

PRECEDING PAGE BLANK-NOT FILMED

Channel 7 Static Thrust Stand

To achieve the higher pressure ratios required for some of the multi-element/annular plug nozzle modes, it was necessary to use the Channel 7 Static Thrust Stand and surround the model with a test cabin. The ambient pressure in the test cabin was controlled by a combination of the pumping action of the test nozzle, inbleeding a small amount of secondary air into the cabin, and throttling with a downstream butterfly valve.

Model total pressure for the Channel 7 tests was maintained between 57 and 75 psia, to obtain the required high pressure ratios and to provide required throat Reynolds numbers greater than 6×10^6.

Channel 12 Static Thrust Stand

The multi-tube preliminary design number three (PD3) model tests were performed in Channel 12 at FluiDyne's Medicine Lake Aerodynamics Laboratory. Channel 12 is a cold-flow axisymmetric free-jet thrust stand. Nozzle thrust is determined from force measurement with a strain gage force balance.

High pressure dried air from the facility storage system was throttled, metered through an ASME long-radius metering nozzle, and discharged through the model to atmosphere. Model total pressure (P_{T8}) was varied from 20 to 50 psia.

Test Data & Instrumentation

The test data obtained in all three facilities consisted of measurements of airflow rate, balance force, nozzle surface static pressures, model total pressure, ambient pressure, meter total temperature and inlet pressures necessary to calculate the stream thrust entering the metric (floating) portion of the model assembly. Pressures were measured with mercury and water manometer banks and bourdon-tube gages, and recorded on Polaroid camera film. Temperatures were measured with iron/constantan thermocouples and recorded on chart recorders.

III. DATA ACQUISITION AND REDUCTION METHODS

III. DATA ACQUISITION AND REDUCTION METHODS

The major portion of the acoustic data and results curves presented in this report were acquired through scale model testing at the General Electric, Evendale, Ohio, Jet Engine Noise Outdoor Test Stand (JENOTS). In addition engine noise data were acquired at the Peebles Site 4D full scale test facility. The basic facilities are discussed in Section II.B and II.C, respectively. The acoustic data acquisition and reduction systems, in addition to methods of data presentation will be discussed in Section III.A - JENOTS and III.B - Peebles Site 4D, for a better understanding of the presented data results.

PRECEDING PAGE BLANK-NOT FILMED

III.A JENOTS DATA ACQUISITION AND REDUCTION

PRECEDING PAGE BLANK-NOT FILMED

III.A JENOTS DATA ACQUISITION AND REDUCTION

During the five year period of model jet suppressor testing at the JENOTS facility, the data acquisition/reduction method underwent major revision only once - during late 1969. The pre-late 1969 system consisted of a standard 40 ft. arc array of microphones at 10° increments from 30° through 90°, with the acoustic signal processed through a Bruel and Kjaer (B&K) Spectrometer and Level Recorder in octave band form. All model test data presented in this report, with the exceptions of Section V.H.2 (Multi-Element Spoke/Chute Model Suppressor Parametric Investigations on Annular Plug Nozzles) and Section VII (General Electric Corporate Research and Development Center's Fundamental Jet Noise Work) were acquired using this system.

In late 1969 additional microphone systems were added on the 40 ft. arc at 20° and from 100° through 160°, at 10° increments. The microphone, cathode follower and power supply system remained the same but the acoustic signals were then processed through an on-line data reduction system consisting of a B&K 1/3 octave band Audio Analyzer with parallel inputs coupled with a DDP-116 computer. Only the JENOTS model data presented in this report as Section V.H.2 were acquired through this system. Method of scaling, consideration of ground reflection and extrapolation techniques remained essentially consistent over the documented five year period.

JENOTS, Pre-Late 1969 (All JENOTS data except Section V.H.2)

In Section II.B, Figure II.B-5 shows a schematic of the JENOTS acoustic arena with microphones located on a 40 ft. radius arc centered at the nozzle exit plane, and at nozzle/facility centerline height of 55". Figure II.B-1 is a photograph of the burner system, test section and microphone array. Prior to late 1969 microphones were located at 30°, 40°, 50°, 60°, 70°, 80°, and 90° to the jet exhaust axis under protective rain shields which were acoustically treated and properly orientated to prohibit acoustic reflection to the microphone. The Bruel and Kjaer (B&K) data acquistion systems, as per Figure III.A-1, consisted of:

PRECEDING PAGE BLANK-NOT FILMED

- Microphones - type 4135
- Adapters - type UA0035
- Cathode Followers - type 2615
- Power Supplys - type 2801
- Audio Frequency Spectrometer - type 2122 (1/3 or 1/1 Octave Band Filters)
- Level Recorder - type 2305 - with 50 dB range potentiometer
- Pistonphone - type 4220 - for calibration

The power supplys and related cables were kept permanently in heated storage boxes at each microphone station as seen in Figures II.B-1 and II.B-5. Shielded cables through conduits to the control room connected the systems to the spectrometer and level-recorder as shown in Figure III.A-2. Using the spectrometer/level-recorder system, data were taken in octave band form through the 31.5 KHz octave band. The system was set to measure the RMS value of the signal. Level recorder adjustments were normally set for 40 mm/sec writing speed, 100 mm/sec paper drive speed, and 12 rpm drive shaft speed. Microphone systems were recorded sequentially requiring approximately 25 seconds per microphone. About 1.5 seconds of data were recorded per octave band. Burner conditions were accurately controlled so that acoustic data were not affected by change in jet conditions during the recording period.

To ascertain that valid acoustic data were obtained from each acoustic test, rigid procedures were followed for equipment calibration prior to test. The calibration of all microphones was checked periodically using an acoustic calibration system built by General Electric and available at the Evendale facilities. All microphones whose voltage output deviated more than $\pm$ 1 dB, as compared to manufacturer specifications during field/laboratory calibration procedures, were not used until a recalibration was done using this facility and until new absolute sensitivity and frequency response characteristic values were assigned, where applicable. Any microphone output deviating by more than $\pm$ 2 dB was returned to the manufacturer for repair and recalibration.

In addition to the periodic laboratory microphone checks, the entire acoustic data acquisition system was calibrated in the field in the following manner. The overall system frequency response was obtained by removing the microphone head and applying a constant-voltage oscillator signal at the center

frequency of each octave band. The response corrections in each octave band are determined for inclusion into the data reduction program.

Immediately prior to and following each day's testing, each microphone system was calibrated using the Model 4220 pistonphone.

The acoustic data were reduced manually, as per Figure III.A-1, by an engineer's assistant to the form of octave band sound pressure levels at the 40 ft. measuring arc for the model frequency range, each microphone system's output adjusted to the proper level using the pre-and post-test pistonphone calibration. The basis on which the model acoustic data were scaled to engine size came from consideration of constant Strouhal number at a given jet velocity. The full scale engine frequency, f_e, was related to the measured model frequency, f_m, by the following:

$$f_e \times D_{8_e} = f_m \times D_{8_m}$$

where D_{8_m} is the equivalent physical exit diameter of the model, and D_{8_e} is the equivalent physical exit diameter of the engine. The above relation assigns the engine jet velocity as that of the model. The scale factor for nozzle diameter, measuring arc, and frequency range was thus defined as the ratio of the engine equivalent physical exit diameter to the model equivalent physical exit diameter and was set at 8:1 for all JENOTS model tests. Thus the measured model octave band sound pressure levels on the 40 ft. arc at 500, 1K, 2K, 4K, 8K, 16K and 31.5 KHz were assigned as the full scale 320 ft. arc octave band sound pressure levels at 63, 125, 250, 500, 1K, 2K, and 4 KHz. The shifting of frequency bands and measuring arcs was part of the manual data reduction process, prior to entering the data into a time-share computer program, which applied the individual microphone system frequency response corrections, calculated arc OASPL and PNL, extrapolated the data to a reference sideline(s) and calculated OASPL and PNL at the sideline(s).

The acoustic levels were reduced on the 40 ft. measuring arc and assigned to the 320 ft. full scale arc in the "as-measured" form (with the exception of microphone system frequency response corrections). The 40 ft. arc atmospheric absorptions at model high-frequencies were assumed equivalent to the full scale 320 ft. arc low-frequency atmospheric absorptions. No adjustments were made to

the model (or full scale) sound pressure levels on the arc to correct to a standard meteorological day, as accurate values of high-frequency atmospheric absorption as a function of test day meteorological conditions were not available. Occasional checks, by correcting model measured data to standard day at the 40 ft. arc and accounting for high-frequency 40 ft. arc to low-frequency 320 ft. arc adjustments in atmospheric absorption, (using extrapolations of the curves in SAE ARP 866) showed minor variance in final PNL levels as compared to the adopted scaling procedure.

The acoustic measurements were not altered for ground reflection interference as the geometry of the source/microphone array nominally set the theoretical first null frequency in the 400 to 500 Hz region, just at the start of the frequency region of interest used for scaling to engine size. In addition, measurements, data reduction, and scaling for all suppressor and baseline nozzles were performed in the same manner, so as not to introduce inconsistencies which would alter the comparative suppression results.

The scaled data, at engine 320 ft. measuring arc and 63 Hz through 4 KHz octave band sound pressure levels were input to a time-share computer program which performed the following:

a) Corrected the individual octave band sound pressure levels for microphone system frequency response (input as a correction table from the system calibrations).

b) Calculated 320 ft. arc OASPL and PNL values.

c) Extrapolated the 320 ft. arc data to the 300 ft. reference sideline using a) inverse square law (hemispherical divergence = 20 log r/R), and b) octave band values for atmospheric absorption per Table III.A-1.

d) Calculated 300 ft. sideline OASPL and PNL values.

e) Repeated steps c) and d) for a 1500 ft. reference sideline.

JENCTS, Post-Late 1969 (JENOTS Data in Section V.H.2)

In late 1969 additional microphones were added to the 40 ft. arc array at 20° and from 100° through 160° from the jet axis at 10° increments, thus filling the arc from 20° through 160°. The same type microphones, cathode followers, and

power supplies were used (Figure III.A-3) and the signal was fed through a selector switch and amplifier system to an on-line data reduction system. The Ithaco Model 442 amplifier was used to set the correct gain/attenuation at the test cell for data reduction. Line drive amplifiers were utilized to drive the signal over approximately 4000 ft. of line t the data reduction quipment in the Instrumentation Data Room (I.D.R.). The amplifiers kept a flat response to 80 KHz. The spectrometer and level recorder in Figure III.A-3 were used only for monitoring purposes in the JENOTS control room.

The on-line data reduction equipment, Figure III.A-4, consisted of a B&K 1/3 octave band Audio Analyzer, which was a parallel filter set with an "average" R.C. network, interfaced with the DDP-116 computer.

A "Quick Look" print-out was obtained from the computer, consisting of scale model 1/3 octave band sound pressure levels through 80 KHz. In addition a digital-magnetic tape was generated for input to the DDP-116 computer for obtaining final scaled and extrapolated data.

Calibration procedures for this system were similar to the pre-late 1969 system, however, frequency response calibrations were done at 1/3 octave band center frequencies instead of octave band. Scaling was done in the same manner using the 8:1 scale factor. The data were uncorrected for ground reflections and were not corrected to a standard meteorological day. The acoustic signals were automatically adjusted for proper level with reference to the pre- and post-test pistonphone calibrations. The individual microphone system's line loss calibration corrections were input to the computer and applied to the measured levels. The computer program then:

a) Scaled the 40 ft. arc model frequency data to the 320 ft. arc engine frequency data.

b) Calculated 320 ft. arc OASPL and PNL values.

c) Extrapolated the 320 ft. arc data to a 300 ft. reference sideline using a) inverse square law (hemispherical divergence = 20 log r/R), b) extra ground attenuation per SAE AIR 923, and c) atmospheric absorption per jointly agreed GE/Boeing values per Table I' . 2.

d) Calculated 300 ft. sideline OASPL and PNL values.

e) Extrapolated the 320 ft. arc data to a 1500 ft. reference sideline using a) inverse square law, and b) atmospheric absorption per Table III.A-2.

f) Calculated 1500 ft. sideline OASPL and PNL values.

g) Repeated steps e) and f) for a 2128 ft. reference sideline.

TABLE III.A-1 OCTAVE BAND ATMOSPHERIC ABSORPTION VALUES

- 77°F; 70% Relative Humidity

Octave Band Center Frequeny	dB/1000 Ft.
63	0
125	0
250	0
500	1.0
1000	1.8
2000	3.9
4000	7.8
8000	11.9

TABLE III.A-2 GE/BOEING AGREED ATMOSPHERIC ABSORPTION VALUES

- 77°F; 70% Relative Humidity

1/3 Octave Band Center Frequency	dB/1000 Ft.	1/3 Octave Band Center Frequency	dB/1000 Ft.
200	0	1600	2.9
250	0.5	2000	3.6
315	0.6	2500	4.7
400	1.0	3150	6.1
500	1.0	4000	7.6
630	1.2	5000	8.8
800	1.4	6300	11.3
1000	1.6	8000	15.0
1250	1.8	10000	19.0

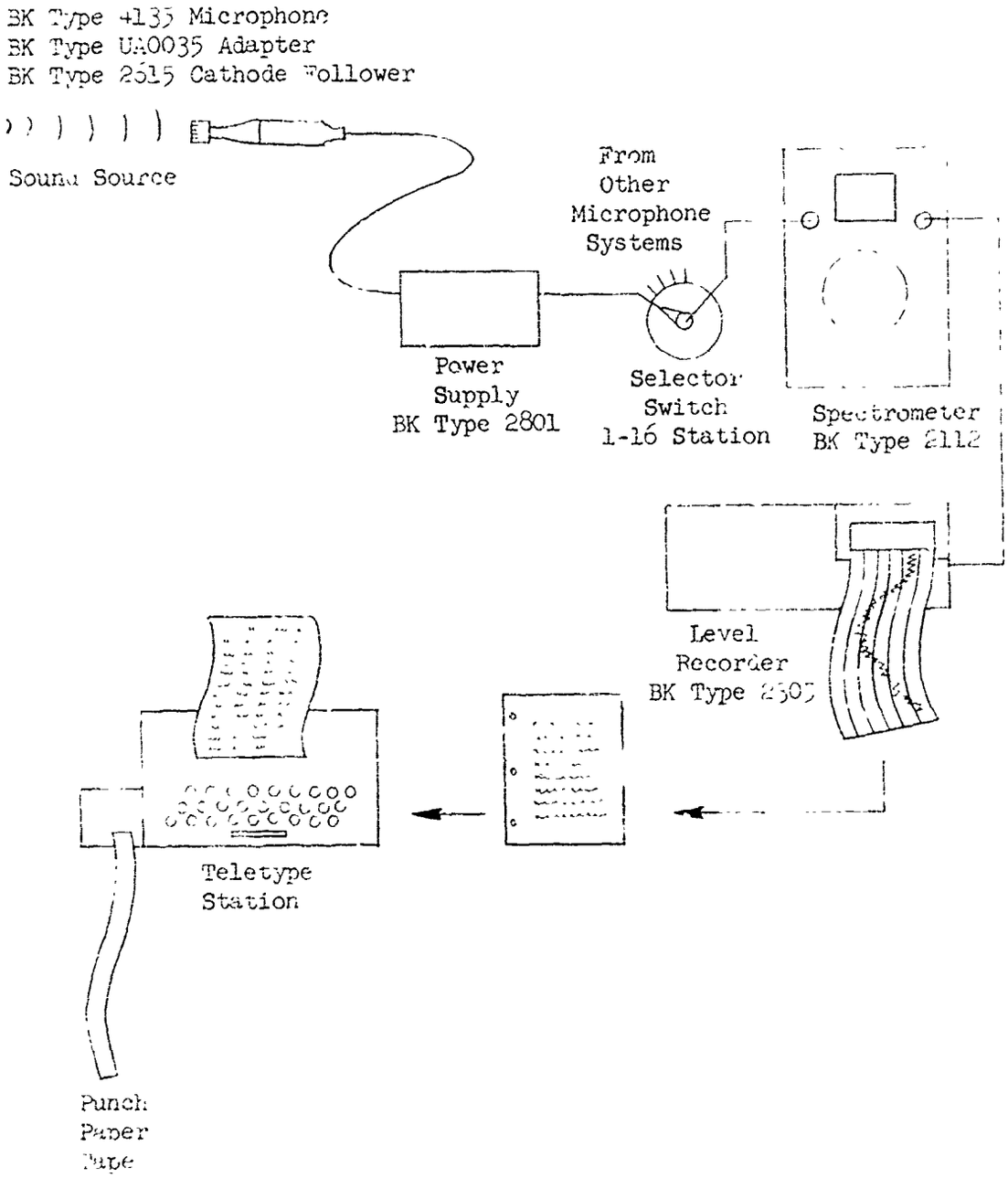

FIGURE III.A-1 SCHEMATIC OF .ENOTS PRE-LATE 1969 ACOUSTIC DATA ACQUISITION/REDUCTION SYSTEM

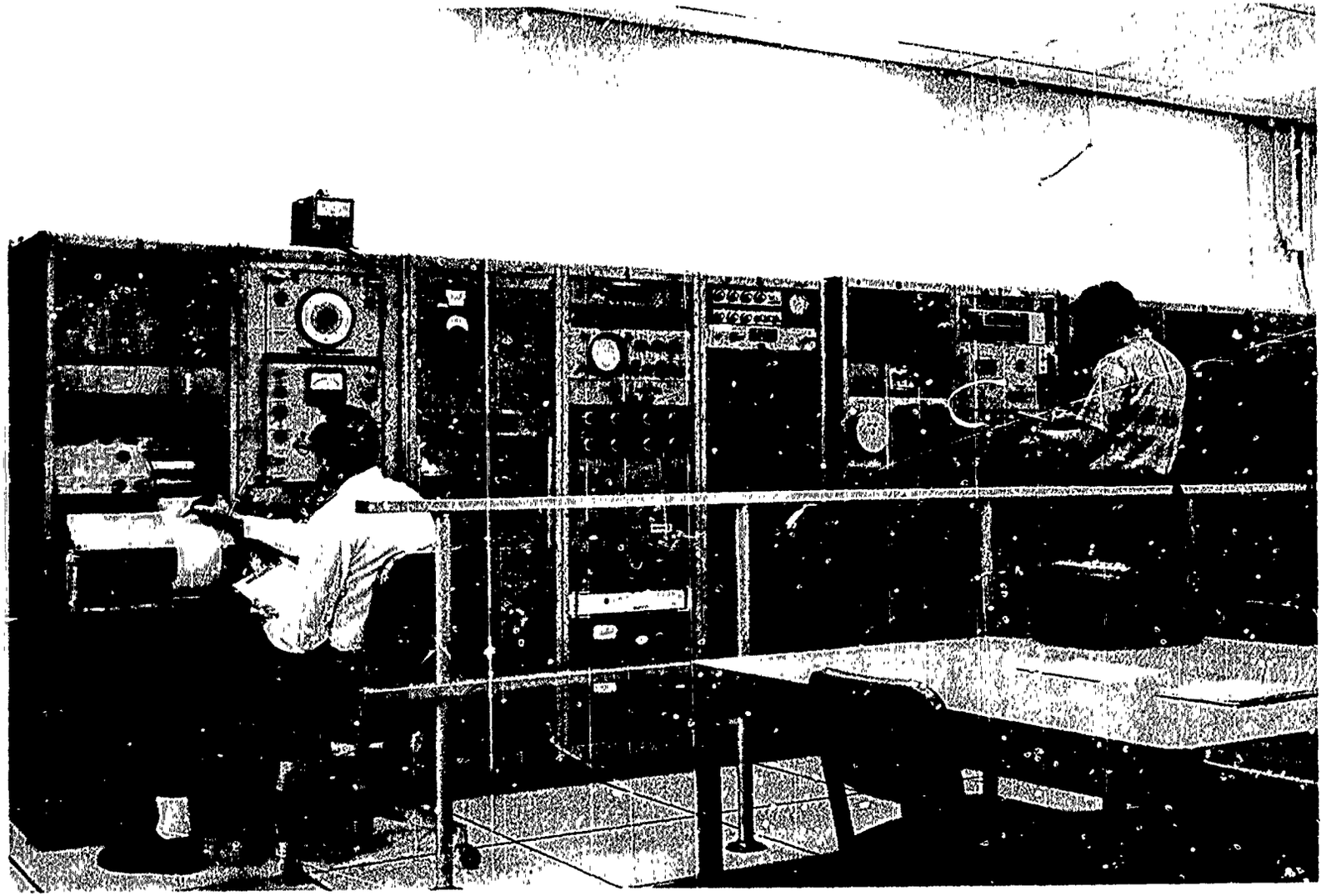

FIGURE III.A-2 JENOTS ACOUSTIC MONITORING AND DIGITAL RECORDING SYSTEMS

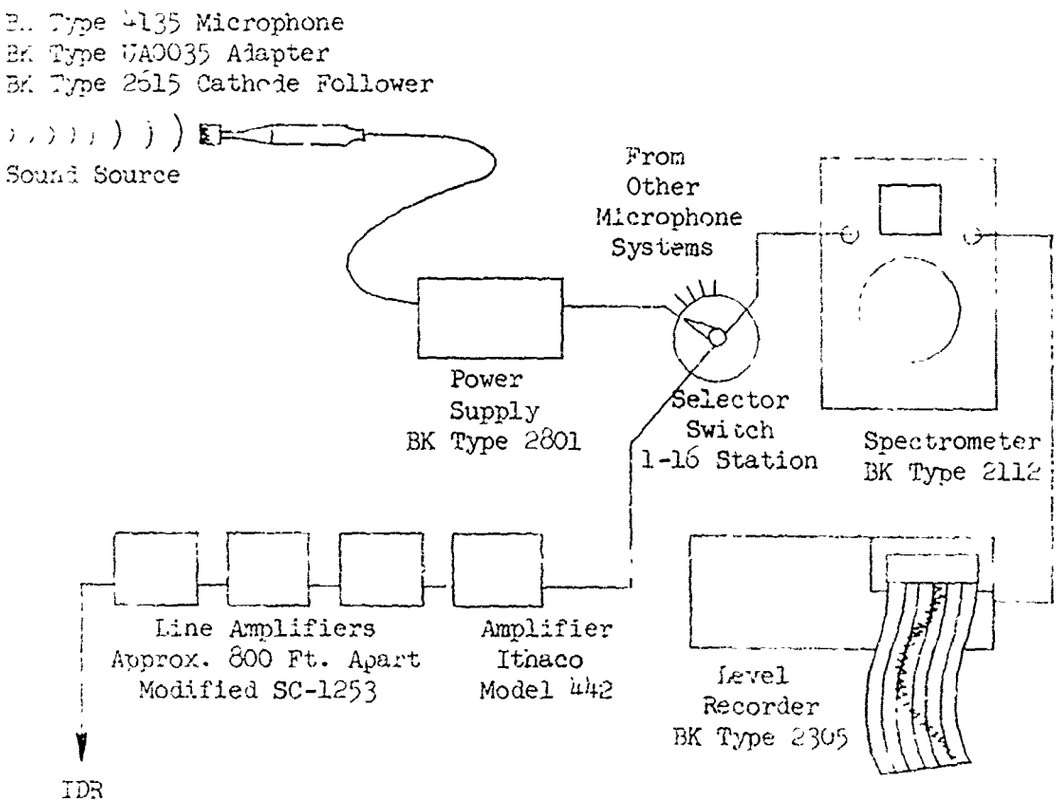

FIGURE III.A-3 SCHEMATIC OF JENOTS POST-LATE 1969
ACOUSTIC DATA ACQUISITION SYSTEM

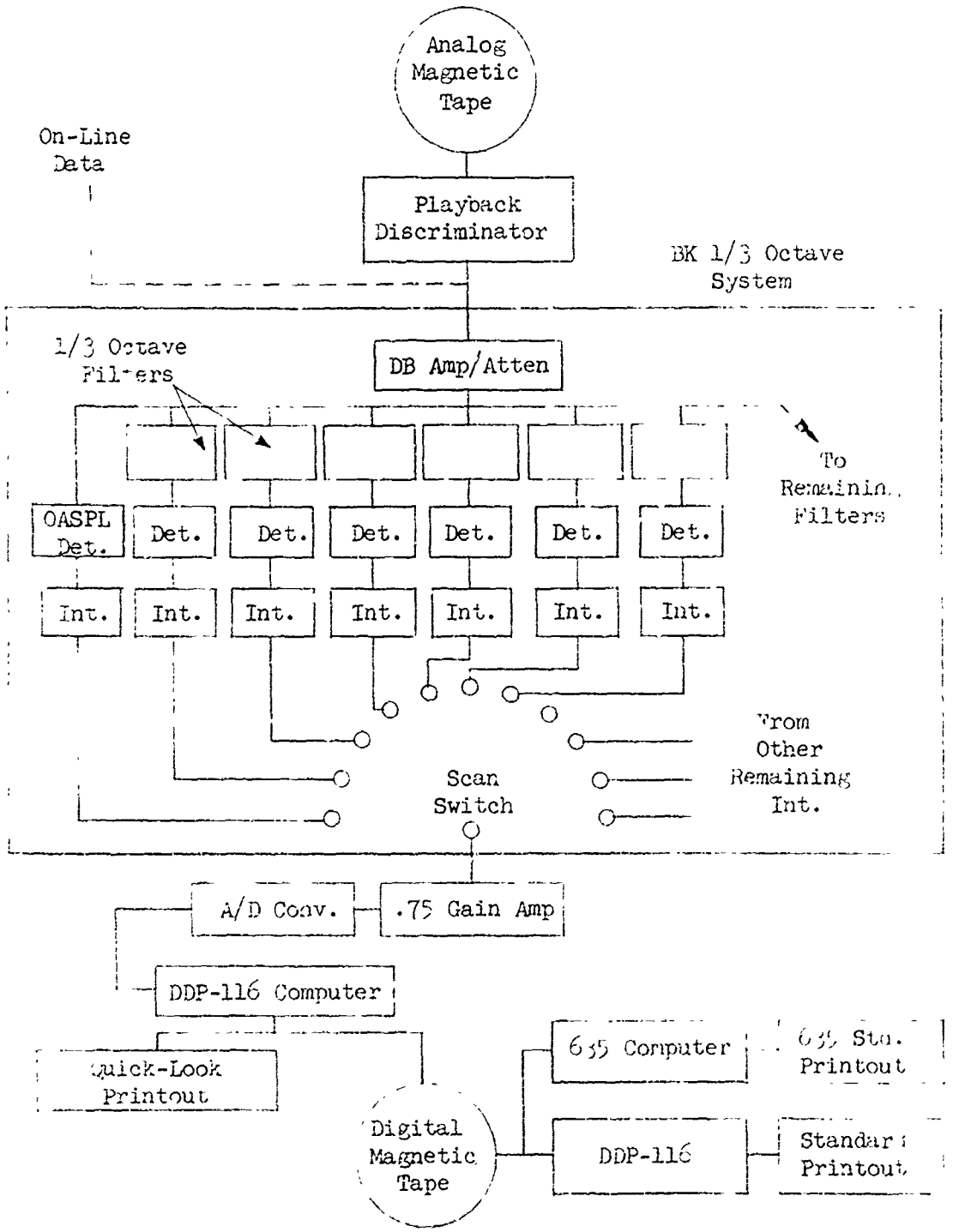

FIGURE III.A-4 SCHEMATIC OF JENOTS POST-LATE 1969 ACOUSTIC DATA REDUCTION SYSTEM

III.B PEEBLES SITE 4D DATA ACQUISITION AND REDUCTION

PRECEDING PAGE BLANK-NOT FILMED

III.B PEEBLES SITE 4D DATA ACQUISITION AND REDUCTION

The Peebles Site 4D acoustic facility is discussed in Section II.C. The sound field consisted of crushed rock over a 250 ft. arc centered about the engine. Far field measurements were taken on a 250 ft. arc with microphones set at engine centerline height of approximately 13 ft., and at each 10° from 0° to 160°, referenced to the inlet. The acoustic recording equipment normally used is shown in Figure III.B-1 and consists of B&K microphone systems and a 28 channel Honeywell or Sangamo tape recorder. All inputs to the recorder were simultaneous, each signal monitored on a separate scope.

The 28 channel Sangamo tape recorder with appropriate amplifiers would simultaneously record 25 channels on FM with frequency response capabilities from 0.5 to 20 KHz, and three direct record channels for voice and vehicle speed data. The Honeywell Model 7600 recorder was available for 28 dynamic signals in the 0.5 to 20 KHz range.

Calibration procedures for each microphone system were similar to that discussed in Section III.A.

The acoustic magnetic tapes were returned to the GE, Evendale Instrumentation Data Room (I.D.R.) for reduction per the schematic of Figure III.B-2, using the I.D.R. data reduction equipment seen in Figures III.B-3 and III.B-4.

The data were reduced in 1/3 octave band form through 10 KHz. The "quick-look" data were corrected to a 59° F standard acoustic day using SAE ARP 866 atmospheric absorption curves. The data were also corrected for individual microphone system calibrations. A digital-magnetic tape of the data was made and processed through the 635 computer program which extrapolated the data to the 300 ft. sideline using inverse square law, SAE ARP 866 atmospheric attenuation for the 59° standard day, and extra ground attenuation per SAE AIR 923. OASPL and PNL calculations were then made at the sideline.

PRECEDING PAGE BLANK-NOT FILMED

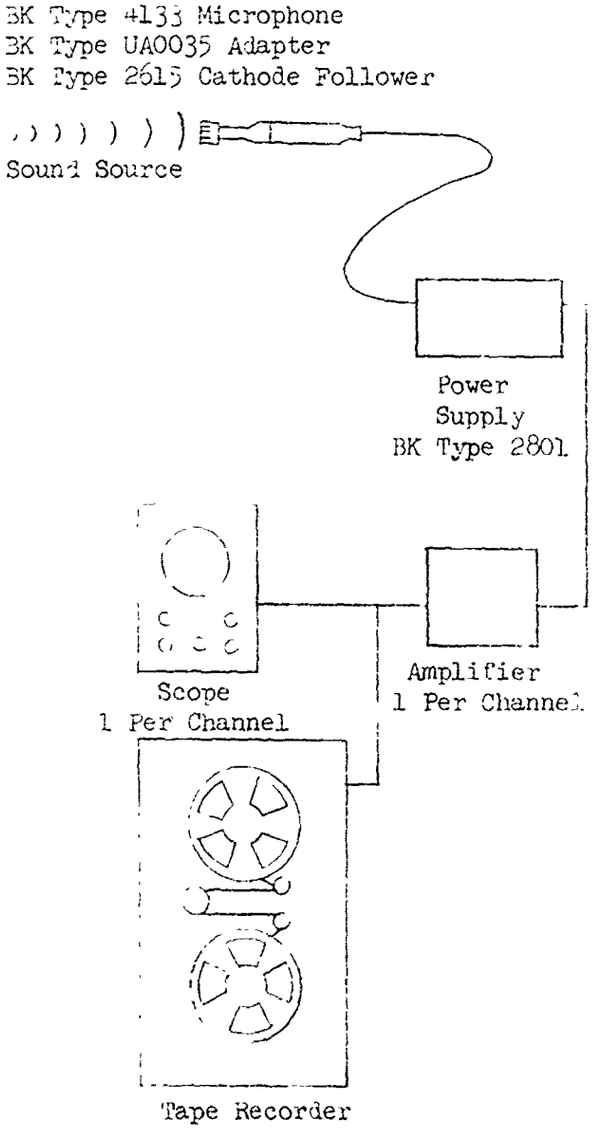

FIGURE III.B-1 SCHEMATIC OF PEEBLES SITE 4D ACOUSTIC DATA ACQUISITION SYSTEM

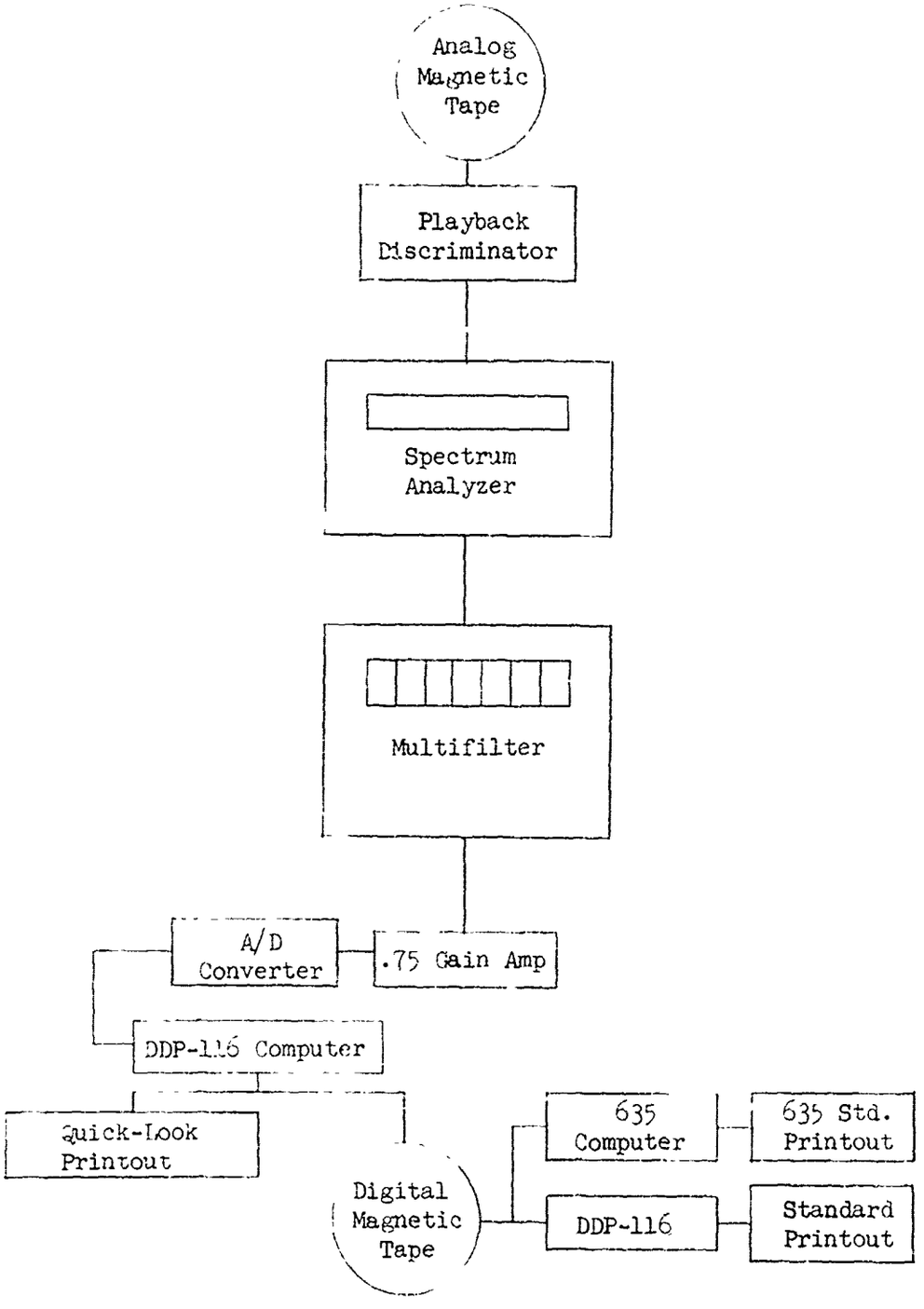

FIGURE III.B-2 SCHEMATIC OF PEEBLES SITE 4D/INSTRUMENTATION DATA ROOM ACOUSTIC DATA REDUCTION SYSTEM

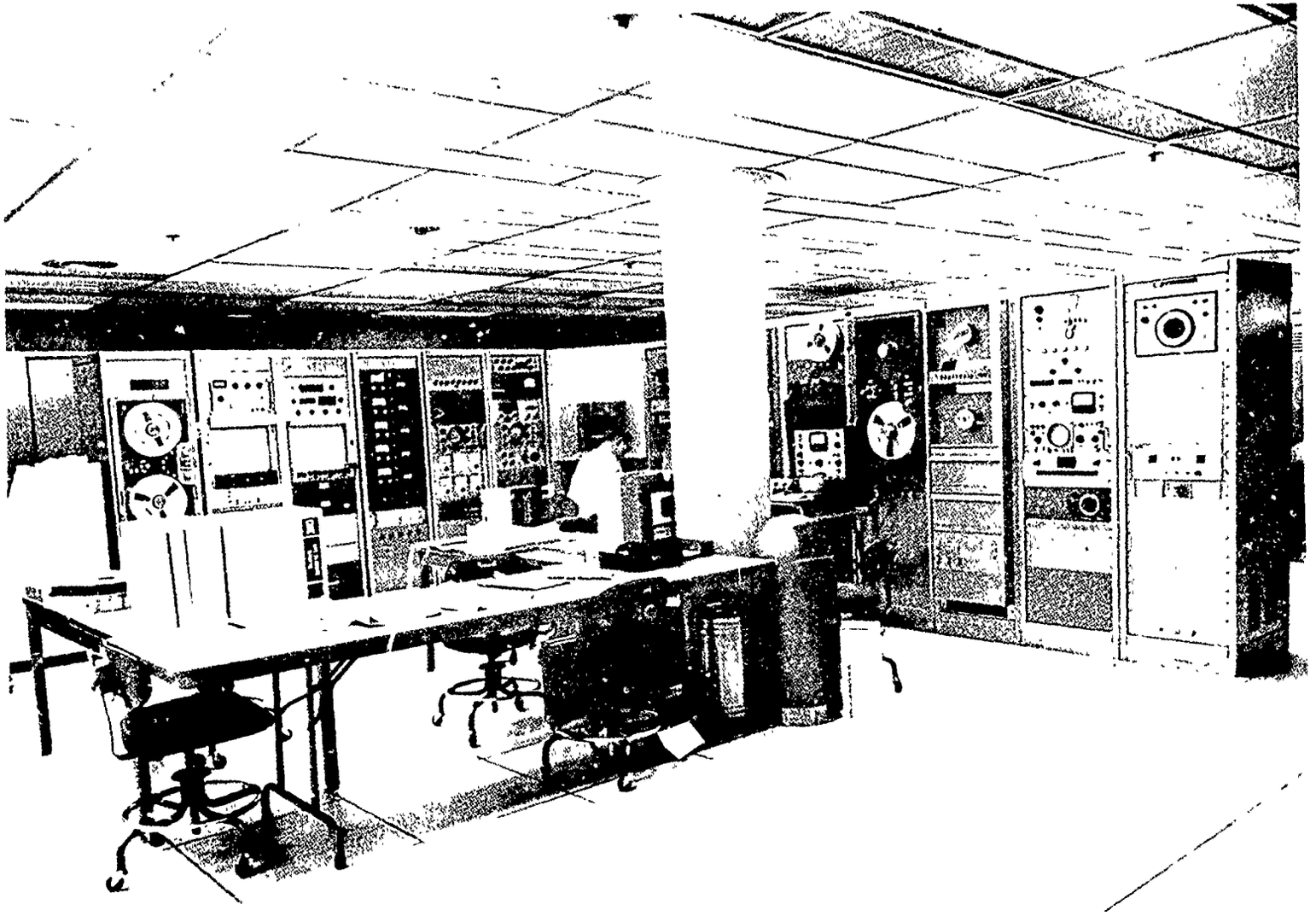

FIGURE III.B-3 INSTRUMENTATION DATA ROOM, ACOUSTIC DATA REDUCTION EQUIPMENT

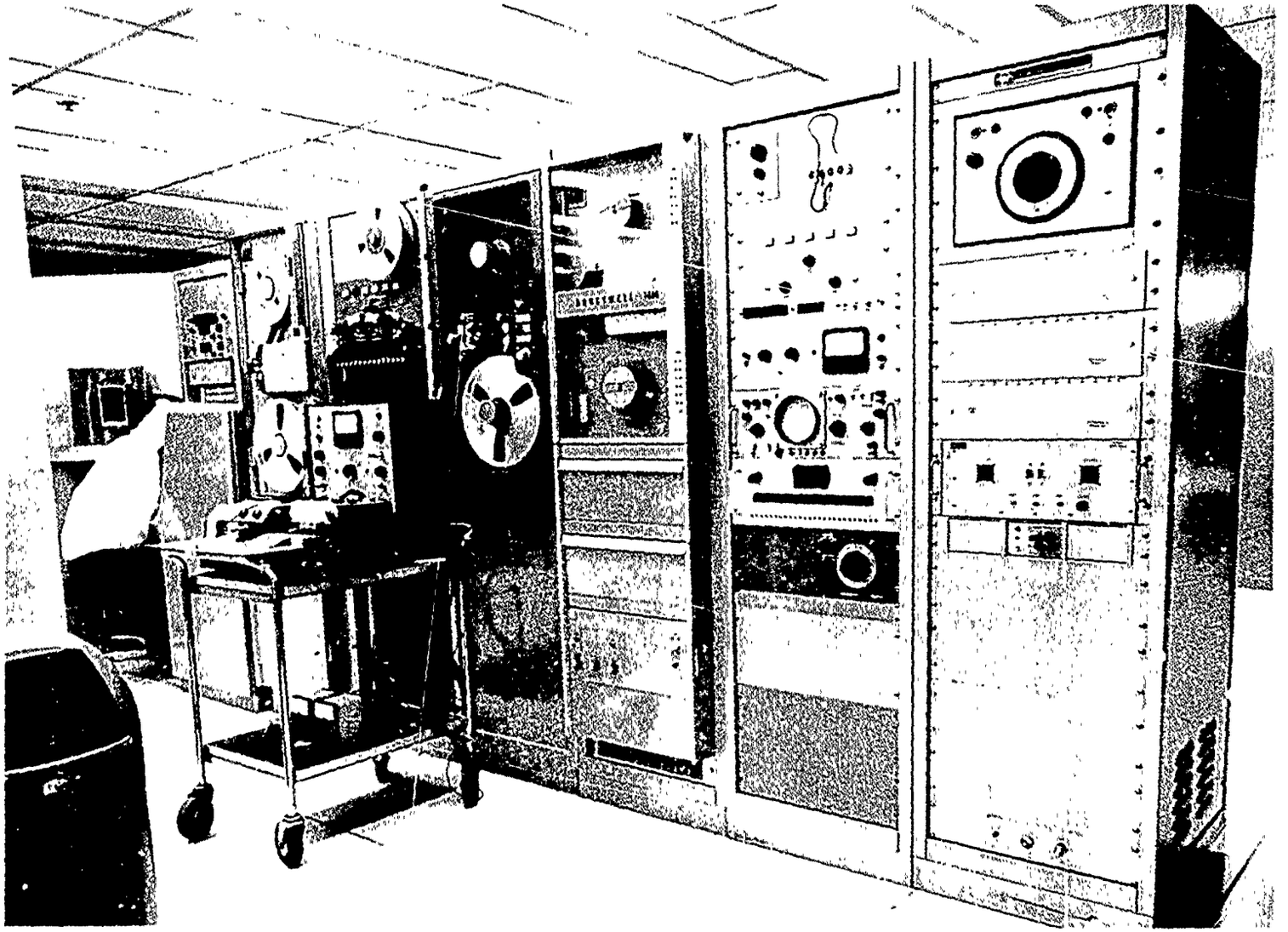

FIGURE III.B-4 INSTRUMENTATION DATA ROOM, ACOUSTIC DATA REDUCTION EQUIPMENT

IV. DATA PRESENTATION, FORM AND PURPOSE

PRECEDING PAGE BLANK-NOT FILMED

IV. DATA PRESENTATION FORM AND PURPOSE

Types of Data Presented

Acoustic data are presented for all of the model configurations, engine tests and system studies reported on in this text. The data included in the different sections of this report are presented in a variety of forms specifically tailored to the content of the sections.

The majority of the jet acoustic data is presented as full scale data with most of it obtained from model scale suppressor measurements. Acoustic measurements, taken on an arc, were scaled by frequency and size to full scale application. Full size engine test data are also included in several sections. Scale model data, unscaled to engine size, are presented in Section VII, which includes several jet acoustic research studies conducted at the Corporate Research and Development Center in Schenectady, New York.

Acoustic results are presented in the form of tabulations and plots of normalized peak perceived noise level (PNL), measured in PNdB, around an arc and at specific sideline distances. The model data, taken on a 40 ft. arc, were scaled by a factor of 8:1 to obtain full scale data on a 320 ft. arc with sideline extrapolations to 300, 1500 ft., and in one case, (Section V.H.2), 2128 ft. PNL suppression comparisons at 300 ft. and 1500 ft. sidelines relative to a baseline conical nozzle, or other baseline reference configuration, are included. Frequency spectra and PNL directivity at increments of velocity are also available for many of the nozzle categories.

Aerodynamic wind tunnel performance tests, for the determination of installed gross thrust coefficients, were conducted on only a limited number of suppressor models. The major portion of the aerodynamic performance data available, and therefore presented, is the result of nozzle base static pressure measurements and includes such items as mean base pressure variations versus nozzle pressure ratio and base drag coefficient. Some static gross thrust coefficients were obtained through aerodynamic tests and are presented.

Test Conditions

The test conditions specified for the majority of the jet suppressor configurations were based on a simulated operating line for the GE4 supersonic transport engine over an ideal jet velocity range from 1000 to 3150 ft/sec.

Several of the suppressor tests were conducted over a matrix of test conditons formed by combinations of exit temperature, T_{T8}, and nozzle pressure ratio, P_{T8}/P_o, to investigate noise generation dependency on these parameters.

Parametric Studies

Several parametric studies were undertaken during the course of the jet suppressor testing. As a result of investigating numerous suppressor configurations, certain geometric parameters were found to have greater suppression effects than others. Investigation of geometric parameters related to each nozzle system included the following:

a. Unsuppressed Nozzles
   - o Pumping Variations

b. Simple Primary Suppressor Systems - Variations of Rod and Tube
   - o Number
   - o Penetration
   - o Blockage
   - o Axial Position

c. Secondary Chute Suppressor Systems - Variations of Chute
   - o Penetration
   - o Blockage
   - o Planform

d. Multi-Element Tube Suppressor System - Variations of Tube
   - o Bundle Compactness
   - o Number
   - o Base and Exit Plane Stagger
   - o Spacing and Size Uniformity
   - o Length and Exit Geometries

e. Multi-Element Spoke/Chute Annular Plug Suppressor Systems - Variations of Element
   - o Blockage Ratio
   - o Number
   - o Planform
   - o Orientation to Flow

The parametric studies were efforts at refining these geometric parameters to optomize the trade between obtainable suppressior and accompanying thrust decrement.

V. JET NOISE SUPPRESSOR CONFIGURATIONS AND PARAMETRIC STUDIES

PRECEDING PAGE BLANK-NOT FILMED

V.A MODEL AND ENGINE SUPPRESSOR CATEGORIES

PRECEDING PAGE

V.A. MODEL AND ENGINE JET SUPPRESSOR CATEGORIES

Model and engine jet suppressor categories are reported on within Section V of this two volume document. The categories include representative selections illustrating the types of suppressor configurations and parametric studies investigated during the GE4/SST development program sponsored by the Federal Aviation Agency. Volume I of this report contains major Sections I through IV and part of Section V (through V.F.10). Volume II contains the remainder of Section V plus the last two major sections of the report, Sections VI and VII. Table V.A-1 lists the Section V suppressor categories by sub-section and summarizes the applicable figures and tables for each category. Table V.A-1 is included in both Volumes I and II for easy reference.

The data in these sections are presented as full scale data obtained from scale model and full size engine measurements. Scale model acoustic measurements were taken on a 40 ft. arc and scaled by frequency and size to full scale application. An 8:1 scale factor relating engine nozzle diameter to model nozzle diameter and engine measuring arc to the 40' model measuring arc was used for scaling. All data presented are therefore of simulated or actual engine size and engine frequency range.

The method of presentation varies for each series of nozzles tested, dependent on the engine type, exhaust nozzle cycle and acoustic measuring location to which the suppressor configuration was intended to apply. The majority of the sections include normalized peak PNL at 300 and 1500 ft. sideline distances (Section V.H.2 includes 2128 ft. sideline PNL data), PNL suppression comparisons referenced to baseline nozzles, and aerodynamic data in the form of mean baseplate pressure and drag coefficient. Some static gross thrust coefficients and a limited amount of wind tunnel data are also presented. Frequency spectra and PNL directivity comparisons are included for most nozzle categories. Within each section is a brief text defining the objectives of the test series, test conditions, baseline comparisons, and suppressor configurations. A brief summary of study results and pertinent conclusions are also included.

Basic two stage ejector nozzle (TSEN) configurations are presented in Section V.B for both model and engine tests. The TSEN system consisted of a primary nozzle (conical or star) with an attached secondary ejector capable of secondary

and tertiary pumping. Baseline comparisons were made without the ejector, using only the primary unsuppressed star or conical nozzle.

Primary suppressor configurations with cylindrical or TSEN ejectors are described in Sections V.C.1, V.C.2 and V.C.3. They include test results on primary radial rods, thrust reverser tabs, and vented primary chutes respectively.

Fluid injectant studies with air and water are reported on briefly in Sections V.D.1, V.D.2 and V.D.3. Hollow radial spokes were investigated with ambient pumping and axial injecting simulated compressor discharge bleed (C.D.B.) in Section V.D.1. Radial and axial air and water injection through hollow spokes is discussed in Section V.D.2, and air and water injection over primary thrust reverser tabs is presented in Section V.D.3.

Secondary suppressor thrust reverser flaps are reviewed in Section V.E.

The largest category of model suppressor configurations reported on in this summary document is multi-tube/hole nozzles presented in Section V.F. This section is composed of ten sub-sections, each documenting a particular suppressor parametric study or related series of model configurations. The various studies and model configuration series document the chronology of multi-tube suppressor technology development and culminates in the multi-tube preliminary design number 3 (PD-3) suppressor study of Section V.F.10. Section V.F.10 is the last section in Volume I of this summary report.

Jet noise suppressor configurations and parametric studies are continued in Volume II with the discussion of acoustically treated ejectors on multi-tube and conical nozzles in Section V.G.

The annular plug nozzle suppressor model studies are presented in Sections V.H.1 and V.H.2. An early series of model configurations using rods, tubes, C.D.B., and flap mechanical blockers was tested on annular plug nozzles with and without secondary ejectors as presented in Section V.H.1. The multi-element spoke/chute model suppressor parametric studies of Section V.H.2 were new efforts to develop that suppressor concept for application to the high-airflow low exhaust velocity cycle of the GE4J6H2 engine. The parallel acoustic and aerodynamic static and wind-on test series resulted in development of design guidelines for future refinement of the multi-element annular plug suppressor concept.

TABLE V.A-1 JET SUPPRESSOR CATEGORIES.

Section	Jet Suppressor Category	Figures	Tables
	Volume I		
V.B.	Two Stage Ejector Nozzle Tests on Suppressor Models and Full Scale Engine	V.B-1 through V.B-23	V.B-1 through V.B-10
V.C.1	Primary Radial Rods Within TSEN-3	V.C.1-1 through V.C.1-16	V.C.1-1 through V.C.1-9
V.C.2	Primary Thrust Reverser Tab Variations for Model and Engine Tests	V.C.2-1 through V.C.2-22	V.C.2-1 through V.C.2-14
V.C.3	Primary Vented Chute Suppressors	V.C.3-1 through V.C.3-6	V.C.3-1 and V.C.3-2
V.D.1	Hollow Radial Spokes with Ambient Pumping and Axial Injecting Simulated Compressor Discharge Bleed	V.D.1-1 through V.D.1-11	None
V.D.2	Hollow Radial Spokes with Radial and Axial Air and Water Injection	V.D.2-1 through V.D.2-5	None
V.D.3	Air and Water Injection Over Primary Thrust Reverser Tabs	V.D.3-1 through V.D.3-3	None
V.E.	Secondary Reverser - Suppressor Flaps	V.E-1 through V.E.-11	None
V.F.1	Comparison of Tube Length, Area Ratio, Secondary Ejector and Secondary Ejector Airflow Effects on 72 Tube/Hole Nozzles	V.F.1-1 through V.F.1-12	V.F.1-1 and V.F.1-2
V.F.2	Baseplate and Tube Exit Plane Stagger Angle Variations on 72 Tube Model Suppressors	V.F.2-1 through V.F.2-24	V.F.2-1 through V.F.2-7
V.F.3	Variations of a 37 Tube Nozzle	V.F.3-1 through V.F.3-24	V.F.3-1 through V.F.3-5

TABLE V.A-1 JET SUPPRESSOR CATEGORIES (Concluded)

Section	Jet Suppressor Category	Figures	Tables
	Volume I (Concluded)		
V.F.4	Tube End Variations on 37 Straight, Convergent, Greatrex and Canted End Tubes	V.F.4-1 through V.F.4-30	V.F.4-1 through V.F.4-8
V.F.5	Tube Internal and External Length To Diameter Studies on an 85 Tube Nozzle	V.F.5-1 through V.F.4-25	V.F.5-1 through V.F.5-8
V.F.6	Hole Shape, Equal and Unequal Hole Size and Spacing Studies on 97 Hole Plates	V.F.6-1 through V.F.6-18	V.F.6-1 through V.F.6-5
V.F.7	Variations of 97 Tube Primary Nozzle with Large and Small Center Hole; Comparisons with Hardwall and 7.5% Open Lined Ejectors	V.F.7-1 through V.F.7-17	V.F.7-1 through V.F.7-4
V.F.8	Geometric Variations of Center Hole Shape on 97 Hole Nozzle; Hardwall and Acoustically Lined Ejector Comparisons; D_S/D_{Td} Variations	V.F.8-1 through V.F.8-35	V.F.8-1 through V.F.8-10
V.F.9	Multi-Hole Nozzle Parametric Variations of Area Ratio, Hole Number, Shroud D_S/D_{Td}, and Shroud Axial Spacing, X_S	V.F.9-1 through V.F.9-67	V.F.9-1 through V.F.9-16
V.F.10	Multi-Tube Preliminary Design Number 3 (PD-3)	V.F.10-1 through V.F.10-27	V.F.10-1 through V.F.10-4
	Volume II		
V.G.	Acoustic Ejectors on Tube and Conical Nozzles	V.G-1 through V.G-25	V.G-1
V.H.1	Rods, Tubes, Chutes, C.D.B and Primary Flaps on Annular Plug Nozzles	V.H.1-1 through V.H.1-23	V.H.1-1 through V.H.1-23
V.H.2	Multi-Element Spoke/Chute Model Suppressor Parametric Investigations on Annular Plug Nozzles	V.H.2-1 through V.H.2-61	V.H.2-1 through V.H.2-15

V.B TWO-STAGE EJECTOR NOZZLE TESTS ON SUPPRESSOR MODELS AND FULL SCALE ENGINE

V.B TWO STAGE EJECTOR NOZZLE TESTS ON SUPPRESSOR MODELS AND FULL SCALE ENGINE

Objectives of Test Series

An acoustic investigation of the GE4 Two Stage Ejector Nozzle (TSEN) design was conducted at the GE, Evendale, JENOTS acoustic facility to determine whether any basic noise reduction would be available due to the ejector nozzles' design effect on pumping and mixing or due to acoustic shielding. To investigate the variables, several test phases and hardware configurations were used. In addition a full scale test at Peebles Site IV, using a GE4 Block I engine, was done to substantiate the TSEN test results.

The test phases and variables investigated were:

- Phase I - TSEN 3 Parametric Variations
  - a) Baseline conical and star primary nozzles
  - b) D_S/D_8 variation within TSEN 3
  - c) Location of D_S aft of the A_8 plane = X_S, within TSEN 3
  - d) Blow-in-door flow area variation within TSEN 3
- Phase II - TSEN 56 D_9/D_S Study
  - a) D_9/D_S variation within TSEN 56
- Phase III - TRSEN 56
  - a) Cylindrical shroud addition to TSEN 56 and shroud length variation
- Phase IV - GE4 Block I Plus TSEN
  - a) Addition of TSEN to GE4 Block I engine with conical and star primary nozzles
  - b) D_S/D_8 variation within the GE4 Block I TSEN

Each study phase will be discussed individually.

Acoustic measurements for model tests at JENOTS were taken on a 40 ft. arc at 10° intervals from 30° through 90° from the jet exhaust axis. The measurements were scaled by frequency and size to full scale application using a scale factor of 8:1. All data presented within this section are, therefore, of simulated engine size and engine frequency range.

PRECEDING PAGE BLANK-NOT FILMED

Test Configurations, Presentation and Discussion of Results

o Phase I - TSEN 3 Parametric Variations

The photograph of Figure V.B-1 shows the TSEN 3 hardware used in this test phase. Figure V.B-2 schematically shows the TSEN 3 hardware set-up, the basic nozzle dimensions and the variable parameter values for each test phase. A 4.99" equivalent D_8 star nozzle plus three conical convergent nozzles of 4.32", 4.82" and 5.14" D_8's were used as baseline reference nozzles. The star nozzle represented the early GE4 primary nozzle design which used a variable A_8 star primary. Around this nozzle the variations of D_S positioning and blow-in-door area were studied. The three conical nozzles were used in the D_S/D_8 variation study.

Tables V.B-1 and V.B-2 summarize the acoustic test results for the star nozzle and conical nozzles, respectively. A plot of the 300 ft. sideline peak normalized PNL as a function of jet velocity is shown as Figure V.B-3. The plot shows the star baseline to be just above the conical nozzle baseline. Both curves will be presented on later plots where results of test series which used the star primary are presented.

To analyze D_S/D_8 effect on TSEN 3 suppression, the three conical convergent nozzles were each used with the fixed D_S = 6.08" TSEN 3 ejector. This gave effective D_S/D_8 ratios of 1.41, 1.26 and 1.18 for the 4.32", 4.82" and 5.14" D_8 nozzles, respectively. TSEN settings of X_S = 1.81" and 10° blow-in-door angle were used as shown in Figure V.B-2. Acoustic test results for these three models are summarized in Table V.B-3 and plotted as 300 ft. sideline normalized peak PNL in Figure V.B-4. This plot also has the baseline conical nozzle data (without TSEN 3) plotted and average baseline curves drawn through the data. In addition a plot of octave band spectra at 60° and 300 ft. sideline normalized PNL directivity are included as Figure V.B-5 for the three D_S/D_8 models plus conical baselines at a P_{T8}/P_o = 2.5 and T_{T8} = 2800° R. The curves of Figure V.B-4 yield no bare TSEN suppression gain through variation of D_S/D_8 and the frequency spectra plus directivity plots of Figure V.B-5 emphasize this.

The evaluation of TSEN nozzle positioning effect on pumping and shielding, the X_S was set at 1.81", 2.81" and 3.81" as shown schematically in Figure V.B-2. X_S is defined as the axial location of the D_S aft of the A_8 plane. In this study

the 4.99" equivalent D_8 star nozzle was used which set an effective D_S/D_8 of 1.22. The 10° blow-in-door angle was maintained for tertiary air pumping. A summary of the acoustic test results for the three models is presented in Table V.B-4. The 300 ft. sideline peak normalized PNL are plotted as a function of jet velocity in Figure V.B-6 and include the star and conical average baseline curves in addition to average curves through the plotted data. Three hundred foot sideline 60° octave band spectra and normalized PNL directivity comparison plots are included as Figure V.B-7 for the three TSEN X_S positions and star baseline, at three exhaust nozzle cycle settings. Inspection of the curves of both figures shows the 3.81" X_S position to be the least noisy with near 2.0 PNdB suppression relative to the star baseline at V_J = 3075 ft/sec (approximately P_{T8}/P_o = 2.8 and T_{T8} = 2800° R). This is about 1.0 PNdB relative to the conical baseline; however, reverse flow commenced at P_{T8}/P_o of 3.0 and T_{T8} of 2800° R. The average curves for the X_S = 2.81" and 1.81" show the 2.81" position louder than the conical baseline; reverse flow occurring at P_{T8}/P_o of 3.5 and T_{T8} of 2800° R. The 1.81" position performed almost identical to the baseline cone.

To determine the acoustic effect of blow-in-door area variation, the D_S/D_8 and X_S were held constant at 1.22 and 1.81", respectively, while setting the blow-in-door angle at 20°, 10° and fully closed, as per Figure V.B-2. Acoustic test results are summarized in Table V.B-5 and acoustic data plots similar to those of the previous study are included as Figures V.B-8 and 9.

The 20° door angle position performed almost identically to the 10° model, both showing about 1.0 PNdB maximum suppression at V_J of 3075 ft/sec (0.3 dB relative to the cone). Closing the blow-in-doors increased high velocity suppression by about 0.3 dB but made the model slightly louder than the cone and star baseline at low jet velocity.

o Phase I - Conclusions

a) Negligible suppression relative to a conical nozzle is realized by optimizing TSEN plus star primary system parameters including D_S/D_8 and tertiary blow-in-door settings.

b) D_S positioning at X_S = 3.81" aft of the A_8 plane yields slight suppression gain but had reverse flow problems.

o Phase II - TSEN 56 D_9/D_S Study

To investigate noise characteristics of the full scale GE4 56" D_S nozzle system, a 1/8 scale model was built. It was designated TSEN 56, having a D_S of 7.0", and is shown photographically in Figures V.B-10 and -11 and schematically in Figure V.B-12. The model was to fully simulate the operating range of the GE4 floating D_9 sector through use of interchangeable fixed D_9 sectors of 7.0, 7.7, 8.4 and 9.1", each adaptable to the basic TSEN structure. Testing with the four sectors yielded D_9/D_S ratios 1.0, 1.1, 1.2 and 1.31. All tests were performed over a P_{T8}/P_o range of 2.0 to 3.0 and a T_{T8} range of 2000 to 2800° R. The D_S/D_8 ratio was held at 1.241 and other parameters are as shown in Figure V.B-12.

A summary of the acoustic test results is done in Tables V.B-6, -7, -8, and -9 for the D_9/D_S settings of 1.0, 1.1, 1.2, and 1.31, respectively. Acoustic data and summary plots are included as Figures V.B-13 through V.B.-15D. Figure V.B-13 presents 300 ft. sideline peak normalized PNdB as a function of jet velocity and D_9/D_S ratio. From these plots it is evident that absolute noise levels varied considerably with primary pressure ratio, therefore, mean noise lines were drawn to favor the higher pressure ratio points, more representative of the engine cycle. The averaged conical baseline is composed of test data at various size conical nozzles, including the 5.6" D_8 cone, and is shown on the D_9/D_S = 1.0 data plot. As such, the mean noise lines for D_9/D_S = 1.0 and the conical nozzle show suppression of about 1.0 PNdB at V_J of 2500 ft/sec, dropping to about 0.3 PNdB at 3050 ft/sec for P_{T8}/P_o = 3.0 and T_{T8} = 2800° R. Within the range of data repeatability this could be considered analogous with the Phase I findings of no inherent suppression in the smaller scale TSEN 3 hardware of identical D_9/D_S and near similar D_S/D_8. The other D_9 variation models will be referenced to the D_9/D_S = 1.0 noise line for quoted suppression.

The mean noise curves of Figure V.B-13 are composited at the top of Figure V.B-14 and from this plot a Δ PNdB suppression plot is shown at the lower left of Figure V.B-14. It shows the 1.1 and 1.2 D_9/D_S models to have near level suppressions of slightly greater than 2.0 PNdB and slightly less than 3.0 PNdB, respectively. The D_9/D_S = 1.3 model shows an increase in suppression with higher jet velocity rather than remaining level as the 1.1 and 1.2 D_9/D_S models did.

The lower right curve of Figure V.B-14 shows the suppression trend with increasing D_9 (relative to $D_9/D_S = 1.0$) at maximum test conditions near $P_{T8}/P_o = 3.0$, $T_{T8} = 2800°$ R and $V_J = 3050$ ft/sec. Leveling of the curve indicates that no additional suppression above 2.8 PNdB is gained by opening the D_9 above a D_9/D_S ratio of about 1.18.

Figures V.B-15A through -15D are data presentations of 300 ft sideline octave band frequency spectra and normalized PNL directivity for $P_{T8}/P_o = 2.7$ and 3.0 at T_{T8} values of 2000, 2500 and 2800° R for the four D_9/D_S models and the reference conical nozzle, where available.

Secondary and tertiary air handling characteristics of the instrumented TSEN 56 are presented in Figure V.B-16. Secondary air flow was measured over a metering section with three total pressure rakes radially spaced 120° apart. Static pressure taps were on the flow path wall in the same vicinity as the total pressure rakes. Tertiary air flow through the 16 blow-in-doors was monitored with total pressure rakes at doors #9 and #12 and static pressure taps on doors #1 and #4. Blow-in-doors were numbered clockwise, aft looking forward, with door #1 at top dead center as per Figure V.B-12. Reference to Figure V.B-16 shows that corrected mass flow ratio increased considerably with D_9/D_S increase from 1.0 to 1.1. Further opening to $D_9/D_S = 1.2$ and 1.3 added only slightly to the secondary and tertiary mass flow ratios.

o Phase II - Conclusions

a) For $D_9/D_S = 1.0$ minor suppression of about 1.0 PNdB at 2500 ft/sec V_J and dropping to about 0.3 PNdB at 3050 ft/sec was experienced. This is analogous to the conclusion of Phase I test of no inherent suppression in the smaller scale TSEN 3 hardware of identical D_9/D_S and near similar D_S/D_8.

b) Additional suppression can be gained by opening the D_9 above $D_9/D_S = 1.0$, however, levels are dependent on V_J. At high V_J a maximum of about 2.8 PNdB additional suppression is seen for D_9/D_S of near 1.18 and further increase gains no further suppression.

c) Air handling characteristics are substantially increased by changing from $D_9/D_S = 1.0$ to 1.1 but further increase adds only slightly to the pumping, synonomous with the acoustic suppression characteristics.

o Phase III - TRESEN 56

Addition of a shroud extension to the TSEN 56 was investigated to form a Three Stage Ejector Nozzle (TRESEN) as shown schematically in Figure V.B-17. Shroud length, L_S, variations of 3.5" and 14" were tested with the TSEN at X_S settings of 2.925" and 2.055". Shroud internal diameter was 1.2 D_9 or 8.4". D_9/D_S of 1.0 and D_S/D_8 of 1.241 were held constant. The shroud leading edge was positioned at the exit plane of the TSEN.

Acoustic test results for the five model configurations, as listed on Figure V.B-17, are summarized in Table V.B-10. Figures V.B-18A and -18B are plots of the 300 ft. sideline peak normalized PNL as a function of jet velocity for each of the models with average noise curves drawn to favor the higher P_{T8}/P_o data. From these plots a summary of the noise suppression effects of the shroud extension is made in Figure V.B-19. The plot shows effects at both X_S positions of 2.925" and 2.055" in addition to the basic TSEN 56 suppression levels, all referenced to the baseline conical nozzle.

With the TSEN at X_S = 2.925", installation of the 3.5" long shroud (L_S = 0.5 D_9 = 3.5") gave suppression of slightly over 1 PNdB compared to the standard conical baseline, at a jet velocity of 3050 ft/sec. The 14" long shroud (L_S = 2 D_9 = 14") produced suppression of slightly greater than 2 PNdB at the same conditions. At the decreased X_S position of 2.055", the 14" long shroud gave slightly lower suppression than with the TSEN at the X_S of 2.925" position.

Octave band frequency spectra and normalized PNL plots at the 300 ft sideline are shown as Figures V.B-20A and -20B for runs at P_{T8}/P_o = 3.1. The addition of the extension shroud caused little change in directivity or spectral shape.

o Phase III - Conclusions

a) Adding a cylindrical shroud extension to the basic TSEN 56 system produced additional suppression of low magnitude. The increment of additional suppression increased with increasing shroud length ranging nominally from 1 to 2 PNdB, depending on shroud length and exhaust velocity.

b) No significant change to spectra or directivity distribution is seen when the shroud is added.

o Phase IV - GE4 Block I Plus TSEN

Measurements were taken with the GE4 Engine 435-002, with and without a Two Stage Ejector Nozzle, to substantiate the acoustic performance levels. Figure V.B-21 shows the engine mounted on the Peebles Site IV acoustic facility. An acoustically treated inlet box was used to isolate forward propagated turbomachinery noise. The TSEN was of fixed D_9 and D_S, therefore, varying D_S/D_8 was accomplished through use of interchangeable primary nozzles. Two primary star configurations of 990 and 1170 in^2 A_8, when used with the TSEN, gave D_S/D_8 values of 1.38 and 1.27, respectively. Four primary nozzles of 917, 1010, 1190 and 1292 in^2 were used as baselines, two of which were tested with the TSEN and gave D_S/D_8 values of 1.26 and 1.37.

Acoustic results are shown as 300 ft. sideline peak normalized PNL plots as a function of jet velocity in Figures V.B-22 and -23, for the systems using conical and star primaries, respectively. Results from the data are in agreement with those of the model tests in Phase I in that negligible change in noise level is seen with the addition of the TSEN to either the star or conical primary nozzles. In addition no suppression gain is seen with the variation of D_S/D_8 within the range of test configurations.

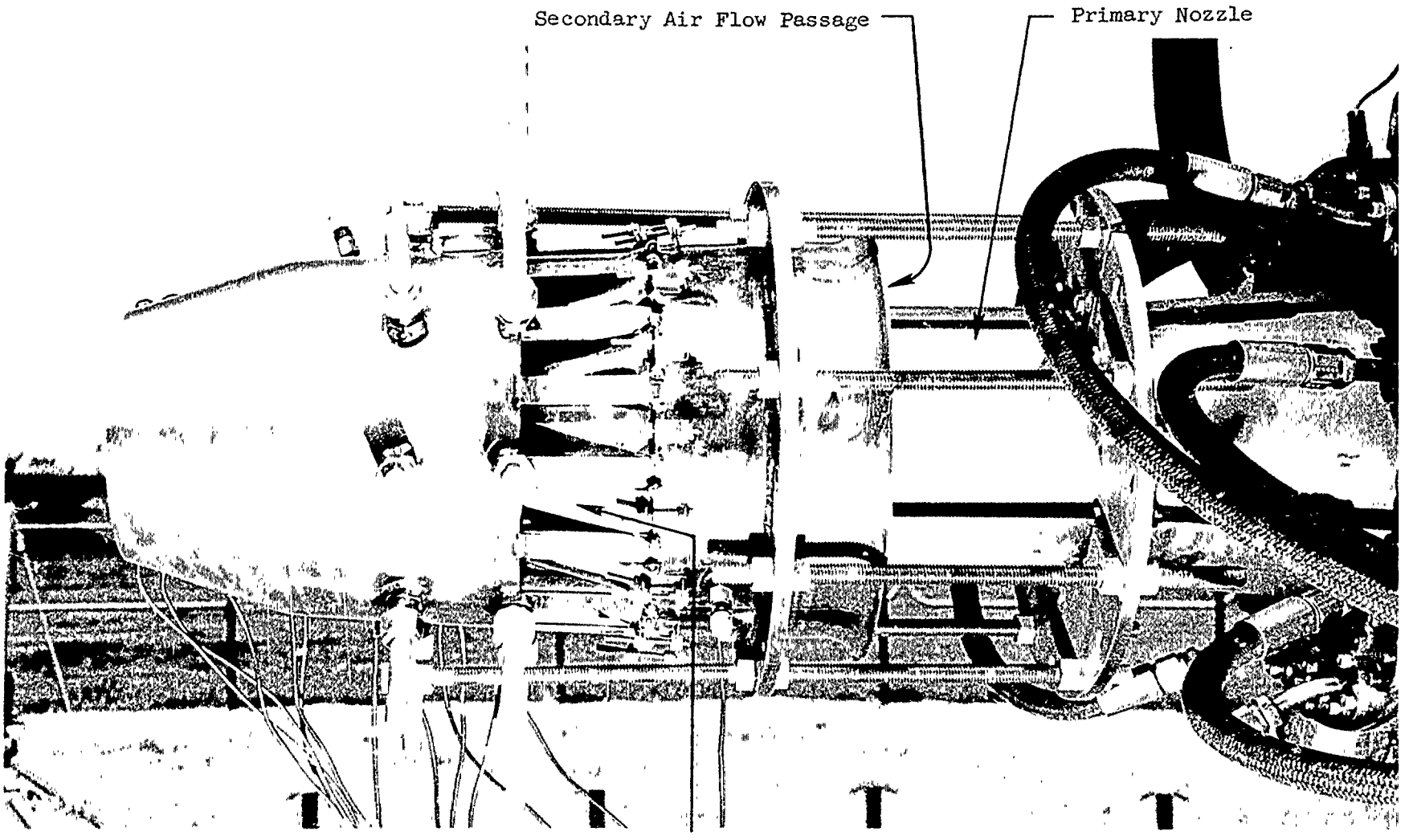

FIGURE V.B-1 TSEN-3 HARDWARE USED FOR INVESTIGATION OF GEOMETRIC VARIATIONS

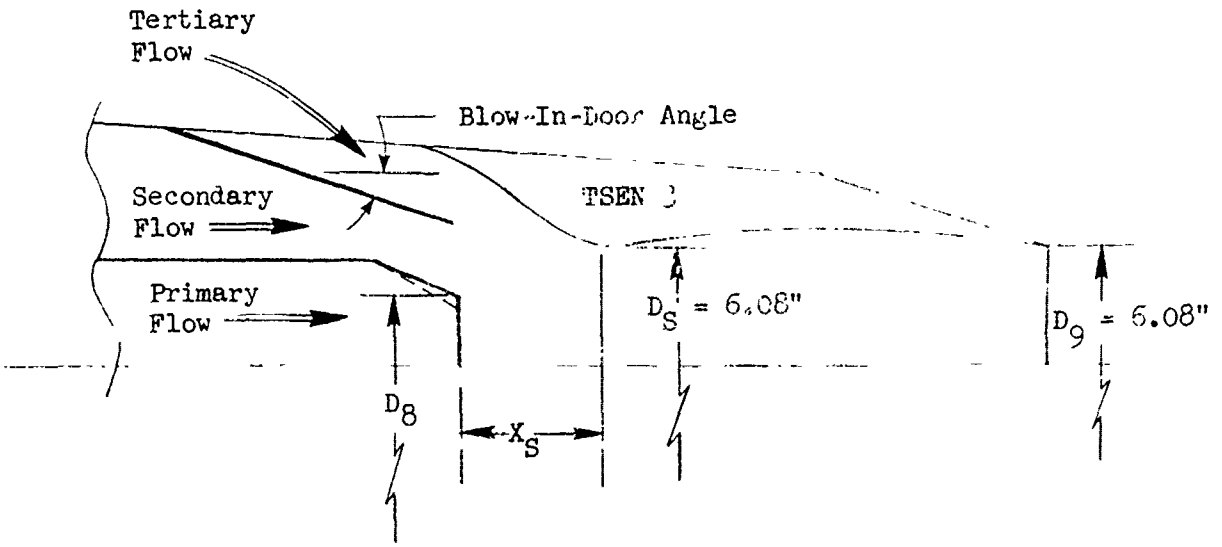

o TSEN = Two Stage Ejector Nozzle

Test Purpose	Model No.	Test Date	Primary Nozzle	D_S/D_8	Blow-In Door Angle	X_S
Star & Conical Baselines	5.1S	2-23-68	4.99" Star	N/A	N/A	N/A
	5.1S	2-24-68	4.99" Star			
	4.32	2-24-68	4.32" Cone			
	4.82	2-24-68	4.82" Cone			
	5.14	2-24-68	5.14" Cone			
D_S/D_8 Variation	4.32-3B	2-24-68	4.32" Cone	1.41	10°	1.81"
	4.82-3B	2-24-68	4.82" Cone	1.26	10°	1.81"
	5.14-3B	2-24-68	5.14" Cone	1.18	10°	1.81"
D_S Positioning = X_S	5.1S-3B	2-14-68	4.99" Star	1.22	10°	2.81"
	5.1S-3B-1	2-14-68	4.99" Star	1.22	10°	1.81"
	5.1S-3B-2	2-16-68	4.99" Star	1.22	10°	3.81"
Blow-In-Door Flow Area Variation	5.1S-3B-1	2-14-68	4.99" Star	1.22	10°	1.81"
	5.1S-3B-4	2-19-68	4.99" Star	1.22	20°	1.81"
	5.1S-3B-5	2-21-68	4.99" Star	1.22	CLOSED	1.81"

FIGURE V.B-2 SCHEMATIC OF TSEN-3 USED FOR INVESTIGATION OF GEOMETRIC VARIATIONS

TABLE V.3-1 TEST SUMMARY

MODEL NO. 5.1 Star

DESCRIPTION: 5.1" Baseline Star Nozzle

DATE: 2/23/68; 2/24/68

SCALE MODEL A_8 = .1362 ft^2

FULL SCALE A_8 = 8.7168 ft^2

SCALE FACTOR = 8:1

o DATA INCLUDES GROUND REFLECTION INTERFERENCE
o ANGLE REFERENCED TO JET EXHAUST

TEST CONDITIONS							ACOUSTIC TEST RESULTS							
							320 FT ARC		300 FT. SIDELINE PNL DIRECTIVITY					
Reg. No.	P_{T8}/P_o	T_{T8} (°F)	V_8 (fps)	W_8 (PPS)	10 $Log p^2_A$	10 Log ϵ_A	PEAK PNdB	PEAK ANGLE	30°	40°	50°	60°	70°	80°	90°
2/23/68															
1	1.99	2800	2476	-	-26.3	-8.4	134.7	50	122.8	128.6	132.6	133.1	129.5	127.2	124.6
2	2.49	2795	2810	-	-25.6	-8.0	138.0	60	124.6	129.7	133.7	137.1	132.9	131.4	130.4
3	3.00	2365	2804	-	-23.6	-6.8	139.1	60	126.0	131.3	135.2	138.2	134.2	133.0	132.5
4	2.99	2000	2577	-	-22.1	-6.1	137.5	50	126.6	131.6	135.4	136.4	133.2	132.2	131.0
5	2.99	2000	2577	-	-22.1	-6.1	138.0	50	126.6	131.7	135.8	136.6	132.6	132.3	131.0
2/24/68															
1	2.02	2800	2494	-	-26.3	-8.4	136.1	50	124.4	129.8	133.9	133.5	130.0	127.2	126.0
2	2.52	2800	2830	-	-25.6	-8.0	138.8	60	127.2	132.5	136.1	137.9	131.8	131.1	129.8
3	3.03	2310	2783	-	-23.3	-6.7	139.4	50	127.9	133.3	137.2	137.9	133.0	131.8	131.5
4	3.03	2010	2597	-	-22.1	-6.1	139.2	50	127.0	135.1	137.1	136.5	132.7	132.1	131.3

TABLE V.B-2 TEST SUMMARY

MODEL NO. 4.32, 4.82, 5.14" I.D. Cones

DESCRIPTION: Baseline Conical Nozzle

DATE: 2/24/68

SCALE MODEL A_8 = Noted

FULL SCALE A_8 = Noted

SCALE FACTOR = 8:1

o DATA INCLUDES GROUND REFLECTION INTERFERENCE
o ANGLE REFERENCED TO JET EXHAUST

TEST CONDITIONS							ACOUSTIC TEST RESULTS								
					$10 \log_{10} A_8^2$	$20 \log V_8$	320 FT ARC		320 FT. SIDELINE PNL DIRECTIVITY						
Rdg. No.	P_{T8}/P_o	T_{T8} (°R)	IDEAL V_8 (fps)	V_8 (PPS)			PEAK PNdB	PEAK ANGLE	30°	40°	50°	60°	70°	80°	90°
	4.32" I.D. Cone						Scale Model A_8 = .1008 ft^2, Full Scale A_8 = 6.4512 ft^2								
1	2.01	2800	2485	-	-27.6	-9.7	134.1	50	124.4	128.7	132.0	132.3	127.4	125.9	123.6
2	2.50	2800	2818	-	-27.0	-9.3	136.0	50	126.2	131.0	133.8	135.1	132.3	130.1	128.1
3	3.01	2430	2847	-	-25.1	-8.3	137.4	50	127.7	131.9	135.2	136.4	133.2	131.8	130.4
4	3.01	2010	2589	-	-23.4	-7.4	138.1	50	127.9	132.0	135.9	135.6	131.7	130.8	129.0
	4.82" I.D. Cone						Scale Model A_8 = .1310 ft^2, Full Scale A_8 = 8.3840 ft^2								
1	2.00	2800	2481	5.01	-26.4	-8.6	135.0	50	124.9	129.5	132.8	132.7	128.8	127.1	130.3
2	2.50	2800	2816	8.26	-25.8	-8.2	137.2	60	125.3	131.0	134.9	136.3	132.0	130.9	130.1
3	3.00	2360	2803	8.07	-23.7	-7.0	138.9	50	127.3	132.6	136.7	137.8	132.8	132.1	131.2
4	3.00	2005	2585	8.96	-22.3	-6.3	138.2	60	127.6	132.6	136.0	135.6	132.6	131.4	130.6
	5.14" I.D. Cone						Scale Model A_8 = .1419 ft^2, Full Scale A_8 = 9.0816 ft^2								
1	2.00	2800	2484	-	-26.1	-8.3	134.8	50	125.2	129.8	132.7	133.1	129.0	127.2	125.5
2	2.50	2800	2817	-	-25.5	-7.8	138.3	60	126.4	131.5	135.6	137.4	132.3	131.2	130.1
3	3.00	2320	2760	-	-23.2	-6.6	139.6	50	128.5	133.2	137.5	137.7	133.4	132.4	132.3
4	3.00	2010	2588	-	-22.0	-6.0	139.7	50	128.3	134.9	137.5	136.6	133.2	132.1	131.3

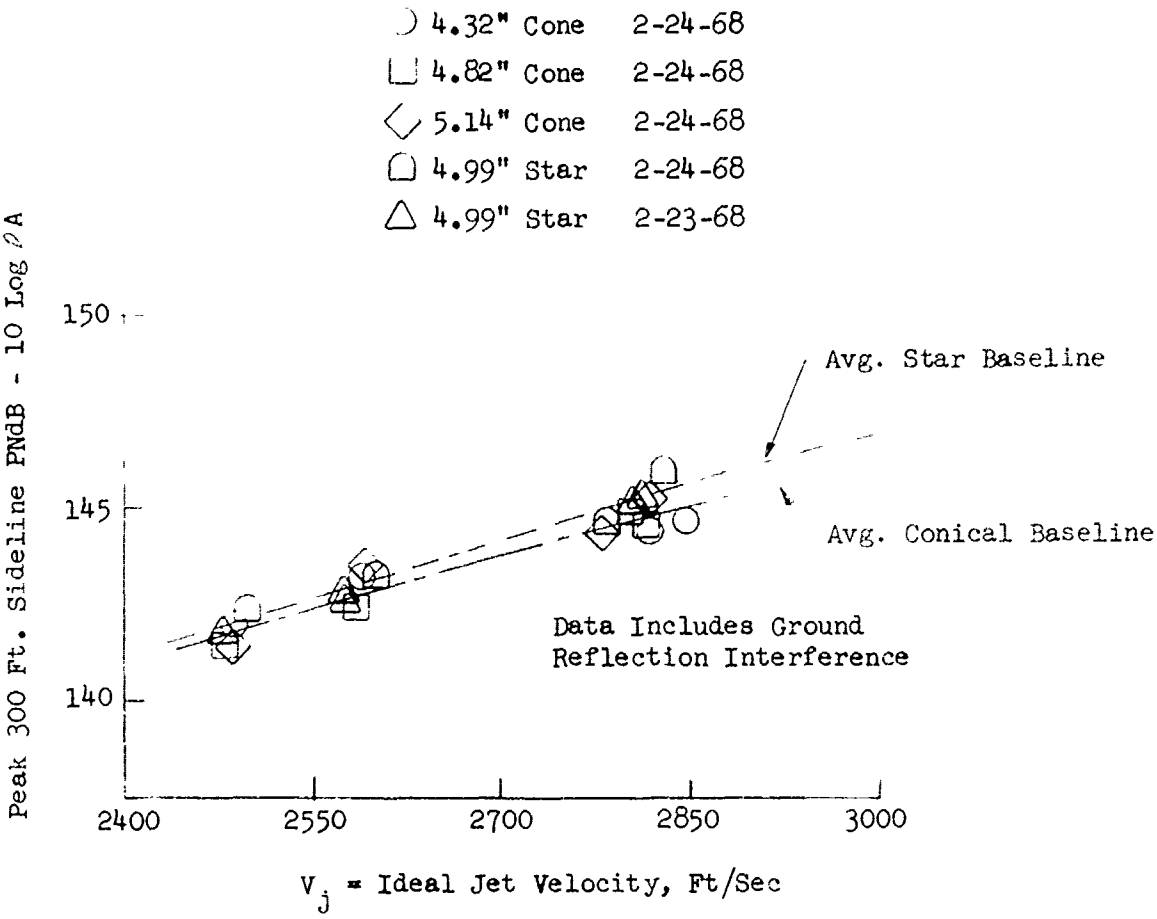

FIGURE V.B-3 COMPARISON OF 300 FT. SIDELINE JET NOISE LEVELS FOR CONE AND STAR PRIMARIES

TABLE V.1-3 TEST SUMMARY

MODEL NO. 4.32-3B, 4.82-3B, 5.14-3B

DESCRIPTION: TSEN 3 + 4.32 Cone; 4.82 Cone; 5.1 Cone; D_S/D_8 Variation

DATE: 2/24/68

SCALE MODEL A_8 = Noted

FULL SCALE A_8 = Noted

SCALE FACTOR = 8:1

o DATA INCLUDES GROUND REFLECTION INTERFERENCE

o ANGLE REFERENCED TO JET EXHAUST

TEST CONDITIONS					$10 \log \frac{P^2}{P_A^2}$	$10 \log \frac{W}{\rho A}$	ACOUSTIC TEST RESULTS							
							320 FT ARC		300 FT. SIDELINE PNL DIRECTIVITY					
Rdg. No.	P_{T8}/P_o	T_{T8} (°R)	IDEAL V_j (fps)	W_8 (PPS)			PEAK PNdB	PEAK ANGLE	30°	40°	50°	60°	70°	80°	90°
	4.32-3B			D_S/D_8 = 1.41			Scale Model A_8 = .1008 ft^2		Full Scale A_8 = 6.451 ft^2						
1	2.00	2800	2484	-	-27.6	-9.7	132.7	50	122.2	126.7	130.5	133.3	128.3	127.0	124.9
2	2.50	2800	2822	-	-27.0	-9.3	137.3	60	125.5	129.1	133.0	136.4	132.1	131.1	128.7
3	3.01	2800	3055	-	-26.3	-8.9	138.8	60	127.0	131.8	135.5	138.0	133.1	132.4	130.8
4	3.01	2500	2888	-	-25.3	-8.4	137.4	60	126.6	131.5	134.9	136.6	132.4	131.4	130.3
5	3.01	2010	2589	-	-23.4	-7.4	137.3	50	127.1	131.5	135.2	134.9	130.9	130.1	129.7
	4.82-3B			D_S/D_8 = 1.26			Scale Model A_8 = .1310 ft^2		Full Scale A_8 = 8.384 ft^2						
1	2.00	2800	2481	-	-26.4	-8.6	134.2	60	122.6	127.7	131.8	133.4	129.1	127.9	126.8
2	2.50	2800	2815	-	-25.8	-8.2	137.7	60	125.2	130.4	134.0	136.8	132.3	131.0	130.4
3	3.00	2800	3054	-	-25.2	-7.7	138.7	60	127.3	131.7	135.1	137.9	133.2	133.5	132.8
4	3.00	2500	2886	-	-24.2	-7.2	138.6	60	127.2	131.7	135.5	137.8	134.3	132.7	132.2
5	3.00	2010	2587	-	-22.3	-6.3	137.2	60	127.4	131.4	134.8	136.3	131.5	131.5	130.5
	5.14-3B			D_S/D_8 = 1.18			Scale Model A_8 = .1419 ft^2		Full Scale A_8 = 9.082 ft^2						
1	2.00	2800	2483	-	-26.1	-8.2	134.7	50	123.0	128.1	132.5	133.8	128.7	127.2	125.9
2	2.50	2810	2820	-	-25.5	-7.9	138.6	60	125.5	130.9	134.7	137.8	132.0	131.5	130.6
3	3.00	2800	3054	-	-24.8	-7.4	139.8	60	127.7	133.4	136.5	138.9	135.7	132.9	132.0
4	3.00	2500	2885	-	-23.9	-6.9	139.5	60	127.0	133.0	137.2	138.7	134.2	132.4	131.2
5	3.00	2010	2588	-	-22.0	-5.9	139.0	60	127.7	132.8	136.8	135.9	132.3	130.8	129.7

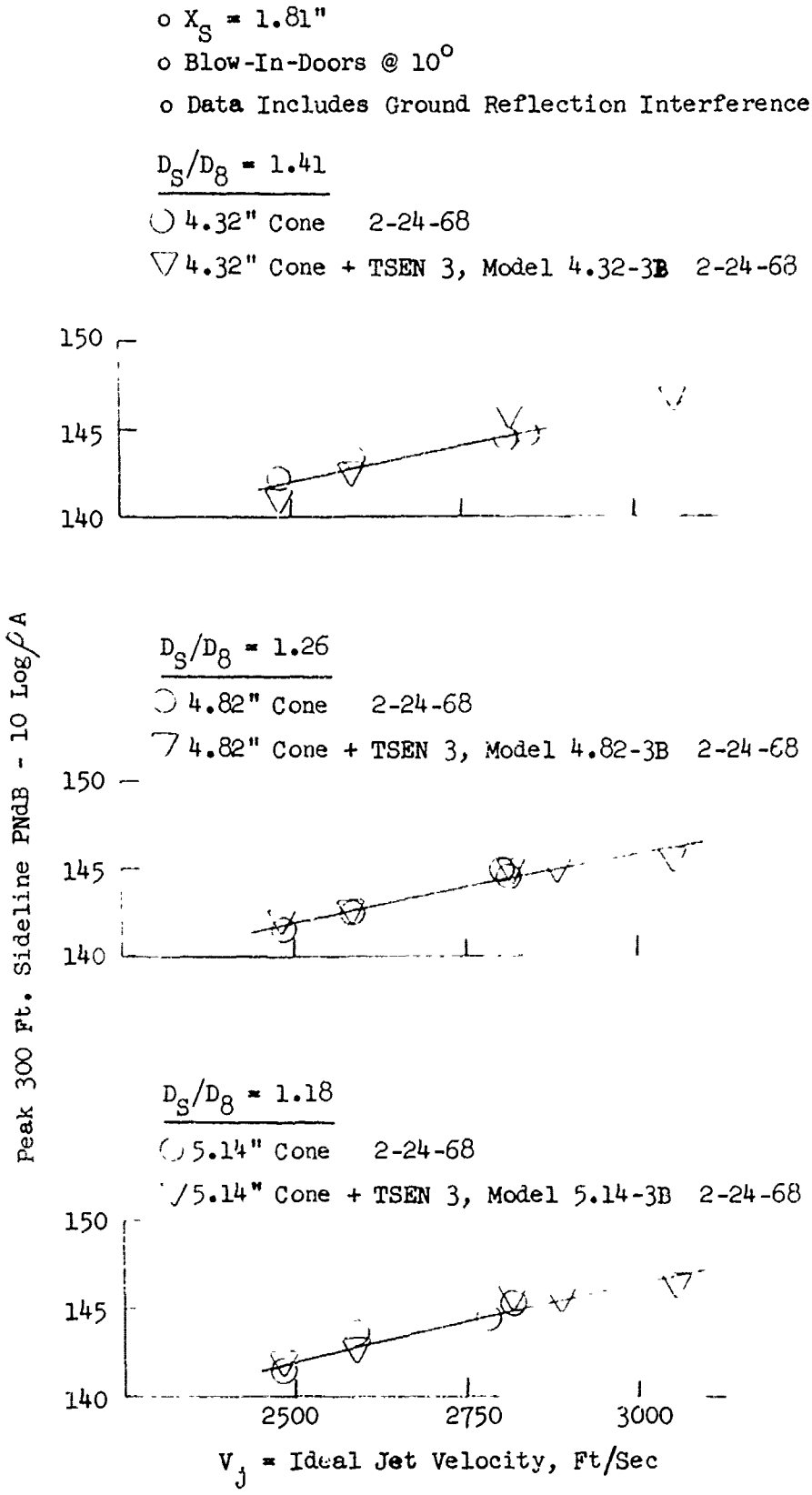

FIGURE V.B-4 EFFECT OF D_S/D_8 VARIATIONS WITHIN TSEN-3 ON 300 FT. SIDELINE JET NOISE LEVELS

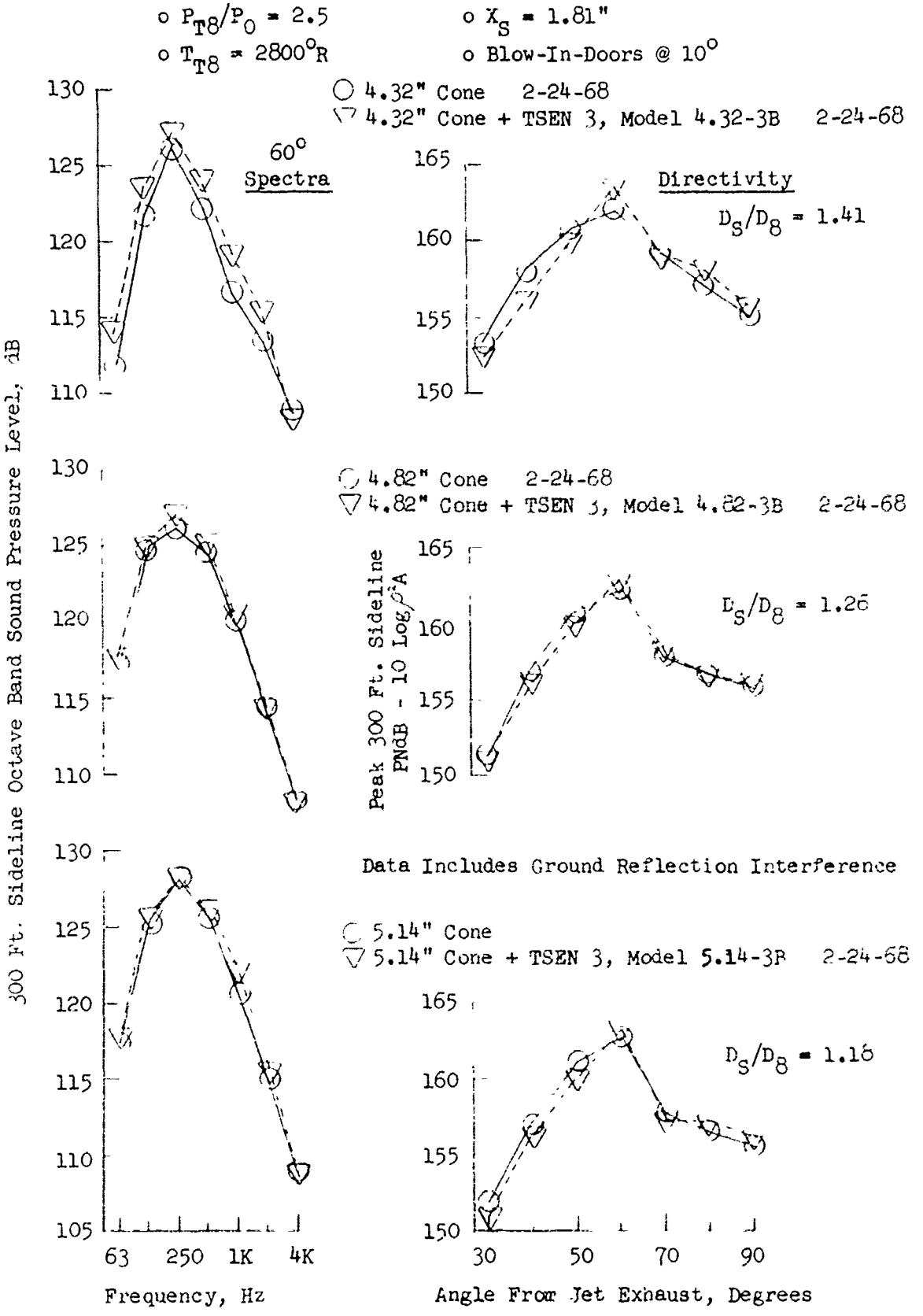

FIGURE V.B-5 EFFECT OF D_S/D_8 VARIATIONS WITHIN TSEN-3 ON SPECTRA AND DIRECTIVITY

TABLE V.B-4 TEST SUMMARY

MODEL NO. 5.1S-3B; 5.1S-3B-1; 5.1S-3B-2

DESCRIPTION: 5.1" Star + TSEN 3; D_S Positioning

DATE: 2/14/68; 2/14/68; 2/16/68

SCALE MODEL A_8 = .1362 ft^2

FULL SCALE A_8 = 8.717 ft^2

SCALE FACTOR = 8:1

- o DATA INCLUDES GROUND REFLECTION INTERFERENCE
- o ANGLE REFERENCED TO JET EXHAUST

TEST CONDITIONS							ACOUSTIC TEST RESULTS							
Rdg. No.	P_{T8}/P_o	T_{T8} (°R)	IDEAL V_j (fps)	W_8 (PPS)	10 $\log_{10} {}^2A$	20 log cA	320 FT ARC PEAK PNdB	320 FT ARC PEAK ANGLE	300 FT. SIDELINE PNL DIRECTIVITY 30°	40°	50°	60°	70°	80°	90°
			2/14/68 D_S @ 2.81 Aft of Plane 8, Doors 10°												
1	3.00	2800	3053	-	-25.0	-7.6	140.0	60	126.4	131.8	136.1	139.2	134.5	133.8	132.9
2	3.00	2500	2886	-	-24.0	-7.1	139.2	60	126.1	131.4	135.4	138.4	133.7	132.3	132.6
3	3.00	2010	2586	-	-22.1	-6.1	137.1	50	126.5	131.6	135.0	135.6	131.9	130.9	129.6
4	3.50	2800	3232	-	-24.4	-7.2	141.1	60	128.2	133.7	137.9	140.3	136.0	134.9	134.2
5	2.50	2800	2818	-	-25.6	-8.0	137.7	60	125.8	130.1	133.2	136.9	133.3	131.9	130.6
6	2.04	2795	2512	-	-26.2	-8.4	135.0	60	122.3	126.4	130.6	134.2	129.0	127.2	126.6
			2/14/68 D_S @ 1.81" Aft of Plane 8, Doors 10°												
1	3.00	2800	3054	-	-25.0	-7.6	138.7	60	126.6	131.1	134.6	137.9	134.4	133.3	131.8
2	3.00	2645	2968	-	-24.5	-7.3	138.6	60	126.6	131.2	134.7	137.8	133.3	132.2	132.2
3	3.00	2020	2593	-	-22.2	-6.2	136.2	50	125.9	131.0	134.1	135.2	131.6	131.7	130.4
4	3.50	2765	3213	-	-24.3	-7.1	141.5	60	128.2	133.4	136.0	140.6	135.9	135.2	134.6
5	2.50	2800	2818	-	-25.6	-8.0	136.2	60	125.5	130.2	134.2	137.4	133.4	131.6	130.0
6	2.00	2800	2489	-	-26.3	-8.4	135.8	60	122.7	127.3	131.4	135.0	129.1	128.3	127.7
			2/16/68 D_S @ 3.81" Aft of Plane 8, Doors 10°												
1	2.00	2800	2480	-	-26.4	-8.5	134.4	60	122.4	126.8	131.0	133.6	129.4	126.8	125.4
2	2.75	2800	2934	-	-25.4	-7.8	138.0	60	125.5	129.5	133.2	137.1	133.9	130.4	129.3
3	3.00	2800	3052	-	-25.1	-7.6	139.0	60	126.2	132.6	135.8	137.1	133.2	130.8	130.6
4	2.99	2500	2881	-	-24.1	-7.1	137.3	60	126.9	131.5	134.9	136.3	131.8	130.0	130.0
5	2.99	2005	2581	-	-22..	-6.2	136.5	50	126.7	131.2	134.3	133.9	131.4	130.1	129.1

- o 4.99" Star + TSEN 3
- o Blow-In-Doors @ 10°
- o Data Includes Ground Reflection Interference

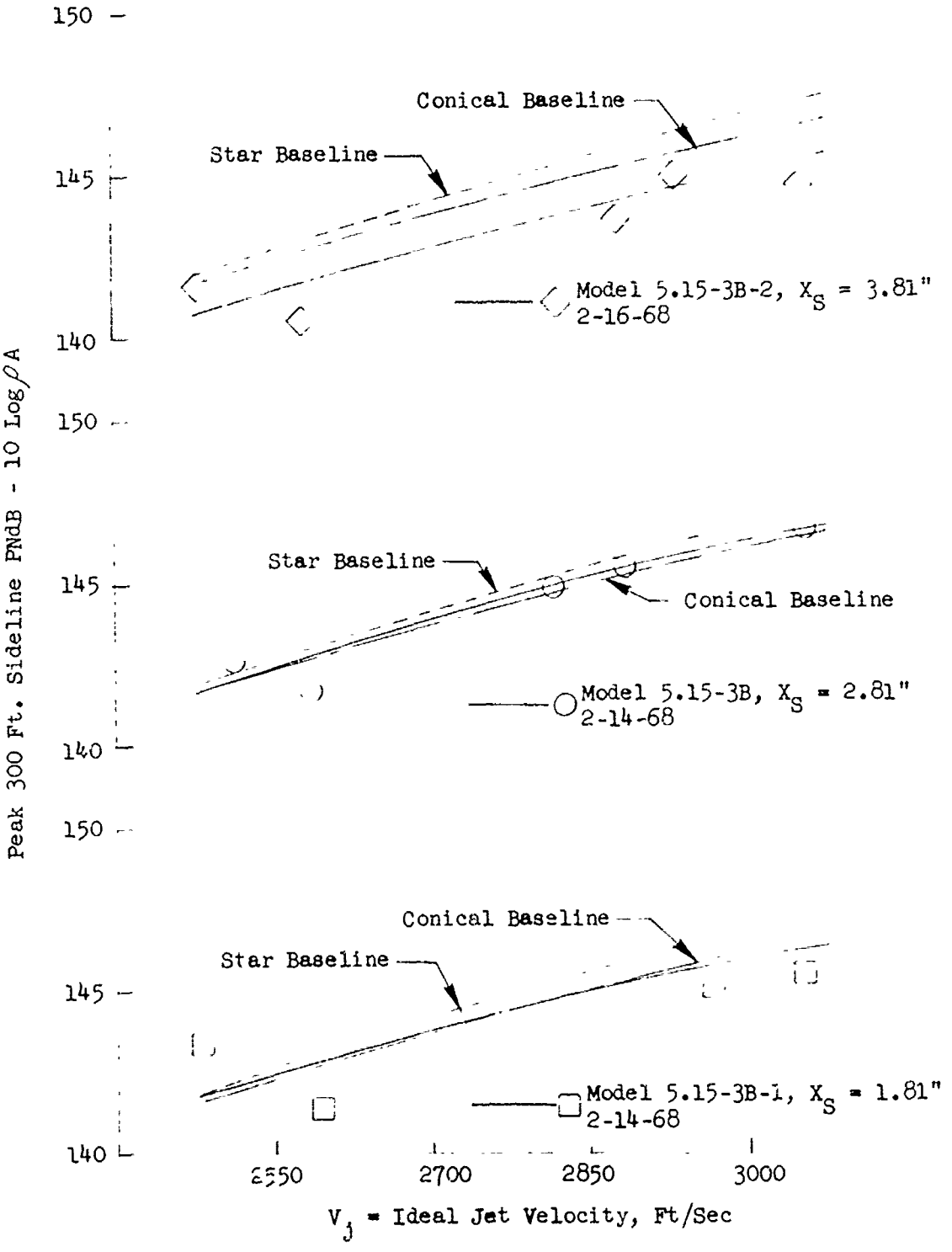

FIGURE V.B-6 EFFECT OF D_S POSITIONING WITHIN TSEN-3 ON 300 FT. SIDELINE JET NOISE LEVELS

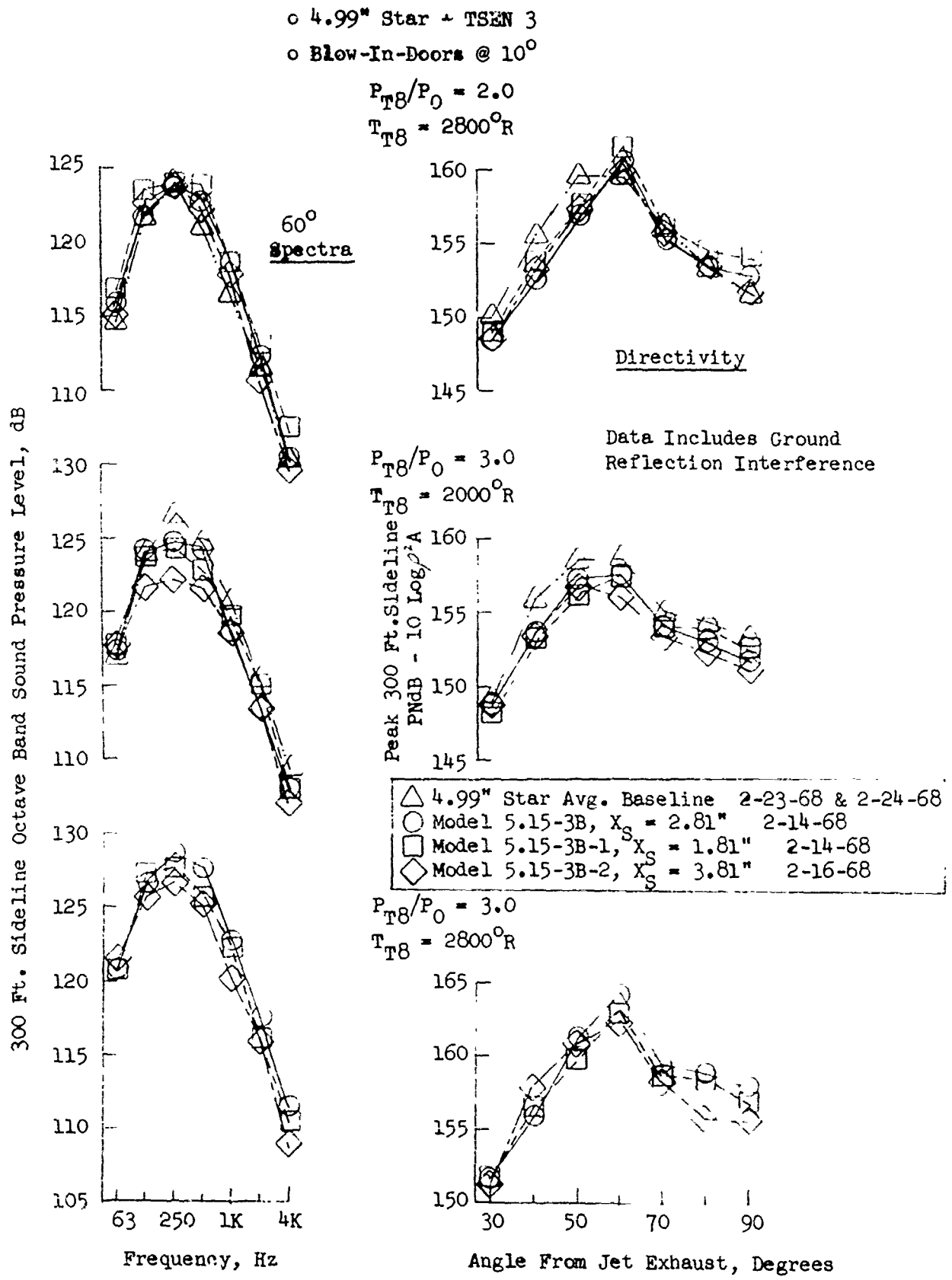

FIGURE V.B-7 EFFECT OF D_S POSITIONING WITHIN TSEN-3 ON SPECTRA AND DIRECTIVITY

TABLE V.B-5 TEST SUMMARY

MODEL NO. 5.1S-3B-4; 5.1S-3B-5

DESCRIPTION: 5.1" Star TSEN 3; Blow-In-Door Variations

DATE: 2/19/68; 2/21/68

SCALE MODEL A_8 = .1362 ft^2

FULL SCALE A_8 = 8.717 ft^2

SCALE FACTOR = 8:1

- o DATA INCLUDES GROUND REFLECTION INTERFERENCE
- o ANGLE REFERENCED TO JET EXHAUST

TEST CONDITIONS							ACOUSTIC TEST RESULTS							
			IDEAL		$10 \log \rho_A V_j^2$	$10 \log \rho_A$	320 FT ARC.		300 FT. SIDELINE PNL DIRECTIVITY					
Rdg. No.	P_{T8}/P_o	T_{T8} (°R)	V_j (fps)	W_8 (PPS)			PEAK PNdB	PEAK ANGLE	30°	40°	50°	60°	70°	80°	90°
	2/19/68 D_S @ 1.81" Aft of Plane 8, Doors @ 20°														
1	2.01	2800	2484	-	-26.5	-8.6	136.1	60	122.4	127.3	131.8	135.2	129.0	128.3	127.1
2	2.51	2800	2819	-	-25.8	-8.2	138.5	60	124.8	130.2	133.9	137.6	132.4	131.1	129.9
3	3.01	2800	3056	-	-25.2	-7.7	138.6	60	126.3	131.0	134.7	137.7	134.1	132.8	131.3
4	3.01	2500	2887	-	-24.2	-7.2	138.1	60	126.3	131.3	135.2	137.2	133.4	131.8	130.5
5	3.01	2010	2589	-	-22.3	-6.3	136.8	50	126.5	131.2	134.6	135.1	131.5	130.5	129.7
	2/21/68 D_S @ 1.81" Aft of Plane 8, Doors Closed														
1	2.01	2800	2485	-	-26.3	-8.4	135.7	60	121.5	126.6	131.1	134.9	133.4	128.3	124.7
2	2.50	2810	2822	-	-25.7	-8.0	135.5	60	123.1	127.9	130.6	134.7	135.1	131.5	129.3
3	3.00	2800	3054	-	-25.0	-7.6	136.8	70	126.2	131.4	135.4	137.9	138.8	133.7	131.8
4	3.01	2500	2887	-	-24.1	-7.1	138.9	60	125.8	130.8	135.6	138.0	137.5	133.0	132.0
5	3.00	2010	2588	-	-22.2	-6.1	136.9	50	125.9	130.9	134.7	135.9	134.4	131.8	131.8

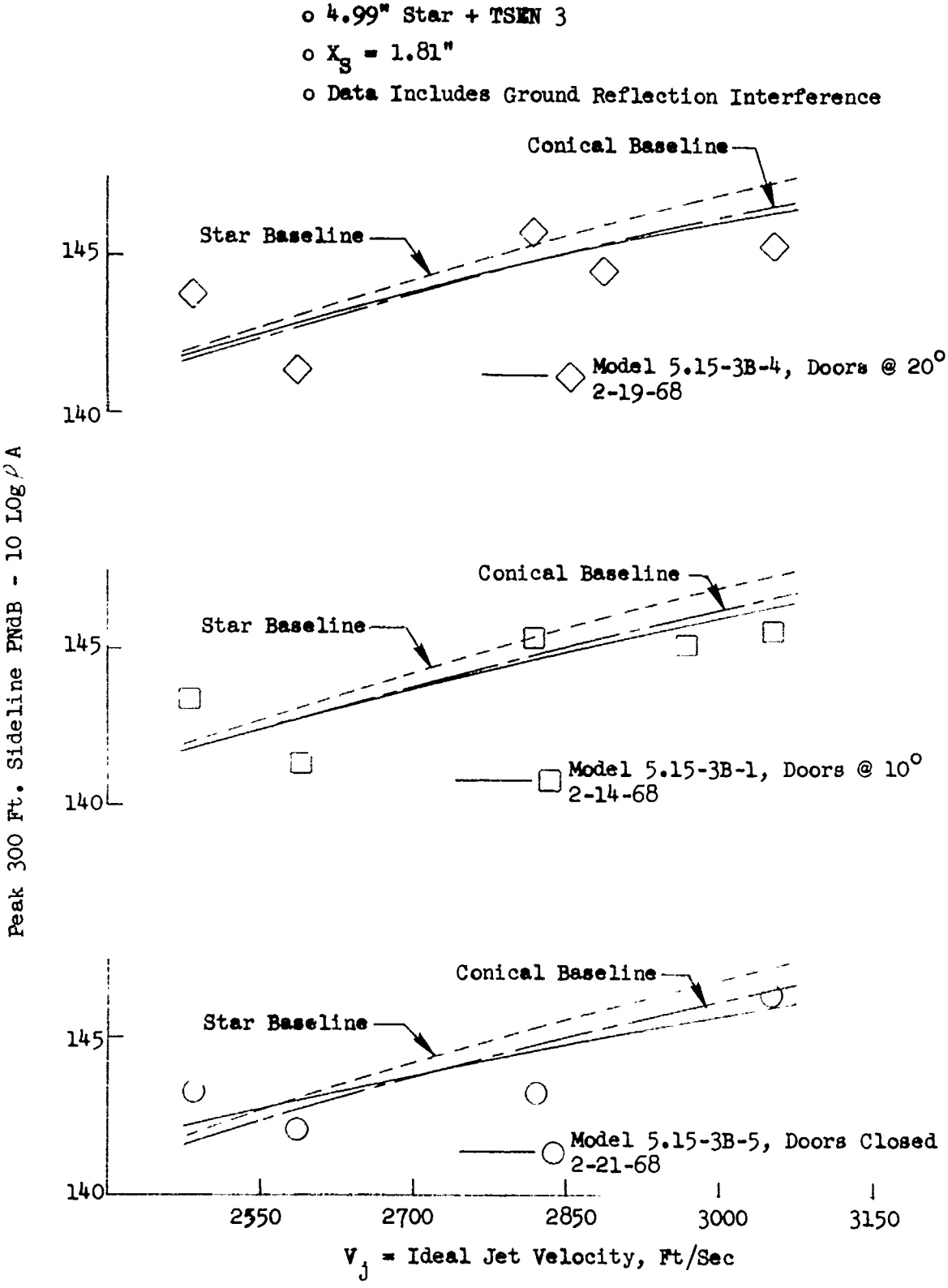

FIGURE V.B-8 EFFECT OF BLOW-IN-DOOR FLOW AREA VARIATION WITHIN TSEN-3 ON 300 FT. SIDELINE JET NOISE LEVELS

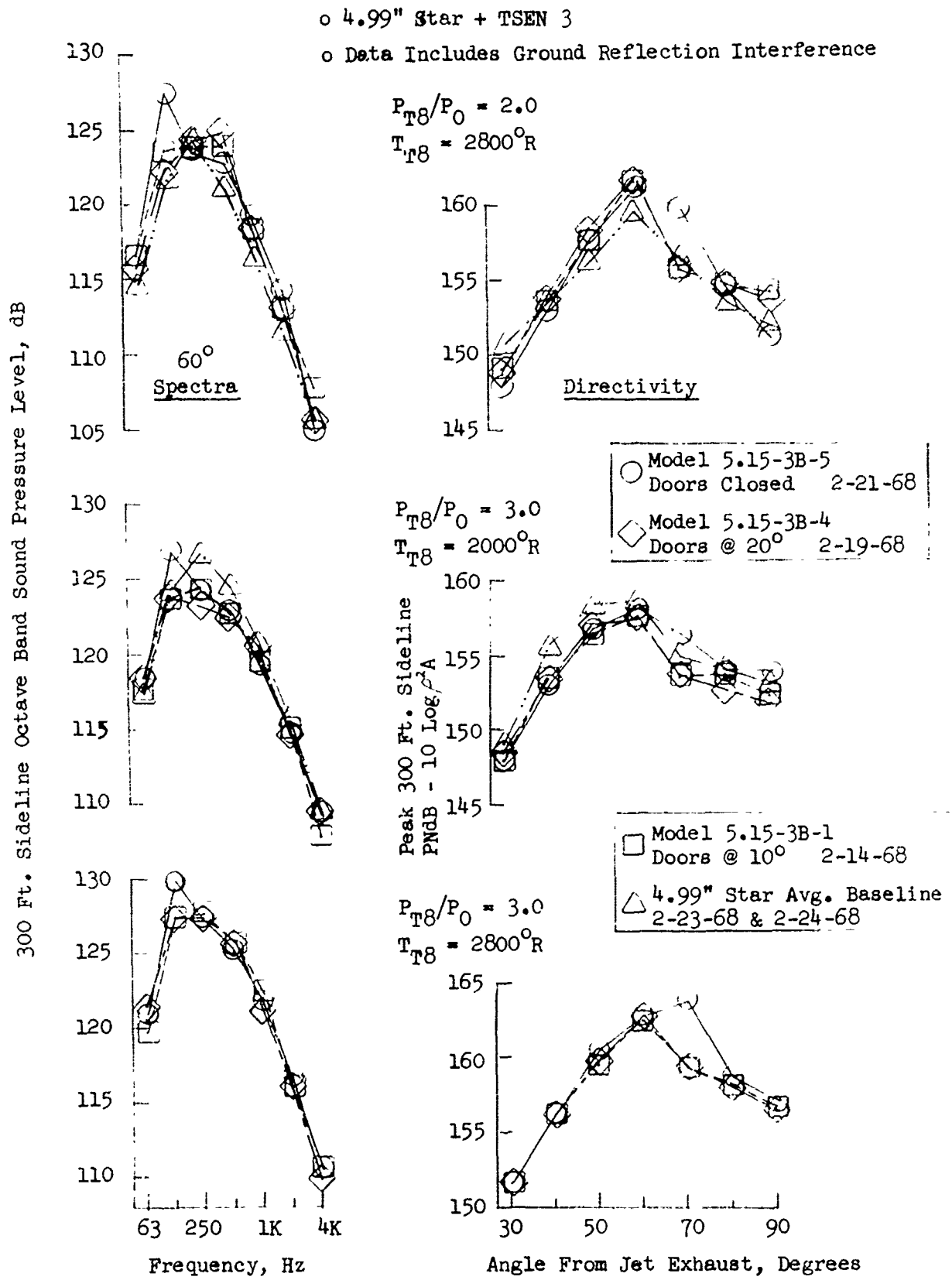

FIGURE V.B-9 EFFECT OF BLOW-IN-DOOR FLOW AREA VARIATION WITHIN TSEN-3 ON SPECTRA AND DIRECTIVITY

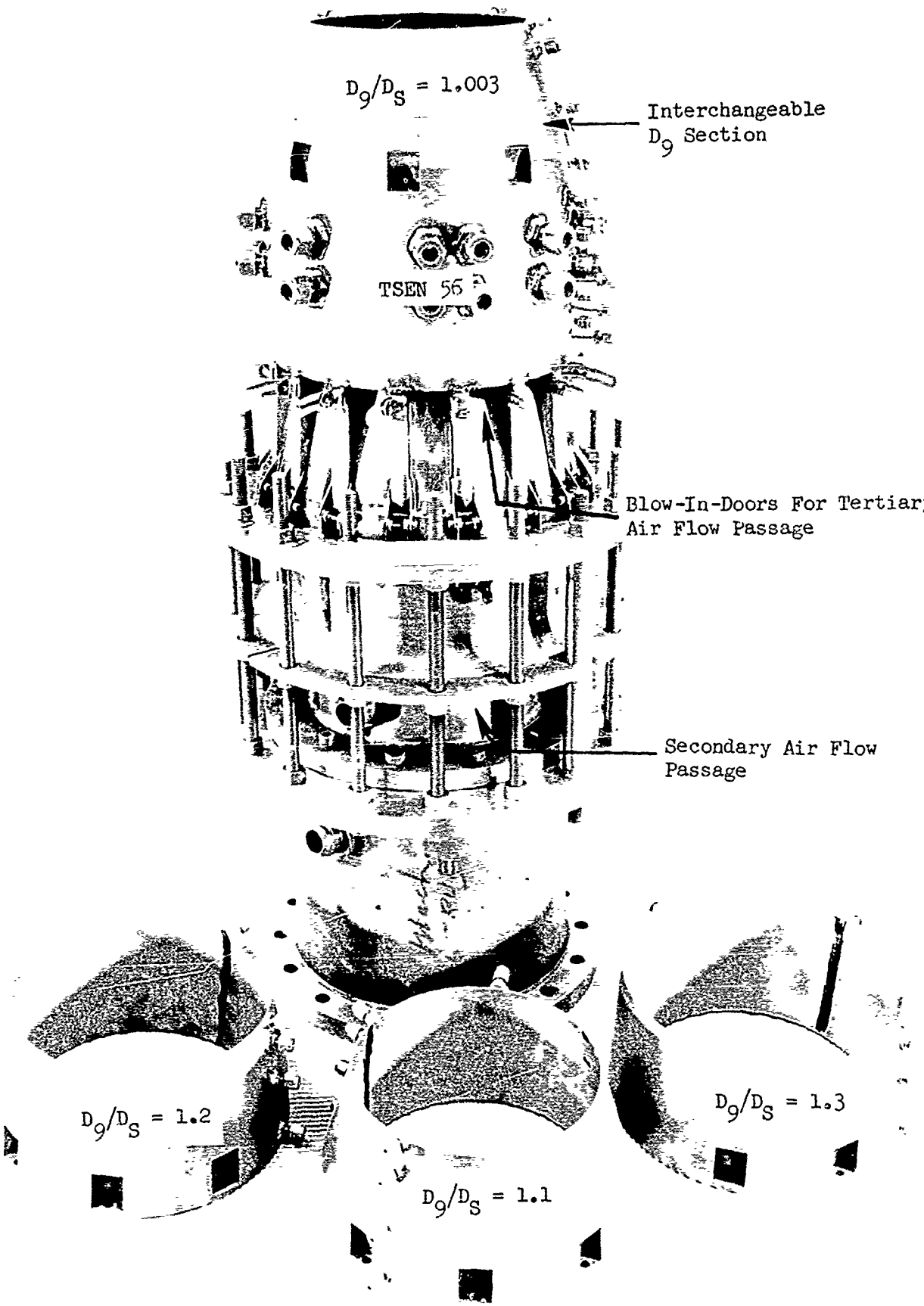

FIGURE V.B-10 TSEN-56 HARDWARE FOR INVESTIGATION OF D_9/D_S VARIATIONS

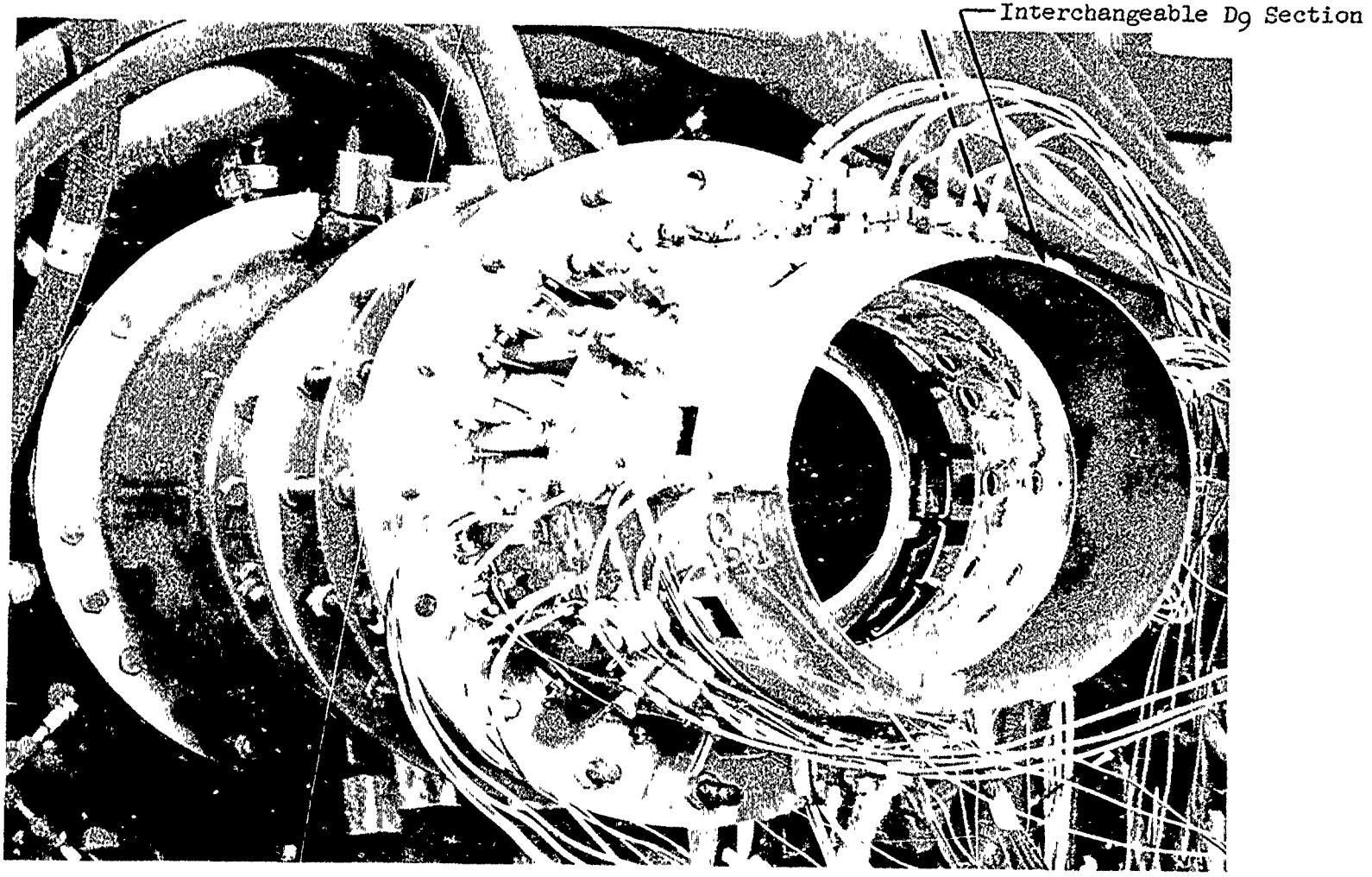

FIGURE V.B-11 TSEN-56 HARDWARE INSTALLATION FOR D_9/D_S INVESTIGATION

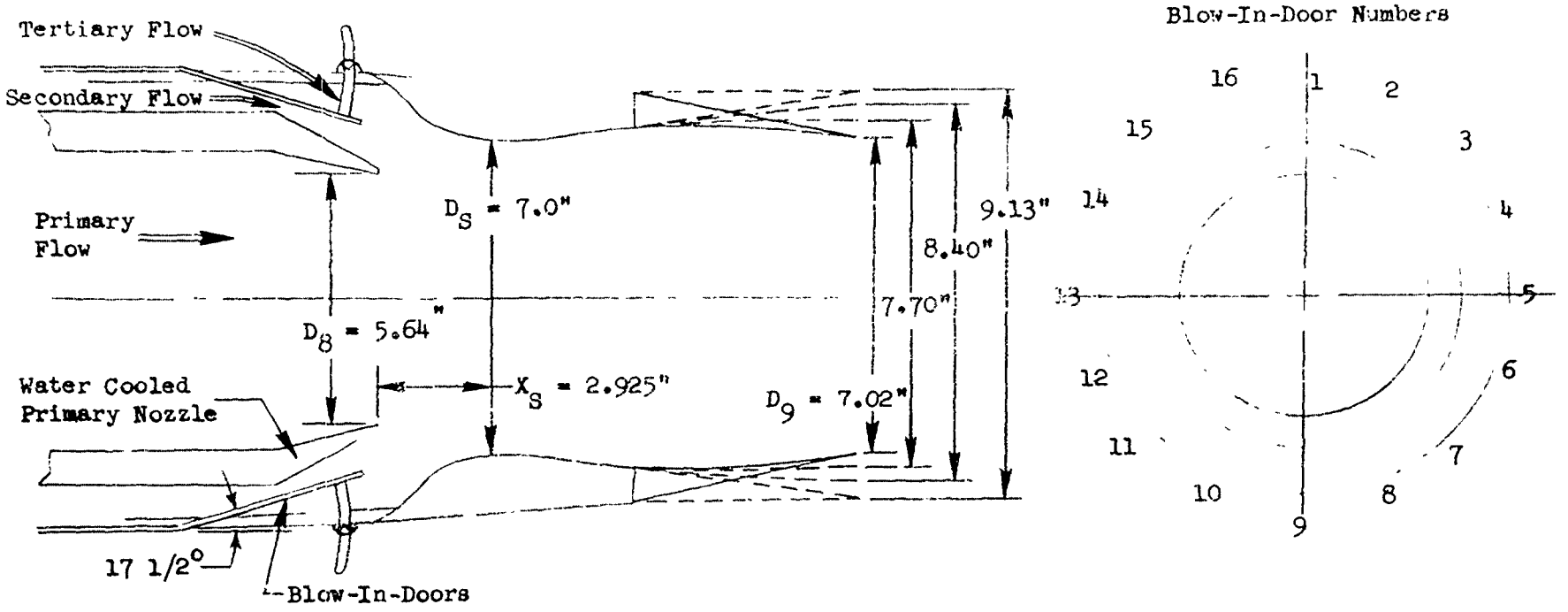

Test No.	Model No.	Test Date	D_S/D_8	Blow-In-Door Area	D_9	D_9/D_S	Secondary Area
1	5.6-56-7	4-1, 4-20 & 4-22-68	1.241	23.5 in.^{2}	7.02"	1.00	7.81 in.^{2}
2	5.6-56-1	4-2-68	1.241	23.5 in.^{2}	7.70"	1.10	7.81 in.^{2}
3	5.6-56-2	4-2-68 & 4-5-68	1.241	23.5 in.^{2}	8.40"	1.20	7.81 in.^{2}
4	5.6-56-3	4-9-68	1.241	23.5 in.^{2}	9.13"	1.31	7.81 in.^{2}

FIGURE V.B-12 SCHEMATIC OF TSEN-56 USED FOR INVESTIGATION OF D_9/D_S VARIATIONS

TABLE V.B-6 TEST SUMMARY

MODEL NO. 5.6-56-7

DESCRIPTION: TSEN 56, D_9/D_S = 1.00

DATE: 4/1/68; 4/20/68

SCALE MODEL A_8 = .1733 ft^2

FULL SCALE A_8 = 11.0912 ft^2

SCALE FACTOR = 8:1

o DATA INCLUDES GROUND REFLECTION INTERFERENCE
o ANGLE REFERENCED TO JET EXHAUST

TEST CONDITIONS							ACOUSTIC TEST RESULTS							
							320 FT ARC		300 FT. SIDELINE PNL DIRECTIVITY					
Rdg. No.	P_{T8}/P_o	T_{T8} (°R)	IDEAL V_j (fps)	W_8 (PPS)	10 Log p^2_A	10 Log ρ_A	PEAK PNdB	PEAK ANGLE	30°	40°	50°	60°	70°	80°	90°
4/1/68															
1	2.06	2783	2518	6.79	-25.0	-7.3	135.3	50.	-	128.3	133.2	134.1	130.0	126.1	128.5
2	2.32	2761	2688	7.67	-24.6	-7.0	138.0	60	-	128.9	133.6	137.1	132.6	130.4	129.1
3	2.58	2782	2851	8.48	-24.4	-6.8	138.3	60	-	132.0	135.3	137.4	134.4	131.2	130.8
4	2.76	2781	2939	9.09	-24.1	-6.7	139.9	60	-	132.4	135.9	139.1	135.0	131.6	131.5
5	2.78	2489	2789	9.64	-23.1	-6.2	138.5	60	-	130.8	136.2	137.6	133.0	131.3	132.0
6	2.78	1957	2472	10.92	-21.1	-5.1	137.7	60	-	131.9	134.1	136.9	136.7	132.8	130.2
7	3.08	1979	2593	12.05	-20.8	-4.9	138.5	50	-	132.8	136.4	135.6	134.1	130.9	131.7
8	3.08	2473	2898	10.75	-22.7	-5.9	139.3	60/70	-	-	135.8	138.5	139.3	135.6	133.1
9	3.10	2756	3067	10.17	-23.6	-6.3	139.3	60	-	133.7	136.8	138.5	135.7	132.9	133.4
4/20/68															
1	2.06	2774	2519	7.17	-25.2	-7.3	135.2	50	123.3	128.4	133.1	133.8	130.5	126.6	126.8
2	2.60	2745	2842	9.05	-24.4	-6.8	138.2	60	126.2	131.6	135.0	137.4	134.7	132.9	131.6
3	3.11	2780	3086	10.67	-23.9	-6.4	139.9	60	128.9	133.2	137.1	139.0	136.3	134.4	134.2
4	3.11	2454	2899	11.31	-22.8	-5.9	139.8	50	128.7	133.5	137.6	138.5	136.1	132.6	132.5
5	3.10	1235	2053	12.58	-16.8	-2.9	139.3	50	128.2	133.4	137.2	137.0	134.1	131.3	132.3

TABLE V.D-7 TEST SUMMARY

MODEL NO. 5.6-56-1

DESCRIPTION: TSEN 56 D_9/D_S = 1.10

DATE: 4/2/68

SCALE MODEL A_8 = .1733 ft^2

FULL SCALE A_8 = 11.0912 ft^2

SCALE FACTOR = 8:1

o DATA INCLUDES GROUND REFLECTION INTERFERENCE
o ANGLE REFERENCED TO JET EXHAUST

TEST CONDITIONS							ACOUSTIC TEST RESULTS								
			IDEAL				320 FT ARC		300 FT. SIDELINE PNL DIRECTIVITY						
Rdg. No.	P_{T8}/P_o	T_{T8} (°R)	V_j (fps)	W_8 (PPS)	10 Log $\rho^2 A$	10 Log ρA	PEAK PNdB	PEAK ANGLE	30°	40°	50°	60°	70°	80°	90°
1	2.04	2738	2490	7.15	-25.0	-7.3	135.0	50	122.8	127.9	132.8	134.0	130.1	127.6	127.5
2	2.27	2828	2696	7.98	-25.0	-7.2	136.1	60	123.9	128.8	133.9	135.2	131.3	128.9	129.7
3	2.56	2720	2812	8.87	-24.3	-6.8	138.0	50	124.7	130.8	135.9	135.9	132.1	132.3	130.7
4	2.77	2747	2927	9.60	-24.1	-6.6	137.0	50	127.4	131.6	134.8	133.4	132.0	132.8	131.1
5	3.08	2761	3063	10.69	-24.0	-6.5	138.8	50	128.7	133.3	136.6	135.8	133.2	133.1	132.3
6	3.06	2457	2882	11.22	-23.0	-6.0	138.2	50	128.3	133.1	136.0	134.1	132.3	131.9	131.6
7	2.77	2442	2758	10.16	-23.2	-6.2	136.9	50	127.2	131.7	134.7	133.0	131.3	130.9	129.7
8	2.76	1993	2486	11.19	-21.5	-5.4	136.4	50	127.4	130.2	134.3	131.6	130.2	128.3	129.3
9	3.08	1990	2600	12.40	-21.1	-5.1	137.8	40	129.3	133.7	135.1	134.3	131.4	131.6	130.5

TABLE V.B-8 TEST SUMMARY

MODEL NO. 5.6-56-2

DESCRIPTION: TSEN 56 D_9/D_S = 1.20

DATE: 4/2/68; 4/5/68

SCALE MODEL A_8 = .1733 ft^2

FULL SCALE A_8 = 11.0912 ft^2

SCALE FACTOR = 8:1

o DATA INCLUDES GROUND REFLECTION INTERFERENCE
o ANGLE REFERENCED TO JET EXHAUST

TEST CONDITIONS							ACOUSTIC TEST RESULTS								
Rdg. No.	P_{T8}/P_o	T_{TS} (°R)	IDEAL V_j (fps)	W_8 (PPS)	10 Log $\rho^2 A$	10 Log ρA	320 FT ARC PEAK PNdB	320 FT ARC PEAK ANGLE	300 FT. SIDELINE PNL DIRECTIVITY 30°	40°	50°	60°	70°	80°	90°
4/2/68															
1	2.05	2787	2515	6.97	-25.4	-7.4	135.5	50	123.2	128.4	133.3	133.0	129.8	128.7	128.3
2	2.11	2779	3083	10.61	-24.0	-6.5	137.6	50	128.8	133.0	135.4	135.0	133.5	132.7	132.7
3	3.03	2476	2882	10.94	-22.9	-6.0	136.6	40	128.4	132.5	134.3	134.1	132.7	133.3	131.4
4/5/68															
1	2.04	2775	2498	7.08	-25.1	-7.3	136.7	50	123.1	129.0	134.6	134.8	130.7	128.0	127.9
2	2.30	2751	2675	8.06	-24.6	-7.0	136.6	50	124.3	129.2	134.5	135.1	131.8	129.9	131.5
3	2.57	2777	2843	9.01	-24.4	-6.8	135.5	40	126.3	131.5	132.9	133.0	131.8	130.2	130.7
4	2.74	2712	2891	9.59	-24.0	6.6	136.9	50	125.6	131.4	134.7	134.1	133.3	132.4	131.7
5	3.06	2716	3032	10.71	-23.6	-6.3	137.6	50	127.9	132.0	135.4	136.1	134.3	132.7	134.0
o	3.06	2435	2871	11.23	-22.6	-5.8	137.6	50	127.4	131.5	135.4	135.1	133.4	132.7	132.8
7	2.75	2436	2747	10.10	-23.0	-6.1	136.3	50	126.9	130.9	134.1	133.3	133.1	130.0	130.9
8	2.76	1951	2462	11.17	-21.1	-5.1	135.0	40	125.4	130.9	132.6	131.1	130.9	129.5	130.0
9	3.06	1978	2587	11.21	-20.8	-4.9	136.2	50	126.7	131.5	134.0	133.2	133.0	131.4	131.5
10	1.52	1481	1426	6.91	-20.1	-4.8	129.4	60	119.5	119.8	[illegible].1	128.6	124.4	123.9	125.2
11	1.52	978	1157	9.15	-16.5	-3.0	112.4	60	105.2	108.0	[illegible]0.0	111.6	110.4	110.4	109.7

TABLE V.3-9 TEST SUMMARY

MODEL NO. 5.6-56-3

DESCRIPTION: TSEN 56 D_9/D_S = 1.31

DATE: 4/9/68

SCALE MODEL A_8 = .1733 ft^2

FULL SCALE A_8 = 11.0912 ft^2

SCALE FACTOR = 8:1

c DATA INCLUDES GROUND REFLECTION INTERFERENCE

o ANGLE REFERENCED TO JET EXHAUST

TEST CONDITIONS							ACOUSTIC TEST RESULTS								
									300 FT. SIDELINE PNL DIRECTIVITY						
Rdg. No.	P_{T8}/P_o	T_{T8} (°R)	IDEAL V_j (fps)	W_8 (PPS)	10 $Log_{10} A^2$	10 Log $_{10}$ A	320 FT ARC PEAK PNdB	PEAK ANGLE	30°	40°	50°	60°	70°	80°	90°
1	2.05	2816	2528	7.14	-25.2	-7.4	135.3	50	122.5	128.5	133.2	133.6	130.7	128.7	127.6
2	2.31	2825	2715	7.94	-24.9	-7.2	136.0	50	125.1	130.0	133.8	134.2	131.5	129.4	130.6
3	2.57	2787	2848	8.89	-24.4	-6.9	137.8	50	127.1	132.6	135.6	134.2	132.7	130.5	130.8
4	2.74	2769	2921	9.54	-24.2	-6.7	137.2	50	127.2	132.7	135.0	134.8	133.2	130.7	130.6
5	3.10	2811	3099	10.63	-23.8	-6.4	137.5	50	127.3	132.2	135.3	136.5	134.9	132.8	133.0
6	3.04	2462	2877	11.09	-22.8	-5.9	137.1	50	126.9	132.4	135.0	135.8	134.3	131.9	131.7
7	2.78	2469	2777	10 05	-23.1	-6.2	141.1	50	130.6	135.6	138.7	137.9	137.4	135.6	134.4
8	2.74	2010	2490	11.08	-21.4	-5.3	136.5	50	127.5	131.7	134.3	135.4	134.0	131.9	129.6
9	3.08	1975	2591	12.50	-20.8	-4.9	137.5	60	128.5	131.7	134.6	136.6	135.0	132.7	130.4

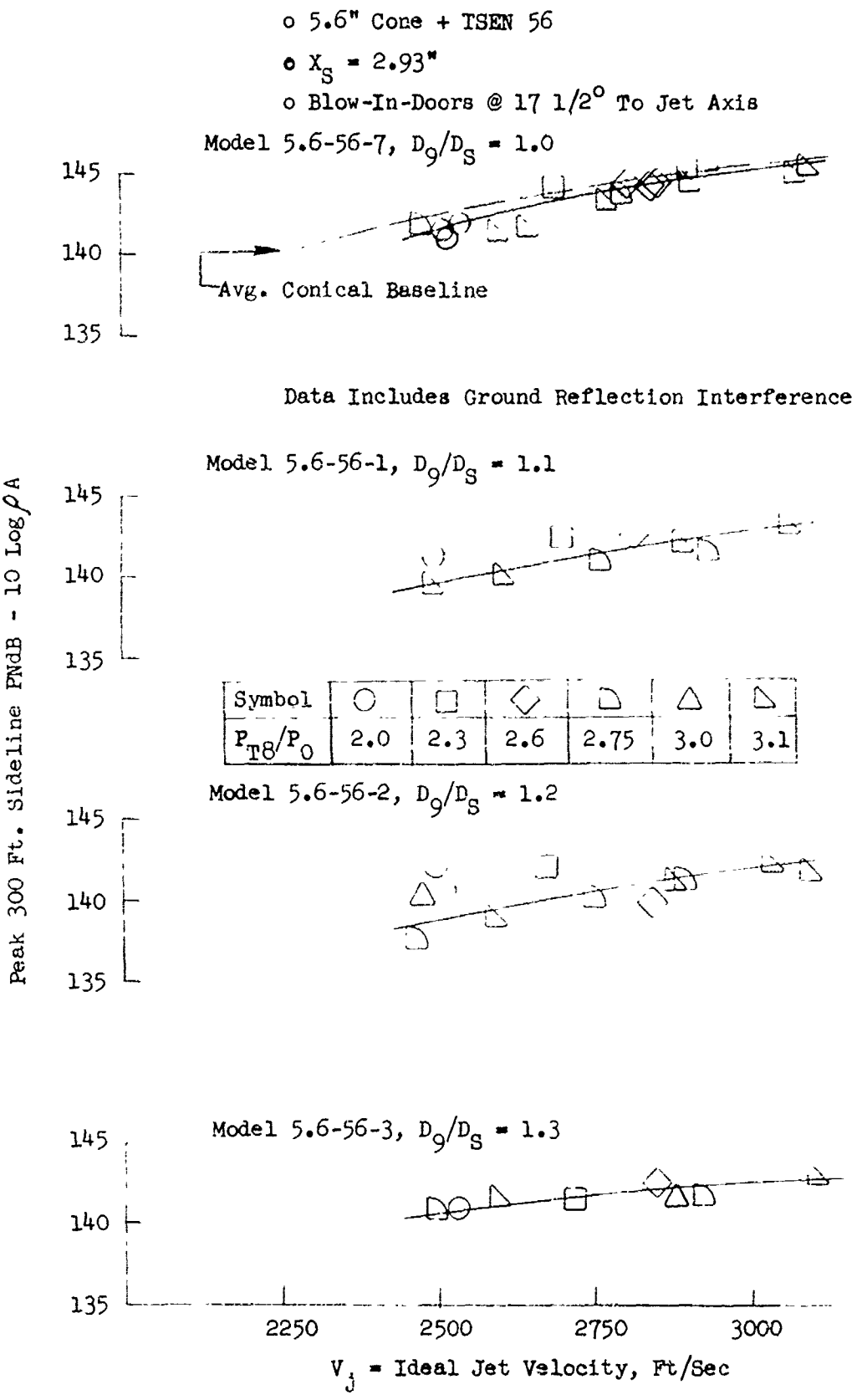

FIGURE V.B-13 EFFECT OF D_9/D_S VARIATION WITHIN TSEN-56 ON 300 FT. SIDELINE JET NOISE LEVELS

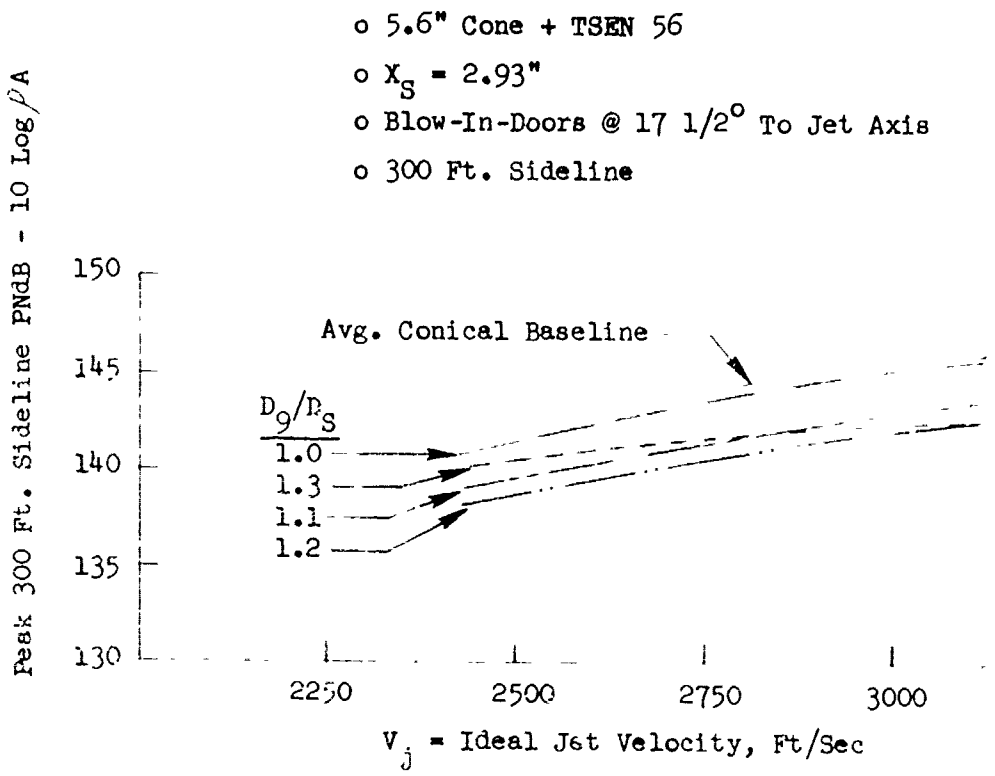

Data Includes Ground Reflection Interference

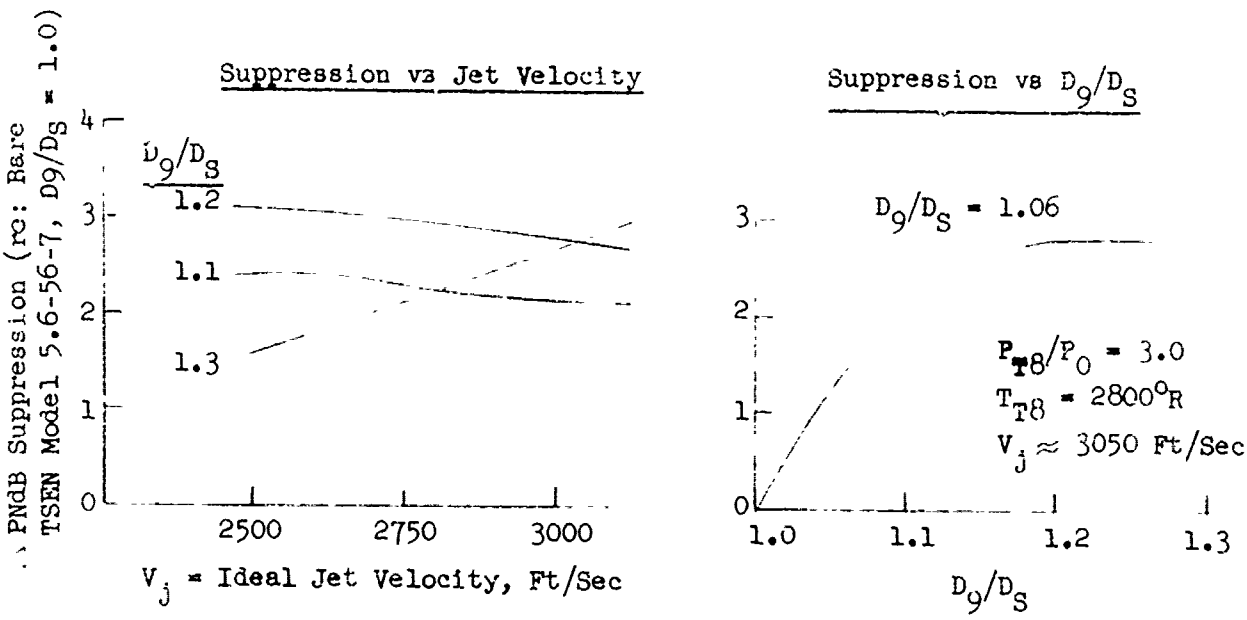

FIGURE V.B-14 EFFECT OF D9/DS VARIATION WITHIN TSEN-56 ON JET NOISE LEVELS AND SUPPRESSION CHARACTERISTICS

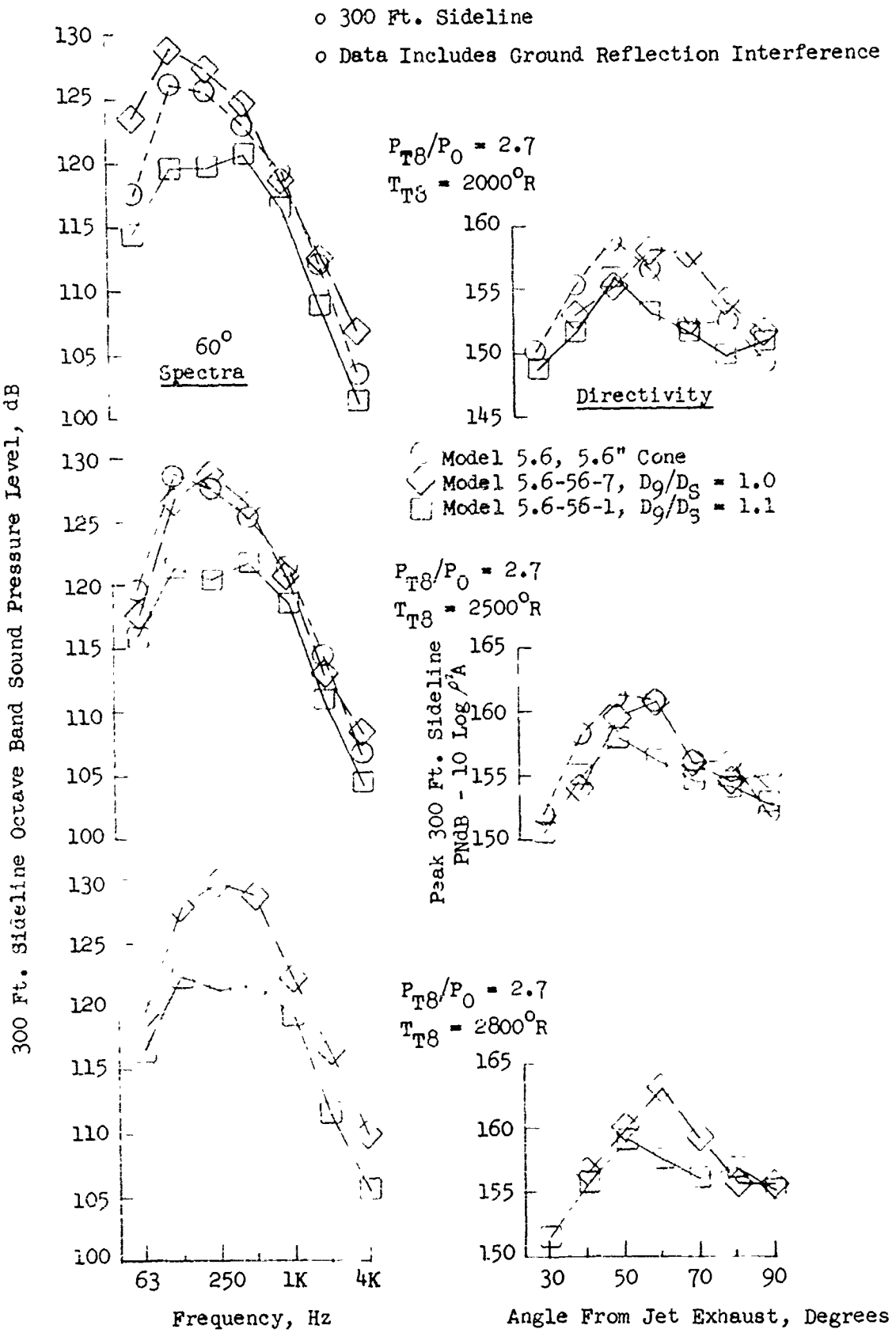

FIGURE V.B-15A EFFECT OF D_9/D_S VARIATION WITHIN TSEN-56 ON SPECTRA AND DIRECTIVITY

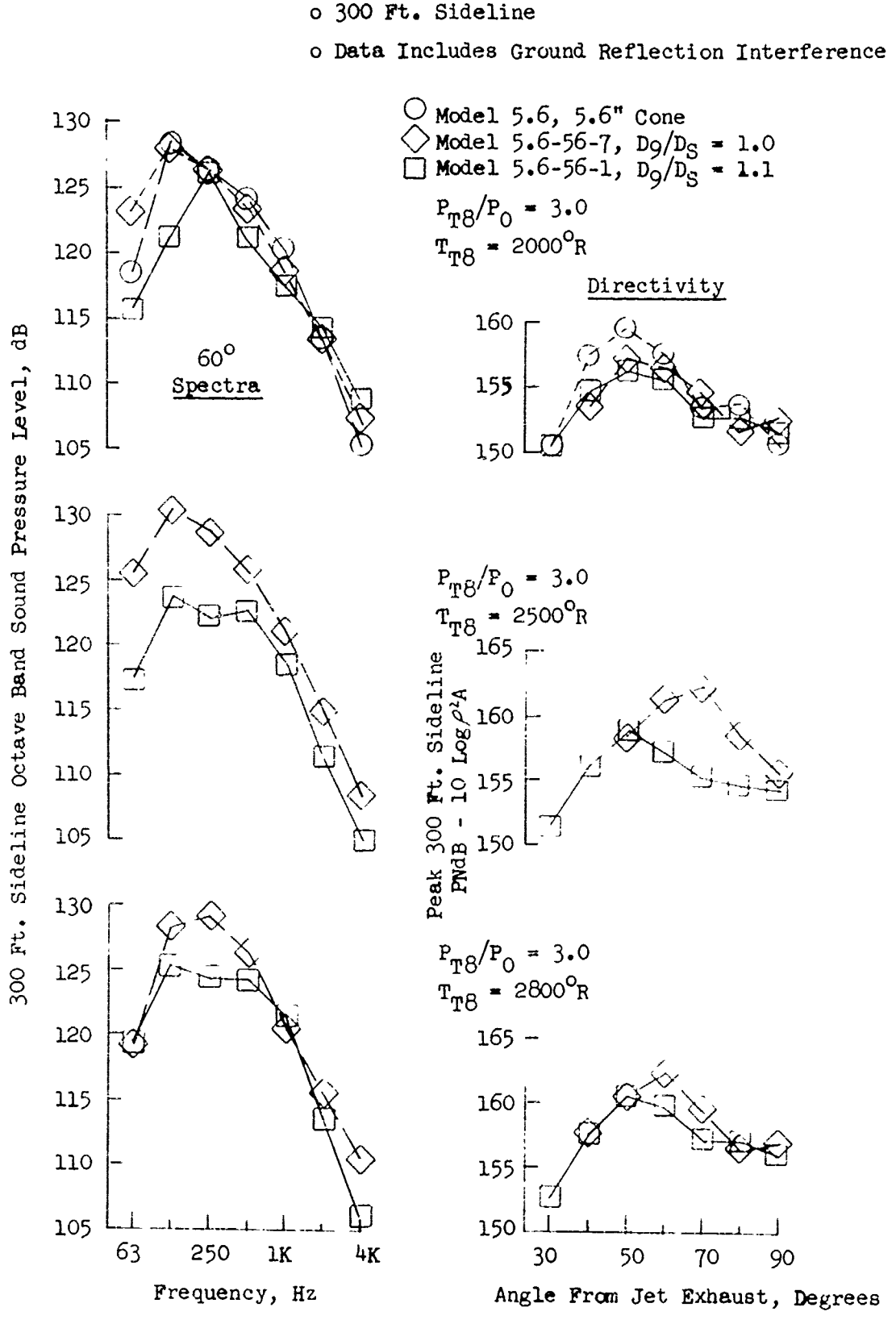

FIGURE V.B-15B EFFECT OF D_9/D_S VARIATION WITHIN TSEN-56 ON SPECTRA AND DIRECTIVITY

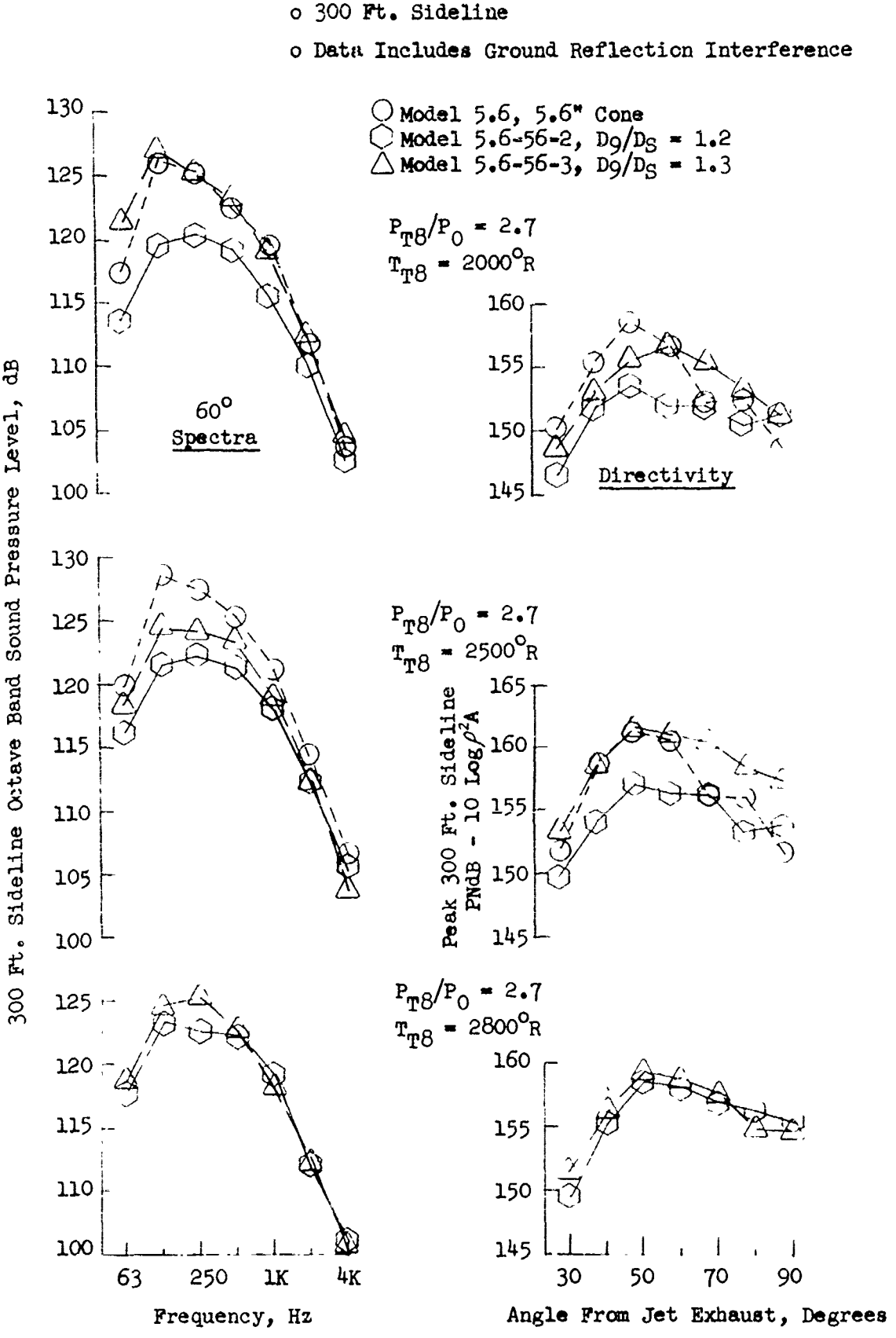

FIGURE V.B-15C EFFECT OF D_9/D_S VARIATION WITHIN TSEN-56 ON SPECTRA AND DIRECTIVITY

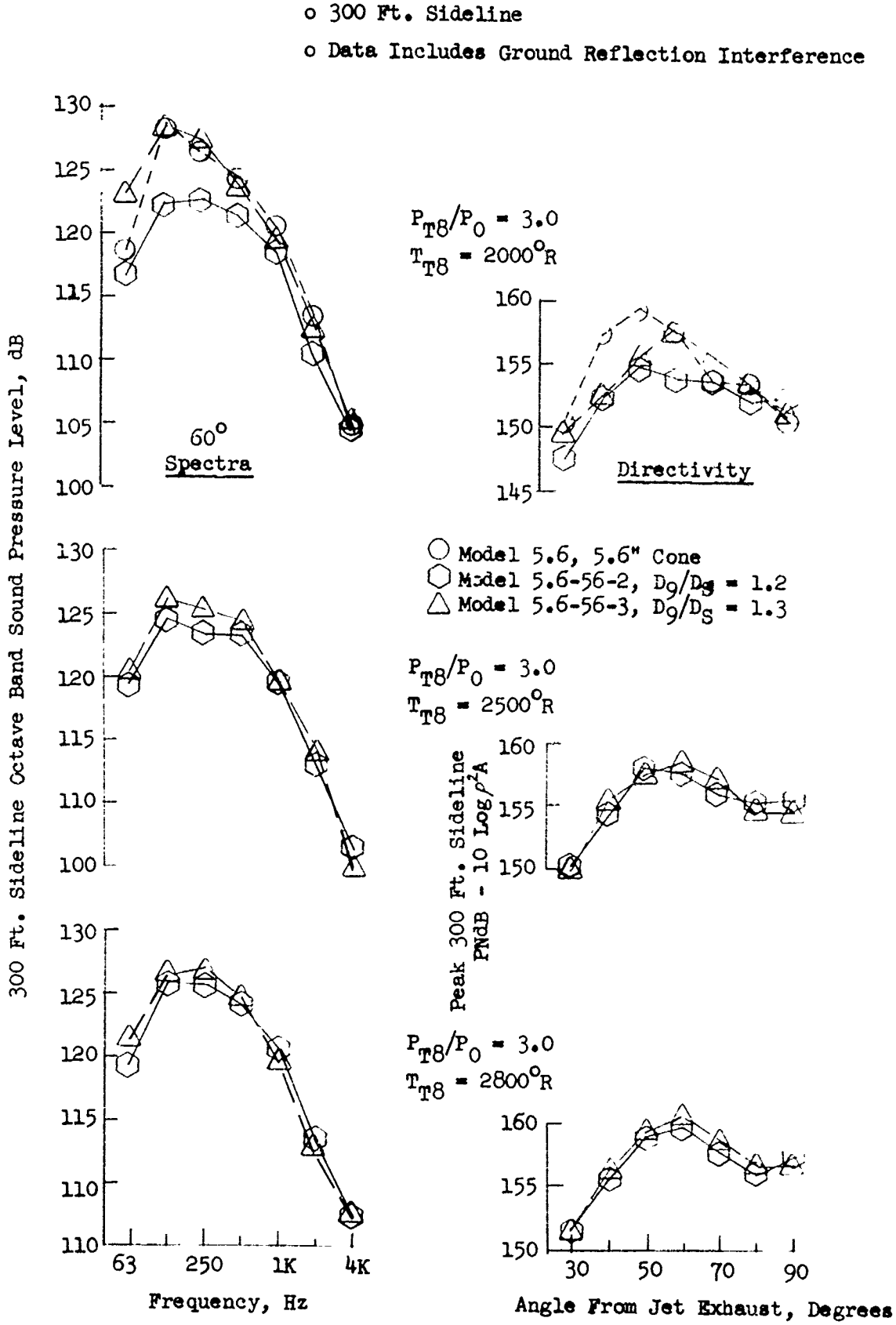

FIGURE V.B-15D EFFECT OF D_9/D_S VARIATION WITHIN TSEN-56 ON SPECTRA AND DIRECTIVITY

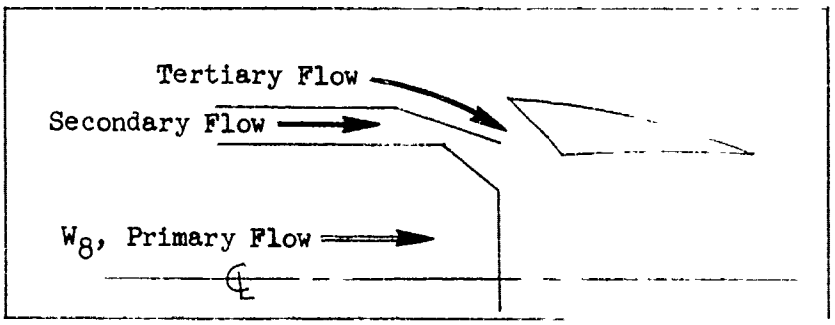

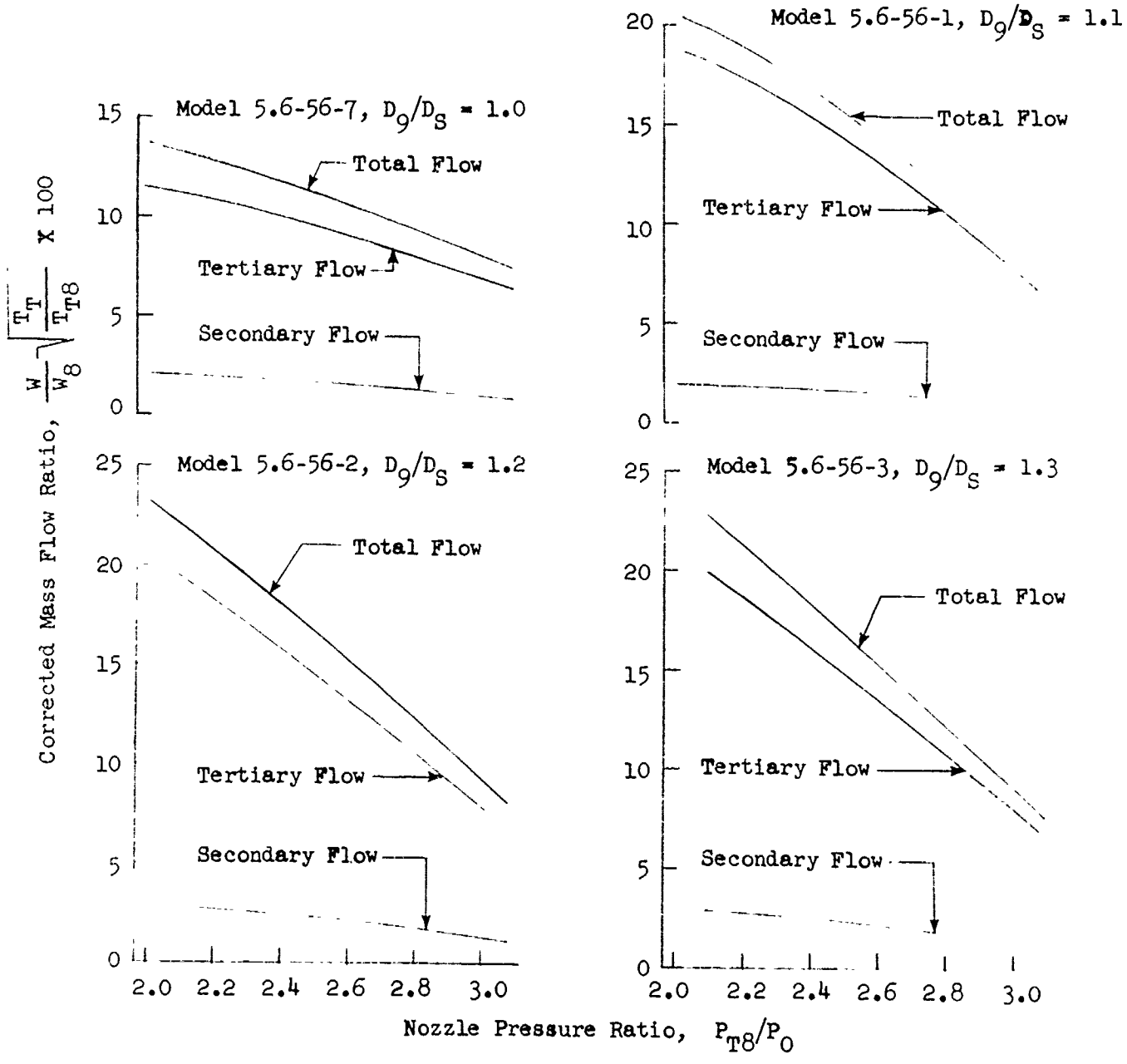

FIGURE V.B-16 TSEN-56 AIR HANDLING CHARACTERISTICS

- o D_9/D_S = 1.0
- o D_S/D_8 = 1.241
- o Blow-In-Door Area = 23.5 in.^{2}; Simulates 1500 in.^{2} Full Scale

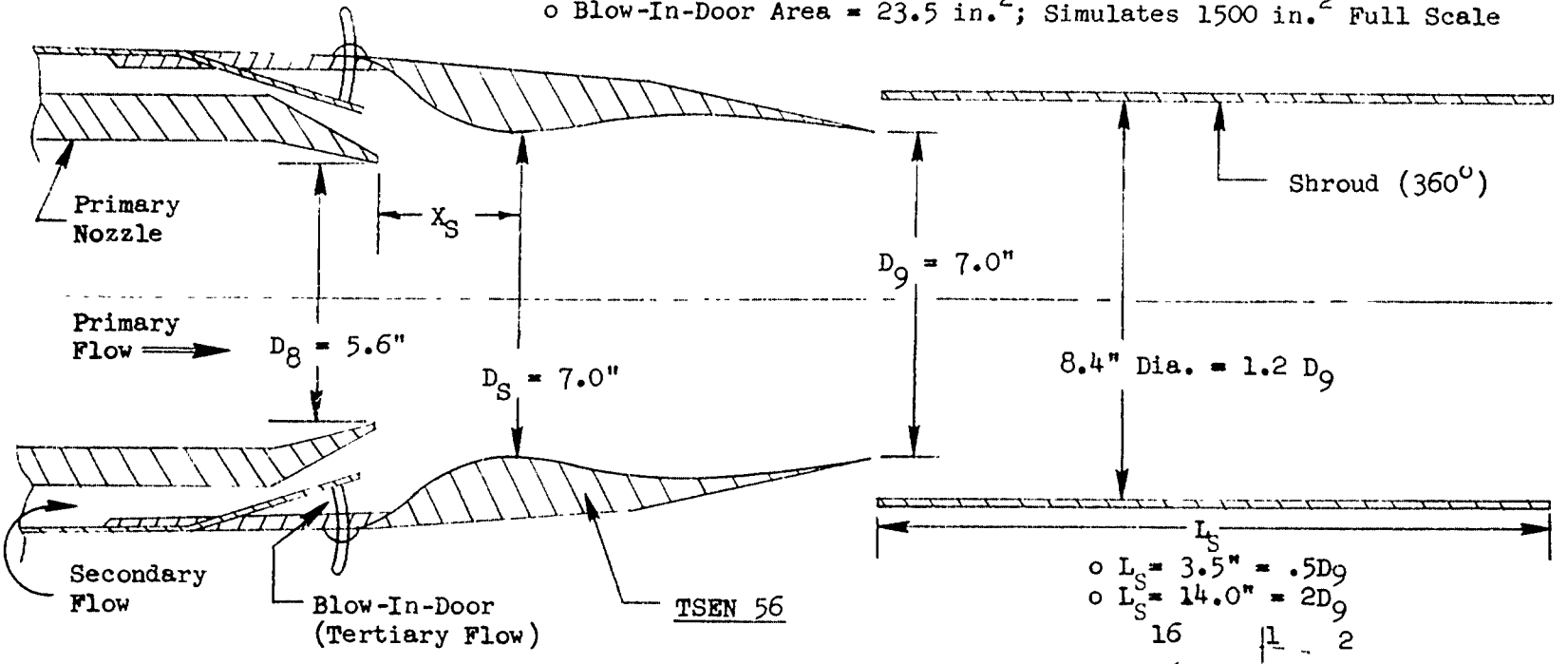

- o L_S = 3.5" = .5D_9
- o L_S = 14.0" = 2D_9

TSEN = Two Stage Ejector Nozzle

Model	Shroud Length "L_S"	X_S
5.6-56B-7	0.0"	2.925"
5.6-56B-8	14.0"	2.925"
5.6-56B-10	3.5"	2.925"
5.6-56B-11	0.0"	2.055"
5.6-56B-12	14.0"	2.055"

Blow-In-Door Numbering Sequence →

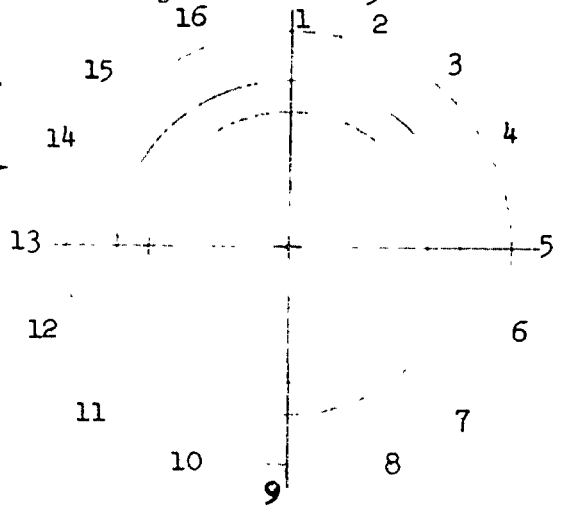

FIGURE V.B-17 SCHEMATIC OF TSEN-56 PLUS SHROUD CONFIGURATIONS

TABLE V.B-10 TEST SUMMARY

MODEL NO. 5.6-56B-7; -8;

DESCRIPTION: TSEN 56 + Shroud; L_S Variation

DATE: 4/22/68; 4/20/68

SCALE MODEL A_8 = .1733 ft^2

FULL SCALE A_8 = 11.0912 ft^2

SCALE FACTOR = 8:1

- o DATA INCLUDES GROUND REFLECTION INTERFERENCE
- o ANGLE REFERENCED TO JET EXHAUST

TEST CONDITIONS							ACOUSTIC TEST RESULTS								
					10 Log $\rho_A V_j^2$	10 Log ρ_A	320 FT ARC		300 FT. SIDELINE PNL DIRECTIVITY						
Rdg. No.	P_{T8}/P_o	T_{T8} (°R)	IDEAL V_j (fps)	W_8 (PPS)			PEAK PNdB	PEAK ANGLE	30°	40°	50°	60°	70°	80°	90°
	4/22/68 5.6-56B-7 X_S = 2.925" L_S = 0														
1	2.06	2832	2540	6.6	-25.3	-7.4	135.3	60	123.4	128.6	132.9	134.4	130.3	127.8	128.5
2	2.59	2687	2807	8.5	-24.2	-6.7	138.5	60	126.0	131.0	135.3	137.6	133.4	130.9	130.4
3	3.09	2246	2767	11.2	-22.0	-5.5	138.7	50	128.4	132.7	136.6	137.7	134.0	131.7	132.1
4	3.10	2041	2639	11.9	-21.2	-5.1	138.7	50	127.6	132.8	136.5	136.1	133.2	130.9	131.6
5	1.59	1268	1378	7.9	-18.8	-4.2	125.9	40	118.6	122.1	119.8	125.0	122.2	122.5	119.9
6	1.36	1140	1076	6.5	-17.9	-3.5	111.1	50	101.8	104.2	106.5	110.2	109.4	109.1	107.8
	4/20/68 5.6-56B-8 X_S = 2.925" L_S = 14"														
1	1.38	1040	1049	7.2	-17.1	-3.1	106.4	30	99.7	101.8	102.5	104.6	104.8	102.6	105.3
2	1.58	1263	1370	8.0	-18.8	-4.1	115.9	30	109.3	111.2	111.7	112.4	112.2	110.6	110.2
3	3.10	2040	2639	12.2	-21.2	-5.1	138.6	50	127.3	132.8	136.5	136.0	132.4	129.3	128.6
4	3.01	2515	2928	10.9	-23.0	-6.0	139.2	50	127.1	132.2	137.0	137.4	133.6	131.0	130.6
5	3.09	2814	3096	10.4	-24.0	-6.5	139.5	50	126.3	132.0	137.3	137.6	134.5	131.6	132.1
6	2.55	2777	2833	8.8	-24.5	-6.9	137.8	60	124.6	130.4	135.4	137.0	132.5	128.7	128.4
7	2.04	2746	2499	7.1	-25.1	-7.3	134.1	50	120.6	126.9	132.0	131.4	128.6	125.8	123.9

TABLE V.B-10 TEST SUMMARY
(Continued)

MODEL NO. 5.6-56B-10; -11; -12

DESCRIPTION: TSEN 56 + SHROUD; L_S Variation

DATE: 4/22/68; 4/29/68; 4/29/68

SCALE MODEL A_8 = .1733 ft^2

FULL SCALE A_8 = 11.0912 ft^2

SCALE FACTOR = 8:1

- o DATA INCLUDES GROUND REFLECTION INTERFERENCE
- o ANGLE REFERENCED TO JET EXHAUST

TEST CONDITIONS							ACOUSTIC TEST RESULTS								
							320 FT ARC		300 FT. SIDELINE PNL DIRECTIVITY						
Rdg. No.	P_{TS}/P_o	T_{T8} (°R)	IDEAL V_j (fps)	W8 (PPS)	V_2 10 Log ρ_8	V_0 10 Log ρ_0	PEAK PNdB	PEAK ANGLE	30°	40°	50°	60°	70°	80°	90°
	4/22/68 5.6-56B-10 X_S = 2.925", L_S = 3.5"														
1	2.04	2797	2512	6.7	-25.2	-7.4	134.2	60	122.3	127.2	131.9	133.4	129.6	127.2	126.5
2	2.56	2799	2849	8.4	-24.6	-6.9	137.7	60	125.3	130.7	135.0	136.9	133.2	131.1	130.7
3	3.07	2476	2896	10.7	-22.9	-6.0	138.4	60	128.3	133.1	136.2	137.5	134.3	132.5	132.4
4	3.08	2811	3090	10.0	-24.0	-6.5	139.4	50	128.5	133.1	137.3	138.4	135.5	132.9	133.6
5	3.08	1987	2599	12.0	-20.9	-5.0	138.5	50	127.3	132.4	136.3	135.9	132.9	131.5	130.7
6	1.58	1266	1371	7.8	-18.8	-4.1	125.6	50	114.6	116.9	123.5	121.0	121.9	119.7	118.1
7	1.36	1116	1065	6.6	-17.7	-3.4	109.6	50	102.0	104.5	107.5	108.6	107.6	108.2	107.3
	4/29/68 5.6-56B-11 X_S = 2.055", L_S = 0														
1	3.10	2812	3098	10.5	-23.9	-6.5	140.8	60	127.9	132.8	138.0	140.0	135.7	132.4	132.2
2	3.08	2509	2921	11.0	-23.0	-6.0	139.7	60	128.1	133.0	137.2	138.9	134.6	132.0	131.9
3	3.10	1991	2608	12.5	-20.9	-5.0	140.5	50	128.2	133.3	138.4	136.9	133.1	130.3	130.0
4	1.57	1237	1346	7.8	-18.6	-4.0	117.7	50	111.2	112.5	115.6	114.6	114.6	112.6	113.3
5	1.37	1024	1034	7.1	-17.0	-3.1	110.5	80	102.9	106.0	107.9	108.5	108.9	110.9	109.8
	4/29/68 5.6-56B-12 X_S = 2.055", L_S = 14"														
1	1.38	1040	1049	7.2	-17.1	-3.1	106.4	30	99.7	101.8	102.5	104.6	104.8	102.6	105.3
2	1.58	1263	1370	8.0	-18.8	-4.1	115.9	30	109.3	111.2	111.7	112.4	112.2	110.6	110.2
3	3.10	2040	2639	12.2	-21.2	-5.1	138.6	50	127.3	132.8	136.5	136.0	132.4	129.3	128.6
4	3.09	2515	2928	10.9	-23.0	-6.0	139.2	50	127.1	132.2	137.0	137.4	133.6	131.0	130.6
5	3.09	2814	3096	10.4	-24.0	-6.5	139.5	50	126.3	132.0	137.3	137.6	134.5	131.6	132.1
6	2.55	2777	2833	8.8	-24.5	-6.9	137.8	60	124.6	130.4	135.4	137.0	132.5	128.7	128.4
7	2.04	2746	2489	7.1	-25.1	-7.3	134.1	50	120.6	126.9	132.0	131.3	128.6	125.8	123.9

- o 5.6" Cone
- o B.J. Doors @ 17 1/2° to ℄
- o D_S/D_8 = 1.24
- o D_9 = 7.0", D_9/D_S = 1.0
- o 8.4" Shroud I.D.
- o D_{Shroud}/D_S = 1.2
- o Leading Edge of Shroud @ D_9

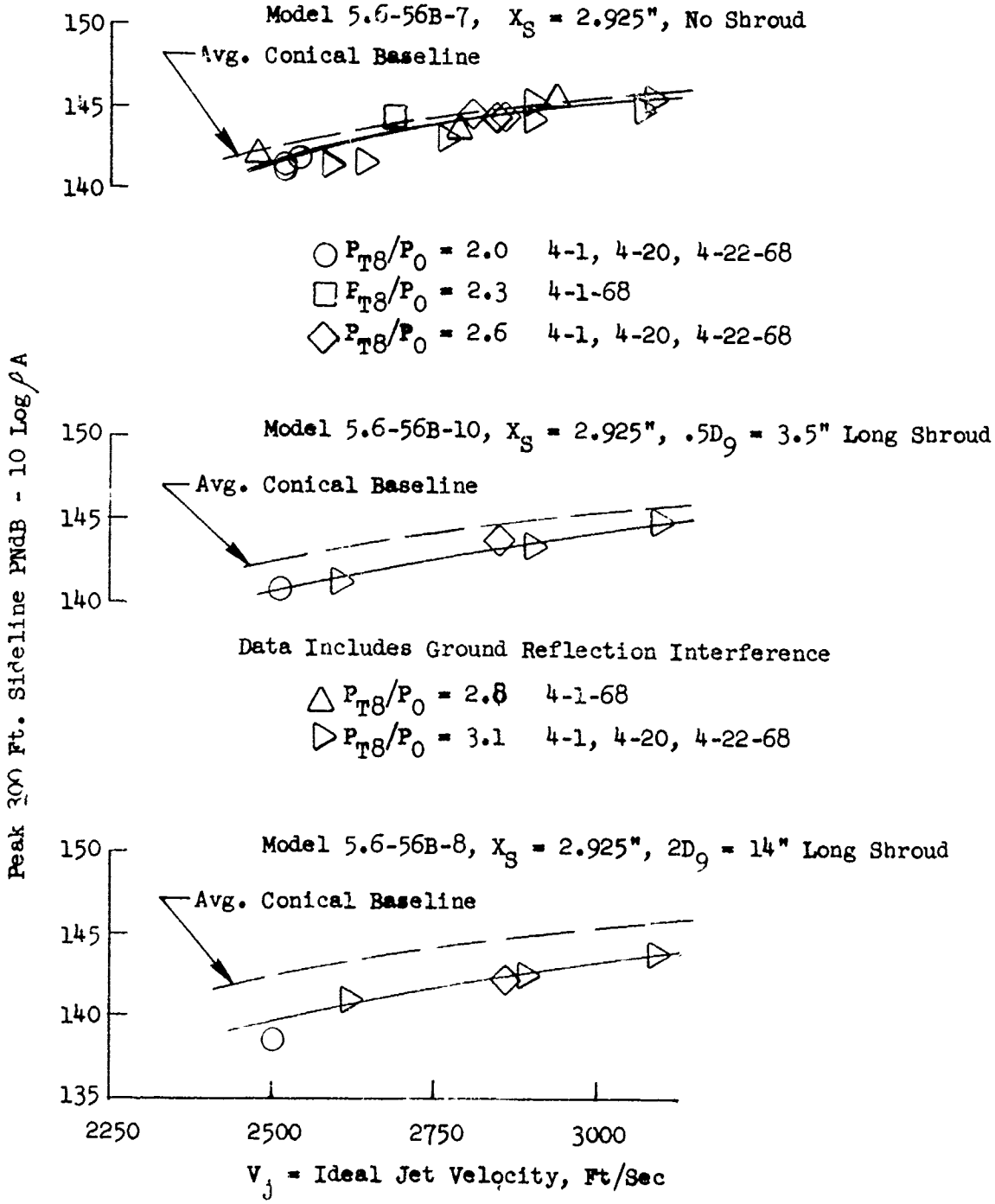

FIGURE V.B-18A 300 FT. SIDELINE JET NOISE LEVELS FOR TSEN-56 PLUS SHROUD CONFIGURATIONS

- o 5.6" Cone
- o B.I. Doors @ 17 1/2° to ℄
- o D_S/D_8 = 1.24
- o D_9 = 7.0"
- o D_9/D_S = 1.0
- o 8.4" Shroud I.D.
- o D_{Shroud}/D_S = 1.2
- o Leading Edge of Shroud @ D_9

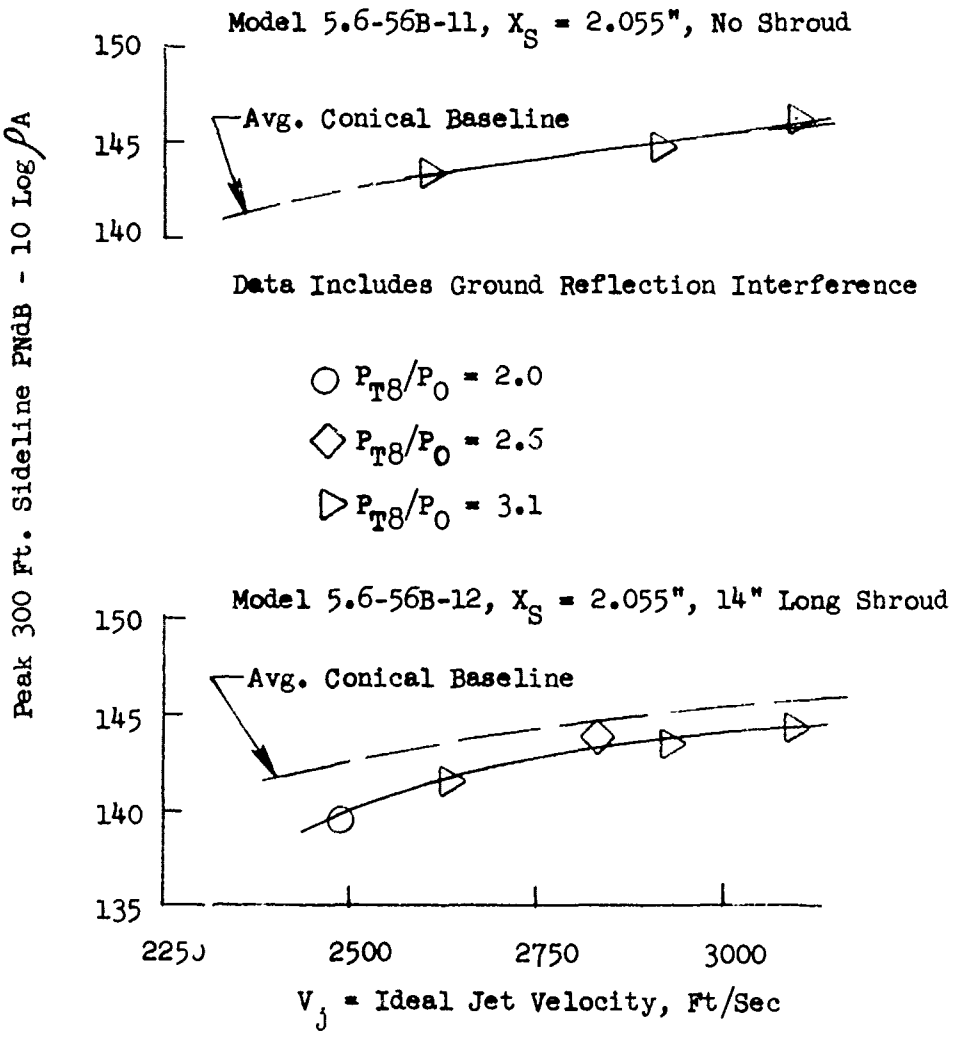

FIGURE V.B-18B 300 FT. SIDELINE JET NOISE LEVELS FOR TSEN-56 PLUS SHROUD CONFIGURATIONS

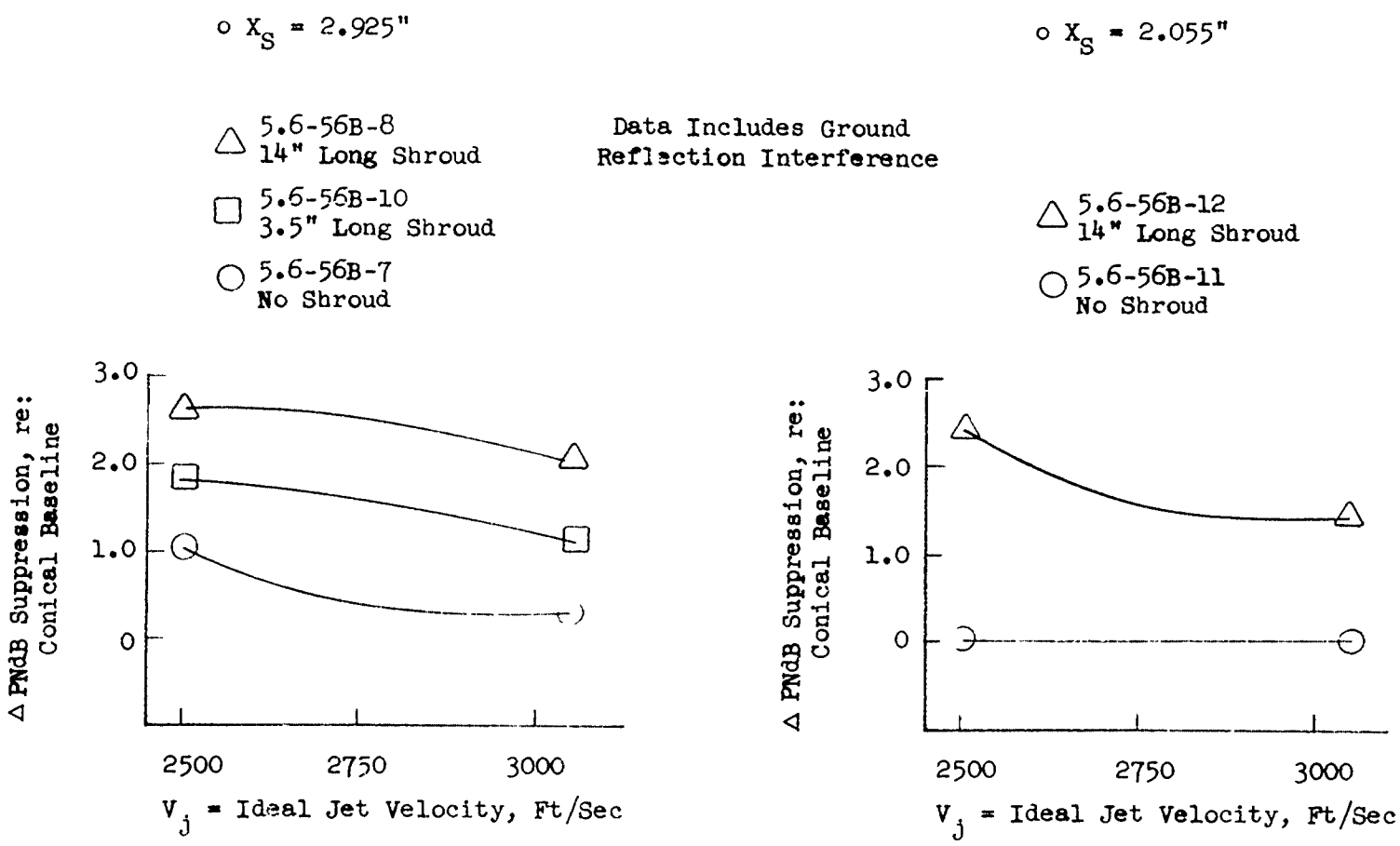

FIGURE V.B-19 EFFECT OF SHROUD ON TSEN-56 PNL SUPPRESSIONS

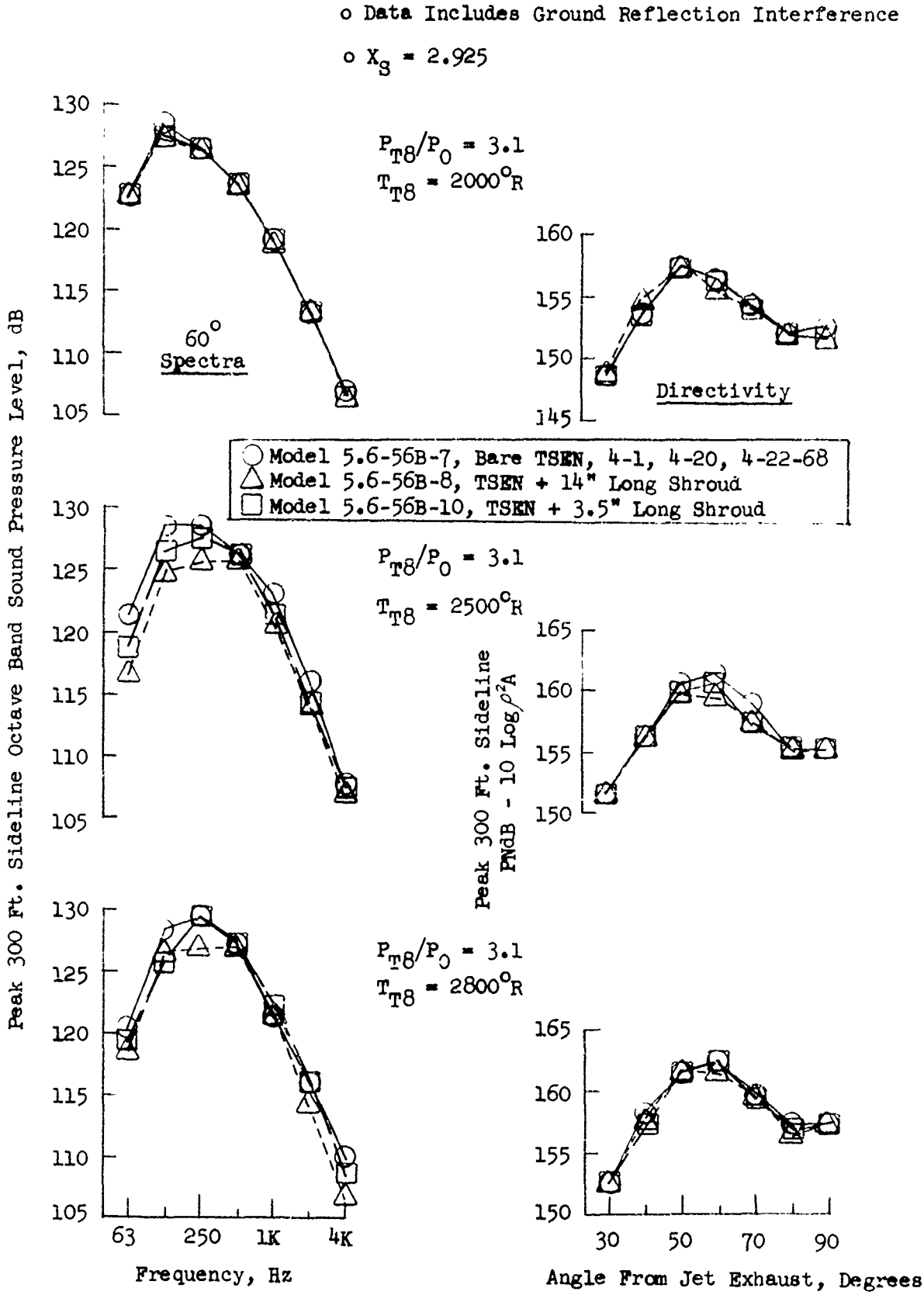

FIGURE V.B-20A EFFECT OF SHROUD ON TSEN-56 SPECTRA AND DIRECTIVITY

X_S = 2.055" — Model 5.6-56B-11, Bare TSEN ●
Model 5.6-56B-12, TSEN + 14" Long Shroud ▲

X_S = 2.925" — Model 5.6-56B-7, Bare TSEN, 4-1, 4-20, 4-22-68 ○
Model 5.6-56B-8, TSEN + 14" Long Shroud △

Data Includes Ground Reflection Interference

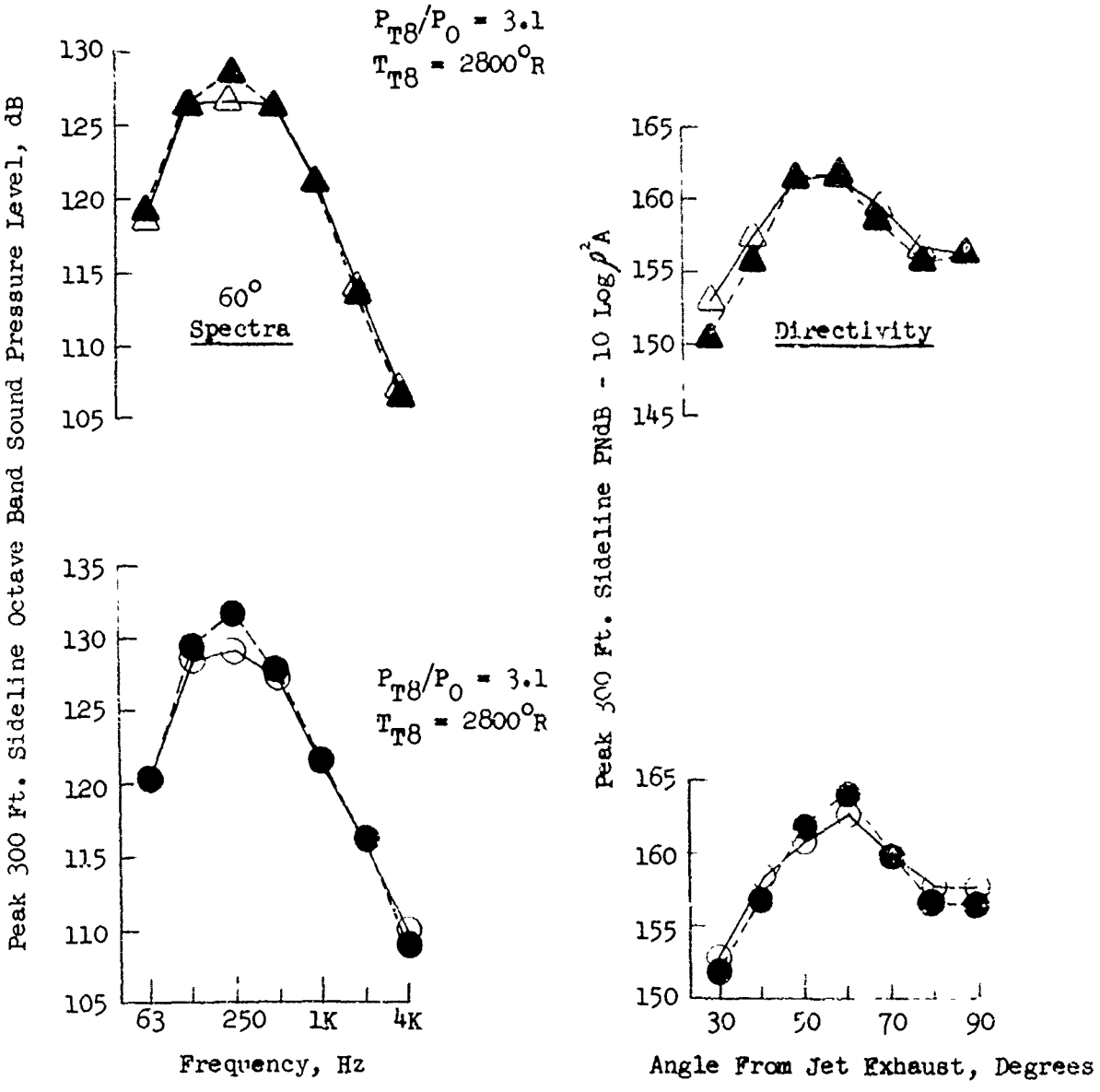

FIGURE V.B-20B EFFECT OF SHROUD CN TSEN-56 SPECTRA AND DIRECTIVITY

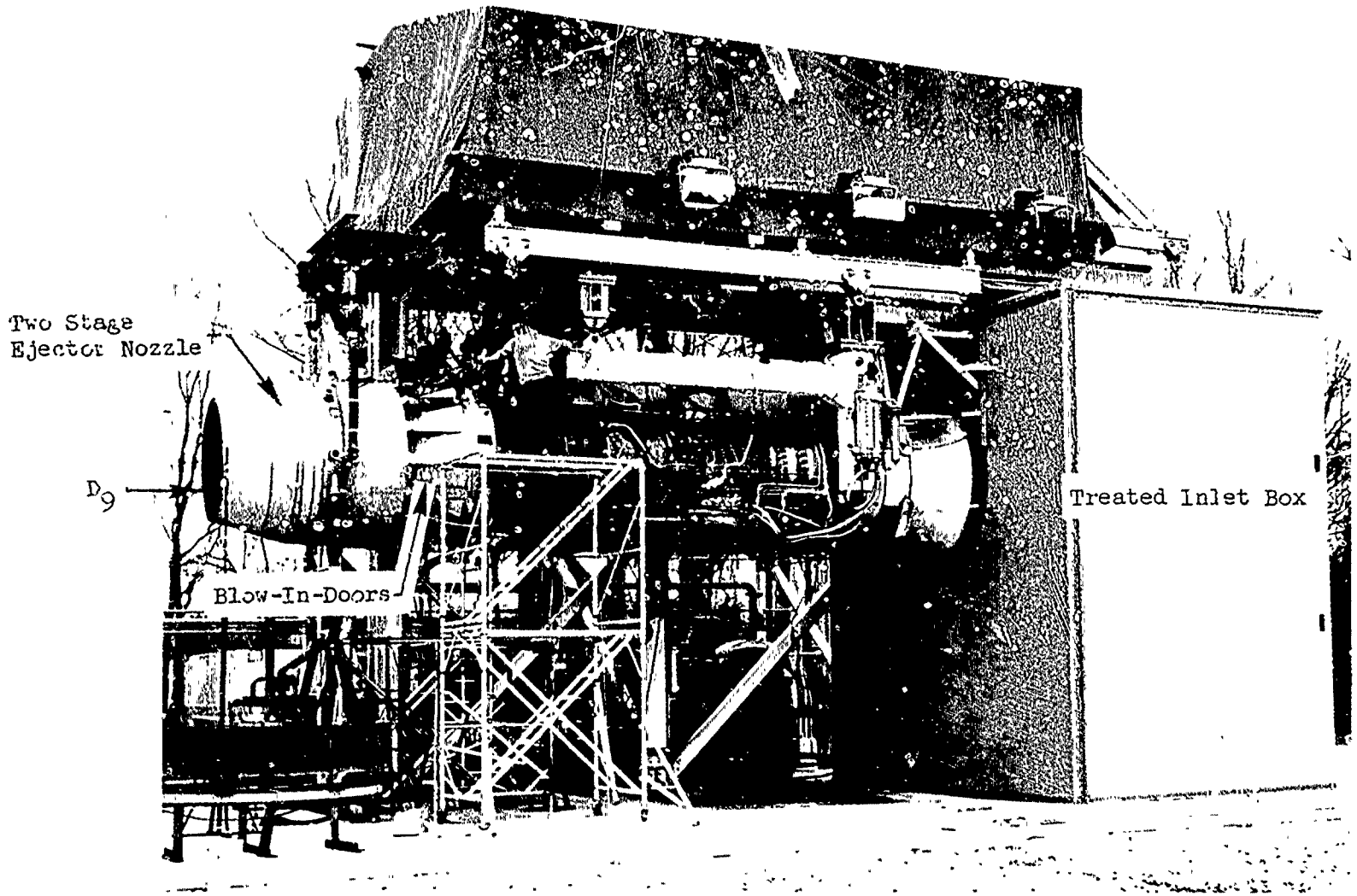

FIGURE V.B-21 GE4/SST ENGINE 435-002 MOUNTED ON PEEBLES SITE IV ACOUSTIC FACILITY

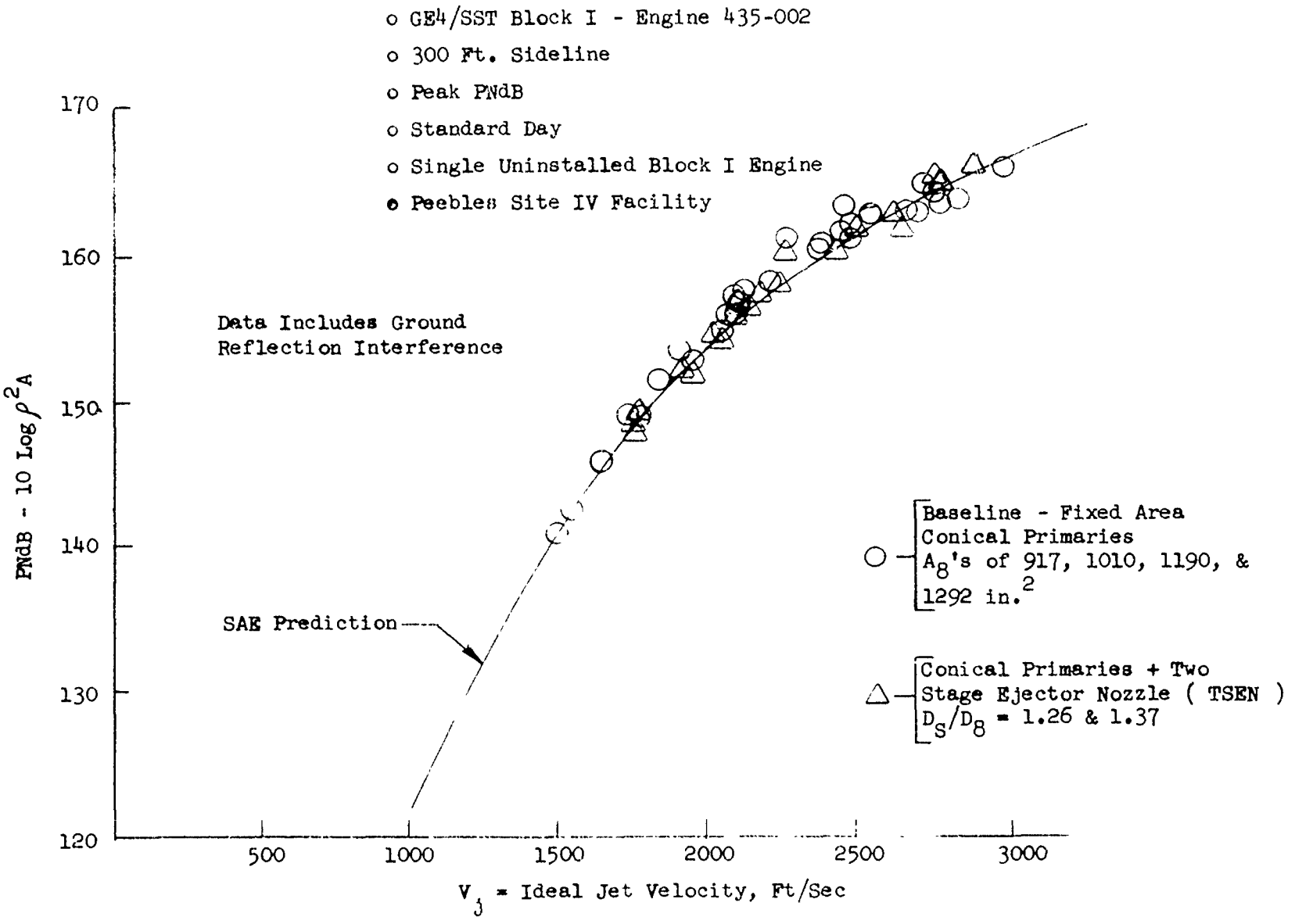

FIGURE V.B-22 GE4 ENGINE NOISE MEASUREMENTS - CONICAL PRIMARY AND CONICAL PRIMARY PLUS TSEN

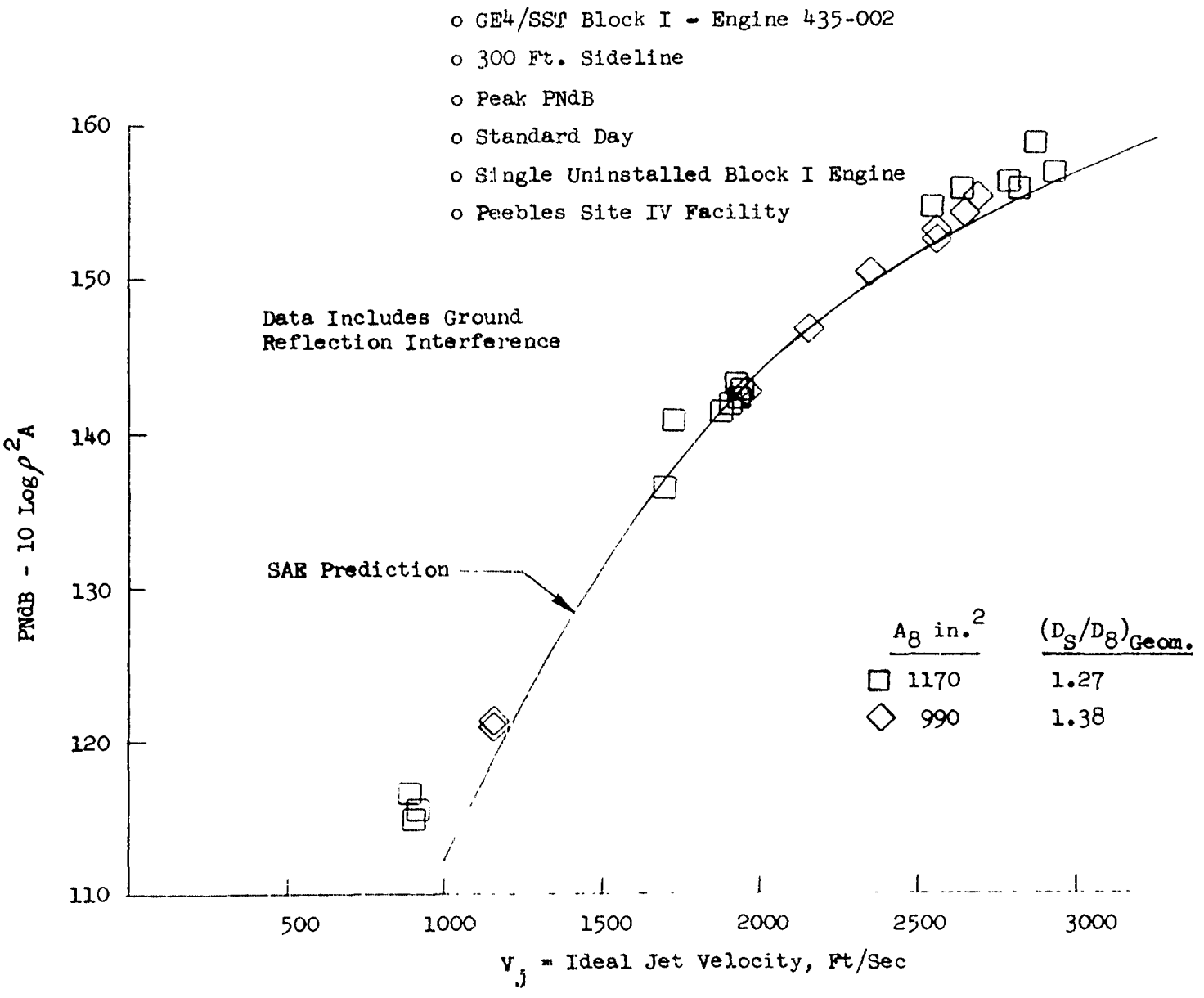

FIGURE V.B-23 GE4 ENGINE NOISE MEASUREMENTS - STAR PRIMARY PLUS TSEN

V.C PRIMARY SUPPRESSOR MODELS WITH CONICAL EJECTORS

V.C. PRIMARY SUPPRESSOR MODELS WITH CONICAL EJECTORS

Primary suppressor configurations with cylindrical ejectors or two stage ejector nozzles (TSEN) are described in Sections V.C.1, V.C.2, and V.C.3. Included within the sections are representative model configurations and results of selective tests relating to primary radial rods and primary thrust reverser tabs within TSEN systems, and a high and low ideal jet velocity study on primary vented chutes, respectively.

Model acoustic data presented in these sections are scaled to engine size.

PRECEDING PAGE BLANK-NOT FILMED

V.C.1 PRIMARY RADIAL RODS WITHIN TSEN-3

PRECEDING PAGE BLANK-NOT FILMED

V.C.1 PRIMARY RADIAL RODS WITHIN TSEN 3

Test Objectives and Setup

Several test series were conducted to determine primary nozzle mechanical obstruction effects on acoustic performance when used within a Two Stage Ejector Nozzle (TSEN) system. Three of the test series were performed at the GE, Evendale JENOTS acoustic facility with model hardware. The fourth was a GE4 Block I engine test at the Peebles Site 4D acoustic facility.

The test phases and variables investigated are as follows:

- Phase I - Star Primary + TSEN 3 + Separate Primary Radial Rods
  - a) Rods located alternately aft of peaks and valleys of star
  - b) Variable penetration of rods at 13, 33 and 53%
- Phase II - Cone Primary + TSEN 3 + Integral Primary Rods
  - a) Variable penetration of rods at 10, 35, 60 and 78%
  - b) Angular location of rods relative to gas stream at 22.5°, 45° and 90°
  - c) TSEN axial positions of X_S = 1.81" and 2.93" with fixed rods
- Phase III - Cone Primary + TSEN 3 + Separate Radial Rods
  - a) Radial rods on conical versus star primary
  - b) Radial rod positioning at D_S and aft of Plane 8
- Phase IV - GE4 Block I Engine - Cone Primary - Separate Radial Rods
  - a) Full scale suppression effect of radial rods

Each study phase will be discussed individually.

Acoustic measurements for the model tests at the JENOTS facility were taken on a 40 ft. arc at 10° intervals from 30° through 90° from the jet exhaust axis. The measurements were scaled by frequency and size to full scale application using a scale factor of 8:1. All data presented within this section are, therefore, of simulated engine size and engine frequency range.

Test conditions for the model series followed a matrix of test conditions over a jet velocity range of 2000 to 3100 ft/sec. A matrix of P_{T8}/P_o and T_{T8} settings was investigated for most of the models with values of P_{T8}/P_o at 2.0, 2.5 and 3.0 and T_{T8}'s at 2000, 2500 and 2800° R.

PRECEDING PAGE BLANK-NOT FILMED

Test Configurations, Presentation and Discussion of Results

o Phase I - Star Primary + TSEN 3 + Separate Primary Radial Rods

Figure V.C.1-1 is a schematic and list of model numbers and hardware details of the five TSEN 3 configurations of this test phase. The system consisted of 8 equally spaced wedge shaped radial rods positioned just aft of the primary nozzle exit plane, (separate rods as opposed to integral) and mounted within the TSEN so as to be alternately in line with the peaks and valleys of the star primary nozzle. Three penetration settings of 13, 33 and 53% of the effective star primary D_8 were tested with rods in line with the star peaks and the latter two penetrations with rods in line with the star valleys.

Table V.C.1-1 summarizes the acoustic test results for the five test configurations. Figure V.C.1-2 is a plot of the 300 ft. sideline peak normalized PNL as a function of jet velocity, rod penetration and rod orientation. Three acoustic baseline model curves are included, namely, a) conical primary alone, b) star primary alone, and c) star primary plus TSEN 3 without radial rods. The peak PNL suppression plot of Figure V.C.1-3, derived from Figure V.C.1-2, shows 1.1, 2.3, and 3.4 PNdB total suppression relative to the star primary for 13, 33 and 53% penetrations, respectively, at V_J of 3075 ft/sec (or 0.4, 1.6, and 2.7 PNdB relative to the conical primary). The same TSEN 3 configuration set-up was used for each of the models with X_S at 2.93" and blow-in-doors at 10°. TSEN contribution to the total suppression is also shown on Figure V.C.1-3. Suppression remained the same with the rods in line with either the peaks or valleys of the star primary. Reverse flow through the tertiary blow-in-doors passages was noted for the high penetration model for primary stream conditions at and above P_{T8}/P_o of 3.0 and T_{T8} of 2000° R. This was partially attributable to the D_S being positioned 2.93" aft of the primary nozzle exit plane.

Peak 300 ft. sideline noise angle spectra plus normalized PNL directivity are included at three primary nozzle conditions as Figures V.C.1-14A and -14B for rods in line with the peaks and valleys of the star, respectively.

o Phase I - Conclusions

a) Primary obstructions just aft of plane 8 gave suppressions up to 2.7 dB

relative to the conical baseline for 53% penetration. Suppression increased almost linearly with the increased rod penetration.

b) Equal suppression levels were attained independent of rod orientation aft of the star peaks or valleys.

o Phase II - Cone Primary + TSEN 3 + Integral Primary Rods

The first part of the Phase II test series was accomplished with the first eight model configurations of Figure V.C.1-5. This was an investigation of the effect of integral rod penetration and location of TSEN aft of the primary exit plane for each rod penetration setting. The radial rod primary nozzles were designed to have the same geometric effective D_8 of 4.9" and the same effective D_S/D_8 of 1.24 while varying rod penetration at setting 10, 35, 60, and 78%. Each model had 16 rods positioned in the A_8 plane and radially perpendicular to the jet axis. Each of the four primary nozzles was tested with the TSEN 3 positioned at X_S= 1.81" and 2.93".

The second part of the Phase II test series was accomplished with model test numbers 5, 6, 9, 10 and 11 of Figure V.C.1-5. This series investigated the effect of varying rod angle of attack to the jet stream, α. The models had a fixed rod penetration of 60% and angular inclinations to the jet axis of α = 22.5°, 45°, and 90°. Again the two TSEN axial locations of X_S= 1.81" and 2.93" were used on all but the α = 45° model, where only X_S of 2.93" was used.

Acoustic test results for the eleven configurations are summarized in Tables V.C.1-2 through V.C.1-7 in the order of which they appear on the listing of Figure V.C.1-5. Jet noise levels, in the form of 300 ft. sideline peak normalized PNL plots as a function of jet velocity, are included as Figures V.C.1-6A through -6D for the first eight configurations which investigated rod penetration and TSEN aixal location. Figures V.C.1-7A and -7B are similar plots for the remaining three models which investigated rod angularity and TSEN axial location. From the plots it is seen that noise levels generated by most of the models were considerably pressure ratio dependent. For the purpose of uniform data comparison, average noise level curves were construted using only the P_{T8}/P_o = 3.0 data. Each of the figures has the individual model's data plotted, the average P_{T8}/P_o curve constructed, and then comparison of the average noise curves to the conical baseline curve (at the top of the figure).

A summary of the acoustic suppression results is shown in Figure V.C.1-8; part a) showing variance of rod penetration and TSEN axial positioning and part b) showing variance of rod angularity and TSEN axial positioning. All data are for P_{T8}/P_o = 3.0, T_{T8} = 2800° R and V_J = 3050 ft/sec and are referenced to the baseline conical nozzle. With the rods within the A_8 plane, Figure V.C.1-8a, highest suppression of about 4.8 PNdB was obtained with maximum penetration tested of 78%. The curves for the two axial TSEN spacings each have a dip in suppression level in the intermediate penetration range and increase to about 2 PNdB suppression at 10% penetration.

Figure V.C.1-8a also shows that best position of the TSEN 3 aft of plane 8 depends on what penetration radial rod primary nozzle is being used. At the maximum tested penetration setting of 78%, D_S positioning nearer plane 8 increased suppression by 1 dB. However, Figure V.C.1-8a suppression curves for the two TSEN positions criss-crossed for low and high penetration values and as such do not define a set "best" position. Reverse flow was not evident for any of the above models at either TSEN position; however, pumping characteristics were better for the X_S = 1.81" setting.

For variation of rod angularity, Figure V.C.1-8b shows a maximum suppression of about 4.7 PNdB was obtained for the 45° model with the TSEN positioned at X_S of 2.93". This TSEN 3 position gave higher suppression for each of the angular positions at the 60% rod penetration. This is reversed from the better 1.81" position of the maximum suppresion 78% penetration radial rod model. The apparent increased suppresion above the radial rod (90°) model for the 22.5° and 45° inclined rod models may be partially attributable to the high reverse flow through the tertiary blow-in-door passages which appeared for both canted rod models at and above P_{T8}/P_o = 2.5, T_{T8} = 2800° R. The reverse flow was due to the large radial flow component imposed on the primary flow by the skewed spokes, especially at higher pressure ratios.

o Phase III - Cone Primary + TSEN 3 + Separate Radial Rods

The two test series convered in this phase, i.e., comparative effect of radial rods on conical versus star primary nozzles and effect of radial rod positioning at D_S as compared to just aft of the A_8 postion, were accomplished with a 4.82" D_8 conical nozzle plus 8 radial rods mounted in TSEN 3. Figure V.C.1-9 shows the specifics of each of the four model configurations. The

First two models had 8 radial rods just aft of plane 8 at alternate penetration settings of 33 and 53%. These were tested for direct comparison to Phase I star primary nozzle tests with the same radial rod location and penetrations and the same TSEN 3 set-up at X_S = 2.93" (see Figure V.C.1-1).

The last two models of Figure V.C.1-9 were identical to the first two except for rod location at the D_S. Effect of axial rod location was the object of these tests.

A summary of the acoustic test results for the four models is presented in Tables V.C.1-8 for the rods just aft of plane 8 and in Table V.C.1-9 for the rods at D_S. Acoustic data plots similar to those of the previous test phase are included on Figures V.C.1-10 and -11, again with mean lines through the P_{T8}/P_o = 3.0 data and with suppression presented at P_{T8}/P_o = 3.0, T_{T8} = 2800° R. Before quoting suppression levels it should be noted that heavy reverse flow through the tertiary blow-in-door passages was present for all four models (all with TSEN at X_S = 2.93") at P_{T8}/P_o = 3.0 for T_{T8}'s of 2000° R and above, just as was present with the Phase I star primary models with high radial rod penetration.

Figure V.C.1-11 shows that rods positioned just aft of plane 8 attain similar suppression levels independent of whether a star or conical primary nozzle is used. Comparison of the 8 radial rod 53% penetration model of Figure V.C.1-11 to a similar 16 integral radial rod model of 60% penetration (Figure V.C.1-8a) shows the attained suppression to be essentially the same at about 2 PNdB. A similar comparison of the 8 rod - 33% penetraton model (Figure V.C.1-11) to the 16 rod - 35% penetration model (Figure V.C.1-8a) shows 1.8 PNdB versus 0.9 PNdB for the 8 and 16 rod models respectively. Trends indicate that, when positioned at or just aft of plane 8, 8 rods will perform acoustically as well as 16 rods. The reverse flow which was present with the 8 rod models and not the 16 rod models is due to the rod positioning; the 8 rods located aft of plane 8 and the 16 rods being an integral part of plane 8.

Moving the 8 radial rods downstream to the D_S position added about 1 PNdB suppression for the 53% penetration model, again accompanied with presence of flow reversal.

Concurrent with the acoustic evaluation, a series of tests were performed at FluiDyne Engineering Corporation to ascertain thrust coefficient characteristics of the radial rod system as a function of a) rod penetration, and b) TSEN exit diameter variation. Figure V.C.1-12 is a photograph of the assembled model and the wedge-shaped leading edge suppressor spokes. The effects of penetration and TSEN diameter ratio (D_9/D_S) on nozzle gross thrust is presented in Figure V.C.1-13. Performance decreases as either the exit diameter (D_9) or rod penetration increase. Thrust losses relative to the baseline TSEN were noted to be about 6% at the P_{T8}/P_o = 3.0 near 45% penetration and above. The radial rod suppressor configuration exhibited pumping characteristics similar to that of the baseline TSEN. The secondary nozzle contour static pressure distribution of the 60% penetration configuration is compared to that of the baseline TSEN in Figure V.C.1-14. The data indicate that the rods had minor effect on the ejector contour static pressure distribution.

o Phase IV - GE4 Block I Engine - Cone Primary - Separate Radial Rods

The test results of the model radial rod suppression system led to radial rod testing on the Block I GE4 engine at Peebles. Figure V.C.1-15 is a photo of the GE4 hardware with the spokes set at 65% penetration. The rods were positioned axially just aft of the A_8 plane. Ceramic rods were initially tested until a material failure necessitated replacement with metallic rods. The leading edge of the spokes was basically wedge-shaped at a total angle of 70° and the spokes were evaluated with the D_S/D_8 = 1.26 TSEN system.

Figure V.C.1-16 (top) presents peak 300 ft. sideline normalized PNdB levels along with the SAE predicted baseline and the GE4 measured baseline. The PNL suppression plot at the bottom of Figure V.C.1-16 shows suppressions in the order of 5.5 PNdB were obtained in 2100 ft/sec velocity range while at the 2900 ft/sec velocity regime suppression dropped off to about 2.5 PNdB. Examination of Figure V.C.1-16 also indicates no discernible acoustic effects due to the material (ceramic vs. metallic) of the rods.

• TSEN = Two Stage Ejector Nozzle

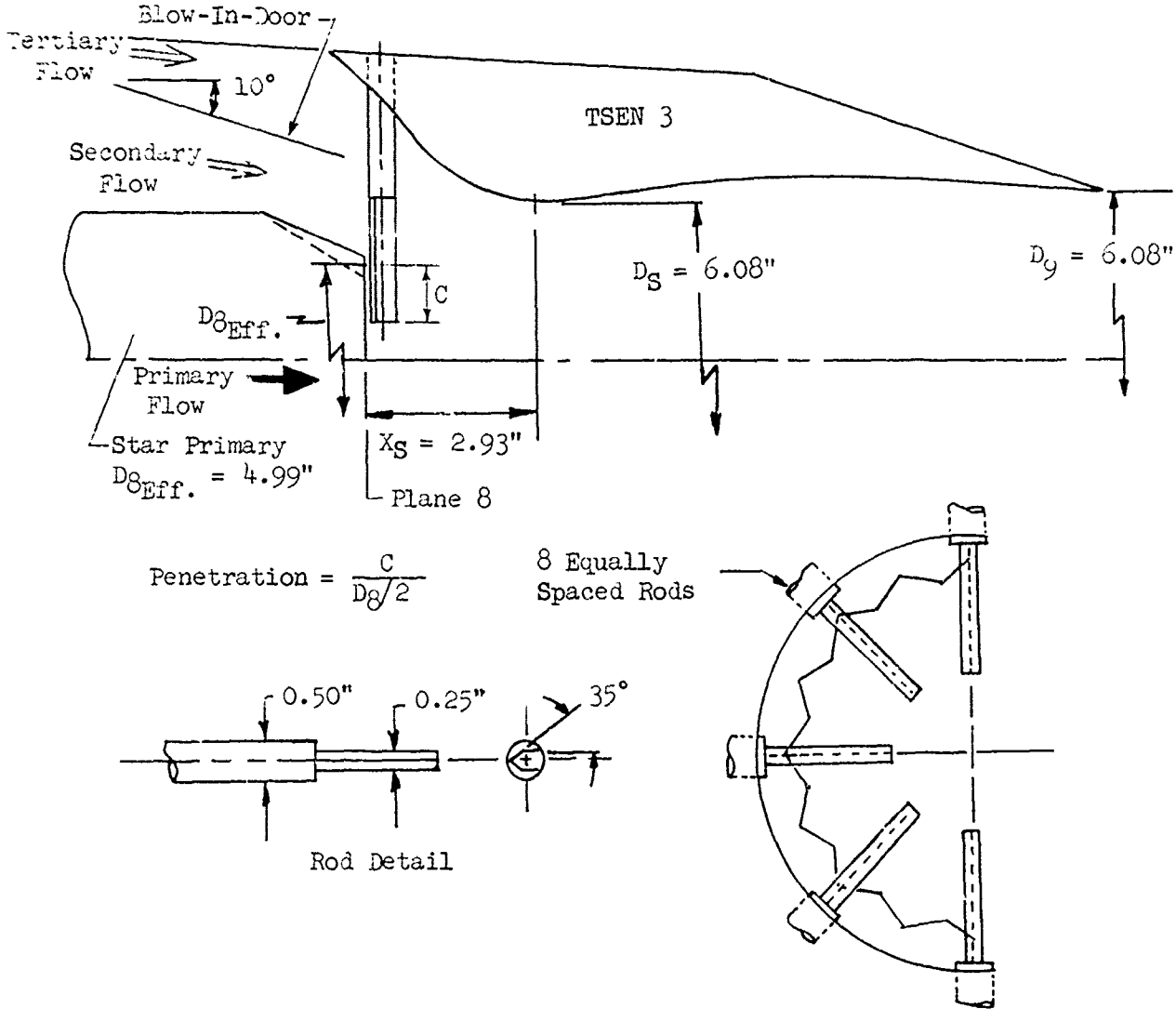

MODEL NO.	TEST DATE	D_S/D_8 PHYS.	NO. OF PRIMARY BLOCKERS	AFT OF PEAKS OR VALLEYS	% PENET.
5.1S-3B-6	2-22-68	1.24	6	Peaks	13
5.1S-3B-7	2-22-68	1.27	8	Peaks	33
5.1S-3B-9	2-24-68	1.27	8	Valleys	33
5.1S-3B-8	2-23-68	1.31	8	Peaks	53
5.1S-3B-10	2-24-68	1.31	8	Valleys	53

FIGURE V.C.1-1 SCHEMATIC OF TSEN 3 WITH (8) RADIAL RODS AFT OF STAR PRIMARY PLANE 8

TABLE V.C.1-1 TEST SUMMARY

MODEL NO. 5.1S-3B-6; -7; -8; -9; -10

DESCRIPTION: 5.1 Stat - TSEN 5, 8 Radial Rods in TSEN 3 Penetrations of 13, 33, 53%

DATE: 2/22/68; 2/23/68; 2/24/68

SCALE MODEL A_8 = Noted

FULL SCALE A_8 = Noted

SCALE FACTOR = 8:1

o DATA INCLUDES GROUND REFLECTION INTERFERENCE

o NOISE RUNS VOIDED DUE TO JET EXIT TEST

TEST CONDITIONS					10 Log $\frac{?}{A}$	10 Log $\frac{}{A}$	ACOUSTIC TEST RESULTS							
							320 FT ARC		300 FT. SIDELINE PNL DIRECTIVITY					
Adg. No.	P_{TS}/P_o	T_{TS} (°R)	IDEAL V_8 (ft^3)	V_8 (FPS)			PEAK PNLB	PEAK ANGLE	30°	40°	50°	60°	70°	80°	90°
	2/22/68	5.1S-3B-6			13% Penetration, Scale Model A_8 = .1344 ft^2, Full Scale A_8 = 8.60 ft^2									
1	2.00	2800	2479	-	-23.3	-8.4	134.4	60	120.6	128.3	130.0	133.5	129.7	127.8	126.6
2	2.50	2800	2814	-	-25.7	-8.0	138.6	60	123.8	129.2	133.9	137.8	133.9	132.0	130.3
3	3.00	2800	3053	-	-25.0	-7.6	138.9	60	125.9	130.9	135.5	139.0	134.0	132.6	131.4
4	3.00	2505	2888	-	-24.1	-7.1	138.9	50	125.4	130.9	135.6	136.8	134.5	133.0	131.4
5	3.00	2010	2587	-	-22.2	-6.1	137.4	50	126.6	131.7	135.3	134.7	133.9	131.6	129.9
	2/22/68	5.1S-3B-7			33% Penetration, Scale Model A_8 = .1283 ft^2, Full Scale A_8 = 8.21									
1	2.00	2800	2482	-	-26.0	-8.4	132.9	60	119.7	124.7	128.7	132.4	129.2	127.1	125.7
2	2.50	2795	2812	-	-25.7	-8.0	136.6	60	124.1	129.2	132.9	136.8	133.2	130.9	131.1
3	3.00	2800	3053	-	-25.1	-7.6	137.2	60	125.9	131.2	134.9	138.6	134.5	132.4	131.2
4	3.00	2500	2884	-	-24.1	-7.1	136.8	60	126.0	130.9	134.3	136.2	133.5	131.4	130.8
5	3.03	2010	2597	-	-22.1	-6.1	135.7	50	125.6	129.8	133.9	133.9	132.3	131.9	129.3
	2/23/68	5.1S-3B-8			53% Penetration, Scale Model A_8 = .122 ft^2, Full Scale A_8 = 7.86									
1	2.00	2800	2464	-	-26.8	-8.9	130.2	60	118.4	123.3	126.9	129.4	126.7	126.4	123.6
2	2.50	2800	2817	-	-26.1	-8.3	134.0	60	123.0	127.3	130.8	134.1	130.8	128.8	128.0
3	3.00	2800	3052	-	-25.5	-7.8	136.1	50	125.0	130.2	133.9	135.1	131.4	131.4	129.8
4	3.00	2700	2[illegible]	-	-24.[illegible]	-7.[illegible]	[illegible].6	60	124.4	129.[illegible]	133.4	135.[illegible]	133.4	131.2	130.1
5	3.00	[illegible]	[illegible]	-	-[illegible]	-[illegible]	134.6	60	124.4	128.6	132.4	134.[illegible]	132.[illegible]	130.1	128.[illegible]
6	3.00	2800	2863	-	-24.5	-7.6	135.4	60	125.2	129.9	135.1	134.5	131.5	130.9	129.5

TABLE V.C.1-1 TEST SUMMARY

(Continued)

MODEL NO. 5.1S-3B-6; -7; -8; -9; -10

DESCRIPTION: 5.1 Star " TSLN 3,8 Radial Rods in TSEN 3 Penetrations of 13, 33, 53%

DATE: 2/22/68; 2/23/68; 2/24/68

SCALE MODEL A_8 = Noted

FULL SCALE A_8 = Noted

SCALE FACTOR = 8:1

o DATA INCLUDES GROUND REFLECTION INTERFERENCE

o ANGLE REFERENCED TO JET EXHAUST

TEST CONDITIONS							ACOUSTIC TEST RESULTS								
Rdg. No.	P_{Tg}/P_o	T_{TS} (°R)	IDEAL V_j (fps)	W_8 (PPS)	10 Log $\rho^2 A$	10 Log ρA	320 FT ARC PEAK PNdB	320 FT ARC PEAK ANGLE	300 FT. SIDELINE PNI DIRECTIVITY 30°	40°	50°	60°	70°	80°	90°
	2/24/68	5.1S-3B-9			33% Penetration, Scale Model A_8 = .1310 ft^2, Full Scale A_8 = 8.38 ft^2										
1	2.02	2800	2495	--	-26.4	-8.6	132.4	60	121.6	125.4	128.7	131.6	128.5	126.3	127.4
2	2.52	2800	2830	--	-25.8	-8.2	136.7	60	124.6	129.2	131.7	135.9	131.9	130.2	128.3
3	3.03	2795	3062	--	-25.2	-7.7	137.3	60	125.4	130.3	134.2	136.4	134.2	132.9	131.1
4	3.03	2500	2896	--	-24.2	-7.2	137.4	60	126.8	131.2	134.8	136.6	132.5	132.2	129.9
5	3.03	2010	2596	--	-22.3	-6.3	135.9	50	126.1	130.8	133.7	133.6	130.8	129.9	128.5
	2/24/68	5.1S-3B-10			53% Penetration, Scale Model A_8 = .1210 ft^2, Full Scale A_8 = 7.74 ft^2										
1	2.02	2800	2497	-	-26.8	-8.9	132.4	60	121.2	125.6	129.4	131.5	127.2	126.2	125.1
2	2.52	2800	2829	-	-26.1	-8.5	135.4	60	124.2	128.7	132.4	135.1	131.2	130.7	128.1
3	3.03	2800	3064	-	-25.5	-8.1	135.8	60	126.6	130.3	133.2	135.0	133.3	131.0	130.3
4	3.03	2500	2895	-	-24.5	-7.6	135.8	60	125.5	130.1	133.3	134.9	132.4	130.7	129.6
5	3.03	2005	2594	-	-22.6	-6.6	134.2	50	124.8	128.0	132.1	132.6	131.4	128.2	127.5

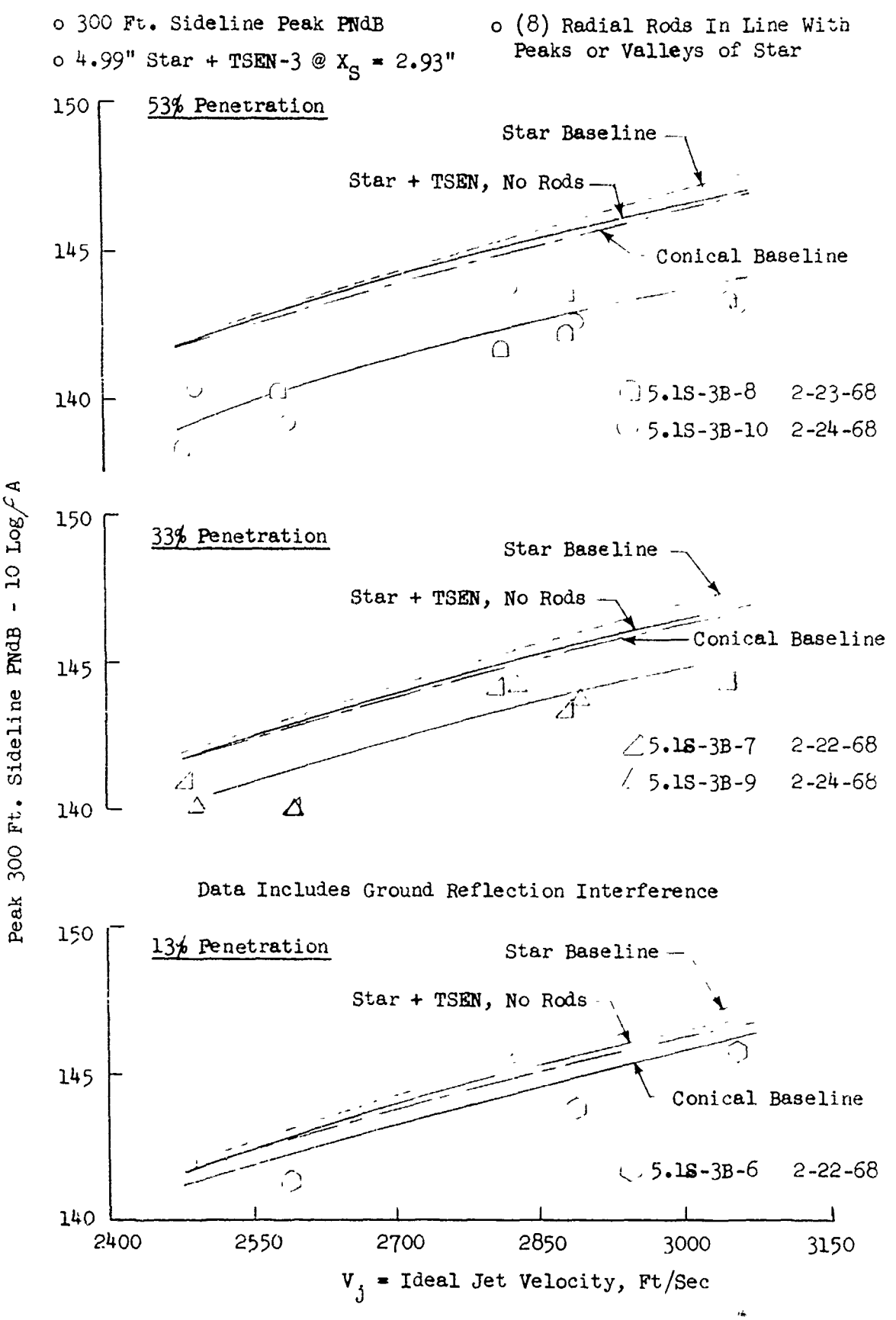

FIGURE V.C.1-2 EFFECT OF RADIAL ROD PENETRATION WITHIN TSEN 3 ON 300 FT. SIDELINE JET NOISE LEVELS

o 300 Ft. Sideline

o 4.99" Star + TSEN-3

Model No.	% Penetration	Rods In Line With
5.1S-3B-6	13	Peak
5.1S-3B-7	33	Peak
5.1S-3B-9	33	Valley
5.1S-3B-8	53	Peak
5.1S-3B-10	53	Valley
5.1S-3B		
Conical Baseline		

Data Includes Ground Reflection Interference

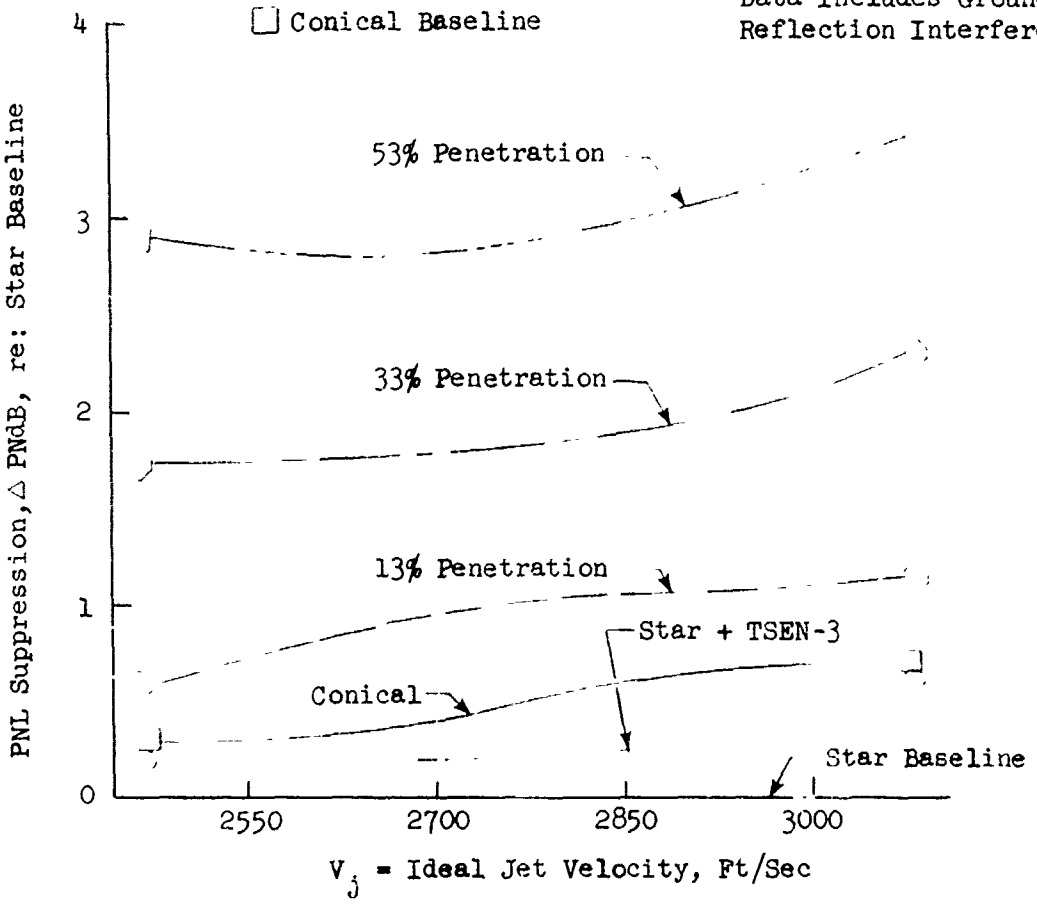

FIGURE V.C.1-3 EFFECT OF RADIAL ROD PENETRATION WITHIN TSEN 3 ON 300 FT. SIDELINE PNL SUPPRESSION

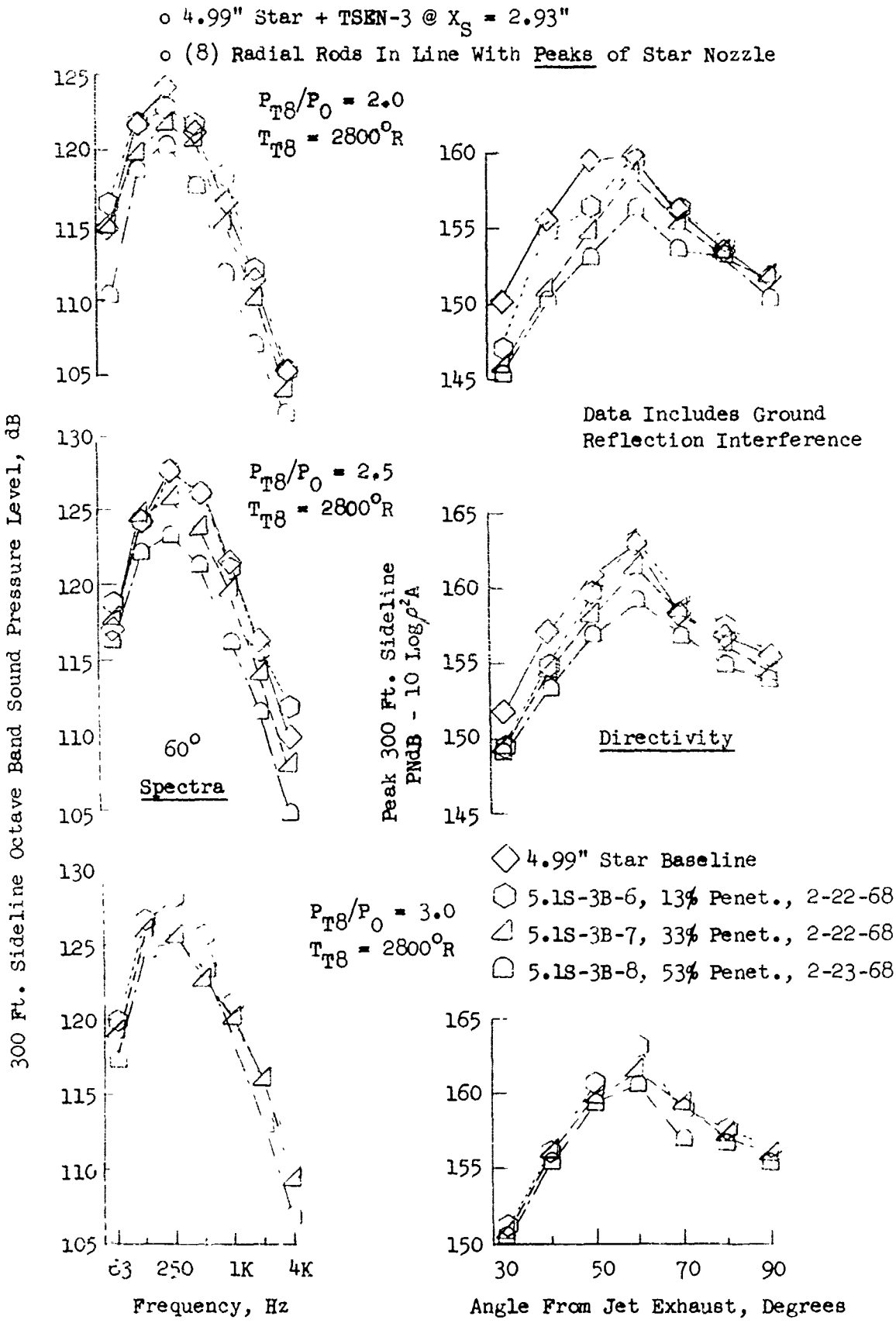

FIGURE V.C.1-4A EFFECT OF RADIAL ROD PENETRATION WITHIN TSEN 3 ON SPECTRA AND DIRECTIVITY

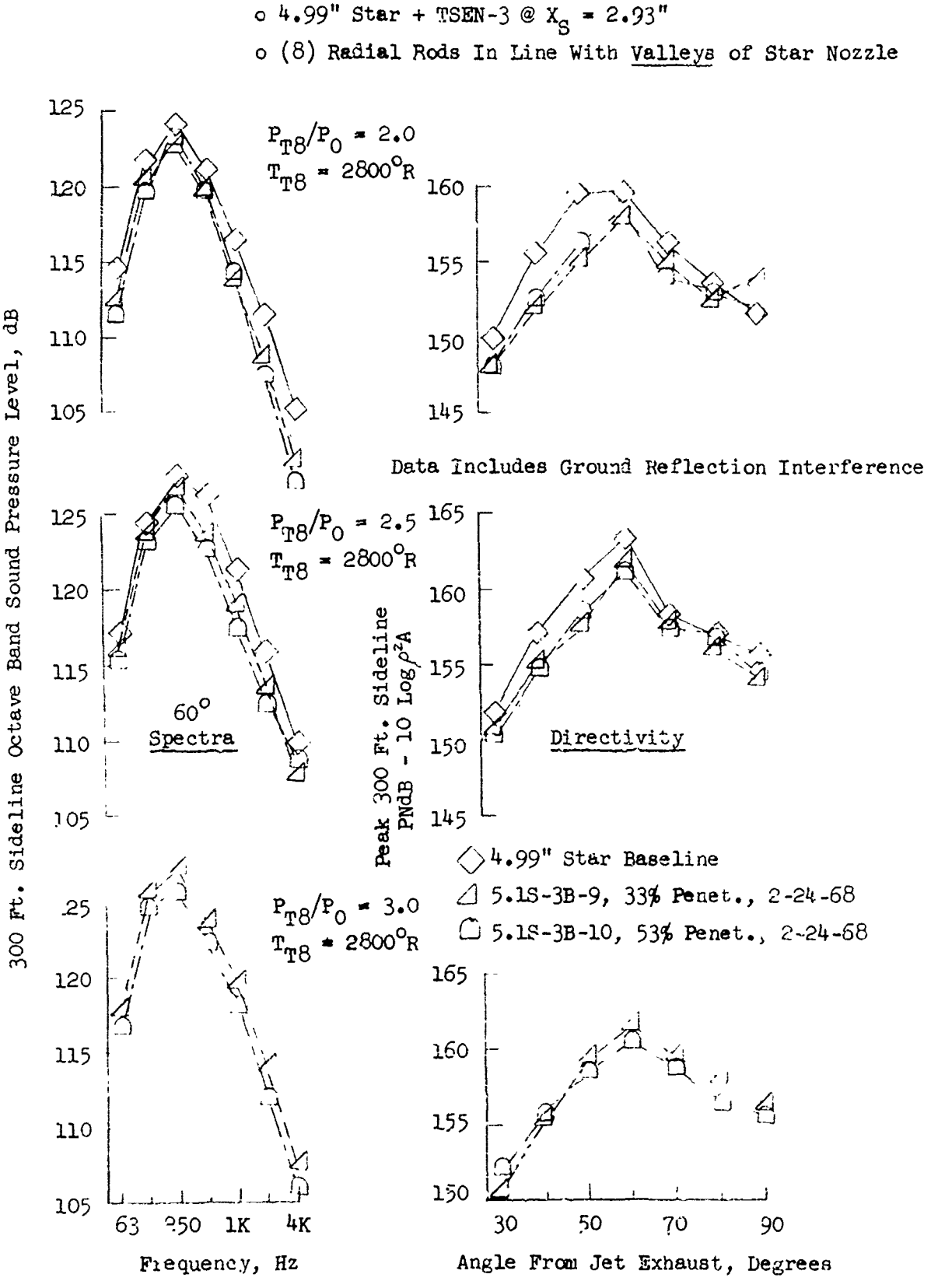

FIGURE V.C.1-4B EFFECT OF RADIAL ROD PENETRATION WITHIN TSEN 3 ON SPECTRA AND DIRECTIVITY

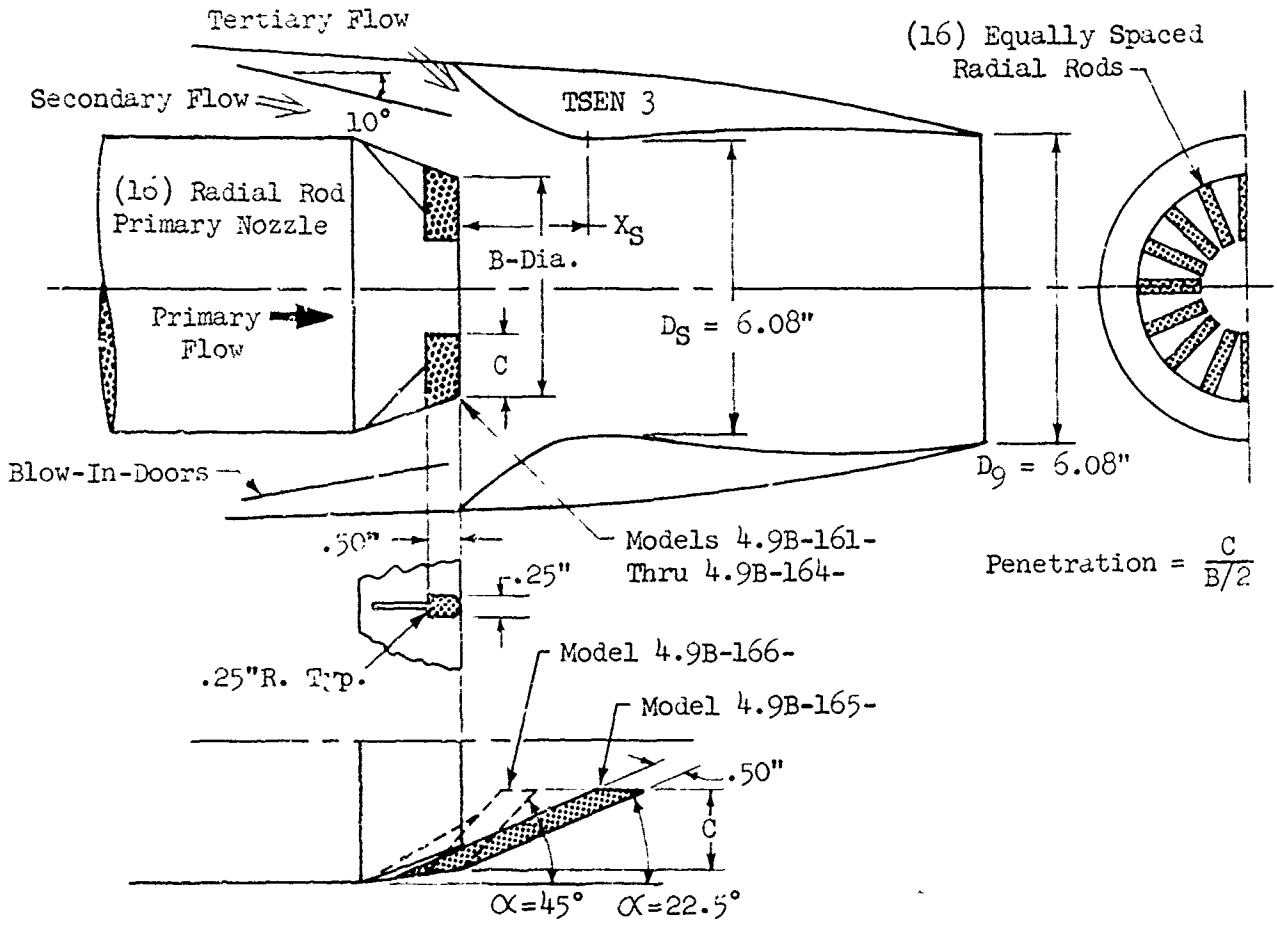

- $D_{8_{Phys.\ Eff.}}$ = 4.9"
- $A_{8_{Phys.\ Eff.}}$ = .1310 Ft^2
- $D_S/D_{8_{Phys.\ Eff.}}$ = 1.24
- TSEN = Two-Stage Ejector Nozzle

TEST NO.	MODEL NO.	TEST DATE	X_S	B	C	% PENET.	∝	% BLOCK. PHYS.	START OF REV. FLOW
1	4.9B-161-3B	3-11-68	2.93"	5.029"	.251"	10	90°	5.1	None
2	4.9B-161-3B-1	3-11-68	1.81"	5.029"	.251"	10	90°	5.1	None
3	4.9B-162-3B	3-13-68	2.93"	5.366"	.939"	35	90°	16.6	None
4	4.9B-162-3B-1	3-13-68	1.81"	5.366"	.939"	35	90°	16.6	None
5	4.9B-163-3B	3-6-68	2.93"	5.723"	1.717"	60	90°	26.7	None
6	4.9B-163-3B-1	3-6-68	1.81"	5.723"	1.717"	60	90°	26.7	None
7	4.9B-164-3B	3-14-68	2.93"	5.993"	2.337"	78	90°	33.1	None
8	4.9B-164-3B-1	3-14-68	1.81"	5.993"	2.337"	78	90°	33.1	None
9	4.9B-165-3B	3-18-68	2.93"	5.723"	1.717"	60	22.5°	26.7	P/R 2.5, 2000°R
10	4.9B-165-3B-1	3-18-68	1.81"	5.723"	1.717"	60	22.5°	26.7	P/R 2.5, 2000°R
11	4.9B-166-3B	3-19-68	2.93"	5.723"	1.717"	60	45°	26.7	P/R 2.5, 2800°R

FIGURE V.C.1-5 SCHEMATIC OF (16) RADIAL ROD PRIMARY NOZZLE PLUS TSEN 3

TABLE V.C.1-2 TEST SUMMARY

TEST NO. 4.9B-161-3B; -3F-1

DESCRIPTION: 4.9 Cone + TSIN 3,16 Rods in Cone, α = 90° 10% Penetration, X_S = 2.93" & 1.81"

DATE: 3/11/68

SCALE MODEL A_8 = .1310 ft^2

FULL SCALE A_8 = 8.38 ft^2

SCALE FACTOR = 8:1

- DATA INCLUDES GROUND REFLECTION INTERFERENCE
- ANGLE REFERENCED TO JET EXHAUST

TEST CONDITIONS							ACOUSTIC TEST RESULTS								
			IDEAL		10 Log $\rho^2 A$	10 Log ρA	320 FT ARC		300 FT. SIDELINE PNL DIRECTIVITY						
Rdg. No.	P_{T8}/P_o	T_{T8} (°R)	V_8 (fps)	W_8 (PPS)			PEAK PNdB	PEAK ANGLE	30°	40°	50°	60°	70°	80°	90°
	4.9B-161-3B X_S = 2.93"														
1	2.00	2790	2472	4.86	-26.4	-8.6	134.6	60	121.4	126.7	131.6	133.7	128.2	124.7	122.5
2	2.50	2795	2812	6.11	-25.8	-8.2	137.9	60	124.3	129.3	133.6	137.1	132.4	129.7	127.4
3	2.99	2790	3043	7.35	-25.2	-7.7	138.7	50	126.4	131.8	136.5	137.2	132.9	129.7	128.3
4	3.00	2500	2883	7.82	-24.2	-7.3	137.7	50	126.5	131.5	135.6	135.9	131.2	130.3	127.8
5	3.00	2010	2585	8.81	-22.3	-6.3	136.9	50	126.2	131.1	134.7	133.1	128.4	128.3	127.4
	4.9B-161-3B-1 X_S = 1.81"														
1	2.99	2010	2584	8.7	-22.3	-6.3	137.0	50	126.2	131.1	134.8	133.3	130.0	127.9	126.9
2	2.99	2590	2933	7.7	-24.5	-7.4	137.1	50	125.8	131.0	135.0	135.8	132.7	128.6	128.3
3	3.00	2790	3045	7.4	-25.2	-7.7	138.2	50	126.3	131.4	136.1	137.1	133.6	130.6	128.6

TABLE V.C.1-3 TEST SUMMARY

MODEL NO. 4.9B-162-3B; -3B-1 SCALE MODEL A_8 = .1319 ft^2

DESCRIPTION: 4.9 Cone + TSEN 3,16 Rods in Cone, α = 90° 35% Penetration, X_S = 2.93" & 1.81" FULL SCALE A_8 = 8.38 ft^2

DATE: 3/13/68 SCALE FACTOR = 8:1

o DATA INCLUDES GROUND REFLECTION INTERFERENCE

o ANGLE IS MEASURED TO JET EXHAUST

TEST CONDITIONS							ACOUSTIC TEST RESULTS								
							320 FT ARC		300 FT. SIDELINE PNL DIRECTIVITY						
Pág. No.	P_{T8}/P_o	T_{T8} (°R)	V_j (fps)	W_8 (PPS)	10 Log $\frac{2}{A}$	10 Log $\frac{}{A}$	PEAK PNdB	PEAK ANGLE	30°	40°	50°	60°	70°	80°	90°
		4.9B-162-3B		X_S = 2.93"											
1	2.00	2790	2472	4.9	-26.4	-8.6	134.7	60	-	125.5	131.2	133.8	128.8	126.9	124.8
2	2.50	2790	2810	6.2	-25.7	-8.1	137.5	60	-	128.8	132.0	136.6	133.0	131.2	129.7
3	3.00	2790	3046	7.4	-25.1	-7.7	138.6	60	-	130.6	134.0	137.9	135.1	133.1	131.0
4	3.00	2500	2883	7.8	-24.2	-7.2	138.4	60	-	131.0	134.9	137.5	134.4	132.8	130.6
5	3.00	2010	2585	8.9	-22.3	-6.3	137.4	50	-	131.2	135.2	135.8	132.8	130.9	128.5
		4.9B-162-3B-1		X_S = 1.81"											
1	2.00	2790	2475	4.9	-26.4	-8.6	134.3	60	-	125.7	130.3	133.5	129.1	126.8	124.9
2	2.50	2790	2809	6.2	-25.7	-8.1	137.8	60	-	128.5	132.7	137.0	133.1	131.0	128.9
3	3.00	2790	3047	7.4	-25.1	-7.7	138.9	60	-	132.3	135.7	138.0	135.9	133.3	132.0
4	3.00	2500	2883	7.8	-24.2	-7.2	138.8	60	-	130.6	134.8	137.9	134.5	132.9	130.8
5	3.00	2010	2585	8.8	-22.3	-6.3	137.7	60	-	130.9	134.9	136.9	133.0	131.2	129.2
6	2.50	2500	2659	6.5	-24.8	-7.7	137.8	60	-	128.6	131.9	136.9	132.4	130.2	128.2
7	2.50	2010	2384	7.4	-22.9	-6.7	135.9	60	-	129.2	133.5	135.1	131.1	128.8	127.1
8	2.00	2010	2038	5.9	-25.5	-7.1	131.7	50	-	125.8	129.6	128.4	125.9	126.8	122.0
9	2.00	2500	2340	5.1	-25.4	-8.1	133.1	60	-	125.9	130.0	132.3	128.0	127.2	124.7

TABLE V.C.1-4 TEST SUMMARY

MODEL NO. 4.9B-163-3B; -3B-1

DESCRIPTION: 4.9 Cone + TSEN 3,16 Rods in Cone, α = 90° 60% Penetration, X_S = 2.93" & 1.81"

DATE: 3/6/68

SCALE MODEL A_S = .1310 ft^2

FULL SCALE A_S = 8.38 ft^2

SCALE FACTOR = S:1

o DATA INCLUDES GROUND REFLECTION INTERFERENCE

o ANGLE REFERENCED TO JET EXHAUST

TEST CONDITIONS							ACOUSTIC TEST RESULTS							
			IDEAL				320 FT ARC		300 FT. SIDELINE PNL DIRECTIVITY					
Rdg. No.	P_{T_S}/P_o	T_{T_S} (°R)	V_8 (fps)	W_8 (PPS)	10 Log $\rho_8 A_8$	10 Log ρ_8	PEAK PNdB	PEAK ANGLE	30°	40°	50°	60°	70°	80°	90°
			4.9B-163-3B		X_S = 2.93"										
1	2.00	2780	2464	4.8	-26.4	-8.6	130.5	50	121.3	125.9	128.4	128.0	125.8	122.6	122.3
2	2.50	2780	2797	6.0	-25.8	-8.2	134.7	50	125.2	128.8	132.5	133.7	129.3	128.9	124.3
3	3.00	2780	3051	7.2	-25.2	-7.7	138.1	60	126.2	130.7	135.0	137.2	133.6	130.4	128.5
4	2.99	2500	2881	7.5	-24.2	-7.3	136.6	50	127.0	131.0	134.4	134.3	132.2	129.7	128.9
5	2.98	2005	2577	8.5	-22.3	-6.3	136.0	40	127.4	132.0	133.8	134.6	129.8	127.6	126.3
			4.9B-163-3B-1		X_S = 1.81"										
1	1.99	2780	2464	4.8	-26.4	-8.6	131.5	50	120.0	125.9	129.4	129.3	126.2	124.7	122.0
2	2.48	2780	2797	6.0	-25.8	-8.2	136.1	60	123.1	130.2	133.1	135.3	130.8	128.0	125.6
3	3.00	2780	3037	7.1	-25.2	-7.7	138.8	60	126.4	130.7	136.2	137.9	133.2	130.9	129.2
4	3.00	2500	2880	7.5	-24.2	-7.3	138.0	50	125.2	131.3	135.8	136.3	131.4	128.9	128.3
5	2.99	2010	2583	8.5	-22.3	-6.3	136.9	50	126.1	131.2	134.8	134.4	130.6	128.2	126.3

TABLE V.C.1-5 TEST SUMMARY

M[illegible] NO. 4.9B-164-3[illegible], -3B-1 SCALE MODEL A_8 = .1310 ft^2

DESCRIPTION: 4.9 Cone + TSEN 3, 16 Rods in Cone, α = 90° 78% Penetration, X_S = 2.93" & 1.81" FULL SCALE A_8 = 8.38 ft^2

DATE: 3/14/68 SCALE FACTOR = 8:1

- o DATA INCLUDES GROUND REFLECTION INTERFERENCE
- o ANGLE REFERENCED TO JET EXHAUST

TEST CONDITIONS							ACOUSTIC TEST RESULTS								
Rdg. No.	P_{TS}/P_o	T_{T8} (°R)	IDEAL V_j (fps)	W_8 (PPS)	20 Log $\rho^2 A$	20 Log ρA	320 FT ARC PEAK PNdB	320 FT ARC PEAK ANGLE	300 FT. SIDELINE PNL DIRECTIVITY 30°	40°	50°	60°	70°	80°	90°
			4.9B-164-3B X_S = 2.93"												
1	2.00	2760	2460	4.8	-26.3	-8.5	127.8	50	120.6	123.6	125.6	125.3	124.2	124.2	122.5
2	2.50	2770	2801	6.2	-25.7	-8.1	133.6	50	124.3	128.1	131.4	131.8	128.9	127.9	125.8
3	3.00	2770	3038	7.2	-25.0	-7.7	135.4	60	126.4	129.7	132.4	134.6	132.0	130.1	128.1
4	3.00	2500	2886	7.7	-24.1	-7.2	136.4	60	125.9	129.8	132.7	135.5	134.4	132.1	126.6
5	3.00	2010	2587	8.5	-22.2	-6.3	133.8	50	125.7	129.6	131.6	131.4	128.7	126.9	125.4
			4.9B-164-3B-1 X_S = 1.81"												
1	3.00	2010	2587	8.6	-22.2	-6.3	134.3	40	126.1	130.3	132.0	131.4	128.8	127.8	126.2
2	3.01	2505	2890	7.6	-24.1	-7.2	134.7	50	126.2	130.4	132.5	133.3	130.4	129.5	127.4
3	3.01	2790	3050	7.2	-25.1	-7.7	135.2	50	125.8	130.2	133.1	134.1	131.4	128.9	127.6
4	2.50	2500	2661	6.4	-24.8	-7.7	133.7	50	124.6	129.3	131.6	130.9	128.4	127.1	125.0
5	2.00	2790	2476	4.8	-26.4	-8.6	128.0	50	120.9	124.1	125.9	125.6	124.1	122.9	121.9

TABLE V.C.1-6 TEST SUMMARY

MODEL NO. 4.9B-165-3B; -3B-1

DESCRIPTION: 4.9 Cone + TSEN 3, 16 Rods in Cone, α = 22.5° 60% Penetration, X_S=2.98" & 1.81"

DATE: 3/18/68

SCALE MODEL A_8 = .1518 ft^2

FULL SCALE A_8 = 9.715 ft^2

SCALE FACTOR = 8:1

- o DATA INCLUDES GROUND REFLECTION INTERFERENCE
- o ANGLE REFERENCED TO JET EXHAUST

TEST CONDITIONS							ACOUSTIC TEST RESULTS								
			IDEAL				320 FT ARC		300 FT. SIDELINE PNL DIRECTIVITY						
Rdg. No.	P_{T8}/P_o	T_{T8} (°R)	V_8 (fps)	W_8 (PPS)	10 Log $\rho_8 V_8^2$	10 Log $\rho_o A_8$	PEAK PNdB	PEAK ANGLE	30°	40°	50°	60°	70°	80°	90°
			4.9B-165-3B		X_S = 2.93"										
1	2.00	2790	2477	5.9	-25.8	-7.9	129.4	50	121.7	125.4	127.3	126.9	125.1	123.6	122.1
2	2.50	2790	2811	7.5	-25.1	-7.5	135.1	50	125.8	130.1	132.9	132.3	129.4	127.7	125.4
3	3.00	2790	3047	8.8	-24.5	-7.1	136.8	50	127.3	131.5	134.6	135.2	131.3	129.5	127.7
4	3.00	2500	2884	9.3	-23.5	-6.6	137.2	50	127.4	131.8	135.0	134.1	131.2	128.5	127.2
5	3.00	2010	2586	10.5	-21.6	-5.6	135.2	50	126.8	130.9	133.0	132.2	128.7	126.5	125.0
			4.9B-165-3B-1		X_S = 1.81"										
1	2.00	2790	2477	5.9	-25.7	-7.9	130.0	50	121.7	125.7	127.8	128.0	125.6	123.9	122.7
2	2.50	2790	2812	7.1	-25.1	-7.5	135.3	50	126.1	130.5	133.1	133.4	130.0	127.8	125.9
3	2.99	2790	3045	8.9	-24.5	-7.1	138.3	50	127.3	132.6	136.2	136.8	132.6	130.7	128.6
4	3.00	2500	2883	9.3	-23.5	-6.6	137.9	50	127.4	132.5	135.8	135.6	131.9	129.8	128.1
5	3.00	2010	2586	10.5	-21.6	-5.6	138.2	40	127.4	133.9	134.4	133.2	129.6	127.8	126.1

TABLE V.C.1-7 TEST SUMMARY

MODEL NO. 4.9B-166-3B

DESCRIPTION: 4.9 Cone + TSEN 3, 16 Rods in Cone, α = 45° 60% Penetration, X_S=2.93"

DATE: 3/18/68

SCALE MODEL A_8 = .1330 ft^2

FULL SCALE A_8 = 8.51 ft^2

SCALE FACTOR = 8:1

- o DATA INCLUDES GROUND REFLECTION INTERFERENCE
- o ANGLE REFERENCED TO JET EXHAUST

TEST CONDITIONS					$10 \log \rho_0 V_0^2$	$10 \log \rho_0 A$	ACOUSTIC TEST RESULTS								
							320 FT ARC		300 FT. SIDELINE PNL DIRECTIVITY						
Rdg. No.	P_{T8}/P_o	T_{T8} (°R)	IDEAL V_8 (fps)	W_8 (PPS)			PEAK PNdB	PEAK ANGLE	30°	40°	50°	60°	70°	80°	90°
1	2.00	2790	2473	5.0	-26.4	-8.5	126.8	40	124.3	122.8	124.1	125.3	124.2	122.8	122.3
2	2.50	2805	2816	6.3	-25.8	-8.1	131.9	50	123.0	127.2	129.8	129.3	127.5	126.7	125.5
3	3.00	2765	3034	2.6	-25.0	-7.6	136.3	50	125.3	130.6	134.1	133.9	131.1	129.6	127.9
4	3.00	2500	2885	8.0	-24.1	-7.2	135.3	50	125.6	130.1	133.1	132.9	130.6	130.2	127.3
5	3.00	2010	2586	8.8	-22.3	-6.2	133.0	40	122.1	128.9	130.8	130.5	128.3	126.6	125.4

- o (16) Radial Rod Primary Nozzle @ 10% Penetration; $\alpha = 90^{\circ}$
- o TSEN-3 @ X_S = 2.93" & 1.81"
- o Mean Curves For $P_{T8}/P_0 = 3.0$

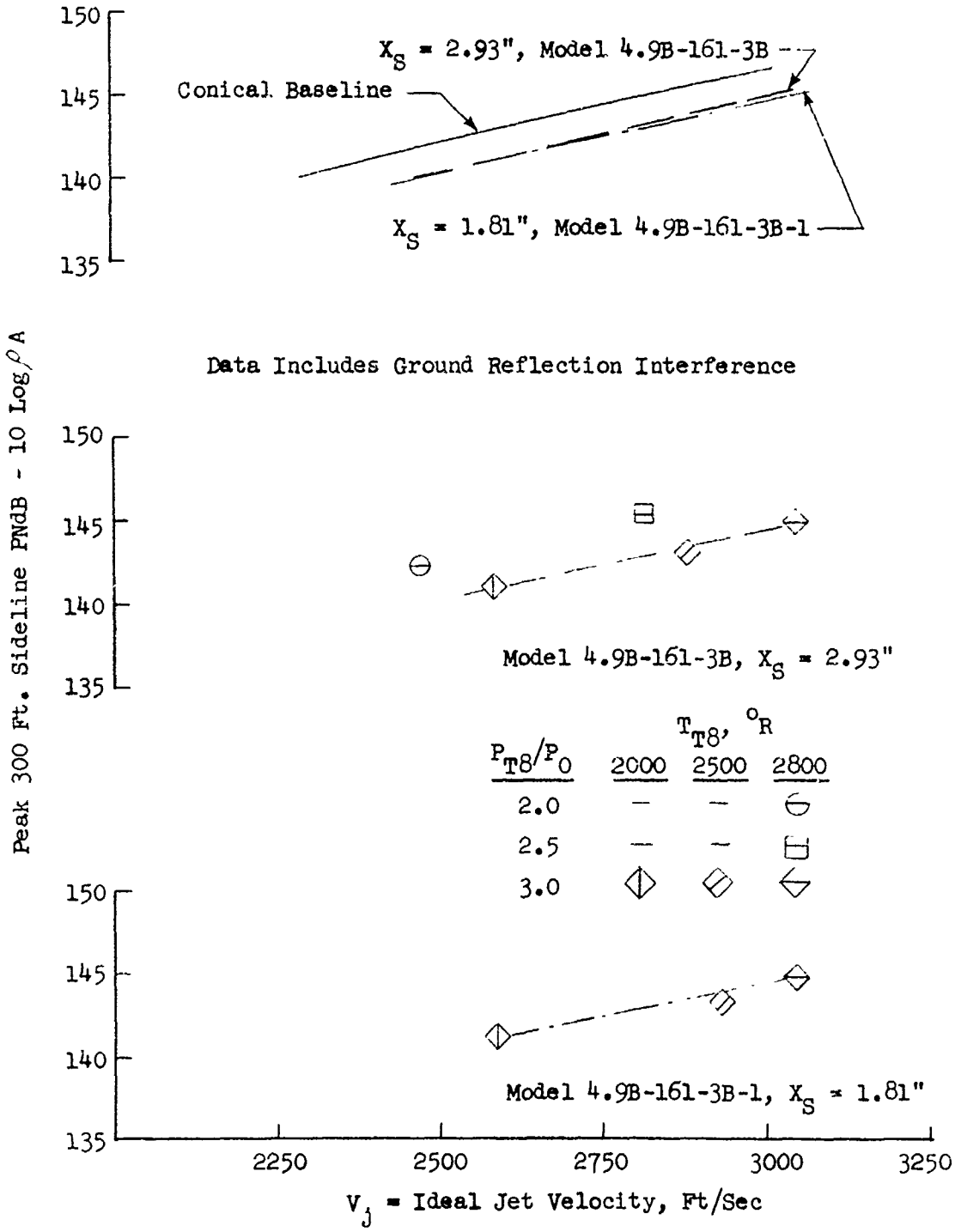

FIGURE V.C.1-6A EFFECT OF RADIAL ROD PENETRATION AND AXIAL SPACING, X_S, OF TSEN 3 ON 300 FT. SIDELINE JET NOISE LEVELS

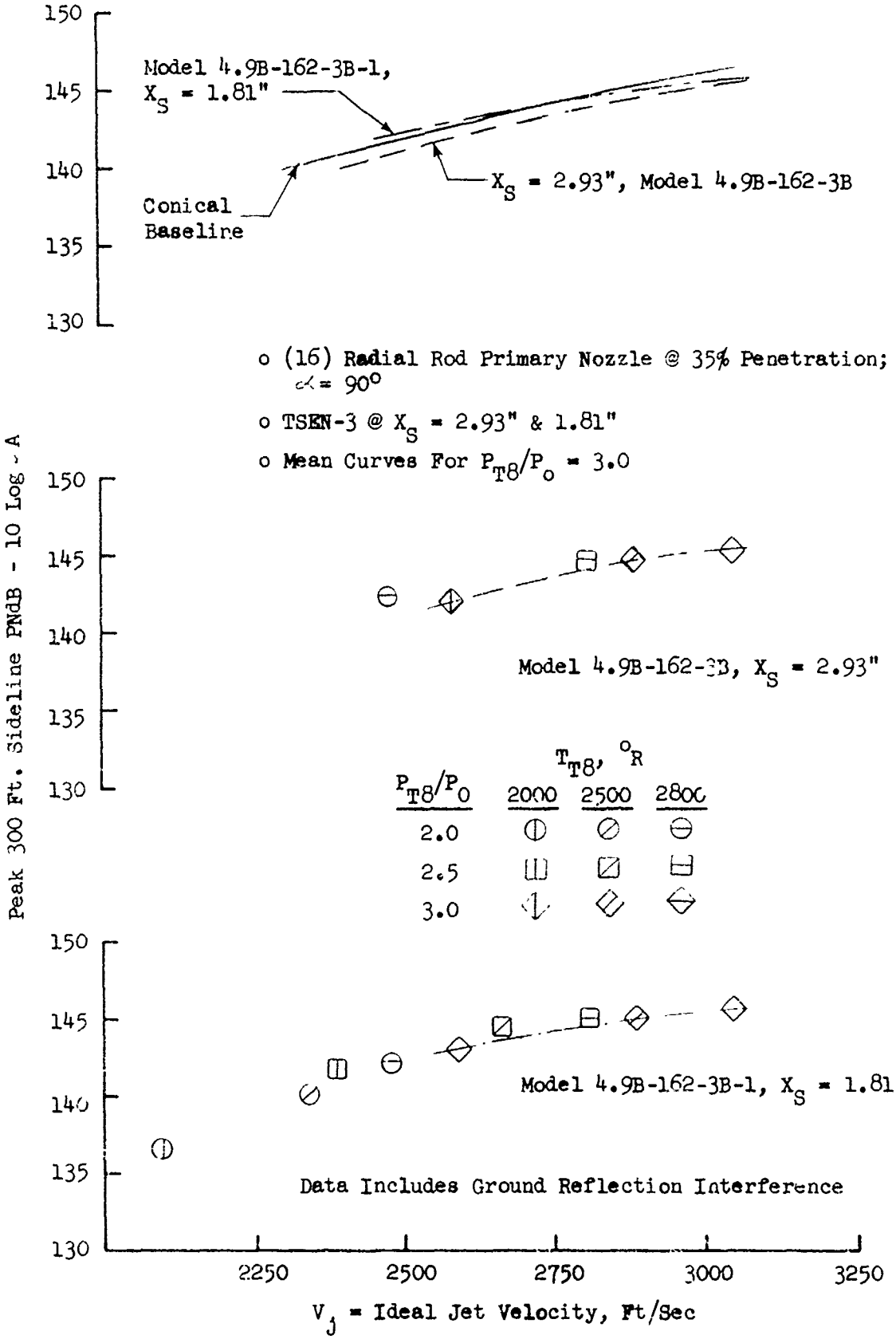

FIGURE V.C.1-6B EFFECT OF RADIAL ROD PENETRATION AND AXIAL SPACING, X_S, OF TSEN 3 ON 300 FT. SIDELINE JET NOISE LEVELS

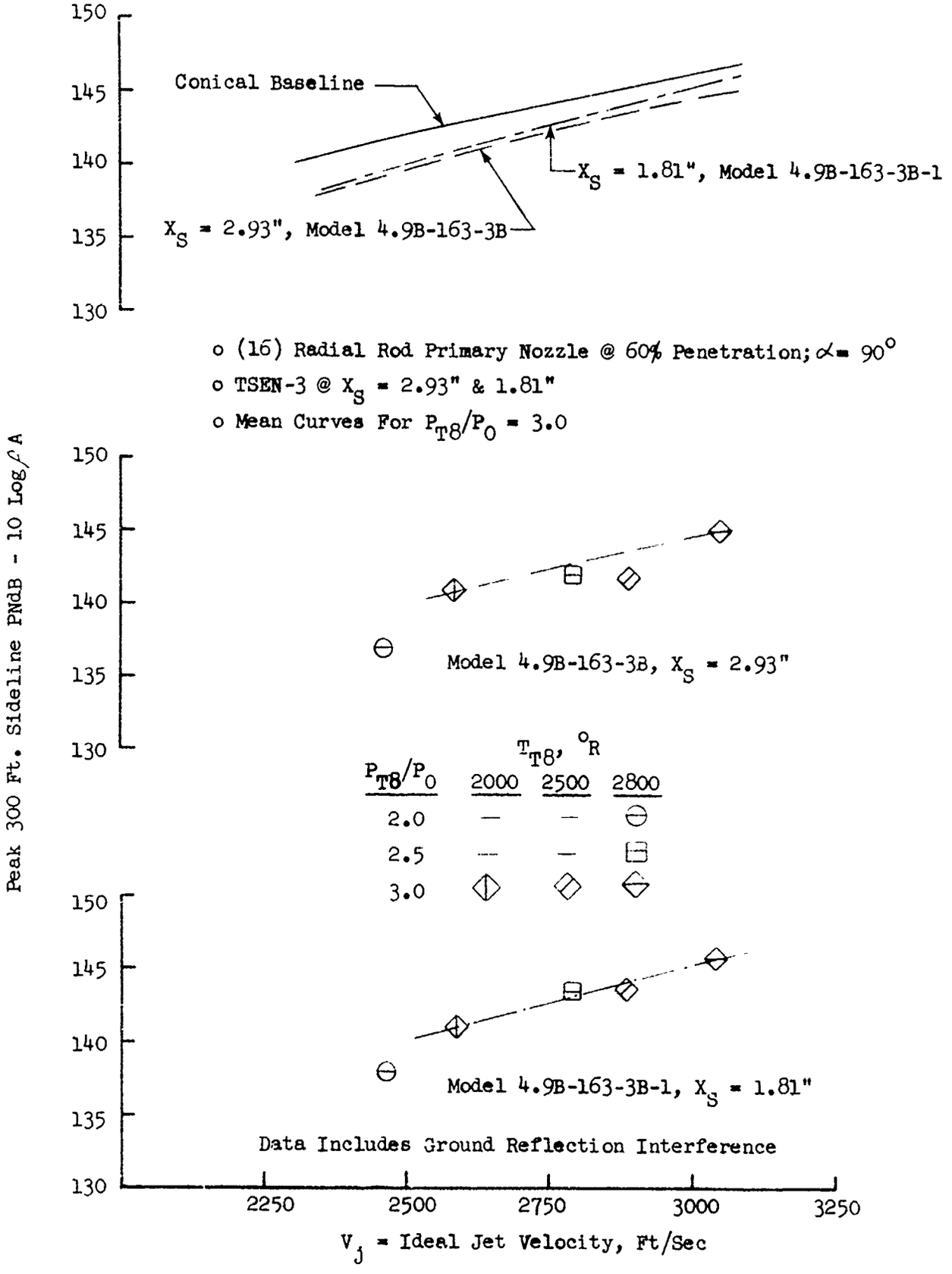

FIGURE V.C.1-6C EFFECT OF RADIAL ROD PENETRATION AND AXIAL SPACING, X_S, OF TSEN 3 ON 300 FT. SIDELINE JET NOISE LEVELS

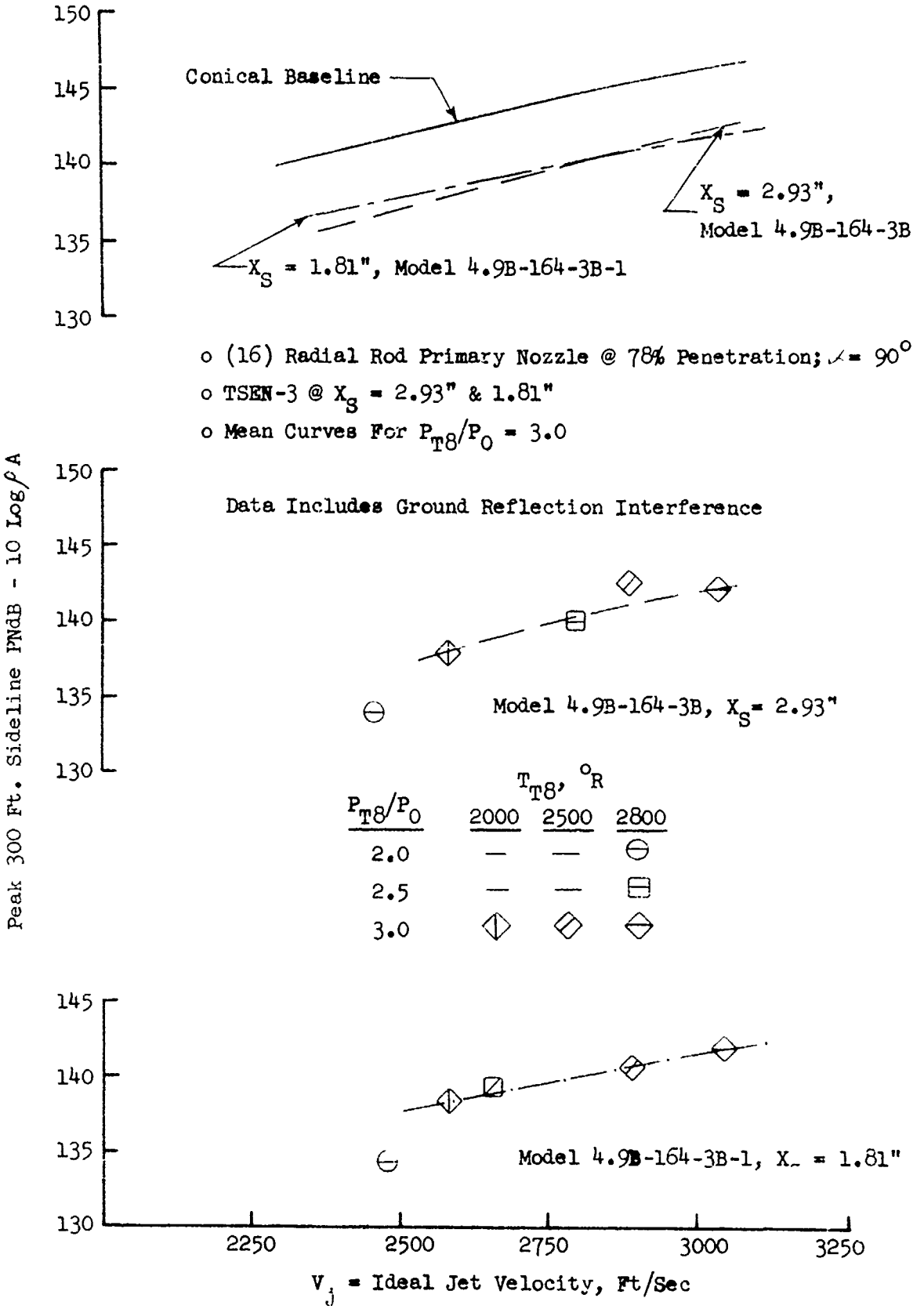

FIGURE V.C.1-6D EFFECT OF RADIAL ROD PENETRATION AND AXIAL SPACING, X_S, OF TSEN 3 ON 300 FT. SIDELINE JET NOISE LEVELS

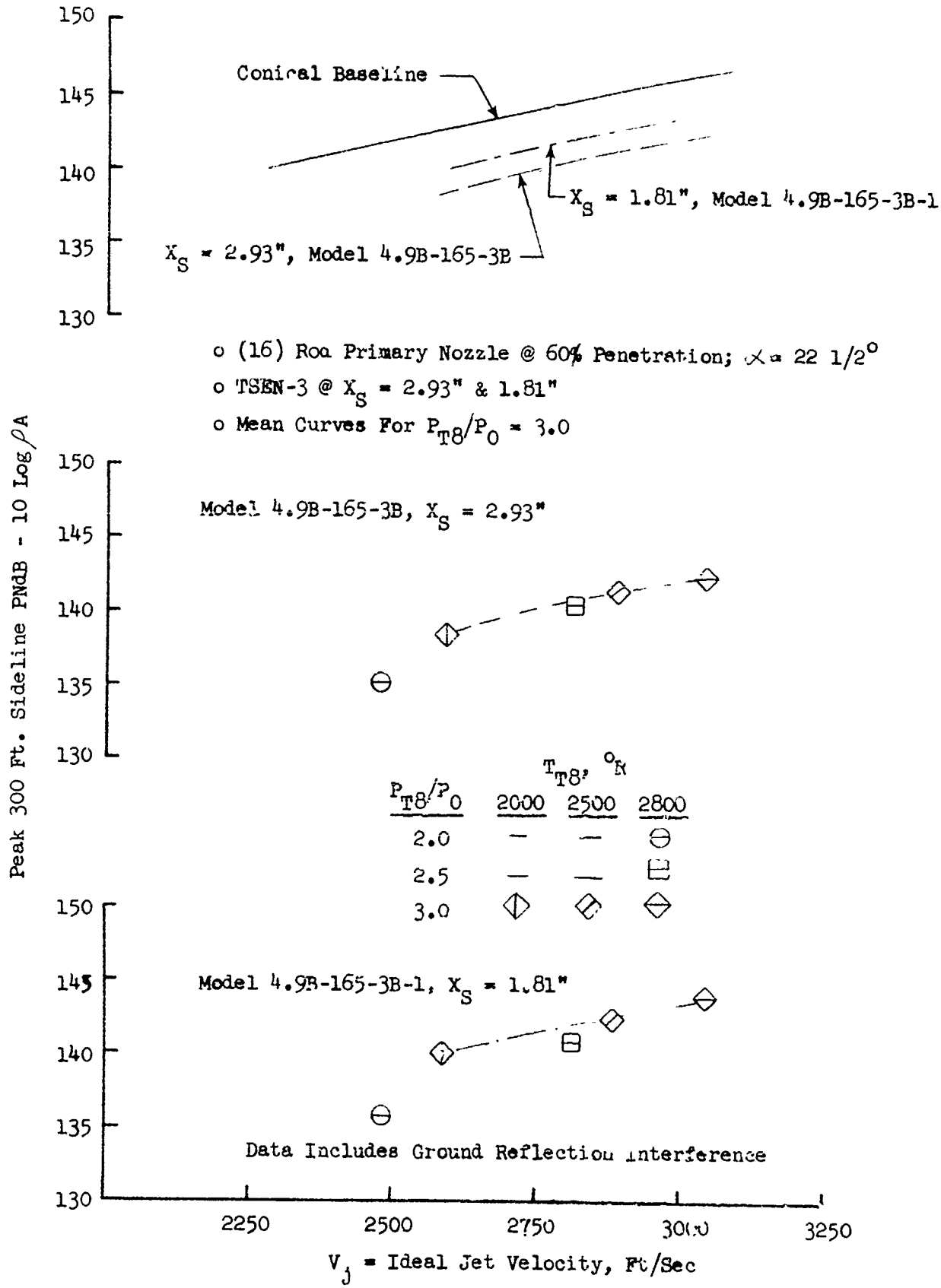

FIGURE V.C.1-7A EFFECT OF RADIAL ROD ANGULARITY AND AXIAL SPACING, X_S, OF TSEN 3 ON 300 FT. SIDELINE JET NOISE LEVELS

- o (16) Radial Rod Primary Nozzle @ 60% Penetration; $\alpha = 45^{\circ}$
- o TSEN-3 @ $X_S = 2.93"$
- o Mean Curves For $P_{T8}/P_0 = 3.0$

Data Includes Ground Reflection Interference

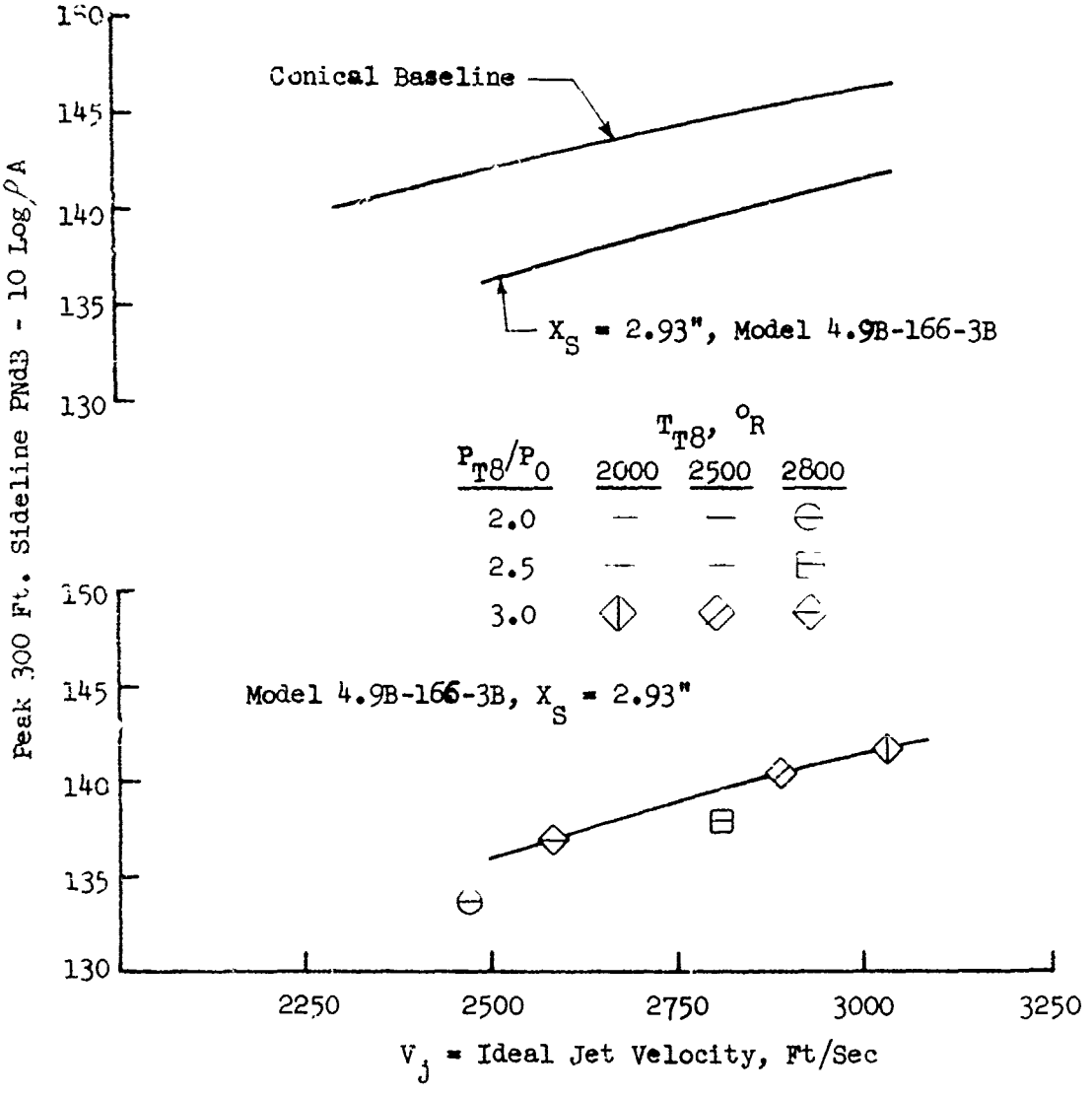

FIGURE V.C.1-7B EFFECT OF RADIAL ROD ANGULARITY AND AXIAL SPACING, X_S, OF TSEN 3 ON 300 FT. SIDELINE JET NOISE LEVELS

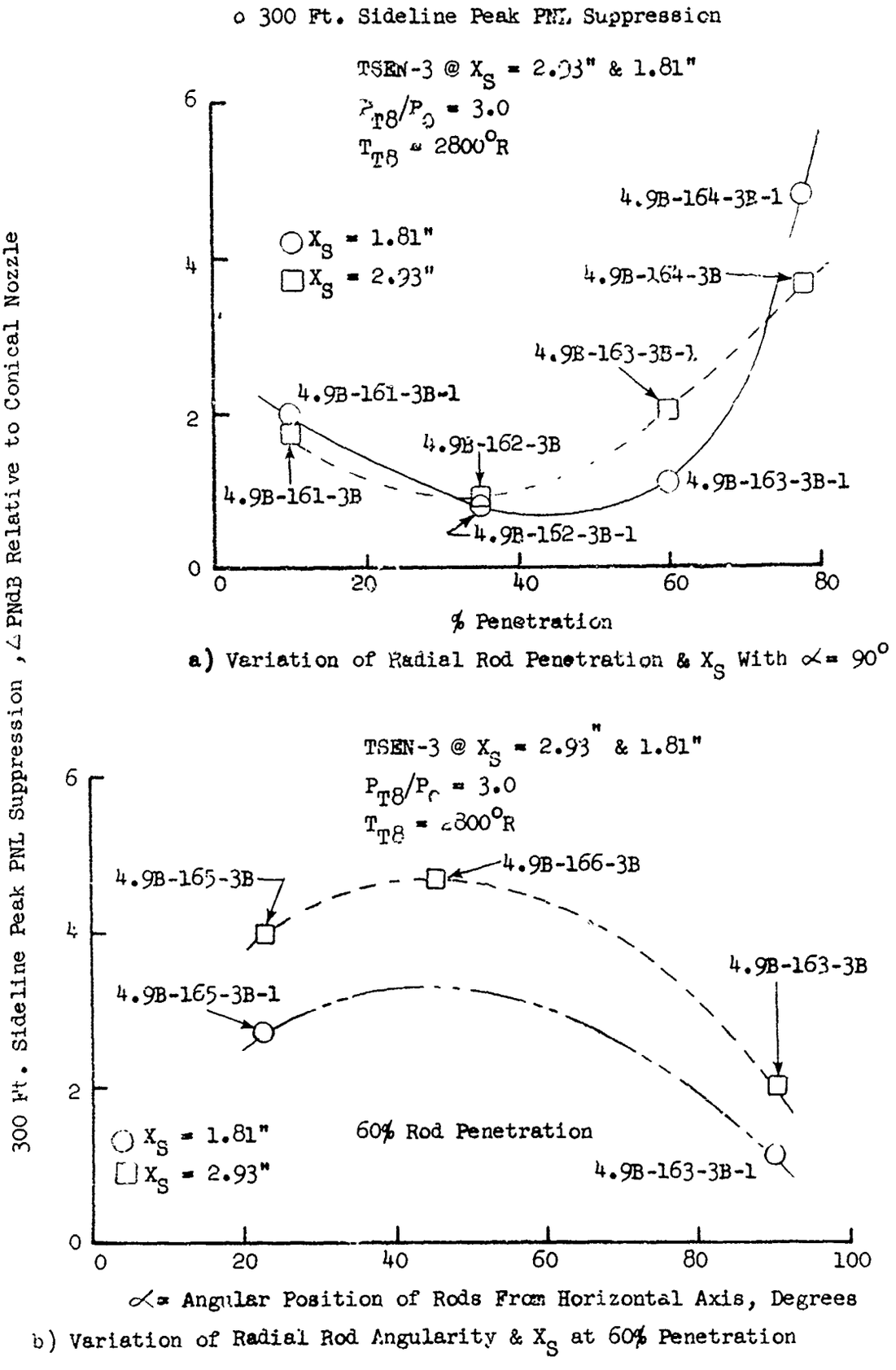

FIGURE V.C.1-8 EFFECT OF RADIAL ROD PENETRATION AND ANGULARITY ON 300 FT. SIDELINE PNL SUPPRESSION

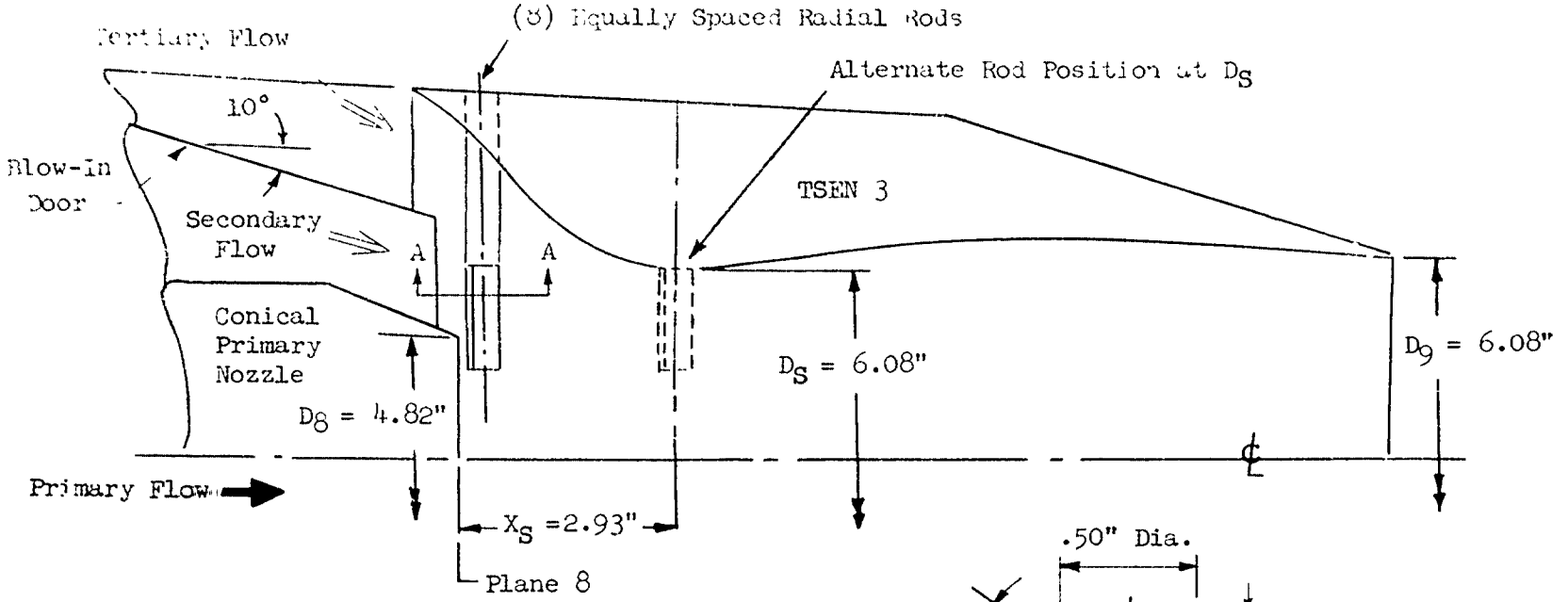

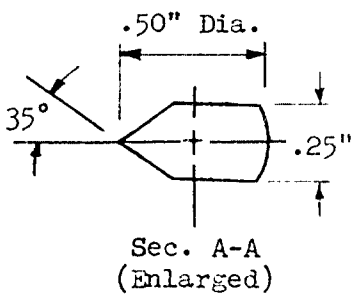

MODEL NO.	TEST DATE	$D_{8_{EFF.}}$ PHYS.	$D_S/D_{8_{EFF.}}$ PHYS.	ROD POSITION	% PENET.	START OF REV. FLOW
4.9-3B-1	3-7-68	4.69"	1.29	Just Aft of A_8	33	P/R 3.0, 2000°R
4.9-3B-2	3-7-68	4.47"	1.36	Just Aft of A_8	53	P/R 3.0, 2000°R
4.9-3B-3	3-8-68	4.82"	1.26	At D_S	33	P/R 3.0, 2000°R
4.9-3B-4	3-8-68	4.82"	1.26	At D_S	53	P/R 3.0, 2000°R

FIGURE V.C.1-9 SCHEMATIC OF TSEN 3 WITH (8) RADIAL RODS AT TWO AXIAL LOCATIONS

TABLE V.C.1-8 TEST SUMMARY

NOZZLE NO. 4.9-3B-1, -3B-2

DESCRIPTION: 4.9 Cone + TSEN 3, 8 Rods Aft of Plane 8 33% & 53% Penetration, X_S = 2.93'

DATE: 3/7/68

SCALE MODEL A_8 = .1310 ft^2

FULL SCALE A_8 = 8.38 ft^2

SCALE FACTOR = 8:1

- DATA INCLUDES GROUND REFLECTION INTERFERENCE
- ANGLE REFERENCED TO JET EXHAUST

TEST CONDITIONS							ACOUSTIC TEST RESULTS								
			IDEAL		20 Log A_8^2	20 Log V_8^6	320 FT ARC		300 FT. SIDELINE PNL DIRECTIVITY						
Rdg. No.	P_{T8}/P_o	T_{T8} (°R)	V_8 (fps)	W_8 (PPS)			PEAK PNdB	PEAK ANGLE	30°	40°	50°	60°	70°	80°	90°
			4.9-3B-1	33% Penetration											
1	2.00	2790	2479	4.6	-26.4	-8.6	132.8	60	120.4	124.2	128.0	131.9	129.9	127.7	126.2
2	2.50	2790	2811	5.7	-25.7	-8.1	136.8	60	124.0	127.9	131.2	135.9	133.5	130.5	129.3
3	3.00	2790	3047	6.9	-25.1	-7.7	137.9	60	126.0	129.5	132.9	137.0	135.4	133.6	131.6
4	3.00	2500	2886	7.4	-24.2	-7.2	138.1	60	125.6	129.6	132.8	137.2	134.8	132.5	130.7
5	3.00	2010	2586	8.3	-22.3	-6.3	136.9	60	125.2	129.1	132.9	136.0	133.5	131.8	130.4
			4.9-3B-2	53% Penetration											
1	2.00	2790	2475	4.3	-26.4	-8.6	130.9	60	118.9	124.2	127.9	130.0	128.8	126.9	125.6
2	2.50	2790	2811	5.4	-25.7	-8.1	135.4	60	123.0	127.0	131.0	134.5	132.1	131.6	132.1
3	3.00	2790	3048	6.5	-25.1	-7.7	137.2	60	125.6	129.4	132.6	136.4	135.1	132.4	131.1
4	3.00	2500	2886	6.9	-24.2	-7.2	137.1	60	125.2	129.1	132.0	136.3	134.4	131.8	130.5
5	3.00	2010	2587	7.8	-22.3	-6.3	136.0	60	124.3	128.8	132.5	135.2	132.2	130.0	129.4

TABLE V.C.1-9 TEST SUMMARY

MODEL NO. 4.9-3B-3, -3B-4

DESCRIPTION: 4.9 Cone + TSEN 3, 8 Rods at D_S 33% & 53% Penetration, X_S = 2.93"

DATE: 3/8/68

SCALE MODEL A_S = .1310 ft^2

FULL SCALE A_S = 8.38 ft^2

SCALE FACTOR = 8:1

o DATA INCLUDES GROUND REFLECTION INTERFERENCE
o ANGLE REFERENCED TO JET EXHAUST

TEST CONDITIONS							ACOUSTIC TEST RESULTS								
							320 FT ARC		300 FT. SIDELINE PNL DIRECTIVITY						
Run No.	P_{T8}/P_o	T_{T8} (°R)	IDEAL V_j (fps)	W_8 (PPS)	10 Log $\frac{A_8}{A_S}$	10 Log $\frac{A_o}{A_S}$	PEAK PNdB	PEAK ANGLE	30°	40°	50°	60°	70°	80°	90°
			4.9B-3B-3	33% Penetration											
1	2.00	2790	2478	5.1	-26.5	-8.6	131.5	60	120.9	124.3	126.4	130.7	126.8	126.0	124.8
2	2.50	2790	2813	6.4	-25.8	-8.2	134.1	60	124.7	128.6	130.4	133.2	130.6	128.1	127.9
3	3.00	2790	3047	7.7	-25.2	-7.8	138.5	50	126.9	131.9	136.3	135.9	132.8	129.9	128.1
4	3.00	2500	2885	8.1	-24.3	-7.3	136.7	50	126.7	131.5	134.5	134.7	132.1	129.0	127.5
5	3.00	2010	2586	9.0	-22.4	-6.3	134.3	50	126.0	130.1	132.1	132.0	130.3	128.4	128.6
			4.9-3B-4	53% Penetration											
1	2.01	2790	2481	4.8	-26.5	-8.6	126.4	40	118.9	122.5	123.9	125.5	124.8	124.8	123.1
2	3.00	2790	3048	7.6	-25.2	-7.8	137.8	50	127.3	132.7	135.6	135.0	131.0	129.4	127.6
3	3.00	2500	2883	8.0	-24.3	-7.3	137.1	50	127.2	132.2	134.9	134.9	131.7	130.1	127.1
4	3.00	2010	2588	9.1	-22.4	-6.3	135.5	40	127.4	131.4	132.7	131.1	127.7	127.9	127.5
5	2.50	2790	2813	6.3	-25.8	-8.2	132.3	40	123.8	128.1	130.1	129.7	128.3	127.0	125.5

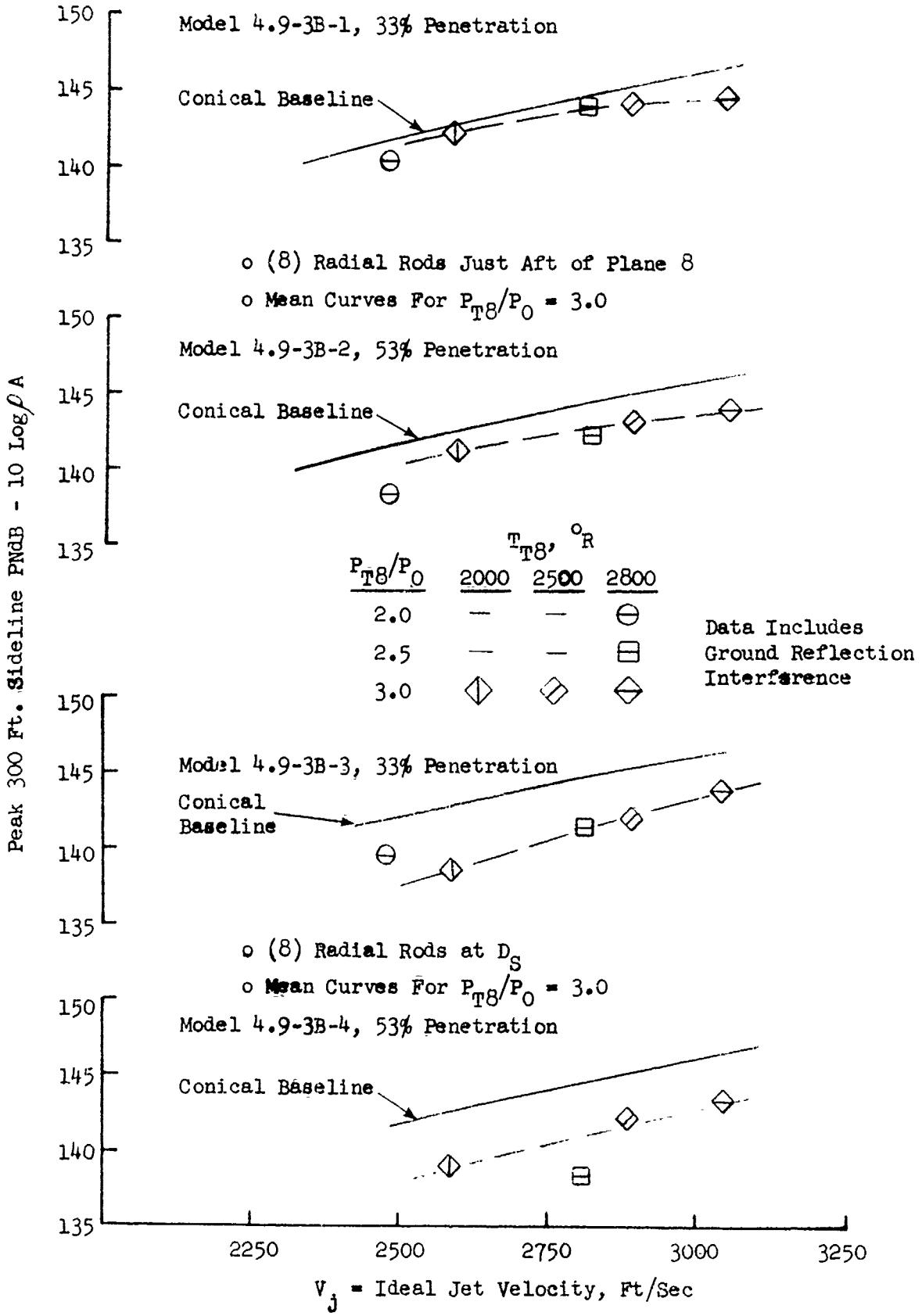

FIGURE V.C.1-10 EFFECT OF RADIAL ROD PENETRATION AT DIFFERENT AXIAL POSITIONS WITHIN TSEN 3 ON 300 FT. SIDELINE JET NOISE LEVELS

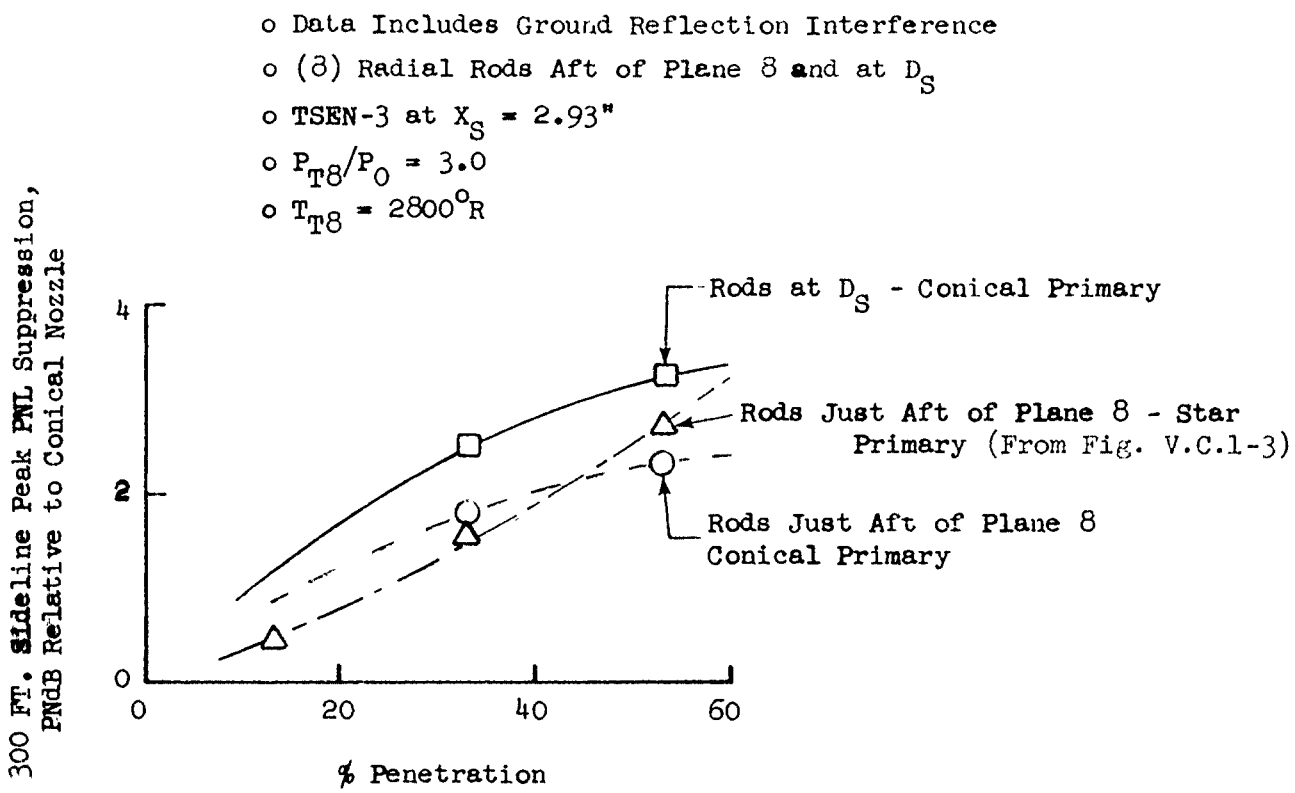

FIGURE V.C.1-11 EFFECT OF RADIAL ROD PENETRATION AND AXIAL LOCATION ON 300 FT. SIDELINE PNL SUPPRESSION

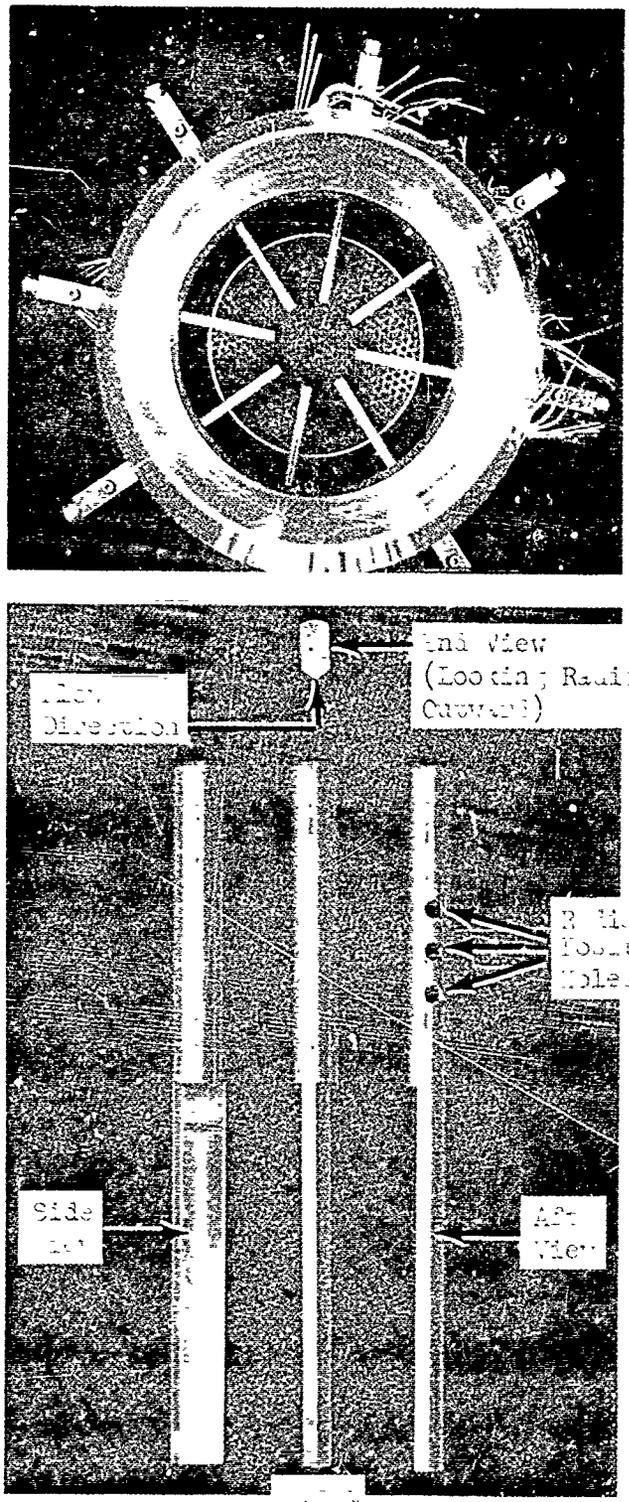

FIGURE V.C.1-12 TWO STAGE EJECTOR NOZZLE AERODYNAMIC MODEL HARDWARE

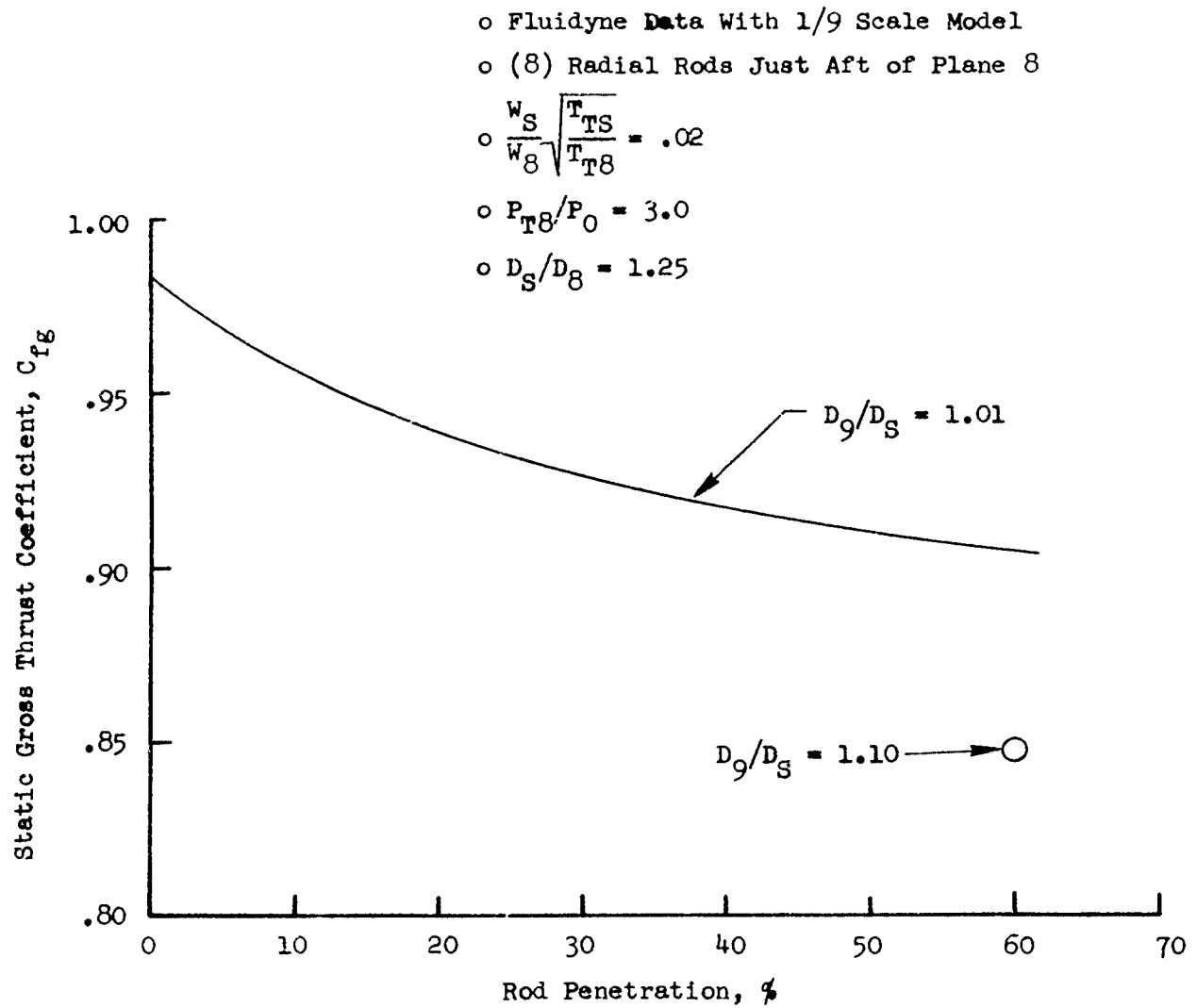

FIGURE V.C.1-13 AERODYNAMIC PERFORMANCE OF TSEN WITH CONICAL PRIMARY AND (8) RADIAL RODS

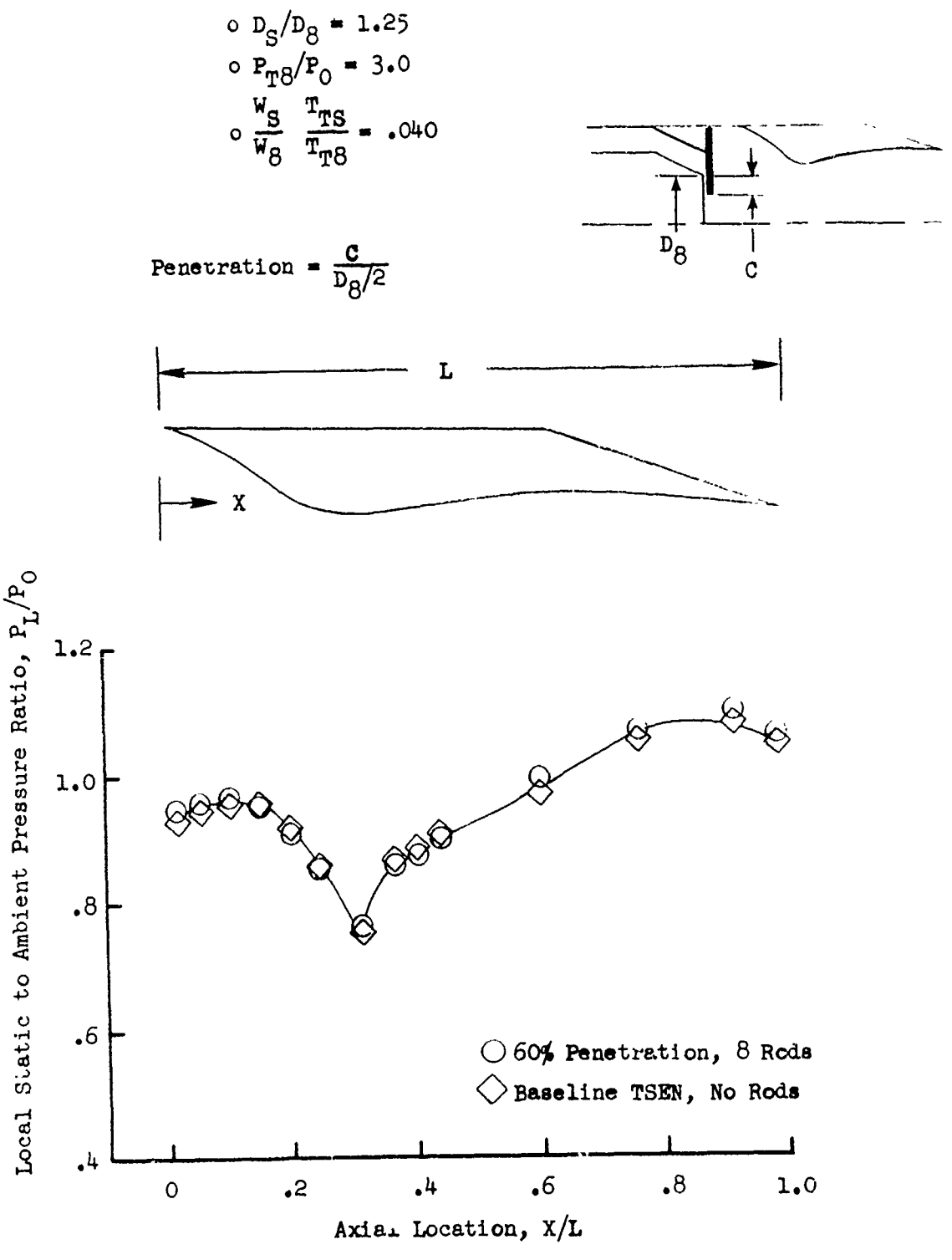

FIGURE V.C.1-14 SECONDARY NOZZLE CONTOUR STATIC PRESSURE DISTRIBUTION OF TSEN WITH AND WITHOUT RADIAL RODS

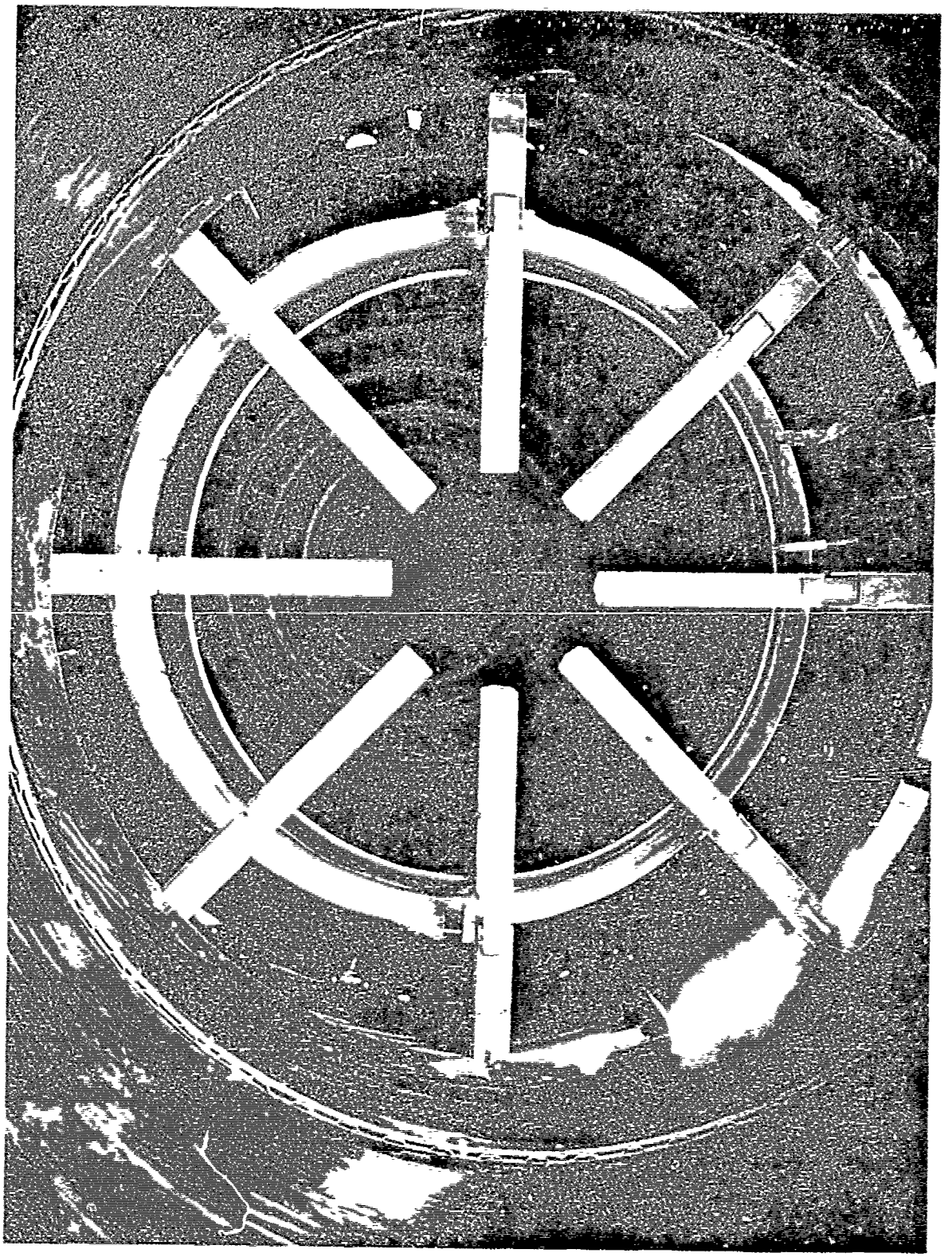

FIGURE V.C.1-15 EXHAUST NOZZLE OF GE4 BLOCK I ENGINE WITH (8) RADIAL RODS AT 65% PENETRATION

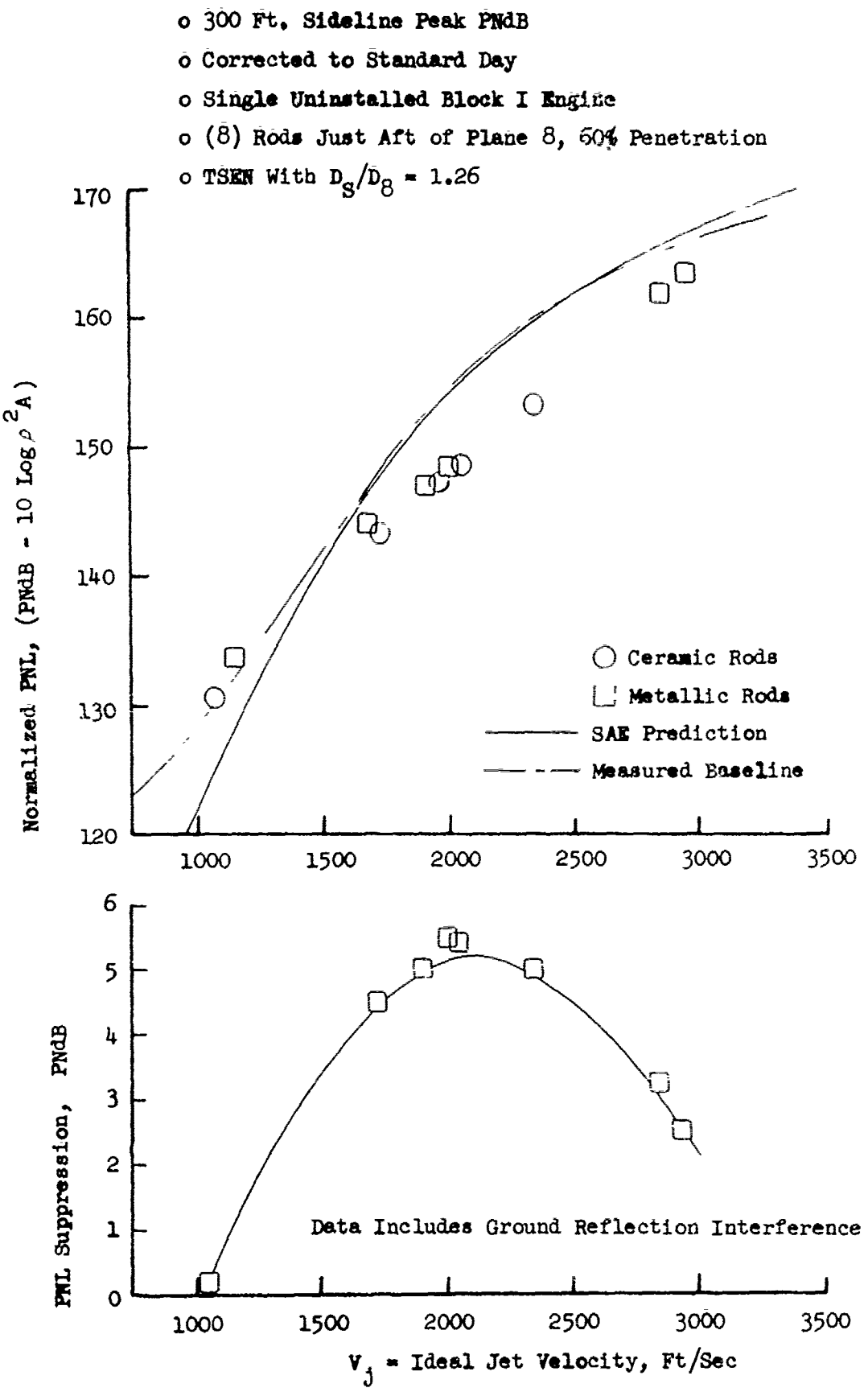

FIGURE V.C.1-16 EFFECT OF (8) RADIAL RODS ON 300 FT. SIDELINE JET NOISE LEVELS AND PNL SUPPRESSION OF GE4 BLOCK I ENGINE

V.C.2 PRIMARY THRUST REVERSER TAB VARIATIONS FOR MODEL AND ENGINE TESTS

PRECEDING PAGE BLANK-NOT FILMED

V.C.2 PRIMARY THRUST REVERSER TAB VARIATIONS FOR MODEL AND ENGINE TESTS

Several test series were performed to establish the acoustic effectiveness of primary thrust reverser tabs as jet noise suppressors. The tabs were an integral part of the full scale primary nozzle thrust reverser system, forming the center of the target when the primary nozzle flaps translated aft and were positioned as the thrust reverser. As the tabs were required hardware for the reverser system, their use as a simple jet suppressor system was investigated. By partial deployment into the jet stream just aft of the A_8 plane, they performed as shock generators and increased the mixing rate of the primary, secondary, and tertiary flows within the two stage ejector system.

Acoustic measurements were primarily at the GE, Evendale, JENOTS facility. In addition, a full scale test at Peebles Site 4D, using a GE4 Block I engine, was done to substantiate model results.

The test phases and system geometric variables investigated are as follows:

- Phase I - Conical Primary + TSEN 4 + Tabs
  - a) Tab Angle Variation (Penetration)
  - b) D_S/D_8 Variation at Fixed Tab Position
  - c) Tab Number Variation
- Phase II - Conical Primary + TSEN 56 + Tabs
  - a) D_9/D_S Variation at Fixed Tab Position
- Phase III - Conical Primary + TSEN + Tabs - Aerodynamic Test
  - a) Tab angle variation (Penetration)
  - b) D_S/D_8 Variation at Fixed Tab Position
  - c) D_9/D_S Variation at Fixed Tab Position
- Phase IV - GE4 Block I Engine - Conical Primary + TSEN + Tabs
  - a) D_S/D_8 Variation at Fixed Tab Position
  - b) Comparison of Model to Engine

Each test phase will be discussed individually.

PRECEDING PAGE BLANK-NOT FILMED

Acoustic measurements for model tests at JENOTS were taken on a 40 ft. arc at 10° intervals from 30° through 90° from the jet exhaust axis. The measurements were scaled by frequency, size, and measuring arc to the full scale application using a scale factor of 8:1. All acoustic data presented within this section are, therefore, of simulated engine size and engine frequency range.

o Phase I - Conical Primary + TSEN 4 + Tabs

The photograph of Figure V.C.2-1 shows the TSEN 4 and primary thrust reverser tab hardware used in this test phase. Figure V.C.2-2 schematically shows the TSEN 4 hardware set-up, basic nozzle dimension, tab planform and positioning, and a test summary of the model configurations.

For the acoustic effect of tab angle, which set penetration into the jet stream, test numbers 4, 2 and 3 are compared. Angles of 11.5°, 18° and 24° were used to set the 16 tabs at penetrations of 4.6%, 11.2% and 15.3%, respectively. The TSEN D_S/D_8 ratio of 1.26 was held by using a 4.82" D_8 conical nozzle with the fixed D_S = 6.08".

For the effect of D_S/D_8 variation with a fixed tab setting, test numbers 1, 4 and 5 are compared. The 16 tabs were held at 11.5° while three primary nozzles of 4.32", 4.82" and 5.14" D_8 were used to obtain the three D_S/D_8 values of 1.41, 1.26 and 1.18, respectively. With the tabs at 11.5° the depth of penetration of the outer jet stream was consistent, however, the percent penetration varies due to the change in D_8.

For tab number effect, test numbers 2, 6 and 7 are compared. The D_S/D_8 was held constant using a 4.82" D_8 conical primary while 16, 8 and 4 tabs were used at 18° or 11.2% penetration.

The three primary nozzles were also used as test numbers 8, 9 and 10 to establish the acoustic baseline to which the suppressors are referenced. Their acoustic test results are summarized in Tables V.C.2-1, -2 and -3 for the 4.32", 4.82" and 5.14" D_8 primary nozzles, respectively. Figure V.C.2-3 is a summary plot of the baseline data as 300 ft. sideline peak normalized PNL as a function of jet velocity. The average conical baseline on this figure is used in subsequent plots and is compared to the baseline data from tests on the same day as the suppressor configurations.

For the tab suppressor models the acoustic test results are presented a) in tabular form and b) as 300 ft. sideline peak normalized PNL plots as a function of jet velocity, as follows:

Test Number	Model Number	Table	Figures
4	4.9-4B-R7	V.C.2-4	V.C.2-4
2	4.9-4B-R7-1	V.C.2-5	V.C.2-5
3	4.9-4B-R7-2	V.C.2-6	V.C.2-6
5	5.1-4B-R2	V.C.2-7	V.C.2-7
1	4.3-4B-R6	V.C.2-8	V.C.2-8
6	4.9-4B-R8	V.C.2-9	V.C.2-9
7	4.9-4B-R8-1	V.C.2-10	V.C.2-9

For comparison of the acoustic suppression variance with a) tab angle, b) D_S/D_8 variation, and c) tab number, the 300 ft. sideline peak PNL suppressions have been plotted in Figures V.C.2-10, -11 and -12, respectively. In general low levels of suppression of 2 to 4 PNdB are gained in the intermediate to high jet velocity range. The variations of tab angle, secondary diameter ratio and number of tabs had minor effect on suppression, especially in the high velocity range, at or above 2750 ft/sec. In some instances, at low jet velocities of 1250 ft/sec or less, various tab configurations became noise generators. For tab angle, (Figure V.C.2-10) the higher penetration settings of 18° and 24° were more beneficial and performed quite similar. For a set tab angle of 11.5°, (Figure V.C.2-11) suppression is enhanced by increasing the D_S/D_8 to the largest value of 1.41. For tab number, (Figure V.C.2-12) results of deployment of part or all of the tabs is somewhat inconclusive showing crossovers of attained suppression in several jet velocity regions.

o Phase II - Conical Primary + TSEN 5D + Tabs

For investigation of D_9/D_S variance within a fixed tab system, the TSEN 5F hardware of Figure V.C.2-14 was used. The conical nozzle and tabs are shown in the photograph of Figure V.C.2-13. The TSEN hardware is the same as that of Section V.B, as shown in Figure V.B-12. The 16 tabs were positioned just aft of plane 8 and set at 18°, equivalent to 14.1% penetration of the 5.637" D_8 primary nozzle. Three D_9 sectors of 7.0", 7.7" and 8.4" I.D. were used to set D_9/D_S at 1.0, 1.1, and 1.2, respectively.

The 5.637" D_8 cone was tested without the TSEN or tabs as baseline reference configuration. Its acoustic test results are summarized in Table V.C.2-11. The tabulated test results for the three tab suppressors are included as Tables V.C.2-12, -13 and -14 for D_9/D_S of 1.0, 1.1 and 1.2, respectively. A plot of the 300 ft. sideline peak normalized PNL as a function of jet velocity is included as Figure V.C.2-15 for the baseline and three suppressor configurations. Average curves are faired through the data and plots of peak PNL suppression are presented as Figure V.C.2-16. Suppression levels of up to 8 PNdB are seen at 2250 ft/sec jet velocity for the D_9/D_S = 1.2 configuration. Thus, the D_9/D_S ratio is the most influencing parameter investigated. For purpose of gauging suppression attributable solely to the tabs, the basic TSEN suppression levels of Section V.B are included in Figure V.C.2-16 as well as the delta suppression of the tabs relative to the cone plus TSEN system. At 2500 ft/sec, about 4.5 PNdB is seen attributable solely to the tabs when used in the D_9/D_S = 1.2 configuration.

o Phase III - Conical Primary + TSEN + Tabs - Aerodynamic Test

Concurrent with the acoustic tests, a cold flow performance test was conducted at the FluiDyne facilities. The purpose of the tests was to investigate a) the effect of tab angle or penetration and b) D_S/D_8 variation in a fixed tab system, and c) D_9/D_S variation in a fixed tab system, on gross thrust coefficient. A photograph of the tab anchor ring assembly aerodynamic hardware is presented as Figure V.C.2-17. Nozzle performance results in the form of a) static gross thrust coefficient. b) primary nozzle flow coefficient, and c) corrected tertiary weight flow ratio, all as a function of primary nozzle pressure ratio, are included as Figure V.C.2-18. At pressure ratios of 2.0 to 3.2 and at 11.5° tab angle, there is no significant effect on performance from changing D_S/D_8 from 1.25 to 1.37. At simulated takeoff conditions, P_{T8}/P_o = 3.2, shallow tab angles of 11-1/2° produced thrust decrements in the order of 4.5% relative to the unsuppressed TSEN, while tertiary pumping and primary flow coefficient characteristics remained essentially unaffected. However, when tab angle and nozzle exit diameter were increased, the gross thrust coefficient was severely affected throughout the entire pressure ratio range. The greatest detrimental effect of increasing nozzle throat diameter was reflected on primary nozzle flow coefficient. Primary nozzle flow coefficient was also reduced by increasing tab penetration angle. The attachment/over-expansion

phenomena when the exit diameter (D_9) is increased is evident at the 2.5 pressure ratio, however, performance is improved when pressure ratio is increased. Generally, none of the acoustic parameters evaluated aerodynamically had any adverse effects on nozzle pumping capability.

o Phase IV - GE4 Block I Engine - Conical Primary + TSEN + Tabs

Measurements were taken with the GE4 Block I Engine plus two stage ejector nozzle plus tab suppressor system to substantiate acoustic performance levels. Sixteen tabs were used at a 11.5° angle which set penetration at 6% of the primary conical nozzle D_8. D_S/D_8 ratios of 1.27 and 1.38 were used. Figure V.C.2-19 is a photograph of the engine tab suppressor system.

Acoustic measurements and results are presented in Figure V.C.2-20 as 300 ft. sideline peak normalized PNL as a function of jet velocity, and in Figure V.C.2-21 as PNL suppression relative to the baseline unsuppressed engine. Model average suppression curves are included on Figure V.C.2-21 at similar D_S/D_8's of 1.41 and 1.26 compared to the engine settings of 1.38 and 1.27. Good agreement between model and engine is seen, particularly up to maximum dry cycle conditions. At the higher jet velocities, corresponding to the engine operating with augmentation, the full scale suppression levels dropped off more rapidly than the scale model counterparts.

Figures V.C.2-22A through V.C.2-22E are included as comparisons of model to engine normalized spectra and PNL directivity. The five curve sets are at incremental increases in jet velocity over the range of 1300 to 3100 ft/sec. The model data have been scaled by the factor of 8:1 and spectra levels have been adjusted for comparison of the octave band model measurements to the engine 1/3 octave band data. The PNL data are seen to agree quite well over the entire velocity range, particularly at angles of peak PNL; the angles at which the spectra comparisons are made. The scaled spectra also match engine data quite closely. They are, however, uncorrected for ground reflection, which accounts for the mis-match in the low frequency range.

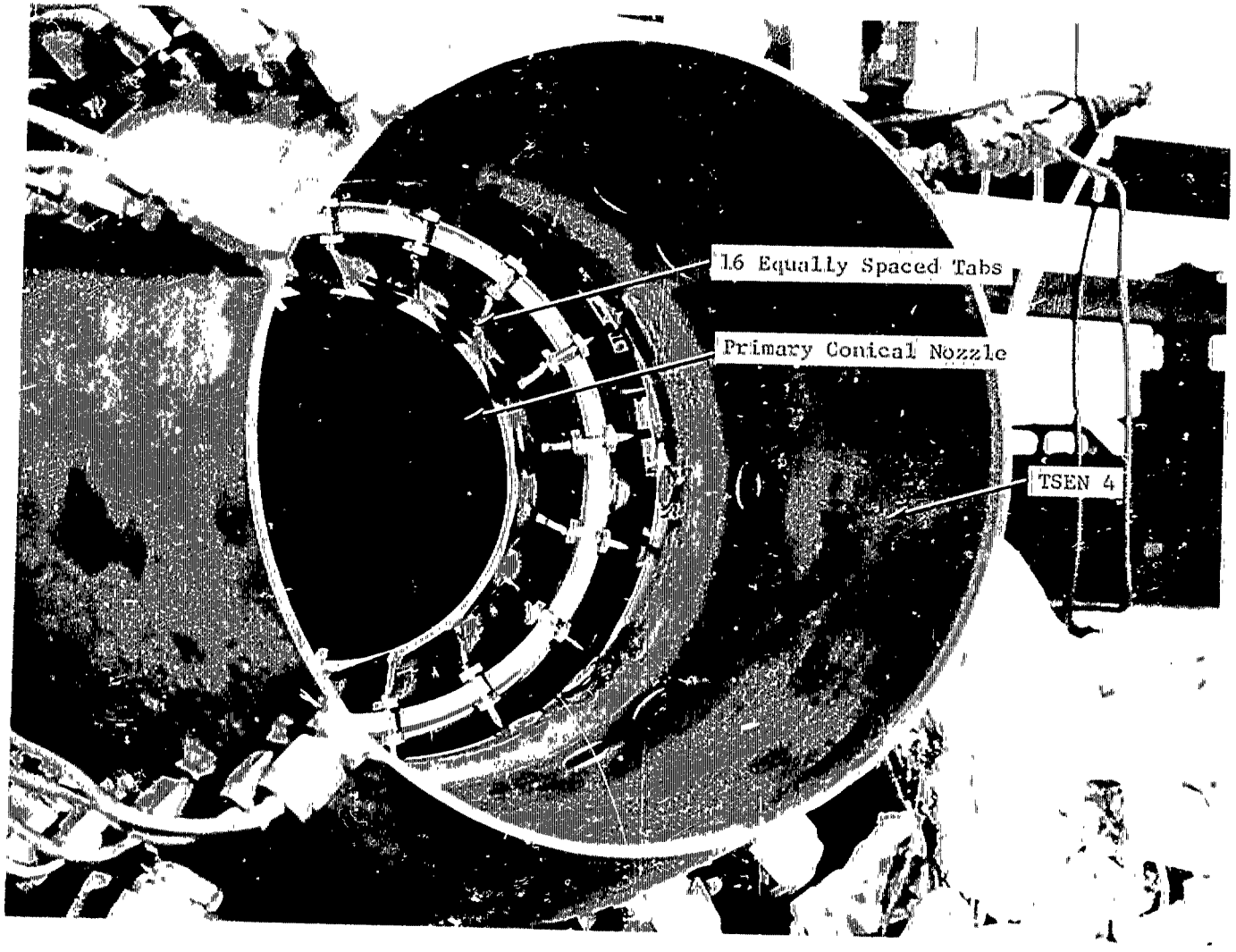

FIGURE V.C.2-1 PRIMARY THRUST REVERSER TABS INSTALLED IN TSEN-4

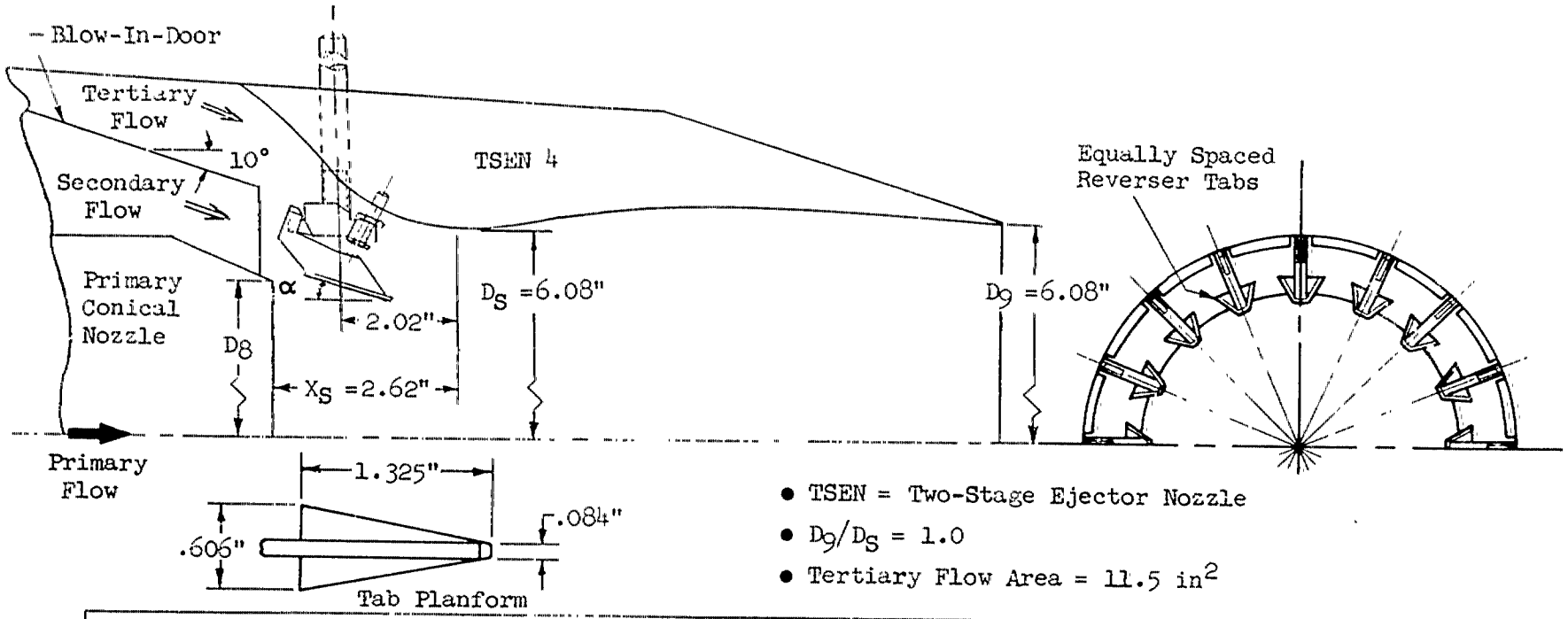

TEST NO.	MODEL NO.	TEST DATE	D_8	D_S/D_8	NUMBER OF TABS	α	% PEN. OF D_8	% BLOCK OF A_8	SECONDARY FLOW AREA
1	4.3-4B-R6	7-11-68	4.32"	1.41	16	11.5°	6.5	3.3	34.8 in^2
2	4.9-4B-R7-1	7-12-68	4.82"	1.26	16	18°	11.2	5.6	41.9 in^2
3	4.9-4B-R7-2	7-15-68	4.82"	1.26	16	24°	15.3	8.3	41.9 in^2
4	4.9-4B-R7	7-16-68	4.82"	1.26	16	11.5°	4.6	1.7	41.9 in^2
5	5.1-4B-R2	10-1-68	5.14"	1.18	16	11.5°	4.7	1.9	34.9 in^2
6	4.9-4B-R8	10-4-68	4.82"	1.26	8	18°	11.2	2.8	41.9 in^2
7	4.9-4B-R8-1	10-7-68	4.82"	1.26	4	18°	11.2	1.4	41.9 in^2
8	Conical	7-11-68	4.32"						
9	Conical	7-12,15,16 10-4 & 7-68	4.82"						
10	Conical	10-1-68	5.14"						

FIGURE V.C.2-2 SCHEMATIC AND LIST OF TEST CONFIGURATIONS OF TSEN 4 WITH PRIMARY THRUST REVERSER TABS

TABLE V.C.2-1 TEST SUMMARY

MODEL NO. 4.32" Cone

DESCRIPTION: Baseline Cone

DATE: 7/11/68

SCALE MODEL A_8 = .1269 ft^2

FULL SCALE A_8 = 8.122 ft^2

SCALE FACTOR = 8:1

- o DATA INCLUDES GROUND REFLECTION INTERFERENCE
- o ANGLE REFERENCED TO JET EXHAUST

TEST CONDITIONS					ACOUSTIC TEST RESULTS					
			IDEAL				320' ARC		300' SIDELINE	
RDG NO.	P_{T8}/P_o	T_{T8} (°R)	V_j (ft/sec)	W_8 (PPS)	10Log $\rho^2 A$	10Log ρA	PEAK PNdB	PEAK ANGLE	PEAK PNdB	PEAK ANGLE
1	3.01	1984	2573	7.04	-23.3	-7.3	140.6	50	138.4	50
2	3.02	2448	2891	6.32	-25.3	-8.3	140.8	50	138.6	50
3	3.02	2580	2937	6.15	-25.6	-8.5	140.8	50	138.6	50/60
4	2.52	2757	2804	4.97	-26.8	-9.2	139.3	50	137.1	50
5	2.01	2795	2484	3.79	-27.5	-9.7	137.5	50	135.3	50
6	1.99	1496	1812	5.25	-22.1	-7.0	131.7	30	126.7	40
7	1.56	1225	1334	4.18	-20.8	-6.3	116.0	30	113.2	50
8	1.34	1125	1042	3.35	-20.0	-5.7	107.3	40	104.5	50

TABLE V.C.2-2 TEST SUMMARY

MODEL NO. 4.82" Cone

DESCRIPTION: Baseline Cone

DATE: 7/12/68; 7/15/68; 7/16/68; 10/4/68; 10/7/68

- o DATA INCLUDES GROUND REFLECTION INTERFERENCE
- o ANGLE REFERENCED TO JET EXHAUST

SCALE MODEL A_8 = .1269 ft^2

FULL SCALE A_8 = 8.122 ft^2

SCALE FACTOR = 8:1

TEST CONDITIONS					ACOUSTIC TEST RESULTS					
							320' ARC		300' SIDELINE	
RDG NO.	P_{T8}/P_o	T_{T8} (°R)	IDEAL V_j (ft/sec)	W_8 (PPS)	10Log $\rho^2 A$	10Log ρA	PEAK PNdB	PEAK ANGLE	PEAK PNdB	PEAK ANGLE
7/12/68										
1	3.00	1996	2590	9.48	-22.4	-6.4	142.2	50	139.9	50
2	3.03	2410	2846	8.68	-28.0	-7.2	142.8	50	140.5	50
3	2.50	2800	2815	6.13	-26.0	-8.3	140.9	50	138.7	50
4	1.99	2800	2472	5.06	-26.6	-8.8	138.7	50	136.4	50
5	2.00	1495	1810	7.15	-21.2	-6.0	131.1	40	127.6	50
6	1.55	1240	1328	5.85	-20.0	-5.4	117.4	30	114.3	60
7	1.35	1130	1055	4.92	-19.1	-4.8	108.7	50	106.5	50
7/15/68										
1	1.33	1119	1026	4.81	-19.0	-4.7	109.5	50	107.2	50
2	1.55	1215	1321	5.77	-19.7	-5.3	118.4	40	115.8	50
3	2.00	1474	1799	7.09	-21.0	-5.9	132.2	40	128.1	40
4	2.02	2674	2436	5.27	-26.1	-8.5	138.3	50	136.1	50
5	2.50	2683	2758	6.57	-25.6	-8.1	140.9	50	139.1	60
6	2.99	2319	2772	8.44	-23.7	-7.1	142.3	50	140.0	50/60
7	2.99	1966	2554	9.25	-22.3	-6.3	142.1	50	139.8	50

TABLE V.C.2-2 TEST SUMMARY

(Continued)

MODEL NO. 4.82" Cone

DESCRIPTION: Baseline Cone

DATE: 7/16/68

SCALE MODEL A_8 = .1269 ft^2

FULL SCALE A_8 = 8.122 ft^2

SCALE FACTOR = 8:1

- o DATA INCLUDES GROUND REFLECTION INTERFERENCE
- o ANGLE REFERENCED TO JET EXHAUST

TEST CONDITIONS					ACOUSTIC TEST RESULTS					
			IDEAL				320' ARC		300' SIDELINE	
RDG NO.	P_{T8}/P_o	T_{T8} (°R)	V_j (ft/sec)	W_8 (PPS)	10Log $\rho^2 A$	10Log ρA	PEAK PNdB	PEAK ANGLE	PEAK PNdB	PEAK ANGLE
7/16/68										
1	1.36	1140	1078	5.20	-19.2	-4.8	109.0	50	107.1	60
2	1.56	1356	1406	5.93	-20.7	-5.8	118.1	30	115.2	50
3	2.00	1500	1814	7.18	-21.2	-6.0	130.2	40	126.9	50
4	2.07	2795	2530	5.10	-26.5	-8.7	137.6	50	135.4	50
5	2.50	2795	2813	6.42	-29.9	-8.3	139.8	60	138.9	60
6	3.00	2410	2833	8.37	-24.1	-7.2	140.8	50	138.8	60
7	3.00	2005	2585	9.16	-22.4	-6.4	141.2	50	138.9	50

TABLE V.C.2-2 TEST SUMMARY

(Continued)

MODEL NO. 4.82" Cone

DESCRIPTION: Baseline Cone

DATE: 10-4/68 & 10-7-68

- o DATA INCLUDES GROUND REFLECTION INTERFERENCE
- o ANGLE REFERENCED TO JET EXHAUST

SCALE MODEL A_8 = .1269 ft^2

FULL SCALE A_8 = 8.122 ft^2

SCALE FACTOR = 8:1

TEST CONDITIONS					ACOUSTIC TEST RESULTS							
							320' ARC		300' SIDELINE		1500' SIDELINE	
RDG NO.	P_{T8}/P_o	T_{T8} (°R)	IDEAL V_j (ft/sec)	W_8 (PPS)	10Log $\rho^2 A$	10Log ρA	PEAK PNdB	PEAK ANGLE	PEAK PNdB	PEAK ANGLE	PEAK PNdB	PEAK ANGLE
		10-4-68										
1	1.35	1130	1059	4.86	-19.1	-4.8	109.7	50	107.6	50	92.3	50
2	1.55	1245	1333	5.82	-20.0	-5.4	117.7	50	115.5	50	100.0	50
3	2.00	1500	1817	7.54	-21.1	-6.0	131.0	40	128.1	50	112.5	50
4	2.00	2760	2465	4.82	-26.4	-8.7	136.7	50	134.5	50	119.0	50
5	2.51	2795	2817	6.32	-25.9	-8.3	138.5	50	136.3	50	121.3	60
6	2.01	2500	2888	8.50	-24.3	-7.4	140.7	50	138.5	50	123.2	50
7	3.00	2005	2585	8.90	-22.4	-6.4	141.0	50	138.8	50	123.2	50
8	2.46	1705	2179	8.07	-21.7	-6.2	137.2	50	135.0	50	119.4	50
		10-7-68										
1	1.34	1130	1050	4.90	-19.1	-4.8	109.0	50	106.9	50	91.6	50
2	1.55	1255	1338	5.82	-20.0	-5.4	119.0	30	116.0	50	100.7	50
3	2.00	1505	1816	7.06	-21.2	-6.0	132.2	40	128.5	50	113.2	50
4	2.00	2790	2790	4.96	-26.5	-8.7	138.0	50	135.8	50	120.2	50
5	2.49	2795	2896	6.30	-26.5	-8.6	140.0	50	138.2	60	122.5	60
6	2.99	2320	2777	8.38	-23.7	-7.1	141.8	50	139.6	50	124.0	50
7	2.99	2005	2579	8.30	-22.4	-6.4	141.5	50	139.3	50	123.7	50
8	2.44	1700	2170	8.26	-21.7	-6.2	137.6	50	135.4	50	119.8	50

TABLE V.C.2-3 TEST SUMMARY

MODEL NO. 5.14" Cone

DESCRIPTION: Baseline Cone

DATE: 10-1-68

SCALE MODEL A_8 = .1443 ft^2

FULL SCALE A_8 = 9.235 ft^2

SCALE FACTOR = 8:1

- o DATA INCLUDES GROUND REFLECTION INTERFERENCE
- o ANGLE REFERENCED TO JET EXHAUST

TEST CONDITIONS					ACOUSTIC TEST RESULTS							
			IDEAL				320' ARC		300' SIDELINE		1500' SIDELINE	
RDG NO.	P_{T8}/P_o	T_{T8} (°R)	V_j (ft/sec)	W_8 (PPS)	10Log $\rho^2 A$	10Log ρA	PEAK PNdB	PEAK ANGLE	PEAK PNdB	PEAK ANGLE	PEAK PNdB	PEAK ANGLE
1	1.35	1130	1060	4.82	-18.6	-4.2	107.7	50	105.6	50	90.6	50
2	1.56	1240	1345	6.00	-19.4	-4.8	118.8	30	114.3	50	99.1	50
3	2.01	1495	1818	7.14	-20.6	-5.5	132.5	40	128.5	40	113.6	40
4	2.01	2795	2485	5.36	-26.1	-8.2	136.7	50	134.5	50	119.1	50
5	2.51	2780	2809	6.48	-25.4	-7.7	138.9	50	137.3	60	121.9	60
6	3.00	2315	2778	8.94	-23.2	-6.5	141.1	50	138.9	50	123.4	50

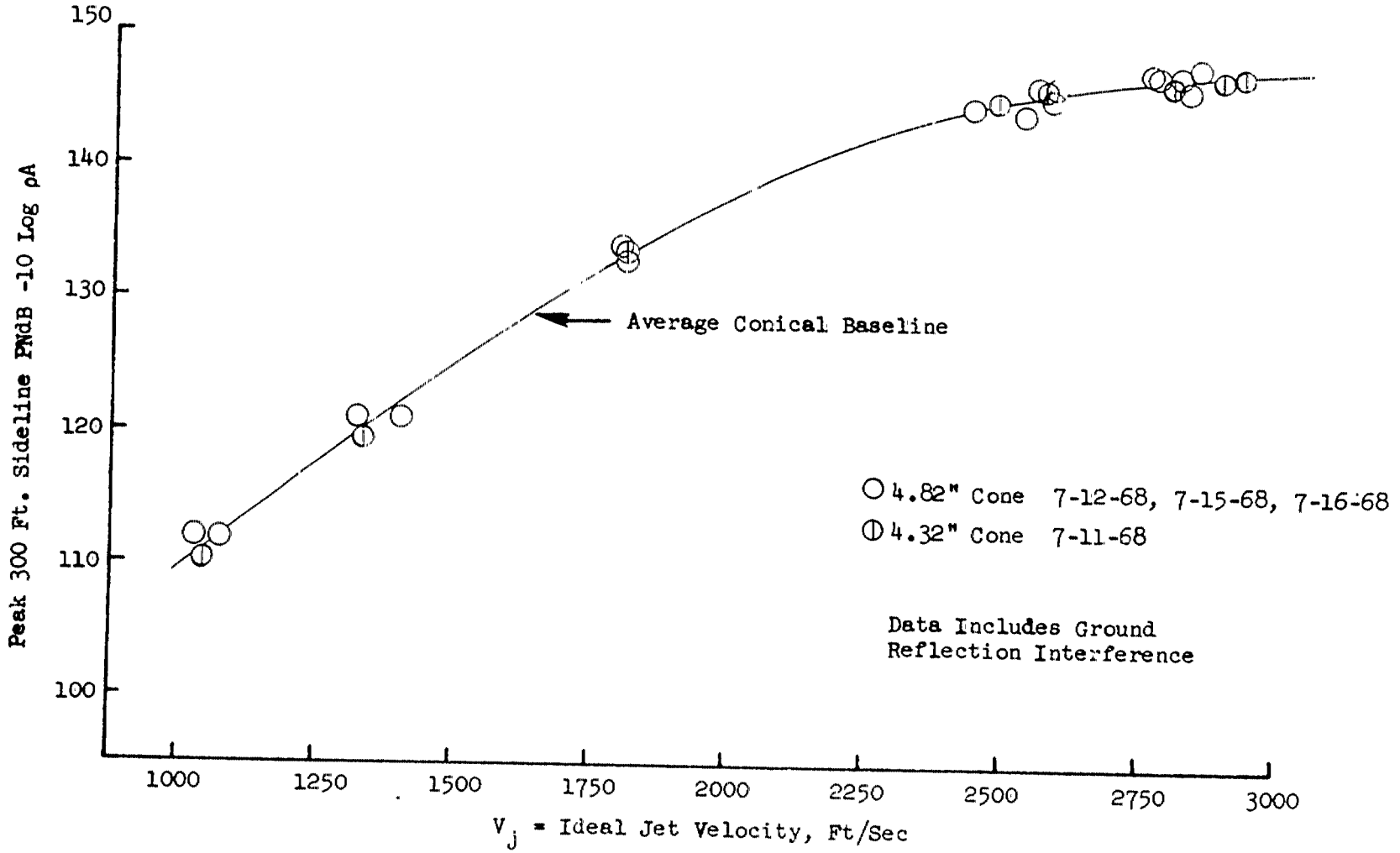

FIGURE V.C.2-3 300 FT. SIDELINE JET NOISE LEVELS FOR AVERAGE CONICAL BASELINE

TABLE V.C.2-4 TEST SUMMARY

MODEL NO. 4.9-4B-R7

DESCRIPTION: 4.82 Cone + TSEN 4,16 Tabs, α = 11.5°

DATE: 7/16/68

SCALE MODEL A_8 = .1269 ft^2

FULL SCALE A_8 = 8.122 ft^2

SCALE FACTOR = 8:1

- o DATA INCLUDES GROUND REFLECTION INTERFERENCE
- o ANGLE REFERENCED TO JET EXHAUST

TEST CONDITIONS					ACOUSTIC TEST RESULTS					
							320' ARC		300' SIDELINE	
RDG NO.	P_{T8}/P_o	T_{T8} (°R)	IDEAL V_j (ft/sec)	W_8 (PPS)	10Log $\rho^2 A$	10Log ρA	PEAK PNdB	PEAK ANGLE	PEAK PNdB	PEAK ANGLE
1	1.36	1360	1178	5.12	-20.7	-5.8	107.8	60	107.5	70
2	1.56	1250	1351	5.99	-20.0	-5.4	116.7	30	114.3	70
3	2.00	1450	1784	7.20	-20.1	-5.9	128.1	50	126.1	70
4	2.00	2780	2471	5.12	-26.5	-8.7	135.0	60	134.1	60
5	2.49	2800	2813	6.36	-26.0	-8.3	138.3	60	137.4	60
6	2.99	2795	3045	7.74	-25.3	-7.9	139.9	60	139.0	60
7	3.00	2520	2897	8.17	-24.4	-7.4	139.6	50	138.3	60
8	3.00	2020	2594	9.12	-22.5	-6.5	138.5	50	137.1	60

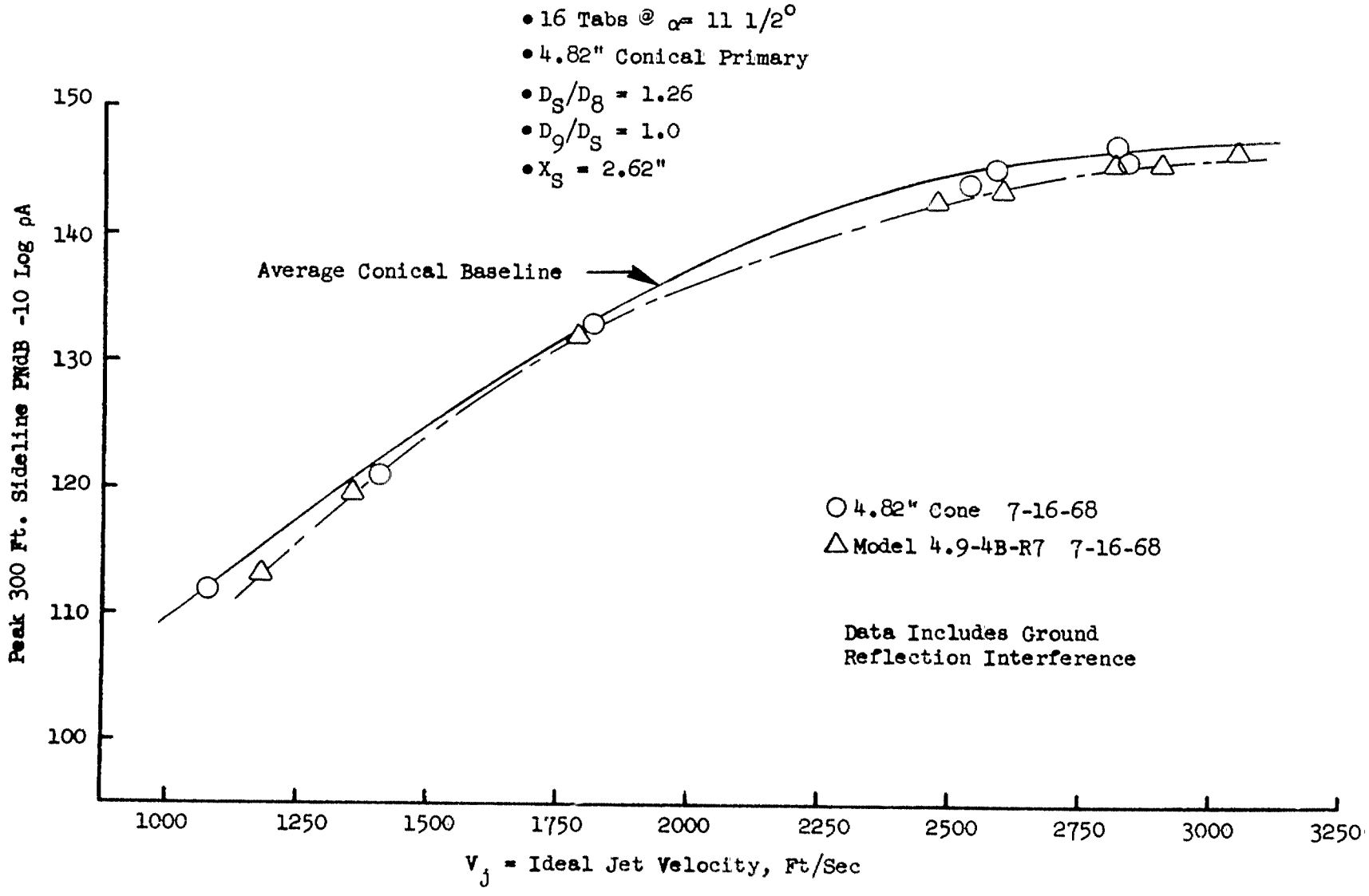

FIGURE V.C.2-4 300 FT. SIDELINE JET NOISE LEVELS FOR TSEN 4 WITH 4.82" CONE AND PRIMARY THRUST REVERSER TABS, α = 11 1/2°

TABLE V.C.2-5 TEST SUMMARY

MODEL NO. 4.9-4B-R7-1

DESCRIPTION: 4.82 Cone + TSEN 4; 16 Tabs, α = 18°

DATE: 7/12/68

SCALE MODEL A_8 = .1269 ft^2

FULL SCALE A_8 = 8.122 ft^2

SCALE FACTOR = 8:1

- o DATA INCLUDES GROUND REFLECTION INTERFERENCE
- o ANGLE REFERENCED TO JET EXHAUST

TEST CONDITIONS					ACOUSTIC TEST RESULTS					
			IDEAL				320' ARC		300' SIDELINE	
RDG NO.	P_{T8}/P_o	T_{T8} (°R)	V_j (ft/sec)	W_8 (PPS)	10Log $\rho^2 A$	10Log ρA	PEAK PNdB	PEAK ANGLE	PEAK PNdB	PEAK ANGLE
1	1.34	1128	1050	4.97	-19.1	-4.8	107.7	60	107.5	70
2	1.57	1224	1338	6.02	-19.8	-5.3	114.6	60	114.8	70
3	2.03	1513	1840	7.30	-21.2	-6.1	127.4	40	125.0	50
4	2.02	2804	2501	5.25	-26.6	-8.7	134.2	60	133.3	60
5	2.54	2787	2834	6.63	-25.9	-8.3	137.8	60	136.5	60
6	3.06	2774	3063	8.03	-25.2	-7.8	139.8	50	138.4	70
7	3.04	2478	2886	8.37	-24.2	-7.3	140.0	50	138.2	60
8	3.04	1995	2590	9.41	-22.4	-6.4	138.7	50	136.5	50

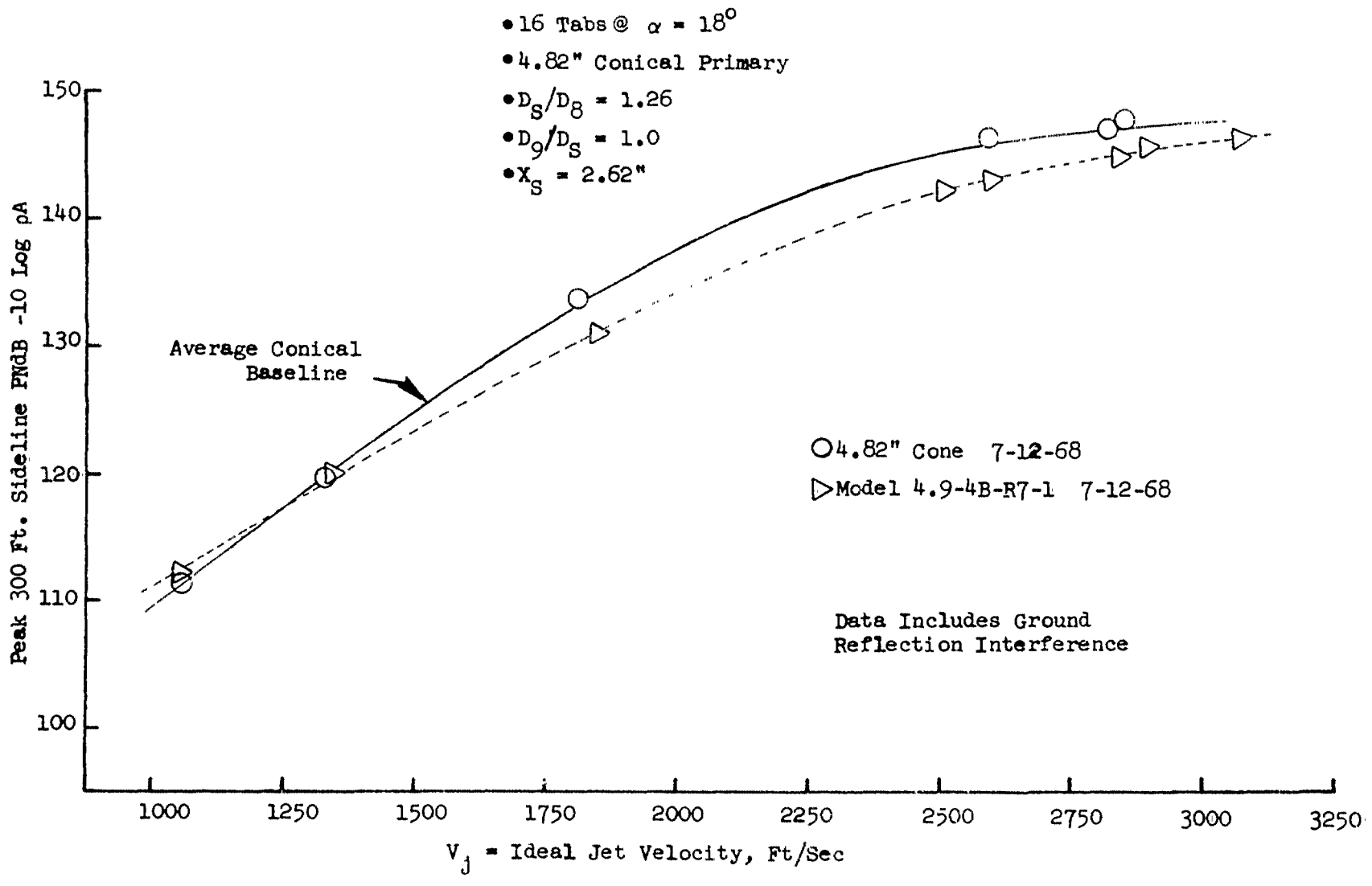

FIGURE V.C.2-5 300 FT. SIDELINE JET NOISE LEVELS FOR TSEN 4 WITH 4.82" CONE PRIMARY THRUST REVERSER TABS, $\alpha = 18^{\circ}$

TABLE V.C.2-6 TEST SUMMARY

MODEL NO. 4.9-4B-K7-2

DESCRIPTION: 4.82 Cone + TSEN 4, 16 Tabs, α = 24°

DATE: 7/15/68

SCALE MODEL A_8 = .1269 ft^2

FULL SCALE A_8 = 8.122 ft^2

SCALE FACTOR = 8:1

- o DATA INCLUDES GROUND REFLECTION INTERFERENCE
- o ANGLE REFERENCED TO JET EXHAUST

TEST CONDITIONS					ACOUSTIC TEST RESULTS					
							320' ARC		300' SIDELINE	
RDG NO.	P_{T8}/P_o	T_{T8} (°R)	IDEAL V_j (ft/sec)	W_8 (PPS)	10Log $\rho^2 A$	10Log ρA	PEAK PNdB	PEAK ANGLE	PEAK PNdB	PEAK ANGLE
1	1.37	1118	1082	5.19	-19.0	-4.8	111.0	60	110.1	60
2	1.57	1212	1330	5.88	-19.7	-5.3	117.5	60	116.6	60/70
3	2.03	1455	1804	7.29	-20.9	-5.9	128.0	40	124.8	50
4	2.01	2684	2438	5.18	-26.2	-8.5	133.6	60	132.7	60
5	2.51	2680	2760	6.52	-25.5	-8.1	137.3	50/60	136.4	60
6	3.03	2676	2994	7.95	-24.9	-7.7	140.3	50	138.8	60
7	3.01	2375	2815	8.38	-23.9	-7.1	139.5	50	137.3	50/60
8	3.00	1949	2548	9.36	-22.2	-6.3	138.0	50	135.8	50

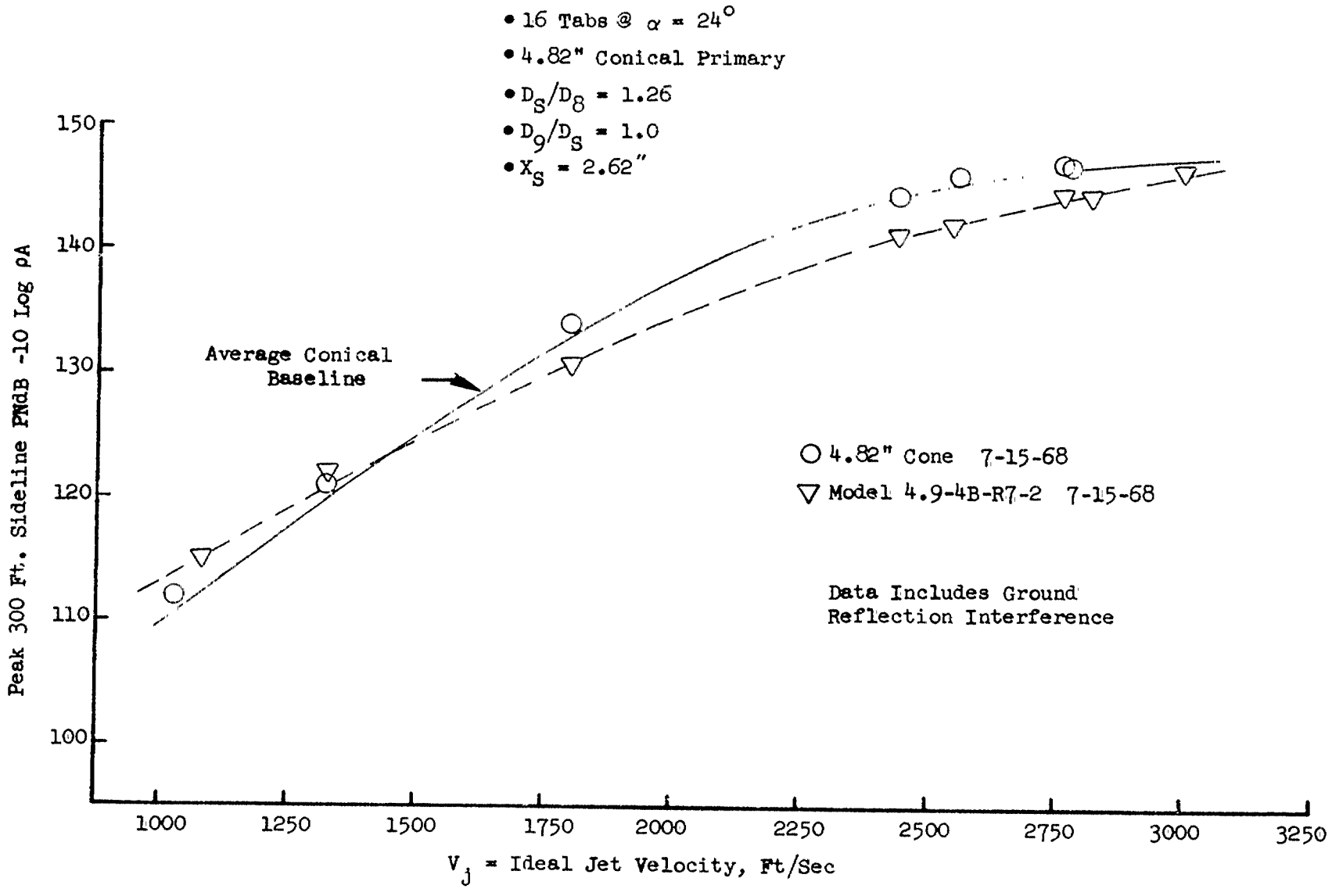

FIGURE V.C.2-6 300 FT. SIDELINE JET NOISE LEVELS FOR TSEN 4 WITH 4.82" CONE PRIMARY THRUST REVERSER TABS, α = 24°

TABLE V.C.2-7 TEST SUMMARY

MODEL NO. 5.1-4B-R2

DESCRIPTION: 5.14 Cone + TSEN 4, 16 Tabs α = 11.5°

DATE: 10/1/68

SCALE MODEL A_8 = .1443 ft^2

FULL SCALE A_8 = 9.235 ft^2

SCALE FACTOR = 8:1

- o DATA INCLUDES GROUND REFLECTION INTERFERENCE
- o ANGLE REFERENCED TO JET EXHAUST

TEST CONDITIONS					ACOUSTIC TEST RESULTS							
RDG NO.	P_{T8}/P_o	T_{T8} (°R)	IDEAL V_j (ft/sec)	W_8 (PPS)	10Log $\rho^2 A$	10Log ρA	320' ARC PEAK PNdB	320' ARC PEAK ANGLE	300' SIDELINE PEAK PNdB	300' SIDELINE PEAK ANGLE	1500' SIDELINE PEAK PNdB	1500' SIDELINE PEAK ANGLE
1	1.35	1135	1066	4.97	-18.5	-4.2	111.4	50	111.5	80	95.9	80
2	1.56	1250	1344	6.03	-19.4	-4.8	120.4	40	119.1	80	104.1	80
3	2.01	1500	1821	7.35	-20.5	-5.4	129.5	40	126.9	50	111.1	50
4	3.01	2785	3048	8.42	-24.7	-7.2	140.6	50	138.5	50	122.9	50
5	2.51	2800	2819	7.20	-25.3	-7.6	139.3	50	137.1	50	121.6	50
6	2.00	2800	2479	5.33	-25.9	-8.0	134.4	50	132.8	60	117.0	50
7	3.01	2490	2882	8.54	-26.6	-6.7	140.5	50	138.3	50	122.8	50
8	3.01	2030	2602	9.67	-21.9	-5.8	139.7	50	137.5	50	122.0	50
9	2.39	1730	2163	8.66	-21.2	-5.6	134.8	50	132.6	50	116.4	50

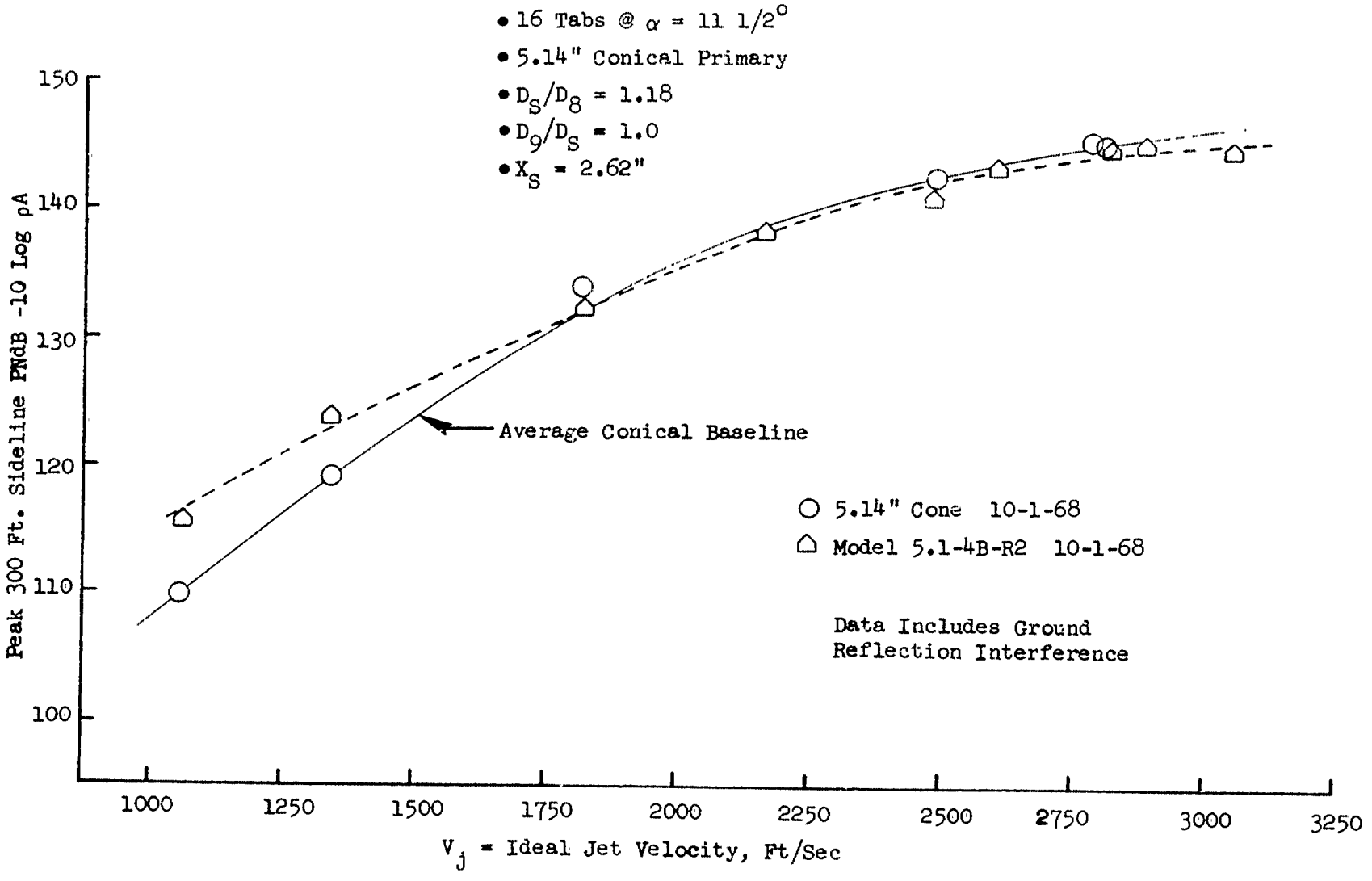

FIGURE V.C.2-7 300 FT. SIDELINE JET NOISE LEVELS FOR TSEN 4 WITH 5.14" CONE AND PRIMARY THRUST REVERSER TABS, D_S/D_8 = 1.18

TABLE V.C.2-8 TEST SUMMARY

MODEL NO. 4.3-4B-R6

DESCRIPTION: 4.32 Cone + TSEN 4/16 Flaps, α = 11.5°

DATE: 7/11/68

SCALE MODEL A_8 =

FULL SCALE A_8 =

SCALE FACTOR = 8:1

- o DATA INCLUDES GROUND REFLECTION INTERFERENCE
- o ANGLE REFERENCED TO JET EXHAUST

TEST CONDITIONS					ACOUSTIC TEST RESULTS					
							320' ARC		300' SIDELINE	
RDG NO.	P_{T8}/P_o	T_{T8} (°R)	IDEAL V_j (ft/sec)	W_8 (PPS)	10Log $\rho^2 A$	10Log ρA	PEAK PNdB	PEAK ANGLE	PEAK PNdB	PEAK ANGLE
1	1.34	1160	1068	3.51	-20.3	-5.8	103.6	50	101.9	60
3	2.01	1509	1828	5.32	-22.2	-7.0	127.3	40/50	125.1	50
4	2.01	2750	2469	3.75	-27.4	-9.6	133.0	50	132.0	60
5	2.52	2762	2810	4.92	-26.7	-9.8	136.5	60	135.6	60
6	3.02	2775	3047	5.95	-26.2	-8.8	138.3	50/60	137.4	60
7	3.03	2487	2887	6.30	-25.2	-8.3	138.4	50	137.1	60
8	3.03	1956	2562	7.06	-23.1	-7.3	137.3	50	135.1	50

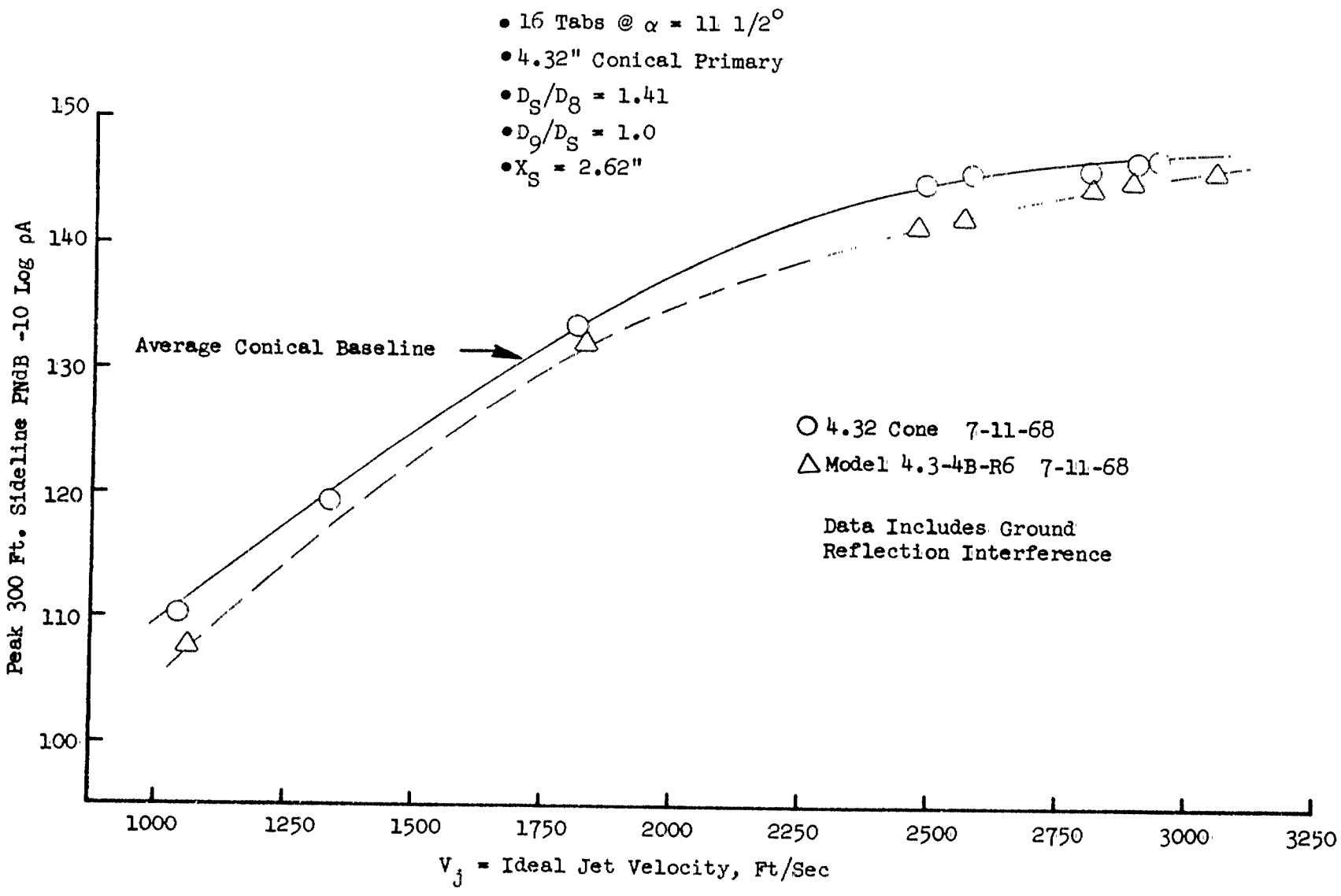

FIGURE V.C.2-8 300 FT. SIDELINE JET NOISE LEVELS FOR TSEN 4 WITH 4.32" CONE AND PRIMARY THRUST REVERSER TABS, D_S/D_8 = 1.41

TABLE V.C.2-9 TEST SUMMARY

MODEL NO. 4.9-4B-R8

DESCRIPTION: 4.82 Cone + TSEN 4, 8 Tabs, α = 18°

DATE: 10/4/68

SCALE MODEL A_8 = .1269 ft^2

FULL SCALE A_8 = 8.122 ft^2

SCALE FACTOR = 8:1

- o DATA INCLUDES GROUND REFLECTION INTERFERENCE
- o ANGLE REFERENCED TO JET EXHAUST

TEST CONDITIONS					ACOUSTIC TEST RESULTS							
							320' ARC		300' SIDELINE		1500' SIDELINE	
RDG NO.	P_{T8}/P_o	T_{T8} (°R)	IDEAL V_j (ft/sec)	W_8 (PPS)	10Log $\rho^2 A$	10Log ρA	PEAK PNdB	PEAK ANGLE	PEAK PNdB	PEAK ANGLE	PEAK PNdB	PEAK ANGLE
1	1.35	1130	1054	4.98	-19.1	-4.8	107.4	50	106.1	60	90.8	60
2	1.55	1250	1335	5.85	-20.0	-5.4	118.4	30	114.7	60	99.5	60
3	2.00	1500	1815	6.86	-21.1	-6.0	128.7	50	126.5	50	110.8	50
4	2.00	2800	2483	4.93	-26.6	-8.7	133.7	50	131.6	50	116.6	60
5	2.50	2790	2810	6.26	-25.9	-8.3	136.4	60	135.6	60	119.7	60
6	3.00	2790	3046	7.50	-25.3	-7.9	136.0	50	134.7	60	119.3	60
7	2.99	2490	2876	7.94	-24.3	-7.4	136.2	50	135.2	60	119.8	60
8	3.01	2010	2589	8.92	-22.4	-6.4	135.3	60	134.4	60	118.7	60
9	2.46	1700	2176	8.03	-21.6	-6.2	133.9	50	131.7	50	115.9	50

TABLE V.C.2-10 TEST SUMMARY

MODEL NO. 4.9-4B-R8-1

DESCRIPTION: 4.82 Cone + TSEN 4, 4 Tabs, α = 18°

DATE: 10/7/68

SCALE MODEL A_8 = .1269 ft^2

FULL SCALE A_8 = 8.122 ft^2

SCALE FACTOR = 8:1

- DATA INCLUDES GROUND REFLECTION INTERFERENCE
- ANGLE REFERENCED TO JET EXHAUST

TEST CONDITIONS					ACOUSTIC TEST RESULTS							
			IDEAL				320' ARC		300' SIDELINE		1500' SIDELINE	
RDG NO.	P_{T8}/P_o	T_{T8} (°R)	V_j (ft/sec)	W_8 (PPS)	10Log $\rho^2 A$	10Log ρA	PEAK PNdB	PEAK ANGLE	PEAK PNdB	PEAK ANGLE	PEAK PNdB	PEAK ANGLE
1	1.35	1140	1063	4.96	-19.1	-4.8	109.1	50	107.6	60	92.4	60
3	1.99	1500	1811	7.10	-21.2	-6.0	129.9	40	127.3	50	112.1	50
4	2.00	2795	2475	4.97	-26.6	-8.7	134.3	60	133.4	60	117.8	60
5	2.50	2795	2813	6.34	-25.9	-8.3	137.5	60	136.7	60	121.1	60
6	2.99	2795	3045	7.57	-25.3	-7.9	138.5	50	136.8	60	121.3	60
7	2.99	2500	2882	8.00	-24.3	-7.4	137.4	60	136.6	60	121.1	60
8	2.98	2005	2578	8.80	-22.4	-6.4	137.3	50	135.3	60	119.7	50
9	2.45	1700	2173	8.74	-21.7	-6.2	135.2	50	133.0	50	117.6	50

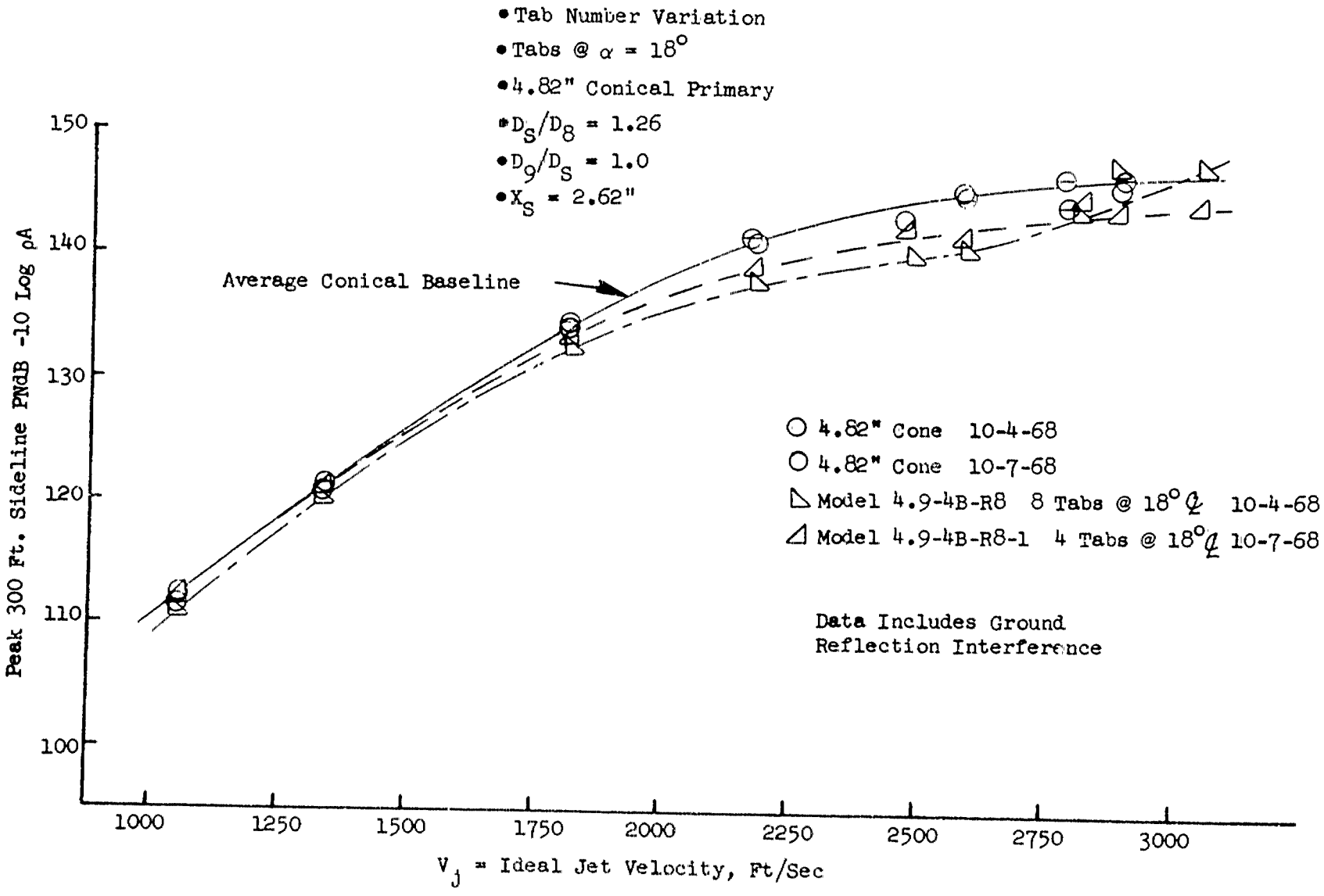

FIGURE V.C.2-9 300 FT. SIDELINE JET NOISE LEVELS FOR 8 AND 4 PRIMARY TABS WITHIN TSEN 4

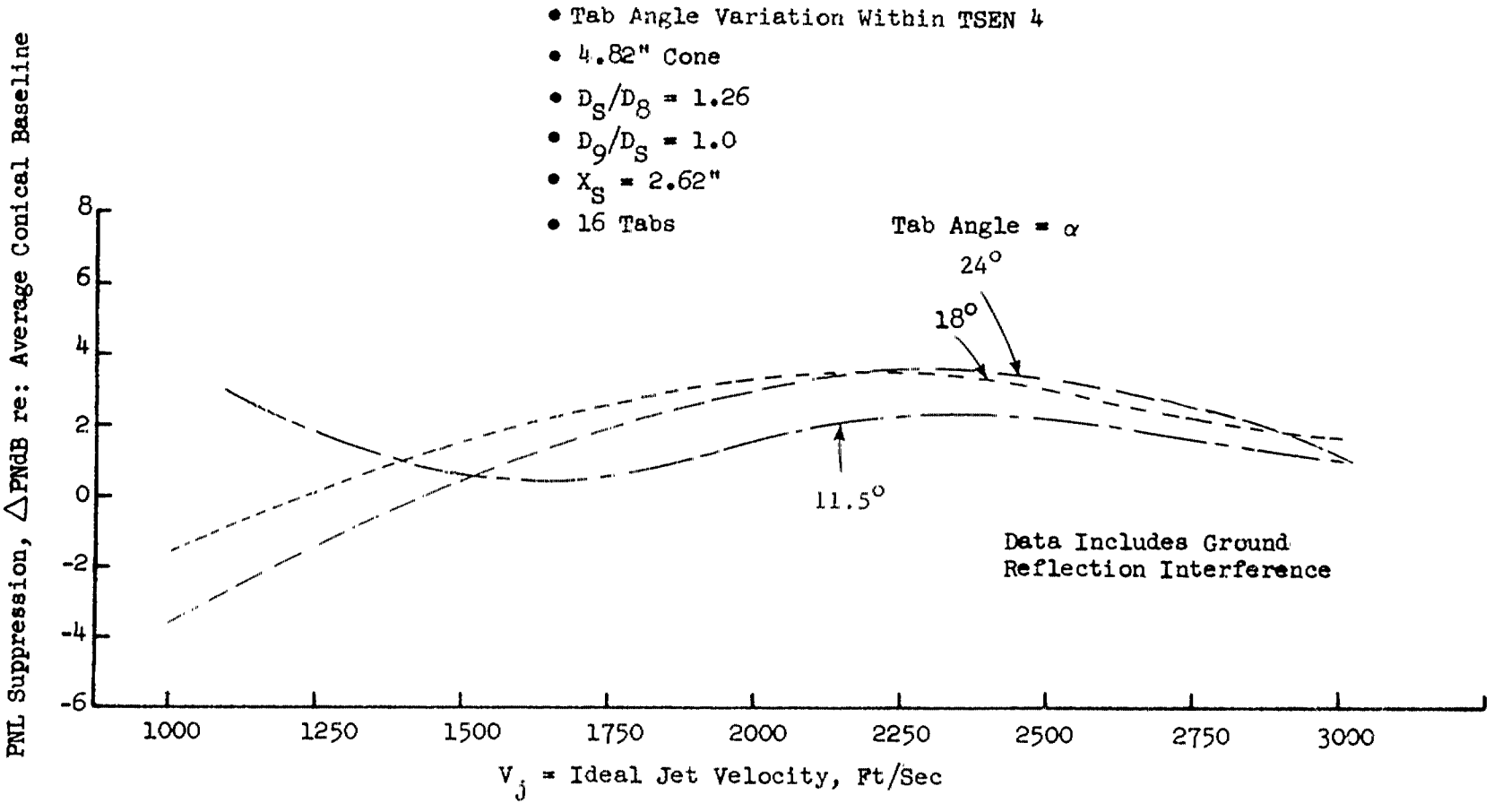

FIGURE V.C.2-10 EFFECT OF PRIMARY THRUST REVERSER TAB ANGLE ON 300 FT. SIDELINE PNL SUPPRESSION

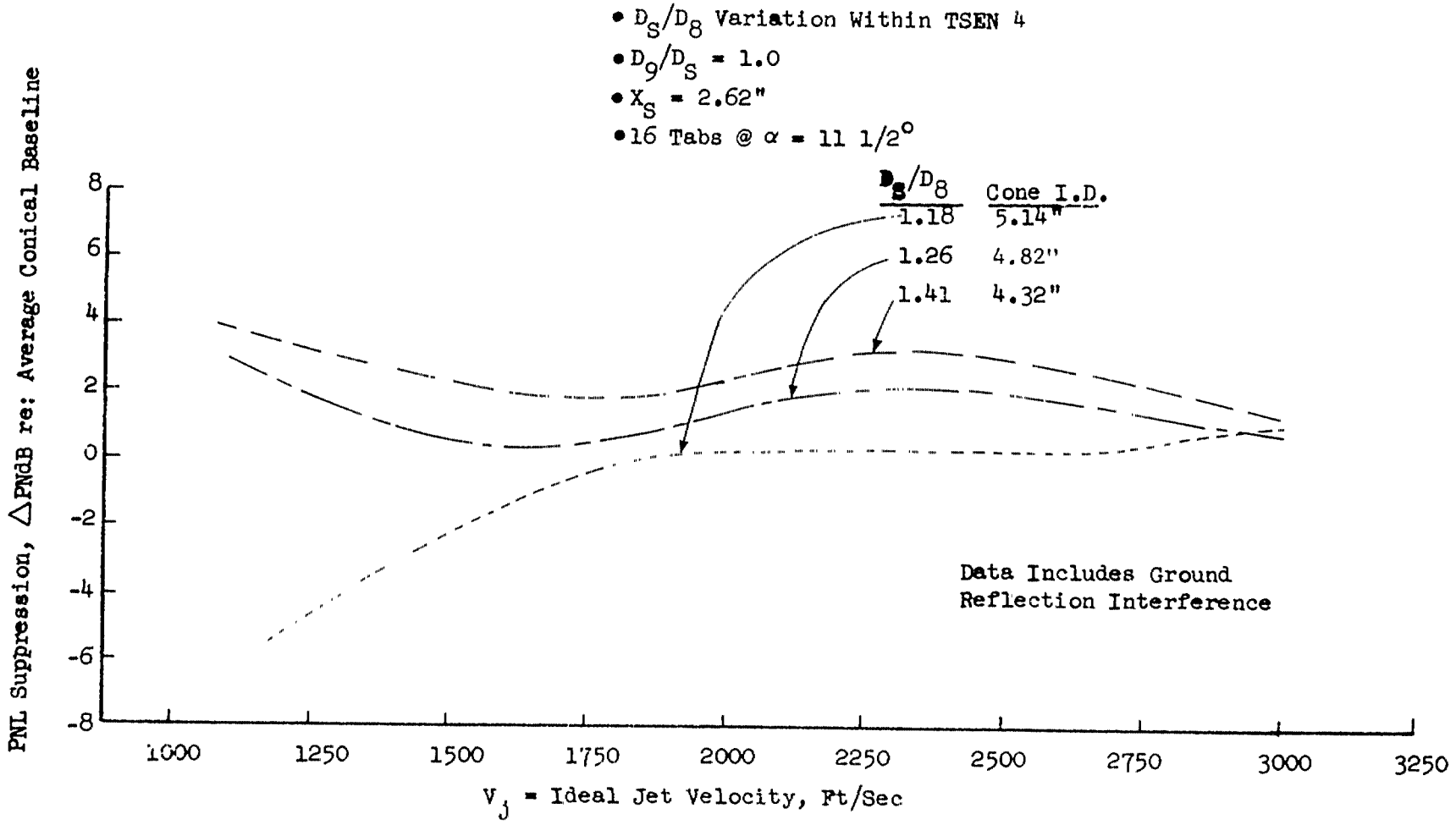

FIGURE V.C.2-11 EFFECT OF PRIMARY THRUST REVERSER TABS AND D_s/D_8 VARIATION WITHIN TSEN 4 ON 300 FT. SIDELINE PNL SUPPRESSION

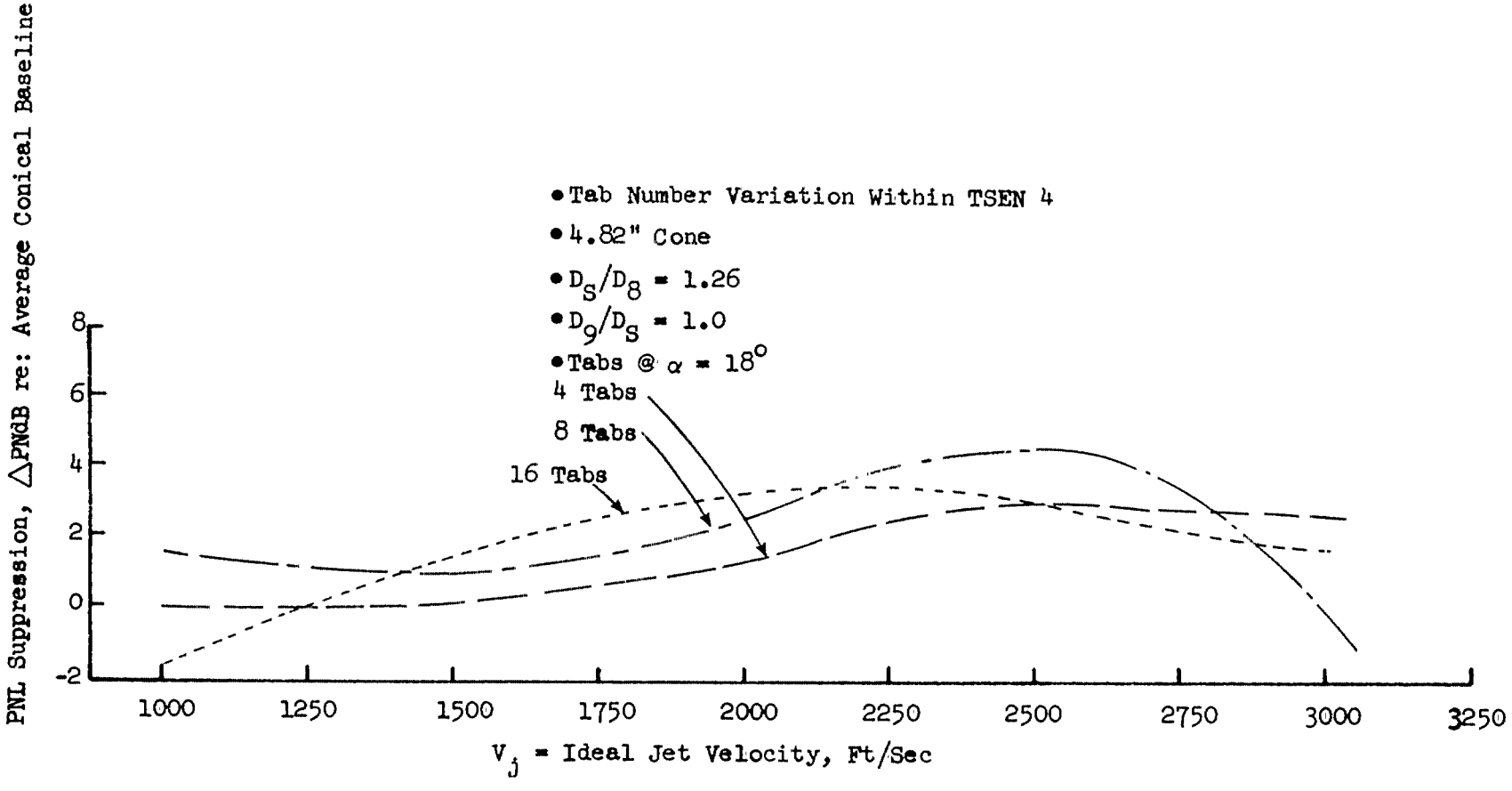

FIGURE V.C.2-12 EFFECT OF PRIMARY THRUST REVERSER TAB NUMBER ON 300 FT. SIDELINE PNL SUPPRESSION

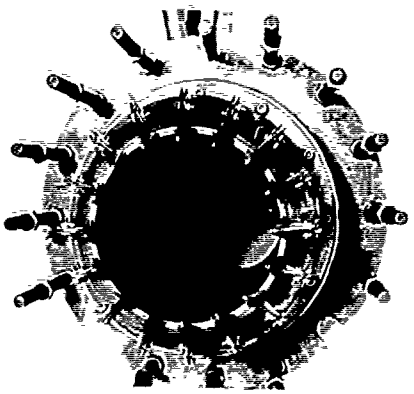

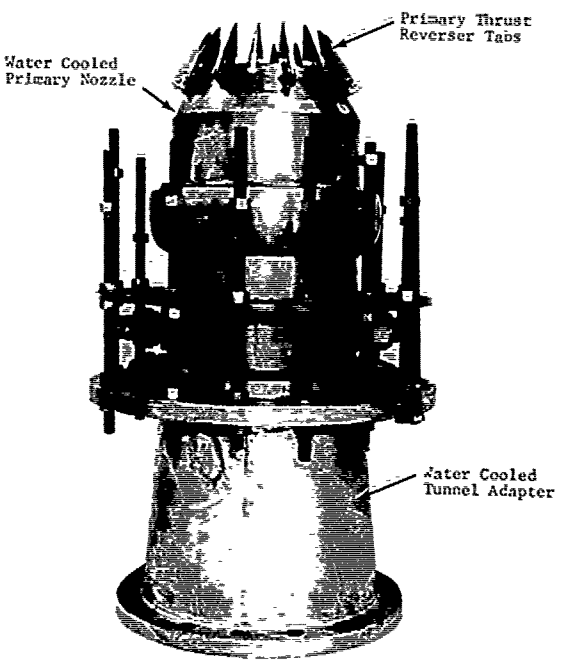

FIGURE V.C.2-13 PRIMARY THRUST REVERSER TABS INSTALLED ON 5.637" I.D. PRIMARY NOZZLE WITHOUT TWO STAGE EJECTOR, TSEN-56

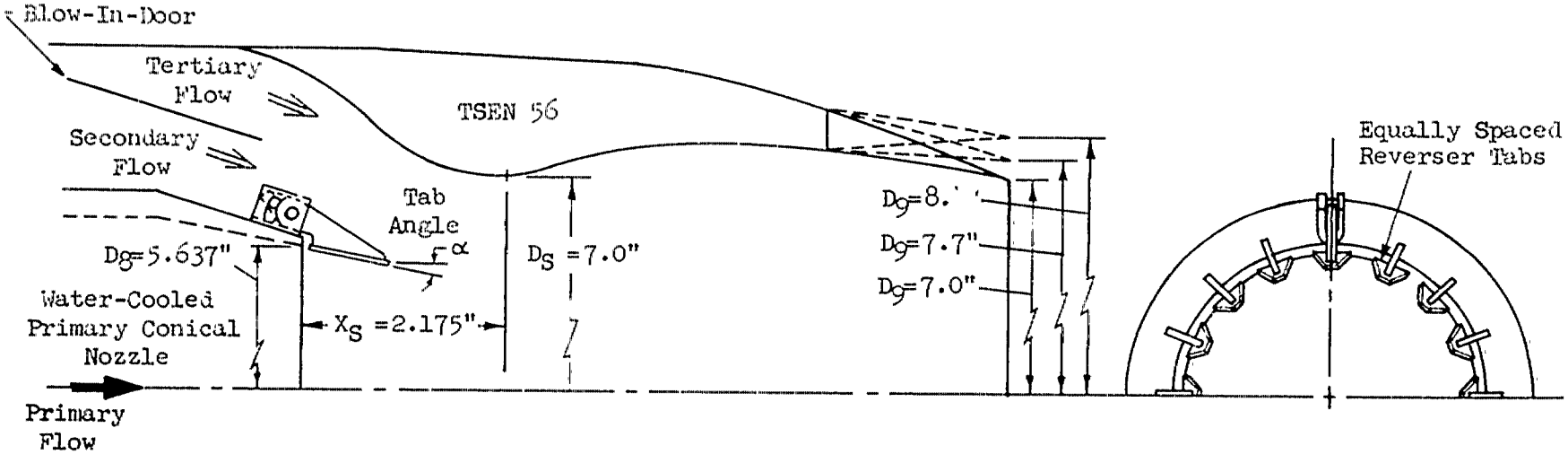

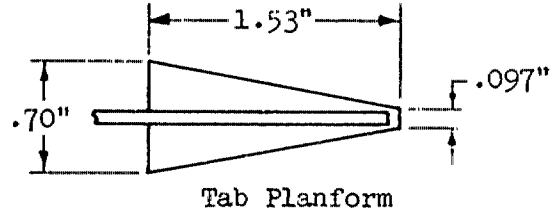

Tab Planform

- TSEN = Two Stage Ejector Nozzle
- D_S/D_8 = 1.241
- 16 Tabs at α = 18°
- 14.1% Penetration of D_8
- 8.8% Blockage of A_8
- Tertiary Flow Area = 16 in^2
- Secondary Flow Area = 7.8 in^2

TEST NO.	MODEL NO.	TEST DATE	D_9	D_9/D_S
1	5.6-56B-14	10-8-68	7.0"	1.0
2	5.6-56B-15	10-9-68	7.7"	1.1
3	5.6-56B-16	10-10-68	8.4"	1.2
4	5.637 Conical	10-8, 9, & 10-10-68		

FIGURE V.C.2-14 SCHEMATIC AND TEST CONFIGURATION SUMMARY OF CONICAL PRIMARY PLUS TSEN 56 WITH (16) PRIMARY THRUST REVERSER TABS

TABLE V.C.2-11 TEST SUMMARY

MODEL NO. 5.637" Cone

DESCRIPTION: Baseline Cone

DATE: 10/8/68 ; 10/9/68; 10/10/68

- o DATA INCLUDES GROUND REFLECTION INTERFERENCE
- o ANGLE REFERENCED TO JET EXHAUST

SCALE MODEL A_8 = .1733 ft^2

FULL SCALE A_8 = 11.091 ft^2

SCALE FACTOR = 8:1

TEST CONDITIONS					ACOUSTIC TEST RESULTS							
			IDEAL				320' ARC		300' SIDELINE		1500' SIDELINE	
RDG NO.	P_{T8}/P_o	T_{T8} (°R)	V_j (ft/sec)	W_8 (PPS)	10Log $\rho^2 A$	10Log ρA	PEAK PNdB	PEAK ANGLE	PEAK PNdB	PEAK ANGLE	PEAK PNdB	PEAK ANGLE
10/8/68												
1	1.34	1135	1056	6.23	-17.8	-3.4	109.2	40	106.9	60	91.8	60
2	1.56	1250	1342	7.52	-18.6	-4.1	119.7	30	115.1	50/60	100.3	40
3	2.00	1495	1812	8.33	-19.8	-4.7	133.5	40	129.4	40	114.3	40
4	2.00	2790	2476	6.58	-25.2	-7.4	138.9	50	136.8	50	121.1	50
5	2.51	2520	2677	8.83	-23.7	-6.5	144.8	50	142.6	50	127.1	50
6	2.99	2210	2710	11.12	-21.9	-5.5	145.1	50	142.9	50	127.3	50
7	2.99	2010	2584	10.65	-21.1	-5.1	144.3	50	142.2	50	126.5	50
8	2.45	1715	2181	10.53	-20.4	-4.9	138.7	50	136.5	50	121.0	50
10/9/68												
1	1.35	1140	1065	6.40	-17.8	-3.5	109.5	40	107.0	60	91.8	50
2	1.55	1250	1338	7.51	-18.7	-4.1	119.9	30	116.0	50	101.0	40
3	2.00	1500	1818	9.20	-19.8	-4.7	134.7	30	130.0	40	115.0	40
4	2.00	1300	1691	6.62	-18.6	-4.1	139.3	50	137.2	50	121.7	50
5	3.00	2015	2590	11.70	-21.1	-5.1	144.5	50	142.2	50	126.3	50
6	2.45	1700	2173	10.45	-20.4	-4.9	139.7	40	136.8	50	121.2	50

TABLE V.C.2-11 TEST SUMMARY

(Continued)

MODEL NO. 5.637" Cone

DESCRIPTION: Baseline Cone

DATE: 10/8/68; 10/9/68; 10/10/68

SCALE MODEL A_8 = .1733 ft^2

FULL SCALE A_8 = 11.091 ft^2

SCALE FACTOR = 8:1

- o DATA INCLUDES GROUND REFLECTION INTERFERENCE
- o ANGLE REFERENCED TO JET EXHAUST

TEST CONDITIONS					ACOUSTIC TEST RESULTS							
							320' ARC		300' SIDELINE		1500' SIDELINE	
RDG NO.	P_{T8}/P_o	T_{T8} (°R)	IDEAL V_j (ft/sec)	W_8 (PPS)	10Log $\rho^2 A$	10Log ρA	PEAK PNdB	PEAK ANGLE	PEAK PNdB	PEAK ANGLE	PEAK PNdB	PEAK ANGLE
10/10/68												
1	1.34	1150	1063	6.23	-17.9	-3.5	109.3	50	107.2	50	92.2	50
2	1.56	1250	1342	7.52	-18.7	-4.1	119.9	30	115.8	50	100.8	50
3	2.00	1495	1812	8.33	-19.8	-6.7	132.9	40	128.9	40	113.7	40
4	2.00	2800	2480	6.58	-25.2	-7.4	138.6	50	136.5	50	121.1	50
5	2.51	2520	2677	8.83	-23.7	-6.5	144.5	50	142.3	50	126.8	50
6	2.99	2220	2716	11.12	-22.0	-5.5	144.4	50	142.3	50	126.7	50
7	2.99	2010	2584	10.65	-21.1	-5.1	143.6	50	141.4	50	125.8	50
8	2.45	1715	2181	10.55	-20.4	-4.9	138.5	60	137.7	60	122.8	60

TABLE V.C.2-12 TEST SUMMARY

MODEL NO. 5.6-56B-14

DESCRIPTION: 5.637 Cone + TSEN 56; 16 Tabs, α = 18°, D_9/D_S = 1.00

DATE: 10/8/68

SCALE MODEL A_8 = .1733 ft^2

FULL SCALE A_8 = 11.091 ft^2

SCALE FACTOR = 8:1

- DATA INCLUDES GROUND REFLECTION INTERFERENCE
- ANGLE REFERENCED TO JET EXHAUST

TEST CONDITIONS					ACOUSTIC TEST RESULTS							
			IDEAL				320' ARC		300' SIDELINE		1500' SIDELINE	
RDG NO.	P_{T8}/P_o	T_{T8} (°R)	V_j (ft/sec)	W_8 (PPS)	10Log $\rho^2 A$	10Log ρA	PEAK PNdB	PEAK ANGLE	PEAK PNdB	PEAK ANGLE	PEAK PNdB	PEAK ANGLE
1	1.34	1130	1054	6.28	-17.7	-3.4	107.5	60	106.7	70	91.3	60
2	1.54	1250	1332	7.46	-18.7	-4.0	117.2	30	114.2	70	98.5	50
3	1.99	1500	1811	8.92	-19.8	-4.7	128.6	40	126.1	50	111.1	50
4	2.00	2885	2515	6.63	-25.5	-7.5	134.7	50/60	133.8	60	118.1	60
5	2.46	1700	2175	10.50	-20.3	-4.8	135.7	50	133.5	50	118.0	50
6	2.56	2795	2816	8.37	-24.6	-7.0	138.3	50	136.9	60	120.8	60
7	3.00	2800	3053	9.86	-24.0	-6.5	141.0	50	139.7	60	124.2	60
8	3.00	2490	2879	10.45	-22.9	-6.0	140.4	50	138.5	60	122.8	50
9	3.00	2005	2582	10.70	-21.1	-5.1	139.4	50	137.2	50	121.8	50

TABLE V.C.2-13 TEST SUMMARY

MODEL NO. 5.6-56B-15

DESCRIPTION: 5.637 Cone + TSEN 56, 16 Tabs, α = 18° D_9/D_S = 1.10

DATE: 10/9/68

SCALE MODEL A_8 = .1733 ft^2

FULL SCALE A_8 = 11.091 ft^2

SCALE FACTOR = 8:1

- o DATA INCLUDES GROUND REFLECTION INTERFERENCE
- o ANGLE REFERENCED TO JET EXHAUST

TEST CONDITIONS					ACOUSTIC TEST RESULTS							
			IDEAL				320' ARC		300' SIDELINE		1500' SIDELINE	
RDG NO.	P_{T8}/P_o	T_{T8} (°R)	V_j (ft/sec)	W_8 (PPS)	10Log $\rho^2 A$	10Log ρA	PEAK PNdB	PEAK ANGLE	PEAK PNdB	PEAK ANGLE	PEAK PNdB	PEAK ANGLE
1	1.35	1125	1061	6.60	-17.7	-3.4	110.2	50	107.9	50	91.4	50
2	1.55	1255	1344	7.66	-18.7	-4.1	117.2	30	116.0	70	98.8	50
3	2.00	1500	1818	8.97	-19.8	-4.7	128.1	50	126.0	50	110.8	50
4	2.00	2790	2477	6.68	-25.2	-7.4	134.1	50	132.2	60	116.7	50
5	2.45	1705	2176	10.45	-20.4	-4.9	130.6	40	127.9	50/70	112.1	50
6	2.51	2800	2820	8.40	-24.6	-7.0	135.8	50	133.7	50	118.4	50
7	3.01	2800	3055	9.95	-24.0	-6.5	140.0	50	137.8	50	122.4	50
8	3.00	2490	2878	10.45	-23.0	-6.0	139.1	50	136.9	50	121.5	50
9	3.00	2005	2584	11.92	-21.1	-5.1	137.5	50	135.4	50	120.0	50

TABLE V.C.2-14 TEST SUMMARY

MODEL NO. 5.6-56B-16

DESCRIPTION: 5.637 Cone + TSEN 56, 16 Tabs, α = 18°, D_9/D_S = 1.20

DATE: 10/10/68

SCALE MODEL A_8 = .1733 ft^2

FULL SCALE A_8 = 11.091 ft^2

SCALE FACTOR = 8:1

- o DATA INCLUDES GROUND REFLECTION INTERFERENCE
- o ANGLE REFERENCED TO JET EXHAUST

TEST CONDITIONS					ACOUSTIC TEST RESULTS							
							320' ARC		300' SIDELINE		1500' SIDELINE	
RDG NO.	P_{T8}/P_o	T_{T8} (°R)	IDEAL V_j (ft/sec)	W_8 (PPS)	10Log $\rho^2 A$	10Log ρA	PEAK PNdB	PEAK ANGLE	PEAK PNdB	PEAK ANGLE	PEAK PNdB	PEAK ANGLE
1	1.34	1130	1054	6.28	-17.7	-3.4	108.8	50	106.7	60	91.1	60
2	1.54	1255	1335	7.46	-18.7	-4.1	117.4	50	115.1	50	99.7	50
3	1.99	1500	1811	8.90	-19.8	-4.7	127.4	50	125.1	50	109.0	50
4	2.00	2780	2469	6.63	-25.2	-7.4	133.4	50	131.3	50	116.3	50
5	2.46	1700	2175	10.50	-20.3	-4.8	128.2	50	127.4	70	110.4	60
6	2.50	2790	2813	8.37	-24.6	-6.9	134.5	50	132.3	50	117.0	50
7	3.00	2795	3050	9.86	-24.5	-6.5	138.6	50	-	-	121.1	50
8	3.00	2500	2885	10.45	-23.8	-6.0	137.8	50	135.7	50	120.4	50
9	3.00	2005	2582	11.70	-21.1	-5.1	134.9	40	132.4	50	116.8	50

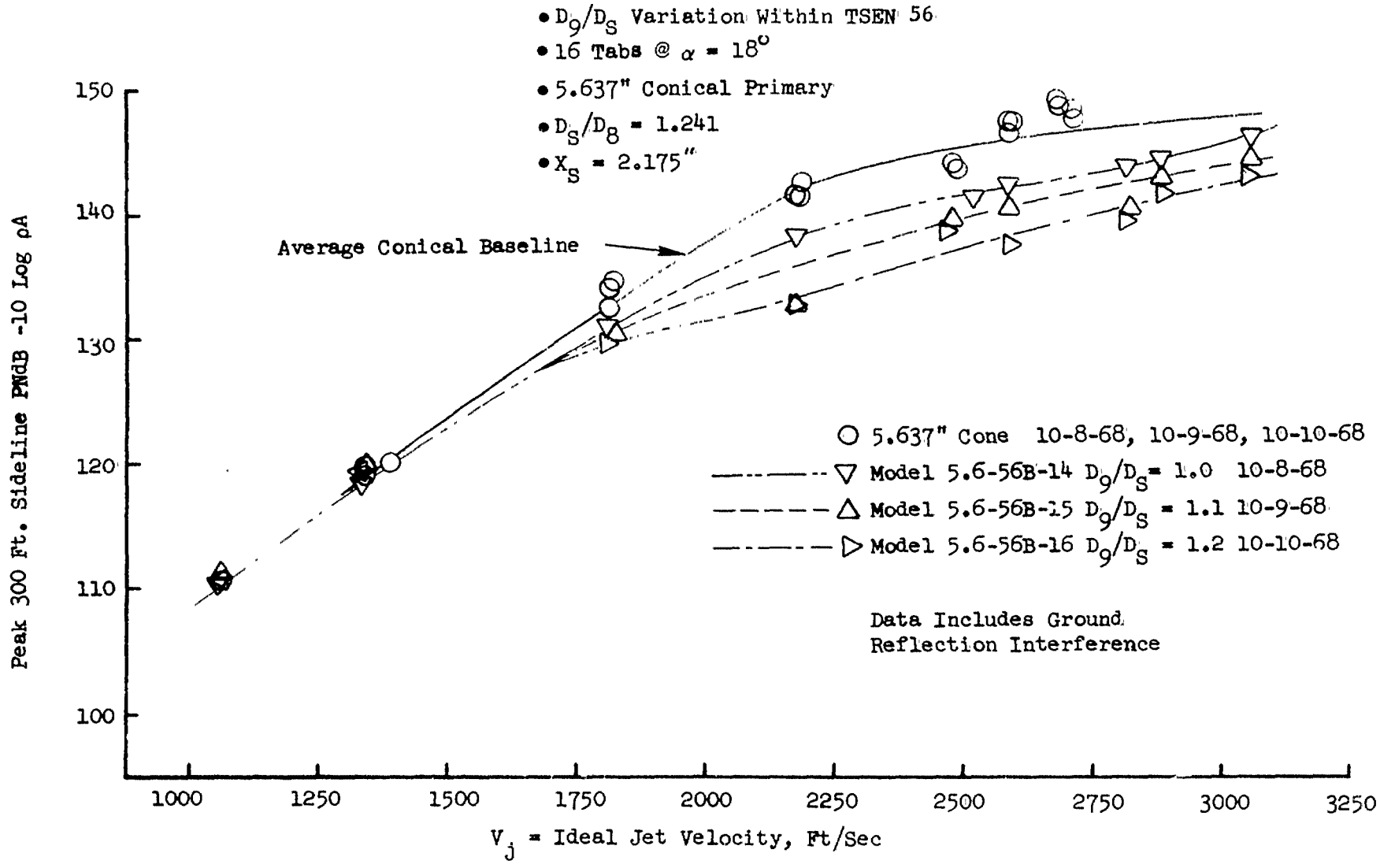

FIGURE V.C.2-15 EFFECT OF PRIMARY THRUST REVERSER TABS AND D_9/D_S VARIATION WITHIN TSEN 56 ON 300 FT. SIDELINE JET NOISE LEVELS

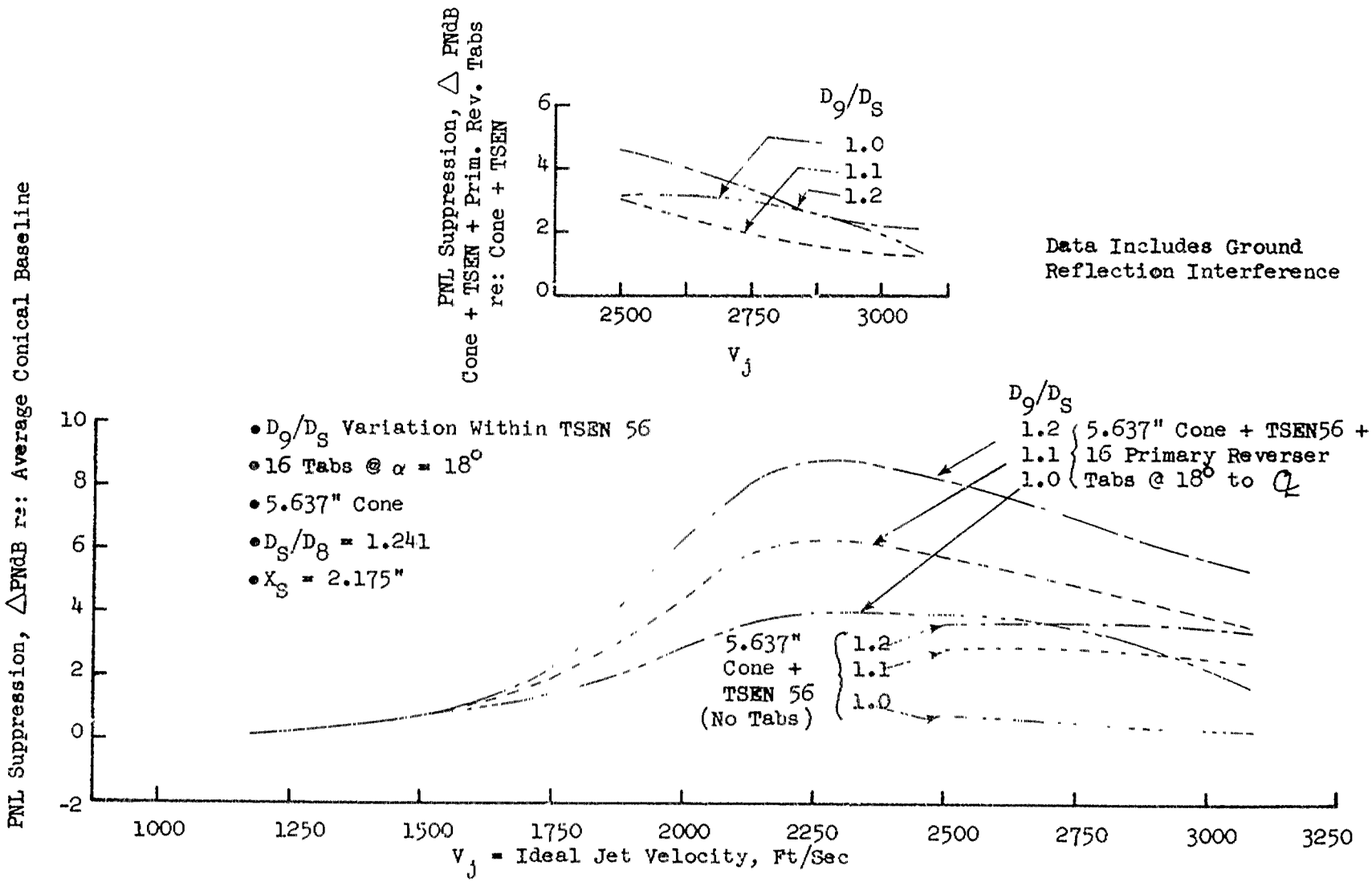

FIGURE V.C.2-16 EFFECT OF PRIMARY THRUST REVERSER TABS AND D_9/D_S VARIATION WITHIN TSEN 56 ON 300 FT. SIDELINE PNL SUPPRESSION

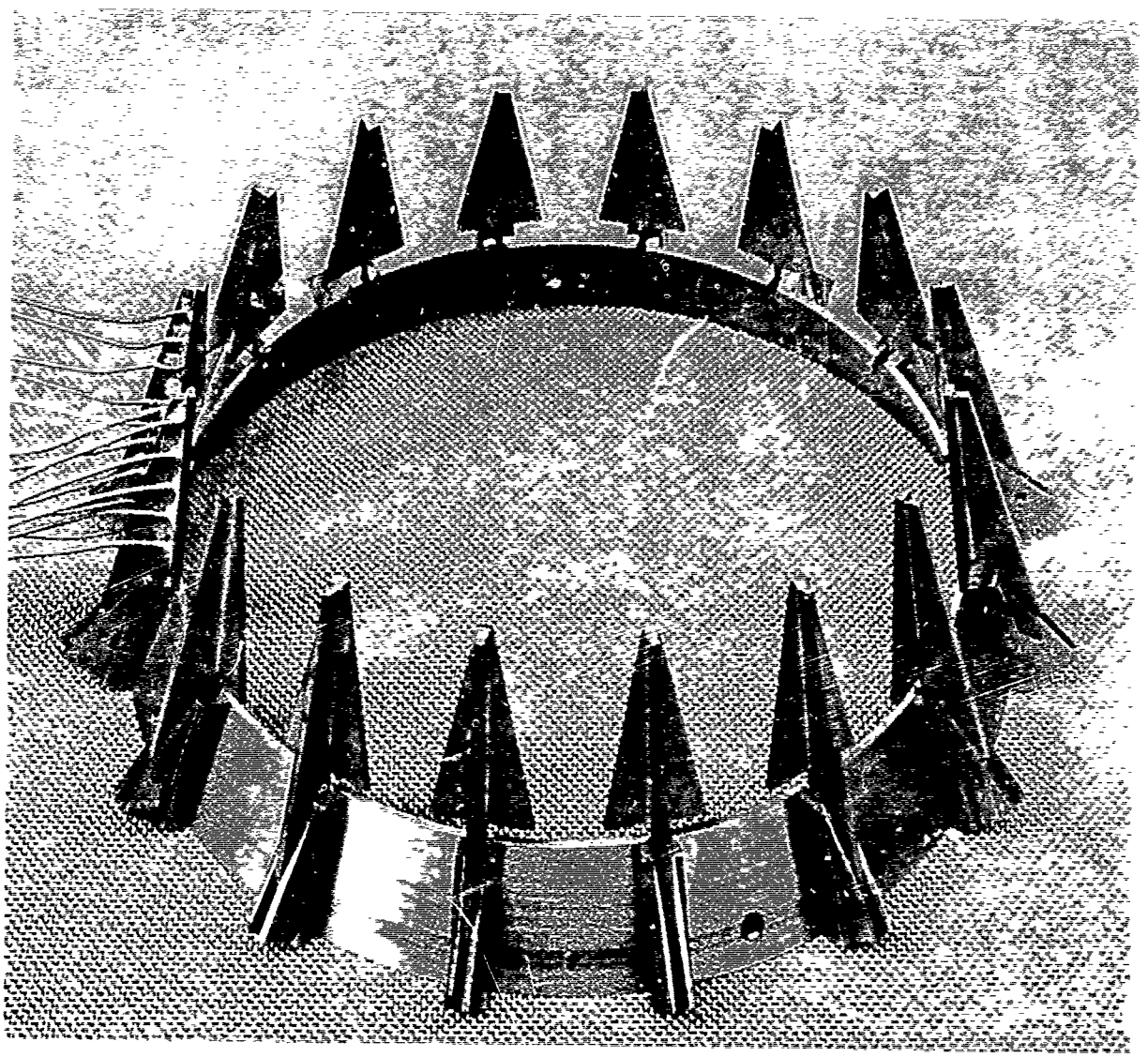

FIGURE V.C.2-17 PRIMARY THRUST REVERSER TAB SYSTEM HARDWARE FOR AERODYNAMIC MODELS

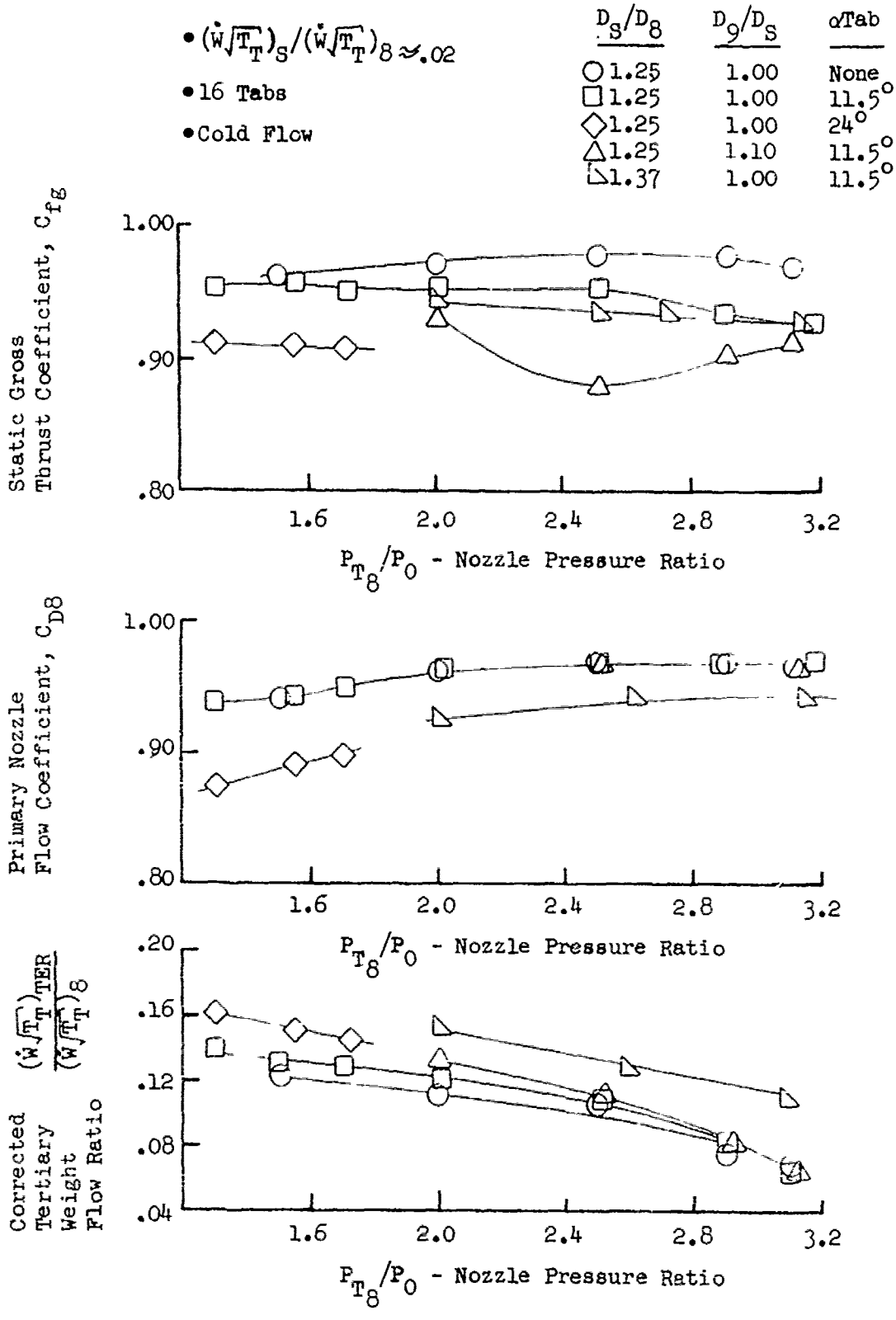

FIGURE V.C.2-18 STATIC PERFORMANCE OF THE PRIMARY REVERSER TAB SUPPRESSOR SYSTEM

• For GE4/SST Block I Engine

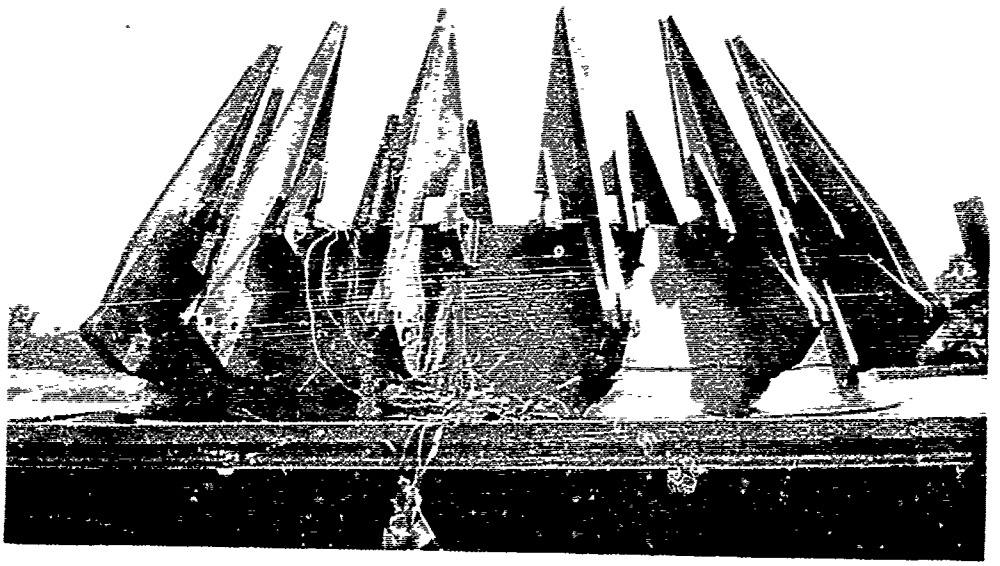

FIGURE V.C.2-19 ENGINE HARDWARE FOR PRIMARY THRUST REVERSER TAB SUPPRESSOR TESTS

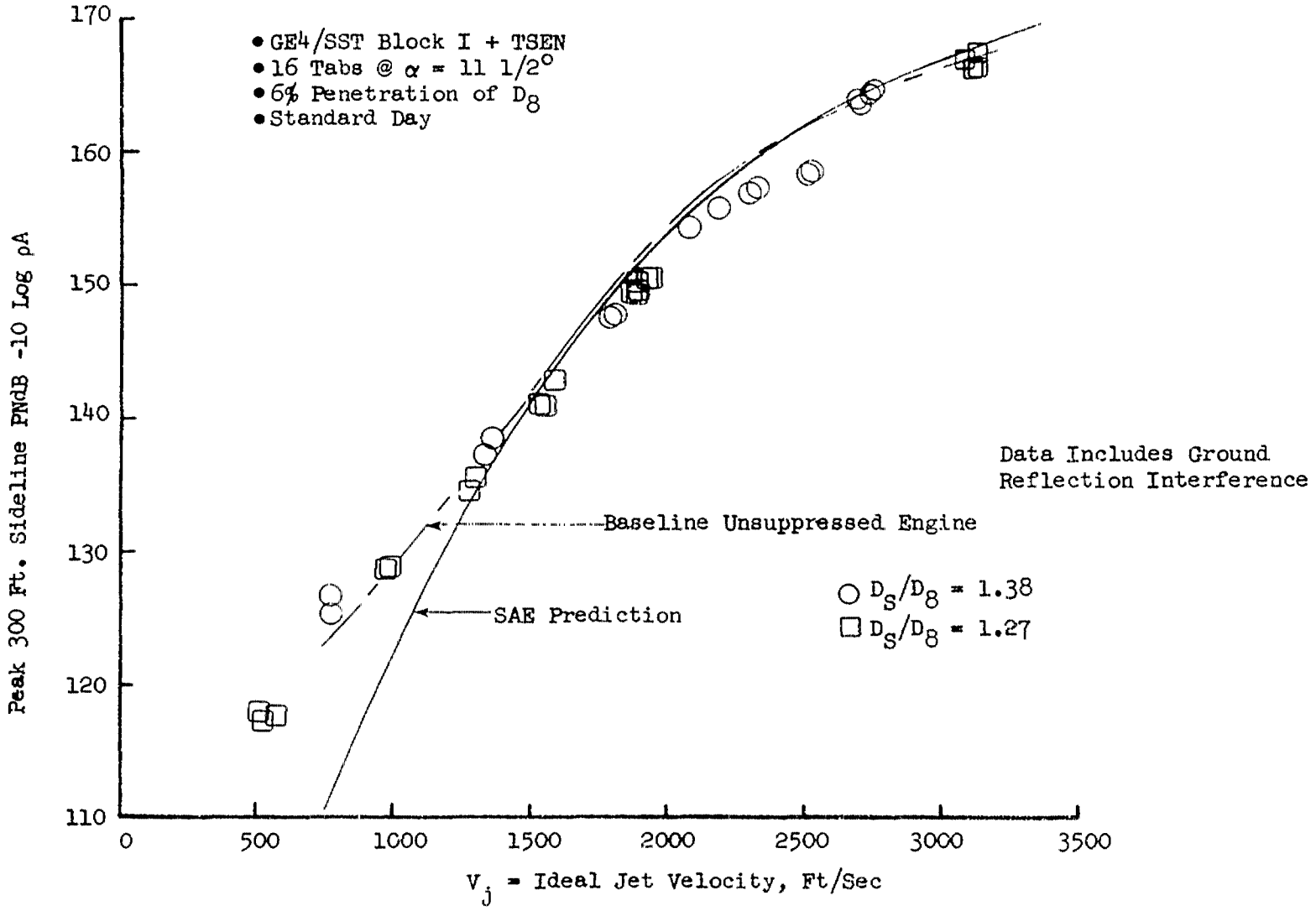

FIGURE V.C.2-20 EFFECT OF PRIMARY THRUST REVERSER TABS WITHIN GE4 BLOCK I ENGINE ON 300 FT. SIDELINE JET NOISE LEVELS

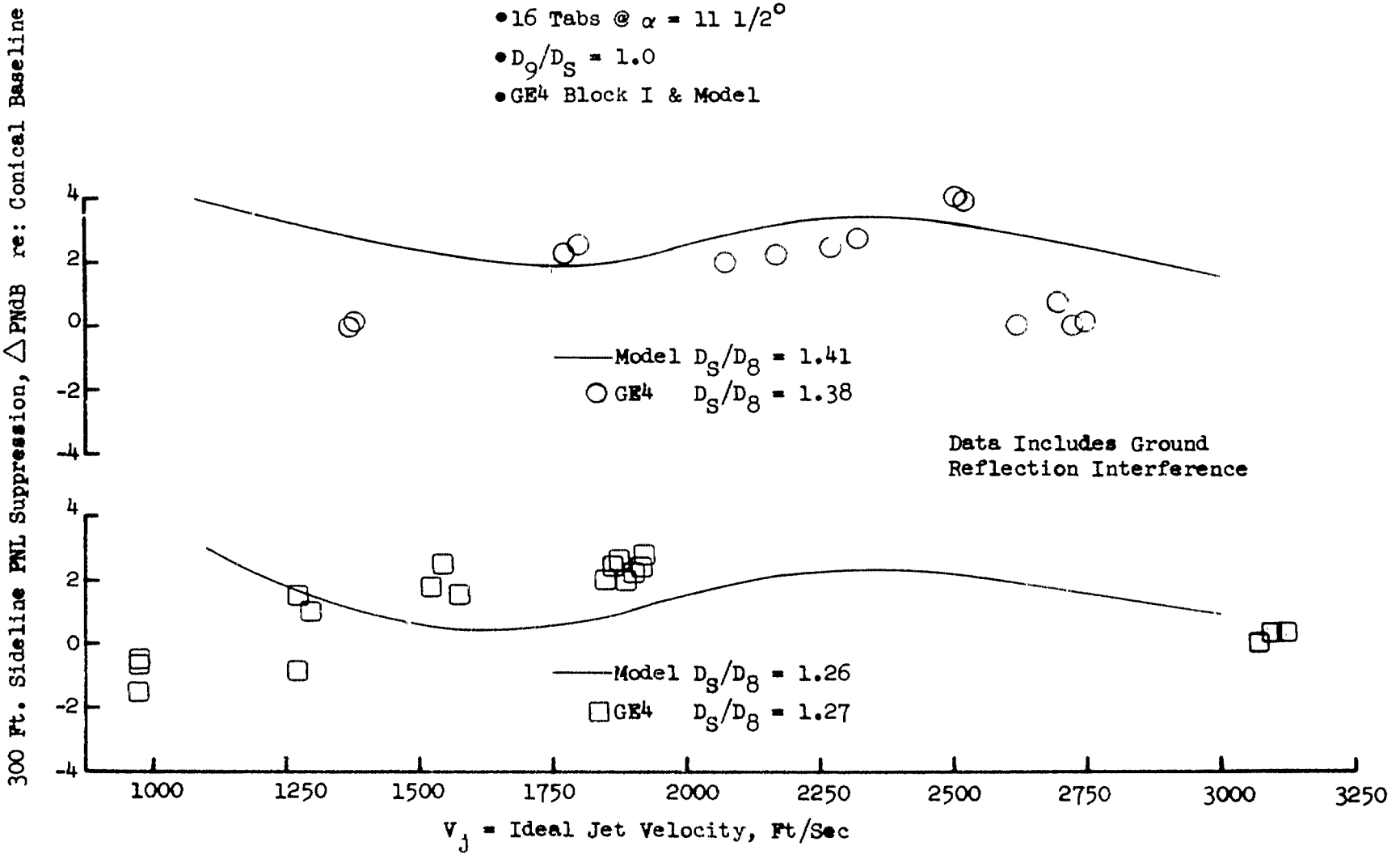

FIGURE V.C.2-21 COMPARISON OF MODEL AND ENGINE PEAK 300 FT. SIDELINE PNL SUPPRESSION WITH PRIMARY THRUST REVERSER TABS

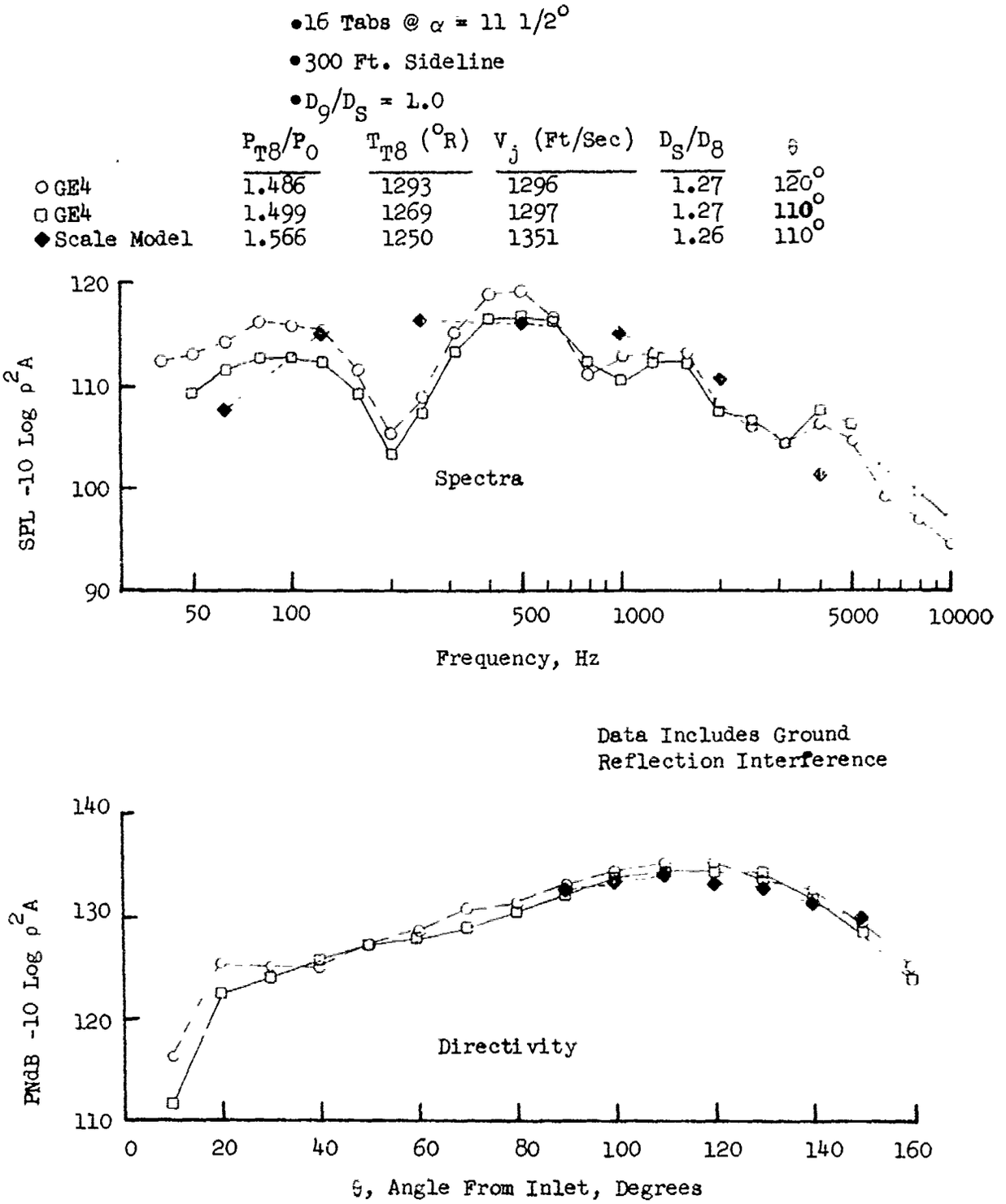

FIGURE V.C.2-22A COMPARISON OF MODEL AND ENGINE SPECTRA AND DIRECTIVITY WITH PRIMARY THRUST REVERSER TABS

- 16 Tabs @ α = 11 1/2°
- 300 Ft. Sideline
- D_9/D_S = 1.0

	P_{T8}/P_0	T_{T8} (°R)	V_j (Ft/Sec)	D_S/D_8	θ
○ GE4	1.918	1542	1788	1.38	120°
□ GE4	1.907	1581	1804	1.38	120°
◆ Scale Model	2.01	1509	1828	1.41	130°

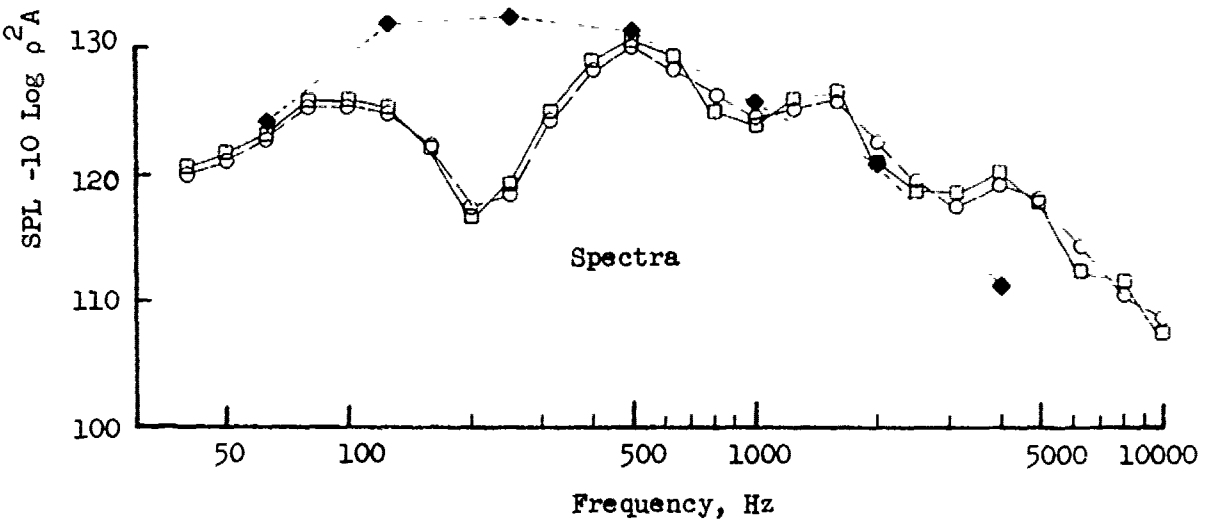

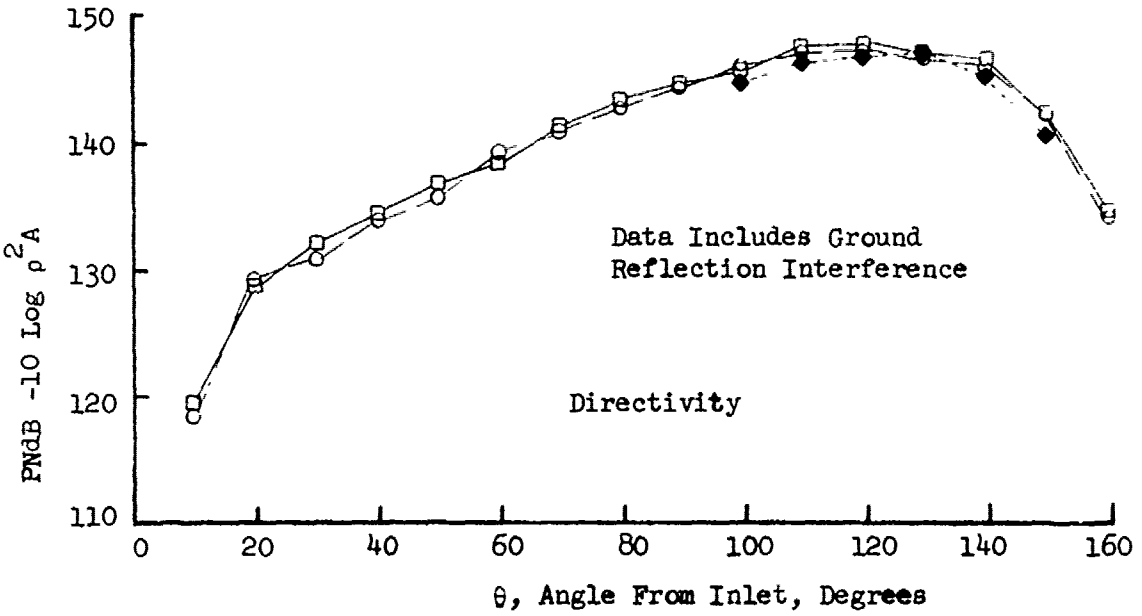

FIGURE V.C.2-22B COMPARISON OF MODEL AND ENGINE SPECTRA AND DIRECTIVITY WITH PRIMARY THRUST REVERSER TABS

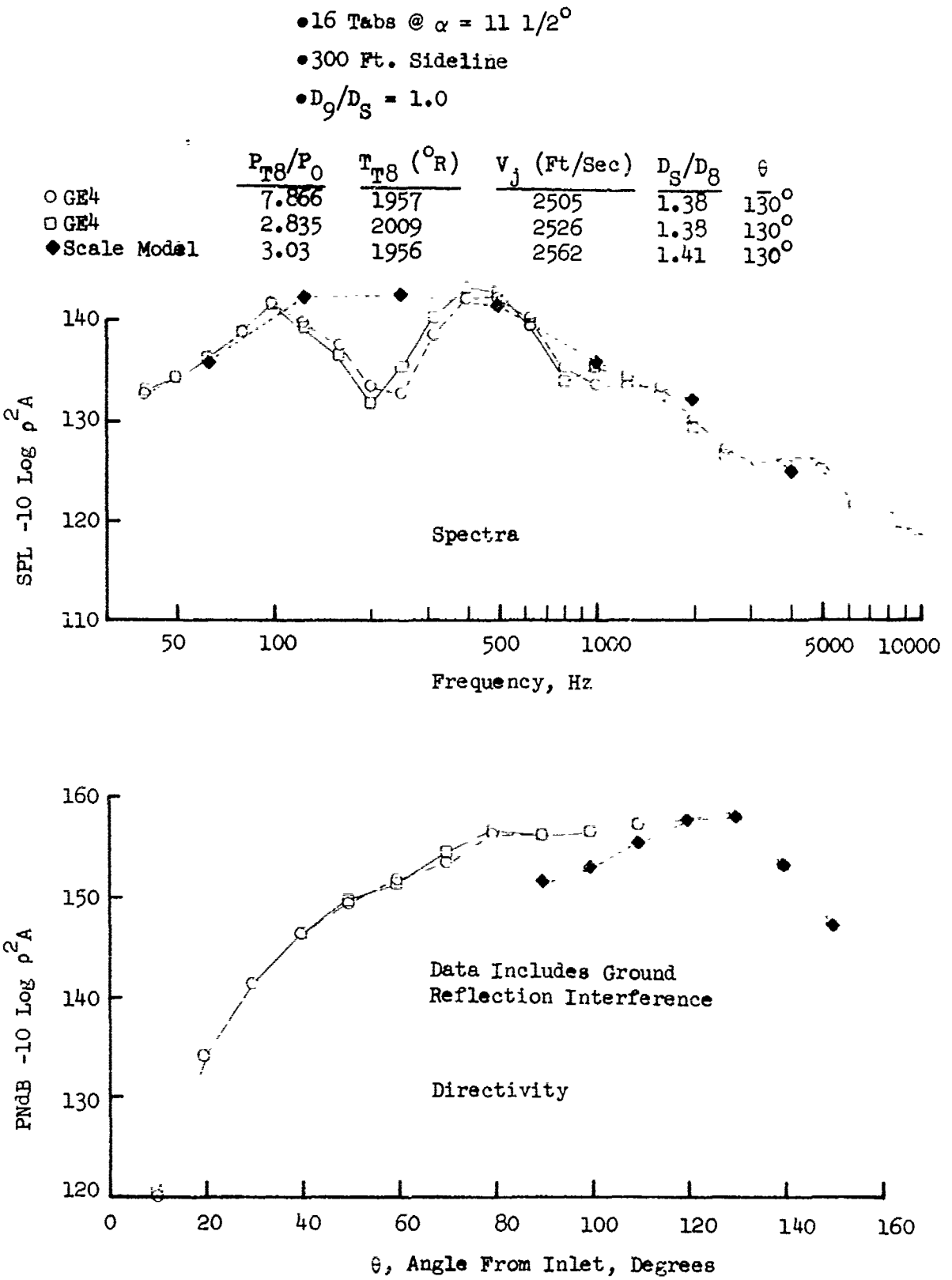

FIGURE V.C.2-22C COMPARISON OF MODEL AND ENGINE SPECTRA AND DIRECTIVITY WITH PRIMARY THRUST REVERSER TABS

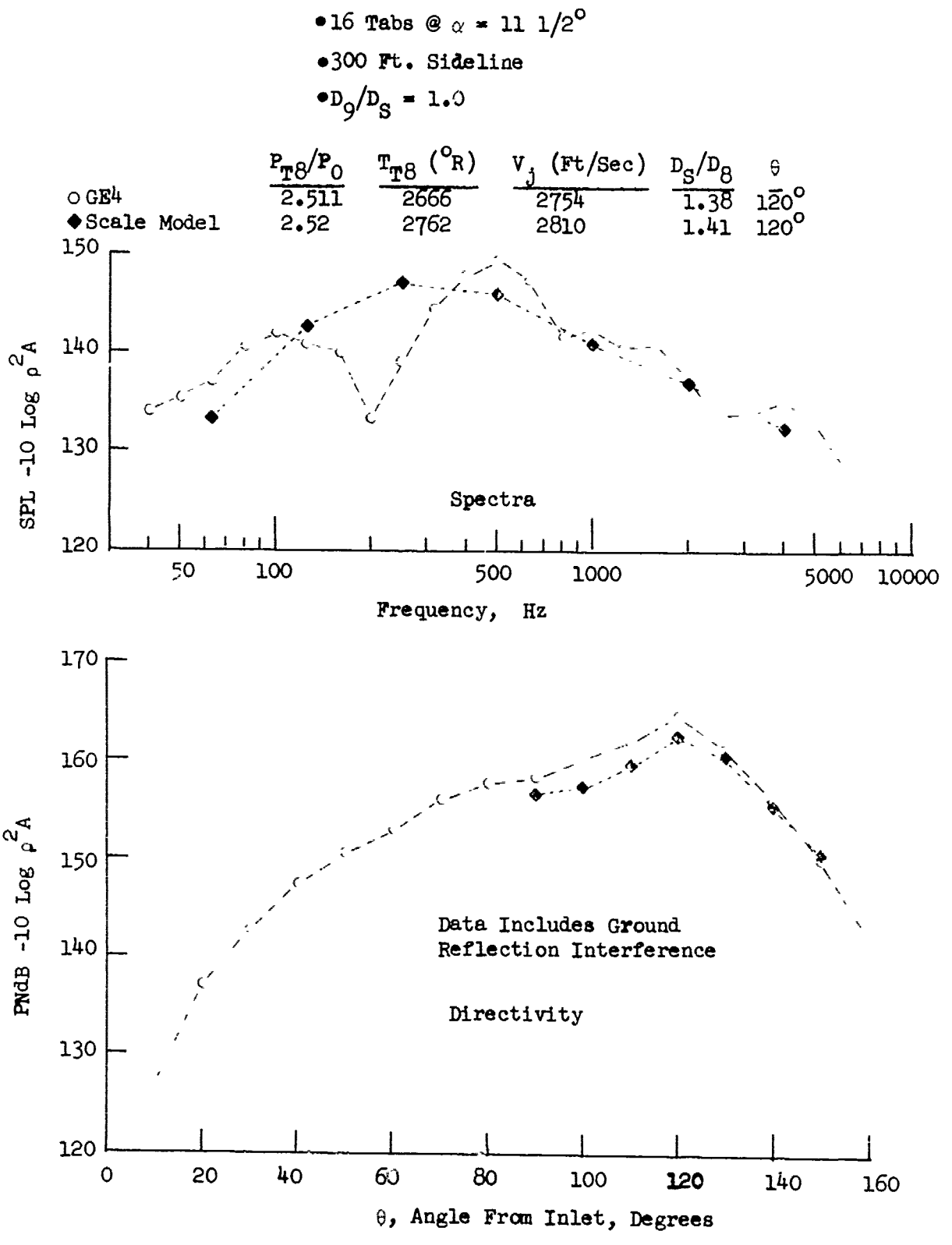

FIGURE V.C.2-22D COMPARISON OF MODEL AND ENGINE SPECTRA AND DIRECTIVITY WITH PRIMARY THRUST REVERSER TABS

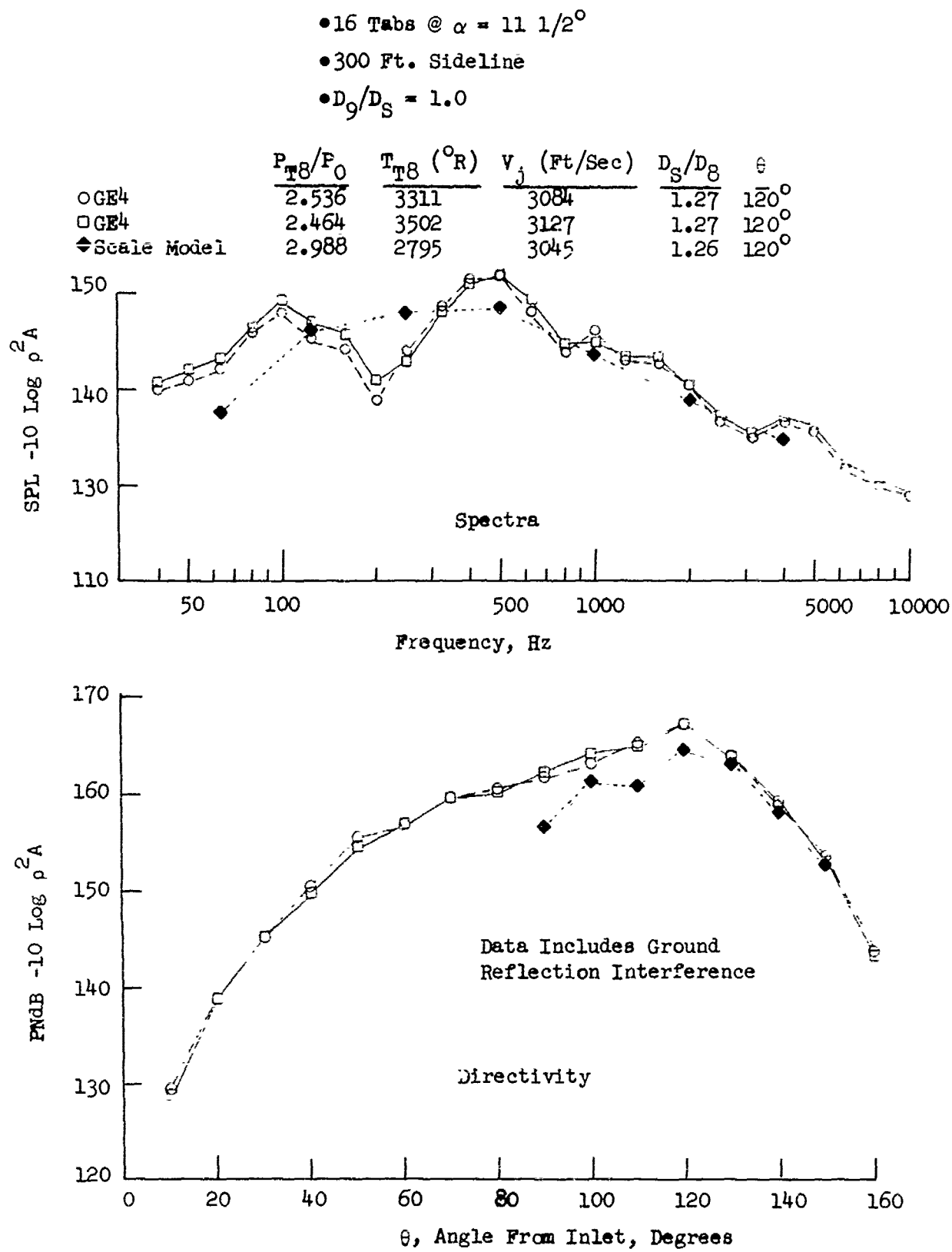

FIGURE V.C.2-22E COMPARISON OF MODEL AND ENGINE SPECTRA AND DIRECTIVITY WITH PRIMARY THRUST REVERSER TABS

V.C.3 PRIMARY VENTED CHUTE SUPPRESSORS

V.C.3 PRIMARY VENTED CHUTE SUPPRESSORS

Objectives of Test Series

The purpose of this test series was to review early jet noise suppression results on primary vented chute suppressors by comparison tests at simulated GE4 reheat operating conditions (high ideal jet velocities) and also to determine the acoustical performance at low velocities simulating GE4 approach and cutback conditions. Other test variables were to include: a) effect of ejector D_9/D_S ratio on suppression and, b) effect of the combinations of P_{T8}/P_0,T_{T8} to attain a particular cycle velocity.

The high velocity test range covered ideal jet velocities from 2000 to 3050 ft/sec. Temperatures of 2000, 2500 and 2800° R were combined with nozzle pressure ratios of 2.0, 2.5 and 3.0 to form a matrix of test conditions.

The region of low velocities investigated included a range from 1050 to 2100 ft/sec for pressure ratios of 1.35 to 2.0 and temperatures of 1100 to 2000° R.

Test Configurations

Two primary vented chute suppressor models were used in this test series, schematically shown in Figure V.C.3-2. A photograph of the basic primary nozzle and primary plus ejector is shown in Figure V.C.3-1; however, the ejector is not the exact hardware used in test as shown in Figure V.C.3-2. Both models used the same primary nozzle which had twelve fully vented chutes at 59% radial penetration into the primary gas stream. The D_S of the two ejector systems, at 5.35" I.D., gave equivalent D_S/D_8 ratios of 1.38. The ejector lengths were also equal at L_S = 7.88", or L_S/D_S = 1.47. To investigate suppression dependency on L_S/D_S, Model III-15 retained the cylindrical ejector the full length for a D_9/D_S of 1.0 while Model III-14's ejector expanded to a D_9 of 6.0" I.D. for a D_9/D_S of 1.12.

Baseline comparisons for the high velocity investigation were made using a 4.0" I.D. conic nozzle. Similarly, for the low velocity study, a 4.32" I.D. conical baseline was employed.

PRECEDING PAGE BLANK-NOT FILMED

Presentation of Test Results

Acoustic measurements were taken on a 40 ft. arc and scaled by frequency and size to full scale application using a scale factor of 8:1. All data presented are, therefore, of simulated engine size and engine frequency range.

Normalized peak PNL, peak PNL suppression, octave band spectra and PNL directivity for a 300 ft. sideline distance, are presented for the high jet velocity test series for both configurations in Figures V.C.3-3 and -4. The same type of data are presented for the low velocity test series in Figures V.C.3-5 and -6. Tables V.C.3-1 and -2 are test summaries for both models, and include data for the high and low jet velocity tests.

Conclusions

- At intermediate and high jet velocities, both models gave substantial jet suppression as seen in Figure V.C.3-3. Model III-15, with $D_9/D_S = 1.0$, shows 11 PNdB suppression at an intermediate V_j of 2100 ft/sec but indicates a rapid loss of suppression (down to 4 PNdB) at the highest test velocity.

- Opening D_9/D_S ratio to 1.12 in Model III-14 did not alter suppression significantly from 2050 to 2500 ft/sec, but then showed gradually increasing suppression up to 4 PNdB at 3050 ft/sec (Figure V.C.3-3) for a total of 8 ΔPNdB at that velocity.

- Prior investigations seemed to indicate that distinct pressure ratio noise generation lines are inherent to specific types of suppressors. Primary chute suppressors have shown to increase noise generation characteristics with higher pressure ratio or to have less suppression potential of operating under a high pressure ratio/low temperature cycle while at a set jet velocity, rather than a low pressure ratio/high temperature cycle. The conical nozzle trends have shown to be opposite to those of the primary suppressors.

  Reference to Figure V.C.3-3 (top) partially bears out this fact for the primary vented chute Models III-14 and III-15 as well as the conical baseline. Peak 300 ft. sideline jet noise levels exhibit lower conical noise generation for increased pressure ratio at the same jet velocity while the two primary chute models show increased

noise generation for the same pressure ratio trend. Consequently, suppression levels (lower half of Figure V.C.3-3) abruptly decrease for Model III-15 with increased pressure ratio lines. Of course, the exception to the rule usually appears and seems to have done so in Model III-14. For the pressure ratio lines of 2.0 and 2.5 suppression increased with increased T_{T8} but then abruptly inverted and started decreasing with the same T_{T8} trend at P/R of 3.0. This is considered to be an aerodynamic effect due to the larger D_9/D_S ratio. Pressure ratio effect, however, is still apparent even though suppression trends may not be consistent.

- At low jet velocities (Figure V.C.3-5) the suppression levels for both models dropped off rapidly with negligible suppression seen at 1500 ft/sec and below. Opening A_9 at these lower velocities with Model III-14 at D_9/D_S = 1.12 gave slightly increased noise levels over the straight ejector, Model III-15 at D_9/D_S = 1.0. Frequency spectra (Figure V.C.3-6) show suppression in the lower frequency bands but greater noise generation than the conical baseline in the higher frequency bands, even when compared at the same angles instead of peak PNL angles.

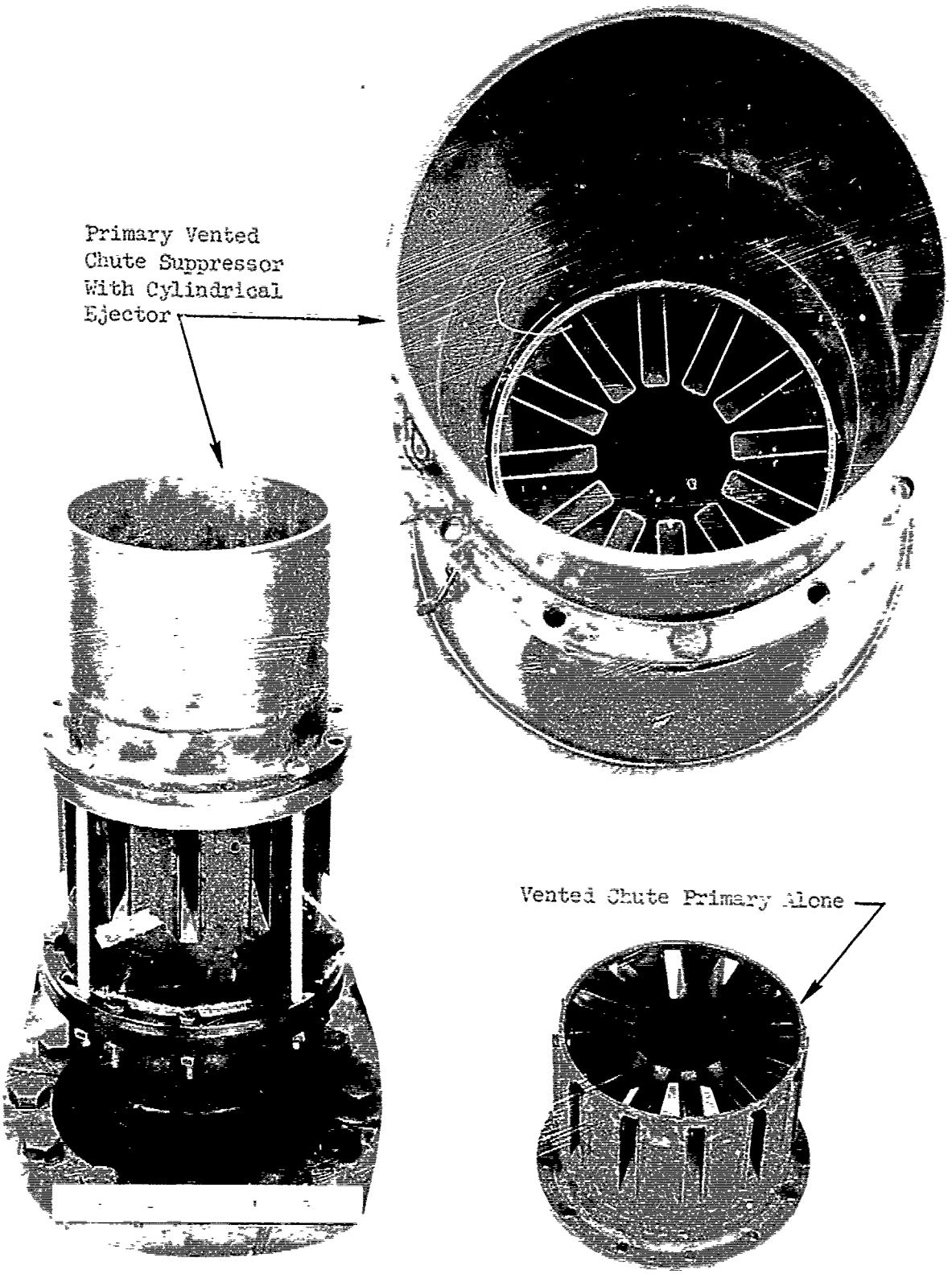

FIGURE V.C.3-1 PRIMARY VENTED CHUTE NOZZLE HARDWARE

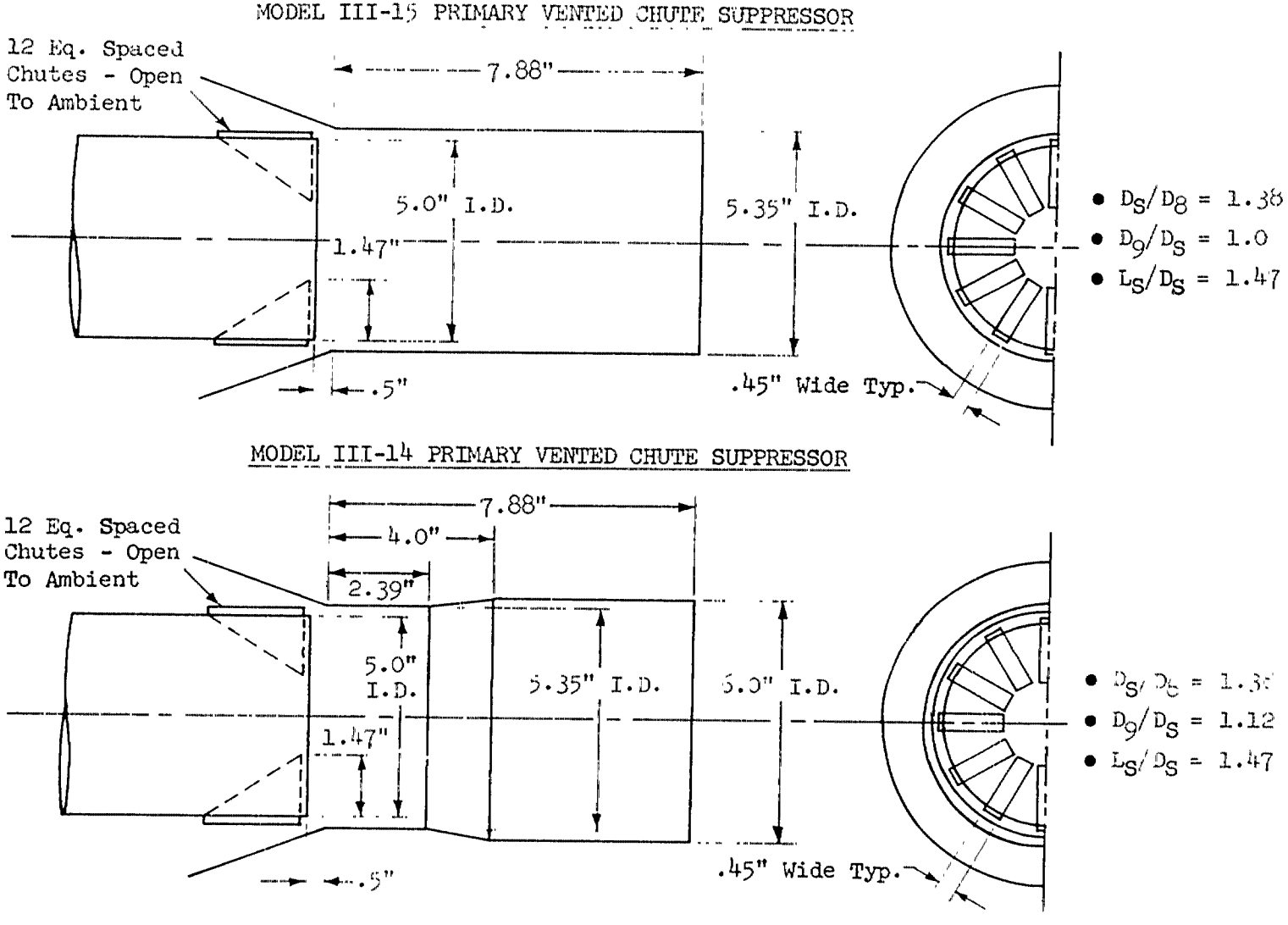

FIGURE V.C.3-2 SCHEMATIC OF PRIMARY VENTED CHUTE SUPPRESSOR CONFIGURATIONS

TABLE V.C.3-1 TEST SUMMARY

MODEL NO. III-14

DESCRIPTION: 12 Primary Vented Chutes, 59% Penet., Ejector D_9=6.0", D_9/D_S=1.12

DATE: 2/26/68 ;
5/13/68 o DATA INCLUDES GROUND REFLECTION INTERFERENCE
o ANGLE REFERENCED TO JET EXHAUST

SCALE MODEL A_8 = .0811 ft^2

FULL SCALE A_8 = 5.190 ft^2

SCALE FACTOR = 8:1

TEST CONDITIONS					ACOUSTIC TEST RESULTS					
							320' ARC		300' SIDELINE	
RDG NO.	P_{T8}/P_o	T_{T8} (°R)	IDEAL V_j (ft/sec)	W_8 (PPS)	10Log $\rho^2 A$	10Log ρA	PEAK PNdB	PEAK ANGLE	PEAK PNdB	PEAK ANGLE
2/26/68										
1	2.00	1995	2093	3.72	-25.6	-9.2	122.3	70	122.3	70
2	2.50	2000	2379	4.68	-25.0	-8.8	126.1	50	125.7	70
3	3.00	2010	2586	4.32	-24.4	-8.4	128.1	50	127.0	60
4	2.99	2500	2882	4.87	-26.3	-9.3	130.7	40	128.6	60
5	2.50	2510	2665	3.97	-27.0	-9.8	126.9	40	125.9	70
6	2.00	2500	2346	5.07	-26.6	-10.2	122.2	70	123.2	80
7	2.00	2800	2483	3.60	-28.5	-10.7	122.0	60	122.2	80
8	2.50	2790	2809	3.84	-27.9	-10.3	126.8	40	124.4	50
9	2.99	2800	3050	4.67	-27.3	-9.8	131.4	40	129.5	60
5/13/68										
1	2.02	1987	2106	4.35	-25.5	-9.2	122.7	70	122.8	70
8	2.01	1460	1796	4.70	-22.8	-7.8	119.7	70	119.8	70
9	2.01	1245	1659	5.00	-21.5	-7.1	118.5	70	118.5	70
10	1.55	1240	1331	3.77	-21.9	-7.3	112.3	60	111.7	70
11	1.35	1130	1056	3.28	-21.0	-6.7	107.0	60	106.7	70

TABLE V.C.3-2 TEST SUMMARY

MODEL NO. 111-15

DESCRIPTION: 12 Primary Vented Chutes. 59% Penet., Ejector D_9=5.35", D_9/D_S=1.0

DATE: 2/6/68; 5/13/68

SCALE MODEL A_8 = .0811 ft^2

FULL SCALE A_8 = 5.190 ft^2

SCALE FACTOR = 8:1

- o DATA INCLUDES GROUND REFLECTION INTERFERENCE
- o ANGLE REFERENCED TO JET EXHAUST

TEST CONDITIONS					ACOUSTIC TEST RESULTS					
							320' ARC		300' SIDELINE	
RDG NO.	P_{T8}/P_o	T_{T8} (°R)	IDEAL V_j (ft/sec)	W_8 (PPS)	10Log $\rho^2 A$	10Log ρA	PEAK PNdB	PEAK ANGLE	PEAK PNdB	PEAK ANGLE
2/6/68										
1	2.00	2020	2109	3.70	-25.7	-9.3	122.4	40	120.0	60
2	3.00	2800	3051	4.75	-27.3	-9.8	134.3	60	133.5	60
3	2.50	2020	2391	4.65	-25.1	-8.8	127.3	40	125.2	60
4	3.00	2000	2578	5.66	-24.4	-8.4	132.4	40	130.2	50
5	3.00	2500	2883	4.93	-26.3	-9.3	133.6	50	132.8	60
6	2.50	2500	2662	4.09	-27.0	-9.8	128.3	60	127.5	60
7	2.01	2500	2348	3.25	-27.6	-10.2	122.7	60	121.9	60
8	2.00	2810	2487	3.01	-28.6	-10.7	125.1	40	123.3	60
9	2.50	2810	2819	3.88	-28.0	-10.3	129.8	60	129.0	60
5/13/68										
1	1.35	1160	1074	3.24	-21.2	-6.8	104.2	60	103.3	60
2	1.58	1257	1367	4.05	-22.0	-7.4	111.1	70	133.1	70
3	2.02	1244	1665	5.20	-21.4	-7.1	116.2	70	116.2	70
4	2.03	1520	1843	4.73	-23.2	-8.0	117.8	40	117.6	70
5	2.02	1995	2109	4.20	-25.5	-9.2	122.0	70	122.0	70

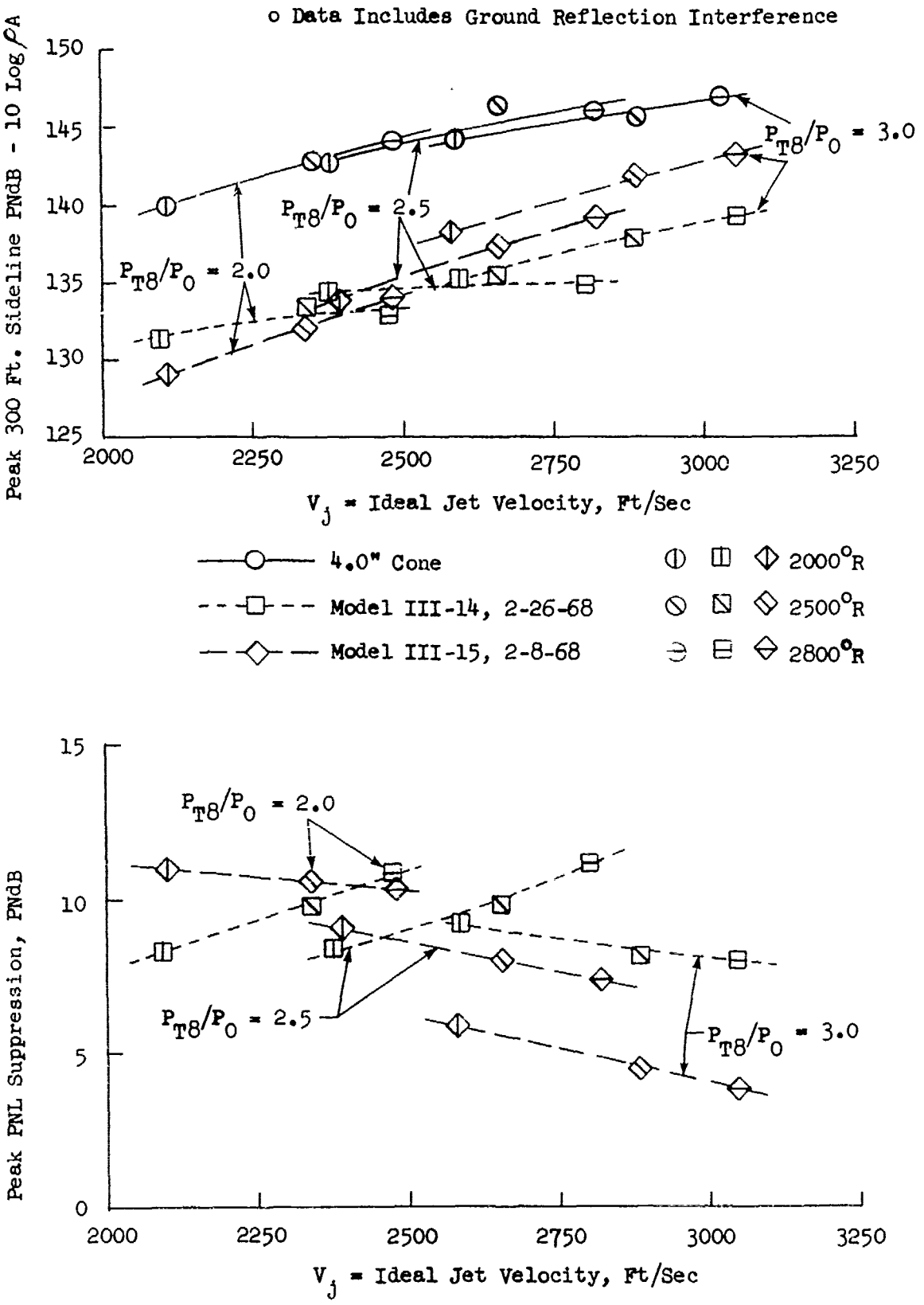

FIGURE V.C.3-3 300 FT. SIDELINE JET NOISE LEVELS & PNL SUPPRESSION AS A FUNCTION OF P_{T8}/P_0 FOR PRIMARY CHUTED SUPPRESSORS AT HIGH IDEAL JET VELOCITIES

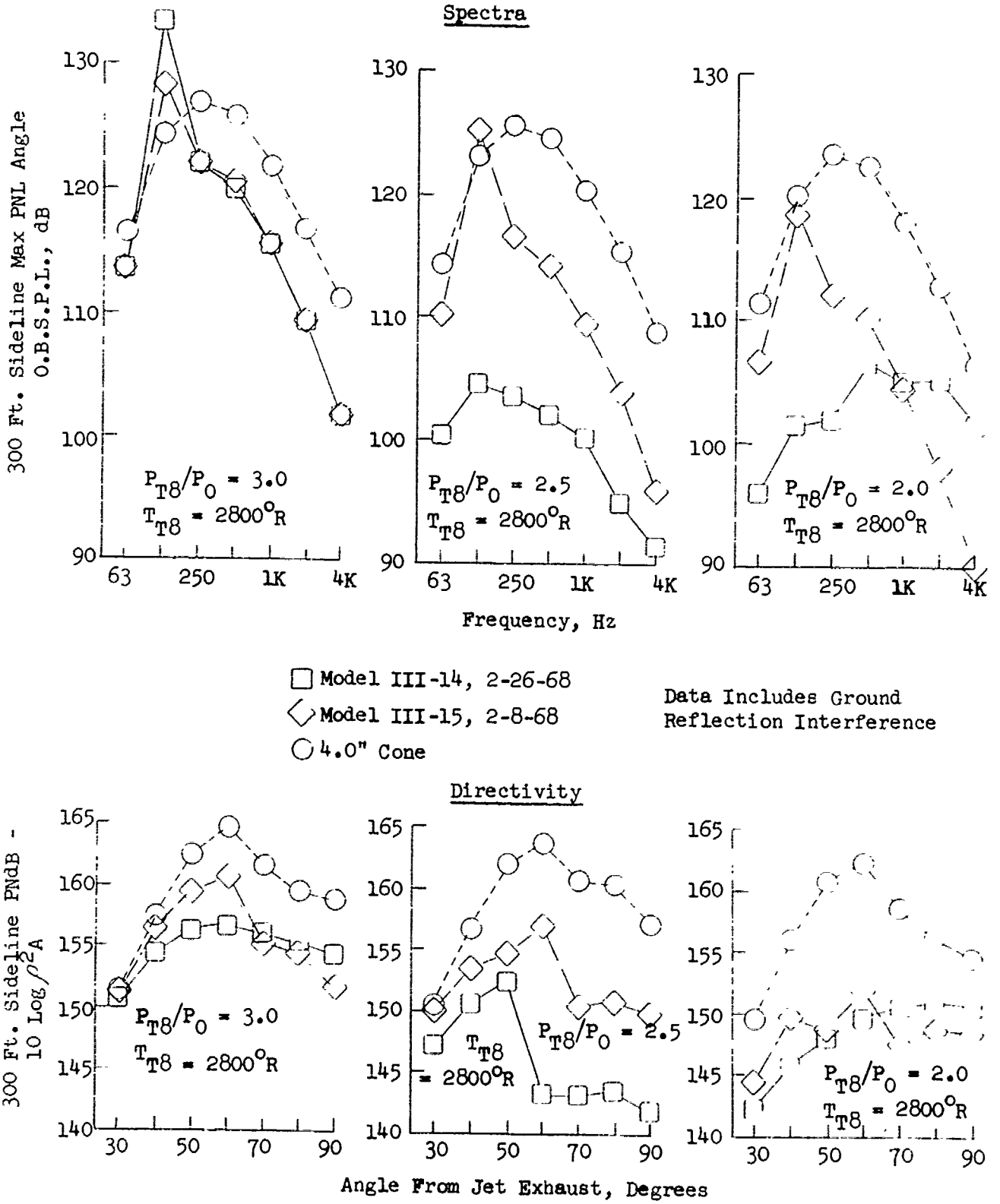

FIGURE V.C.3-4 300 FT. SIDELINE SPECTRA AND DIRECTIVITY FOR PRIMARY CHUTED SUPPRESSORS AT HIGH IDEAL JET VELOCITIES

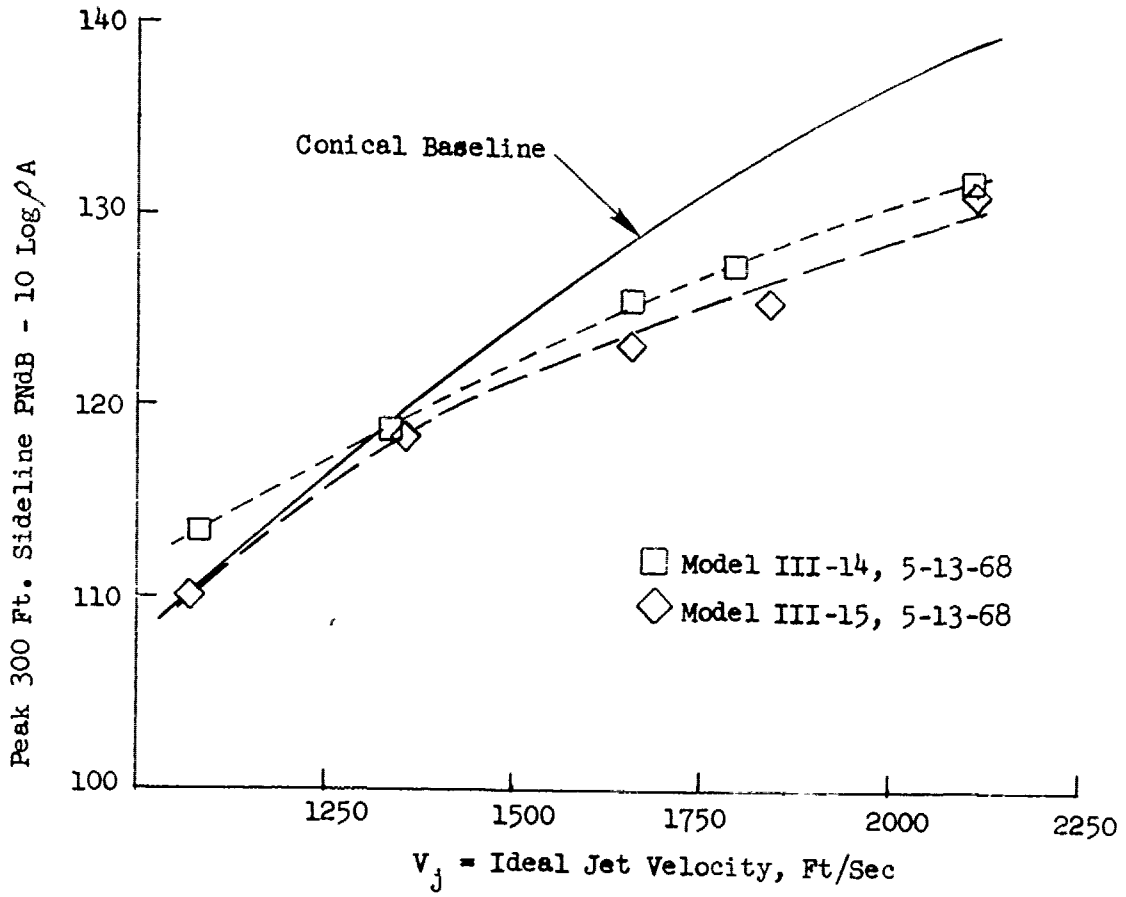

Data Includes Ground Reflection Interference

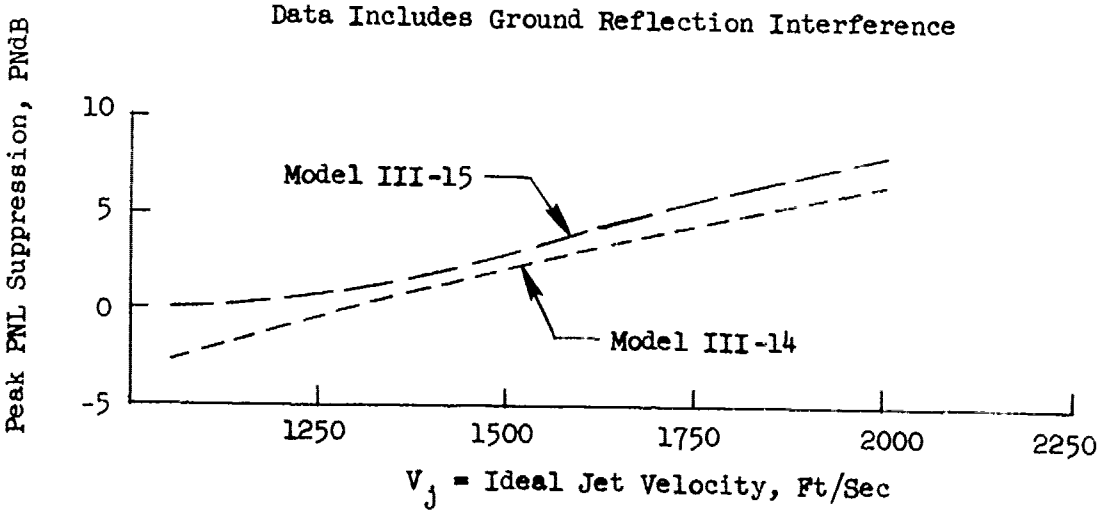

FIGURE V.C.3-5 300 FT. SIDELINE JET NOISE LEVELS AND PNL SUPPRESSION FOR PRIMARY CHUTED SUPPRESSORS AT LOW IDEAL JET VELOCITIES

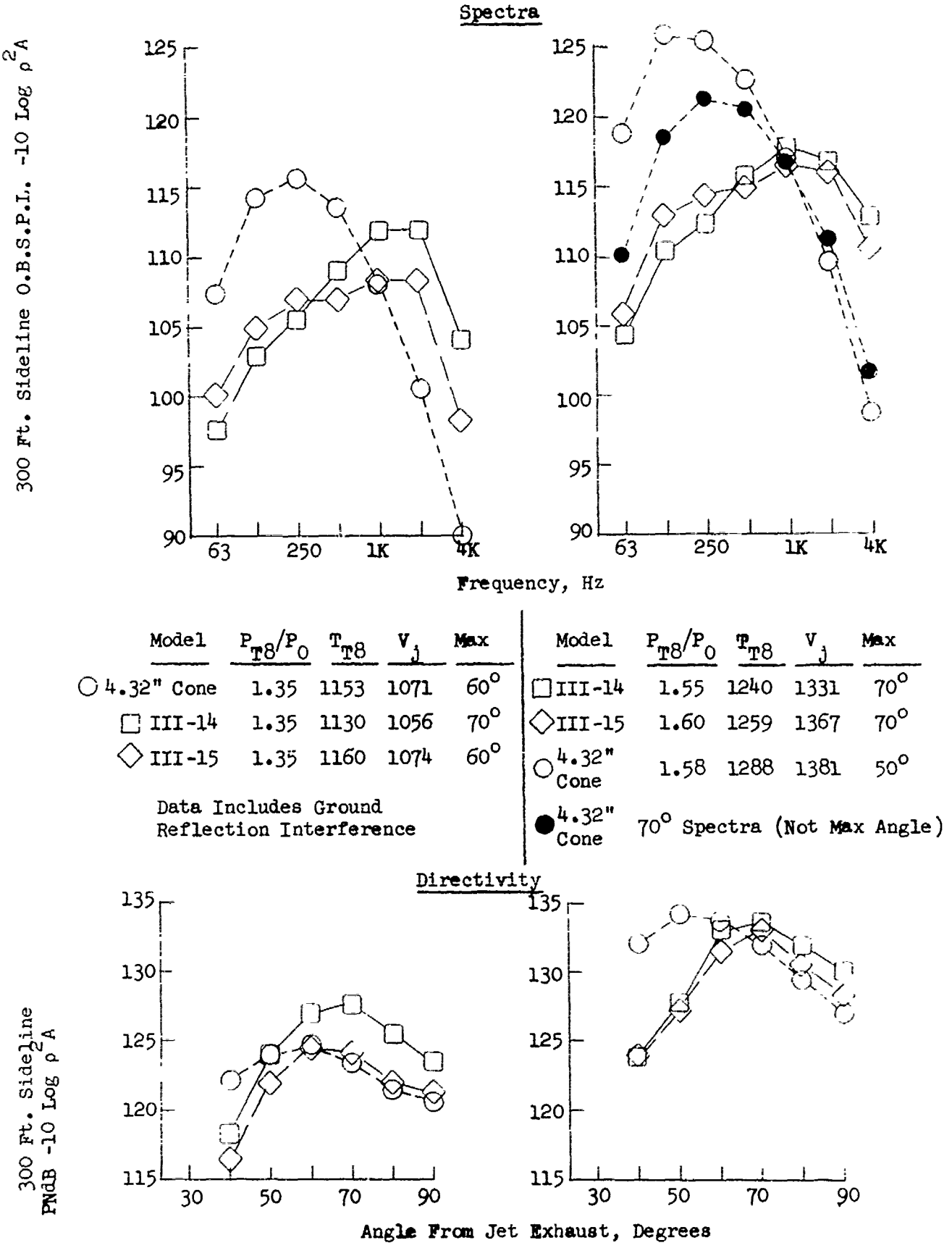

FIGURE V.C.3-6 300 FT. SIDELINE SPECTRA AND DIRECTIVITY FOR PRIMARY CHUTED SUPPRESSORS AT LOW IDEAL JET VELOCITIES

V.D FLUID INJECTANT SUPPRESSORS

PRECEDING PAGE BLANK-NOT FILME

V.D FLUID INJECTANT SUPPRESSORS

Several series of tests were performed to evaluate the effectiveness of fluid injectants as noise suppression schemes. Emphasis was primarily on their use in conjunction with simple mechanical suppressor systems such as primary radial rods and primary thrust reverser tabs. The tests were conducted with model systems on the GE, Evendale, JENOTS acoustic facility and are considered within the following topics.

- Hollow radial spokes with ambient pumping and axial injecting simulated compressor discharge bleed (Section V.D.1)
- Hollow radial spokes with radial and axial air and water injection (Section V.D.2)
- Air and water injection over primary thrust reverser tabs (Section V.D.3)

PRECEDING PAGE BLANK-NOT FILMED

V.D.1 HOLLOW RADIAL SPOKES WITH AMBIENT PUMPING AND AXIAL INJECTING SIMULATED COMPRESSOR DISCHARGE BLEED

PRECEDING PAGE BLANK-NOT FILMED

V.D.1 HOLLOW RADIAL SPOKES WITH AMBIENT PUMPING AND AXIAL INJECTING SIMULATED COMPRESSOR DISCHARGE BLEED

Purpose of Tests

In a continuing effort to realize additional suppression from the radial spoke suppressor concept, the feasibility of inducing ambient air and/or injecting compressor discharge bleed (C.D.B.) air from the back side of the spoke into the core jet stream was investigated. Such flow could serve the multiple purpose of radial spoke cooling, reduced spoke drag, hence low thrust loss, as well as possible additional noise abatement above that attained with solid radial spokes.

Test Set Up and Procedure

Hardware configurations and test schedule for the vented/pressurized radial spoke investigation are shown in Figure V.D.1-1. Detailed spoke designs are shown in Figure V.D.1-2 and photographs of the spoke are shown in Figures V.D.1-3 and -4. Two spoke designs were tested, designated T1 and T3, identical with the exception of trailing edge web length. The longer .35 inch web of the T3 spoke was believed would have a lower thrust loss than the .03 inch web design of the T1 spoke.

The TSEN 4 ejector system was used with X_S spacing of 2.62 inches and tertiary blow-in-door area of 12 square inches to directly simulate the GE4 Block II 57 inch D_S nozzle system with 1,000 square inch tertiary blow-in-door area. Each of the tests tabulated on Figure V.D.1-1 was run with (8) equally spaced hollow radial spokes located .30 inches aft of plane 8 and at 53% penetration of the primary conical nozzle on a 2.26 inch spoke tip I.D.

Each spoke design was tested over a range of primary nozzle conditions within a jet velocity range of 950 to 3050 ft/sec with the hollow spokes open to ambient. Calculations from an instrumented metering section connected to one of the vented spokes and located outside of the TSEN nozzle, showed that the spokes pumped ambient flow under all conditions. The amount of ambient pumping varied between .75 and 1.1 percent of the primary nozzle total flow. The hollow spokes were then connected to a common circular plenum chamber fed

PRECEDING PAGE BLANK-NOT FILMED

by a metered and controlled secondary air supply, independent of the primary flow system. For each spoke type and for three primary tunnel conditions simulating approach, cutback and takeoff, the secondary plenum was pressurized with plant facility air at ambient temperature to settings of or near 25, 50, 75, 100 and 120 psia and acoustic data were recorded. The various plenum settings defined a wide percentage range of simulated compressor discharge bleed (C.D.B.) flow being injected into the core jet stream. Each of the spokes had a design exit area of .0375 square inches or .30 square inches total physical flow area for an 8 spoke model. A calibration curve of total spoke C.D.B. flow versus plenum static pressure is shown in Figure V.D.1-5.

Presentation Discussion of Test Results

Peak 300 foot sideline jet noise levels for the T1 spokes are shown in Figure V.D.1-6 and for the T3 spokes in Figure V.D.1-7. Each of the figures also show conical baseline data run on the same day as the suppressor. The solid curves are the average conical baselines and the dashed curves are baselines of the spokes vented to ambient with no pressurized flow, drawn to favor P_{T8}/P_o = 3.0 data. The data points flagged with numbers are with pressurized secondary flow through the spokes, the numbers represent the plenum static pressure in pounds per square inch absolute, (psia). The numbers can be used in Figure V.D.1-5 to determine the actual air flow being passed by the pressurized hollow spokes.

From the jet noise levels of Figures V.D.1-6 and -7, 300 ft. sideline suppression is plotted in Figure V.D.1-8. Hollow T1 and T3 spoke suppression curves are also directly compared to previously tested solid radial rods in a similar physical hardware setup. In the higher jet velocity range of 2400 to 3100 ft/sec the attained suppression of the vented spokes is almost identical to that of the solid rods, being in the 3 PNdB range. The T3 spokes did show slightly more suppression than the T1 spokes when both were vented to ambient. In the low jet velocity range the T1 and T3 spokes proved inferior to the solid rods and became noisier than the conical baseline below jet velocities of 1330 and 1000 ft/sec respectively.

Considering induced spoke flow, points of minimum and maximum percent simulated C.D.B. flow for both the T1 and T3 spokes, at the three tested conditions, are shown in Figure V.D.1-8. General conclusions are:

- o At high jet velocity near 3000 ft/sec, a 2% total flow rate, similar to that considered practical on the full scale engine, produced no more than 1/2 dB additional suppression over the vented to ambient hollow spokes. Increasing the C.D.B. flow to 12% added only 1 dB suppression to the T3 spokes and 2 dB to the T1 spokes.
- o In the low jet velocity range of simulated cutback and approach, low C.D.B. flow of 3 to 4 percent quieted the T1 spoke system by 1/2 to 1 dB but had an average nil effect on the T3 spokes. Gradually increasing flow only served to increase the absolute noise levels, rather than obtaining suppression. This is attributed to the C.D.B. flow through the spokes producing noise levels of sufficient magnitude to directly add to the primary jet noise levels. These results fall in line with previous scale model and full scale C.D.B. tests.

Figure V.D.1-9 shows the suppression effects of C.D.B. injection more clearly when suppression relative to spokes vented to ambient is plotted against percent C.D.B. flow. Results follow the general conclusions as mentioned above.

To show how generated jet noise spectra are effected, Figures V.D.1-10A through -10C and Figures V.D.1-11A through -11C are included. Each has a 300 ft. sideline frequency spectra for the basic hollow spokes vented to ambient on the upper part of the page. The lower part of each page shows octave band suppression relative to the vented to ambient spectra for the various pressurized C.D.B. flow settings. Each of these spectra can be referenced back to Figure V.D.1-9 to find the PNdB levels relative to the vented to ambient spokes. Generalized observations from the spectra plots are:

- o At low primary nozzle jet velocities, pressurized C.D.B. flow somewhat suppressed all but the high octave bands using the T1 spokes. (Figures V.D.1-10A and -10B.) Suppression decreased with increasing C.D.B. flow. The suppressor increased SPL's in the high octave bands for high C.D.B. flow. The T3 spokes (Figures V.D.1-11A and -11B) showed no significant spectra suppression with increasing C.D.B. flow.

- At high primary nozzle jet velocity, pressurized C.D.B. flow through T1 or T3 spokes normally suppressed all frequency bands. (Figures V.D.1-10C and V.D.1-11C.) Suppression increased with higher octave bands and generally increased with greater C.D.B. flow.

Summary and Conclusions

Application of radial spokes as a jet noise suppressor introduces a feasible means of pumping ambient air and/or injecting compressor discharge bleed air into the core jet stream. Such flow could possibly serve a dual purpose of radial spoke cooling along with additional noise abatement. A test series was performed to evaluate the concept and conclusions are as follows:

- To attain any significant suppression gain of 1 to 2 dB in the takeoff mode over suppression of solid radial rods, high bleed flow rates of near 12% of the total primary flow must be injected into the core stream.
- When opened to ambient, the hollow spokes pumped ambient flow for all primary conditions but gave no suppression gain over the non-vented solid radial rods.
- At simulated low velocity approach and cutback conditions, neither vented to ambient or forced flow spokes performed acoustically as well as solid radial rods. Noise levels became increasingly higher than the conical baseline as the percentage of spoke flow was increased.
- Axial injection of C.D.B. air at some penetration within the jet stream is not as effective as radial injection, where the C.D.B. jets also simulate an aerodynamic blocker similar to the effect of mechanical blockers.

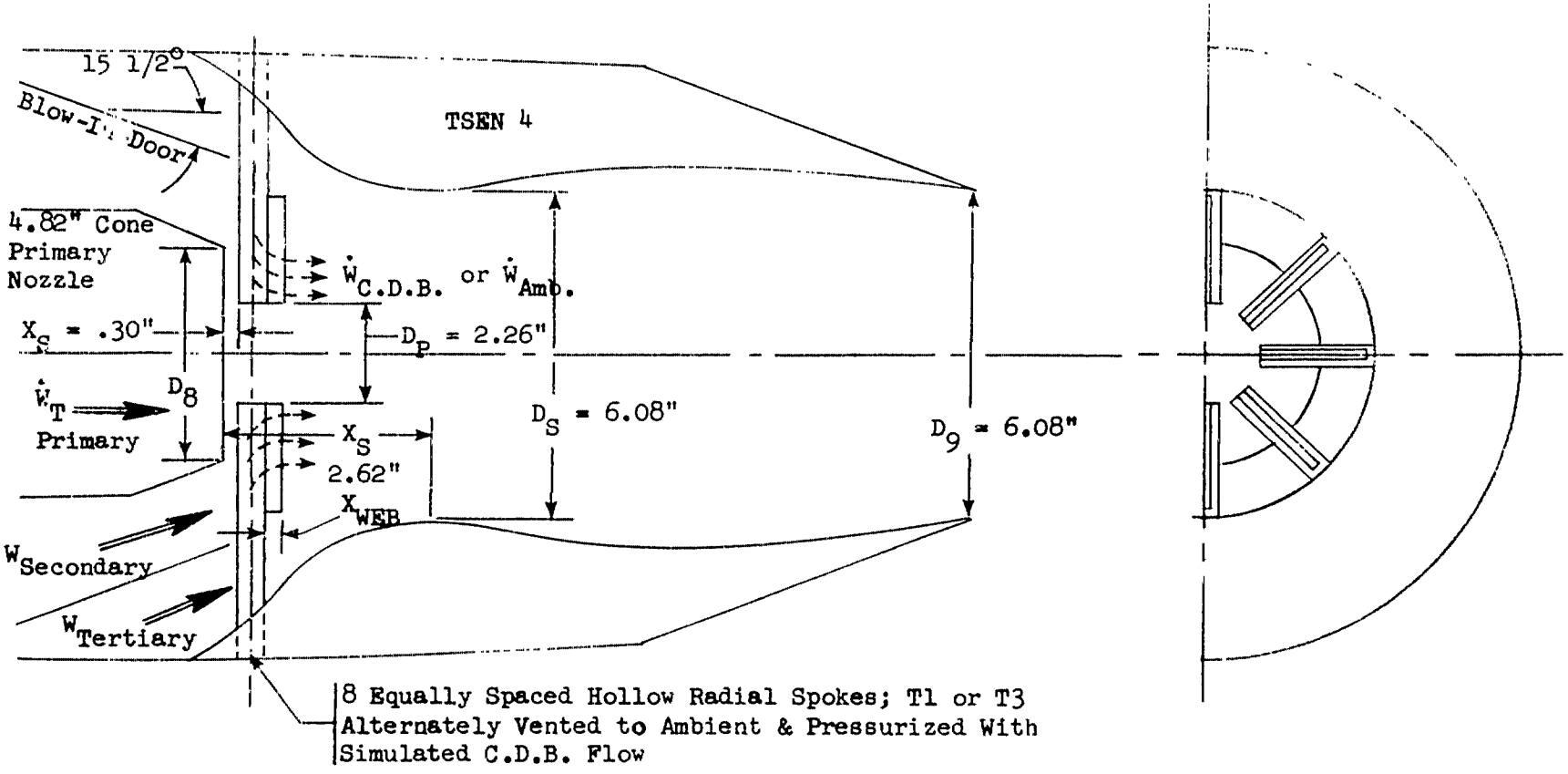

Test No.	Model No.	Test Date	Cone I.D.	A_8 Eff.	Remarks
1	4.9-4B-8T1-E	6-19 & 6-24-68	4.82	.1142	Spokes Vented To Ambient
2	4.9-4B-8T1-E-1	6-24-68	4.82	.1142	Spokes With C.D.B.
3	4.9	6-19-68	4.82	.1269	Baseline For Tests 1 & 2
4	4.9-4B-8T3-E	6-20 & 6-21-68	4.82	.1142	Spokes Vented To Ambient
5	4.9-4B-8T3-E-1	6-21-68	4.82	.1142	Spokes With C.D.B.
6	4.9	6-20-68	4.82	.1269	Baseline For Tests 4 & 5

FIGURE V.D.1-1 SCHEMATIC OF TEST HARDWARE FOR VENTED & SIMULATED C.D.B. INJECTANT STUDY

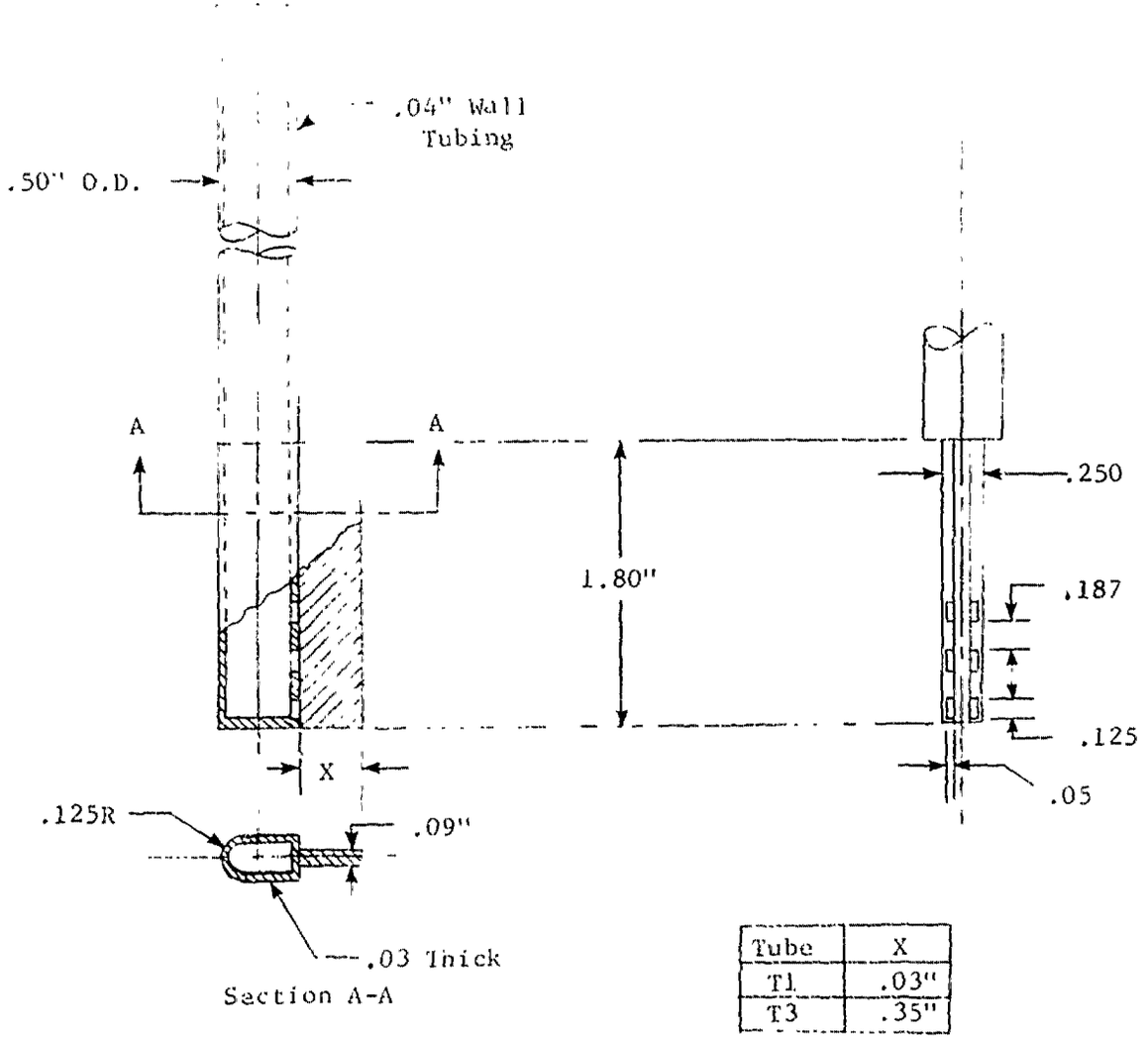

Tube	X
T1	.03"
T3	.35"

FIGURE V.D.1-2 HOLLOW SPOKE DESIGN FOR INJECTANT STUDY

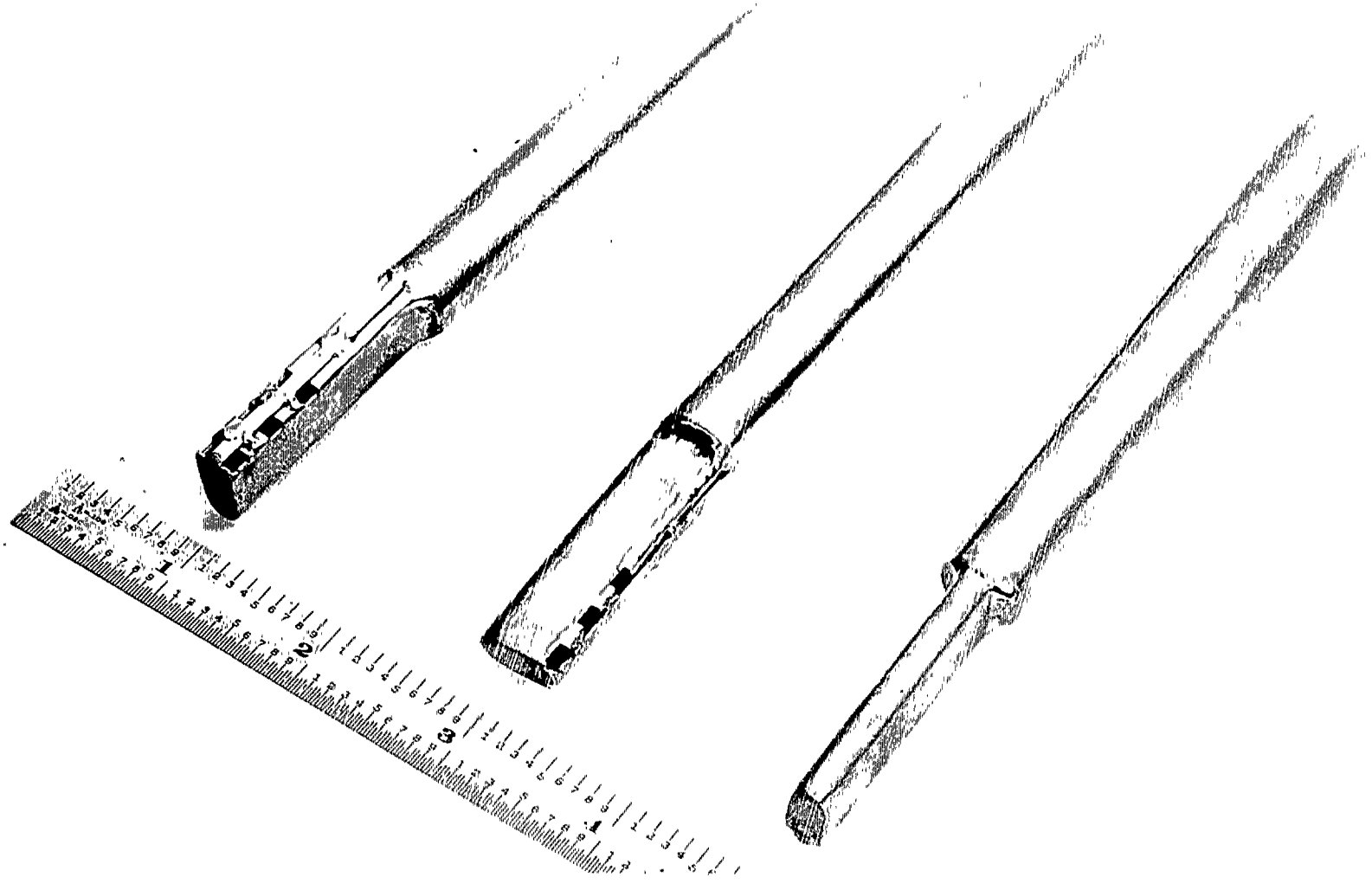

FIGURE V.D.1-3 HOLLOW RADIAL SPOKE - DESIGN T1

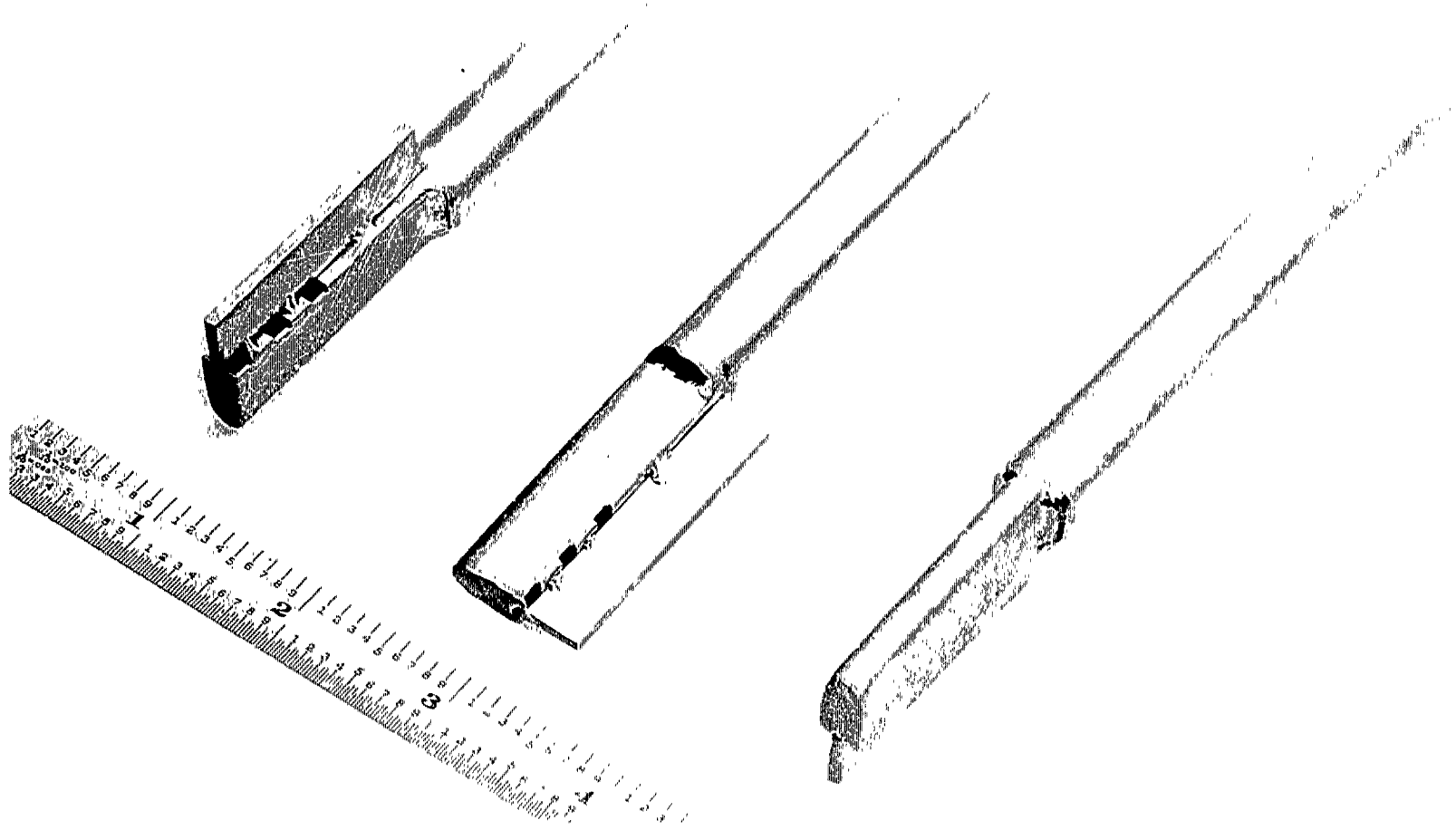

FIGURE V.D.1-4 HOLLOW RADIAL SPOKE - DESIGN T3

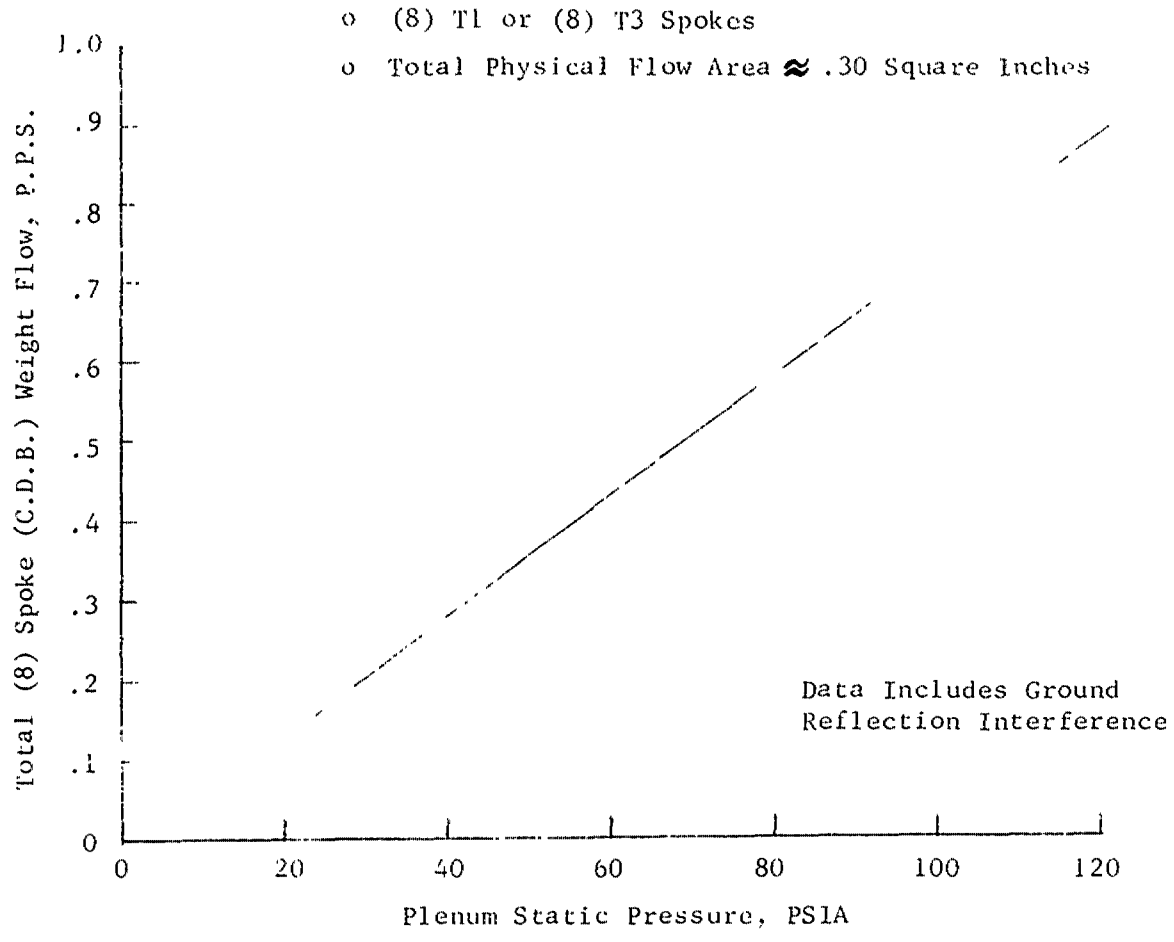

FIGURE V.D.1-5 HOLLOW RADIAL SPOKE C.D.B. FLOW CALIBRATION

- o Baseline & (8) T1 Spokes
- o Vented to Amb. or with Simulated C.D.B.
- o Numbers Beside Flagged Symbols are Plenum Static Pressure in PSIA

△ Model 4.9-4B-8T1-E 6-19-68 (8) T1 Spokes Vented to Ambient

▼ Model 4.9-4B-8T1-E-1 6-24-68 (8) T1 Spokes With Simulated C.D.B.

○ 4.82" Cone 6-19-68

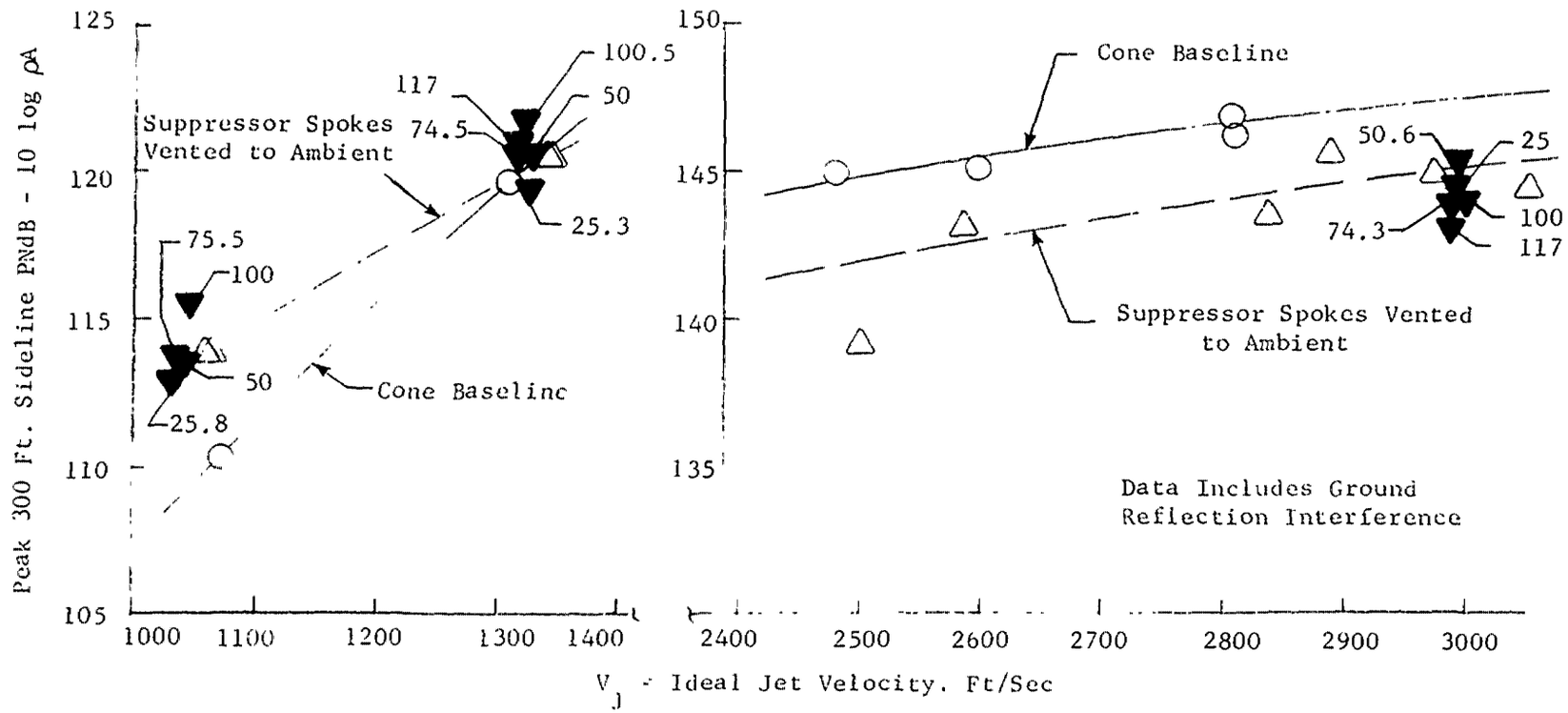

FIGURE V.D.1-5 300 FT. SIDELINE PEAK JET NOISE LEVELS USING T1 HOLLOW SPOKES

- o Baseline & (8) T3 Spokes
- o Vented to Amb. or with Simulated C.D.B.
- o Numbers Beside Flagged Symbols are Plenum Static Pressure in PSIA

◇ Model 4.9-4B-8T3-E 6-20-68 (8) T3 Spokes Vented to Ambient

◆ Model 4.9-4B-8T3-E-1 6-21-68 (8) T3 Spokes With Simulated C.D.B.

○ 4.82" Cone 6-20-68

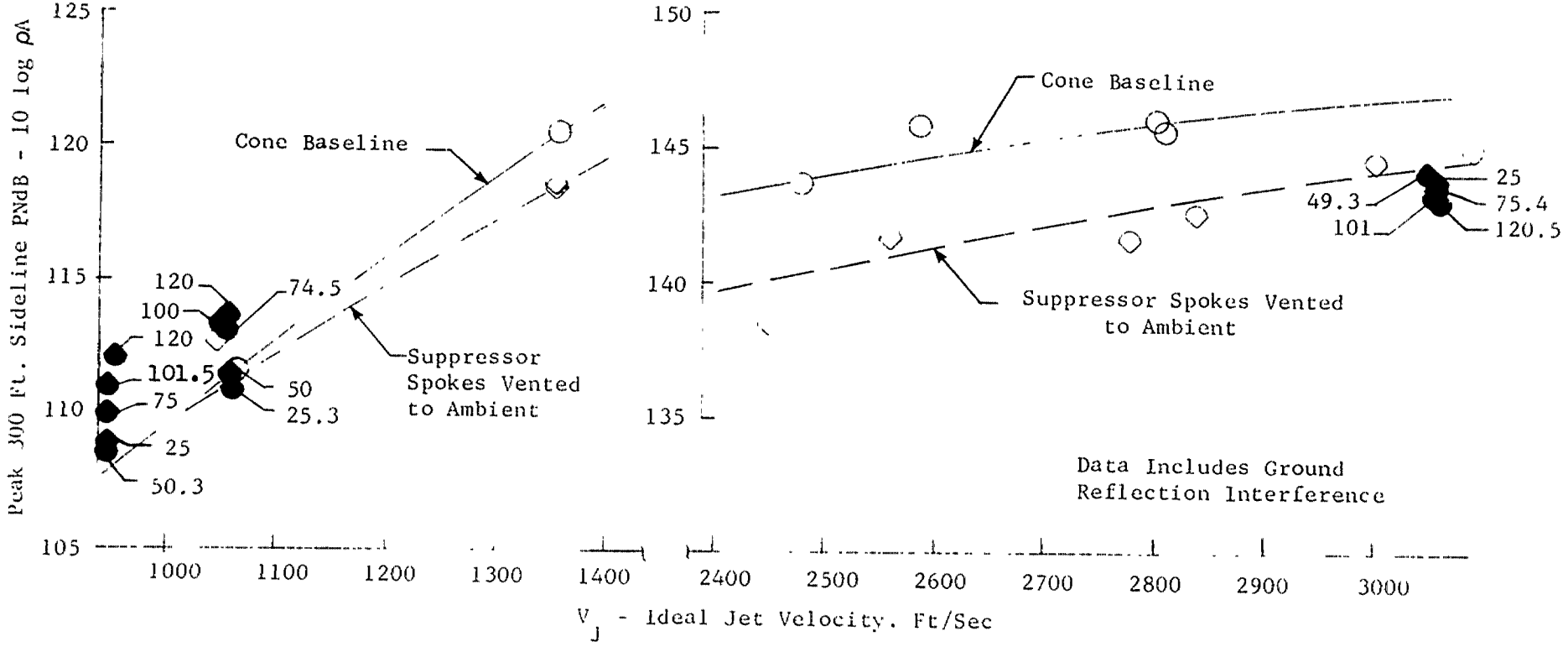

FIGURE V.D.1-7 300 FT. SIDELINE PEAK JET NOISE LEVELS USING T3 HOLLOW SPOKES

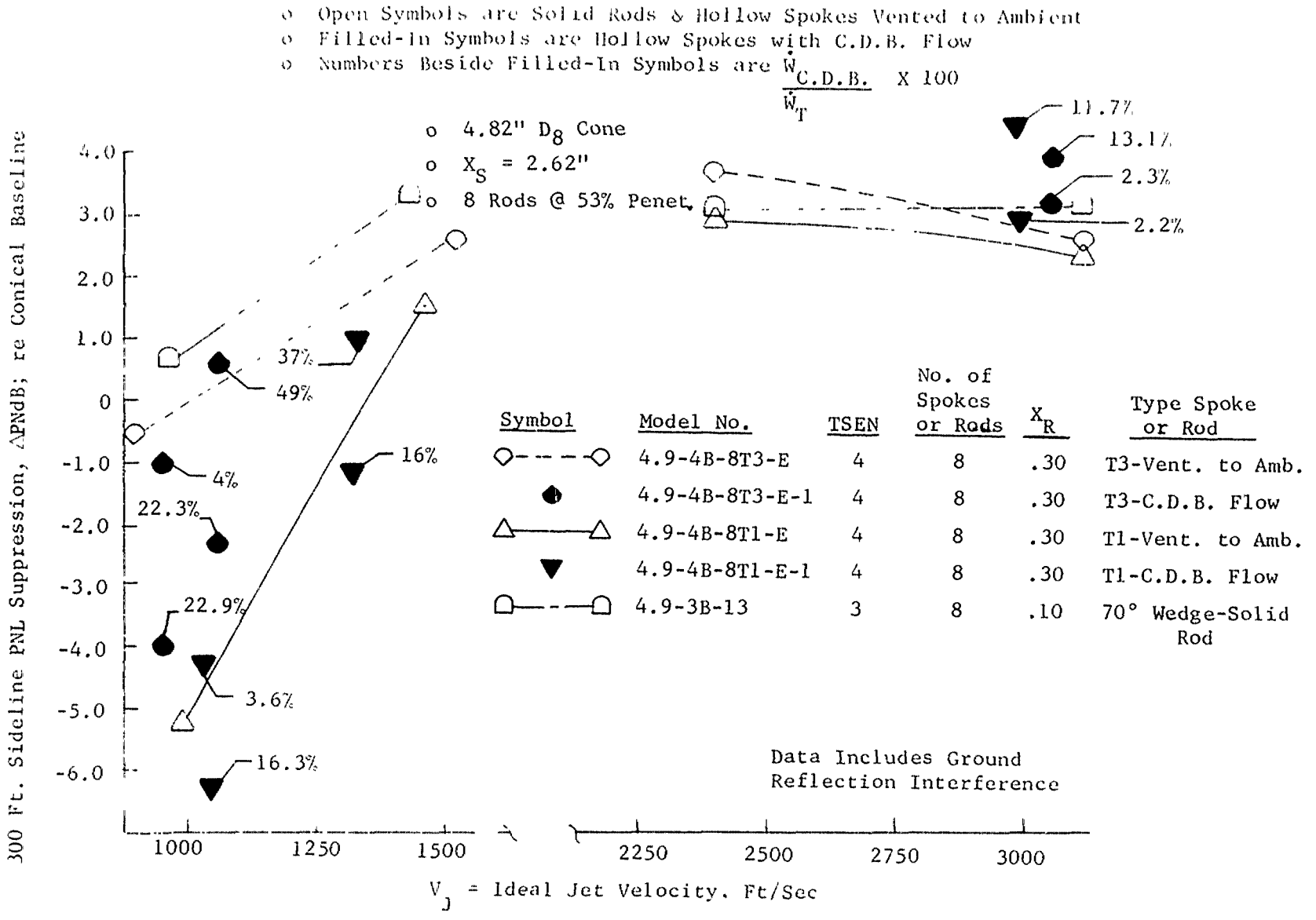

FIGURE V.D.1-8 300 FT. SIDELINE PEAK PNL SUPPRESSION OF VENTED & PRESSURIZED SPOKE SYSTEMS

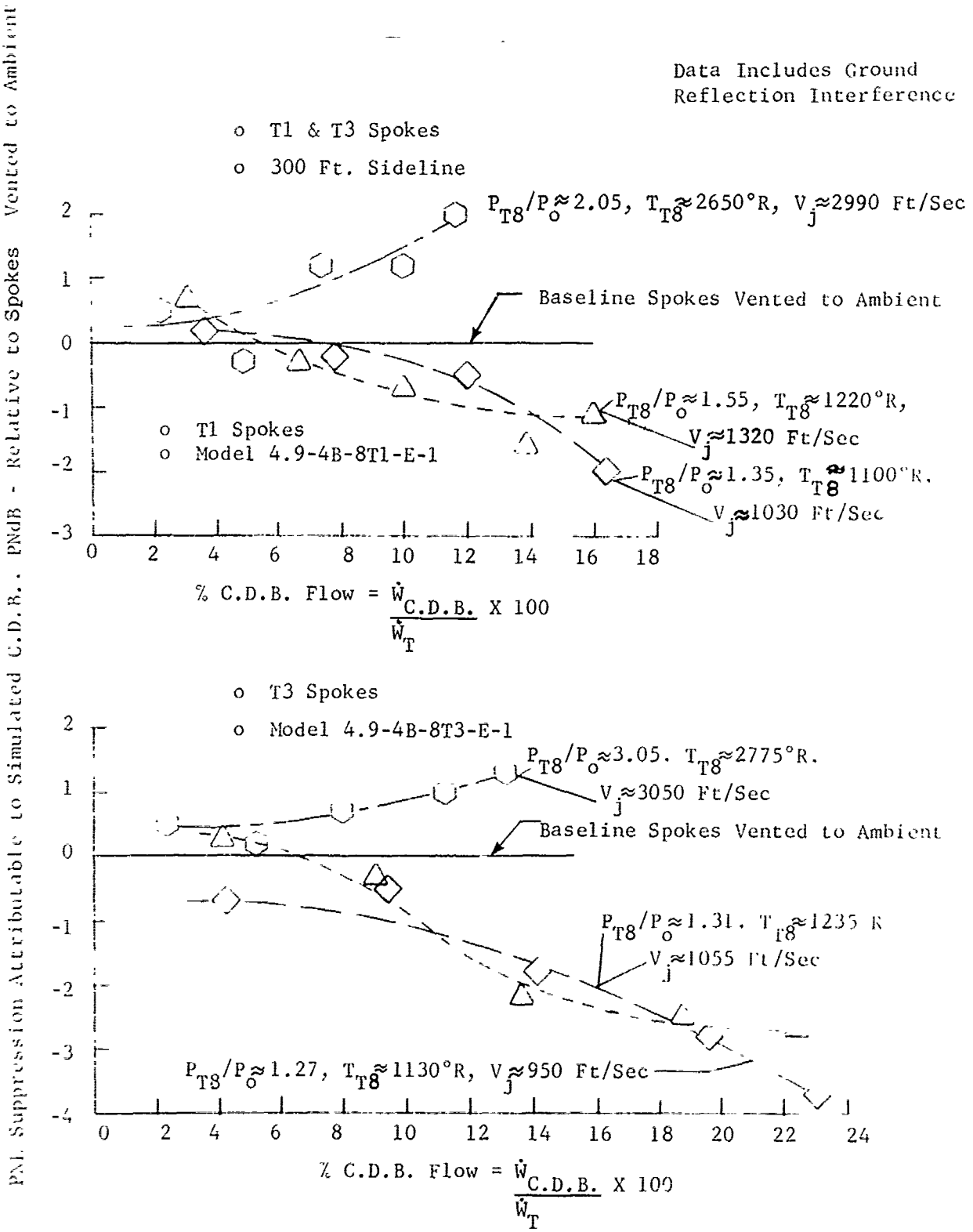

FIGURE V.D.1-9 300 FT. SIDELINE SUPPRESSION EFFECT OF SIMULATED COMPRESSOR DISCHARGE BLEED

- T1 Tubes – Model 4.9-4B-8T1-E-1
- $P_{T8}/P_o \approx 1.35$
- $T_{T8} \approx 1100°R$
- $V_j \approx 1030$ Ft/Sec
- 70° From Jet Exhaust

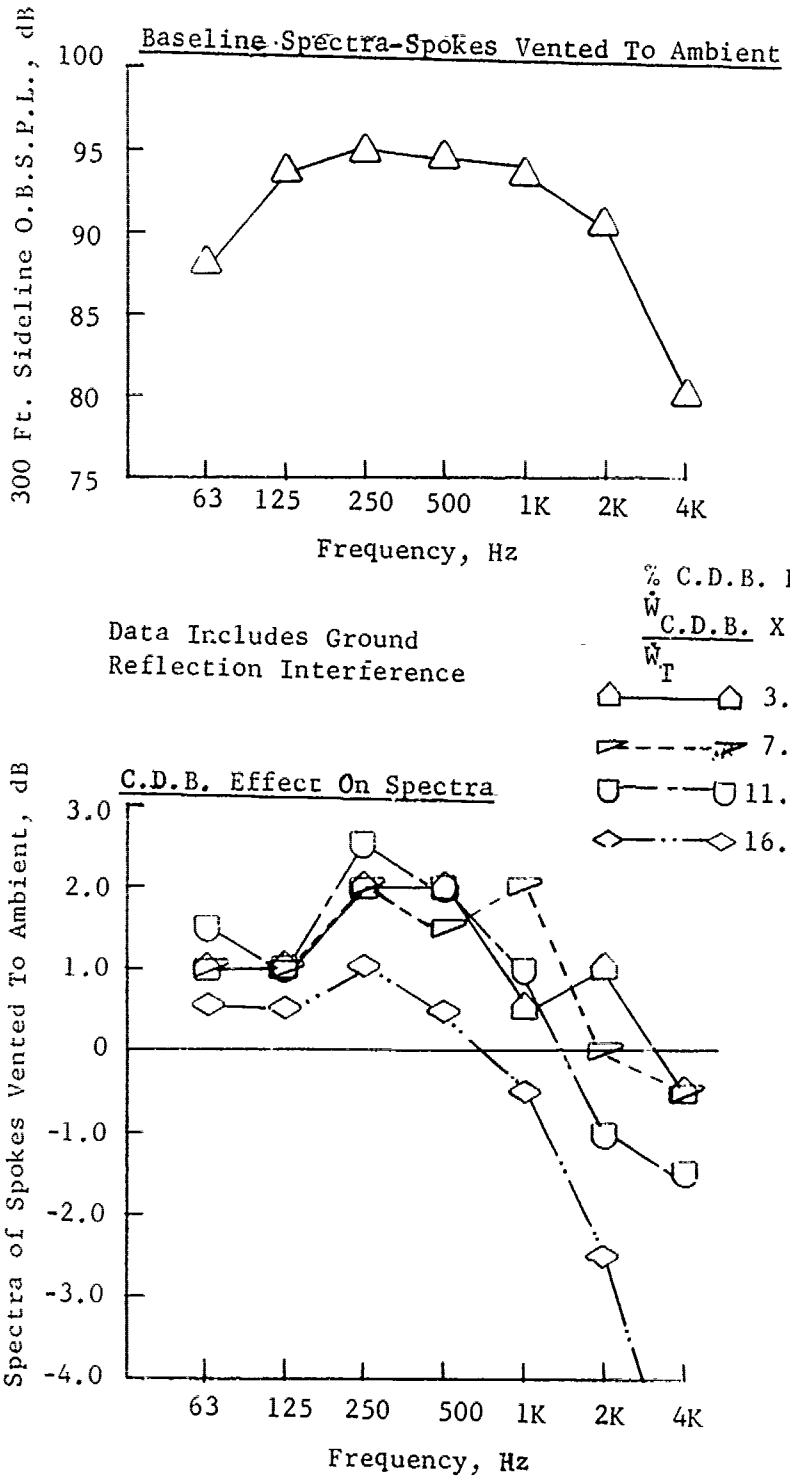

FIGURE V.D.1-10A EFFECT OF SIMULATED C.D.B. ON SPECTRA SUPPRESSION WITH T1 HOLLOW SPOKES

- o T1 Spokes – Model 4.9-4B-8T1-E-1
- o $P_{T8}/P_o \approx 1.55$
- o $T_{T8} \approx 1220°R$
- o $V_j \approx 1320$ Ft/Sec
- o 70° From Jet Exhaust

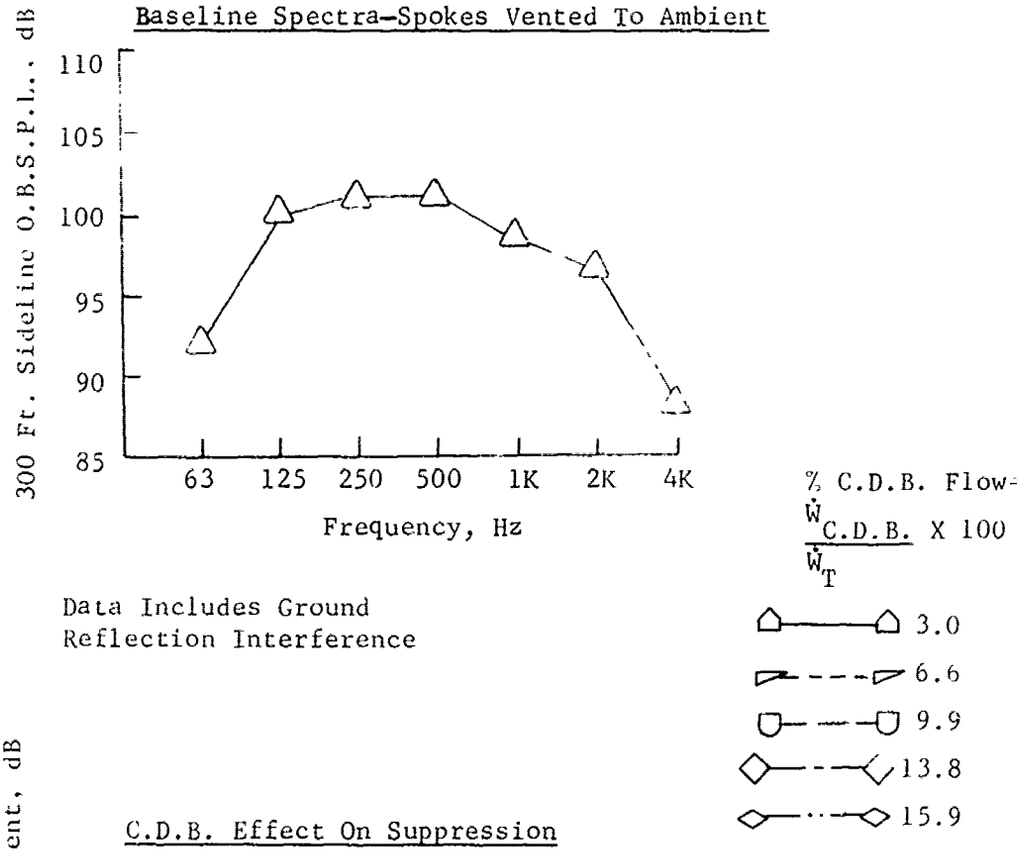

FIGURE V.D.1-10B EFFECT OF SIMULATED C.D.B. ON SPECTRA SUPPRESSION WITH T1 HOLLOW SPOKES

- o T1 Spokes - Model 4.9-4B-8T1-E-1
- o $P_{T8}/P_o \approx 3.05$
- o $T_{T8} \approx 2650°R$
- o $V_j \approx 2990$ Ft/Sec
- o 60° From Jet Exhaust

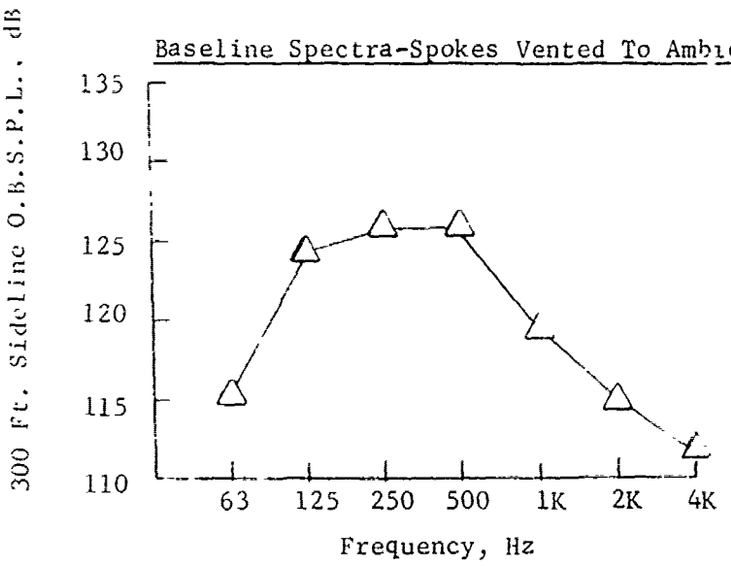

Data Includes Ground Reflection Interference

% C.D.B. Flow= $\frac{\dot{W}_{C.D.B.}}{\dot{W}_T} \times 100$

2.2
4.9
7.4
10.0
11.7

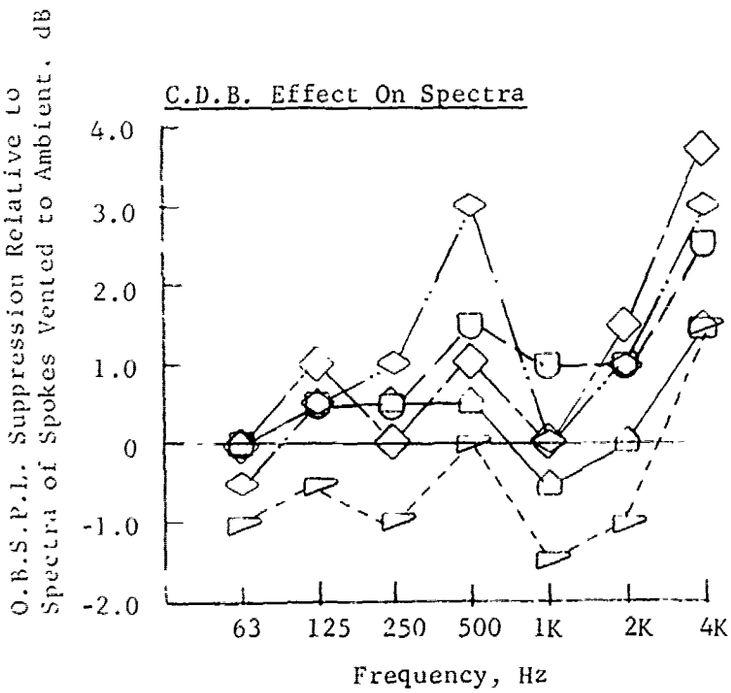

FIGURE V.D.1-10C EFFECT OF SIMULATED C.D.B. ON SPECTRA SUPPRESSION WITH T1 HOLLOW SPOKES

- o T3 Spokes – Model 4.9-4B-8T3-E-1
- o $P_{T8}/P_o \approx 1.27$
- o $T_{T8} \approx 1130°R$
- o $V_j \approx 950$ Ft/Sec
- o 70° From Jet Exhaust

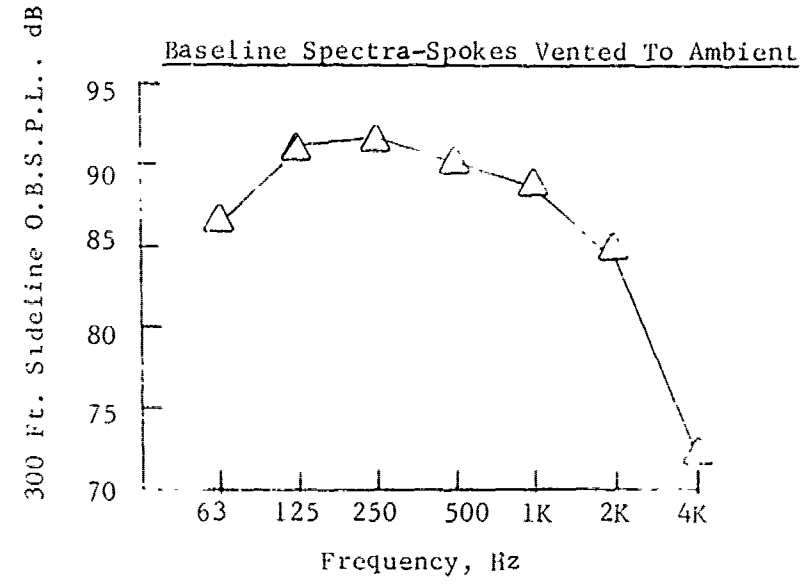

Data Includes Ground Reflection Interference

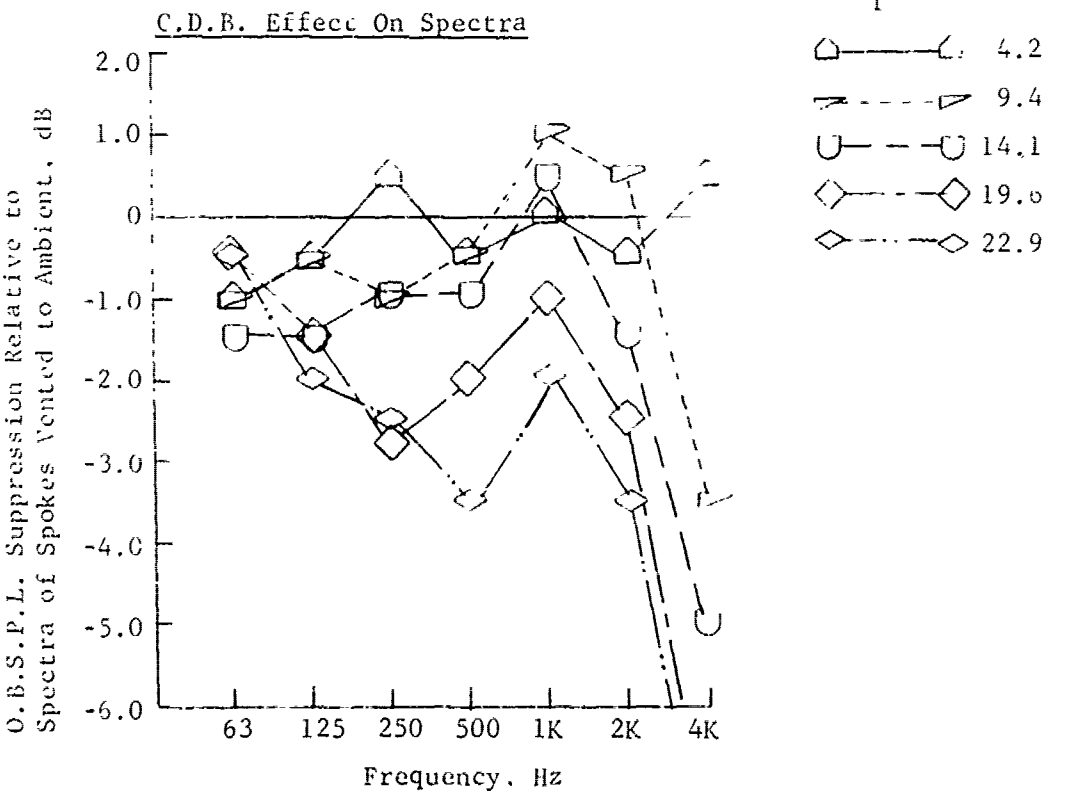

FIGURE V.D.1-11A EFFECT OF SIMULATED C.D.B. ON SPECTRA SUPPRESSION WITH T3 HOLLOW SPOKES

- o T3 Spokes – Model 4.9-4B-8T3-E-1
- o $P_{T8}/P_o \approx 1.31$
- o $T_{T8} \approx 1235°R$
- o $V_j \approx 1055$ Ft/Sec
- o 70° From Jet Exhaust

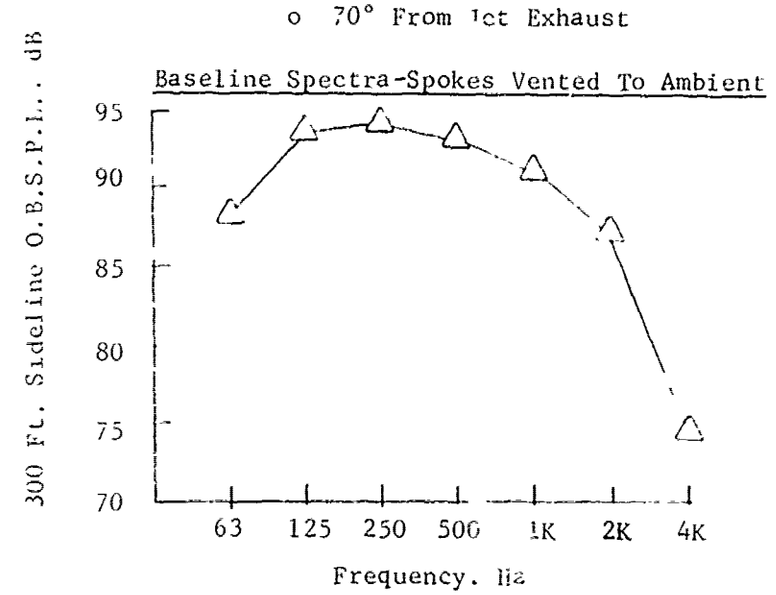

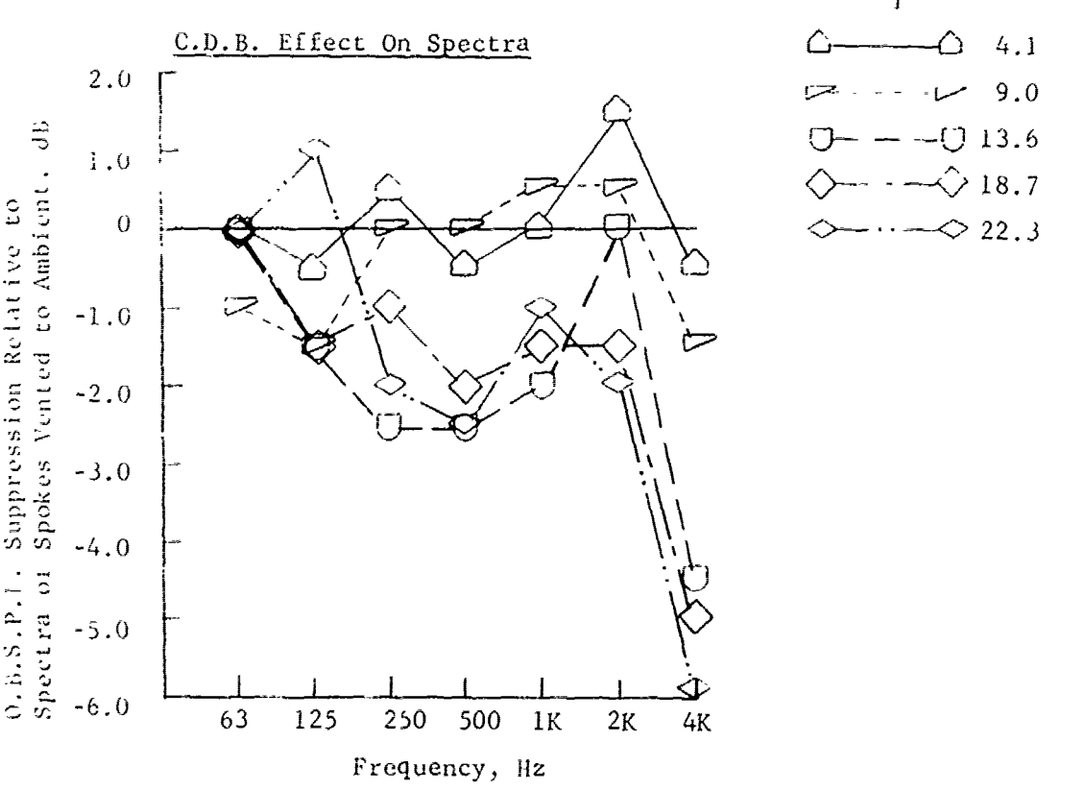

FIGURE V.D.1-11B EFFECT OF SIMULATED C.D.B. ON SPECTRA SUPPRESSION WITH T3 HOLLOW SPOKES

- o T3 Spokes - Model 4.9-4B-8T3-E-1
- o $P_{T8}/P_o \approx 3.05$
- o $T_{T8} \approx 2775°R$
- o $V_j \approx 3050$ Ft/Sec
- o 60° From Jet Exhaust

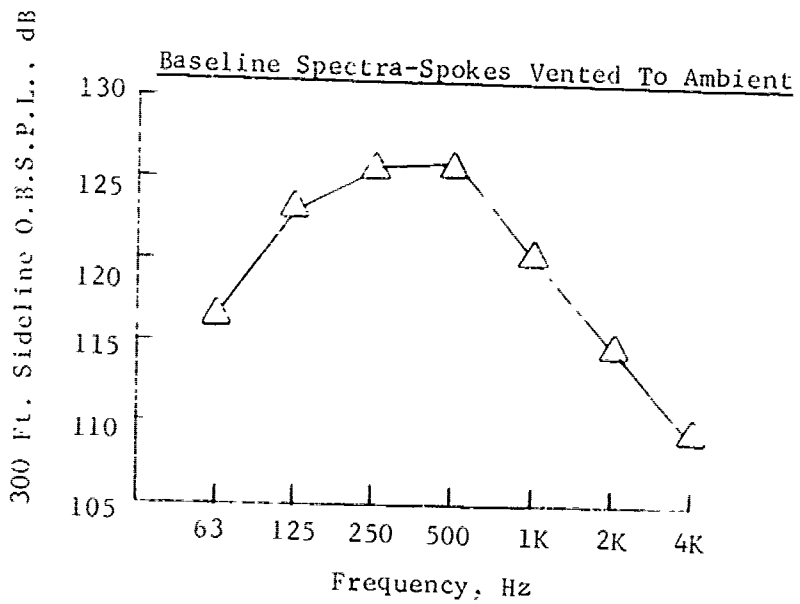

Data Includes Ground Reflection Interference

% C.D.B. Flow = $\frac{\dot{W}_{C.D.B.}}{\dot{W}_T} \times 100$

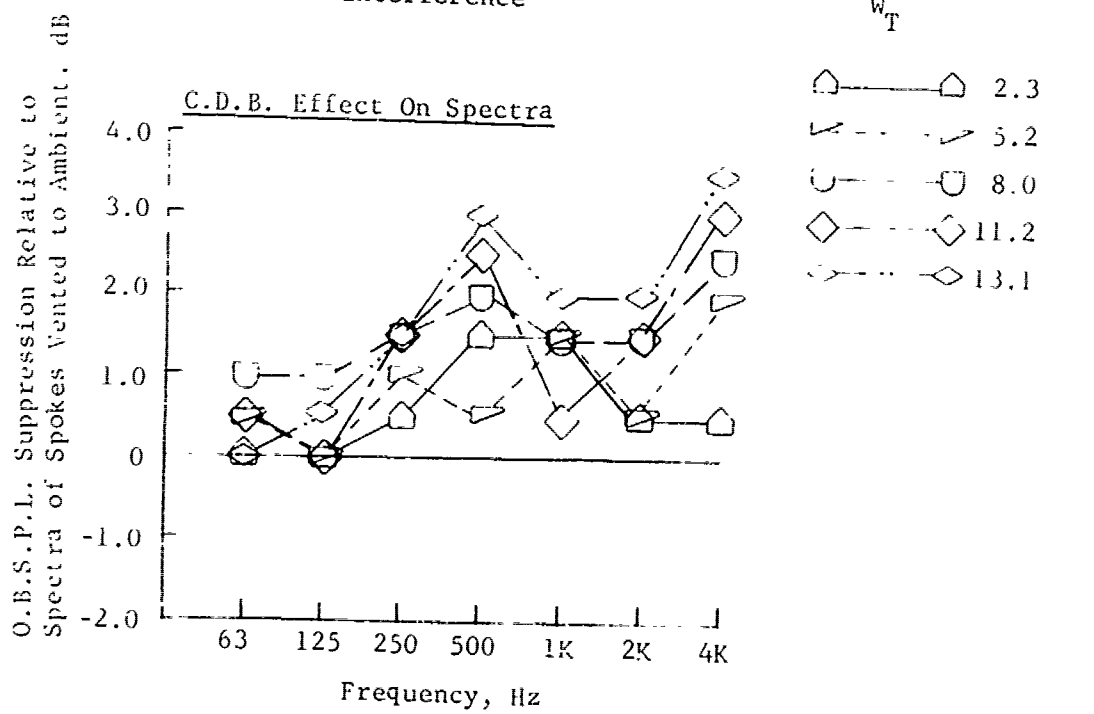

FIGURE V.D.1-11C EFFECT OF SIMULATED C.D.B. ON SPECTRA SUPPRESSION WITH T3 HOLLOW SPOKES

V.D.2 HOLLOW RADIAL SPOKES WITH RADIAL AND AXIAL AIR AND WATER INJECTION

V.D.2 HOLLOW RADIAL SPOKES WITH RADIAL AND AXIAL AIR AND WATER INJECTION

Purpose of Tests

Other variations of injectants were studied in the attempt to improve noise suppression of the radial spoke suppressor concept. Those covered in this section are a) radial injection of air and water through hollow spokes set at 53% penetration of the primary jet, and b) upstream directed axial injection of air and water through similar hollow spokes.

Test Set Up and Procedure

Basic hardware was similar to that of Figure V.D.1-1 of Section V.D.1 and is shown in Figure V.D.2-1. The same T1 spoke design of Figure V.D.1-2 was used for axial injection, however, they were turned to inject forward instead of aft. For radial injection of air and water, the T3 spoke design of Figure V.D.1-2 was altered to block the axial injectant passages and bleed holes were opened in the end of the spokes.

The TSEN 4 ejector system was used with X_S spacing of 2.62 inches and tertiary blow-in-door area of 12 square inches. Each test configuration had 8 equally spaced hollow radial spokes located aft of plane 8 at 53% penetration of the primary conical nozzle on a 2.26 inch spoke tip I.D. For both radial and axial injection, the tests covered a wide range of weight flow. Injectant flow rate is measured in pounds per second and expressed as a percentage of the primary gas stream.

Presentation and Discussion of Test Results

Air injection test results are seen in Figure V.D.2-2 as 300 and 1500 ft. sideline peak PNL suppressions. The data are for four test jet velocities of 1090, 1350, 1750 and 3050 ft/sec with axial and radial air injection ranging from 0.5 to 22.5% of the primary jet stream. The PNL suppression values shown are referenced to the conical primary/TSEN/radial spoke system without bleed flow and, therefore, are attributable to air injection alone. At low and intermediate jet velocities, both radial and axial air injection had minor suppression effect and normally increased the generated total noise levels. At high velocity the radial injectant was ineffective and the axial injectant attained several PNdB suppression but only with high percentage of mass flow.

PRECEDING PAGE BLANK-NOT FILMED

Figure V.D.2-3 shows the spectral change due to the axial and radial air injection at the 3050 ft/sec jet velocity condition. The top of the figure shows the basic spectra for the 8 hollow spoke system and the bottom shows the variation around that spectra due to the air injectant. The radial injectant shows greater noise produced in all intermediate octave bands with suppression only in the 63 Hz and 4 KHz bands. For axial injection, suppression is gained in all octave bands.

Considering water injection, Figure V.D.2-4 shows the resultant 300 and 1500 ft. sideline PNL suppression. Again the test points were set at 1090, 1350, 1750 and 3050 ft/sec but with an injectant range of 18 to 208% of the primary gas stream expressed as $(\dot{W}_{water}/\dot{W}_{primary})X\ 100$ where $\dot{W}$'s are measured in pounds-per-second. Radial injection gained about 6 PNdB suppression for the high V_j point with 40% injectant flow. Axial injection attained similar levels but with much greater mass flow of water.

The spectral changes with radial and axial water injection are shown for the high V_j point in Figure V.D.2-5. Major suppression is attained in the low frequency bands from 63 to 500 Hz.

Conclusions

- Suppression of approximately 2 PNdB was obtained for axial air injection flow rates in the order of 13%. Radial air injection at these low flow rates was ineffectual.
- Water injection, radial and axial, proved to be effective at high velocity conditions with suppressions reaching 6 PNdB using 40% $\dot{W}$ radial and 100% $\dot{W}$ axial injection, respectively.
- In summary, the results of this series of tests indicate that low fluid injection rates, relative to the primary flow, will not enhance the suppression potential of the primary spoke system.

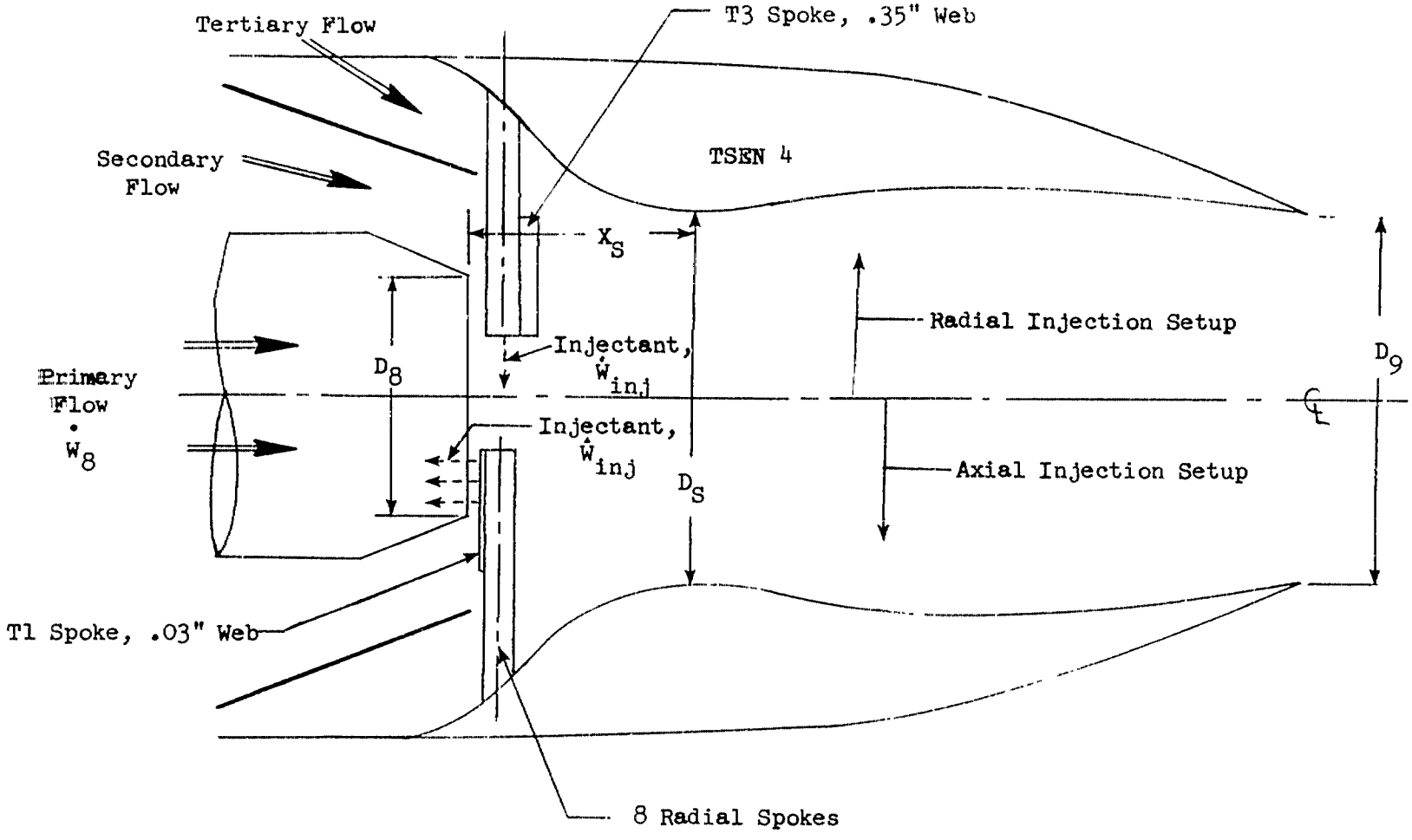

FIGURE V.D.2-1 SCHEMATIC OF PRIMARY SPOKE/FLUID INJECTION SUPPRESSOR SYSTEM

- (8) Radial Hollow Spokes at 53% Penetration

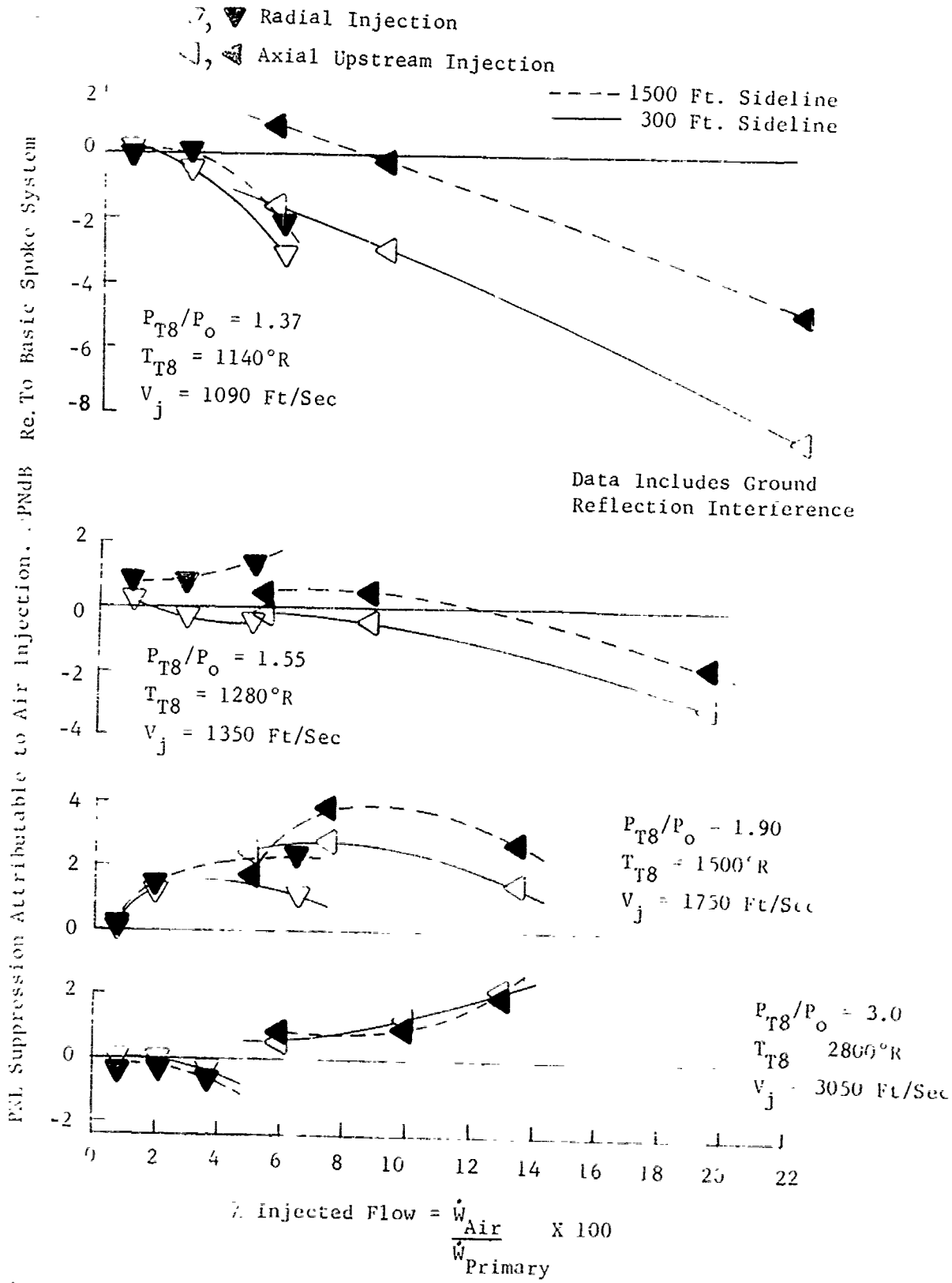

Figure D.7-2 EFFECT OF AIR INJECTION ON 300 & 1500 FT. SIDELINE PNL SUPPRESSION CHARACTERISTICS OF PRIMARY SPOKE SYSTEM

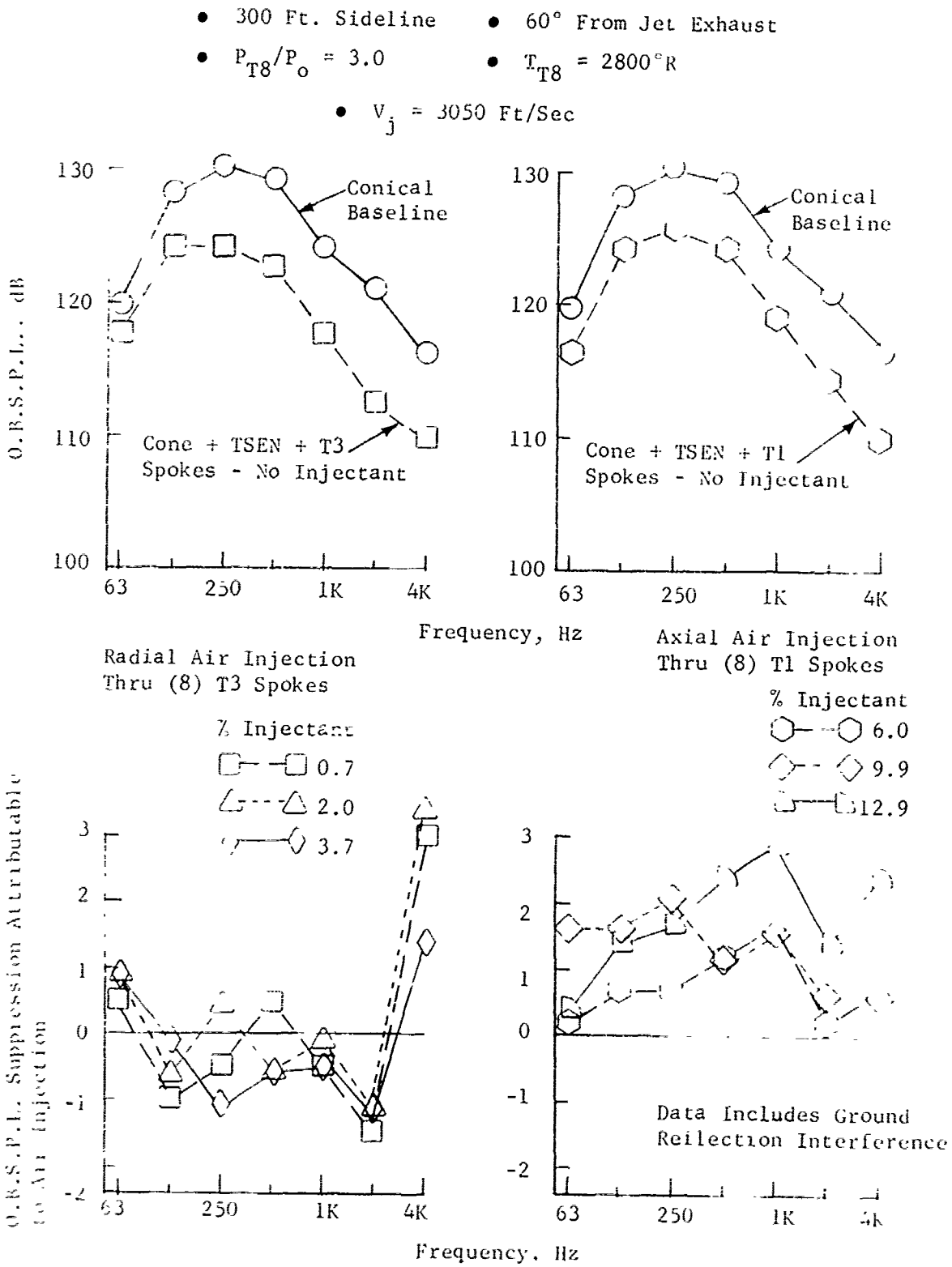

Figure D.2-3 EFFECT OF AIR INJECTION ON 300 FT. SIDELINE SPECTRAL CHARACTERISTICS OF PRIMARY SPOKE SYSTEM

- (8) Radial Hollow Spokes at 53% Penetration

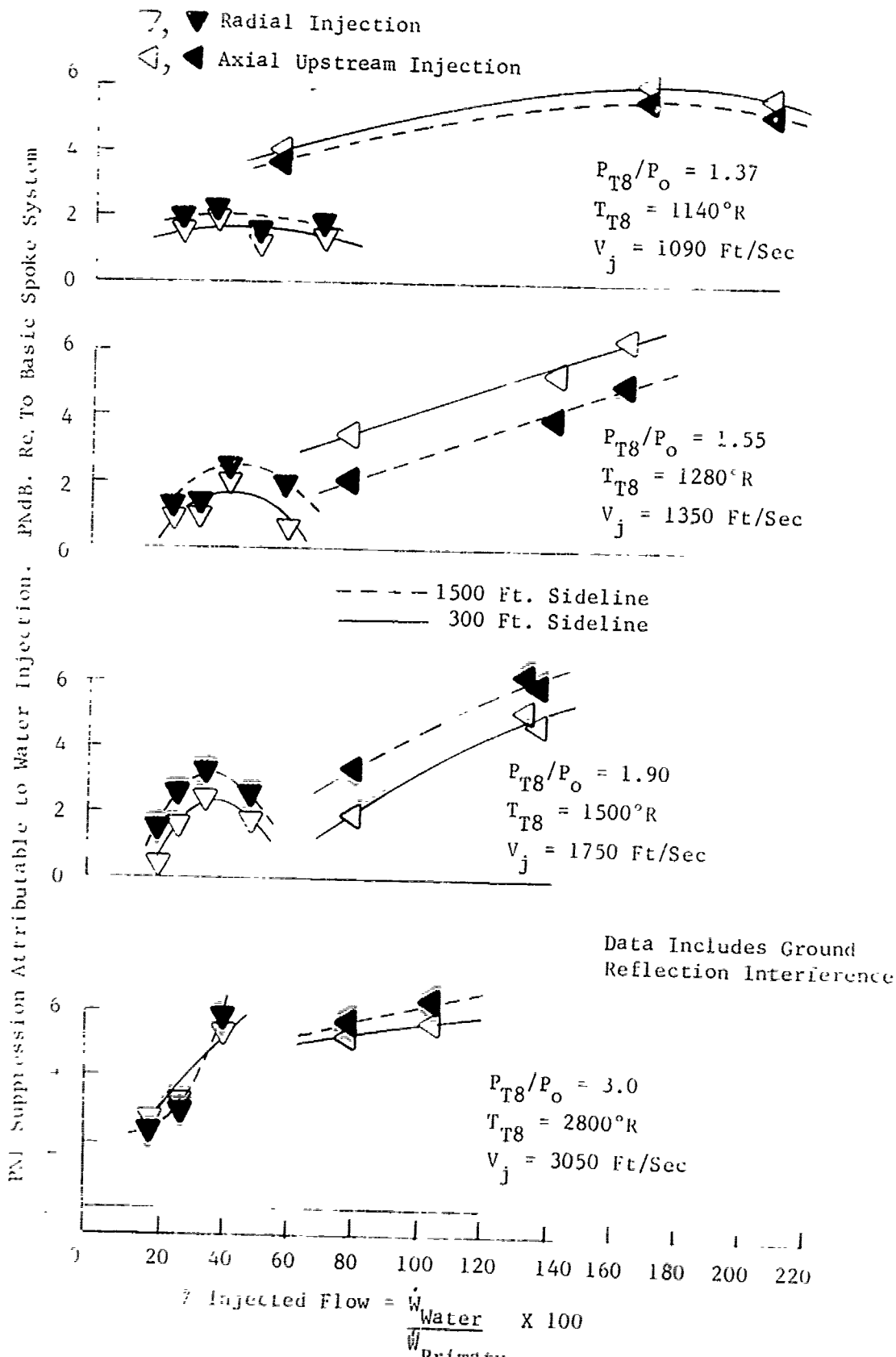

5.2-4 EFFECT OF WATER INJECTION ON 300 & 1500 FT. SIDELINES PNL SUPPRESSION CHARACTERISTICS OF PRIMARY SPOKE SYSTEM

- 300 Ft. Sideline
- 60° From Jet Exhaust
- P_{T8}/P_o = 3.0
- T_{T8} = 2800°R
- V_j = 3050 Ft/Sec

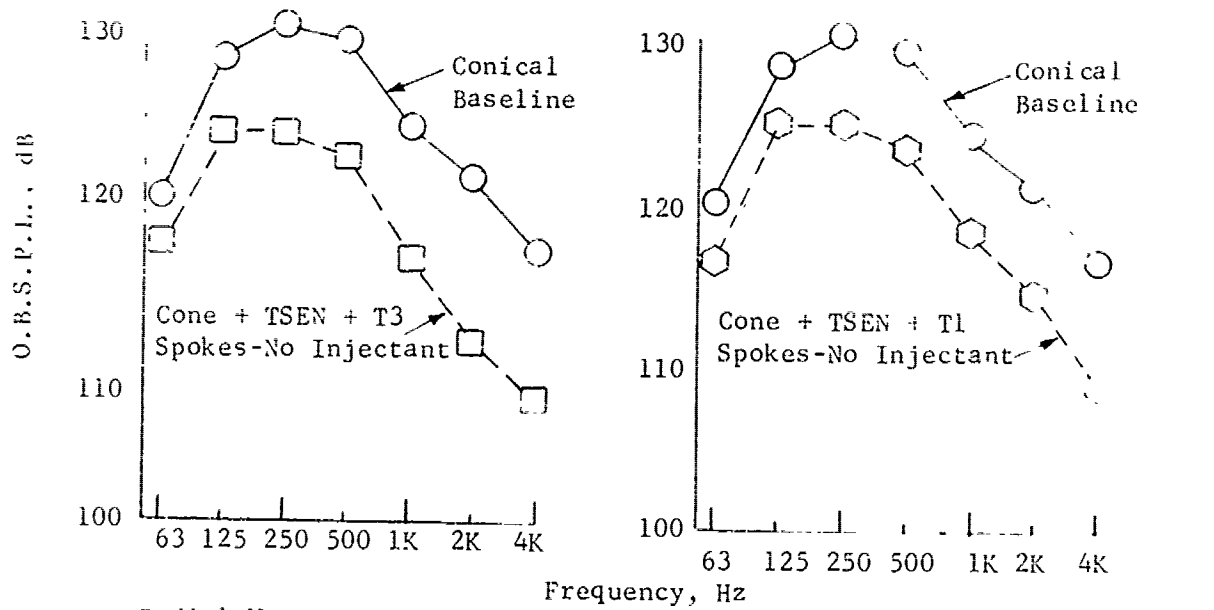

Radial Water Injection Thru (8) T3 Spokes

Axial Water Injection Thru (8) T1 Spokes

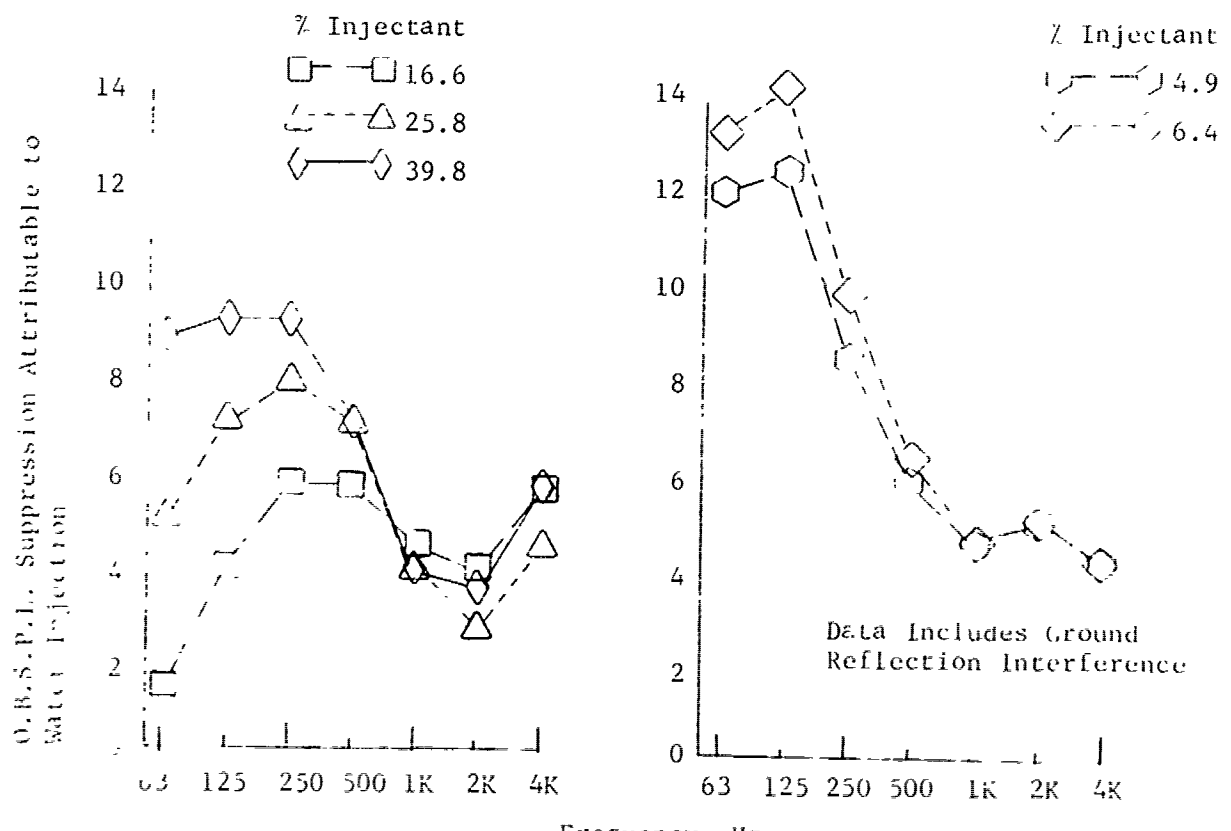

Fig. 4.0.2-5 EFFECT OF WATER INJECTION ON 300 FT. SIDELINE SPECTRAL CHARACTERISTICS OF PRIMARY SPOKE SYSTEM

V.D.3 AIR AND WATER INJECTION OVER PRIMARY THRUST REVERSER TABS

PRECEDING PAGE BLANK-NOT FILMED

V.D.3 AIR AND WATER INJECTION OVER PRIMARY THRUST REVERSER TABS

Purpose of Test

In an effort to realize additional suppression from the primary thrust reverser tab system (see Section V.C.2), the feasibility of injecting simulated compressor discharge bleed (C.D.B.) air and water over the tabs and into the jet stream was investigated.

Test Set Up and Procedure

Basic test hardware was similar to that of Figure V.C.2-14 of Section V.C.2, and is shown in Figure V.D.3-1. The 5.637" D_8 conical primary with TSEN 56 was used for a D_s/D_8 of 1.241 and a D_9/D_s of 1.0. As the 16 equally spaced tabs at an 18° stream penetration angle were acoustically beneficial, this tab setting was chosen for application of injectants. At 18° the tabs penetrated D_8 by 14.1% and formed 8.8% projected blockage of A_8. The tab planform shape is shown in Figure V.C.2-14. The air and water injections were accomplished through 16 hollow tubes of .170" I.D. The tubes were fastened to the back rib of each tab and terminated in the plane of the tab face.

Plant facility air was manifolded and injected through the tubes to simulate compressor discharge bleed at flow rates from 0.5 to 9% of the primary stream. Water injection flow rates ranged from about 2 to 65%. Water injection was used for heated primary stream jet velocities of 1085, 1360, 2850 and 2995 ft/sec. Air injection was used at the first three velocity conditions. The system without injectants was also tested as reference, so that noise generation changes could be gauged and attributed solely to the injectants.

Presentation of Test Results

Results of both air and water injection are shown as 300 and 1500 ft. sideline peak PNL suppressions in Figures V.D.3-2 and -3, respectively. The data are for the jet velocities of 1085, 1360, 2850 and 2995 ft/sec and are referenced to the cone + TSEN + tabs without injectants. Therefore the suppression is attributable solely to fluid injection.

Conclusions

- Air injection over the tabs proved ineffective in gaining additional suppression when used with flow rates from 0.5 to 9%. At high velocity negligible gains were seen over the basic suppressor system. At low jet velocity, the noise generated by the air jets was sufficient to increase the total noise of the system.
- With water injection, substantial gains of 2 to 3 PNdB were not seen until large flow rates of 15% and higher were used.

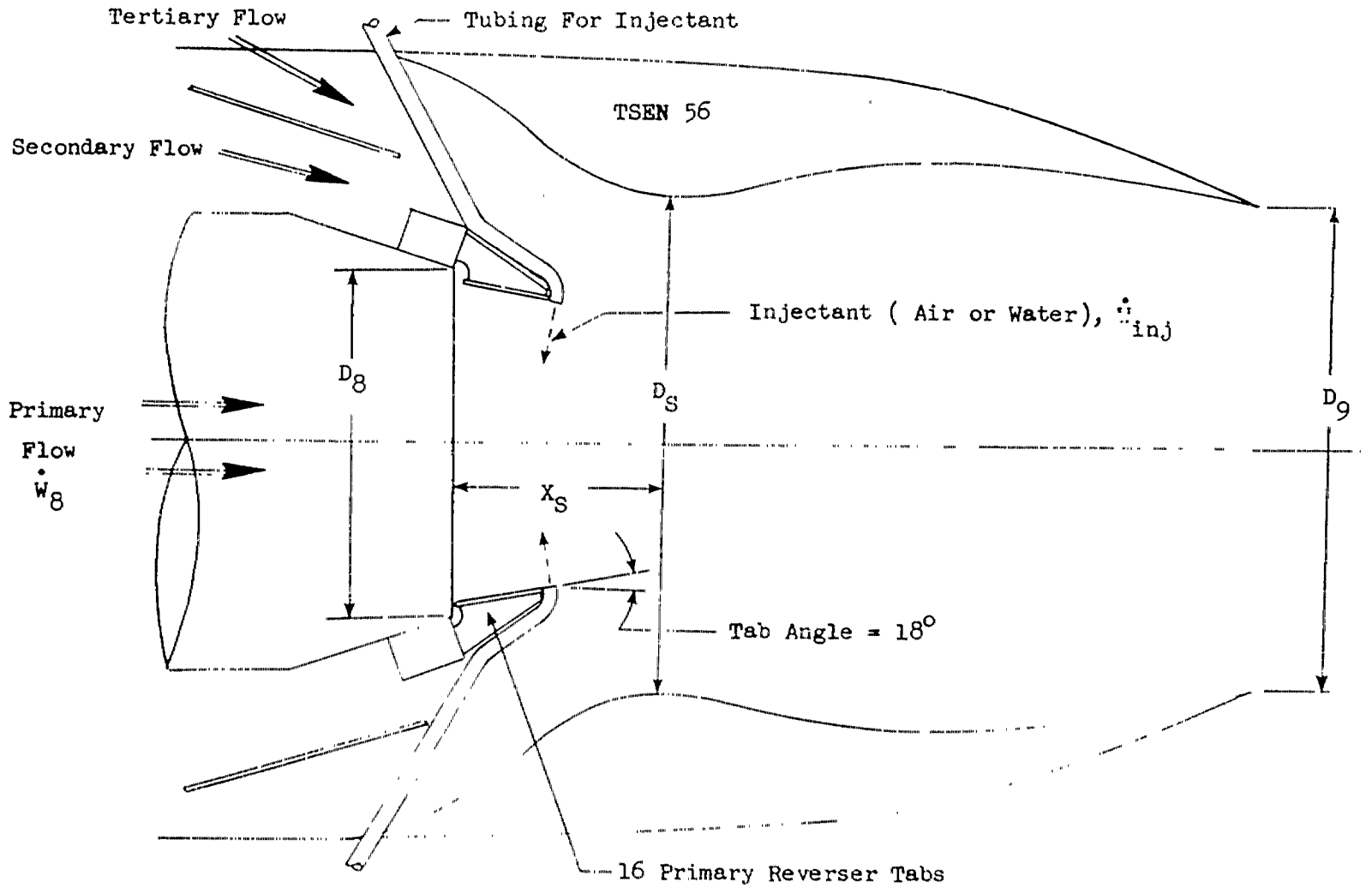

FIGURE V.D.3-1 SCHEMATIC OF PRIMARY TAB/FLUID INJECTION SUPPRESSOR SYSTEM

o 300 Ft. Sideline
o 16 Primary Tabs @ 18°

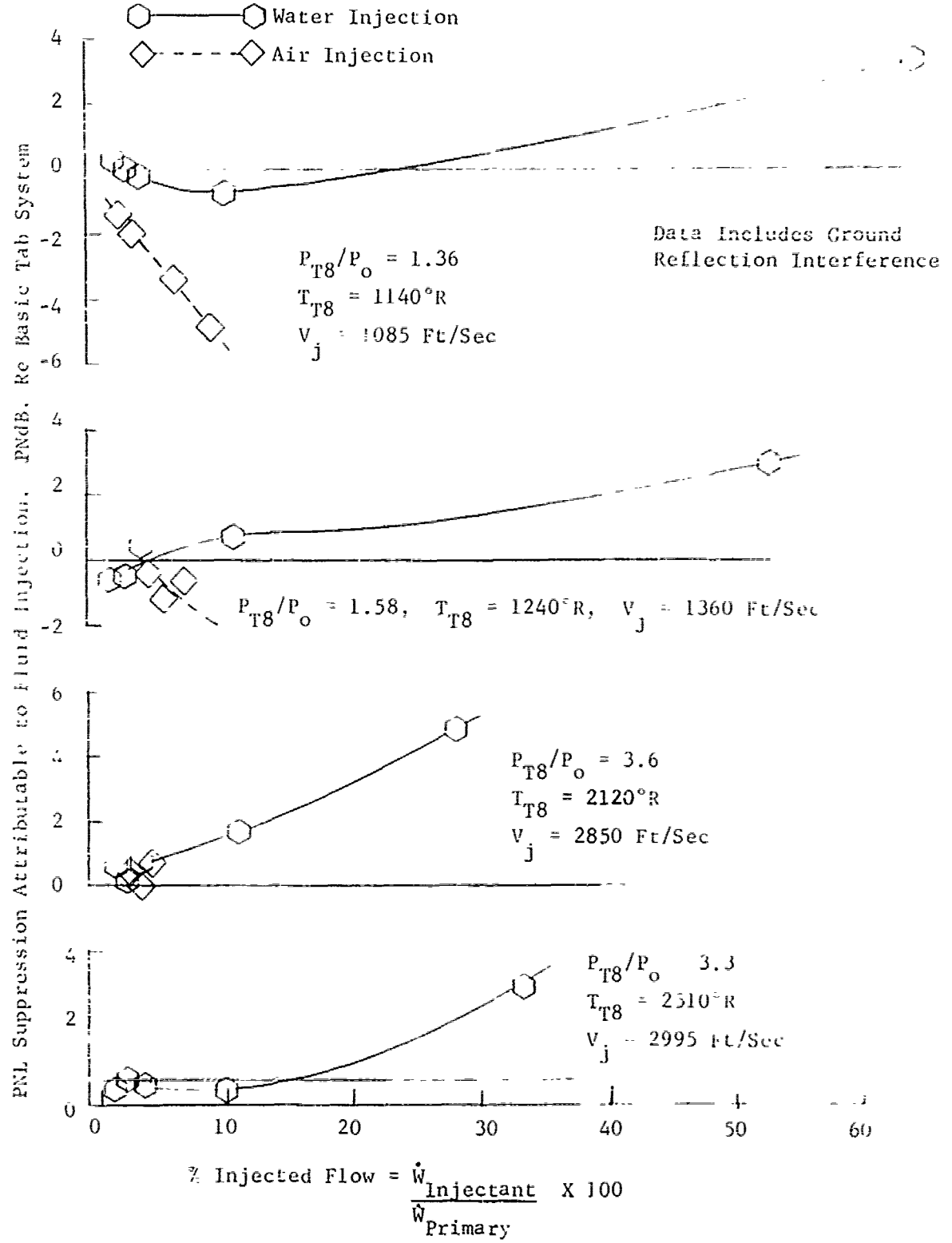

FIGURE V.D.3-2 EFFECT OF AIR AND WATER INJECTION ON 300 FT. SIDELINE PNL SUPPRESSION CHARACTERISTICS OF PRIMARY THRUST REVERSER TAB SYSTEM

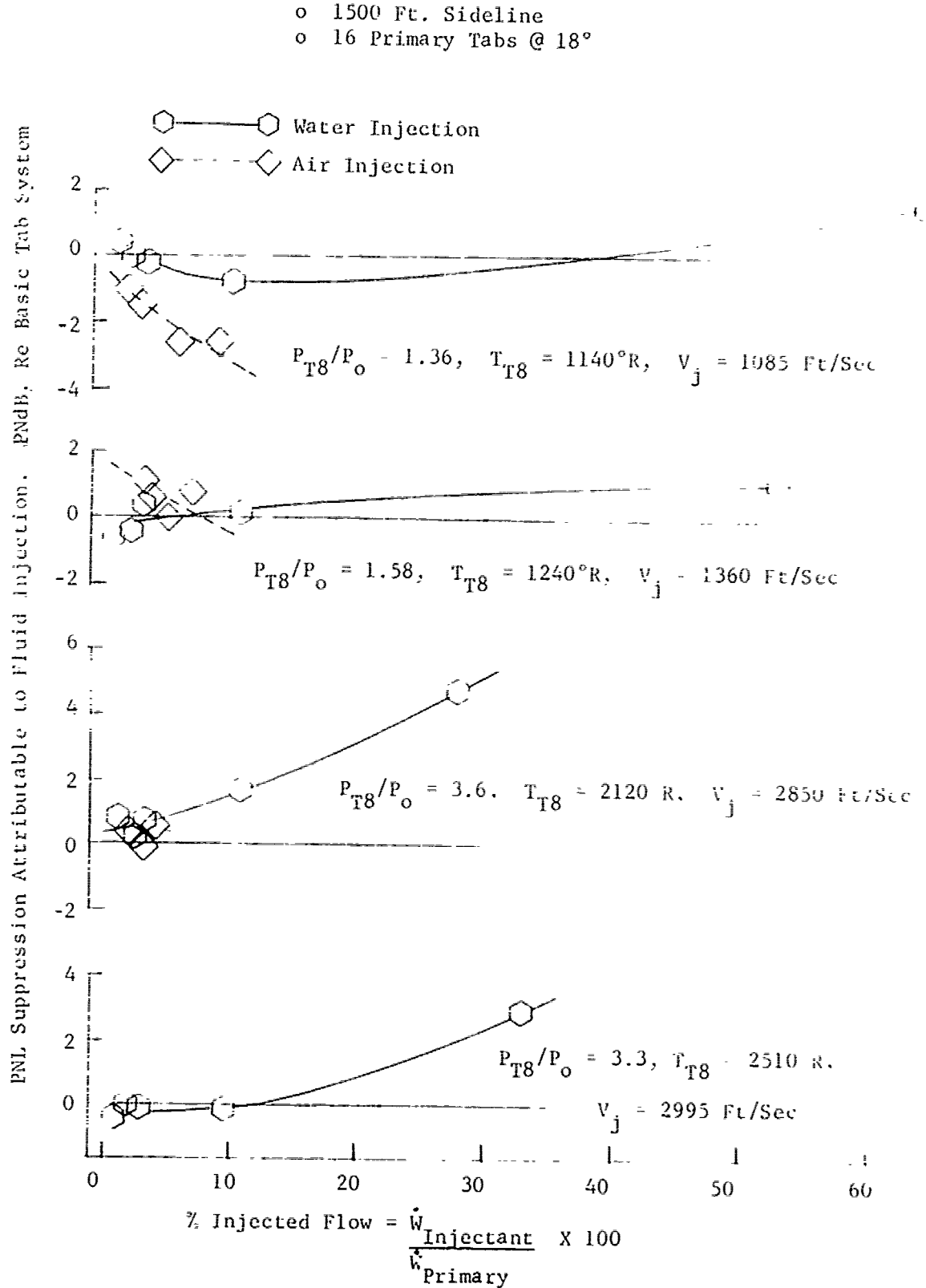

FIGURE V.D.3-3 EFFECT OF AIR AND WATER INJECTION ON 1500 FT. SIDELINE PNL SUPPRESSION CHARACTERISTICS OF PRIMARY THRUST REVERSER TAB SYSTEM

V.E SECONDARY REVERSER - SUPPRESSOR FLAPS

PRECEDING PAGE BLANK-NOT FILMED

V.E SECONDARY REVERSER-SUPPRESSOR FLAPS

Introduction and Test Purpose

In the design of the full scale engine thrust reverser system, a target type reverser was considered; to be deployed from the inner flowpath of the Two-Stage Ejector Nozzle (TSEN). A 16 flap arrangement was to be used which would form a full target reverser, exiting the gas stream through the fully open blow-in-doors. These reverser flaps were investigated to determine their benefit as acoustic suppressors. By partially deploying six or eight of the flaps into the primary jet stream, a suppressor system could be available with no additional weight penalty to the engine.

The system variables were investigated through a series of model tests. Representative model results are presented in this section through a selection of the flap designs designated F1, F7 and F15. These models were tested at the GE, Evendale, JENOTS facility. Acoustic performance dependency on a) flap planform shape, and b) secondary to primary diameter ratio, D_S/D_8, were investigated.

Test Configurations

Three secondary flap designs, F1, F7 and F15 (See Figure V.E-1) were used in a Two-Stage Ejector Nozzle system designated TSEN 3. The TSEN had a fixed D_S and D_9 of 6.09". To vary the D_S/D_8 ratio, simulating the range of engine operation with a variable conical primary, three primary nozzles of 4.32, 4.82 and 5.14" D_8 were used, resulting in D_S/D_8 ratios of 1.41, 1.26 and 1.18, respectively. The position of the flap leading edge was held constant aft of the D_S, both axially and radially for each model, as were the flap mount angle of 32.7° and blow-in-door angle of 14.5°. The 14.5° setting simulated an equivalent 1500 square inch blow-in-door area of the full scale engine design. Six flaps were used for each configuration, located on an 8 equally spaced pattern, but with a gap at the top and bottom vertical positions. (See Figure V.E-1.)

The three primary nozzles of D_8 = 4.32, 4.82 and 5.14" were each tested without the TSEN/suppressor system to establish the reference conical baseline to which suppression is quoted. Simulated engine cycle conditions over a jet

PRECEDING PAGE BLANK-NOT FILMED

velocity range of 2450 through 3050 ft/sec were used since this was the velocity range of interest for the suppressor system application.

Acoustic measurements, taken on a 40 ft. arc, were scaled by frequency and size to full scale application using a scale factor of 8:1. All data presented are, therefore, of simulated engine size and engine frequency range.

Presentation and Discussion of Results

Acoustic results are presented in the form of 300 ft. sideline normalized peak PNL as a function of ideal jet velocity in Figures V.E-2, -3 and -4. The figures are for the F1, F7 and F15 designs, respectively, and each shows variation with D_S/D_8 at the values of 1.41, 1.26 and 1.18. Baseline conical nozzle curves for the 4.32, 4.82 and 5.14" D_8 nozzles are also on each of the figures, the curves coming from the data plots of Figure V.E-5.

To show the absolute suppression levels as a function of flap design, cycle setting and D_S/D_8, Figure V.E-6 presents the 300 ft sideline peak PNL suppression for the F1, F7 and F15 flaps as a function of D_S/D_8 at 2000, 2500, 2800 and 3000° R for P_{T8}/P_o settings of 2.7 and 3.0. Each of the three flap configurations showed increasing suppression with increasing D_S/D_8. Pressure ratio increase from 2.7 to 3.0 also slightly improved suppression of the F1 and F7 flaps. However, with the F15 flaps, P_{T8}/P_o increase tended to lower suppression by .2 to .4 PNdB in the higher temperature range of 2800 to 3000° R. The F1 flaps show a crossover effect of P_{T8}/P_o at D_S/D_8 of about 1.22 for T_8 range of 2800 to 3000° R. Decreasing D_S/D_8 by use of larger primary conical nozzles shows suppression decreases 1.2 to 1.6 PNdB at 3000° R from 1.41 to 1.18.

A better feel of jet exhaust temperature effect on suppression is derived from Figure V.E-7 where jet noise suppression is plotted against temperature for constant D_S/D_8 ratios. Data were cross plotted and D_S/D_8 ratios of 1.20, 1.25, 1.36 and 1.43 were chosen for presentation. Separate curves for P/R of 3.0 and 2.7 are shown for each of the flap types. The F7 flaps show increasing suppression for temperature in the plotted P_{T8}/P_o range. The F1 flaps show an almost level or no effect with temperature increase. The general trend for the F15 flaps is for higher temperature to slightly decrease suppression in the plotted P/R range. Again the effect of increasing suppression with larger D_S/D_8 is emphasized by this figure.

Presentation of frequency spectra for T_{T8} of 2800° R and P_{T8}/P_o of 2.7 and 3.0 is shown in Figures V.E-8 through -11. Each shows the F7, F1 and F15 data in a different manner or combination. Peak 300 ft. sideline data is plotted on Figures V.E-8 and -9, Figure V.E-8 comparing the three different suppression spectra for the same D_S/D_8 ratio and Figure V.E-9 varying D_S/D_8 for each flap configuration. Large variations in spectra shape on these two figures are due to peak angle variation and not increased suppression. To better analyze spectra suppression, Figure V.E-10 and -11 have data at a constant 60° angle corrected to a 300 ft sideline. Figure V.E-10 again compares the three flap spectra for the same D_S/D_8 ratio whereas Figure V.E-11 shows variation of D_S/D_8 for each flap configuration. Conical baseline data are also plotted on Figure V.E-10 and maximum suppressed frequency bands can readily be spotted.

Conclusions

- Representative configurations of the secondary reverser/suppressor flap system in the form of F1, F7 and F15 designs have shown to produce sideline PNL suppression up to 8 PNdB at high jet velocity.
- The F7 "wide-diamond" planform produced better suppression than the "triangular" F1 or "narrow-diamond" F15 designs.
- Suppression is strongly influenced by D_S/D_8 ratio, increasing as D_S/D_8 increases. Suppression is generally increased with increase of P_{T8}/P_o at a set T_{T8}, within the test range.

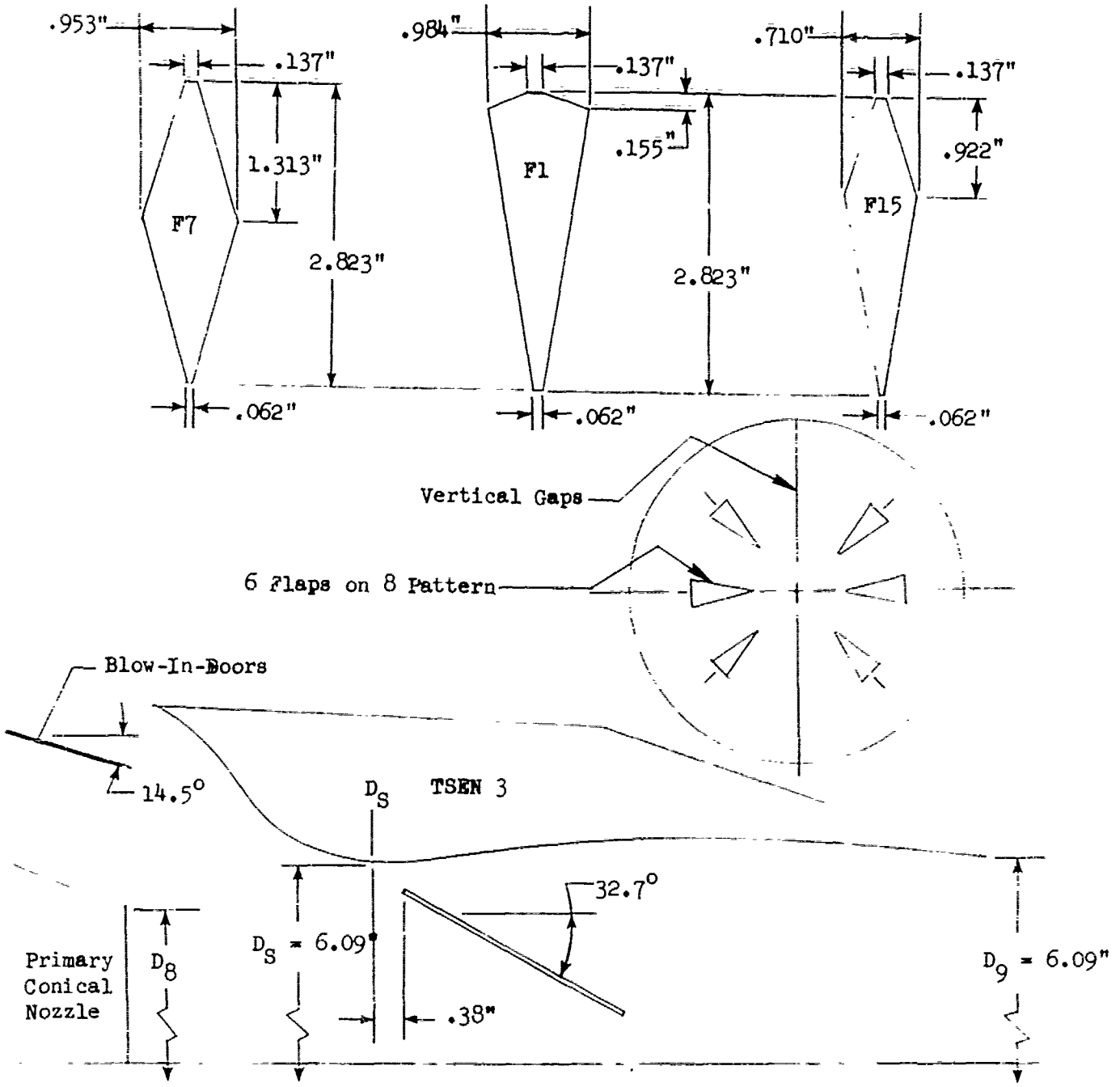

Chute	Planform	D_8	D_S/D_8	% Penet.	*% Blockage
F7	Wide Diamond	4.32	1.41	42	33.1
		4.82	1.26	48	25.5
		5.14	1.18	51	23.5
F1	Triangular	4.32	1.41	42	33.1
		4.82	1.26	48	25.5
		5.14	1.18	51	23.5
F15	Narrow Diamond	4.32	1.41	42	25.1
		4.82	1.26	48	19.3
		5.14	5.14	51	17.8

* % Blockage = Total Chute Projected Area/ A_8

FIGURE V.E-1 SCALE MODEL SECONDARY REVERSER - SUPPRESSOR FLAP CONFIGURATIONS

o Data Includes Ground Reflection Interference

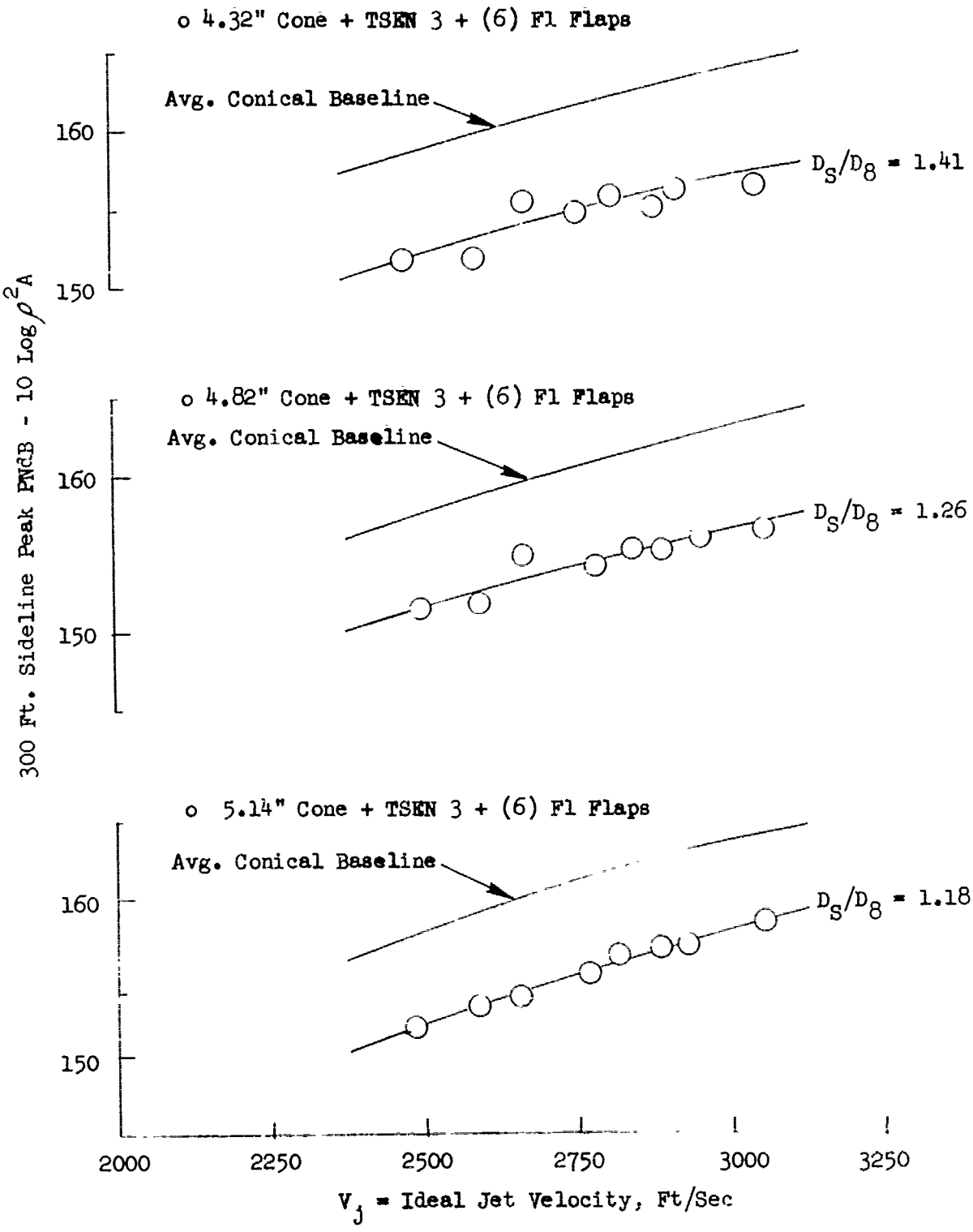

FIGURE V.E-2 300 FT. SIDELINE PEAK PNL LEVELS FOR F1 FLAPS WITH D_S/D_8 = 1.41, 1.26 & 1.18

o Data Includes Ground Reflection Interference

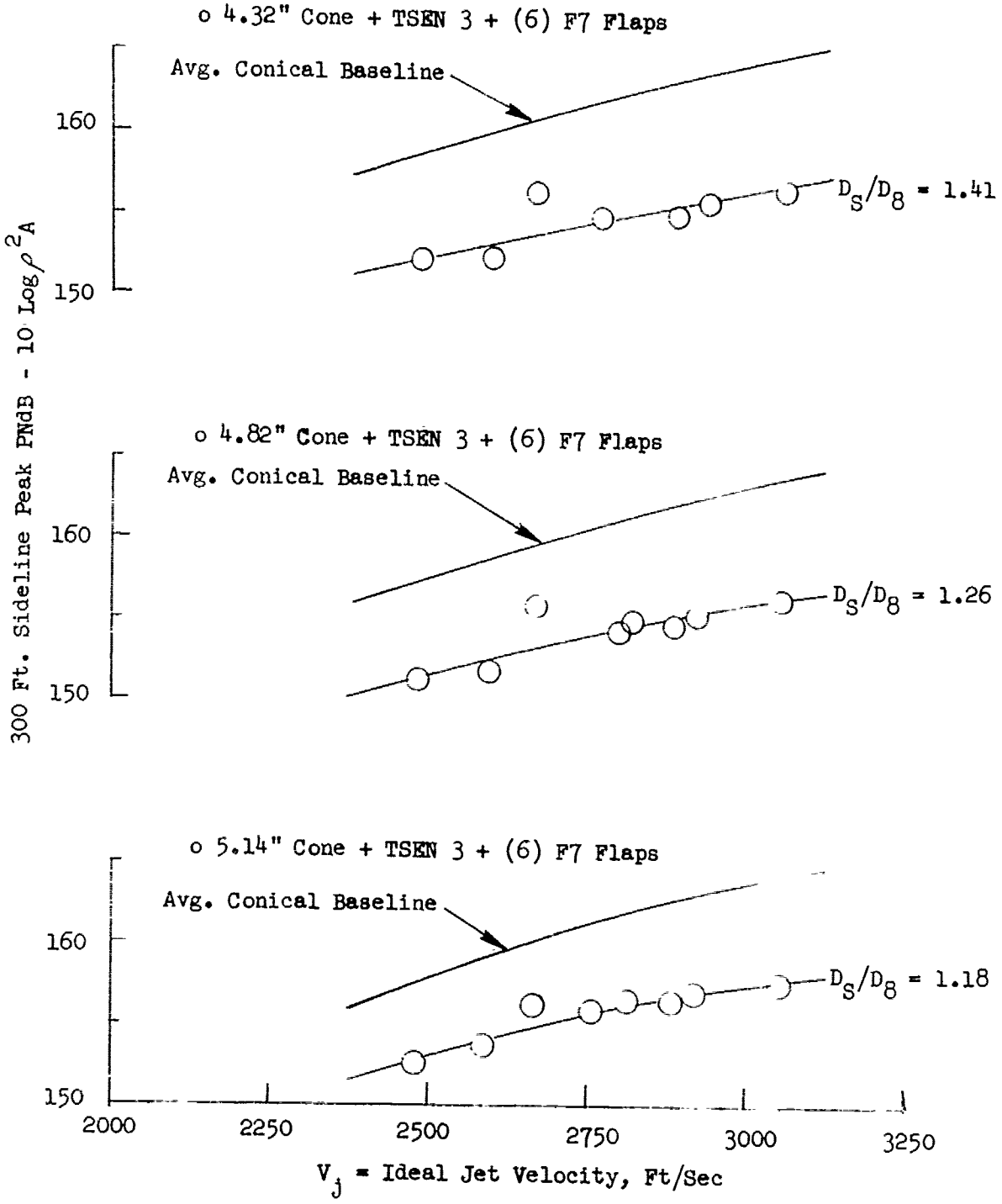

FIGURE V.E-3 300 FT. SIDELINE PEAK PNL LEVELS FOR F7 FLAPS WITH D_S/D_8 = 1.41, 1.26 & 1.18

o Data Includes Ground Reflection Interference

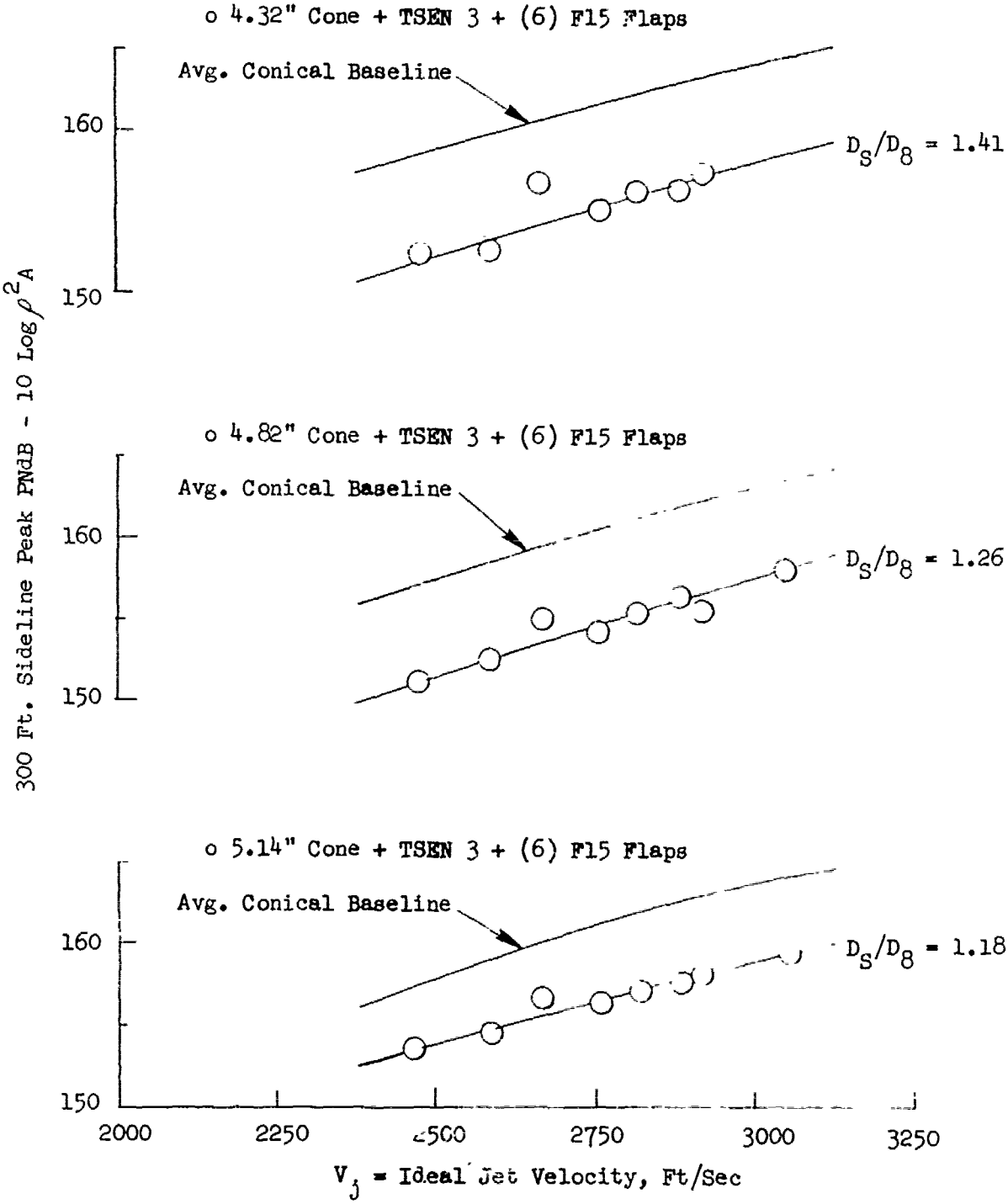

FIGURE V.E-4 300 FT. SIDELINE PEAK PNL LEVELS FOR F15 FLAPS WITH D_S/D_8 = 1.41, 1.26 & 1.18

o Data Includes Ground Reflection Interference

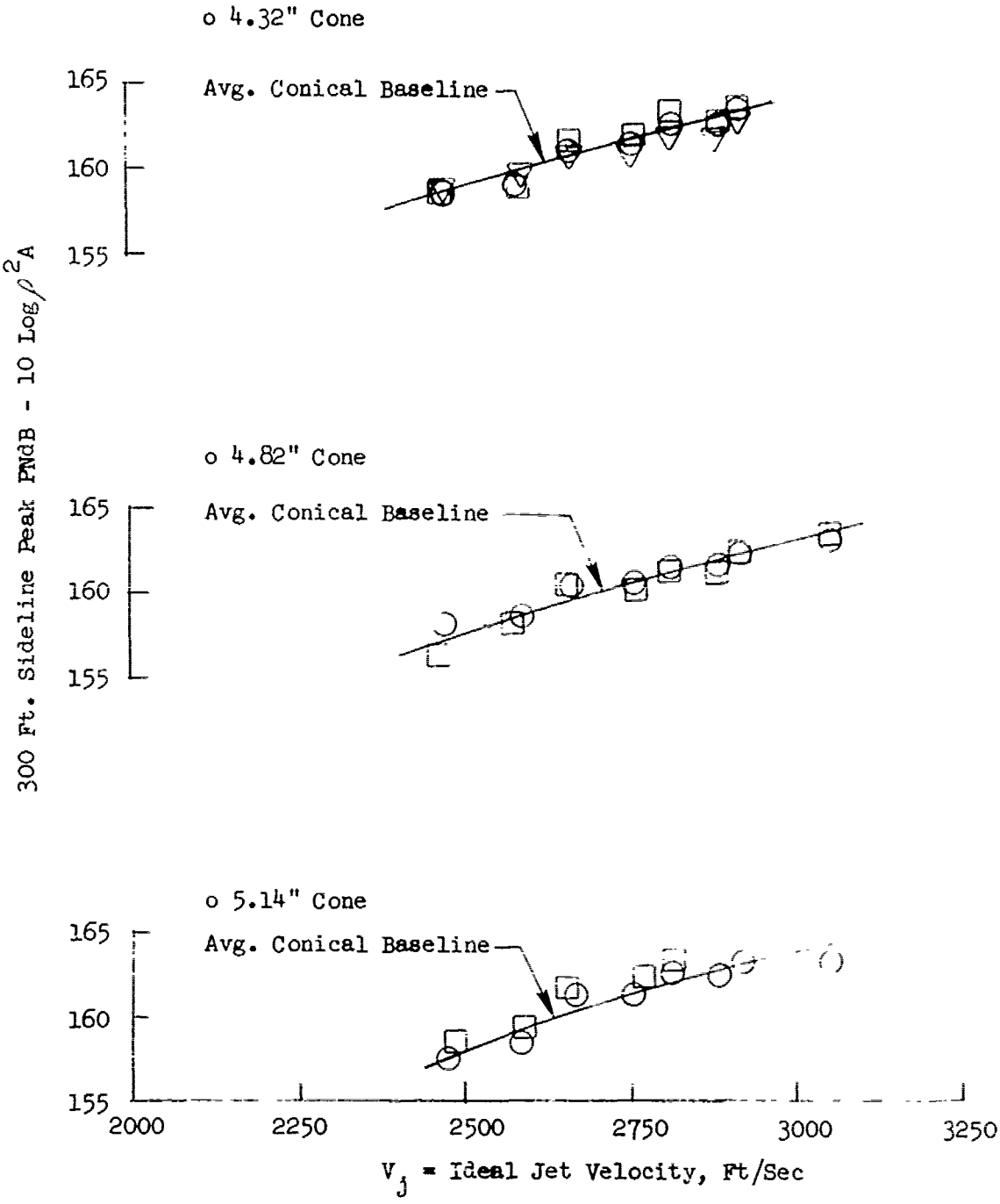

FIGURE V.E-5 300 FT. SIDELINE PEAK PNL LEVELS FOR 4.32", 4.82" & 5.14" D_8 CONES

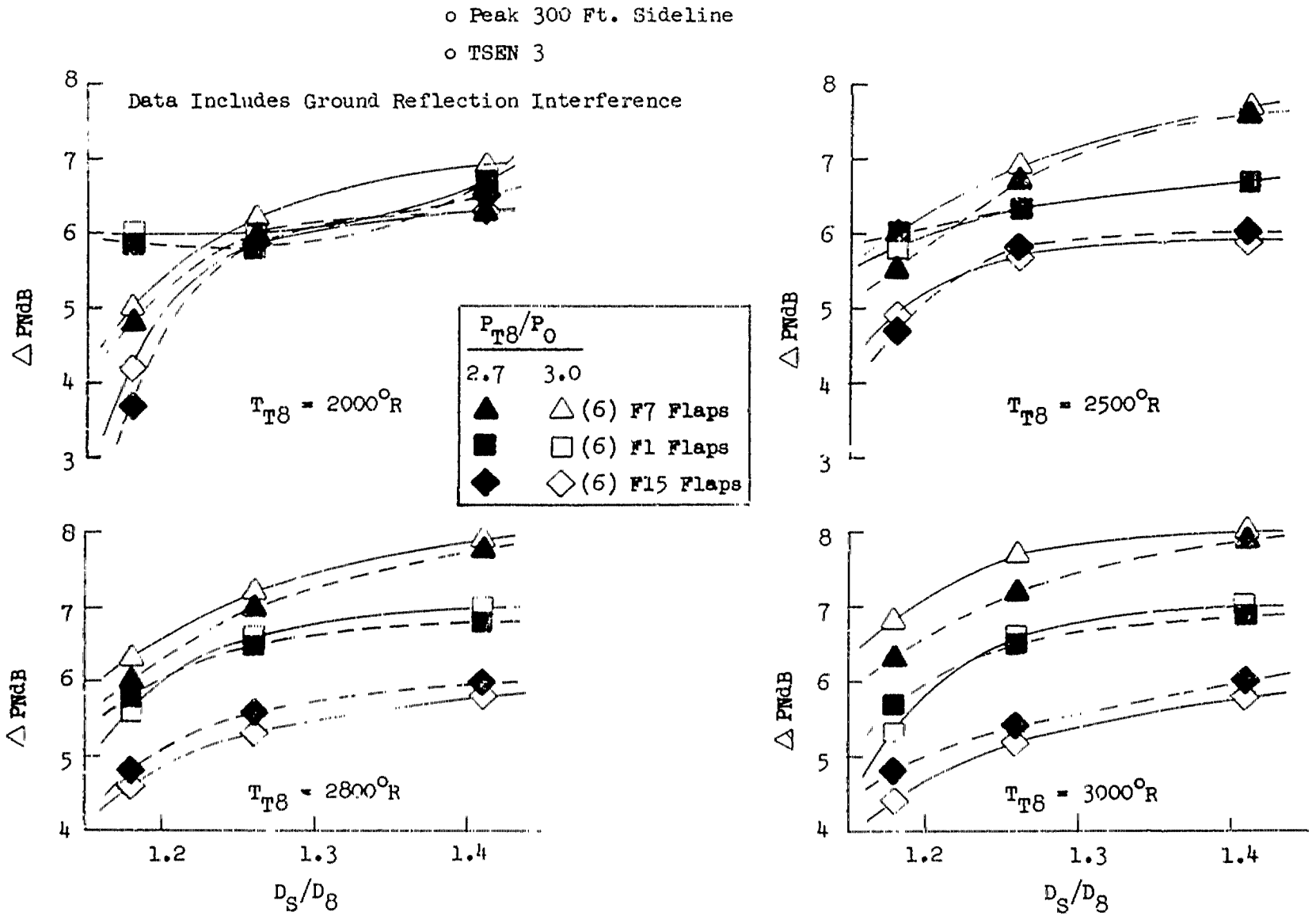

FIGURE V.E-6 EFFECT OF D_S/D_8 ON PNL SUPPRESSION FOR F1, F7 & F15 REVERSER - SUPPRESSOR FLAPS

o 6 on 8 Flap Pattern o TSEN 3 o Peak 300 Ft. Sideline

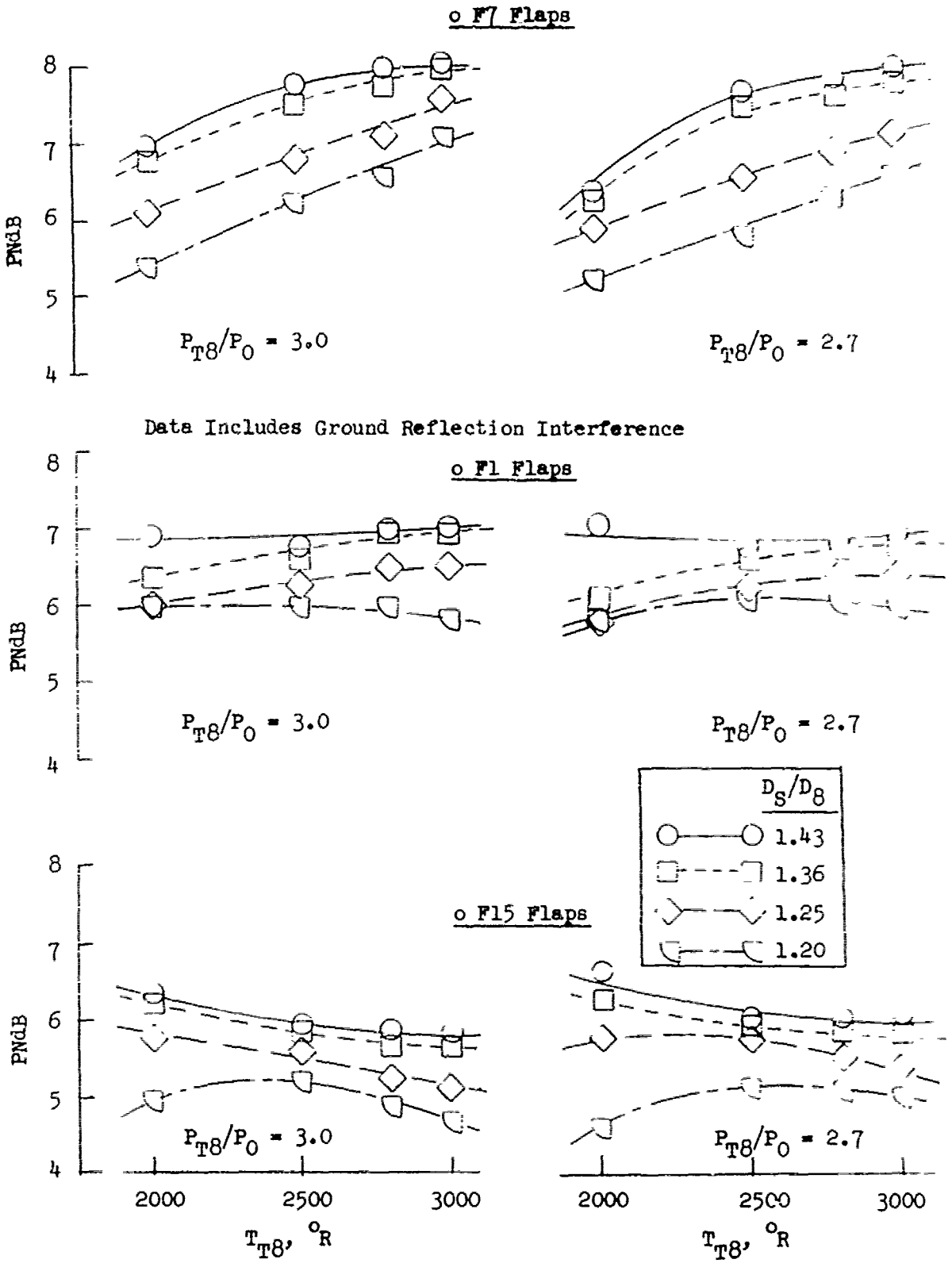

FIGURE V.E-7 EFFECT OF T_{T8} ON PNL SUPPRESSION FOR F1, F7 & F15 REVERSER - SUPPRESSOR FLAPS

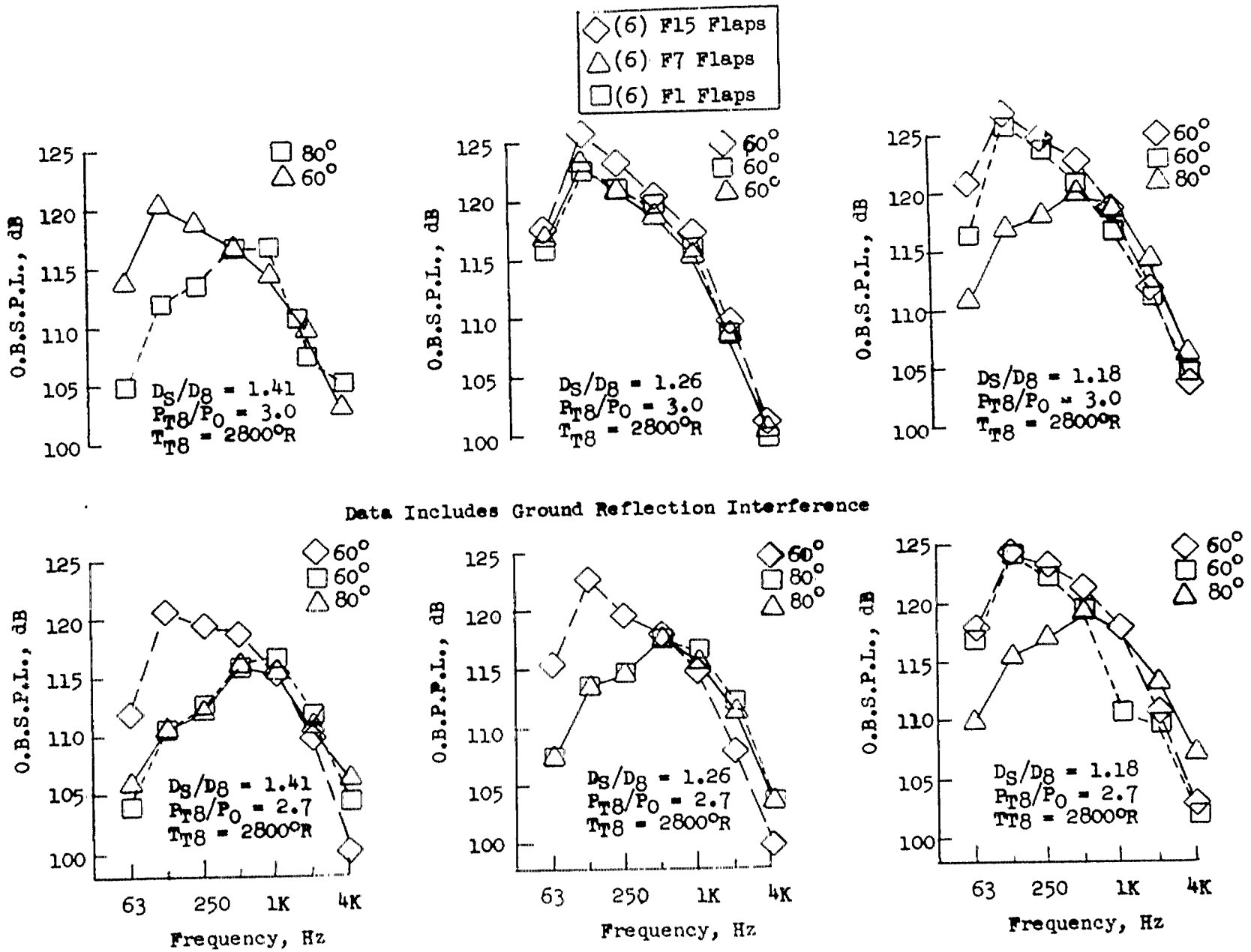

FIGURE V.E-8 EFFECT OF FLAP PLANFORM ON 300 FT. SIDELINE PEAK PNL SPECTRA AT D_S/D_8 = 1.41, 1.26 & 1.18

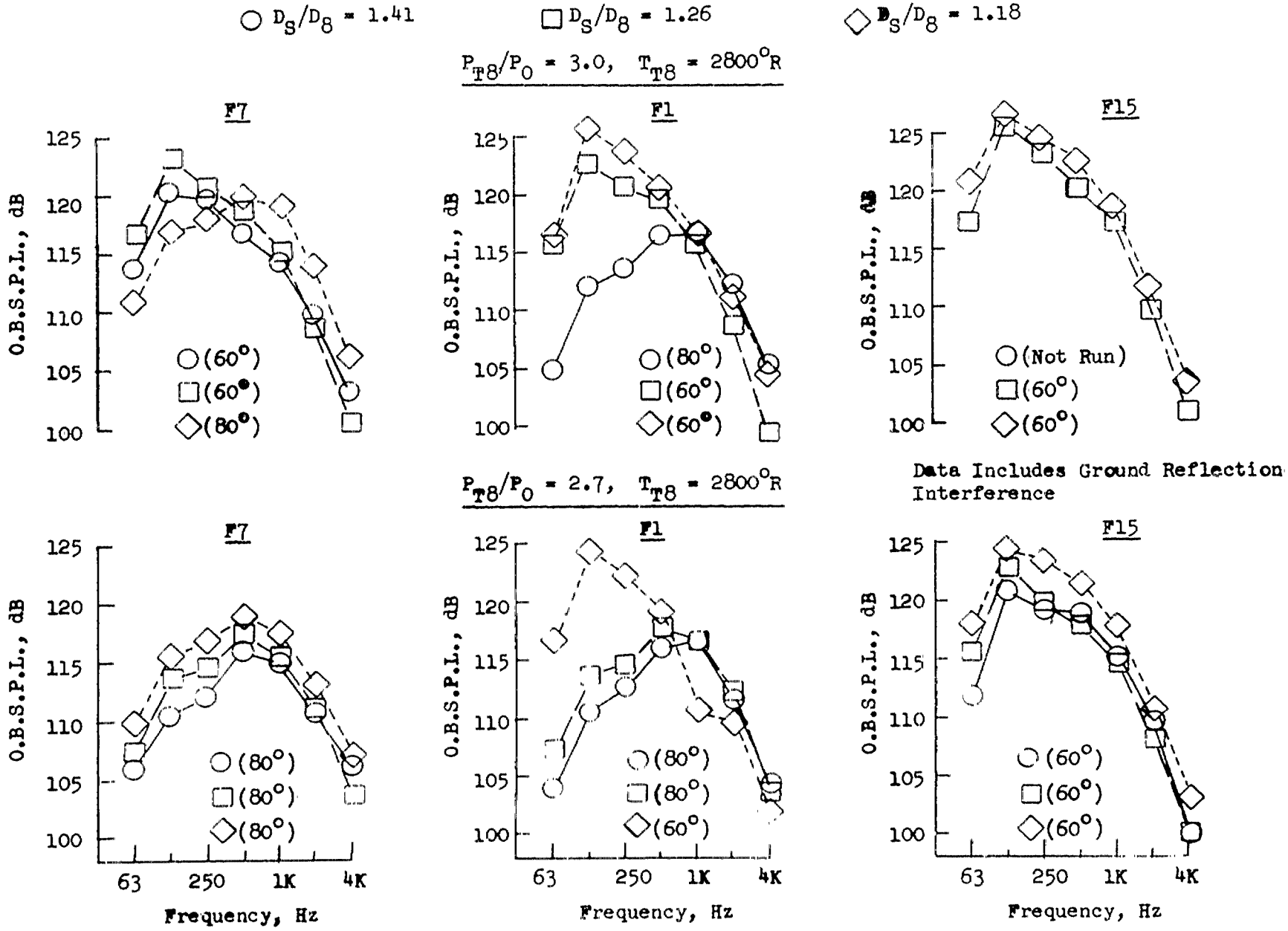

FIGURE V.E-9 EFFECT OF D_S/D_8 ON 300 FT. SIDELINE PEAK PNdB ANGLE SPECTRA FOR F1, F7 & F15 FLAPS

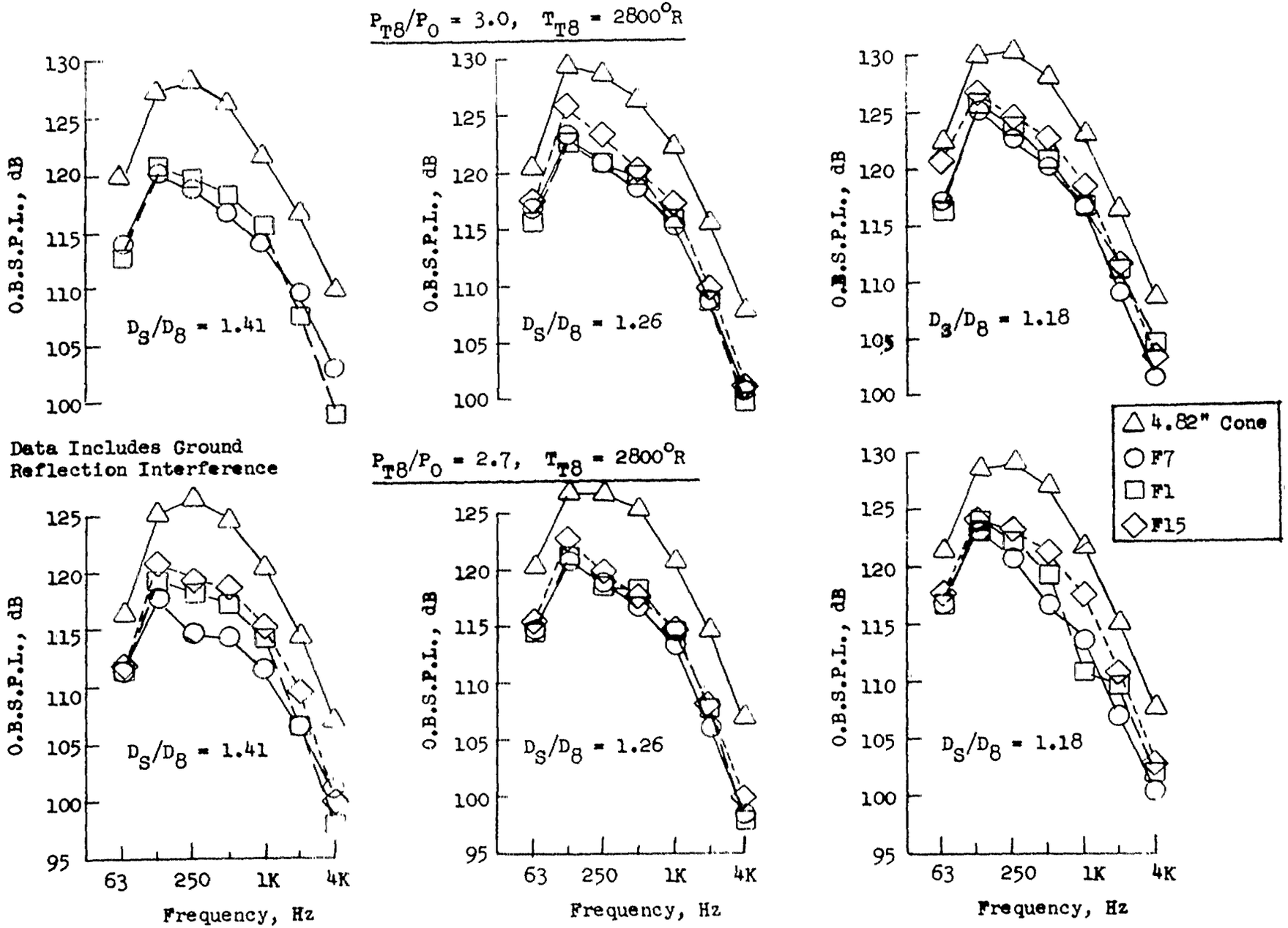

FIGURE V.E-10 EFFECT OF FLAP PLANFORM ON 300 FT. SIDELINE 60° SPECTRA AT D_S/D_8 = 1.41, 1.26 & 1.18

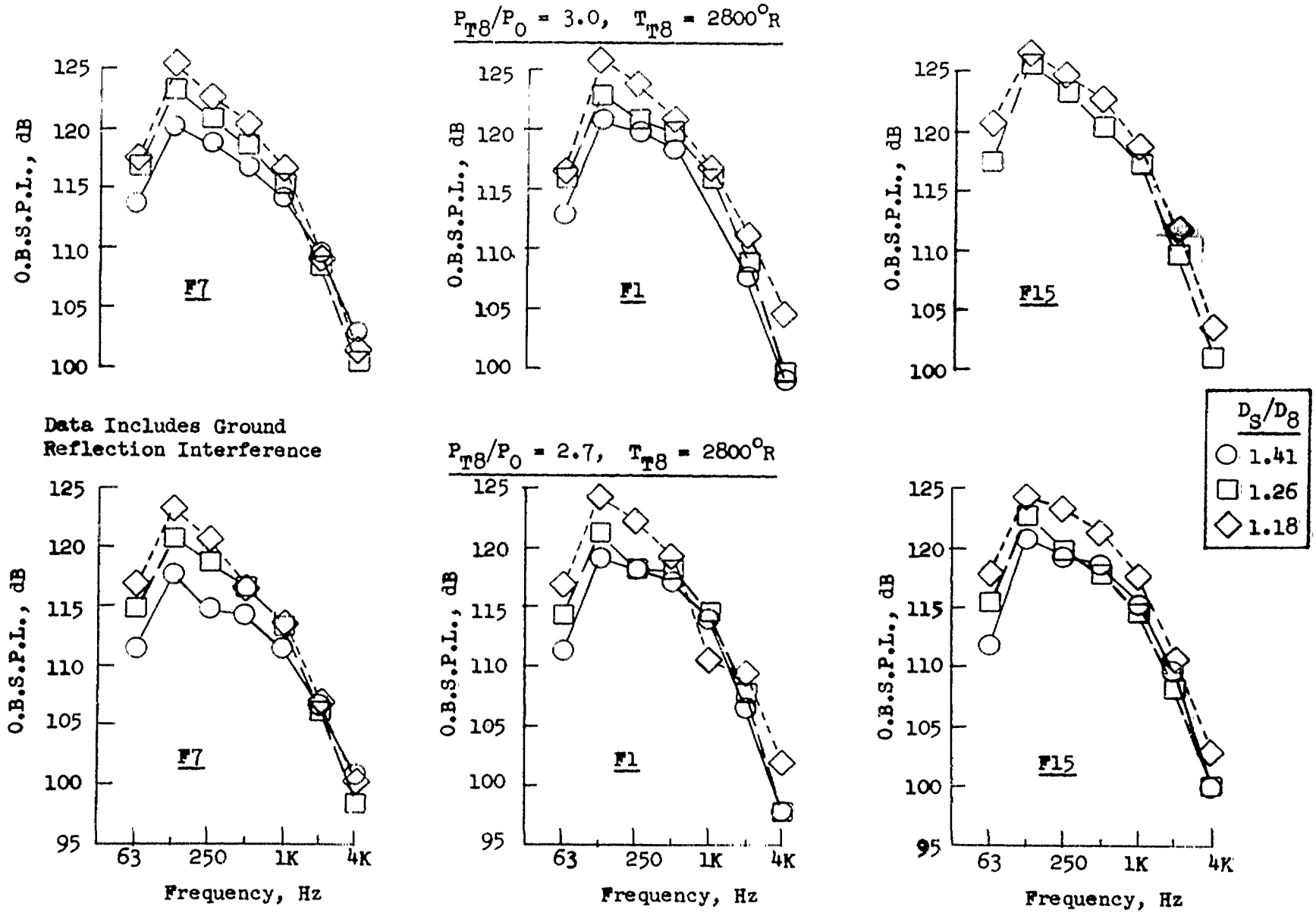

Data Includes Ground Reflection Interference

FIGURE V.E-11 EFFECT OF D_S/D_8 ON 300 FT. SIDELINE 60° SPECTRA FOR F1, F7 & F15 FLAPS

V.F MULIT-TUBE/HOLE SUPPRESSOR MODEL STUDIES

V.F MULTI-TUBE/HOLE SUPPRESSOR MODEL STUDIES

The multi-tube/hole nozzles presented in Sections V.F.1 through V.F.10 comprise the largest category of model suppressor configurations reported on this summary document. These ten sections each document a particular suppressor parametric study or related series of model configurations. The various studies and model configuration series document the chronology of multi-tube suppressor technology development, which is culminated in the multi-tube preliminary design number 3 (PD-3) study of Section V.F.10.

Section V.F.1 presents results of 72 tube/hole nozzle comparisons of a) tube length, b) area ratio, c) secondary ejector, and d) secondary ejector air flow effects on 72 tube/hole nozzles. Another series of tests in Section V.F.2 investigates baseplate and tube exit plane stagger angle variations on 72 tube nozzle suppressors.

Section V.F.3 and V.F.4 document the results of tests on 37 tube nozzles. Section V.F.3 presents results of a high temperature/jet velocity study on 37 tube nozzles, while tube end variations on 37 straight, convergent, Greatrex and canted end tubes are documented in Section V.F.4.

Section V.F.5 presents the results of a parametric study on tube internal and external length to diameter ratio variations on an 85 hole nozzle.

Investigations with 97 hole plates of a) hole shape, and b) equal and unequal hole size and spacing are presented in Section V.F.6.

Sections V.F.7 and V.F.8 document results of tests with 97 tube and 97 hole nozzles, respectively. Variations of a 97 tube primary nozzle with a) large and small center hole, and b) comparisons with hardwall and 7.5% open lined ejectors are presented in Section V.F.7. Results of tests conducted on a 97 hole nozzle with geometric variations of a) center hole shape, b) hardwall versus acoustically lined ejectors, and c) D_S/D_{Td} variations, are documented in Section V.F.8.

Parametric investigations on multi-hole nozzles are documented in Section V.F.9. It includes variations of a) area ratio, b) hole number, c) shroud D_S/D_{Td}, and d) shroud axial spacing, X_S.

PRECEDING PAGE BLANK-NOT FILMED

Section V.F.10 presents the results of the multi-tube preliminary design number 3 (designated, PD-3) study and is the last section in Volume I of this summary report. All acoustic data are presented as applicable to full size engine.

V.F.1 COMPARISON OF TUBE LENGTH, AREA RATIO, SECONDARY EJECTOR AND SECONDARY EJECTOR AIR FLOW EFFECTS ON 72 TUBE/HOLE NOZZLES

V.F.1 COMPARISON OF TUBE LENGTH, AREA RATIO, SECONDARY EJECTOR AND SECONDARY EJECTOR AIR FLOW EFFECTS ON 72 TUBE/HOLE NOZZLES

Objectives of Test Series

This test series was conducted in two phases. The purpose of this test series was to establish multi-tube suppression dependency in Phase I on:

a) Tube external length to internal diameter ratio, L_t/D_t;

b) Area Ratio, defined as the circumscribed tube bundle area/physical flow area, AR_d;

and in Phase II on:

a) Addition of secondary ejector;

b) Secondary ejector pumping variations.

This was an initial test series on early 72 tube and 72 hole nozzle hardware studying a limited range of the variables compared. At later dates, more detailed parametric tests were conducted to study a wider range of the same variables. Section V.F.5 will further treat variation of L_t/D_t and L_{ti}/D_t. Section V.F.9 further studies area ratio variations, addition of a secondary ejector and axial location of secondary ejector for pumping variations, all on 85 hole nozzle hardware.

Specific comparisons within this test series include those for Phase I:

a) 72 tube nozzle at L_t/D_t = 1.69 and 1.74 to 72 hole nozzle at L_t/D_t = 0; each at AR_d = 2.65;

b) 72 hole nozzles at AR_d's of 2.65 and 2.0, each at L_t/D_t = 0;

and for Phase II:

a) 72 tube nozzle at AR_d = 2.65 and L_t/D_t = 1.69, with and without secondary cylindrical ejector;

b) 72 tube nozzle at AR_d = 2.65 and L_t/D_t = 1.69, with secondary cylindrical ejector; secondary air flow passages open and blocked to pumping flow.

PRECEDING PAGE BLANK-NOT FILMED

Acoustic testing was done on the GE, Evendale, JENOTS test facility. Nozzle conditions were representative of a GE4 engine operating line with exhaust cycle ranging over nozzle pressure ratios of 1.4 to 4.0 , exit gas temperatures of 1100 to 2700° R, and ideal jet velocities of 1100 to 3000 ft/sec.

Acoustic measurements were taken on a 40 ft. arc and scaled by frequency and size to full scale application using a scale factor of 8:1. All data presented are, therefore, of simulated engine size and engine frequency range.

Test Configurations

o Phase I

Three model configurations were tested in Phase I investigating external tube length to internal tube diameter ratio (L_t/D_t) and area ratio (AR_d) variations with 72 tube/hole nozzles. They are described as follows:

o Model 4.0T72- was tested under several model numbers, (referred to in this section as Models 4.0T72, 4.0T72-1, 4.0T72-4 and 4.0T72-5) and the data and results are presented in Section V.F.2 (Baseplate and Tube Exit Plane Stagger Angle Variations on 72 Tube Model Suppressors). Within that section the model is shown photographically in Figure V.F.2-1 and schematically in Figure V.F.2-2 as Models 4.0T72-4 and 4.0T72-5. The basic configuration was a 72 tube nozzle with 1.5" long seamless tubes pressed into a flat circular baseplate of 3/4" thickness. Model 4.0T72-4 had 0.444" I.D. tubes and Model 4.0T72-5 had 0.430" I.D. tubes. With the exposed length of 3/4", the L_t/D_t for the two models was 1.69 and 1.74, respectively. The nozzle physical A_8 of 11.15 in^2 has the equivalent flow area of a 3.77" I.D. conical nozzle. The plenum chamber just forward of the tube baseplate had an 8" I.D. for an area ratio of A_8/A_{plenum} = 0.222. Tube inlets were flared to provide a smooth transition for the jet flow. The tube bundle is spaced at an area ratio of 2.65.

  Within Section V.F.2 the test summary and acoustic data plots for Model 4.0T72-4 are presented as Table V.F.2-2 and Figures V.F.2-5 and -6. For Model 4.0T72-5 the summary and plots are Table V.F.2-3 and Figures V.F.2-7 and -8. In addition to this baseplate/tube configuration being

tested as the above two model numbers in 1969, it was also used in 1968 as Model 4.0T72-1. All of the test data have been scaled to full size and are summarized in Section V.F.2 as Figures V.F.2-9 and -10 in which average curves of 300 and 1500 ft sideline peak PNL suppression are derived. These average curves will be presented in this section to compare variation of suppression with L_t/D_t change.

- Model 4.0H72 of Figure V.F.1-1 is a 3/4" thick flat circular baseplate with 72, 0.444" I.D. holes in an area ratio of 2.65 design. It has no external tube length; therefore, $L_t/D_t = 0$.
- Model 4.88H121-72 of Figure V.F.1-2 was a 72 hole baseplate similar to Model 4.0H72 but of area ratio of 2.0. It also had no external tube length; therefore, $L_t/D_t = 0$.
- Phase II

Two further model configurations were tested in Phase II investigating the addition of a cylindrical secondary ejector to the 72 tube primary suppressor and the effect of blocking the secondary air flow passage of any pumped air. They are:

- Model 4.0T72-7.28CS of Figure V.F.1-10 (top); consisting of the same primary tube system of Model 4.0T72 with $L_t/D_t = 1.69$ plus a 7.28" I.D. cylindrical ejector with an effective D_S/D_8 of 1.93 and positioned at $X_S = 1.787$". This model had sleeves over the support rods between the primary and secondary flanges to allow secondary air flow to pump through this inlet passage.
- Model 4.0T72-7.28CS-1 of Figure V.F.1-10 (bottom); identical to Model 4.0T72-7.28CS except the support sleeves were replaced with a solid spacer ring to block the flow of secondary air through the inlet passage.

For acoustic suppression reference, a 4.32" I.D. conical convergent nozzle was tested as the baseline for both phases. In addition, several of the models were tested at the FluiDyne Engineering Corporation for static thrust performance.

Presentation and Discussion of Test Results - Phases I and II

The following tables and figures present the acoustic test summaries and data results for the two test phases.

Model	Table	Figure
4.0T72-4	V.F.2-2	V.F.2-5,-6,-9 and -10
4.0T72-5	V.F.2-3	V.F.2-7,-8,-9 and -10
4.0H72	V.F.1-1	V.F.1-1,-2 and -3
4.88H121-72	V.F.1-2	V.F.1-4,-5 and -6
4.0T72-7.28CS		V.F.1-11
4.0T72-7.28CS-1		V.F.1-11

For a comparative effect of external tube length to internal tube diameter, L_t/D_t, the Model 4.0T72 series is compared to Model 4.0H72 in Figures V.F.1-7. This shows 300 and 1500 ft. sideline full scale peak PNL suppressions, using the average curve from the 4.0T72 series of models (from Figures V.F.2-9 and -10) and the data for Model 4.0H72 (from Figures V.F.1-2 and -3). The curves suggest that decreasing L_t/D_t within the range of 1.69-1.74 to 0 results in a suppression decrease ranging from 2 to 0 PNdB, dependent upon jet velocity. In general, the suppression levels are within 1 PNdB of each other.

The curve also suggests, as is true with most multi-element suppressors, that suppression is somewhat higher at the more distant sideline. This is caused by the characteristic double-hump spectra and high frequency dominance of the multi-element nozzle compared to the low frequency dominated spectra of the conical reference nozzle. High frequencies attenuate at a greater rate than low frequencies due to atmospheric absorption. The high frequency content of the reference conical nozzle, which was not controlling PNL at the 300 ft sideline distance, became even less influencing at the 1500 ft. sideline, leaving the low frequency content to still control PNL. For the multi-element nozzles, high frequency controls PNL at the 300 ft. sideline but becomes less dominant at the 1500 ft. sideline, causing a greater PNL change than that of the reference nozzle.

For comparing the change in area ratio from 2.65 to 2.0, Figure V.F.1-8 shows Model 4.0H72 suppression from Figures V.F.1-2 and -3 and Model 4.0H72 suppression from Figures V.F.1-5 and -6. The peak PNL suppression changes very slightly within this area ratio range but does support results seen in Section V.F.9. This shows increasing area ratio increases suppression at high jet velocity and decreases suppression at low jet velocity. The jet velocity at which crossover occurs depends on the sideline to which the data is extrapolated.

For performance variance with L_t/D_t and area ratio, Figure V.F.1-9 shows static gross thrust coefficient, C_{fg}, as a function of primary nozzle pressure ratio, P_{T8}/P_o. Decreasing the tube length from L_t/D_t of 1.69 to 0 results in approximately 7% C_{fg} decrease at $P_{T8}/P_o = 3.0$, due to the increased base drag. With no external tube length, ventilation of the base area between the holes becomes a problem, lowering the base pressures below ambient and increasing base drag.

Changing area ratio from 2.65 (Model 4.0H72) to 2.0 (Model 4.88H121-72) at $L_t/D_t = 0$ has the same cause and end effect as shortening tube length, (see Figure V.F.1-9). The more compact hole pattern of the smaller area ratio limits the available space between holes through which ambient air can be pumped to ventilate the base area and to prevent base pressures from going below ambient pressure. Therefore, the smaller area ratio has greater base drag and higher thrust loss, by about 2 to 3% C_{fg}, increasing loss with higher pressure ratios.

With the addition of the cylindrical secondary ejector to the 72 tube nozzle (Figure V.F.1-10), acoustic suppression has been shown to decrease (Figure V.F.1-4) below that attained by the primary suppressor alone. Acoustic results are not compatible with the more detailed study of ejector suppression done in Sections V.F.9 and V.F.10 and should not be used in lieu of those studies. The major emphasis of this test is the lack of major change in suppression due to blocking the secondary air passage. As seen in Figure V.F.1-11, suppression was decreased only at intermediate and low jet velocity and then by 1 to 2 PNdB. Suppression attained at high jet velocity was unchanged.

Aerodynamically, the open secondary air passage model was tested at FluiDyne and results are compared to the primary alone in Figure V.F.1-12. An increase in static performance of near 5% C_{fg} at $3.0 \leq P_{T8}/P_o \leq 3.5$ is seen due to the ejector action.

Conclusions

- Decreasing L_t/D_t within the test range of 1.7 to 0 results in about 1 PNdB less suppression at the 300 and 1500 ft. sidelines and an additional loss of about 7% C_{fg} at $P_{T8}/P_o = 3.0$.
- Multi-tube suppression is slightly greater at 1500 ft. sideline than at 300 ft. sideline.
- Lowering area ratio from 2.65 to 2.0 decreases suppression slightly at high jet velocity and increases suppression slightly at low jet velocity, in line with results of Section V.F.9. Aerodynamically, the higher area ratio has better performance by 2 to 3% C_{fg}, dependent on P_{T8}/P_o.
- Adding the cylindrical ejector indicates a loss of suppression; however, a more reliable acoustic study is reported on in Sections V.F.9 and V.F.10. Ejector action increased static aerodynamic performance by about 5% C_{fg} at high P_{T8}/P_o.
- Depriving the ejector of secondary air flow lowered PNL suppression by 1 to 2 PNdB, but only at low and intermediate jet velocities.

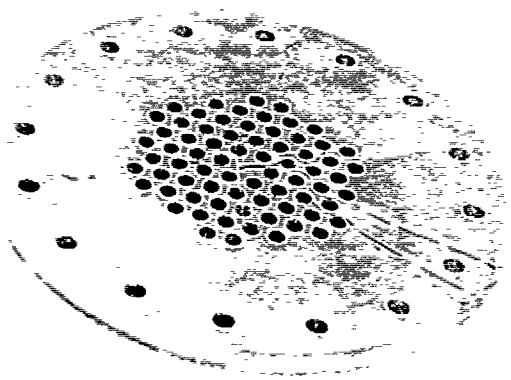

Model 4.0-H-72

Model 4.0-H-72 was a 72 Hole Flat Baseplate with .444" I.D. Holes. Plate Thickness was .75". $L_t/D_t = 0$, $AR_d = 2.65$, Scale Model $A_8 = 0.774\ ft^2$, Full Scale $A_8 = 4.9536\ ft^2$ Scale Factor = 8:1

TABLE V.F.1-1 TEST SUMMARY

MODEL NO. 4.0 H 72

DESCRIPTION: 72 Hole Plate with .444" ID Holes, $AR_d = 2.65$

DATE: 8/19/68

SCALE MODEL $A_8 = .0774\ ft^2$

FULL SCALE $A_8 = 4.9536\ ft^2$

SCALE FACTOR = 8:1

- DATA INCLUDES GROUND REFLECTION INTERFERENCE
- ANGLE REFERENCED TO JET EXHAUST

RDG NO.	TEST CONDITIONS				ACOUSTIC TEST RESULTS						
						320' ARC		300' SIDELINE		1500' SIDELINE	
	P_{TS}/P_o	T_{TS} (°R)	IDEAL V_j (ft/sec)	W_8 (FPS)	10 log ρA	PEAK PNdB	PEAK ANGLE	PEAK PNdB	PEAK ANGLE	PEAK PNdB	PEAK ANGLE
1	2.44	1670	2150	4.16	-8.28	126.7	50	124.3	50	106.0	50
2	2.00	2300	2251	2.64	-10.04	125.7	40	123.3	70	105.1	70
3	2.50	2310	2257	3.64	-9.64	127.7	50	125.3	50	107.4	50
4	2.49	1960	2352	3.99	-8.94	127.5	50	125.0	50	106.9	50
5	2.50	1480	2047	4.50	-7.71	124.4	40	126.9	70	103.7	70
6	2.99	1480	2216	5.51	-7.28	126.7	50	124.3	50	106.2	50
7	3.00	1980	2567	4.57	-8.53	128.9	50	126.6	50	109.4	50
8	2.99	2310	2768	3.74	-9.21	130.1	50	127.8	50	111.0	50
9	3.84	2300	3021	4.84	-8.49	131.7	50	129.4	50	112.9	50/60
10	3.35	2680	3115	4.38	-9.55	132.5	50	130.2	50	114.6	50
11	3.35	2420	2954	4.47	-9.11	132.1	50	129.8	50	114.1	50
12	3.34	2300	2883	4.61	-8.89	131.3	50	129.0	50	112.7	50
13	1.99	1940	2057	3.10	-9.31	123.7	50	122.0	70	103.7	70
14	1.99	1490	1805	3.51	-8.16	121.8	50	119.3	50	100.7	50
15	1.62	1320	1437	3.15	-7.81	115.9	40	94.3	70	95.9	70

FIGURE V.F.1-1 72 HOLE PLATE HARDWARE, DESCRIPTION AND TEST SUMMARY

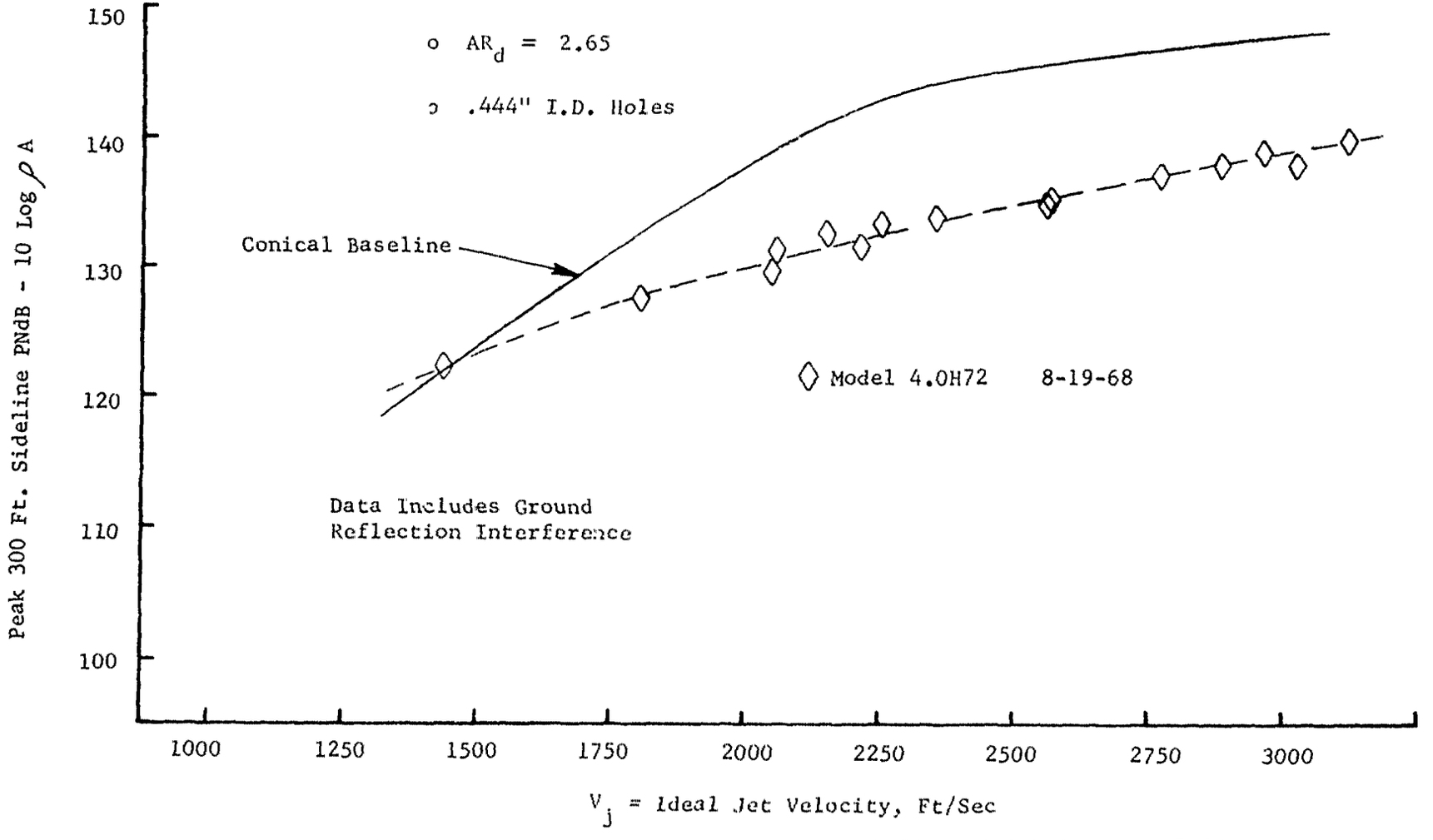

FIGURE V.F.1-2 300 FT. SIDELINE JET NOISE LEVELS FOR A 72 HOLE PLATE, AR_d = 2.65

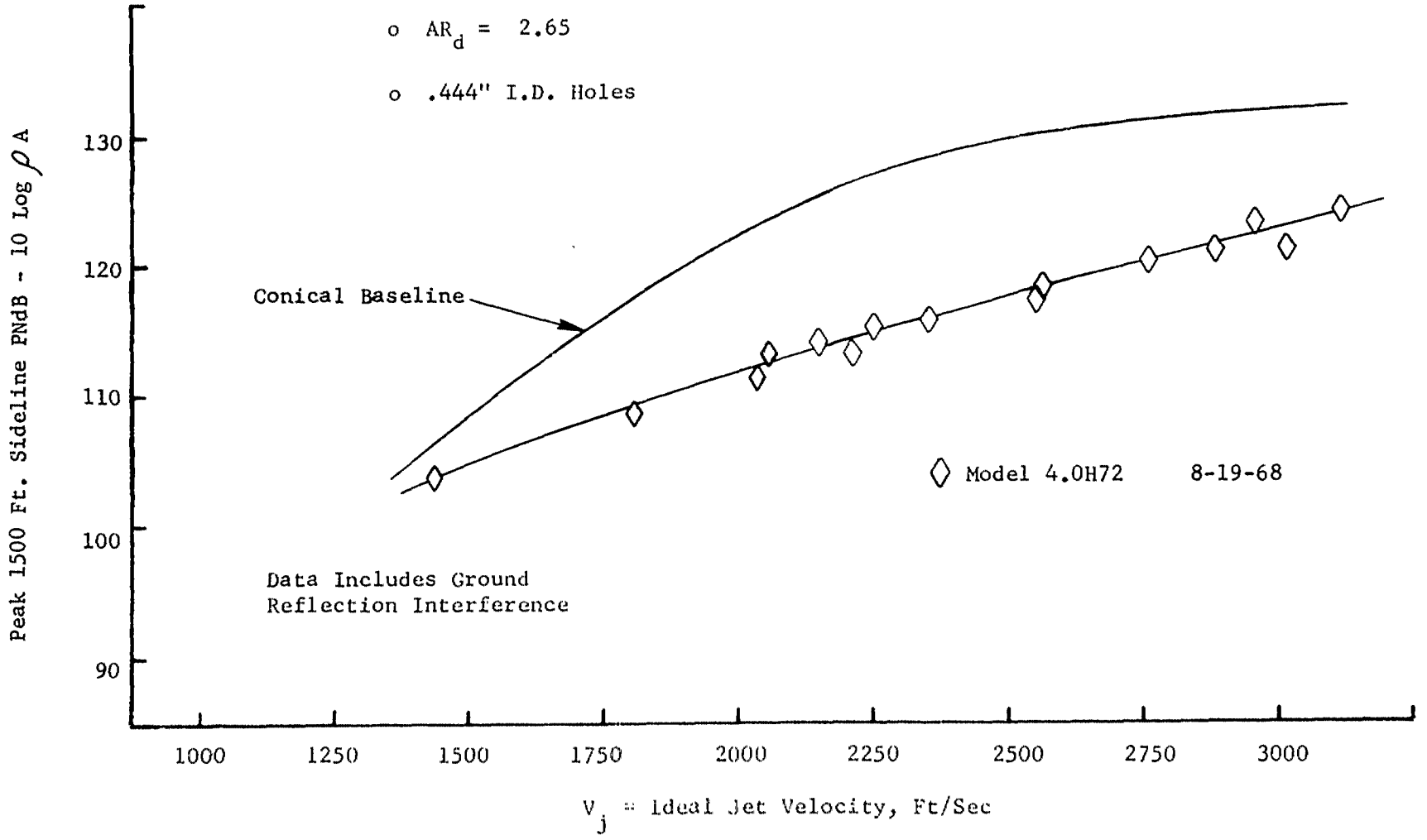

FIGURE V.F.1-3 1500 FT. SIDELINE JET NOISE LEVELS FOR A 72 HOLE PLATE, AR_d = 2.65

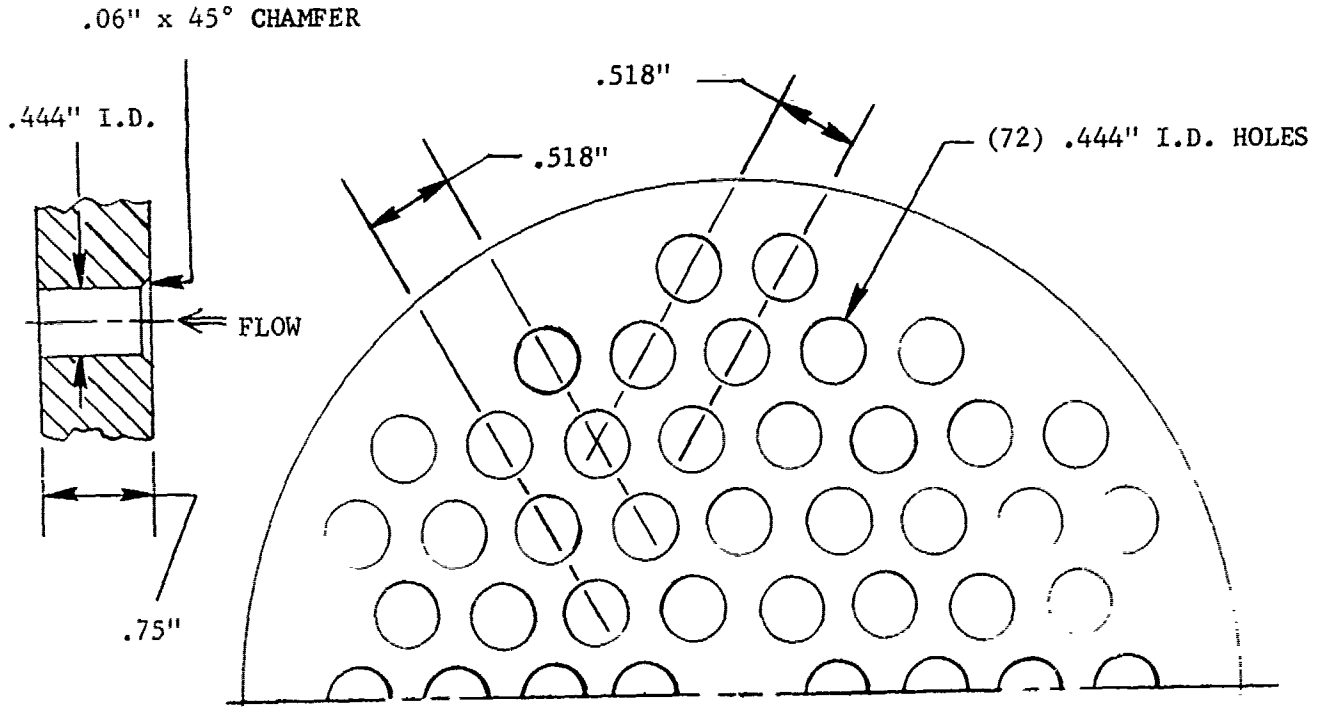

TABLE V.F.1-2 TEST SUMMARY

MODEL NO. 4.88-H-121-72
DESCRIPTION: 72 Hole Plate, .444" I.D. Holes, AR_d = 2.0
DATE: 8/21/68

SCALE MODEL A_8 = .0774 ft^2
FULL SCALE A_8 = 4.954 ft^2
SCALE FACTOR = 8:1

- DATA INCLUDES GROUND REFLECTION INTERFERENCE
- ANGLE REFERENCED TO JET EXHAUST

	TEST CONDITIONS				ACOUSTIC TEST RESULTS						
			IDEAL			320' ARC		300' SIDELINE		1500' SIDELINE	
EDG NO.	P_{T8}/P_o	T_{T8} (°R)	V_j (ft/sec)	W_8 (PPS)	10 log ρA	PEAK PNdB	PEAK ANGLE	PEAK PNdB	PEAK ANGLE	PEAK PNdB	PEAK ANGLE
1	1.63	1350	1463	3.22	-7.9	115.8	50	113.9	60/70	95.6	70
2	1.99	1540	1839	3.68	-8.3	120.9	40	118.9	60/70	100.8	70
3	2.00	1955	2073	3.21	-9.3	124.1	50	121.9	50	103.7	50
4	2.00	2300	2249	2.82	-10.0	124.3	50	121.9	50	104.2	50
5	2.46	1720	2188	4.24	-8.4	124.7	40	122.5	70	105.0	50
6	2.50	2295	2547	3.51	-9.6	128.9	50	126.6	50	111.0	50
7	2.50	1970	2364	4.02	-8.9	126.9	40	124.3	50	108.0	50
8	2.51	1480	2051	4.73	-7.7	124.3	50	122.0	50	104.2	50
9	2.98	1500	2230	5.58	-7.3	124.9	40	122.3	50	105.1	50
10	2.99	1960	2550	4.80	-8.5	128.2	40	123.8	40	108.0	40
11	2.98	2295	2757	4.29	-9.2	126.2	60	127.0	50	111.6	50
12	3.19	2395	2893	4.56	-9.0	131.0	50	128.9	50	113.4	50
13	3.20	2450	2927	4.28	-9.3	132.0	50	129.7	50	113.9	50
14	3.20	2650	3044	4.18	-9.6	132.5	50	130.4	50	114.8	50
15	4.01	2295	3059	5.10	-8.3	137.6	50	135.3	50	119.4	50

FIGURE V.F.1-4 SCHEMATIC OF 72 HOLE PLATE AND TEST SUMMARY

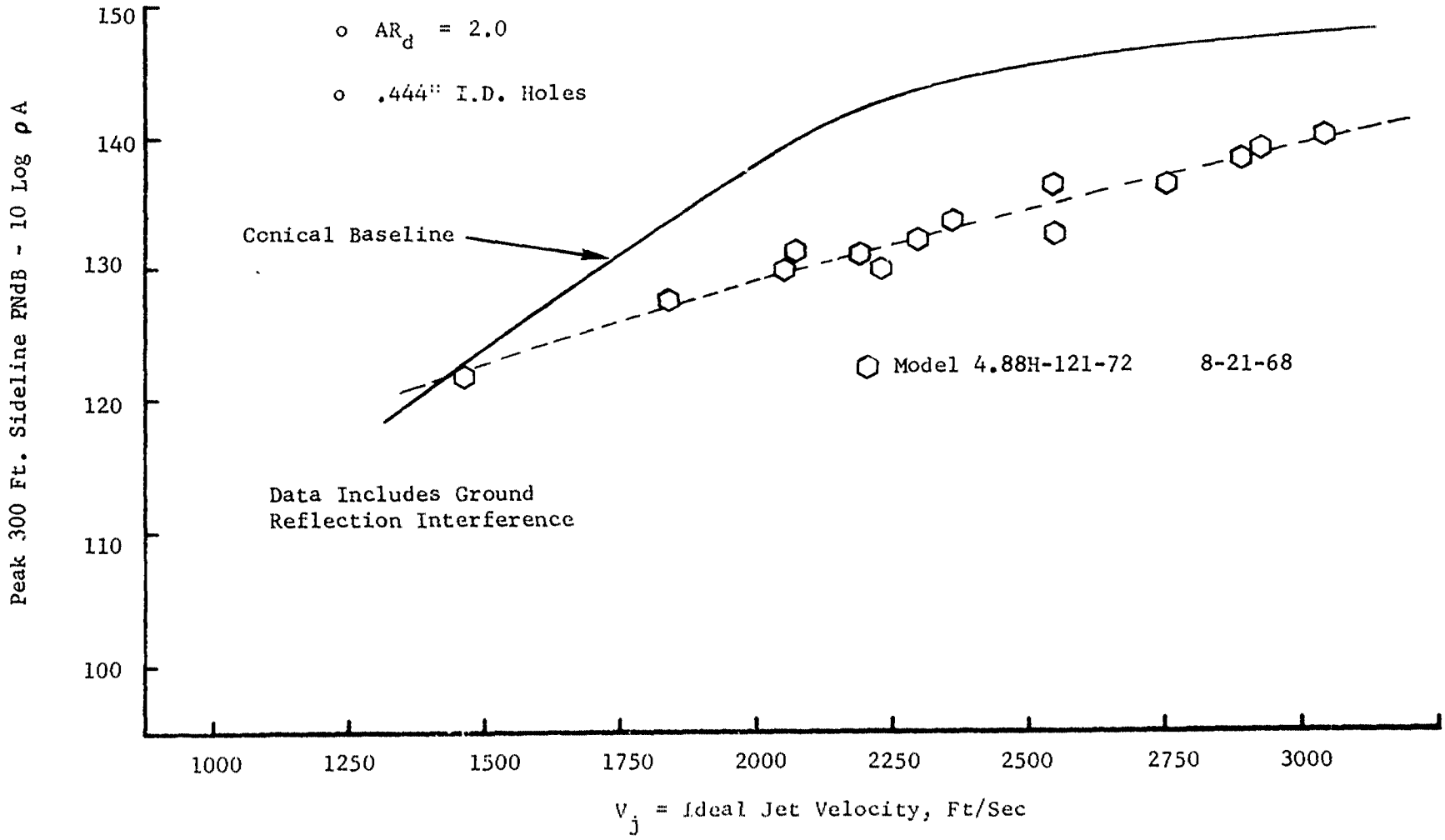

FIGURE V.F.1-5 300 FT. SIDELINE JET NOISE LEVELS FOR A 72 HOLE PLATE, AR_d = 2.0

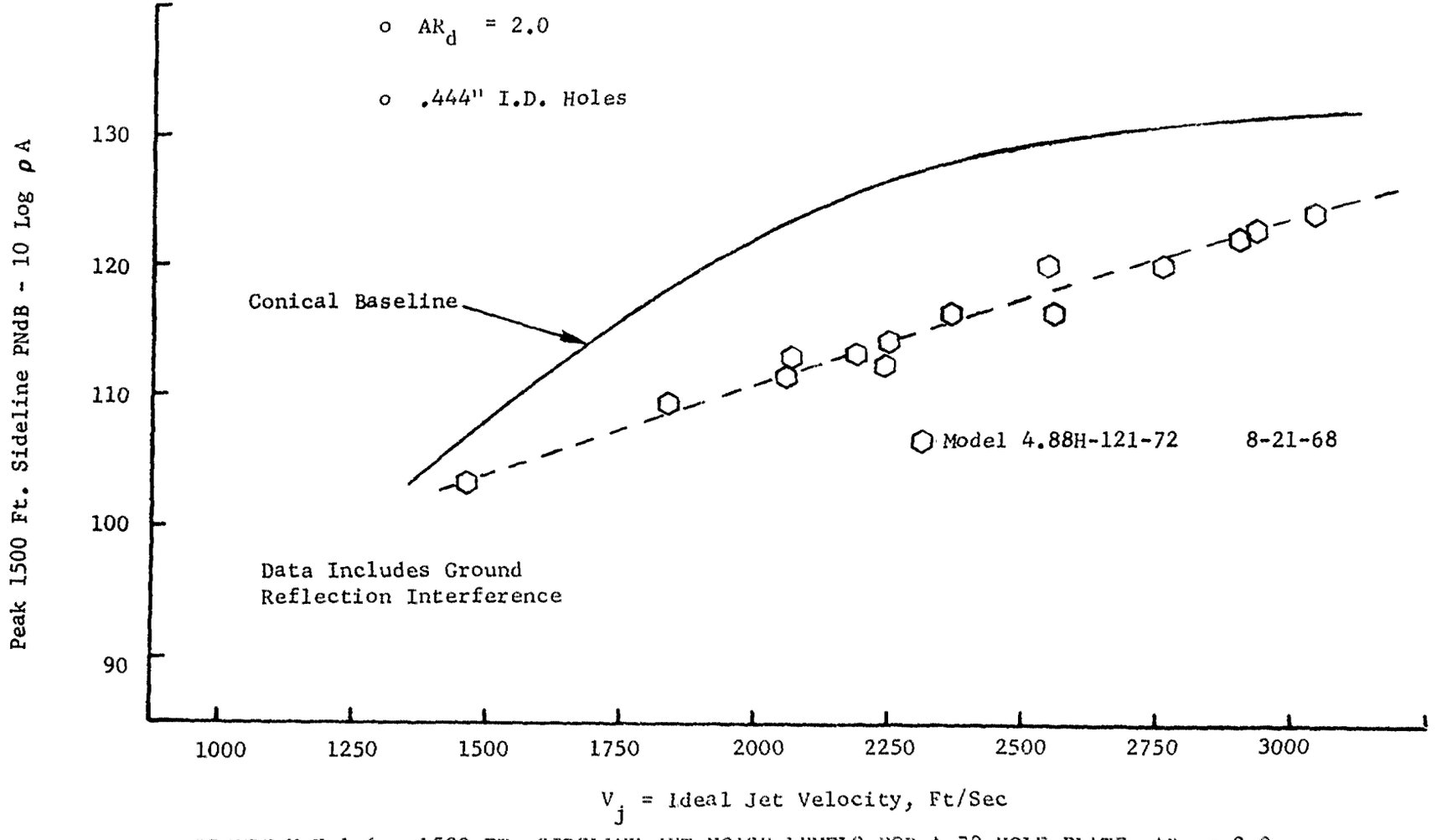

FIGURE V.F.1-6 1500 FT. SIDELINE JET NOISE LEVELS FOR A 72 HOLE PLATE, AR_d = 2.0

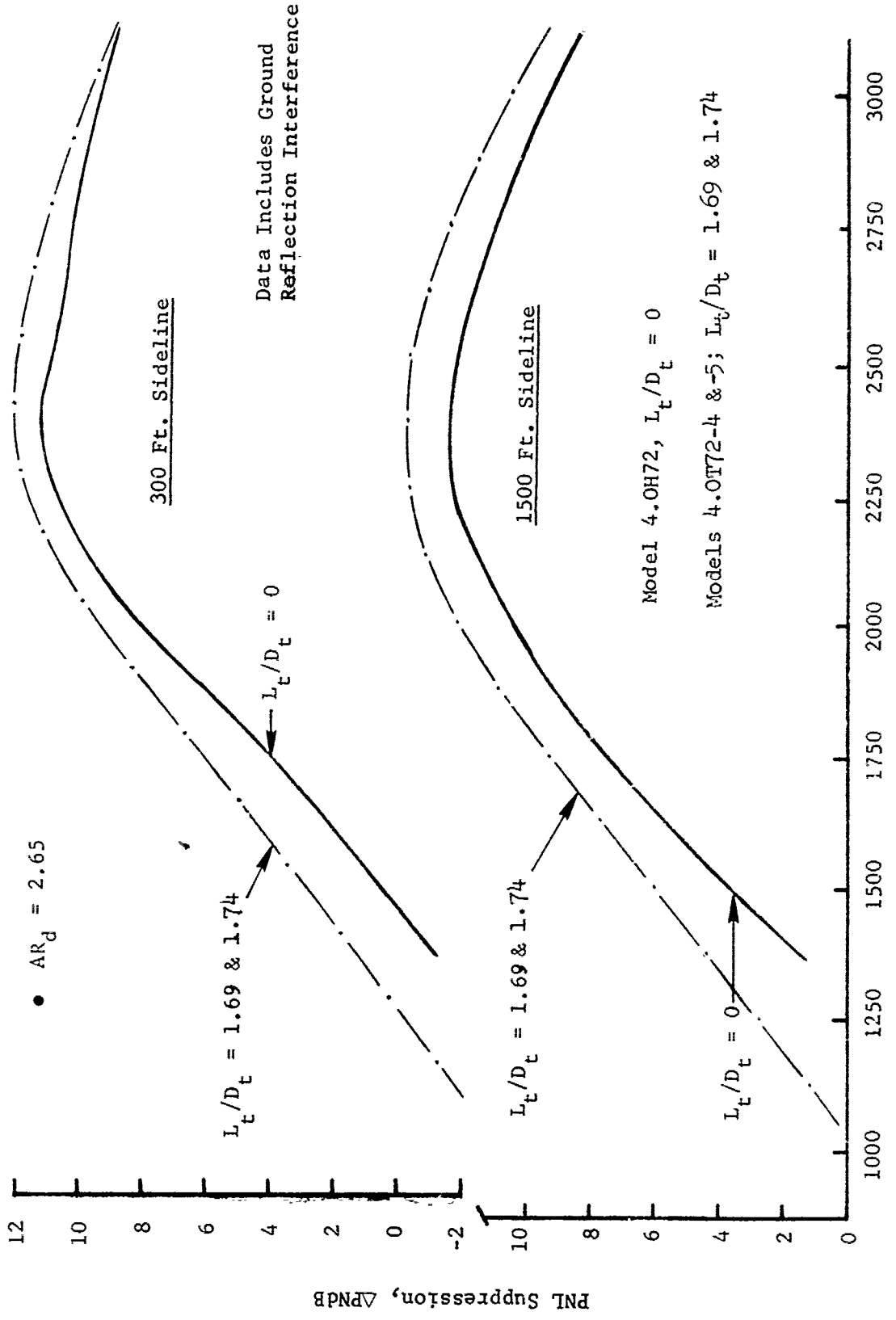

FIGURE V.F.1-7 EFFECT OF EXTERNAL TUBE LENGTH TO TUBE INTERNAL DIAMETER ON 300 FT. AND 1500 FT. SIDELINE PNL SUPPRESSIONS FOR 72 TUBE/HOLE NOZZLES

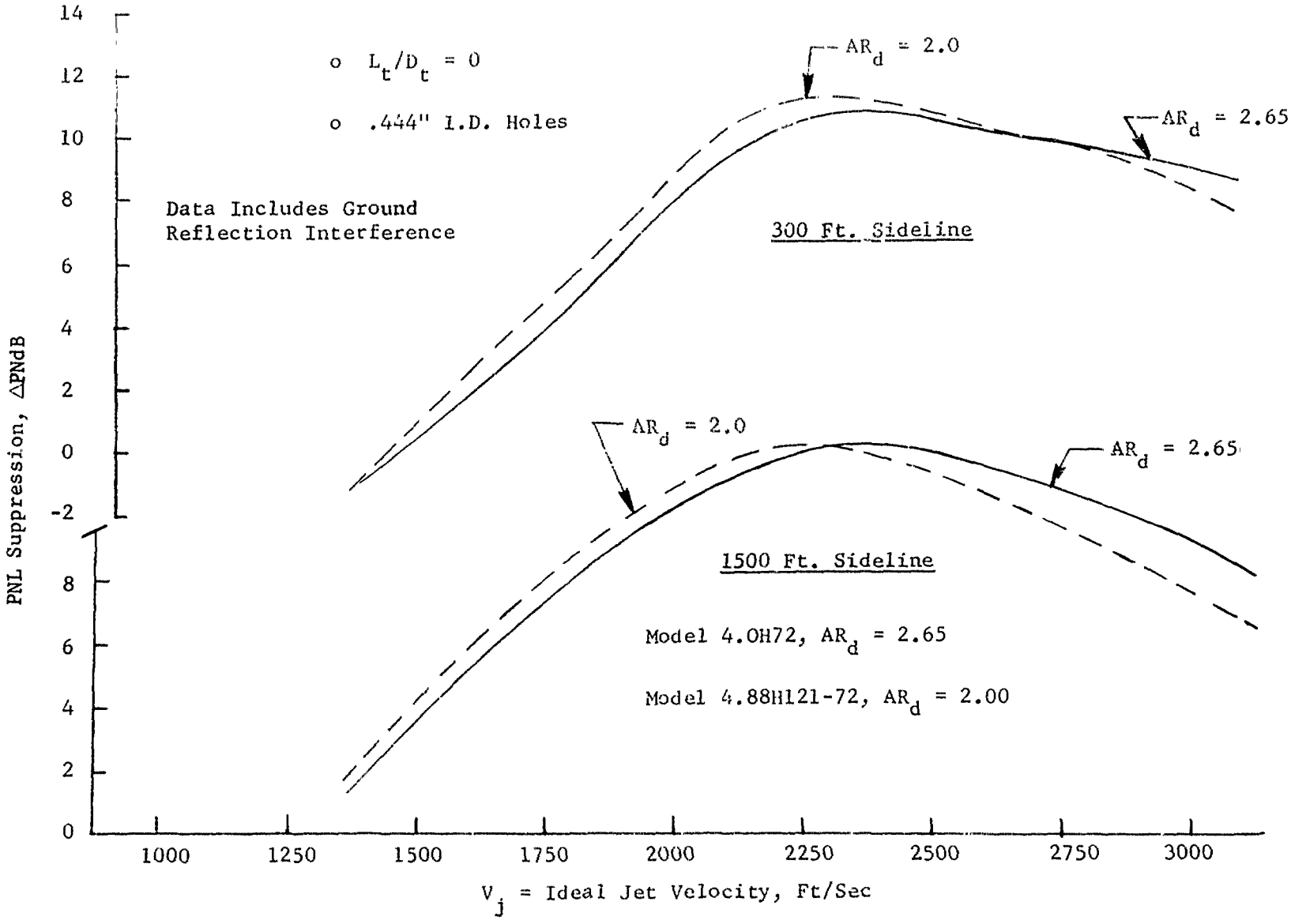

FIGURE V.F.1-8 EFFECT OF AREA RATIO ON 300 FT. AND 1500 FT. SIDELINE PNL SUPPRESSIONS FOR 72 HOLE PLATES

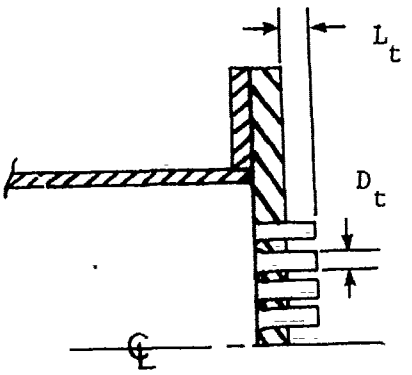

○ Model 4.0T72, 72 Tube, AR_d = 2.65, L_t/D_t = 1.69
□ Model 4.0H72, 72 Hole, AR_d = 2.65, L_t/D_t = 0
△ Model 4.88H121-72, 72 Hole, AR_d = 2.0, L_t/D_t = 0

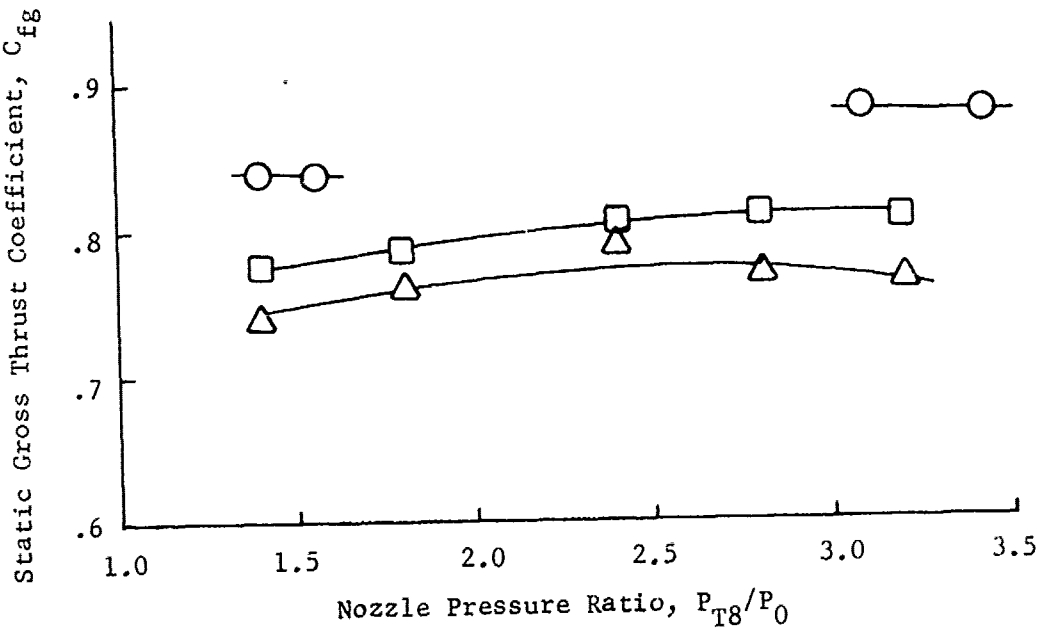

FIGURE V.F.1-9 EFFECT OF AREA RATIO AND TUBE LENGTH ON AERODYNAMIC PERFORMANCE FOR 72 TUBE/HOLE NOZZLES

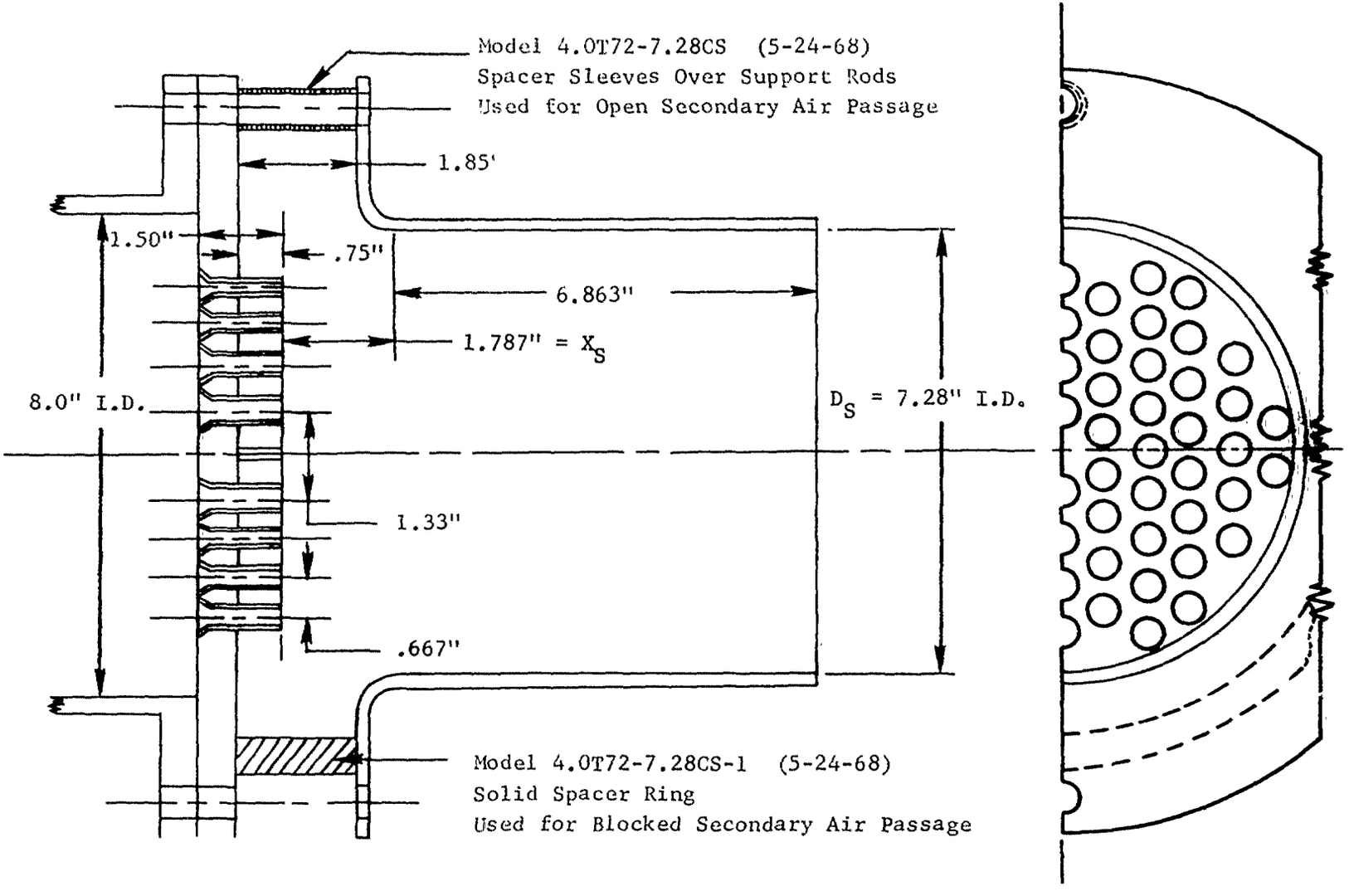

FIGURE V.F.1-10 SCHEMATIC OF 72 TUBE PRIMARY NOZZLE PLUS CYLINDRICAL EJECTOR (SHROUD) CONFIGURATIONS USED WITH AND WITHOUT SECONDARY FLOW

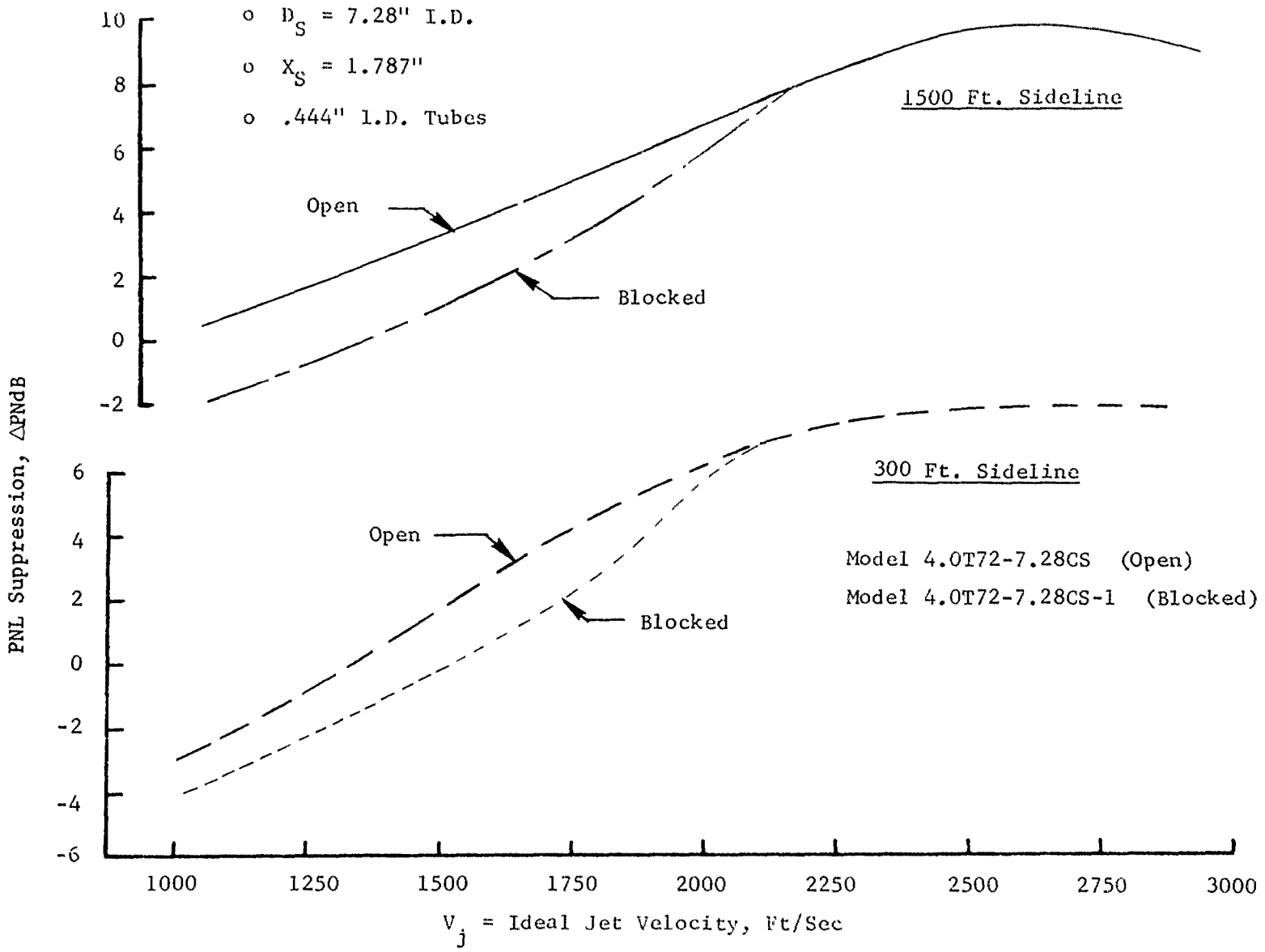

FIGURE V.F.1-11 EFFECT OF OPEN AND BLOCKED SECONDARY AIR PASSAGES ON 300 FT. AND 1500 FT. SIDELINE PNL SUPPRESSIONS FOR A 72 TUBE PRIMARY NOZZLE WITH CYLINDRICAL EJECTOR

- $AR_d = 2.65$
- $D_S/D_{Td} = 1.12$
- $L_t/D_t = 1.69$

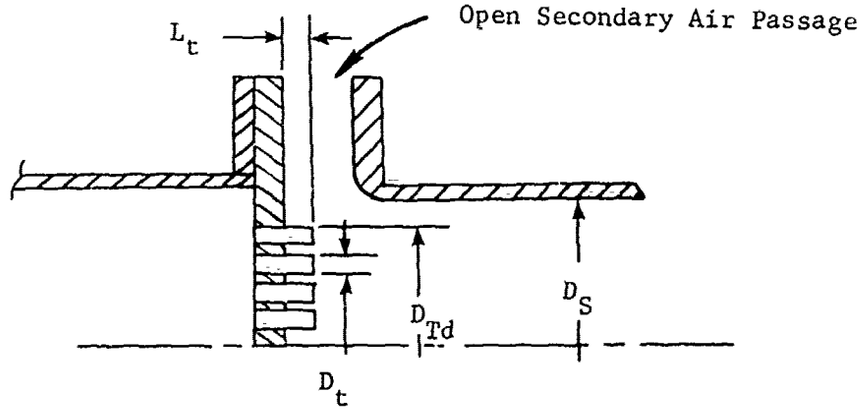

○ Model 4.0T72, 72 Tube Primary

● Model 4.0T72-7.28CS, 72 Tube Primary Plus Ejector

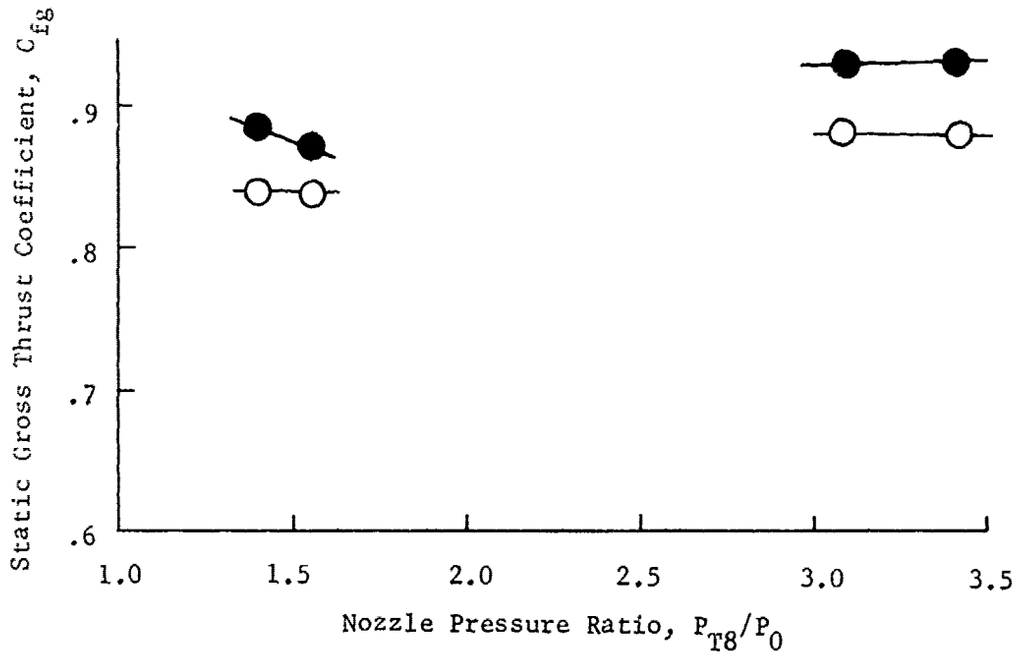

FIGURE V.F.1-12 EFFECT OF SECONDARY CYLINDRICAL EJECTOR ON AERODYNAMIC PERFORMANCE FOR A 72 TUBE NOZZLE

V.F.2 BASEPLATE AND TUBE EXIT PLANE STAGGER ANGLE VARIATIONS ON 72 TUBE MODEL SUPPRESSORS

V.F.2. BASEPLATE AND TUBE EXIT STAGGER ANGLE VARIATIONS ON 72 TUBE MODEL SUPPRESSORS

Objectives of Test Series

The purpose of this test series was to establish the dependency of acoustic suppression and aerodynamic performance on:

- o Tube bundle baseplate cant (stagger) angle.
- o Tube bundle exit plane cant (stagger) angle.

Initial tests with several 37 tube nozzles had indicated that suppression and aerodynamic performance levels varied somewhat by changing tube exit plane angle and baseplate orientation angle from the conventional coplanar and flat configurations, respectively. The tests also indicated that a controlled test series was necessary to establish the direction and magnitude of changes. The controlled series reported in this section was therefore designed to investigate combinations of tube and baseplate stagger angles up to 60° sweep angle from the coplanar plane.

Acoustic testing was done on the GE, Evendale, JENOTS test facility. Nozzle test conditions were representative of a GE4 engine operating line with an exhaust cycle range of P_{T8}/P_o from 1.4 to 3.4, T_{T8} from 1100 to 2680°R and V_j from 1100 to 3150 ft/sec.

Acoustic measurements were taken on a 40 ft. arc and scaled by frequency and size to full scale application using a scale factor of 8:1. All data presented are, therefore, of simulated engine size and engine frequency range.

In addition, a 4.3" D_8 conical convergent nozzle was run as an unsuppressed baseline to which the models are referenced for suppression.

Test Configurations

Five suppressor systems were tested within the series as shown pictorially in Figure V.F.2-1 and schematically in Figure V.F.2-2. The systems were:

- o Coplanar Tube Exit, Flat Baseplate, Models 4.0T72-4 and 4.0T72-5
- o Coplanar Tube Exit, 30° Baseplate, Model 4.0T72-30-1
- o Coplanar Tube Exit, 60° Baseplate, Model 4.0T72-60-1
- o 30° Tube Exit Stagger, 30° Baseplate, Model 4.0T72-30
- o 60° Tube Exit Stagger, 60° Baseplate, Model 4.0T72-60

PRECEDING PAGE BLANK-NOT FILMED

Each model had 72 tubes on a hexagonal pattern with 0.58" spacing between centers. Internal tube diameters changed slightly between models using 0.430", 0.444" or 0.437" I.D. tubing, depending on the particular model. This varied the area ratio (AR_d) from 2.87 to 3.06, however, a nominal AR_d of 3.0 is quoted for the study. The first system, coplanar tube exits within a flat baseplate, was tested in 1969 with 0.444" I.D. tubes as Model 4.0T72-4 and with 0.430" I.D. tubes as Model 4.0T72-5. In addition, several earlier tests in 1968 were made with the 0.444" I.D. tube/baseplate system as Model 4.0T72-1. Results of these tests are included with the 1969 results to establish average acoustic performance of this system. The other systems each had a singular test in 1969. Specifics of each suppressor system and test dates are included on Figure V.F.2-2.

Presentation and Discussion of Test Results

The following tables and figures present the acoustic test summaries and data plots for the baseline conical nozzle and the five suppressor systems.

Model	Table	Figures
4.3" I.D. Cone	V.F.2-1	V.F.2-3 and -4
4.0T72-4	V.F.2-2	V.F.2-5 and -6
4.0T72-5	V.F.2-3	V.F.2-7 and -8
4.0T72-30-1	V.F.2-4	V.F.2-11 and -12
4.0T72-60-1	V.F.2-5	V.F.2-13 and -14
4.0T72-30	V.F.2-6	V.F.2-15 and -16
4.0T72-60	V.F.2-7	V.F.2-17 and -18

The figures consist of 300 and 1500 ft. sideline plots of full scale peak normalized PNL as a function of jet velocity, for each model tested. The 4.3" I.D. conical nozzle was tested for acoustic baseline on each day of suppressor testing. Results of several test dates are plotted on Figures V.F.2-3 and -4 and average curves are drawn through the data. These average curves are included on each suppressor configurations data plots, as are the daily baseline data and daily baseline curve. The suppressions quoted are to the daily baselines, unless they are identical to the average baseline curves.

For the flat baseplate, coplanar tube exit system (tested as Models 4.0T72-4 and -5 in 1969 and as Model 4.0T72-1 in 1968) the 300 and 1500 ft. sidelines peak PNL suppression curves are individually plotted in Figures V.F.2-9 and -10, respectively. Repeatability of suppression levels is very consistent, within $\pm$ 1 PNdB at all jet velocities. Average curves are drawn through the results of the four individual tests and are used for comparison to the canted baseplate and staggered tube exit systems.

For comparative results of all five systems, Figures V.F.2-19 and -20 present the 300 and 1500 ft. sideline peak PNL suppressions, respectively; taken as deltas from the individual PNL data plots and from Figures V.F.2-9 and -10. Inspection of the plots indicates, particularly at high jet velocity, that a wide range of suppression is achievable with the basic 72 tube system, magnitude depending strongly on tube base and exit plane orientations. If the model is staggered both at the base and tube exit planes, suppression decreases, a larger decrease resulting from the greater stagger (60°). For a coplanar tube bundle exit plane, suppression increases with increased canting of the baseplate.

For comparing basic measurements, Figures V.F.2-21A through -21G present octave band sound pressure level spectra and PNL directivity of the five suppressor systems plus the baseline nozzle at seven incremental jet velocity settings from 1155 to 3130 ft/sec. No abrupt changes in either spectra or directivity are seen from model to model, only gradual shifting of levels as geometry varies. The high frequency predominance at low jet velocity is gradually replaced by low frequency predominance at high jet velocity. Spectra shape at high jet velocity is similar to, but lower than, the unsuppressed baseline jet. At low jet velocity the shapes differ considerably and only low frequencies are suppressed.

Aerodynamic test results for the nozzle series are based on static pressure measurements on the baseplate of each model. The base pressure profiles were used to calculate the mean base pressure by integrating the measured static pressures over their respective incremental base areas and then dividing the total value by the total base area acted upon. Mean base pressure ratio, $\bar{P}_B/P_o$, versus nozzle pressure ratio, P_{T8}/P_o, is presented in Figure V.F.2-22.

Figure V.F.2-23 presents $P_{T8}/\bar{P}_B$ as a function of nozzle pressure ratio. Figure V.F.2-24 presents base drag coefficient as a function of P_{T8}/P_o and nozzle geometry.

The flat baseplate, coplanar tube exit plane system (Models 4.0T72-4 and -5) had the lowest $\bar{P}_B/P_o$, and consequently the highest base drag coefficients, due to inability to ventilate the base area between the tubes. The 60° baseplate, coplanar tube exit system (Model 4.0T72-60-1) had the highest mean base pressure ratios, and consequently the lowest base drag. The long tube lengths at the outer periphery of the tube bundle allowed for pumping of ambient air to the center of the baseplate, pressurizing the base area and minimizing loss due to base drag.

Conclusions

- Major suppression changes are seen to be attributable to the particulars of tube exit plane and baseplate design. Within the range of geometry variance of the test series, sideline peak PNL suppression change ranged up to 6 PNdB at high jet velocity. Each of the models had 72 tubes and was near AR_d = 3.0 design, therefore, suppression variance was attributable only to baseplate and tube exit plane changes.
- The suppression and aerodynamic data show that if the model is staggered at both base and tube exit planes, suppression decreases and base pressure increases as stagger angle is increased.
- For a coplanar tube bundle exit plane, both base pressure and suppression increase with increased base stagger. The increased base pressure results in lower base drag and total aerodynamic thrust loss.
- The best suppressor configuration was the coplanar tube exit plane model with high base stagger angle, yielding 2 to 3 ΔPNdB additional suppression at high jet velocity over the flat baseplate coplanar tube exit plane system.

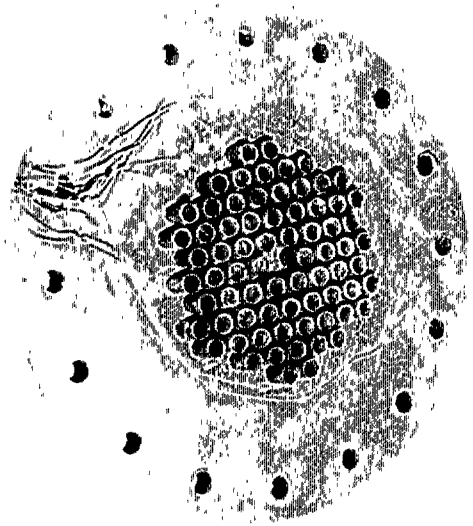

① & ② 0° Base Stagger
Coplanar Tube Exit

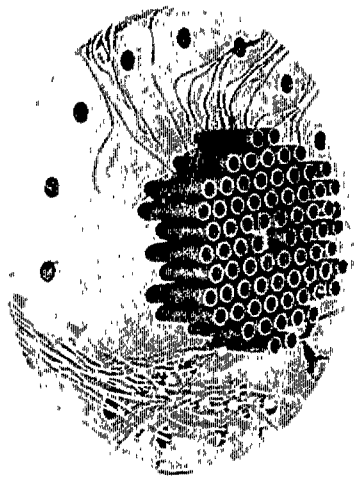

③ 30° Base Stagger
Coplanar Tube Exit

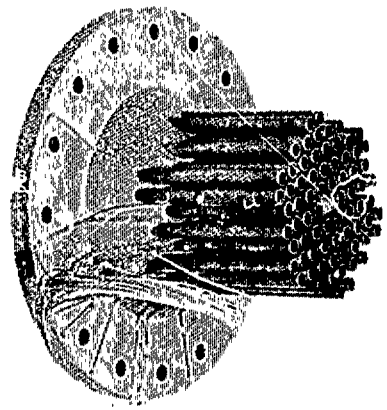

④ 60° Base Stagger
Coplanar Tube Exit

⑤ 30° Base Stagger
30° Tube Exit Stagger

⑥ 60° Base Stagger
60° Tube Exit Stagger

FIGURE V.F.2-1 72 TUBE NOZZLE HARDWARE FOR BASEPLATE AND TUBE EXIT PLANE STAGGER CONFIGURATIONS

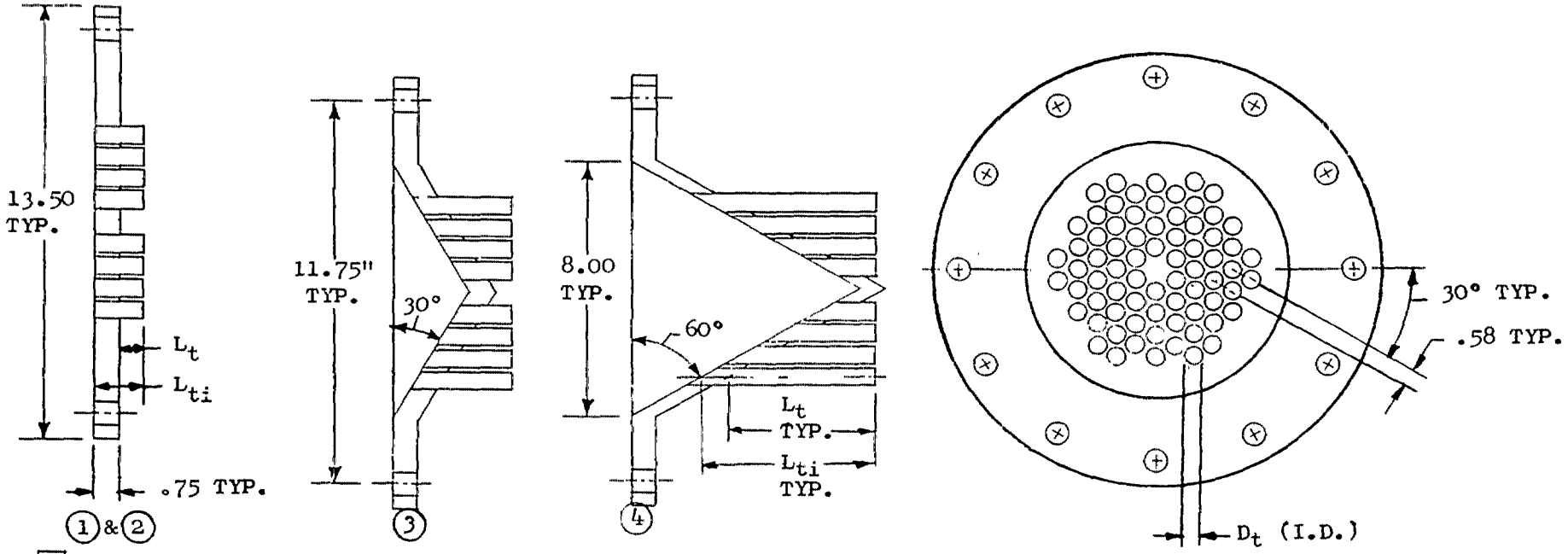

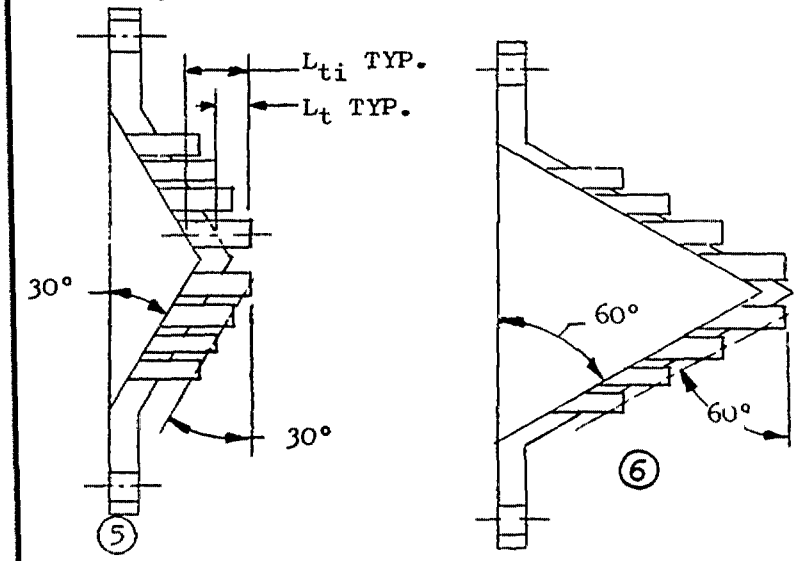

	Model No.	D_t	L_t/D_t	L_{t_i}/D_t	AR_d	Test Date
①	4.0T72-4	.444"	1.69	3.38	2.87	5-6-69
②	4.0T72-5	.430"	1.74	3.49	3.06	8-29-69
③	4.0T72-30-1	.430"	1.74 to 4.75	3.49 to 6.50	3.06	8-14-69
④	4.0T72-60-1	.430"	1.74 to 10.76	3.49 to 12.51	3.06	8-28-69
⑤	4.0T72-30	.437"	1.72	3.43	2.96	5-6-69
⑥	4.0T72-60	.437"	1.72	3.43	2.96	5-7-69

FIGURE V.F.2-2 SCHEMATIC OF 72 TUBE NOZZLE CONFIGURATIONS FOR BASEPLATE AND TUBE EXIT PLANE STAGGER VARIATIONS

TABLE V.F.2-1 TEST SUMMARY

MODEL NO. 4.3" Cone

DESCRIPTION: Baseline Conical Nozzle, 4.3" I.D.

DATE: 5/6/69; 5/7/69

SCALE MODEL A_8 = .102 ft^2

FULL SCALE A_8 = 6.528 ft^2

SCALE FACTOR = 8:1

- o DATA INCLUDES GROUND REFLECTION INTERFERENCE
- o ANGLE REFERENCED TO JET EXHAUST

RDG NO.	TEST CONDITIONS				ACOUSTIC TEST RESULTS						
			IDEAL			320' ARC		300' SIDELINE		1500' SIDELINE	
	P_{T8}/P_o	T_{T8} (°R)	V_j (ft/sec)	W_8 (PPS)	10 log ρA	PEAK PNdB	PEAK ANGLE	PEAK PNdB	PEAK ANGLE	PEAK PNdB	PEAK ANGLE
5/6/69											
1	1.41	1157	1149	3.71	-6.0	110.4	30	108.1	50	92.5	50
2	2.01	1499	1820	5.23	-7.0	130.9	30	126.3	40	110.9	40
3	2.46	1640	2140	6.37	-7.0	135.5	40/50	133.3	50	117.7	50
4	2.66	1778	2310	6.43	-7.2	138.0	50	135.8	50	120.1	50
5	3.13	1299	2750	6.70	-7.7	141.1	50	138.9	50	123.2	50
5/7/69											
1	1.43	1164	1181	3.92	-6.0	110.8	50	108.6	50	93.2	50
2	2.00	1509	1825	5.20	-7.0	130.7	30	126.5	50	118.1	50
3	2.50	1645	2145	6.22	-7.0	136.2	50	134.0	50	125.2	50
4	2.70	1763	2320	6.62	-7.1	139.2	40	136.7	50	128.1	50
5	3.11	2220	2757	6.74	-7.7	142.3	50	140.1	50	132.2	50

TABLE V.F.2-1 (Continued) TEST SUMMARY

MODEL NO. 4.3" Cone

DESCRIPTION: Baseline Conical Nozzle, 4.3" I.D.

DATE: 8/14/69; 8/28/69

SCALE MODEL A_8 = .102 ft^2

FULL SCALE A_8 = 6.528 ft^2

SCALE FACTOR = 8:1

- o DATA INCLUDES GROUND REFLECTION INTERFERENCE
- o ANGLE REFERENCED TO JET EXHAUST

RDG NO.	TEST CONDITIONS				ACOUSTIC TEST RESULTS						
			IDEAL			320' ARC		300' SIDELINE		1500' SIDELINE	
	P_{T8}/P_o	T_{T8} (°R)	V_j (ft/sec)	W_8 (PPS)	10 log ρA	PEAK PNdB	PEAK ANGLE	PEAK PNdB	PEAK ANGLE	PEAK PNdB	PEAK ANGLE
8/14/69											
1	1.44	1159	1178	3.80	-6.0	110.7	50	108.6	50	93.3	50
2	1.76	1536	1673	4.50	-7.2	126.3	30	121.4	50	106.1	50
3	2.02	1516	1834	5.26	-7.0	132.6	30	125.7	40/50	110.3	40
4	2.31	1600	2044	6.02	-7.0	134.1	40	130.3	50	114.9	50
5	2.72	1799	2350	6.79	-7.2	138.2	50	136.0	50	120.2	50
6	3.13	2264	2790	6.65	-7.8	140.9	50	138.7	50	123.0	50
8/28/69											
1	1.44	1138	1166	3.80	-5.9	110.5	50	108.3	50	93.1	50
2	2.01	1500	1821	5.24	-7.0	130.8	30	126.1	40	110.9	40
3	2.71	1750	2312	6.64	-7.0	138.1	50	135.9	50	120.2	50
4	3.14	2200	2754	6.67	-7.7	140.8	50	138.6	50	123.0	50
5	3.23	2408	2914	6.56	-8.0	141.3	50	139.2	50	123.6	50
6	2.47	1618	2127	6.27	-6.9	135.2	50	132.7	50	117.1	50
7	2.30	1549	2006	6.00	-6.9	133.7	40	130.8	50	115.2	50
8	1.75	1499	1644	4.43	-7.1	125.9	30	121.4	50	106.2	50
9	1.56	1499	1470	3.64	-7.1	118.8	50	116.7	50	101.4	50
10	1.63	1220	1392	4.27	-6.2	116.9	30	114.4	50	98.9	50
11	2.93	2105	2623	6.21	-7.6	140.3	50	138.2	50	122.5	50
12	2.56	2105	2470	5.39	-8.0	138.9	50	136.7	50	120.9	50

TABLE V.F.2-1 TEST SUMMARY

(Continued)

MODEL NO. 4.3" Cone

DESCRIPTION: Baseline Conical Nozzle, 4.3" I.D.

DATE: 8/29/69

SCALE MODEL A_8 = .102 ft^2

FULL SCALE A_8 = 6.528 ft^2

SCALE FACTOR = 8:1

- o DATA INCLUDES GROUND REFLECTION INTERFERENCE
- o ANGLE REFERENCED TO JET EXHAUST

RDG NO.	TEST CONDITIONS				ACOUSTIC TEST RESULTS						
			IDEAL			320' ARC		300' SIDELINE		1500' SIDELINE	
	P_{T8}/P_o	T_{T8} (°R)	V_j (ft/sec)	W_8 (PPS)	10 log ρA	PEAK PNdB	PEAK ANGLE	PEAK PNdB	PEAK ANGLE	PEAK PNdB	PEAK ANGLE
8/29/69											
1	1.44	1175	1191	3.58	-6.0	111.1	50	108.9	50	93.6	50
2	2.03	1508	1841	5.22	-7.0	130.2	30	125.8	50	110.5	50
3	2.72	1798	2349	6.58	-7.1	138.2	50	135.8	50	120.0	50
4	3.12	2113	2693	6.67	-7.5	141.0	50	138.8	50	123.2	50
5	3.23	2417	2918	6.59	-8.0	140.8	50	138.6	50	123.0	50
6	2.46	1669	2155	6.06	-7.1	135.8	50	133.5	50	117.8	50
7	2.29	1551	2003	5.88	-6.9	133.5	40	130.2	50	114.6	50
8	1.74	1520	1648	4.24	-7.2	125.0	30	121.9	50	106.6	50
9	1.53	1486	1440	3.35	-7.1	118.7	50	116.5	50	100.9	50
10	1.62	1236	1388	4.06	-6.3	116.6	50	114.4	50	99.1	50
11	2.92	2093	2611	6.15	-7.6	140.8	50	138.4	50	122.7	50

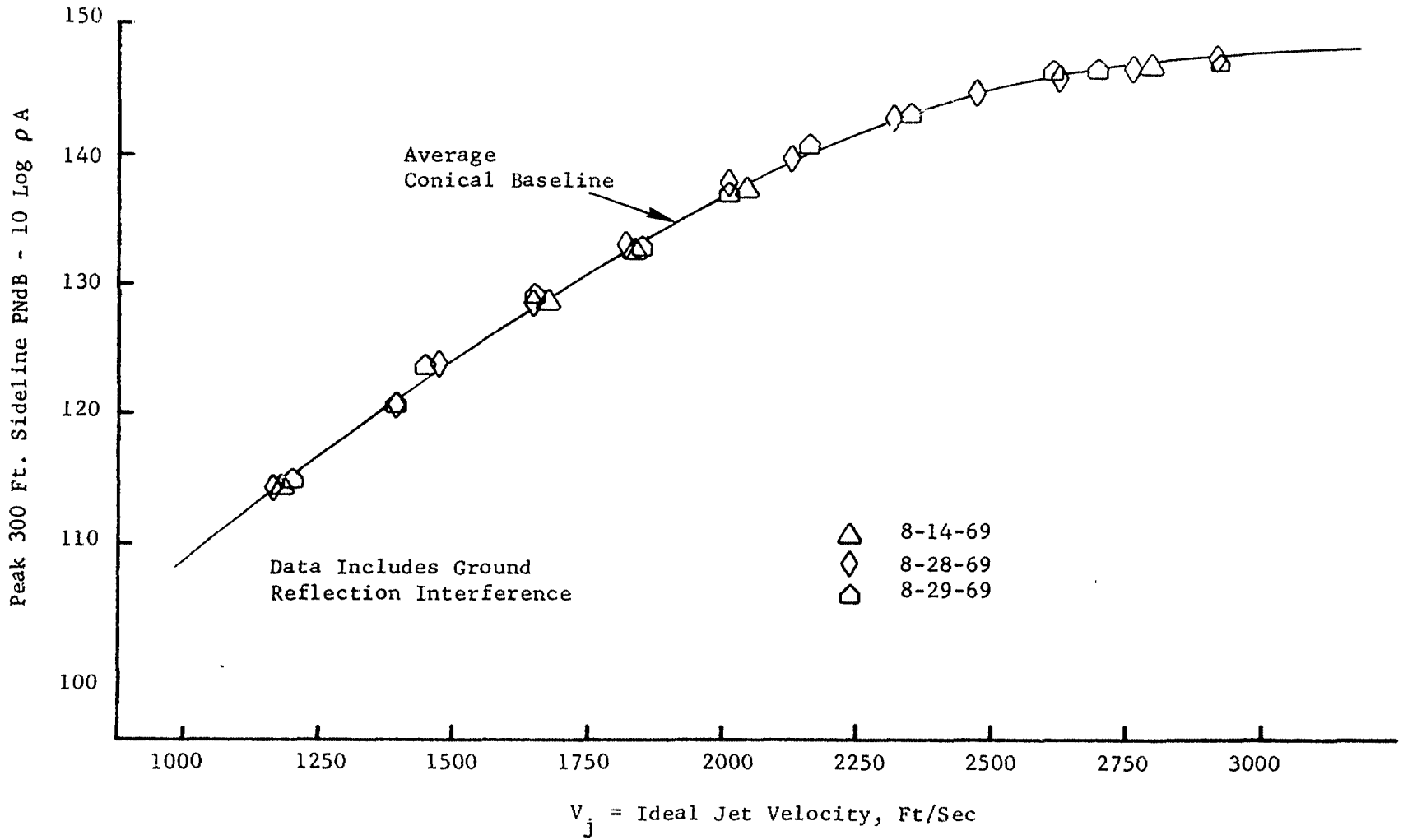

FIGURE V.F.2-3 300 FT. SIDELINE JET NOISE LEVELS FOR AVERAGE BASELINE CONICAL NOZZLE

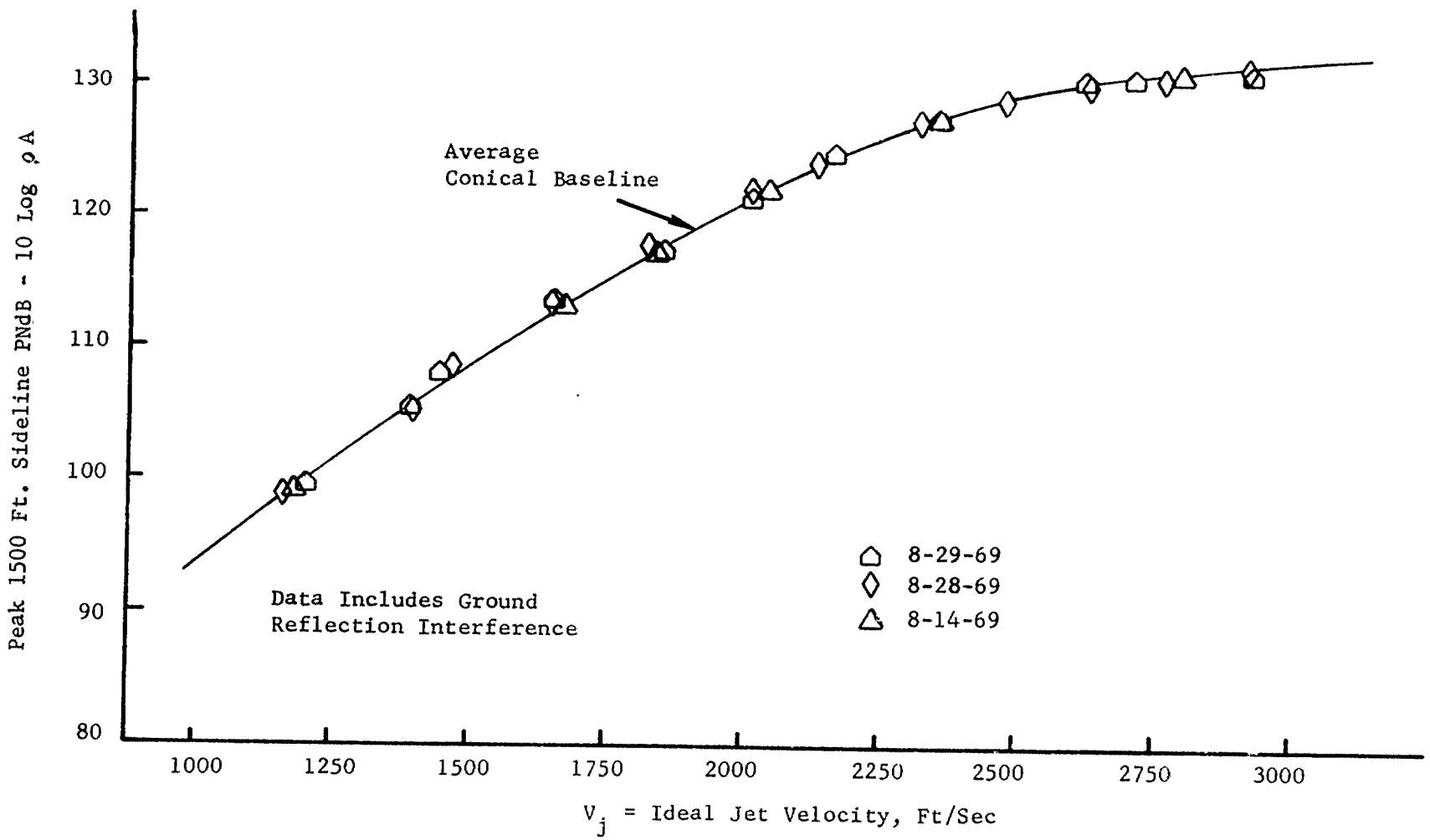

FIGURE V.F.2-4 1500 FT. SIDELINE JET NOISE LEVELS FOR AVERAGE BASELINE CONICAL NOZZLE

TABLE V.F.2-2 TEST SUMMARY

MODEL NO. 4.0T72-4

DESCRIPTION: 0° Base Stagger, Coplanar Tube Exit, 72 Tube Nozzle

DATE: 5/6/69

SCALE MODEL A_8 = .0774 ft^2

FULL SCALE A_8 = 4.954 ft^2

SCALE FACTOR = 8:1

- o DATA INCLUDES GROUND REFLECTION INTERFERENCE
- o ANGLE REFERENCED TO JET EXHAUST

	TEST CONDITIONS				ACOUSTIC TEST RESULTS						
			IDEAL			320' ARC		300' SIDELINE		1500' SIDELINE	
RDG NO.	P_{T8}/P_o	T_{T8} (°R)	V_j (ft/sec)	W_8 (PPS)	10 log ρA	PEAK PNdB	PEAK ANGLE	PEAK PNdB	PEAK ANGLE	PEAK PNdB	PEAK ANGLE
1	1.42	1151	1152	2.62	-7.1	107.3	60	106.4	60	88.9	60
2	1.53	1555	1467	2.64	-8.5	113.0	50	111.6	80	94.2	80
3	1.62	1238	1390	3.14	-7.5	112.5	50	116.4	60	93.0	60
4	1.74	1527	1654	3.00	-8.4	116.1	50	113.7	70	96.8	70
5	2.01	1512	1831	3.60	-8.2	118.8	50	116.7	80	99.2	80
6	2.29	1558	2008	3.87	-8.1	120.8	50	118.4	50	100.8	50
7	2.47	1660	2156	4.19	-8.2	121.6	50	119.5	80	102.1	80
8	2.51	2106	2449	3.58	-9.2	123.4	50	121.2	80	103.9	80
9	2.71	1787	2336	4.56	-8.4	123.4	50	121.1	80	103.8	80
10	2.93	2109	2624	4.24	-8.9	126.5	50	124.2	50	107.4	50
11	3.14	2217	2766	4.67	-8.9	127.9	50	125.5	50	108.4	50
12	3.22	2396	2904	4.44	-9.2	129.1	50	126.8	50	110.1	50
13	3.22	2611	3028	4.40	-9.6	129.3	50	127.0	50	110.5	50
14	3.40	2656	3117	4.38	-9.5	130.6	50	128.3	50	111.6	50

- o AR_d = 2.87
- o D_t = .444"
- o L_t/D_t = 1.69
- o L_{ti}/D_t = 3.38

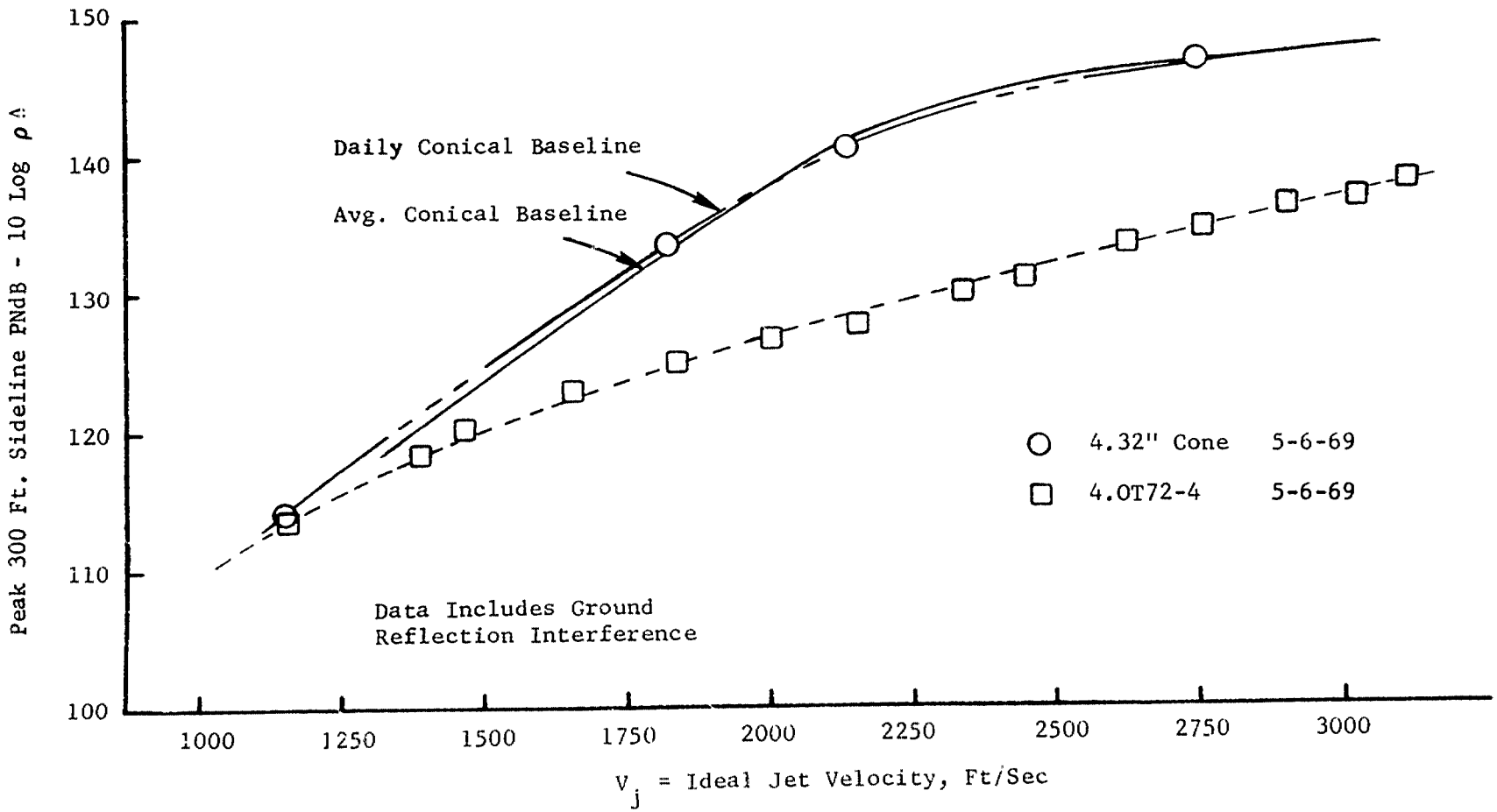

FIGURE V.F.2-5 300 FT. SIDELINE JET NOISE LEVELS FOR A 72 TUBE NOZZLE WITH FLAT BASEPLATE AND COPLANER TUBE EXIT

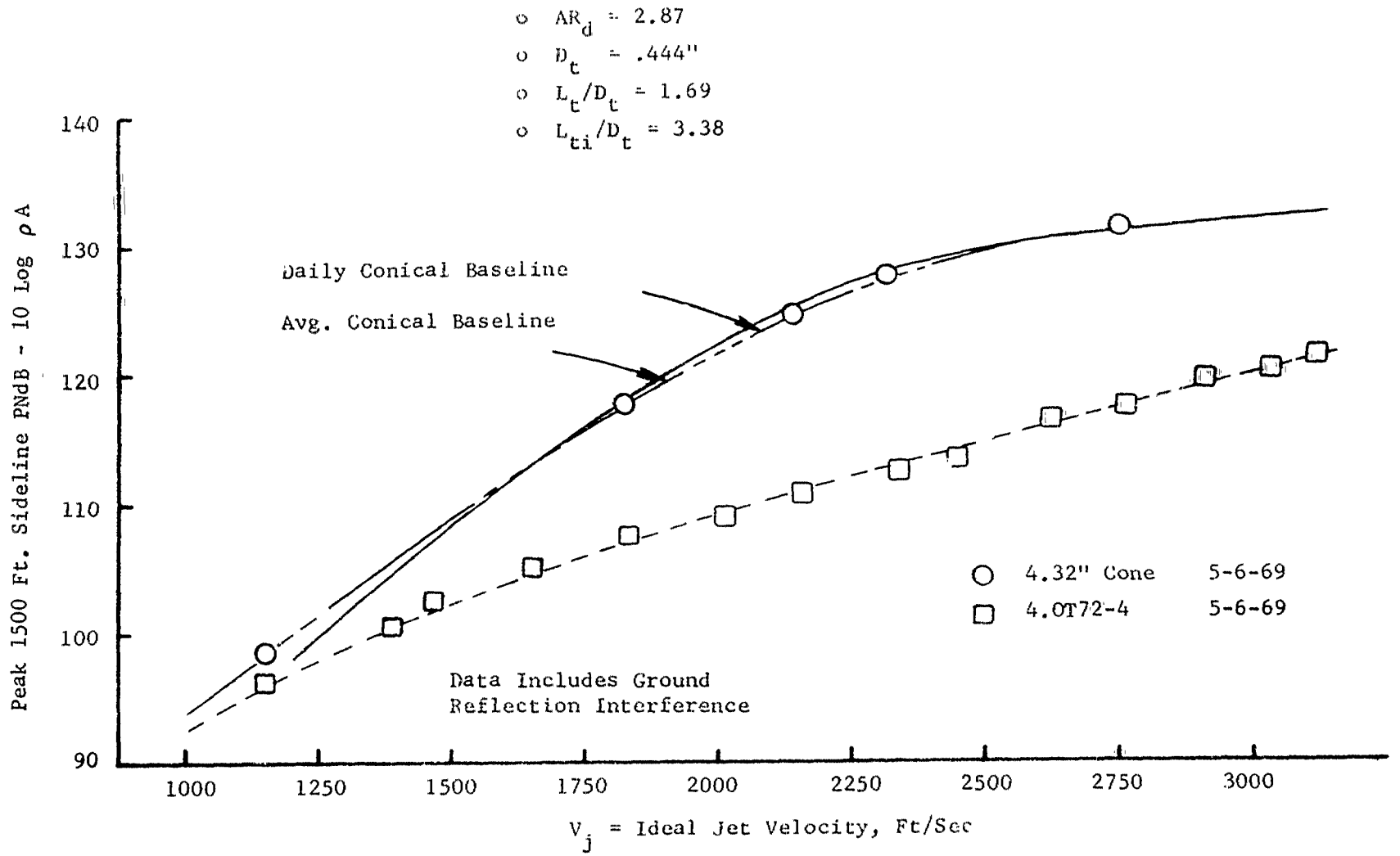

FIGURE V.F.2-6 1500 FT. SIDELINE JET NOISE LEVELS FOR A 72 TUBE NOZZLE WITH FLAT BASEPLATE AND COPLANER TUBE EXIT

TABLE V.F.2-3 TEST SUMMARY

MODEL NO. 4.0T72-5

DESCRIPTION: 0° Base Stagger, Coplanar Tube Exit, 72 Tube Nozzle

DATE: 8/29/69

SCALE MODEL A_8 = .0726 ft^2

FULL SCALE A_8 = 4.646 ft^2

SCALE FACTOR = 8:1

- o DATA INCLUDES GROUND REFLECTION INTERFERENCE
- o ANGLE REFERENCED TO JET EXHAUST

RDG NO.	TEST CONDITIONS				ACOUSTIC TEST RESULTS						
			IDEAL			320' ARC		300' SIDELINE		1500' SIDELINE	
	P_{T8}/P_o	T_{T8} (°R)	V_j (ft/sec)	W_8 (PPS)	10 log ρA	PEAK PNdB	PEAK ANGLE	PEAK PNdB	PEAK ANGLE	PEAK PNdB	PEAK ANGLE
1	1.43	1150	1162	3.10	-7.4	108.1	60	107.2	60	89.7	60
2	1.58	1514	1497	2.94	-8.7	114.3	50	112.2	60	94.8	60
3	1.63	1235	1403	3.41	-7.8	112.3	50	110.8	70	93.6	70
4	1.74	1526	1650	3.24	-8.7	117.5	50	115.1	50	97.4	50
5	2.02	1484	1817	3.83	-8.4	119.5	50	117.2	50	98.7	50
6	2.30	1538	1998	4.21	-8.3	122.3	50	119.9	50	102.3	50
7	2.45	1625	2122	4.37	-8.4	123.1	50	120.7	50	103.3	50
8	2.52	2132	2467	3.84	-9.5	125.9	50	123.5	50	106.2	50
9	2.71	1779	2330	4.73	-8.6	125.3	50	122.9	50	105.7	50
10	2.93	2130	2637	4.58	-9.2	127.3	50	124.9	50	108.2	50
11	3.13	2224	2766	4.79	-9.2	129.2	50	126.9	50	110.9	50
12	3.30	2422	2943	4.78	-9.4	129.5	40	127.2	50	111.4	50
13	3.21	2620	3032	4.48	-9.8	130.8	50	128.7	50	113.2	50
14	3.41	2661	3122	4.69	-9.7	133.2	50	131.0	50	115.5	50

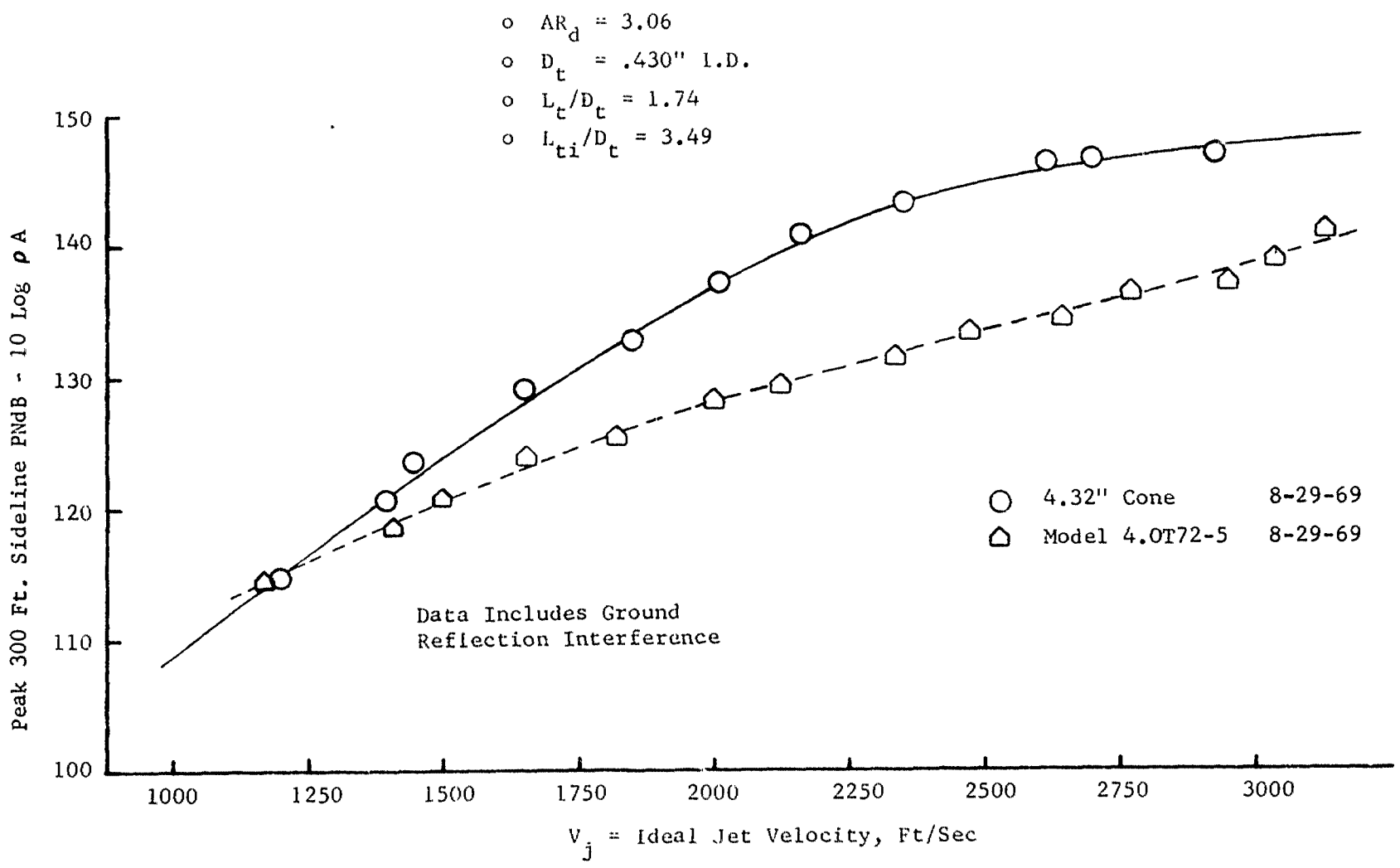

FIGURE V.F.2-7 300 FT. SIDELINE JET NOISE LEVELS FOR A 72 TUBE NOZZLE WITH FLAT BASEPLATE AND COPLANER TUBE EXIT

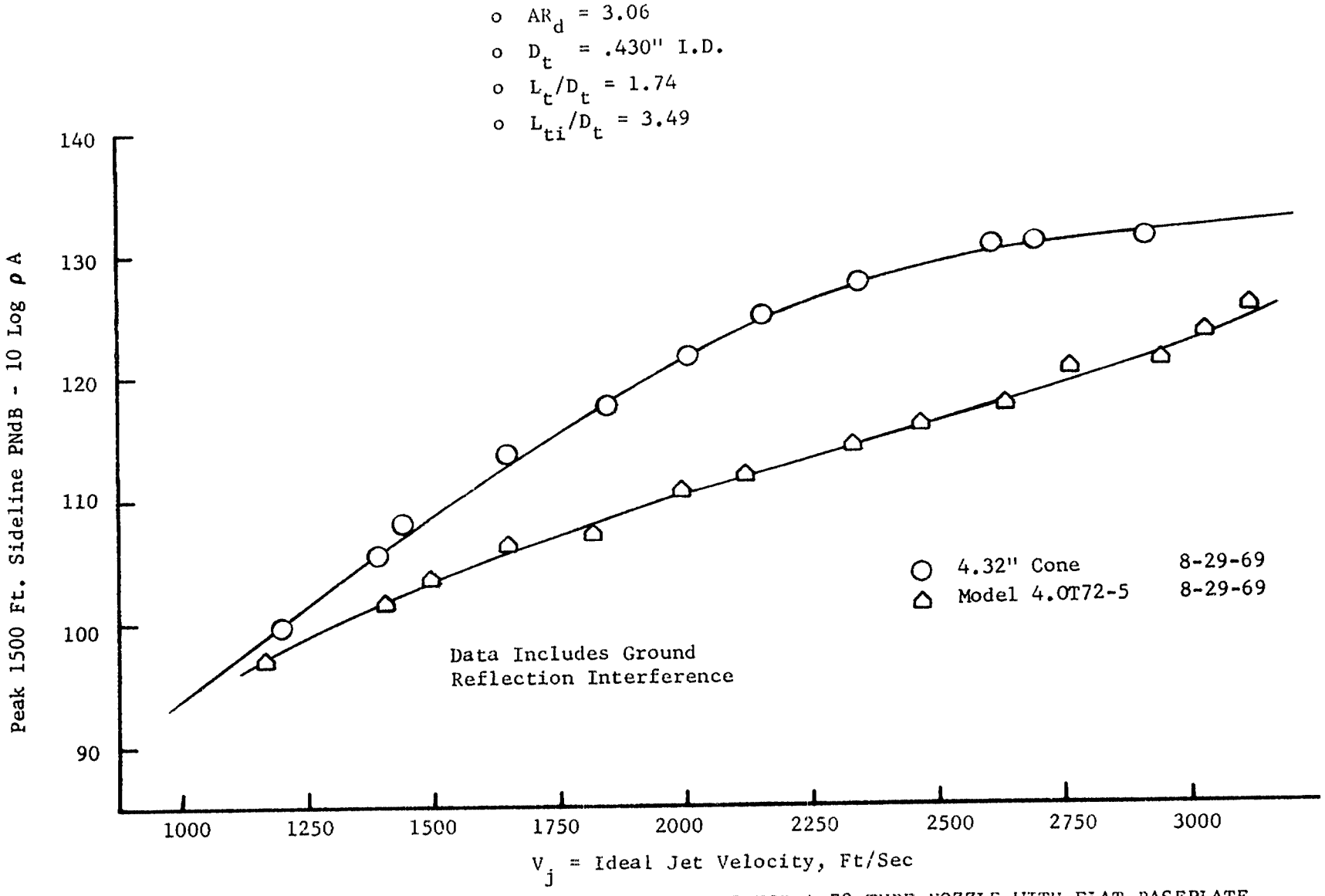

FIGURE V.F.2-8 1500 FT. SIDELINE JET NOISE LEVELS FOR A 72 TUBE NOZZLE WITH FLAT BASEPLATE AND COPLANER TUBE EXIT

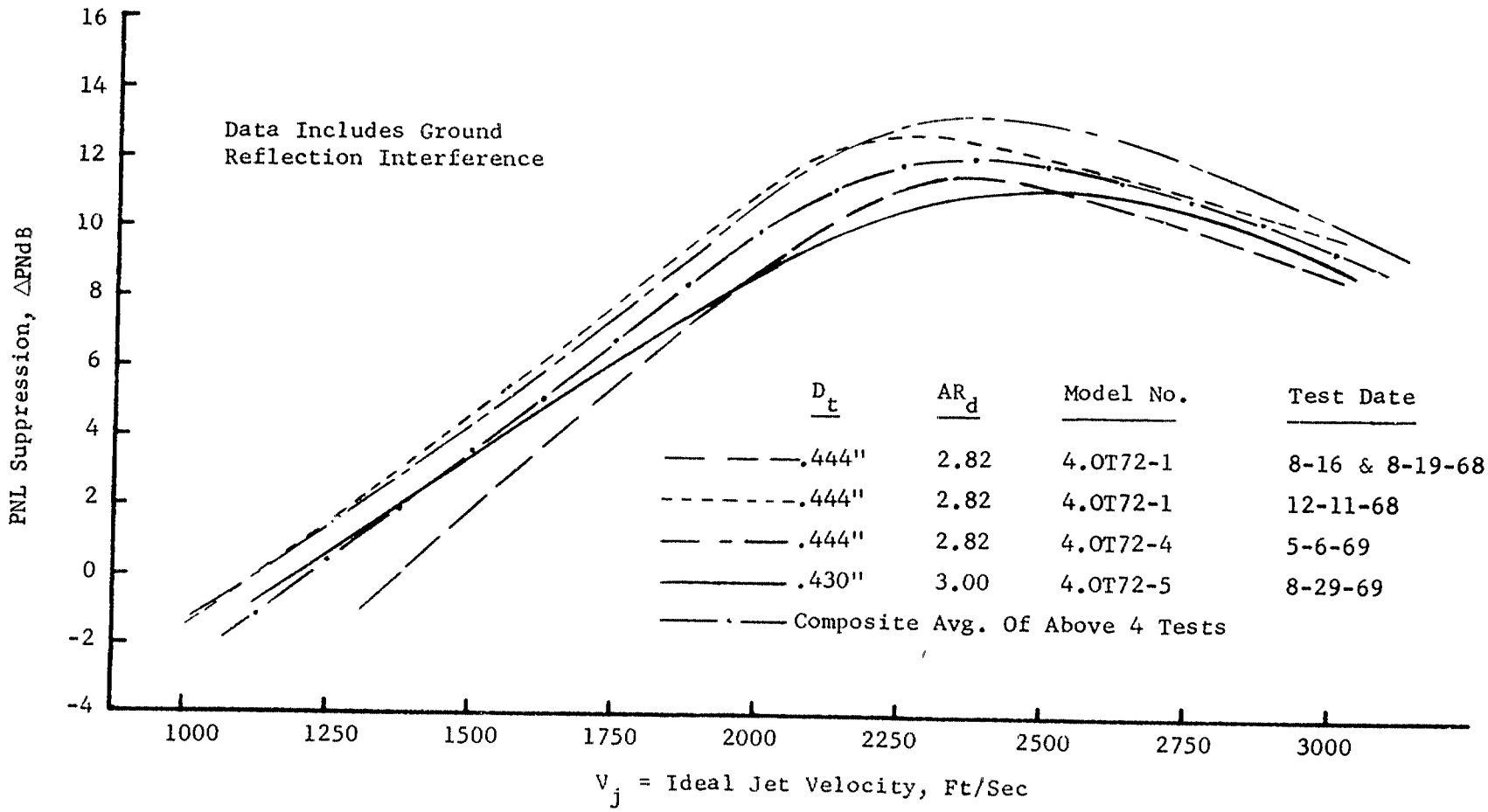

FIGURE V.F.2-9 300 FT. SIDELINE PNL SUPPRESSION COMPARISONS FOR 72 TUBE NOZZLES WITH FLAT BASEPLATES AND COPLANER EXITS

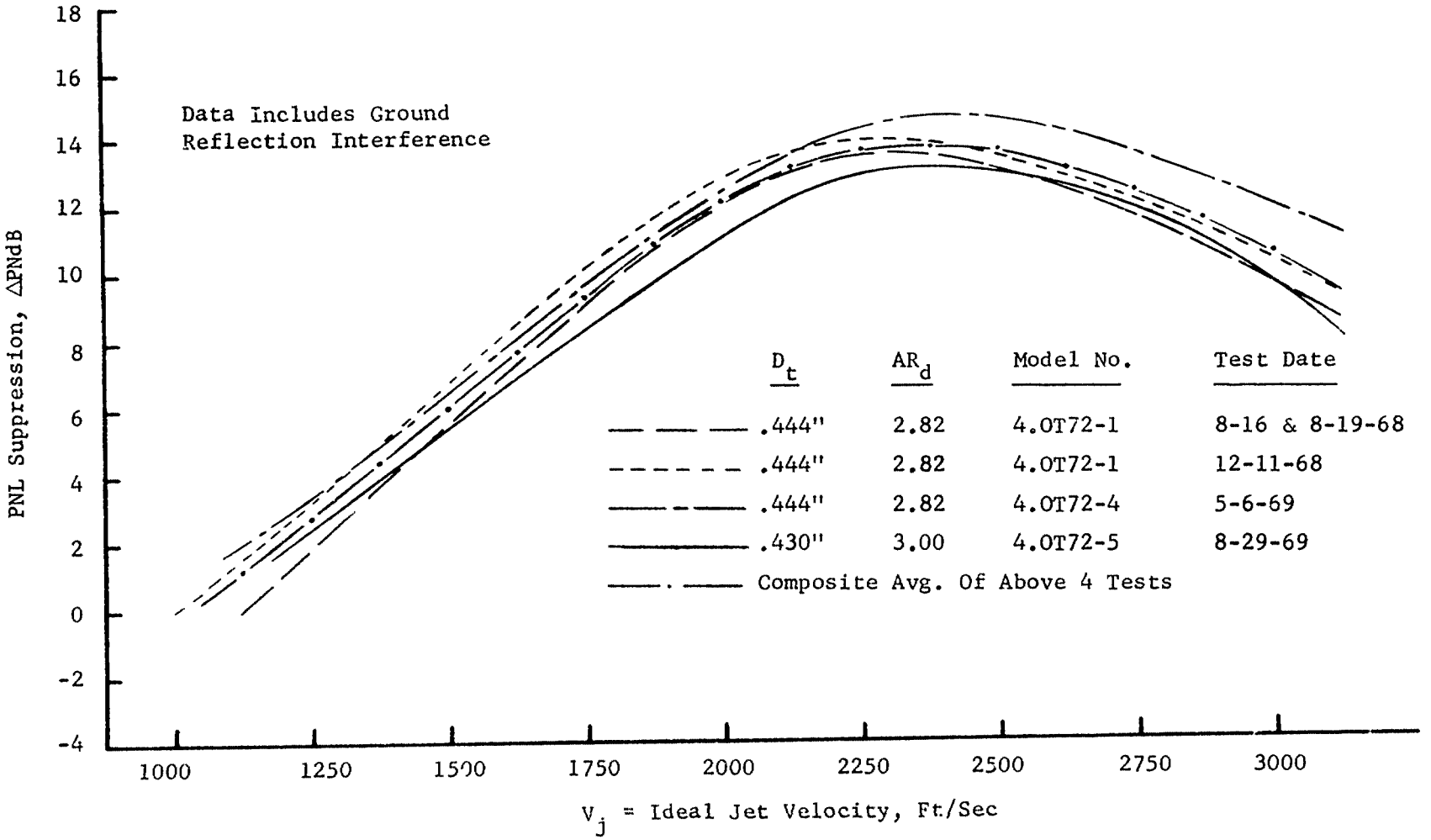

FIGURE V.F.2-10 1500 FT. SIDELINE PNL SUPPRESSION COMPARISONS FOR 72 TUBE NOZZLES WITH FLAT BASEPLATES AND COPLANER EXITS

TABLE V.F. 2-4 TEST SUMMARY

MODEL NO. 4.0T72-30-1

DESCRIPTION: 30° Base Stagger, Coplanar Tube Exit, 72 Tube Nozzle

DATE: 8/14/69

SCALE MODEL A_8 = .0726 ft^2

FULL SCALE A_8 = 4.646 ft^2

SCALE FACTOR = 8:1

- o DATA INCLUDES GROUND REFLECTION INTERFERENCE
- o ANGLE REFERENCED TO JET EXHAUST

	TEST CONDITIONS				ACOUSTIC TEST RESULTS						
			IDEAL			320' ARC		300' SIDELINE		1500' SIDELINE	
RDG NO.	P_{T8}/P_o	T_{T8} (°R)	V_j (ft/sec)	W_8 (PPS)	10 log ρA	PEAK PNdB	PEAK ANGLE	PEAK PNdB	PEAK ANGLE	PEAK PNdB	PEAK ANGLE
1	1.43	1132	1153	2.90	-6.3	111.7	30	106.6	80	90.5	80
2	1.56	1531	1488	2.84	-7.7	114.1	50	112.4	70	95.0	70
3	1.63	1242	1403	3.28	-6.7	112.3	50	111.2	60	93.7	60
4	1.75	1500	1642	-	-7.6	116.1	50	113.7	50	96.3	60
5	2.00	1517	1827	3.70	-7.5	119.1	50	116.8	60	99.2	60
6	2.31	1552	2012	4.26	-8.4	130.7	60	129.8	60	112.6	60
7	2.47	1646	2147	4.37	-8.5	122.5	50	120.1	50	102.5	50
8	2.49	2108	2439	3.73	-9.5	124.9	50	122.5	50	105.0	50
9	2.71	1801	2345	4.53	-8.7	124.2	50	121.9	50	104.4	50
10	2.91	2147	2639	4.35	-9.2	125.5	50	123.2	50	105.9	50
11	3.13	2247	2780	4.52	-9.2	127.6	50	125.3	50	108.6	50
12	3.22	2441	2929	4.46	-9.5	128.2	50	125.9	50	108.8	50
13	3.23	2641	3050	4.40	-9.9	128.0	50	125.6	50	108.9	50
14	3.41	2685	3135	4.62	-9.8	130.0	50	127.7	50	109.2	50

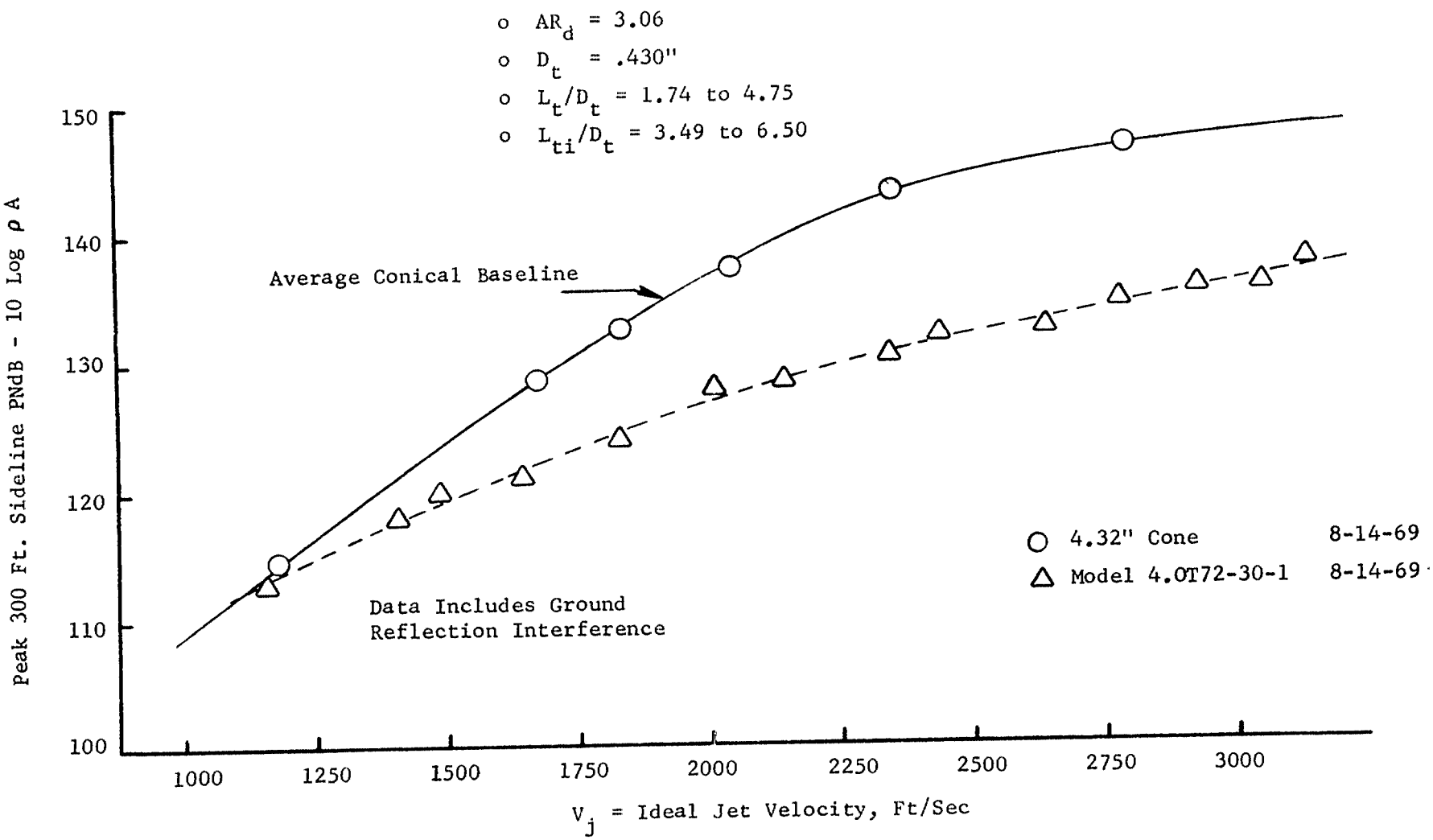

FIGURE V.F.2-11 300 FT. SIDELINE JET NOISE LEVELS FOR A 72 TUBE NOZZLE WITH 30° BASEPLATE STAGGER AND COPLANER TUBE EXIT

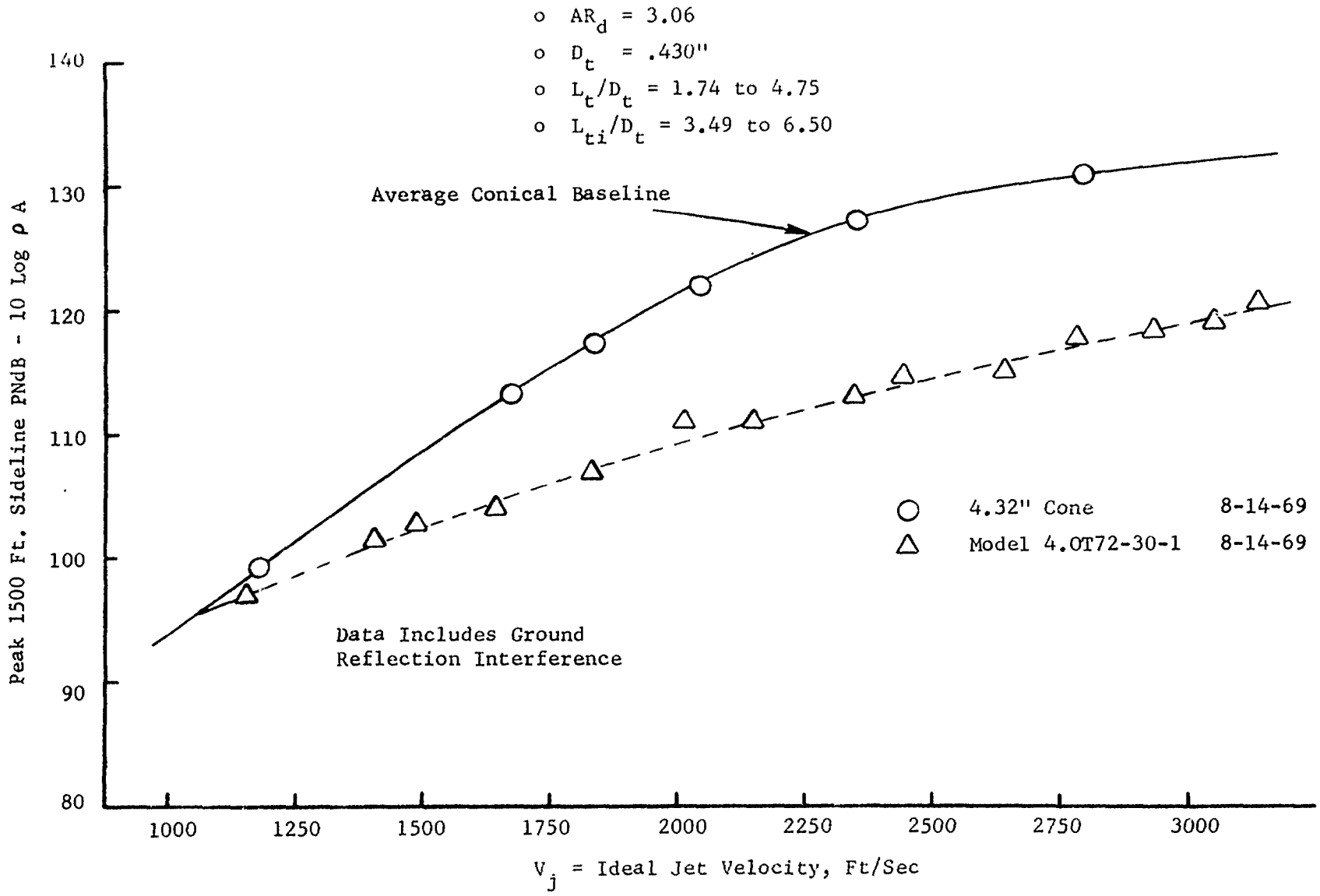

FIGURE V.F.2-12 1500 FT. SIDELINE JET NOISE LEVELS FOR A 72 TUBE NOZZLE WITH 30° BASEPLATE STAGGER AND COPLANER TUBE EXIT

TABLE V.F.2-5 TEST SUMMARY

MODEL NO. 4.0T72-60-1

DESCRIPTION: 60° Base Stagger, Coplanar Tube Exit, 72 Tube Nozzle

DATE: 8/28/69

SCALE MODEL A_8 = .0726 ft^2

FULL SCALE A_8 = 4.646 ft^2

SCALE FACTOR = 8:1

- o DATA INCLUDES GROUND REFLECTION INTERFERENCE
- o ANGLE REFERENCED TO JET EXHAUST

RDG NO.	TEST CONDITIONS				ACOUSTIC TEST RESULTS						
			IDEAL			320' ARC		300' SIDELINE		1500' SIDELINE	
	P_{T8}/P_o	T_{T8} (°R)	V_j (ft/sec)	W_8 (PPS)	10 log ρA	PEAK PNdB	PEAK ANGLE	PEAK PNdB	PEAK ANGLE	PEAK PNdB	PEAK ANGLE
1	1.37	1139	1092	2.85	-7.3	103.4	60	102.5	60	85.0	60
2	1.55	1502	1469	2.54	-8.6	110.0	50	108.4	60	91.0	60
3	1.62	1220	1384	2.70	-7.7	109.4	60	108.4	60	91.8	70
4	1.75	1502	1645	2.95	-8.6	114.1	50	111.7	50/60	94.3	60
5	2.00	1530	1833	3.65	-8.5	117.3	50	114.9	50	97.2	50
6	2.29	1559	2007	4.13	-8.4	118.7	50	116.3	50	98.8	70
7	2.49	1640	2151	4.28	-8.4	121.2	50	118.8	50	101.3	50
8	2.50	2119	2452	3.76	-9.5	123.1	50	120.8	50	103.4	50
9	2.71	1768	2324	4.34	-8.5	122.7	50	120.3	50	102.9	50
10	2.92	2115	2624	4.35	-9.1	124.8	50	122.5	50	105.3	50
11	3.12	2226	2763	4.58	-9.2	126.3	50	124.0	50	107.0	50
12	3.22	2422	2917	4.54	-9.5	127.4	50	125.0	50	108.0	50
13	3.22	2602	3023	4.31	-9.8	127.6	50	125.3	50	108.5	50
14	3.40	2682	3131	4.54	-9.8	129.3	50	127.0	50	110.6	50

- o AR_d = 3.06
- o D_t - .430"
- o L_t/D_t = 1.74 to 10.76
- o L_{ti}/D_t = 3.49 to 12.51

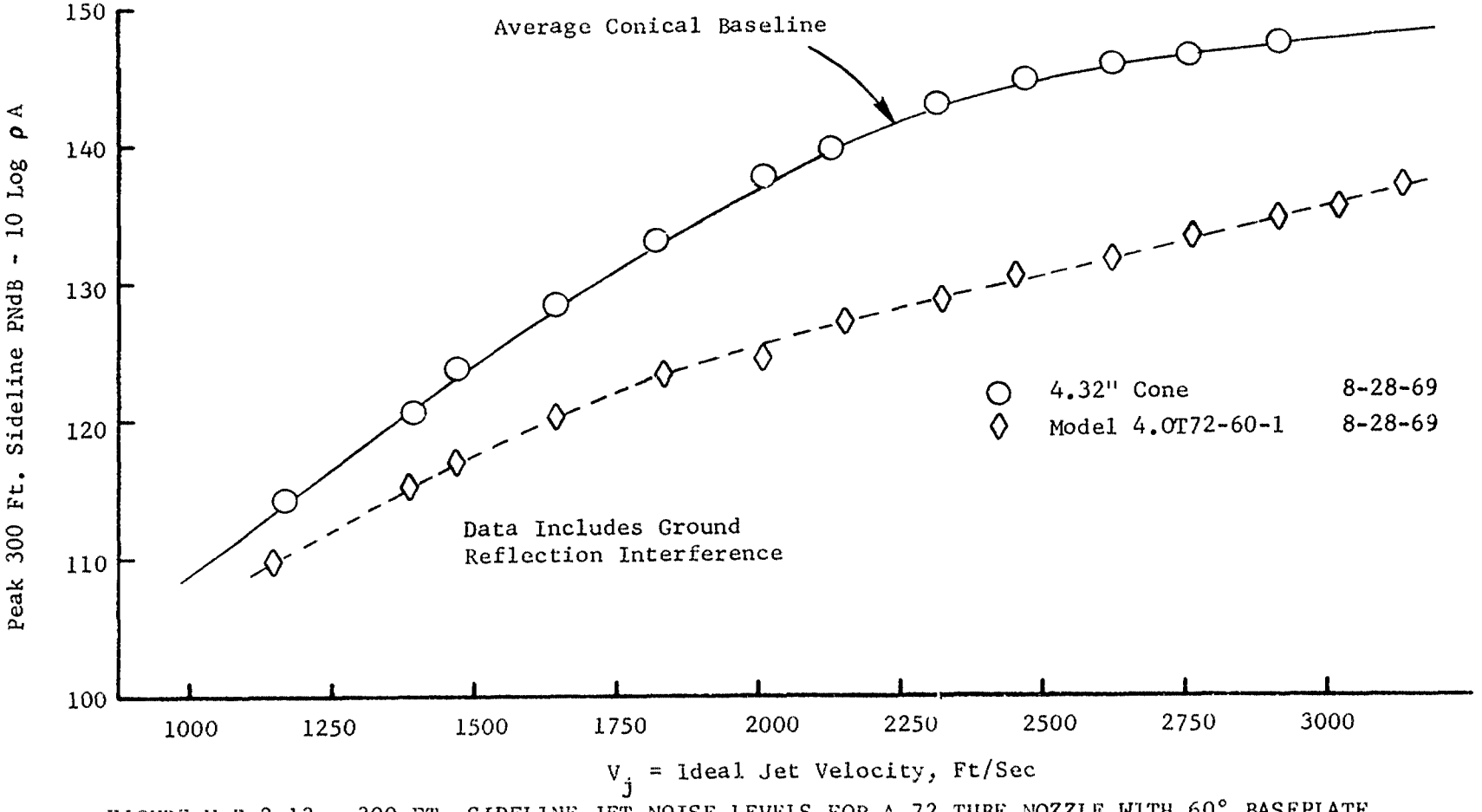

FIGURE V.F.2-13 300 FT. SIDELINE JET NOISE LEVELS FOR A 72 TUBE NOZZLE WITH 60° BASEPLATE STAGGER AND COPLANER TUBE EXIT

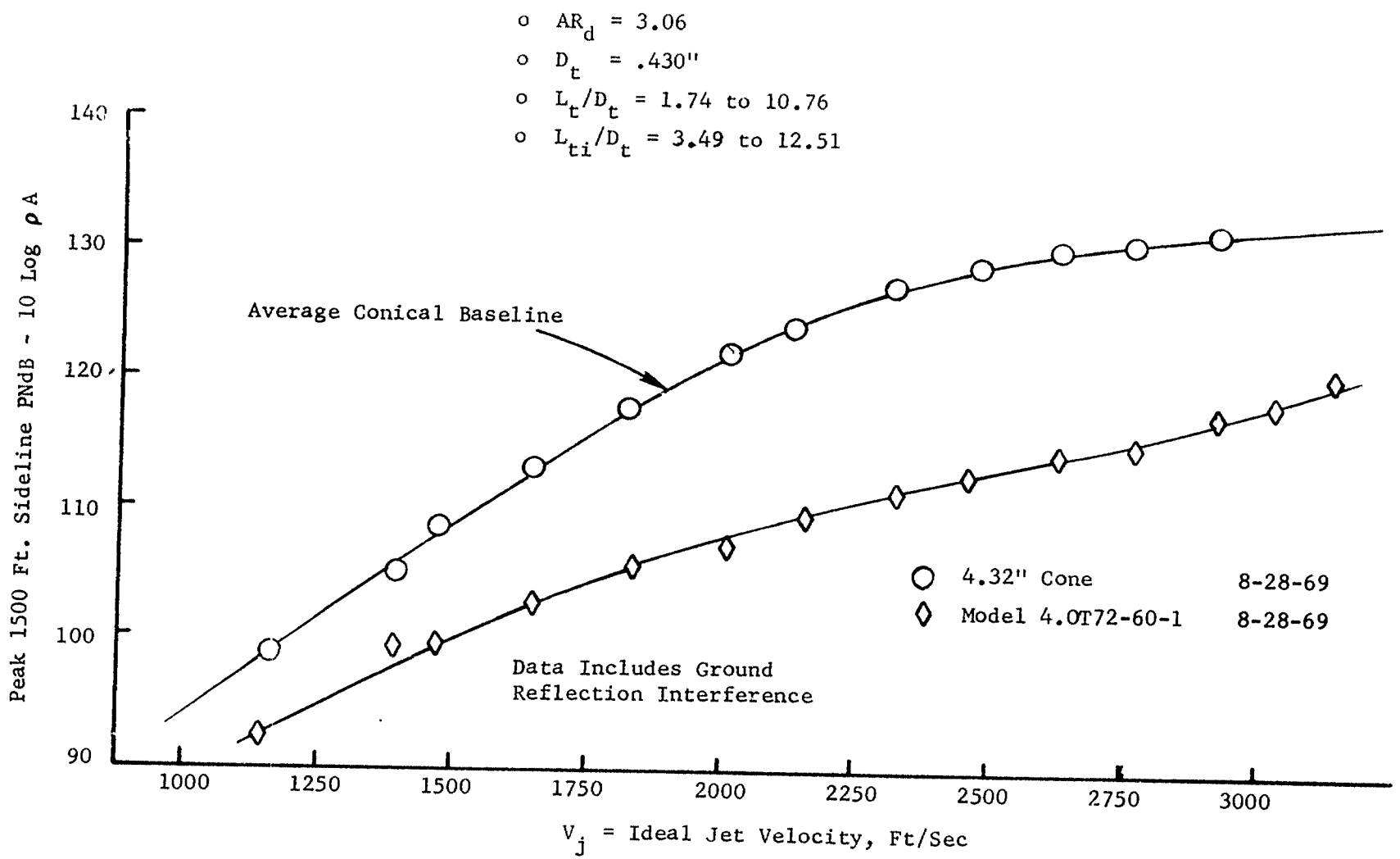

FIGURE V.F.2-14 1500 FT. SIDELINE JET NOISE LEVELS FOR A 72 TUBE NOZZLE WITH 60° BASEPLATE STAGGER AND COPLANER TUBE EXIT

TABLE V.F.2-6 TEST SUMMARY

MODEL NO. 4.0T72-30

DESCRIPTION: 30° Base and Tube Exit Stagger, 72 Tube Nozzle

DATE: 5/6/69

SCALE MODEL A_8 = .075 ft^2

FULL SCALE A_8 = 4.80 ft^2

SCALE FACTOR = 8:1

- o DATA INCLUDES GROUND REFLECTION INTERFERENCE
- o ANGLE REFERENCED TO JET EXHAUST

RDG NO.	TEST CONDITIONS				ACOUSTIC TEST RESULTS						
			IDEAL			320' ARC		300' SIDELINE		1500' SIDELINE	
	P_{T8}/P_o	T_{T8} (°R)	V_j (ft/sec)	W_8 (PPS)	10 log ρA	PEAK PNdB	PEAK ANGLE	PEAK PNdB	PEAK ANGLE	PEAK PNdB	PEAK ANGLE
1	1.43	1157	1163	2.96	-7.2	107.3	50	107.1	80	89.5	80
2	1.55	1519	1471	2.97	-8.4	111.8	50	111.5	80	94.1	80
3	1.63	1241	1402	3.39	-7.6	111.1	60	110.2	60	92.7	60/80
4	1.76	1487	1644	3.49	-8.3	116.5	30	114.7	80	97.3	80
5	2.02	1529	1847	4.04	-8.3	120.8	50	118.4	50	100.7	50
6	2.30	1566	2020	4.44	-8.1	122.5	40	119.0	50	101.7	50
7	2.47	1635	2138	4.71	-8.2	124.4	50	122.0	50	104.7	50
8	2.51	2099	2445	4.14	-9.2	125.8	50	123.5	50	106.4	50
9	2.72	1817	2360	4.84	-8.4	126.2	50	123.9	50	107.3	50
10	2.92	2138	2640	4.58	-8.9	128.0	40	125.3	50	109.3	50
11	3.11	2242	2772	4.95	-9.0	129.9	40	127.1	50	111.6	50
12	3.23	2422	2922	5.07	-9.2	131.0	50	128.8	50	113.3	50
13	3.22	1605	2375	4.68	-7.4	132.6	50	130.4	50	114.9	50
14	3.40	1629	2441	5.04	-7.4	133.0	50	130.9	50	115.5	50

- o AR_d = 2.96
- o D_t = .437"
- o L_t/D_t = 1.72
- o L_{ti}/D_t = 3.43

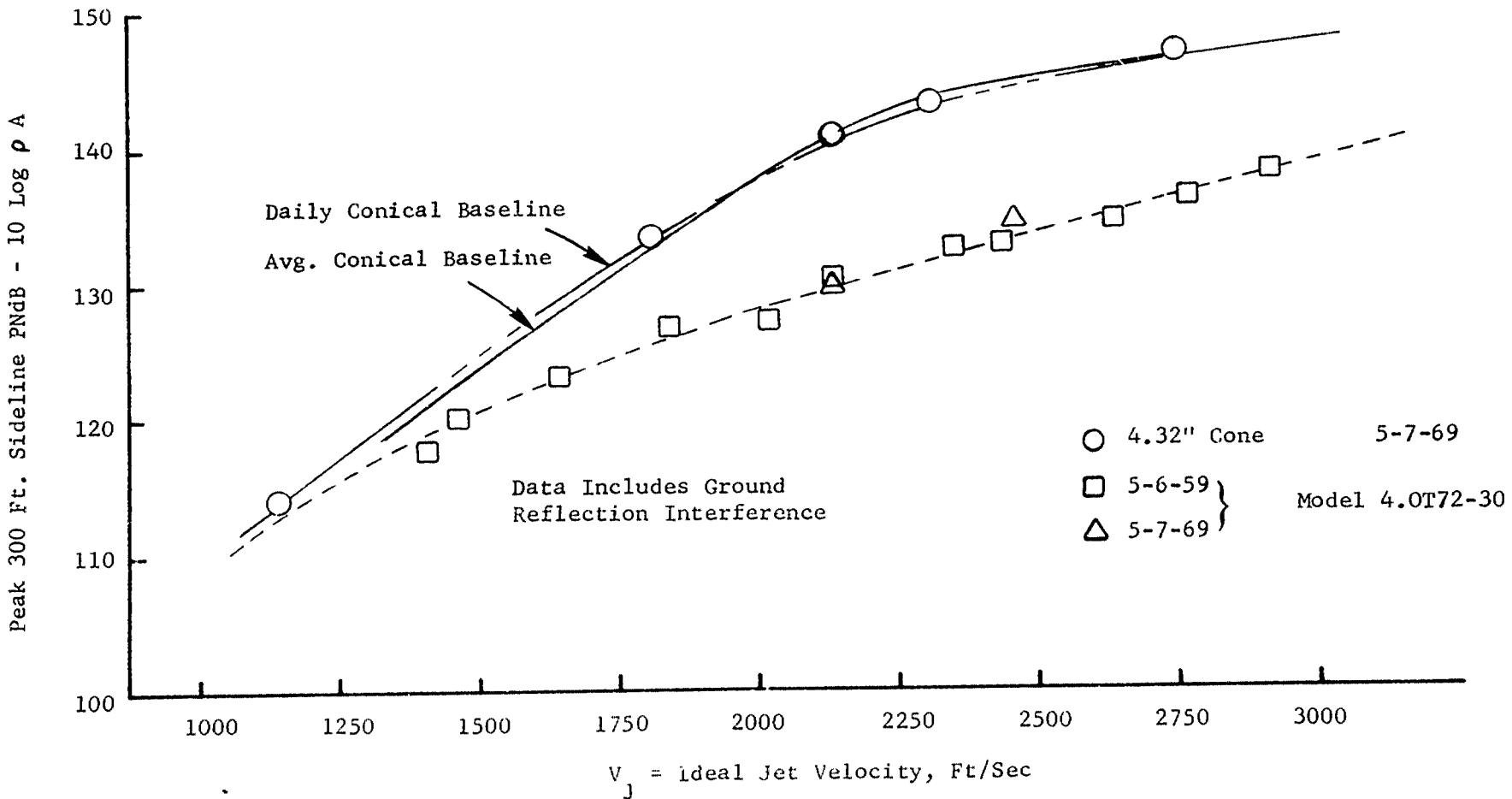

FIGURE V.F.2-15 300 FT. SIDELINE JET NOISE LEVELS FOR A 72 TUBE NOZZLE WITH 30° BASEPLATE AND TUBE EXIT STAGGER

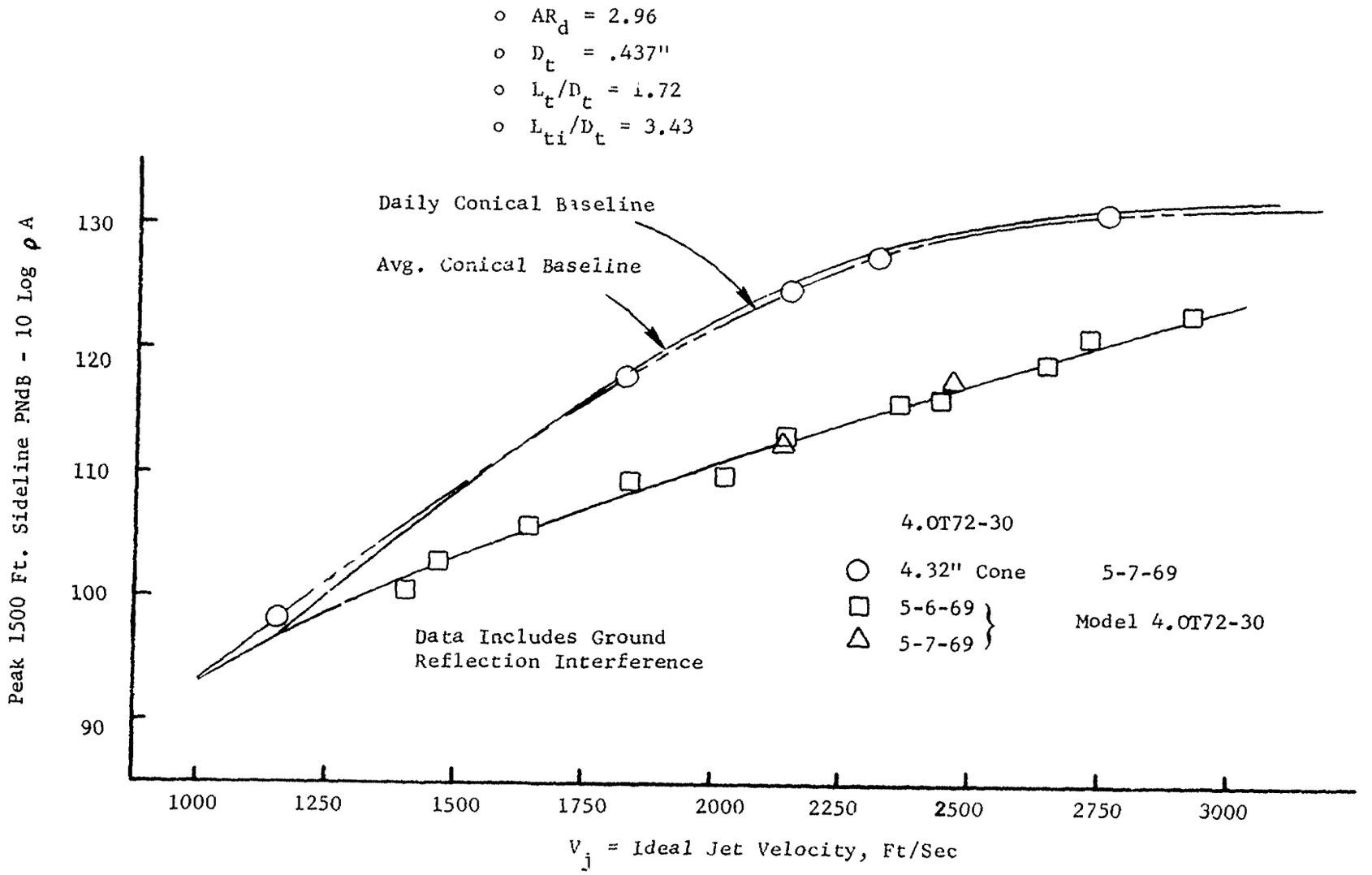

FIGURE V.F.2-16 1500 FT. SIDELINE JET NOISE LEVELS FOR A 72 TUBE NOZZLE WITH 30° BASEPLATE AND TUBE EXIT STAGGER

TABLE V.F.2-7 TEST SUMMARY

MODEL NO. 4.0T72-60

DESCRIPTION: 60° Base and Tube Exit Stagger, 72 Tube Nozzle

DATE: 5/7/69

SCALE MODEL A_8 = .075 ft^2

FULL SCALE A_8 = 4.80 ft^2

SCALE FACTOR = 8:1

- o DATA INCLUDES GROUND REFLECTION INTERFERENCE
- o ANGLE REFERENCED TO JET EXHAUST

RDG NO.	TEST CONDITIONS				ACOUSTIC TEST RESULTS						
			IDEAL			320' ARC		300' SIDELINE		1500' SIDELINE	
	P_{T8}/P_o	T_{T8} (°R)	V_j (ft/sec)	W_8 (PPS)	10 log ρA	PEAK PNdB	PEAK ANGLE	PEAK PNdB	PEAK ANGLE	PEAK PNdB	PEAK ANGLE
1	1.44	1160	1182	3.33	-7.1	109.6	60	109.3	80	91.7	80
2	1.60	1504	1469	3.16	-8.4	114.6	50	112.9	80	95.5	80
3	1.60	1255	1392	7.80	-7.6	114.3	50	112.8	80	95.2	80
4	1.80	1501	1644	3.73	-8.3	117.6	50	115.7	60	98.2	60
5	2.01	1523	1841	4.07	-8.2	121.8	40	118.9	50	101.5	50
6	2.30	1557	2012	4.54	-8.1	123.8	50	121.4	50	104.0	50
7	2.46	1660	2153	4.81	-8.2	126.0	40	122.3	50	105.2	50
8	2.71	2102	2535	4.39	-9.1	129.0	40	126.5	50	110.9	50
9	2.71	1807	2351	5.05	-8.3	128.3	40	126.0	50	109.3	50
10	2.93	2155	2633	4.78	-9.0	130.7	50	128.5	50	113.0	50
11	3.12	2228	2767	4.90	-9.0	132.7	50	130.5	50	115.0	50
12	3.21	2403	2906	5.05	-9.1	134.5	50	132.3	50	116.6	50
13	3.21	2616	3030	4.65	-10.0	135.1	50	132.9	50	117.3	50
14	3.40	2666	3124	5.23	-9.4	135.8	50	133.6	50	117.9	50

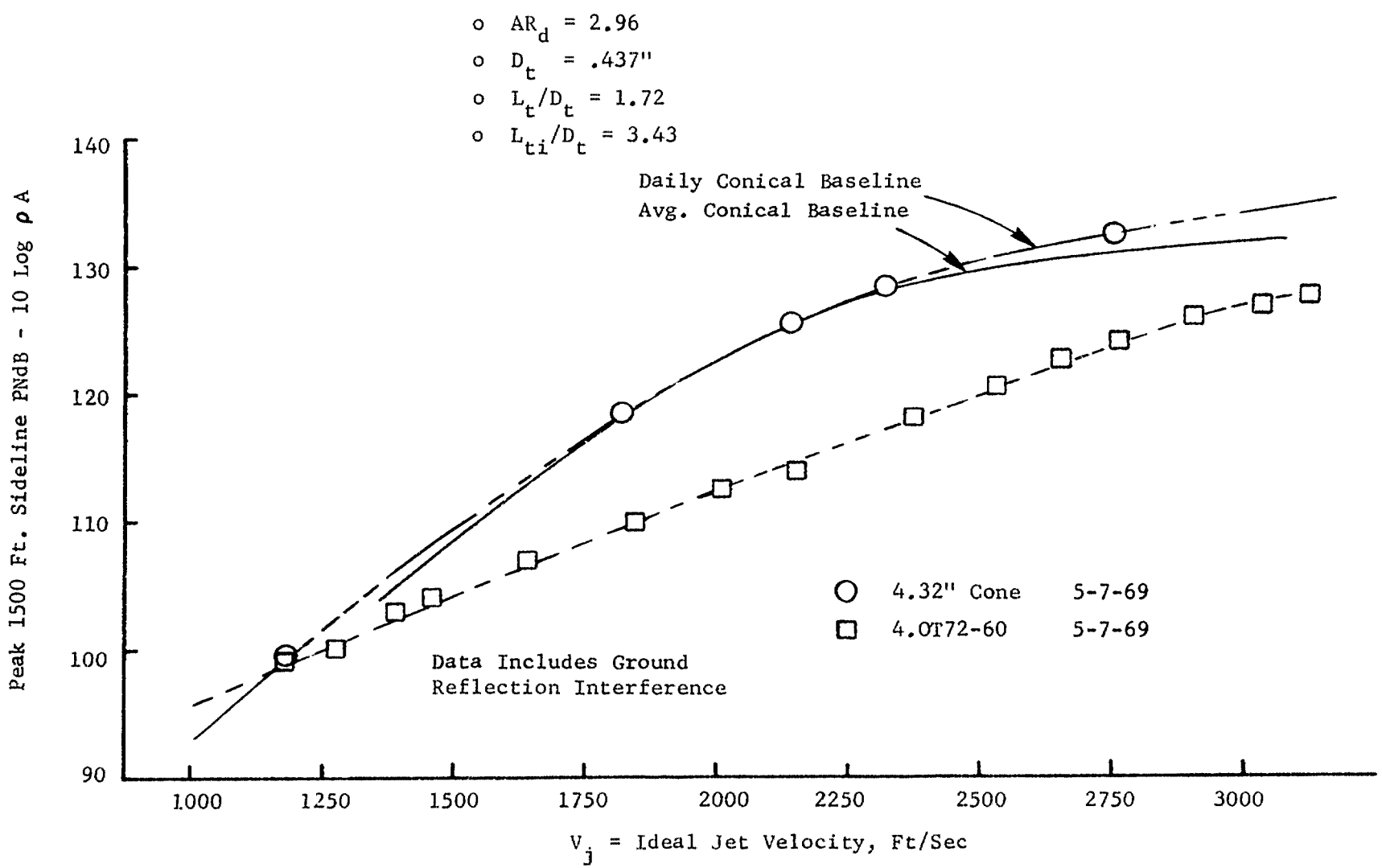

FIGURE V.F.2-18 1500 FT. SIDELINE JET NOISE LEVELS FOR A 72 TUBE NOZZLE WITH 60° BASEPLATE AND TUBE EXIT STAGGER

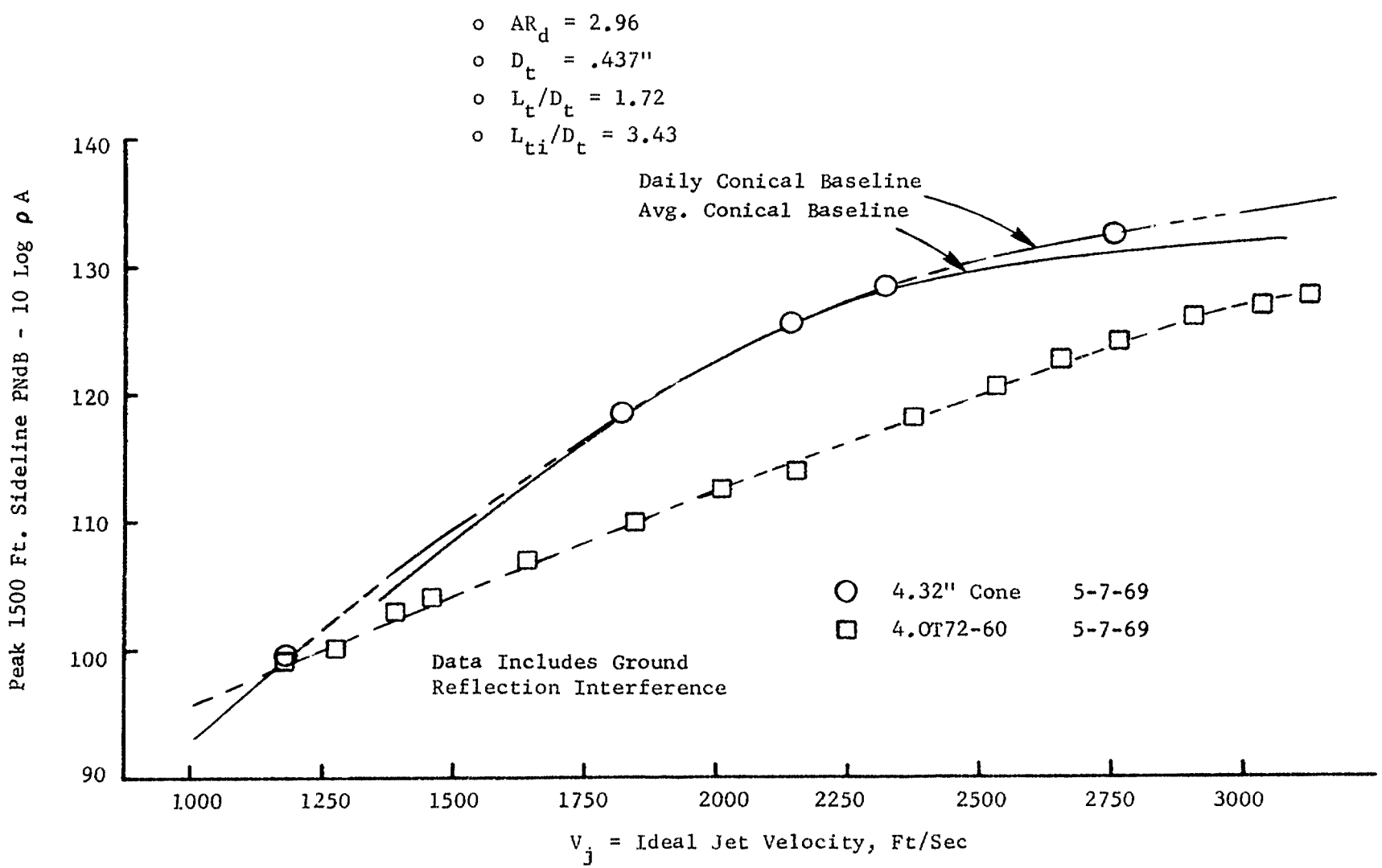

FIGURE V.F.2-18 1500 FT. SIDELINE JET NOISE LEVELS FOR A 72 TUBE NOZZLE WITH 60° BASEPLATE AND TUBE EXIT STAGGER

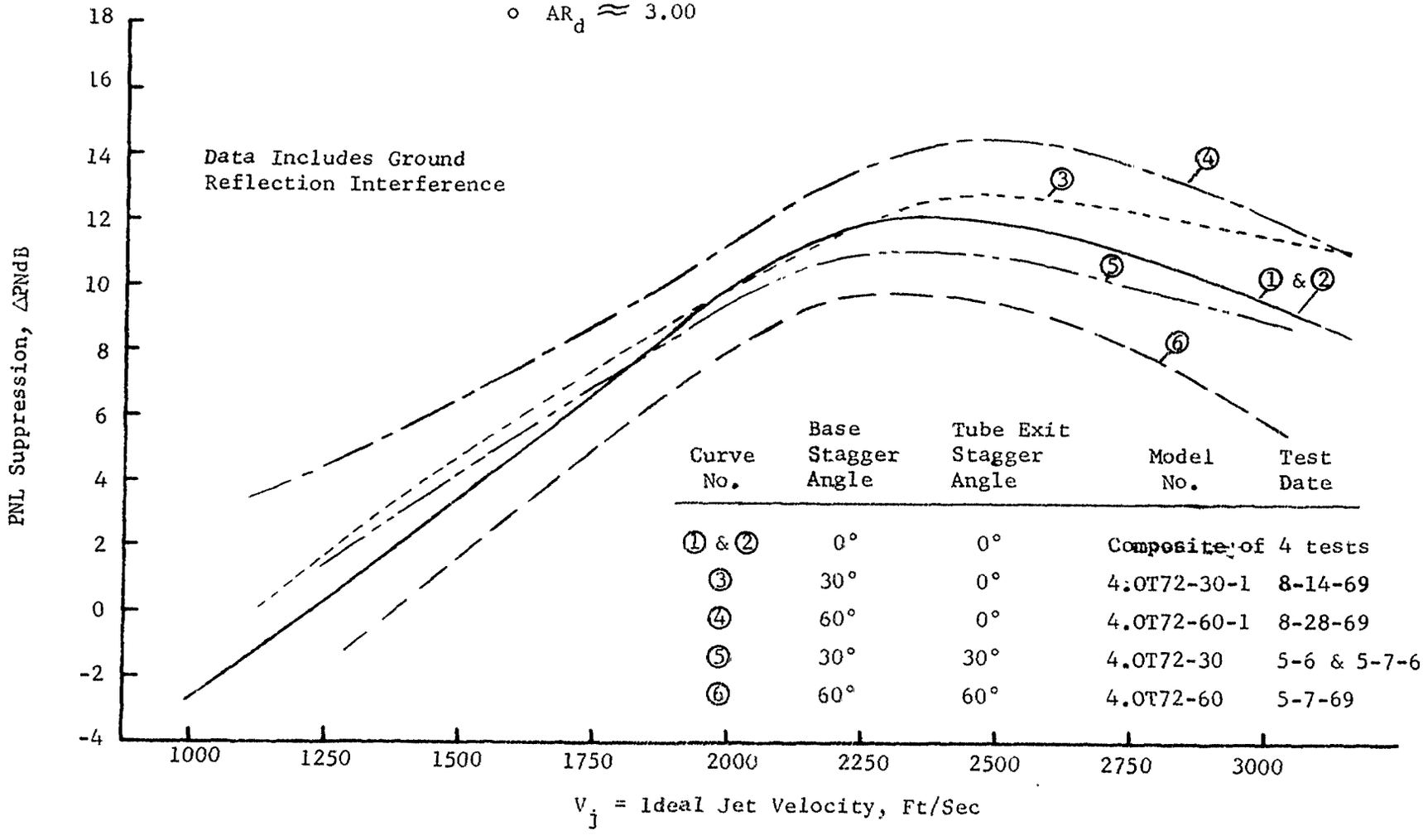

FIGURE V.F.2-19 EFFECT OF BASEPLATE AND TUBE EXIT PLANE STAGGER ON 300 FT. SIDELINE PNL SUPPRESSIONS FOR A 72 TUBE NOZZLE

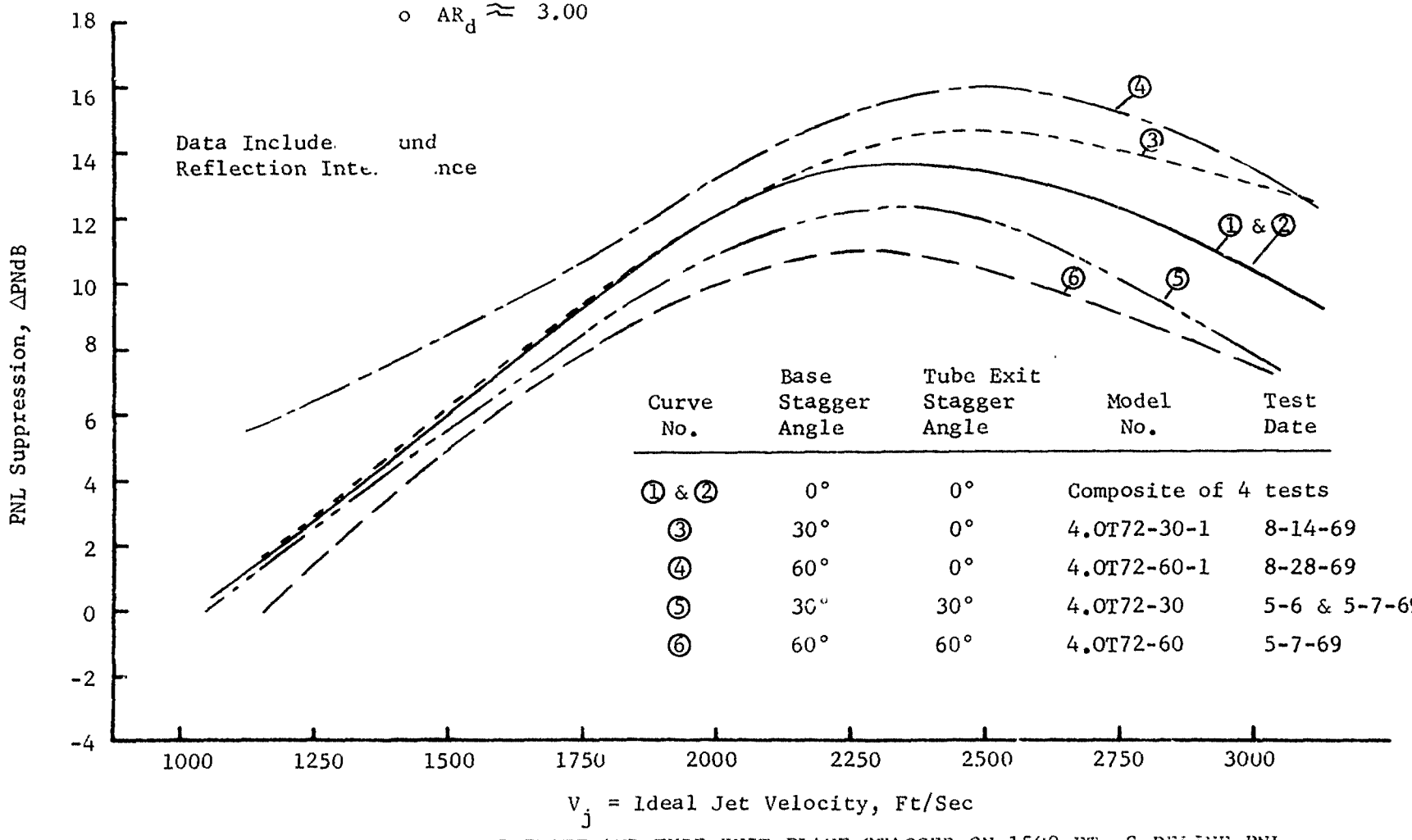

FIGURE V.F.2-20 EFFECT OF BASEPLATE AND TUBE EXIT PLANE STAGGER ON 1500 FT. SIDELINE PNL SUPPRESSIONS FOR A 72 TUBE NOZZLE

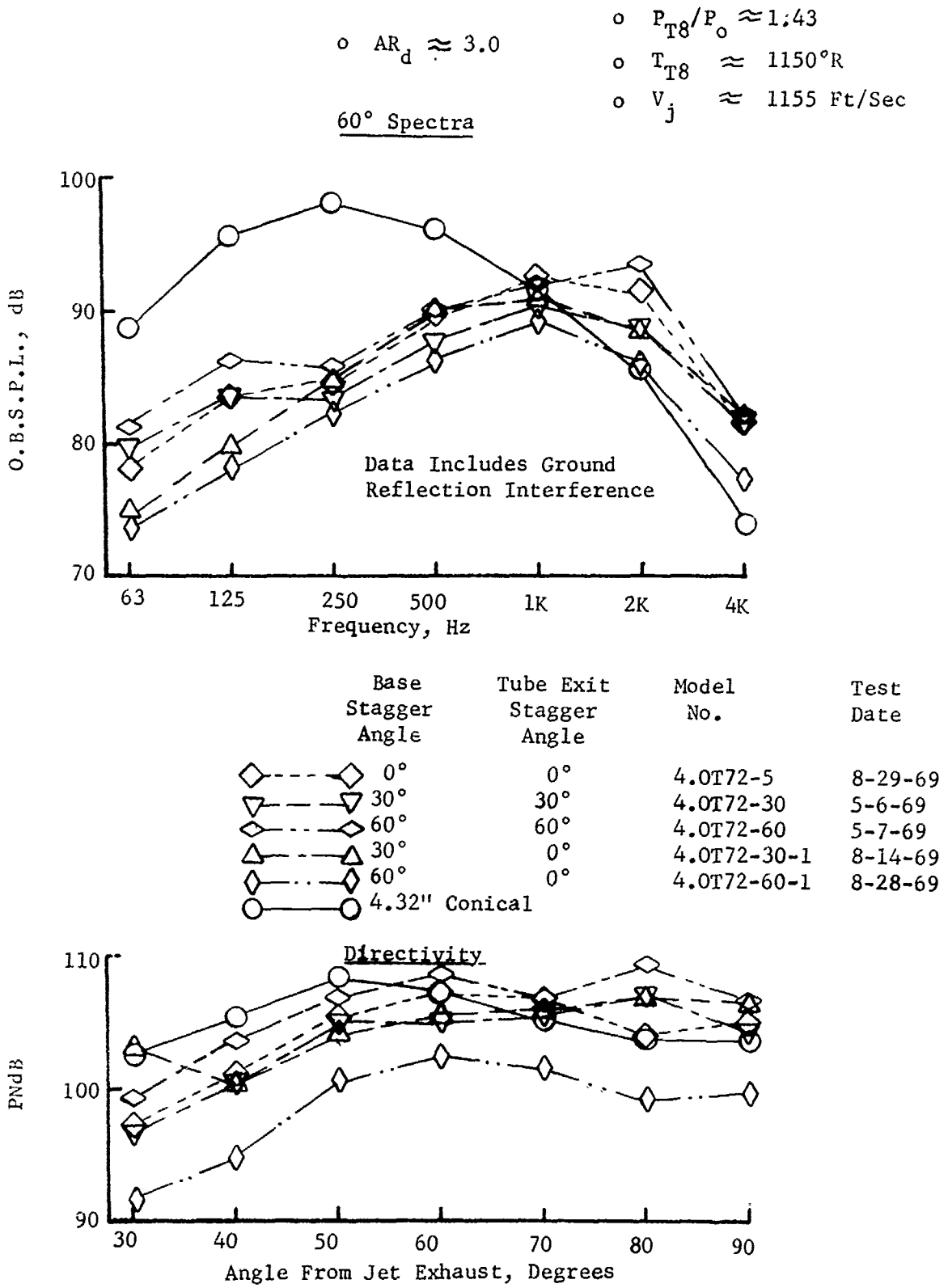

FIGURE V.F.2-21A EFFECT OF BASEPLATE AND TUBE EXIT PLANE STAGGER ON 300 FT. SIDELINE SPECTRA AND DIRECTIVITY

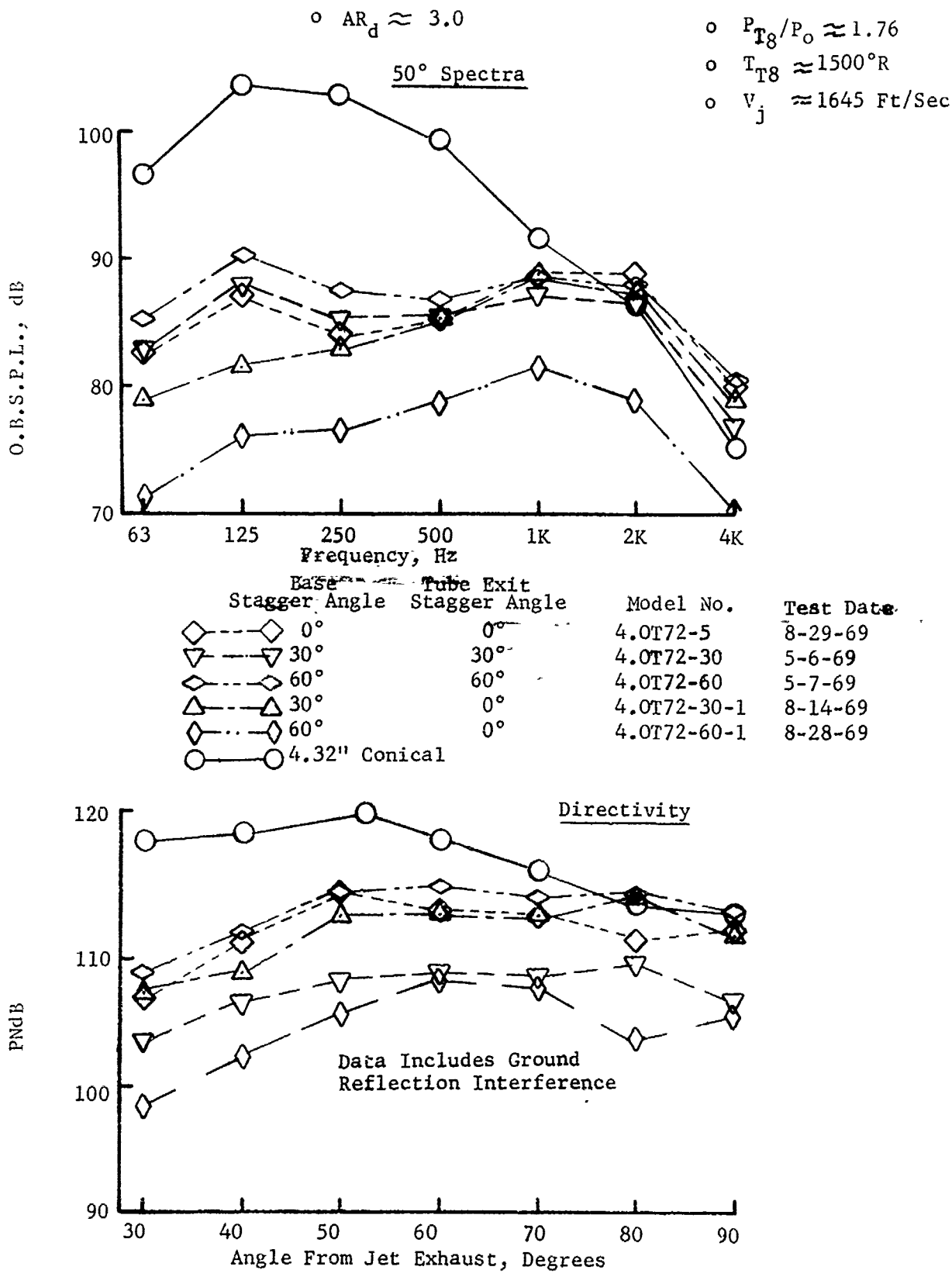

FIGURE V.F.2-21B EFFECT OF BASEPLATE AND TUBE EXIT PLANE STAGGER ON 300 FT. SIDELINE SPECTRA AND DIRECTIVITY

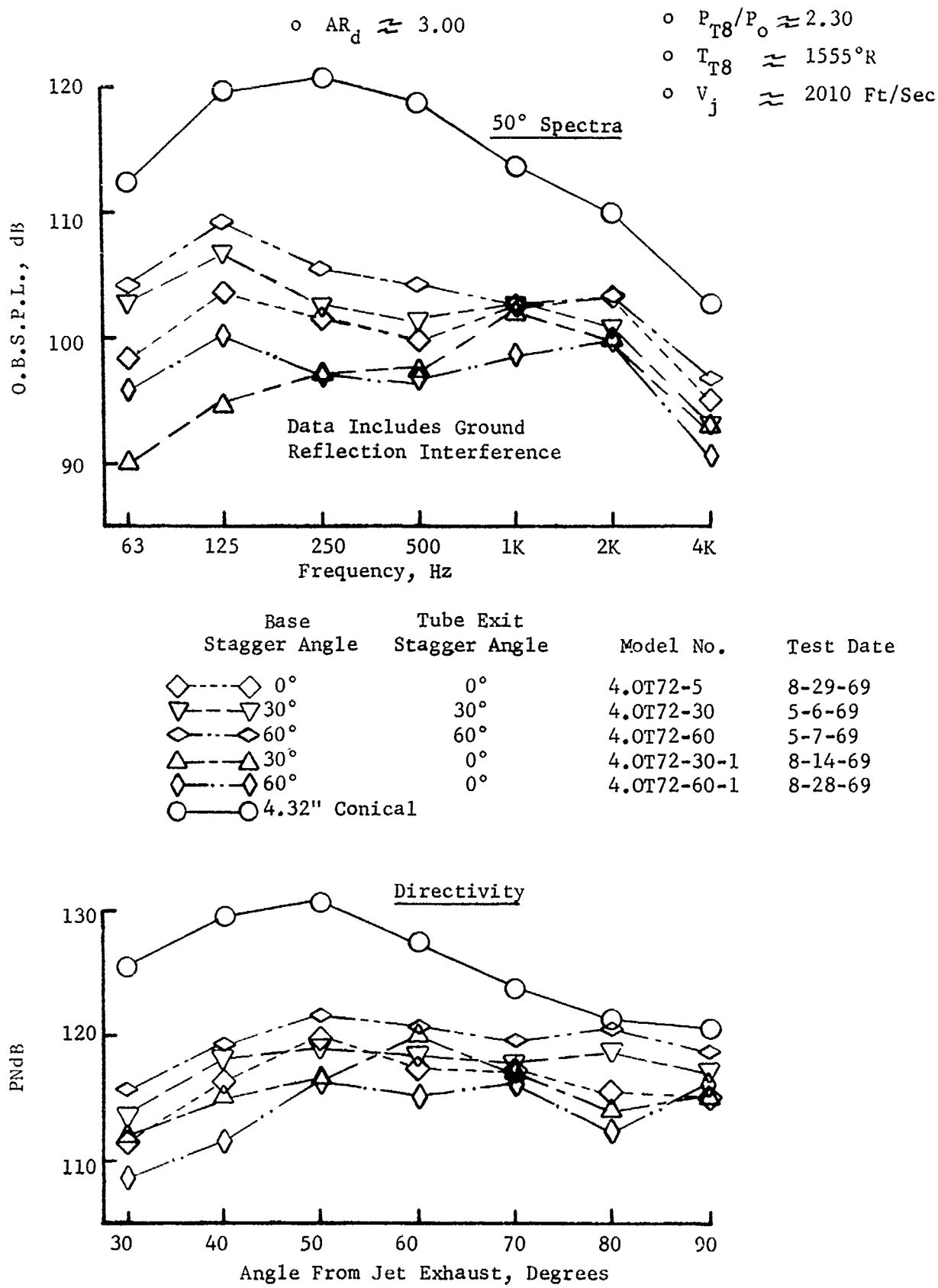

FIGURE V.F.2-21C EFFECT OF BASEPLATE AND TUBE EXIT PLANE STAGGER ON 300 FT. SIDELINE SPECTRA AND DIRECTIVITY

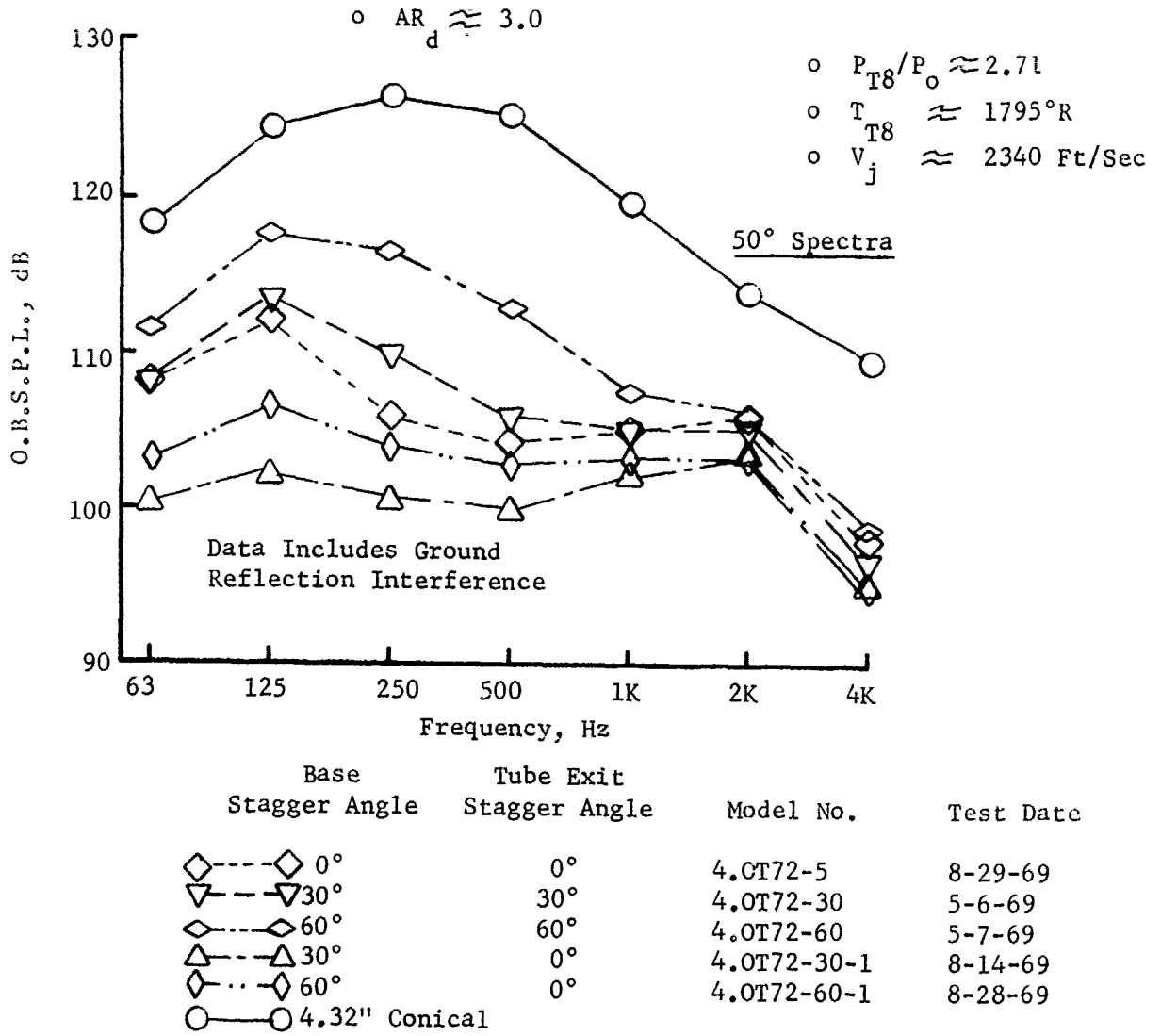

Base Stagger Angle	Tube Exit Stagger Angle	Model No.	Test Date
0°	0°	4.0T72-5	8-29-69
30°	30°	4.0T72-30	5-6-69
60°	60°	4.0T72-60	5-7-69
30°	0°	4.0T72-30-1	8-14-69
60°	0°	4.0T72-60-1	8-28-69
4.32" Conical			

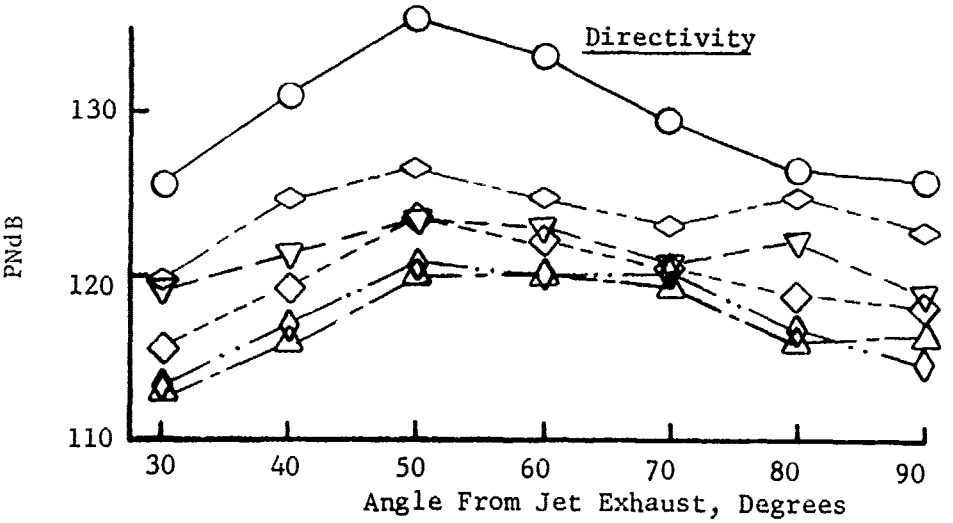

FIGURE V.F.2-21D EFFECT OF BASEPLATE AND TUBE EXIT PLANE STAGGER ON 300 FT. SIDELINE SPECTRA AND DIRECTIVITY

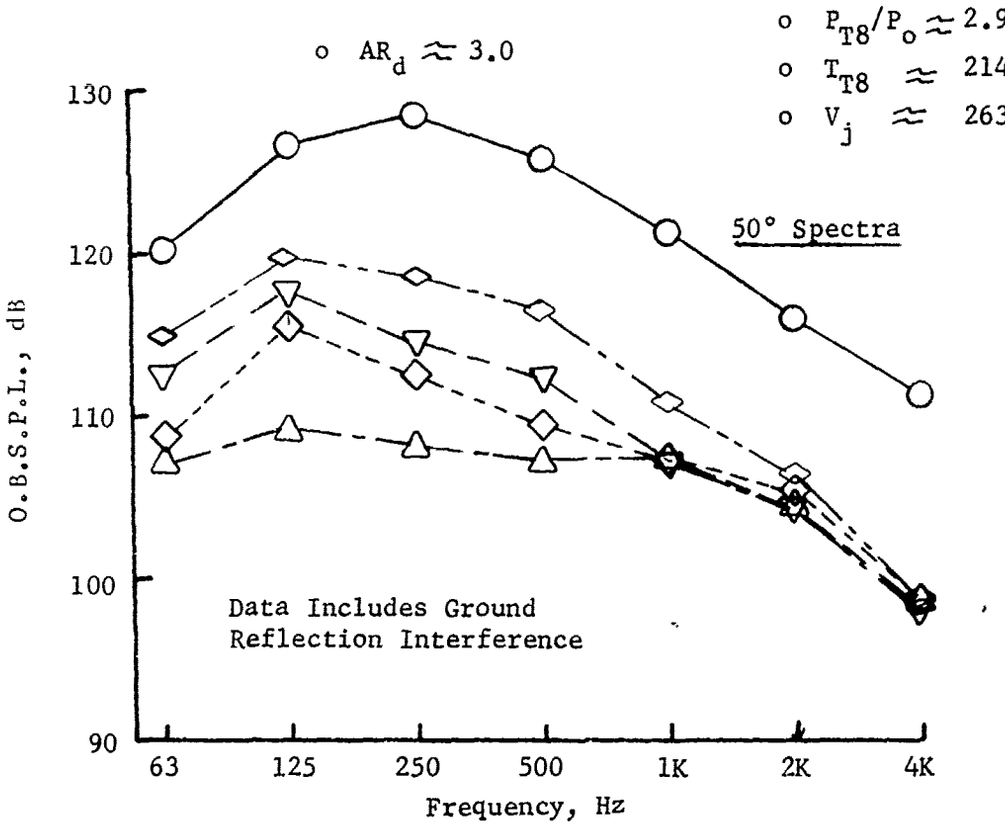

o For Symbol Designation, See Previous Figure

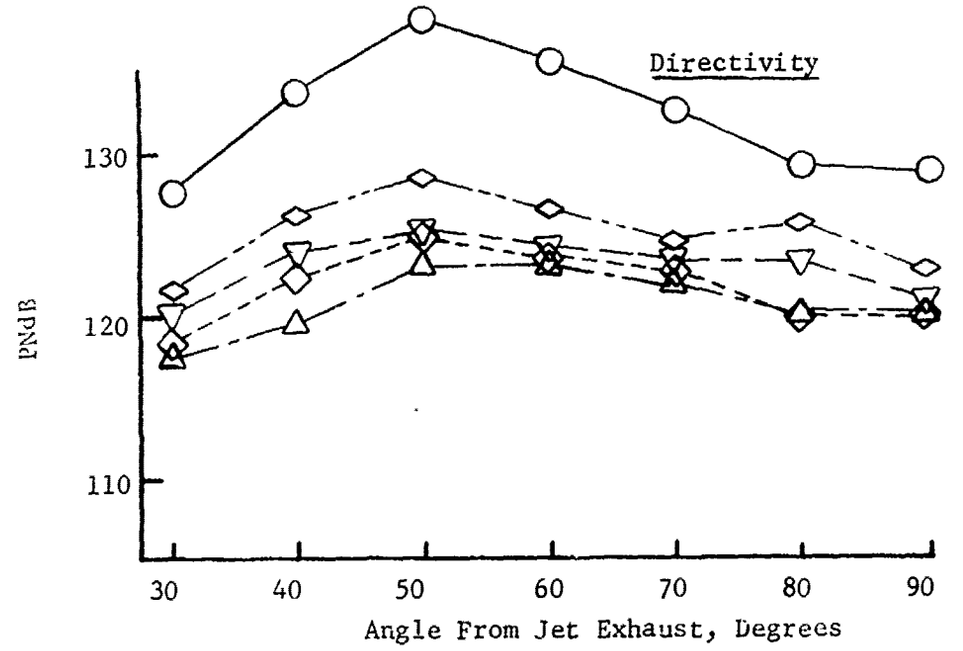

FIGURE V.F.2-21E EFFECT OF BASEPLATE AND TUBE EXIT PLANE STAGGER ON 300 FT. SIDELINE SPECTRA AND DIRECTIVITY

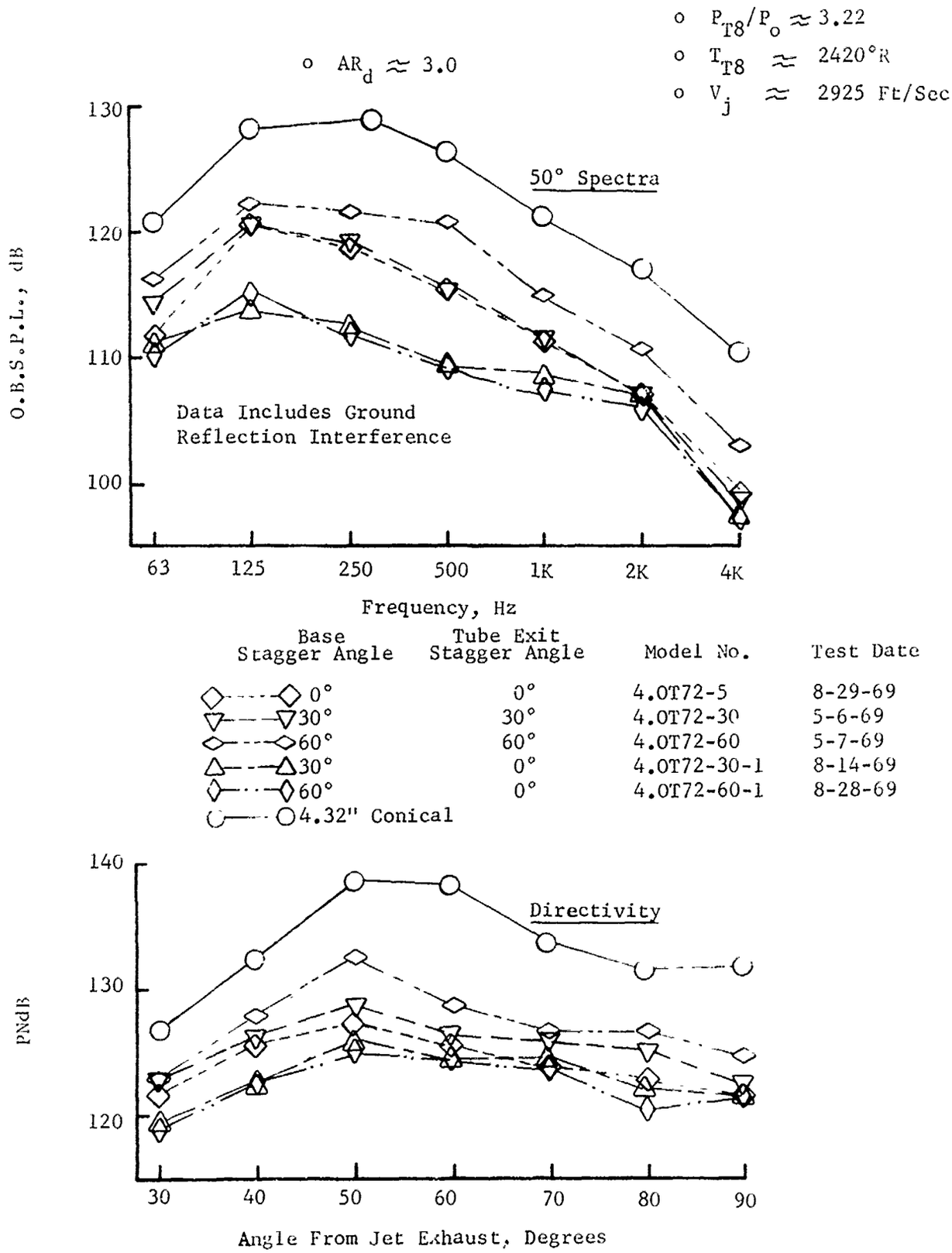

FIGURE V.F.2-21F EFFECT OF BASEPLATE AND TUBE EXIT PLANE STAGGER ON 300 FT. SIDELINE SPECTRA AND DIRECTIVITY

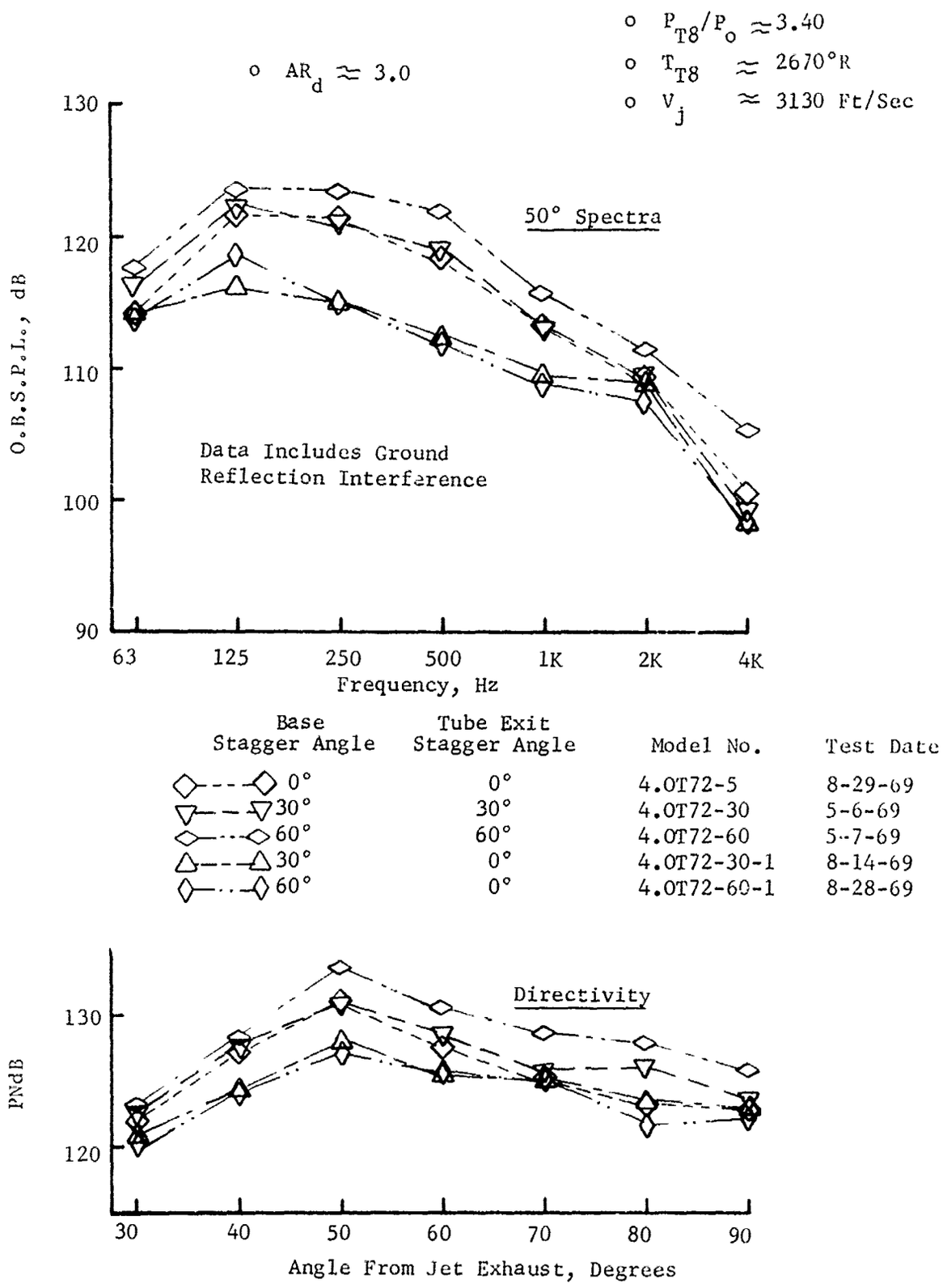

FIGURE V.F.2-216 EFFECT OF BASEPLATE AND TUBE EXIT PLANE STAGGER ON 300 FT. SIDELINE SPECTRA AND DIRECTIVITY

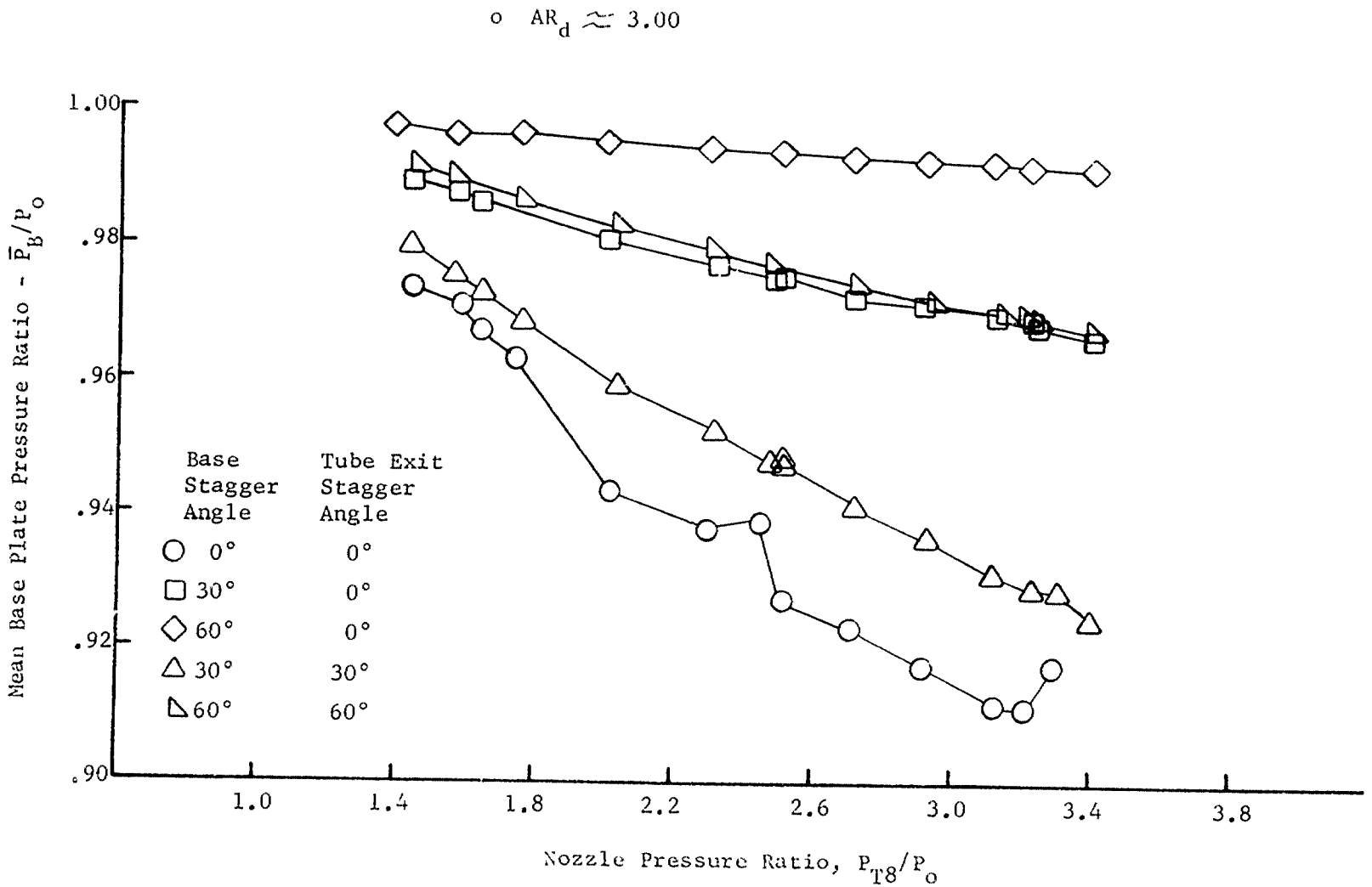

FIGURE V.F.2-22 EFFECT OF BASEPLATE AND TUBE EXIT PLANE STAGGER ON MEAN BASEPLATE PRESSURE RATIO

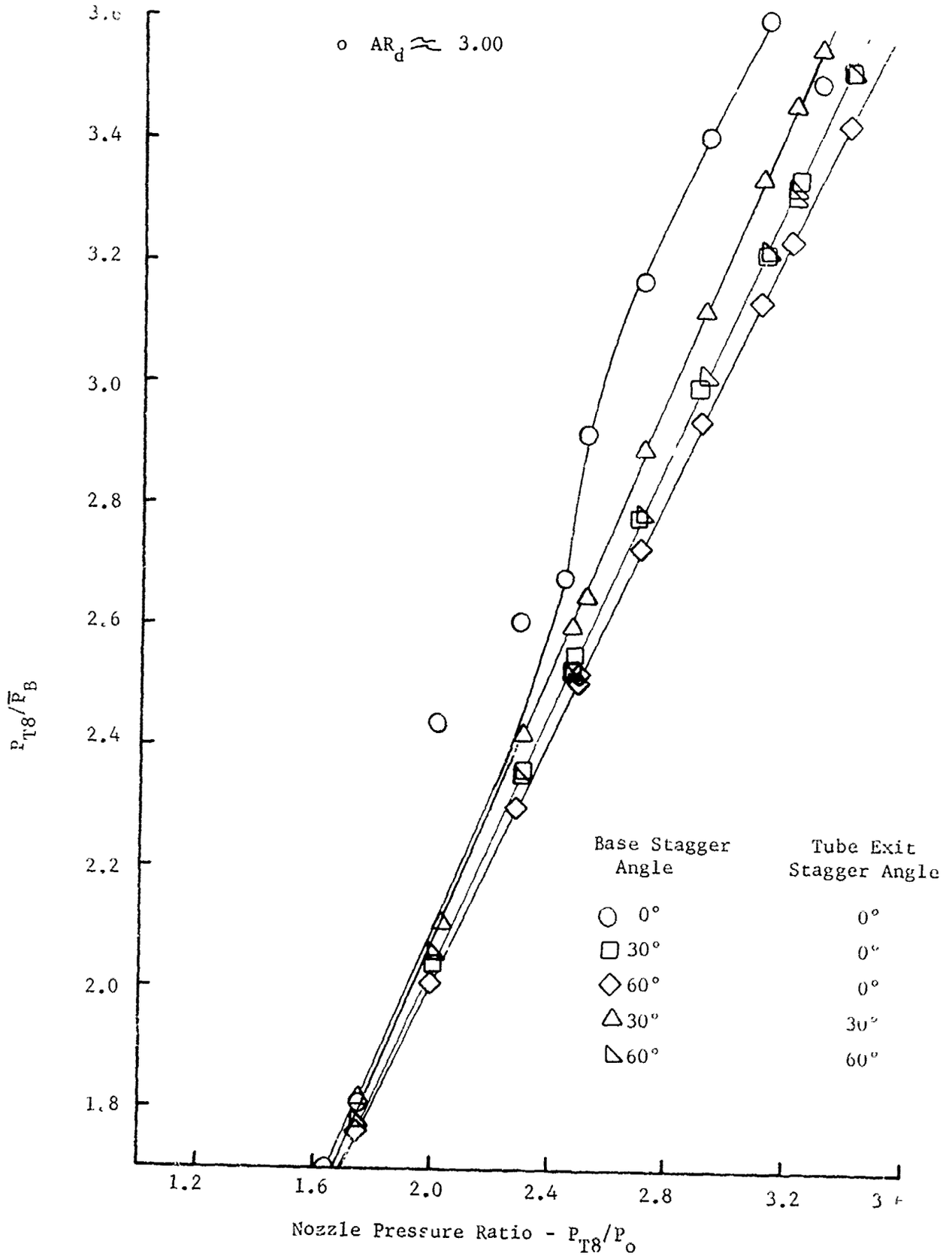

FIGURE V.F.2-23 EFFECT OF BASEPLATE AND TUBE EXIT PLANE STAGGER ON NOZZLE EXIT TO MEAN BASEPLATE PRESSURE RATIO

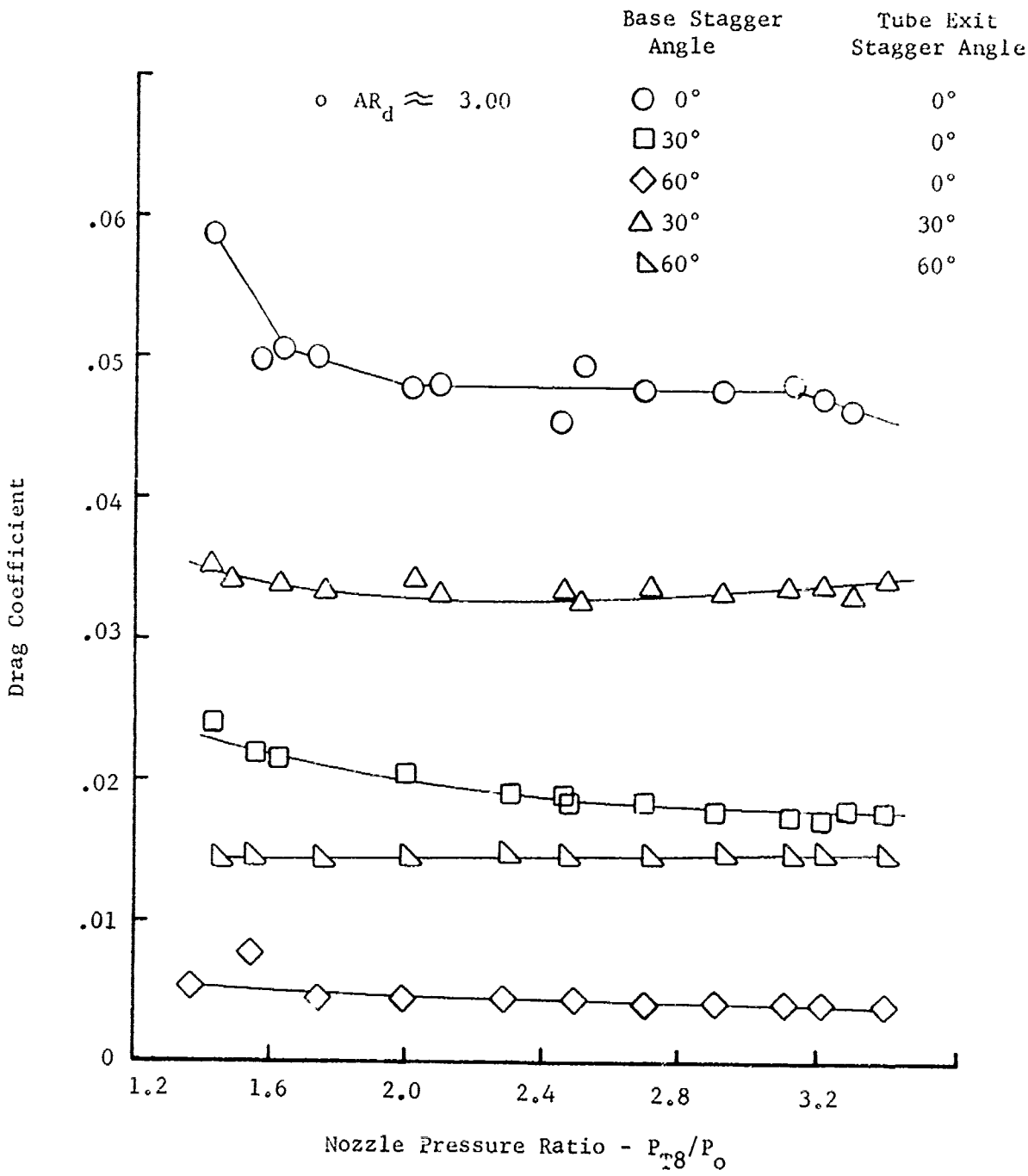

FIGURE V.F.2-24 EFFECT OF BASEPLATE AND TUBE EXIT PLANE STAGGER ON BASEPLATE DRAG COEFFICIENT

V.F.3 VARIATIONS OF A 37 TUBE NOZZLE

PRECEDING PAGE BLANK-NOT FILMED

V.F.3 VARIATIONS OF 37 TUBE NOZZLE

Introduction and Test Purpose

A significant number of suppressor configurations were investigated around a basic array of 37 long tubes. The bulk of the basic hardware was borrowed from The Boeing Company. The major items consisted of:

- A non-cooled baseplate assembly with an area ratio of 4.0.
- Three water-cooled baseplate assemblies at area ratios of 3.5, 4.1 and 5.3 (Figure V.F.3-9).
- A set of 37 Greatrex tubes for the non-cooled baseplate (Figure V.F.4-4).
- A set of columbium-coated high-temperature tubes for the water cooled baseplates.
- A bulk fiberglass lined ejector (Figure V.F.3-1).

The baseplate hardware formed the basic building block. By making various sets of 37 tubes, studies were performed to investigate tube exit geometric variations including Greatrex, straight, convergent and canted. An additional non-cooled baseplate with an area ratio (AR_d) of 3.0 was made to complement the Boeing baseplate (area ratio of 4.0). Tube exit geometric variations were studied at both area ratios. These tube exit variations are completely documented in Section V.F.4, the tube designs being shown in Figure V.F.4-1 and an assembly schematic and photograph of hardware appearing in Figures V.F.-2 and -4, respectively.

A second study involved the basic 37 Greatrex end tube design in the non-cooled baseplate (AR_d = 4.0). It served as one of the primary nozzle systems within an acoustic ejector study. Boeing's Fiberglass lined cylindrical ejector was used (Figure V.F.3-1) in addition to a Rigimesh lined ejector (Figure V.G-7) and a Cerafelt-packed porous face-plate ejector (Figure V.G-18). The acoustic ejector study is fully documented in Section V.G, showing the additional suppression gain attributable to treatment application. The absolute levels of suppression attained by the total system of primary suppressor, secondary ejector, and acoustic treatment, are documented in this section for the Fiberglass and Rigimesh liners.

PRECEDING PAGE BLANK-NOT FILMED

A third study involving the basic 37 tube array used the three Boeing water cooled baseplate assemblies for area ratios of 3.5, 4.1 and 5.3. (Figure V.F.3-9). A set of 37 convergent end stainless steel tubes was built and tested within each baseplate. Prior to this series, all tests with an array of 37 long tubes were temperature limited, the hardware capable of withstanding only 1500° F (1960 ° R). Combined with the cycle pressure ratio range of interest, a maximum jet velocity of about 2500 ft/sec was attainable. However, the acoustic range of interest was up to about 3100 ft/sec.

The Boeing water cooled baseplate hardware was tested to a maximum of 2700° R and 3150 ft/sec jet velocity. (Baseplate hole nozzles within other parametric studies, e.g., Section V.F.9, were normally tested to 2650° R and 3150 ft/sec V_j). Thus, particular points of interest could be studied; namely, a) to determine whether attainable suppression at very high jet velocity dropped considerably with the low number of long tubes, and b) to determine whether area ratio influence at very high jet velocity was as significant for a low number of long tubes as it was for a higher number of holes within a baseplate. The study with 37 tubes at high temperature/ jet velocity is documented in this section.

Scale model acoustic measurements were taken on the General Electric, Evendale, JENOTS facility around a 40 ft. arc. These measurements were then scaled by frequency and size to full scale application using a scale factor of 8:1. All data presented are, therefore, of simulated engine size and engine frequency range.

Test Configurations and Results

o 37 Greatrex Tube Primary with Acoustic Ejectors

The 37 Greatrex tube primary nozzle of area ratio = 4.0 was fitted with a Fiberglass packed acoustic ejector as Model 4.1 T37-10CS in Figure V.F.3-1. A photograph of the primary nozzle is shown in Figure V.F.4-4 and a schematic of the Greatrex convolutions is shown on the right side of Figure V.F.10-23. Without the tube cover, as was this configuration, the external tube length to equivalent tube flow diameter, L_t/D_t, was 8.0. The ejector was tightly spaced with respect to the circumscribed tube diameter at D_S/D_{Td} = 1.55. The Fiberglass was retained in a 1" cavity with 40% open mesh.

The same primary nozzle, but using the tube cover for an $L_t/D_t = 1.5$, was fitted with a Rigimesh lined acoustic ejector as Model 4.1T37-10.8CSEL in Figure V.F.3-5. The ejector was cylindrical of 10.4" I.D. and of shroud length to internal diameter ratio, L_S/D_S, of 1.25 and of $D_S/D_{Td} = 1.20$.

Acoustic results of the tube-Fiberglass ejector system are summarized in Table V.F.3-1 and plotted in Figures V.F.3-2, -3 and -4. Table V.F.3-2 and Figures V.F.3-6, -7 and -8 contain similar information for the Rigimesh ejector system. The nozzles were tested at the JENOTS acoustic facility using a matrix of four P_{T8}/P_o points from nominal 1.46 to 2.70 and three T_{T8}'s of nominal 1140, 1500 and 1960° R at each P_{T8}/P_o point. The matrix was to establish dependency of suppression on pressure ratio and temperature rather than to follow an engine cycle running line.

The measurements for the two nozzles indicate:

- The combination of multi-elements, Greatrex convolutions, secondary ejector, and bulk Fiberglass absorption material, forms a highly effective suppression system, attaining up to 26 peak PNdB suppression within the test range.
- The shorter Rigimesh ejector is a more practical design and was also a highly effective suppressor system. It attained peak PNL suppression just under that of the Fiberglass ejector, the lower level possibly due to the shorter length of treatment.
- The noise generation and subsequent suppression levels attained by the multi-element systems is very dependent on the pressure ratio/temperature combination used to attain a specific jet velocity. For example, with the Rigimesh system at a velocity of 2000 ft/sec, 3.5 PNdB additional suppression is gained at the 1500 ft. sideline by testing at the pressure ratio of 1.85 instead of 2.7 with the corresponding change in T_8 to attain that velocity. In general the suppression is decreased with increase in pressure ratio at a chosen jet velocity.
- The 1500 ft. sideline peak PNL suppressions are above those at the 300 ft. sideline due to the additional high frequency attenuation with increased distance.

o 37 Tube High Temperature Nozzles, AR_d = 3.5, 4.1, & 5.3

The baseplates and tube hardware for the high temperature tube study are shown in Figure V.F.3-9 with a schematic of the nozzle system in Figure V.F.3-10. Specifics of each tube bundle are tabulated on the schematic, the only major difference being the spacing between tubes which sets the area ratio. The three nozzles were acoustically tested at JENOTS using an engine cycle running line P_{T8}/P_o of 1.4 to 3.4, T_{T8} of 1150 to 2700° R and V_j range of 1175 to 3150 ft/sec. In addition, a 4.32" I.D. conical convergent nozzle was tested each day as the reference baseline.

The 300 and 1500 ft. sideline normalized peak PNL plots, forming the baseline to which the suppressor configurations are referenced, are presented in Figures V.F.3-11 and -12. For the suppressor configuration, the tabulated data, normalized peak PNL plots, and suppression plots are as follows:

AR_d = 3.5, Table V.F.3-3, Figures V.F.3-13, -14 & -15
AR_d = 4.1, Table V.F.3-4, Figures V.F.3-16, -17 & -18
AR_d = 5.3, Table V.F.3-5, Figures V.F.3-19, -20 & -21

Composites of the PNL suppression levels are done for the 300 and 1500 ft. sidelines in Figures V.F.3-22 and -23, respectively, to compare to area ratio effect. Spectra and directivity comparisons at the 300 ft. sideline, for the three area ratio models and the conical baseline, are presented in Figure V.F.3-24A through -24H. The plots are at incremental V_j points from 1170 to 3145 ft/sec.

Comparison of acoustic results from the three nozzles indicate:

o The suppression levels attained by the long tubes are quite high, particularly at the higher jet velocites, suppression at the 1500 ft. sideline being about 2 PNdB above the 300 ft. sideline.

By comparing the 37 long tube results of Figure V.F.3-23 to the results of the 85 hole nozzle parametric area ratio study in Figure V.F.9-21, several trends due to area ratio are seen.

a. Suppression drop-off rates from V_j of peak suppression to maximum V_j are of similar magnitudes for the long-tube area ratio of 3.5 and 4.1 models and the 85-hole (short tube) parametric results.

b. The 37 tube model with the largest area ratio of 5.3 retained its peak suppression at high V_j with no drop-off; however, no similar AR_d model was tested in the 85-hole nozzle series for comparison, the largest being $AR_d = 4.0$. The extrapolated ($AR_d = 4.5$) suppression level in Figure V.F.9-21 may be conservatively low at high V_j and very large area ratios may retain their peak suppressions into the high V_j range.

c. Again, as in the 85-hole parametric area ratio investigation, all high area-ratio suppression curves converge at low V_j, suggesting little relevance of that parameter at low V_j for an area ratio greater than 3.0.

o Study of the spectra plots in Figures V.F.3-24A through -24H, particularly in the range of high jet velocity, shows that the content of high frequency is nearly the same for the three area ratio nozzles. The low frequency levels are significantly more predominant with lower area ratio, the $AR_d = 3.5$ model being highest. The more compact spacing of tubes with low area ratio causes earlier coalescense of individual tube flows into a single jet producing the predominant low frequency noise.

• Model 4.1T37-10CS Acoustic Treated Ejector

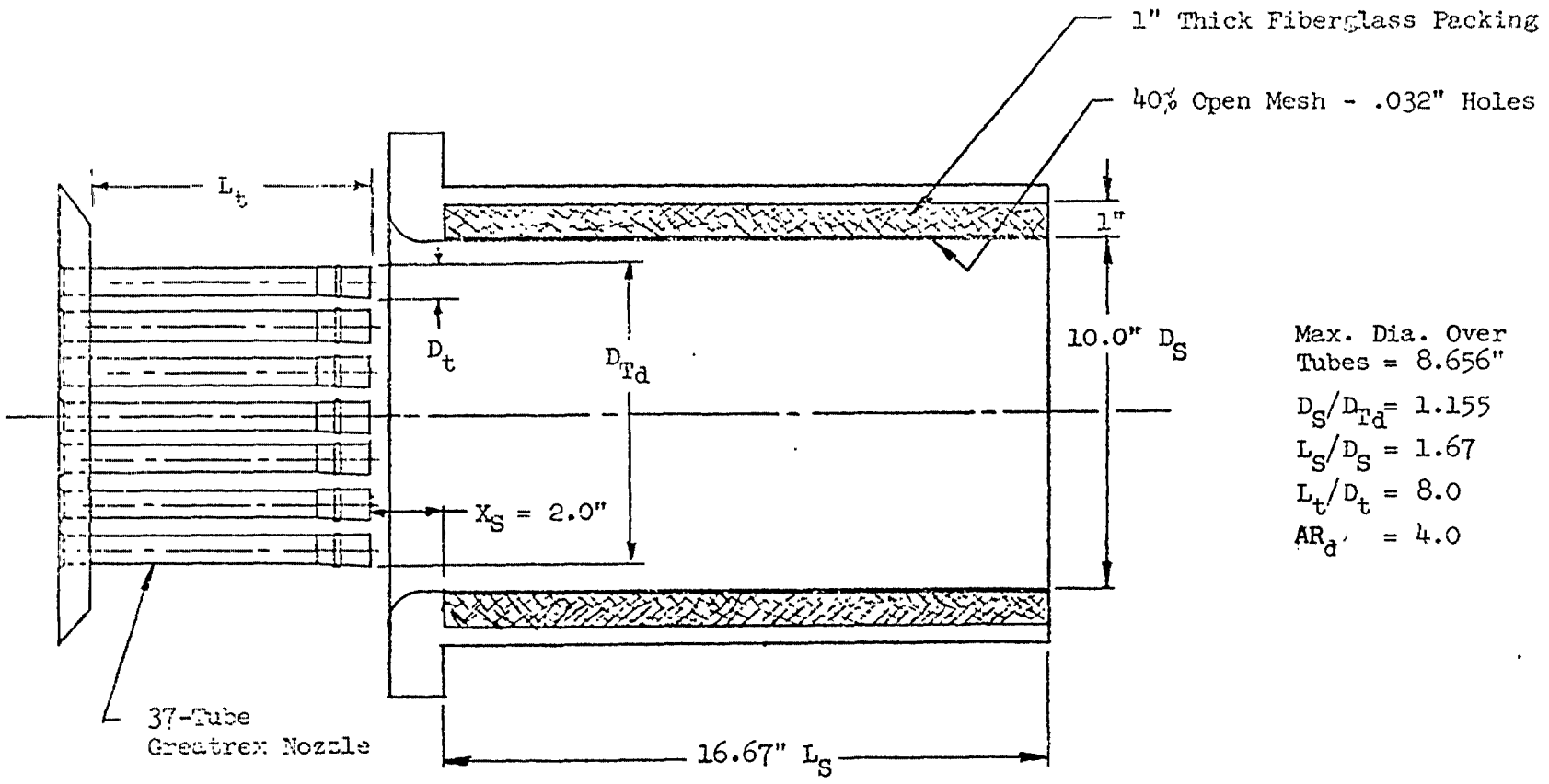

FIGURE V.F.3-1 SCHEMATIC OF 37 GREATREX TUBE NOZZLE WITH FIBERGLASS LINED EJECTOR

TABLE V.F.3-1 TEST SUMMARY

MODEL NO. 4.1-T37-10CS

DESCRIPTION: 37 Greatrex Tubes, AR_d=4.0, Fiberglass Lined Cylindrical Ejector

DATE: 8/6/68

SCALE MODEL A_8 = .0917 ft^2

FULL SCALE A_8 = 5.869 ft^2

SCALE FACTOR = 8:1

- o DATA INCLUDES GROUND REFLECTION INTERFERENCE
- o ANGLE REFERENCED TO JET EXHAUST

TEST CONDITIONS					ACOUSTIC TEST RESULTS							
			IDEAL				320' ARC		300' SIDELINE		1500' SIDELINE	
RDG NO.	P_{T8}/P_o	T_{T8} (°R)	V_j (ft/sec)	W_8 (PPS)	10Log $\rho^2 A$	10Log ρA	PEAK PNdB	PEAK ANGLE	PEAK PNdB	PEAK ANGLE	PEAK PNdB	PEAK ANGLE
1	1.45	1140	1176	3.76	-20.9	-6.6	102.1	50	99.7	50	81.0	50
2	1.83	1130	1477	4.91	-20.3	-6.3	107.2	50	105.2	70	87.2	70
3	2.25	1140	1701	6.19	-19.9	-6.0	111.9	50	109.5	50/70	91.6	70
4	2.68	1130	1850	7.51	-19.2	-5.6	114.6	50	112.2	50/70	94.4	70
5	2.69	1495	2131	6.33	-21.7	-6.8	114.8	50	112.9	70	95.2	70
6	2.26	1495	1950	5.18	-22.2	-7.2	111.7	50	110.3	70	92.5	70
7	1.83	1480	1695	4.10	-22.7	-7.5	108.5	50	106.3	60	88.0	60
8	1.46	1480	1354	3.02	-23.1	-7.7	101.9	50	99.5	50	80.9	50
9	2.69	1750	2306	5.80	-23.0	-7.5	115.1	50	113.2	60	95.2	60
10	2.69	1960	2439	5.40	-24.0	-8.0	114.3	50	113.7	70	96.0	70
11	2.26	1960	2233	4.49	-24.6	-8.4	111.5	50	110.7	70	92.1	70
12	1.84	1960	1952	3.53	-25.1	-8.7	107.8	50	106.4	70	88.5	70
13	1.46	1950	1557	2.58	-25.5	-8.9	101.3	50	99.4	70	81.5	70

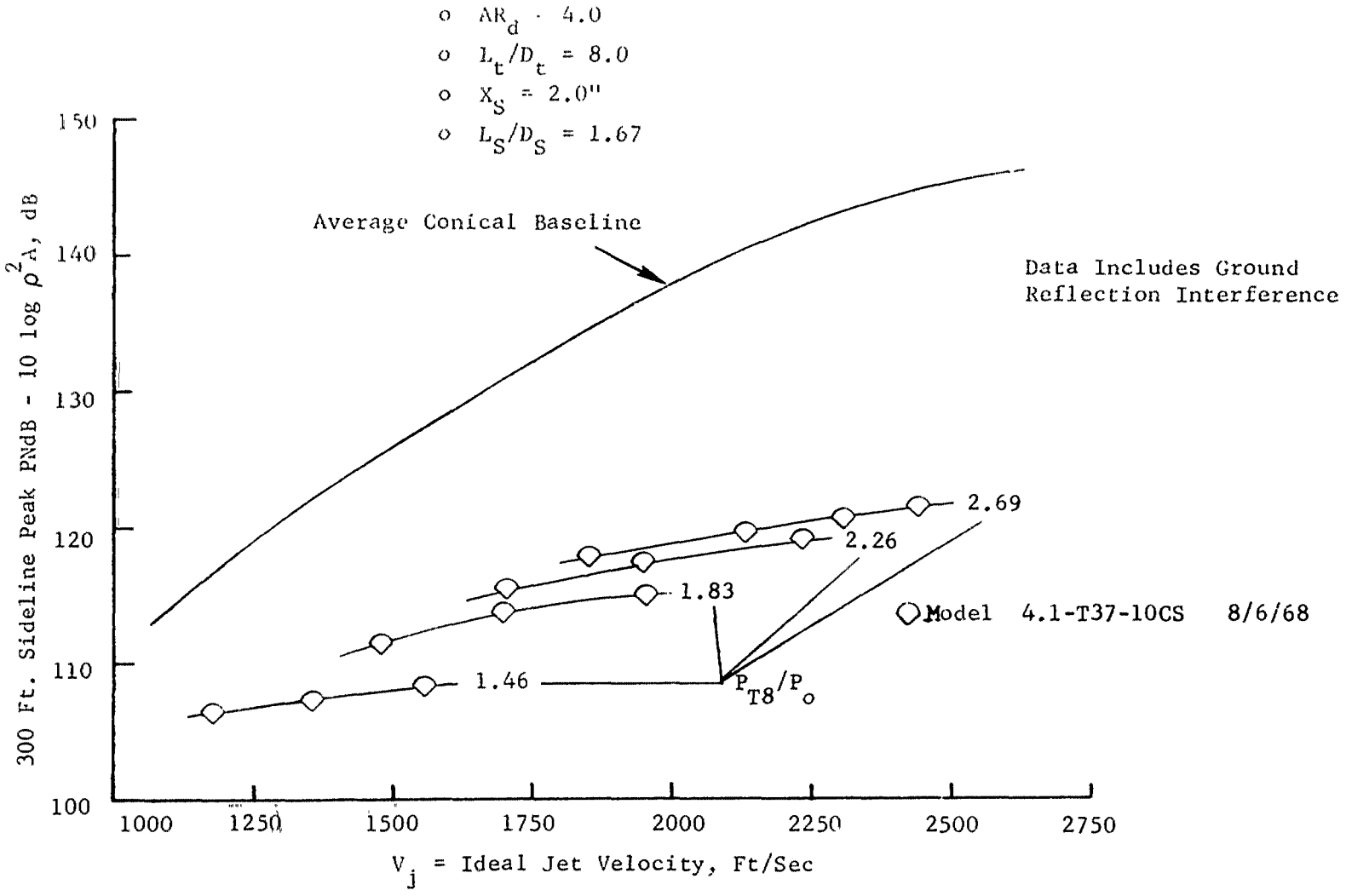

FIGURE V.F.3-2 300 FT. SIDELINE JET NOISE LEVELS FOR 37 GREATREX TUBE + FIBERGLASS EJECTOR

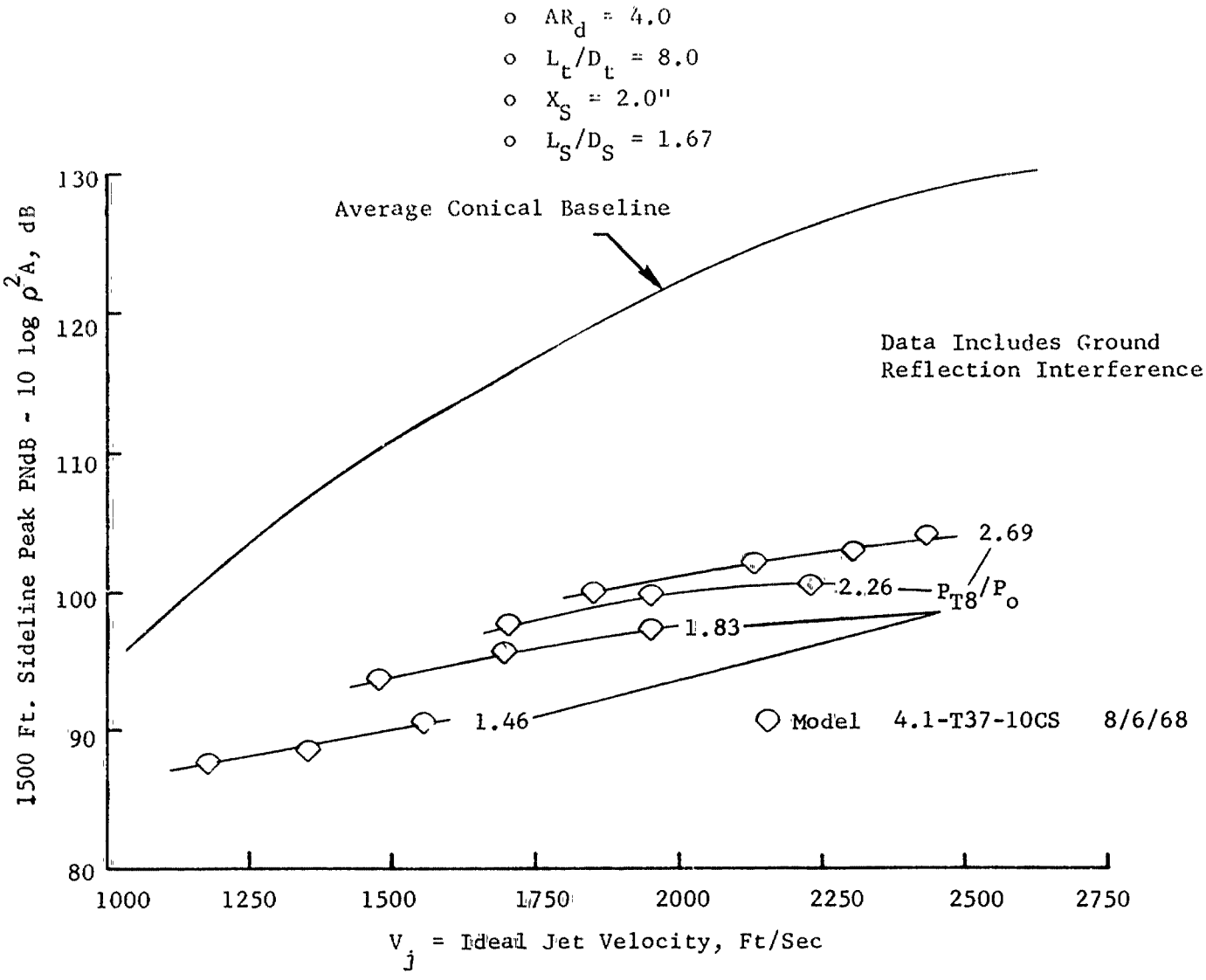

FIGURE V.F.3-3 1500 FT. SIDELINE JET NOISE LEVELS FOR 37 GREATREX TUBE + FIBERGLASS EJECTOR

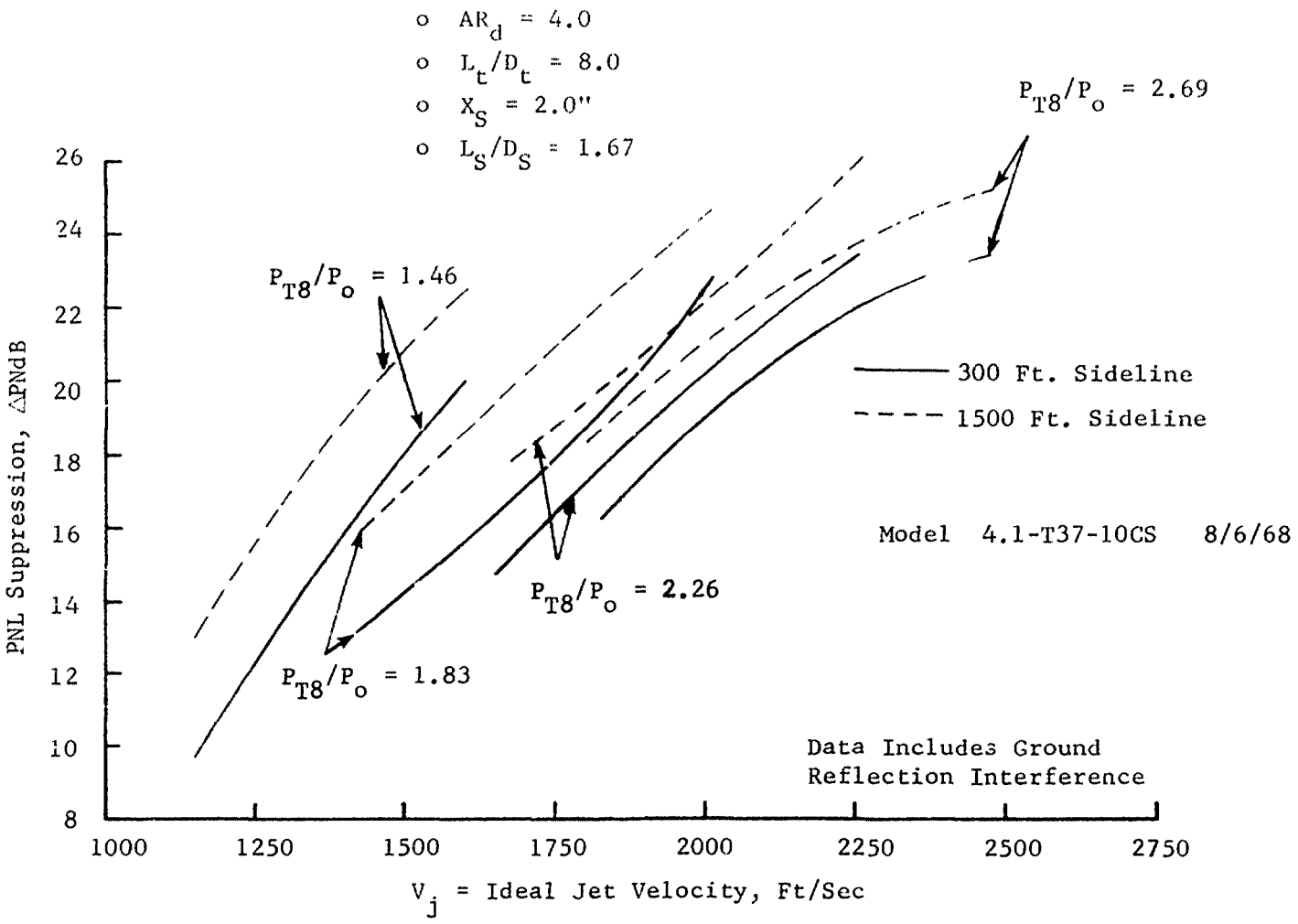

FIGURE V.F.3-4 300 & 1500 FT. SIDELINE PNL SUPPRESSION LEVELS FOR 37 GREATREX TUBE + FIBERGLASS EJECTOR

• Model 4.1T37-10.8 CSEL - 13" L_S Rigimesh Ejector

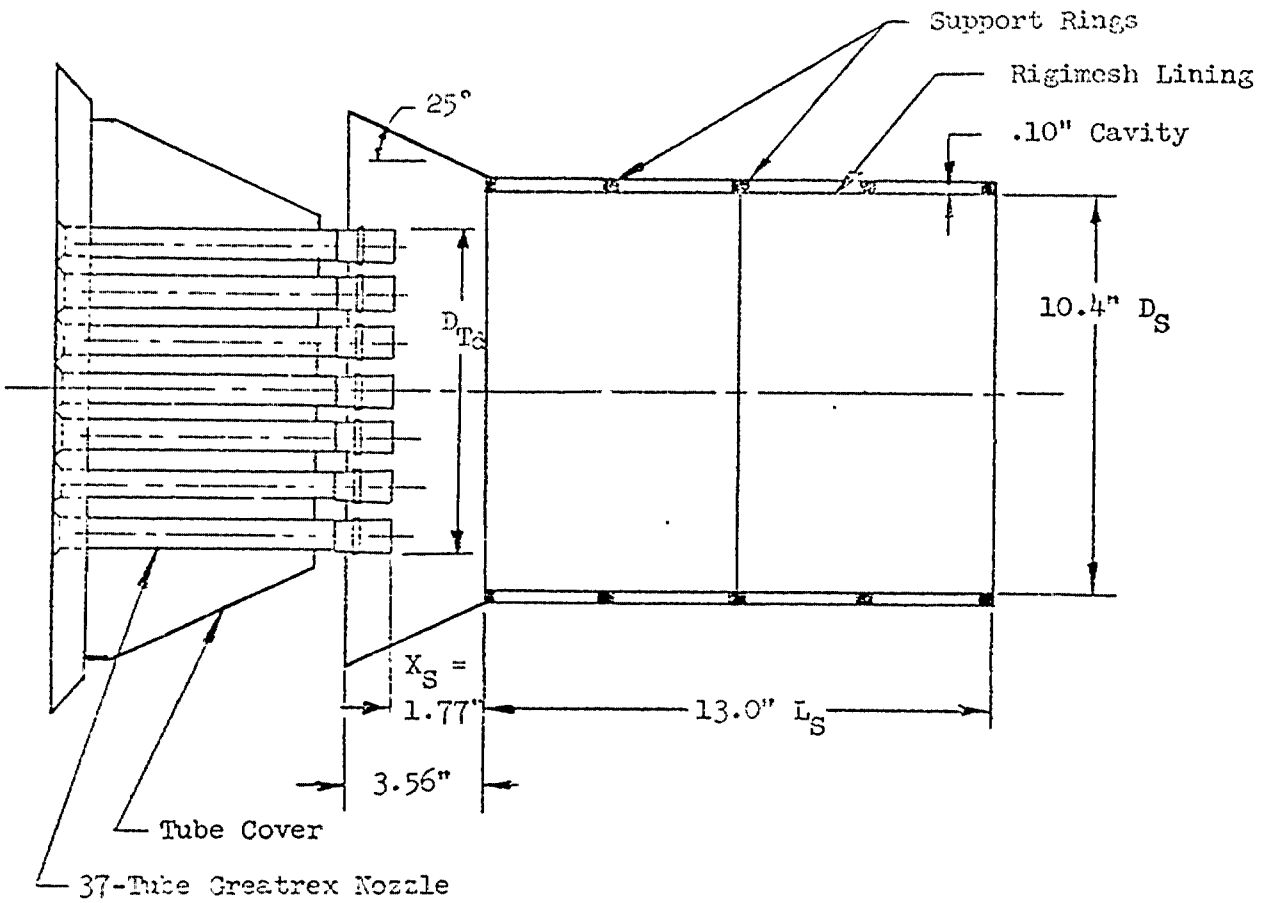

D_{Td} = Max. Dia.
Over Tubes = 8.656"

D_S/D_{Td} = 1.20
L_t/D_t = 1.5
AR_d = 4.0
L_S/D_S = 1.25

FIGURE V.F.3-5 SCHEMATIC OF 37 GREATREX TUBE NOZZLE WITH RIGIMESH LINED EJECTOR

TABLE V.F.3-2 TEST SUMMARY

MODEL NO. 4.1-T37-10CSEL

DESCRIPTION: 37 Greatrex Tubes, AR_d=4.0, Rigimesh Lined Cylindrical Ejector

DATE: 8/12/68

SCALE MODEL A_8 = .0917 ft^2

FULL SCALE A_8 = 5.869 ft^2

SCALE FACTOR = 8:1

- o DATA INCLUDES GROUND REFLECTION INTERFERENCE
- o ANGLE REFERENCED TO JET EXHAUST

TEST CONDITIONS					ACOUSTIC TEST RESULTS							
			IDEAL				320' ARC		300' SIDELINE		1500' SIDELINE	
RDG NO.	P_{T8}/P_o	T_{T8} (°R)	V_j (ft/sec)	W_8 (PPS)	10Log $\rho^2 A$	10Log ρA	PEAK PNdB	PEAK ANGLE	PEAK PNdB	PEAK ANGLE	PEAK PNdB	PEAK ANGLE
1	1.46	1140	1194	3.31	-20.9	-6.6	102.6	50	100.2	50	82.2	50
2	1.87	1150	1513	3.71	-20.5	-6.4	108.1	50	105.8	60	87.8	60
3	2.31	1145	1728	4.66	-19.9	-6.0	112.1	50	110.0	60	92.6	70
4	2.70	1145	1866	6.18	-19.4	-5.7	114.4	50	112.9	60	95.3	70
5	2.69	1505	2137	7.33	-21.8	-6.9	114.9	50	113.6	70	96.2	60
6	2.25	1490	1946	5.15	-22.2	-7.2	111.2	50	110.1	60	92.7	60/70
7	1.83	1505	1707	4.00	-22.8	-7.6	107.0	50	106.3	70	88.7	70
8	1.46	1505	1365	3.05	-23.3	-7.8	101.9	50	100.3	60	82.7	60
9	2.70	1765	2316	6.35	-23.1	-7.6	114.6	50	113.5	70	97.1	60
10	2.70	1960	2441	5.37	-24.0	-8.0	115.0	50	114.3	70	97.7	70
11	2.26	1960	2233	4.41	-24.6	-8.4	111.1	50	111.1	70	94.1	60
12	1.84	1960	1951	3.40	-25.1	-8.7	107.5	50	106.4	70	89.3	60
13	1.47	1950	1575	2.53	-25.5	-8.9	101.3	60	100.6	70	83.5	60

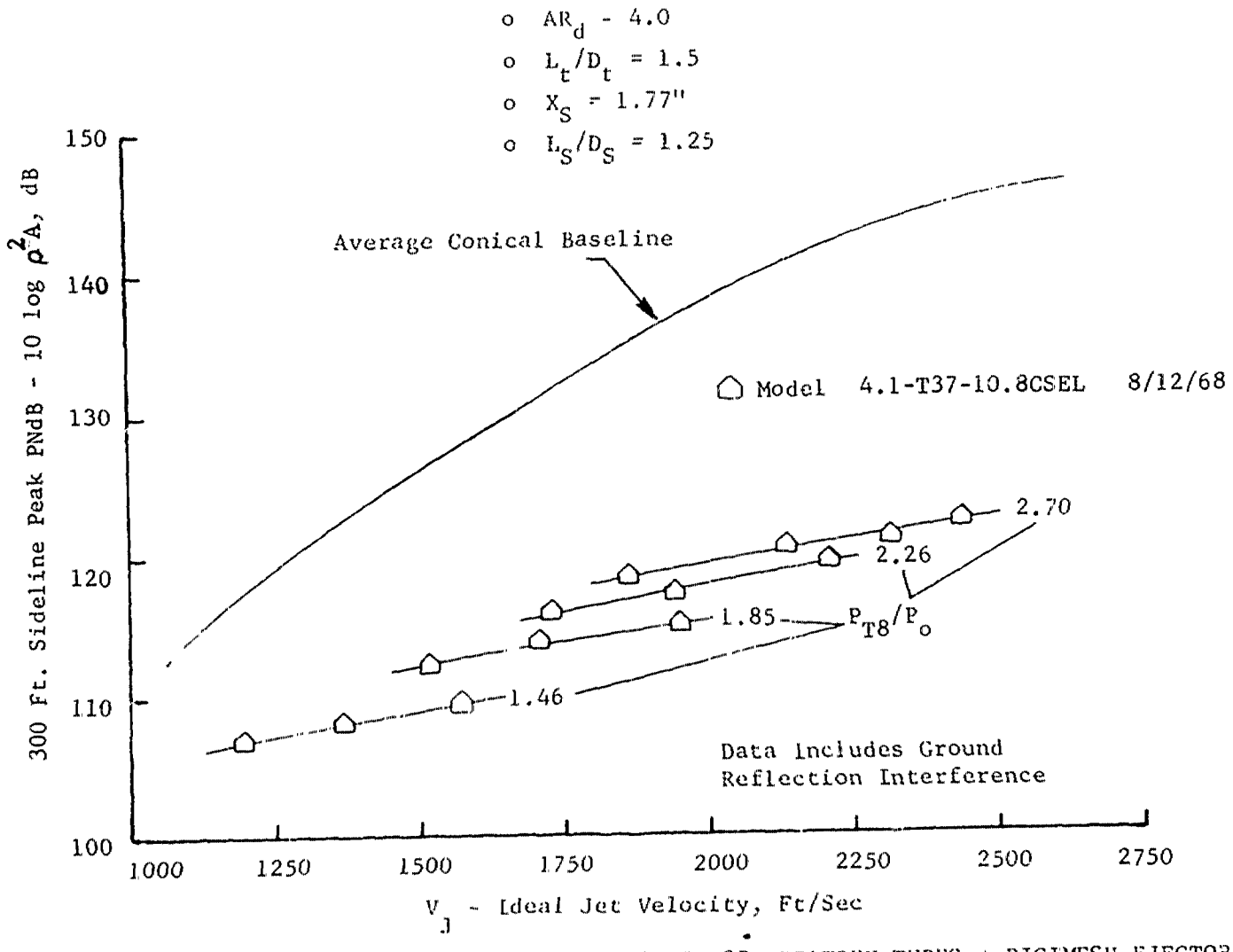

FIGURE V.F.3-6 300 FT. SIDELINE JET NOISE LEVELS FOR 37 GREATREX TUBES + RIGIMESH EJECTOR

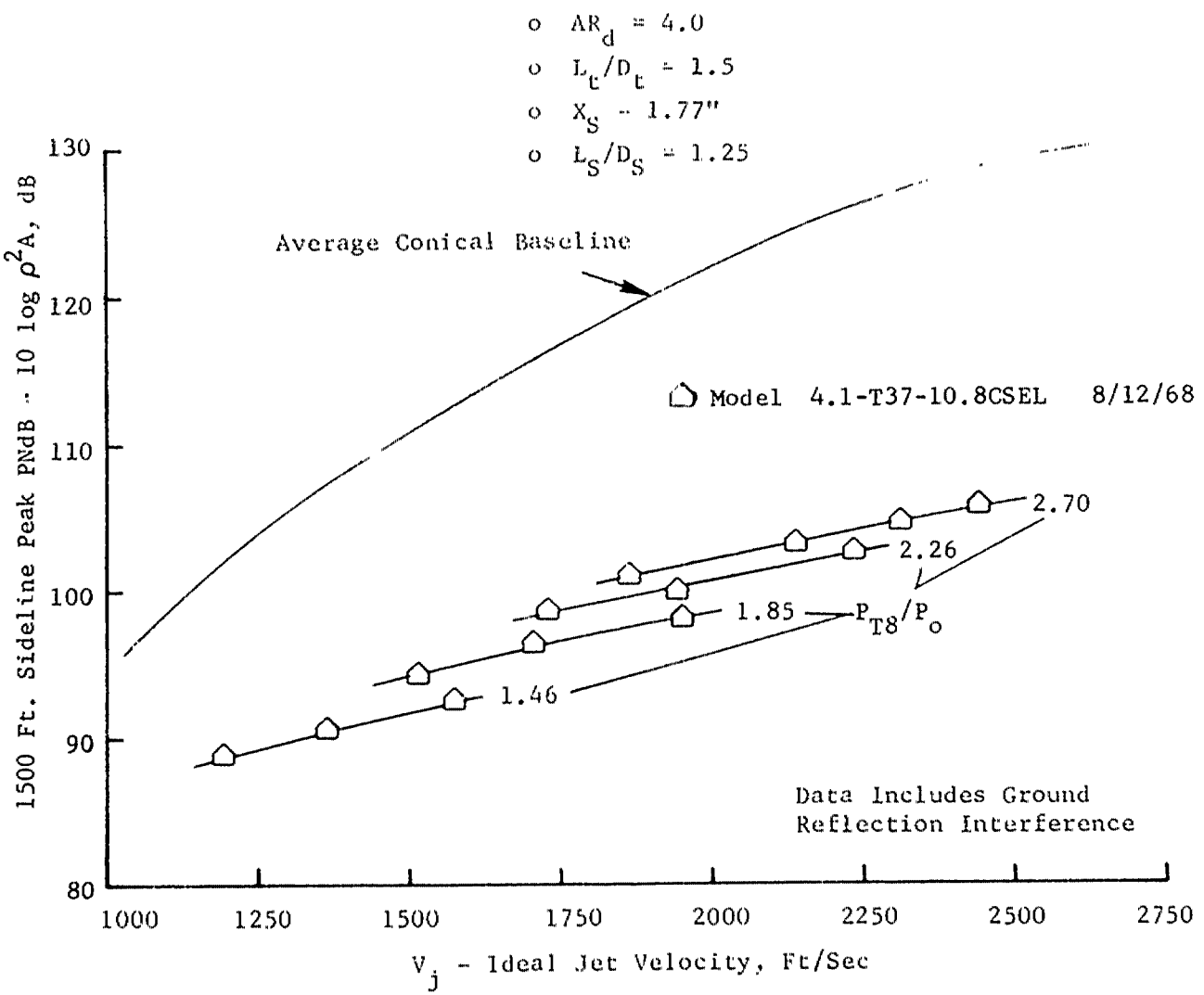

FIGURE V.F.3-7 1500 FT. SIDELINE JET NOISE LEVELS FOR 37 GREATREX TUBES + RIGIMESH EJECTOR

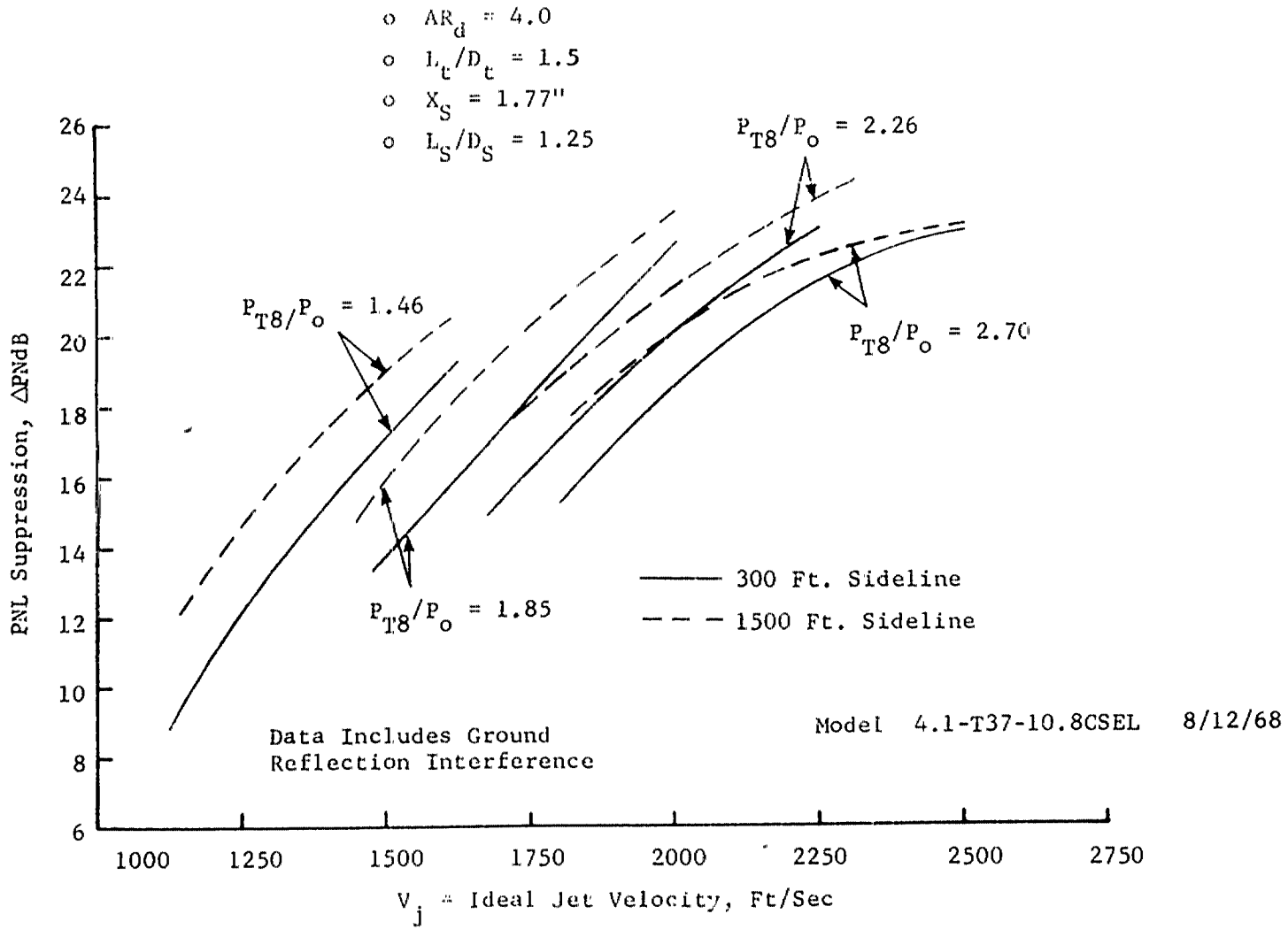

FIGURE V.F.3-8 300 & 1500 FT. SIDELINE PNL SUPPRESSION FOR 37 GREATREX TUBE + RIGIMESH EJECTOR

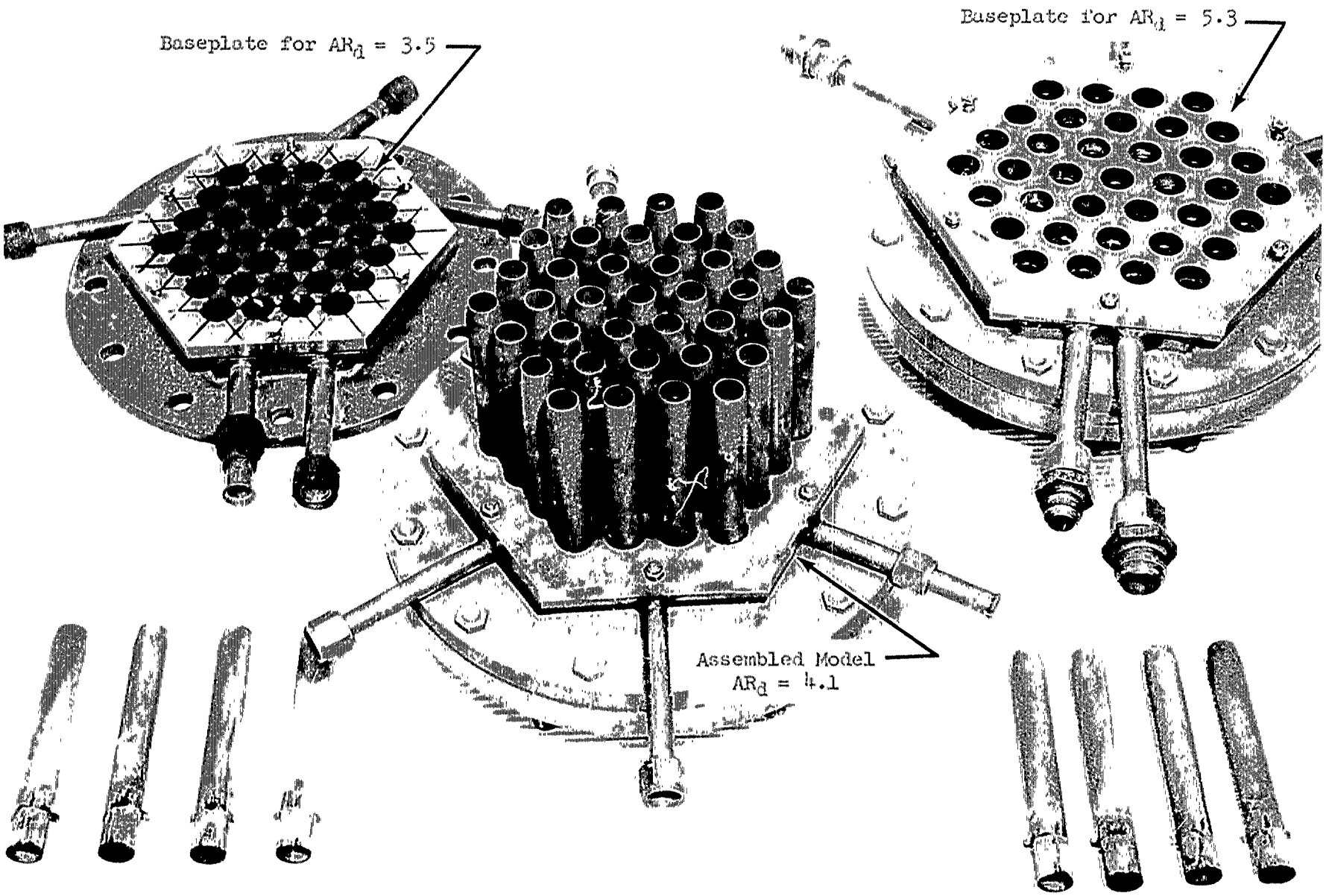

FIGURE V.F.3-9 HARDWARE FOR 37 TUBE HIGH TEMPERATURE MODELS

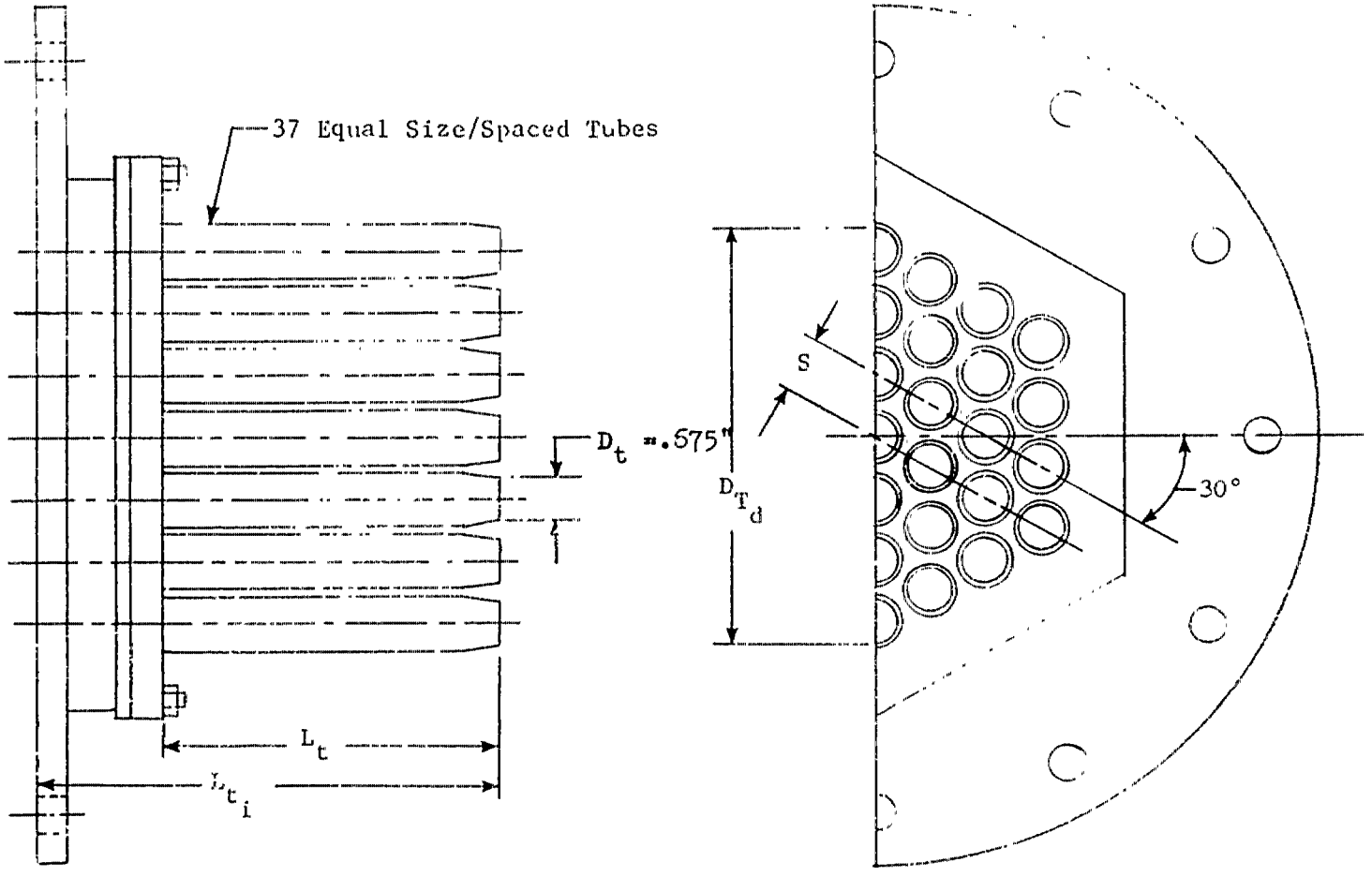

Model No.	AR_d	Test Date	S	D_{Td}	L_t	L_t/D_t	L_{ti}	L_{ti}/D_t
4.1-T37-3.5	3.5	8/8	1.011"	7.68"	5.29"	7.84	7.14"	10.58
4.1-T37-4.1	4.1	8/5	1.109"	8.36"	5.26"	7.79	7.51"	11.13
4.1-T37-5.3	5.3	8/6 8/7	1.264"	9.43"	5.26"	7.79	7.51"	11.13

FIGURE V.F.3-10 SCHEMATIC OF HARDWARE FOR 37 TUBE HIGH TEMPERATURE MODELS

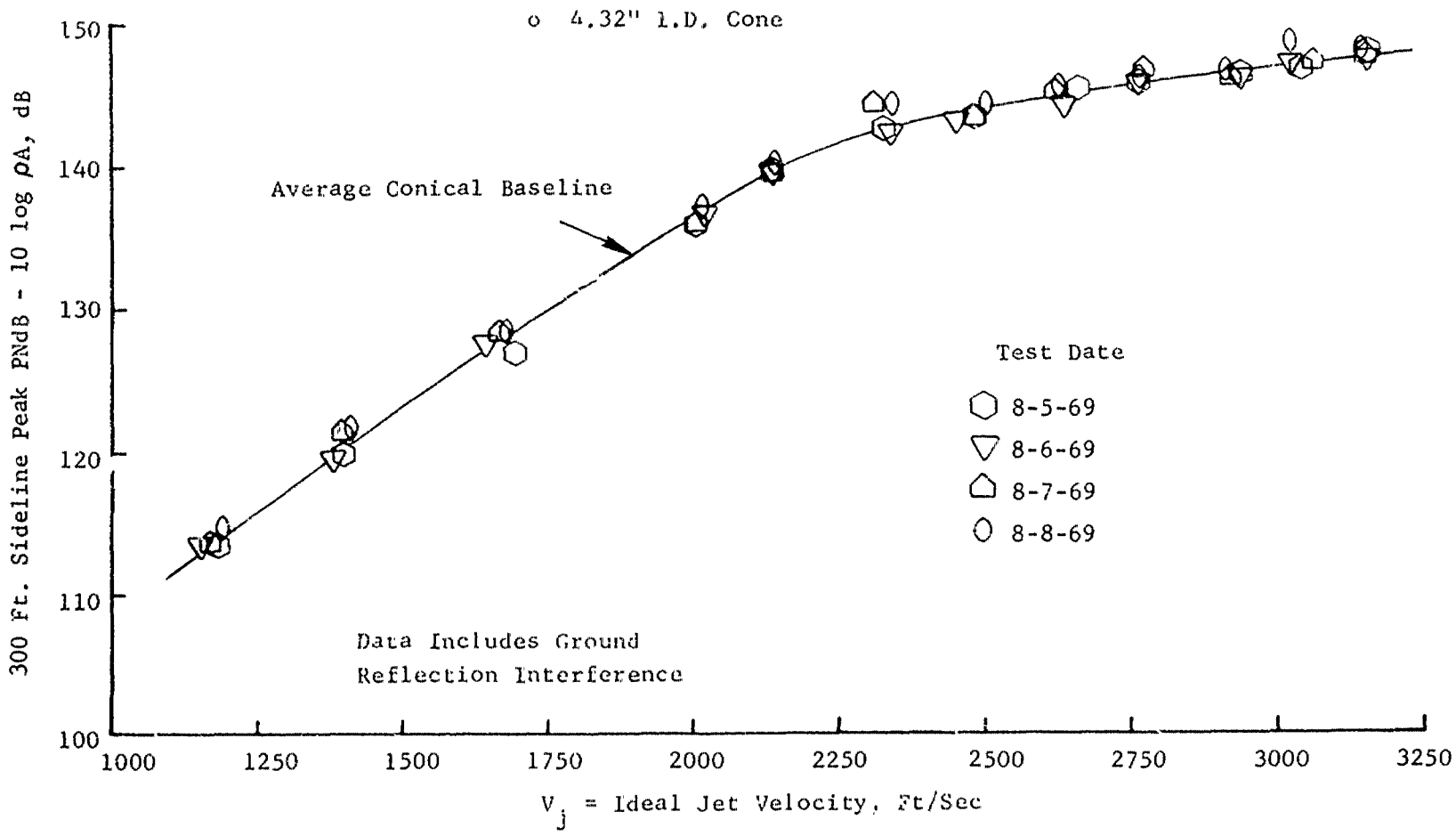

FIGURE V.F.3-11 300 FT. SIDELINE JET NOISE LEVELS FOR THE 4.32" I.D. BASELINE CONICAL NOZZLE

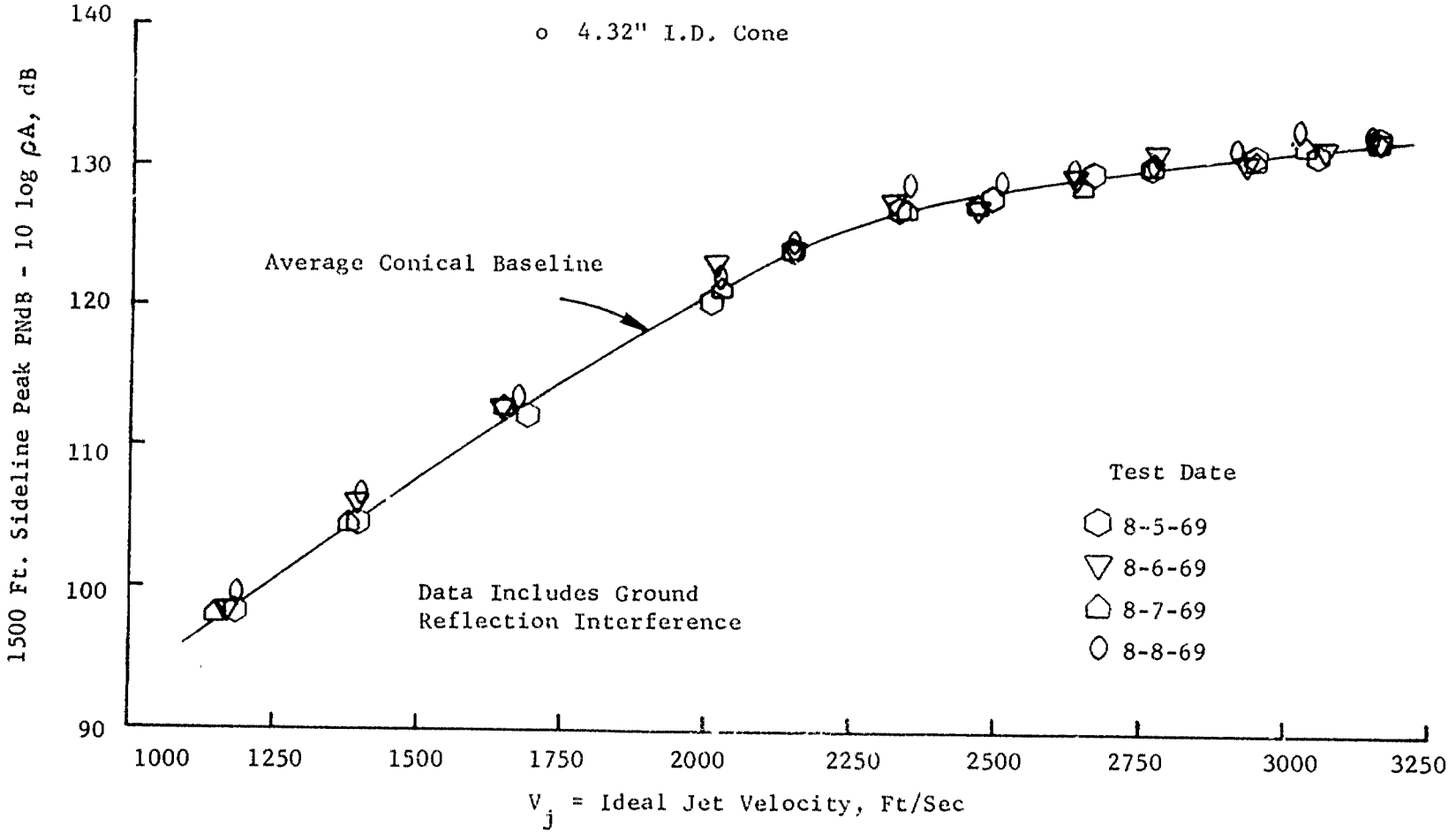

FIGURE V.F.3-12 1500 FT. SIDELINE JET NOISE LEVELS FOR THE 4.32"I.D. BASELINE CONICAL NOZZLE

TABLE V.F.3-3 TEST SUMMARY

MODEL NO. 4.1-T37-3.5

DESCRIPTION: 37 Convergent End Tubes, AR_d=3.5

DATE: 8/8/69

SCALE MODEL A_8 = .0919 ft^2

FULL SCALE A_8 = 5.882 ft^2

SCALE FACTOR = 8:1

- o DATA INCLUDES GROUND REFLECTION INTERFERENCE
- o ANGLE REFERENCED TO JET EXHAUST

TEST CONDITIONS							ACOUSTIC TEST RESULTS					
							320' ARC		300' SIDELINE		1500' SIDELINE	
RDG NO.	P_{T8}/P_o	T_{T8} (°R)	IDEAL V_j (ft/sec)	W_8 (PPS)	10Log $\rho^2 A$	10Log ρA	PEAK PNdB	PEAK ANGLE	PEAK PNdB	PEAK ANGLE	PEAK PNdB	PEAK ANGLE
1	3.44	2683	3145	6.73	-25.9	-8.8	132.6	60	131.7	60	114.6	60
2	3.23	2395	2903	6.72	-25.2	-8.4	132.8	50	133.1	50	115.6	50
3	2.94	2113	2632	6.75	-24.4	-8.1	130.5	50	128.1	50	111.0	50
4	2.72	1757	2319	6.94	-23.1	-7.5	128.9	50	126.5	50	109.1	50
5	2.28	1549	1998	6.19	-22.6	-7.4	125.3	50	122.9	50	105.4	50/60
6	1.75	1521	1658	4.76	-23.0	-7.7	118.3	40	116.2	60	98.9	60
7	1.61	1233	1379	4.70	-21.4	-6.9	114.3	50	112.7	70	95.4	70
8	1.44	1150	1173	4.18	-21.0	-6.7	109.3	60	108.4	60	91.1	60
9	3.26	2608	3043	6.48	-25.9	-8.8	134.6	70	134.7	60	117.3	60
10	3.15	2220	2770	7.01	-24.6	-8.2	132.1	60	131.2	60	114.1	60
11	2.53	2113	2462	5.77	-24.9	-8.5	129.1	50	126.8	50	109.4	50
12	2.46	1633	2135	6.61	-22.8	-7.4	126.9	50	124.6	50/60	107.3	60

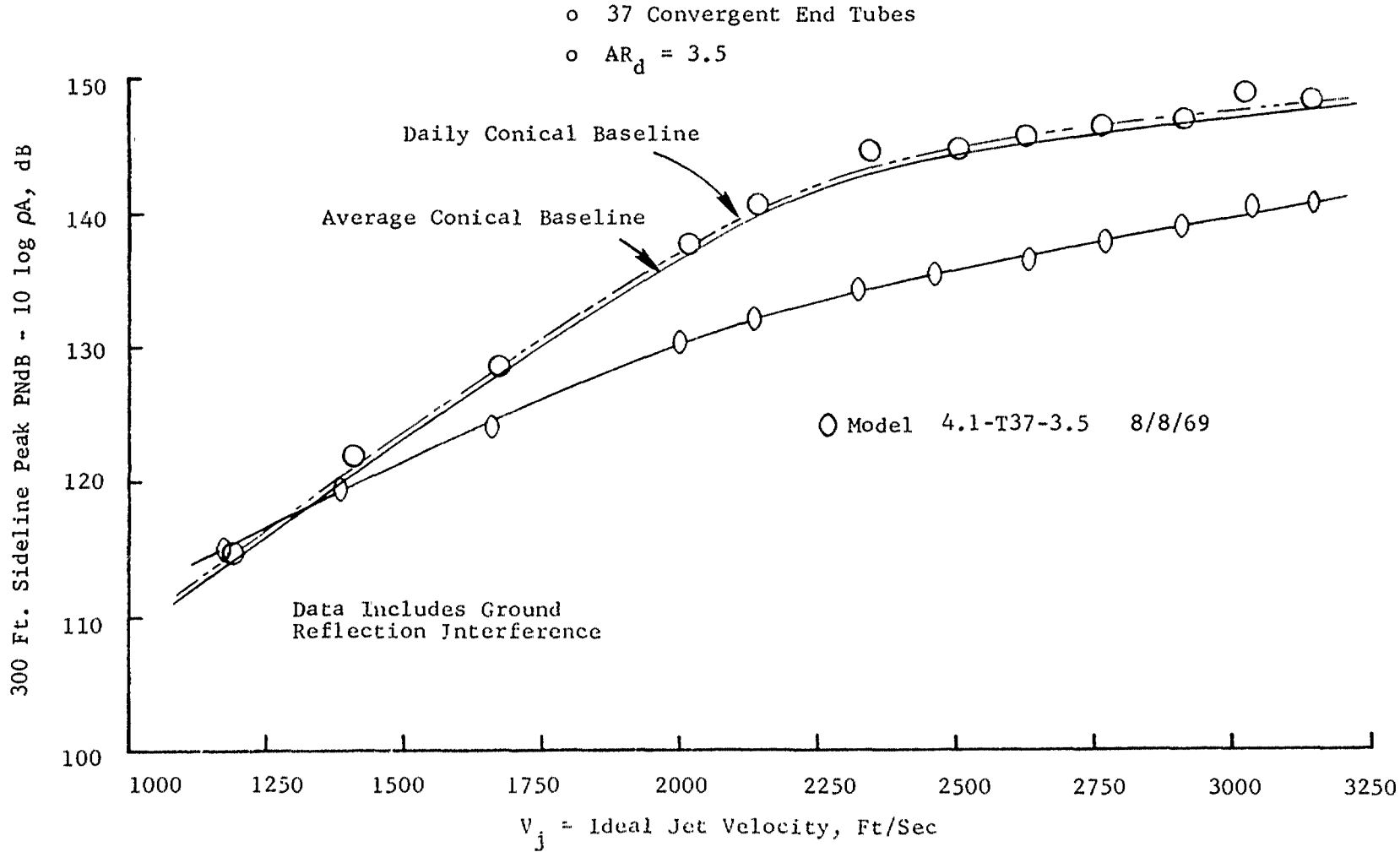

FIGURE V.F.3-13 300 FT. SIDELINE JET NOISE LEVELS FOR 37 TUBE HIGH TEMPERATURE MODEL, AR_d = 3.5

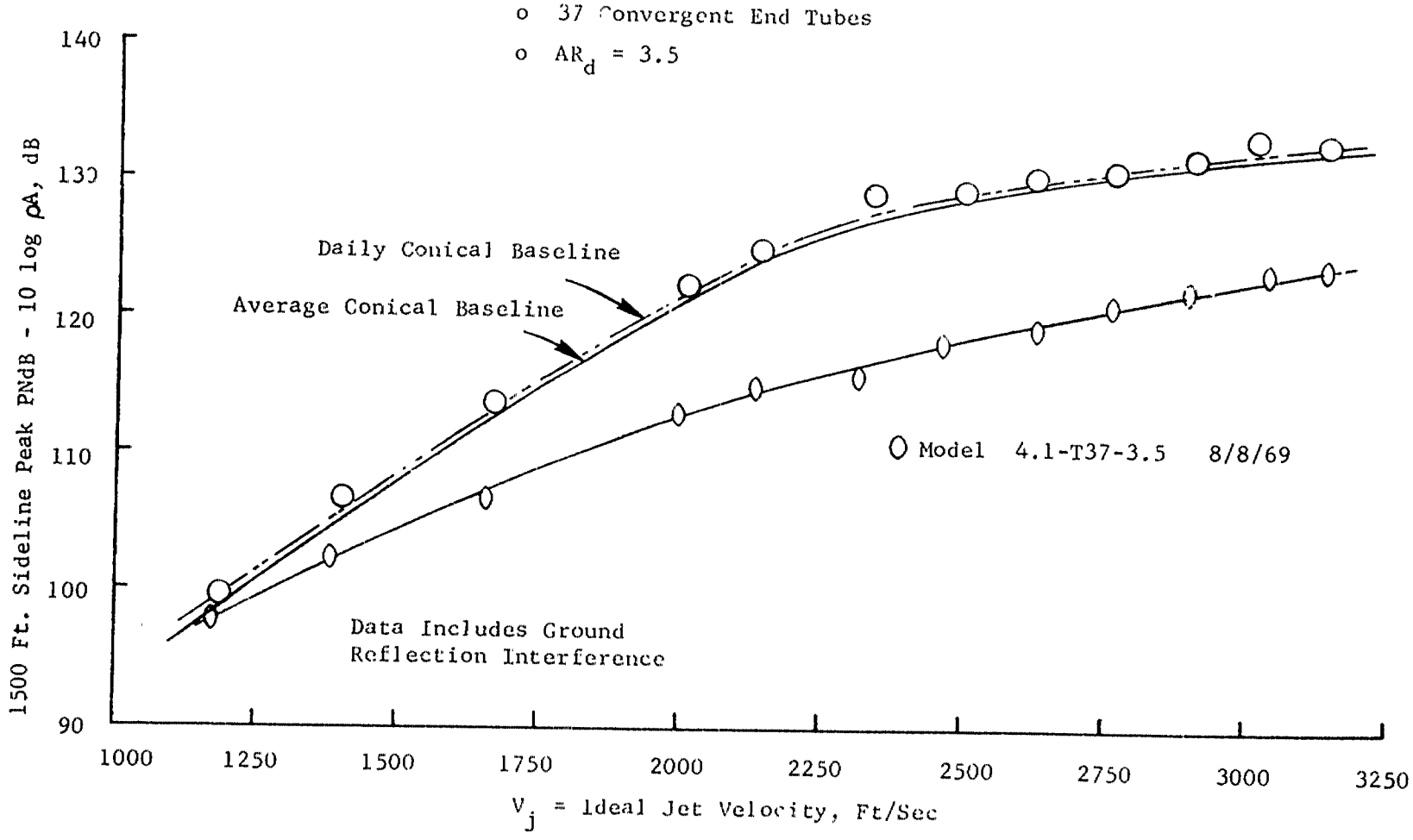

FIGURE V.F.3-14 1500 FT. SIDELINE JET NOISE LEVELS FOR 37 TUBE HIGH TEMPERATURE MODEL, AR_d = 3.5

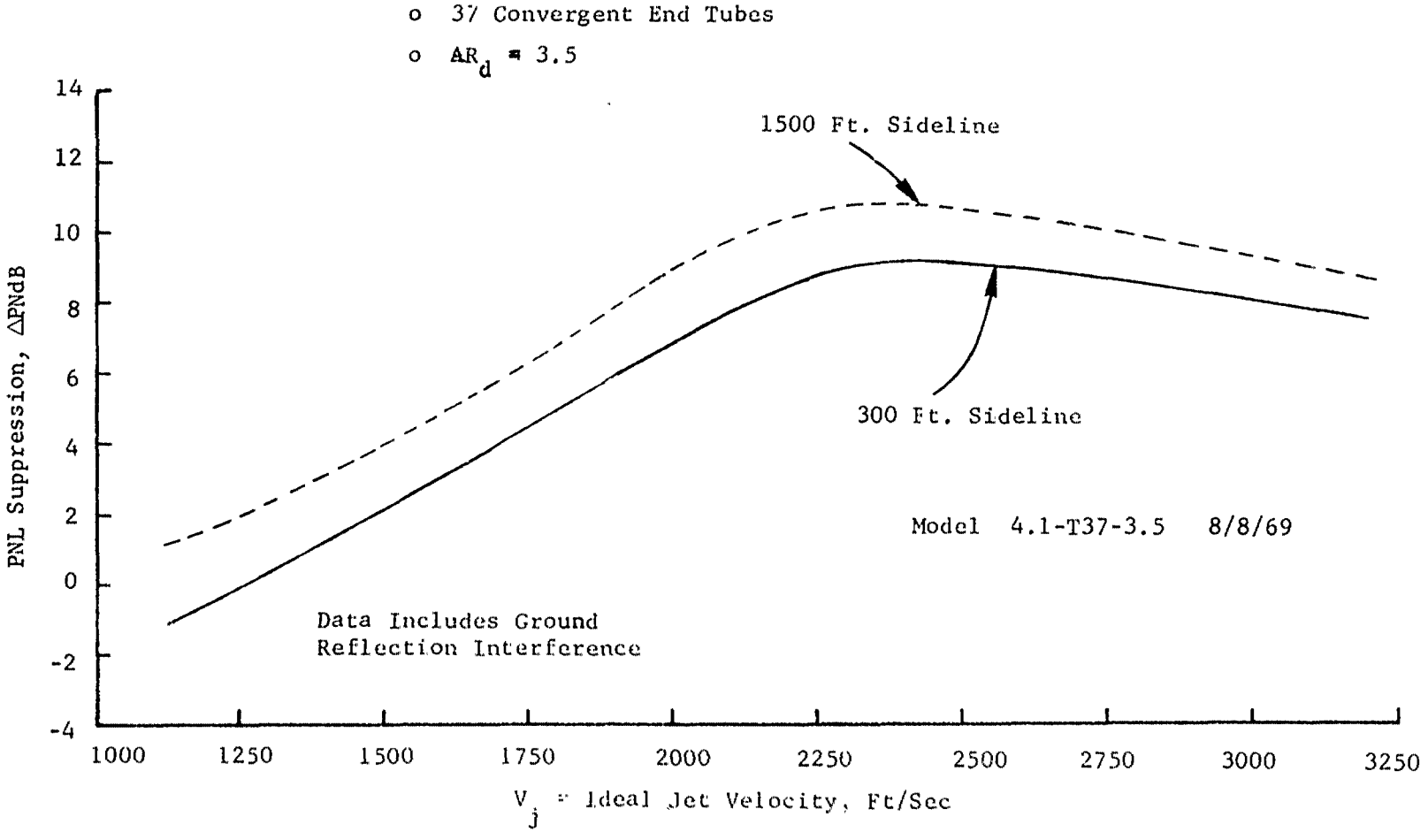

FIGURE V.F.3-15 300 & 1500 FT. SIDELINE PNL SUPPRESSIONS FOR 37 TUBE HIGH TEMPERATURE MODEL, AR_d = 3.5

TABLE V.F.3-4 TEST SUMMARY

MODEL NO. 4.1-T37-4.1

DESCRIPTION: 37 Convergent End Tubes, AR_d=4.1

DATE: 8/5/69

SCALE MODEL A_8 = .0919 ft^2

FULL SCALE A_8 = 5.882 ft^2

SCALE FACTOR = 8:1

- o DATA INCLUDES GROUND REFLECTION INTERFERENCE
- o ANGLE REFERENCED TO JET EXHAUST

TEST CONDITIONS					ACOUSTIC TEST RESULTS							
RDG NO.	P_{T8}/P_o	T_{T8} (°R)	IDEAL V_j (ft/sec)	W_8 (PPS)	10Log $\rho^2 A$	10Log ρA	320' ARC PEAK PNdB	320' ARC PEAK ANGLE	300' SIDELINE PEAK PNdB	300' SIDELINE PEAK ANGLE	1500' SIDELINE PEAK PNdB	1500' SIDELINE PEAK ANGLE
1	3.41	2673	3129	6.32	-25.9	-8.8	135.4	50	131.9	60	114.8	60
2	3.22	2413	2911	6.31	-25.2	-8.5	133.5	50	131.1	60	113.8	60
3	2.93	2114	2627	6.28	-24.4	-8.1	133.0	50	129.6	60	112.3	60
4	2.74	1793	2353	6.31	-23.2	-7.6	131.2	50	128.9	60	111.9	70
5	2.29	1568	2015	5.82	-22.6	-7.4	123.7	50	121.6	70	104.1	70
6	1.75	1527	1660	4.35	-23.0	-7.7	119.1	60	118.2	60	100.7	60
7	1.61	1247	1391	4.39	-21.3	-6.8	113.8	50	112.4	60	95.0	60
8	1.44	1146	1175	3.83	-20.7	-6.4	109.4	60	108.5	60	90.9	60
9	3.23	2621	3039	6.06	-25.9	-8.8	130.4	50	128.3	60	111.1	60
10	3.12	2224	2762	6.39	-24.6	-8.2	129.3	50	127.9	60	110.6	60
11	2.52	2129	2468	5.30	-25.0	-8.5	131.2	50	124.0	60	106.9	70
12	2.48	1630	2139	6.20	-22.7	-7.4	125.3	50	123.5	60	106.1	60

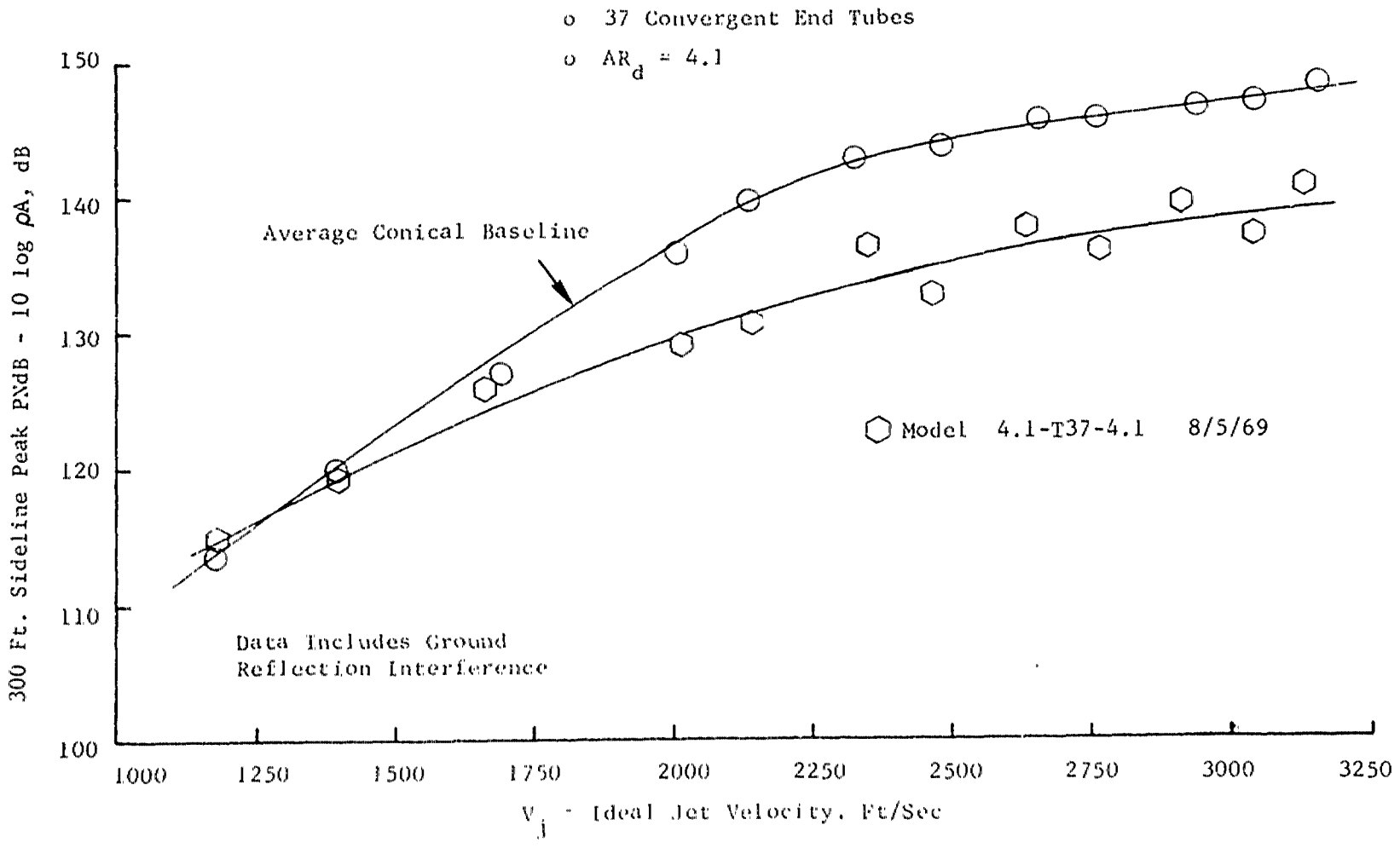

FIGURE V.F.3-16 300 FT. SIDELINE JET NOISE LEVELS FOR 37 TUBE HIGH TEMPERATURE MODEL, AR_d = 4.1

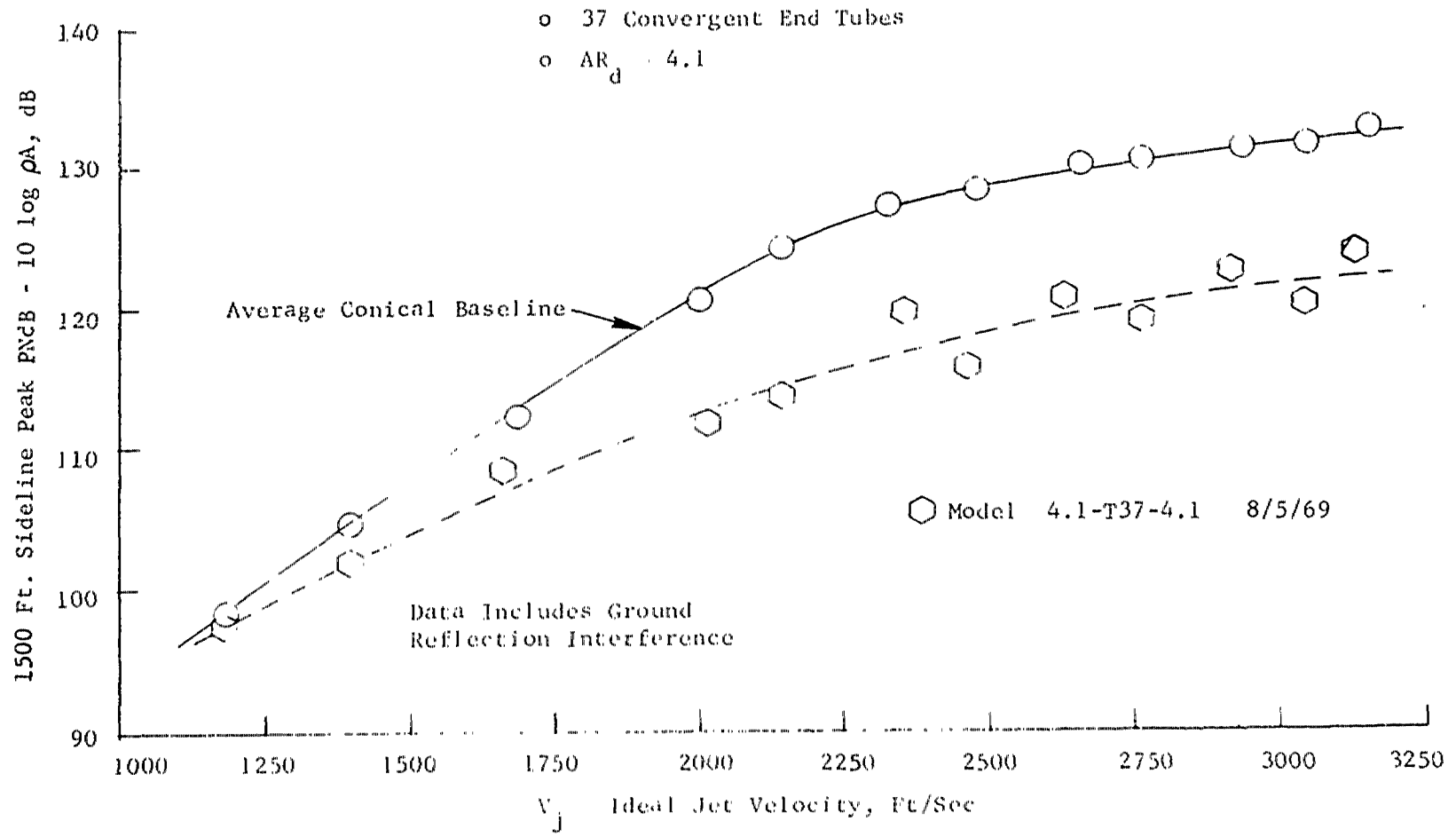

FIGURE V.F.3-17 1500 FT. SIDELINE JET NOISE LEVELS FOR 37 TUBE HIGH TEMPERATURE MODEL, AR_d = 4.1

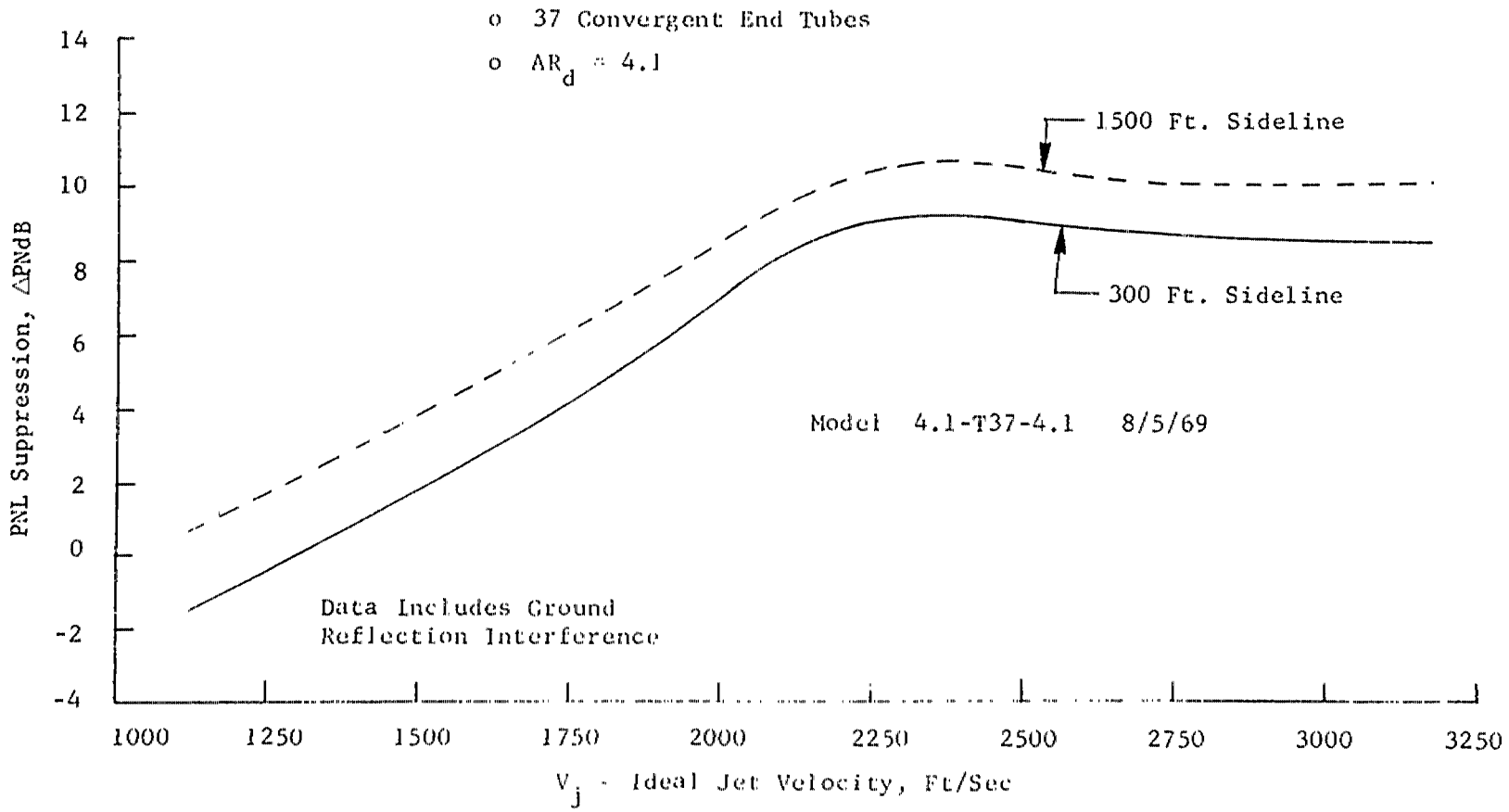

FIGURE V.F.3-18 300 & 1500 FT. SIDELINE PNL SUPPRESSIONS FOR 37 TUBE HIGH TEMPERATURE MODEL, AR_d = 4.1

TABLE V.F.3-5 TEST SUMMARY

MODEL NO. 4.1-T37-5.3

DESCRIPTION: 37 Convergent End Tubes. AR_d=5.3

DATE: 8/6 & 8/7/69

SCALE MODEL A_8 = .0919 ft^2

FULL SCALE A_8 = 5.882 ft^2

SCALE FACTOR = 8:1

- o DATA INCLUDES GROUND REFLECTION INTERFERENCE
- o ANGLE REFERENCED TO JET EXHAUST

TEST CONDITIONS							ACOUSTIC TEST RESULTS					
							320' ARC		300' SIDELINE		1500' SIDELINE	
RDG NO.	P_{T8}/P_o	T_{T8} (°R)	IDEAL V_j (ft/sec)	W_8 (PPS)	10Log $\rho^2 A$	10Log ρA	PEAK PNdB	PEAK ANGLE	PEAK PNdB	PEAK ANGLE	PEAK PNdB	PEAK ANGLE
8/6/69												
1	3.41	2695	3143	6.40	-25.9	-8.8	129.9	50	129.1	70	111.8	70
2	3.25	2426	2931	6.24	-25.2	-8.5	129.4	50	128.6	70	111.3	70
3	2.92	2113	2623	6.37	-24.4	-8.1	127.5	50	126.8	70	109.4	70
4	2.77	1793	2364	6.35	-23.2	-7.6	127.1	50	125.6	60	108.2	60
5	2.29	1558	2009	5.83	-22.5	-7.4	124.5	50	123.0	70	105.5	70
8/7/69												
1	3.43	2688	3145	6.36	-25.9	-8.8	129.8	50	127.9	60	110.8	60
2	3.25	2423	2928	6.35	-25.2	-8.5	129.0	50	128.0	70	110.6	70
3	2.93	2136	2640	6.12	-24.5	-8.2	128.5	50	126.9	70	109.5	70
4	2.75	1774	2341	6.27	-23.1	-7.5	126.6	60	126.4	70	108.9	70
5	2.30	1563	2015	5.56	-22.6	-7.4	123.3	50	122.7	70	105.2	70
6	1.76	1528	1665	4.40	-23.0	-7.7	118.8	60	117.9	60	100.5	60
7	1.61	1239	1381	4.34	-21.4	-6.9	114.0	50	112.8	60	95.5	60
8	1.43	1149	1159	3.86	-21.0	-6.6	108.9	50	107.5	60	90.7	50
9	3.25	2617	3042	6.02	-25.9	-8.8	129.1	50	128.6	70	111.3	70
10	3.14	2251	2785	6.29	-24.7	-8.2	128.3	50	127.0	70	109.7	70

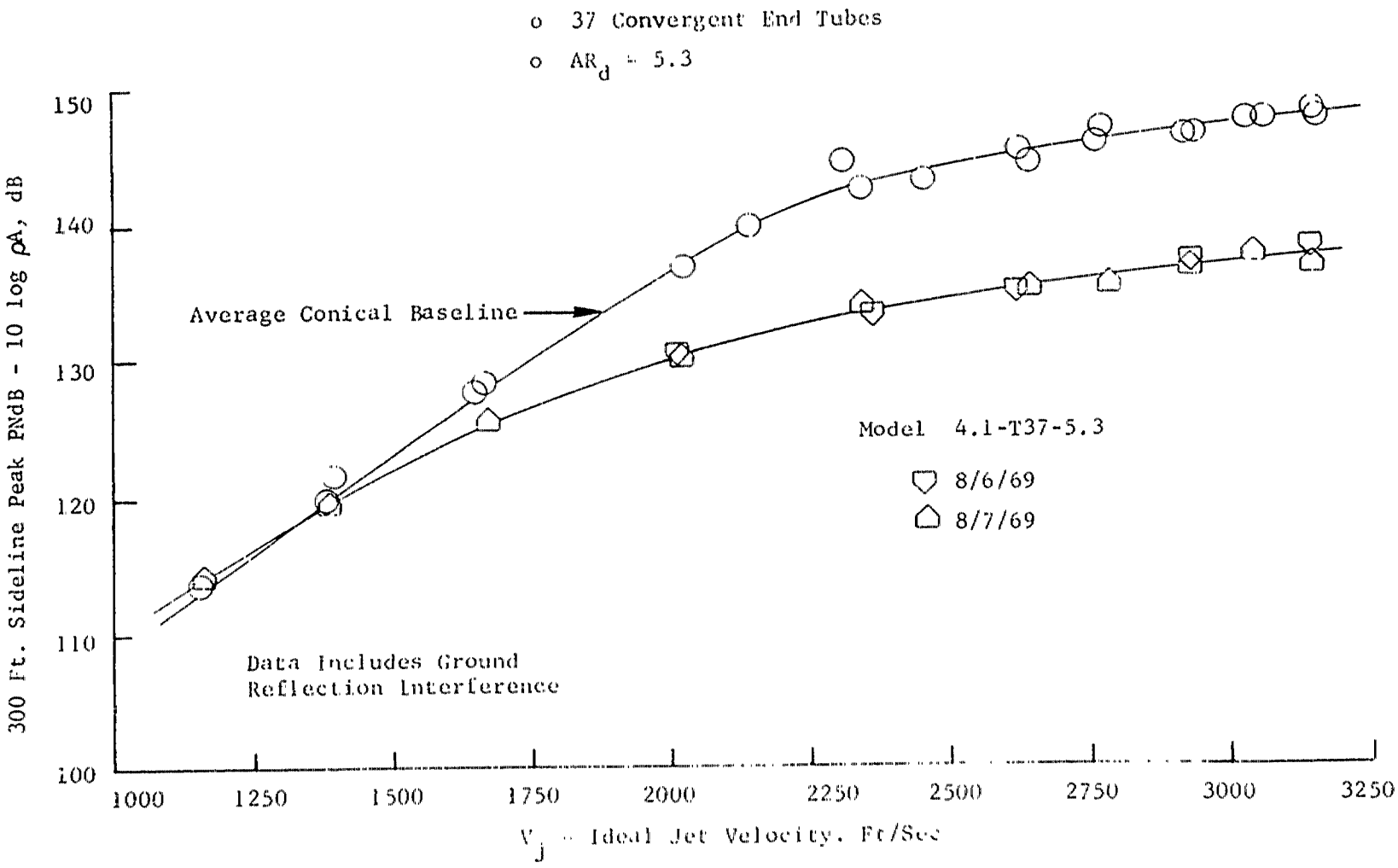

FIGURE V.F.3-19 300 FT. SIDELINE JET NOISE LEVELS FOR 37 TUBE HIGH TEMPERATURE MODEL, AR_d 5.3

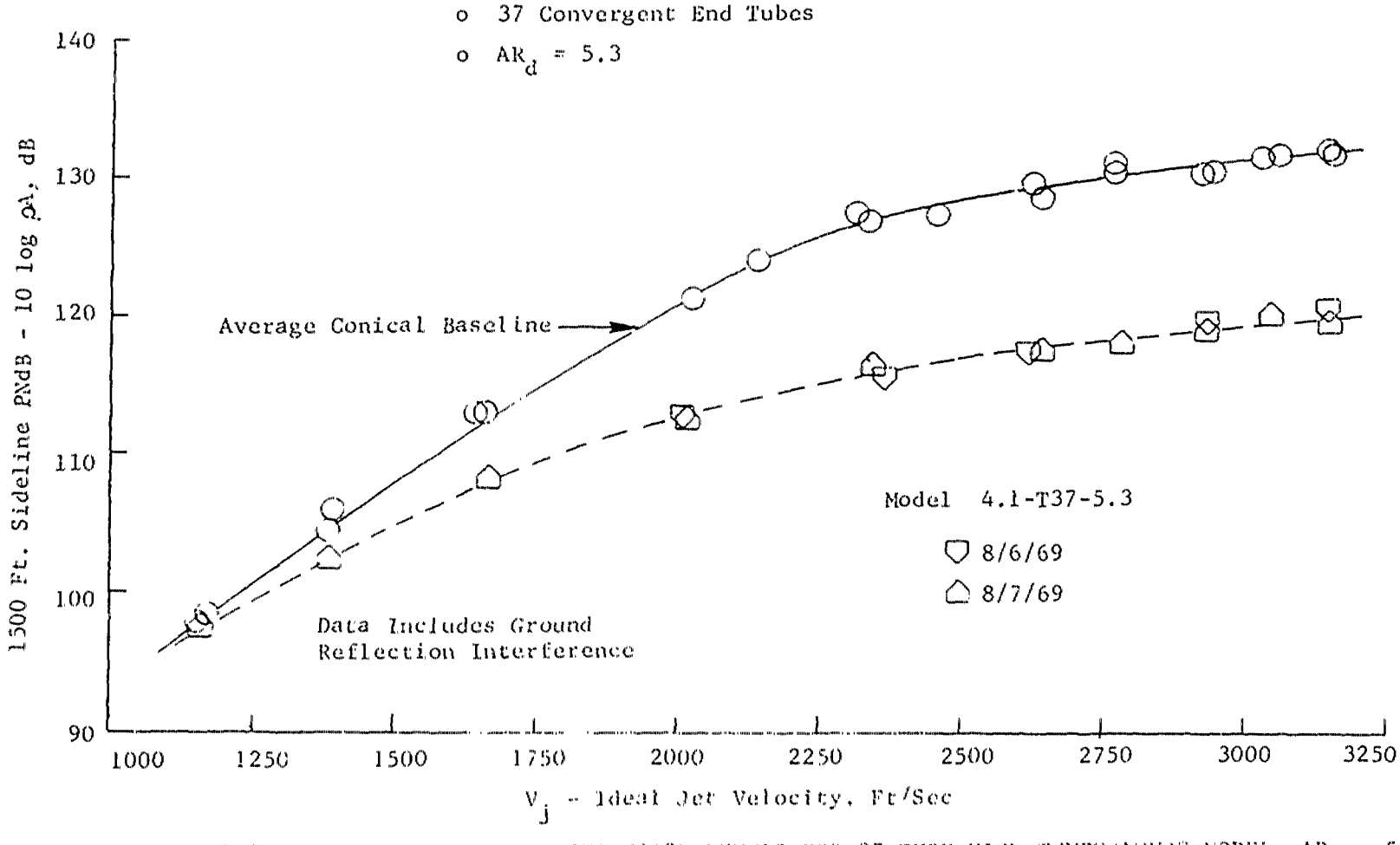

FIGURE V.F.3-20 1500 FT. SIDELINE JET NOISE LEVELS FOR 37 TUBE HIGH TEMPERATURE MODEL, AR_d = 5.3

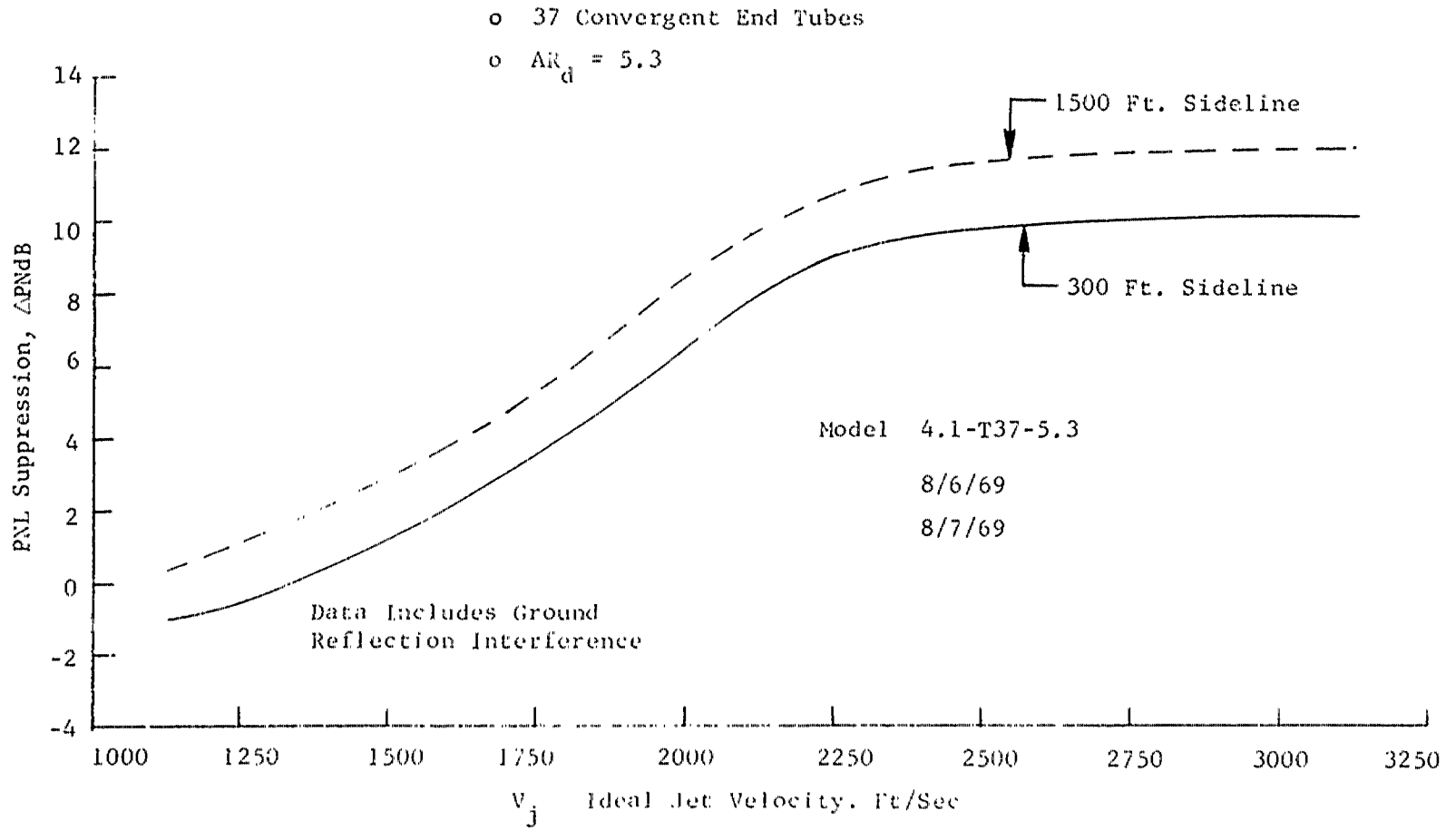

FIGURE V.F.3-21 300 & 1500 FT. SIDELINE PNL SUPPRESSIONS FOR 37 TUBE HIGH TEMPERATURE MODEL, AR_d = 5.3

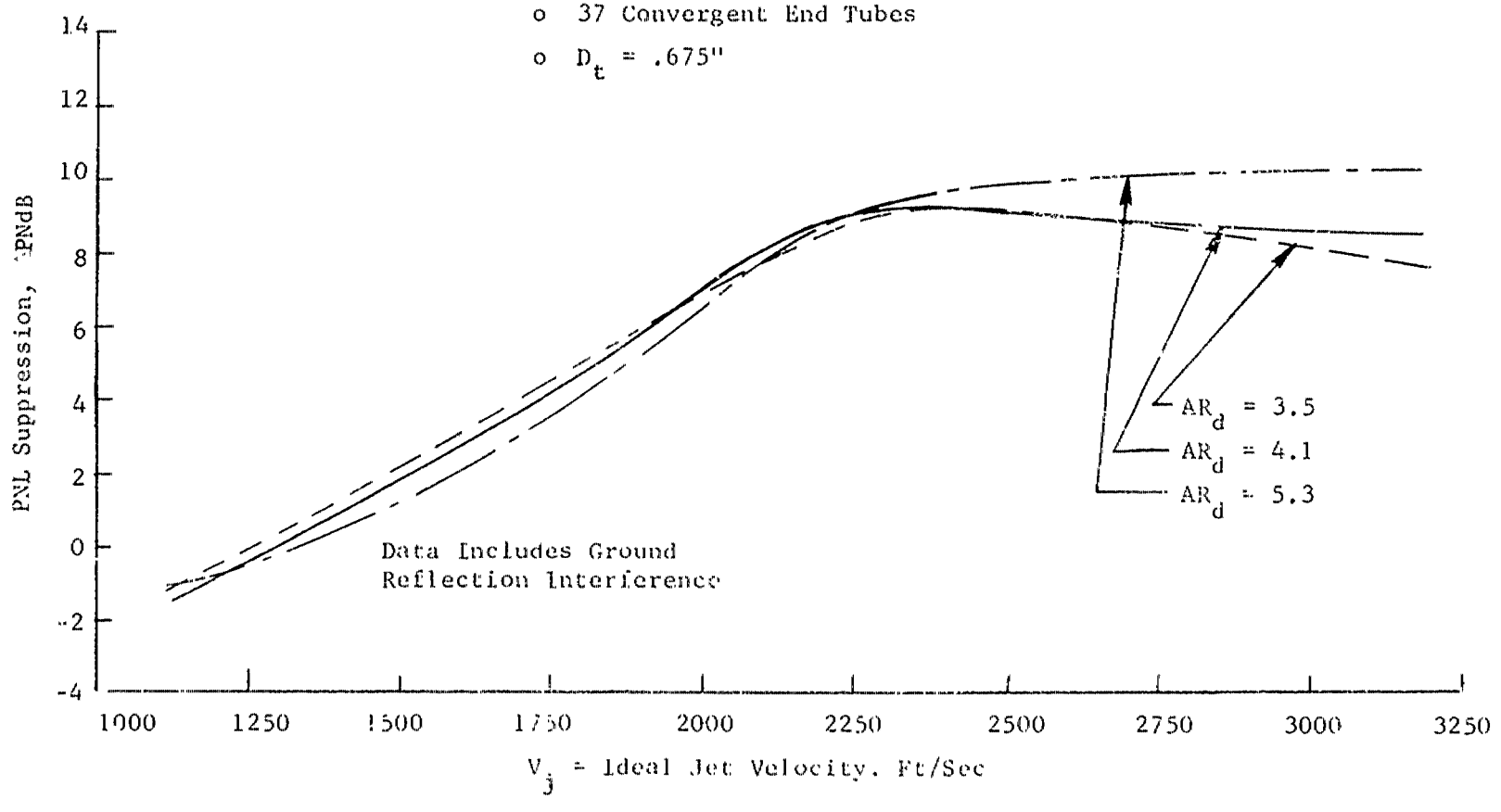

FIGURE V.F.3-22 300 FT. SIDELINE PNL SUPPRESSION COMPARISON FOR 37 TUBE HIGH TEMPERATURE MODELS, AR_d = 3.5, 4.1 & 5.3

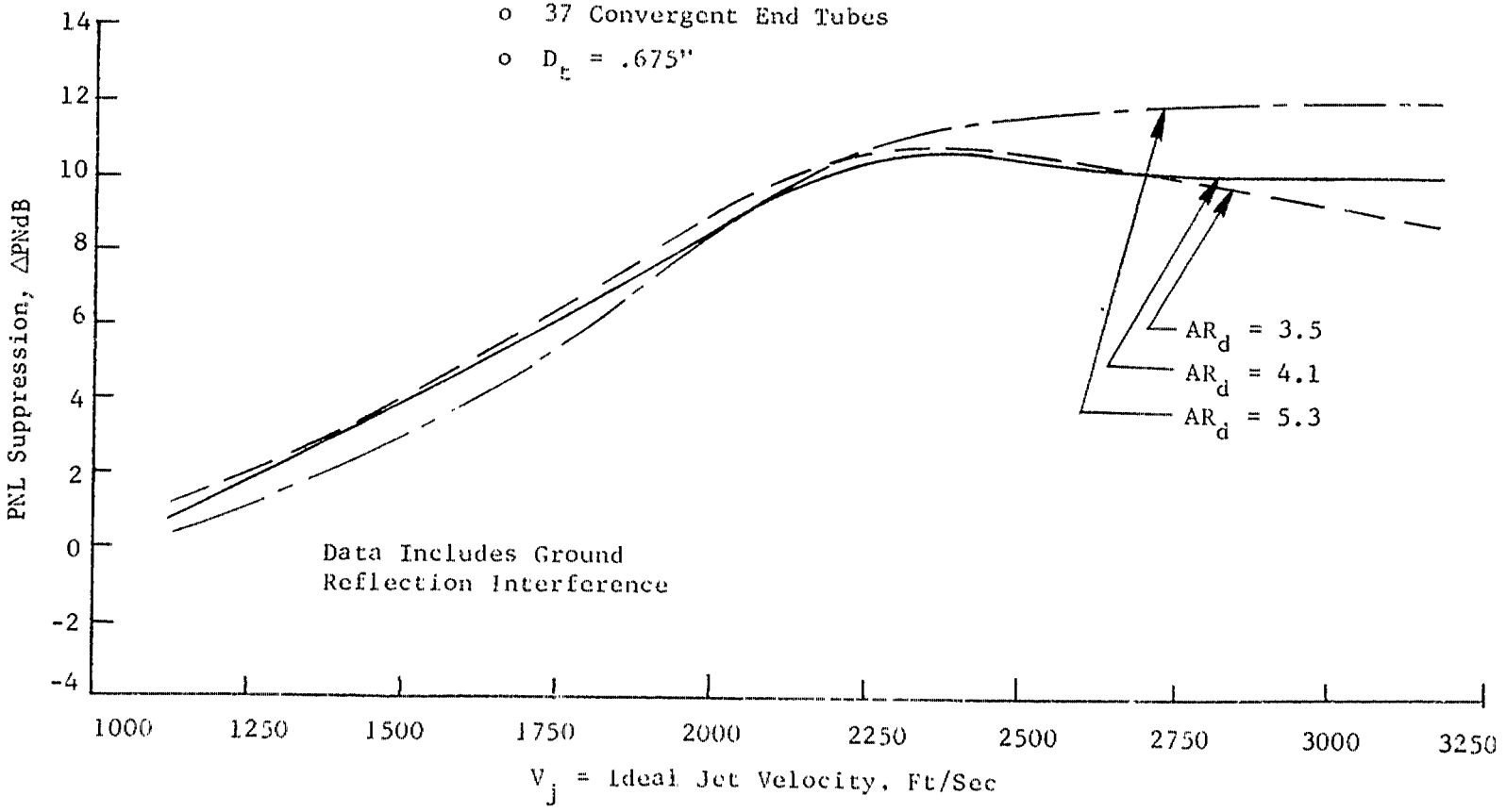

FIGURE V.F.3-23 1500 FT. SIDELINE PNL SUPPRESSION COMPARISON FOR 37 TUBE HIGH TEMPERATURE MODELS, AR_d = 3.5, 4.1 & 5.3

- o 37 Convergent End Tubes
- o 300 Ft. Sideline

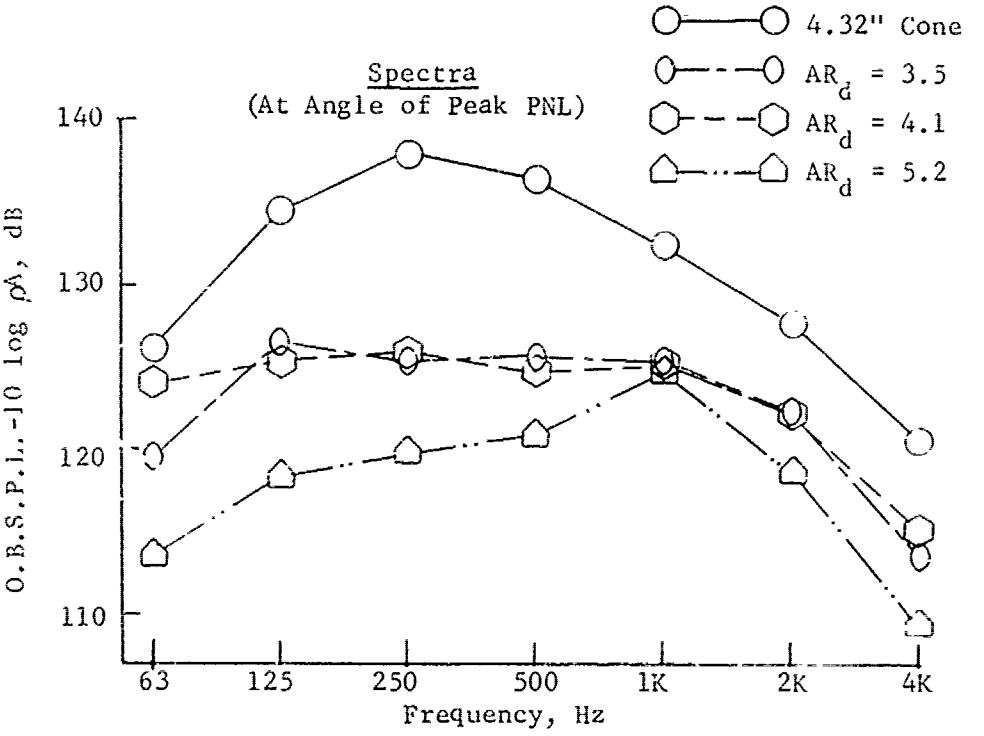

Data Includes Ground
Reflection Interference

$P_{T8}/P_o \approx 3.42$
$T_{T8} \approx 2680°R$
$V_j \approx 3145$ Ft/Sec

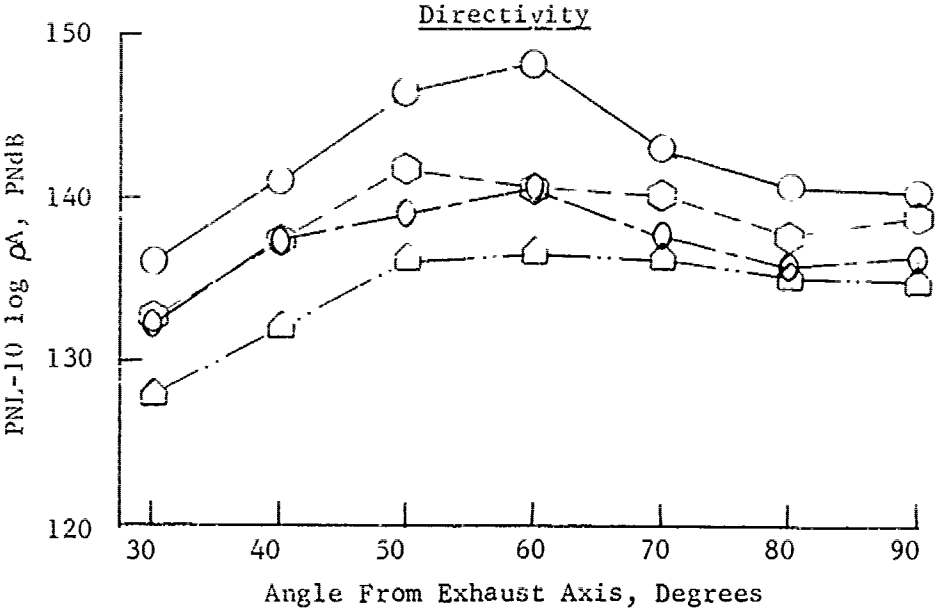

FIGURE V.F.3-24A 300 FT. SIDELINE SPECTRA & DIRECTIVITY COMPARISON FOR 37 TUBE HIGH TEMPERATURE MODELS

- o 37 Convergent End Tubes
- o 300 Ft. Sideline

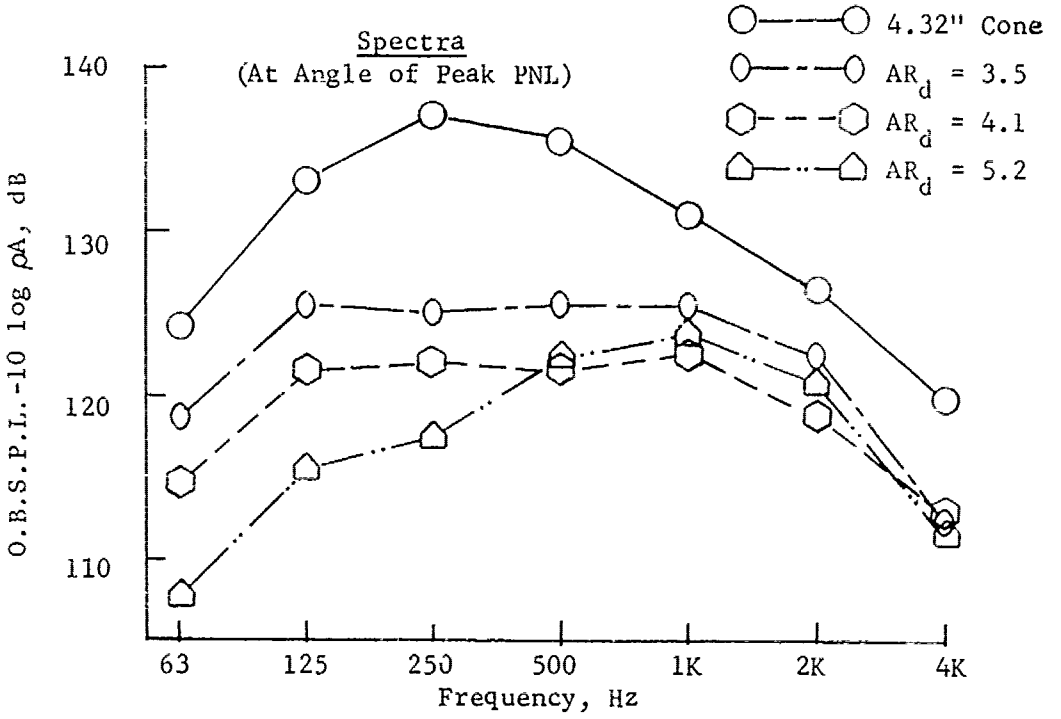

Data Includes Ground Reflection Interference

$P_{T8}/P_o \approx 3.24$
$T_{T8} \approx 2620°R$
$V_j \approx 3040$ Ft/Sec

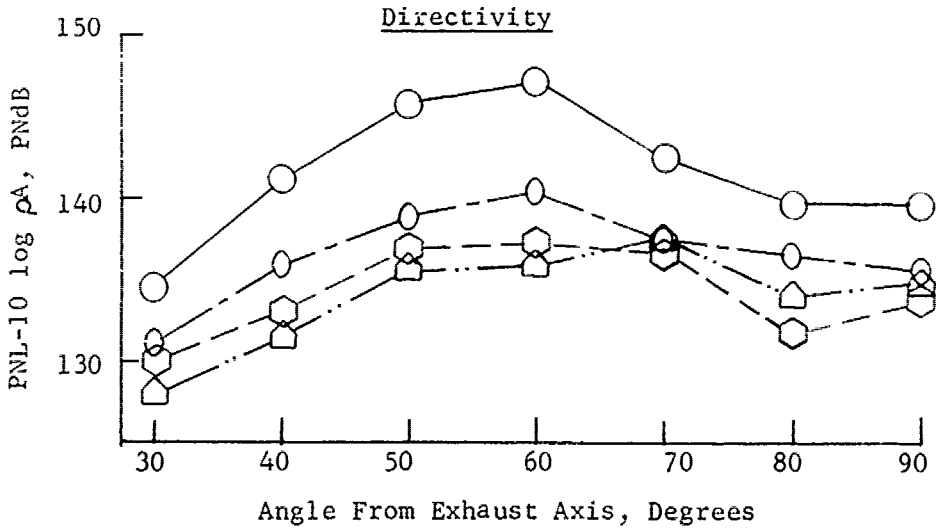

FIGURE V.F.3-24B 300 FT. SIDELINE SPECTRA & DIRECTIVITY COMPARISON FOR 37 TUBE HIGH TEMPERATURE MODELS

- o 37 Convergent End Tubes
- o 300 Ft. Sideline

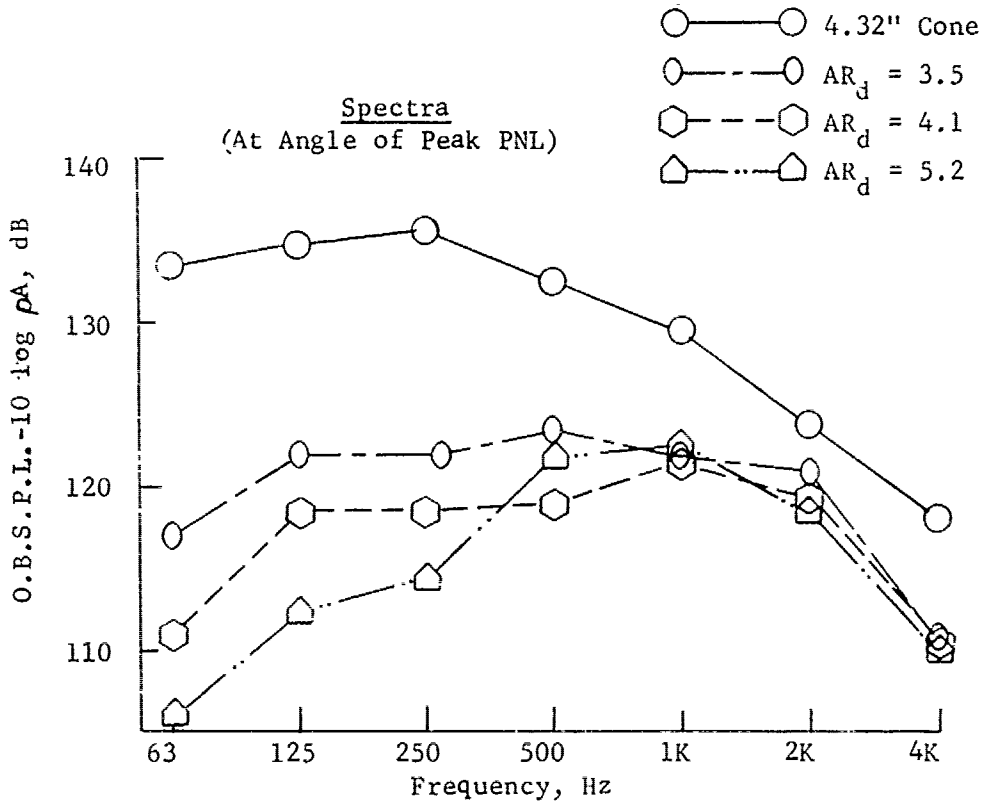

Data Includes Ground
Reflection Interference

$P_{T8}/P_o \approx 3.12$
$T_{T8} \approx 2220°R$
$V_j \approx 2770$ Ft/Sec

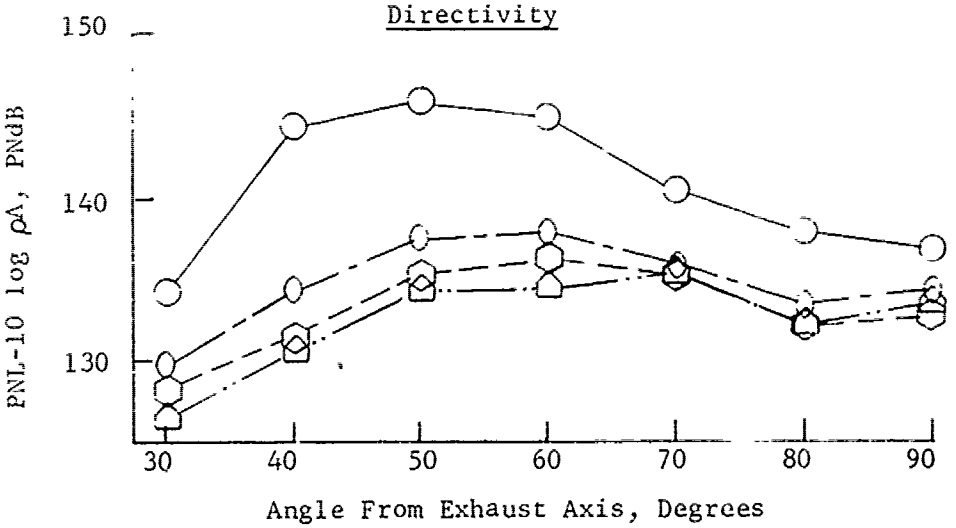

FIGURE V.F.3-24C 300 FT. SIDELINE SPECTRA & DIRECTIVITY COMPARISON FOR 37 TUBE HIGH TEMPERATURE MODELS

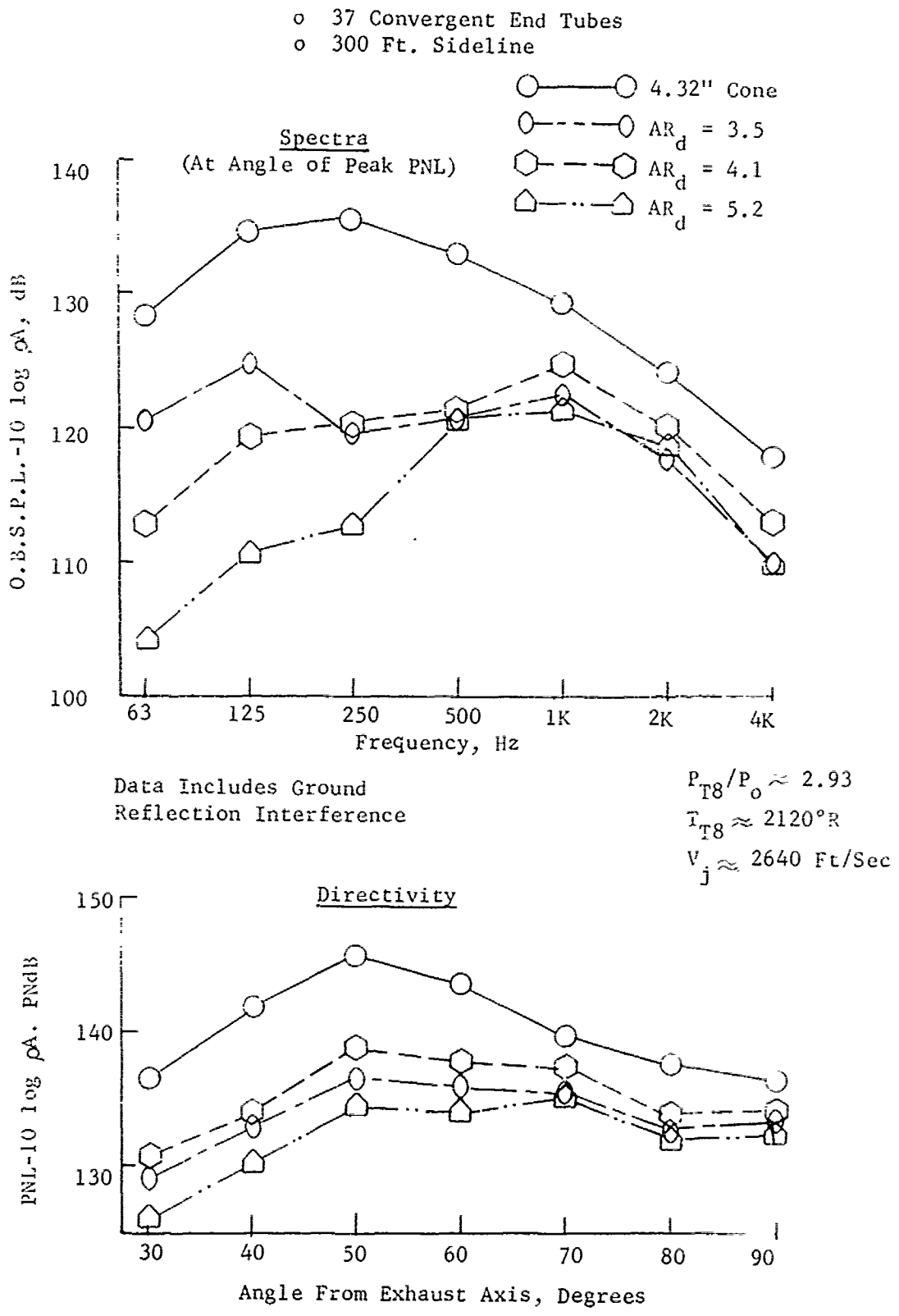

FIGURE V.F.3-24D 300 FT. SIDELINE SPECTRA & DIRECTIVITY COMPARISON FOR 37 TUBE HIGH TEMPERATURE MODELS

- o 37 Convergent End Tubes
- o 300 Ft. Sideline

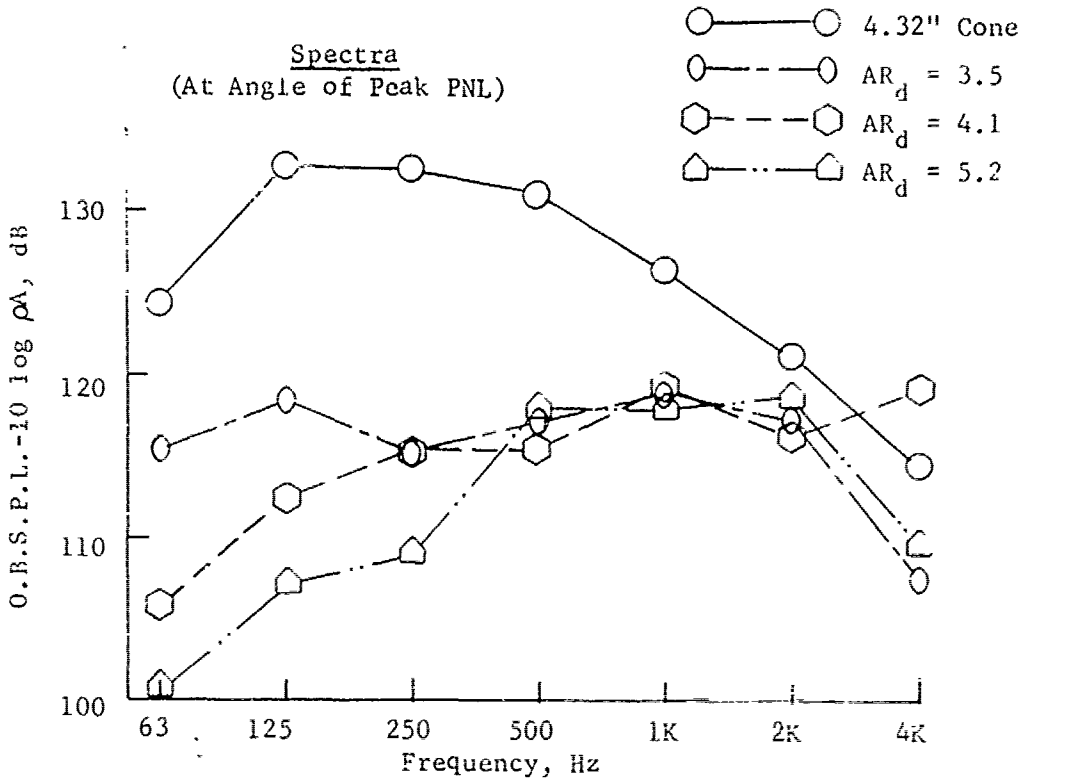

Data Includes Ground Reflection Interference

$P_{T8}/P_o \approx 2.75$

$T_{T8} \approx 1770°R$

$V_j \approx 2540$ Ft/Sec

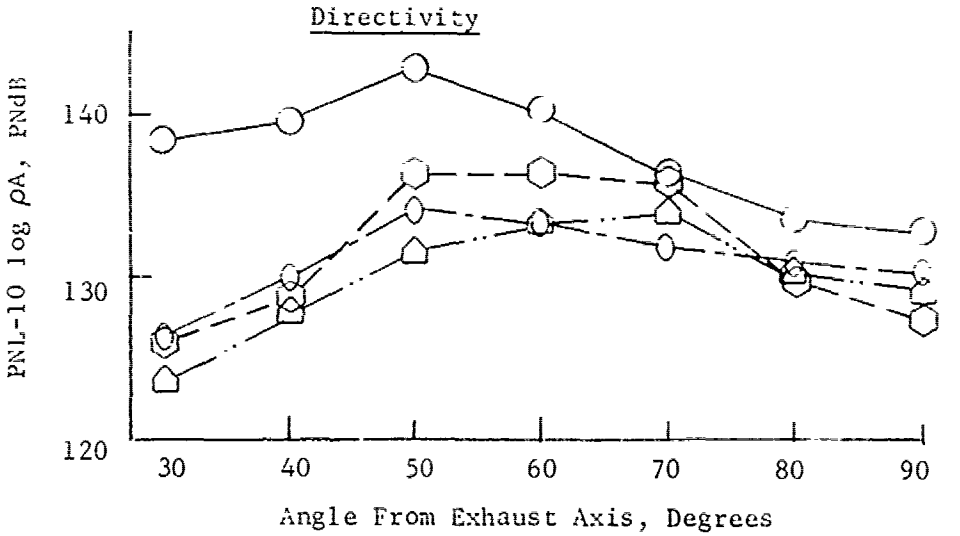

FIGURE V.F.3-24E 300 FT. SIDELINE SPECTRA & DIRECTIVITY COMPARISON FOR 37 TUBE HIGH TEMPERATURE MODELS

- o 37 Convergent End Tubes
- o 300 Ft. Sideline

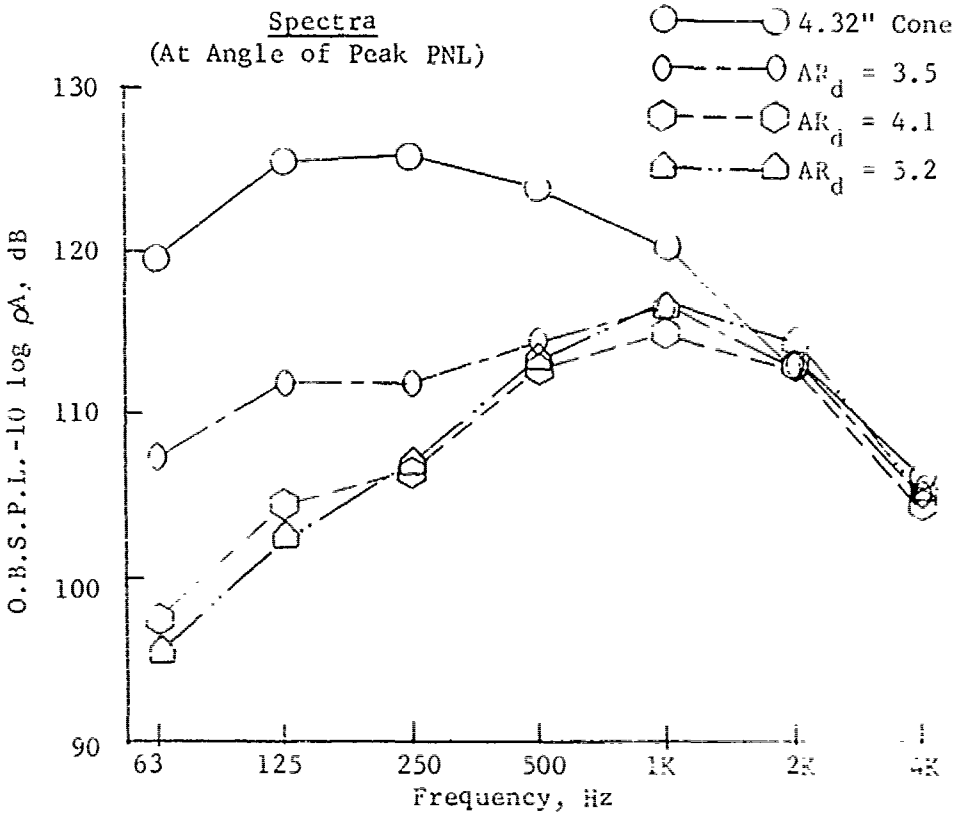

Data Includes Ground
Reflection Interference

$P_{T8}/P_o \approx 2.29$
$T_{T8} \approx 1560°R$
$V_j \approx 2010$ Ft/Sec

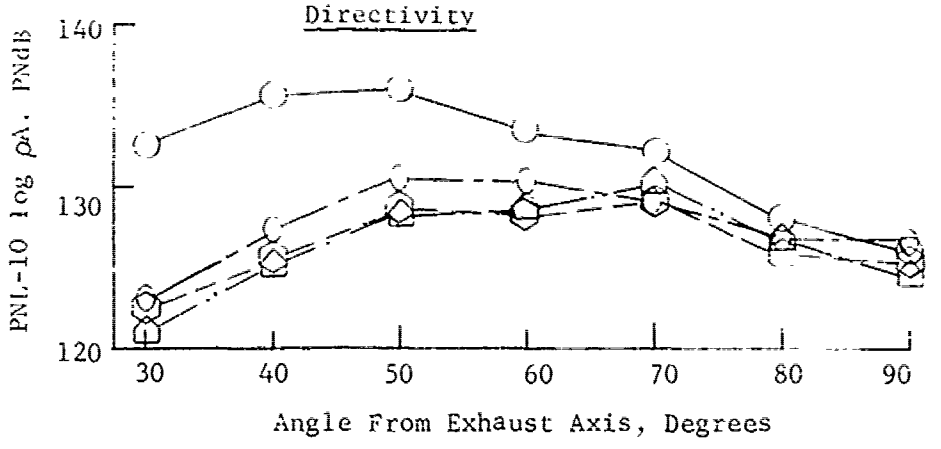

FIGURE V.F.3-24F 300 FT. SIDELINE SPECTRA & DIRECTIVITY COMPARISON FOR 37 TUBE HIGH TEMPERATURE MODELS

- o 37 Convergent End Tubes
- o 300 Ft. Sideline

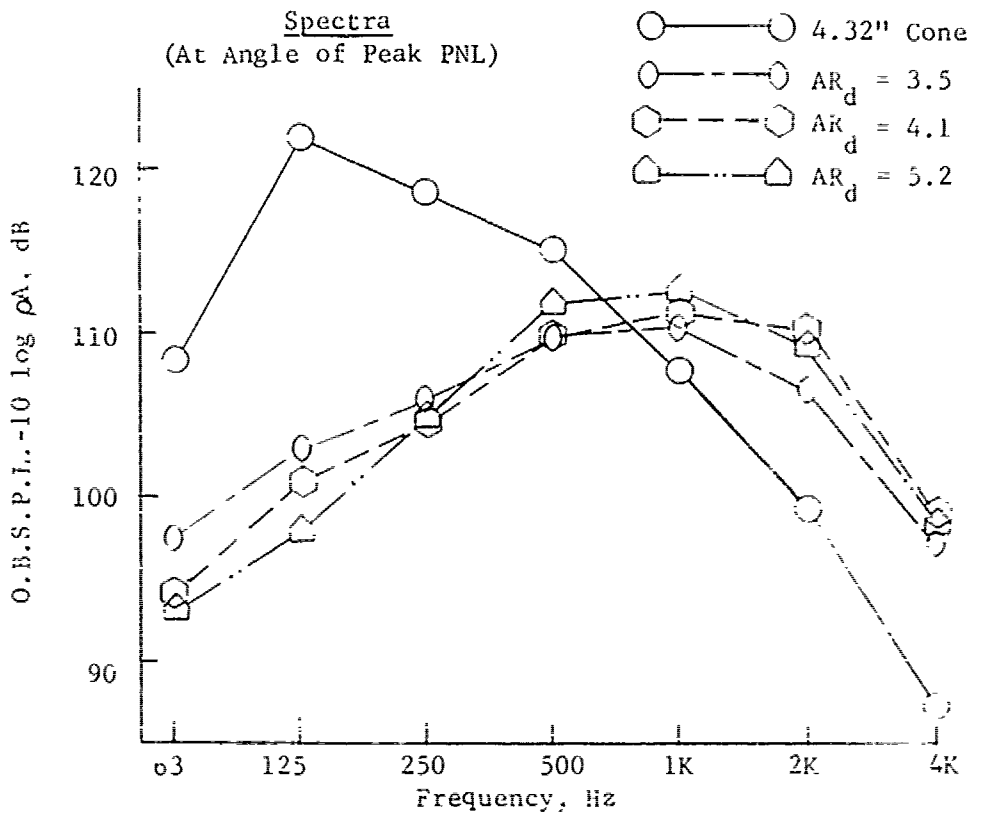

Data Includes Ground Reflection Interference

$P_{T8}/P_o \approx 1.76$

$T_{T8} \approx 1530°R$

$V_j \approx 1660$ Ft/Sec

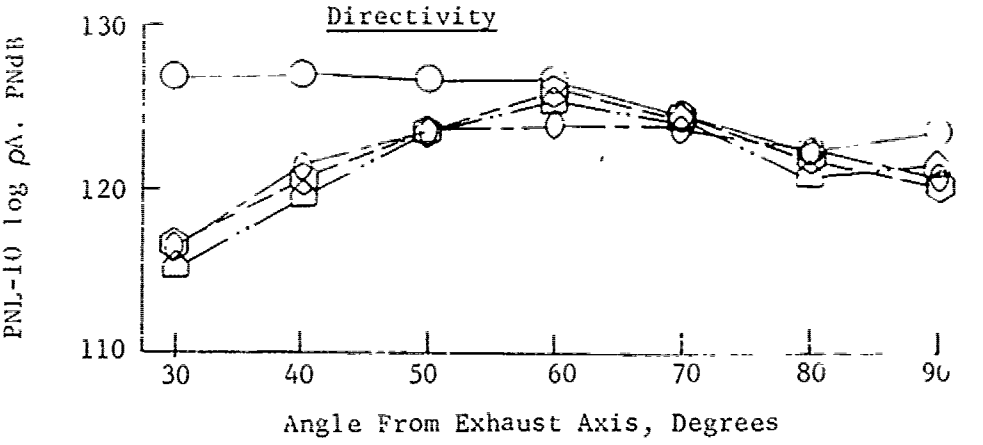

FIGURE V.F.3-24G 300 FT. SIDELINE SPECTRA & DIRECTIVITY COMPARISON FOR 37 TUBE HIGH TEMPERATURE MODELS

- o 37 Convergent End Tubes
- o 300 Ft. Sideline

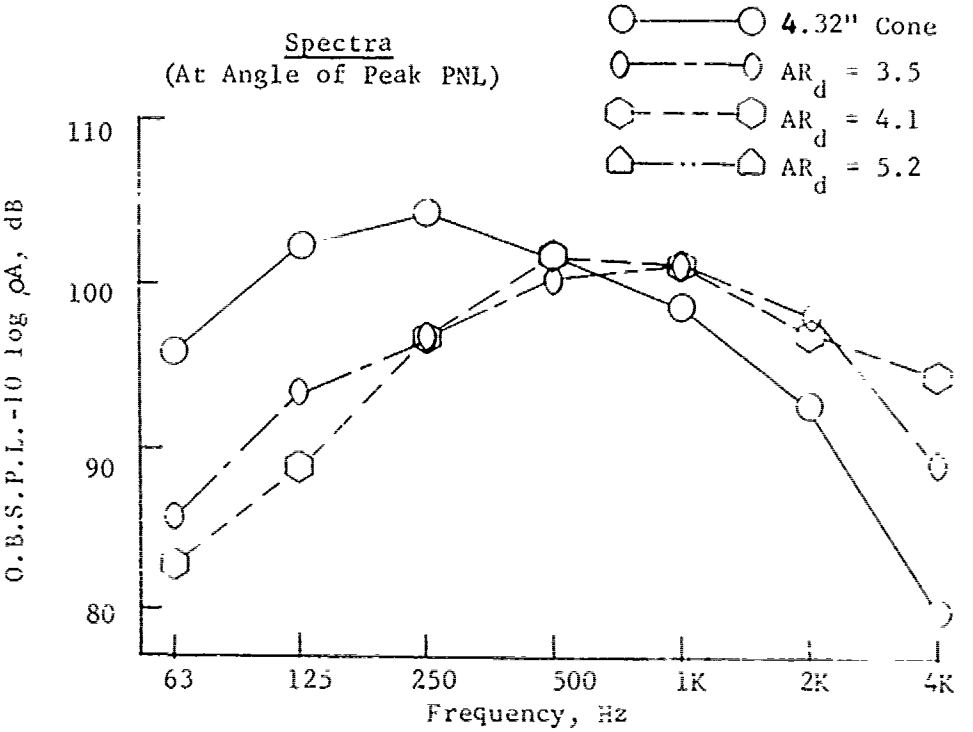

Data Includes Ground Reflection Interference

$P_{T8}/P_o \approx 1.44$

$T_{T8} \approx 1150°F$

$V_j \approx 1170$ Ft/Sec

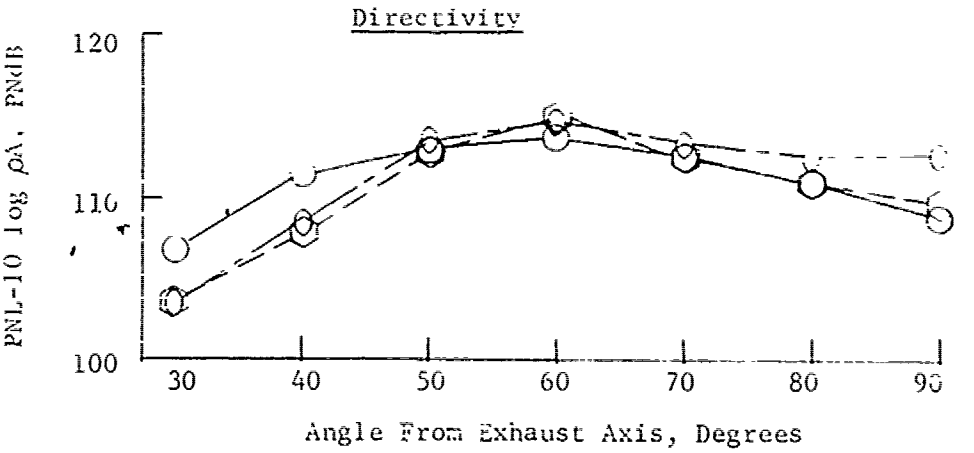

FIGURE V.F.3-24H 300 FT. SIDELINE SPECTRA & DIRECTIVITY COMPARISON FOR 37 TUBE HIGH TEMPERATURE MODELS

V.F.4 TUBE END VARIATIONS ON 37 STRAIGHT, CONVERGENT, GREATREX AND CANTED END TUBES

PRECEDING PAGE BLANK-NOT FILMED

V.F.4 TUBE END VARIATIONS ON 37 STRAIGHT, CONVERGENT, GREATREX AND CANTED END TUBES

A study was performed to evaluate tube end variations within multi-element nozzles; tube end designs being Greatrex, convergent, straight and canted as per tube numbers 1 through 4 of Figure V.F.4-1. The tubes were made in sets of 37, to be interchangeable within baseplate hardware typical of Figure V.F.4-2. To study tube end effects at several area ratios, several baseplate configurations were made available. A baseplate with an area ratio of 4, borrowed from The Boeing Company, was used in the 1968 test series with Greatrex and convergent end tubes. Specifics of these models and others are listed on Figure V.F.4-1, including pertinent physical parameters, model numbers and test dates. For pictorial definition of physical parameters such as L_t, L_{ti}, D_t, etc., see Figure V.F.4-2. The early AR_d of 4 baseplate hardware was replaced by a thinner baseplate used in the 1969 test models; therefore, parameters of L_t and L_t/D_t changed slightly while using the same Greatrex tubes. The thinner AR_d of 4 baseplate and a new AR_d of 3 baseplate were each used for the Greatrex, straight and canted end tube models. Area ratio is referred to as 3.0 and 4.0 within this section although it changed slightly with individual tube end design, even though common baseplate hardware was used.

Figure V.F.4-3 shows the Greatrex and convergent end tubes; tube numbers 1 and 2 of Figure V.F.4-1. Figure V.F.4-4 is a typical hardware setup showing 37 Greatrex end tubes in the AR_d of 4 baseplate without the tube cover. The tube cover, shown in Figure V.F.4-4, was used on all models to bring the ratio of external tube length to internal tube diameter (L_t/D_t) within the range of practical application for study of base pressure variation with tube end design.

Table V.F.4-1 is a summary of all the test models and test dates within this study. Models 4.1T37-1 and 4.1T37-4 are the Greatrex and convergent end tubes tested in 1968. They will only be used to substantiate the increased suppression effectiveness of the Greatrex end tube within the 1969 test series. The others, Models 4.1T37-23, -27, -31, -29, -21 and -25, are straight, canted and Greatrex ends tested within the newer AR_d of 3 and 4 baseplate and tube cover hardware. The straight end tube design was used as the baseline configuration in the test series, referring changes in suppression due to Greatrex and canted ends to the straight end design.

PRECEDING PAGE BLANK-NOT FILMED

The major aerodynamic performance problem of multiple tube nozzle design is the accompanying low base pressure. As a possible means to alleviate drag loss due to low base pressure, the canted end tube was investigated. This design (tube number 4 of Figure V.F.4-1) is similar to the straight end tube but with the tube end canted or staggered. The angle varied from 0° to 5° depending on its location within the tube bundle. When properly assembled within the area ratio of 3 or 4 baseplate, see Figure V.F.4-5, the tube exits project to a common intersection point at the apex of a 10° total included angle cone.

Model acoustic tests were conducted on the General Electric Evendale, JENOTS Facility where acoustic measurements were taken on a 40 ft. arc and scaled by frequency and size to full scale application using a scale factor of 8:1. All data presented are, therefore, of simulated engine size and engine frequency range.

A 4.148" I.D. conical convergent nozzle was used to generate reference baseline data to which the multi-element nozzles are referenced for suppression. This data is tabulated in Table V.F.4-2 and plotted as 300 and 1500 ft. sideline normalized peak PNL as a function of jet velocity, in Figures V.F.4-6 and V.F.4-7. Average curves through this data are then used as baseline curves on the suppressor data plots.

For the suppressor nozzles, with the exception of the Greatrex and convergent end tests in 1968, 300 and 1500 ft. sideline normalized peak PNL versus V_j plots are presented, per the listing in Table V.F.4-1, as Figures V.F.4-8 through V.F.4-19. Composites of the 300 and 1500 ft. sideline peak PNL suppression levels are shown in Figures V.F.4-20 and -21, respectively, illustrating the acoustic performance levels of all three tube end designs relative to the conical baseline. The Greatrex end and canted end tube performance relative to the baseline straight end tube model is also shown, as well as a comparison of AR_d of 3 to AR_d of 4 performance for each tube type.

Area Ratio Effect

Considering area ratio effect, Figures V.F.4-20 and -21 show that for all three tube end configurations, at both sidelines, the AR_d of 3 models attained slightly greater peak PNL suppression than the AR_d of 4 models for jet velocities

below the range of 2300 to 2500 ft/sec. A plot of this Δ suppression attributable to area ratio change is shown in Figure V.F.4-22. With the exception of the Greatrex end tubes (see Figures V.F.4-20 and -21), the crossover point, beyond which the AR_d of 4 attains PNL suppression above the AR_d of 3, occurs in the jet velocity range between 2300 to 2500 ft/sec. The Greatrex end tube shows no convergence of suppression between AR_d of 3 and 4 and suggests that if a crossover exists where the larger area ratio becomes more effective it will not occur until very high jet velocity is attained.

Explanation for the existence of a crossover point hinges on the tube nozzle jet noise spectral content and its change with jet velocity. In the high jet velocity region, spectra of all area ratio tube models are primarily low frequency dominated, meaning the primary noise source is from the coalesced flow region where the individual tube flows have merged to a common stream, similar to a conical nozzle. The location of this coalesced region for any pressure ratio/jet velocity point, and hence the change in mixing length before coalescense, is dependent upon area ratio. The greater the area ratio, the further downstream the merging occurs; therefore, a greater mixing region, a lower noise level and higher suppression. In the low jet velocity region, spectra of all area ratio tube models are primarily high frequency dominated, meaning the primary noise source is from the region of individual tube flows rather than the coalesced tube flow. Classical subsonic theory would indicate that noise generation location aft of the individual tube exits remains essentially constant at velocities below choking. Thus a low area ratio would be favored since the streams from the closer spaced tubes would coalesce much sooner to a jet similar to a conical nozzle than a high area ratio with large spacing between individual streams. The sooner the coalescence, the lower the content of the predominately PNdB weighted high frequency noise produced by the noncoalesced tube flow.

The non-existence of the crossover point of peak PNL suppression for the AR_d of 3 and 4 Greatrex tube configurations (Figures V.F.4-20 and -21) can probably be explained through interpretation of their spectra content (see Figures V.F.4-26A through -26F). The area ratio of 4 continues to retain its predominant high frequency noise at the maximum tested V_j whereas the AR_d of 3 has a more balanced high and low frequency content. The retained greater

PNdB weighted high frequency content raises the AR_d of 4 PNdB level above that of AR_d of 3. High frequency retention in AR_d of 4 and not in the AR_d of 3 would be due to the more rapid coalescence of individual jet streams to a simulated conical stream in the AR_d of 3. Predominance of the high frequency content of the Greatrex tube spectra compared to a plain tube spectra, which normally shows low frequency predominance, would have to be a phenomena of the lobes of the Greatrex end tubes causing small individual high frequency generating jet streams.

A second possible explanation for non-existence of the crossover point is that the Greatrex models comprise a system of higher aerodynamic loss and, since all acoustic plots are presented on an ideal jet velocity basis, shifting of jet velocity for loss corrections would mean a lower measured jet velocity attained on the Greatrex end tubes than on the other models.

PNL Suppression - Canted End Tubes

Using the data from Figures V.F.4-20 and 21, a plot of PNL suppression attributable to canting the tube ends (with reference to the straight end tubes as baseline) is shown as Figure V.F.4-23. Canting the tube ends is seen to reduce the PNL suppression attainable by use of all straight end tubes. The magnitude of reduction varies with jet velocity and area ratio, the greater reduction for the larger area ratio. In general, 0.5 to 1.5 PNdB suppression reduction is seen for the AR_d of 3 and 1.5 to 2.5 Δ PNdB for the AR_d of 4. The suppression loss is explained through examination of spectra for the straight and canted end tubes, shown as 300 ft. sideline comparative spectra and directivity plots on Figures V.F.4-26A through -26F, and especially on Figure V.F.4-26F. The canted end tubes show levels of high frequency noise equal to the straight end tubes, but a greater content of low frequency noise. This suggests that by canting the tube ends, coalescence of individual stream flows into a simulated convergent nozzle stream occurs more rapidly than it would for straight end tubes, hence, the shorter mixing length and the greater low frequency noise content generated from the coalesced flow. This loss of suppression by canting is somewhat offset by better aerodynamic performance as seen later.

Greatrex End Effects

To illustrate the PNL suppression gain attributable to the Greatrex end tubes (design No. 1 of Figure V.F.4-1) over the baseline straight end tubes (design No. 3), the difference in Δ PNL levels from the suppression comparisons on Figures V.F.4-20 and 21 are shown on Figure V.F.4-24. The curves are a peak to peak PNL comparison and show an additional 1 to 2 PNdB suppression gain for the more compact tube array at AR_d of 3 above the AR_d of 4. This gain is due to the effect of Greatrex ends at that area ratio rather than a gain due to area ratio change alone.

As a check of suppression repeatability the PNL suppression curves relative to a conical baseline, generated from testing the Greatrex end tubes in the early AR_d of 4 baseplate on 8-5-68 (see Figure V.F.4-1 and Table V.F.4-1), are superimposed in Figure V.F.4-25 on the curves generated by testing the same tubes within the AR_d of 4 baseplate on 6-5-69. The two models are the same except for a slight change in L_t/D_t and the curves show very good agreement.

To further verify the PNL suppression gain attributable solely to the Greatrex ends, the suppression levels for the early AR_d of 4 Greatrex model were compared to those of the convergent end tube design No. 2 (see Figure V.F.4-1) in the AR_d of 4 baseplate within the 1968 test series. This is the third curve set on Figure V.F.4-24 and shows quite good agreement with the Greatrex to straight tube comparison. Thus, the Greatrex ends produce from 4 to 7 PNdB suppression gain above straight ends, the magnitude fluctuating with area ratio and jet velocity.

As mentioned, Figures V.F.4-26A through 26F are 300 ft. sideline spectra and directivity comparisons for straight, canted, and Greatrex end tubes; arranged in order of increasing jet velocity.

Design curves for estimating spectra change due to addition of Greatrex ends to straight or convergent end tubes are presented on Figure V.F.4-27, the upper curve set showing the same angle comparison and the lower curve set showing the peak to peak comparison. Both curve sets show most suppression is attained in the 250, 500 and 1000 Hz octave bands.

Aero Analysis - Base Pressure and Base Drag

Each of the tube nozzles had base pressure instrumentation (static taps) applied per Figure V.F.4-2. The basic pressure profiles were used to calculate the mean base pressures by integrating the measured static pressures over their respective incremental base areas and dividing the total value by the total base area acted upon. This data is presented for all six tube configurations in Figure V.F.4-28 as the mean base pressure ratio ($\bar{P}_{base}/P_o$) versus the nozzle pressure ratio (P_{T8}/P_o). Canting the tube ends to a projected common intersection point at the apex of a 10° included angle cone increased the flow of ventilating air causing higher base pressures than the straight end tubes. The Greatrex end tubes were more highly starved of ventilating air toward the center tubes causing the mean base pressure to be lowered significantly with reference to the straight end tubes. The mean base pressure increased with the larger area ratio for all three tube configurations, since more area was available between tubes for entraining air and ventilating the base region. However, with increasing pressure ratio, mean base pressure ratio steadily decreased due to two opposing effects; a) the greater degree of entrainment made possible with increased pressure ratio and, b) the decreased available ventilation area, especially above a pressure ratio of 2.0, due to the increased plume width between the outer row of holes. The much higher rate of mean base pressure decrease for the Greatrex end tubes can be attributed to the more rapid increase in plume width since each tube has twelve separate flared-out flow paths at the exit.

The mean base pressure, $\bar{P}_{base}$, variation is presented in a different manner in Figure V.F.4-29 as a function of P_{T8} in the form of $P_{T8}/\bar{P}_{Base}$ versus P_{T8}/P_o. However, in this form the trends are not as straightforward since they are a function of P_{T8}. The small changes in base pressure do not show up as well or as consistent as the mean base pressure ratio presentation in Figure V.F.4-28, due to the large range of P_{T8} compared to the magnitude of change between mean base pressure and ambient pressure.

Figure V.F.4-30 presents a comparison of the baseplate drag coefficient versus nozzle pressure ratio, P_{T8}/P_o, for the three tube end configurations at each area ratio. The drag coefficient is defined as the ratio of drag force per unit area

to the velocity pressure per unit area of the approaching stream using the equation:

$$C_D = \frac{F_D}{\frac{1}{2g} A_P \rho V^2}$$

Through substitution of Mach number and density definitions the equation changes to:

$$C_D = \frac{+ \quad F_D}{\frac{1}{2} A_P P_o k M^2}$$

The drag force, F_D, is calculated from the mean base pressure data. The velocity pressure of the approaching stream is calculated from the stream parameters of P_{T8} and T_{T8} for Mach number, M, and using:

A_P = projected base area exclusive of tube flow area
P_o = ambient pressure
k = specific heat ratio

Presented in this form the trends are the same as the mean base pressure ratio trends showing a higher loss or greater drag coefficient for the Greatrex end tubes and a lower drag coefficient or lower loss for the canted end tubes than for the baseline straight end tubes.

Conclusions

- Canting the tube ends to a projected common intersection point at the apex of a 10° included angle cone decreased PNL suppression attainable, with reference to straight end tubes, by 0.5 to 2.5 PNdB; exact magnitude dependent on jet velocity and area ratio. Offsetting this suppression loss is a significant gain in base pressurization.
- Addition of Greatrex ends acquired a total PNL suppression gain of 4 to 7 PNdB, the magnitude again dependent on jet velocity and area ratio. In addition to the basic area ratio effect causing suppression change, the Greatrex end tubes showed 1 to 2 PNdB additional suppression gain when used in the more compact area ratio of 3 tube array than in the AR_d of 4.

PNL suppression repeatability of the Greatrex end tube model through comparison of 1968 to 1969 tests proved very satisfactory.

- Aerodynamically, the Greatrex end tube configurations were highly starved of ventilating air toward the center tubes causing the mean base pressure to be lowered significantly and base drag to increase greatly with reference to the straight end tubes.
- Design curves for future application when estimating spectral suppression attainable through addition of Greatrex end tubes have been developed. They show predominant suppression in the 250, 500 and 1000 Hz octave bands.
- Addition of Greatrex ends shifts the peak PNL angle from it dominant 60° position to a constant 80° angle from the jet exhaust axis.
- Decrease in area ratio from 4 to 3 increased suppression on all three tube type configurations within the jet velocity range below 2300 to 2500 ft/sec. The crossover point in increasing V_j, where the higher area ratio becomes more effective in PNL suppression, occurred for the straight end and canted end tubes but not for the Greatrex end tubes, a phenomena which may well exist or may just be delayed until higher jet velocity.
- Aerodynamically, the area ratio increase from 3 to 4 produced higher base pressurization for all three tube types, resulting from the greater area available between tubes for entraining air and ventilating the base region.

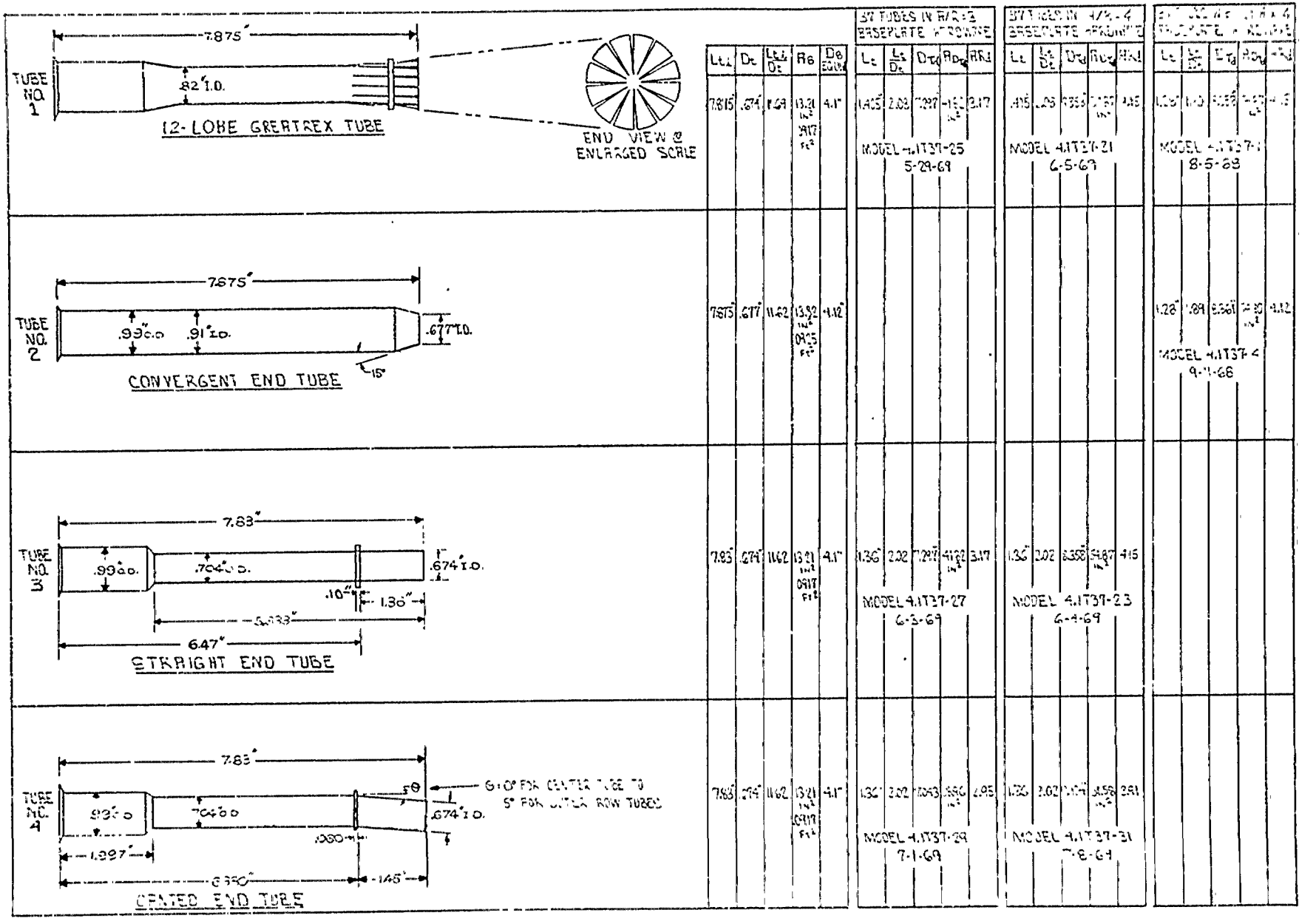

	L_{t_1}	D_t	L_{t_1}/D_t	R_B	D_B EQUIV.
12-LOBE GREATREX TUBE	7.815"	.674"	11.59	13.21 in² .0917 ft²	4.17"
CONVERGENT END TUBE	7.875"	.677"	11.62	13.32 in² .0925 ft²	4.12"
STRAIGHT END TUBE	7.83"	.674"	11.62	13.21 in² .0917 ft²	4.17"
CANTED END TUBE	7.83"	.674"	11.62	13.21 in² .0917 ft²	4.17"

37 TUBES IN R/B=3 BASEPLATE ARRANGE

	L_t	L_t/D_t	D_{T_d}	R_{D_T}	R_{N_d}
12-LOBE GREATREX TUBE	1.405"	2.08	7.297"	4.12 in²	3.17
CONVERGENT END TUBE					
STRAIGHT END TUBE	1.36"	2.02	7.297"	4.12 in²	3.17
CANTED END TUBE	1.36"	2.02	7.043"	3.86 in²	2.95

MODEL 4.1T37-25 5-29-69
MODEL 4.1T37-27 6-3-69
MODEL 4.1T37-29 7-1-69

37 TUBES IN R/B=4 BASEPLATE ARRANGE

	L_t	L_t/D_t	D_{T_d}	R_{D_T}	R_{N_d}
12-LOBE GREATREX TUBE	.415	2.08	8.358"	5.487 in²	4.15
CONVERGENT END TUBE					
STRAIGHT END TUBE	1.36"	2.02	8.358"	5.487 in²	4.15
CANTED END TUBE	1.36"	2.02	8.104"	5.258 in²	3.91

MODEL 4.1T37-21 6-5-69
MODEL 4.1T37-23 6-4-69
MODEL 4.1T37-31 7-8-69

37 TUBES IN R/B=4 BASEPLATE + NOZZLES

	L_t	L_t/D_t	D_{T_d}	R_{D_T}	R_{N_d}
12-LOBE GREATREX TUBE	1.405"	2.08	8.358"	5.487 in²	4.15
CONVERGENT END TUBE	1.28"	1.89	8.358"	5.30 in²	4.12
STRAIGHT END TUBE					
CANTED END TUBE					

MODEL 4.1T37-1 8-5-68
MODEL 4.1T37-4 9-11-68

FIGURE V.F.4-1 SCHEMATIC OF TUBE NOZZLE HARDWARE SPECIFICS FOR TUBE END STUDY

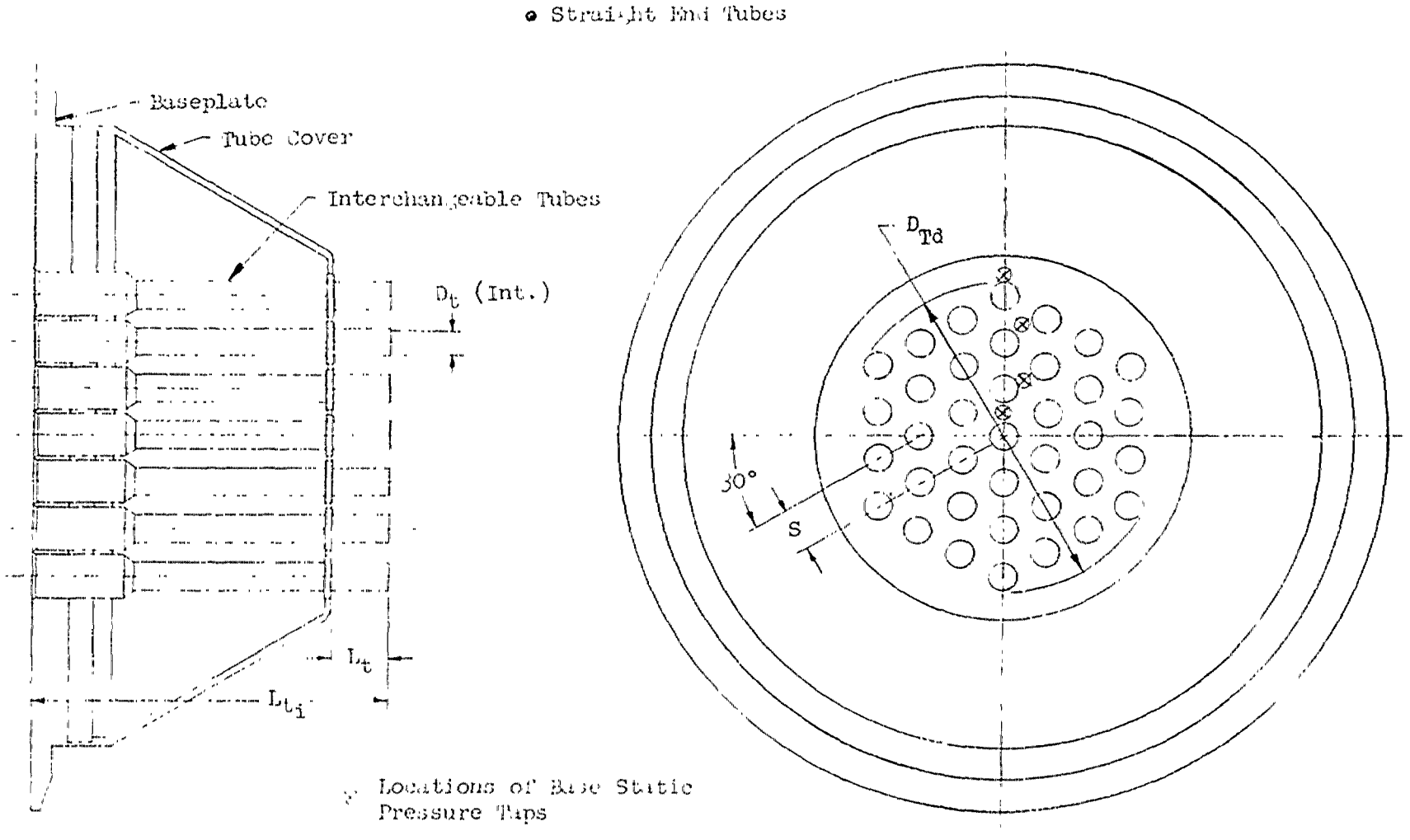

FIGURE V.F.4-2 SCHEMATIC OF 37 TUBE NOZZLE CONFIGURATION WITH STRAIGHT END TUBES

Tube No. 1

12-Lobe Greatrex Tube

Tube No. 2

Convergent End Tube

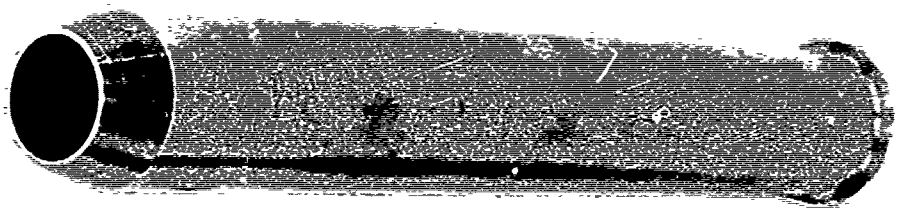

FIGURE V.F.4-3 TYPICAL TUBE HARDWARE FOR END VARIATION STUDY

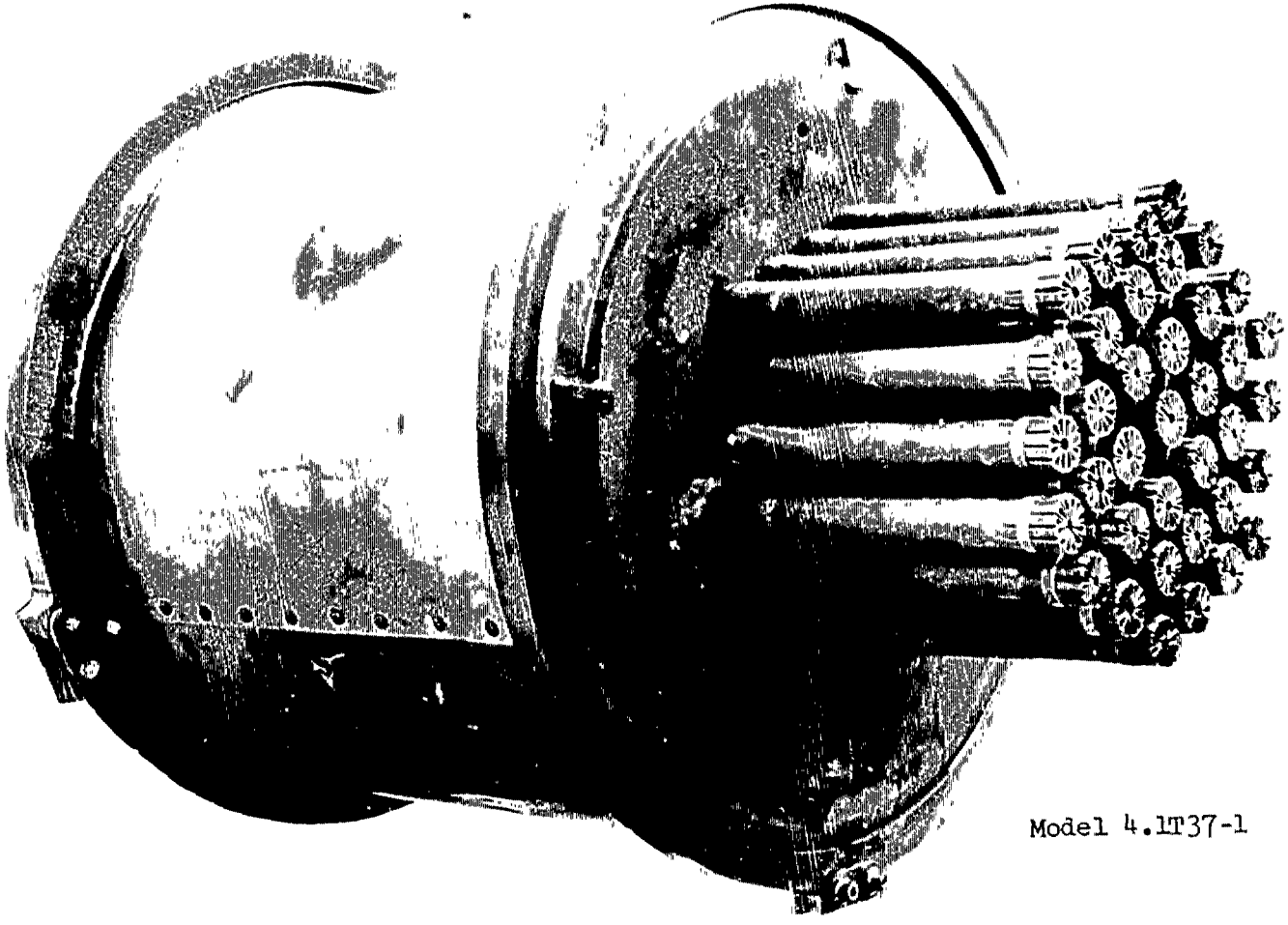

FIGURE V.F.4-4 37 GREATREX END TUBES IN AR_d = 4 BASEPLATE

TABLE V.F.4-1 TEST CONFIGURATION SUMMARY

TUBE NO.	TUBE DESCRIPTION	AR_d	MODEL NO.	TEST DATA	REMARKS	ACOUSTIC DATA ON SECTION V.F.4 FIGURES	TABLES
1	37 GREATREX END	4.0	4.1T37-1	8-05-68	TEST DATA USING EARLY AR_d = 4 BASEPLATE	-	-
2	37 CONVERGENT END	4.0	4.1T37-4	9-11-68		-	-
3	37 STRAIGHT END	4.0	4.1T37-23	6-04-69	TEST DATA USING AR_d = 3 AND 4 BASEPLATES	8 & 9	3
3	37 STRAIGHT END	3.0	4.1T37-27	6-03-69		10 & 11	4
4	37 CANTED END	4.0	4.1T37-31	7-08-69		12 & 13	5
4	37 CANTED END	3.0	4.1T37-29	7-01-69		14 & 15	6
1	37 GREATREX END	4.0	4.1T37-21	6-05-69		16 & 17	7
1	37 GREATREX END	3.0	4.1T37-25	5-29-69		18 & 19	8
	MODEL 4.1 (4.148" I.D. CONVERGENT NOZZLE) TESTED ON EACH ABOVE DATE AS ACOUSTIC BASELINE FOR SUPPRESSOR MODEL.					6 & 7	2

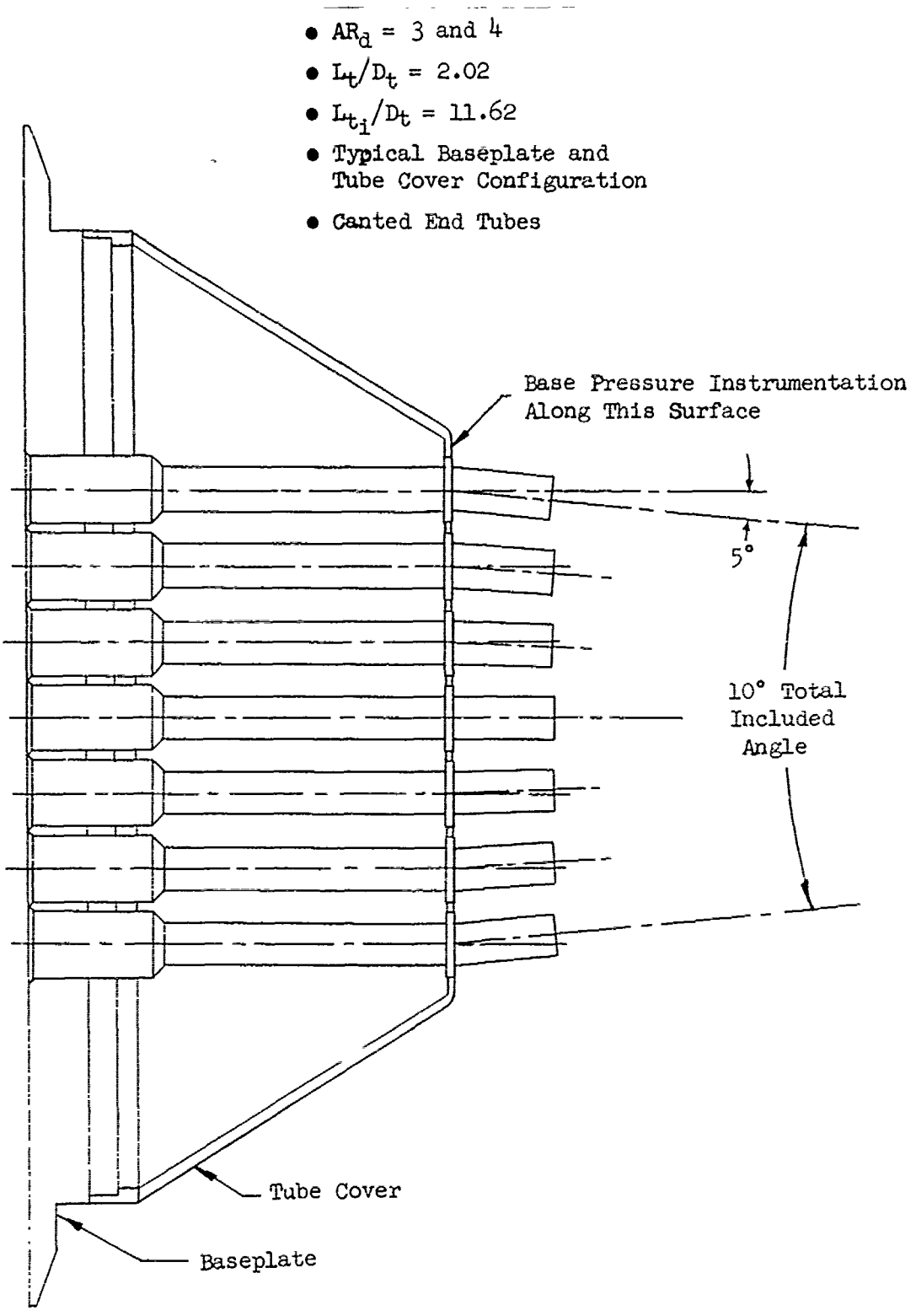

FIGURE V.F.4-5 SCHEMATIC OF 37 TUBE NOZZLE CONFIGURATION WITH CANTED END TUBES

TABLE V.F.4-2 TEST SUMMARY

MODEL NO. 4.1" Cone

DESCRIPTION: 4.148" I.D. Baseline Conical Nozzle

DATE: 4/11/69; 6/5/69

SCALE MODEL A_8 = .0938 ft^2

FULL SCALE A_8 = 6.003 ft^2

SCALE FACTOR = 8:1

- o DATA INCLUDES GROUND REFLECTION INTERFERENCE
- o ANGLE REFERENCED TO JET EXHAUST

RDG NO.	TEST CONDITIONS				ACOUSTIC TEST RESULTS						
			IDEAL			320' ARC		300' SIDELINE		1500' SIDELINE	
	P_{T8}/P_o	T_{T8} (°R)	V_j (ft/sec)	W_8 (PPS)	10 log oA	PEAK PNdB	PEAK ANGLE	PEAK PNdB	PEAK ANGLE	PEAK PNdB	PEAK ANGLE
4/11/69											
1	1.36	1160	1092	3.53	-6.6	110.4	50	108.2	50	92.6	50
2	1.89	1506	1748	4.82	-7.4	128.8	30	124.3	40	108.8	40
3	2.82	1515	2188	7.41	-6.7	137.0	40	134.4	50	118.9	50
4	2.82	1766	2363	6.84	-7.3	139.2	50	137.0	50	121.2	50
5	2.85	1993	2520	6.28	-7.8	138.3	50	136.2	50	120.6	50
6/5/69											
1	1.37	1164	1100	3.54	-6.8	108.3	50	106.1	50/60	90.6	50
2	1.87	1541	1758	4.78	-7.6	127.0	40	124.0	50	108.6	50
3	2.83	1518	2195	7.39	-6.7	136.4	40	133.4	50	117.6	50
4	2.85	1989	2520	6.29	-7.9	139.9	50	137.6	50	121.6	50

TABLE V.F.4-2 TEST SUMMARY

(Cont.)

MODEL NO. 4.1" Cone

DESCRIPTION: 4.148" I.D. Baseline Conical Nozzle

DATE: 5/29/69; 6/3/69; 6/4/69

SCALE MODEL A_8 = .0938 ft^2

FULL SCALE A_8 = 6.003 ft^2

SCALE FACTOR = 8:1

- o DATA INCLUDES GROUND REFLECTION INTERFERENCE
- o ANGLE REFERENCED TO JET EXHAUST

RDG NO.	TEST CONDITIONS				ACOUSTIC TEST RESULTS						
			IDEAL			320' ARC		300' SIDELINE		1500' SIDELINE	
	P_{T8}/P_o	T_{T8} (°R)	V_j (ft/sec)	W_8 (PPS)	10 log ρA	PEAK PNdB	PEAK ANGLE	PEAK PNdB	PEAK ANGLE	PEAK PNdB	PEAK ANGLE
5/29/69											
1	1.36	1158	1084	3.90	-6.7	108.4	50	106.2	50	90.7	50
2	1.83	1516	1718	5.10	-7.6	-	-	123.3	50	107.7	50
3	2.86	1512	2199	7.47	-6.8	135.3	40	132.8	50	116.9	50
4	2.85	1985	2516	6.57	-7.9	137.9	50	135.7	50	119.9	50
6/3/69											
1	1.35	1141	1060	3.53	-6.6	-	-	105.6	80	89.8	80
2	1.88	1515	1746	4.50	-7.5	-	-	123.1	50	107.7	50
3	2.82	1512	2186	7.36	-6.7	-	-	134.4	50	118.6	50
4	2.83	2008	2524	6.10	-7.9	-	-	137.3	50	121.5	50
6/4/69											
1	1.31	1167	1026	3.60	-6.7	108.2	30	105.9	50	90.6	50
2	1.88	1519	1752	4.90	-7.5	126.9	30	122.8	50	107.3	50
3	2.82	1517	2190	7.42	-6.7	135.7	40	132.4	50	116.6	50
4	2.86	1946	2494	6.40	-7.8	139.1	50	136.9	50	121.0	50

TABLE V.F.4-2 TEST SUMMARY

(Cont.)

MODEL NO. 4.1" Cone

DESCRIPTION: 4.148" I.D. Baseline Conical Nozzle

DATE: 7/1/69; 7/8/69

SCALE MODEL A_8 = .0938 ft^2

FULL SCALE A_8 = 6.003 ft^2

SCALE FACTOR = 8:1

- o DATA INCLUDES GROUND REFLECTION INTERFERENCE
- o ANGLE REFERENCED TO JET EXHAUST

	TEST CONDITIONS				ACOUSTIC TEST RESULTS						
						320' ARC		300' SIDELINE		1500' SIDELINE	
RDG NO.	P_{T8}/P_o	T_{T8} (°R)	IDEAL V_j (ft/sec)	W_8 (PPS)	10 log ρA	PEAK PNdB	PEAK ANGLE	PEAK PNdB	PEAK ANGLE	PEAK PNdB	PEAK ANGLE
7/1/69											
1	1.34	1154	1052	3.51	-6.6	106.9	50	104.7	50	89.0	50
2	1.47	1469	1362	3.59	-7.6	116.3	50	114.1	50	98.7	50
3	1.88	1523	1748	5.04	-7.5	126.7	30	124.3	50	108.6	50
4	2.82	1512	2186	7.68	-6.7	136.6	40	133.6	50	117.9	50
5	2.84	1997	2520	6.43	-7.9	140.0	50	137.9	50	122.2	50
6	2.52	1794	2264	6.27	-7.7	138.6	40	134.1	40	116.3	50
7	2.82	1775	2368	7.01	-7.4	139.4	50	137.1	50	121.0	50
8	2.30	1645	2069	6.08	-7.5	133.0	40	130.5	50	114.7	50
9	2.14	1514	1906	5.89	-7.3	133.9	70	127.6	50	112.1	50
10	1.64	1534	1562	4.35	-7.6	121.8	30	119.3	50	103.7	50
11	1.52	1247	1304	4.39	-6.8	115.5	40	112.5	50	96.9	50
7/8/69											
1	1.38	1140	1098	3.73	-6.5	108.9	50	106.7	50	91.0	50
2	1.88	1498	1742	5.08	-7.4	129.1	30	123.4	50	107.7	50
3	2.83	1516	2194	7.59	-6.7	137.4	40	134.2	50	118.1	50
4	2.86	1984	2518	6.28	-7.8	139.7	50	137.4	50	121.5	50

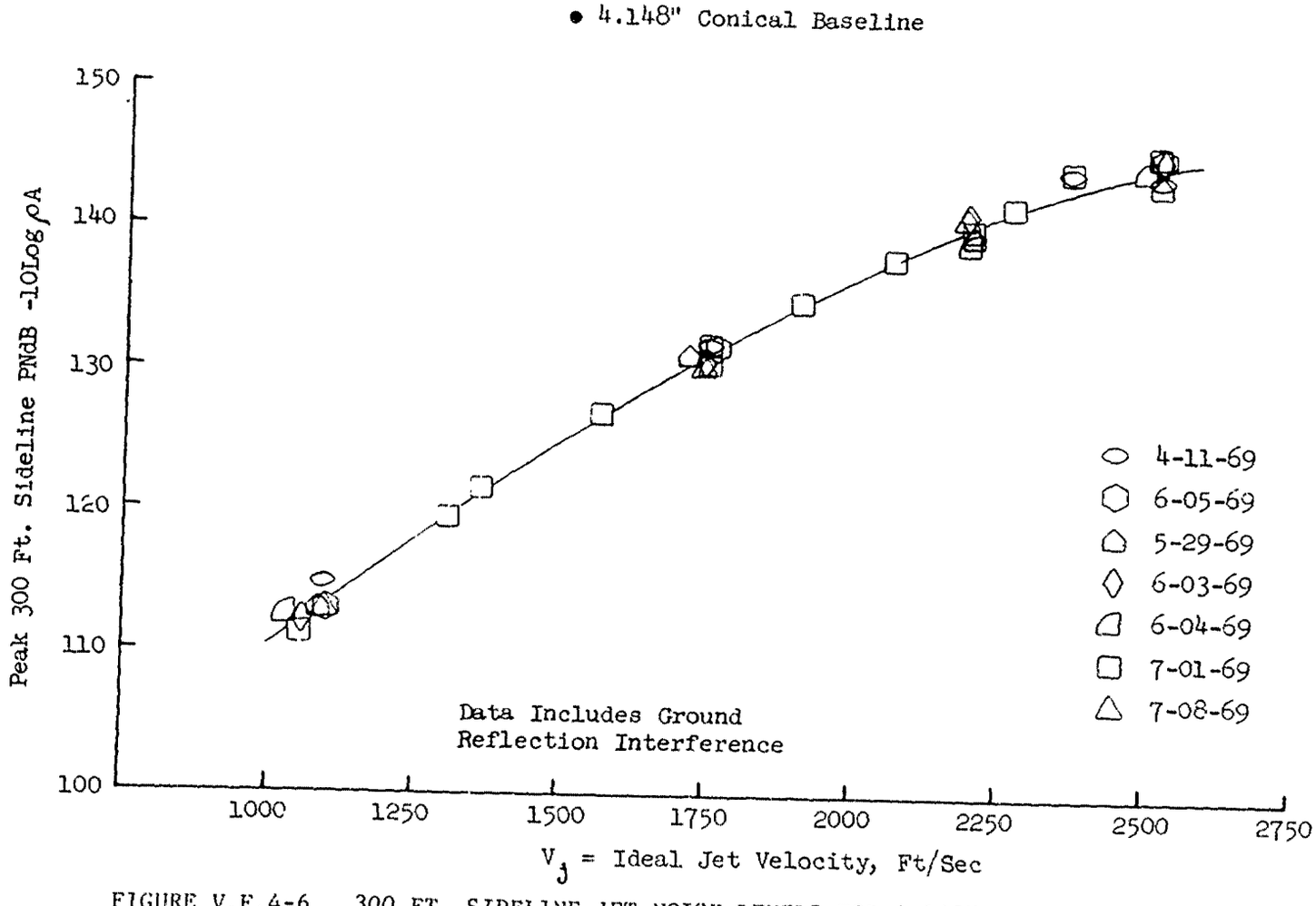

FIGURE V.F.4-6 300 FT. SIDELINE JET NOISE LEVELS FOR 4.148" CONE

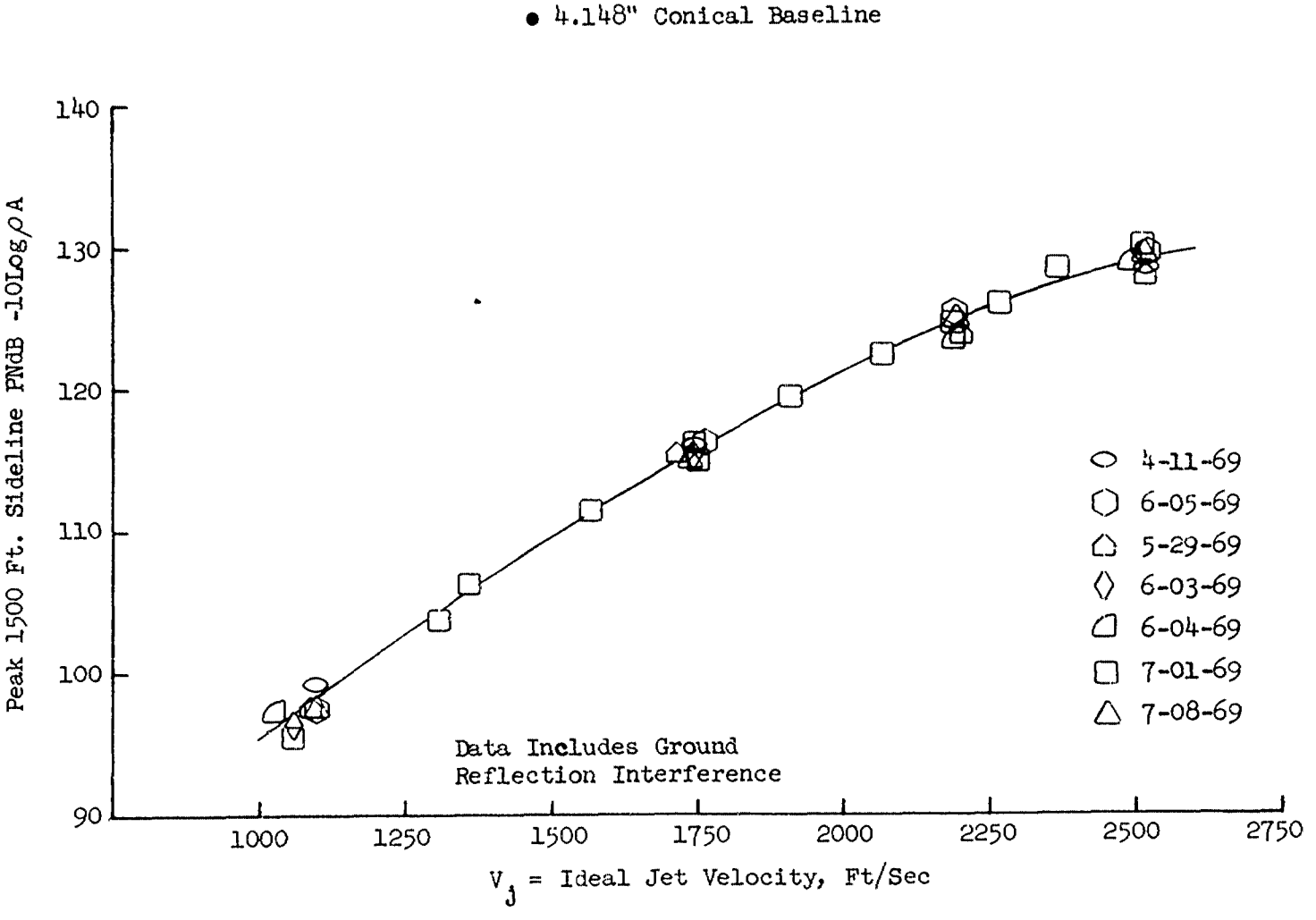

FIGURE V.F.4-7 1500 FT. SIDELINE JET NOISE LEVELS FOR 4.148" CONE

TABLE V.F.4-3 TEST SUMMARY

MODEL NO. 4.1T37-23

DESCRIPTION 37 Straight End Tubes, .624" I.D. AR_d = 4

DATE: 6/4/69

SCALE MODEL A_8 = .0917 ft^2

FULL SCALE A_8 = 5.869 ft^2

SCALE FACTOR = 8:1

- o DATA INCLUDES GROUND REFLECTION INTERFERENCE
- o ANGLE REFERENCED TO JET EXHAUST

	TEST CONDITIONS				ACOUSTIC TEST RESULTS						
			IDEAL			320' ARC		300' SIDELINE		1500' SIDELINE	
RDG NO.	P_{TS}/P_o	T_{T8} (°R)	V_j (ft/sec)	W_8 (PPS)	10 log ρA	PEAK PNdB	PEAK ANGLE	PEAK PNdB	PEAK ANGLE	PEAK PNdB	PEAK ANGLE
1	1.37	1156	1097	3.29	-6.7	108.2	50	105.9	50	88.7	50
2	1.48	1514	1397	3.42	-7.8	113.0	50	110.6	50	93.6	50
3	1.53	1234	1310	4.08	-6.9	112.5	50	110.4	80	92.9	80
4	1.68	1523	1594	4.04	-7.7	117.3	50	115.2	60	97.7	60
5	1.90	1519	1764	4.76	-7.6	120.4	50	118.3	60	100.8	60
6	2.16	1582	1947	5.35	-7.6	122.9	50	121.6	60	104.1	60
7	2.33	1653	2086	5.70	-7.6	123.8	30/40	121.7	60	104.2	60
8	2.55	1774	2265	6.00	-7.7	125.3	30	123.8	80	106.2	80
9	2.85	1519	2210	7.26	-6.8	125.8	30	124.2	60	106.7	60
10	2.84	1787	2398	6.67	-7.5	126.8	50	124.9	80	107.4	80
11	2.87	1983	2523	6.17	-7.9	128.3	40	125.5	80	108.1	80

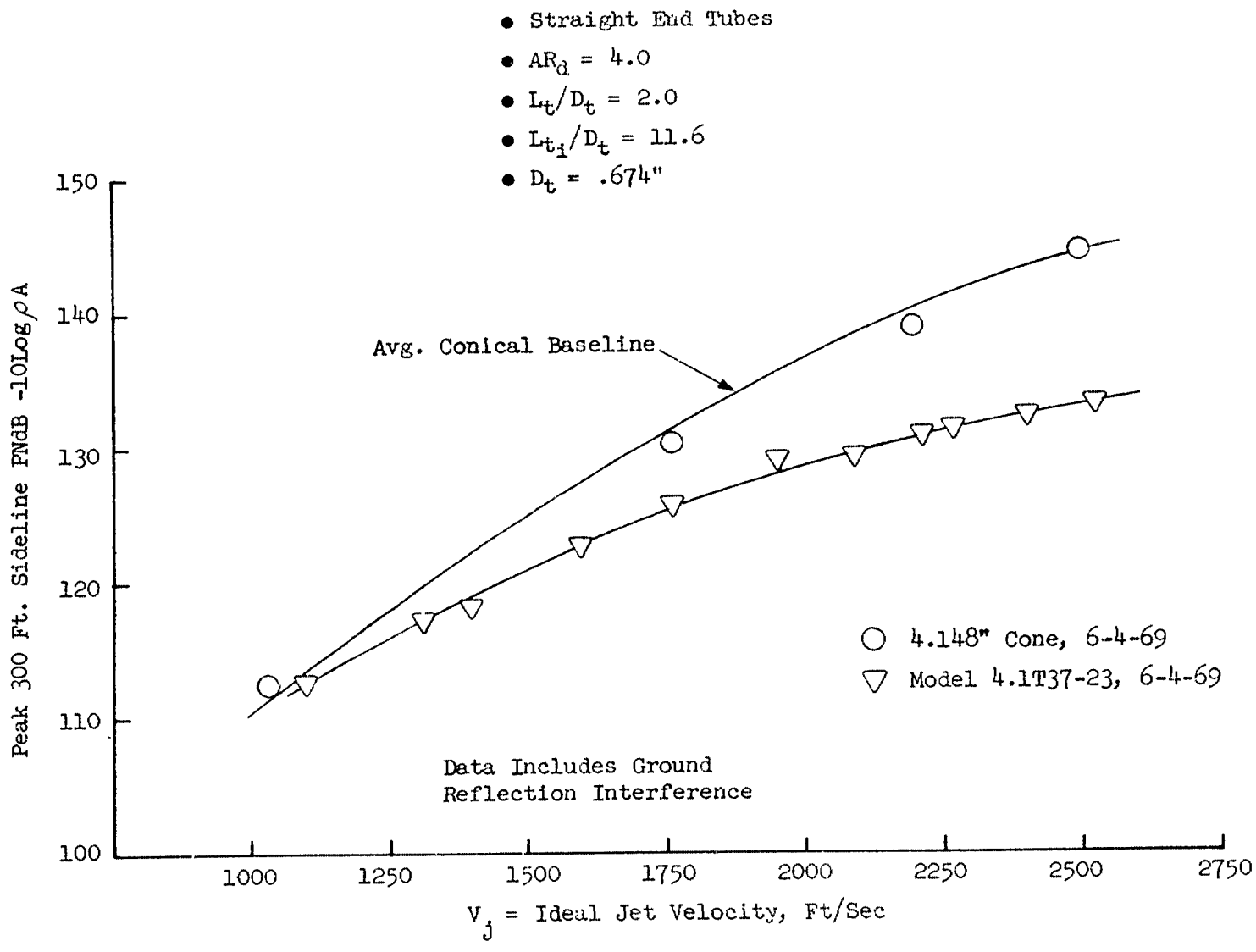

FIGURE V.F.4-8 300 FT. SIDELINE JET NOISE LEVELS FOR 37 STRAIGHT END TUBE NOZZLE, AR_d=4 0

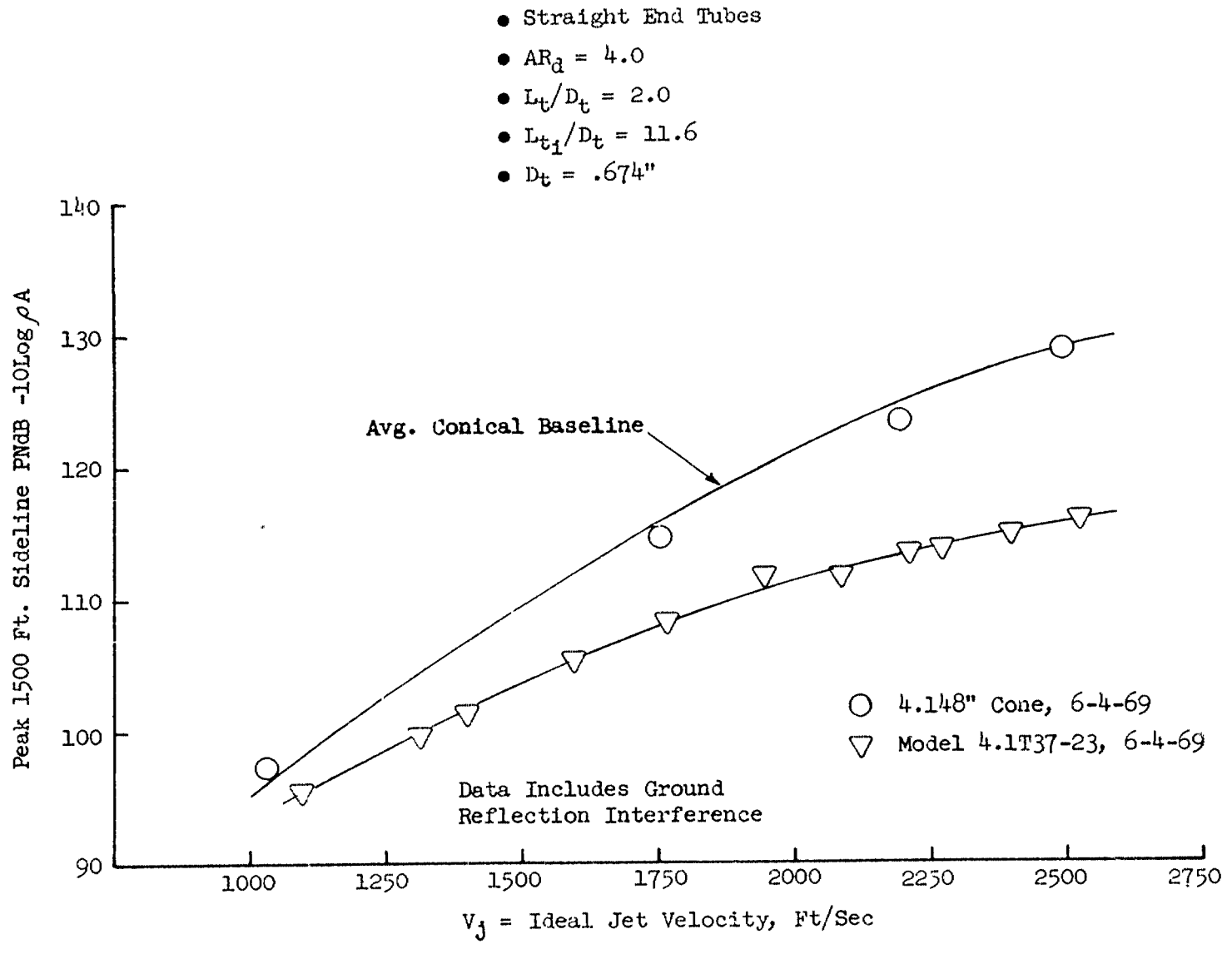

FIGURE V.F.4-9 1500 FT. SIDELINE JET NOISE LEVELS FOR 37 STRAIGHT END TUBE NOZZLE, AR_d=4.0

TABLE V.F.4-4 TEST SUMMARY

MODEL NO. 4.1T37-27

DESCRIPTION: 37 Straight End Tubes, $AR_d = 3$

DATE: 6/3/69

SCALE MODEL A_8 = .0917 ft^2

FULL SCALE A_8 = 5.869 ft^2

SCALE FACTOR = 8:1

- o DATA INCLUDES GROUND REFLECTION INTERFERENCE
- o ANGLE REFERENCED TO JET EXHAUST

	TEST CONDITIONS				ACOUSTIC TEST RESULTS						
			IDEAL			320' ARC		300' SIDELINE		1500' SIDELINE	
RDG NO.	P_{TS}/P_c	T_{T8} (°R)	V_j (ft/sec)	W_8 (PPS)	10 log ρA	PEAK PNdB	PEAK ANGLE	PEAK PNdB	PEAK ANGLE	PEAK PNdB	PEAK ANGLE
1	1.30	1143	998	3.42	-6.7	105.5	50	103.2	60	86.9	50
2	1.49	1485	1391	3.42	-7.7	111.3	60	110.3	60	93.2	60
3	1.54	1235	1317	3.88	-6.9	111.2	50	109.1	60	91.7	60
4	1.66	1500	1566	3.93	-7.7	115.7	50	113.4	50/60	96.1	60
5	1.90	1516	1763	4.64	-7.6	119.2	50	117.4	60	100.0	60
6	2.14	1562	1936	5.12	-7.5	122.0	50	120.9	60	103.3	60
7	2.33	1641	2078	5.46	-7.6	129.8	50	121.1	70/80	103.6	70/80
8	2.55	1772	2260	5.67	-7.7	125.5	30	122.6	60	105.3	60
9	2.83	1521	2196	6.84	-6.8	125.9	30/50	123.5	50	106.5	50
10	2.86	1771	2382	6.23	-7.4	127.7	40	124.2	80	106.8	60/80
11	2.88	1986	2527	5.62	-7.9	129.5	50	127.2	50	109.9	50

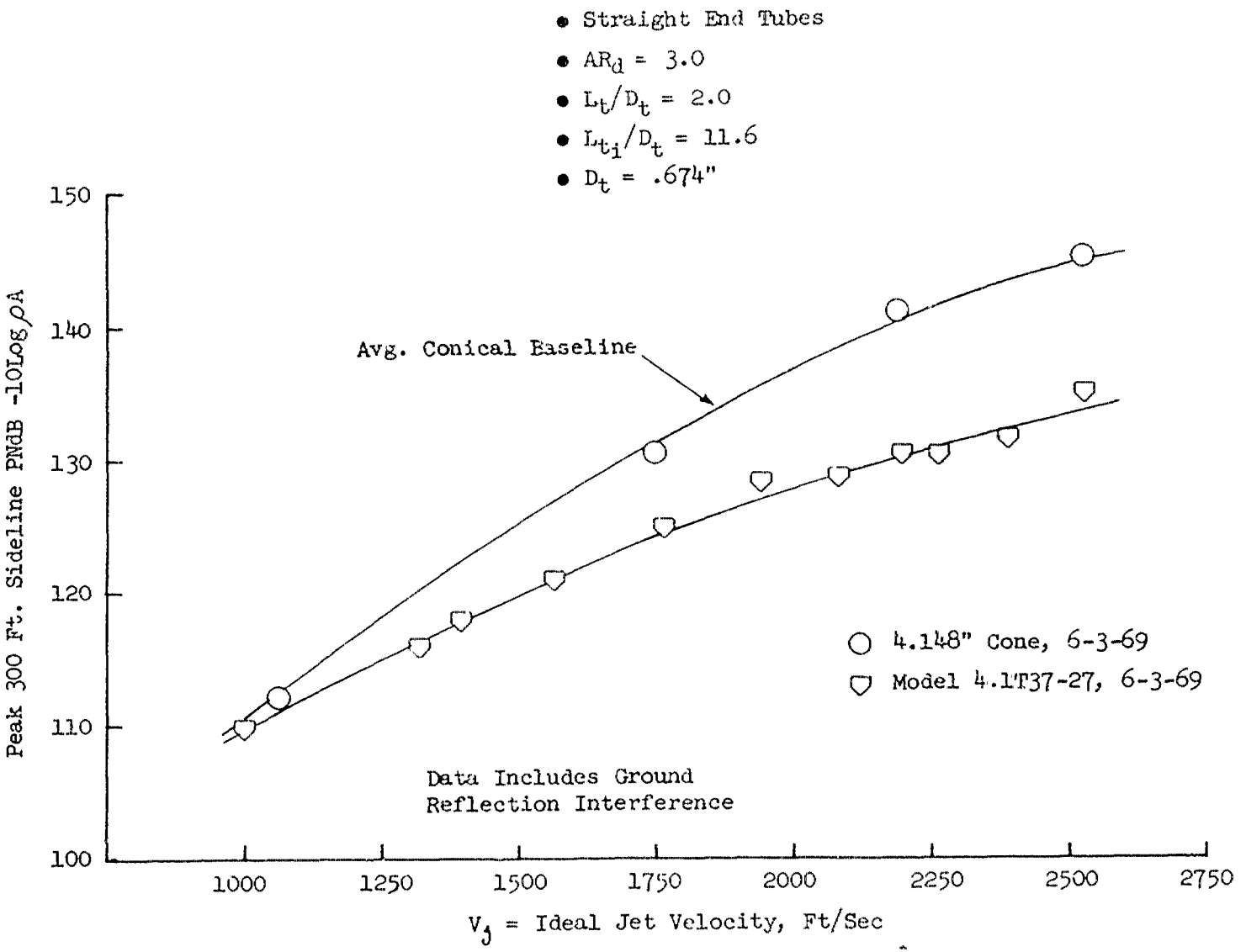

FIGURE V.F.4-10 300 FT. SIDELINE JET NOISE LEVELS FOR 37 STRAIGHT END TUBE NOZZLE, AR_d=3.0

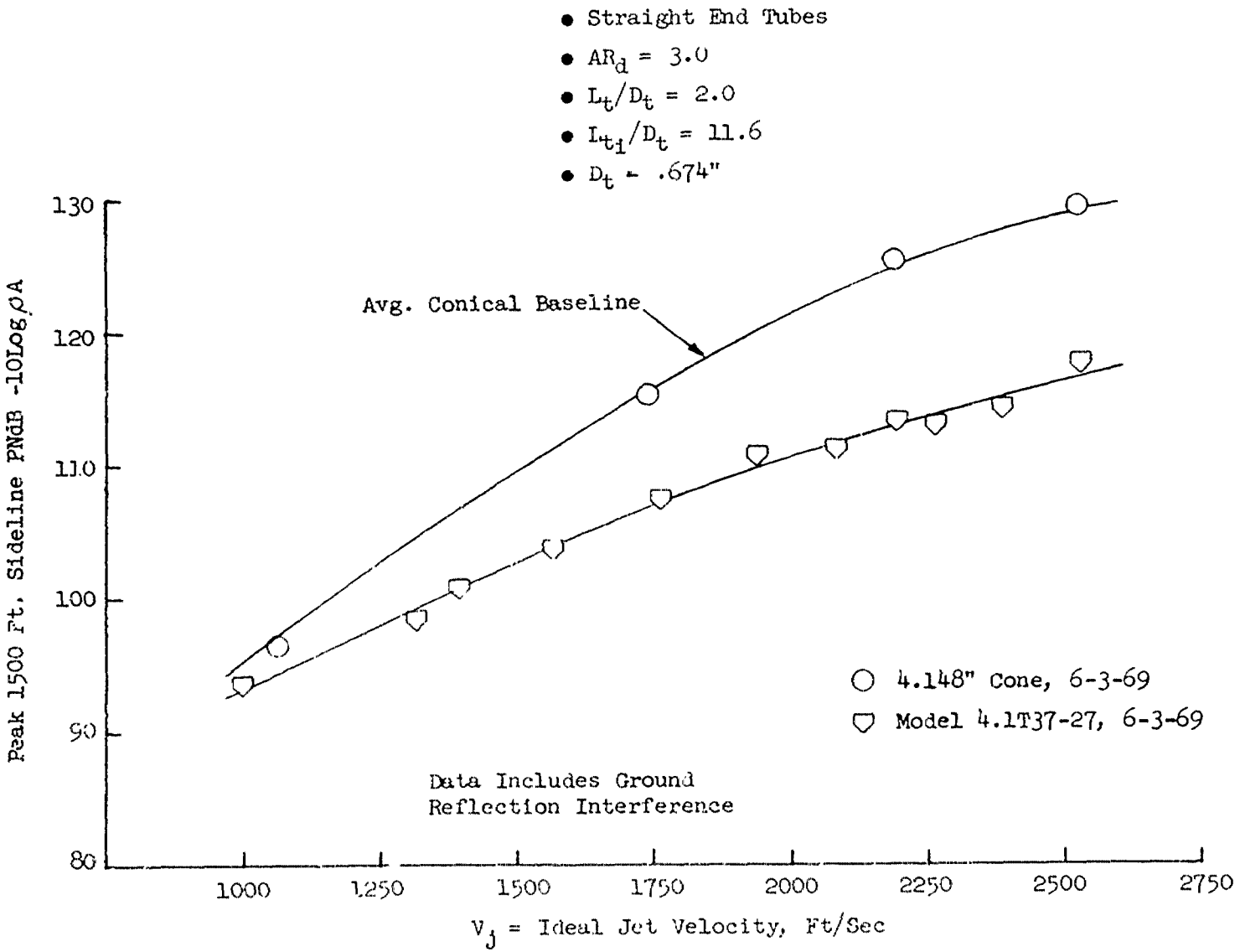

FIGURE V.F.4-11 1500 FT. SIDELINE JET NOISE LEVELS FOR 37 STRAIGHT END TUBE NOZZLE, AR_d=3.0

TABLE V.F.4-5 TEST SUMMARY

MODEL NO. 4.1T37-31

DESCRIPTION: 37 Canted End Tubes, $AR_d = 4$

DATE: 7/8/79

SCALE MODEL A_8, = .0917 ft^2

FULL SCALE A_8 = 5.869 ft^2

SCALE FACTOR = 8:1

- o DATA INCLUDES GROUND REFLECTION INTERFERENCE
- o ANGLE REFERENCED TO JET EXHAUST

	TEST CONDITIONS				ACOUSTIC TEST RESULTS						
			IDEAL			320' ARC		300' SIDELINE		1500' SIDELINE	
RDG NO.	P_{T8}/P_o	T_{T8} (°R)	V_j (ft/sec)	W_8 (PPS)	10 log oA	PEAK PNdB	PEAK ANGLE	PEAK PNdB	PEAK ANGLE	PEAK PNdB	PEAK ANGLE
1	1.38	1149	1100	3.39	-6.7	108.0	60	107.1	60	89.8	60
2	1.49	1508	1405	3.42	-7.8	115.2	60	114.3	60	96.9	60
3	1.54	1242	1320	4.12	-6.9	114.1	60	113.2	60	95.7	60
4	1.68	1512	1592	4.07	-7.7	119.4	50	117.5	60	100.0	60
5	1.92	1488	1755	4.65	-7.5	121.7	50	120.5	60	102.9	60
6	2.18	1559	1940	5.23	-7.5	123.7	40	122.7	60	105.1	60
7	2.36	1645	2094	5.47	-7.6	126.7	30	123.9	50	106.1	50
8	2.38	1771	2275	5.74	-7.7	127.4	40	124.7	70	107.2	70
9	2.89	1521	2215	6.98	-6.7	128.2	30	125.6	60	108.1	60
10	2.86	1765	2378	6.59	-7.4	128.3	50	126.4	60	108.9	60
11	2.87	1989	2526	6.00	-7.9	129.4	40	127.1	60	109.7	60

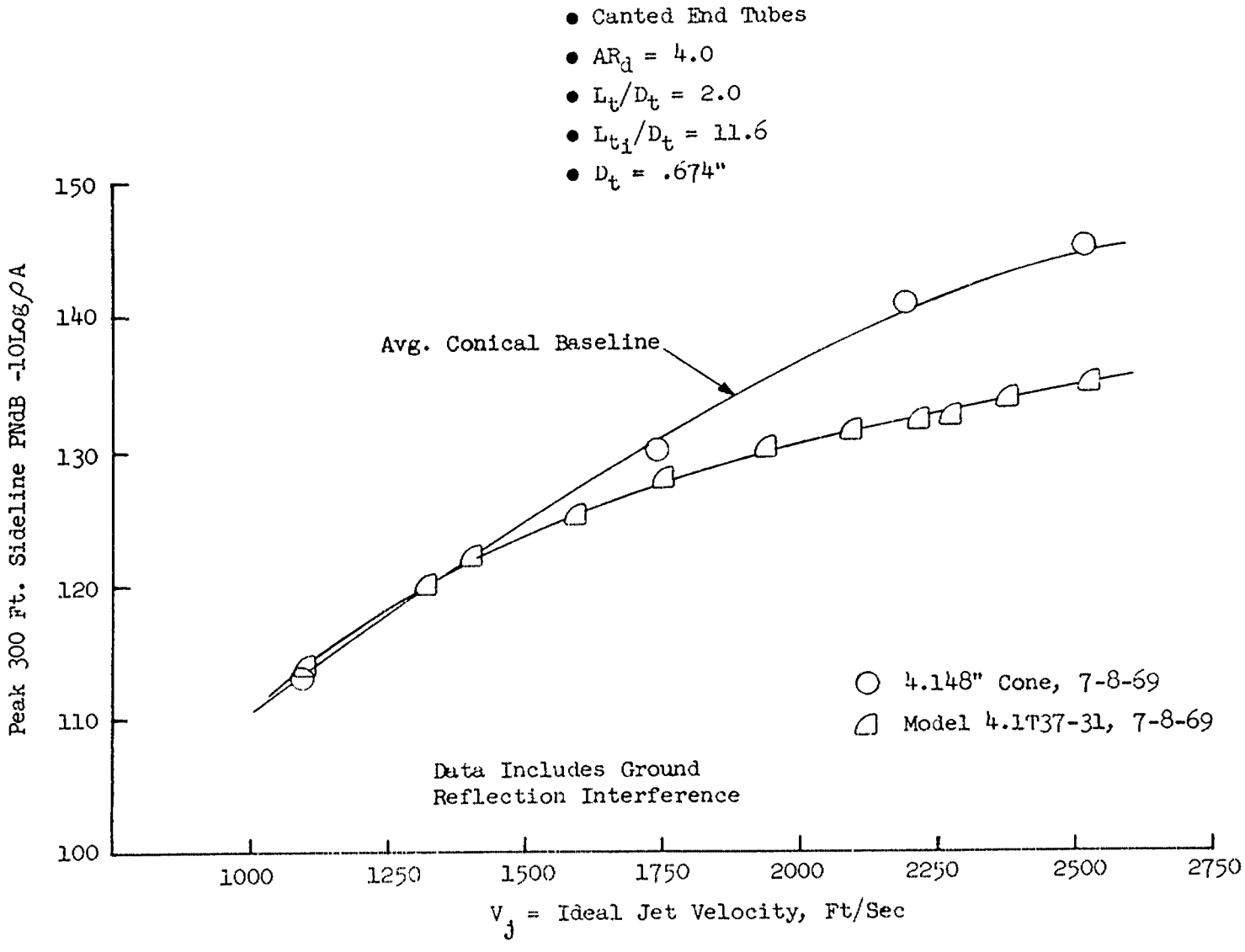

FIGURE V.F.4-12 300 FT. SIDELINE JET NOISE LEVELS FOR 37 CANTED END TUBE NOZZLE, AR_d=4.0

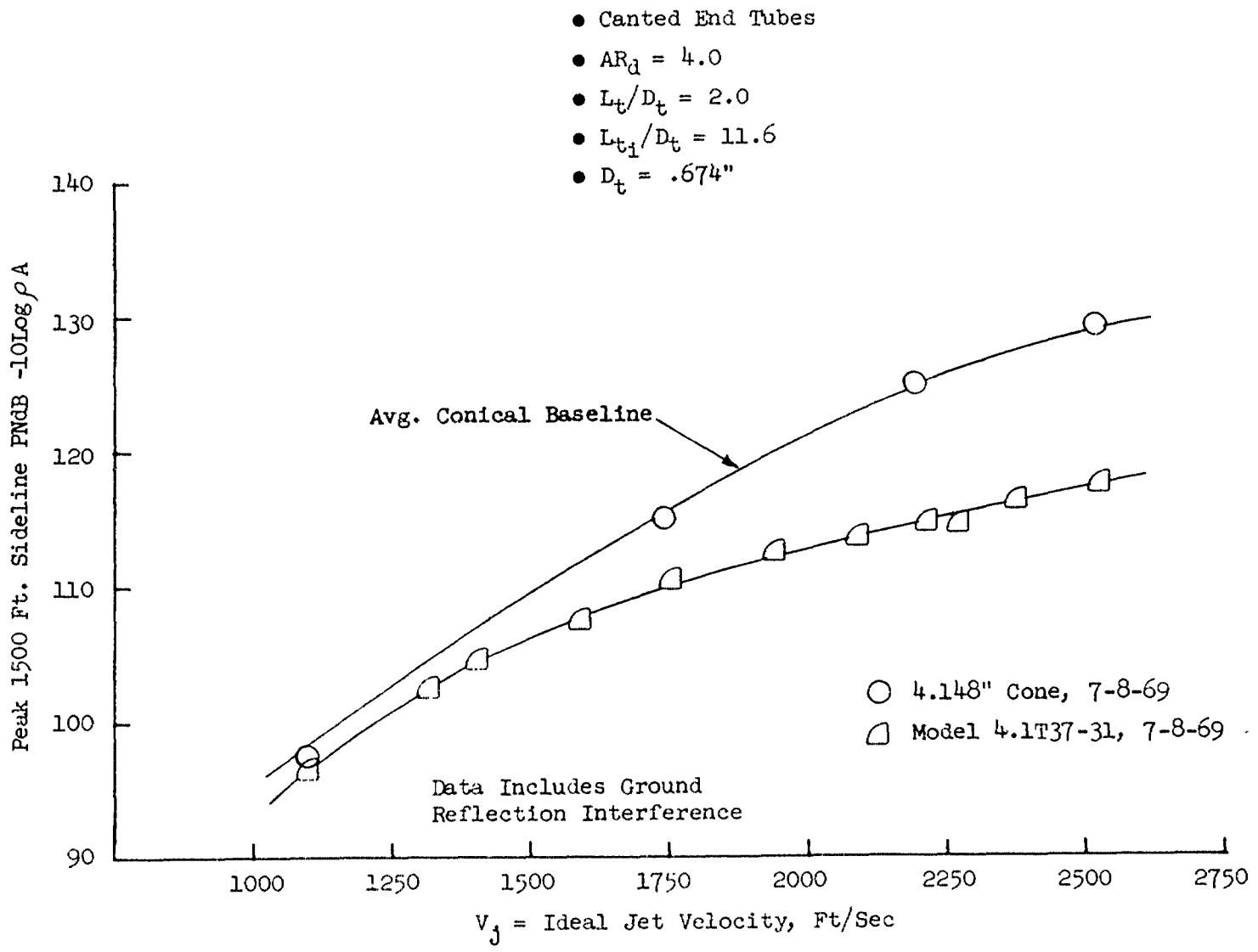

FIGURE V.F.4-13 1500 FT. SIDELINE JET NOISE LEVELS FOR 37 CANTED END TUBE NOZZLE, AR_d=4.0

TABLE V.F.4-6 TEST SUMMARY

MODEL NO. 4.1T37-29

DESCRIPTION: 37 Canted End Tubes, AR_d = 3

DATE: 6/30/69; 7/1/69

SCALE MODEL A_8 = .0917 ft^2

FULL SCALE A_8 = 5.869 ft^2

SCALE FACTOR = 8:1

- o DATA INCLUDES GROUND REFLECTION INTERFERENCE
- o ANGLE REFERENCED TO JET EXHAUST

	TEST CONDITIONS				ACOUSTIC TEST RESULTS						
			IDEAL			320' ARC		300' SIDELINE		1500' SIDELINE	
RDG NO.	P_{T8}/P_o	T_{T8} (°R)	V_j (ft/sec)	W_8 (PPS)	10 log σA	PEAK PNdB	PEAK ANGLE	PEAK PNdB	PEAK ANGLE	PEAK PNdB	PEAK ANGLE
6/30/69											
1	1.37	1151	1096	3.52	-6.7	105.6	60	104.7	60	87.3	60
2	1.43	1527	1336	3.23	-7.9	110.5	60	109.6	60	92.1	60
3	1.55	1256	1337	3.98	-6.9	111.6	50	110.4	60	92.9	60
4	1.67	1516	1586	4.04	-7.7	120.0	40	114.7	60	97.3	60
5	1.91	1529	1778	4.64	-7.6	116.4	30	117.5	60	100.0	60
6	2.16	1557	1940	5.22	-7.5	123.3	50	120.9	50	103.5	50
7	2.33	1655	2089	5.49	-7.6	126.4	40	123.1	60	105.5	60
7/1/69											
1	1.38	1159	1116	3.61	-6.7	105.8	50	103.5	50	86.2	50
2	1.48	1531	1409	3.54	-7.8	112.1	60	111.2	60	93.9	60
3	1.55	1218	1321	3.70	-6.8	110.9	50	109.4	60	92.1	60
4	1.66	1517	1582	4.08	-7.7	92.1	60	116.3	60	97.7	60
5	1.90	1512	1761	4.69	-7.5	120.9	40	116.1	40/50/60	98.9	50/60
6	2.17	1586	1964	5.22	-7.5	123.3	40	119.9	60	102.5	60
7	2.33	1658	2087	5.59	-7.6	125.0	40	121.2	60	103.9	60
8	2.57	1792	2282	5.84	-7.7	127.9	50	125.5	50	108.2	50
9	3.00	1500	2235	5.50	-6.6	127.5	40	123.4	50	106.8	50
10	2.85	1771	2378	6.53	-7.4	129.7	40	126.1	50	109.1	50
11	2.86	2002	2532	5.83	-7.9	130.6	40	127.2	50	110.8	50

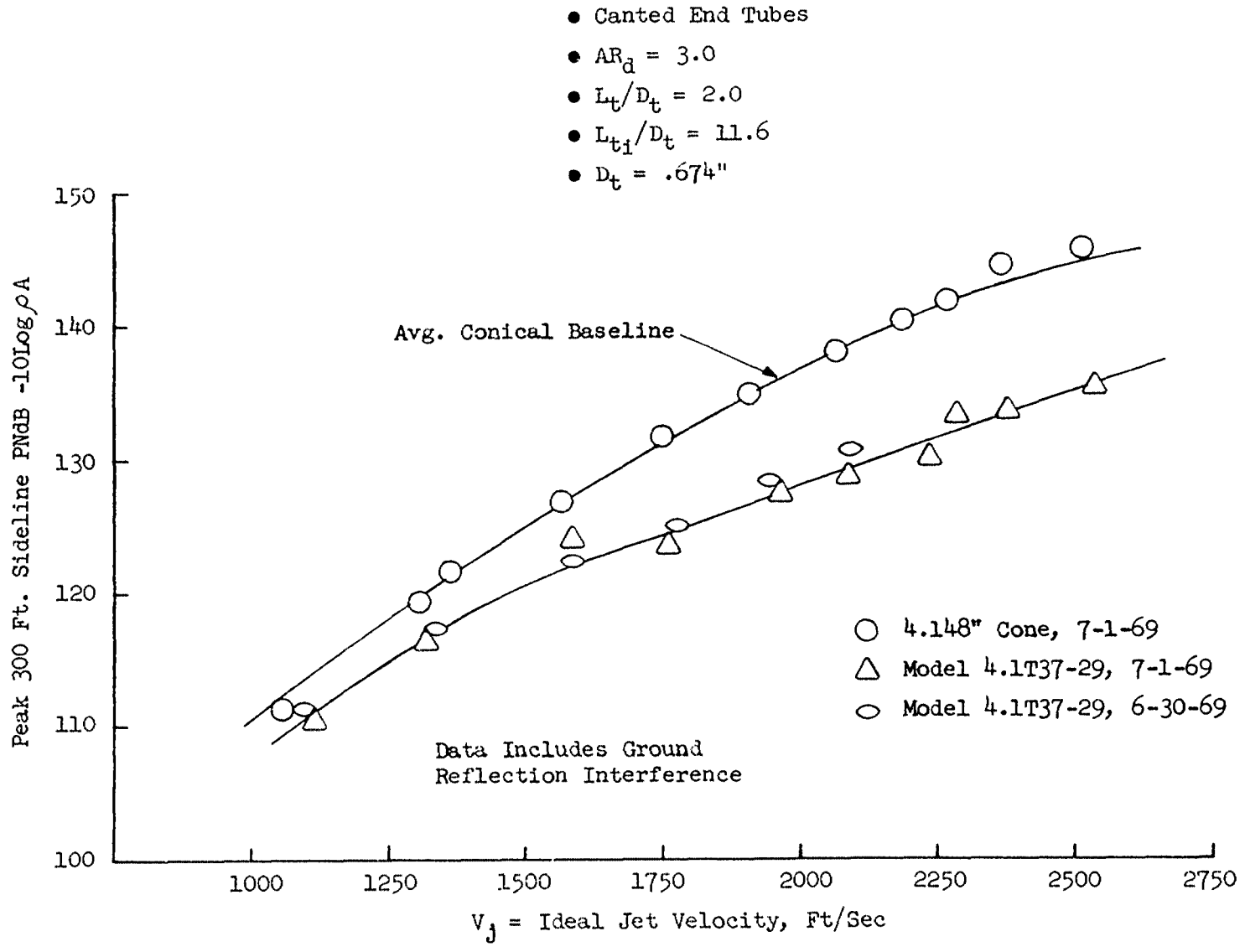

FIGURE V.F.4-14 300 FT. SIDELINE JET NOISE LEVELS FOR 37 CANTED END TUBE NOZZLE, AR_d=3.0

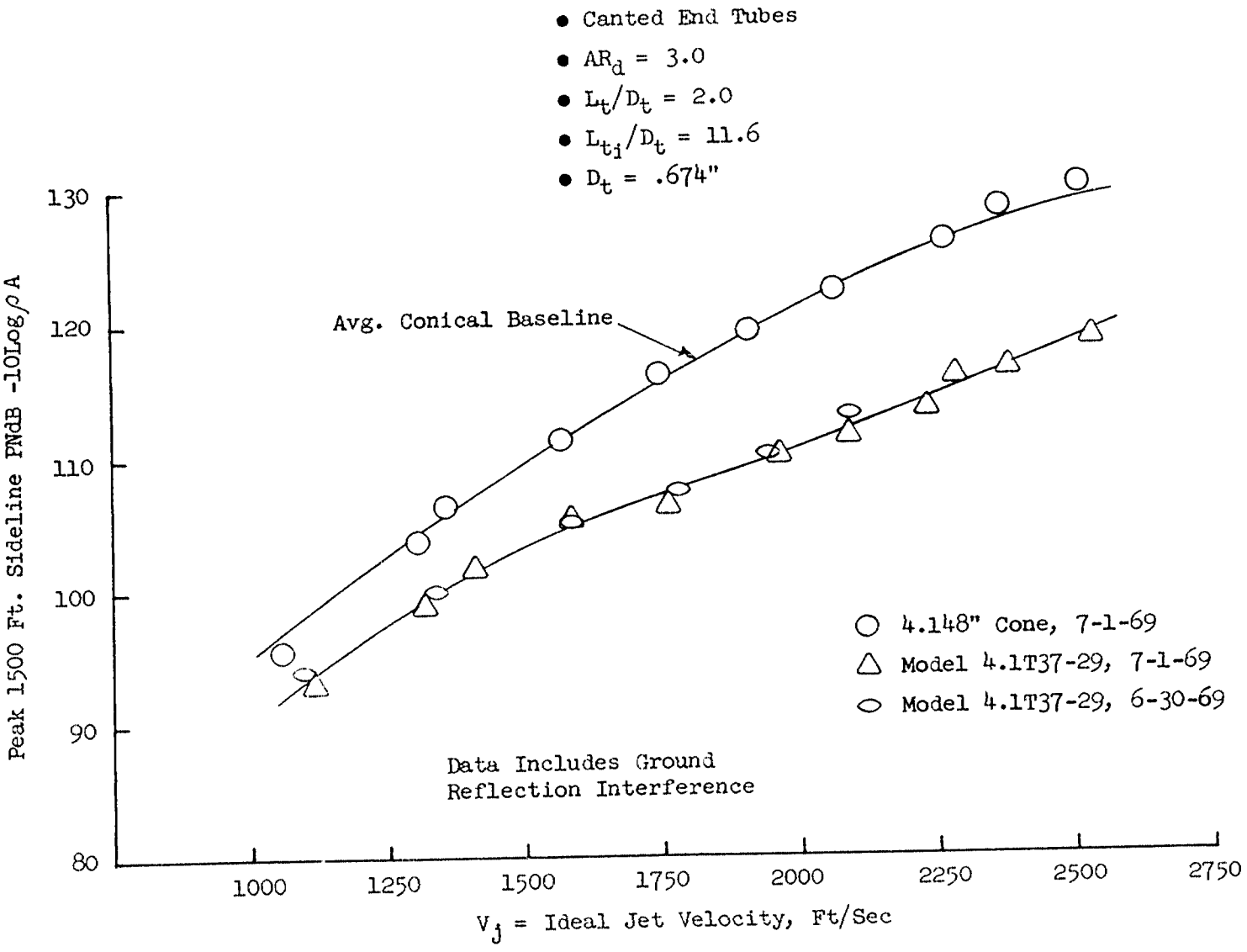

FIGURE V.F.4-15 1500 FT. SIDELINE JET NOISE LEVELS FOR 37 CANTED END TUBE NOZZLE, AR_d=3.0

TABLE V.F.4-7 TEST SUMMARY

MODEL NO. 4.1T37-21

DESCRIPTION: 37 Greatrex End Tubes, AR_d = 4

DATE: 6/5/69

SCALE MODEL A_8 = .0917 ft^2

FULL SCALE A_8 = 5.869 ft^2

SCALE FACTOR = 8:1

- o DATA INCLUDES GROUND REFLECTION INTERFERENCE
- o ANGLE REFERENCED TO JET EXHAUST

RDG NO.	TEST CONDITIONS				ACOUSTIC TEST RESULTS						
			IDEAL			320' ARC		300' SIDELINE		1500' SIDELINE	
	P_{T8}/P_o	T_{T8} (°R)	V_j (ft/sec)	W_8 (PPS)	10 log ρA	PEAK PNdB	PEAK ANGLE	PEAK PNdB	PEAK ANGLE	PEAK PNdB	PEAK ANGLE
2	1.56	1526	1491	3.20	-7.8	109.1	60	108.2	60	90.3	60
3	1.56	1236	1335	3.64	-6.9	107.2	50	106.9	80	89.3	80
4	1.69	1497	1590	3.57	-7.7	110.9	60	109.9	60	92.2	60
5	1.93	1522	1785	4.15	-7.6	113.4	50	112.6	80	94.9	80
6	2.20	1573	1973	4.70	-7.5	115.4	50	115.2	80	97.5	80
7	2.36	1657	2106	4.93	-7.6	117.2	50	116.8	80	99.1	80
8	2.56	1790	2279	5.20	-7.8	118.7	60	118.5	80	100.9	80
9	2.89	1518	2214	6.46	-6.8	120.1	60	119.8	80	102.2	80
10	2.89	1785	2401	5.92	-7.5	122.0	50	120.4	80	102.8	80
11	2.89	1987	2533	5.51	-7.9	122.4	50	122.1	80	104.5	80

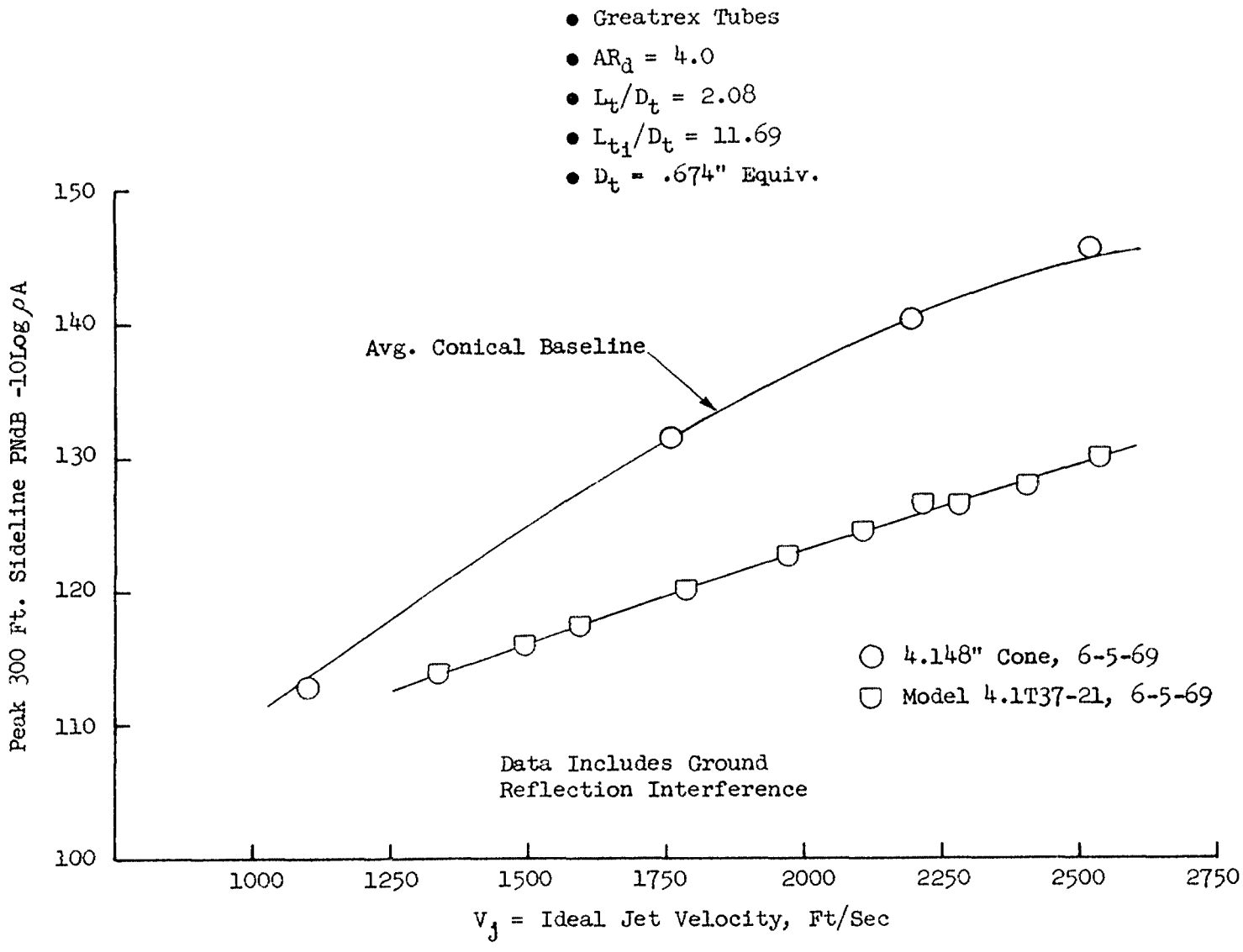

FIGURE V.F.4-16 300 FT. SIDELINE JET NOISE LEVELS FOR 37 GREATREX END TUBE NOZZLE, AR_d=4.0

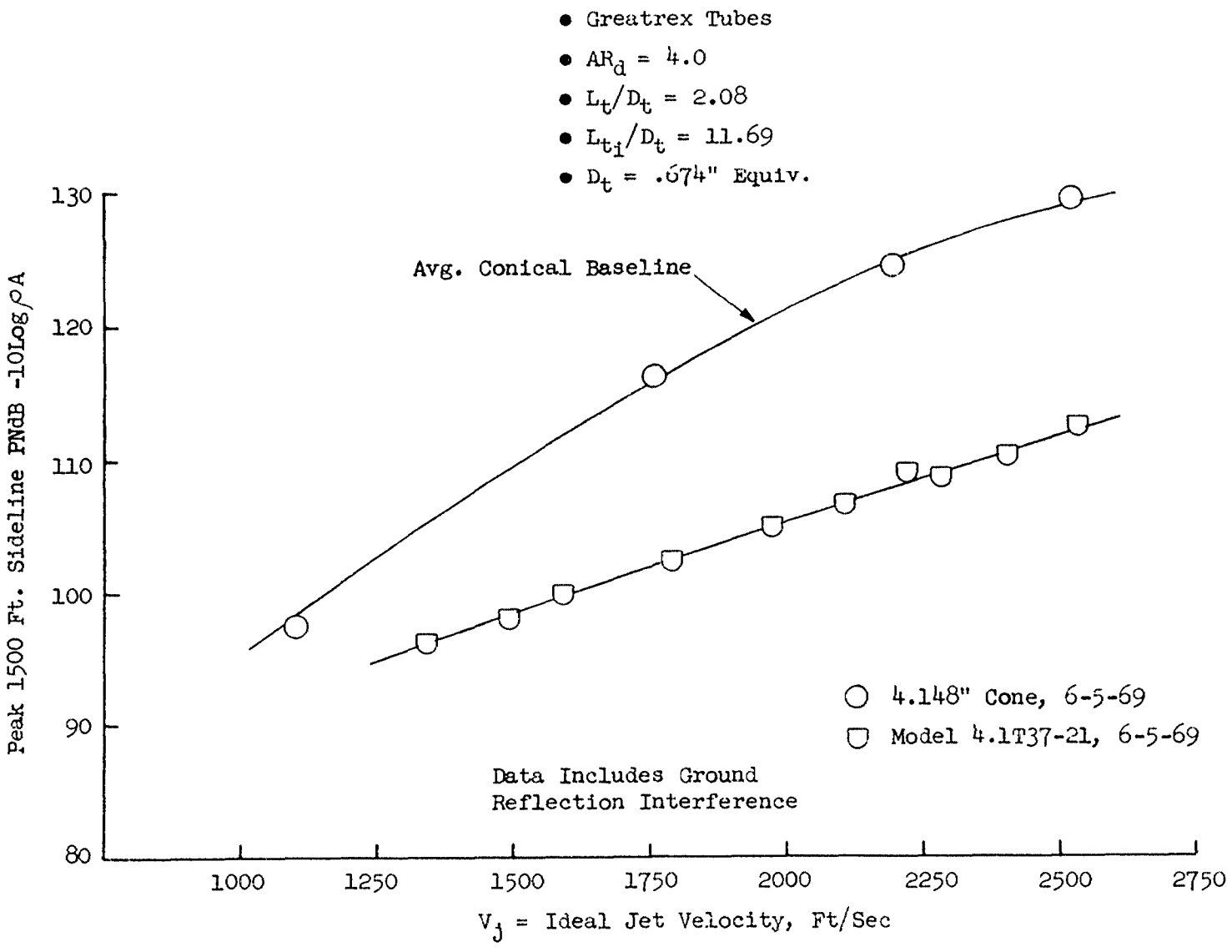

FIGURE V.F.4-17 1500 FT. SIDELINE JET NOISE LEVELS FOR 37 GREATREX END TUBE NOZZLE, AR_d=4.0

TABLE V.F.4-8 TEST SUMMARY

MODEL NO. 4.1T37-25

DESCRIPTION: 37 Greatrex End Tubes, AR_d = 3

DATE: 5/29/69

SCALE MODEL A_8 = .0917 ft^2

FULL SCALE A_8 = 3.869 ft^2

SCALE FACTOR = 8:1

- o DATA INCLUDES GROUND REFLECTION INTERFERENCE
- o ANGLE REFERENCED TO JET EXHAUST

	TEST CONDITIONS				ACOUSTIC TEST RESULTS						
			IDEAL			320' ARC		300' SIDELINE		1500' SIDELINE	
RDG NO.	P_{T8}/P_o	T_{TS} (°R)	V_j (ft/sec)	W_8 (PPS)	10 log ρA	PEAK PNdB	PEAK ANGLE	PEAK PNdB	PEAK ANGLE	PEAK PNdB	PEAK ANGLE
2	1.49	1508	1407	3.21	-7.8	104.0	80	104.6	80	87.0	80
3	1.55	1229	1325	3.75	-6.9	105.0	80	105.5	80	88.1	80
4	1.70	1521	1611	3.76	-7.7	107.1	50	107.1	80	89.6	80
6	2.19	1551	1954	4.87	-7.5	112.0	50	113.0	80	95.6	80
7	2.37	1647	2103	5.14	-7.6	115.2	50	114.6	80	97.2	80
8	2.60	1773	2285	5.48	-7.7	117.0	50	115.9	80	98.5	80
9	2.89	1506	2206	6.58	-6.7	117.7	50	117.6	80	100.2	80
10	2.89	1782	2400	6.00	-7.4	119.0	40	118.5	80	101.2	80
11	2.90	1968	2522	5.73	-7.9	120.7	50	119.6	80	102.2	80

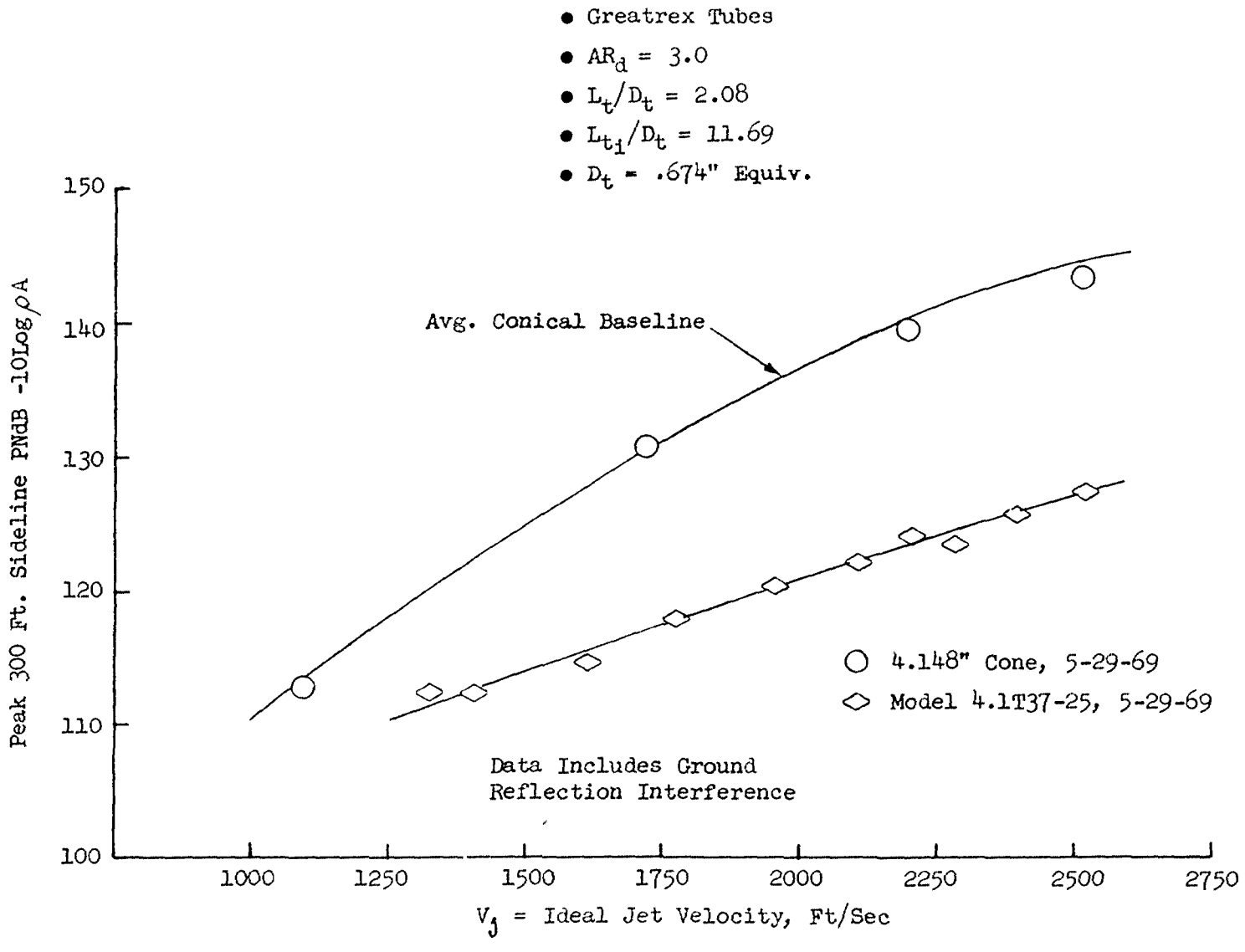

FIGURE V.F.4-18 300 FT. SIDELINE JET NOISE LEVELS FOR 37 GREATREX END TUBE NOZZLE, AR_d=3.0

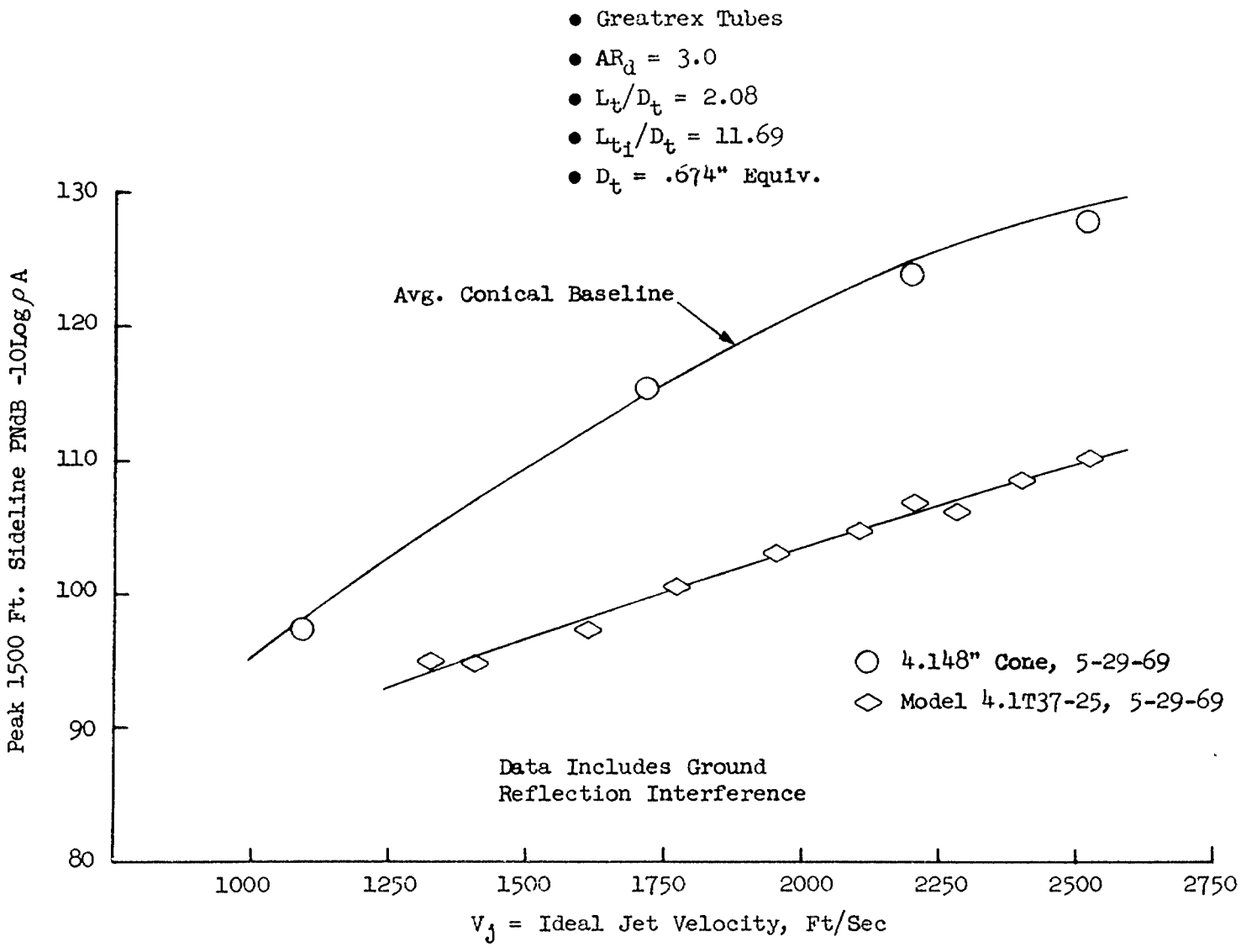

FIGURE V.F.4-19 1500 FT. SIDELINE JET NOISE LEVELS FOR 37 GREATREX END TUBE NOZZLE, AR_d=3.0

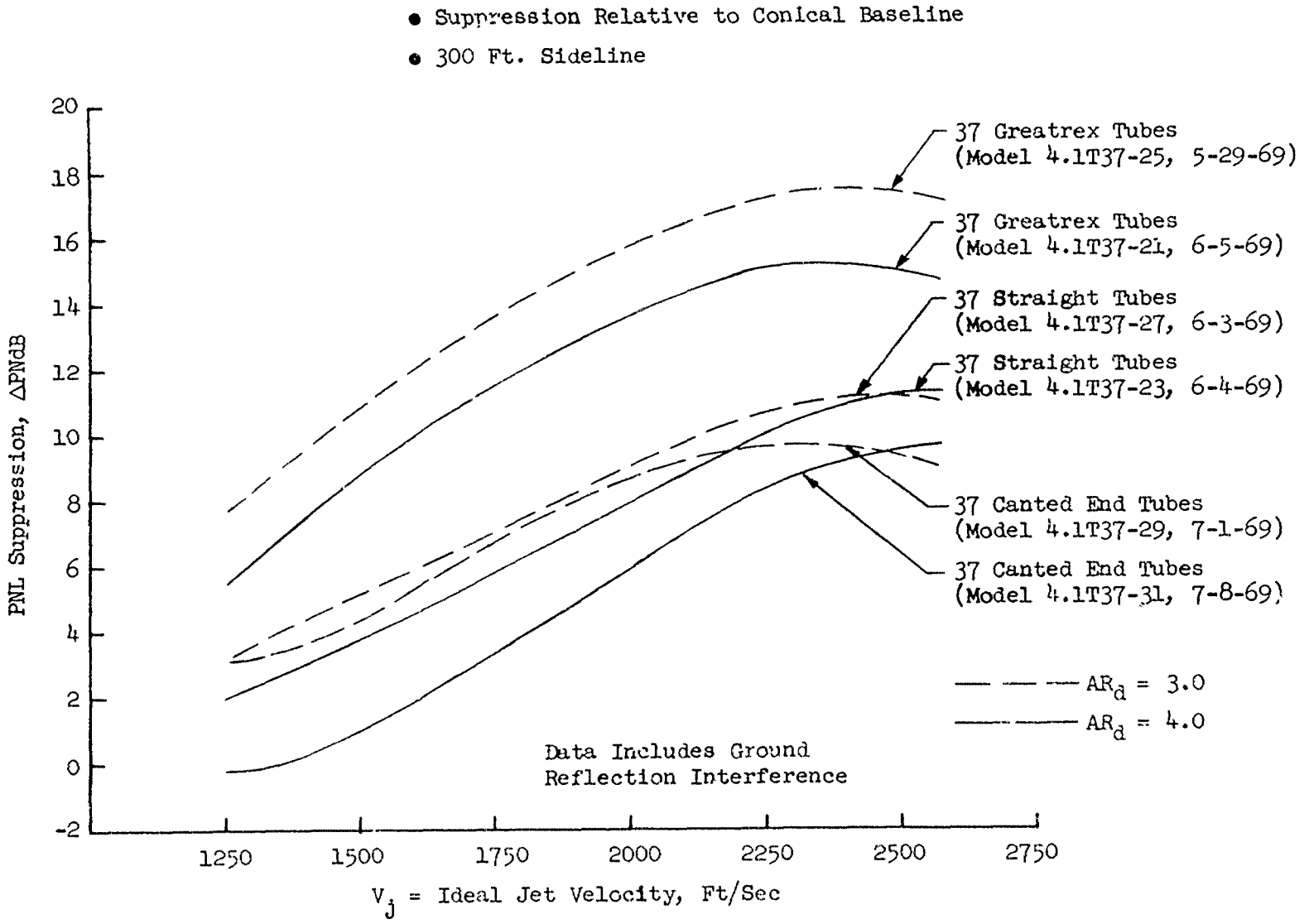

FIGURE V.F.4-20 COMPARISON OF 300 FT. SIDELINE PNL SUPPRESSIONS FOR STRAIGHT, GREATREX, AND CANTED END TUBES

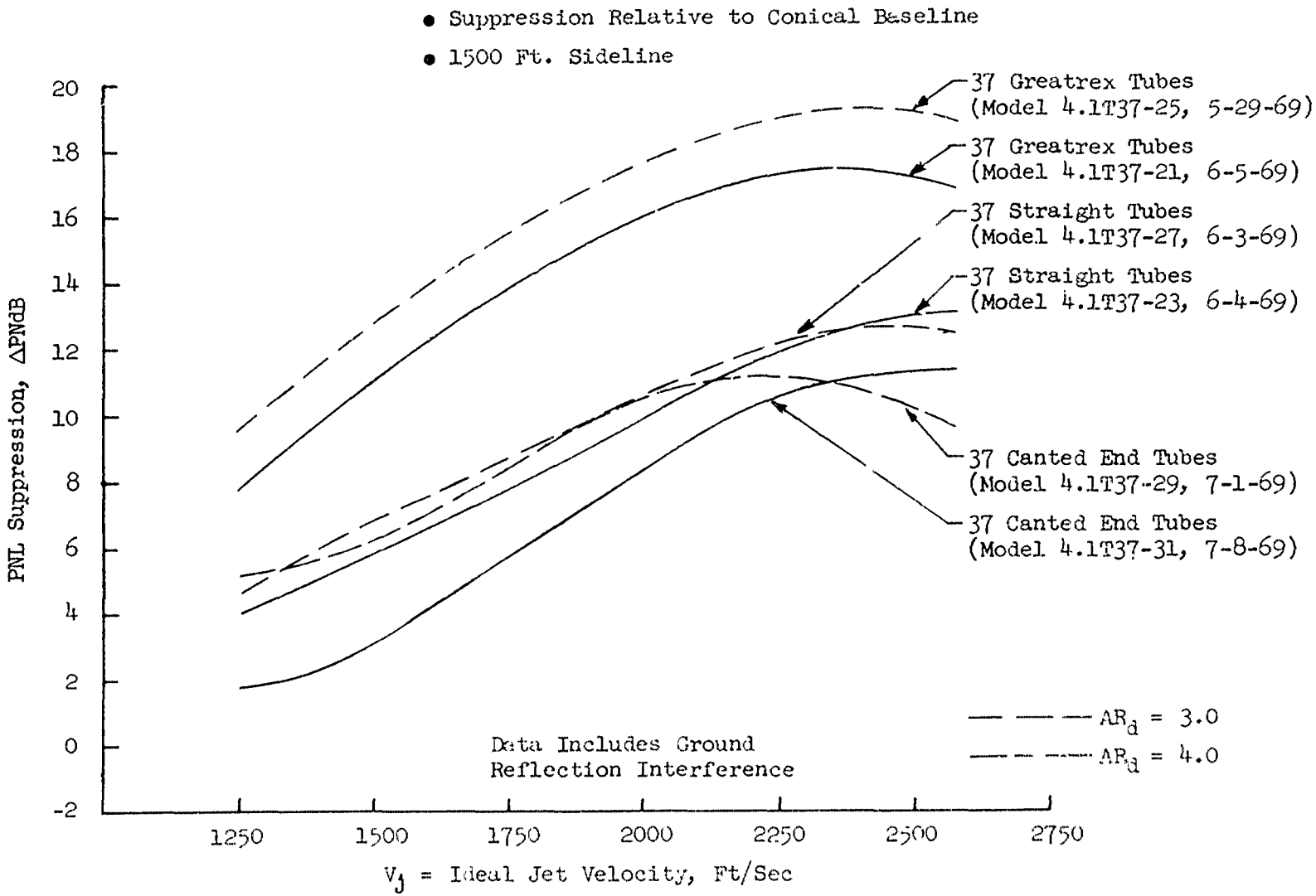

FIGURE V.F.4-21 COMPARISON OF 1500 FT. SIDELINE PNL SUPPRESSIONS FOR STRAIGHT, GREATREX, AND CANTED END TUBES

- Comparison of Straight, Canted, and Greatrex End Tubes, Each at AR_d = 3 & 4
- + = Increase in Suppression by Decreasing AR_d

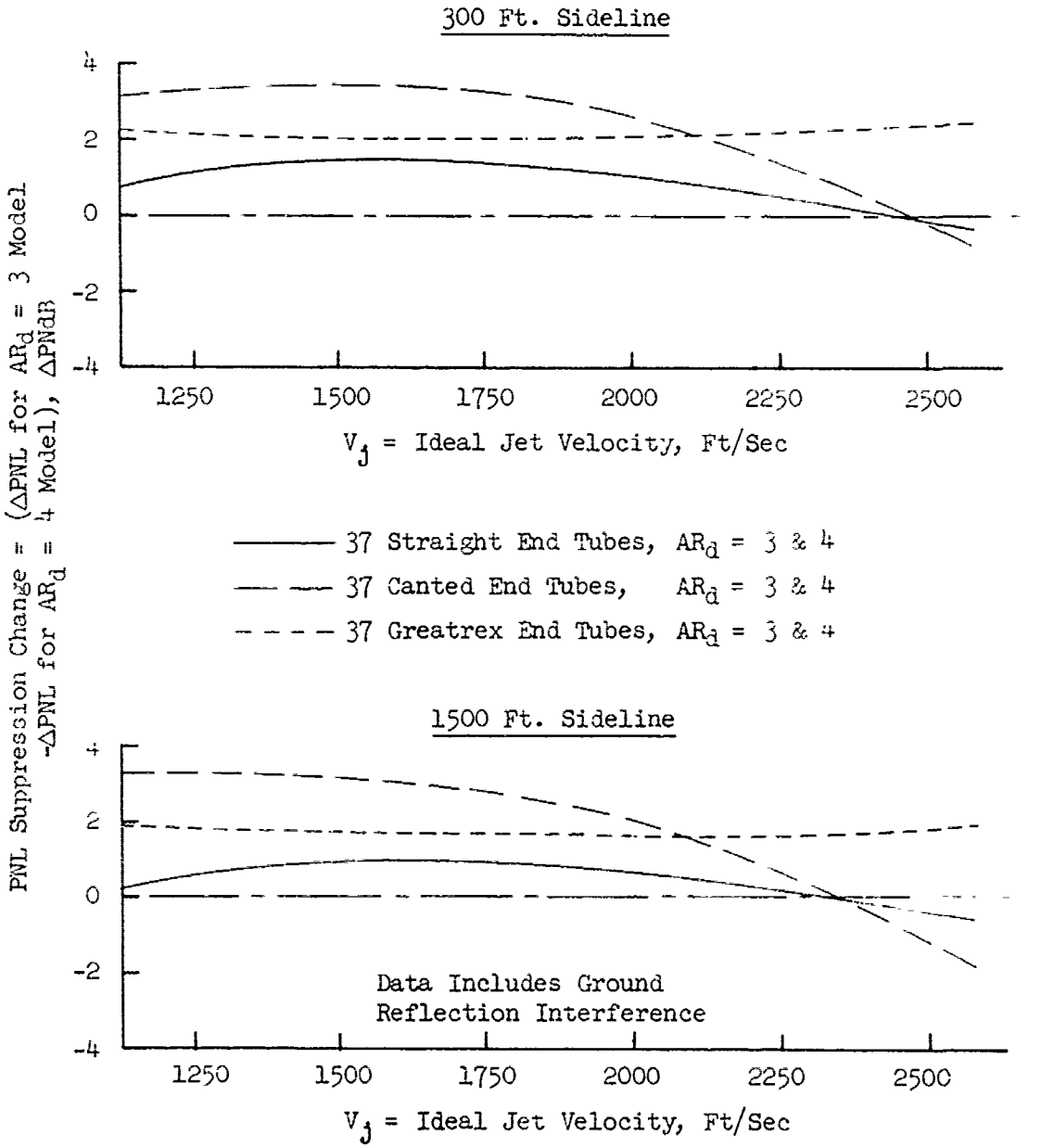

FIGURE V.F.4-22 CHANGE IN PNL SUPPRESSION DUE TO AREA RATIO VARIATION

- AR_d = 3 & 4 Models with Tube Exits Canted to Form a Projected Intersection on a 10° Total Included Angle Cone
- + = Suppression Increase by Canting
- Suppression Relative to 37 Straight End Tubes at Same AR_d

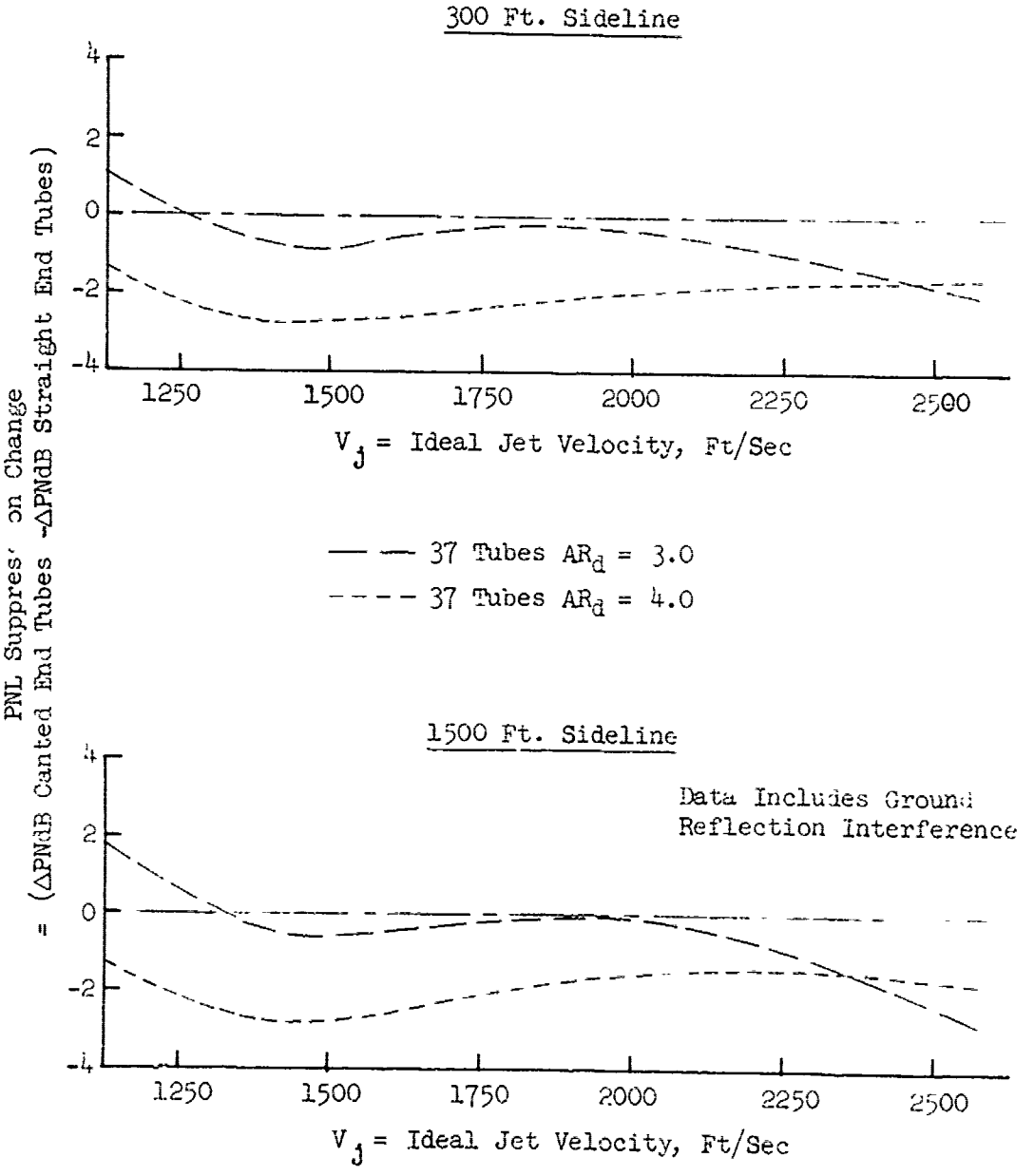

FIGURE V.F.4-23 CHANGE IN PNL SUPPRESSION DUE TO TUBE EXIT CANT

- Comparison of Greatrex Ends to Straight and Convergent Ends at AR_d = 3 & 4
- Peak to Peak PNL Comparison
- + = Suppression Increase with Greatrex Ends

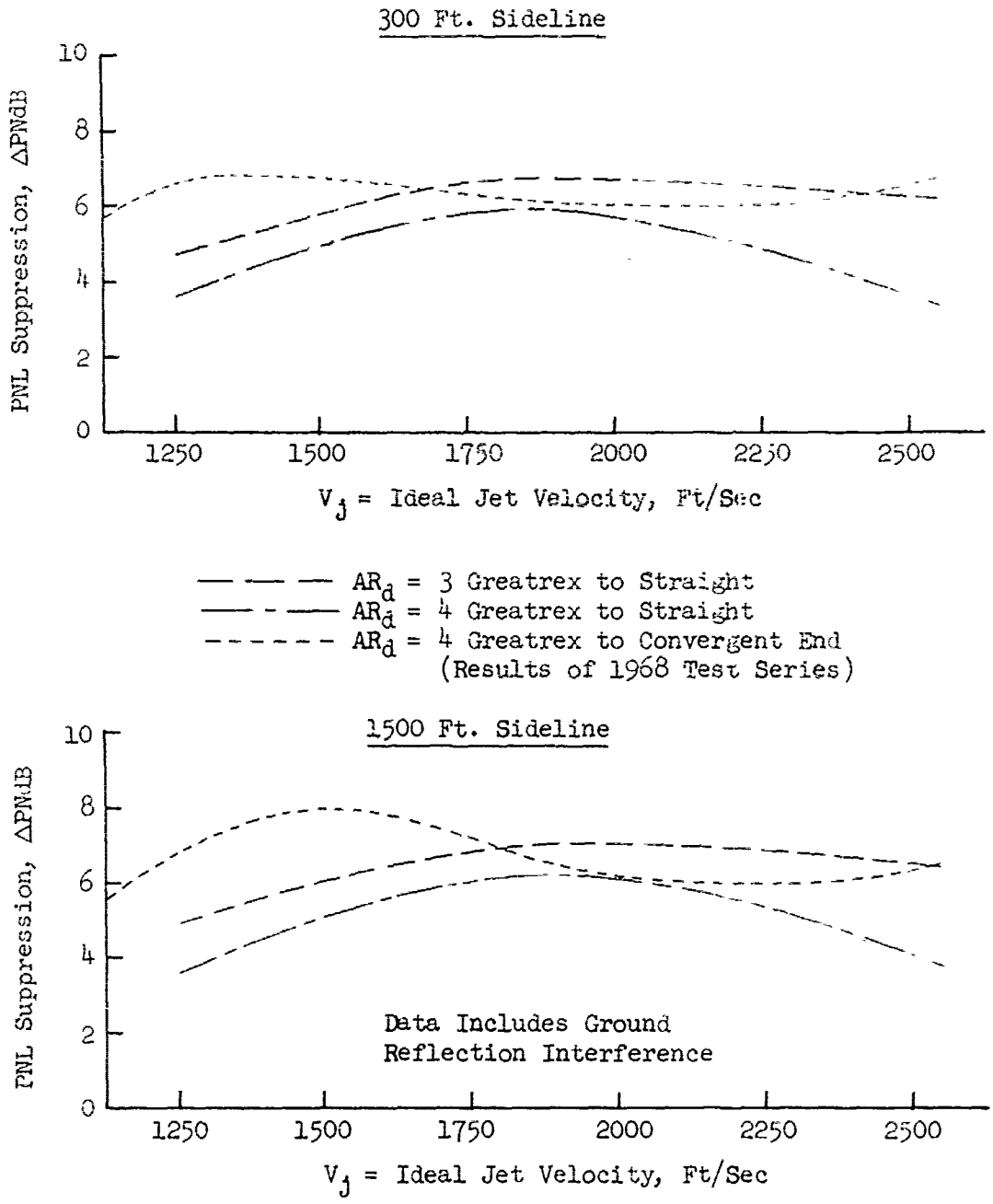

FIGURE V.F.4-24 GAIN IN PNL SUPPRESSION DUE TO GREATREX END TUBES

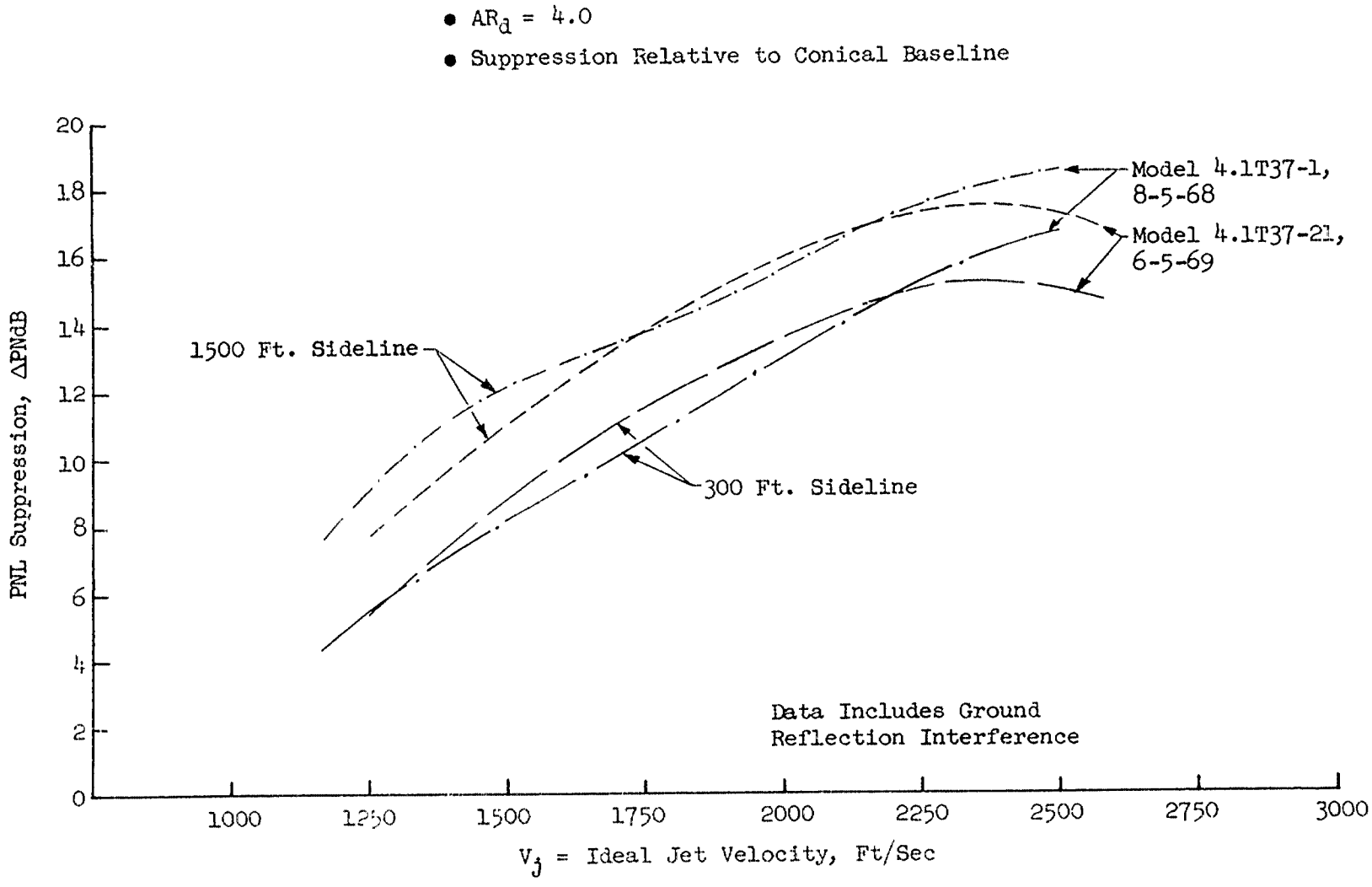

FIGURE V.F.4-25 COMPARISON OF PNL SUPPRESSION FOR 1968 & 1969 TEST RESULTS ON 37 GREATREX END TUBES

- Spectra at Peak PNdB Angle
- 300 Ft. Sideline
- $P_{T8}/P_o \approx 1.55$
- $T_{T8} \approx 1230°R$
- $V_j \approx 1325$ Ft/Sec

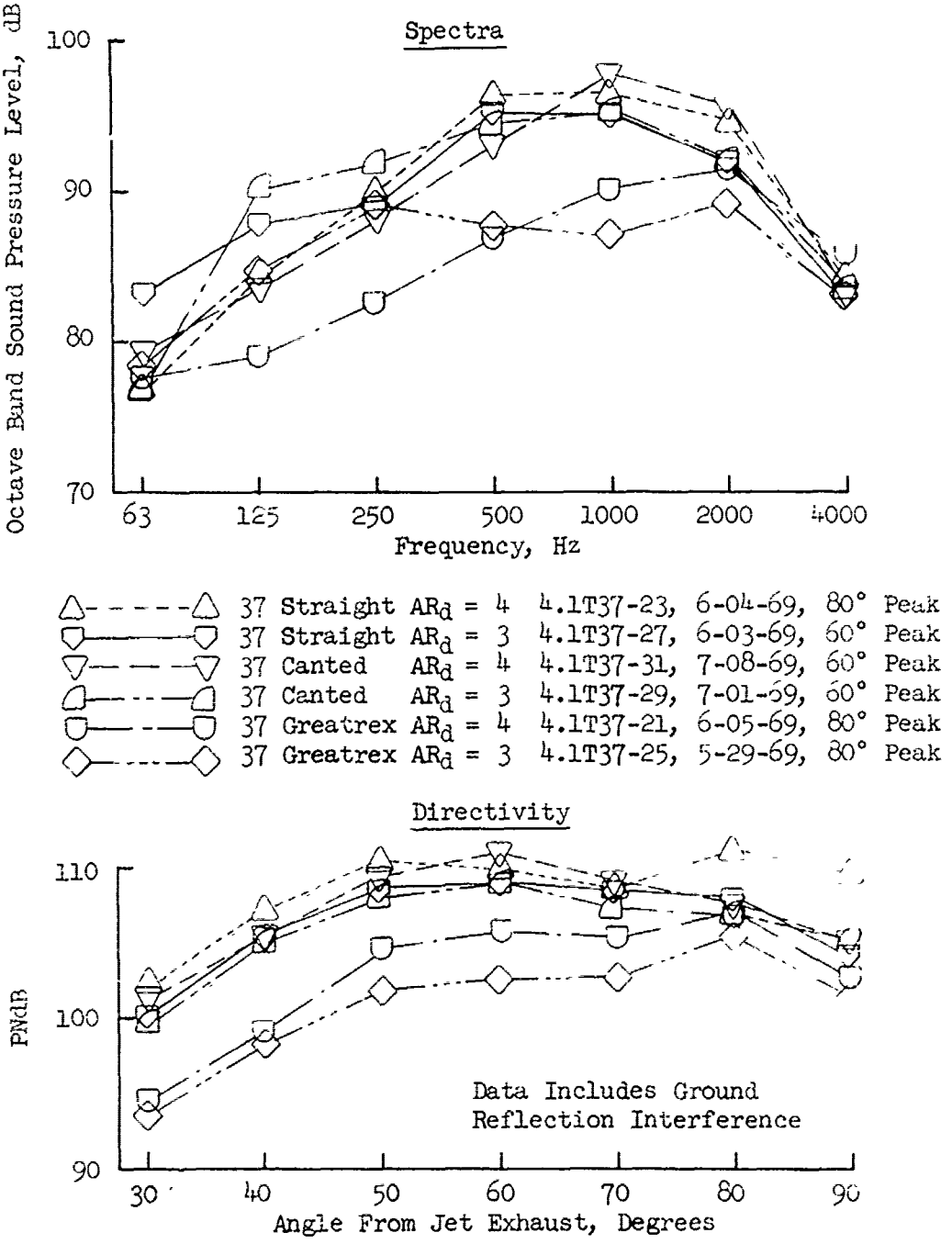

FIGURE V.F.4-26A EFFECT OF STRAIGHT, GREATREX AND CANTED END TUBES ON SPECTRA AND DIRECTIVITY

- Spectra at Peak PNdB Angle
- 300 Ft. Sideline
- $P_{T8}/P_o \approx 1.68$
- $T_{T8} \approx 1520°R$
- $V_j \approx 1590$ Ft/Sec

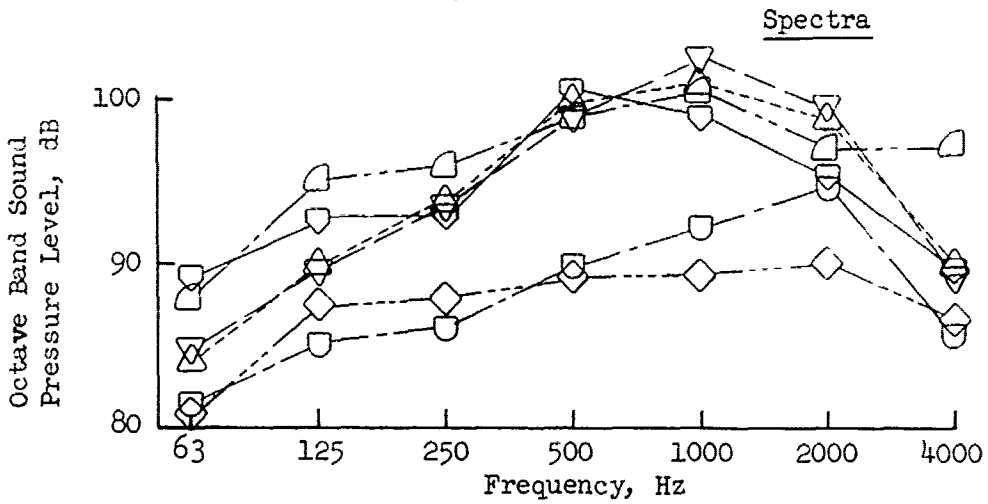

37 Straight	$AR_d = 4$	4.1T37-23, 6-04-69, 60° Peak
37 Straight	$AR_d = 3$	4.1T37-27, 6-03-69, 60° Peak
37 Canted	$AR_d = 4$	4.1T37-31, 7-08-69, 60° Peak
37 Canted	$AR_d = 3$	4.1T37-29, 7-01-69, 60° Peak
37 Greatrex	$AR_d = 4$	4.1T37-21, 6-05-69, 60° Peak
37 Greatrex	$AR_d = 3$	4.1T37-25, 5-29-69, 80° Peak

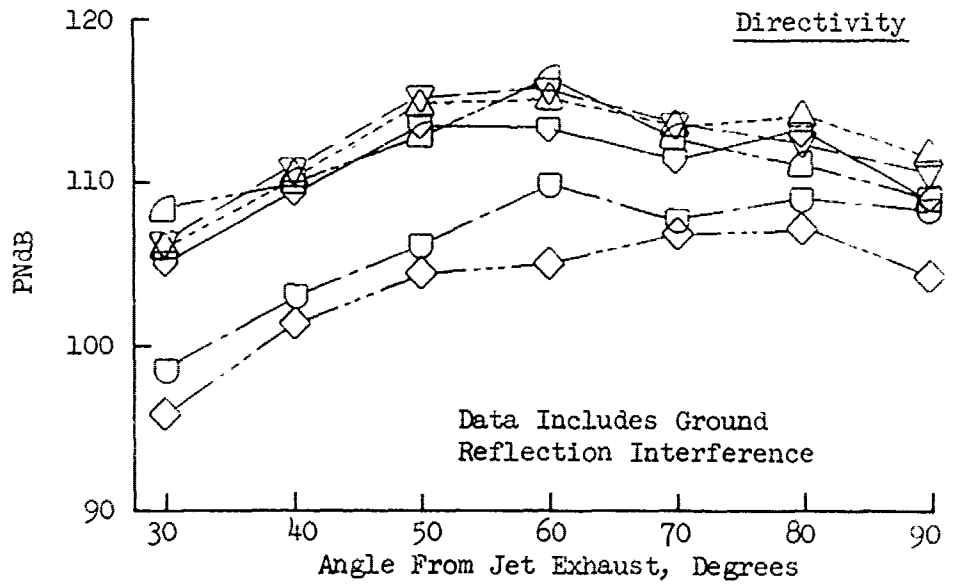

FIGURE V.F.4-26B EFFECT OF STRAIGHT, GREATREX AND CANTED END TUBES ON SPECTRA AND DIRECTIVITY

- Spectra at Peak PNdB Angle
- 300 Ft. Sideline
- $P_{T8}/P_o \approx 2.18$
- $T_{T8} \approx 1575°R$
- $V_j \approx 1950$ Ft/Sec

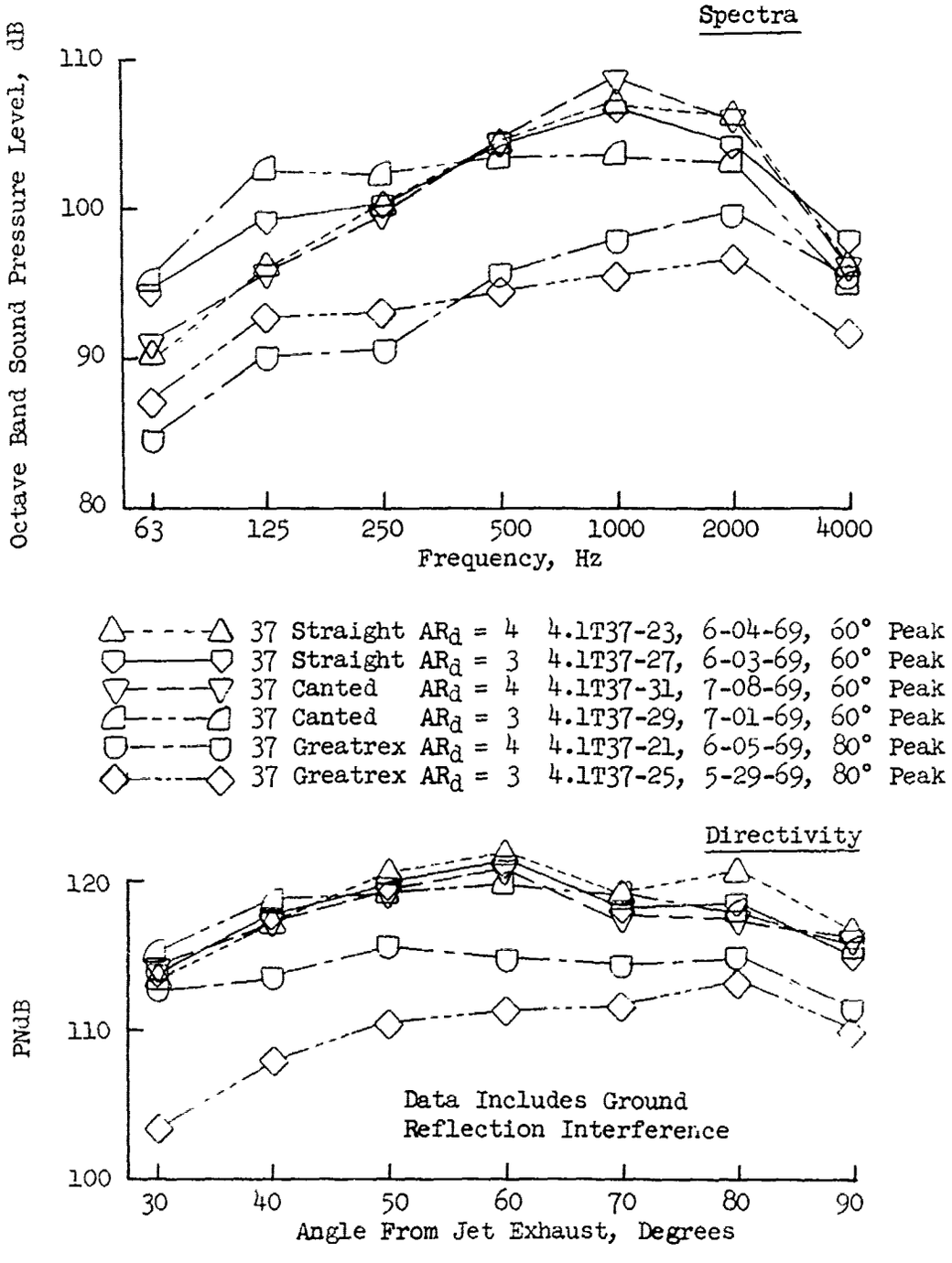

FIGURE V.F.4-26C EFFECT OF STRAIGHT, GREATREX AND CANTED END TUBES ON SPECTRA AND DIRECTIVITY

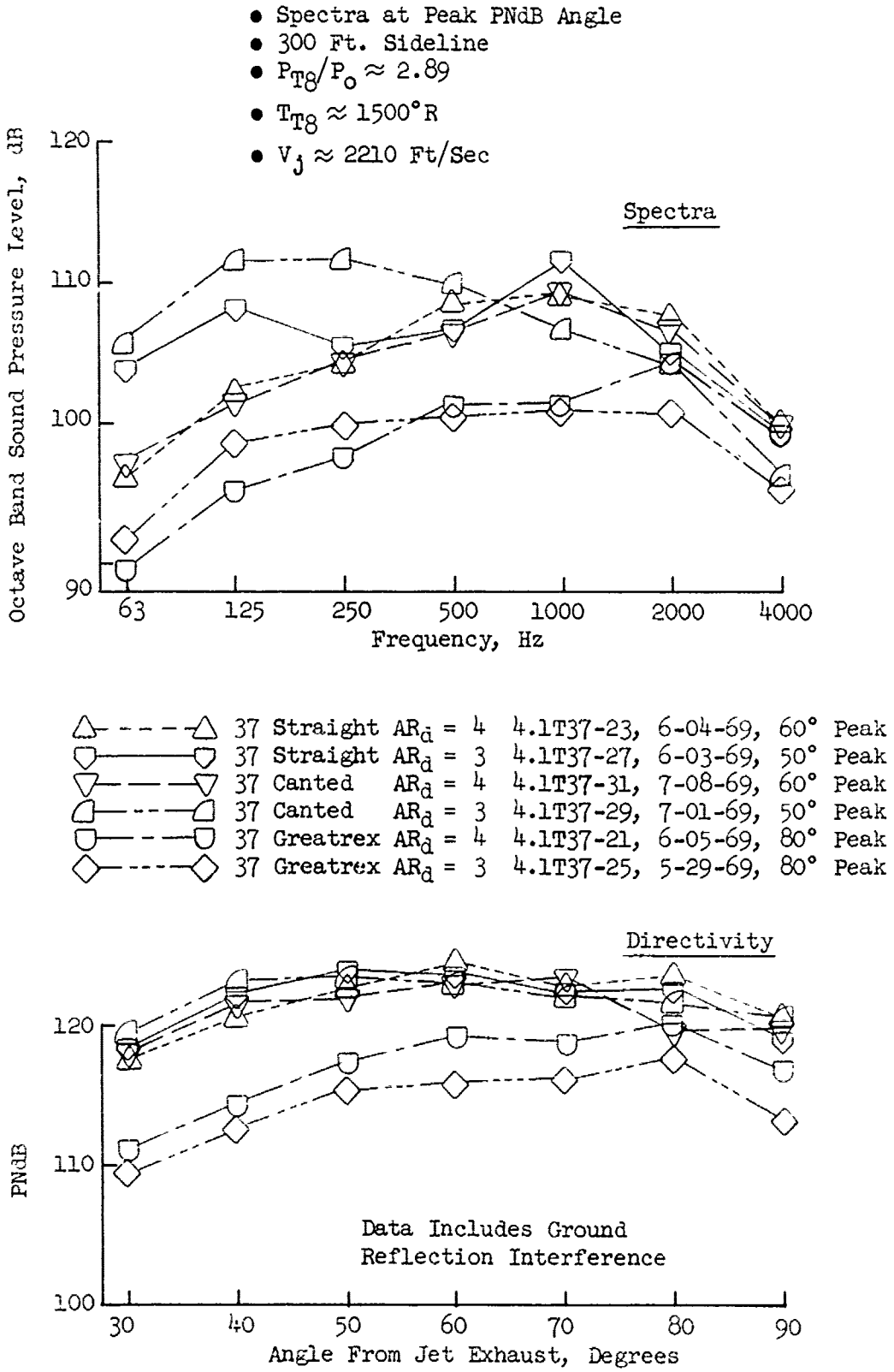

FIGURE V.F.4-26D EFFECT OF STRAIGHT, GREATREX AND CANTED END TUBES ON SPECTRA AND DIRECTIVITY

- Spectra at Peak PNdB Angle
- 300 Ft. Sideline
- $P_{T8}/P_o \approx 2.86$
- $T_{T8} \approx 1775°R$
- $V_j \approx 2400$ Ft/Sec

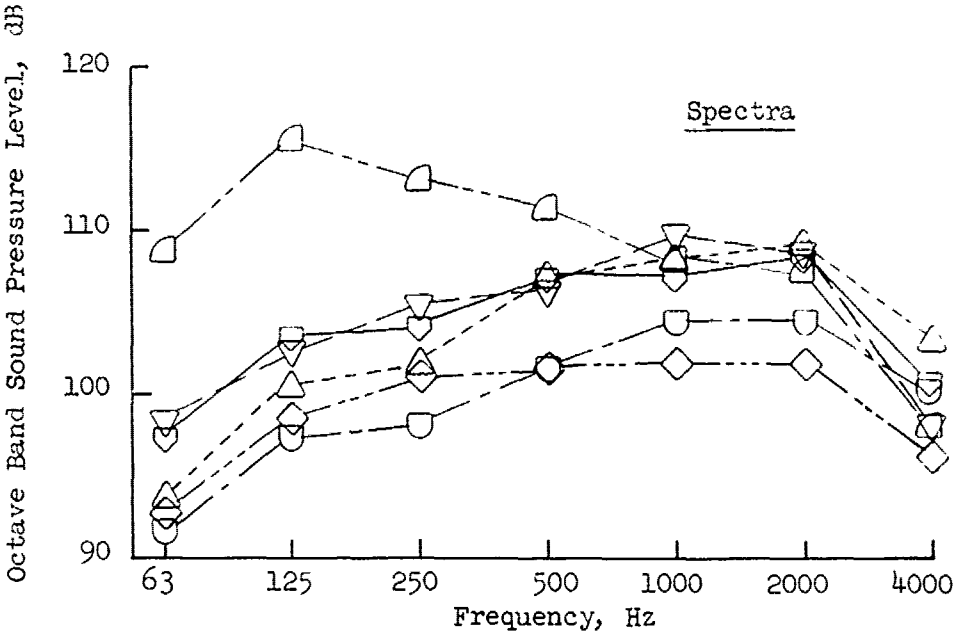

37 Straight	$AR_d = 4$	4.1T37-23, 6-04-69,	80° Peak
37 Straight	$AR_d = 3$	4.1T37-27, 6-03-69,	80° Peak
37 Canted	$AR_d = 4$	4.1T37-31, 7-08-69,	60° Peak
37 Canted	$AR_d = 3$	4.1T37-29, 7-01-69,	50° Peak
37 Greatrex	$AR_d = 4$	4.1T37-21, 6-05-69,	80° Peak
37 Greatrex	$AR_d = 3$	4.1T37-25, 5-29-69,	80° Peak

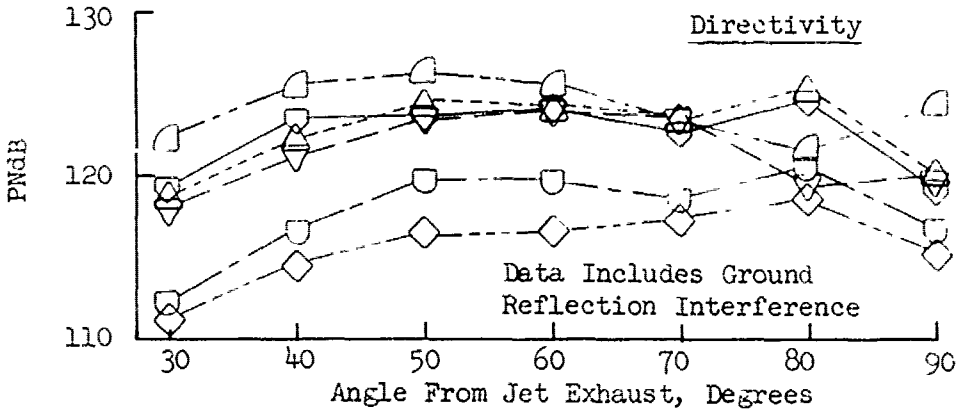

FIGURE V.F.4-26E EFFECT OF STRAIGHT, GREATREX AND CANTED END TUBES ON SPECTRA AND DIRECTIVITY

- Spectra at Peak PNdB Angle
- 300 Ft. Sideline
- $P_{T8}/P_o \approx 2.87$
- $T_{T8} \approx 1985°R$
- $V_j \approx 2525$ Ft/Sec

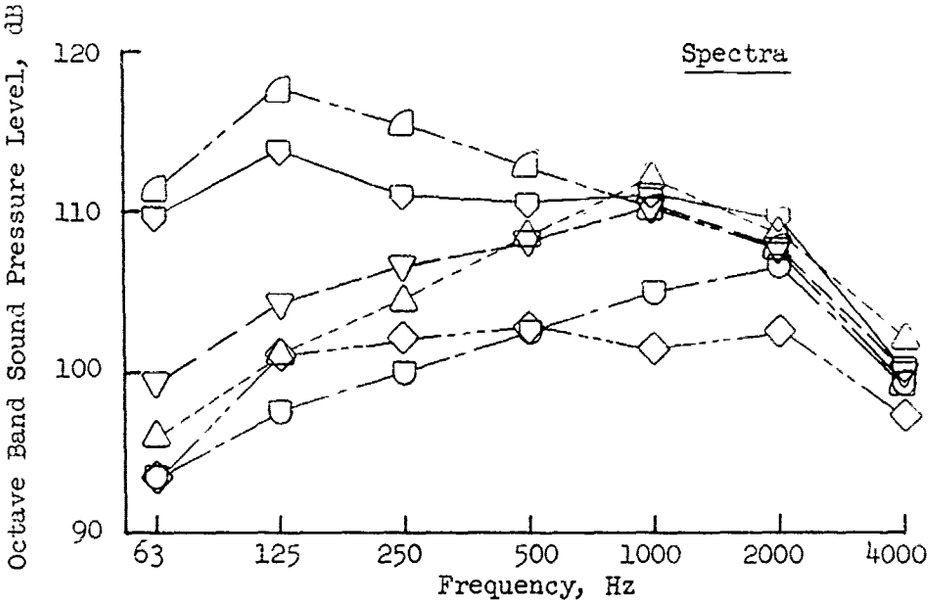

37 Straight	$AR_d = 4$	4.1T37-23, 6-04-69,	80° Peak
37 Straight	$AR_d = 3$	4.1T37-27, 6-03-69,	50° Peak
37 Canted	$AR_d = 4$	4.1T37-31, 7-08-69,	60° Peak
37 Canted	$AR_d = 3$	4.1T37-29, 7-01-69,	50° Peak
37 Greatrex	$AR_d = 4$	4.1T37-21, 6-05-69,	80° Peak
37 Greatrex	$AR_d = 3$	4.1T37-25, 5-29-69,	80° Peak

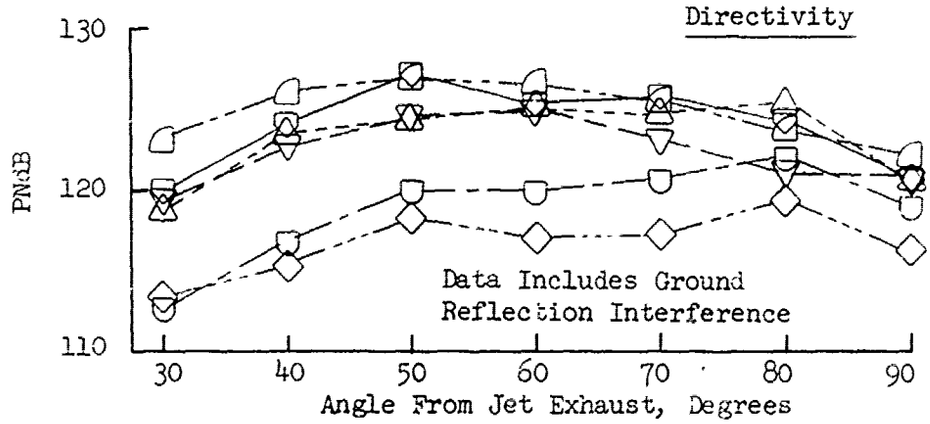

FIGURE V.F.4-26F EFFECT OF STRAIGHT, GREATREX AND CANTED END TUBES ON SPECTRA AND DIRECTIVITY

- 12-Lobe Greatrex Vs. Straight & Convergent Ends
- AR_d = 3.0 and 4.0
- Applies to 300 or 1500 Ft. Sideline

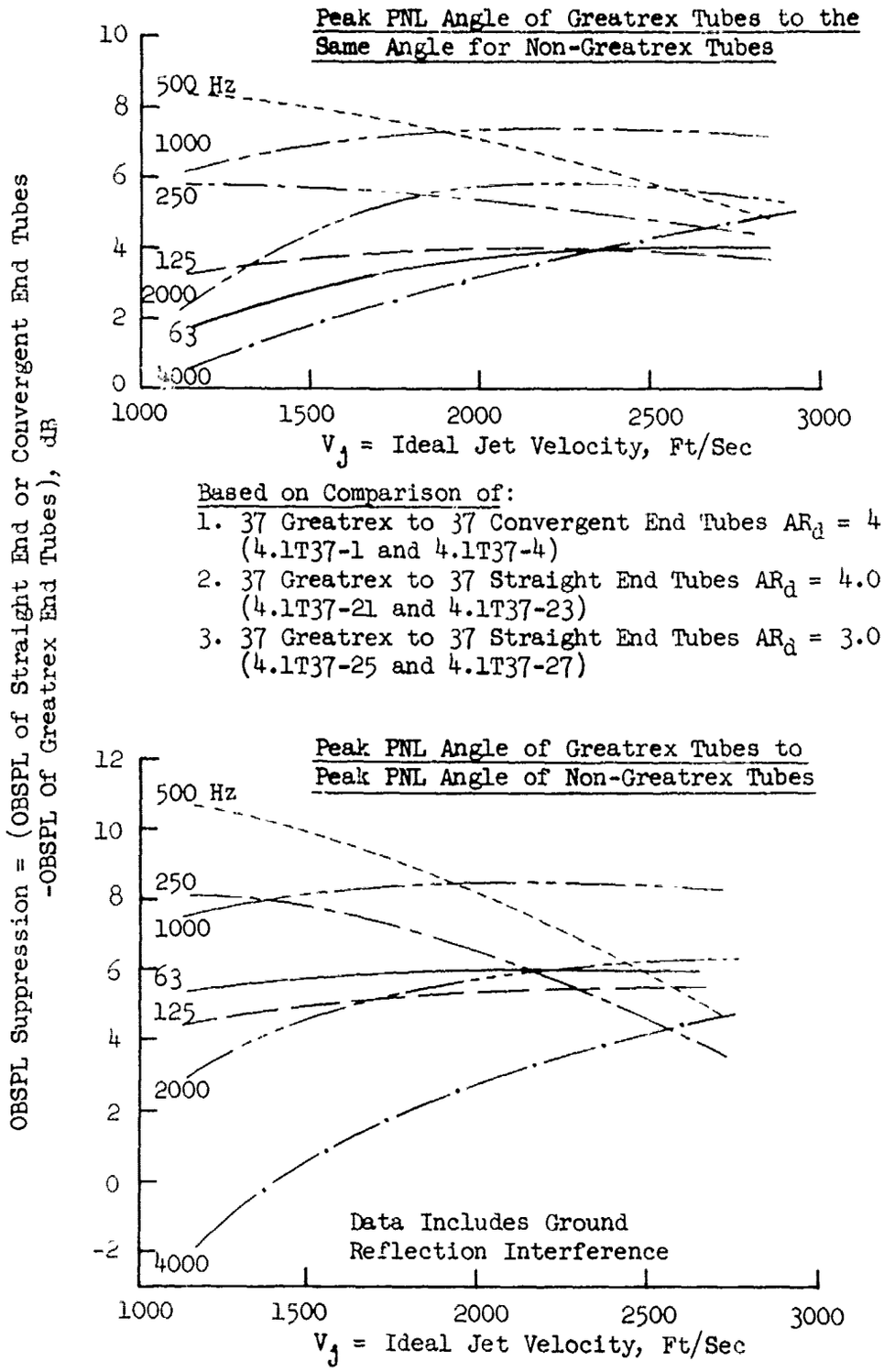

FIGURE V.F.4-27 OCTAVE BAND SPECTRAI SUPPRESSION ATTRIBUTABLE TO ADDITION OF GREATREX TUBE ENDS

• 37 Tubes; AR_d = 3 and 4

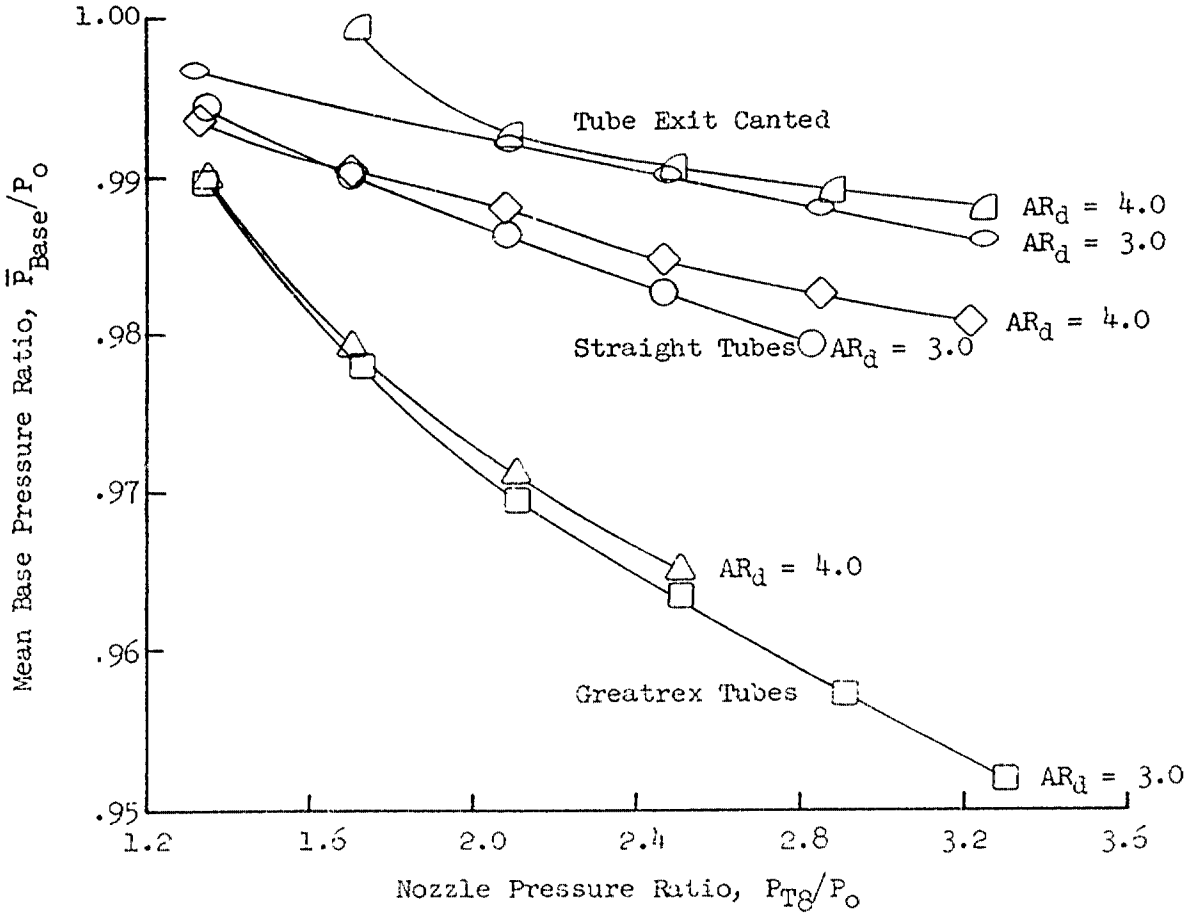

FIGURE V.F.4-28 EFFECT OF TUBE END VARIATIONS ON MEAN BASE PRESSURE RATIO

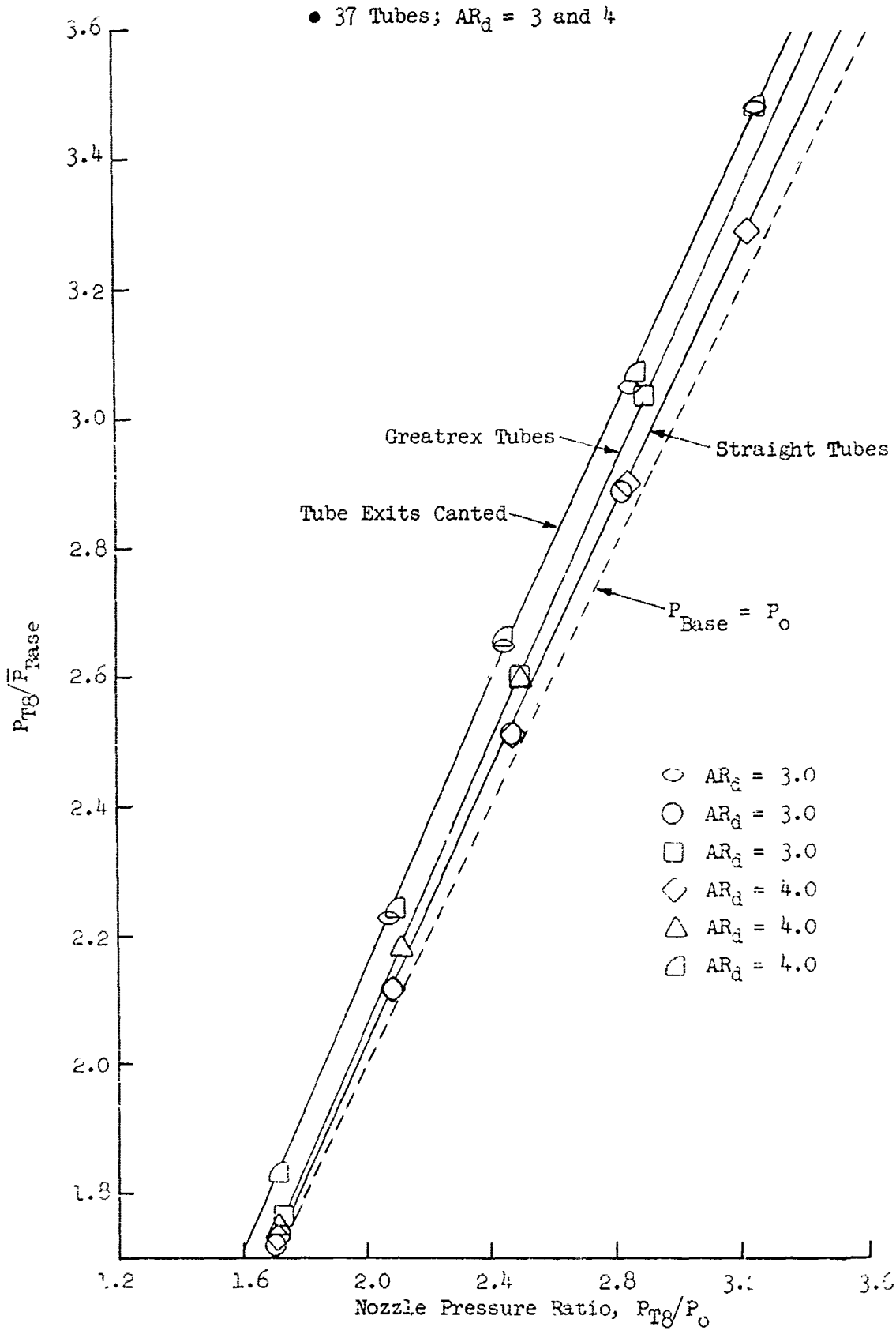

FIGURE V.F.4-29 EFFECT OF TUBE END VARIATIONS ON NOZZLE EXIT TO MEAN BASE PRESSURE RATIO

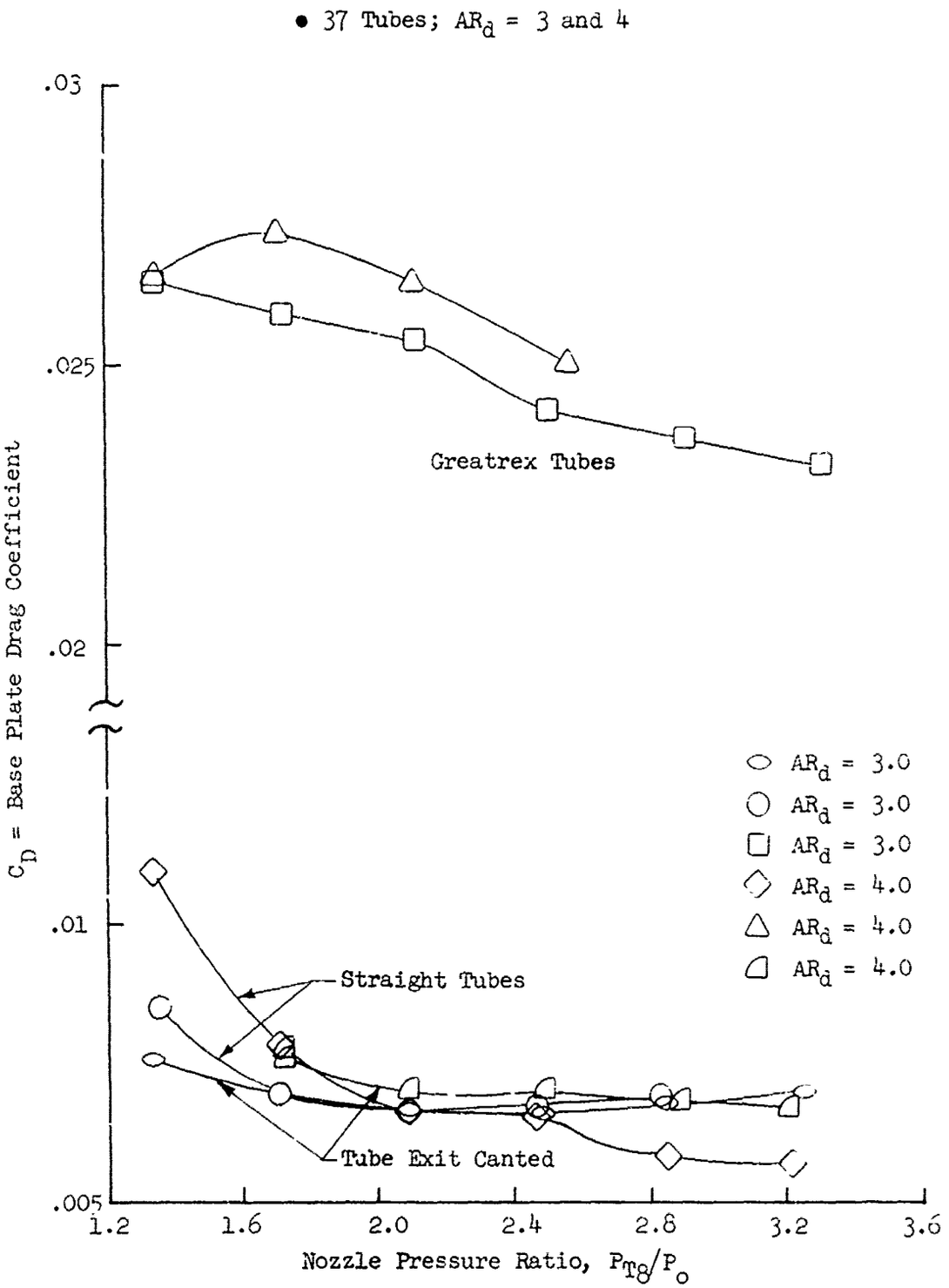

FIGURE V.F.4-30 EFFECT OF TUBE END VARIATIONS ON BASEPLATE DRAG COEFFICIENT

V.F.5 TUBE INTERNAL AND EXTERNAL LENGTH TO DIAMETER STUDIES ON AN 85 TUBE NOZZLE

BLANK NOT FILMED

V.F.5 TUBE INTERNAL AND EXTERNAL LENGTH TO DIAMETER STUDIES ON AN 85 TUBE NOZZLE

Objectives of Test Series

A study was conducted to investigate the aero/acoustic effects of tube internal/external length-to-diameter ratio (L_{ti}/D_t) on multi-tube suppressors.

The tests on the hot flow acoustic models were conducted on the GE, Evendale, JENOTS facility obtaining accustic measurements and static base pressures for determination of aerodynamic performance. The acoustic measurements were taken on a 40 ft. arc and scaled by frequency and size to full scale application using a scale factor of 8:1. All data presented are, therefore, of simulated engine size and engine frequency range. Test conditions were selected along a GE4 engine operating line with nozzle pressure ratios of 1.4 to 3.5, exit gas temperatures of 1000 to 2600° R and ideal jet velocities ranging from 1130 to 3130 ft/sec.

Test Configurations

An 85 tube nozzle with .430" I.D. tubes of 4.5" length was fabricated at AR_d of 3.19. The nozzle was similar to that of the 85 hole nozzle used in the area ratio study of Section V.F.9 and was meant to continue accumulation of tube nozzle design technology to determine tube length effects past the baseplate hardware used in that section. The tube pattern was held uniform, equally spacing the 85 tubes on a hexagonal pattern, and using coplanar tube exits. A photograph of the initial configuration, with 4.5" long tubes, is shown in Figure V.F.5-1. A total of seven models were tested in the series by shortening the tubes in increments of 1/2 , 3/4, or 1 inch until a baseplate remained as the last configuration. Figure V.F.5-2 is a schematic of the nozzle defining the pertinent geometric variables. It also contains a configuration listing and tube dimensions. The internal length-to-diameter ratio, was varied from 10.47 to 1.74 and the external length-to-diameter ratio, L_t/D_t, was varied from 8.72 to 0.

Baseline nozzle for the test series was a 4.32" I.D. conical convergent nozzle tested each day to insure that minor changes in noise suppression anticipated from the cutback tube nozzle were discernable over daily changes

PRECEDING PAGE BLANK-NOT FILMED

due to meteorological conditions. Average baseline PNL curves were established for the 300 and 1500 ft. sidelines as a function of jet velocity, and the same day baseline test points were compared to the average curves for a gauge of variance. The suppressed nozzle measurements were then referenced to the daily conical baseline. To present the effect of varying L_{ti}/D_t, the longest tube configuration (L_{ti} = 4.5", L_{ti}/D_t = 10.47) was chosen as the basis for comparison.

Presentation of Test Results

Table V.F.5-1 presents the primary nozzle test parameters and acoustic results for the baseline conical nozzle. Similarly, Tables V.F.5-2 through -8 present the same for the seven tube models in order of decreasing tube length. Figures V.F.5-3 through -18 are plots of 300 ft. and 1500 ft. sidelines normalized peak PNL full scale data as a function of ideal jet velocity for the conical and seven suppressor models. Figure V.F.5-19 summarizes the 300 ft. sideline variation in peak PNL suppression as the tubes were shortened, referenced to the longest tube model. The curve shows variations are minor across the jet velocity range with maximum suppression gain in the velocity range of 1600 to 2200 ft/sec. To determine more closely the effect of L_{ti}/D_t at a specific design velocity, Figures V.F.5-20A and 20B show PNL suppression change as a function of L_{ti}/D_t at velocity increments of 250 ft/sec, from 1250 to 3000 ft/sec. Average curves through the data variations indicate the optimum design in the intermediate L_{ti}/D_t range, peaking most frequently at 5 to 6, but with the magnitude of suppression gain varying with jet velocity. A maximum of about 2 PNL gain is seen from the average curves, this being a gain in suppression over that achieved by the longest tube nozzle.

Spectra and directivity curves at various cycle points from 1170 to 3120 ft/sec are presented at 300 ft. sideline in Figures V.F.5-21A through 21H.

Aerodynamic test results are based on static pressure measurements on the baseplate of the models and are presented in Figures V.F.5-22 through 25. The base pressure profiles were used to calculate the mean base pressures by integrating the measured static pressures over their respective incremental base areas and then dividing the total value by the total base area acted upon.

Mean base pressure ratio, $\bar{P}_B/P_o$, versus nozzle pressure ratio, P_{T8}/P_o, is presented in Figure V.F.5-22. As the tubes were shortened, $\bar{P}_B/P_o$ decreased uniformly until $L_{ti}/D_t = 3.49$, meaning the base drag force increased. Further cutback of the baseplate model ($L_{ti}/D_t = 1.74$) significantly lowered the mean base pressure ratio. Figure V.F.5-23 presents $P_{T8}/\bar{P}_{MEAN\ BASE}$ as a function of P_{T8}/P_o. Figure V.F.5-24, base drag coefficient variation with P_{T8}/P_o and L_{ti}/D_t, shows baseplate drag increasing as tube length is decreased, synonymous with mean base pressure data. The change in pressure ratio and drag coefficient per incremental $\Delta\ L_{ti}/D_t$ is approximately constant, except for the shorter tubes which show a much greater increment of change for the same amount of cutback. In the range of $1.5 \leq P_{T8}/P_o \leq 3.4$, the change in pressure ratio has little effect on the drag coefficient except for the baseplate model. Therefore, a design curve is presented in Figure V.F.5-25 showing base drag coefficient change as a function of L_{ti}/D_t, independent of P_{T8}/P_o for the measured range.

Conclusions

- Acoustically, minor suppression changes are seen to be attributable to tube length variation, as long as the tubes are of equal size, uniformly spaced, and form a coplanar exit plane. Slight suppression gain (over baseplate or long tubes) is achieved by tube design in the intermediate L_{ti}/D_t and jet velocity.
- Aerodynamically, the trends are more definite. As the tubes are shortened the mean base pressure ratio decreases uniformly over the range of $10.47 \leq L_{ti}/D_t \leq 3.49$, thus increasing base drag. For the final cutback from $L_{ti}/D_t = 3.49$ to the $L_{ti}/D_t = 1.74$ baseplate, there was a sharp reduction in mean base pressure and associated increase in base drag. A design curve was formed showing change in base drag coefficient with L_{ti}/D_t, independent of P_{T8}/P_o.

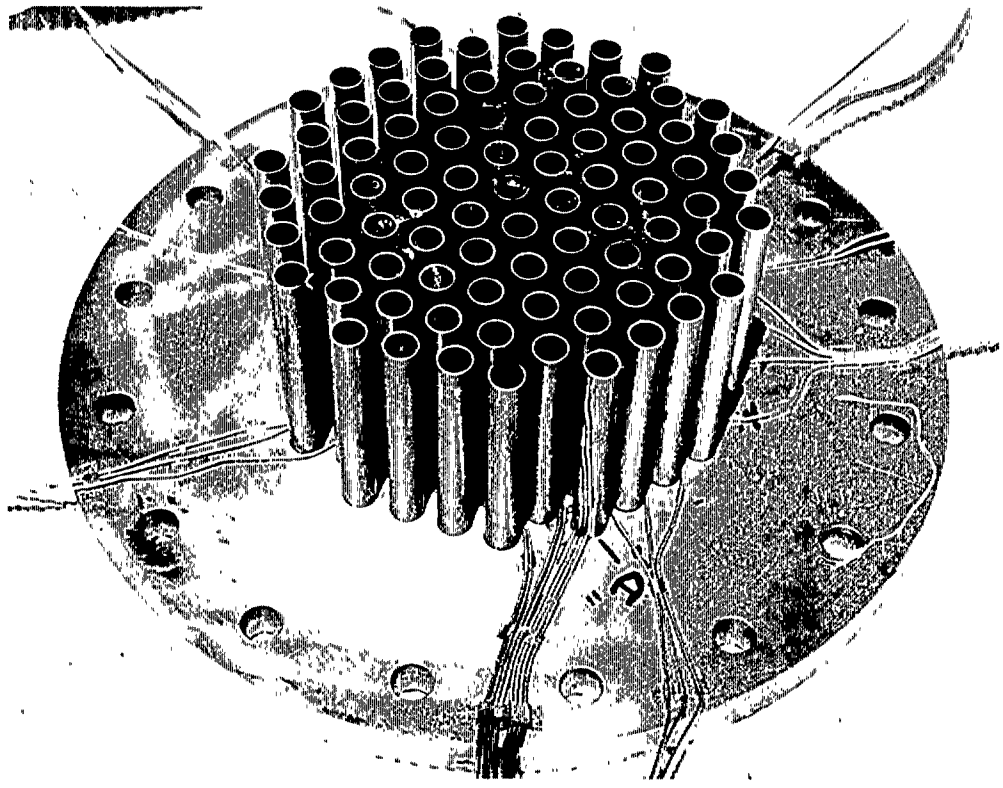

FIGURE V.F.5-1 BASIC 85 TUBE HARDWARE CONFIGURATION USED IN THE EXTERNAL/ INTERNAL TUBE LENGTH VARIATION STUDY

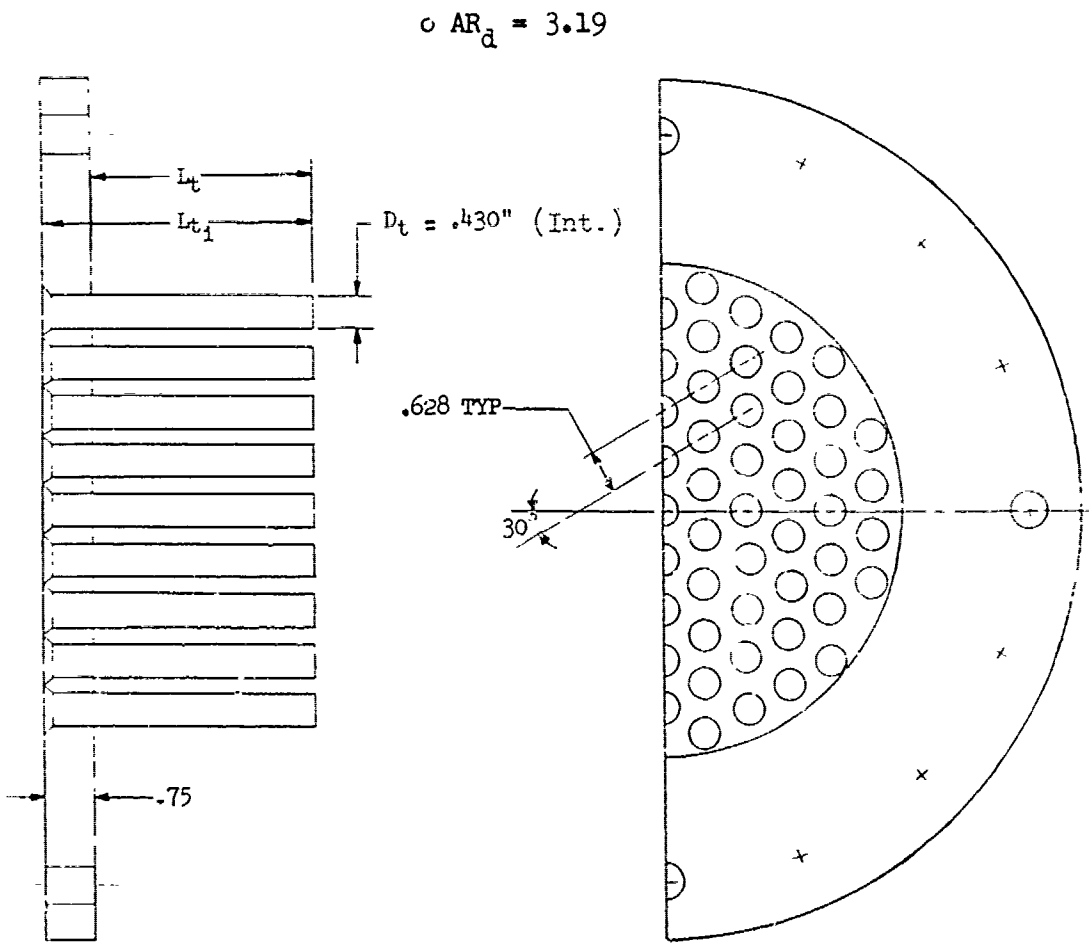

Model No.	Test Date	L_t	L_t/D_t	L_{ti}	L_{ti}/D_t
3.4T85	6-12-69	3.75"	8.72	4.5"	10.47
3.4T85-1	8-12-69	2.75"	6.40	3.5"	8.14
3.4T85-2	8-18-69	2.25"	5.23	3.0"	6.98
3.4T85-3	8-26-69	1.75"	4.07	2.5"	5.81
3.4T85-4	9-04-69	1.25"	2.91	2.0"	4.65
3.4T85-5	10-28-69	.75"	1.74	1.5"	3.49
3.4T85-6	11-21-69	0	0	.75"	1.74

FIGURE V.F.5-2 SCHEMATIC OF 85 TUBE NOZZLE USED IN EXTERNAL/ INTERNAL TUBE LENGTH STUDY

TABLE V.F.5-1 TEST SUMMARY

MODEL NO. 4.3" Cone

DESCRIPTION: Baseline Conical Nozzle

DATE: 6/12/69; 8/12/69

SCALE MODEL A_8 = .1020 ft^2

FULL SCALE A_8 = 6.528 ft^2

SCALE FACTOR = 8:1

- DATA INCLUDES GROUND REFLECTION INTERFERENCE
- ANGLE REFERENCED TO JET EXHAUST

RDG NO.	TEST CONDITIONS				ACOUSTIC TEST RESULTS						
			IDEAL			320' ARC		300' SIDELINE		1500' SIDELINE	
	P_{TS}/P_o	T_{T8} (°R)	V_j (ft/sec)	W_8 (PPS)	10 log ρA	PEAK PNdB	PEAK ANGLE	PEAK PNdB	PEAK ANGLE	PEAK PNdB	PEAK ANGLE
6/12/69											
1	1.42	1151	1157	3.76	-5.9	111.1	50	108.9	50	93.3	50
2	1.99	1524	1825	5.15	-7.1	128.9	50	126.7	50	111.1	50
8/12/69											
1	1.44	1161	1185	3.88	-6.0	110.2	50	108.0	50	92.7	50
2	2.01	1536	1845	5.27	-7.1	132.2	30	126.6	50	111.2	50
3	2.71	1803	2348	6.71	-7.2	138.7	50	136.5	50	120.9	50
4	3.13	2279	2015	6.77	-5.0	140.7	50	138.6	50	123.0	50
5	3.40	2689	3143	6.82	-8.3	141.1	50	140.0	60	124.1	60
6	3.20	2420	2915	6.79	-8.0	140.7	50	138.5	50	122.9	50
7	2.49	1640	2149	6.44	-7.0	136.1	50	134.0	50	118.3	50

TABLE V.F.5-1 (Cont.) TEST SUMMARY

NOZZLE NO. 4.3" Cone

DESCRIPTION: Baseline Conical Nozzle

DATE: 8/18/69; 8/26/69; 9/4/69

SCALE MODEL A_8 = .1020 ft^2

FULL SCALE A_8 = 6.528 ft^2

SCALE FACTOR = 8:1

- DATA INCLUDES GROUND REFLECTION INTERFERENCE
- ANGLE REFERENCED TO JET EXHAUST

RUN NO.	TEST CONDITIONS				ACOUSTIC TEST RESULTS						
	P_{TS}/P_o	T_{T8} (°R)	IDEAL V_j (ft/sec)	W_8 (PPS)	10 log ρA	320' ARC PEAK PNdB	320' ARC PEAK ANGLE	300' SIDELINE PEAK PNdB	300' SIDELINE PEAK ANGLE	1500' SIDELINE PEAK PNdB	1500' SIDELINE PEAK ANGLE
8/18/69											
2	2.02	1542	1851	5.13	-7.1	131.4	30	126.7	40	111.3	40
3	2.72	1779	2334	6.60	-7.1	139.4	50	137.2	50	121.5	50
4	3.10	2232	2762	6.56	-7.8	140.8	50	138.5	50/60	122.7	50/60
5	3.41	2705	3147	6.50	-8.4	141.8	50	140.4	60	124.5	60
6	3.21	2406	2916	6.48	-8.1	141.3	50	139.2	50	123.5	50
7	2.46	1677	2162	6.03	-7.1	136.6	50	134.4	50	118.4	50
8/26/69											
1	1.43	1157	1168	3.63	-6.0	108.9	50	107.8	60	92.3	60
2	2.01	1502	1825	5.20	-7.0	129.6	30/40	126.3	50	110.8	50
3	2.72	1768	2329	6.73	-7.1	138.5	50	136.4	50	120.7	50
4	3.13	2220	2765	6.72	-7.7	141.0	50	138.8	50	123.0	50
5	3.22	2410	2911	6.62	-8.0	141.1	50	138.9	50	123.3	50
6	3.42	2662	3127	6.67	-8.3	141.0	60	140.1	60	124.4	60
7	2.47	1624	2132	6.17	-6.9	135.6	50	133.4	50	117.8	50
9/4/69											
[illegible]	2.01	1495	1819	5.28	-7.0	130.2	30	125.3	50	110.0	40

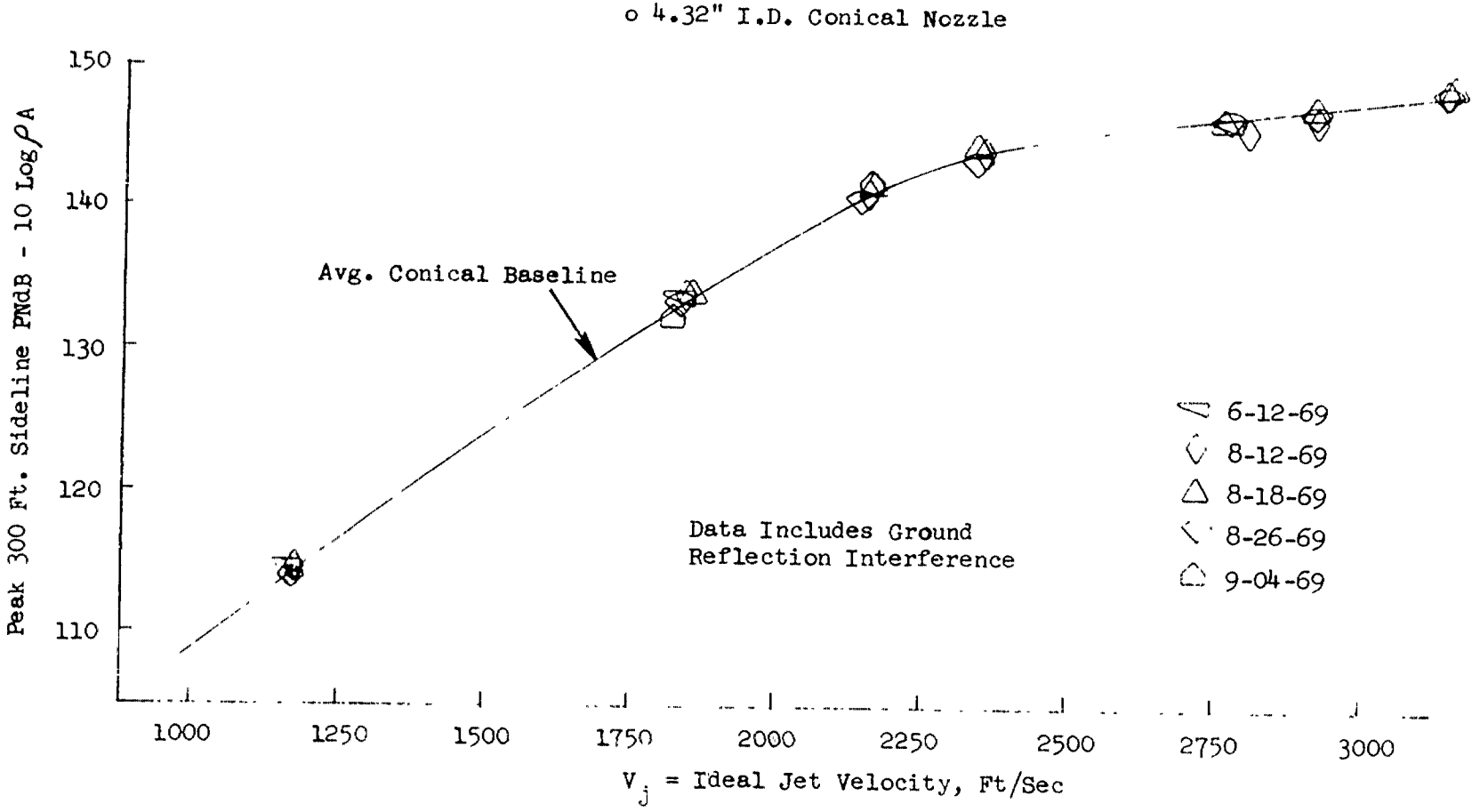

FIGURE V.F.5-3 300 FT. SIDELINE JET NOISE LEVELS FOR AVERAGE CONICAL BASELINE

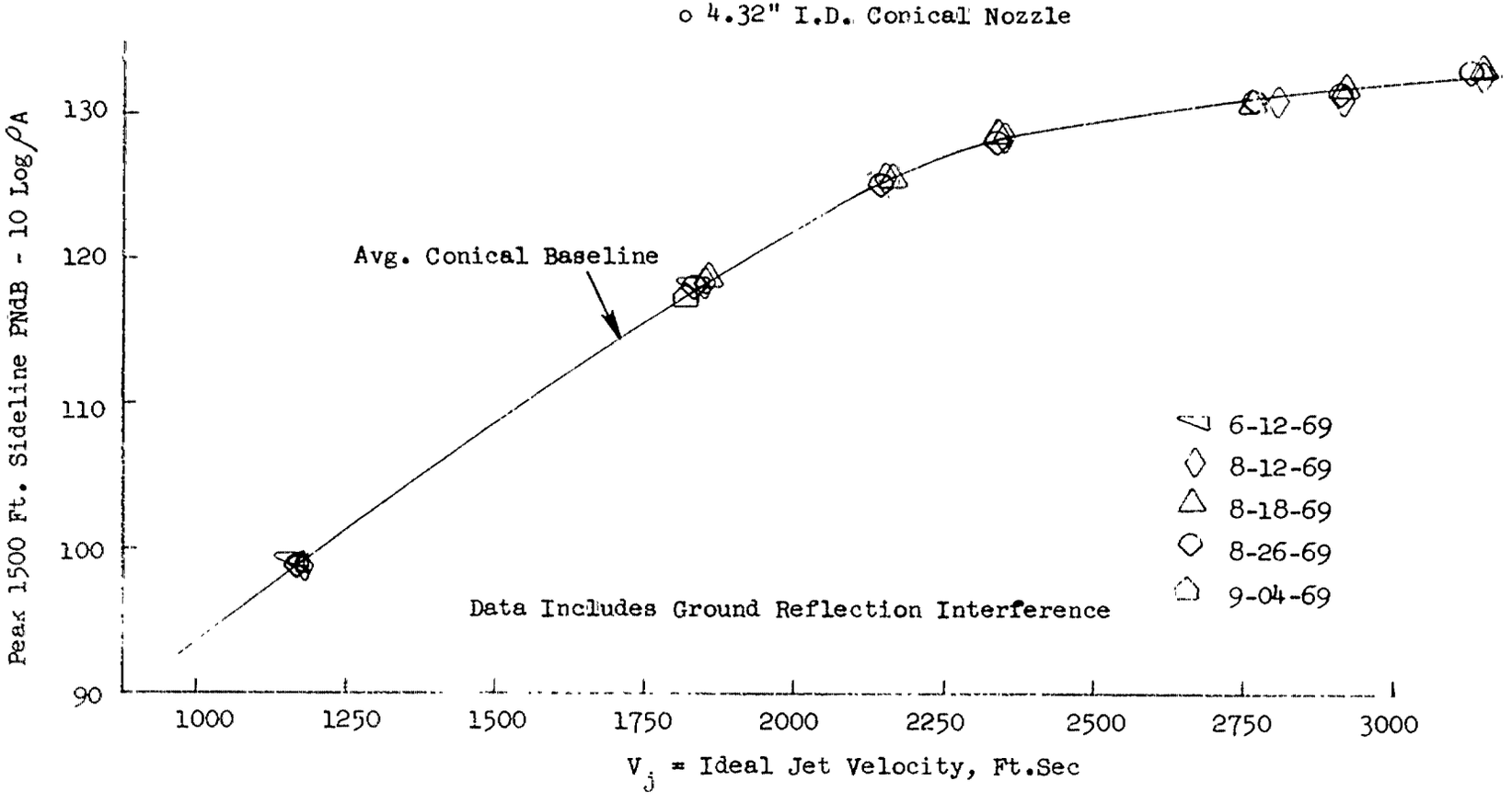

FIGURE V.F.5-4 1500 FT. SIDELINE JET NOISE LEVELS FOR AVERAGE CONICAL BASELINE

TABLE V.B-2 TEST SUMMARY

MODEL NO. 3.4 T 85

DESCRIPTION: 85 Tube, .430" I.D. Equal Size and Length, L_{ti}/D_t = 10.47, AR_d = 3.19

DATE: 6/12/69

SCALE MODEL A_8 = .0857 ft^2

FULL SCALE A_8 = 5.485 ft^2

SCALE FACTOR = 8:1

- o DATA INCLUDES GROUND REFLECTION INTERFERENCE
- o ANGLE REFERENCED TO JET EXHAUST

	TEST CONDITIONS				ACOUSTIC TEST RESULTS						
			IDEAL			320' ARC		300' SIDELINE		1500' SIDELINE	
RDG NO.	P_{T8}/P_o	T_{T8} (°R)	V_j (ft/sec)	W_8 (PPS)	10 log ρA	PEAK PNdB	PEAK ANGLE	PEAK PNdB	PEAK ANGLE	PEAK PNdB	PEAK ANGLE
1	1.43	1143	1161	3.25	-6.7	108.3	50/60	107.4	60	89.6	60
2	1.62	1517	1544	3.30	-8.0	116.3	60	115.3	60	97.6	60
3	1.62	1243	1391	3.56	-7.1	114.9	50	112.8	60	95.0	60
4	1.75	1516	1652	3.55	-8.0	118.8	60	117.9	60	100.0	60
5	2.00	1512	1823	4.18	-7.8	121.5	50	120.0	60	102.3	60
6	2.00	2115	2159	3.32	-9.3	123.5	50	121.6	60	103.9	60
7	2.30	1571	2020	4.93	-7.7	122.7	50	120.5	60	102.8	60
8	2.45	1649	2140	4.96	-7.8	124.1	50	121.8	60	104.1	60
9	2.51	2091	2440	4.35	-8.8	125.4	50	123.7	70	106.2	70
10	2.70	1766	2319	5.19	-7.9	125.8	50	123.4	50	105.8	50
11	2.91	2137	2634	5.01	-8.5	126.8	50	125.2	60	107.7	60
12	3.12	2218	2758	5.20	-8.5	128.7	40	126.2	70	108.8	70
13	3.21	2424	2917	5.14	-8.8	128.9	40	127.0	60	109.7	60
14	3.21	2620	3031	4.85	-9.1	129.6	40	127.2	70	109.8	70
15	3.39	2661	3117	5.19	-9.1	130.4	40	127.8	50	110.6	50
16	3.41	2122	2789	5.91	-8.1	129.0	30	126.4	60	109.0	60

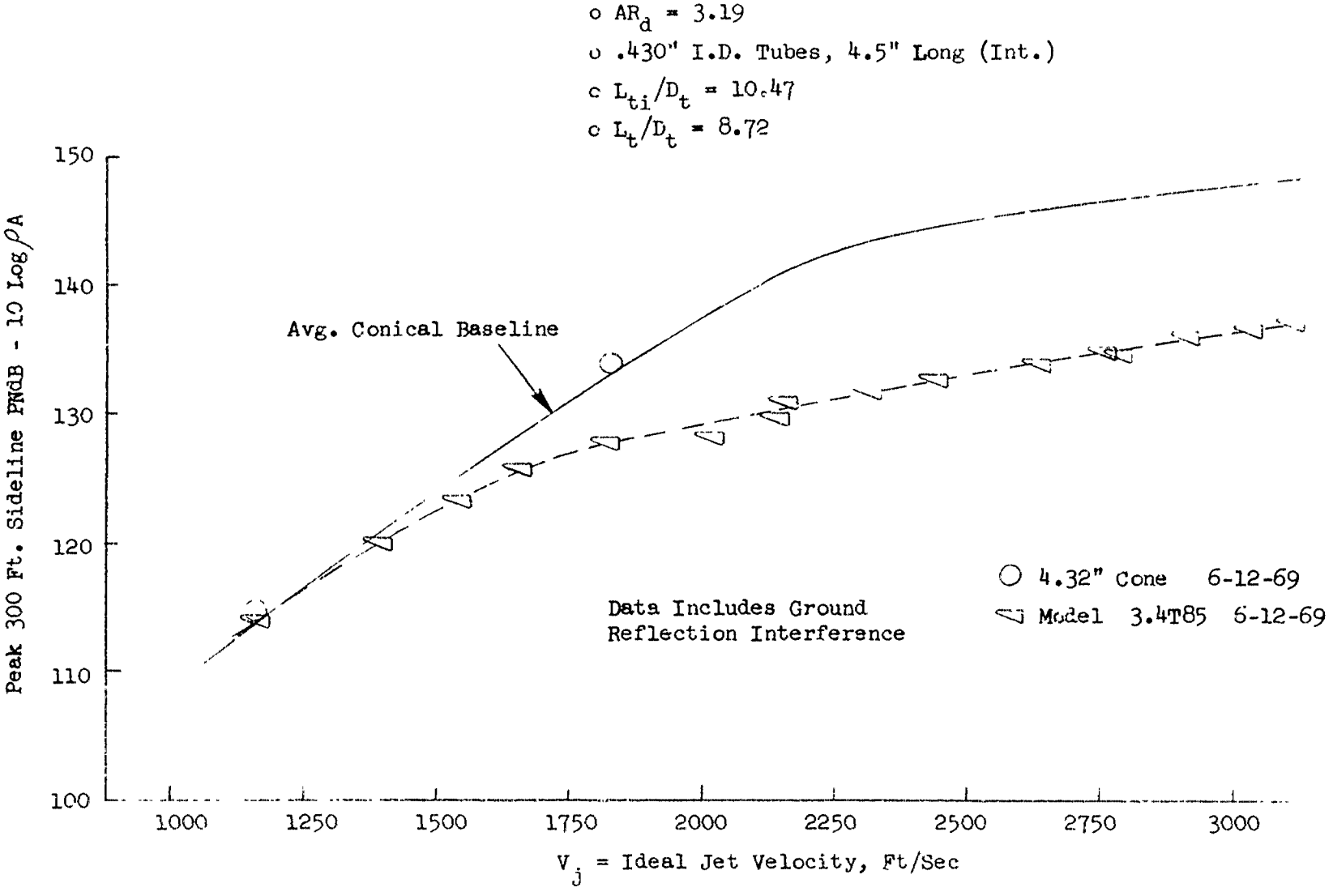

FIGURE V.F.5-5 300 FT. SIDELINE JET NOISE LEVELS FOR AN 85 TUBE NOZZLE, L_{ti}/D_t = 10.47

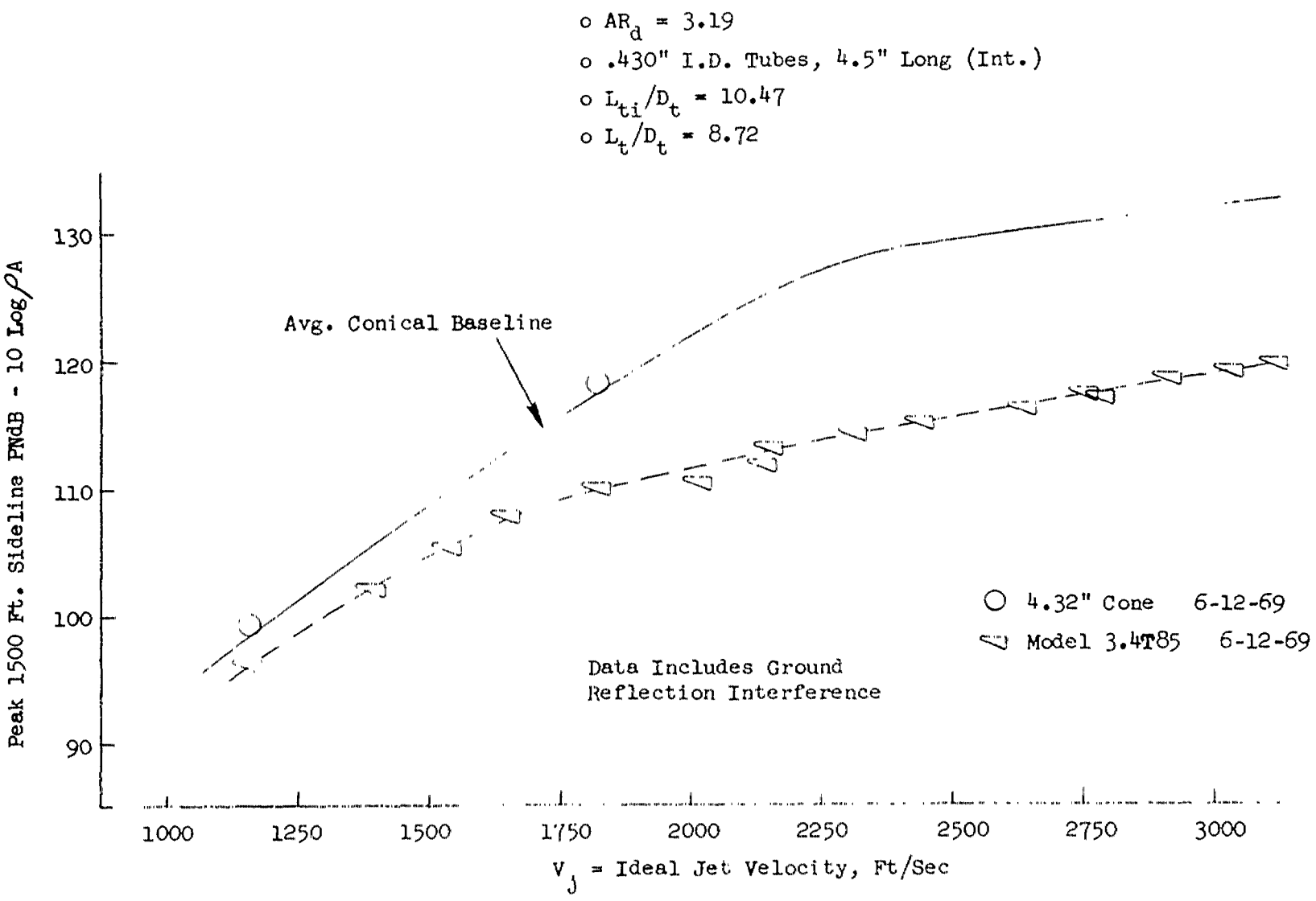

FIGURE V.F.5-6 1500 FT. SIDELINE JET NOISE LEVELS FOR AN 85 TUBE NOZZLE, L_{ti}/D_t = 10.47

TABLE V.F.5-3 TEST SUMMARY

MODEL NO. 3.4 T 85-1

DESCRIPTION: 85 Tube, .430" I.D. Equal Size and Length, L_{ti}/D_t = 8.14, AR_d = 3.19

DATE: 8/12/69

SCALE MODEL A_8 = .0857 ft^2

FULL SCALE A_8 = 5.485 ft^2

SCALE FACTOR = 8:1

- o DATA INCLUDES GROUND REFLECTION INTERFERENCE
- o ANGLE REFERENCED TO JET EXHAUST

RDG NO.	TEST CONDITIONS				ACOUSTIC TEST RESULTS						
			IDEAL			320' ARC		300' SIDELINE		1500' SIDELINE	
	P_{T8}/P_o	T_{T8} (°R)	V_j (ft/sec)	W_8 (PPS)	10 log ρA	PEAK PNdB	PEAK ANGLE	PEAK PNdB	PEAK ANGLE	PEAK PNdB	PEAK ANGLE
1	1.44	1142	1167	3.38	-6.7	108.0	50	106.4	60	88.8	60
2	1.56	1499	1463	3.28	-7.9	113.5	50	112.2	60	94.8	60
3	1.62	1221	1386	3.83	-7.0	114.0	50	111.6	50	93.9	50
4	1.76	1533	1671	3.82	-8.0	116.2	60	115.2	60	97.8	60
5	2.02	1498	1824	4.36	-7.7	119.6	50	117.2	50	99.5	50
6	2.00	2116	2152	3.46	-9.2	122.3	50	119.9	50	102.1	50
7	2.31	1612	2052	4.81	-7.8	121.8	50	119.4	50	101.7	50
8	2.48	1634	2142	5.09	-7.7	122.3	50	120.7	60	103.3	60
9	2.53	2197	2509	4.31	-9.0	125.2	50	122.8	50	105.3	50
10	2.71	1785	2336	5.10	-7.9	124.7	50	122.4	50	104.9	50
11	2.90	2160	2645	4.98	-8.5	126.7	50	124.3	50	106.9	50
12	3.12	2198	2745	5.30	-8.4	126.4	50	124.6	60	107.3	60
13	3.23	2439	2931	5.18	-8.8	128.4	50	126.0	50	108.8	50
14	3.22	2650	3051	5.05	-9.2	127.5	50	126.2	60	108.1	50/60
15	3.44	2660	3131	-	-9.0	128.6	50	126.3	50	109.4	50
16	3.47	2105	2795	-	-7.9	127.9	50	125.6	50	108.4	50

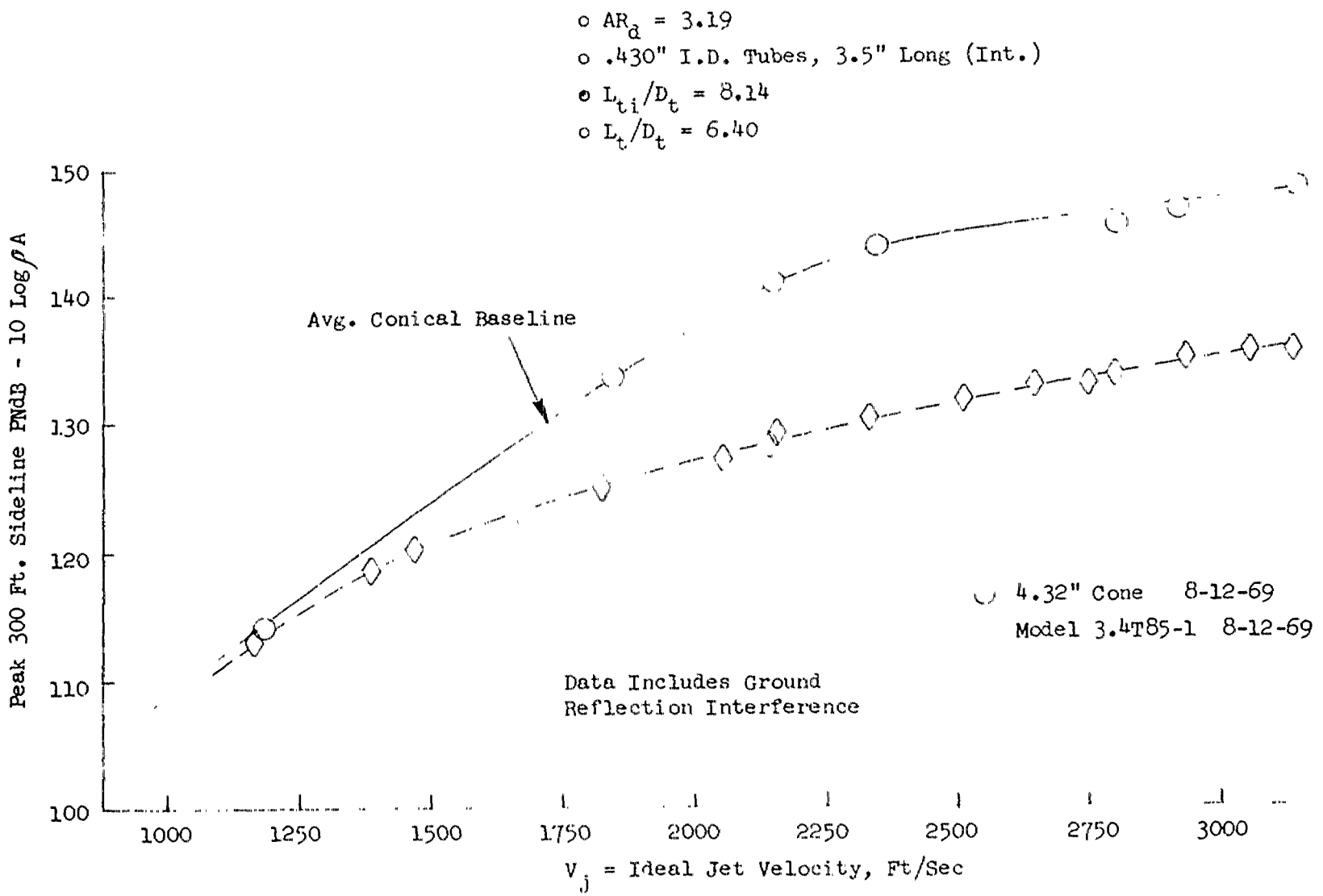

FIGURE V.F.5-7 300 FT. SIDELINE JET NOISE LEVELS FOR AN 85 TUBE NOZZLE, L_{ti}/D_t = 8.14

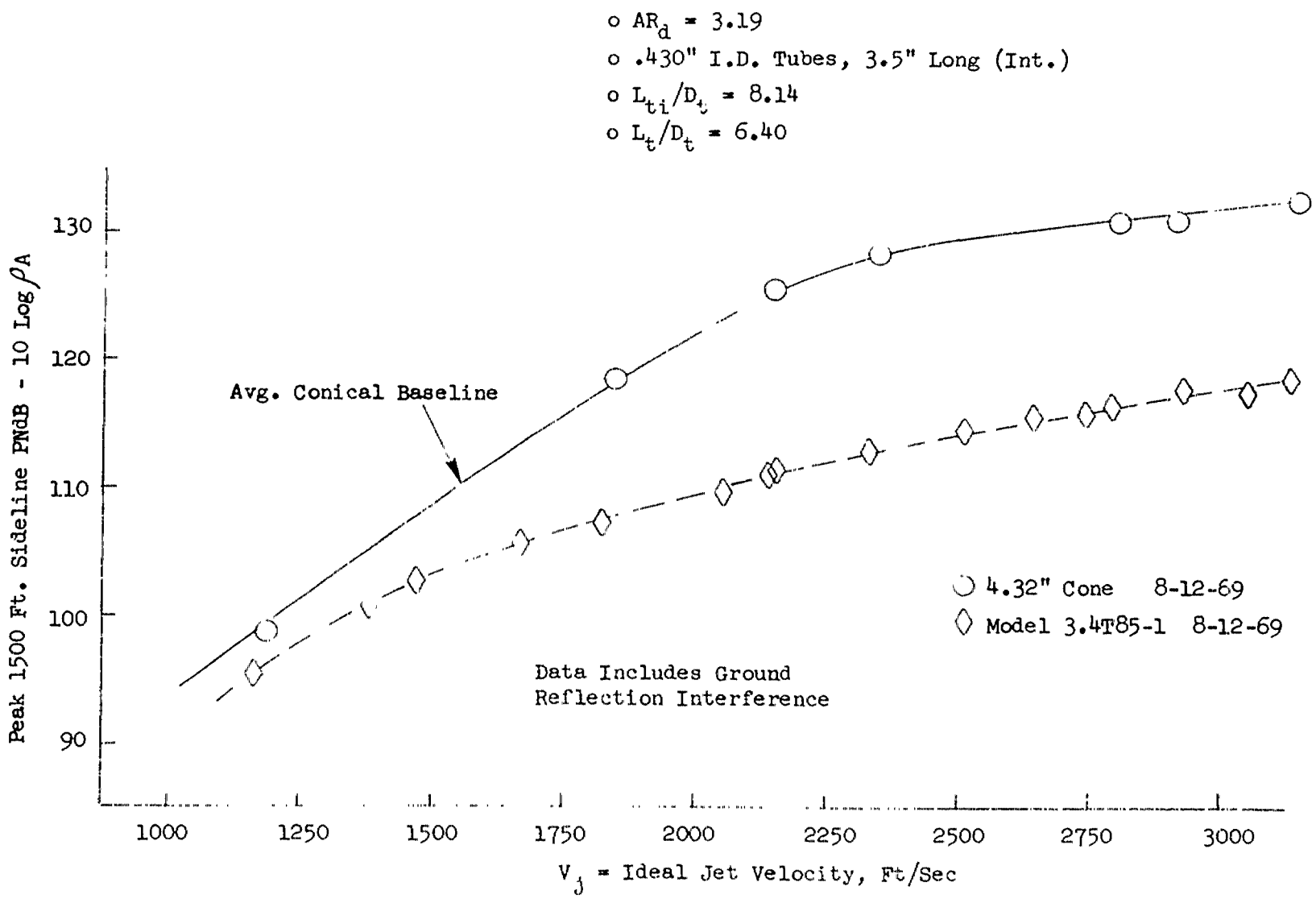

FIGURE V.F.5-8 1500 FT. SIDELINE JET NOISE LEVELS FOR AN 85 TUBE NOZZLE, L_{ti}/D_t = 8.14

TABLE V.F.5-4 TEST SUMMARY

MODEL NO. 3.4 T 85-2

DESCRIPTION: 85 Tube, .430" I.D. Equal Size and Length, L_{ti}/D_t = 6.98, AR_d = 3.19

DATE: 8/18/69

SCALE MODEL A_8 = .0857 ft^2

FULL SCALE A_8 = 5.485 ft^2

SCALE FACTOR = 8:1

- o DATA INCLUDES GROUND REFLECTION INTERFERENCE
- o ANGLE REFERENCED TO JET EXHAUST

	TEST CONDITIONS				ACOUSTIC TEST RESULTS						
			IDEAL			320' ARC		300' SIDELINE		1500' SIDELINE	
RDG NO.	P_{T8}/P_o	T_{T8} (°R)	V_j (ft/sec)	W_8 (PPS)	10 log ρA	PEAK PNdB	PEAK ANGLE	PEAK PNdB	PEAK ANGLE	PEAK PNdB	PEAK ANGLE
1	1.44	1148	1174	3.42	-6.7	108.5	60	107.6	60	89.9	60
2	1.55	1532	1482	3.15	-8.0	114.8	60	113.9	60	96.3	60
3	1.75	1256	1503	4.12	-7.1	116.0	60	115.1	60	97.4	60
4	1.76	1523	1664	3.58	-8.0	117.5	60	116.6	60	99.0	60
5	2.01	1533	1843	4.18	-7.8	119.6	60	118.7	60	101.2	60
6	2.02	2076	2152	3.42	-9.1	123.0	50	120.7	60	103.2	60
7	2.28	1570	2010	4.79	-7.7	121.7	50	120.5	60	103.0	60
8	2.49	1665	2167	4.99	-7.8	123.4	50	121.1	60	103.7	60/70
9	2.51	2153	2474	4.19	-8.9	124.4	50	123.1	60	105.6	60/70
10	2.72	1788	2342	5.28	-7.9	124.6	50	123.3	60	105.8	60
11	2.92	2143	2643	5.17	-8.5	126.8	50	125.3	60	108.0	60
12	3.13	2246	2781	5.33	-8.5	127.3	50	125.7	60	108.4	60
13	3.21	2446	2928	5.26	-8.8	129.0	50	126.6	50/60	109.5	60
14	3.23	2642	3051	5.09	-9.2	129.3	50	127.7	60	110.5	60
15	3.40	2665	3123	5.48	-9.1	129.8	30	127.8	70	110.6	70
16	3.42	2129	2796	6.08	-8.1	129.1	50	127.1	60	109.8	60

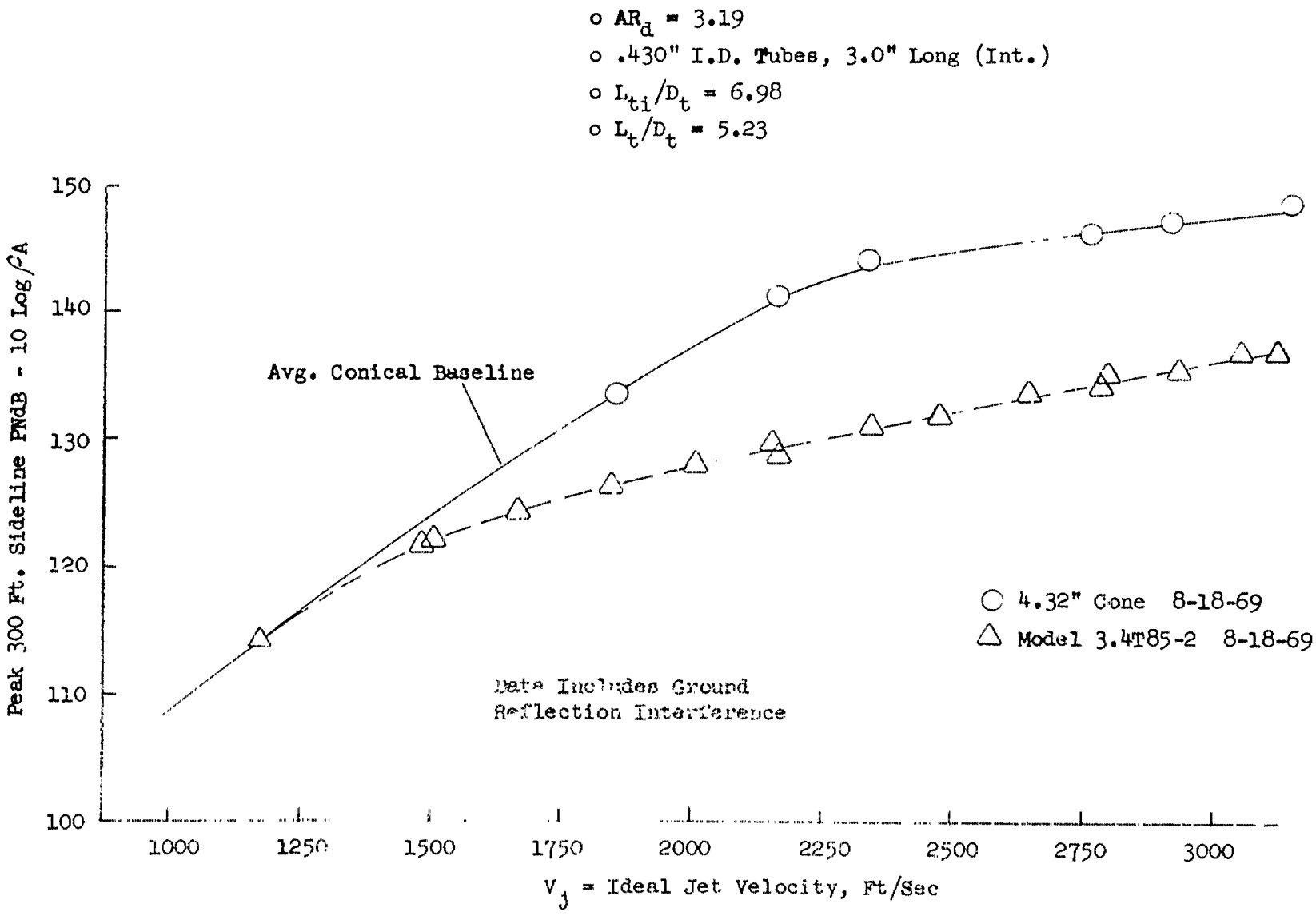

FIGURE V.F.5-9 300 FT. SIDELINE JET NOISE LEVELS FOR AN 85 TUBE NOZZLE, L_{ti}/D_t = 6.98

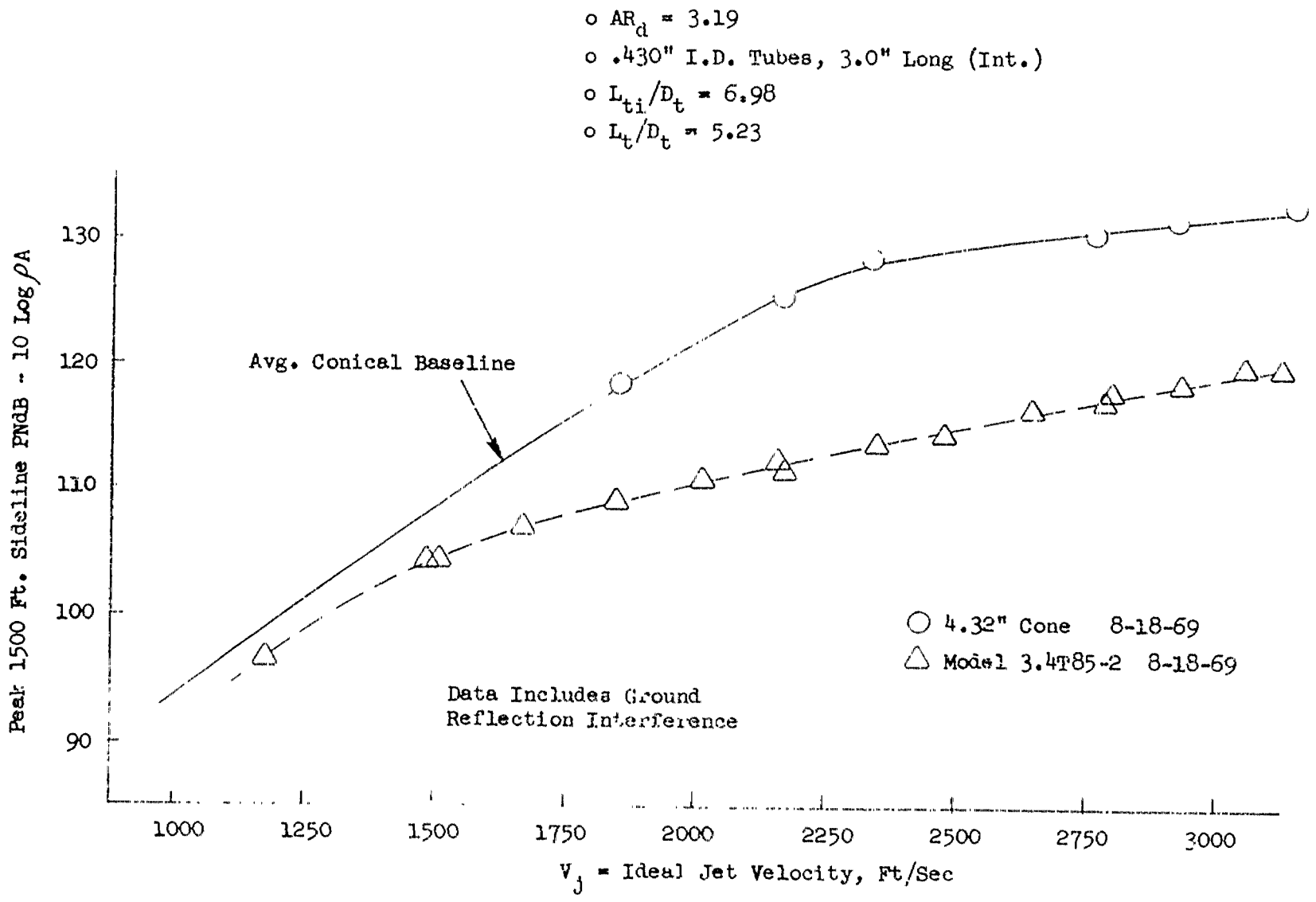

FIGURE V.F.5-10 1500 FT. SIDELINE JET NOISE LEVELS FOR AN 85 TUBE NOZZLE, L_{ti}/D_t = 6.98

TABLE V.F.5-5 TEST SUMMARY

MODEL NO. 3.4 T 85-3

DESCRIPTION: 85 Tube, .430" I.D., Equal Size and Length, L_{ti}/D_t = 5.81, AR_d = 3.19

DATE: 8/26/69

SCALE MODEL A_8 = .0857 ft^2

FULL SCALE A_8 = 5.485 ft^2

SCALE FACTOR = 8:1

- o DATA INCLUDES GROUND REFLECTION INTERFERENCE
- o ANGLE REFERENCED TO JET EXHAUST

RDG NO.	TEST CONDITIONS				ACOUSTIC TEST RESULTS						
			IDEAL			320' ARC		300' SIDELINE		1500' SIDELINE	
	P_{T8}/P_o	T_{T8} (°R)	V_j (ft/sec)	W_8 (PPS)	10 log oA	PEAK PNdB	PEAK ANGLE	PEAK PNdB	PEAK ANGLE	PEAK PNdB	PEAK ANGLE
1	1.43	1161	1172	3.50	-6.7	107.9	50	106.8	60	89.2	60
2	1.57	1498	1478	3.29	-7.9	113.7	60	112.8	60	95.2	60
3	1.62	1296	1400	3.89	-7.1	113.6	60	112.6	60	95.0	60
4	1.69	1499	1594	3.83	-7.9	117.8	50	115.4	50	97.7	60
5	2.01	1497	1822	4.47	-7.7	119.0	50	117.5	70	99.9	70
6	2.00	2089	2141	3.55	-9.2	120.7	50	119.6	70	102.2	70
7	2.32	1543	2015	4.92	-7.6	121.6	50	119.2	50	101.4	50/70
8	2.44	1656	2138	5.00	-7.8	123.2	50	120.8	50	103.0	50
9	2.51	2098	2443	4.36	-8.8	124.1	50	122.6	70	105.2	70
10	2.70	1766	2320	5.31	-7.8	123.5	50	121.1	50	103.7	70
11	2.91	2114	2619	5.13	-8.4	125.6	50	123.2	50	105.9	50/70
12	3.12	2232	2767	5.33	-8.5	126.3	50	124.0	50	106.8	50
13	3.20	2410	2903	5.29	-8.8	127.1	50	124.8	50/60	107.9	50
14	3.21	2598	3018	5.12	-9.1	127.5	50	125.3	60	108.2	60
15	3.42	2654	3120	5.44	-9.0	128.6	50	126.3	50	109.2	50
16	3.41	2092	2769	6.06	-8.0	128.0	50	125.6	50	108.4	50

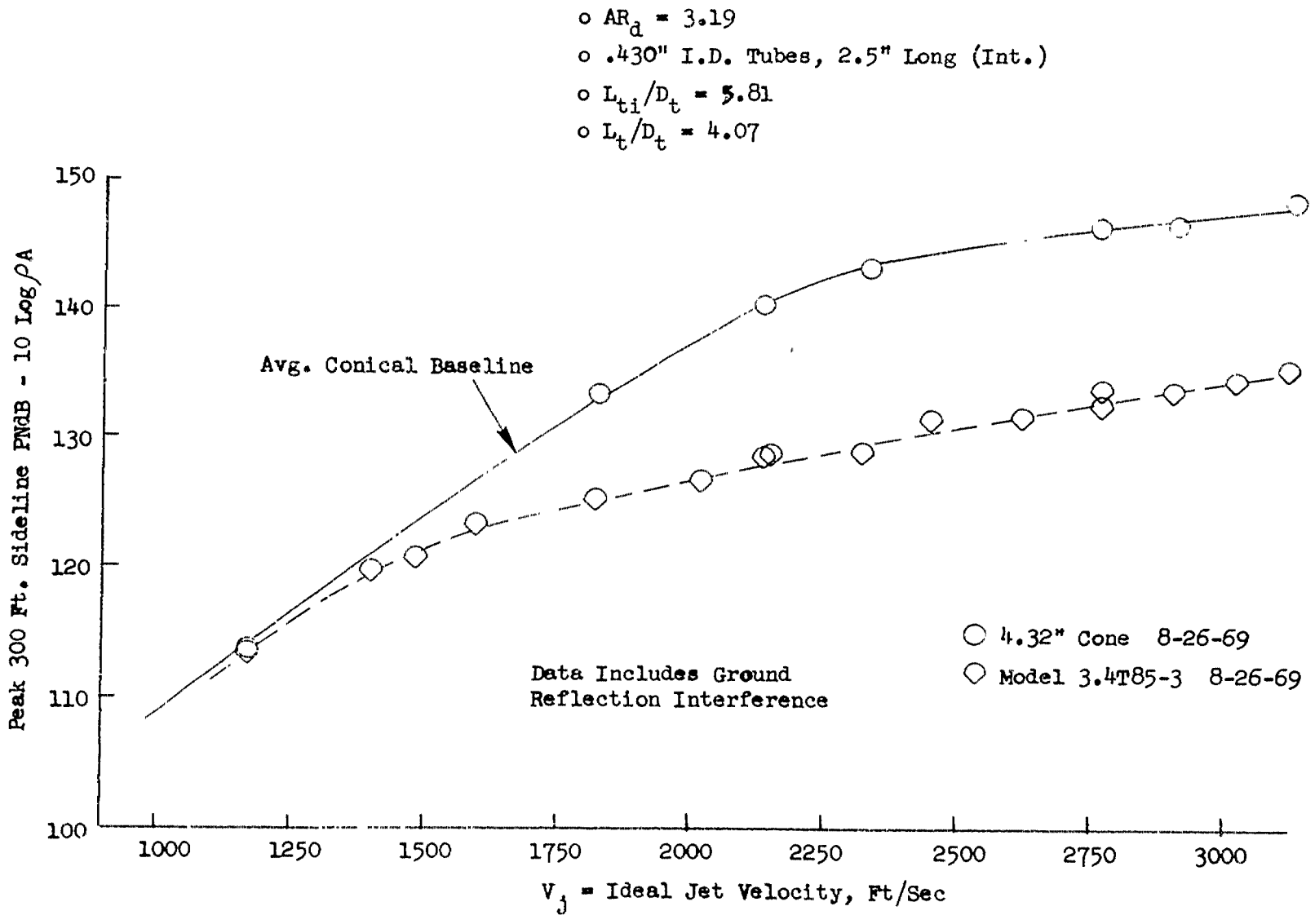

FIGURE V.F.5-11 300 FT. SIDELINE JET NOISE LEVELS FOR AN 85 TUBE NOZZLE, L_{ti}/D_t = 5.81

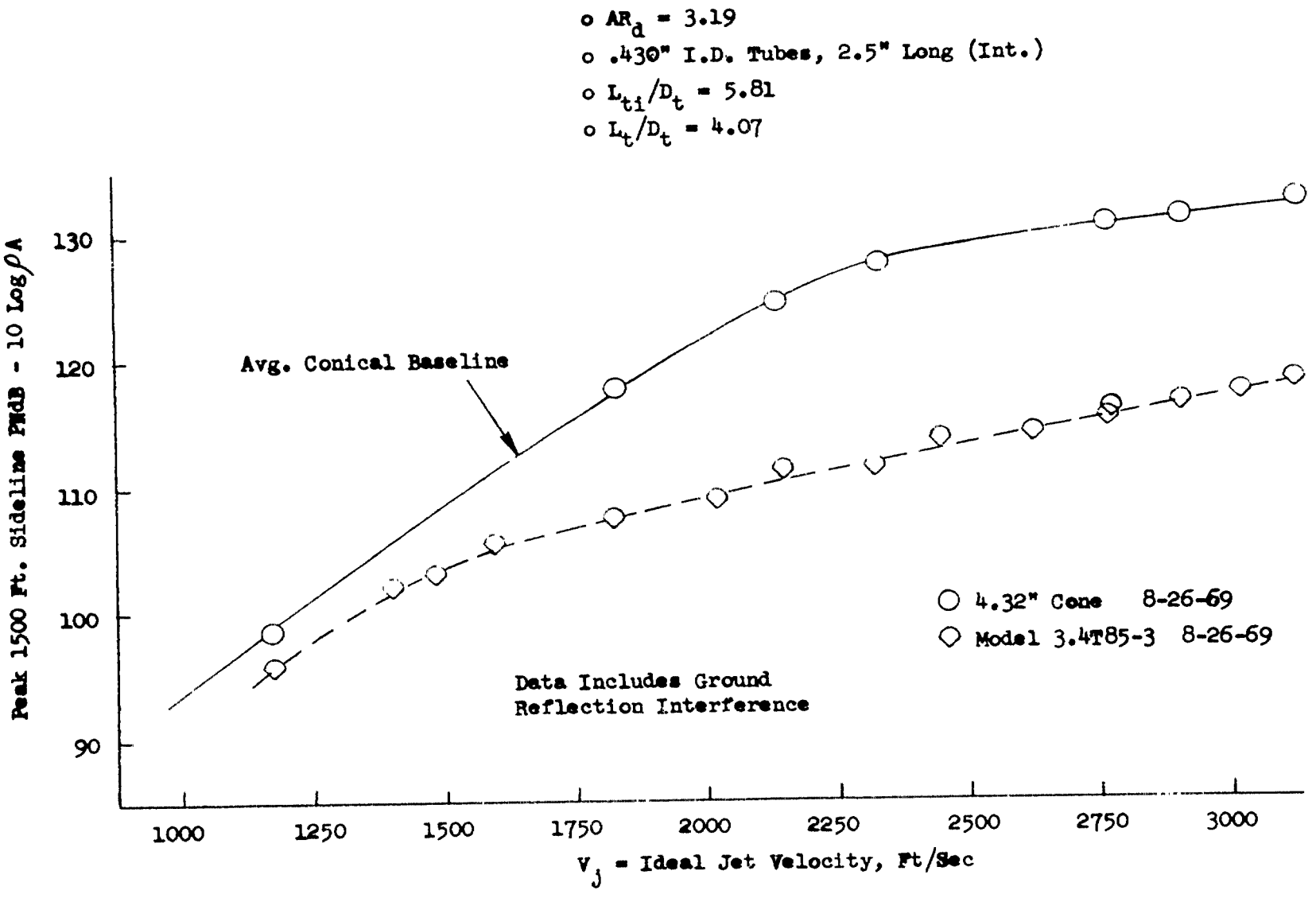

FIGURE V.F.5-12 1500 FT. SIDELINE JET NOISE LEVELS FOR AN 85 TUBE NOZZLE, L_{ti}/D_t = 5.81

TABLE V.F.5-6 TEST SUMMARY

MODEL NO. 3.4 T 85-4

DESCRIPTION: 85 Tube, .430" I.D. Equal Size and Length, L_{ti}/D_t = 4.65, AR_d = 3.19

DATE: 9/4/69

SCALE MODEL A_8 = .0859 ft^2

FULL SCALE A_8 = 5.485 ft^2

SCALE FACTOR = 8:1

- o DATA INCLUDES GROUND REFLECTION INTERFERENCE
- o ANGLE REFERENCED TO JET EXHAUST

	TEST CONDITIONS				ACOUSTIC TEST RESULTS						
			IDEAL			320' ARC		300' SIDELINE		1500' SIDELINE	
RDG NO.	P_{T8}/P_o	T_{T8} (°R)	V_j (ft/sec)	W_8 (PPS)	10 log ρA	PEAK PNdB	PEAK ANGLE	PEAK PNdB	PEAK ANGLE	PEAK PNdB	PEAK ANGLE
1	1.42	1111	1132	3.54	-6.5	108.2	50	107.1	60	89.5	60
2	1.54	1495	1456	3.15	-7.9	115.2	50	113.3	60	95.7	60
3	1.60	1239	1376	3.72	-7.1	113.8	50	112.8	60	95.1	60
4	1.76	1501	1651	3.81	-7.9	118.8	50	116.9	60	99.3	60
5	2.00	1502	1818	4.23	-7.7	119.8	50	117.7	60	100.0	60
6	1.99	2142	2165	3.41	-9.3	122.6	50	121.5	90	104.1	90
7	2.29	1560	2009	4.77	-7.7	121.4	50	119.7	60/90	102.4	60/90
8	2.45	1591	2103	5.06	-7.6	122.9	50	121.3	90	104.0	90
9	2.50	2095	2437	4.27	-8.8	124.8	50	123.0	60	105.5	60
10	2.71	1742	2305	5.33	-7.8	124.2	50	121.9	70	104.5	70
11	2.92	2132	2634	5.16	-8.5	125.2	50	124.0	60	106.8	60/90
12	3.12	2197	2746	5.35	-8.4	127.3	50	124.9	50	107.6	50
13	3.20	2388	2892	5.15	-8.7	127.8	50	126.0	60	108.8	60
14	3.24	2601	3031	5.13	-9.1	128.4	50	126.1	60/90	109.1	60
15	3.41	2641	3109	5.23	-9.0	129.6	50	127.3	50	110.1	50
16	3.40	2101	2773	5.94	-8.0	128.4	50	126.1	50	108.8	50

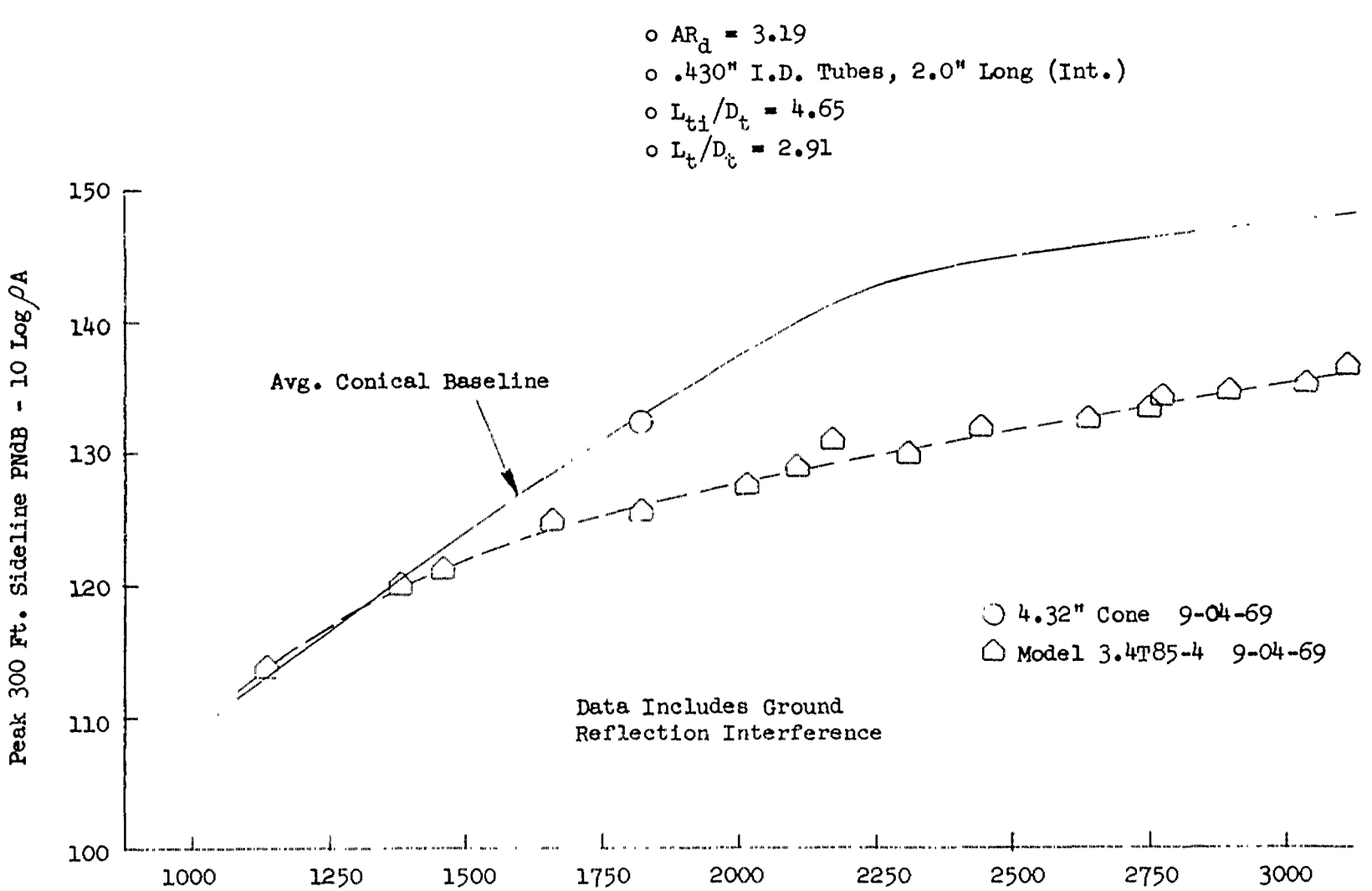

FIGURE V.F.5-13 300 FT. SIDELINE JET NOISE LEVELS FOR AN 85 TUBE NOZZLE, L_{ti}/D_t = 4.65

- AR_d = 3.19
- .430" I.D. Tubes, 2.0" Long (Int.)
- L_{ti}/D_t = 4.65
- L_t/D_t = 2.91

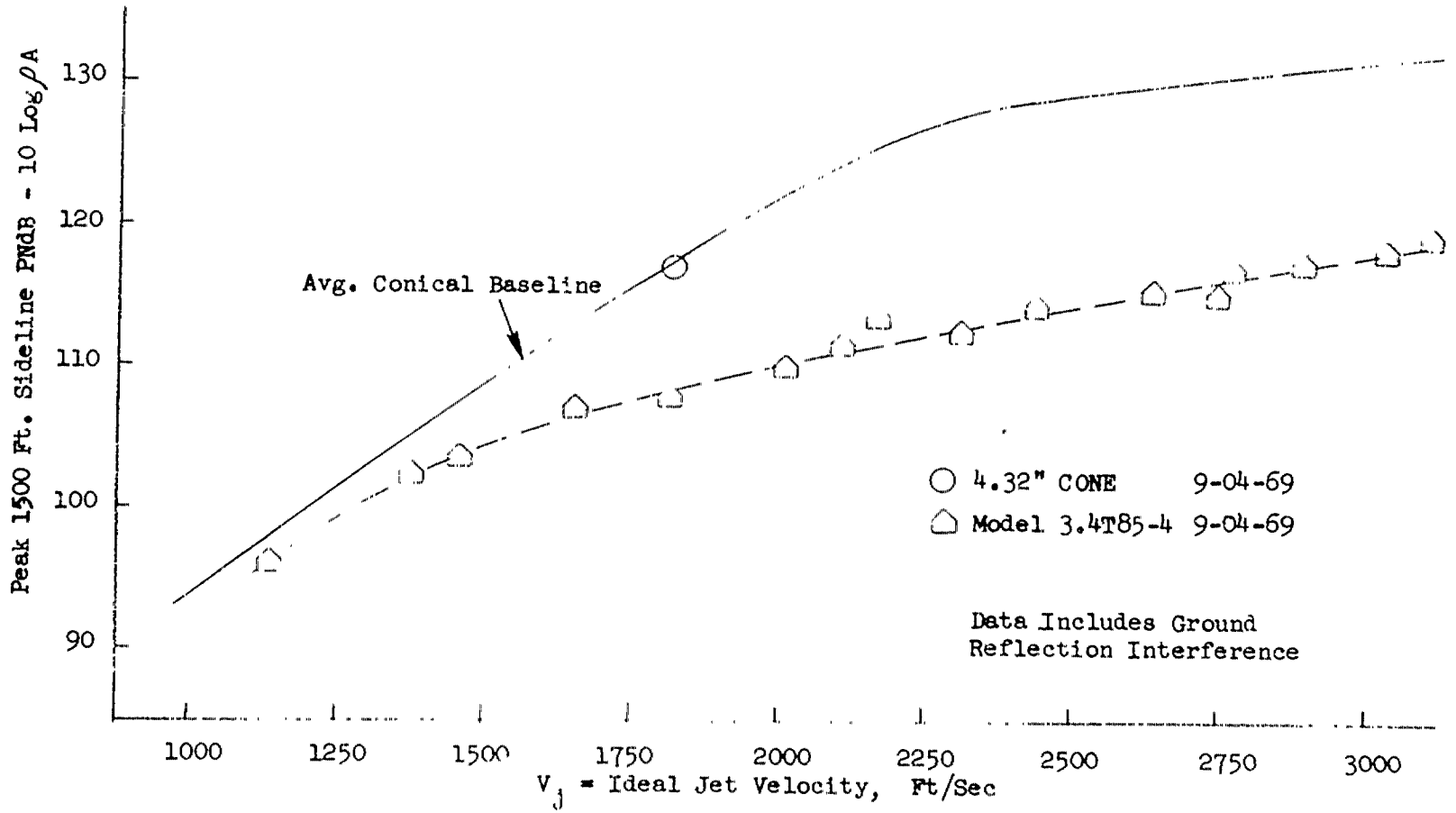

FIGURE V.F.5-14 1500 FT. SIDELINE JET NOISE LEVELS FOR AN 85 TUBE NOZZLE, L_{ti}/D_t = 4.65

TABLE V.F.5-7 TEST SUMMARY

MODEL NO. 3.4 T 85-5

DESCRIPTION: 85 Tube, .430" I.D., Equal Size and Length, L_{ti}/D_t = 3.49
AR_d = 3.19

DATE: 10/28/69

SCALE MODEL A_8 = .0857 ft^2

FULL SCALE A_8 = 5.485 ft^2

SCALE FACTOR = 8:1

- o DATA INCLUDES GROUND REFLECTION INTERFERENCE
- o ANGLE REFERENCED TO JET EXHAUST

RDG NO.	TEST CONDITIONS				ACOUSTIC TEST RESULTS						
			IDEAL			320' ARC		300' SIDELINE		1500' SIDELINE	
	P_{T8}/P_o	T_{T8} (°R)	V_j (ft/sec)	W_8 (PPS)	10 log ρA	PEAK PNdB	PEAK ANGLE	PEAK PNdB	PEAK ANGLE	PEAK PNdB	PEAK ANGLE
1	1.43	1168	1176	3.15	-6.7	110.0	60	109.1	60	91.4	60
2	1.51	1518	1426	2.57	-7.9	114.8	60	113.9	60	96.3	60
3	1.61	1242	1388	3.57	-7.0	114.1	60	113.2	60	95.4	60
4	1.75	1545	1668	3.38	-8.0	117.5	60	116.6	60	98.9	60
5	2.00	1507	1823	4.18	-7.7	119.0	60	118.1	60	100.4	60
6	1.99	2136	2159	3.20	-9.2	123.1	50	120.7	50	102.7	50/70
7	2.28	1557	2001	4.55	-7.6	121.1	50	119.7	60	102.2	60
8	2.46	1613	2154	4.75	-7.8	122.4	50	120.8	60	103.3	60
9	2.50	2103	2439	4.28	-8.7	123.9	50	122.4	60	105.1	60
10	2.70	1790	2335	5.17	-7.9	122.4	50/60	121.5	70	104.2	60
11	2.98	2137	2658	4.94	-8.4	125.3	50	123.2	60	105.9	60
12	3.11	2256	2778	5.09	-8.5	128.3	70	124.6	60	107.5	60
13	3.20	2422	2912	4.74	-8.7	128.1	30	125.7	60	108.8	50
14	3.21	2601	3020	4.83	-9.0	128.1	50	125.9	60	108.9	50
15	3.36	2693	3123	5.01	-9.1	132.5	50	126.6	60	110.1	60
16	3.40	2135	2793	5.65	-8.0	127.8	50	125.7	60	108.7	60

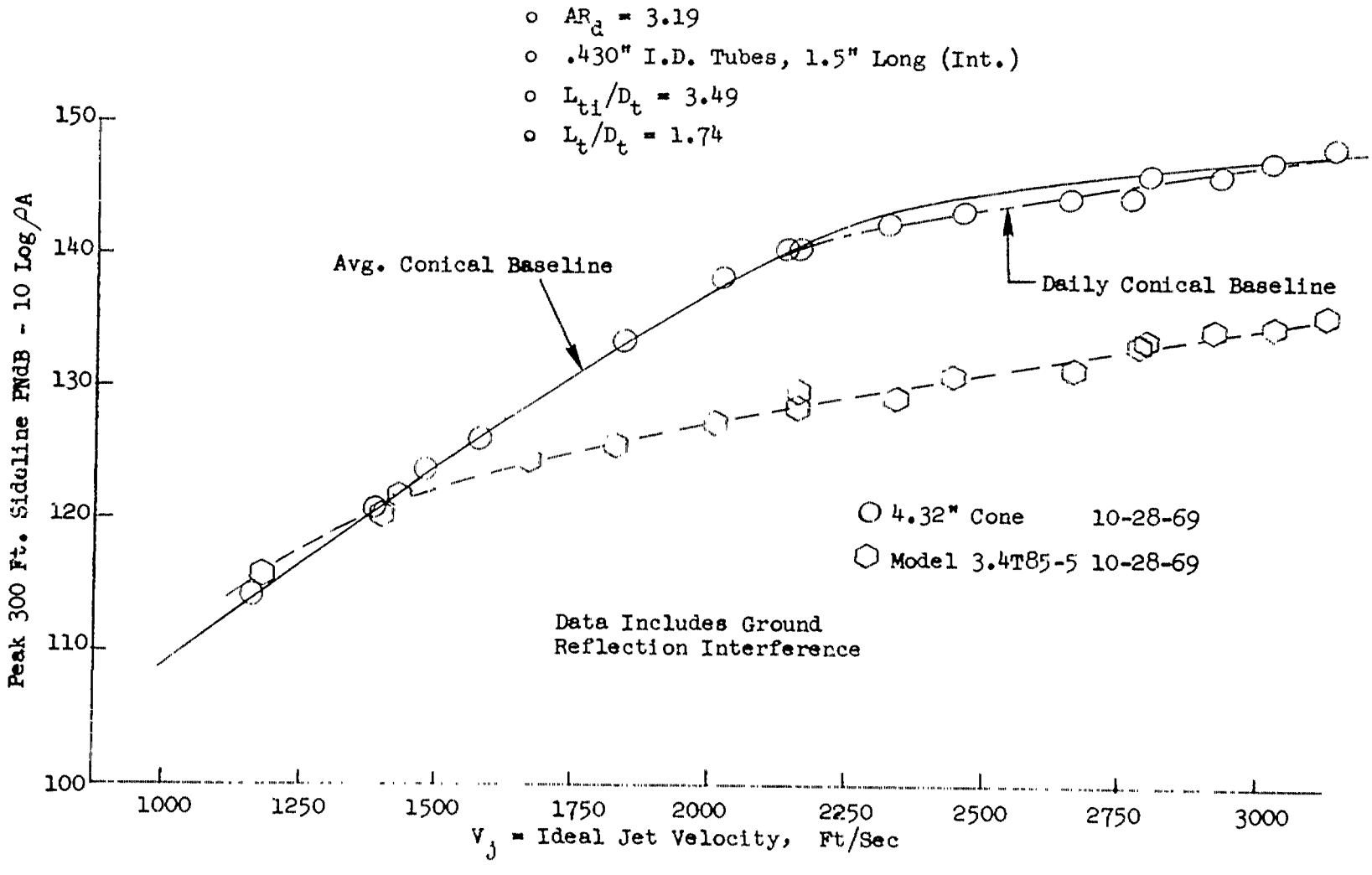

FIGURE V.F.5-15 300 FT. SIDELINE JET NOISE LEVELS FOR AN 85 TUBE NOZZLE, L_{ti}/D_t = 3.49

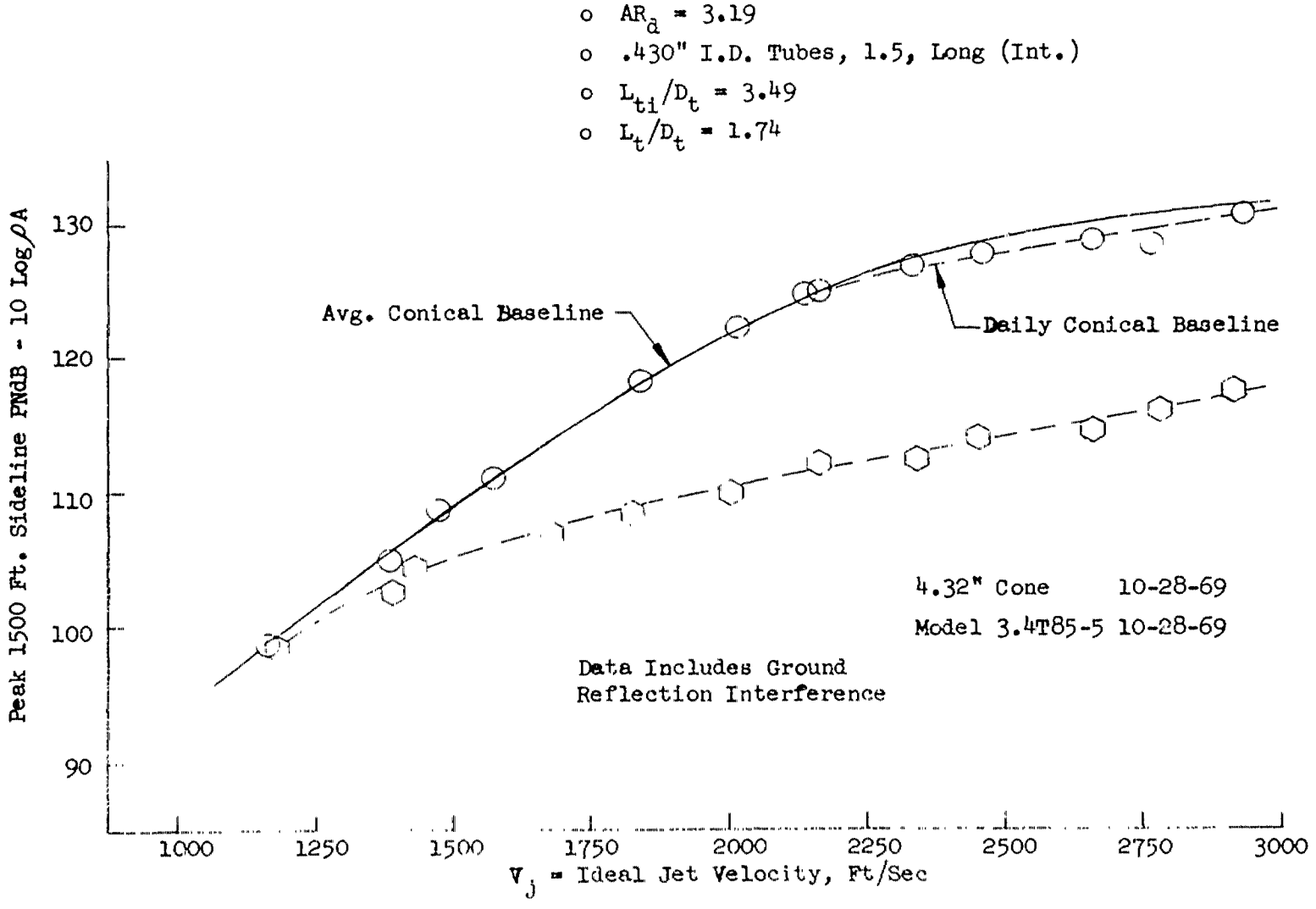

FIGURE V.F.5-16 1500 FT. SIDELINE JET NOISE LEVELS FOR AN 85 TUBE NOZZLE, L_{ti}/D_t = 3.49

TABLE V.F.5-8 TEST SUMMARY

MODEL NO. 3.4 T 85-6

DESCRIPTION: 85 Tube, .430" I.D., Equal Size and Length, L_{ti}/D_t = 1.74

DATE: 11/21/69 AR_d = 3.19

SCALE MODEL A_8 = .0857 ft^2

FULL SCALE A_8 = 5.485 ft^2

SCALE FACTOR = 8:1

- o DATA INCLUDES GROUND REFLECTION INTERFERENCE
- o ANGLE REFERENCED TO JET EXHAUST

	TEST CONDITIONS				ACOUSTIC TEST RESULTS						
			IDEAL			320' ARC		300' SIDELINE		1500' SIDELINE	
RDG NO.	P_{T8}/P_o	T_{T8} (°R)	V_j (ft/sec)	W_8 (PPS)	10 log ρA	PEAK PNdB	PEAK ANGLE	PEAK PNdB	PEAK ANGLE	PEAK PNdB	PEAK ANGLE
1	1.45	1181	1196	3.41	-6.8	114.3	30	111.8	60	93.9	60
2	1.58	1521	1499	3.54	-7.9	117.5	60	116.5	60	98.6	60
4	1.77	1526	1673	3.95	-7.9	119.9	30	118.1	60/90	100.4	90
5	2.02	1553	1857	4.41	-7.8	121.3	30	119.8	60	101.9	60
6	2.02	2138	2178	3.79	-9.2	123.4	50	122.1	60	104.4	60
7	2.30	1581	2027	4.99	-7.7	123.1	30/40	121.7	60	103.5	60
8	2.49	1667	2167	5.19	-7.7	123.8	40	121.2	50/60	103.7	60
9	2.53	2137	2473	4.59	-8.8	125.0	50	123.1	60	105.7	60
10	2.71	1781	2332	5.39	-7.8	126.2	30	124.0	60	106.5	60
11	2.93	2159	2654	5.19	-8.5	128.0	30	125.1	60	107.8	60
12	3.14	2215	2766	5.52	-8.4	128.6	30	126.0	50	109.4	50
13	3.23	2441	2932	5.39	-8.8	129.2	30	126.5	50	110.2	50
14	3.24	2609	3036	5.17	-9.0	129.4	30	126.5	50	110.5	50
15	3.41	2690	3139	5.47	-9.0	130.1	40	127.4	50	111.5	50
16	3.42	2107	2782	6.01	-8.0	129.1	30	126.1	50	109.4	50

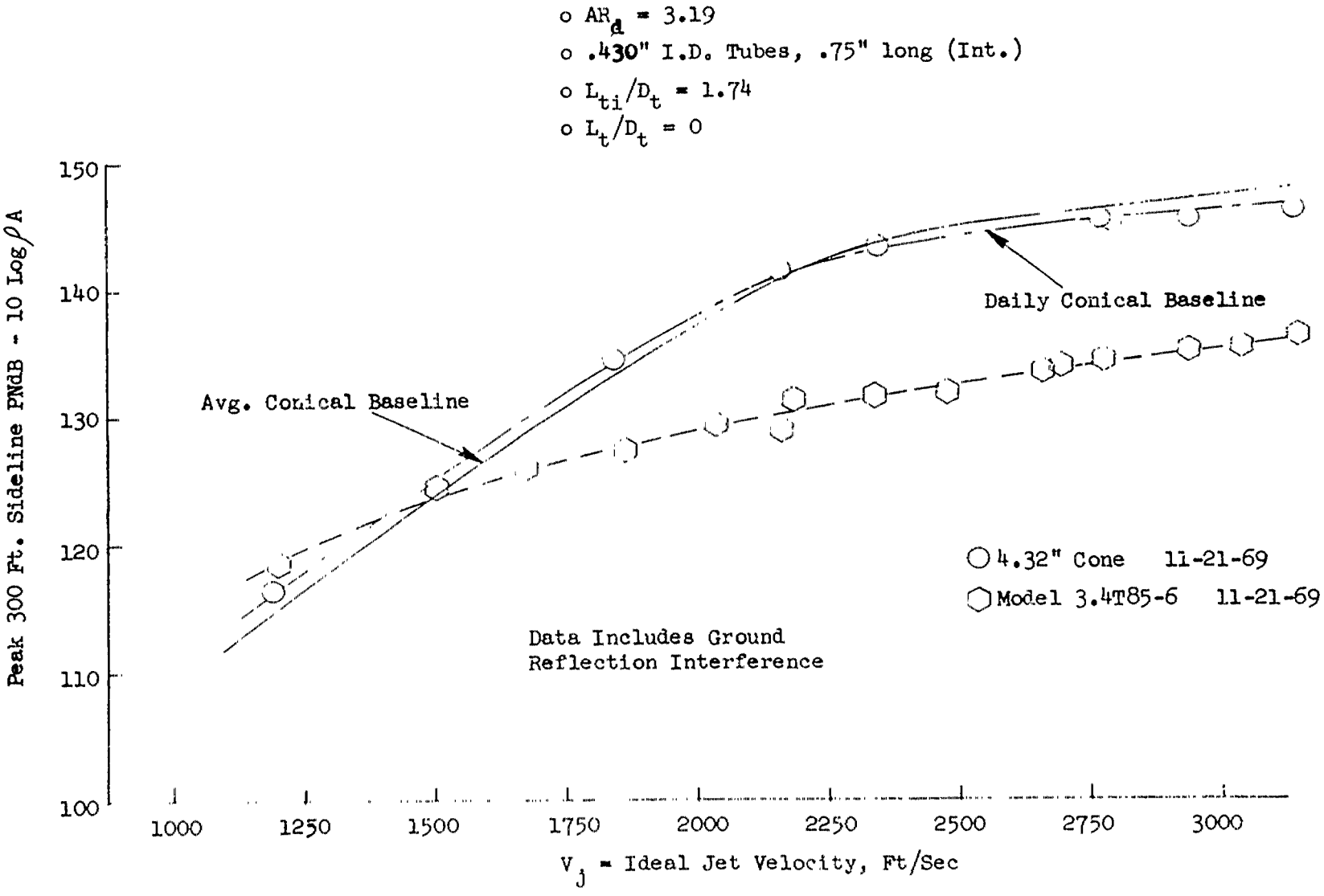

FIGURE V.F.5-17 300 FT. SIDELINE JET NOISE LEVELS FOR AN 85 TUBE NOZZLE, L_{ti}/D_t = 1.74

- o AR_d = 3.91
- o .430" I.D. Tubes, .75" Long (Int.)
- o L_{ti}/D_t = 1.74
- o L_t/D_t = 0

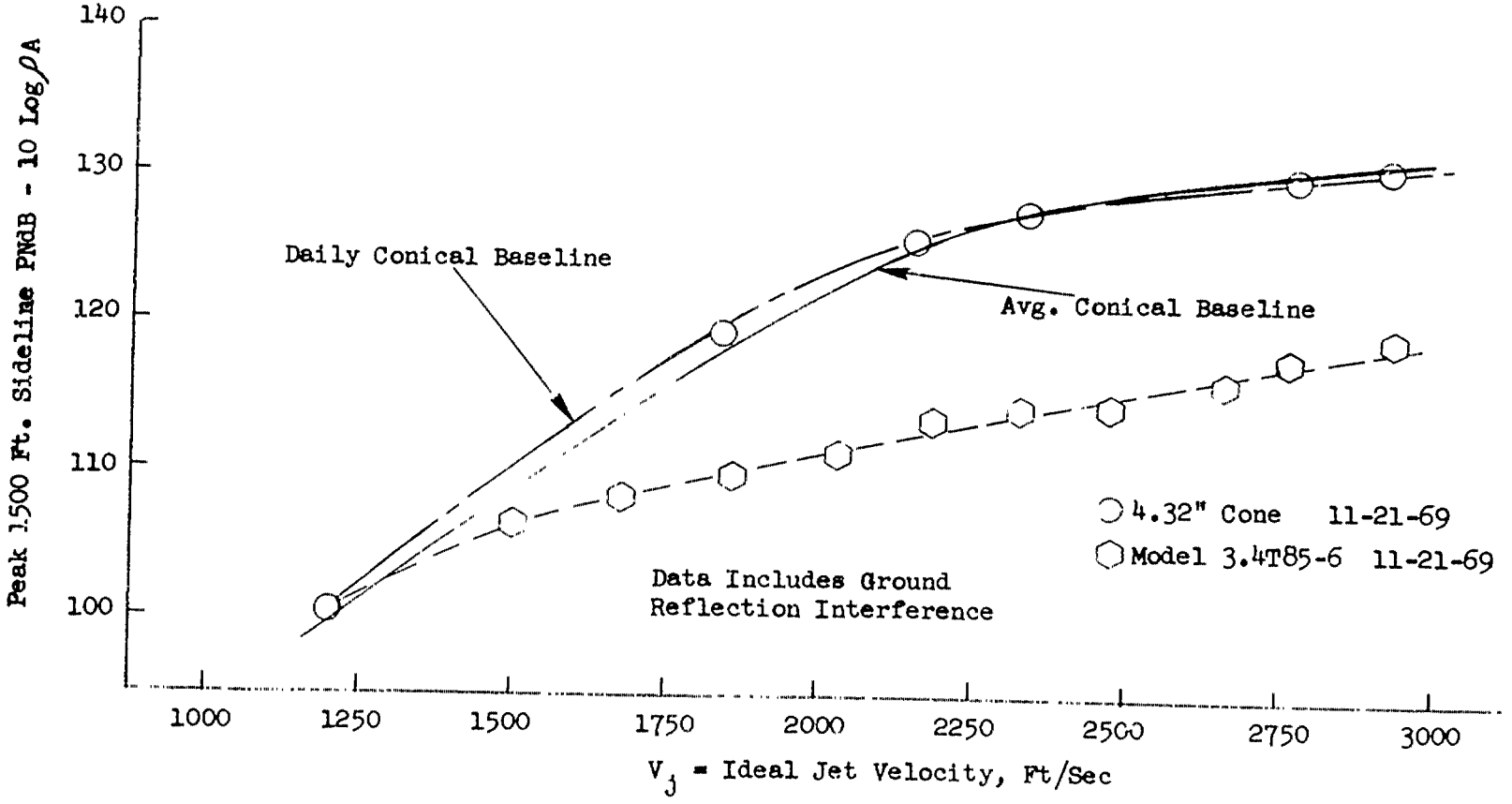

FIGURE V.F.5-18 1500 FT. SIDELINE JET NOISE LEVELS FOR AN 85 TUBE NOZZLE, L_{ti}/D_t = 1.74

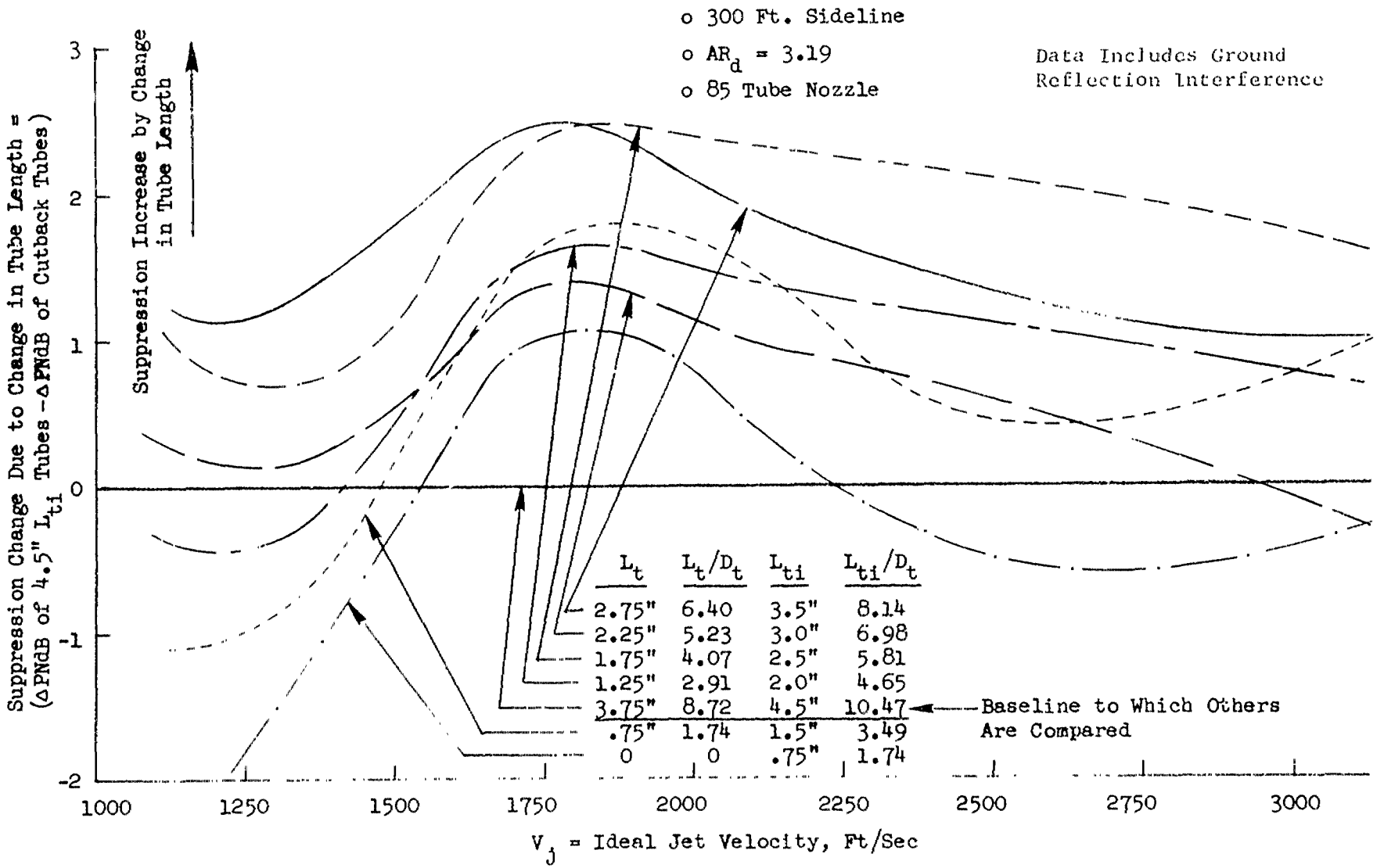

FIGURE V.F.5-19 EFFECT OF INTERNAL/EXTERNAL TUBE LENGTH TO TUBE INTERNAL DIAMETER RATIO ON PNL SUPPRESSION

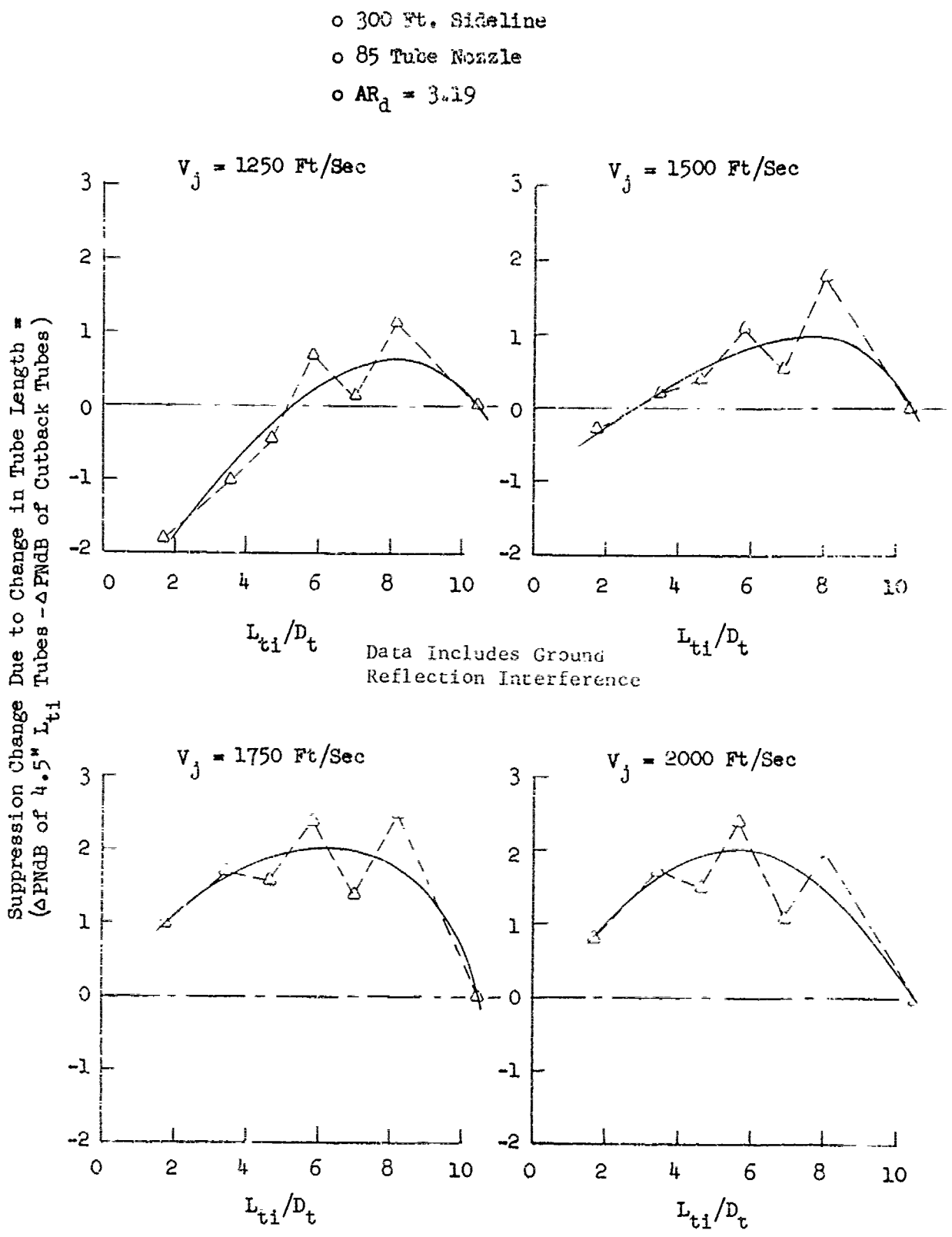

FIGURE V.F.5-20A EFFECT OF TUBE INTERNAL LENGTH TO TUBE INTERNAL DIAMETER, L_{ti}/D_t, ON PNL SUPPRESSIONS FOR DIFFERENT JET VELOCITIES

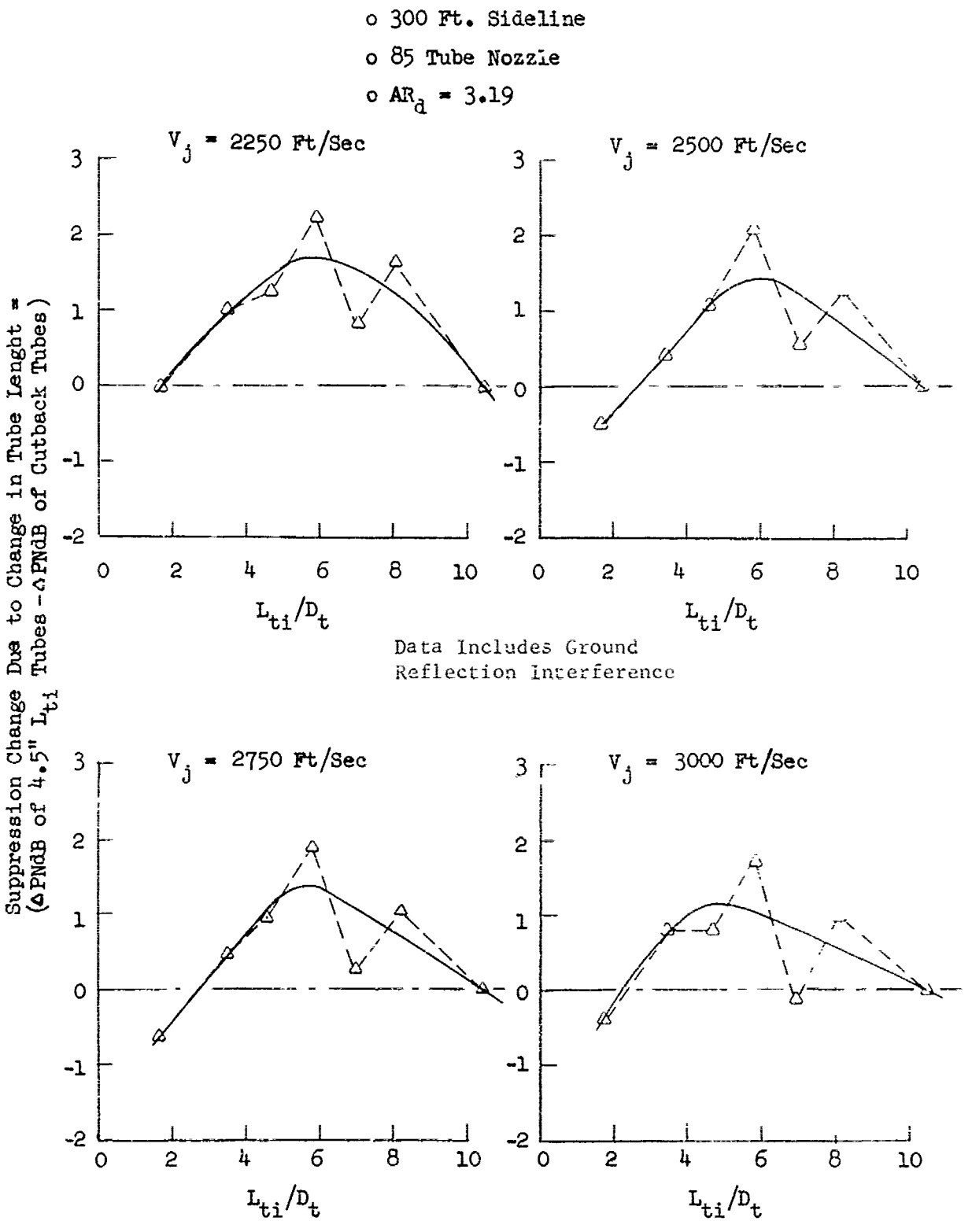

FIGURE V.F.5-20B EFFECT OF TUBE INTERNAL LENGTH TO TUBE INTERNAL DIAMETER, L_{ti}/D_t, ON PNL SUPPRESSIONS FOR DIFFERENT JET VELOCITIES

$P_{T8}/P_0 \approx 1.44$
$T_{T8} \approx 1140^{\circ}R$
$V_j \approx 1170$ Ft/Sec

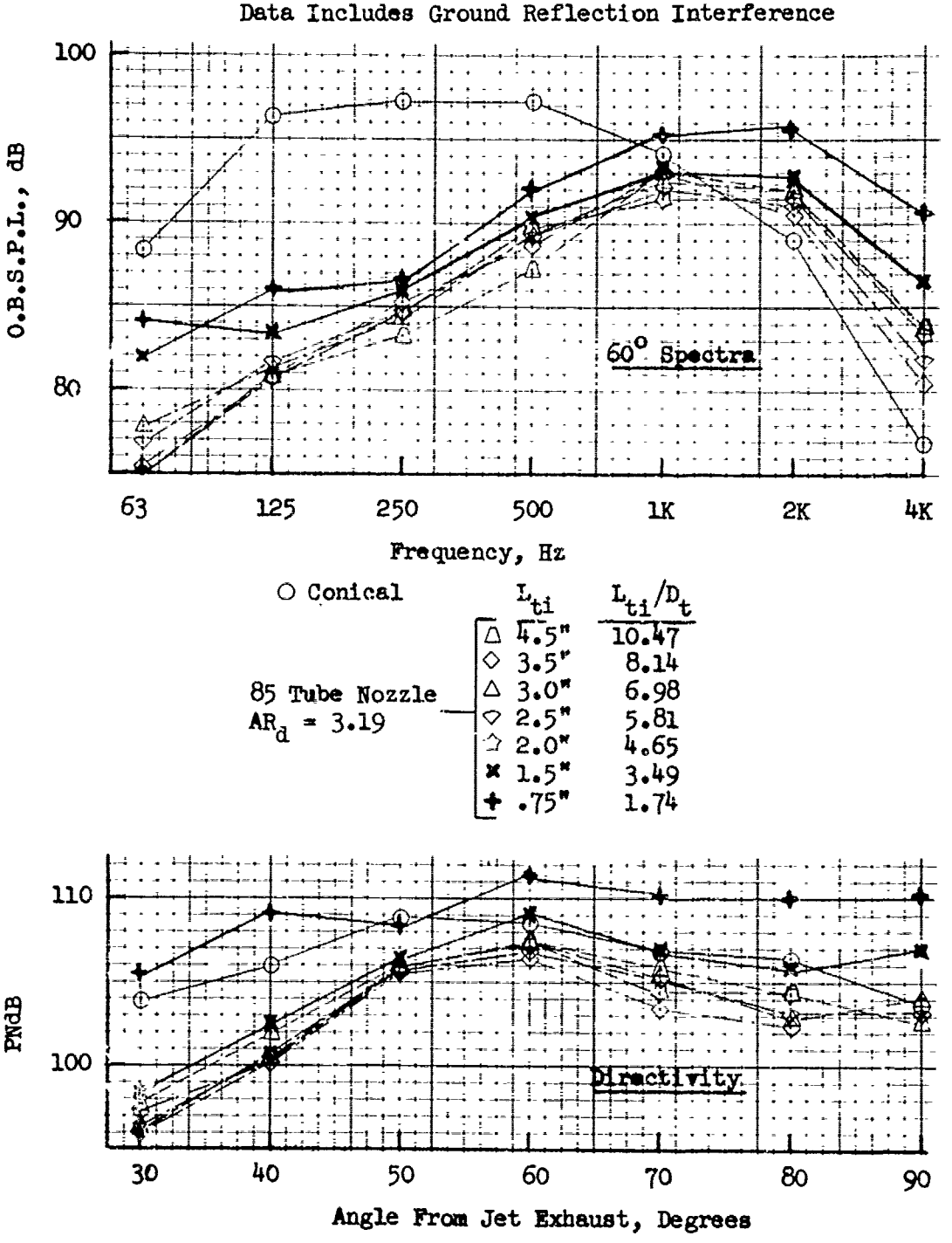

FIGURE V.F.5-21A EFFECT OF TUBE LENGTH TO TUBE DIAMETER RATIO ON 300 FT. SIDELINE SPECTRA AND DIRECTIVITY

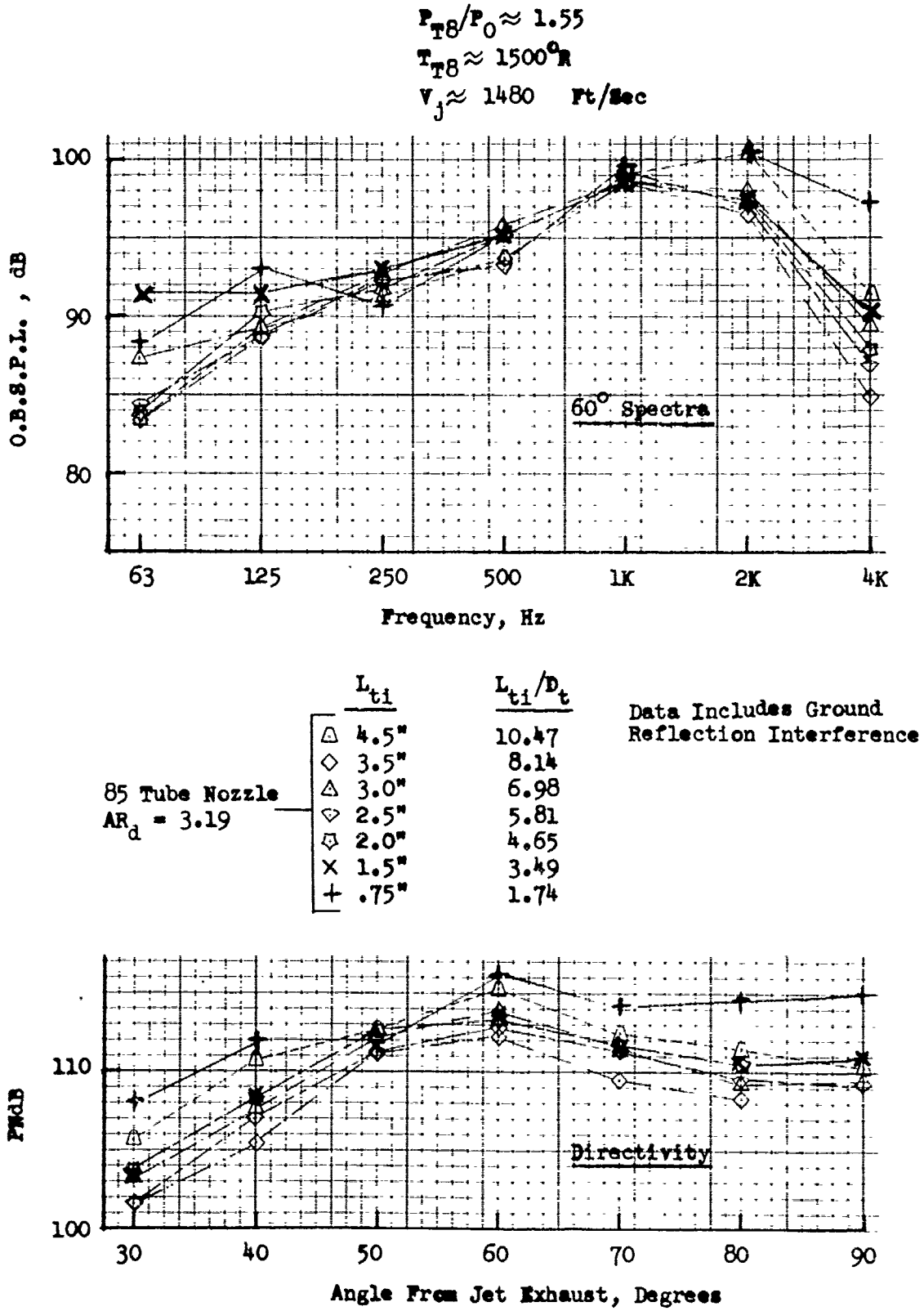

FIGURE V.F.5-21B EFFECT OF TUBE LENGTH TO TUBE DIAMETER RATIO ON 300 FT. SIDELINE SPECTRA AND DIRECTIVITY

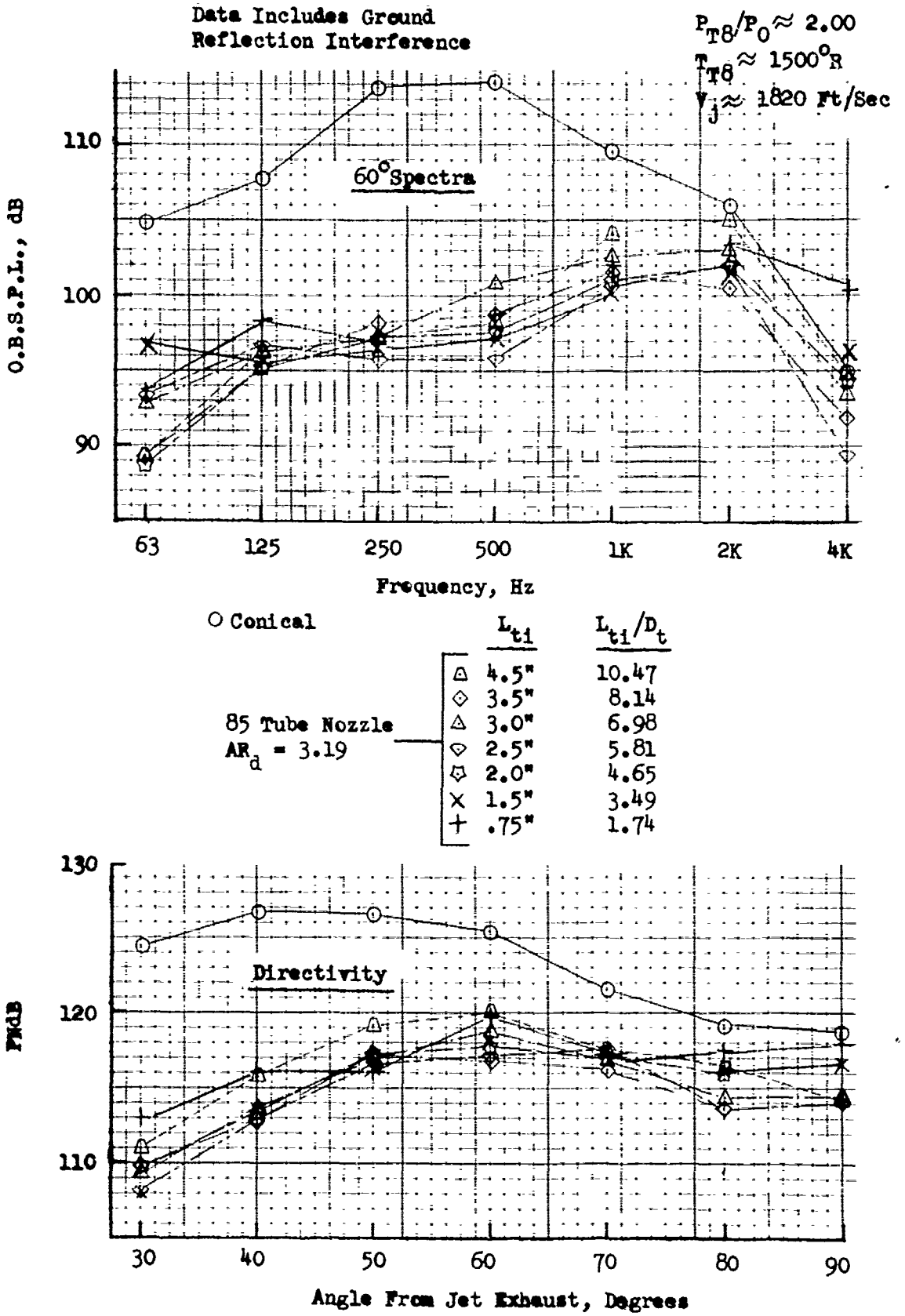

FIGURE V.F.5-21C EFFECT OF TUBE LENGTH TO TUBE DIAMETER RATIO ON 300 FT. SIDELINE SPECTRA AND DIRECTIVITY

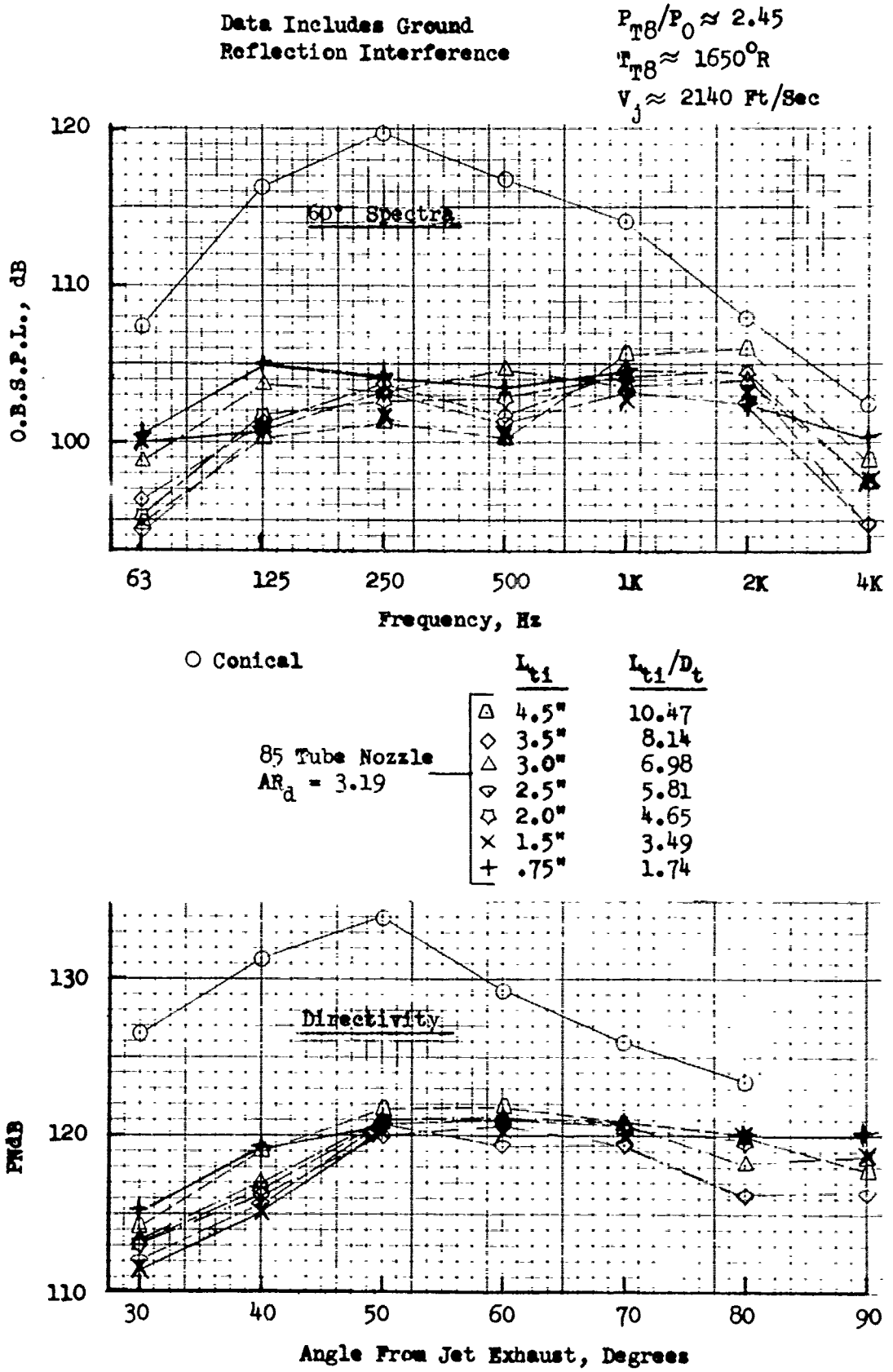

FIGURE V.F.5-21D EFFECT OF TUBE LENGTH TO TUBE DIAMETER RATIO ON 300 FT. SIDELINE SPECTRA AND DIRECTIVITY

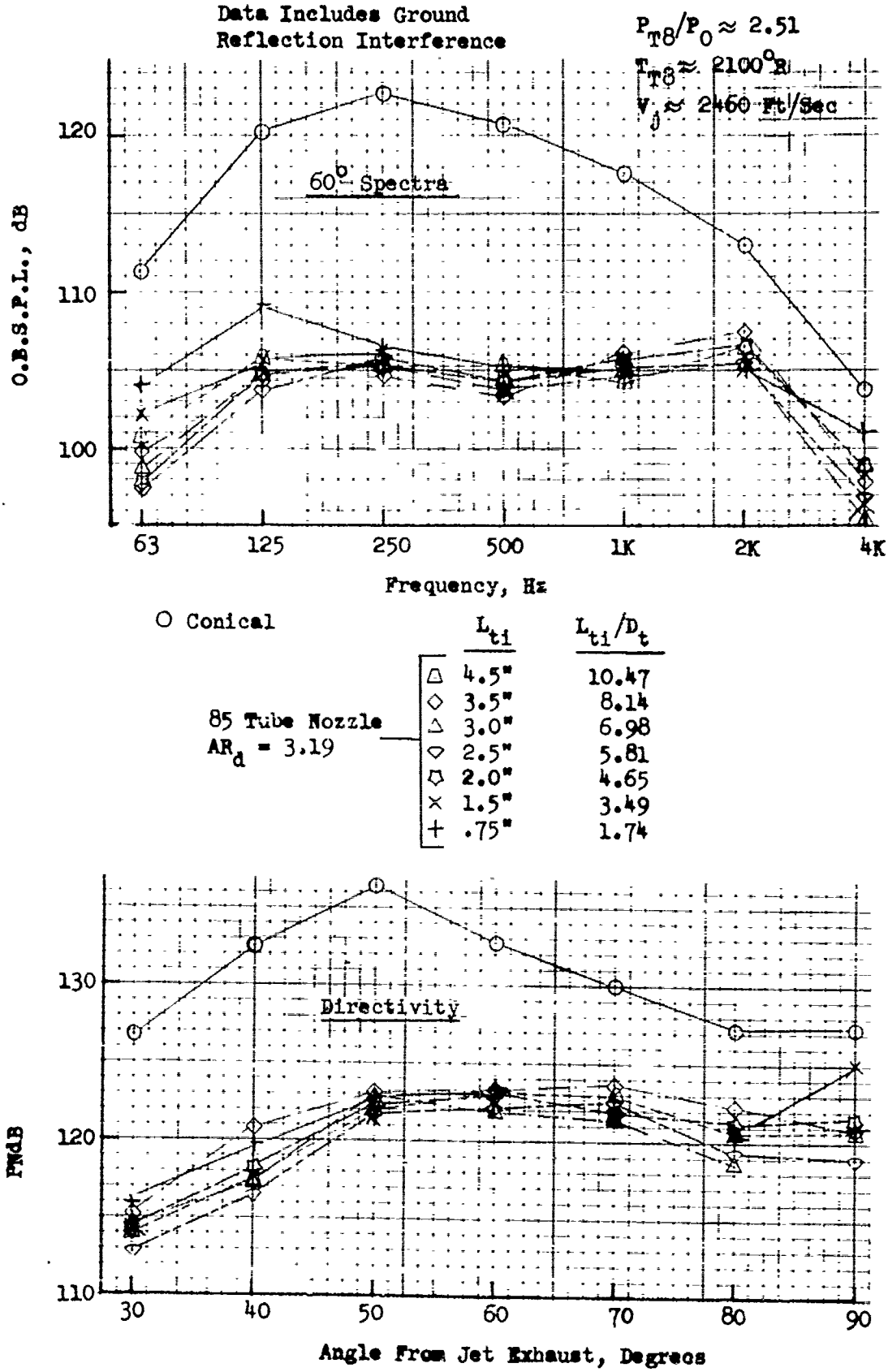

FIGURE V.F.5-21E EFFECT OF TUBE LENGTH TO TUBE DIAMETER RATIO ON 300 FT. SIDELINE SPECTRA AND DIRECTIVITY

$P_{T8}/P_0 \approx 3.12$
$T_{T8} \approx 2200^{\circ}R$
$V_j \approx 2750$ Ft/Sec

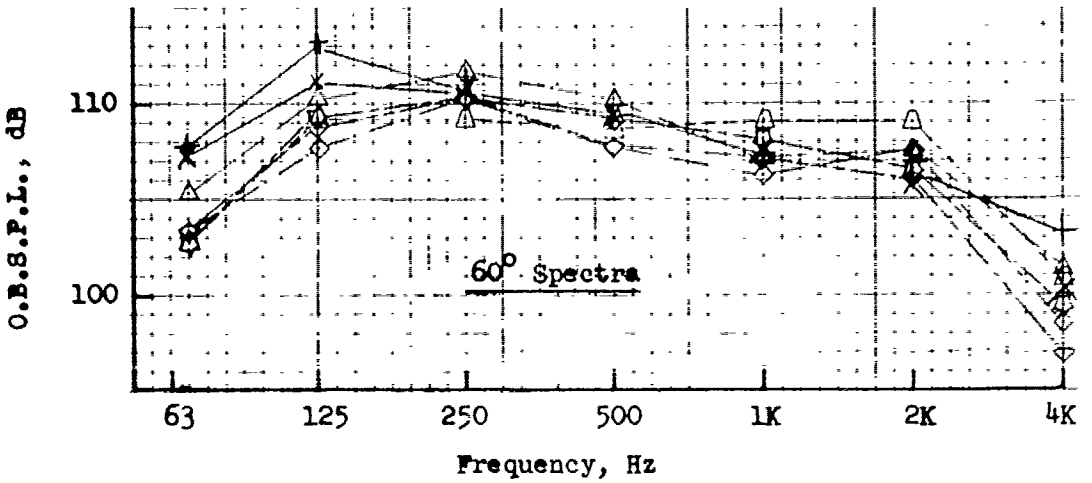

○ Conical

85 Tube Nozzle
AR_d = 3.19

	L_{ti}	L_{ti}/D_t
△	4.5"	10.47
◇	3.5"	8.14
△	3.0"	6.98
◇	2.5"	5.81
◇	2.0"	4.65
×	1.5"	3.49
+	.75"	1.74

Data Includes Ground Reflection Interference

Directivity

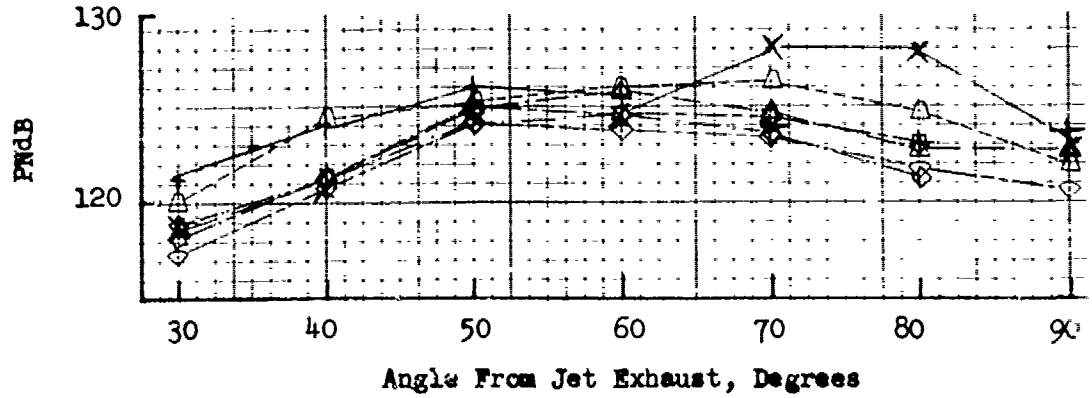

FIGURE V.F.5-21F EFFECT OF TUBE LENGTH TO TUBE DIAMETER RATIO ON 300 FT. SIDELINE SPECTRA AND DIRECTIVITY

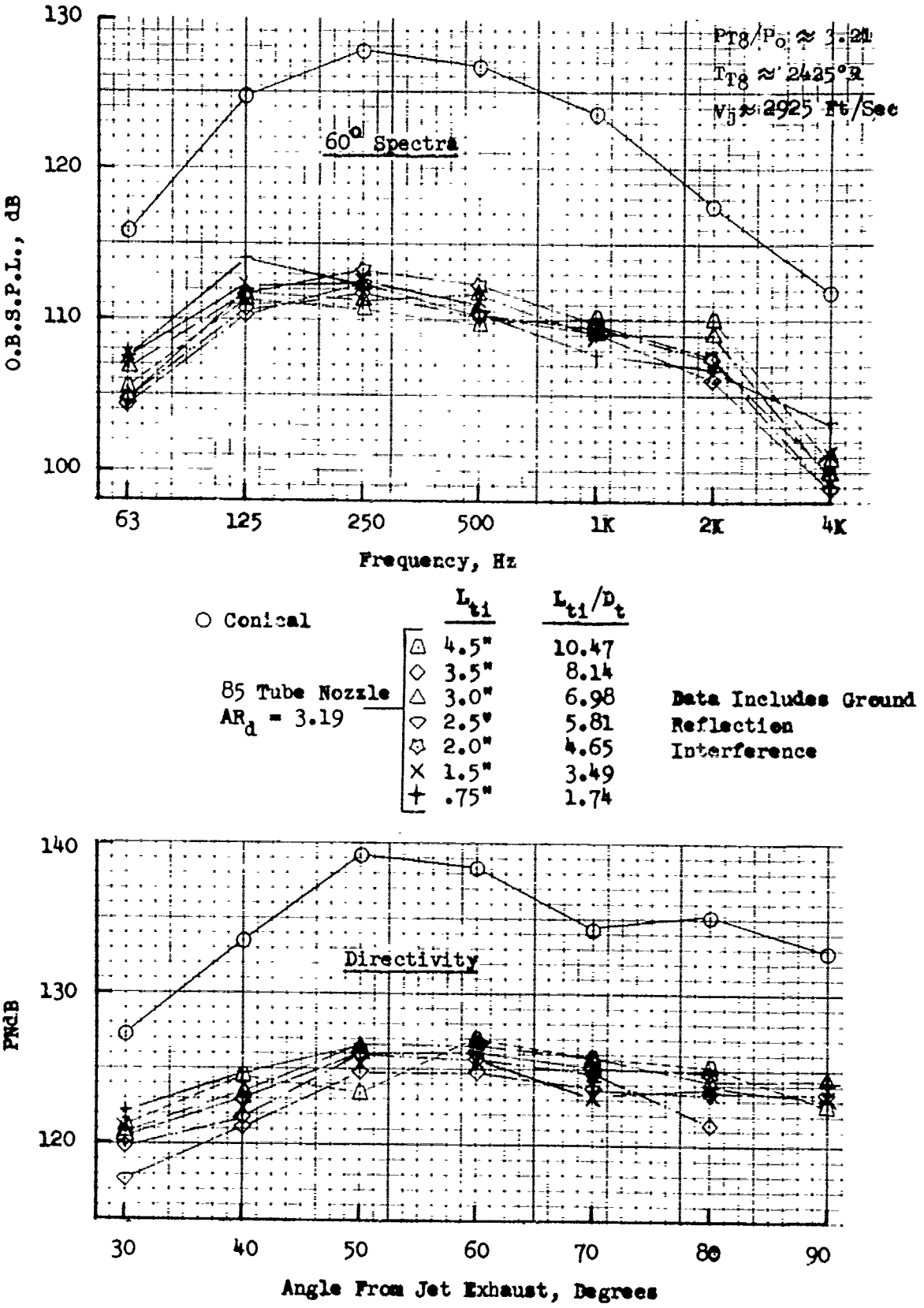

FIGURE V.F.5-21G EFFECT OF TUBE LENGTH TO TUBE DIAMETER RATIO ON 300 FT. SIDELINE SPECTRA AND DIRECTIVITY

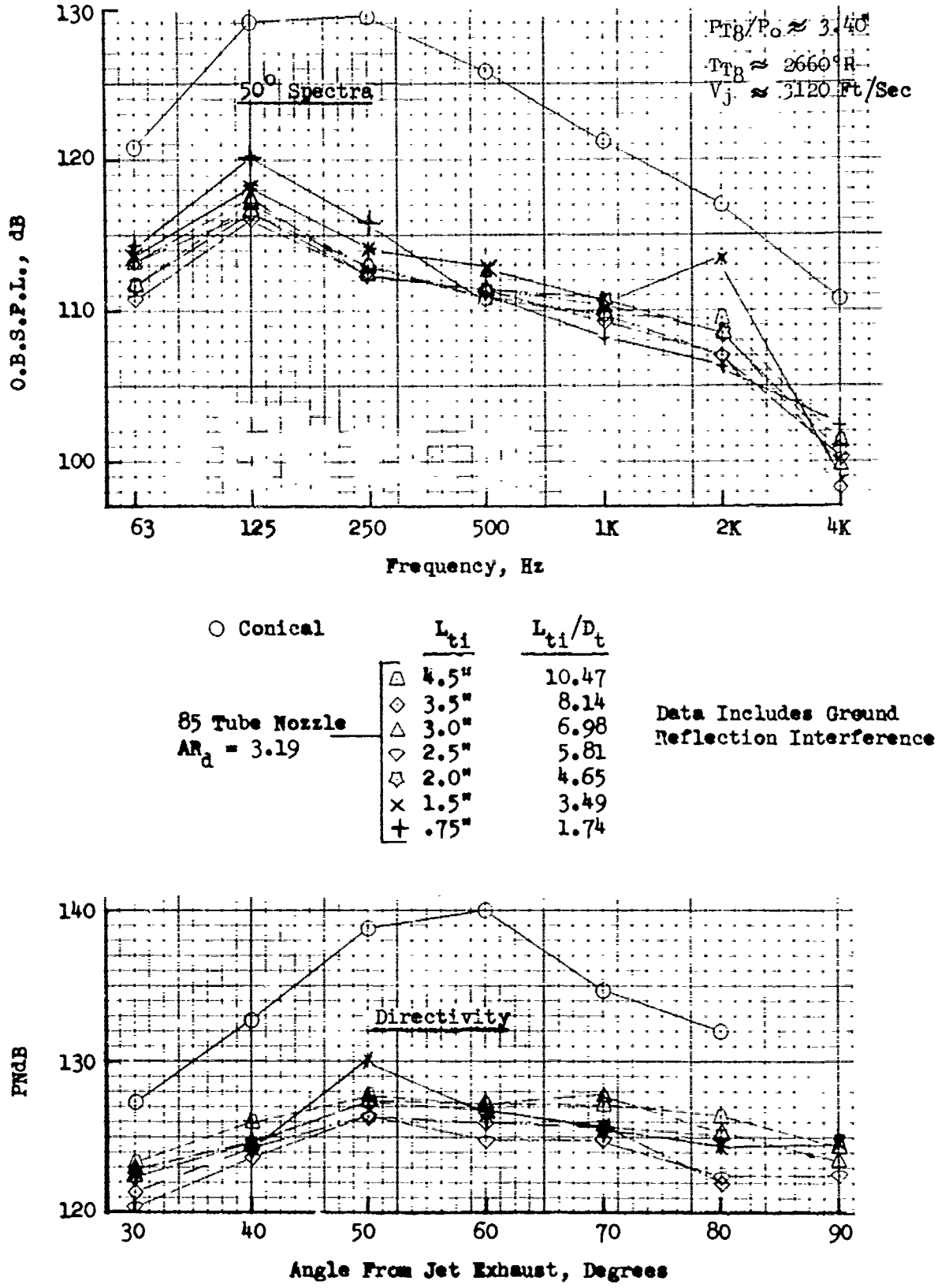

FIGURE V.F.5-21H EFFECT OF TUBE LENGTH TO TUBE DIAMETER RATIO ON 300 FT. SIDELINE SPECTRA AND DIRECTIVITY

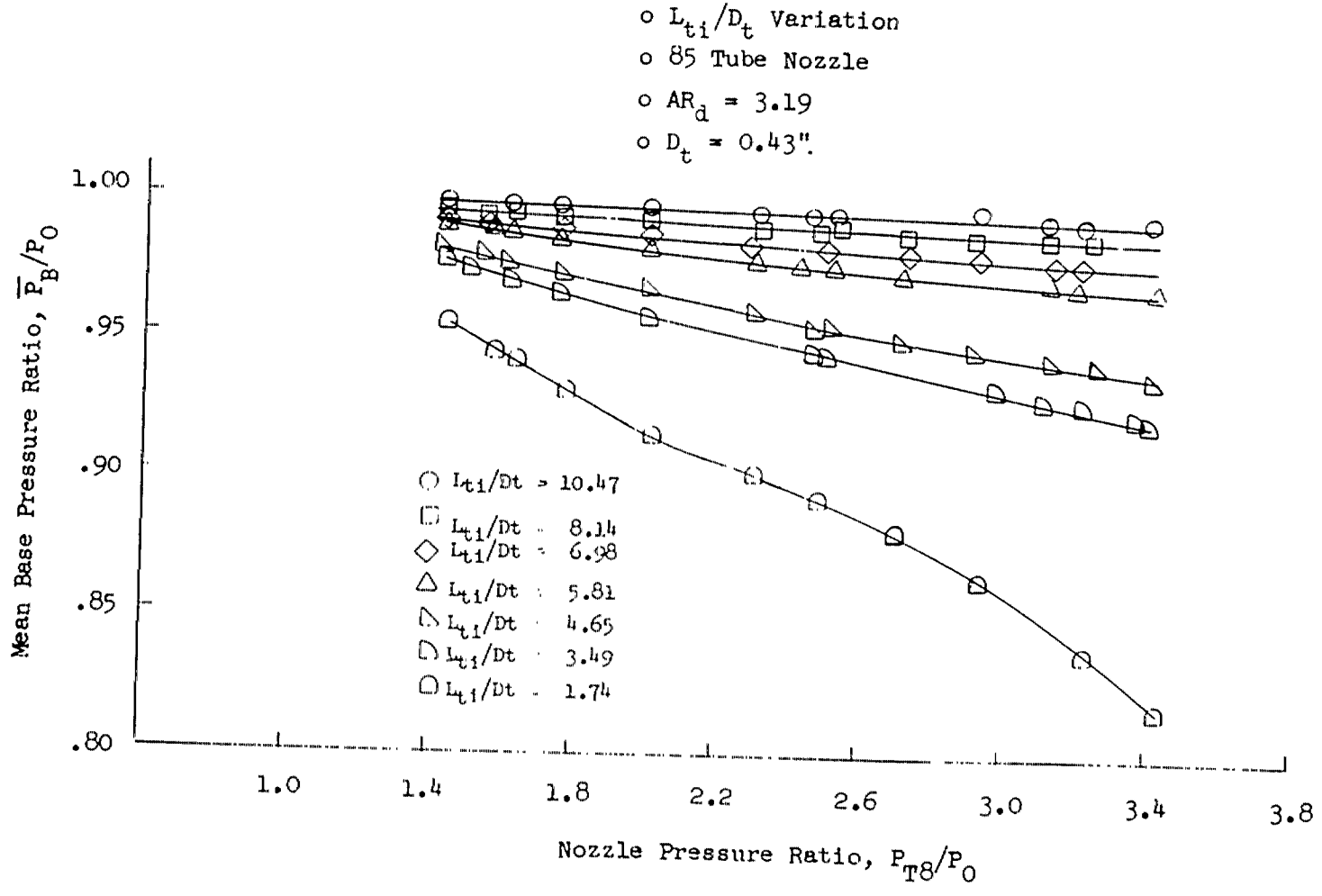

FIGURE V.F.5-22 EFFECT OF TUBE LENGTH TO TUBE DIAMETER RATIO ON MEAN BASEPLATE PRESSURE RATIO

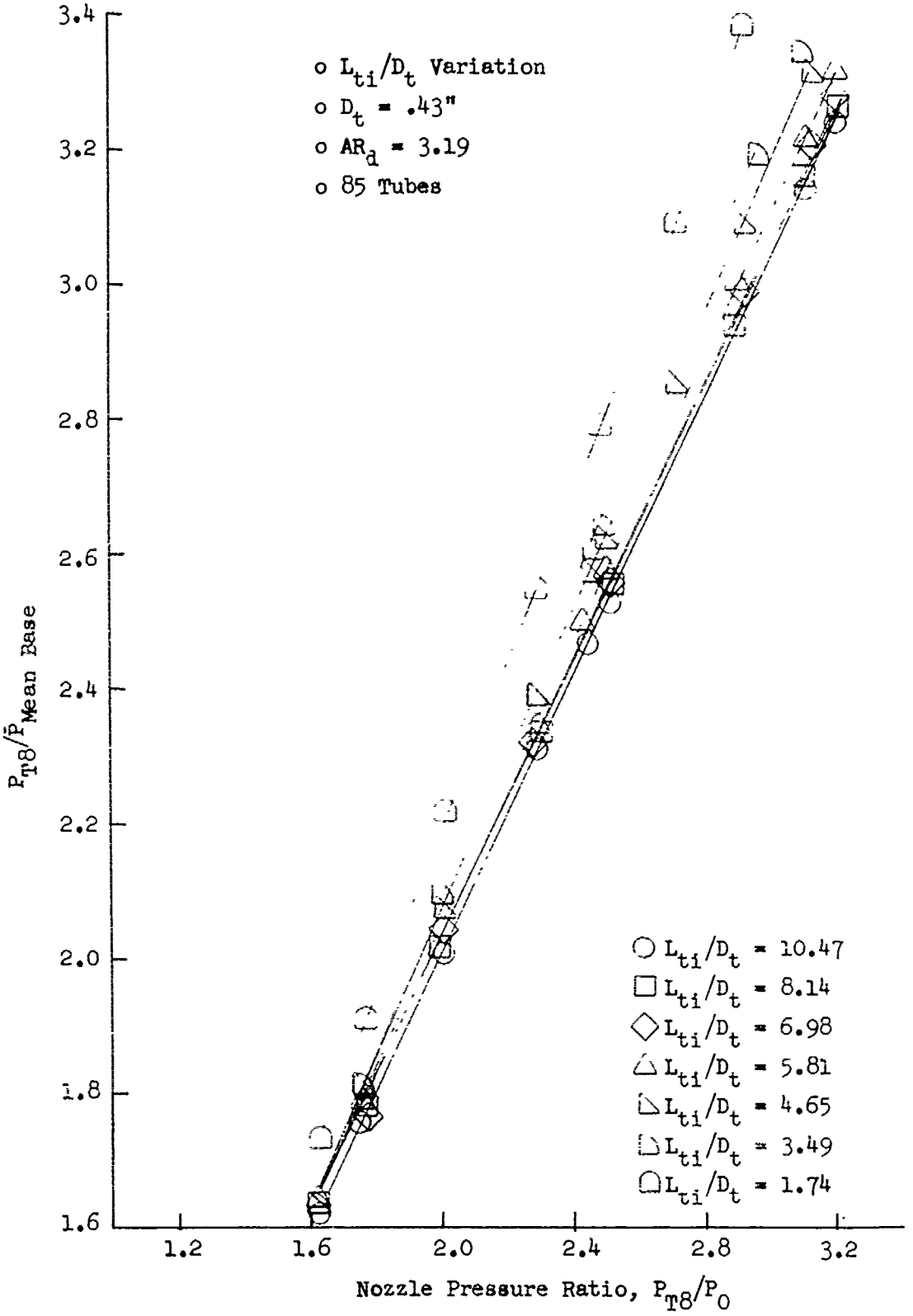

FIGURE V.F.5-23 EFFECT OF TUBE LENGTH TO TUBE DIAMETER RATIO ON NOZZLE EXIT TO MEAN BASEPLATE PRESSURE RATIO

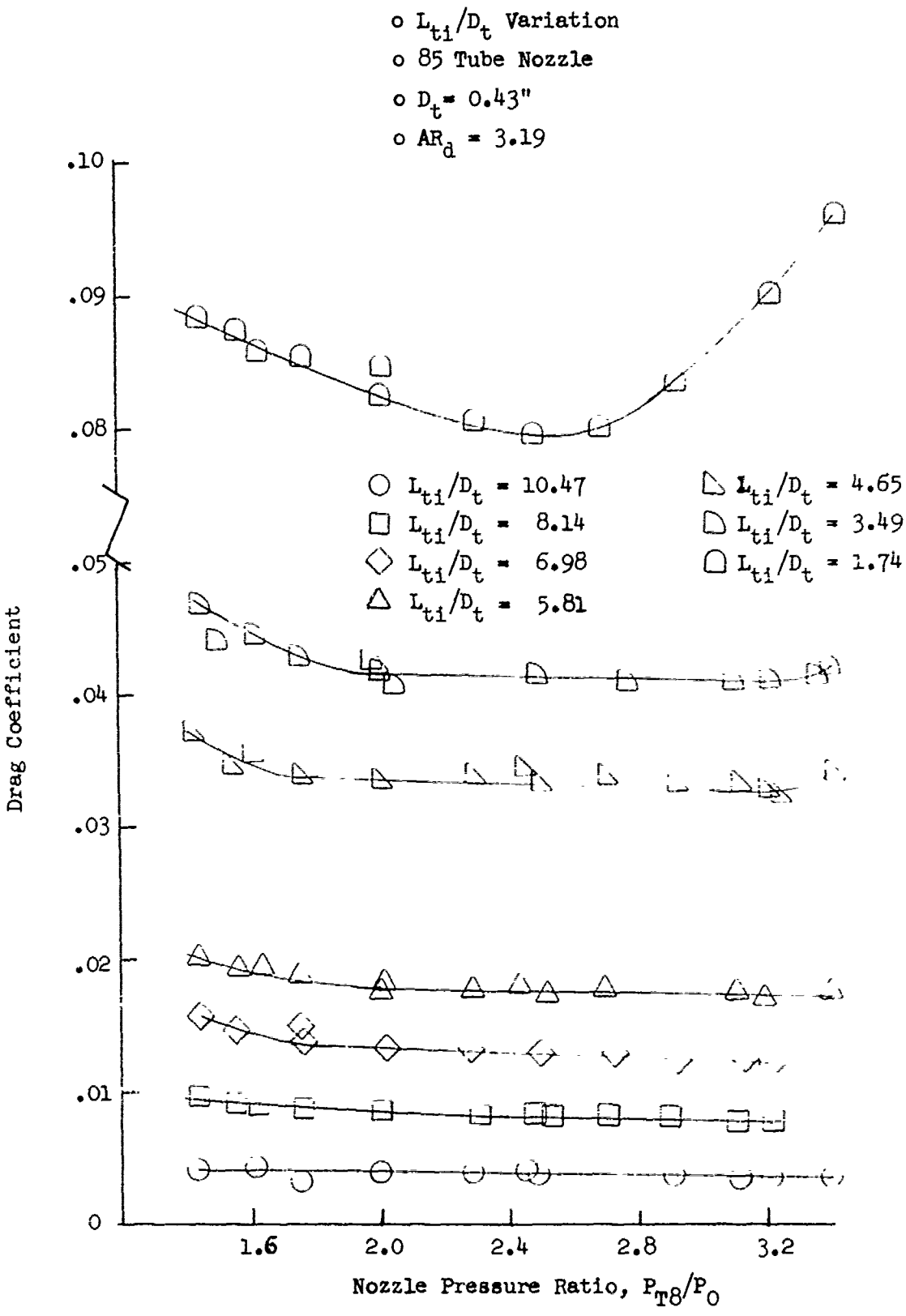

FIGURE V.F.5-24 EFFECT OF TUBE LENGTH TO TUBE DIAMETER RATIO ON BASEPLATE DRAG COEFFICIENT

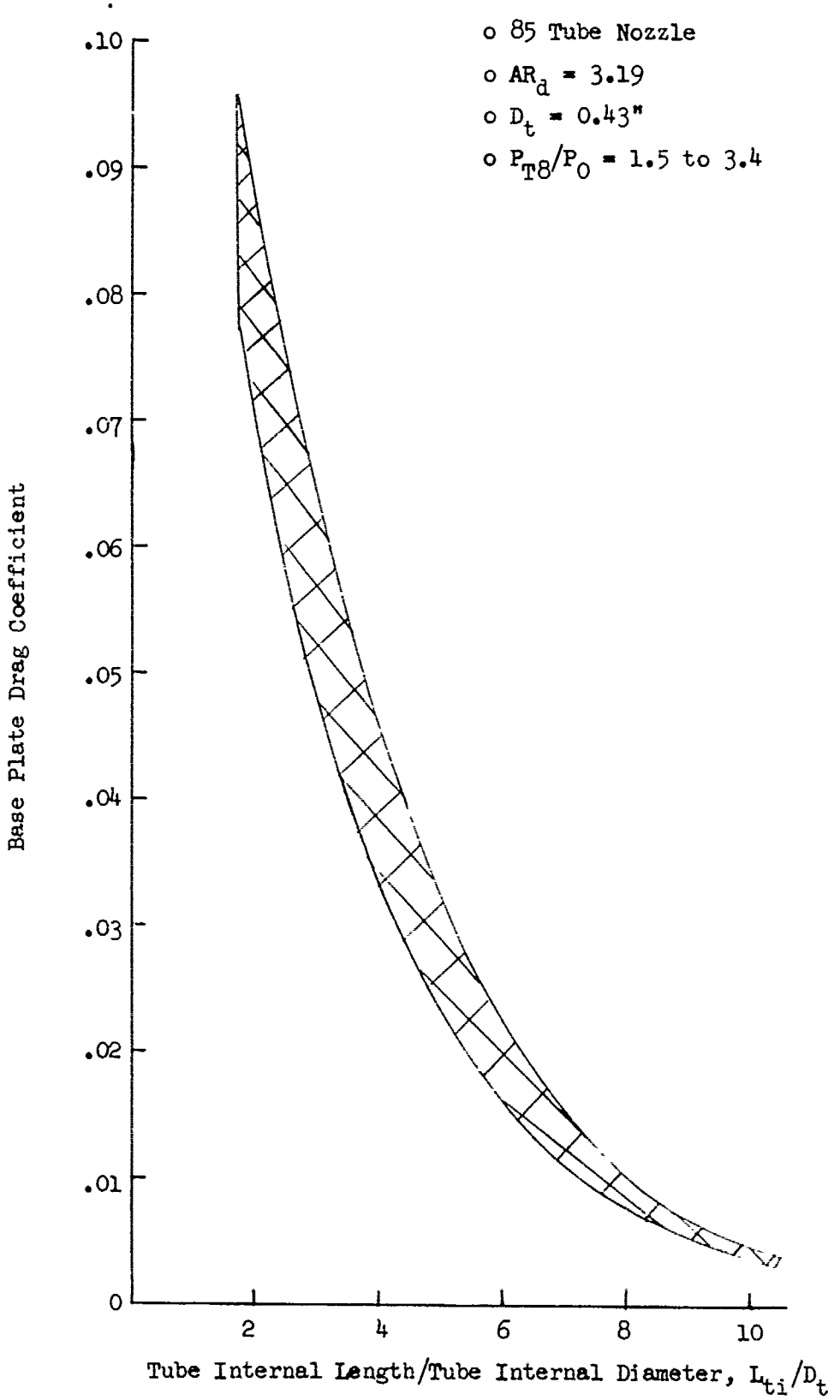

FIGURE V.F.5-25 BASEPLATE DRAG COEFFICIENT AS A FUNCTION OF TUBE INTERNAL LENGTH TO TUBE INTERNAL DIAMETER RATIO

V.F.6 HOLE SHAPE, EQUAL AND UNEQUAL HOLE SIZE AND SPACING STUDIES ON 97 HOLE PLATES

PRECEDING PAGE BLANK-NOT FILMED

V.F.6 HOLE SHAPE, EQUAL AND UNEQUAL HOLE SIZE AND SPACING STUDIES ON 97 HOLE PLATES

Objectives of Test Series

The purpose of this series of tests was to evaluate the suppression effects of hole shape, equal and unequal hole size, and uniform vs. random spacing. The tests were conducted in two phases. Phase I compared trapezoidal and circular hole patterns. Phase II compared equal and unequal hole size plus uniform and random spacing patterns.

Acoustic measurements were taken on a 40 ft. arc and scaled by frequency and size to full scale application using a scale factor of 3:1. All data presented are therefore of simulated engine size and engine frequency range.

Test conditions covered a range of nozzle pressure ratios from 1.4 to 4.0, and temperatures from 1200 to 2600° R, which yielded ideal jet velocities from 1100 to 3100 ft/sec.

Phase I Test Configurations

Two equal flow area 97 hole flat baseplate models were tested in Phase I of this series. The first model (4.26SH97) had 96 trapezoidal shaped holes plus a Greatrex center. The second model (4.2H97-1) had 96 circular holes plus the common Greatrex center pattern. Each configuration was designed for area ratio of 2.0 and was to simulate a tube or hole pattern on a full scale retractable suppressor utilizing 16 flaps of unequal lengths. In the suppressed mode the unequal flap lengths created the center hole Greatrex pattern. Figure V.F.6-1 shows a comparative schematic and photo of the 97 trapezoidal hole plate and its equal area counterpart, the 97 circular hole plate.

Both configurations were tested at JENOTS to substantiate their acoustic performance. The trapezoidal hole/tube design in simulating a full scale 16 flap nozzle system was believed would perform better acoustically for several reasons: a) It would allow a straighter, smoother flowpath in the simulated flap edge region through which more ambient air could be pumped to a deeper penetration into the core of the hot jet; b) Trapezoidal holes increase the peripheral flow area for the same total flow area (15% more than for the

PRECEDING PAGE BLANK-NOT FILMED

circular holes on this model) and allow for quicker and more complete mixing of the ambient air with the high temperature jet. The increased flow rate and improved mixing could possibly reduce the noise generation potential of the jet stream.

Acoustic comparisons were made with a baseline 4.32" I.D. conical nozzle for both Phases I and II.

Presentation of Phase I Test Results

Phase I results are found in Figures V.F.6-2 through V.F.6-7D with individual model test summaries (listing the data scaled to engine size) included in Tables V.F.6-2 and -3 show 300 ft. and 1500 ft. sideline normalized peak jet noise levels for the trapezoidal plate. Similar data are illustrated in Figures V.F.6-4 and -5 for the circular hole plate.

Figure V.F.6-6 is a comparison of the 300 ft. and 1500 ft. sideline peak PNL suppression levels attained by the two nozzles. Trapezoidal hole suppression was only slightly greater in the intermediate and low jet velocity region, 1/2 to 1 dB greater at peak suppression and then identical to the circular hole plate above 2500 ft/sec.

A comparison of spectra and directivity for a series of engine running line test points from P_{T8}/P_o of 1.6 through 3.2 are shown on Figures V.F.6-7A through -7D; spectra, the upper plot on each figure, and directivity, the lower plot. The four figures show a random crossover of data for both spectra and directivity, indicating no pattern of preferential suppression for either. Location of peak noise angle and the typical spectra shape and change in spectra shape with increasing P_{T8}/P_o for a circular hole/tube nozzle are retained by the trapezoidal hole nozzle.

Phase II Test Configurations

Three 97 hole flat baseplate models were tested in Phase II of the test series. Figure V.F.6-8 is a schematic of the 97 hole baseplate configurations showing equal and unequal circular hole sizes and spacing patterns. The first model (Model 4.88H121-97) had equal hole size (0.444" I.D.) and uniform spacing. The second (4.2H97) and third (4.39H97) models employed different

hole patterns of unequal size and non-uniform spacings. All three models had equal area ratios, $AR_d = 2.0$.

Presentation of Phase II Test Results

Test summaries showing acoustic data scaled to engine size for the individual models are presented in Tables V.F.6-3, -4, and -5. Peak 300 ft. and 1500 ft. sideline jet noise levels and PNL suppressions are found in Figures V.F.6-9 through V.F.6-17. The effect of hole size and spacing on PNL suppressions is shown in Figure V.F.6-18 for both sizeline distances. The equal hole size and spacing configuration gave 2 to 6 PNL greater suppression in the medium-to-high velocity range over the non-uniform configurations.

Conclusions

- Little difference (.5 - 1 dB) in suppression levels was observed between trapezoidal and circular hole patterns. The suppressions for trapezoidal shaped holes were greater in the low to mid-high V_j range, but fell below the circular holes in the high V_j region.
- Equality of hole/tube size and uniformity of spacing between tubes or holes appears to be a major parameter in refining a suppressor design. The more uniformly sized and spaced tube bundle produces significantly higher suppression than a randomly size and spaced array.

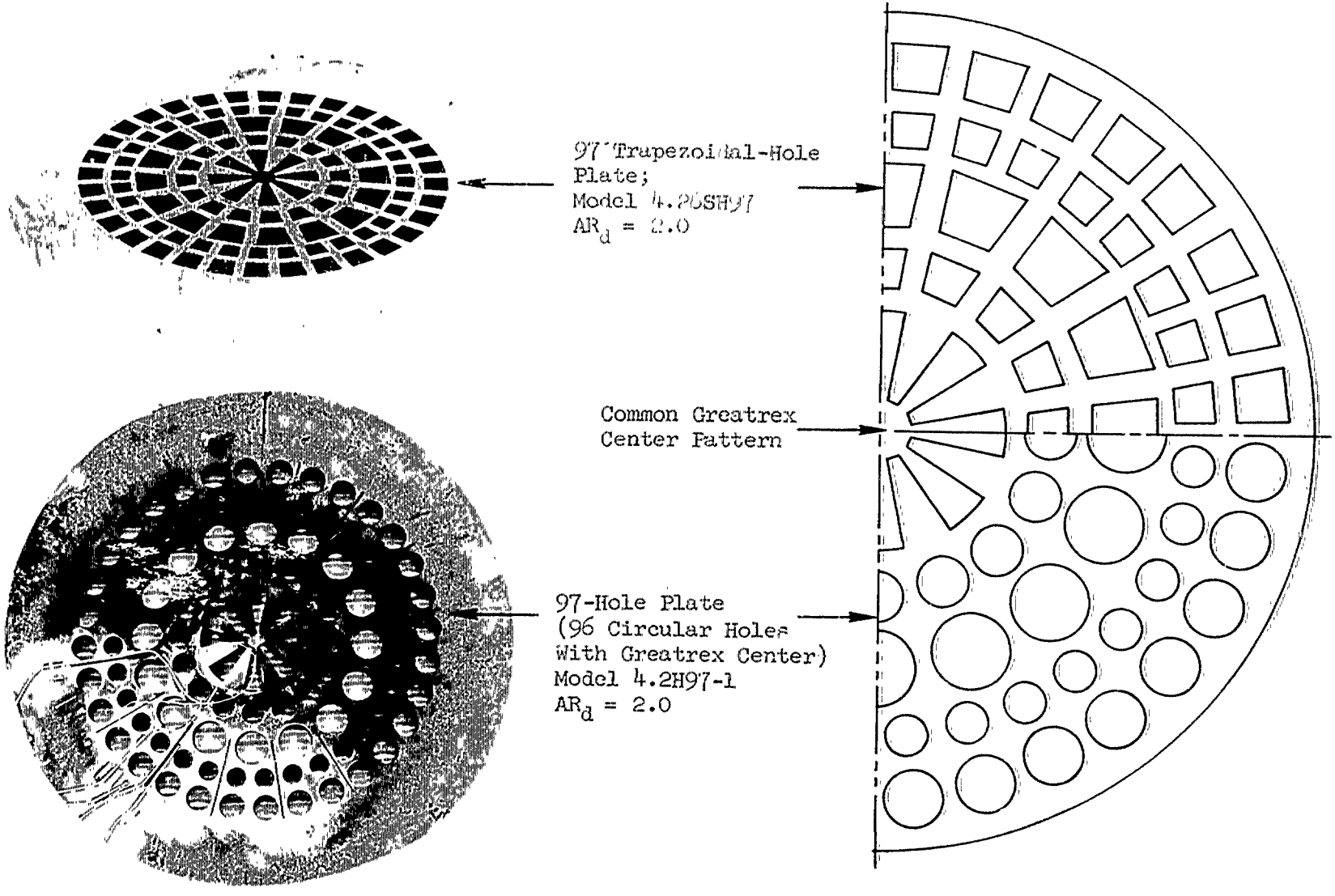

FIGURE V.F.6-1 HARDWARE AND SCHEMATIC OF 97 HOLE BASEPLATES WITH TRAPEZOIDAL AND CIRCULAR HOLE PATTERNS

TABLE V.F.6-1 TEST SUMMARY

MODEL NO. 4.26SH97

DESCRIPTION: 97 Trapezoidal Hole Plate with Greatrex Center

DATE: 5/12/69

SCALE MODEL A_8 = .0994 ft^2

FULL SCALE A_8 = 6.362 ft^2

SCALE FACTOR = 8:1

- o DATA INCLUDES GROUND REFLECTION INTERFERENCE
- o ANGLE REFERENCED TO JET EXHAUST

	TEST CONDITIONS				ACOUSTIC TEST RESULTS						
			IDEAL			320' ARC		300' SIDELINE		1500' SIDELINE	
RDG NO.	P_{T8}/P_o	T_{T8} (°R)	V_j (ft/sec)	W_8 (PPS)	10 log ρA	PEAK PNdB	PEAK ANGLE	PEAK PNdB	PEAK ANGLE	PEAK PNdB	PEAK ANGLE
1	1.44	1154	1173	3.88	-6.1	111.7	50	110.5	80	93.0	80
2	1.56	1524	1481	3.72	-7.3	115.2	40	114.2	60	96.5	60
3	1.65	1224	1410	4.50	-6.4	114.7	50	113.2	60	95.5	60
4	1.79	1492	1668	4.32	-7.2	118.4	50	116.0	50	98.5	60
5	2.00	1508	1827	4.86	-7.1	119.7	50	117.5	60	100.4	60
6	2.30	1572	2021	5.49	-7.0	122.9	30	120.0	60	103.0	60
7	2.46	1649	2144	5.71	-7.1	124.9	30	121.5	60	105.1	50
8	2.52	2104	2451	4.91	-8.1	129.4	30	125.3	50	109.6	50
9	2.73	1771	2332	6.01	-7.2	125.7	30	125.1	50	109.0	50
10	2.94	2126	2639	5.70	-7.8	132.7	40	128.6	40	113.3	40
11	3.11	2214	2752	5.87	-7.8	135.0	40	131.2	50	115.7	50
12	3.21	2456	2935	5.70	-8.2	135.7	50	133.5	50	117.8	50
13	3.22	2595	3019	5.57	-8.4	136.4	50	134.3	50	118.7	50
14	3.41	2677	3131	5.84	-8.4	137.7	50	135.5	50	119.7	50

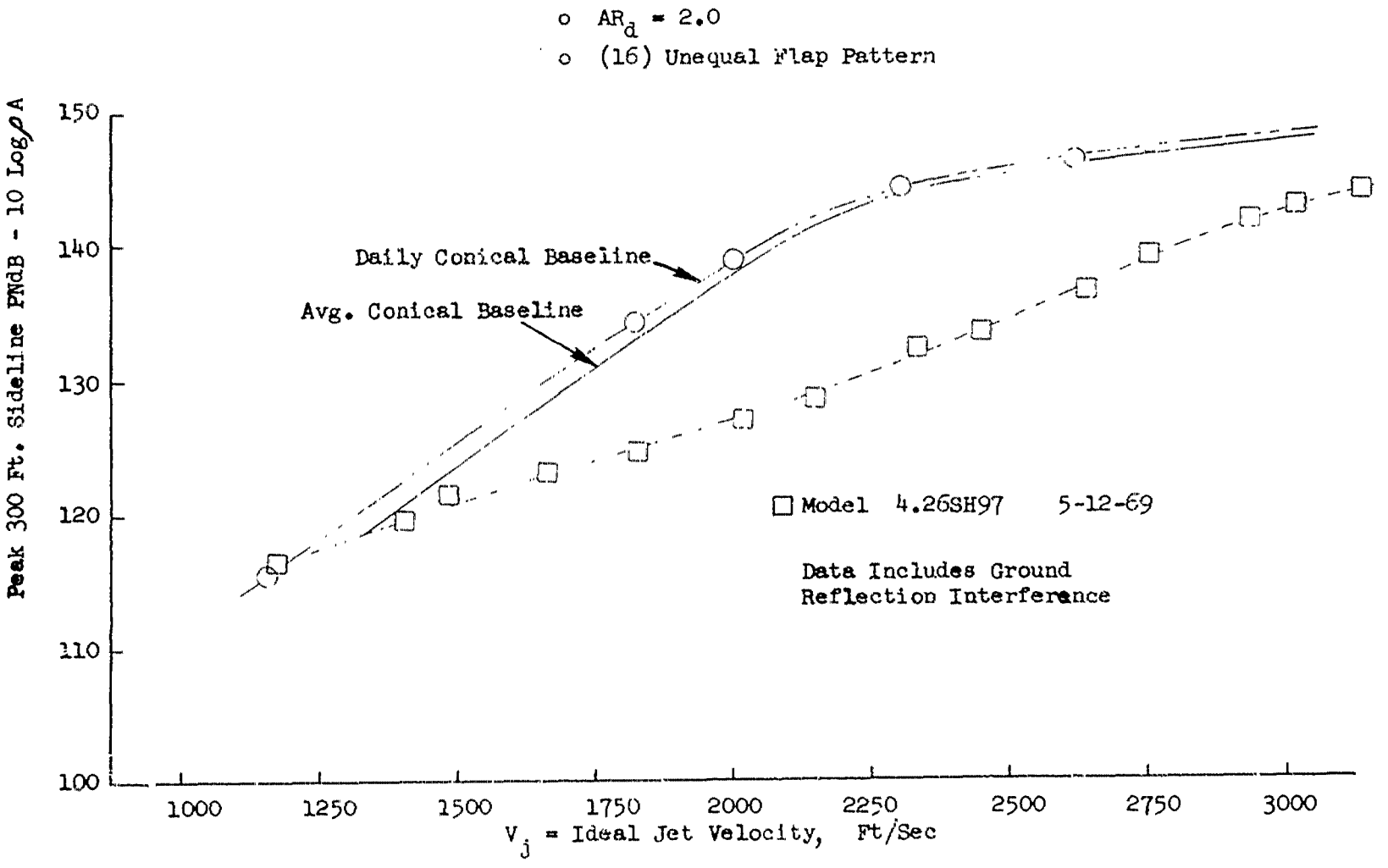

FIGURE V.F.6-2 300 FT. SIDELINE JET NOISE LEVELS FOR A 97 TRAPEZOIDAL HOLE PLATE WITH GREATREX CENTER

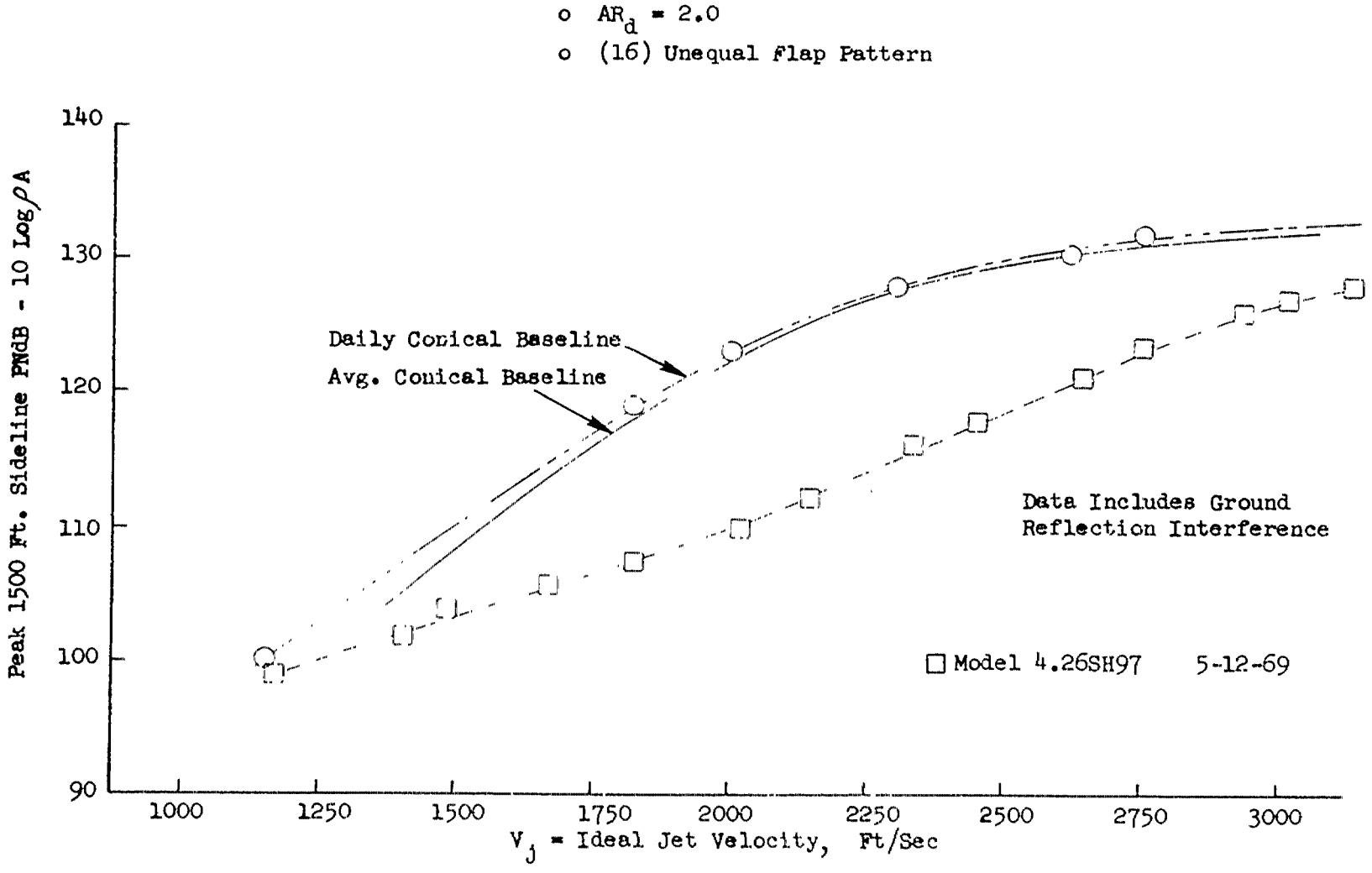

FIGURE V.F.6-3 1500 FT. SIDELINE JET NOISE LEVELS FOR A 97 TRAPEZOIDAL HOLE PLATE WITH GREATREX CENTER

TABLE V.F.6-2 TEST SUMMARY

MODEL NO. 4.2H97-1

DESCRIPTION: 97 Hole Plate with 96 Circular Holes of Various Size, Greatrex Center

DATE: 9/4/68

SCALE MODEL A_8 = .0994 ft^2

FULL SCALE A_8 = 6.362 ft^2

SCALE FACTOR = 8:1

- o DATA INCLUDES GROUND REFLECTION INTERFERENCE
- o ANGLE REFERENCED TO JET EXHAUST

	TEST CONDITIONS				ACOUSTIC TEST RESULTS						
			IDEAL			320' ARC		300' SIDELINE		1500' SIDELINE	
RDG NO.	P_{T8}/P_o	T_{T8} (°R)	V_j (ft/sec)	W_8 (PPS)	10 log ρA	PEAK PNdB	PEAK ANGLE	PEAK PNdB	PEAK ANGLE	PEAK PNdB	PEAK ANGLE
1	1.63	1300	1446	4.24	-7.3	115.5	40/50	113.1	50	94.9	70
2	2.45	1700	2173	5.59	-7.3	126.1	40	122.8	50	105.8	40/50
3	2.00	1500	1817	4.84	-7.1	121.0	40	118.0	50	100.1	50
4	2.00	1960	2077	4.17	-8.3	123.4	30	120.4	50	102.9	40
5	2.00	2280	2239	3.77	-8.9	124.2	40	121.7	50	104.5	50
6	2.51	2310	2562	4.70	-8.6	129.8	40	125.8	50	110.2	40
7	2.50	2000	2380	5.20	-7.9	127.7	40	124.7	50	108.4	40
8	2.50	1500	2062	6.08	-6.7	123.9	40/50	121.6	50	104.0	50
9	2.99	1500	2233	7.25	-6.2	127.7	30	123.9	50	107.6	40
10	3.00	1970	2563	6.18	-7.4	132.0	30	127.6	50	111.9	40/50
11	3.00	2310	2773	5.62	-8.1	133.1	40	130.1	50	114.5	50
12	3.21	2300	2839	6.02	-7.9	134.8	40	130.9	50	115.5	40
13	3.21	2460	2938	5.82	-8.2	135.0	40	132.5	50	116.7	50
14	3.21	2650	3049	5.56	-8.5	133.8	50	133.6	50	117.9	50

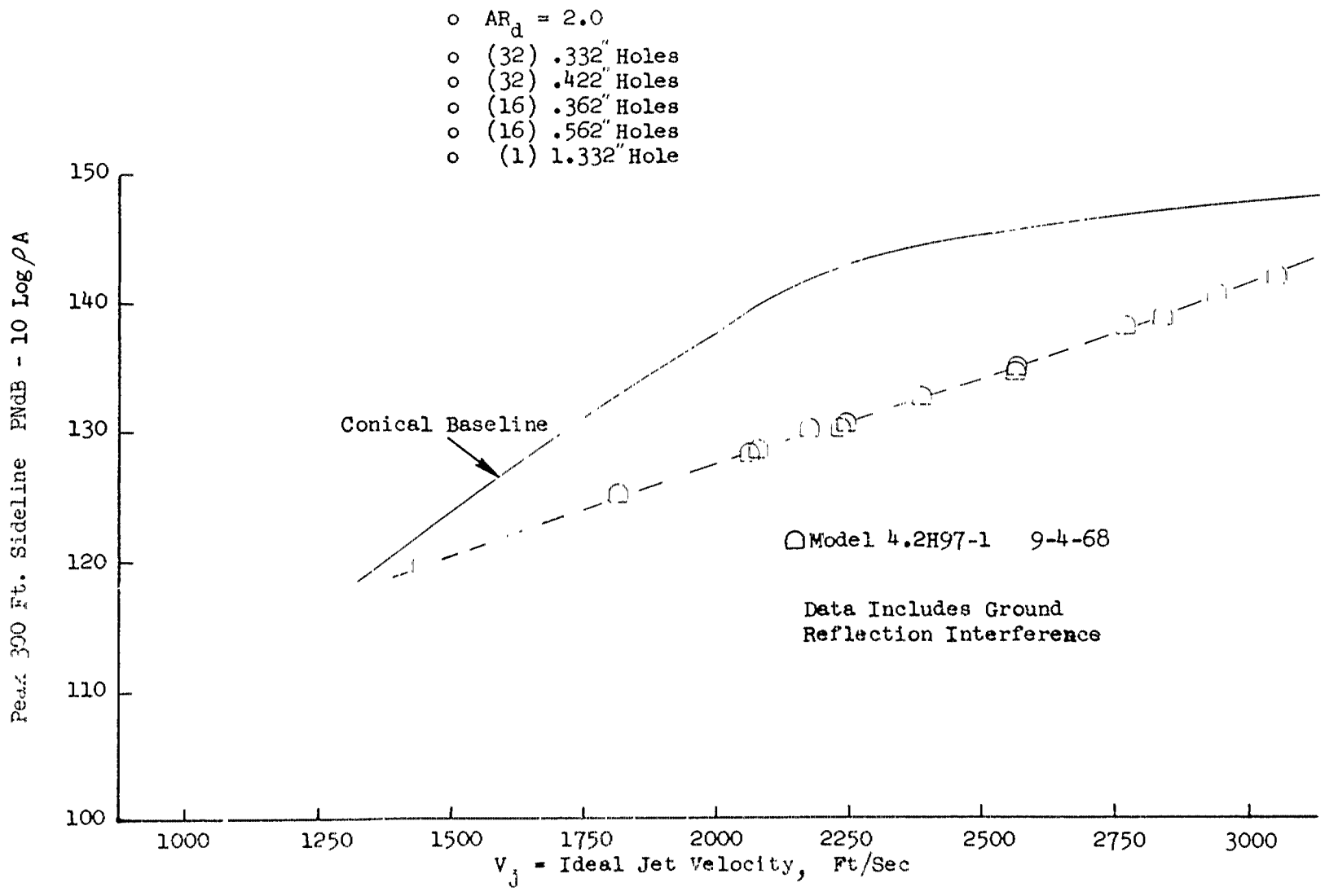

FIGURE V.F.6-4 300 FT. SIDELINE JET NOISE LEVELS FOR A 97 HOLE PLATE WITH 96 CIRCULAR HOLES PLUS GREATREX CENTER

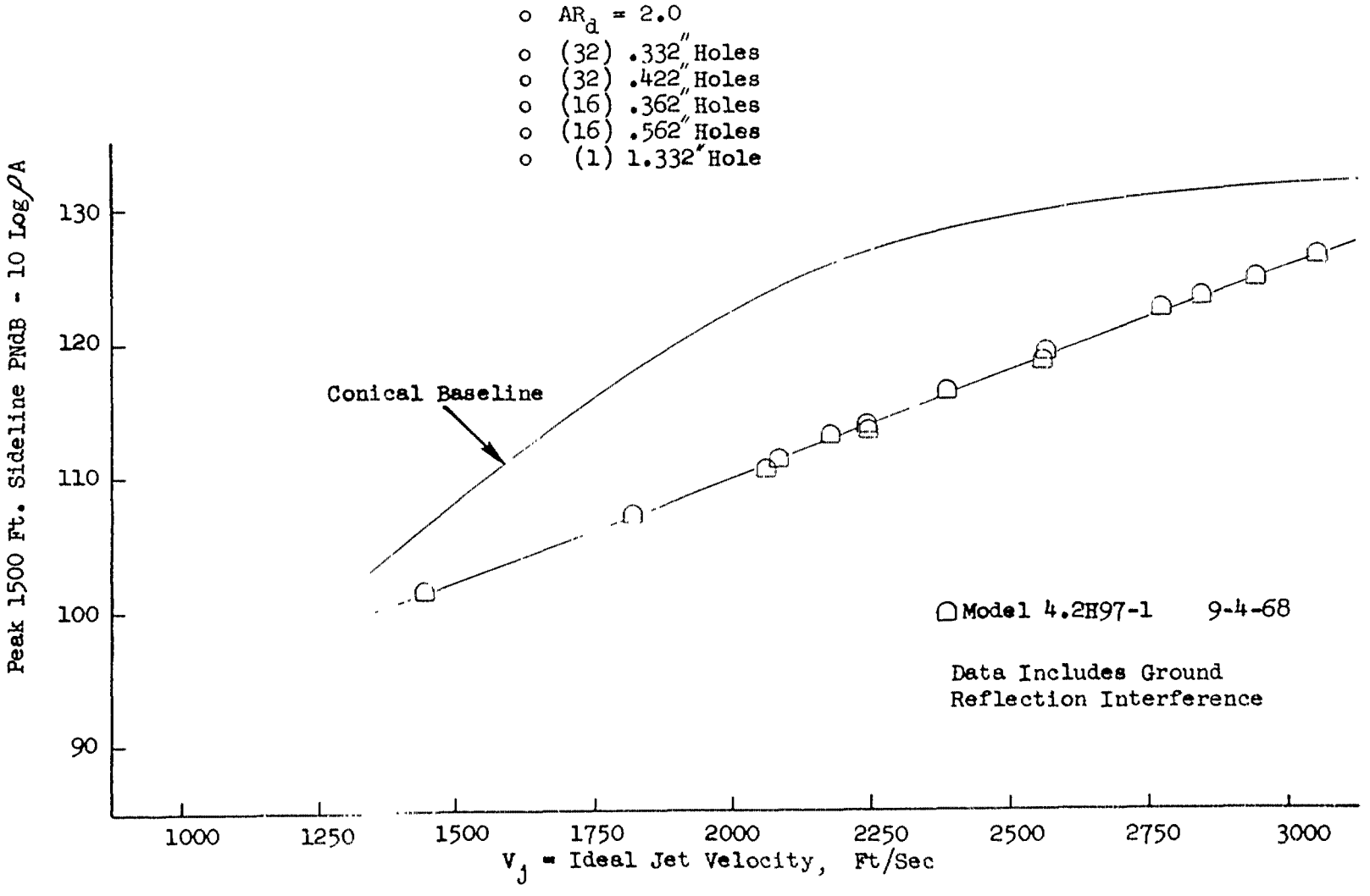

FIGURE V.F.6-5 1500 FT. SIDELINE JET NOISE LEVELS FOR A 97 HOLE PLATE WITH 96 CIRCULAR HOLES PLUS GREATREX CENTER

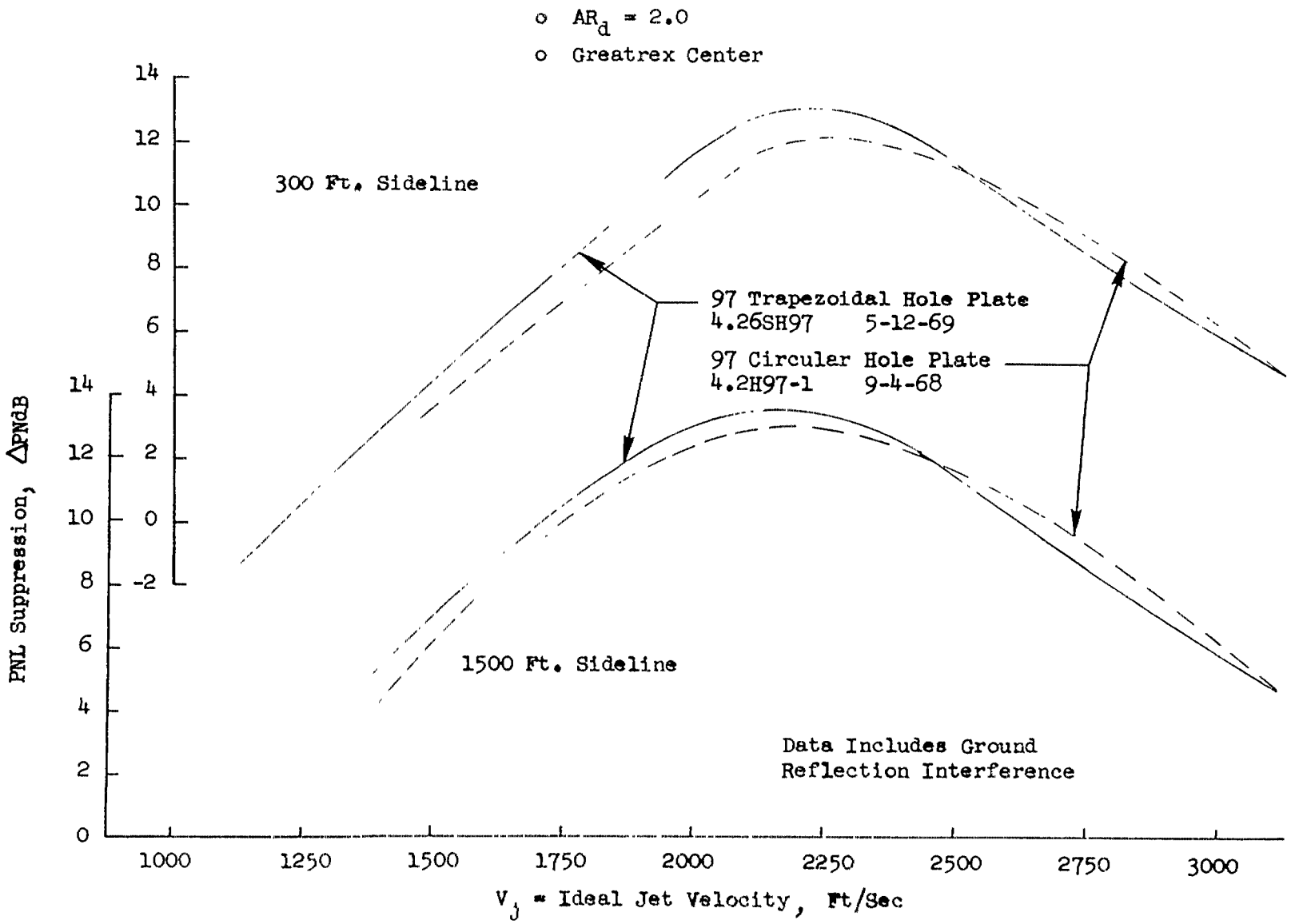

FIGURE V.F.6-6 EFFECT OF TRAPEZOIDAL AND CIRCULAR HOLE SHAPES ON 300 FT. AND 1500 FT. SIDELINE PNL SUPPRESSIONS FOR 97 HOLE PLATE NOZZLES

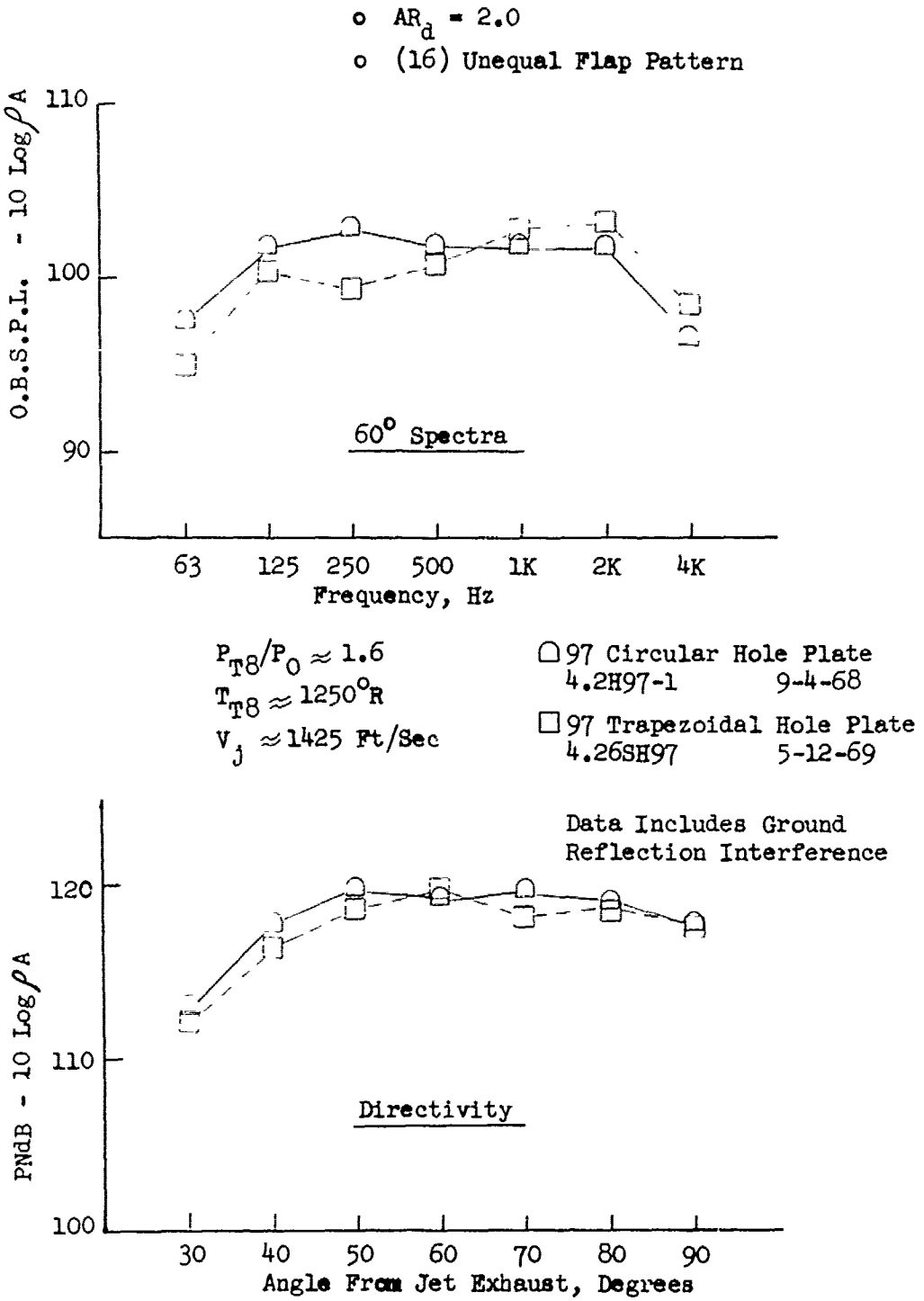

FIGURE V.F.6-7A EFFECT OF TRAPEZOIDAL AND CIRCULAR HOLE SHAPES ON 300 FT. SIDELINE SPECTRA AND DIRECTIVITY

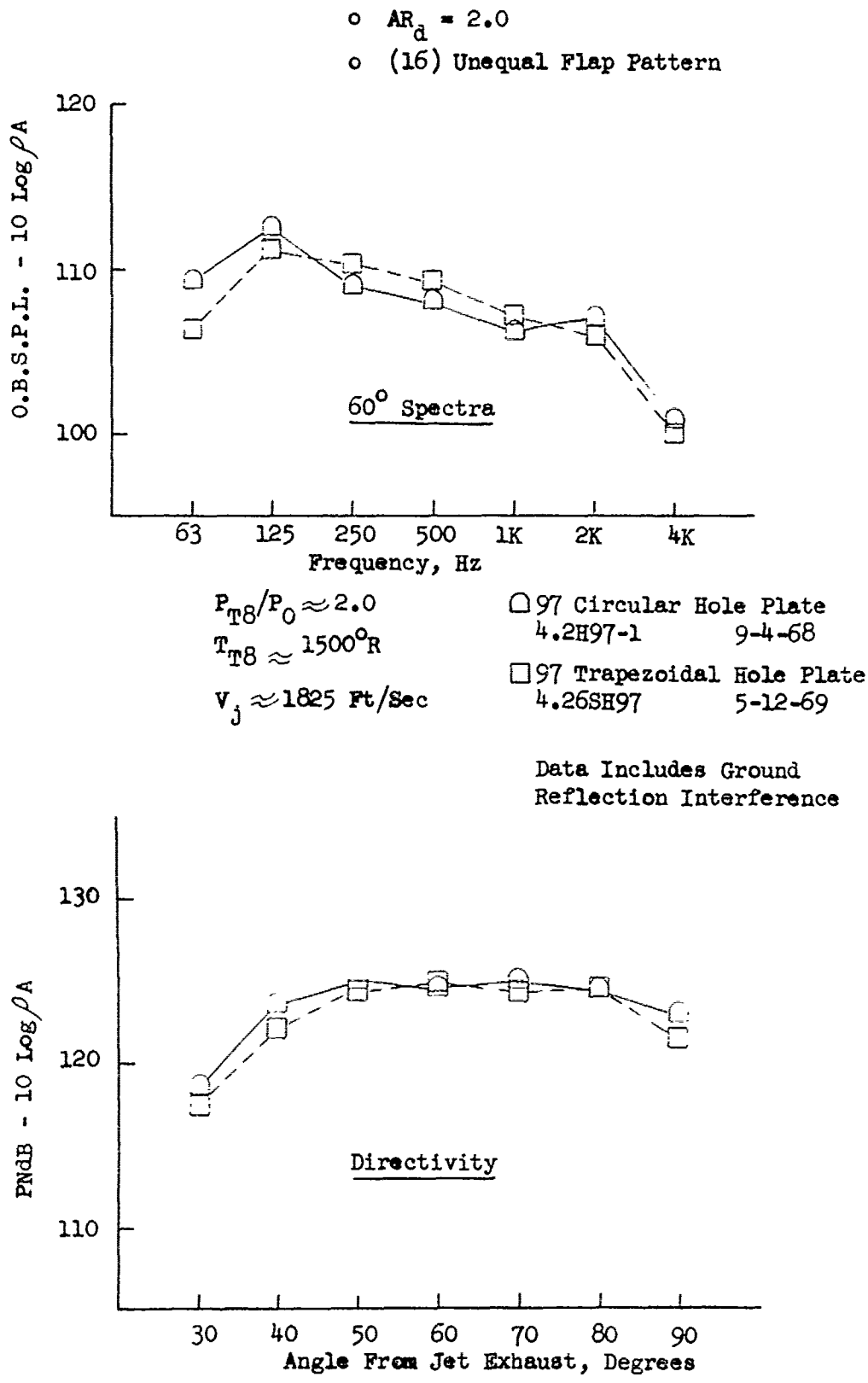

FIGURE V.F.6-7B EFFECT OF TRAPEZOIDAL AND CIRCULAR HOLE SHAPES ON 300 FT. SIDELINE SPECTRA AND DIRECTIVITY

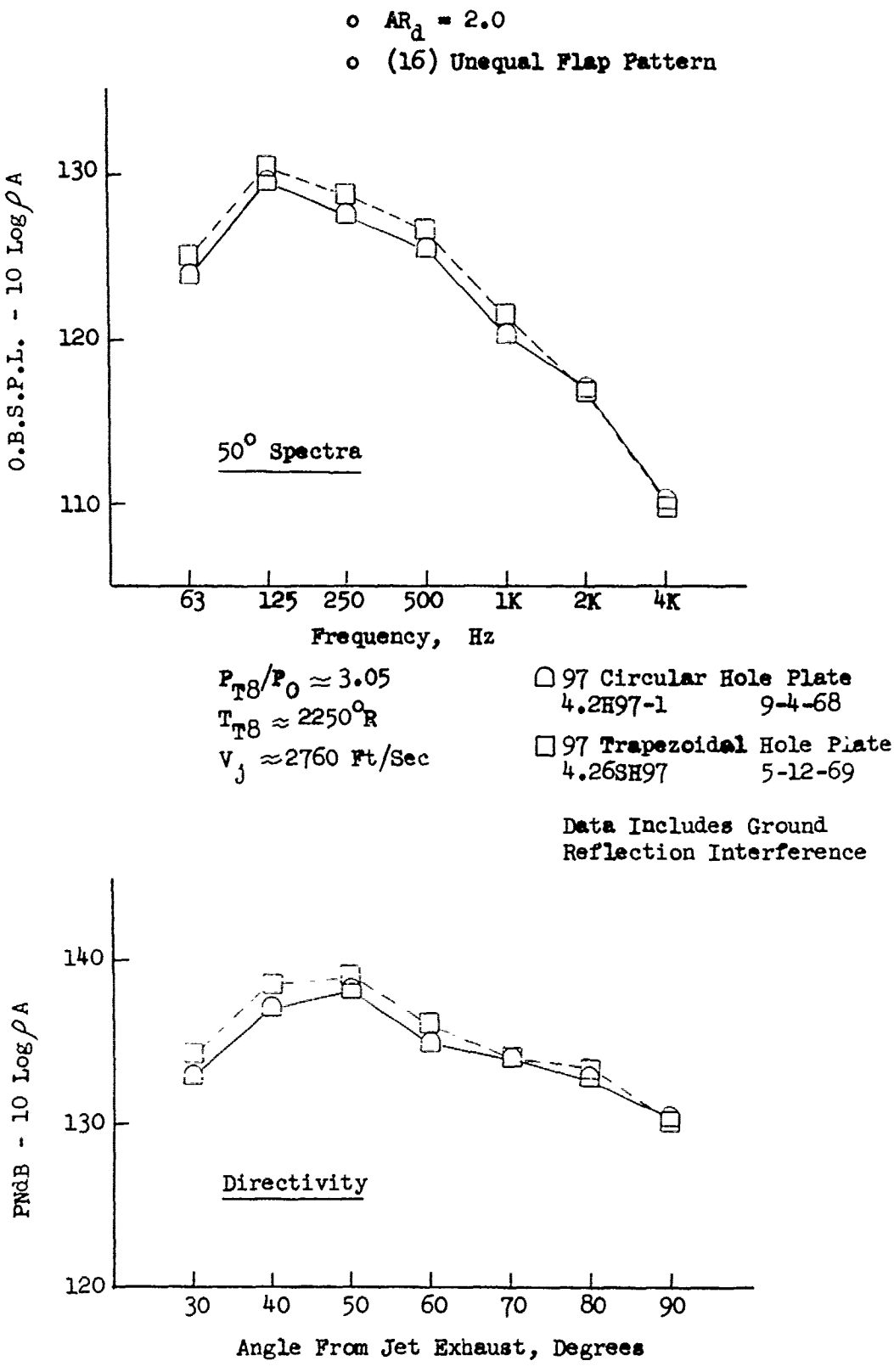

FIGURE V.F.6-7C EFFECT OF TRAPEZOIDAL AND CIRCULAR HOLE SHAPES ON 300 FT. SIDELINE SPECTRA AND DIRECTIVITY

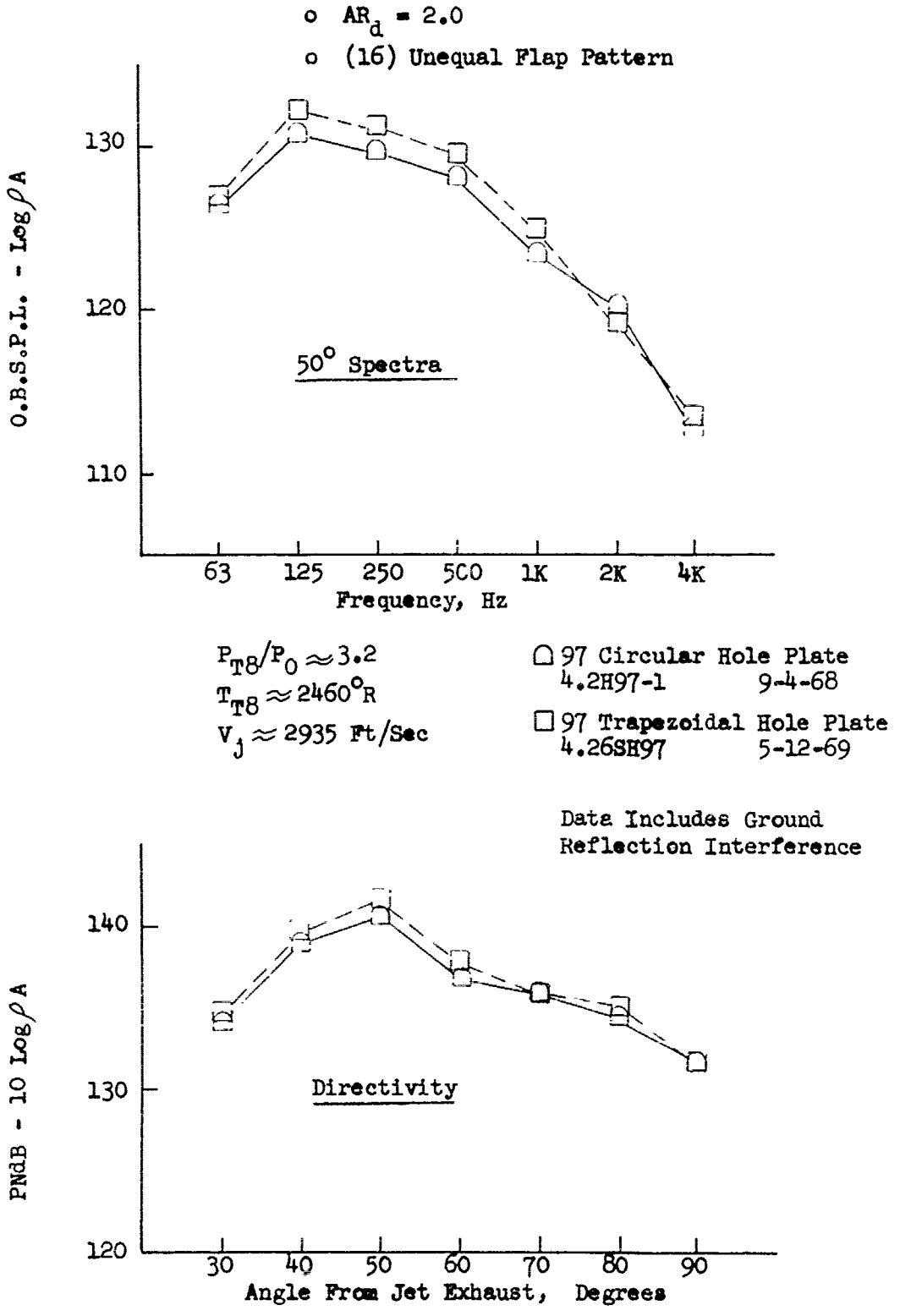

FIGURE V.F.6-7D EFFECT OF TRAPEZOIDAL AND CIRCULAR HOLE SHAPES ON 300 FT. SIDELINE SPECTRA AND DIRECTIVITY

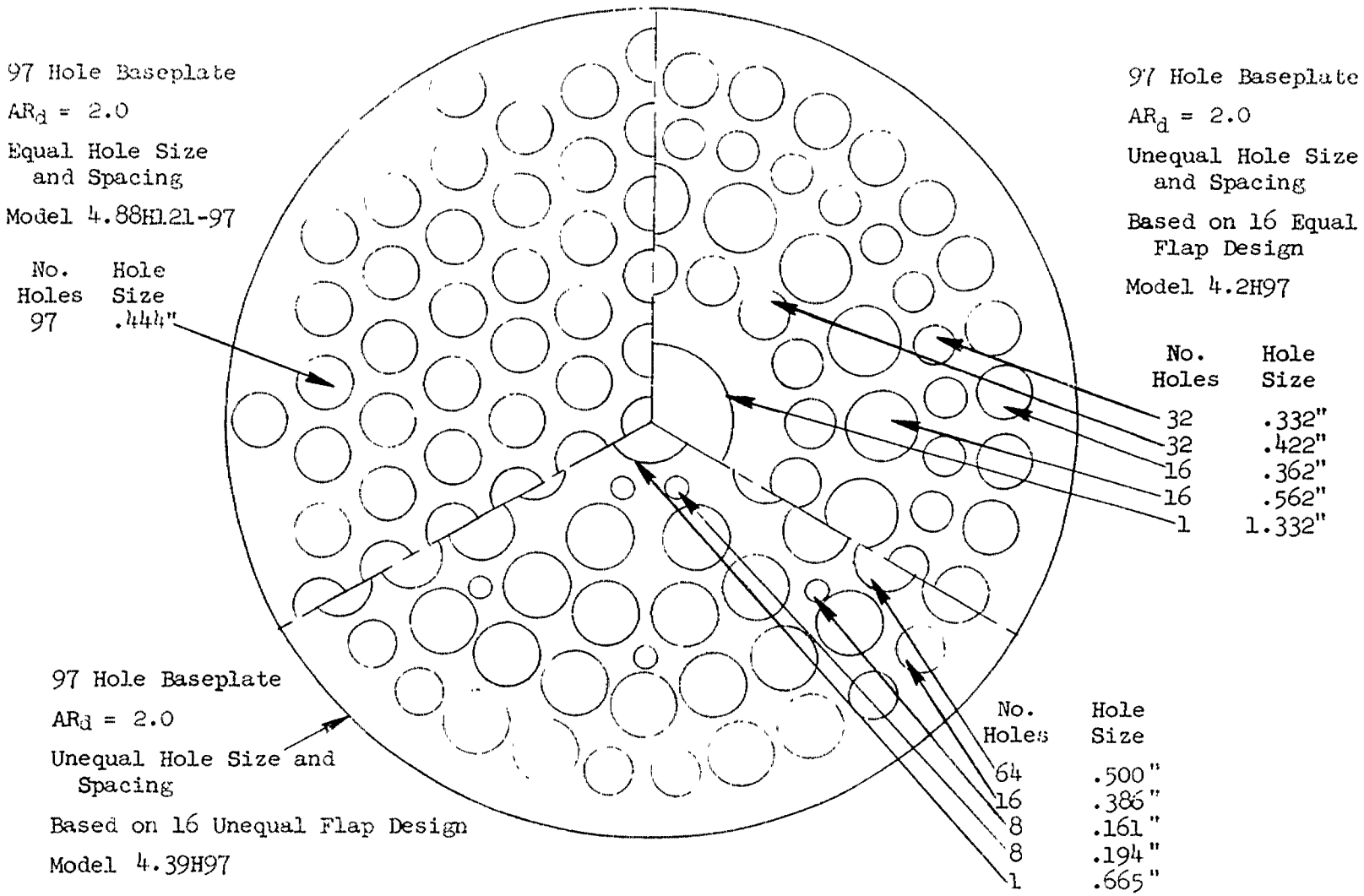

FIGURE V.F.6-8 SCHEMATIC OF 97-HOLE BASEPLATE COMPOSITE SHOWING EQUAL AND UNEQUAL CIRCULAR HOLE SIZES AND SPACING PATTERNS

TABLE V.F.6-3 TEST SUMMARY

MODEL NO. 4.88H121-97

DESCRIPTION: 97 Hole Plate with Equally Spaced .444" I.D. Holes, AR_d = 2.0

DATE: 9/9/68

SCALE MODEL A_8 = .1043 ft^2

FULL SCALE A_8 = 6.675 ft^2

SCALE FACTOR = 8:1

- o DATA INCLUDES GROUND REFLECTION INTERFERENCE
- o ANGLE REFERENCED TO JET EXHAUST

	TEST CONDITIONS				ACOUSTIC TEST RESULTS						
			IDEAL			320' ARC		300' SIDELINE		1500' SIDELINE	
RDG NO.	P_{T8}/P_o	T_{T8} (°R)	V_j (ft/sec)	W_8 (PPS)	10 log ρA	PEAK PNdB	PEAK ANGLE	PEAK PNdB	PEAK ANGLE	PEAK PNdB	PEAK ANGLE
2	3.19	2645	3040	5.58	-8.4	134.1	40	130.9	50	115.0	50
3	3.20	2455	2931	5.81	-8.0	133.3	40	129.0	40	113.7	40
4	1.63	1320	1448	4.69	-6.5	116.5	50	115.0	70	96.8	70
5	2.01	1505	1823	4.98	-6.9	122.6	50	120.2	50	101.8	50
6	2.66	1990	2094	4.24	-8.1	122.9	50	120.5	50	103.6	70
7	2.01	2300	2252	3.63	-8.8	124.1	50	122.0	70	104.2	70
8	2.45	1720	2187	5.62	-7.1	125.1	30	122.7	50	104.9	50
9	2.49	1500	2059	6.19	-6.5	124.4	40	121.9	50	103.9	50
10	2.50	1965	2361	5.12	-7.7	126.9	40	124.2	50	107.0	40
11	2.50	2320	2564	4.61	-8.4	128.3	40	125.7	80	108.6	50
12	3.00	2320	2779	5.57	-8.0	130.3	40	127.3	50	110.5	50
13	3.00	1965	2559	6.20	-7.2	129.3	40	125.9	50	109.2	40
14	3.00	1500	2234	7.37	-6.1	125.7	40	122.9	50	105.1	50
15	3.20	2315	2846	5.99	-7.8	131.5	30	128.6	50	112.0	50

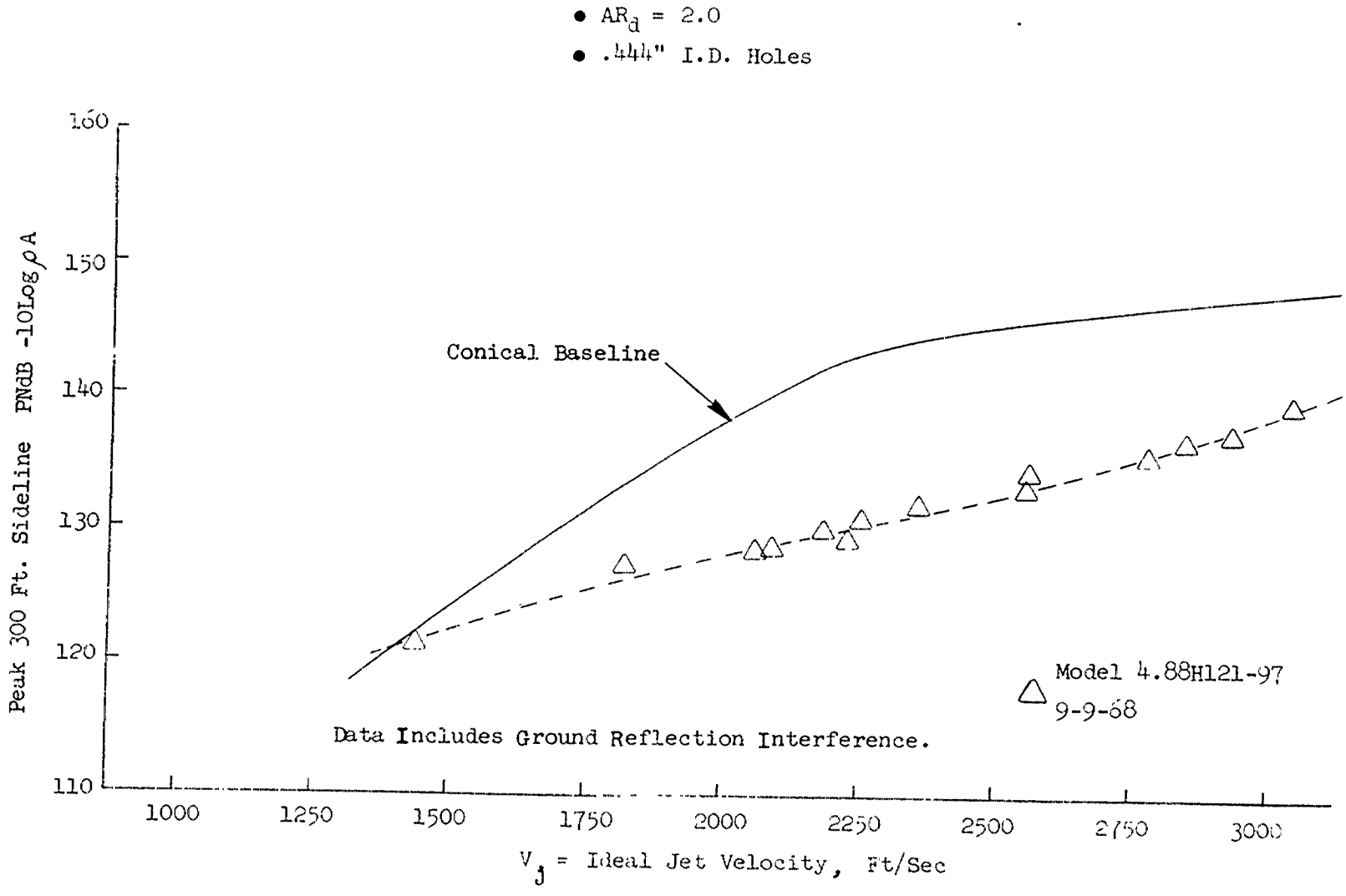

FIGURE V.F.6-9 300 FT. SIDELINE JET NOISE LEVELS FOR A 97 HOLE PLATE WITH EQUAL HOLE SIZES AND SPACING

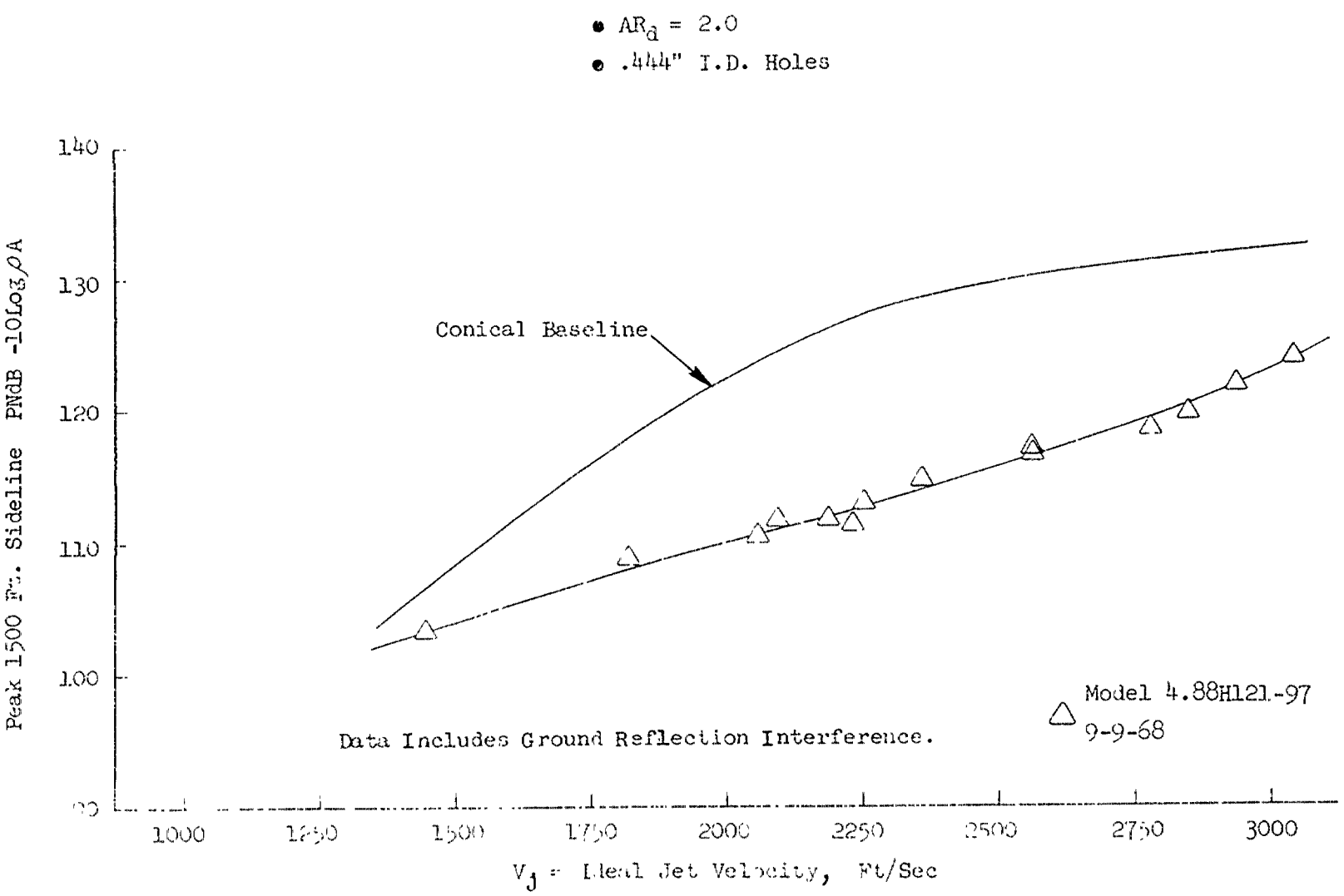

FIGURE V.F.6-10 1500 FT. SIDELINE JET NOISE LEVELS FOR A 97 HOLE PLATE WITH EQUAL HOLE SIZES AND SPACING

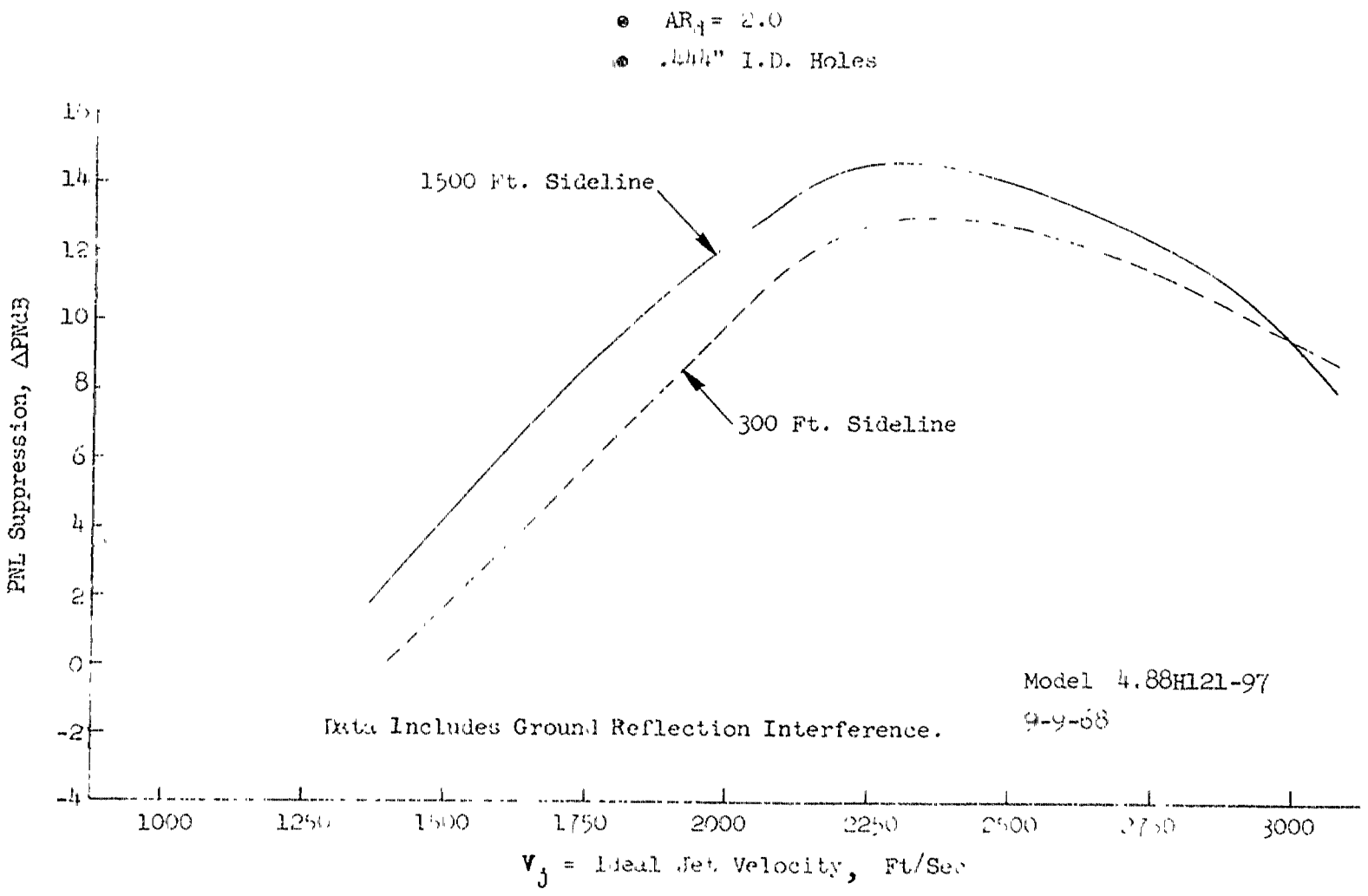

FIGURE V.F.6-11 COMPARISON OF 300 FT. AND 1500 FT. SIDELINE PNL SUPPRESSIONS FOR A 97 HOLE PLATE WITH EQUAL HOLE SIZES AND SPACING

TABLE V.F.6-4 TEST SUMMARY

MODEL NO. 4.2H97

DESCRIPTION: 97 Hole Plate with Unequal Hole Sizes and Spacing, AR_d = 2.0

DATE: 8/22/68

SCALE MODEL A_8 = .0994 ft^2

FULL SCALE A_8 = 6.362 ft^2

SCALE FACTOR = 8:1

- o DATA INCLUDES GROUND REFLECTION INTERFERENCE
- o ANGLE REFERENCED TO JET EXHAUST

RDG NO.	TEST CONDITIONS				ACOUSTIC TEST RESULTS						
			IDEAL			320' ARC		300' SIDELINE		1500' SIDELINE	
	P_{T8}/P_o	T_{T8} (°R)	V_j (ft/sec)	W_8 (PPS)	10 . g ρA	PEAK PNdB	PEAK ANGLE	PEAK PNdB	PEAK ANGLE	PEAK PNdB	PEAK ANGLE
1	1.64	1322	1453	4.29	-6.7	115.5	50	113.9	70	95.8	70
2	2.00	1492	1808	5.03	-7.1	120.9	40	118.6	70	100.7	70
3	2.62	1954	2084	4.37	-8.2	124.0	40	121.4	70	104.5	60
4	1.99	2268	2221	3.91	-8.9	125.6	30	122.5	50	106.0	50
5	2.47	1728	2198	5.76	-7.3	127.0	40	123.4	50	107.6	50
6	2.54	1474	2057	6.44	-6.6	126.0	40	121.7	50	106.0	40
7	2.50	1966	2360	5.42	-7.8	128.6	40	125.5	50	110.0	50
8	2.52	2273	2548	4.97	-8.5	130.4	40	126.9	50	111.5	50
9	3.02	2283	2763	5.94	-8.0	133.9	50	131.7	50	116.2	50
10	3.02	1950	2553	6.54	-7.4	132.4	40	129.7	50	114.2	50
11	3.03	1497	2243	7.68	-6.2	129.4	30	124.9	50	109.4	40
12	3.22	1508	2303	8.09	-6.1	130.2	30	126.5	50	110.9	50
13	3.20	1961	2619	6.92	-7.2	133.2	40	130.6	50	115.1	50
14	3.22	2317	2855	6.20	-7.9	135.5	50	133.4	50	117.9	50
15	3.22	2437	2926	6.03	-8.2	135.6	50	133.5	50	118.1	50
16	3.20	2632	3035	5.77	-8.5	136.9	50	134.7	50	119.0	50
17	3.52	2278	2922	6.90	-7.6	137.6	50	135.4	50	119.7	50
18	4.05	2270	3051	7.92	-7.2	139.1	50	136.9	50	121.1	50

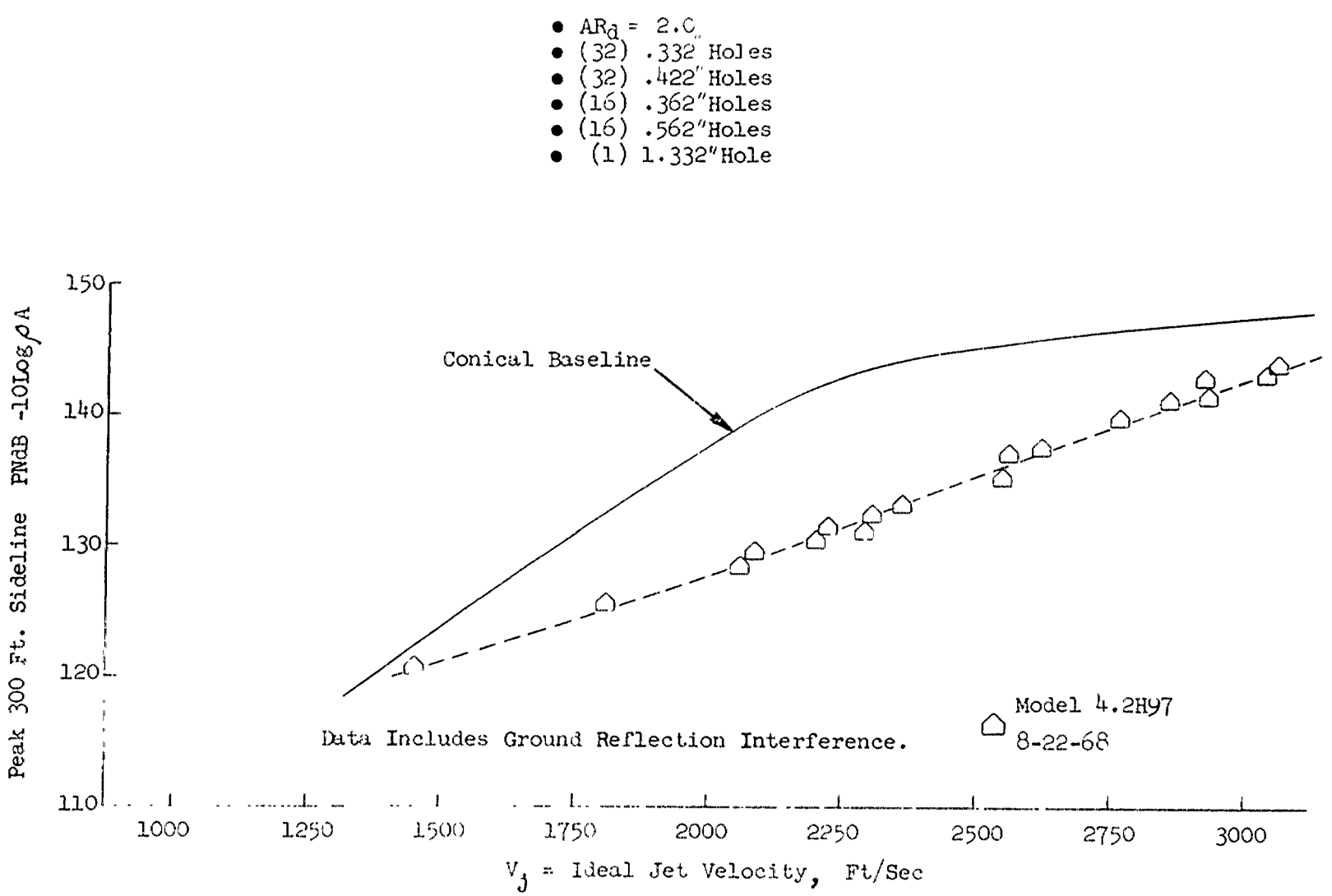

FIGURE V.F.6-12 300 FT. SIDELINE JET NOISE LEVELS FOR A 97 HOLE PLATE WITH UNEQUAL HOLE SIZES AND SPACING

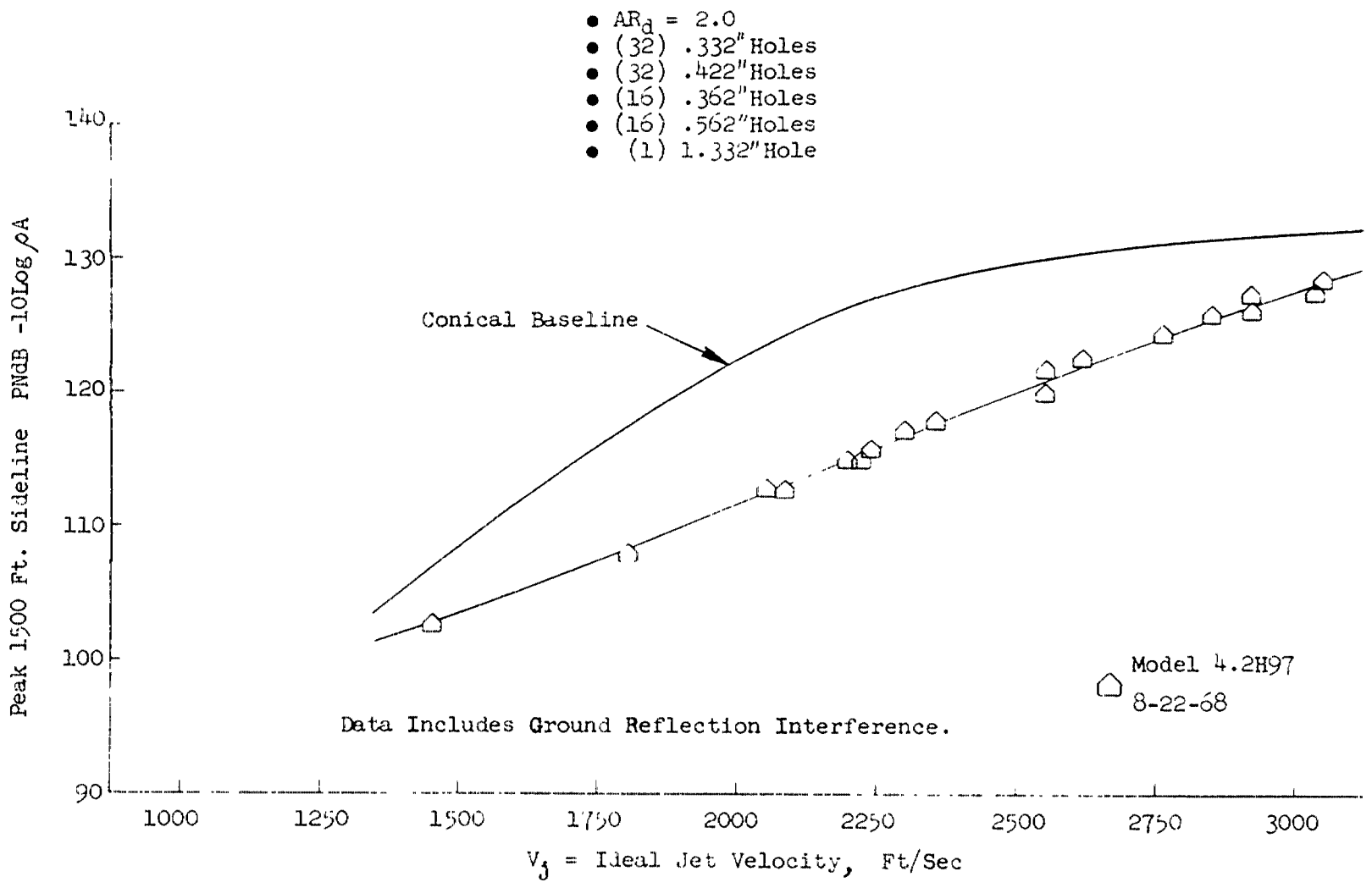

FIGURE V.F.6-13 1500 FT. SIDELINE JET NOISE LEVELS FOR A 97-HOLE PLATE WITH UNEQUAL HOLE SIZES AND SPACING

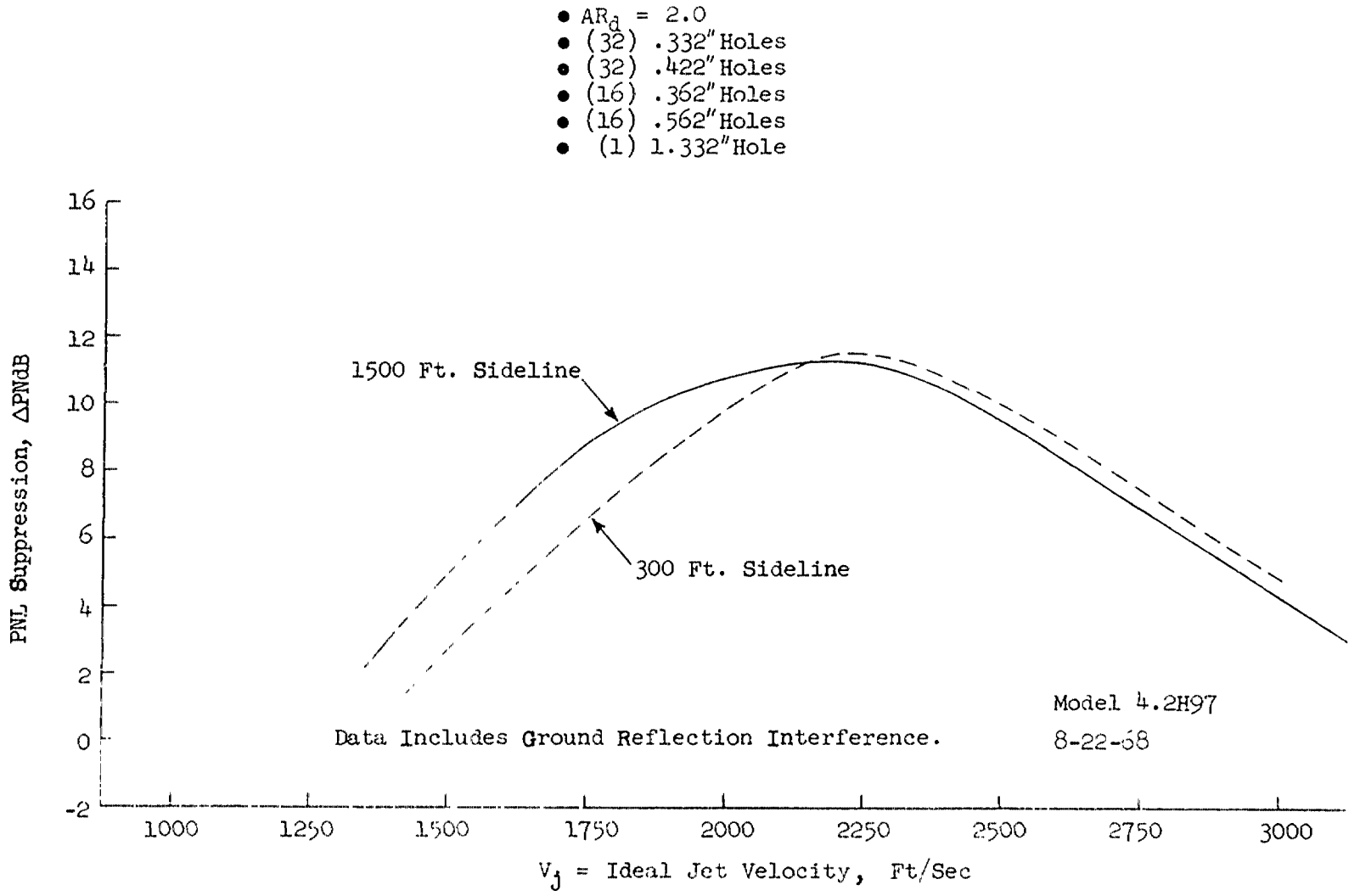

FIGURE V.F.6-14 COMPARISON OF 300 FT. AND 1500 FT. SIDELINE PNL SUPPRESSIONS FOR A 97 HOLE PLATE WITH UNEQUAL HOLE SIZES AND SPACING

TABLE V.F. 6-5 TEST SUMMARY

MODEL NO. 4.39H97

DESCRIPTION: 97 Hole Plate with Unequal Hole Sizes and Spacings, AR_d = 2.0

DATE: 10/11/68 ; 10/14/68

SCALE MODEL A_8 = .1051 ft^2

FULL SCALE A_8 = 6.726 ft^2

SCALE FACTOR = 8:1

- o DATA INCLUDES GROUND REFLECTION INTERFERENCE
- o ANGLE REFERENCED TO JET EXHAUST

RDG NO.	TEST CONDITIONS				ACOUSTIC TEST RESULTS						
			IDEAL			320' ARC		300' SIDELINE		1500' SIDELINE	
	P_{T8}/P_o	T_{T8} (°R)	V_j (ft/sec)	W_8 (PPS)	10 log ρA	PEAK PNdB	PEAK ANGLE	PEAK PNdB	PEAK ANGLE	PEAK PNdB	PEAK ANGLE
1	1.39	1200	1145	3.68	-5.9	110.1	50	108.7	70	90.6	70
2	1.53	1255	1317	4.16	-6.2	113.7	50	111.3	70	93.4	70
3	1.62	1320	1437	4.37	-6.5	115.9	50	113.5	50	95.5	50
4	2.00	1505	1815	5.08	-6.9	121.2	50	118.9	50	101.5	50
5	1.99	1985	2083	4.28	-8.1	123.7	50	121.4	50	104.8	50
6	2.00	2310	2252	3.77	-8.7	125.6	50	123.2	50	106.8	50
7	2.21	1620	2008	5.35	-5.4	123.9	30	121.5	50	104.9	50
8	2.45	1700	2171	5.72	-5.4	127.7	30	123.9	50	107.8	50
9	2.51	1970	2366	5.34	-7.6	130.0	40	126.0	40/50	110.7	40
10	2.49	2280	2539	4.87	-8.2	131.0	40	127.9	50	112.5	50
11	3.00	2310	2775	5.74	-7.9	135.0	50	132.9	50	117.3	50
12	3.01	1975	2567	6.50	-7.2	133.2	40	130.1	50	114.6	50
10/14/68											
1	1.63	1320	1444	4.32	-6.5	115.6	50	113.2	50	95.2	50
2	2.45	1685	2161	5.74	-7.0	126.9	50	124.4	50	107.5	50
3	2.50	2305	2565	4.79	-8.3	130.6	40	127.4	50	111.6	50
4	3.40	2305	2903	6.62	-7.5	136.3	50	134.1	50	118.4	50
5	3.20	2305	2841	6.23	-7.7	135.5	50	133.3	50	117.7	50

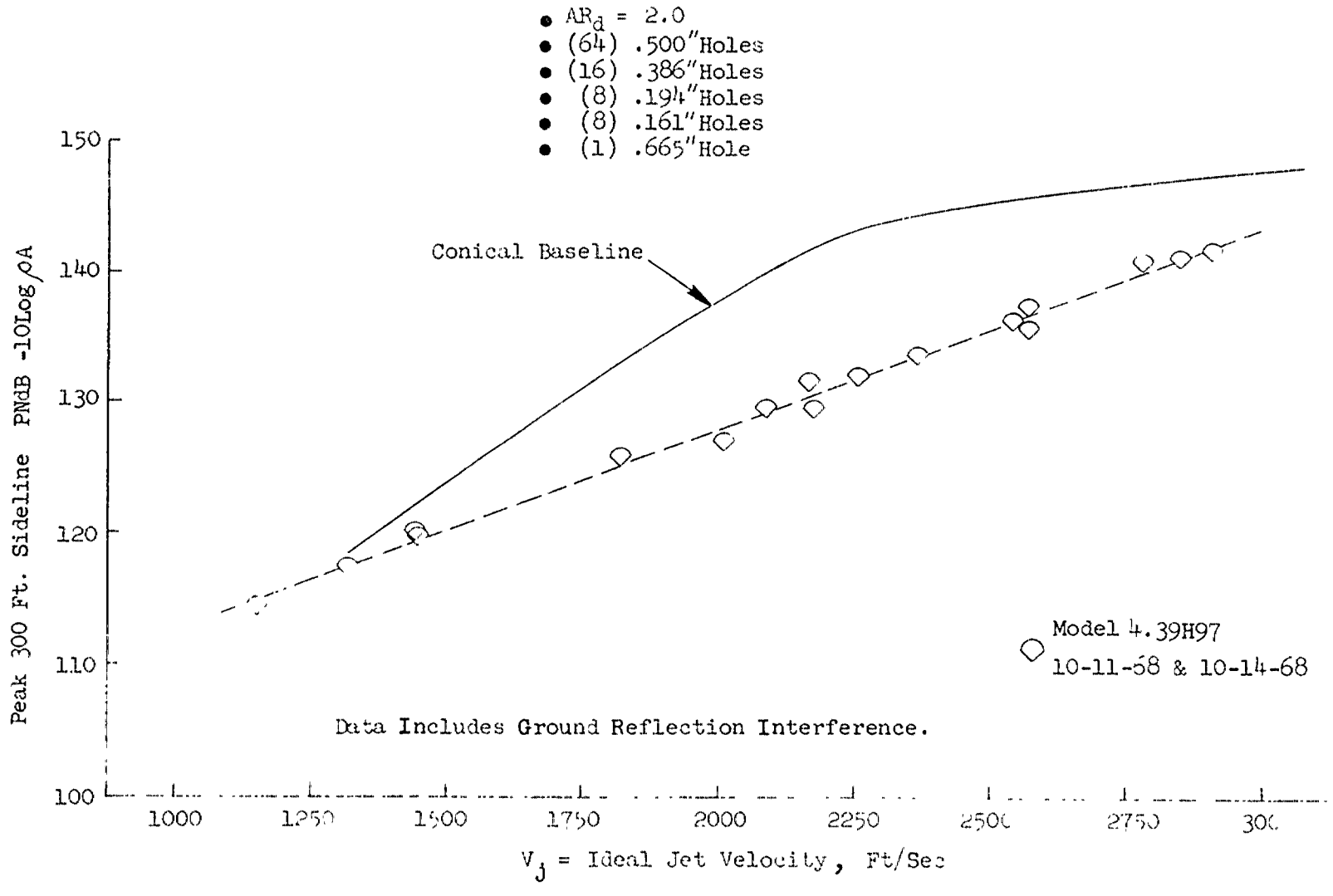

FIGURE V.F.6-15 300 FT. SIDELINE JET NOISE LEVELS FOR A 97 HOLE PLATE WITH UNEQUAL HOLE SIZES AND SPACING

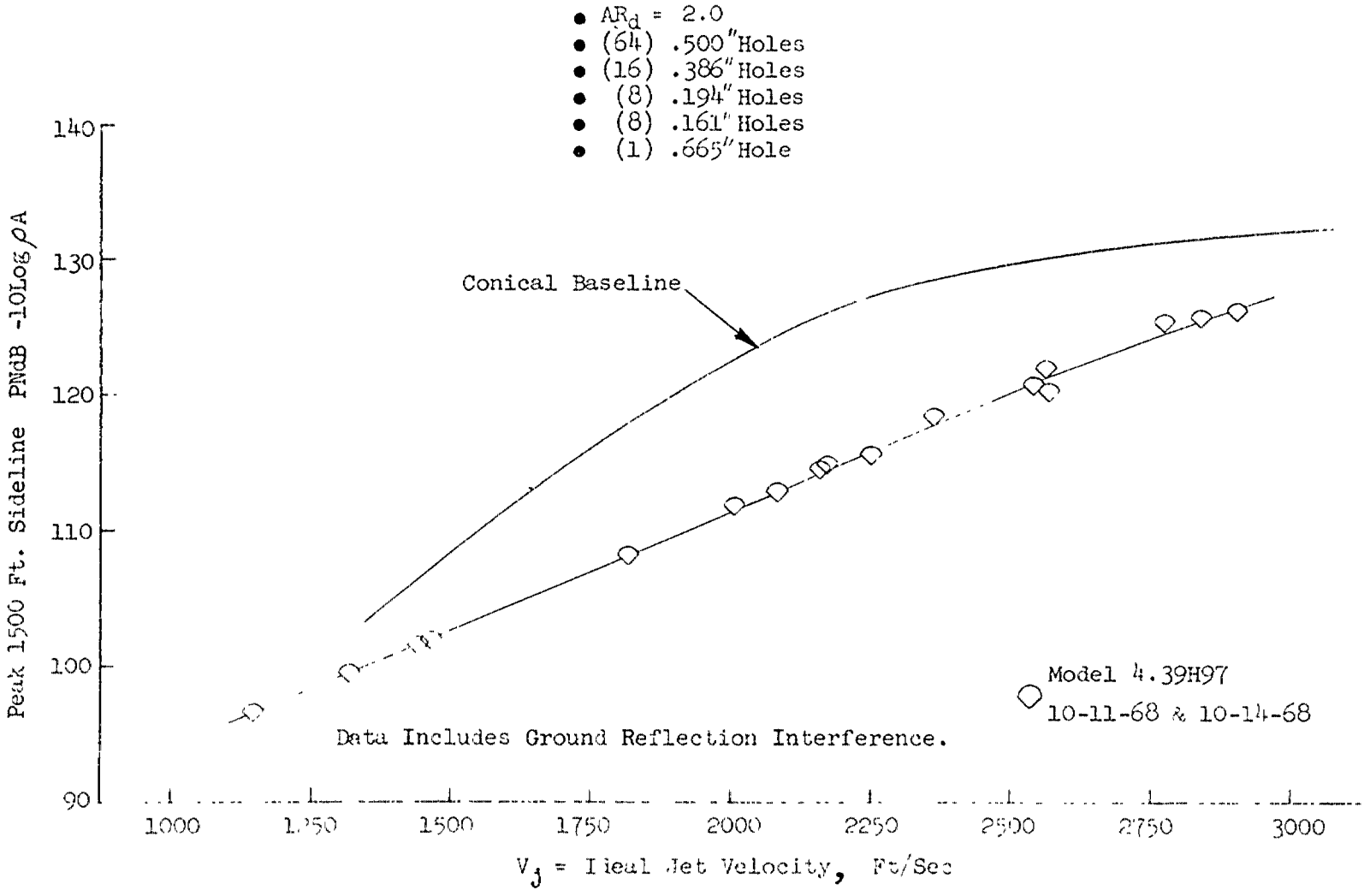

FIGURE V.F.6-16 1500 FT. SIDELINE JET NOISE LEVELS FOR A 97 HOLE PLATE WITH UNEQUAL HOLE SIZES AND SPACING

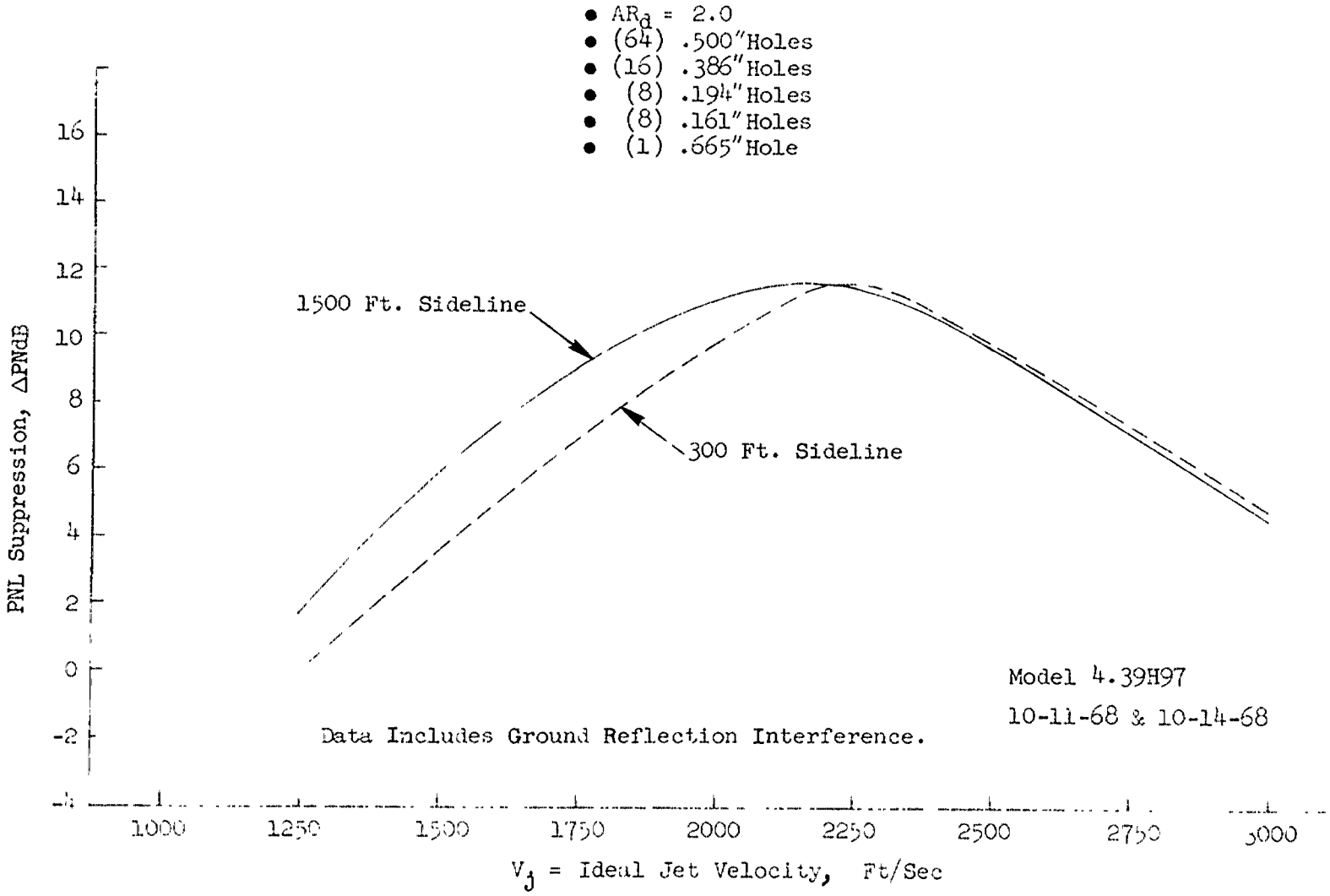

FIGURE V.F.6-17 COMPARISON OF 300 FT. AND 1500 FT. SIDELINE PNL SUPPRESSIONS FOR A 97 HOLE PLATE WITH UNEQUAL HOLE SIZES AND SPACING

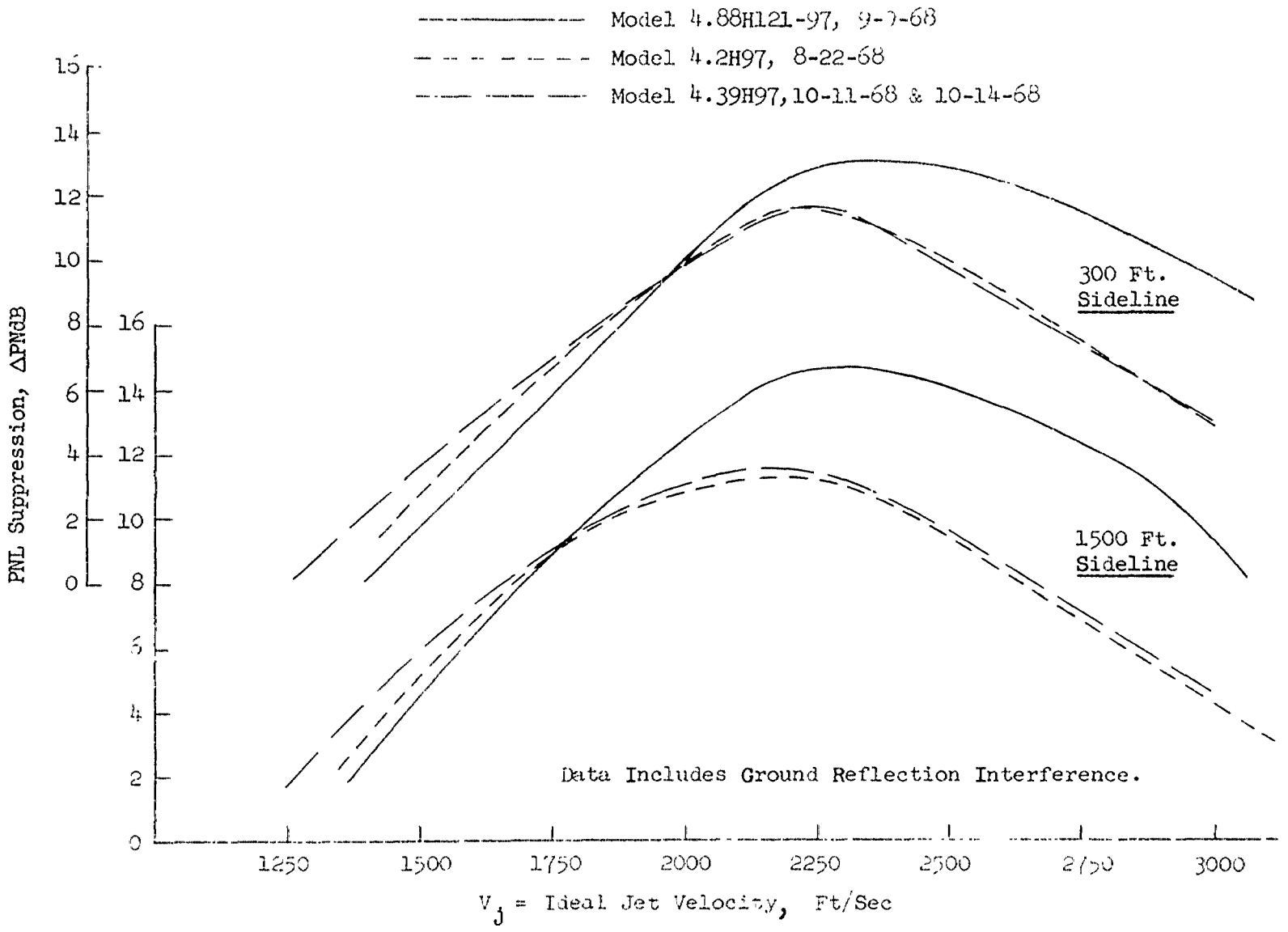

FIGURE V.F.6-18 EFFECT OF HOLE SIZE AND SPACING ON 300 FT. AND 1500 FT. SIDELINE PNL SUPPRESSIONS FOR 97 HOLE PLATE NOZZLES

V.F.7 VARIATIONS OF 97 TUBE PRIMARY NOZZLE WITH LARGE AND SMALL CENTER HOLE; COMPARISONS WITH HARDWALL AND 7.5% OPEN LINED EJECTORS

PRECEDING PAGE BLANK-NOT FILMED

V.F.7 VARIATIONS OF 97 TUBE PRIMARY NOZZLE WITH LARGE AND SMALL CENTER HOLE; COMPARISONS WITH HARDWALL AND 7.5% OPEN LINED EJECTORS

Objectives of Test Series

The purpose of this test series was to investigate the acoustic and aerodynamic performance of a practical tube nozzle design for a viable engine application. The system consisted of a 97 tube nozzle (96 tubes plus center hole) with a practical length and diameter cylindrical ejector. Initially the primary nozzle had a large center hole but was altered to a smaller center hole when the core jet through the center hole was found to predominate the generated noise. In addition to the hardwall cylindrical ejector, an acoustically treated ejector was tested. The comparative results of the treated versus hardwall ejector are presented in Section V.G "Acoustic Ejectors on Multi-Tube and Conical Nozzles". The absolute noise levels and total system suppression are presented in this study.

Acoustic tests were performed at the GE, Evendale, JENOTS facility. Measurements were taken on a 40 ft. arc at 10° increments from 30° through 90° from the jet exhaust axis and over a frequency range to 40 KHz (31.5 KHz octave band). The data were scaled to full scale engine application using a scale factor of 8:1 for frequency, nozzle size and measuring arc. Therefore, all data are presented as simulated engine size and frequency range.

The acoustic tests were conducted over a simulated engine running line with P_{T8}/P_o from 1.4 to 4.0, T_{T8} from 1140 to 2325° R and V_J from 1120 to 3070 ft/sec.

Individual acoustic comparisons within the test series include:

a) 97 tube primary nozzle with 1.764" I.D. versus 1.415" I.D. center holes
b) Addition of a hardwall (non-acoustically treated) ejector to the primary nozzle system.
c) Effect of 7.5% open performated acoustic liner referenced to the hardwall ejector.

Aerodynamic testing was performed at the FluiDyne Engineering Corporation on the 97 tube, large center hole + hardwall ejector configuration, Model 4.2 T97-7.7CS, to evaluate the basic nozzle systems static thrust performance.

PRECEDING PAGE BLANK-NOT FILMED

Test Configurations

Several photographs of the 97 tube primary and the primary plus cylindrical ejector system are included as Figures V.F.7-1 and -2. A total of four model configurations were tested as shown schematically in Figure V.F.7-3. The basic configuration, Model 4.2T97 was a 97 tube primary nozzle (96 tubes plus center hole) with various size internal tube diameters and a 1.764" center hole. The tube exit plane was staggered 15° from the vertical plane. Tube bundle compactness was set at AR_d = 2.0. Using this primary nozzle, a cylindrical hardwall ejector of L_S= 7.965, L_S/D_S = 1.03 and D_S/D_{Td} = 1.185, was added as Model 4.2T97-7.7CS. The interchangeable ejector hardwall insert of this model was replaced with an acoustic liner of 7.5% open perforated sheet metal with a 0.22" cavity depth behind the perforated sheet. This was designated Model 4.2T97-7.7CS-1. Following these tests, a filler plug was added to alter the center hole to a 1.415" I.D.. The small center hole primary alone was tested as Model 4.2T97-1.

Baseline reference nozzle curves for the test series were obtained from prior tests on a 4.32" D_8 conical convergent nozzle.

Presentation of Data and Discussion of Results

For each of the models, in order of their listing on Figure V.F.7-3, acoustic test results are included as a) tabular form, b) 300 and 1500 ft. sidelines peak normalized PNL plots as a function of jet velocity, and c) 300 and 1500 ft. sidelines peak normalized PNL suppression curves, as follows:

Model No.	Table	Figures
4.2T97	V.F.7-1	V.F.7-4, -5 and -6
4.2T97-1	V.F.7-2	V.F.7-7, -8 and -9
4.2T97-7.7CS	V.F.7-3	V.F.7-10, -11, and -12
4.2T97-7.7CS-1	V.F.7-4	V.F.7-13, -14 and -15

For comparison purpose, Figure V.F.7-16 composites the 300 and 1500 ft. sidelines individual model PNL suppression curves, all suppression levels being referenced to the baseline conical nozzle. The comparisons show:

- o A maximum suppression of near 13 PNdB was attained in the 2250 ft/sec jet velocity region with the acoustic ejector system on the large

center hole primary. Suppression rates drop off considerably and uniformly above and below the velocity at peak suppression.

- Reducing the center-hole size from 1.764" to 1.415" I.D. increased suppression by about 2 PNdB fairly uniformly over the tested velocity range.
- The hardwall cylindrical ejector can provide about 2 PNdB suppression increase over the basic multi-tube configuration over the tested velocity range.
- The addition of the acoustically treated ejector did not gain appreciable suppression over the hardwall ejector, with about 1.5 PNdB increase at low V_j and 0.5 PNdB at high V_j. The relative ineffectiveness of the liner, particularly at high jet veloicty was thought to be due to the high acoustic power generated by the large center hole, which appeared to dominate the spectrum.

The 97 tube configuration with the large center-hole and hardwall ejector, Model 4.2T97-7.7CS, was subjected to cold flow tests at FluiDyne Engineering Corporation to obtain its static performance. Figure V.F.7-17 summarizes the gross nozzle thrust coefficient and primary nozzle flow coefficient characteristics as a function of pressure ratio. A maximum gross thrust coefficient of 0.89 was obtained at simulated climbout/takeoff conditions ($P_{T8}/P_o \approx 3.2$). Primary nozzle flow coefficient remained essentially constant at about 0.90 down to about tube choking pressure ratios.

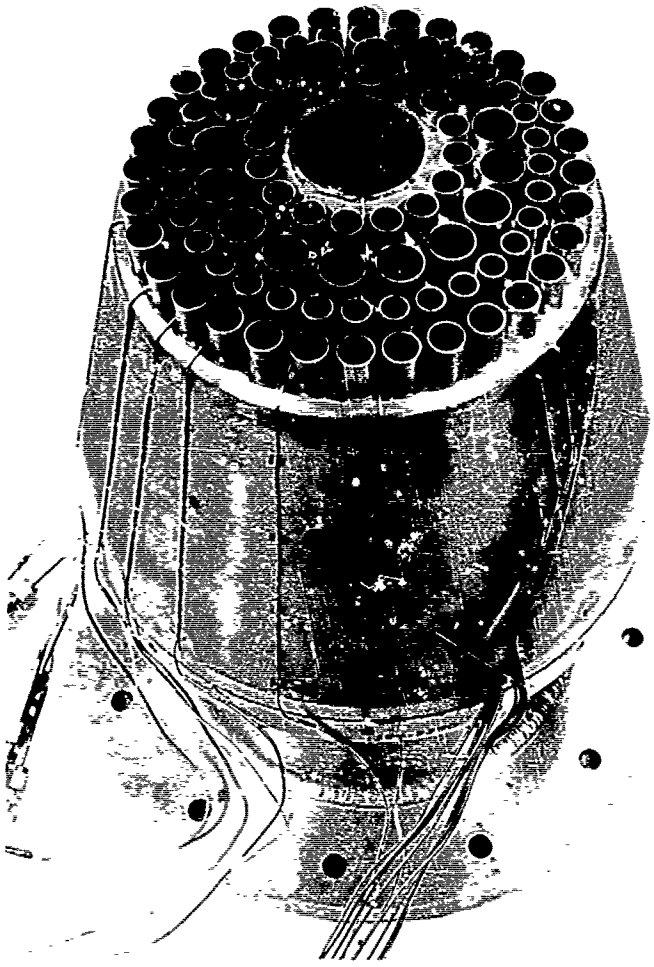

FIGURE V.F.7-1 97 TUBE PRIMARY NOZZLE HARDWARE, $AR_d = 2.0$

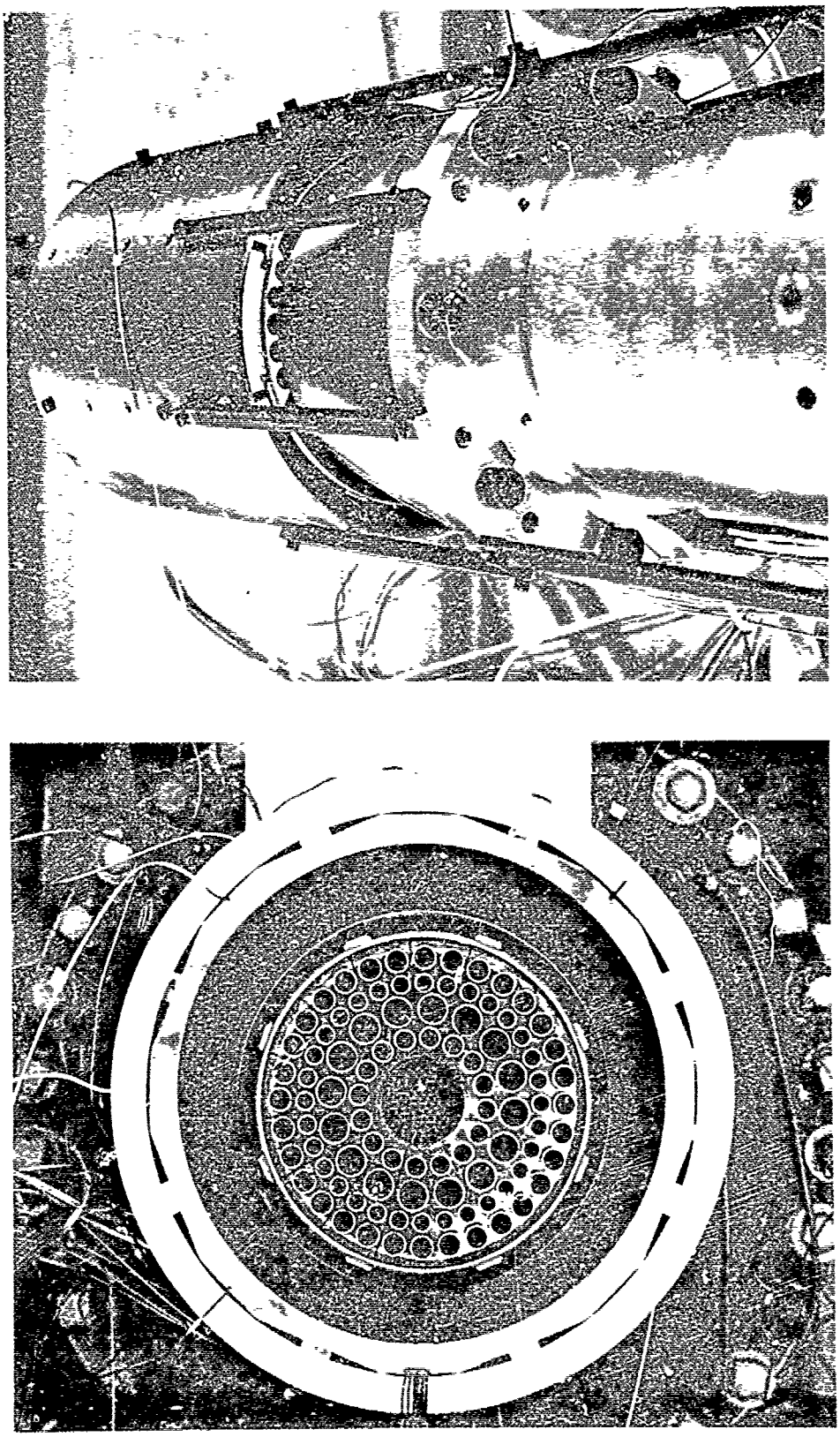

FIGURE V.F.7-2 97 TUBE PRIMARY NOZZLE WITH HARDWALL EJECTOR

- D_S/D_{Td} = 1.185
- L_S/D_S = 1.03
- AR_d = 2.0
- 15° Stagger Angle
- All Tubes Equally Spaced Circumferentially

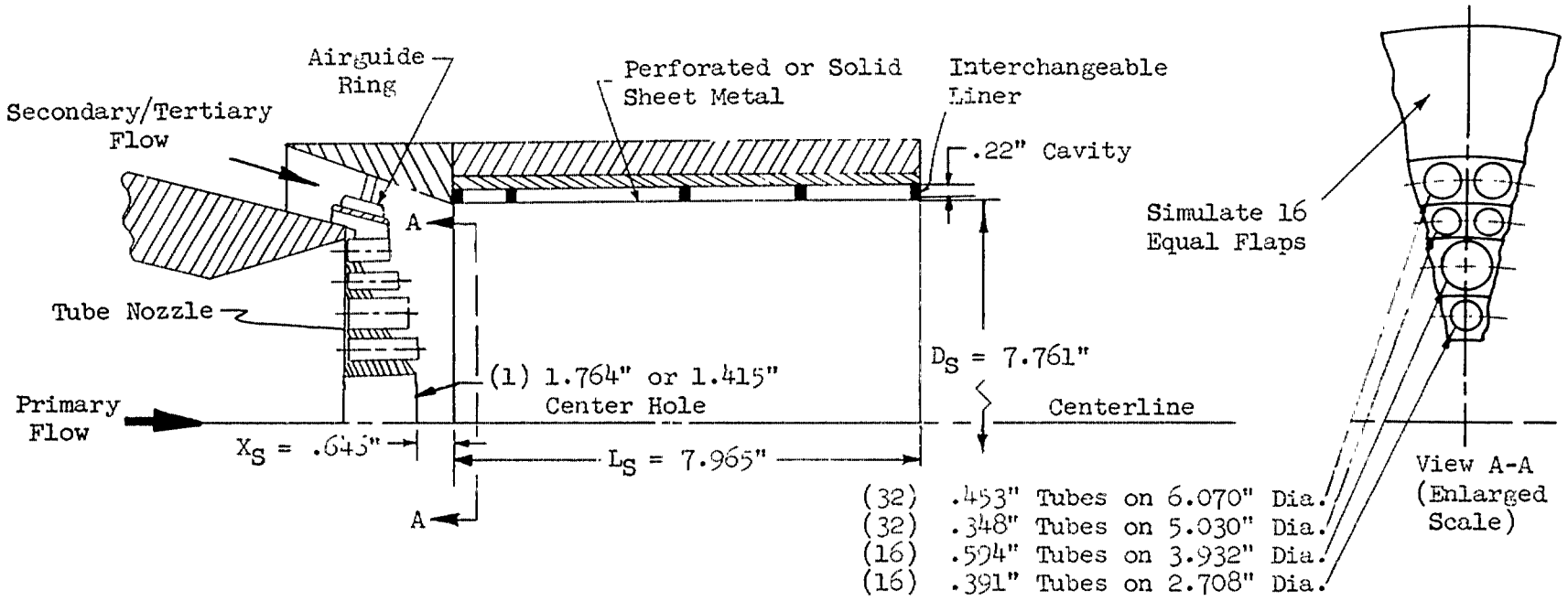

MODEL NO.	TEST DATE	DESCRIPTION
4.2T97	9-19-68	Primary with 1.764" Center Hole; No Ejector
4.2T97-1	9-27-68	Primary with 1.415" Center Hole; No Ejector
4.2T97-7.7CS	9-20-68	Primary with 1.764" Center Hole; Hardwall Ejector
4.2T97-7.7CS-1	9-23-68	Primary with 1.764" Center Hole; 7.5% Open Perforated-Lined Ejector

FIGURE V.F.7-3 SCHEMATIC OF 97 TUBE NOZZLE WITH HARDWALL AND ACOUSTICALLY TREATED EJECTOR

TABLE V.F.7-1 TEST SUMMARY

MODEL NO. 4.2T97

DESCRIPTION: 97 Tube Nozzle (15° Stagger), 1.764" I.D. Centerhole, AR_d = 2.0

DATE: 9/19/68

SCALE MODEL A_8 = .1180 ft^2

FULL SCALE A_8 = 7.552 ft^2

SCALE FACTOR = 8:1

- o DATA INCLUDES GROUND REFLECTION INTERFERENCE
- o ANGLE REFERENCED TO JET EXHAUST

	TEST CONDITIONS				ACOUSTIC TEST RESULTS						
			IDEAL			320' ARC		300' SIDELINE		1500' SIDELINE	
RDG NO.	P_{T8}/P_o	T_{T8} (°R)	V_j (ft/sec)	W_8 (PPS)	10 log ρA	PEAK PNdB	PEAK ANGLE	PEAK PNdB	PEAK ANGLE	PEAK PNdB	PEAK ANGLE
1	1.40	1140	1126	4.47	-5.2	111.1	40/50	110.2	70	92.2	70
2	1.53	1280	1329	4.71	-5.8	115.3	50	113.7	70	95.8	70
3	1.62	1320	1440	5.08	-5.9	116.9	30/40	116.2	70	98.2	70
4	2.01	1480	1807	5.56	-6.3	121.4	50	119.1	50	101.6	70
5	2.01	1960	2080	5.19	-7.5	126.3	50	124.0	50	107.0	50
6	1.99	2310	2248	4.43	-8.2	127.5	40	124.6	50	108.5	50
7	2.22	1520	1949	6.54	-6.2	126.3	40	122.6	50	106.4	50
8	2.45	1690	2166	6.82	-7.0	128.4	30/40	125.5	70	109.6	50
9	2.50	1490	2054	7.03	-5.9	128.0	30	124.4	50	108.2	50
10	2.50	1970	2363	6.33	-7.1	130.4	40	127.9	50	112.4	50
11	2.51	2301	2559	6.92	-7.8	131.7	50	129.6	50	114.1	50
12	3.00	2311	2778	7.56	-7.3	135.8	50	133.6	50	118.1	50
13	2.99	1980	2564	7.56	-7.3	133.8	50	131.7	50	116.2	50
14	3.01	1500	2237	8.75	-5.5	131.6	30	128.8	50	113.4	50
15	3.21	2305	2842	7.38	-7.2	136.9	50	134.7	50	119.2	50
16	3.40	2310	2906	7.82	-7.0	137.7	50	135.5	50	120.0	50
17	4.00	2310	3066	9.15	-6.5	140.4	50	138.3	50	122.6	50

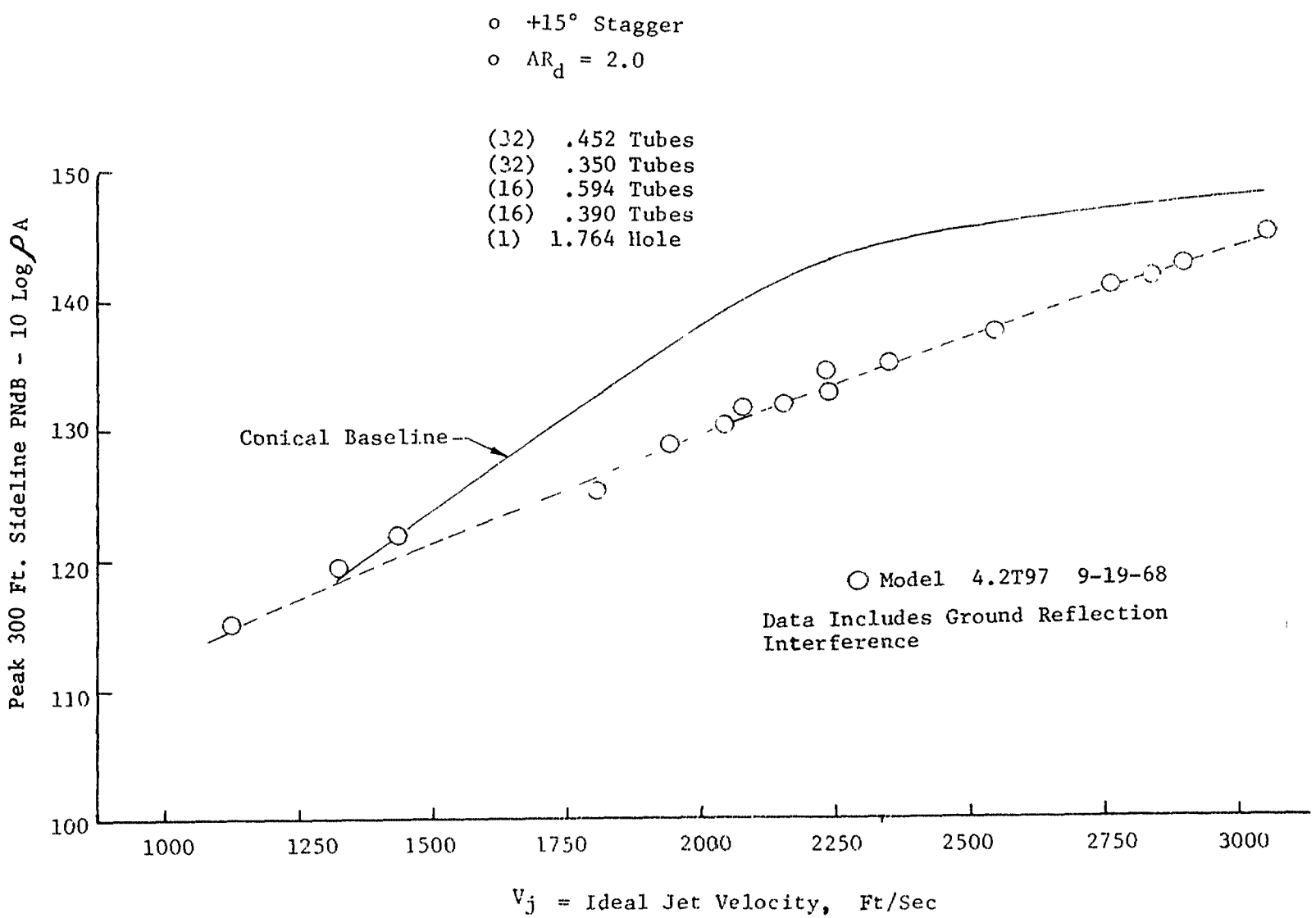

FIGURE V.F.7-4 300 FT SIDELINE JET NOISE LEVELS FOR A 97 TUBE NOZZLE WITH LARGE CENTERHOLE

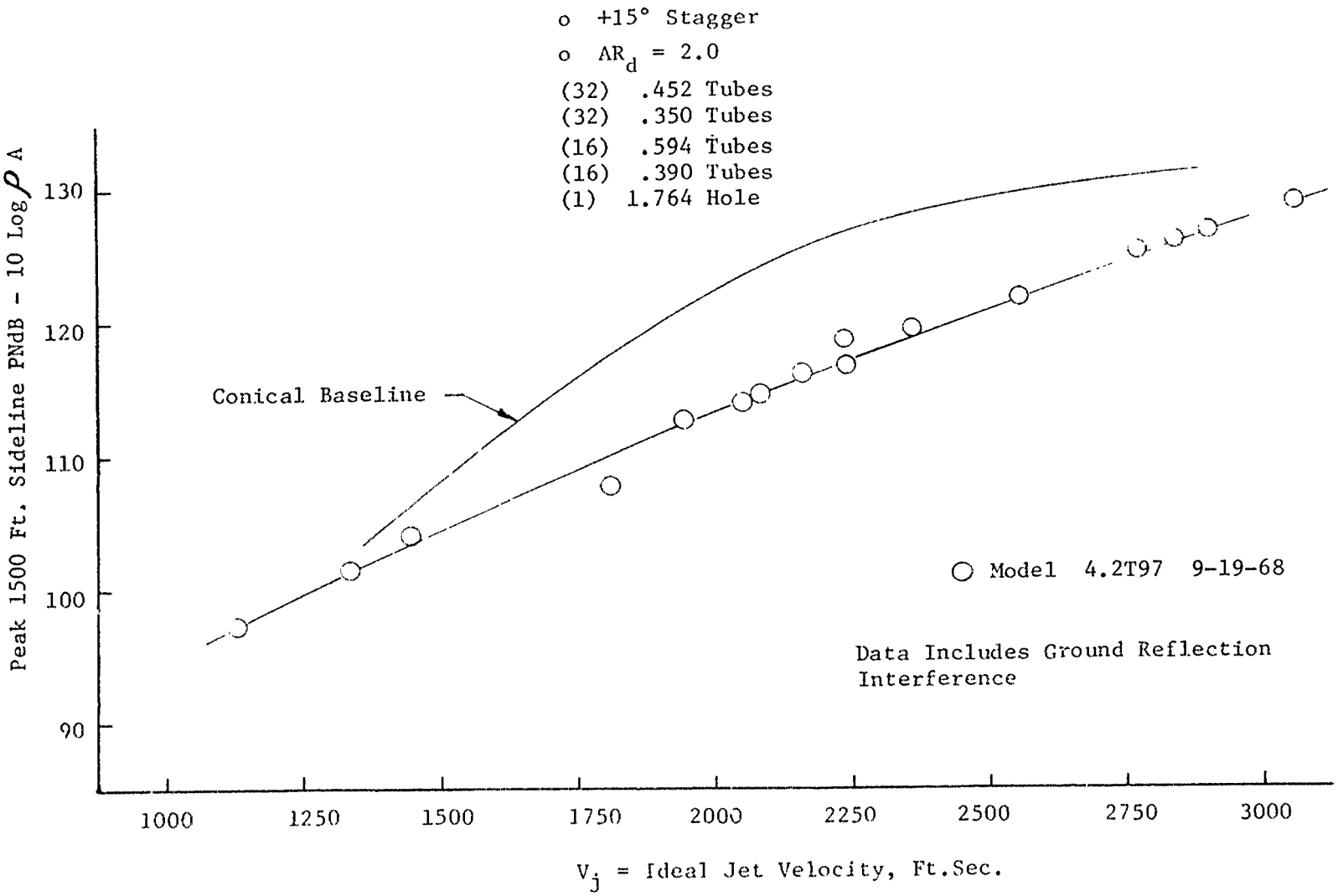

FIGURE V.F.7-5 1500 FT. SIDELINE JET NOISE LEVELS FOR A 97 TUBE NOZZLE WITH LARGE CENTERHOLE

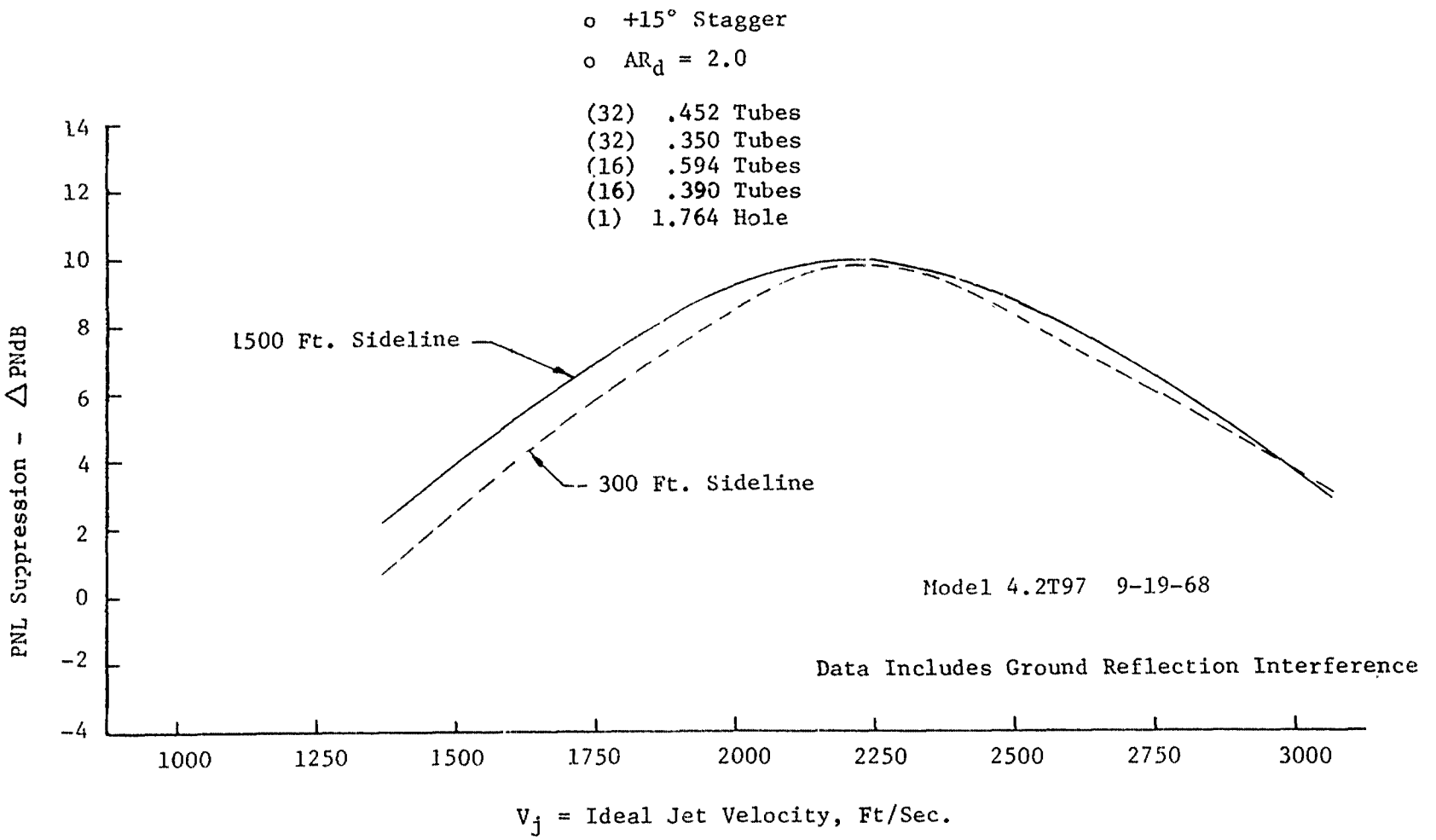

FIGURE V.F.7-6 300 FT. AND 1500 FT. SIDELINE PNL SUPPRESSIONS FOR A 97 TUBE NOZZLE WITH LARGE CENTERHOLE

TABLE V.F.7-2 TEST SUMMARY

MODEL NO. 4.2T97-1

DESCRIPTION: 97 Tube Nozzle (15° Stagger) 1.15" I.D. Centerhole, AR_d = 2.0

DATE: 9/27/68

SCALE MODEL A_8 = .1120 ft^2

FULL SCALE A_8 = 7.168 ft^2

SCALE FACTOR = 8:1

- o DATA INCLUDES GROUND REFLECTION INTERFERENCE
- o ANGLE REFERENCED TO JET EXHAUST

RDG NO.	TEST CONDITIONS				ACOUSTIC TEST RESULTS						
			IDEAL			320' ARC		300' SIDELINE		1500' SIDELINE	
	P_{T8}/P_o	T_{T8} (°R)	V_j (ft/sec)	W_8 (PPS)	10 log ρA	PEAK PNdB	PEAK ANGLE	PEAK PNdB	PEAK ANGLE	PEAK PNdB	PEAK ANGLE
1	1.40	1140	1120	4.26	-5.5	109.1	50	106.7	50	89.6	70
2	1.53	1270	1332	4.62	-6.0	113.8	50	111.4	50	93.9	70
3	1.64	1330	1458	4.88	-6.2	116.3	50	113.9	50	96.0	70
4	2.00	1505	1817	5.56	-6.6	121.7	50	119.3	50	101.5	70
5	2.00	1980	2087	4.92	-7.8	123.2	40	121.3	70	104.2	50
6	2.00	2310	2256	4.37	-8.5	125.4	50	123.1	70	106.6	50
7	2.20	1660	2025	5.83	-6.9	125.0	40	122.9	70	105.8	50
8	2.45	1715	2183	6.35	-6.8	125.8	40	123.5	50	108.0	50
9	2.50	1495	2058	6.18	-6.2	125.6	40	122.4	50	105.8	40
10	2.50	1965	2361	6.02	-7.3	128.3	40	125.2	50	109.8	50
11	2.50	2310	2560	5.46	-8.0	129.9	40	127.3	50	111.9	40
12	3.00	2310	2771	6.57	-7.6	133.1	50	130.9	50	115.6	50
13	3.00	1980	2568	7.20	-6.9	130.8	40	128.5	50	113.2	50
14	3.00	1495	2231	8.76	-5.7	128.8	40	125.2	50	109.8	50
15	3.19	2315	2844	6.94	-7.4	134.4	50	132.3	50	117.0	50
16	3.30	2310	2875	7.44	-7.3	135.2	50	133.1	50	117.7	50
17	3.99	2280	3043	8.74	-6.7	137.5	50	135.3	50	119.9	50

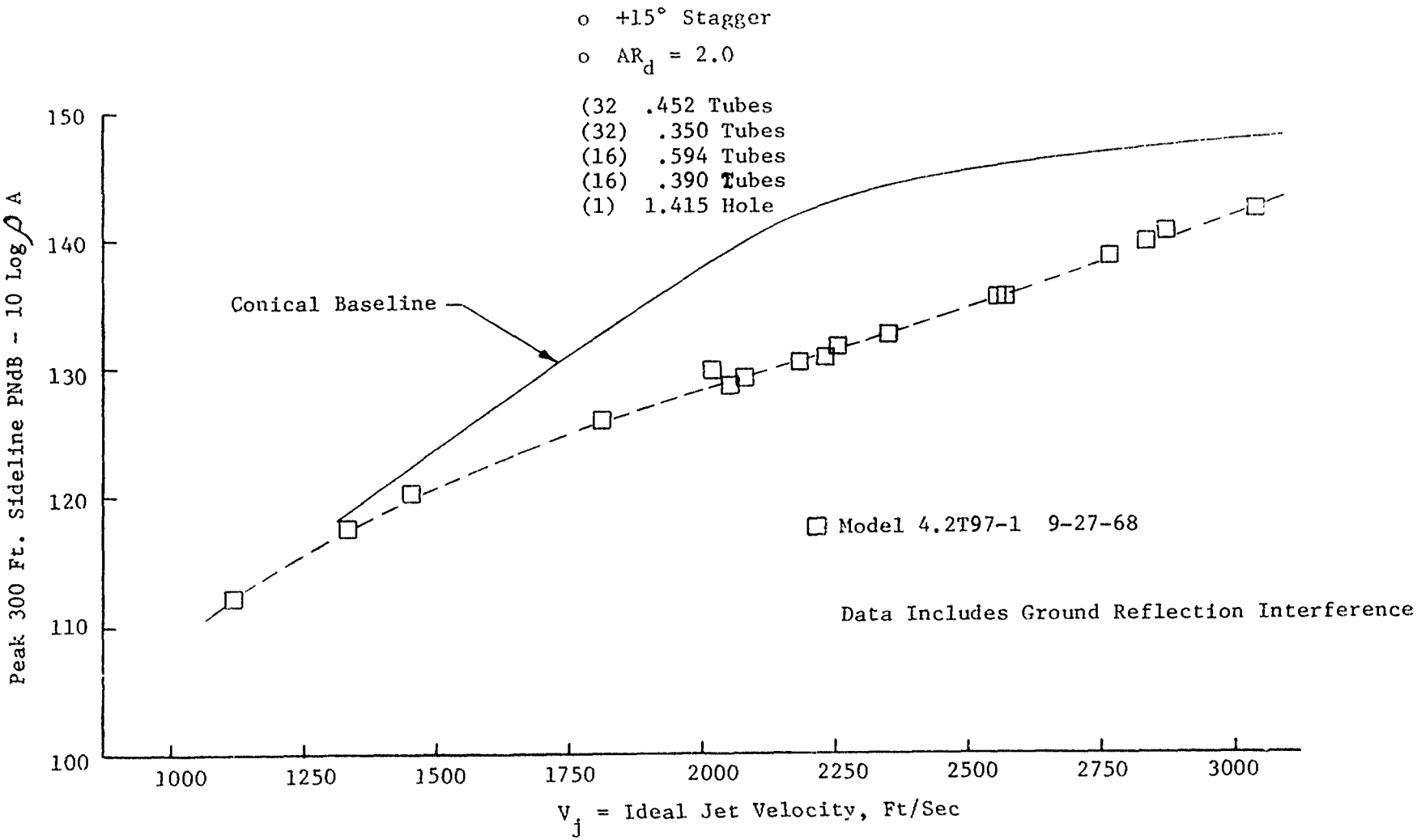

FIGURE V.F.7-7 300 FT. SIDELINE JET NOISE LEVELS FOR A 97 TUBE NOZZLE WITH SMALL CENTERHOLE

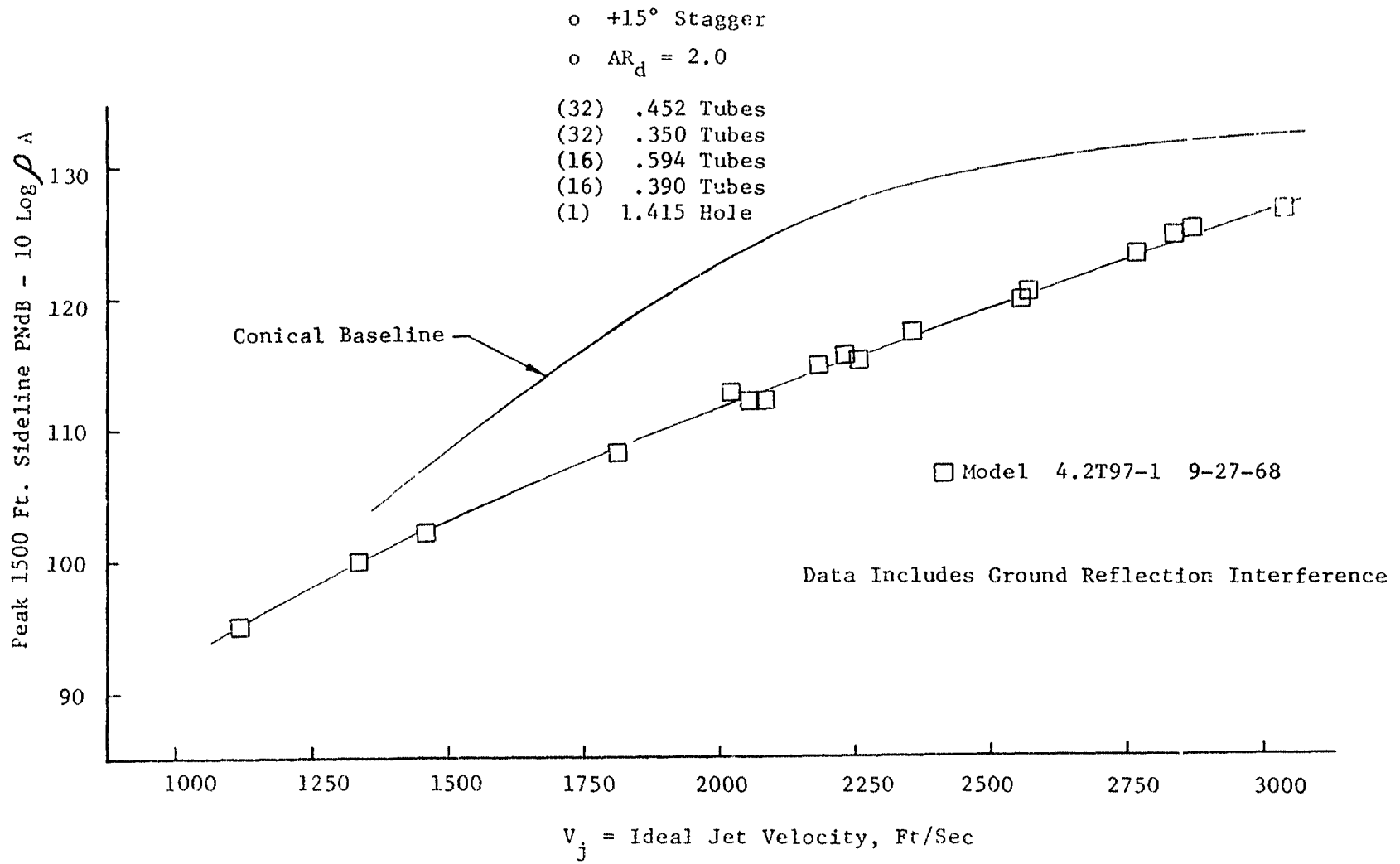

FIGURE V.F.7-8 1500 FT. SIDELINE JET NOISE LEVELS FOR A 97 TUBE NOZZLE WITH SMALL CENTERHOLE

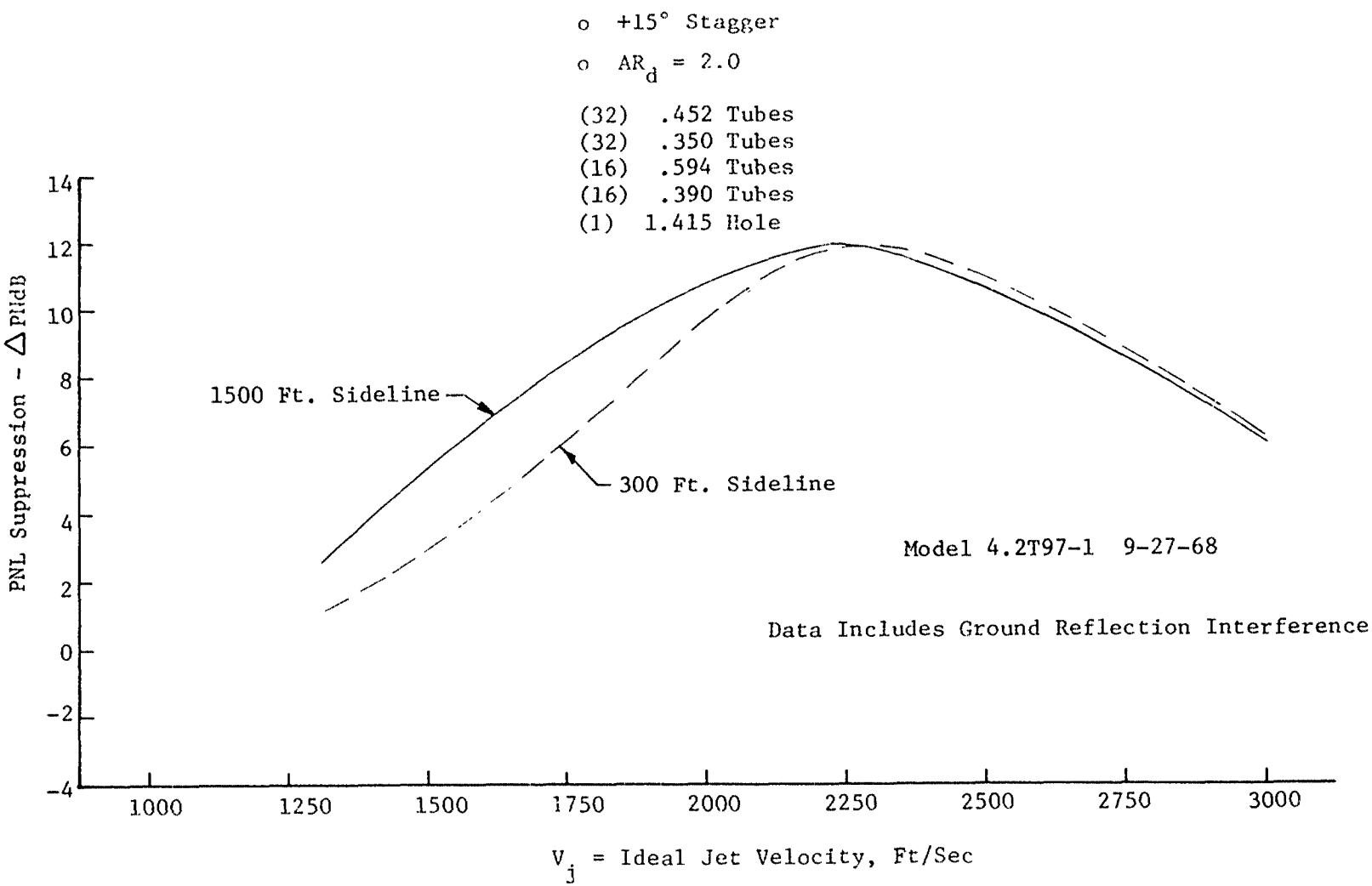

FIGURE V.F.7-9 300 FT. AND 1500 FT. SIDELINE PNL SUPPRESSIONS FOR A 97 TUBE NOZZLE WITH SMALL CENTERHOLE

TABLE V.F.7-3 TEST SUMMARY

NOTE NO. 4.2T97-7.7CS

DESCRIPTION: 97 Tube Primary (15° Stagger), 1.764" I.D. Centerhole, AR_d = 2.0; Hardwall Ejector.

DATE: 9-20-68

SCALE MODEL A_8 = .1180 ft^2

FULL SCALE A_8 = 7.552 ft^2

SCALE FACTOR = 8:1

- o DATA INCLUDES GROUND REFLECTION INTERFERENCE
- o ANGLE REFERENCED TO JET EXHAUST

	TEST CONDITIONS				ACOUSTIC TEST RESULTS						
			IDEAL			320' ARC		300' SIDELINE		1500' SIDELINE	
RUN NO.	P_{T8}/P_o	T_{T8} (°R)	V_j (ft/sec)	W_8 (PPS)	10 log ρA	PEAK PNdB	PEAK ANGLE	PEAK PNdB	PEAK ANGLE	PEAK PNdB	PEAK ANGLE
1	1.40	1180	1149	4.92	-5.3	110.1	50	109.7	70	91.8	70
2	1.54	1270	1336	4.87	-5.8	112.9	50	112.5	70	94.7	70
3	1.64	1320	1456	5.22	-5.9	115.0	70	115.0	70	97.2	70
4	1.99	1500	1811	5.90	-6.3	120.6	50	119.5	70	101.7	70
5	2.00	1960	2073	-	-7.5	123.0	50	122.4	70	104.7	70
6	2.00	2320	2258	4.58	-8.2	123.4	50	123.3	70	105.8	50
7	2.21	1620	2005	6.29	-6.5	122.6	50	121.6	70	104.4	50
8	2.46	1705	2178	6.83	-6.5	125.2	40	122.7	50	107.3	50
9	2.50	1500	2060	7.41	-5.9	124.5	50	122.3	50	107.0	50
10	2.50	1965	2358	6.36	-7.1	127.9	50	125.7	50	110.4	50
11	2.50	2300	2554	5.83	-7.8	129.1	50	127.0	50	111.9	50
12	3.01	2325	2786	7.03	-7.4	133.9	50	131.8	50	116.7	50
13	3.00	1965	2557	7.56	-6.6	131.9	50	129.8	50	114.7	50
14	3.01	1500	2236	8.82	-5.4	128.2	40	125.7	50	110.7	50
15	3.21	2300	2841	7.32	-7.1	134.5	50	132.3	50	117.2	50
16	3.41	2310	2909	7.76	-7.0	136.6	50	134.4	50	119.2	50
17	4.01	2305	3066	9.20	-6.5	140.6	50	138.4	50	122.9	50

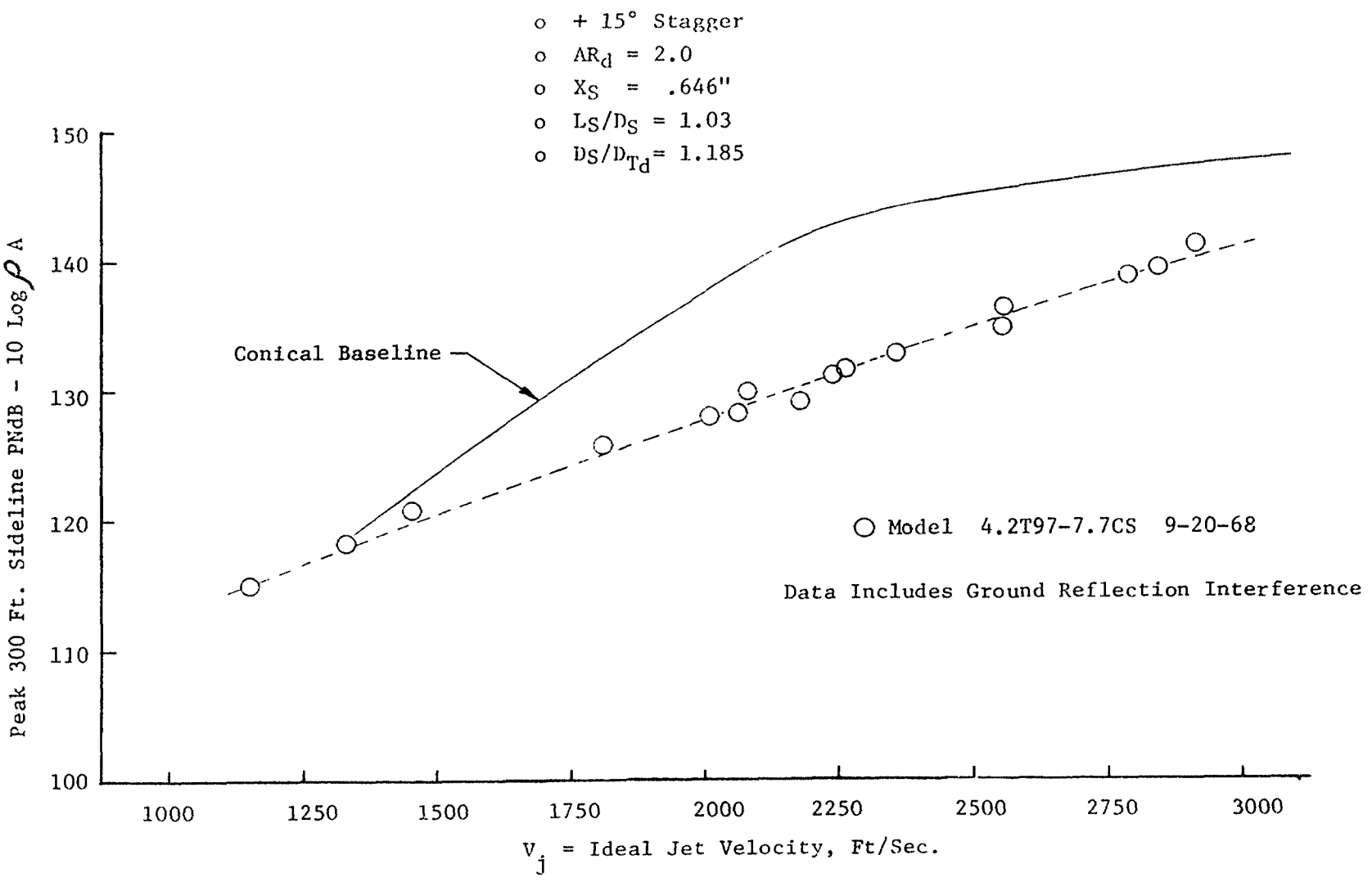

FIGURE V.F.7-10 300 FT. SIDELINE JET NOISE LEVELS FOR A 97 TUBE NOZZLE WITH LARGE CENTERHOLE PLUS HARDWALL EJECTOR

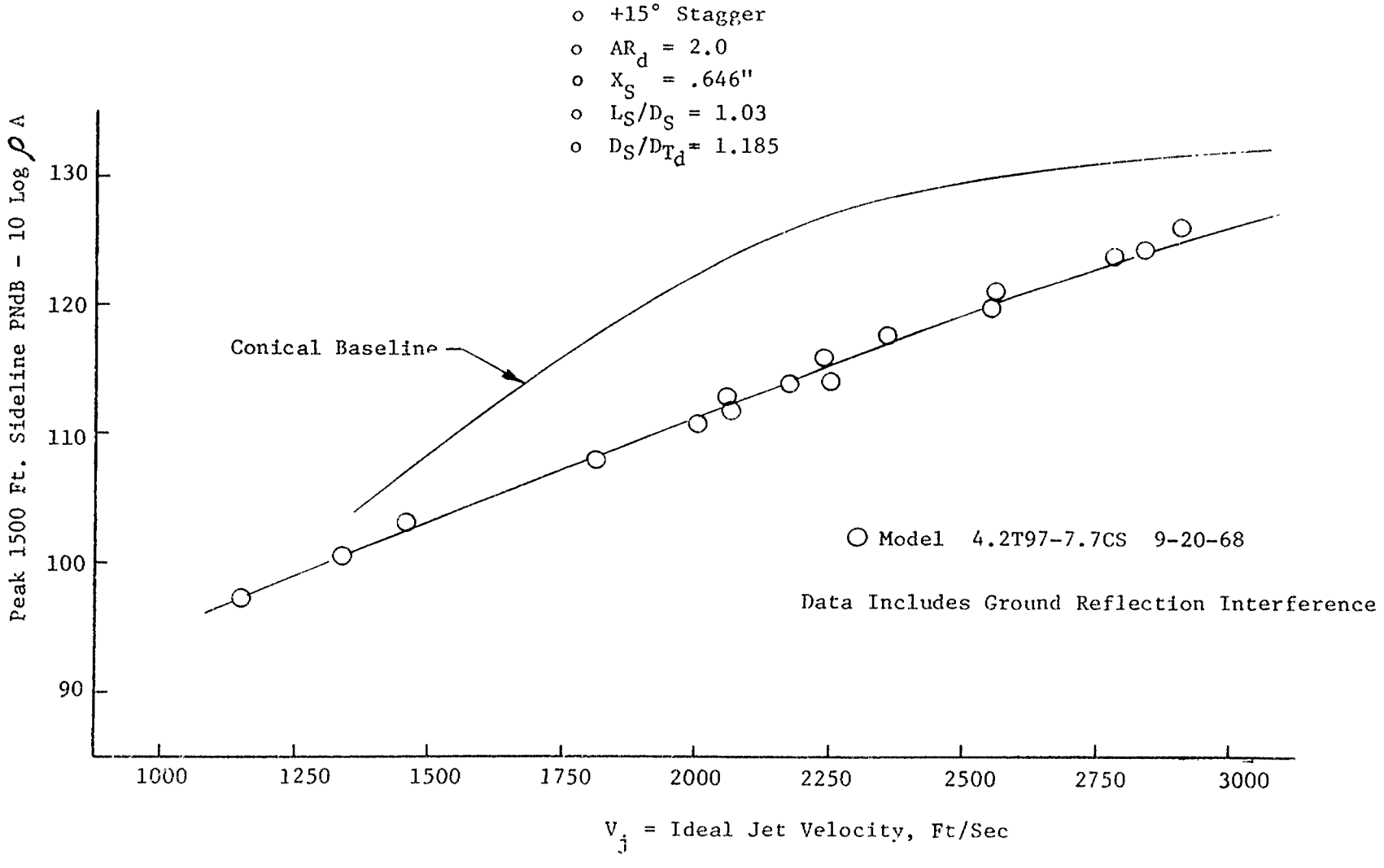

FIGURE V.F.7-11 1500 FT. SIDELINE JET NOISE LEVELS FOR A 97 TUBE NOZZLE WITH LARGE CENTERHOLE PLUS HARDWALL EJECTOR

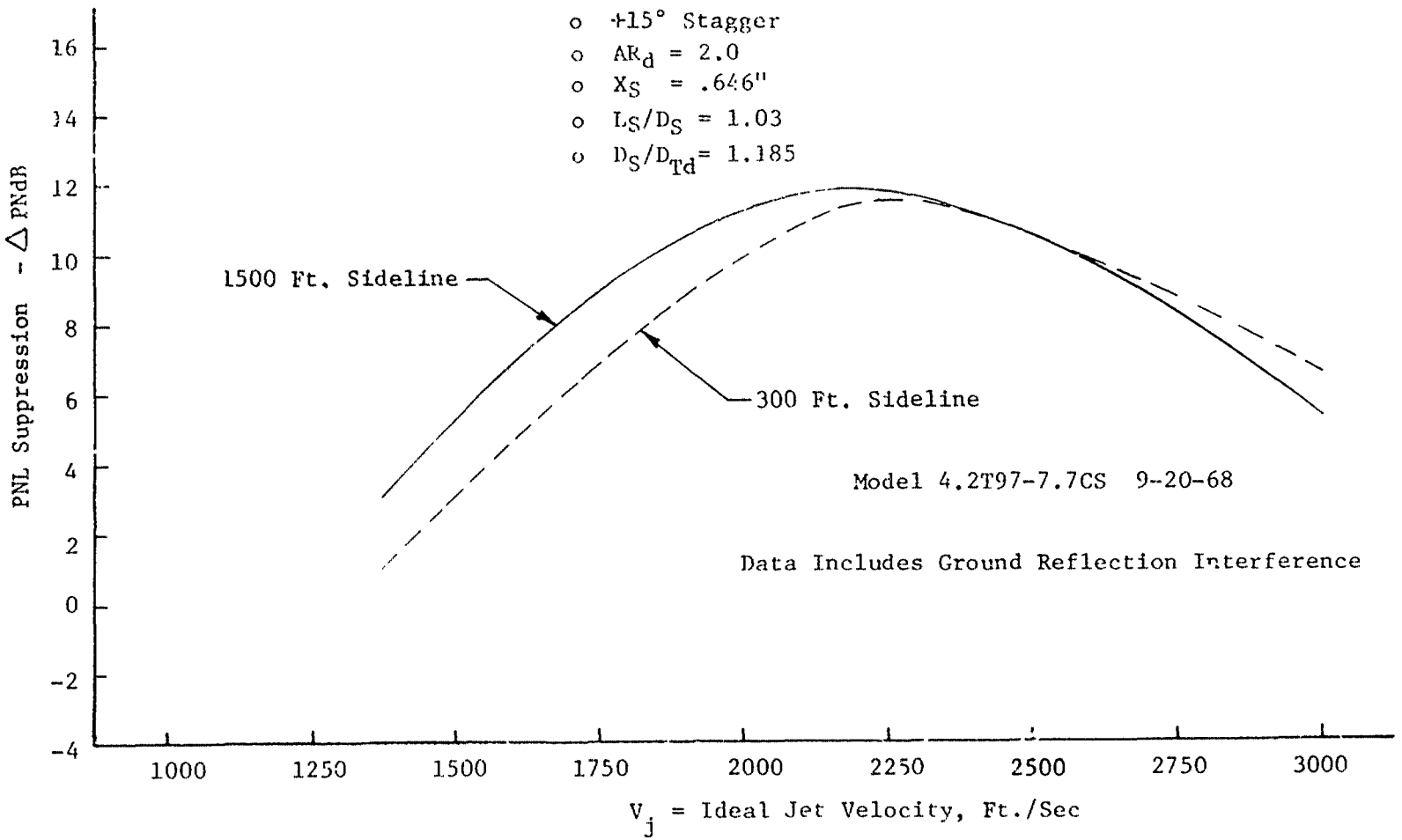

FIGURE V.F.7-12 300 FT. AND 1500 FT. SIDELINE PNL SUPPRESSIONS FOR A 97 TUBE NOZZLE WITH LARGE CENTERHOLE PLUS HARDWALL EJECTOR

TABLE V.E.7-4 TEST SUMMARY

MODEL NO. 4.2T97-7.7CS-1

DESCRIPTION: 97 Tube Primary (15° Stagger) 1.764" I.D. Centerhole, AR_d = 2.0. Perforated Lined Ejector 7.5% open

DATE: 9/23/68

SCALE MODEL A_8 = .1180 ft^2

FULL SCALE A_8 = 7.552 $ft.^2$

SCALE FACTOR = 8:1

o DATA INCLUDES GROUND REFLECTION INTERFERENCE

o ANGLE REFERENCED TO JET EXHAUST

RPG NO.	TEST CONDITIONS				ACOUSTIC TEST RESULTS						
			IDEAL			320' ARC		300' SIDELINE		1500' SIDELINE	
	P_{T8}/P_o	T_{T8} (°R)	V_j (ft/sec)	W_8 (PPS)	10 log ρA	PEAK PNdB	PEAK ANGLE	PEAK PNdB	PEAK ANGLE	PEAK PNdB	PEAK ANGLE
1	1.40	1140	1125	3.80	-5.2	107.5	70	107.5	70	89.7	70
2	1.62	1305	1433	5.21	-5.9	113.1	70	113.1	70	95.2	70
3	2.00	1990	2091	5.01	-7.5	120.8	40	119.5	70	103.3	50
4	1.99	1480	1797	5.86	-6.3	118.0	30	116.9	70	99.7	50
5	2.49	2310	2553	5.69	-7.8	127.9	50	125.8	50	110.9	50
6	3.00	2325	2782	6.85	-7.4	132.3	50	130.2	50	115.2	50
7	2.45	1710	2178	6.69	-6.5	124.7	40	122.2	50	107.0	50
8	2.49	1500	2057	7.38	-5.9	123.4	40	121.1	50	105.9	50
9	3.19	2315	2841	7.33	-7.2	134.1	50	131.9	50	116.9	50
10	2.99	1970	2558	7.52	-6.6	131.0	50	128.9	50	114.0	50

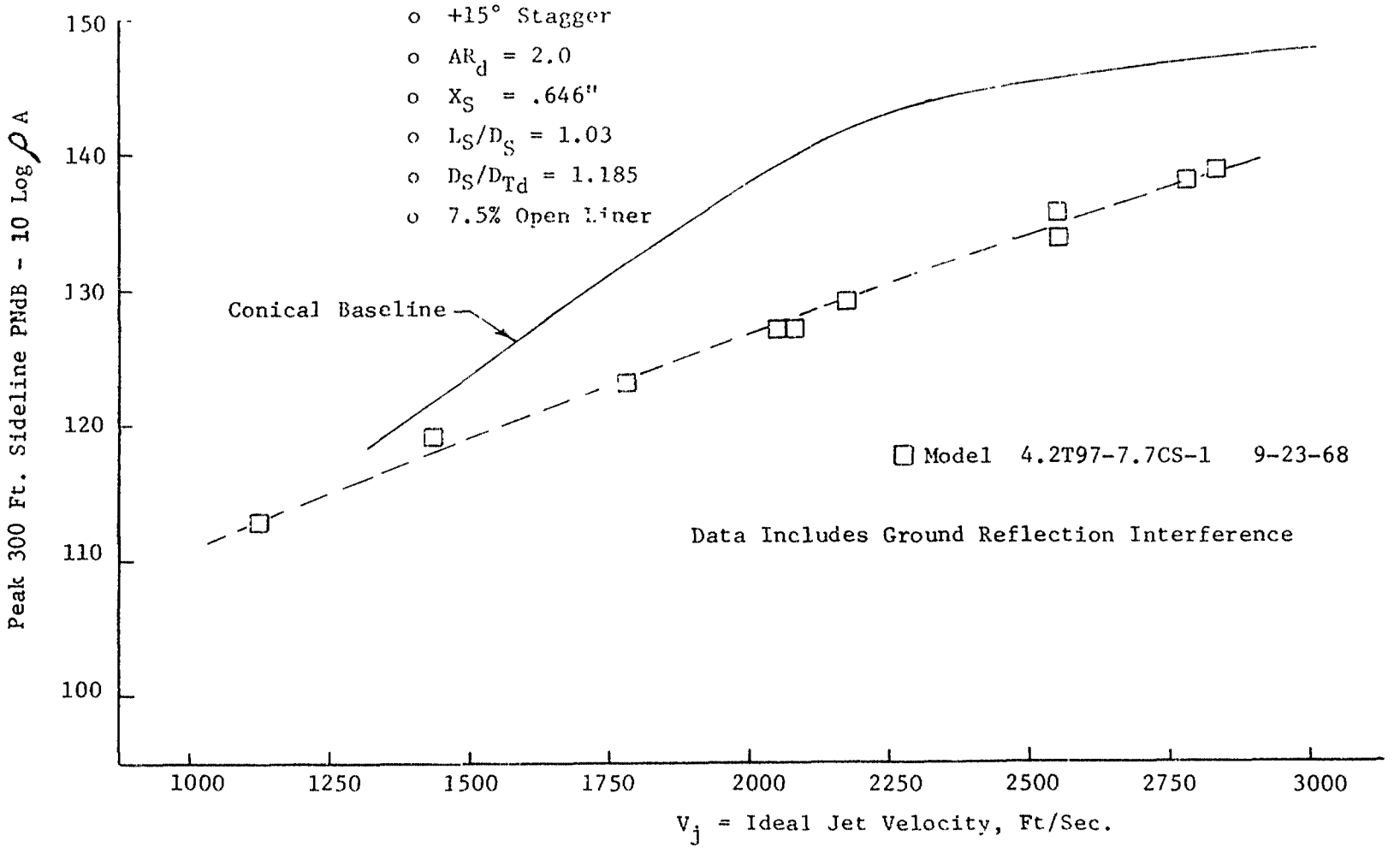

FIGURE V.F.7-13 300 FT. SIDELINE JET NOISE LEVELS FOR A 97 TUBE NOZZLE WIT' ARGE CENTERHOLE PLUS LINED EJECTOR

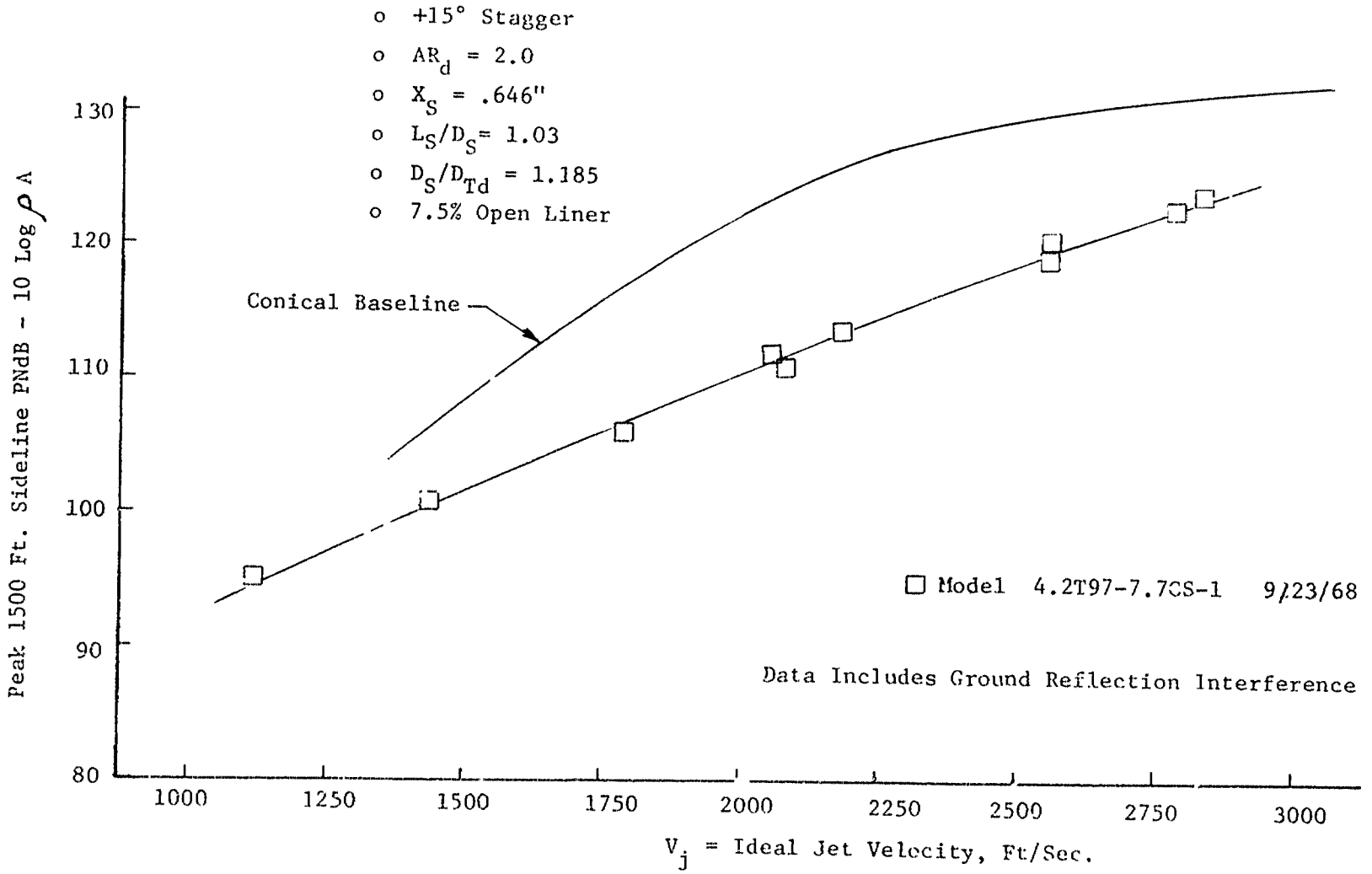

FIGURE V.F.7-14 1500 FT. SIDELINE JET NOISE LEVELS FOR A 97 TUBE NOZZLE WITH LARGE CENTERHOLE PLUS LINED EJECTOR

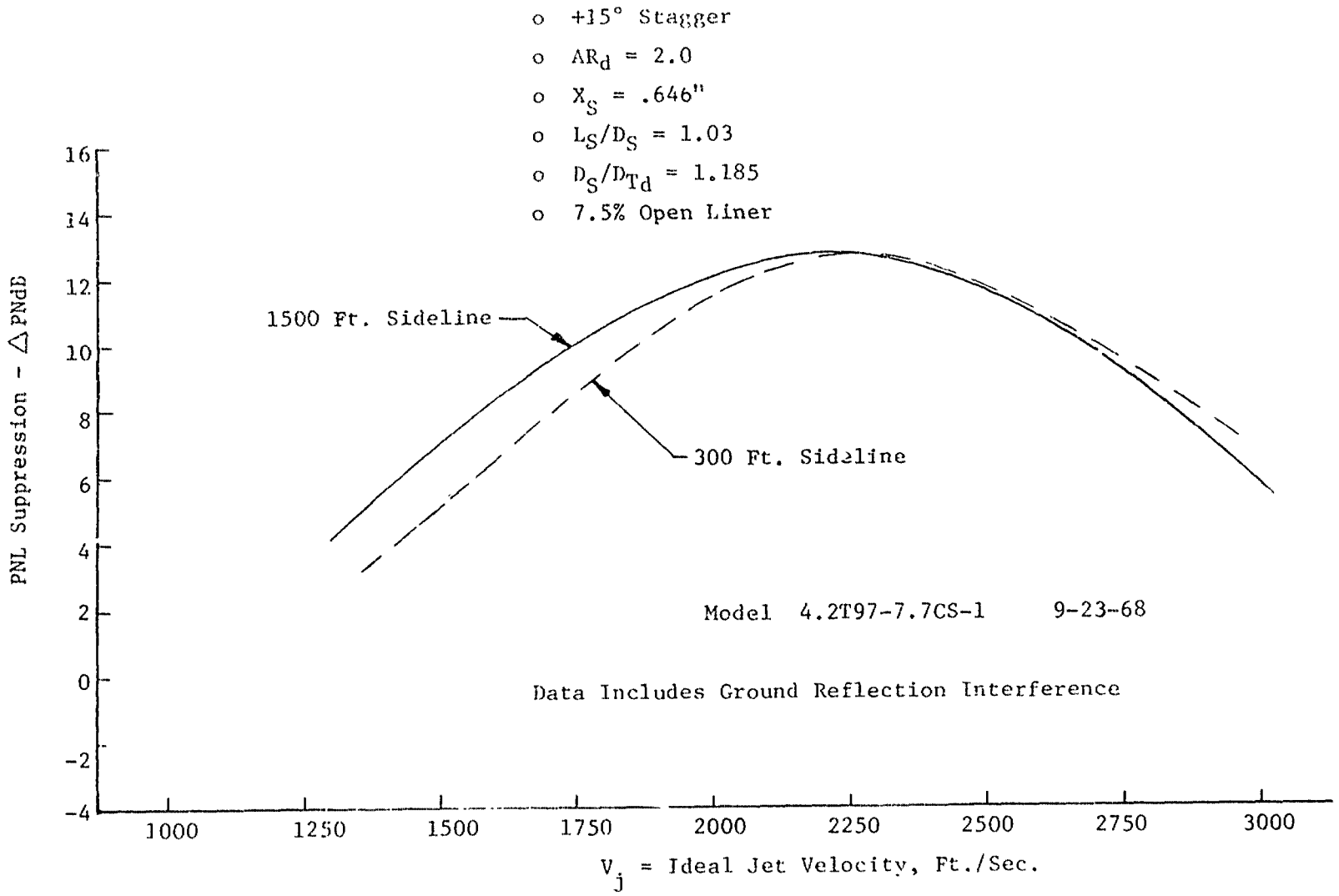

FIGURE V.F.7-15 300 FT. AND 1500 FT. SIDELINE PNL SUPPRESSIONS FOR A 97 TUBE NOZZLE WITH LARGE CENTERHOLE PLUS LINED EJECTOR

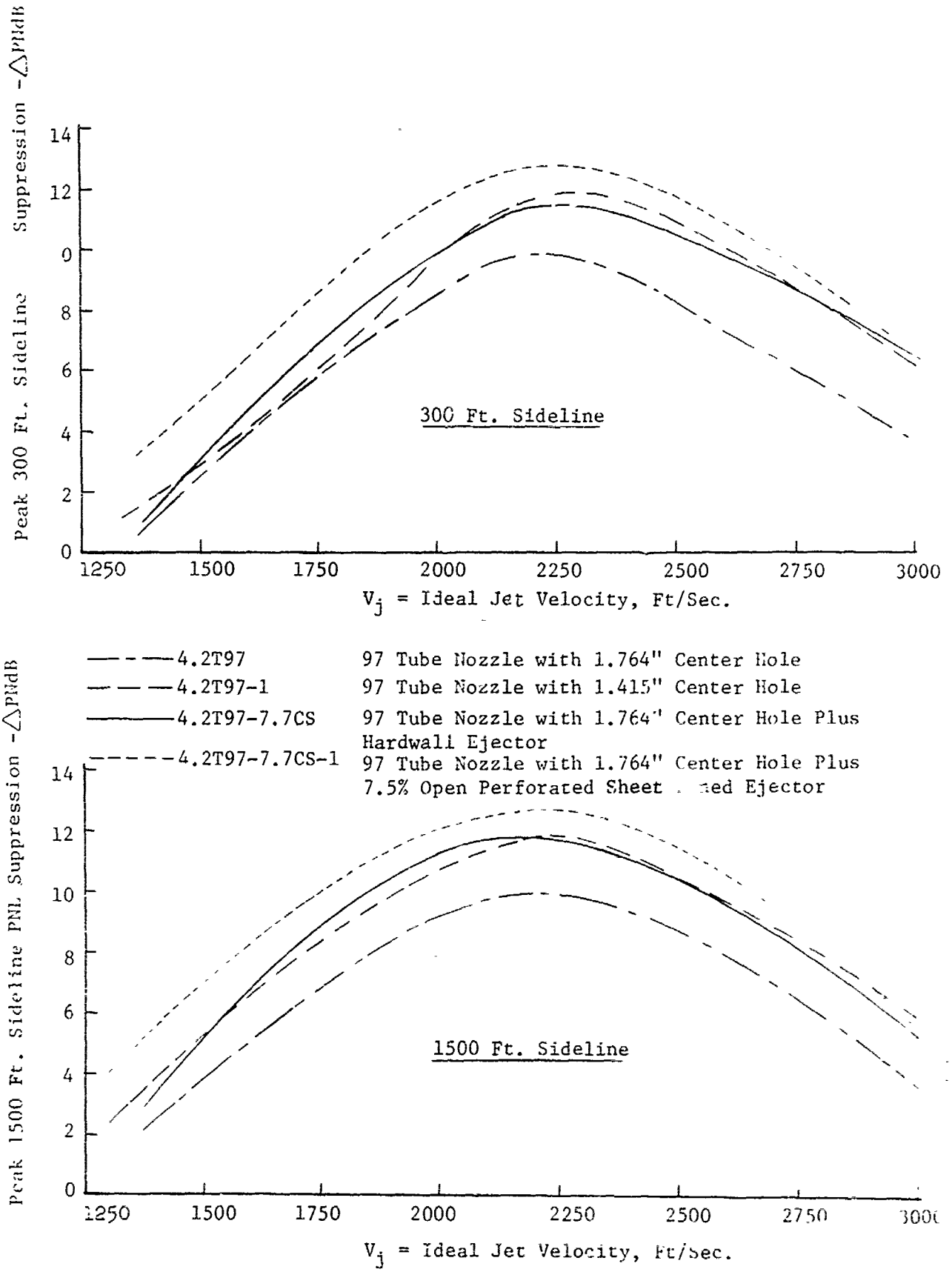

FIGURE V.F.7-16 COMPARISON OF PNL SUPPRESSIONS FOR VARIATIONS OF 97 TUBE NOZZLE

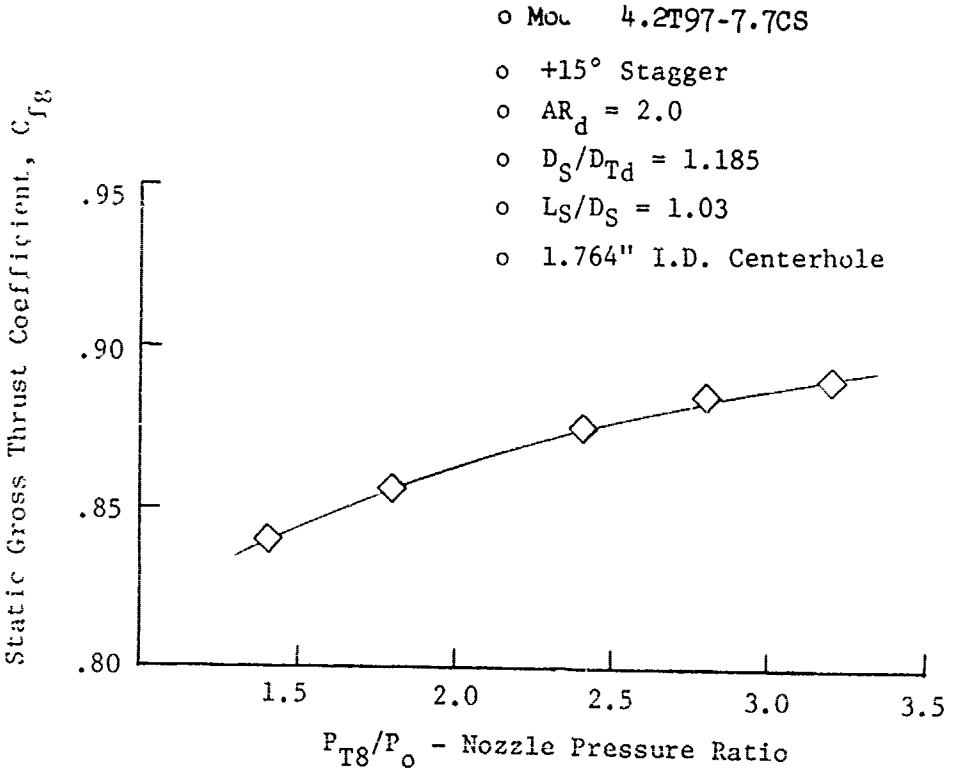

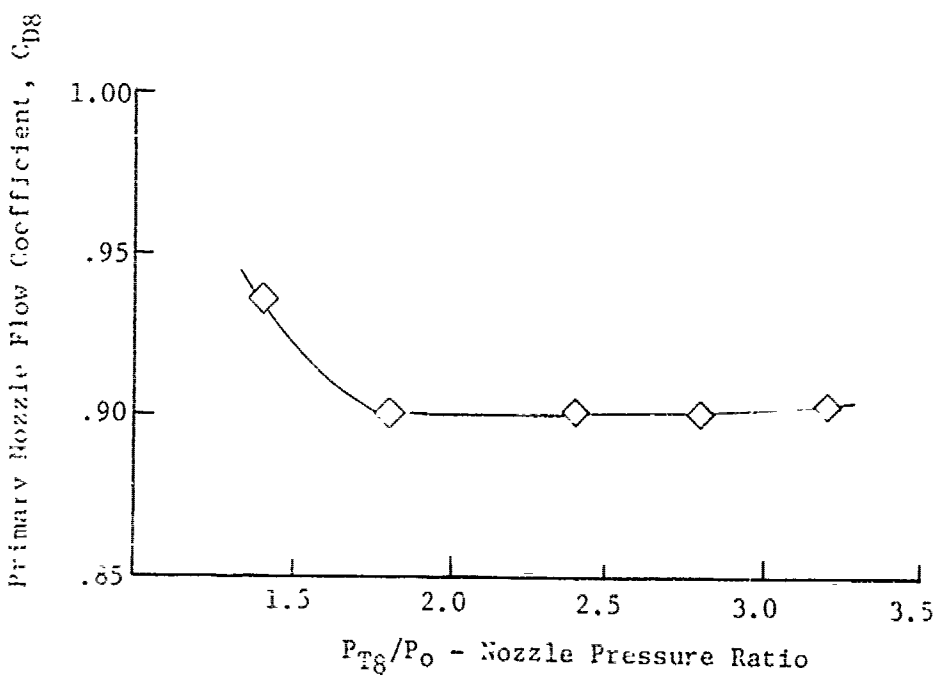

FIGURE V.F.7-17 AERODYNAMIC STATIC PERFORMANCE OF 97 TUBE NOZZLE WITH LARGE CENTERHOLE PLUS HARDWALL EJECTOR

V.F.8 GEOMETRIC VARIATIONS OF CENTER HOLE SHAPE ON 97 HOLE NOZZLES; HARDWALL AND ACOUSTICALLY LINED EJECTOR COMPARISONS; D_S/D_{Td} VARIATIONS

V.F.5 GEOMETRIC VARIATIONS OF CENTER HOLE SHAPE ON 97 HOLE NOZZLE; HARDWALL AND ACOUSTICALLY LINED EJECTOR COMPARISONS; D_S/D_{Td} VARIATIONS

Objectives of Test Series

Before an extensive test series planned for the 97 tube primary nozzle of Section V.F.7 was complete, the nozzle failed. It was replaced with a similar nozzle, designated the 97 hole nozzle as shown schematically in Figure V.F.8-1, and the planned tests were continued. Specific objectives of this test series were:

a) To determine the acoustic effect of replacing the nozzle center hole with a convoluted (Greatrex) center.

b) To establish the effect of adding a hardwall cylindrical secondary ejector to the 97 hole primary.

c) To establish acoustic suppression dependency on the ratio of ejector internal diameter to circumscribed tube bundle diameter, D_S/D_{Td}.

d) To investigate the efficiency of a series of acoustically treated liners within the cylindrical secondary ejector. The comparative results of the treated versus hardwall ejectors are discussed in more detail in Section V.G, "Acoustic Ejectors on Multi-Tube and Conical Nozzles". The absolute noise levels and total system suppressions are found in this section.

Acoustic tests were performed at the GE, Evendale, JENOTS facility. Measurements were taken on a 40 ft. arc at 10° increments from 30° through 90° from the jet exhaust axis and over a frequency range to 40 KHz (31.5 KHz octave band). The data were scaled to full scale engine application using a scale factor of 8:1 for frequency, nozzle size and measuring arc. Therefore, all data are presented as simulated engine size and frequency range.

The acoustic tests were conducted over a simulated engine running line with P_{T8}/P_o from 1.4 to 3.4, T_{T8} from 1250 to 2340° R, and V_J from 1150 to 2930 ft/sec.

A 4.32" D_8 conical nozzle was used as the unsuppressed reference to establish baseline acoustic curves.

PRECEDING PAGE BLANK-NOT FILMED

Test Configurations

Nine model suppressor configurations were tested using variations around the 97 hole primary and cylindrical secondary system as shown in Figure V.F.8-1. The basic 97 hole nozzle configuration was identical to the 97 tube nozzle (Section V.F.7, Figures V.F.7-1, -2 and -3) in area ratio, hole size and spacing, internal tube length, and tube exit plane stagger; but was a thick baseplate design with no external tube length. The model simulated a full scale design in which 16 flaps, on which the tubes were mounted, would be deployed to form the suppressor system. The round center hole remained after the flaps joined together (Model 4.2H97N-1). The convoluted (Greatrex) center simulated a set of uneven flap lengths, 8 of the 16 flaps projecting deeper into the central area (Model 4.2H97N-2).

For the study of shroud diameter effect, three hardwall cylindrical ejectors of 7.357", 7.554", and 7.76" I.D.'s were used. These were designated Models 4.2H97N-CS-2, 4.2H97N-CS-3 and 4.2H97N-CS with D_S/D_{Td}'s of 1.125, 1.155, and 1.185, respectively.

For the acoustically treated ejector study, the D_S/D_{Td} of 1.185 ejector was used, replacing the removable hardwall section with acoustic liners. Four liners were used, the first three consisting of porous sheet metal of 4%, 7.5%, and 15% open area with 0.22" cavity depth. These are designated as Models 4.2H97N-CS-4, 4.2H97N-CS-1, and 4.2H97N-CS-5, respectively. The fourth configuration, Model 4.2H97N-CS-6 used 22.5% porous plate and with the cavity packed with Cerafelt.

Presentation of Data

The baseline conical nozzle test results are summarized in Table V.F.8-1 and plotted as 300 and 1500 ft. sidelines peak normalized PNL plots as a function of jet velocity in Figures V.F.8-2 and -3. The conical baseline was tested on each day of suppressor nozzle testing. The average baseline curves of Figures V.F.8-2 and -3 are somewhat biased at low jet velocity by previous test results. The curves are duplicated on each of the suppressor data plots and referenced to for quoting suppression levels.

For each of the suppressor models, in order of their listing on Figure V.F.8-1, acoustic test results are included as a) tabular form, b) 300 and 1500 ft. sidelines

peak normalized PNL plots as a function of jet velocity, and c) 300 and 1500 ft. sidelines peak normalized PNL suppression curves, as follows:

Model No.	Table	Figures
4.2H97N-1	V.F.8-2	V.F.8-4, -5, and -6
4.2H97N-2	V.F.8-3	V.F.8-7, -8, and -9
4.2H97N-CS-2	V.F.8-4	V.F.8-10, -11, and -12
4.2H97N-CS-3	V.F.8-5	V.F.8-13, -14, and -15
4.2H97N-CS	V.F.8-6	V.F.8-16, -17, and -18
4.2H97N-CS-4	V.F.8-7	V.F.8-19, -20, and -21
4.2H97N-CS-1	V.F.8-8	V.F.8-22, -23, and -24
4.2H97N-CS-5	V.F.8-9	V.F.8-25, -26, and -27
4.2H97N-CS-6	V.F.8-10	V.F.8-28, -29, and -30

Discussion of Test Results

Composites of the individual suppression curves are included as Figures V.F.8-31 through -35 to evaluate the test series objectives. Figure V.F.8-31 compares the round center hole to the Greatrex center, showing that by segmenting the center slug of jet flow, approximately 2 PNdB additional suppression is gained across the tested jet velocity range.

For the effect of hardwall ejector addition and D_S/D_{Td} ratio of the hardwall ejector, comparisons are in Figures V.F.8-32 and -33. The comparison indicates that nominally from 1 to 2 PNdB additional suppression can be gained with the hardwall ejector, the magnitude of gain being greatest for the small shroud D_S/D_{Td} of 1.125. A maximum suppression level between 13 and 14 PNL is seen near 2250 ft/sec jet velocity.

Figures V.F.8-34 and -35 summarize the effects of the acoustically treated ejectors in comparison to the hardwall ejector of D_S/D_{Td} = 1.185. The purpose of presenting these models' data was to show the absolute suppression levels attained by the total nozzle systems. Effect of the treatment alone, with respect to the hardwall ejector, is discussed more thoroughly in Section V.G. Reference to Figures V.F.8-34 and -35, however, shows negligible change due to acoustic lining. As pointed out in Section V.G, this is attributable to the particular primary nozzle configuration generating the major noise aft of the shroud exit plane, past the acoustic treatment. The low suppression gain does not imply a poor treatment design.

MODEL NO.	TEST DATE	CENTER HOLE	SECONDARY	D_S	D_S/D_{Td}	L_S/D_S
4.2H97N-1	1-13-69	Round	--	--	--	--
4.2H97N-2	11-25-68	Greatrex	--	--	--	--
4.2H97N-CS-2	12-2-68	Greatrex	Hardwall	7.357"	1.125	1.082
4.2H97N-CS-3	12-4-68	Greatrex	Hardwall	7.554"	1.155	1.052
4.2H97N-CS	11-29-68	Greatrex	Hardwall	7.76"	1.185	1.03
4.2H97N-CS-4	1-14-69	Greatrex	4% Open Liner	7.76"	1.185	1.03
4.2H97N-CS-1	11-22-68	Greatrex	7.5% Open Liner	7.76"	1.185	1.03
4.2H97N-CS-5	1-20-69	Greatrex	15% Open Liner	7.76"	1.185	1.03
4.2H97N-CS-6	2-13-69	Greatrex	22.5% Open + Cerafelt Packed	7.76"	1.185	1.03

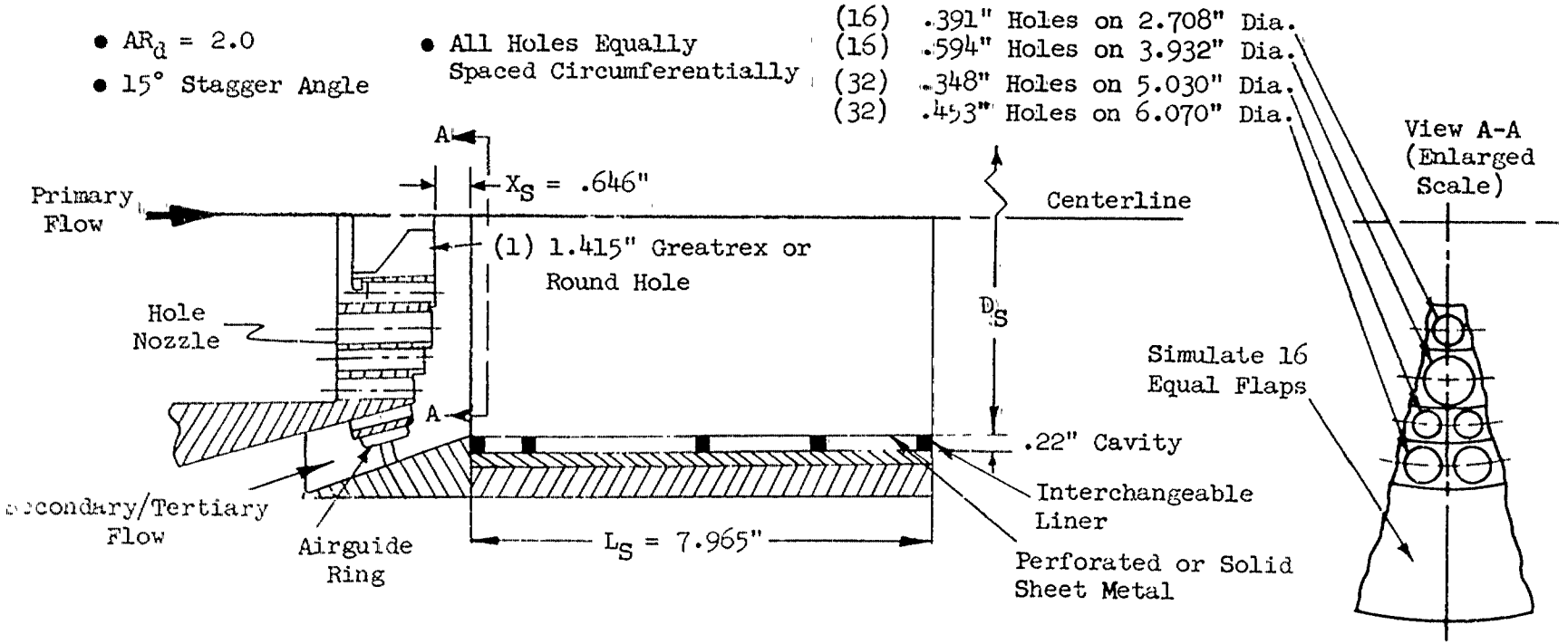

FIGURE V.F.8-1 SCHEMATIC OF 97 HOLE NOZZLE WITH HARDWALL AND ACOUSTICALLY TREATED EJECTOR

TABLE V.F.8-1 TEST SUMMARY

MODEL NO. 4.3"Cone

DESCRIPTION: Baseline 4.32" I.D. Conical Nozzle

DATE: 11/29/68; 1/14/69

SCALE MODEL A_8 = .1020 ft^2

FULL SCALE A_8 = 6.528 ft^2

SCALE FACTOR = 8:1

- o DATA INCLUDES GROUND REFLECTION INTERFERENCE
- o ANGLE REFERENCED TO JET EXHAUST

RUN NO.	TEST CONDITIONS				ACOUSTIC TEST RESULTS						
			IDEAL			320' ARC		300' SIDELINE		1500' SIDELINE	
	P_{T8}/P_o	T_{T8} (°R)	V_j (ft/sec)	W_8 (PPS)	10 log ρA	PEAK PNdB	PEAK ANGLE	PEAK PNdB	PEAK ANGLE	PEAK PNdB	PEAK ANGLE
11/29/68											
1	1.64	1334	1460	4.19	-6.6	122.0	30	118.2	50	102.8	50
2	2.01	2329	2272	4.08	-8.8	136.4	50	134.2	50	118.4	50
3	2.22	1665	2041	5.56	-7.2	135.6	50	133.4	50	117.7	50
4	2.49	1505	2062	6.68	-6.5	137.1	50	134.9	50	119.3	50
5	3.23	2318	2857	6.81	-7.8	141.3	50	139.3	60	123.5	50
6	3.01	1516	2249	8.24	-6.1	139.7	50	137.5	50	121.7	50
1/14/69											
1	1.63	1321	1449	4.19	-6.6	121.0	40	117.7	50	102.4	50
2	2.00	1906	2045	4.82	-8.0	135.1	50	132.9	50	117.1	50
3	2.50	2312	2559	6.37	-8.4	138.9	50	137.5	60	121.0	50/60
4	3.00	2252	2734	6.31	-7.8	140.5	50	139.4	60	122.9	60

TABLE V.F.8-1 TEST SUMMARY
(Continued)

MODEL NO. 4.3" Cone

DESCRIPTION: Baseline 4.32" I.D. Conical Nozzle

DATE: 11/22/68; 1/20/69 ; 2/13/69

SCALE MODEL A_8 = .1020 ft^2

FULL SCALE A_8 = 6.528 ft^2

SCALE FACTOR = 8:1

- o DATA INCLUDES GROUND REFLECTION INTERFERENCE
- o ANGLE REFERENCED TO JET EXHAUST

	TEST CONDITIONS				ACOUSTIC TEST RESULTS						
			IDEAL			320' ARC		300' SIDELINE		1500' SIDELINE	
RUN NO.	P_{T8}/P_o	T_{T8} (°R)	V_j (ft/sec)	W_8 (PPS)	10 log ρA	PEAK PNdB	PEAK ANGLE	PEAK PNdB	PEAK ANCLE	PEAK PNdB	PEAK ANGLE
11/22/68											
1	3.02	1541	2270	8.00	-6.2	138.7	50	136.5	50	120.8	50
2	2.52	1497	2067	6.74	-6.6	135.4	50	133.2	50	117.5	50
3	2.01	1491	1816	5.34	-7.0	130.7	40	126.6	50	111.2	40/50
4	2.21	1661	2029	5.59	-7.3	134.3	50	132.2	50	116.6	50
5	2.53	1935	2353	5.99	-7.7	138.0	50	135.8	50	120.2	50
6	3.22	2325	2862	6.95	-7.8	140.1	50	138.9	60	122.8	60
1/20/69											
1	2.00	2318	2258	3.90	-8.0	137.8	50	135.6	50	119.7	50
2	2.50	2312	2558	5.00	-7.6	139.7	50	137.5	50	121.7	50
2/13/69											
1	2.51	1984	2375	5.91	-7.2	138.4	50	136.1	50	120.1	50
2	3.26	2312	2864	6.94	-7.7	140.4	60	139.5	60	123.5	60
3	3.03	1974	2573	7.03	-7.3	140.1	50	137.9	50	122.1	50
4	2.44	1732	2188	6.11	-7.2	138.5	50	136.2	50	119.9	50

TABLE V.1.8-1 TEST SUMMARY
(Continued)

MODEL NO. 4.3" Cone

DESCRIPTION: Baseline 4.32" I.D. Conical Nozzle

DATE: 1/13/69; 11/25/68; 12/2/68; 12/4/68

SCALE MODEL A_8 = .1020 ft^2

FULL SCALE A_8 = 6.528 ft^2

SCALE FACTOR = 8:1

- o DATA INCLUDES GROUND REFLECTION INTERFERENCE
- o ANGLE REFERENCED TO JET EXHAUST

RDG NO.	TEST CONDITIONS				ACOUSTIC TEST RESULTS						
		IDEAL				320' ARC		300' SIDELINE		1500' SIDELINE	
	P_{T8}/P_o	T_{T8} (°R)	V_j (ft/sec)	W_8 (PPS)	10 log ρA	PEAK PNdB	PEAK ANGLE	PEAK PNdB	PEAK ANGLE	PEAK PNdB	PEAK ANGLE
1/13/69											
1	1.40	1203	1153	3.48	-5.6	112.7	50/30	110.7	50/60	94.7	50
2	1.63	1324	1448	4.17	-6.2	122.5	30	118.9	50	103.3	50
11/25/68											
1	1.53	1295	1341	3.90	-6.5	118.5	30	115.2	60	99.6	50
2	2.51	2325	2571	5.21	-8.4	139.4	50	137.5	60	121.6	50
3	3.39	2318	2904	7.14	-7.2	146.1	40	142.0	40	126.7	40
12/2/68											
1	2.54	2015	2406	5.43	-7.8	138.9	50	136.7	50	121.0	50
2	3.02	2320	2786	6.25	-8.0	140.4	60	139.6	60	123.6	60
3	2.43	1743	2212	5.84	-7.2	137.9	50	135.7	50	120.0	50
4	3.03	2034	2614	6.87	-7.4	140.5	50	138.3	60	122.6	50
5	2.02	1539	1849	5.02	-6.7	132.8	40	129.0	50	113.5	50
12/4/68											
1	2.52	1984	2379	5.76	-7.8	137.8	60	137.0	60	120.7	60
2	3.42	2337	2930	7.21	-7.7	141.3	50	140.4	60	124.5	60
3	3.03	2315	2787	6.44	-8.0	140.2	50	138.6	60	122.6	60
4	2.53	2319	2577	5.41	-8.5	138.9	50	137.1	60	121.2	60
5	2.02	1979	2101	4.78	-8.2	135.5	50	133.3	50	117.7	50

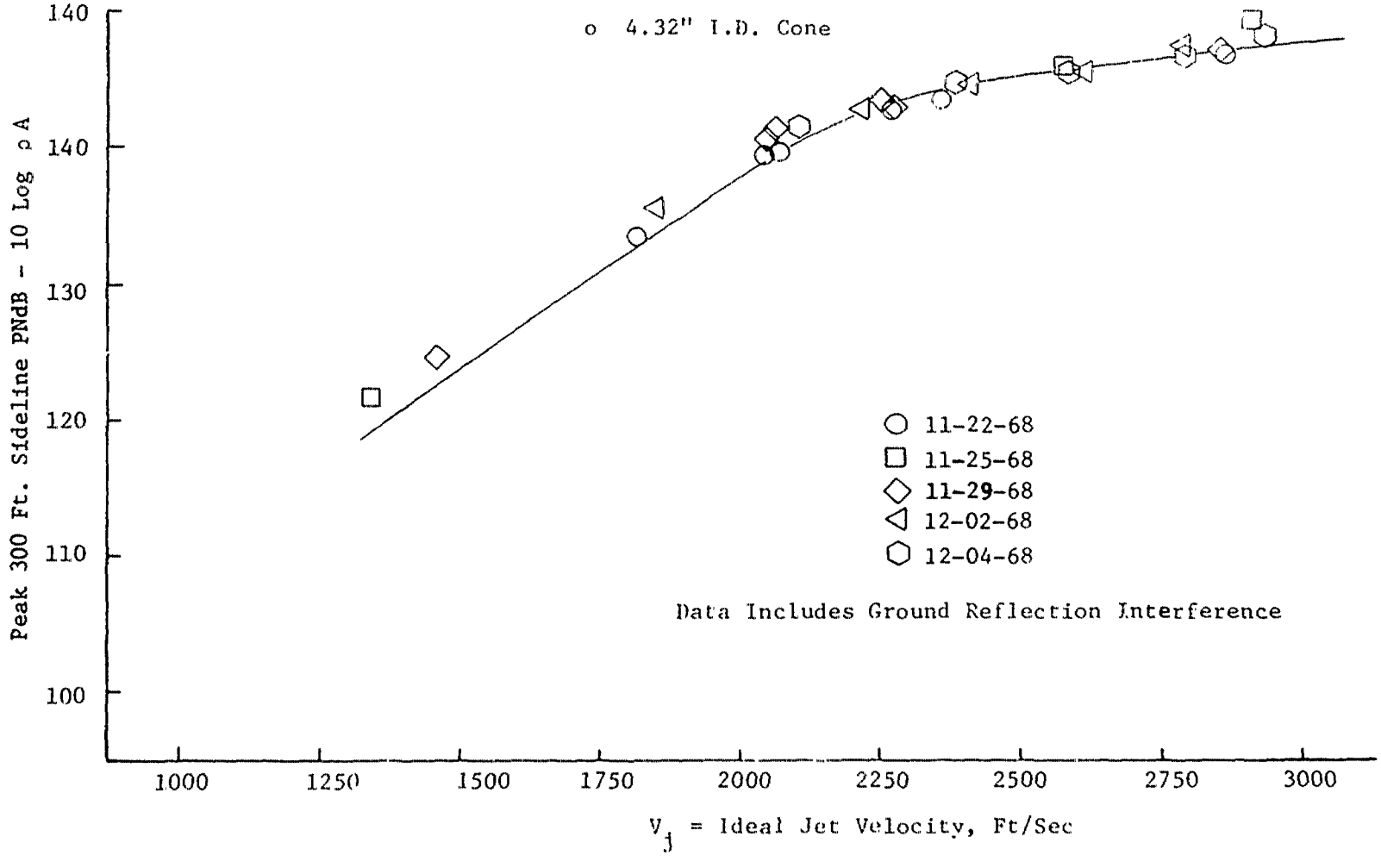

FIGURE V.F.8-2 300 FT. SIDELINE JET NOISE LEVELS FOR THE 4.32" I.D. BASELINE CONICAL NOZZLE

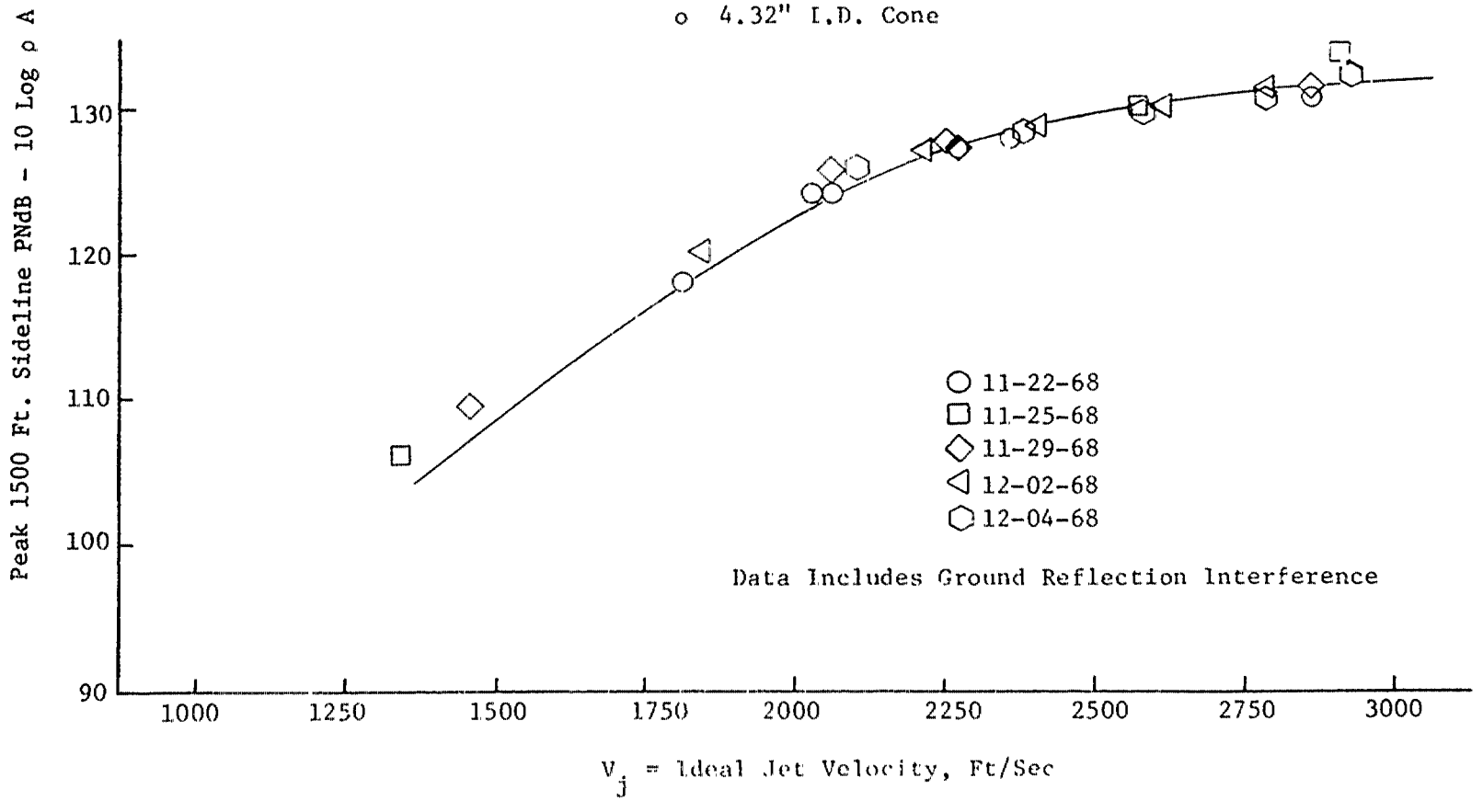

FIGURE V.F.8-3 1500 FT.SIDELINE JET NOISE LEVELS FOR THE 4.32" I.D. BASELINE CONICAL NOZZLE

TABLE V.F.8-2 TEST SUMMARY

MODEL NO. 4.2H97N-1

DESCRIPTION: 97 Hole Nozzle with 1.415" I.D. Centerhole, $AR_d = 2.0$

DATE: 1-13-69

SCALE MODEL A_8 = .1120 ft^2

FULL SCALE A_8 = 7.168 ft^2

SCALE FACTOR = 8:1

- o DATA INCLUDES GROUND REFLECTION INTERFERENCE
- o ANGLE REFERENCED TO JET EXHAUST

RDG NO.	TEST CONDITIONS				ACOUSTIC TEST RESULTS						
			IDEAL			320' ARC		300' SIDELINE		1500' SIDELINE	
	P_{T8}/P_o	T_{T8} (°R)	V_j (ft/sec)	W_8 (PPS)	10 log ρA	PEAK PNdB	PEAK ANGLE	PEAK PNdB	PEAK ANGLE	PEAK PNdB	PEAK ANGLE
1	3.01	1496	2233	8.60	-5.6	131.7	40	129.0	50	113.4	50
2	3.22	2326	2862	7.80	-7.4	137.1	50	134.9	50	119.2	50
3	3.25	2328	2869	7.90	-7.4	138.4	50	136.2	50	120.5	50
4	3.41	2330	2923	8.13	-7.2	139.3	50	137.1	50	121.5	50
5	3.02	1980	2572	10.41	-6.8	134.8	50	132.6	50	117.0	50
6	3.02	2339	2796	14.08	-7.6	137.1	50	134.9	50	119.2	50
7	2.50	2333	2571	18.99	-8.0	133.0	50	130.8	50	115.2	50
8	2.50	1991	2373	16.93	-7.3	131.7	40	128.1	50	112.5	50
9	2.51	1518	2077	12.62	-6.1	128.6	30	124.6	50	108.5	50
10	2.45	1700	2171	6.58	-6.7	129.9	30	126.4	50	110.5	50
11	2.19	1662	2024	6.10	-6.8	126.8	40	123.7	70	107.3	50
12	2.00	2305	2250	4.82	-8.4	127.7	40	125.3	50	109.3	50
13	2.00	1956	1956	5.21	-7.7	126.9	30	123.8	50	107.8	50
14	2.00	1502	1815	5.90	-6.5	123.9	30/50	121.6	50	104.3	50
15	1.64	1306	1444	5.22	-6.1	117.2	40/50	115.5	60	97.9	60
16	1.52	1269	1321	4.97	-6.0	114.3	50	112.9	60	95.4	60
17	1.40	1215	1158	4.17	-5.7	111.1	50	110.0	60	92.5	60

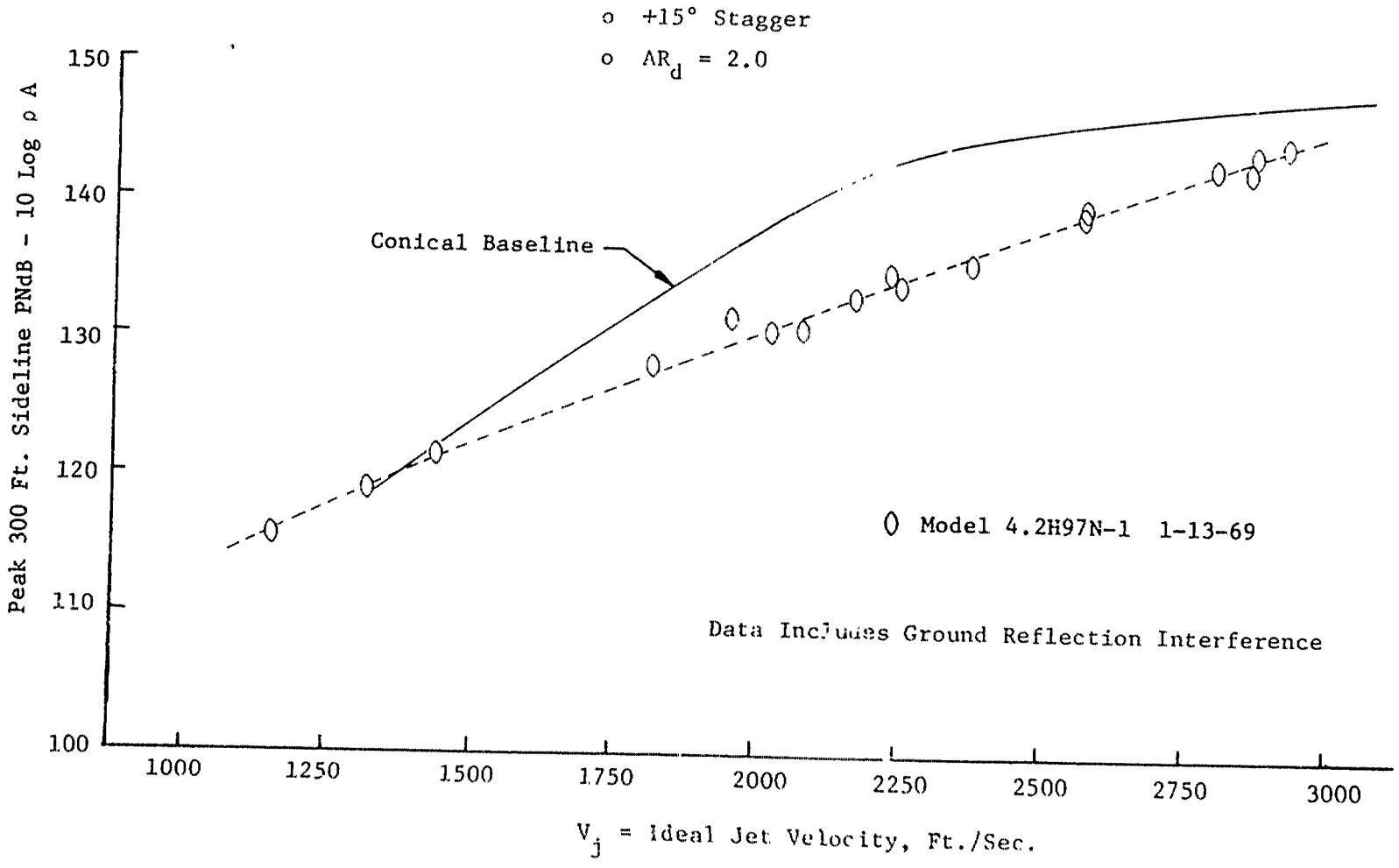

FIGURE V.F.8-4 300 FT. SIDELINE JET NOISE LEVELS FOR A 97 HOLE NOZZLE WITH SMALL ROUND CENTERHOLE

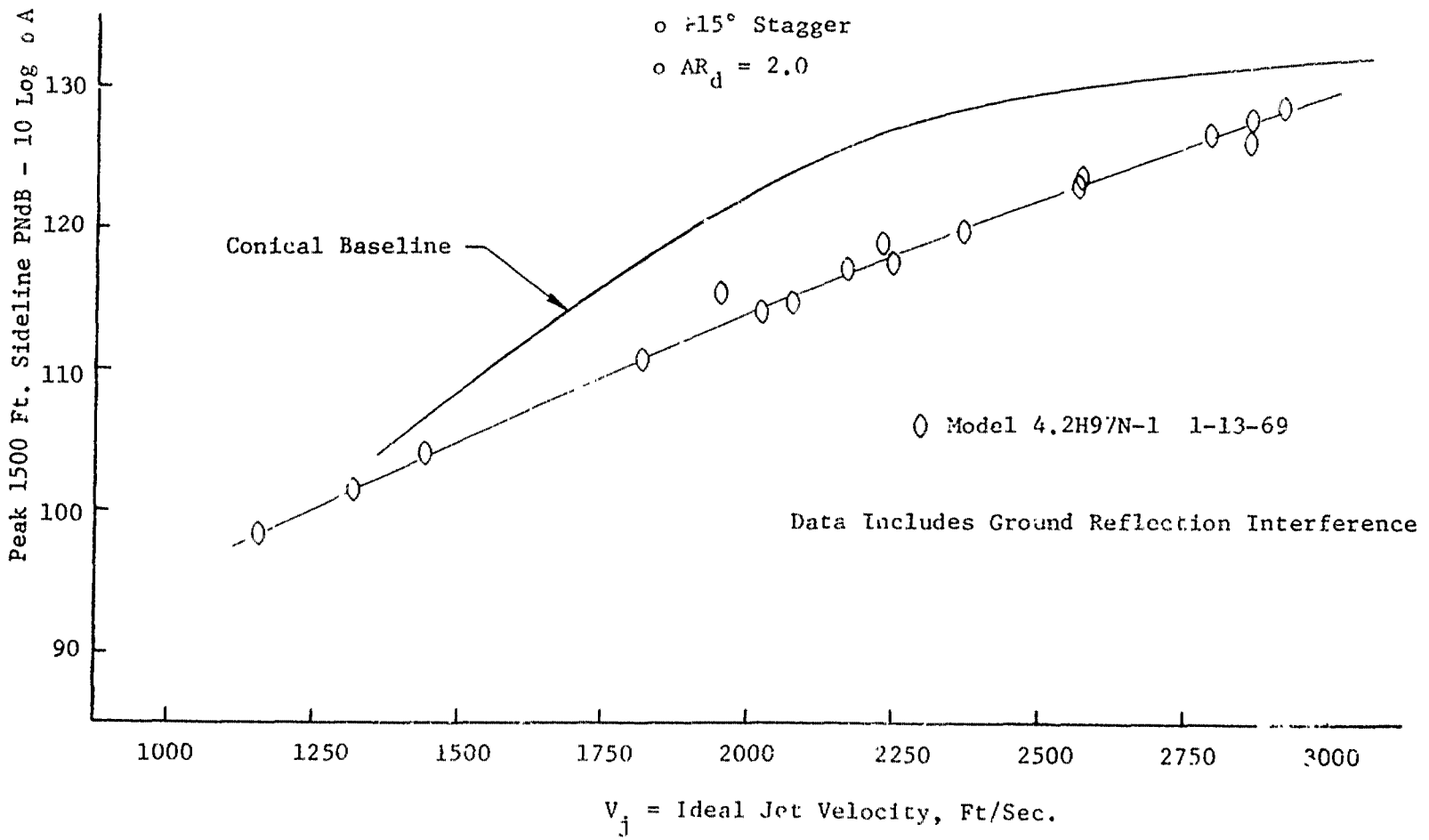

FIGURE V.F.8-5 1500 FT. SIDELINE JET NOISE LEVELS FOR A 97 HOLE NOZZLE WITH SMALL ROUND CENTERHOLE

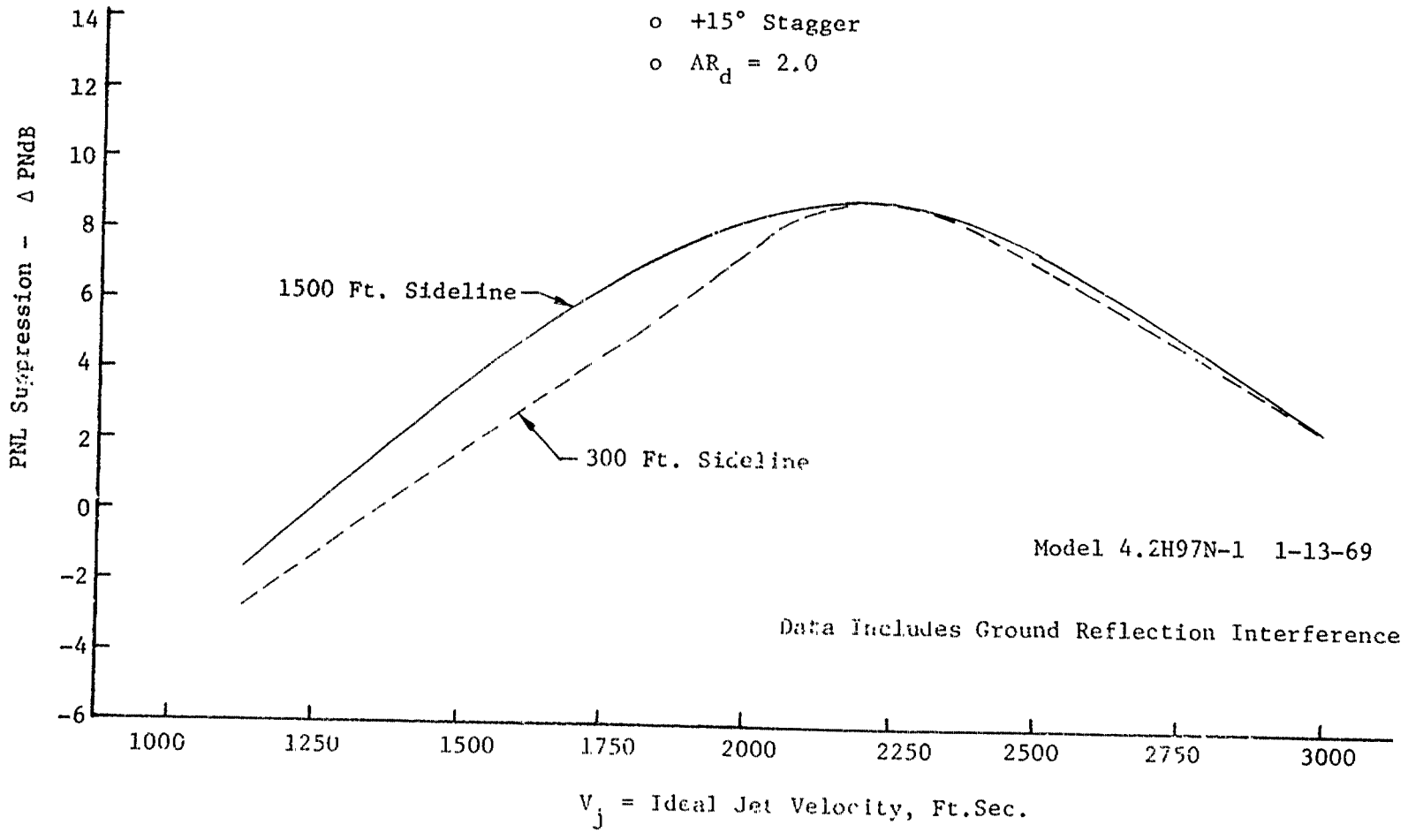

FIGURE V.F.8-6 300 FT AND 1500 FT. SIDELINE PNL SUPPRESSIONS FOR A 97 HOLE NOZZLE WITH SMALL ROUND CENTERHOLE

TABLE V.F.8-3 TEST SUMMARY

MODEL NO. 4.2H97N-2

DESCRIPTION: 97 Hole Nozzle with Greatrex Center, AR_d = 2.0

DATE: 11/25/68

SCALE MODEL A_8 = .1120 ft^2

FULL SCALE A_8 = 7.168 ft^2

SCALE FACTOR = 8:1

- o DATA INCLUDES GROUND REFLECTION INTERFERENCE
- o ANGLE REFERENCED TO JET EXHAUST

RDG NO.	TEST CONDITIONS				ACOUSTIC TEST RESULTS						
			IDEAL			320' ARC		300' SIDELINE		1500' SIDELINE	
	P_{T8}/P_o	T_{T8} (°R)	V_j (ft/sec)	W_8 (PPS)	10 log ρA	PEAK PNdB	PEAK ANGLE	PEAK PNdB	PEAK ANGLE	PEAK PNdB	PEAK ANGLE
1	1.40	1200	1155	4.17	-5.7	108.5	50	107.4	70	89.9	60/70
2	1.53	1275	1328	4.59	-6.0	112.3	50	110.6	60	93.3	60
3	1.63	1315	1444	4.86	-6.2	114.8	50	113.7	60	96.4	60
4	2.00	1500	1812	5.69	-6.6	121.0	50	118.9	60	101.8	60
5	1.99	1960	2069	4.89	-7.7	124.6	30	121.3	60	105.2	50
6	2.00	2300	2247	4.47	-8.5	126.4	30	122.5	50	106.5	50
7	2.20	1653	2021	5.95	-6.8	125.6	30	121.5	50	105.2	40
8	2.45	1715	2181	6.42	-6.8	129.0	30	124.1	50	108.5	40/50
9	2.51	1495	2060	7.09	-6.1	127.4	30	123.0	50	107.2	50
10	2.49	1983	2368	6.04	-7.4	130.0	40	126.3	50	110.8	50
11	2.51	2300	2555	5.52	-8.0	131.4	40	128.6	50	113.1	50
12	3.00	2300	2769	6.42	-7.6	134.5	40	132.0	50	116.5	50
13	3.39	2310	2904	7.60	-7.2	146.1	40	142.0	40	127.6	40

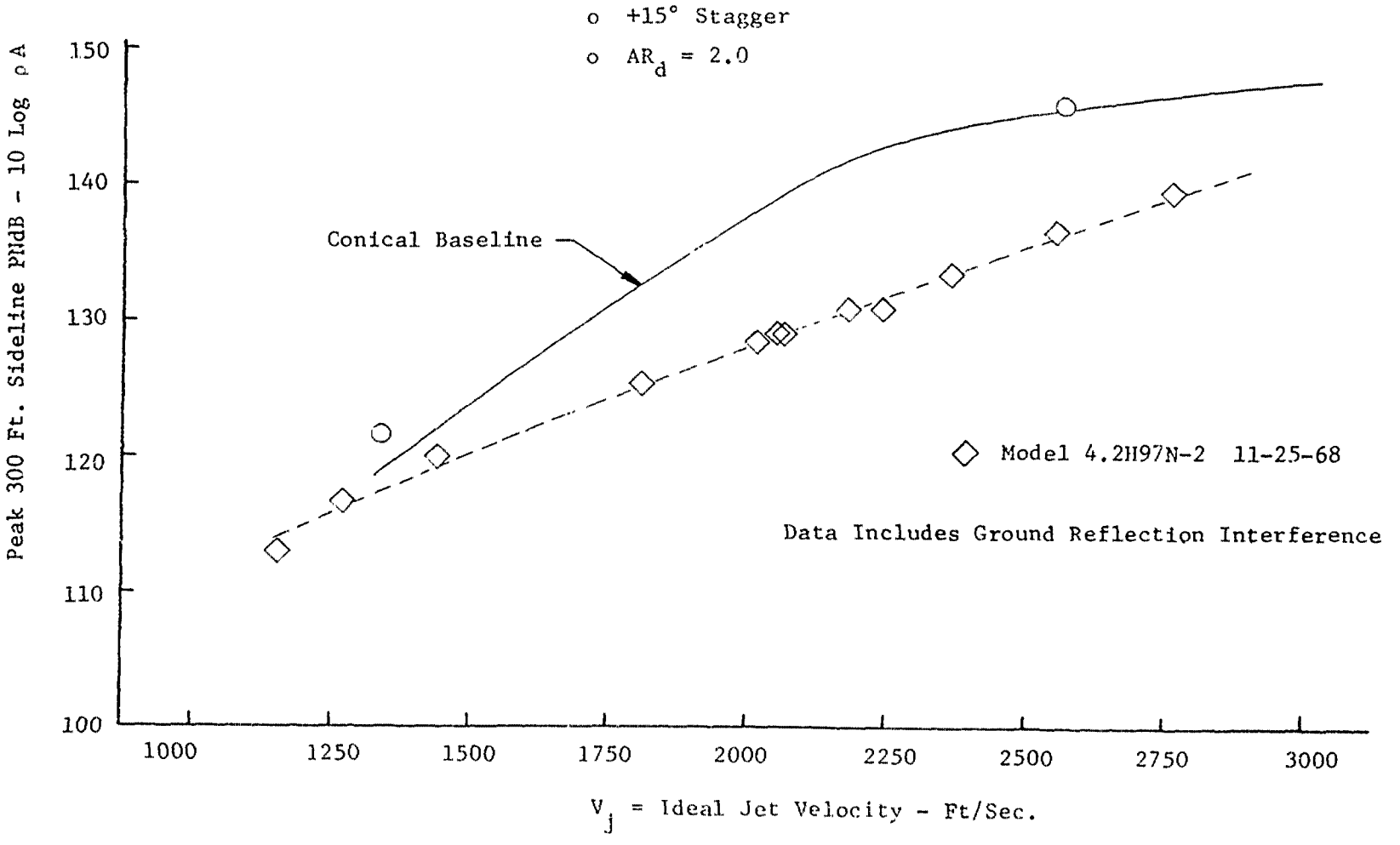

FIGURE V.F.8-7 300 FT. SIDELINE JET NOISE LEVELS FOR A 97 HOLE NOZZLE WITH GREATREX CENTER

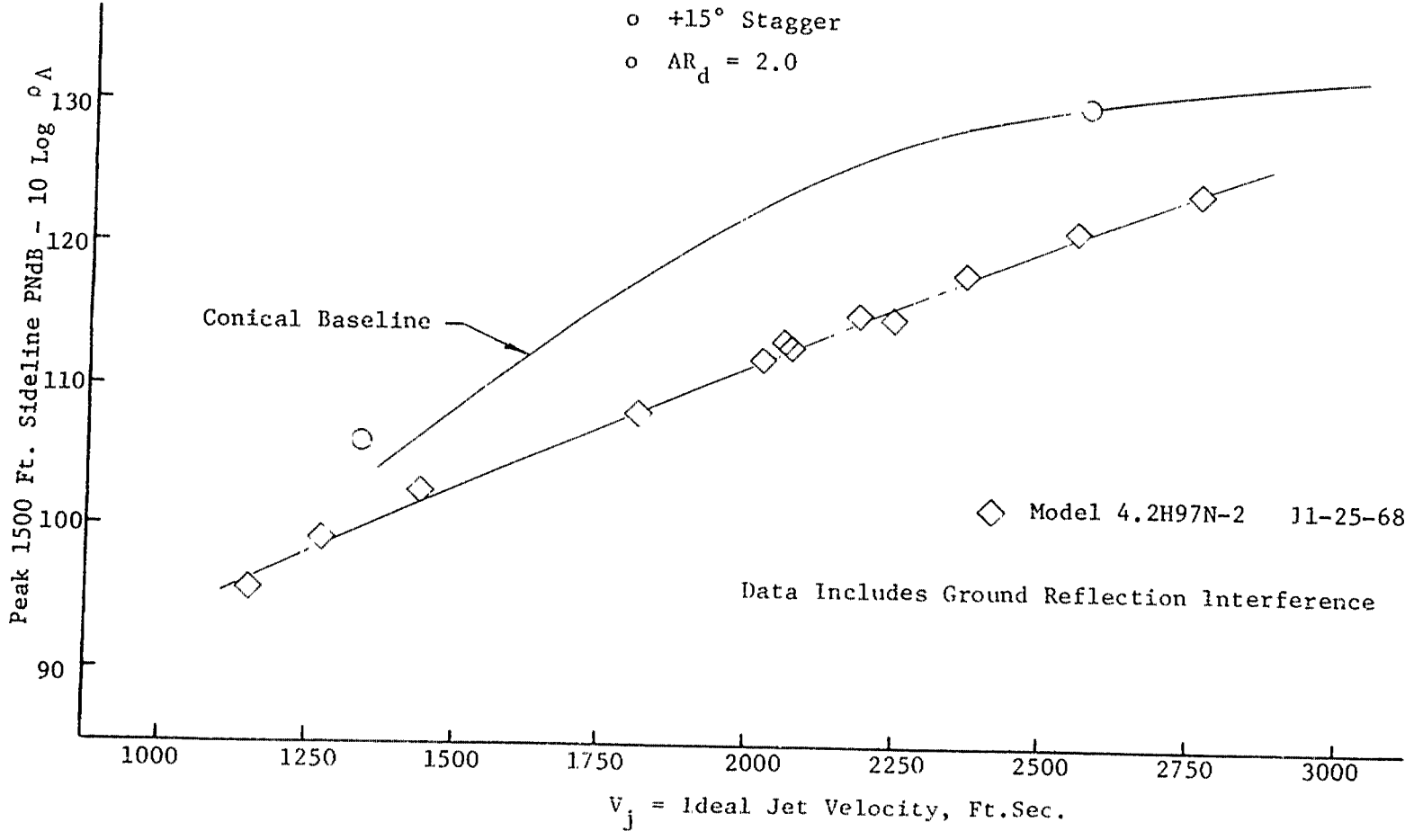

FIGURE V.F.8-8 1500 FT. SIDELINE JET NOISE LEVELS FOR A 97 HOLE NOZZLE WITH GREATREX CENTER

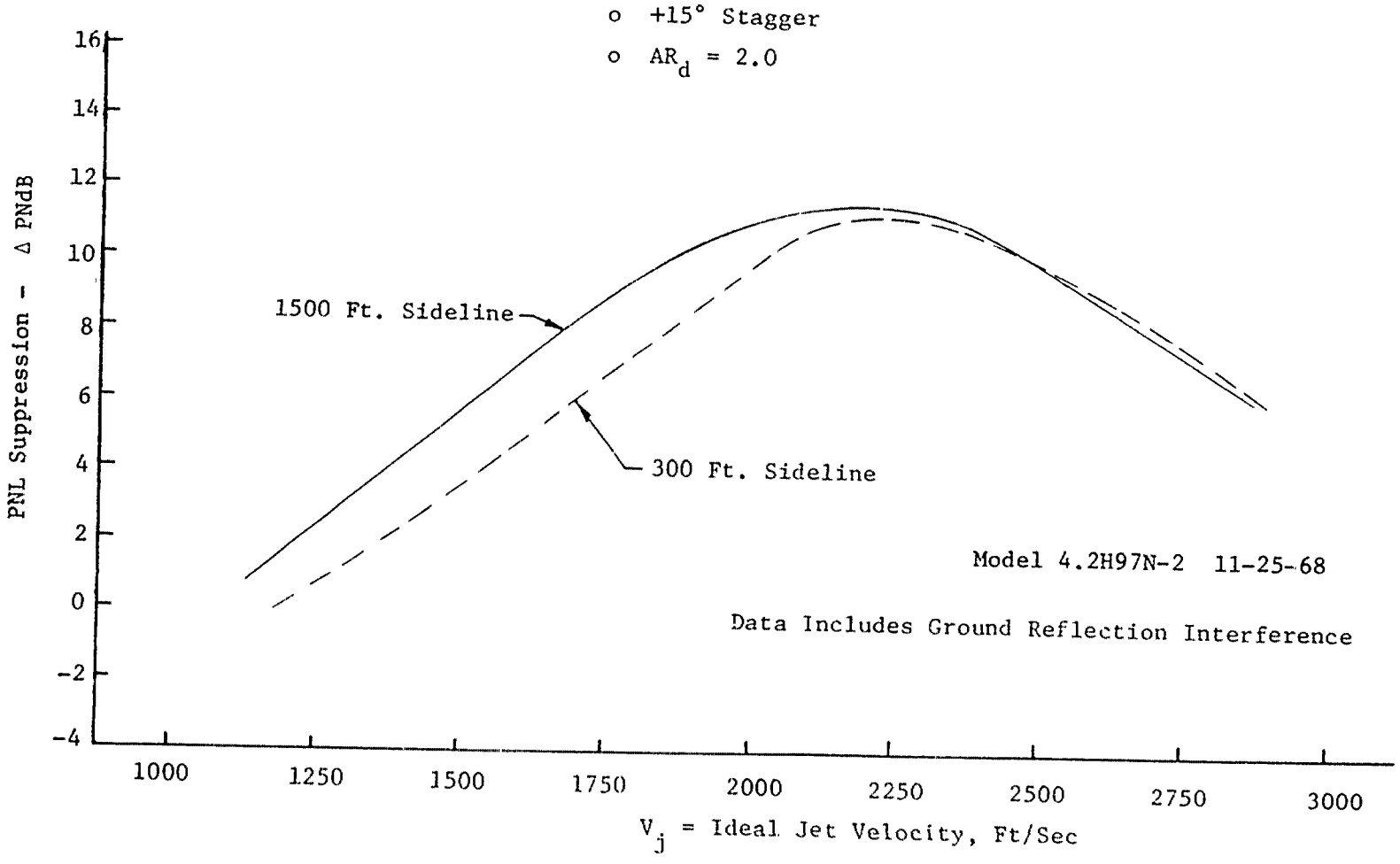

FIGURE V.F.8-9 300 FT. AND 1500 FT. SIDELINE PNL SUPPRESSIONS FOR A 97 HOLE NOZZLE WITH GREATREX CENTER

TABLE V.F.8-4 TEST SUMMARY

MODEL NO. 4.2H97N-CS-2

DESCRIPTION: 97 Hole Nozzle with Greatrex Center, Hardwall Ejector D_s/D_{Td} = 1.125

DATE: 12/2/68

SCALE MODEL A_8 = .1120 ft^2

FULL SCALE A_8 = 7.168 ft^2

SCALE FACTOR = 8:1

- o DATA INCLUDES GROUND REFLECTION INTERFERENCE
- o ANGLE REFERENCED TO JET EXHAUST

	TEST CONDITIONS				ACOUSTIC TEST RESULTS						
			IDEAL			320' ARC		300' SIDELINE		1500' SIDELINE	
RDG NO.	P_{T8}/P_o	T_{T8} (°R)	V_j (ft/sec)	W_8 (PPS)	10 log σA	PEAK PNdB	PEAK ANGLE	PEAK PNdB	PEAK ANGLE	PEAK PNdB	PEAK ANGLE
4	2.01	1530	1842	5.71	-6.7	118.7	50	117.5	80	100.4	80
5	2.01	1997	2102	4.90	-7.8	122.0	30	120.3	70	103.2	50/70
6	2.00	2336	2268	4.59	-8.5	124.0	40	121.1	70	105.1	50
7	2.22	1661	2040	6.06	-6.8	122.5	30	120.4	60	104.0	50
8	2.47	1714	2188	6.47	-6.8	125.4	40	122.6	60	106.8	60
9	2.54	1533	2103	7.21	-6.2	124.9	40	121.7	60	106.1	40
10	2.53	1983	2386	6.15	-7.3	127.8	40	124.4	50	109.2	50
11	2.51	2287	2552	5.68	-8.0	129.3	50	127.2	50	112.1	50
12	3.02	2333	2796	6.88	-7.6	133.2	50	131.0	50	115.7	50
13	3.02	1981	2574	7.31	-6.9	131.8	50	129.5	50	114.3	50
14	3.03	1517	2257	8.84	-5.7	128.4	30	124.3	50	109.1	50
15	2.55	2295	2575	5.87	-8.0	129.4	40	126.4	50	111.3	50
16	2.59	2313	2603	5.96	-8.0	129.3	50	127.3	50	112.1	50
17	3.42	2321	2920	7.69	-7.3	136.8	50	134.6	50	119.1	50

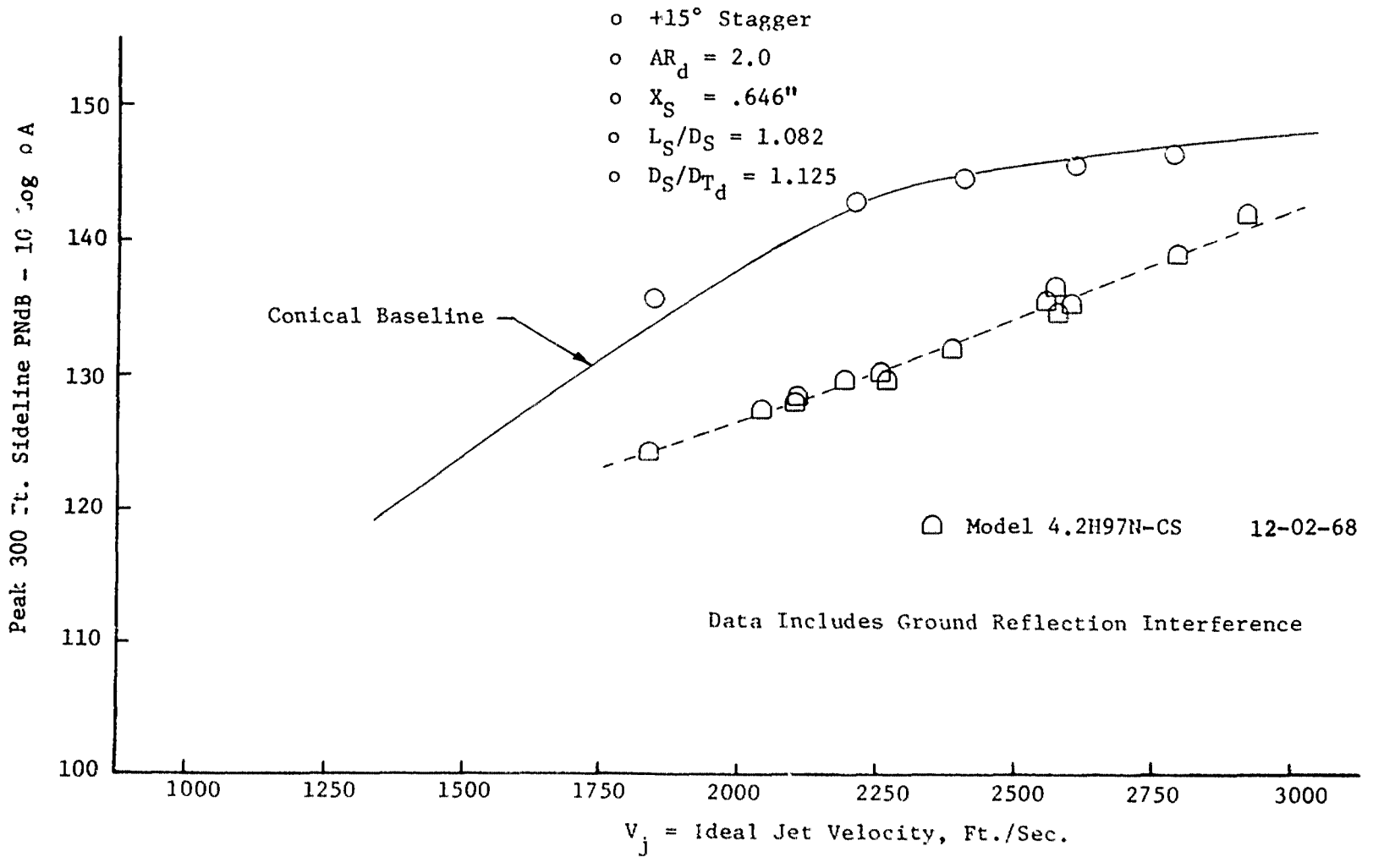

FIGURE V.F.8-10 300 FT. SIDELINE JET NOISE LEVELS FOR A 97 HOLE NOZZLE WITH GREATREX CENTER PLUS HARDWALL EJECTOR, D_S/D_{Td} = 1.125

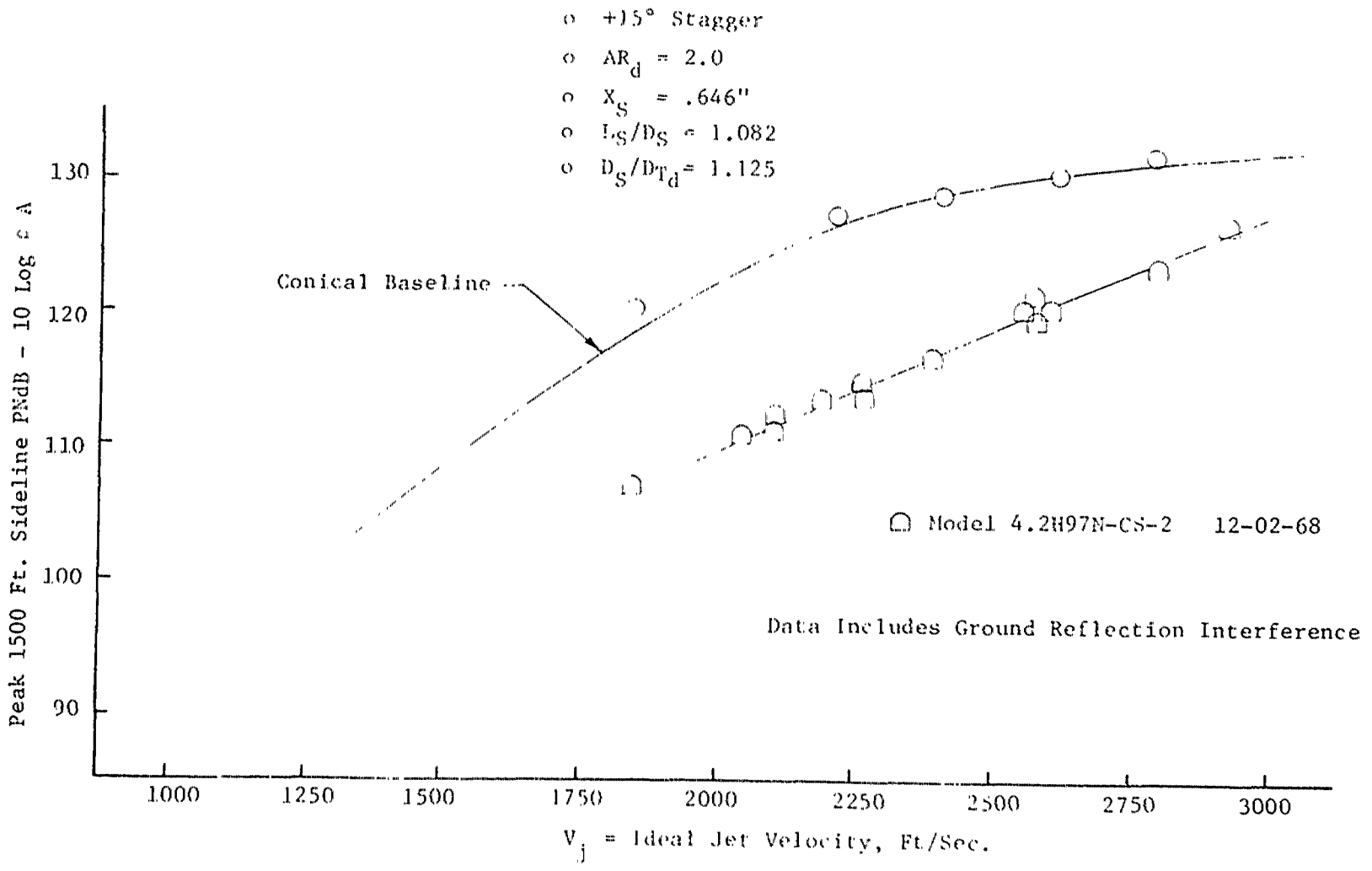

FIGURE V.F.8-11 1500 FT. SIDELINE JET NOISE LEVELS FOR A 97 HOLE NOZZLE WITH GREATREX CENTER PLUS HARDWALL EJECTOR, D_S/D_{Td} = 1.125

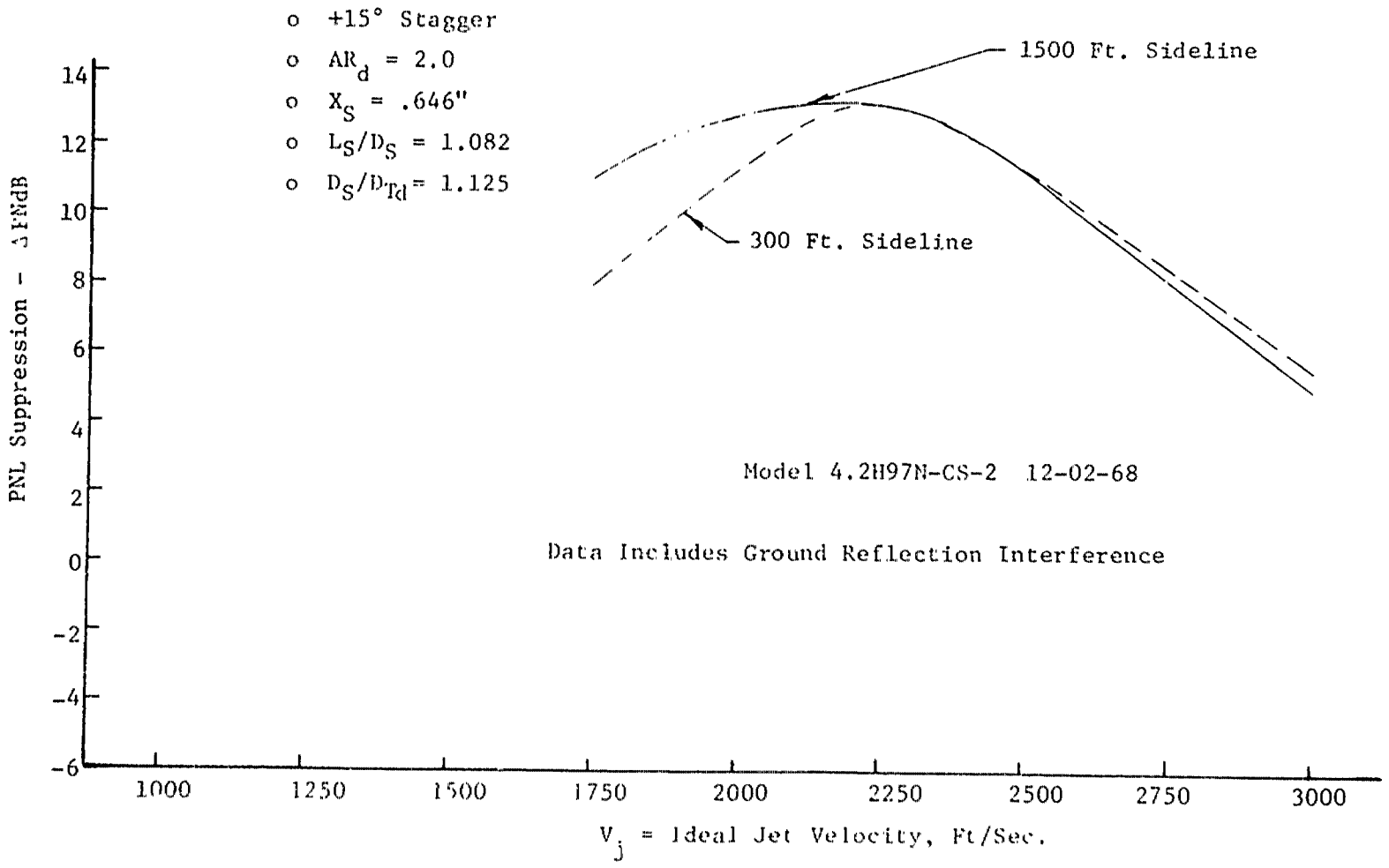

FIGURE V.F.8-12 300 FT. AND 1500 FT. SIDELINE PNL SUPPRESSIONS FOR A 97 HOLE NOZZLE WITH GREATREX CENTER PLUS HARDWALL EJECTOR, D_S/D_{Td} = 1.125

TABLE V.F.8-5 TEST SUMMARY

MODEL NO. 4.2H97N-CS-3

DESCRIPTION: 97 Hole Nozzle with Greatrex Center, Hardwall Ejector, D_s/D_{Td} = 1.155

DATE: 12/4/68

SCALE MODEL A_8 = .1120 ft^2

FULL SCALE A_8 = 7.168 ft^2

SCALE FACTOR = 8:1

- o DATA INCLUDES GROUND REFLECTION INTERFERENCE
- o ANGLE REFERENCED TO JET EXHAUST

	TEST CONDITIONS				ACOUSTIC TEST RESULTS						
						320' ARC		300' SIDELINE		1500' SIDELINE	
RDG NO.	P_{T8}/P_o	T_{T8} (°R)	IDEAL V_j (ft/sec)	W_8 (PPS)	10 log ρA	PEAK PNdB	PEAK ANGLE	PEAK PNdB	PEAK ANGLE	PEAK PNdB	PEAK ANGLE
4	1.99	1505	1812	5.50	-6.6	119.3	50	119.0	70	101.8	70
5	2.00	2006	2098	4.90	-7.9	123.0	30	121.5	70	103.0	50
6	2.01	2303	2254	4.47	-8.5	124.7	40	122.1	70	106.1	50
7	2.70	1669	2031	6.04	-6.9	123.1	40	121.1	70	104.8	50
8	2.46	1762	2216	6.85	-6.9	126.3	30/40	123.6	50	108.2	50
9	2.49	1495	2054	7.10	-6.2	125.4	30	121.4	50	105.9	50
10	2.69	1990	2370	5.94	-7.4	127.8	40	125.2	50	109.9	50
11	2.49	2310	2555	4.60	-8.1	129.5	40	127.1	50	111.8	50
12	3.00	2315	2775	6.50	-7.6	134.5	50	132.4	50	117.0	50
13	2.88	1975	2521	7.10	-7.1	132.2	40	130.0	50	114.7	50
14	2.99	1495	2227	8.50	-5.8	128.5	40	124.9	50	109.5	50
15	3.20	2320	2848	6.96	-7.5	133.5	40	134.0	50	118.6	50
16	3.22	2310	2851	7.07	-7.4	135.9	50	133.7	50	118.4	50
17	3.39	2310	2904	7.46	-7.3	137.8	50	135.7	50	120.2	50

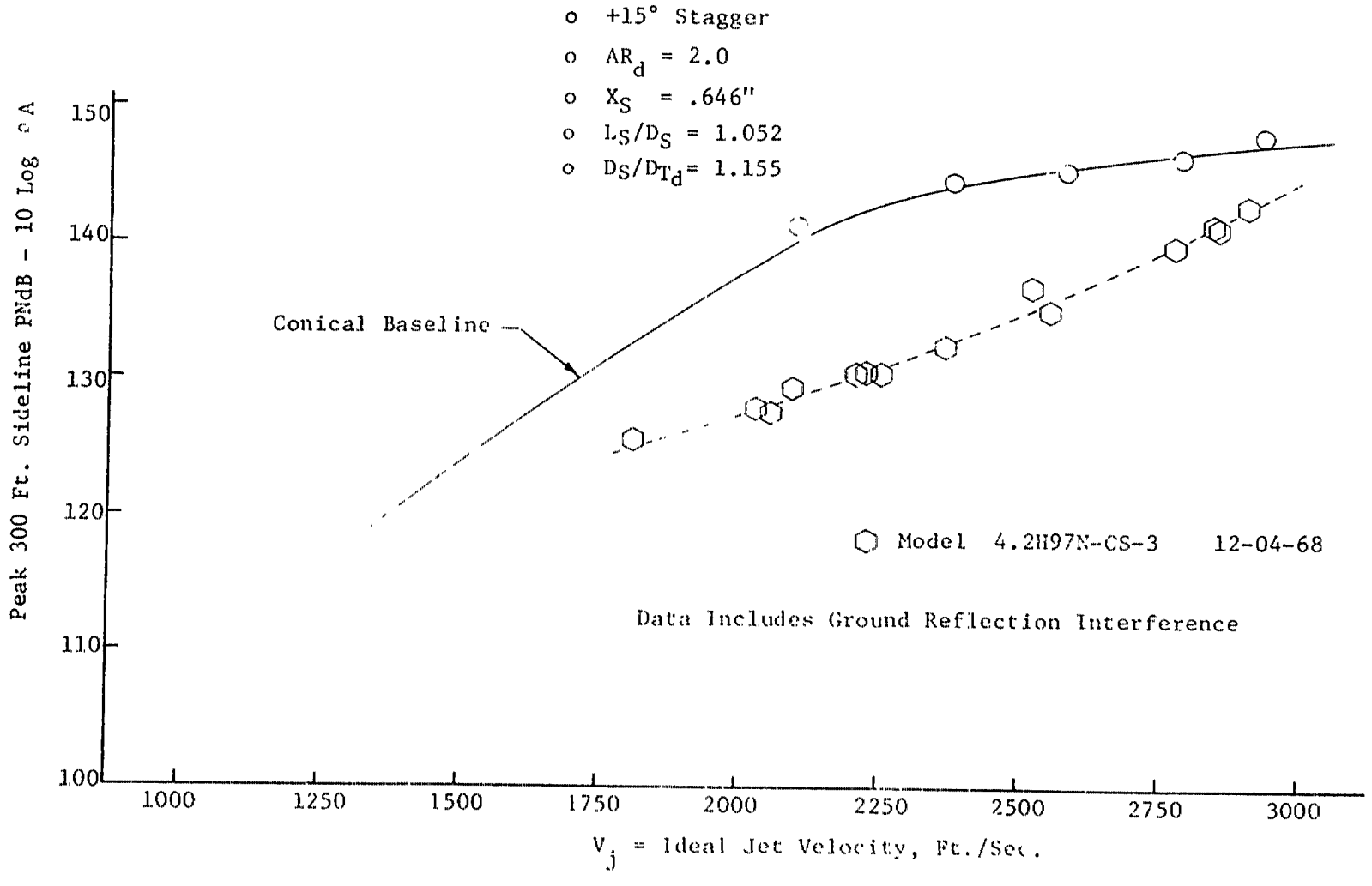

FIGURE V.F.8-13 300 FT. SIDELINE JET NOISE LEVELS FOR A 97 HOLE NOZZLE WITH GREATREX CENTER PLUS HARDWALL EJECTOR, D_S/D_{Td} = 1.155

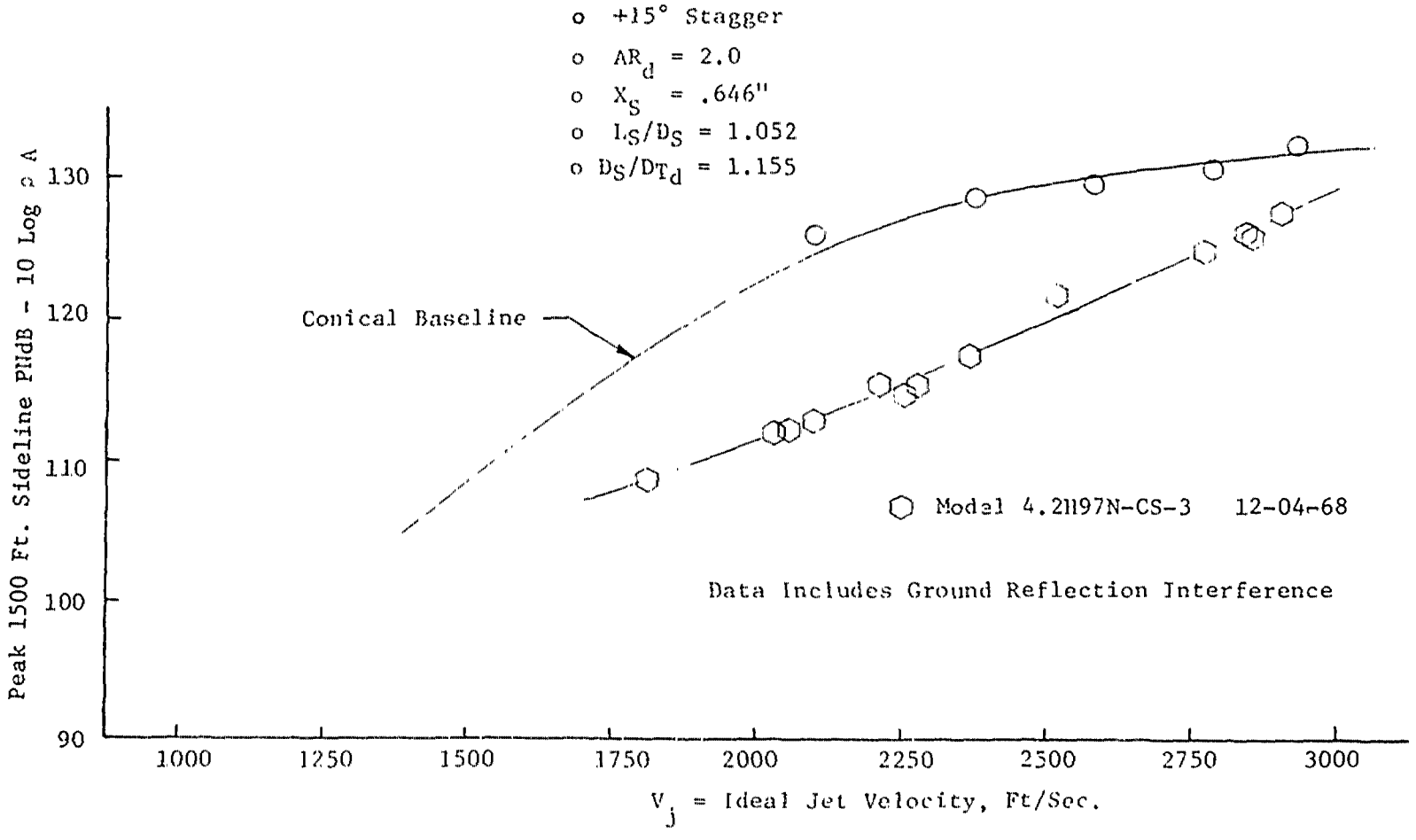

FIGURE V.F.8-14 1500 FT. SIDELINE JET NOISE LEVELS FOR A 97 HOLE NOZZLE WITH GREATREX CENTER PLUS HARDWALL EJECTOR, D_S/D_{Td} = 1.155

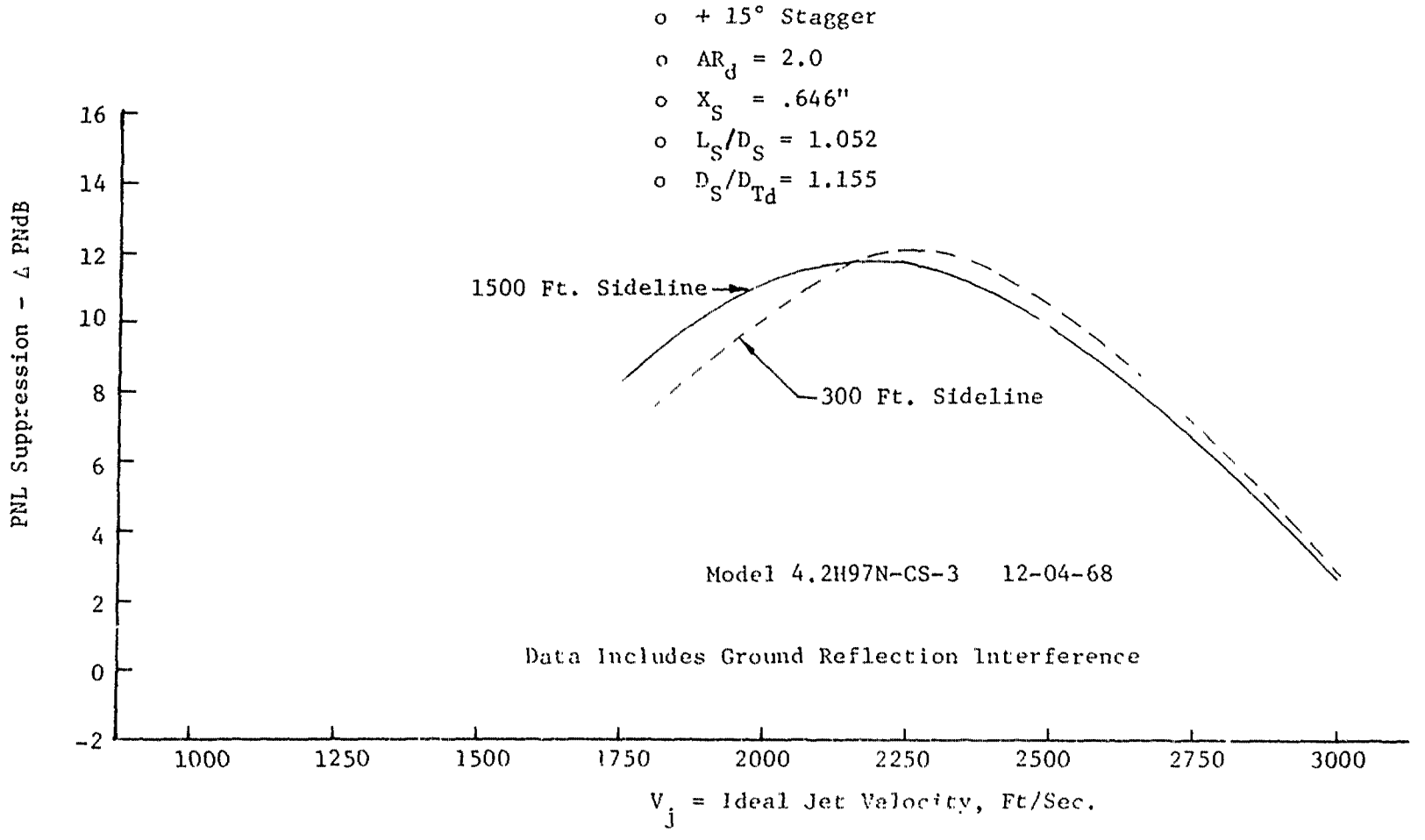

FIGURE V.F.8-15 300 FT. AND 1500 FT. SIDELINE PNL SUPPRESSIONS FOR A 97 HOLE NOZZLE WITH GREATREX CENTER PLUS HARDWALL EJECTOR, D_S/D_{Td} = 1.155

TABLE V.F.8-6 TEST SUMMARY

MODEL NO. 4.2H97N-CS

DESCRIPTION: 97 Hole Nozzle with Greatrex Center, Hardwall Ejector, $D_S / D_{Td} = 1.185$

DATE: 11/29/68

SCALE MODEL A_8 = .1120 ft^2

FULL SCALE A_8 = 7.168 ft^2

SCALE FACTOR = 8:1

- o DATA INCLUDES GROUND REFLECTION INTERFERENCE
- o ANGLE REFERENCED TO JET EXHAUST

	TEST CONDITIONS				ACOUSTIC TEST RESULTS						
			IDEAL			320' ARC		300' SIDELINE		1500' SIDELINE	
RDG NO.	P_{T8}/P_o	T_{T8} (°R)	V_j (ft/sec)	W_8 (PPS)	10 log ρA	PEAK PNdB	PEAK ANGLE	PEAK PNdB	PEAK ANGLE	PEAK PNdB	PEAK ANGLE
1	1.40	1235	1173	4.69	-5.8	109.8	70/80	110.3	80	95.0	80
2	1.54	1293	1349	4.76	-6.1	113.0	60	113.4	80	97.9	80
3	1.62	1341	1447	4.96	-6.2	115.5	60	114.7	60	99.2	60
4	2.01	1525	1834	5.71	-6.6	119.2	50	118.0	70	101.0	50
5	2.00	2028	2108	4.96	-7.9	121.9	30/40	119.9	80	104.2	50
6	2.01	2324	2269	4.59	-8.4	123.6	30	121.4	50	105.9	50
7	2.22	1622	2013	6.13	-6.7	123.0	30	119.6	70	103.9	50
8	2.49	1759	2228	6.63	-6.8	127.0	40	123.1	60	108.3	40
9	2.49	1508	2061	7.24	-6.2	124.1	40	121.2	50	105.7	50
10	2.53	1964	2371	6.17	-7.3	128.3	40	125.3	50	110.0	50
11	2.52	2301	2562	5.60	-8.0	129.3	40	127.0	50	111.7	50
12	3.03	2333	2798	6.83	-7.6	134.7	50	132.8	50	117.2	50
13	3.03	1972	2574	7.44	-6.8	132.5	50	130.4	50	115.0	50
14	3.03	1534	2268	8.73	-5.7	129.1	40	125.8	50	110.4	50
15	3.22	2311	2852	7.33	-7.4	135.7	50	133.5	50	118.1	50
16	3.27	2320	2873	7.40	-7.3	136.2	50	134.1	50	118.6	50
17	3.44	2331	2932	7.78	-7.2	137.5	50	135.4	50	119.7	50

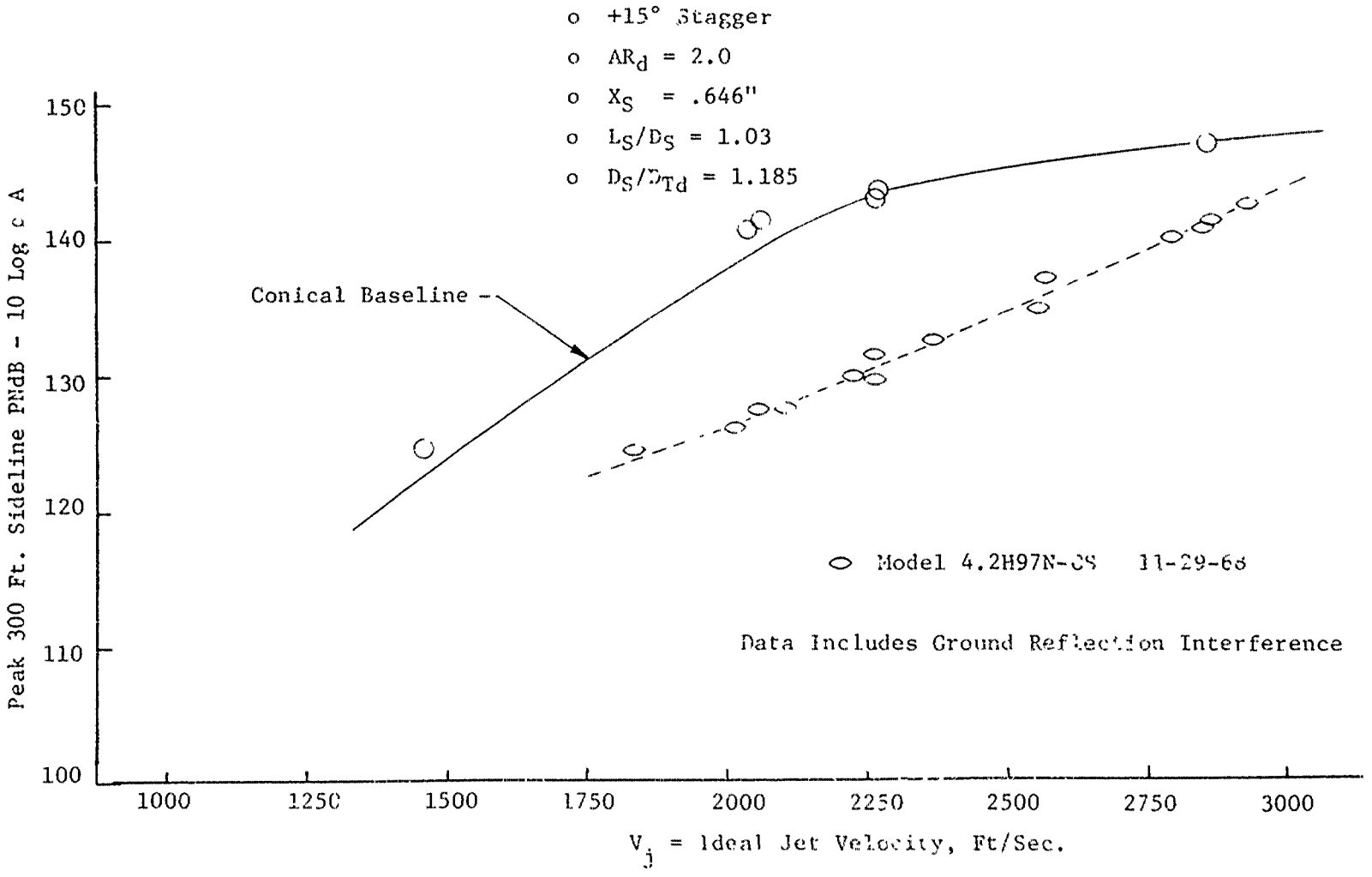

FIGURE V.F.8-16 300 FT. SIDELINE JET NOISE LEVELS FOR A 97 HOLE NOZZLE WITH GREATREX CENTER PLUS HARDWALL EJECTOR, D_S/D_{Td} = 1.185

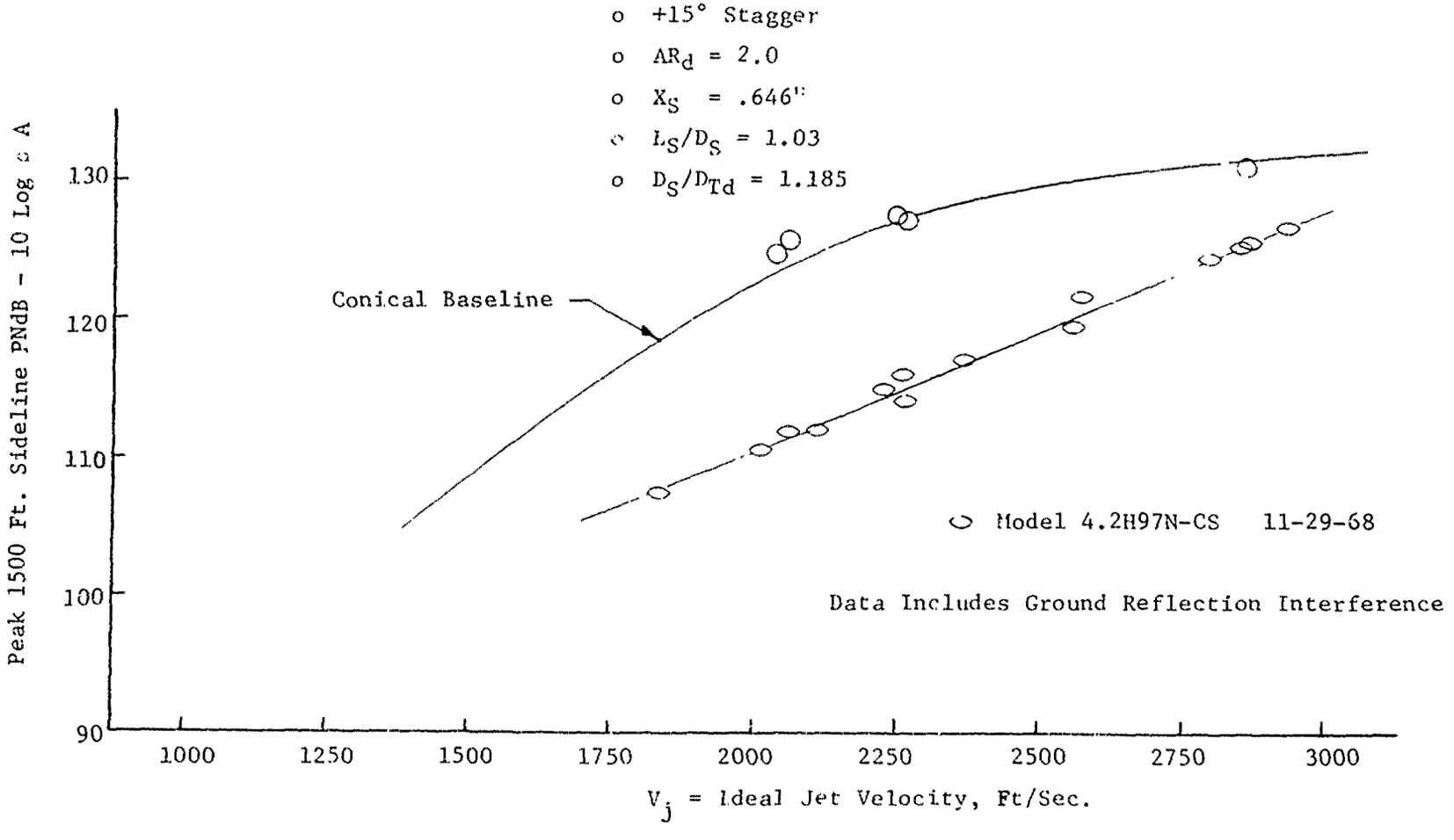

FIGURE V.F.8-17 1500 FT. SIDELINE JET NOISE LEVELS FOR A 97 HOLE NOZZLE WITH GREATREX CENTER PLUS HARDWALL EJECTOR, D_S/D_{Td} = 1.185

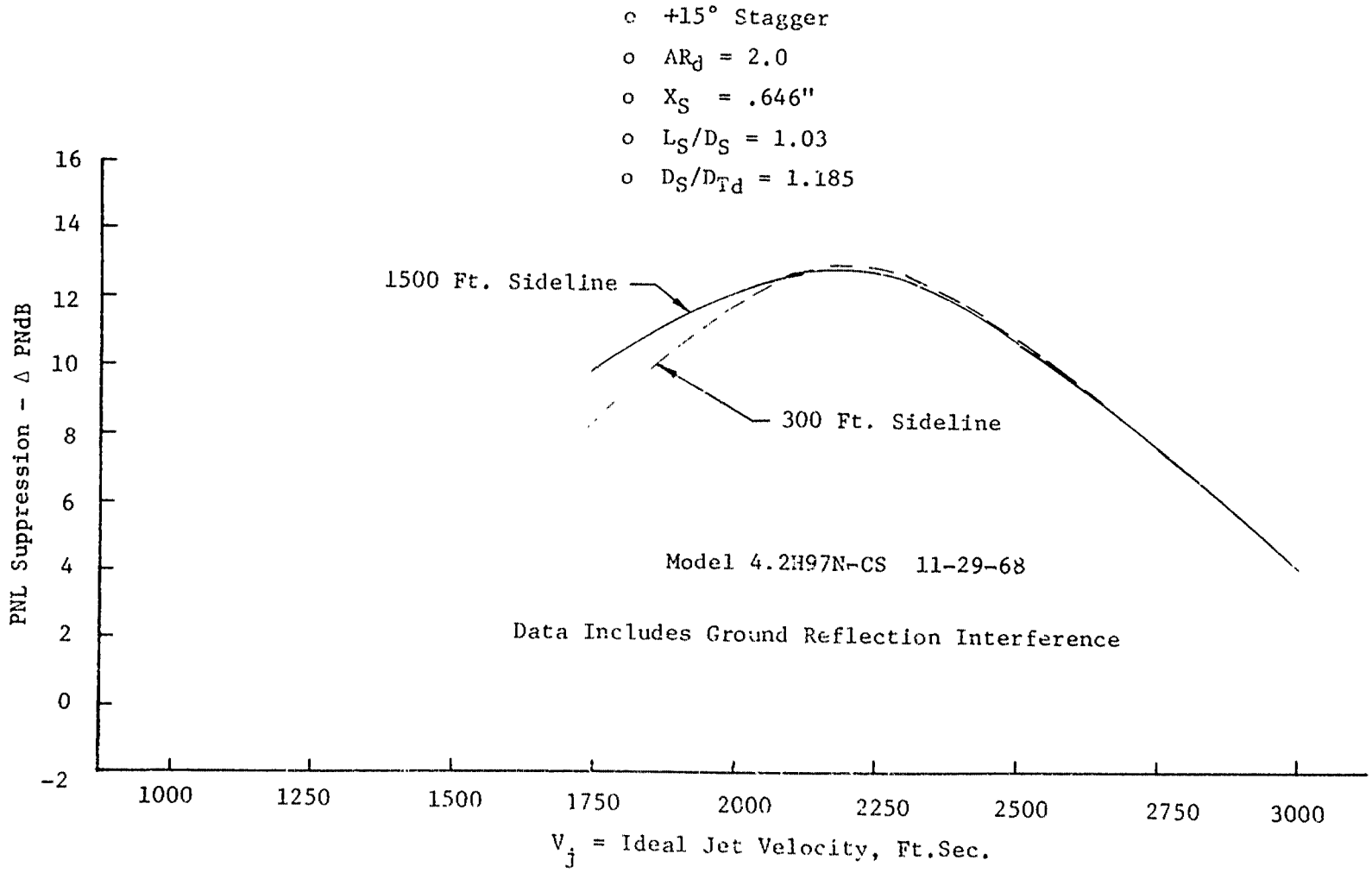

FIGURE V.F.8-18 300 FT. AND 1500 FT. SIDELINE PNL SUPPRESSIONS, FOR A 97 HOLE NOZZLE WITH GREATREX CENTER PLUS HARDWALL EJECTOR, D_S/D_{Td} = 1.185

TABLE V.F.8-7 TEST SUMMARY

MODEL NO. 4.2H97N-CS-4

DESCRIPTION: 97 Hole Nozzle with Greatrex Center, 4% Open Lined Ejector
D_S/D_{Td} = 1.185

DATE: 1-14-69

SCALE MODEL A_8 = .1120 ft^2

FULL SCALE A_8 = 7.168 ft^2

SCALE FACTOR = 8:1

- DATA INCLUDES GROUND REFLECTION INTERFERENCE
- ANGLE REFERENCED TO JET EXHAUST

	TEST CONDITIONS				ACOUSTIC TEST RESULTS						
			IDEAL			320' ARC		300' SIDELINE		1500' SIDELINE	
RDG NO.	P_{T8}/P_o	T_{T8} (°R)	V_j (ft/sec)	W_8 (PPS)	10 Log ρA	PEAK PNdB	PEAK ANGLE	PEAK PNdB	PEAK ANGLE	PEAK PNdB	PEAK ANGLE
1	1.39	1213	1143	4.42	-5.6	109.4	70	109.4	70	93.1	70
2	1.53	1270	1340	5.08	-6.0	112.4	60	112.8	80	95.7	80
3	1.63	1337	1460	5.37	-6.2	113.9	70	113.9	70	96.4	70
4	1.99	1572	1852	5.99	-6.7	119.5	60	119.0	70	101.6	70
5	2.02	2018	2122	5.19	-7.8	122.4	30	121.5	70	104.2	70
6	2.03	2344	2290	4.91	-8.4	123.7	40	122.4	70	105.7	50
7	2.23	1663	2045	6.50	-6.8	123.1	40	121.6	70	104.4	70
8	2.51	1738	2223	7,03	-6.7	126.3	30	123.4	50	107.8	50
9	2.53	1508	2079	7.78	-6.1	124.7	30	121.9	70	105.6	50
10	2.53	1991	2389	6.70	-7.3	128.1	40	125.1	50	109.6	50
11	2.52	2308	2566	6.15	-7.9	129.7	40/50	127.5	50	112.1	50
12	3.02	2336	2797	7.33	-7.6	134.7	50	132.5	50	117.0	50
13	3.03	2012	2598	7.91	-6.9	132.9	50	130.8	50	115.3	50
14	3.02	1518	2250	9.27	-5.7	127.7	50	125.5	50	110.0	50/60
15	3.24	2310	2860	7.83	-7.3	136.2	50	134.0	50	118.4	50
16	3.22	2313	2851	7.88	-7.3	136.6	50	134.4	50	118.8	50
17	3.43	2311	2915	8.22	-7.2	134.8	40	135.5	50	120.3	50

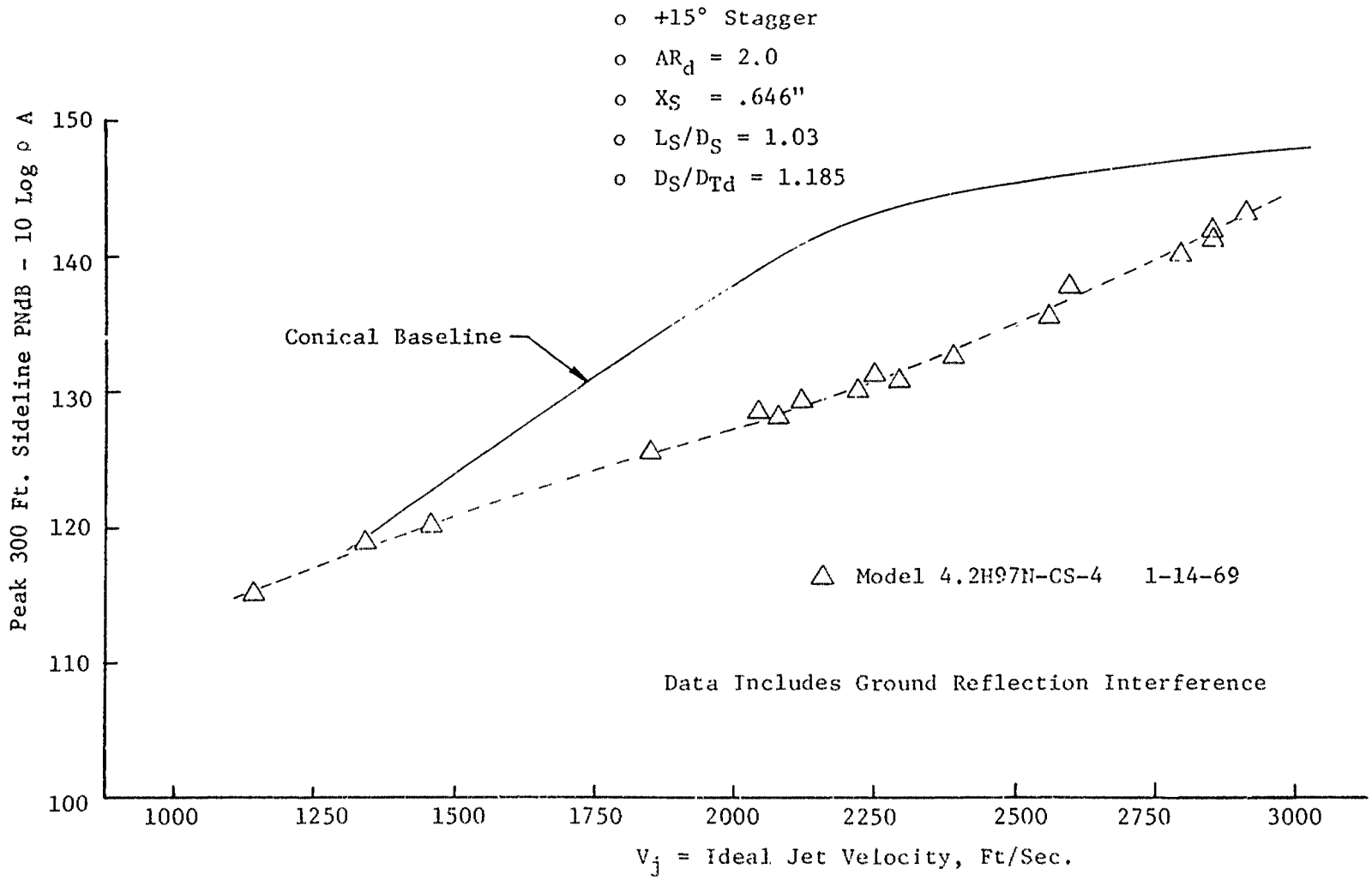

FIGURE V.F.8-19 300 FT. SIDELINE JET NOISE LEVELS FOR A 97 HOLE NOZZLE WITH GREATREX CENTER PLUS 4% OPEN LINED EJECTOR, D_S/D_{Td} = 1.185

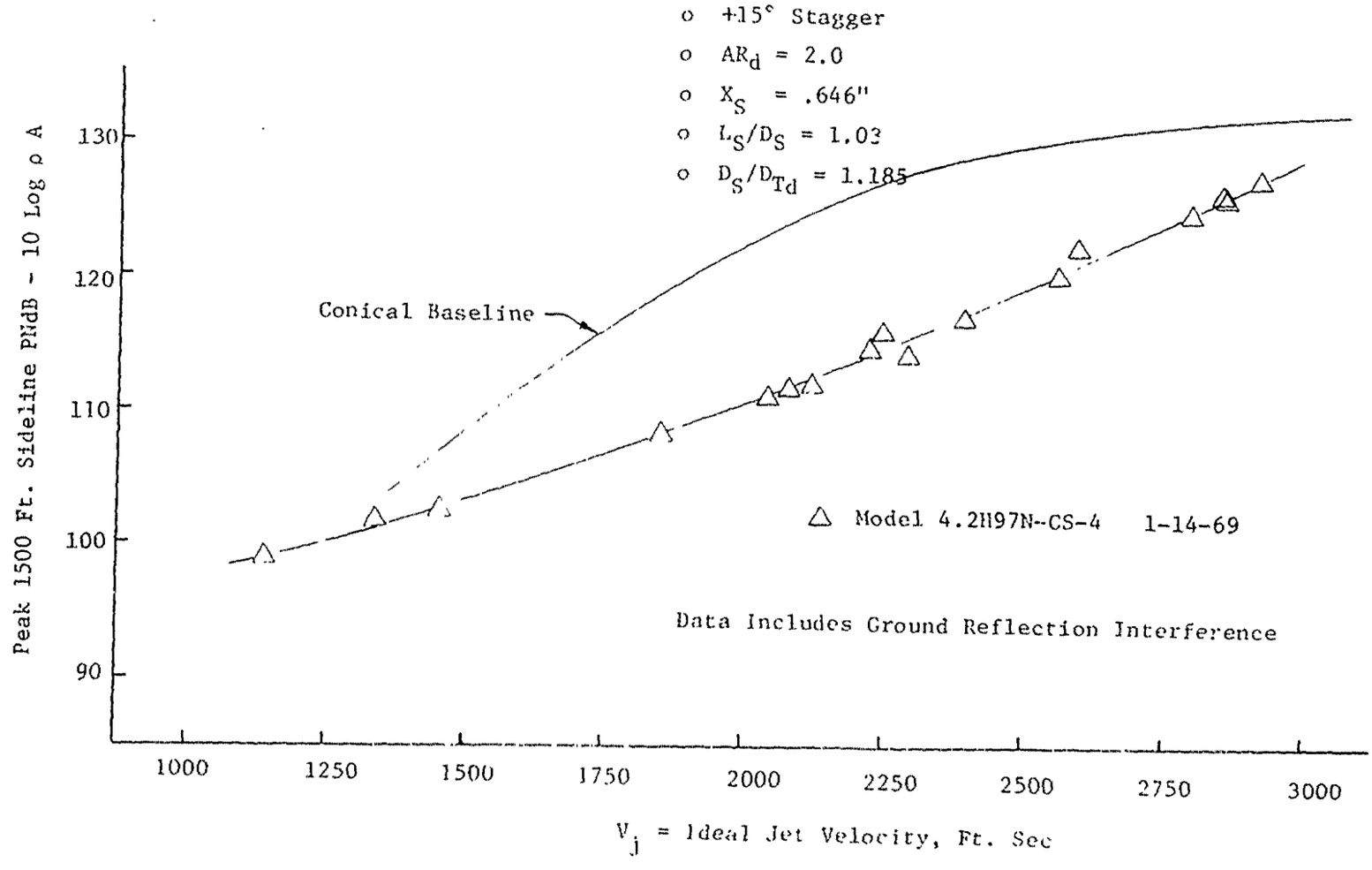

FIGURE V.F.8-20 1500 FT. SIDELINE JET NOISE LEVELS FOR A 97 HOLE NOZZLE WITH GREATREX CENTER PLUS 4% OPEN LINED EJECTOR, D_S/D_{Td} = 1.185

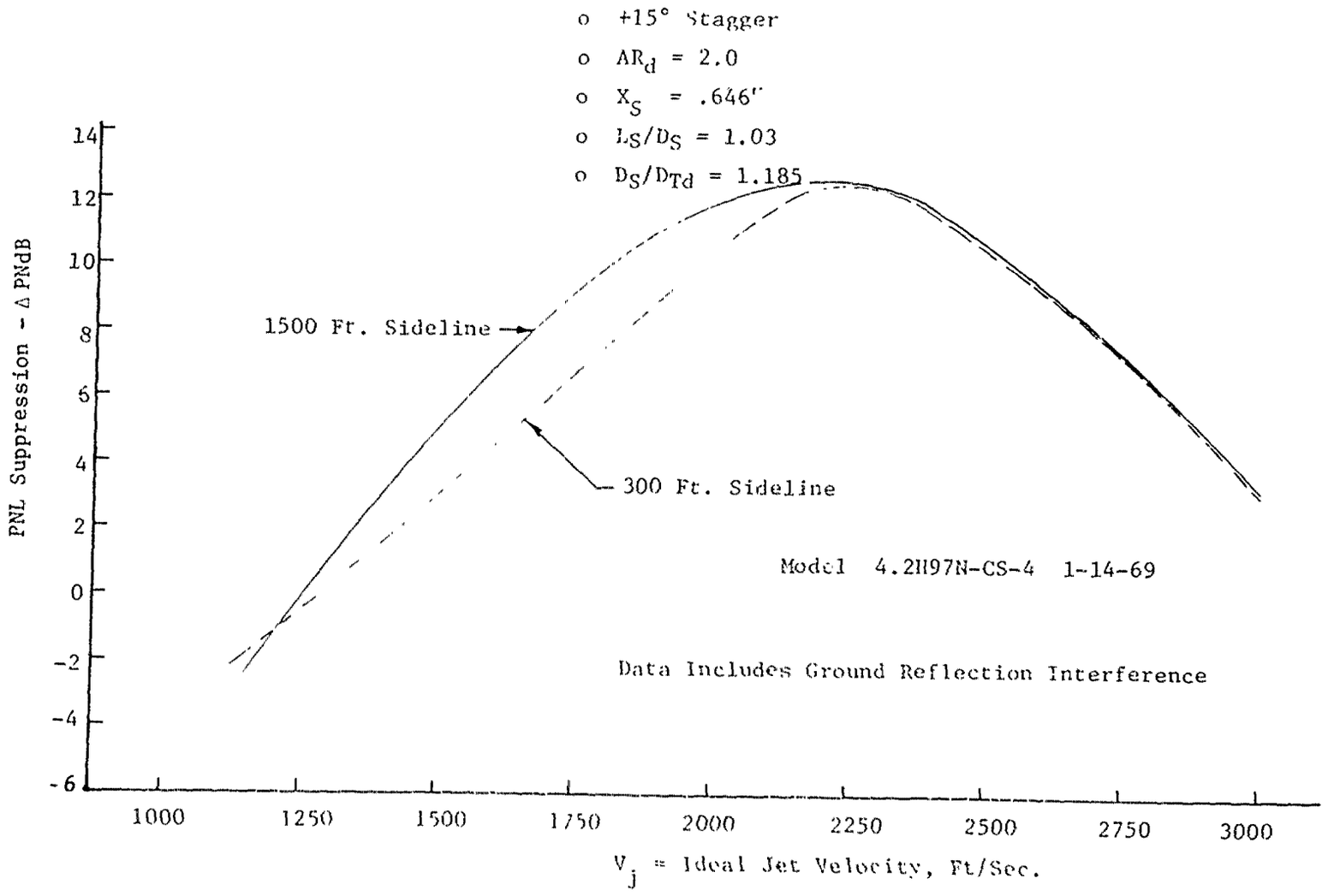

FIGURE V.F.8-21 300 FT. AND 1500 FT. SIDELINE PNL SUPPRESSIONS FOR A 97 HOLE NOZZLE WITH GREATREX CENTER PLUS 4% OPEN LINED EJECTOR, D_S/D_{Td} = 1.185

TABLE V.F.8-8 TEST SUMMARY

MODEL NO. 4.2H97N-CS-1

DESCRIPTION: 97 Hole Nozzle with Greatrex Center, 7.5% Open Lined Ejector, D_S/D_{Td} = 1.185

DATE: 11/22/68

SCALE MODEL A_8 = .1120 ft^2

FULL SCALE A_ϵ = 7.168 ft^2

SCALE FACTOR = 8:1

- DATA INCLUDES GROUND REFLECTION INTERFERENCE
- ANGLE REFERENCED TO JET EXHAUST

RDG NO.	TEST CONDITIONS				ACOUSTIC TEST RESULTS						
	P_{T8}/P_o	T_{T8} (°R)	IDEAL V_j (ft/sec)	W_8 (PPS)	10 log ρA	320' ARC PEAK PNdB	320' ARC PEAK ANGLE	300' SIDELINE PEAK PNdB	300' SIDELINE PEAK ANGLE	1500' SIDELINE PEAK PNdB	1500' SIDELINE PEAK ANGLE
4	2.01	1530	1842	5.79	-6.6	118.5	30	116.1	70	100.4	50
5	1.97	1987	2066	5.07	-7.7	121.9	40	118.6	50	103.2	50
6	1.96	2340	2234	4.66	-8.4	123.1	40	120.6	60	104.9	60
7	2.22	1686	2053	6.11	-6.9	122.9	30	121.0	70	104.5	70
8	2.47	1709	2185	6.77	-6.7	124.9	30	121.8	60	106.0	50
9	2.52	-	2052	6.35	-7.3	124.4	30	119.9	60	104.5	40
10	2.52	1966	2371	6.35	-7.3	127.2	40	123.7	50	108.4	40
11	2.52	2296	2560	5.87	-8.0	129.1	40	125.6	50	110.3	40
12	3.03	2330	2797	7.03	-7.6	133.6	50	131.4	50	116.1	50
13	3.04	1986	2583	7.65	-6.9	131.1	40	128.9	50	113.6	50
14	3.02	1507	2245	8.86	-5.7	127.5	30	123.7	50	108.4	40/50
15	3.22	2312	2851	7.43	-7.4	134.6	50	132.5	50	117.1	50
16	3.27	2322	2874	7.55	-7.4	135.4	50	133.2	50	117.8	50
17	3.44	2330	2930	7.85	-7.3	136.1	50	133.9	50	118.5	50

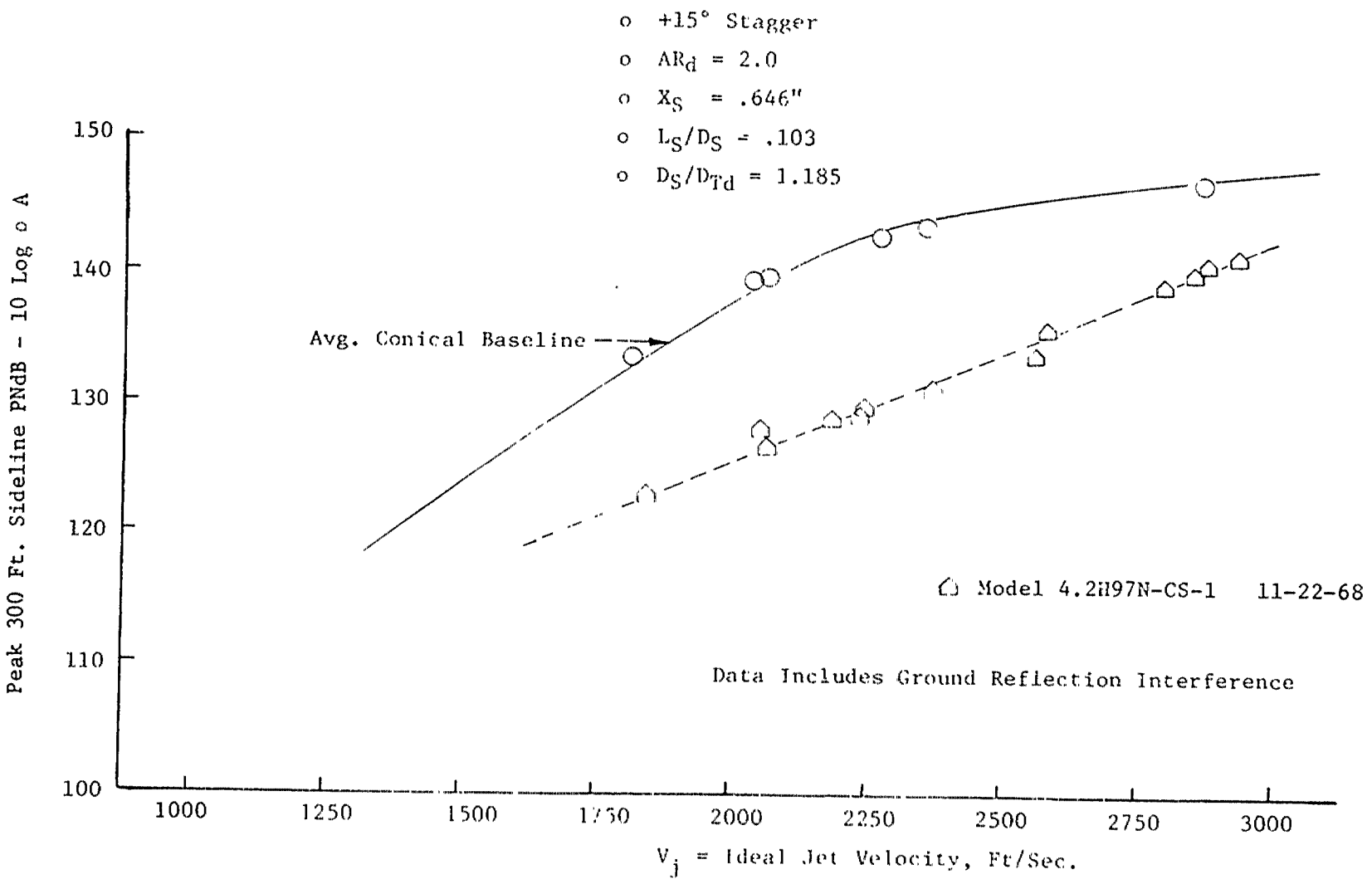

FIGURE V.F.8-22 300 FT. SIDELINE JET NOISE LEVELS FOR A 97 HOLE NOZZLE WITH GREATREX CENTER PLUS 7.5% OPEN LINED EJECTOR, D_S/D_{Td} = 1.185

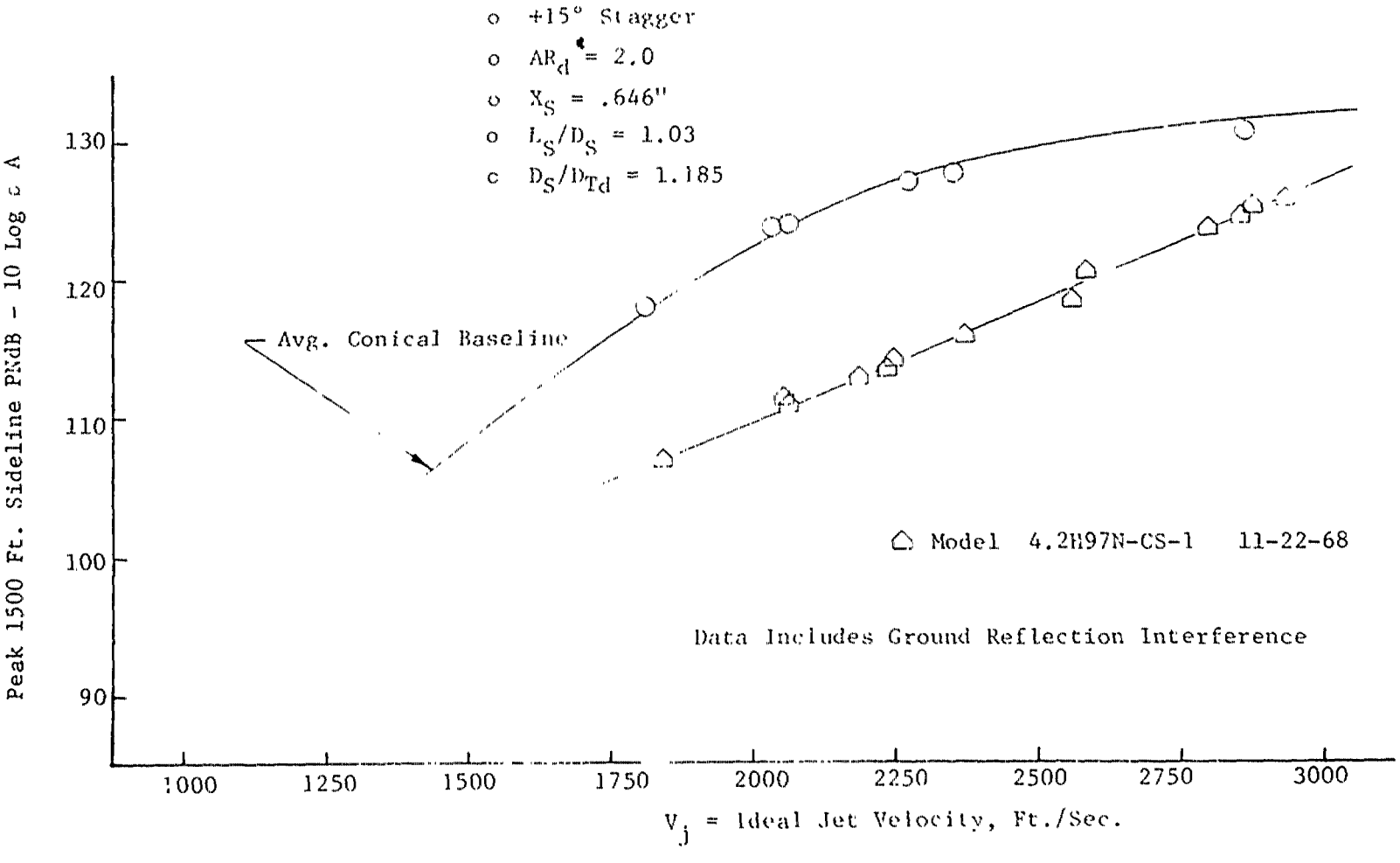

FIGURE V.F.8-23 1500 FT. SIDELINE JET NOISE LEVELS FOR A 97 HOLE NOZZLE WITH GREATREX CENTER PLUS 7.5% OPEN LINED EJECTOR, D_S/D_{Td} = 1.185

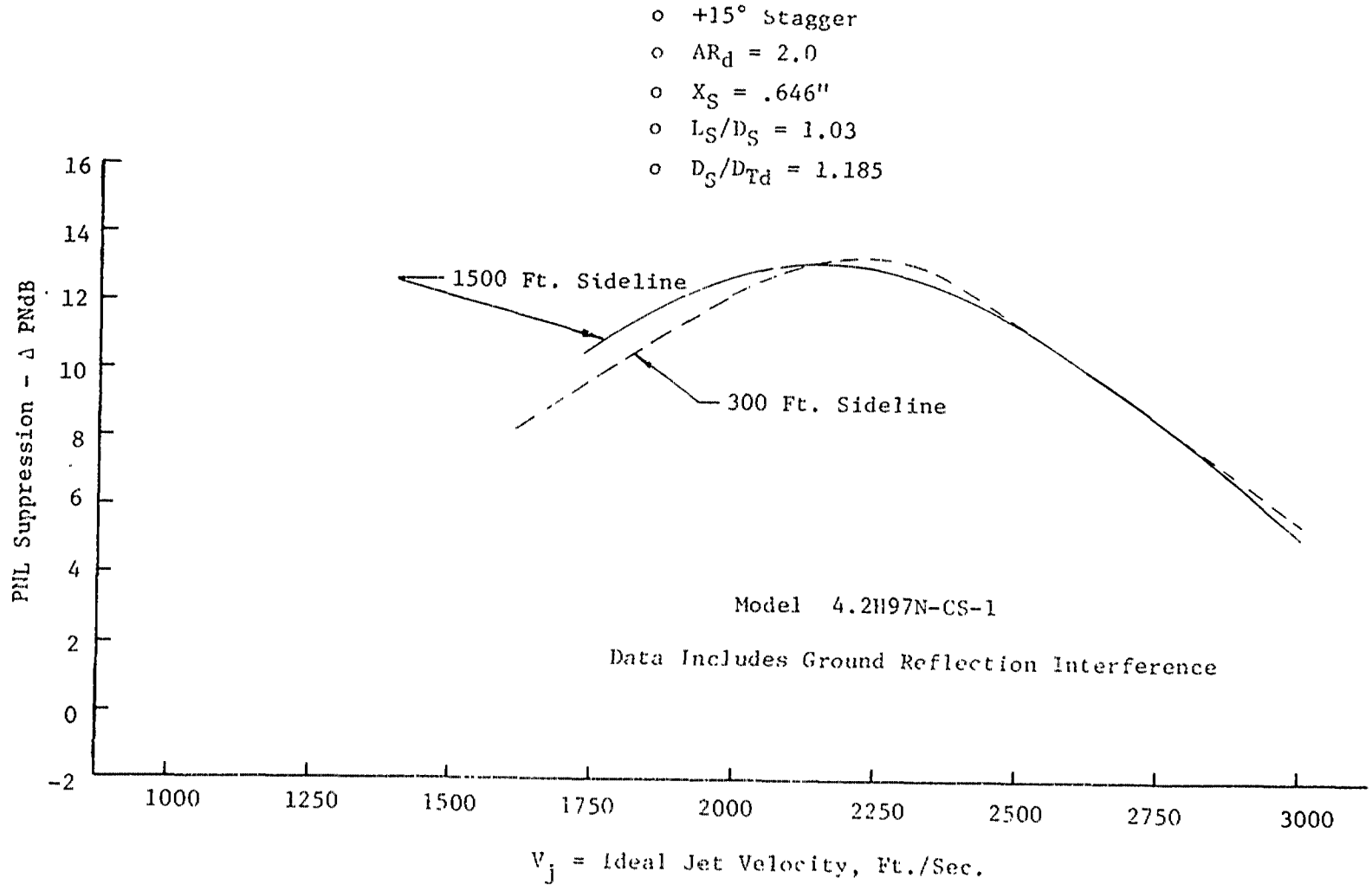

FIGURE V.F.8-24 300 FT. AND 1500 FT. SIDELINE PNL SUPPRESSIONS FOR A 97 HOLE NOZZLE WITH GREATREX CENTER PLUS 7.5% OPEN LINED EJECTOR, D_S/D_{Td} = 1.185

TABLE V.F.8-9 TEST SUMMARY

MODEL NO. 4.2H97N-CS-5

DESCRIPTION: 97 Hole Nozzle with Greatrex Center, 15% Open Lined Ejector

DATE: 1-20-69 D_S/D_{Td} = 1.185

SCALE MODEL A_8 = .1120 ft^2

FULL SCALE A_8 = 7.168 ft^2

SCALE FACTOR = 8:1

- o DATA INCLUDES GROUND REFLECTION INTERFERENCE
- o ANGLE REFERENCED TO JET EXHAUST

	TEST CONDITIONS					ACOUSTIC TEST RESULTS					
			IDEAL			320' ARC		300' SIDELINE		1500' SIDELINE	
RDG NO.	P_{T8}/P_o	T_{T8} (°R)	V_j (ft/sec)	W_8 (PPS)	10 Log ρA	PEAK PNdB	PEAK ANGLE	PEAK PNdB	PEAK ANGLE	PEAK PNdB	PEAK ANGLE
4	2.00	1502	1816	5.80	-6.6	117.8	40	117.5	70	100.7	60
5	2.00	1989	2089	5.02	-7.8	121.9	30	119.5	70	103.3	50
6	2.00	2305	2252	4.65	-8.5	123.4	40	120.5	70	105.2	50
7	2.23	1688	2058	6.40	-6.9	123.1	40	119.8	60/70	104.3	40
8	2.32	1714	2119	6.70	-6.9	125.7	40	122.1	50	106.9	40
9	2.51	1508	2069	7.40	-6.2	124.1	30	120.9	60	105.3	50
10	2.50	1983	2369	6.30	-7.4	128.0	40	124.5	50	109.3	50
11	2.49	2305	2554	5.75	-8.0	129.4	40	126.8	50	111.5	40
12	2.99	2312	2772	6.92	-7.6	134.4	50	132.3	50	116.9	50
13	3.00	1978	2566	7.60	-6.9	131.5	40	128.3	50	112.9	50
14	3.00	1485	2223	8.91	-5.7	129.1	30	124.8	50	109.6	40
15	3.20	2305	2840	7.48	-7.4	136.5	50	134.4	50	118.9	50
16	3.23	2312	2854	7.18	-7.4	136.7	50	138.5	50	119.0	50
17	3.41	2312	2910	7.46	-7.3	138.0	50	135.9	50	120.3	50

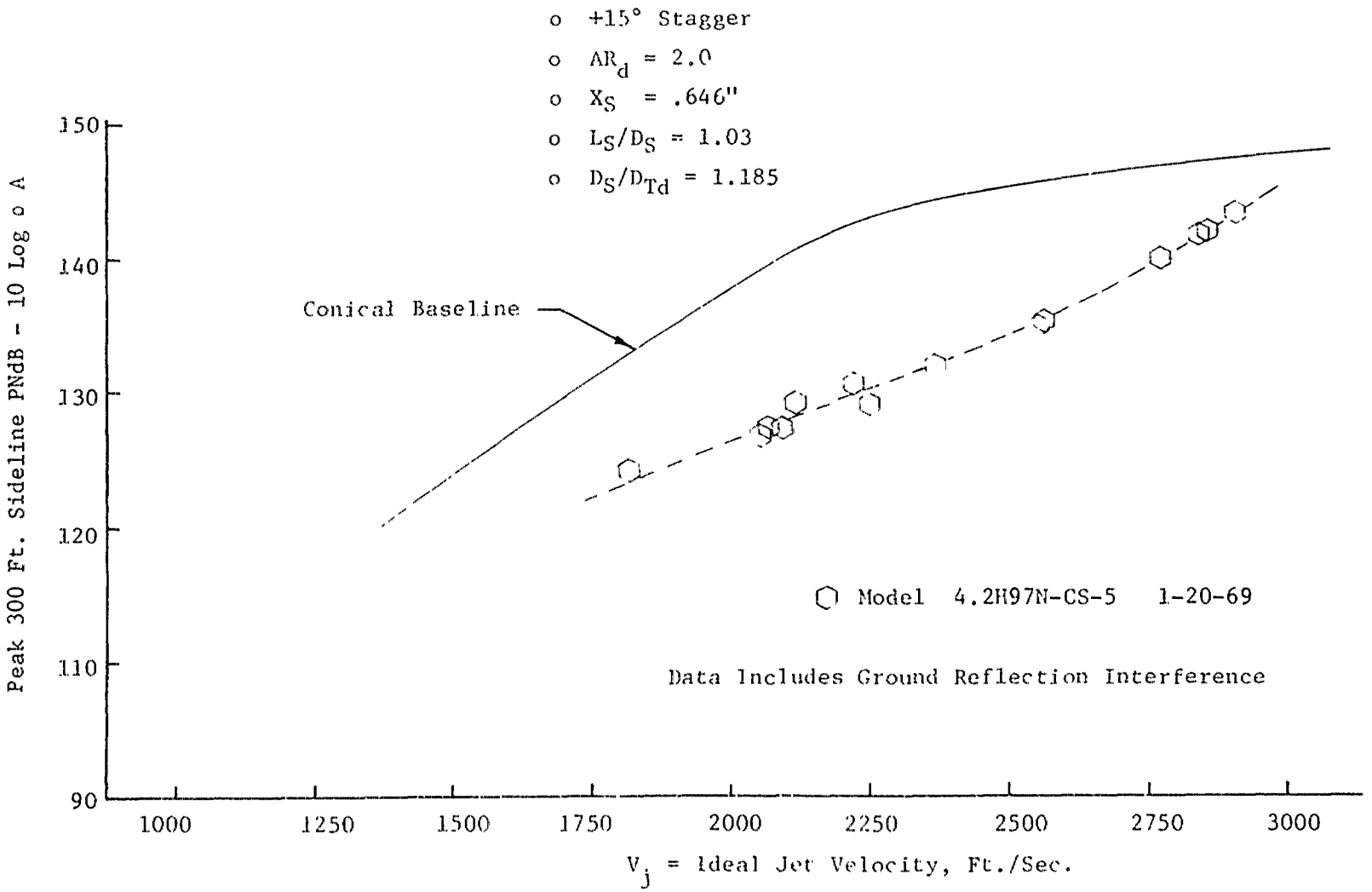

FIGURE V.F.8-25 300 FT. SIDELINE JET NOISE LEVELS FOR A 97 HOLE NOZZLE WITH GREATREX CENTER PLUS 15% OPEN LINED EJECTOR, D_S/D_{Td} = 1.185

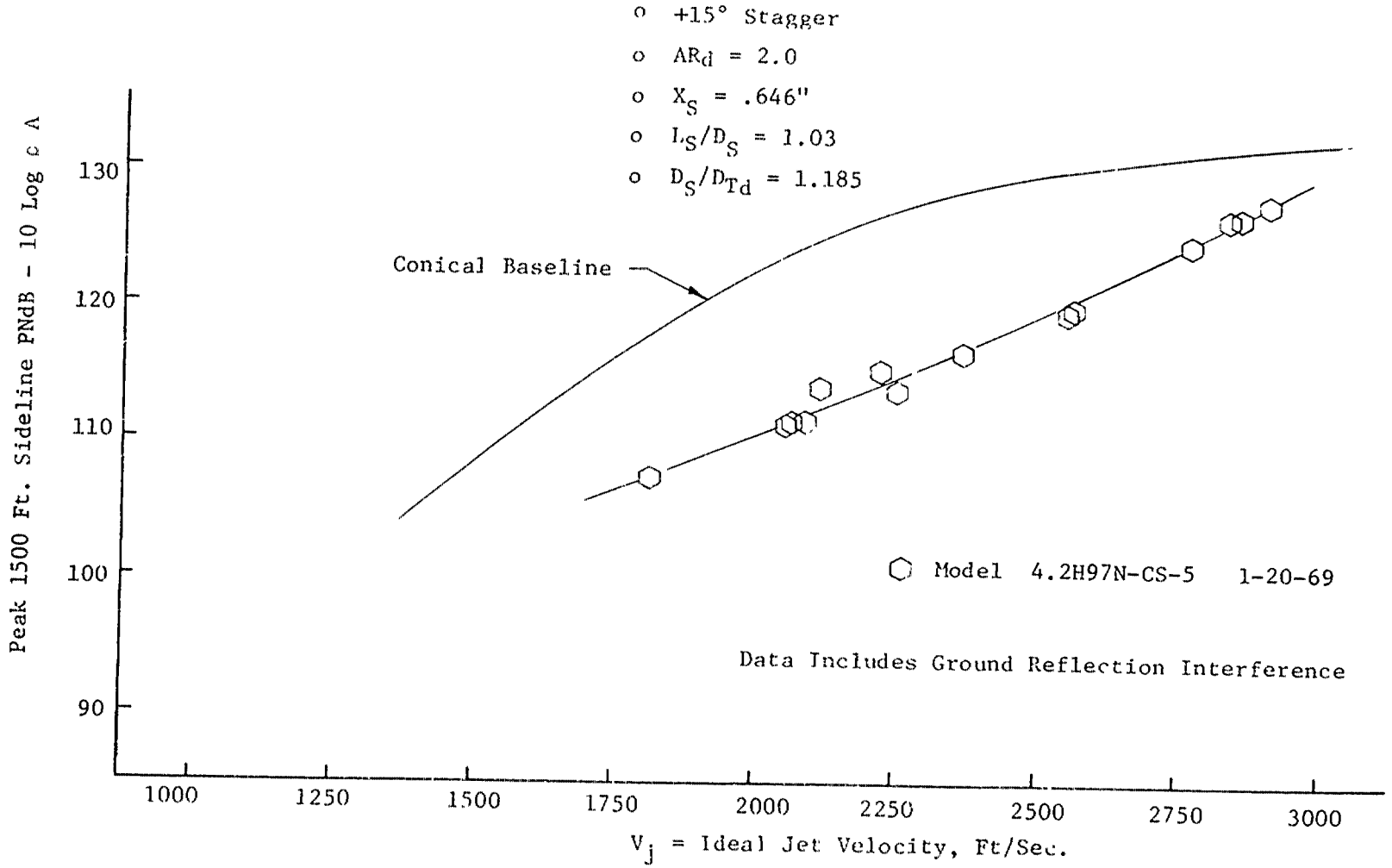

FIGURE V.F.8-26 1500 FT. SIDELINE JET NOISE LEVELS FOR A 97 HOLE NOZZLE WITH GREATREX CENTER PLUS 15% OPEN LINED EJECTOR, D_S/D_{Td} = 1.185

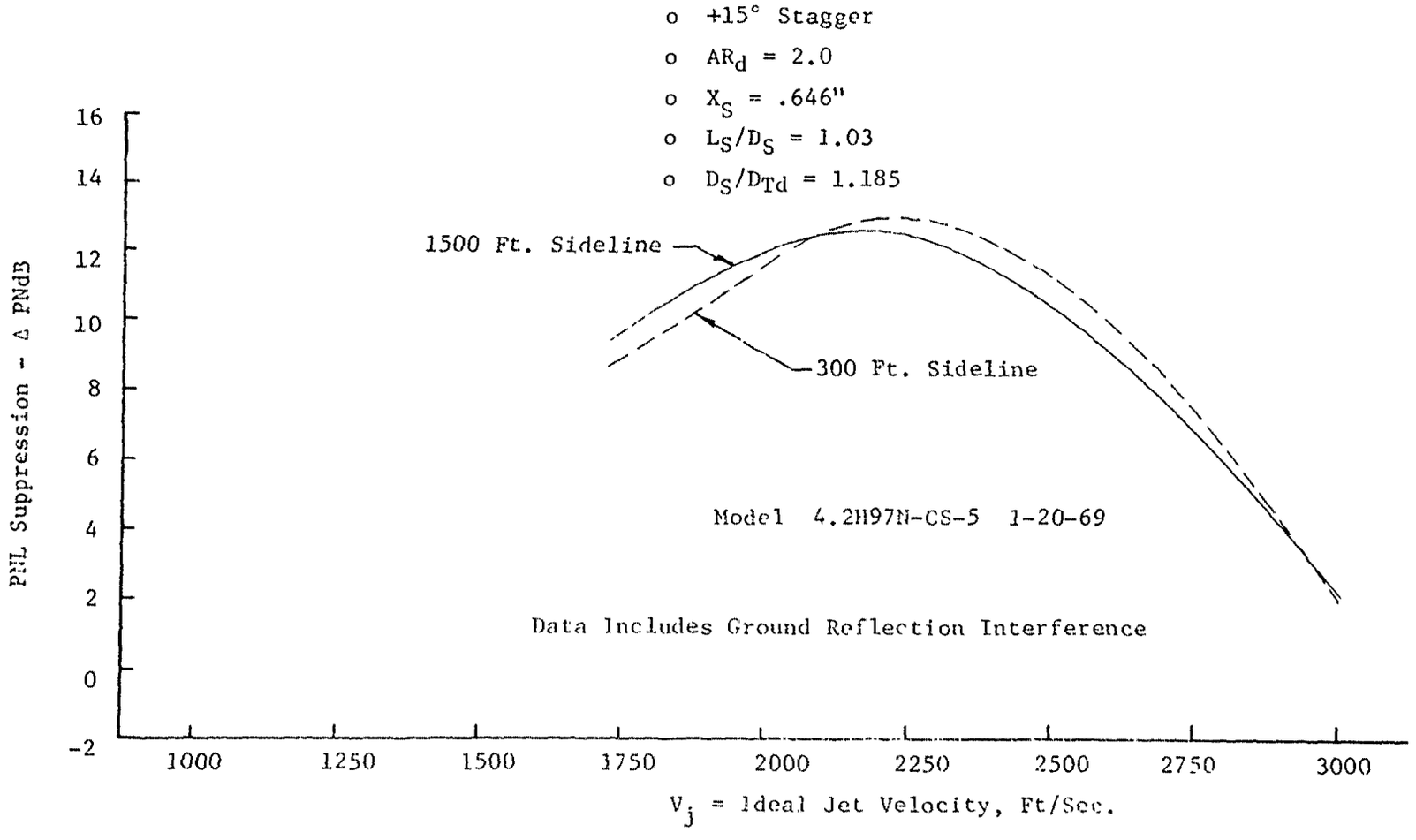

FIGURE V.F.8-27 300 FT. AND 1500 FT. SIDELINE PNL SUPPRESSIONS FOR A 97 HOLE NOZZLE WITH GREATREX CENTER PLUS 15% OPEN LINED EJECTOR, D_S/D_{Td} = 1.185

TABLE V.F.8-10 TEST SUMMARY

MODEL NO. 4.2H97N-CS-6

DESCRIPTION: 97 Hole Nozzle with Greatrex Center, 22.5% Open Lined, Cerafelt Packed, D_S/D_{Td} = 1.185

DATE: 2/11/69; 2/13/69

SCALE MODEL A_8 = .1120 ft^2

FULL SCALE A_8 = 7.168 ft^2

SCALE FACTOR = 8:1

- o DATA INCLUDES GROUND REFLECTION INTERFERENCE
- o ANGLE REFERENCED TO JET EXHAUST

	TEST CONDITIONS				ACOUSTIC TEST RESULTS						
			IDEAL			320' ARC		360' SIDELINE		1500' SIDELINE	
RDG NO.	P_{T8}/P_o	T_{T8} (°R)	V_j (ft/sec)	W_8 (PPS)	10 log ρA	PEAK PNdB	PEAK ANGLE	PEAK PNdB	PEAK ANGLE	PEAK PNdB	PEAK ANGLE
2/11/69											
4	2.01	1533	1841	5.79	-6.7	117.1	40	115.1	70	99.0	60
5	2.02	1992	2107	5.14	-7.8	120.5	40	118.0	50	102.8	50
2/13/69											
1	2.00	2320	2255	4.63	-8.4	123.3	50	121.3	60	106.2	50
2	2.21	1706	2058	6.41	-6.9	121.5	30/40	119.0	60	103.4	60
3	2.47	1730	2199	6.95	-6.8	125.4	40	123.0	50	107.7	50
4	2.53	1512	2082	7.76	-6.1	123.9	30	120.8	50	105.3	50
5	2.52	1974	2373	6.57	-7.3	128.2	40	125.8	50	110.6	50
6	2.50	2314	2560	7.97	-8.0	130.1	50	128.0	50	112.7	50
7	2.99	2328	2781	7.10	-7.6	134.6	50	122.5	50	117.0	50
8	3.02	1991	2581	7.82	-6.9	132.1	50	129.9	50	114.5	50
9	3.00	1538	2261	9.13	-5.8	128.8	40	125.7	50	110.4	50
10	3.22	2269	2825	7.78	-7.3	137.2	50	135.0	50	119.5	50
11	3.25	2660	3069	7.34	-8.0	138.1	50	135.9	50	120.3	50
12	3.44	2331	2931	8.34	-7.2	138.4	50	136.3	50	120.7	50
16	2.00	1522	1829	6.08	-6.6	117.1	40/50	115.9	70	99.4	50
17	2.04	1950	2098	5.35	-7.6	121.5	40	119.0	50	103.6	50

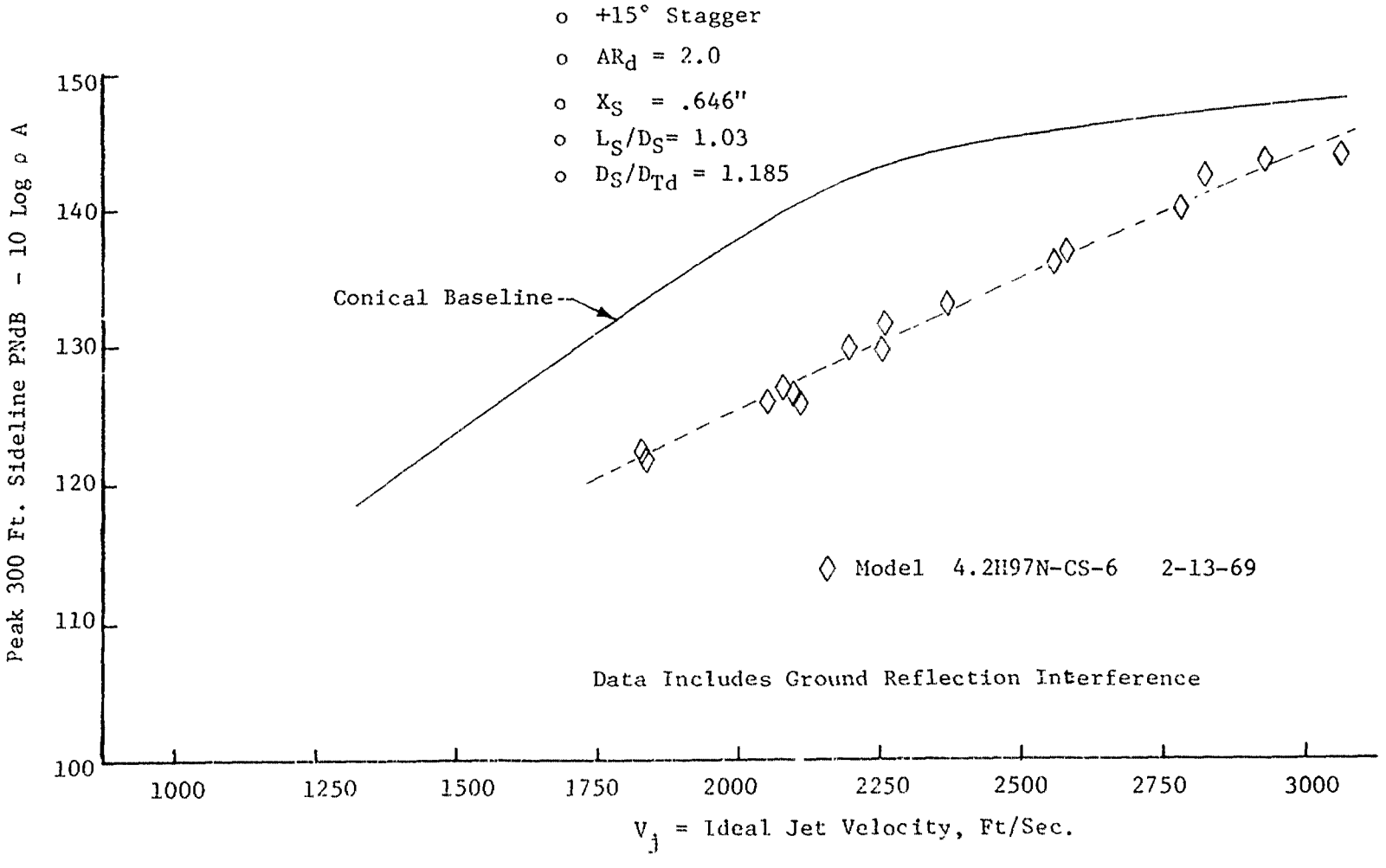

FIGURE V.F.8-28 300 FT. SIDELINE JET NOISE LEVELS FOR A 97 HOLE NOZZLE WITH GREATREX CENTER PLUS 22.5% OPEN LINED, CERAFELT PACKED, EJECTOR, D_S/D_{Td} = 1.185

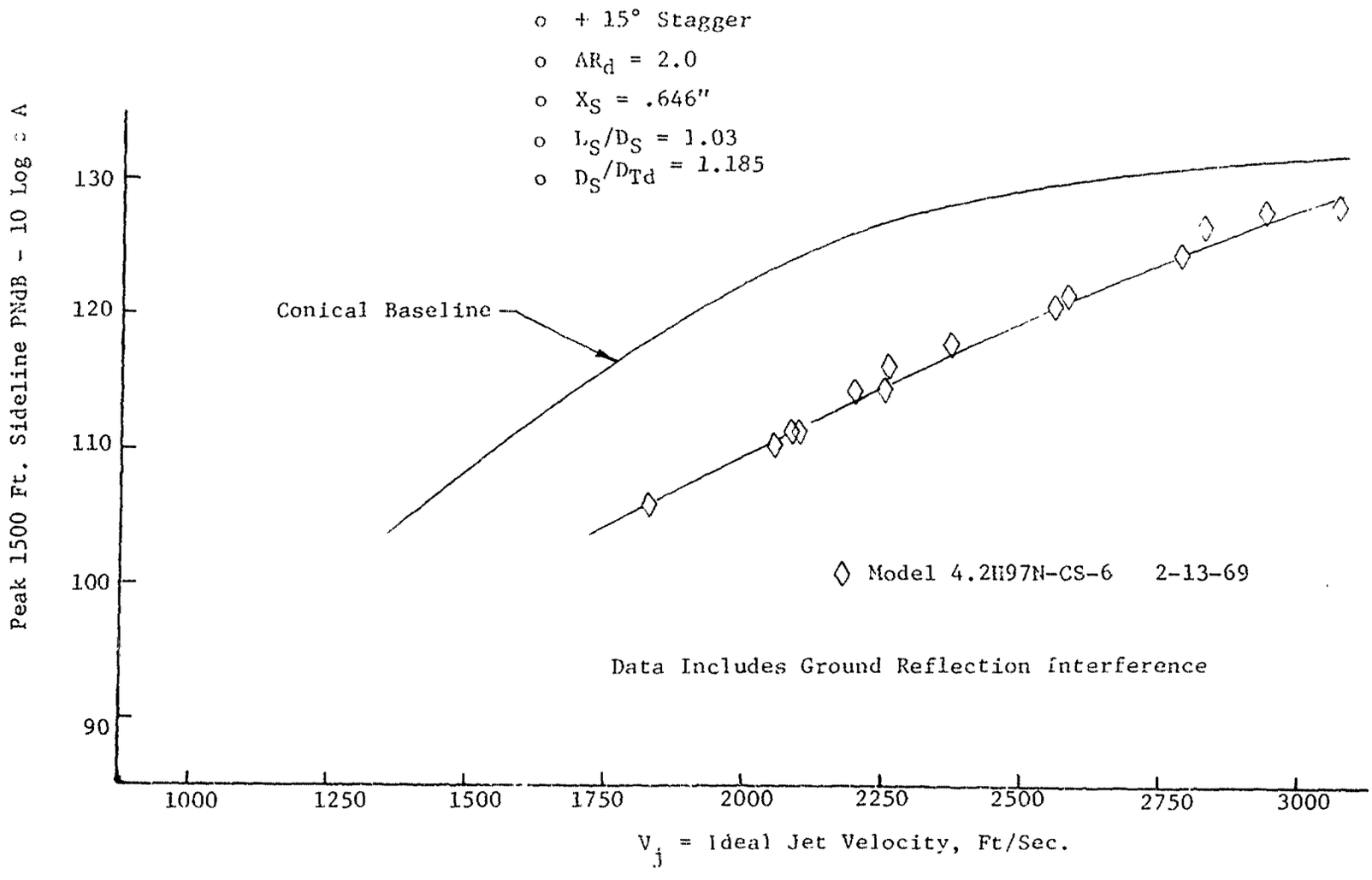

FIGURE V.F.8-29 1500 FT. SIDELINE JET NOISE LEVELS FOR A 97 HOLE NOZZLE WITH GREATREX CENTER PLUS 22.5% OPEN LINED, CERAFELT PACKED, EJECTOR, D_S/D_{Td} = 1.185

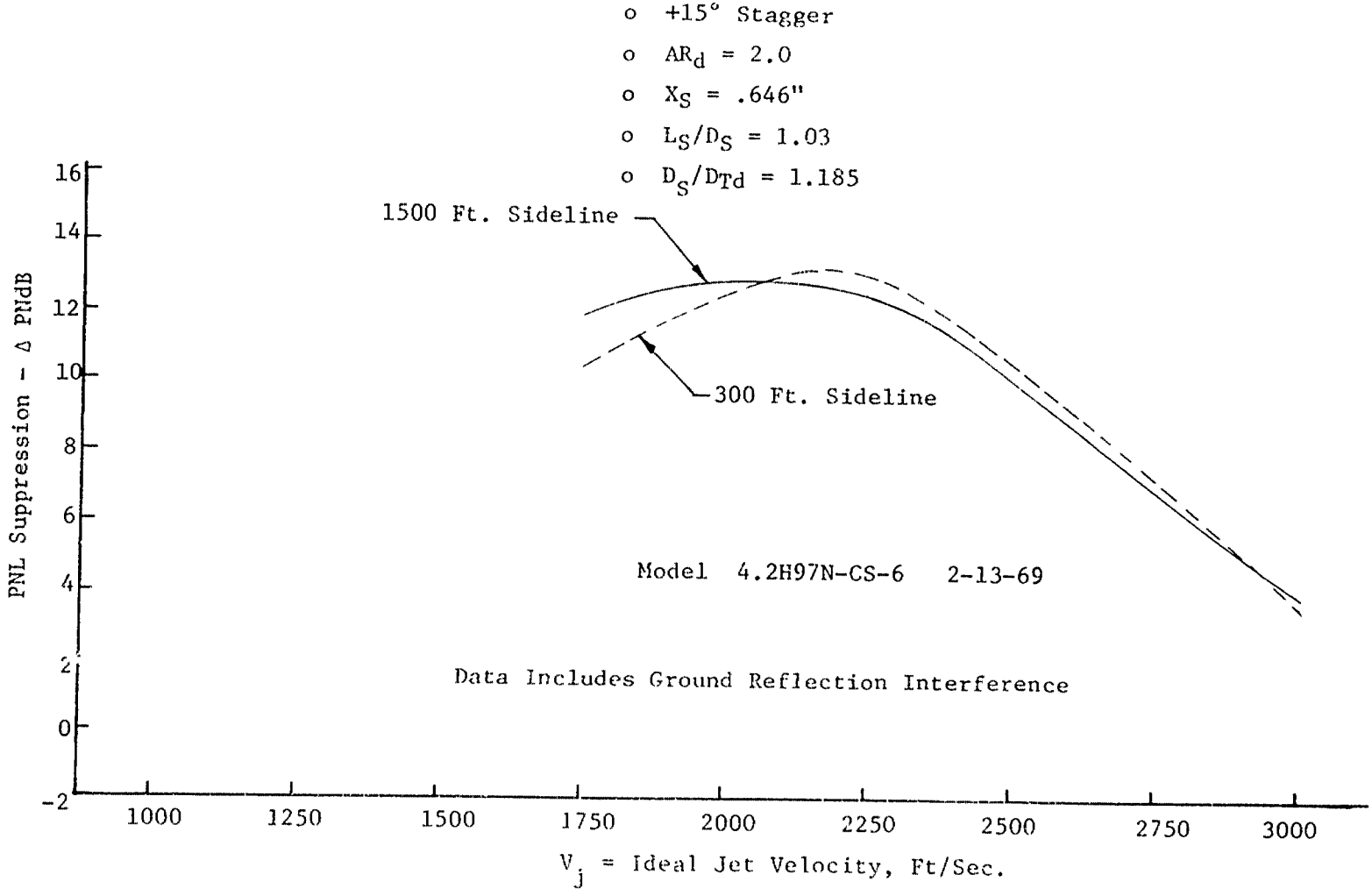

FIGURE V.F.8-30 300 FT. AND 1500.0 FT. SIDELINE PNL SUPPRESSIONS FOR A 97 HOLE NOZZLE WITH GREATREX CENTER PLUS 22.5% OPEN LINED, CERAFELT PACKED, EJECTOR, D_S $_{Td}$ = 1.185

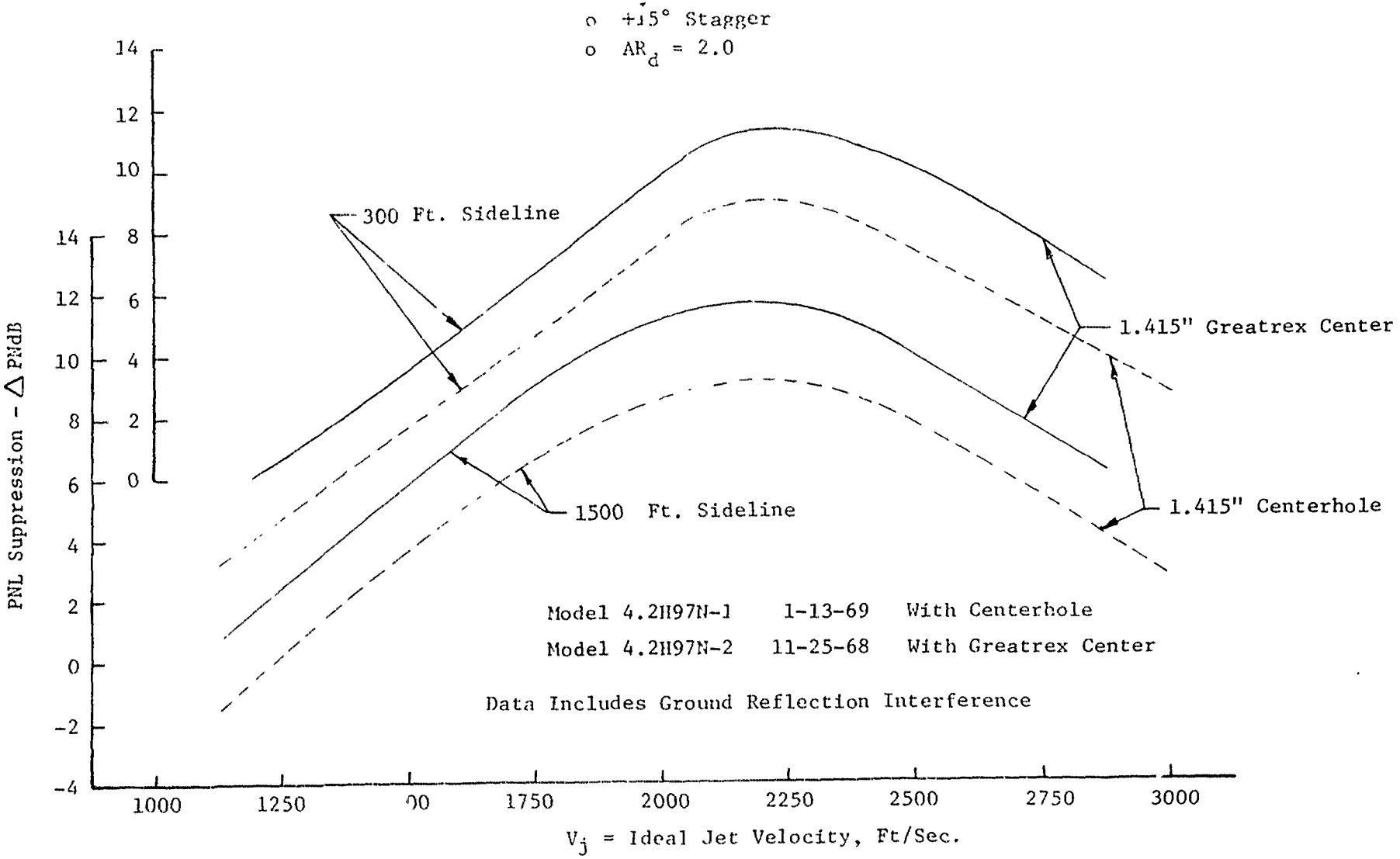

FIGURE V.F.8-31 COMPARISON OF 300 FT. AND 1500 FT. SIDELINE PNL SUPPRESSIONS FOR A 97 HOLE NOZZLE WITH AND WITHOUT A CENTRAL GREATREX

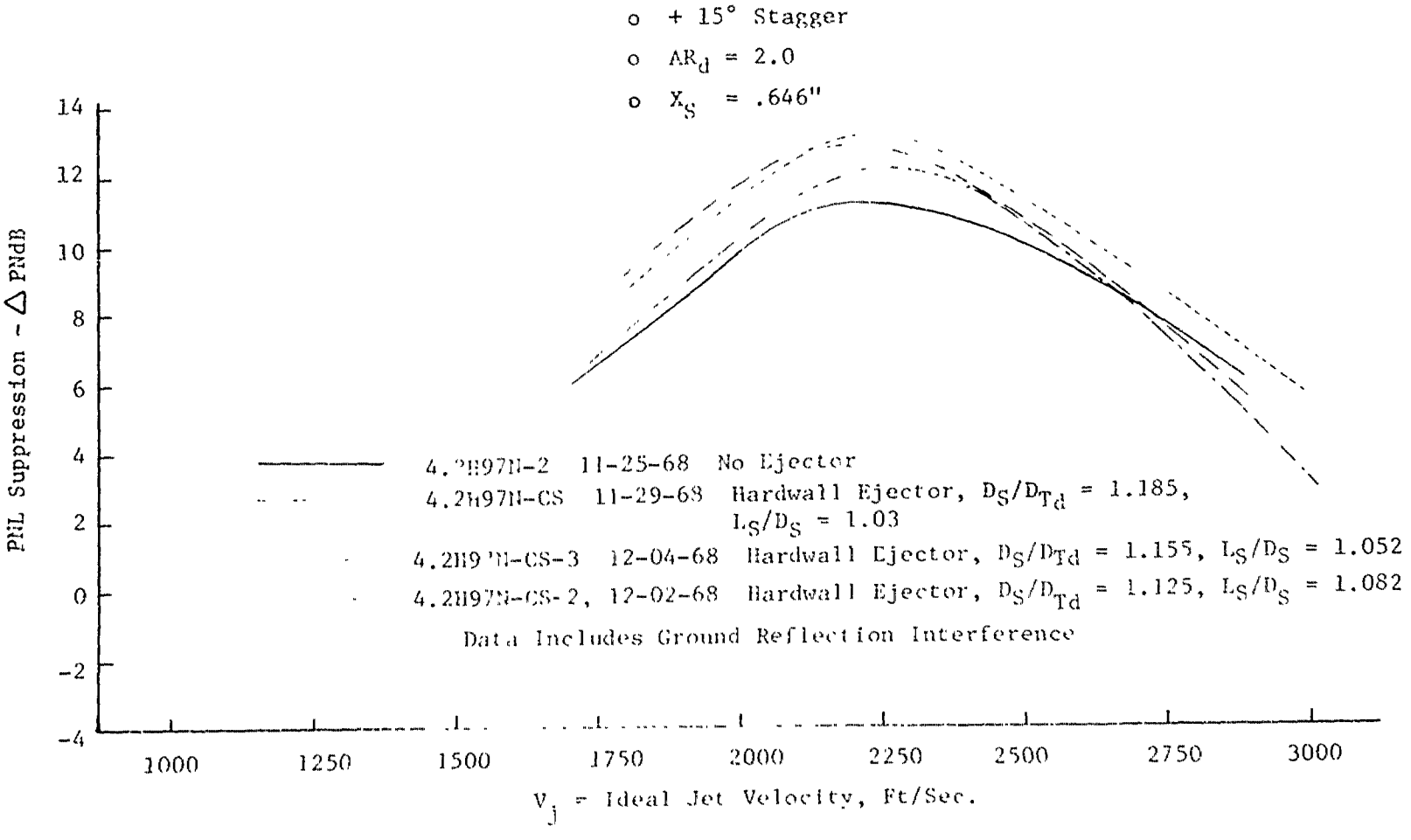

FIGURE V.F.8-32 EFFECT OF SECONDARY HARDWALL EJECTOR D_S/D_{Td} VARIATION ON 300 FT. SIDELINE PNL SUPPRESSIONS FOR 97 HOLE NOZZLES WITH GREATREX CENTER

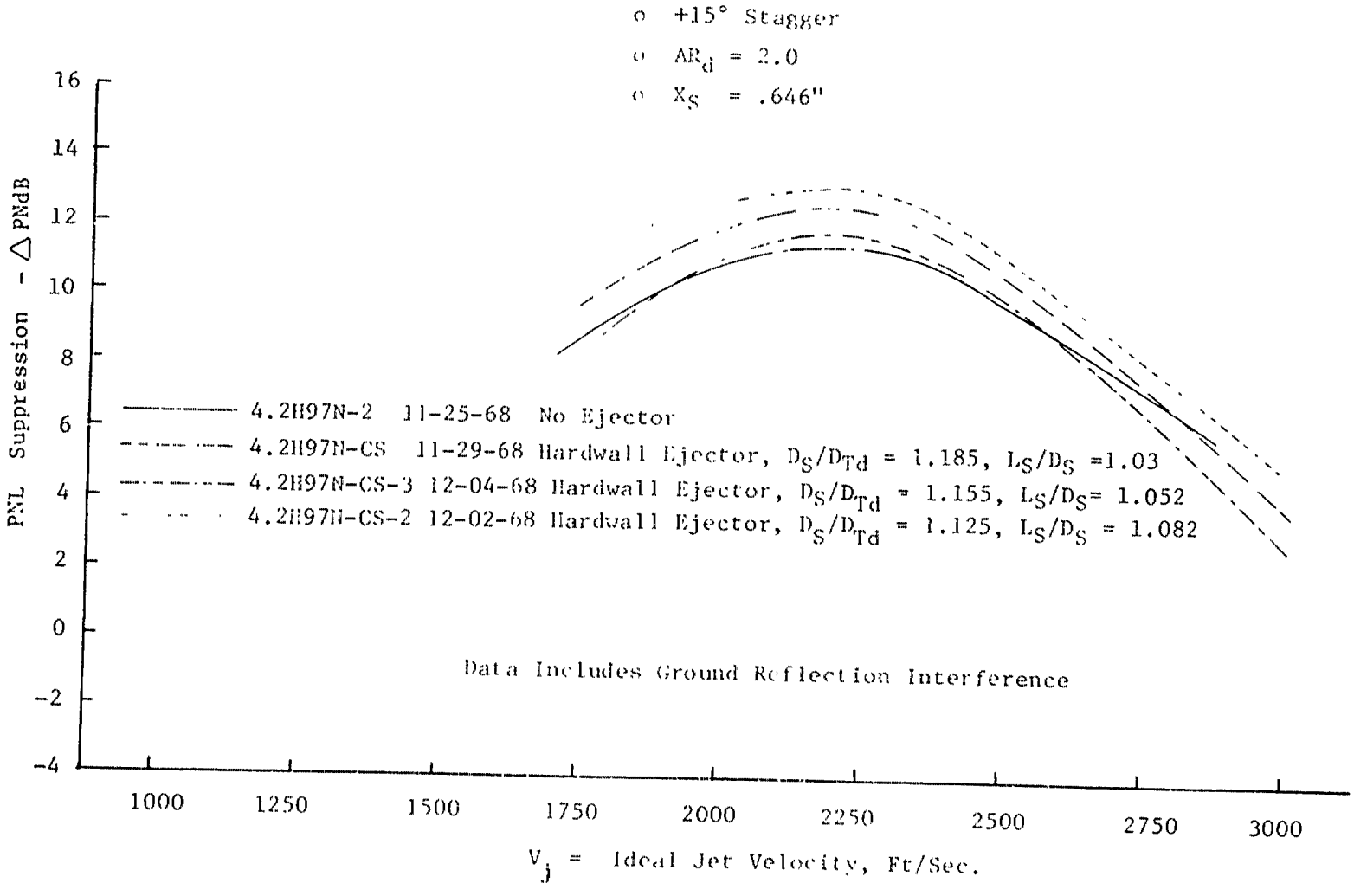

FIGURE V.F.8-33 EFFECT OF SECONDARY HARDWALL EJECTOR D_S/D_{Td} VARIATION ON 1500 FT SIDELINE PNL SUPPRESSIONS FOR 97 HOLE NOZZLES WITH GREATREX CENTER

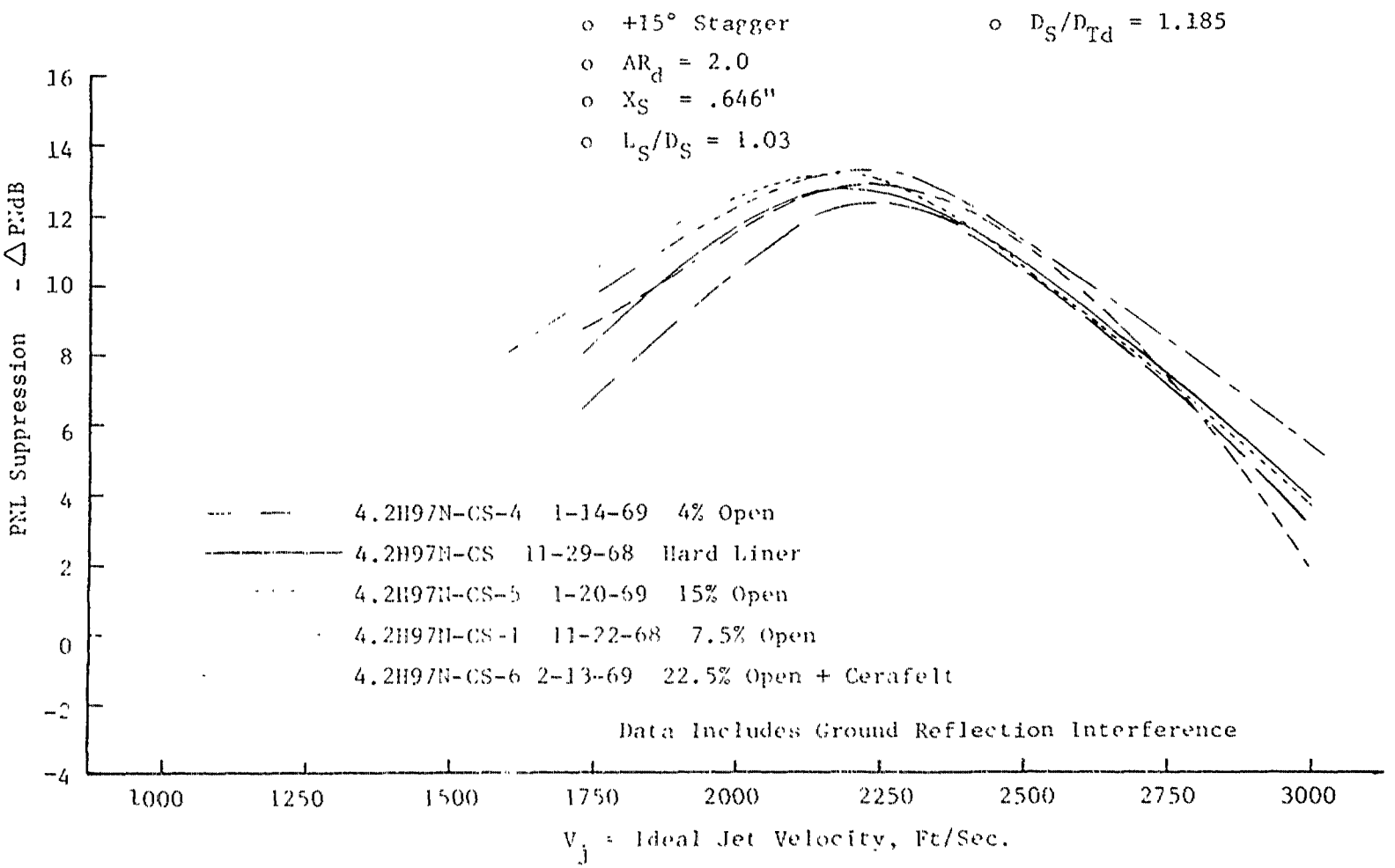

FIGURE V.F.8-34 EFFECT OF ACOUSTICALLY LINED EJECTOR VARIATIONS ON 300 FT. SIDELINE PNL SUPPRESSIONS FOR 97 HOLE NOZZLES WITH GREATREX CENTER

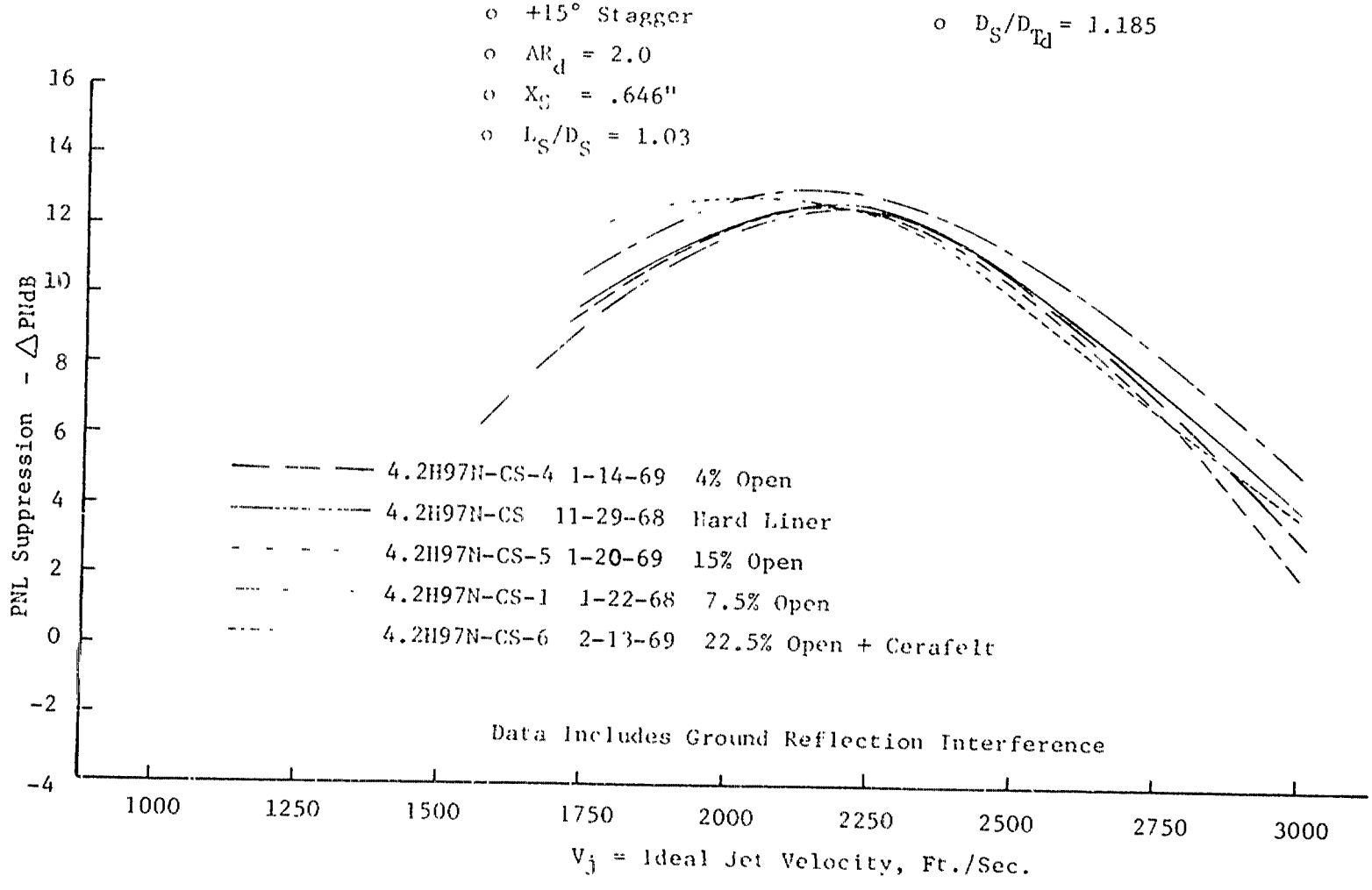

FIGURE V.F.8-35 EFFECT OF ACOUSTICALLY LINED EJECTOR VARIATIONS ON 1500 FT. SIDELINE PNL SUPPRESSIONS FOR 97 HOLE NOZZLES WITH GREATREX CENTER

V.F.9 MULTI-HOLE NOZZLE PARAMETRIC VARIATIONS OF AREA RATIO, HOLE NUMBER, SHROUD D_S/D_{Td}, AND SHROUD AXIAL SPACING, X_S

V.F.9 MULTI-HOLE NOZZLE PARAMETRIC VARIATIONS OF AREA RATIO, HOLE NUMBER, SHROUD D_S/D_{Td}, AND SHROUD AXIAL SPACING, X_S

For a more thorough understanding of tube/hole nozzle acoustic and aerodynamic performance dependency on fundamental nozzle geometry, a comprehensive scale model test program was performed. The program was divided into several phases, each phase (with the exception of Phase I) investigating aerodynamic and acoustic performance dependency on a basic tube nozzle geometric parameter. The phases will be discussed individually within this section and include:

Phase I - Baseline Conical Convergent Nozzle Noise Levels; Figures V.F.9-1 through V.F.9-3 and Table V.F.9-1.

Phase II - Multi-Hole Nozzles, Area Ratio Variation; Figures V.F.9-4 through V.F.9-26 and Tables V.F.9-2 through V.F.9-8

Phase III- Multi-Hole Nozzle, Hole Number Variation; Figures V.F.9-27 through V.F.9-41 and Tables V.F.9-9 through V.F.9-11

Phase IV - Multi-Hole Nozzle, Shroud D_S/D_{T_d} Variation; Figures V.F.9-42 through V.F.9-56 and Tables V.F.9-12 through V.F.9-14

Phase V - Multi-Hole Nozzle, Shroud Axial Spacing, X_S, Variation; Figures V.F.9-57 through V.F.9-67 and Tables V.F.9-15 and V.F.9-16

All acoustic and aerodynamic base pressure data were measured while testing at the G.E., Evendale, JENOTS acoustic facility. Acoustic data were taken on a 40 ft. arc at 10° increments from 30° through 90° from the jet exhaust axis and over a frequency range to 40 KHz (31.5 KHz octave band). The data were scaled to full scale engine application using a scale factor of 8:1 for frequency, nozzle size and measuring arc. Therefore all data are presented as simulated engine size and frequency range.

A simulated engine running line was used to set exhaust nozzle conditions. These normally ranged from P_{T8}/P_o of 1.4 to 3.5, T_{T8} of 1150 to 2690° R, and V_j of 1150 to 3160 ft/sec.

Each of the hole nozzle configurations had base pressure instrumentation applied in the form of static taps. The base pressure profiles were used to calculate the mean base pressures by integrating the measured static pressures

PRECEDING PAGE BLANK-NOT FILMED

over their respective incremental base areas and dividing the total value by the total base area acted upon. This data will be presented in each parametric study in the form of mean base pressure ratio ($\bar{P}_{Base}/P_o$) versus the nozzle pressure ratio (P_{T8}/P_o). The mean base pressure, $\bar{P}_{Base}$, variation will also be presented as a function of P_{T8} in the form of $P_{T8}/\bar{P}_{Base}$ versus P_{T8}/P_o. However, in this form the trends are not as straightforward since they are a function of P_{T8}. The small changes in base pressure do not show up as well or as consistently as the mean base pressure ratio presentations due to the large range of P_{T8} compared to the magnitude of change between mean base pressure and ambient pressure.

As a gauge of base pressure influence on overall nozzle aerodynamic performance, baseplate drag coefficient curves were generated for each parametric study. The drag coefficient is defined as the ratio of drag force per unit area to the velocity pressure per unit area of the approaching stream using the equation:

$$C_D = \frac{F_D}{\frac{1}{2g} A_P \rho V^2}$$

Through substitution of Mach number and density definitions the equation changes to:

$$C_D = \frac{F_D}{\frac{1}{2} A_P P_o k M^2}$$

The drag force, F_D, is calculated from the mean base pressure data. The velocity pressure of the approaching stream is calculated from the stream parameters of P_{T8} and T_{T8} for Mach number, M, and using:

A_P = Projected base area exclusive of hole flow area
P_o = Ambient pressure
k = Specific heat ratio

o Phase I - Baseline Conical Convergent Nozzle Noise Levels

For uniform comparison of test data, a 5.7" D_8 water cooled conical convergent primary nozzle of Figure V.F.9-1 was tested as the baseline

noise source on each day of suppressor testing. A thorough check-out, with data tabulated in Table V.F.9-1 and plotted in Figures V.F.9-2 and -3, established the average peak normalized PNL curves for the 300 ft. and 1500 ft. sidelines, respectively. The normalized curves also agree well with previous baseline curves developed for smaller size nozzles. Thus, confidence is added to the extrapolation beyond 2750 ft/sec jet velocity where measured data were not obtained.

Each day of suppressor testing was accompanied with a baseline nozzle test, the measured noise data being compared to the average baseline curves. On occasion when meteorological conditions changed sufficiently to appreciably alter the daily noise levels, daily conical baseline curves were established and are shown on the suppressor data figures. All suppression values are then quoted to the daily baseline since all measured noise levels within the same time period would have correspondingly shifted. Daily baseline data variation never averaged greater than 1.5 dB from the average baseline and then were always consistently either high or low for the day. Suppression levels are then quoted between average noise curves of the conical and suppressor models, rather than on a point-to-point basis between the two configurations. Several of the suppressor models were retested to ascertain data repeatability. Final suppression levels quoted for these models are the average of both test runs.

o Phase II - Multi-Hole Nozzle, Area Ratio Variation

The parametric area ratio study, as well as the hole number, D_S/D_{Td} and X_S studies, was conducted using simple baseplate models, i.e., holes instead of tubes, since previous results had implied that tube external length does not appreciably influence noise generation. A photograph of the multi-hole configurations in Figure V.F.9-4 shows six of the seven primary nozzles used for the four parametric studies. The hardware schematic of Figure V.F.9-5 lists the specifics of the models used within the area ratio study. This study consisted of five models, each with 85 holes of .651" I.D. arranged in a hexagonal pattern. Area ratio was changed by varying the spacing between holes, S, which altered the compactness of hole array. Area ratio for tube or hole nozzles, AR_d, is defined as the

ratio of area within a circle which circumscribes the hole array to the physical flow area. This was set at AR_d = 2.0, 2.3, 2.7, 3.1 and 4.0. An 85 hole system was representative of a full scale design. The range of area ratio variation extended below and above a practical configuration design. Each model was tested once over a simulated engine running line with the exception of area ratio of 2.0 and 4.0 models. These models had repeat tests to gauge data repeatability. Data results are included in tabular form and as plots of 300 and 1500 ft. sideline normalized peak PNL as follows:

Area Ratio	Tables	Figures
2.0	V.F.9-2 & -3	V.F.9-6 through -9
2.3	V.F.9-4	V.F.9-10 & -11
2.7	V.F.9-5	V.F.9-12 & -13
3.1	V.F.9-6	V.F.9-14 & -15
4.0	V.F.9-7 & -8	V.F.9-16 through -19

To generate design curves for area ratio effect on PNL suppression as a function of jet velocity, peak PNL suppression curves were obtained from the individual normalized peak PNL plots. These were then cross plotted against area ratio at incremental jet velocities to remove any data anomalies and re-read at even increments of area ratio. The resultant generalized suppression characteristic curves are presented in Figures V.F.9-20 and -21 at 300 and 1500 ft. sidelines, respectively.

Figures V.F.9-22A through -22C are 1500 ft. sideline composite spectra plots for comparison of area ratio variation, in order of increasing jet velocity, with measured conical baseline spectra, where available. Following the spectra plots are composite 1500 ft. sideline PNL directivity plots in Figures V.F.9-23A through -23C. These show variation with area ratio at the same jet velocity points as the spectra. Again, baseline nozzle PNL directivity are included where available.

In the high jet velocity region above choking pressure ratio, spectra for all area ratio configurations (Figure V.F.9-22C) are low frequency dominated, meaning the primary noise source is from the coalesced flow region where the individual tube flows have merged to a common stream similar to a conical nozzle.

The location of this coalesced region for any pressure ratio/jet velocity point, and hence the change in mixing length before coalescence, is dependent on area ratio. The greater the area ratio the further downstream the merging occurs, therefore a greater mixing region, a lower noise level and higher suppression. The spectra indicate this by decreasing content of the predominant low frequency noise as area ratio is increased. PNL suppression curves of Figures V.F.9-20 and -21 reflect this with greater suppression for the high area ratios.

At the high jet velocity the change in suppression becomes less as area ratio increases, probably approaching a point beyond which further increase in area ratio will no longer gain suppression. The limiting factor seems to be the amount of pumping of ambient air to the center region of the tube bundle. Total mixing of the available pumped air may be accomplished for the high area ratio models before coalescence is complete. A trade-off point should exist where increase in area ratio, or available mixing region, and increase pumped flow, or actual mixing region, are best matched. Beyond that point no increase in suppression would be expected.

In the low jet velocity region below choking pressure ratio, spectra for all area ratio configurations are high frequency dominated (Figure V.F.9-22A) meaning the primary noise source is from the region of individual tube flows rather than the coalesced tube flow. Classical subsonic theory would indicate that noise generation location aft of the individual tube exits remains essentially constant at velocities below choking (approximately 2000 ft/sec). Thus a low area ratio would be favored since it would coalesce much sooner to a jet similar to that of a conical nozzle than would a high area ratio nozzle with large spacing between individual streams. The sooner the coalescence, the lower the content of the predominantly PNdB weighted high frequency noise produced by the non-merged tube flow. This is indicated in the low jet velocity spectra of Figure V.F.9-22A where the high frequency content of noise decreases as area ratio decreases. The PNL suppression curves of Figures V.F.9-20 and -21 reflect the spectra change with much higher suppression for low area ratio in the low jet velocity range.

As a gauge of aerodynamic performance variation with area ratio, the following data are included.

Figure V.F.9-24; Mean base pressure ratio, $\bar{P}_{Base}/P_o$ versus nozzle pressure ratio, P_{T8}/P_o

Figure V.F.9-25; $P_{T8}/\bar{P}_{Base}$ versus P_{T8}/P_o

Figure V.F.9-26; Base Plate Drag Coefficient versus P_{T8}/P_o

As readily seen, mean base pressure ratio steadily decreased and base drag coefficient steadily increased as area ratio was changed from 4.0 to 2.0. This is due to the increased compactness of the hole bundle limiting the available area between holes which act as air passages for the pumped ambient flow. The wide spacing at high area ratios allows for increased pumping and therefore high base pressures and lower base drag.

o Phase III - Multi-Hole Nozzle, Hole Number Variation

For the parametric hole number study the three primary nozzles of Figure V.F.9-27 were used. Each was at AR_d=2.7, as shown on the schematic of Figure V.F.9-28. Hole numbers were set at 55, 85, and 121, holding the total physical flow area constant by setting hole size at .809", .651", and .546" I.D., respectively.

Data results are included in tabular form and as plots of 300 and 1500 ft. sideline normalized peak PNL as a function of jet velocity, as follows:

Hole Number	Tables	Figures
55	V.F.9-9 & 10	V.F.9-29 through -32
85	V.F.9-5	V.F.9-12 & -13
121	V.F.9-11	V.F.9-33 & -34

The 85 hole, AR_d = 2.7, model data is that of the previous area ratio study. To formulate generalized suppression characteristic curves as a function of hole number, peak PNL suppression plots as a function of jet velocity were made from the individual normalized peak PNL plots. They were then cross plotted against hole number at incremental jet velocities to remove any data anomalies and re-read at even increments of hole number. Thus, the generalized curves of Figures V.F.9-35 and -36 were formed to show peak PNL suppression at the 300 and 1500 ft. sidelines, respectively.

Figures V.F.9-37A through -37C are 1500 ft. sideline composite spectra plots for comparison of hole number in order of increasing jet velocity. Figures V.F.9-38A through -38C are composite 1500 ft. sideline PNL directively plots at the same jet velocity points. Baseline conical nozzle spectra and PNL directivity are included where available.

Inspection of the acoustic curves shows increased suppression with higher hole number, the level of increase being nearly consistent across the jet velocity range. The spectra show that the noise level changes are across the frequency range, not just in the high frequency bands.

Aerodynamic data for parametric hole number variation is presented as follows:

Figure V.F.9-39; Mean base pressure ratio, $\bar{P}_B/P_o$, versus nozzle pressure ratio, P_{T8}/P_o

Figure V.F.9-40; $P_{T8}/\bar{P}_{Base}$ versus P_{T8}/P_o

Figure V.F.9-41; Base Plate Drag Coefficient versus P_{T8}/P_o

Inspection of these plots and the schematic of Figure V.F.9-28 shows that for identically the same base area (since area ratio is constant at 2.7 and total flow area is constant) the fineness of segmentation changes the flow channels through which ambient air is pumped. The coarsely divided 55 hole baseplate has larger passageways between holes for pumping ambient air to the center of the hole array than do the more finely divided 85 and 121 hole nozzles. The finer the division, the lower the base pressure becomes toward the center of the array and consequently the higher the base drag.

o Phase IV - Multi-Hole Nozzle, Shroud D_S/D_{Td} Variation

The primary nozzle for this series was the 85 hole, AR_d of 2.7, configuration. Secondary shrouds were cylindrical and of internal diameters, D_S of 10.352", 10.845" and 11.338" to give D_S/D_{Td} values of 1.05, 1.10 and 1.15, respectively. Figure V.F.9-42 shows a photograph of the shrouds while Figure V.F.9-43 is a schematic of the primary-secondary systems with pertinent physical dimensions. Location of the shroud aft of the primary nozzle was held constant at X_S = 1.73". The purposes of the series were to determine the acoustic effectiveness of an untreated shroud and at what diameter ratio, D_S/D_{Td}, the acoustic suppression to aerodynamic loss was optimum.

Acoustic and aerodynamic data are presented in the same format as the area ratio and hole number studies as follows:

D_S/D_{Td}	Tables	Figures
1.05	V.F.9-12	V.F.9-44 & -45
1.10	V.F.9-13	V.F.9-46 & -47
1.15	V.F.9-14	V.F.9-48 & -49

Figures V.F.9-50 & 51; Peak PNL suppression at 300 and 1500 ft. sidelines

Figures V.F.9-52A through -52C; 1500 ft. sideline spectra comparisons

Figures V.F.9-53A through -53C; 1500 ft. sideline PNL directivity comparisons.

Figure V.F.9-54; Mean base pressure ratio, $\bar{P}_B/P_o$ versus nozzle pressure ratio, P_{T8}/P_o

Figure V.F.9-55; $P_{T8}/\bar{P}_{Base}$ versus P_{T8}/P_o

Figure V.F.9-56; Base Plate Drag Coefficient versus P_{T8}/P_o

The PNL suppression plots of Figures V.F.9-50 &-51 are taken directly from the individual peak PNL data plots against jet velocity, not from cross plotting as were the area ratio and hole number generalized suppression curves.

In general the addition of a hardwall cylindrical shroud enhanced the suppression in the higher jet velocity region. Decreasing the diameter ratio, D_S/D_{Td}, increased suppression. This implies that the 1.05 diameter ratio shroud is inhibiting the induced flow, and the primary flow expands as if it were a no-flow ejector or dump diffuser. The base pressure data (Figure V.F.9-54) and the base drag coefficient plot (Figure V.F.9-56) tend to verify this contention. For a given axial spacing, increasing shroud diameter ratio tends to produce induced flow conditions approaching the non-shrouded configuration. This, in turn, suggests that the base pressure will be higher with the larger diameter ratio, implying better overall aerodynamic performance.

o Phase V - Multi-Hole Nozzle, Shroud Axial Spacing, X_S, Variation

This test phase again used the 85 hole, AR_d of 2.7, primary nozzle. The D_S/D_{Td} of 1.10 cylindrical shroud, shown in Figure V.F.9-57, was used at three axial spacings, X_S of 1.73", 4.73" and 7.47", as shown schematically in Figure V.F.9-58. The X_S= 1.73" configuration and data are from the preceding study of D_S/D_{Td}. The purpose of the test series was to obtain generalized aerodynamic and acoustic information on the effect of increasing/decreasing the auxiliary flow on a multi-hole (or tube) suppressor system. Instrumentation was included in the auxiliary flow inlet to measure pumping characteristics.

Acoustic and aerodynamic data are presented in the same format as the previous sections, as follows:

X_S	Tables	Figures
1.73"	V.F.9-13	V.F.9-46 & -47
4.73"	V.F.9-15	V.F.9-59 & -60
7.47"	V.F.9-16	V.F.9-61 & -62

Figures V.F.9-63 & 64; Peak PNL suppression at 300 & 1500 ft. sidelines

Figure V.F.9-65; Mean base pressure ratio, $\bar{P}_B/P_o$, versus nozzle pressure ratio, P_{T8}/P_o

Figure V.F.9-66; $P_{T8}/\bar{P}_{Base}$ versus P_{T8}/P_o

Figure V.F.9-67; Base Plate Drag Coefficient versus P_{T8}/P_o

The PNL suppression curves of Figures V.F.9-63 and -64 are again taken directly from the individual peak PNL data plots, not from cross plotting as were the area ratio and hole number generalized suppression curves. The intermediate and the shortest spacing configuration, X_S = 4.73" and 1.73", exhibited almost identical suppression trends while, as expected, the largest axial spacing of 7.47" produced suppression levels approaching the no-shroud configuration. The implication is that increased auxiliary flow had minor effects on the noise generation.

The short axial spacing produced very low base pressures (Figure V.F.9-65) which increased the base drag component of thrust loss (Figure V.F.9-67). Translating the shroud downstream provided more induced flow and regained much of the base pressure loss, nearly simulating a no-shroud configuration and thereby reducing base drag significantly. (The aerodynamic data for the X_S= 4.73" model were not available.) In general, the data suggest that the addition of a suitably located hard shroud may increase suppression for a slight increase in base drag.

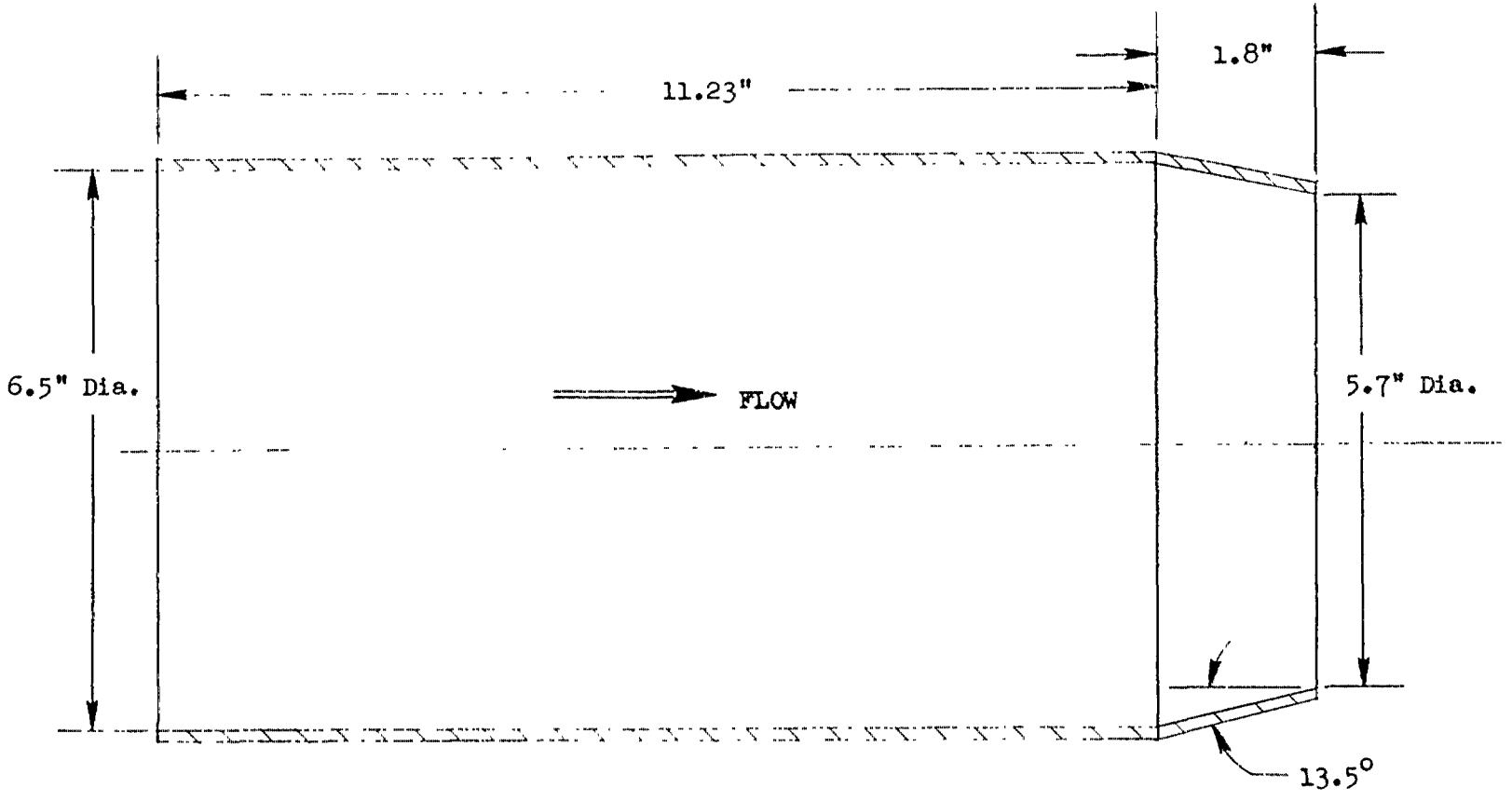

FIGURE V.F.9-1 SCHEMATIC OF 5.7" I.D. CONICAL NOZZLE USED IN BASELINE COMPARISONS

TABLE V.F.9-1 TEST SUMMARY

MODEL NO. 5.7" ID Cone

DESCRIPTION: Baseline Conical Nozzle

DATE: 3/3/69

SCALE MODEL A_8 = .178 ft^2

FULL SCALE A_8 = 11.392 ft^2

SCALE FACTOR = 8:1

- o DATA INCLUDES GROUND REFLECTION INTERFERENCE
- o ANGLE REFERENCED TO JET EXHAUST

	TEST CONDITIONS				ACOUSTIC TEST RESULTS						
			IDEAL			320' ARC		300' SIDELINE		1500' SIDELINE	
RDG NO.	P_{T8}/P_o	T_{T8} (°R)	V_j (ft/sec)	W_8 (PPS)	10 log ρA	PEAK PNdB	PEAK ANGLE	PEAK PNdB	PEAK ANGLE	PEAK PNdB	PEAK ANGLE
3/3/69											
1	1.42	1136	1140	7.67	-3.4	119.6	30	113.0	30	98.4	30
2	1.57	1196	1329	8.44	-3.8	119.6	30	116.0	70	100.2	60
3	1.65	1246	1423	8.71	-3.9	122.9	30	118.6	50	103.2	50
4	1.72	1396	1565	8.74	-4.4	126.7	30	121.2	50	105.8	50
5	1.74	1300	1523	9.16	-4.1	125.7	30	120.5	50	105.3	40
6	1.90	1390	1686	9.72	-4.3	130.0	30	124.7	50	109.2	50
7	1.94	1396	1714	9.96	-4.3	131.7	30	126.7	40	111.3	40
8	1.98	1523	1819	9.57	-4.6	133.1	30	128.9	40	113.6	40
9	2.08	1672	1967	9.65	-5.0	136.3	40	132.1	40	116.5	40
10	2.29	1666	2074	10.54	-4.8	137.2	40	135.0	50	119.4	50
11	2.36	1560	2043	11.36	-4.4	137.0	40	133.7	50	118.1	50
12	2.43	1819	2240	10.51	-5.1	139.5	50	137.3	50	121.4	50
13	2.75	1848	2390	12.13	-4.8	143.0	40	140.3	50	124.6	50
14	3.09	1829	2495	13.50	-4.5	142.9	50	140.7	50	125.0	50
15	3.29	2021	2688	13.74	-4.8	142.8	50	140.7	50	125.7	50
16	3.55	1902	2678	15.26	-4.3	143.7	50	141.5	50	125.7	50

TABLE V.F.9-1 TEST SUMMARY
(Cont.)

MODEL NO. 5.7" ID Cone

DESCRIPTION: Baseline Conical Nozzle

DATE: 3/18/69; 3/19/69

SCALE MODEL A_8 = .178 ft^2

FULL SCALE A_8 = 11.392 ft^2

SCALE FACTOR = 8:1

- o DATA INCLUDES GROUND REFLECTION INTERFERENCE
- o ANGLE REFERENCED TO JET EXHAUST

	TEST CONDITIONS				ACOUSTIC TEST RESULTS						
			IDEAL			320' ARC		300' SIDELINE		1500' SIDELINE	
RDG NO.	P_{T8}/P_o	T_{T8} (°R)	V_j (ft/sec)	W_8 (PPS)	10 log ρA	PEAK PNdB	PEAK ANGLE	PEAK PNdB	PEAK ANGLE	PEAK PNdB	PEAK ANGLE
3/18/69											
1	2.05	1514	1851	9.8	-4.6	134.1	40	130.1	40	114.8	40
2	2.75	1779	2348	12.0	-4.7	141.0	50	138.8	50	122.9	50
3	2.98	2128	2653	11.5	-5.3	142.9	50	140.7	50	125.0	50
4	2.53	1622	2155	11.5	-4.5	139.2	40	135.9	50	120.2	50
5	1.43	1154	1164	7.8	-3.8	113.9	40	111.5	60	95.9	50/60
3/19/69											
1	2.05	1512	1857	10.10	-4.6	133.7	30	128.9	40	113.8	40
2	2.79	1778	2362	12.28	-4.6	141.1	50	138.9	50	123.2	50
3	2.97	2126	2651	12.06	-5.3	143.2	50	141.0	50	125.4	50
4	2.53	1640	2168	11.87	-4.5	139.1	50	137.0	50	121.3	50
5	2.58	2099	2475	10.41	-5.6	141.4	50	139.2	50	123.5	50
6	2.30	1550	2007	10.91	-4.5	136.8	40	132.6	40	117.2	40
7	1.79	1517	1684	8.61	-4.8	128.7	30	124.5	40	109.7	40
8	1.57	1515	1489	7.33	-4.8	122.6	30	118.4	50	103.2	50
9	1.65	1243	1423	8.88	-3.9	121.2	30	116.7	50	101.2	40/50
10	1.46	1130	1185	7.75	-3.7	112.8	40	110.5	50	95.1	50

TABLE V.F.9-1 TEST SUMMARY

(Cont.)

MODEL NO. 5.7" ID Cone

DESCRIPTION: Baseline Conical Nozzle

DATE: 3/27/69; 3/31/69

SCALE MODEL A_8 = .178 ft^2

FULL SCALE A_8 = 11.392 ft^2

SCALE FACTOR = 8:1

- o DATA INCLUDES GROUND REFLECTION INTERFERENCE
- o ANGLE REFERENCED TO JET EXHAUST

	TEST CONDITIONS				ACOUSTIC TEST RESULTS						
			IDEAL			320' ARC		300' SIDELINE		1500' SIDELINE	
RDG NO.	P_{T8}/P_o	T_{T8} (°R)	V_j (ft/sec)	W_8 (PPS)	10 log ρA	PEAK PNdB	PEAK ANGLE	PEAK PNdB	PEAK ANGLE	PEAK PNdB	PEAK ANGLE
3/27/69											
1	2.03	1511	1839	10.05	-4.7	133.3	40	129.3	40	114.0	40
2	2.03	1490	1839	10.05	-4.7	133.8	40	129.7	40	114.3	40
3	2.74	1760	2330	12.49	-4.8	141.7	50	139.5	50	123.8	50
4	2.96	2124	2644	11.95	-5.4	142.7	50	140.5	50	124.8	50
5	2.48	1631	2142	11.81	-4.7	139.7	50	137.5	50	121.8	50
6	1.40	1145	1130	7.65	-3.9	113.3	40	110.9	60	95.3	60
3/31/69											
1	2.03	1522	1845	10.2	-4.5	134.1	30/40	130.1	50	114.6	40/50
2	2.50	1630	2149	12.1	-4.5	140.2	50	138.0	50	122.3	50
3	2.94	2108	2629	12.4	-5.2	143.3	50	141.1	50	125.4	50
4	2.74	1754	2326	12.7	-4.6	147.2	50	140.0	50	124.2	50
5	1.76	1498	1653	8.9	-4.7	129.7	30	125.1	50	109.7	40/50
6	1.59	1507	1498	7.5	-4.8	124.4	30	120.2	50	104.8	50
7	1.63	1237	1397	8.9	-3.9	122.7	30	118.5	50	103.2	40
8	1.42	1140	1145	7.8	-3.7	114.8	50	112.6	50	97.1	50

TABLE V.F.9-1 TEST SUMMARY

(Cont.)

MODEL NO. 5.7" ID Cone

DESCRIPTION: Baseline Conical Nozzle

DATE: 4/2/69; 4/3/69; 4/7/69

SCALE MODEL A_8 = .178 ft^2

FULL SCALE A_8 = 11.392 ft^2

SCALE FACTOR = 8:1

- o DATA INCLUDES GROUND REFLECTION INTERFERENCE
- o ANGLE REFERENCED TO JET EXHAUST

	TEST CONDITIONS				ACOUSTIC TEST RESULTS					
			IDEAL			320' ARC		300' SIDELINE		1500' SIDELINE
RDG NO.	P_{T8}/P_o	T_{T8} (°R)	V_j (ft/sec)	W_8 (PPS)	10 log ρA	PEAK PNdB	PEAK ANGLE	PEAK PNdB	PEAK ANGLE	PEAK PNdB	PEAK ANGLE
4/2/69											
1	1.43	1154	1166	7.81	-3.5	115.0	50	112.9	50	97.6	50
2	2.04	1519	1845	10.00	-4.6	133.2	30	130.1	50	114.7	50
3	2.52	1651	2172	11.79	-4.5	139.8	50	137.6	50	122.0	50
4	2.96	2146	2658	12.06	-5.3	144.5	50	142.2	50	126.4	50
5	2.72	1761	2323	12.62	-4.6	141.8	50	139.6	50	124.0	50
4/3/69											
1	1.43	1152	1160	7.84	-3.5	112.9	50	110.8	50	95.5	50
2	2.06	1509	1855	10.22	-4.5	132.2	30/40	129.2	40	114.0	40
3	2.76	1794	2360	12.50	-4.7	142.0	50	139.8	50	124.1	50
4	2.51	1632	2153	11.87	-4.5	138.5	40/50	136.3	50	120.7	50
4/7/69											
1	1.43	1156	1162	7.71	-3.5	113.1	30/50	111.2	60	95.8	50/60
2	2.03	1528	1850	10.03	-4.6	133.4	40	129.3	40	114.0	40
3	2.51	1649	2167	11.74	-4.5	138.8	50	137.6	60	121.8	60
4	2.80	1786	2369	12.59	-4.6	141.9	50	139.7	50	124.0	50

TABLE V.F.9-1 TEST SUMMARY

(Cont.)

MODEL NO. 5.7" ID Cone

DESCRIPTION: Baseline Conical Nozzle

DATE: 4/8/69; 5/5/69

SCALE MODEL A_8 = .178 ft^2

FULL SCALE A_8 = 11.392 ft^2

SCALE FACTOR = 8:1

- o DATA INCLUDES GROUND REFLECTION INTERFERENCE
- o ANGLE REFERENCED TO JET EXHAUST

	TEST CONDITIONS				ACOUSTIC TEST RESULTS						
			IDEAL			320' ARC		300' SIDELINE		1500' SIDELINE	
RDG NO.	P_{T8}/P_o	T_{T8} (°R)	V_j (ft/sec)	W_8 (PPS)	10 log ρA	PEAK PNdB	PEAK ANGLE	PEAK PNdB	PEAK ANGLE	PEAK PNdB	PEAK ANGLE
4/8/69											
1	1.43	1163	1172	7.87	-3.6	113.0	30	110.7	50	95.4	50
2	1.58	1527	1507	7.60	-4.8	122.9	30	118.4	50	103.3	50
3	1.64	1250	1415	8.85	-3.9	120.1	30	116.0	50	100.8	50
4	1.79	1516	1684	8.81	-4.7	128.5	30	123.0	50	108.2	40
5	2.03	1529	1852	9.90	-4.6	133.2	30	128.4	40	113.3	40
6	2.29	1562	2010	11.21	-4.5	136.4	40	132.4	40	117.0	40
7	2.51	1648	2164	11.89	-4.5	138.5	40	136.0	50	120.4	50
8	2.57	2121	2485	10.49	-5.6	141.7	50	139.6	50	123.9	50
9	2.75	1762	2336	12.50	-4.6	141.4	50	139.2	50	123.6	50
10	2.98	2127	2655	12.17	-5.2	143.6	50	141.4	50	125.8	50
5/5/69											
1	1.42	1141	1143	7.78	-3.5	113.1	50	111.0	50	95.7	50
2	2.04	1505	1842	10.10	-4.6	133.2	30	128.5	40	113.2	40
3	2.52	1643	2166	11.86	-4.5	138.6	40	136.1	50	120.5	50
4	2.77	1752	2336	12.53	-4.6	141.4	50	139.2	50	123.6	50
5	2.60	2104	2485	10.80	-5.6	142.1	50	139.9	50	124.2	50

TABLE V.F.9-1 TEST SUMMARY

(Cont.)

MODEL NO. 5.7" ID Cone

DESCRIPTION: Baseline Conical Nozzle

DATE: 5/14/69; 6/17/69

SCALE MODEL A_8 = .178 ft^2

FULL SCALE A_8 = 11.392 ft^2

SCALE FACTOR = 8:1

- o DATA INCLUDES GROUND REFLECTION INTERFERENCE
- o ANGLE REFERENCED TO JET EXHAUST

RDG NO.	TEST CONDITIONS				ACOUSTIC TEST RESULTS						
			IDEAL			320' ARC		300' SIDELINE		1500' SIDELINE	
	P_{T8}/P_o	T_{T8} (°R)	V_j (ft/sec)	W_8 (PPS)	10 log ρA	PEAK PNdB	PEAK ANGLE	PEAK PNdB	PEAK ANGLE	PEAK PNdB	PEAK ANGLE
5/14/69											
1	1.44	1170	1187	8.38	-3.6	113.2	40/50	111.3	60	96.0	60
2	2.05	1522	1860	10.64	-4.6	132.9	30	128.4	40	113.2	40
3	2.77	1806	2371	13.21	-4.7	141.4	50	139.2	50	123.5	50
4	2.98	2130	2655	12.95	-5.2	143.0	50	140.9	50	125.3	50
5	1.57	1516	1491	7.96	-4.8	122.3	30	118.4	50	103.4	40
6	1.65	1251	1422	9.45	-3.9	120.9	30	117.0	50	101.8	50
7	1.79	1519	1685	9.38	-4.7	128.1	30	123.1	40	108.2	40
8	2.34	1571	2038	11.94	-4.5	137.0	40	132.9	40	117.5	40
9	2.52	1657	2174	12.58	-4.6	138.6	40	136.2	50	120.6	50
6/17/69											
1	2.05	1321	1734	11.03	-3.4	128.5	40	124.5	40	109.6	40
2	2.05	2950	2586	7.27	-7.5	139.2	50	137.1	50	121.6	50
3	2.50	2117	2487	10.87	-5.6	141.7	50	139.6	50	123.9	50
4	2.06	1507	1857	10.34	-4.6	132.8	30	128.3	40	113.2	40

TABLE V.F.9-1 TEST SUMMARY

(Cont.)

MODEL NO. 5.7" ID Cone

DESCRIPTION: Baseline Conical Nozzle

DATE: 6/26/69 ; 7/10/69

SCALE MODEL A_8 = .178 ft^2

FULL SCALE A_8 = 11.392 ft^2

SCALE FACTOR = 8:1

- o DATA INCLUDES GROUND REFLECTION INTERFERENCE
- o ANGLE REFERENCED TO JET EXHAUST

RDG NO.	TEST CONDITIONS				ACOUSTIC TEST RESULTS						
	P_{T8}/P_o	T_{T8} (°R)	IDEAL V_j (ft/sec)	W_8 (PPS)	10 log ρA	320' ARC PEAK PNdB	320' ARC PEAK ANGLE	300' SIDELINE PEAK PNdB	300' SIDELINE PEAK ANGLE	1500' SIDELINE PEAK PNdB	1500' SIDELINE PEAK ANGLE
6/26/69											
1	1.42	1208	1186	-	-3.7	113.8	30/40	111.8	60	96.1	60
2	2.05	1517	1852	-	-4.6	135.4	30	129.4	40	114.1	40
3	2.78	1782	2358	-	-4.7	141.8	50	139.5	50	123.7	50
4	2.56	2099	2468	-	-5.6	141.8	50	139.6	50	123.8	50
5	2.33	1579	2039	-	-4.5	137.6	40	135.0	40	118.0	40
7/10/69											
1	1.43	1149	1161	7.83	-3.5	113.0	50	111.5	60	94.0	60
2	2.05	1513	1855	10.07	-4.6	132.5	40	128.5	40	113.4	40
3	2.79	1788	2367	12.67	-4.7	141.3	50	139.1	50	123.6	50
4	2.98	2111	2645	12.18	-5.2	143.3	50	141.2	50	125.7	50
5	2.57	2150	2499	10.47	-5.7	142.6	50	140.4	50	124.9	50

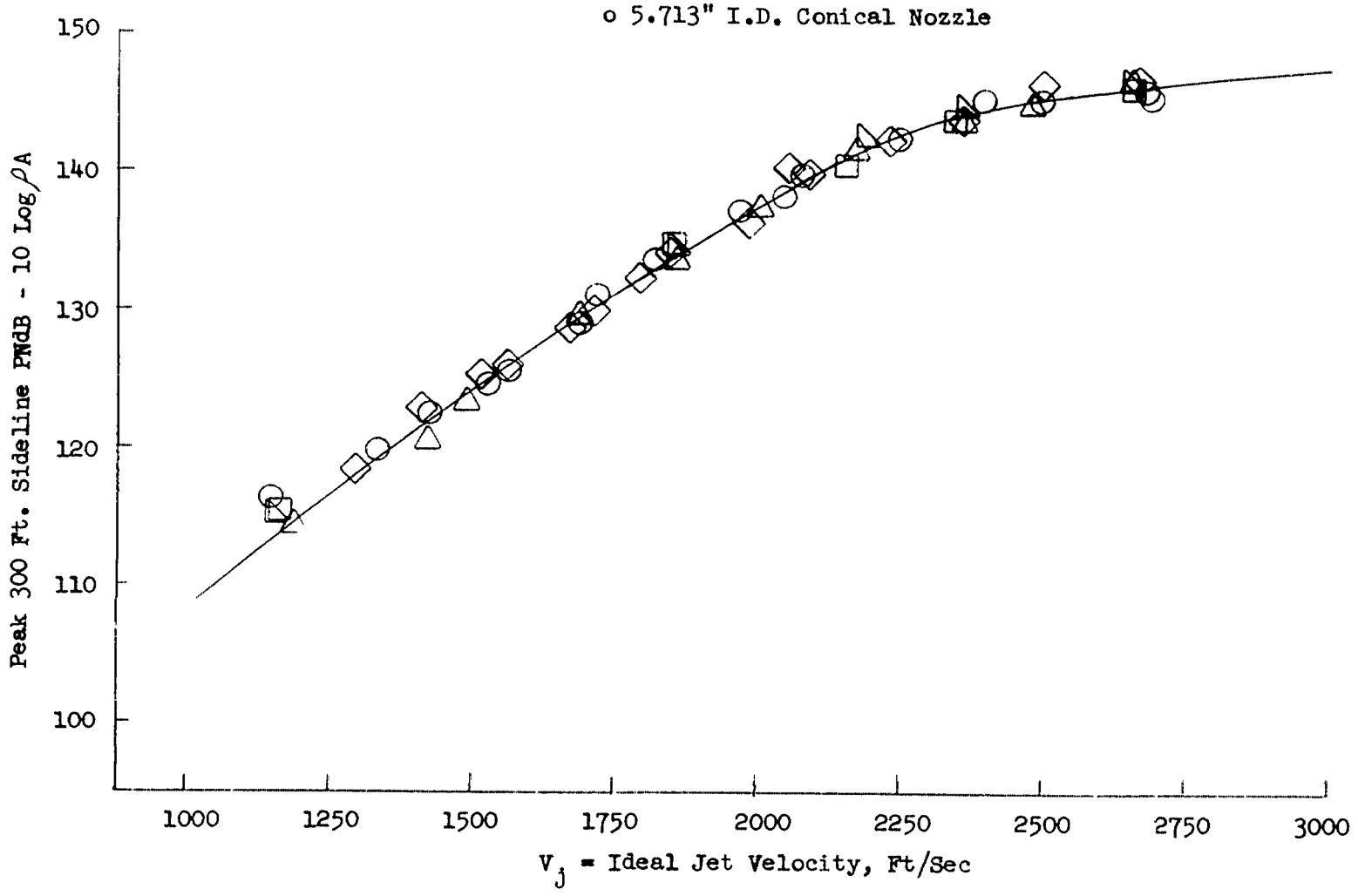

FIGURE V.F.9-2 300 FT. SIDELINE JET NOISE LEVELS FOR AVERAGE BASELINE CONICAL NOZZLE

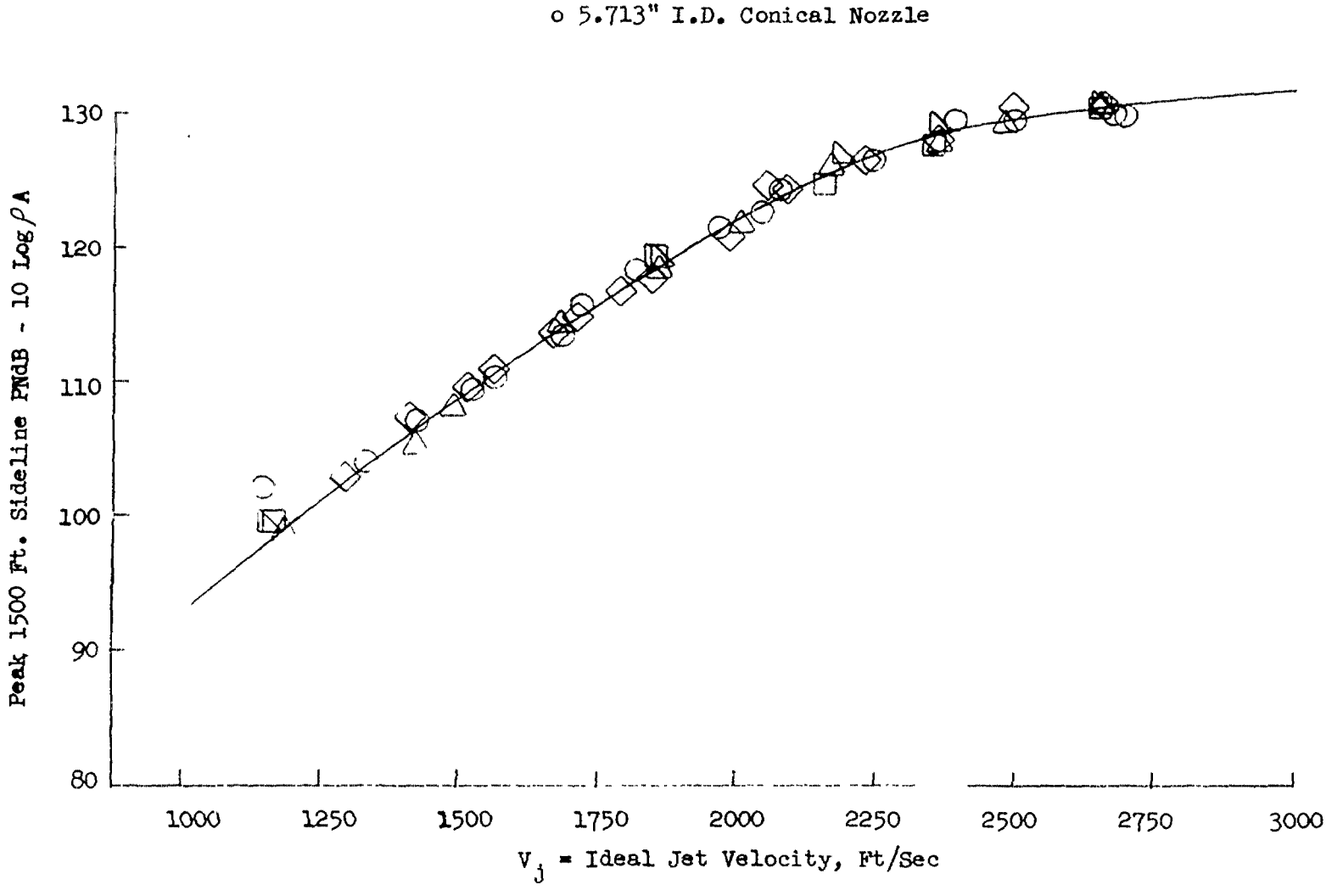

FIGURE V.F.9-3 1500 FT. SIDELINE JET NOISE LEVELS FOR AVERAGE BASELINE CONICAL NOZZLE

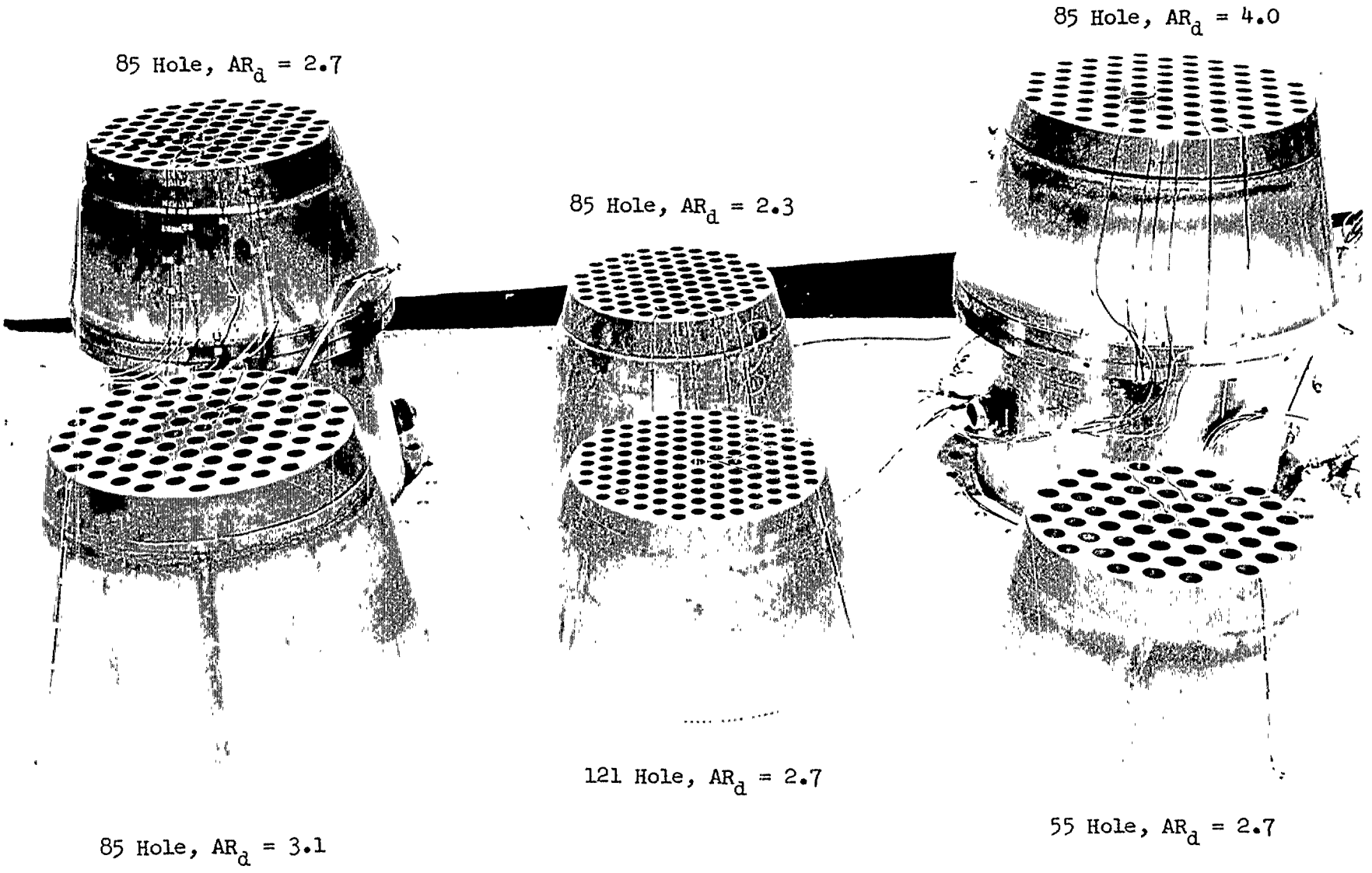

FIGURE V.F.9-4 MULTI-HOLE NOZZLE HARDWARE USED IN PARAMETRIC INVESTIGATIONS OF AREA RATIO AND HOLE NUMBER

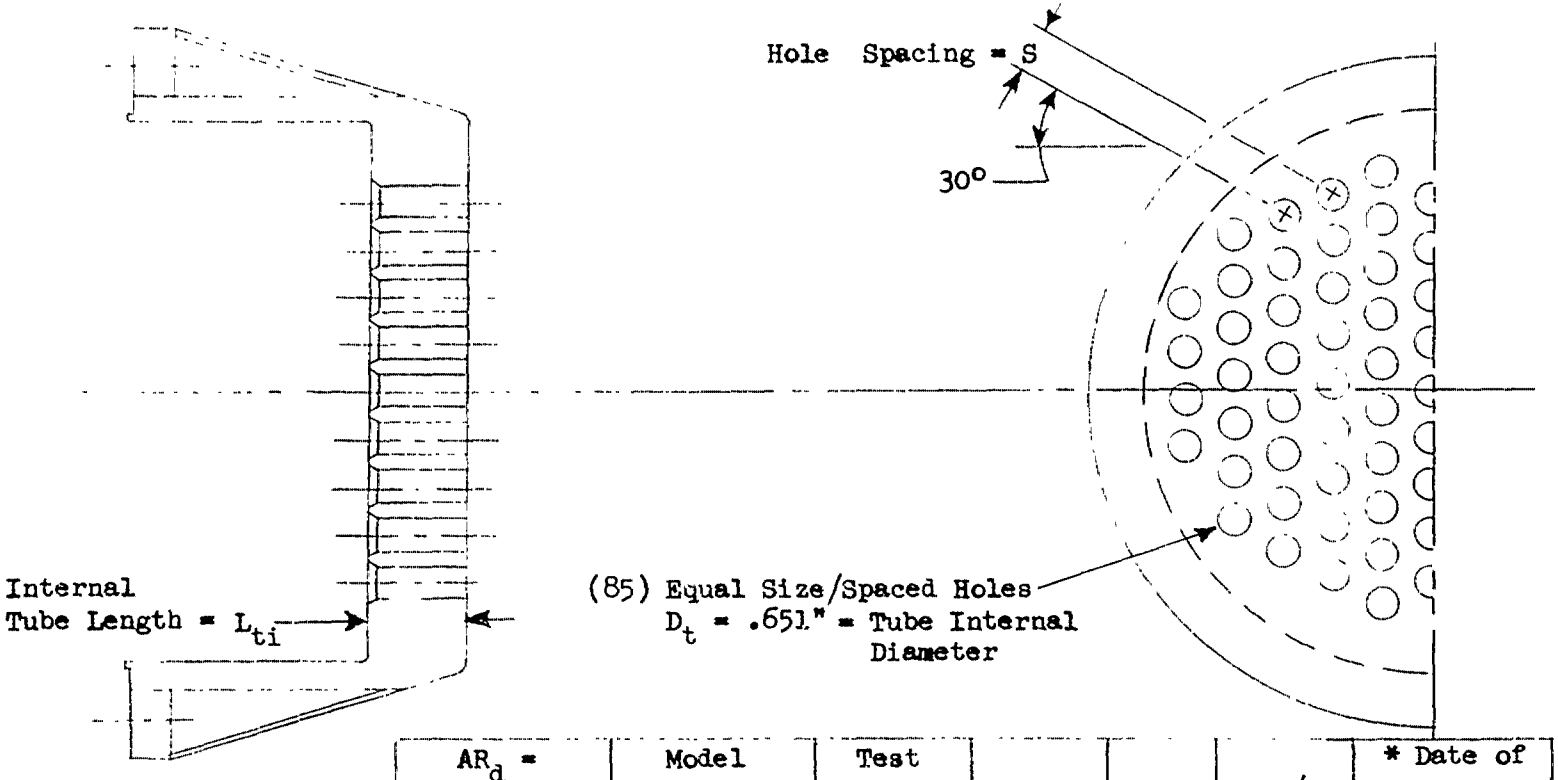

AR_d = Area Ratio	Model No.	Test Date	S	L_{ti}	L_{ti}/D_t	* Date of Repeat Run
2.0	6.0H85-2.0	4-02-69*	.741"	1.45	2.23	6-17-69
2.3	6.0H85-2.3	3-18-69	.799"	1.45	2.23	
2.7	6.0H85-2.7	3-06-69	.870"	1.49	2.29	
3.1	6.0H85-3.1	3-19-69	.937"	1.45	2.23	
4.0	6.0H85-4.0	4-03-69*	1.072"	1.49	2.29	5-14-69

FIGURE V.F.9-5 SCHEMATIC OF 85 HOLE NOZZLE USED IN PARAMETRIC INVESTIGATION OF AREA RATIO

TABLE V.F.9-2 TEST SUMMARY

MODEL NO. 6.0 H85-2.0

DESCRIPTION: 85 Hole Plate with Equally Spaced .651" ID Holes, AR_d = 2.0

DATE: 4/02/69

SCALE MODEL A_8 = .1965 ft^2

FULL SCALE A_8 = 12.576 ft^2

SCALE FACTOR = 8:1

- o DATA INCLUDES GROUND REFLECTION INTERFERENCE
- o ANGLE REFERENCED TO JET EXHAUST

	TEST CONDITIONS				ACOUSTIC TEST RESULTS						
			IDEAL			320' ARC		300' SIDELINE		1500' SIDELINE	
RDG. No.	P_{T8}/P_o	T_{T8} (°R)	V_j (ft/sec)	W_8 (PPS)	10 log ρA	PEAK PNdB	PEAK ANGLE	PEAK PNdB	PEAK ANGLE	PEAK PNdB	PEAK ANGLE
1	3.44	2626	3111	13.03	-5.3	139.8	50	137.7	50	122.2	50
2	3.18	2471	2935	12.27	-5.3	139.8	50	137.5	50	122.0	50
3	3.19	2203	2771	12.98	-4.8	136.4	50	134.2	50	118.8	50
4	3.00	2131	2665	12.38	-4.8	136.4	30	131.8	50	116.5	50
5	2.80	1809	2383	11.91	-4.3	132.1	40	129.0	50	113.4	50
6	2.58	2138	2497	10.62	-5.2	132.2	40	129.4	50	113.9	50
7	2.53	1638	2165	12.12	-4.1	129.0	50	126.7	50	110.3	50
8	2.31	1557	2015	11.22	-4.0	126.9	30	123.8	50	107.8	50
9	2.07	1534	1875	10.15	-4.2	123.7	50	121.9	70	104.7	70
10	1.77	1530	1678	8.71	-4.4	121.1	50	119.1	80	101.9	80
11	1.58	1529	1514	7.96	-4.4	117.0	40	116.8	80	99.6	80
12	1.45	1166	1193	8.55	-3.2	112.8	50	111.9	80	94.7	80

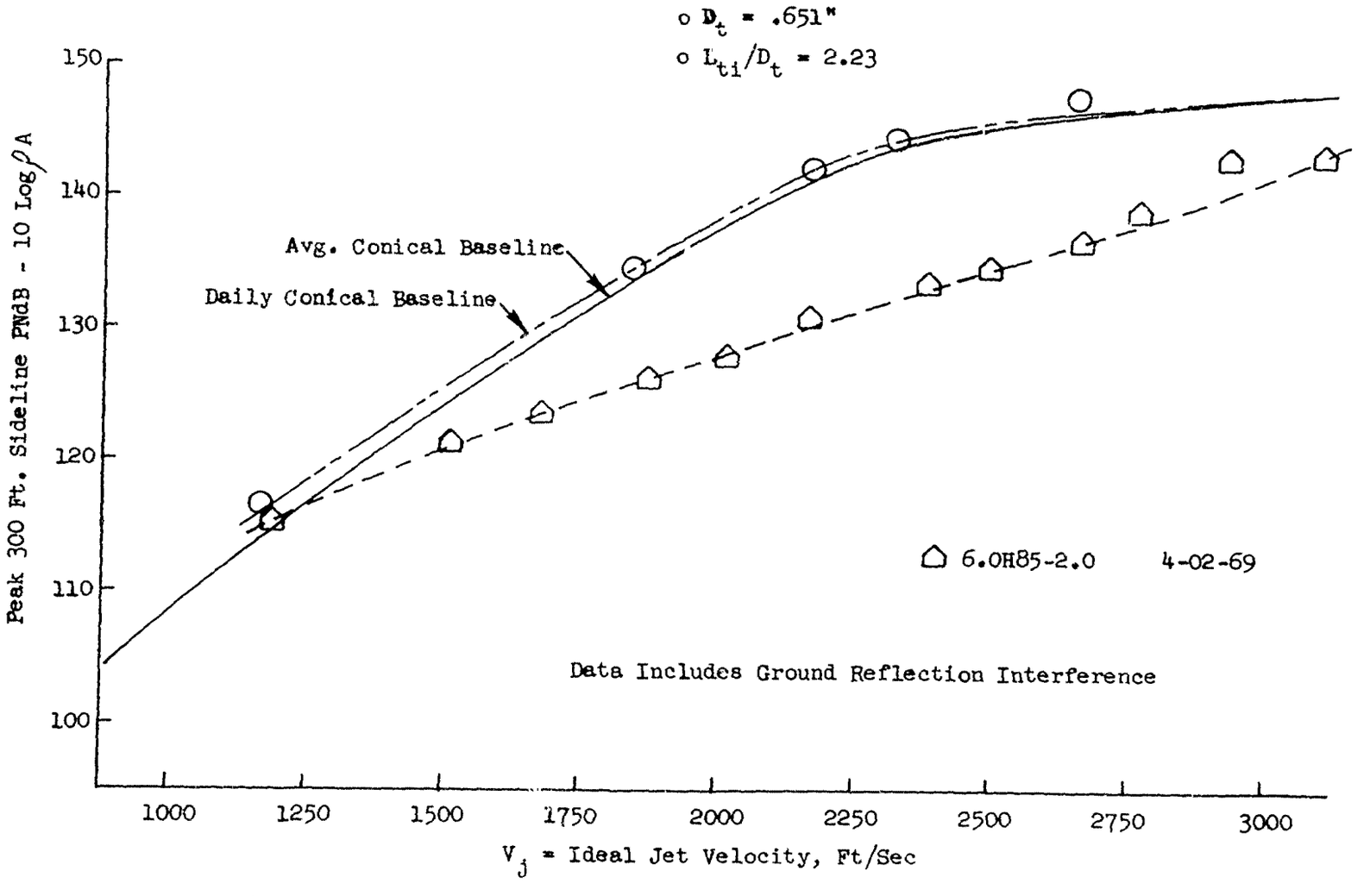

FIGURE V.F.9-6 300 FT. SIDELINE JET NOISE LEVELS FOR AN 85 HOLE NOZZLE, AR_d = 2.0

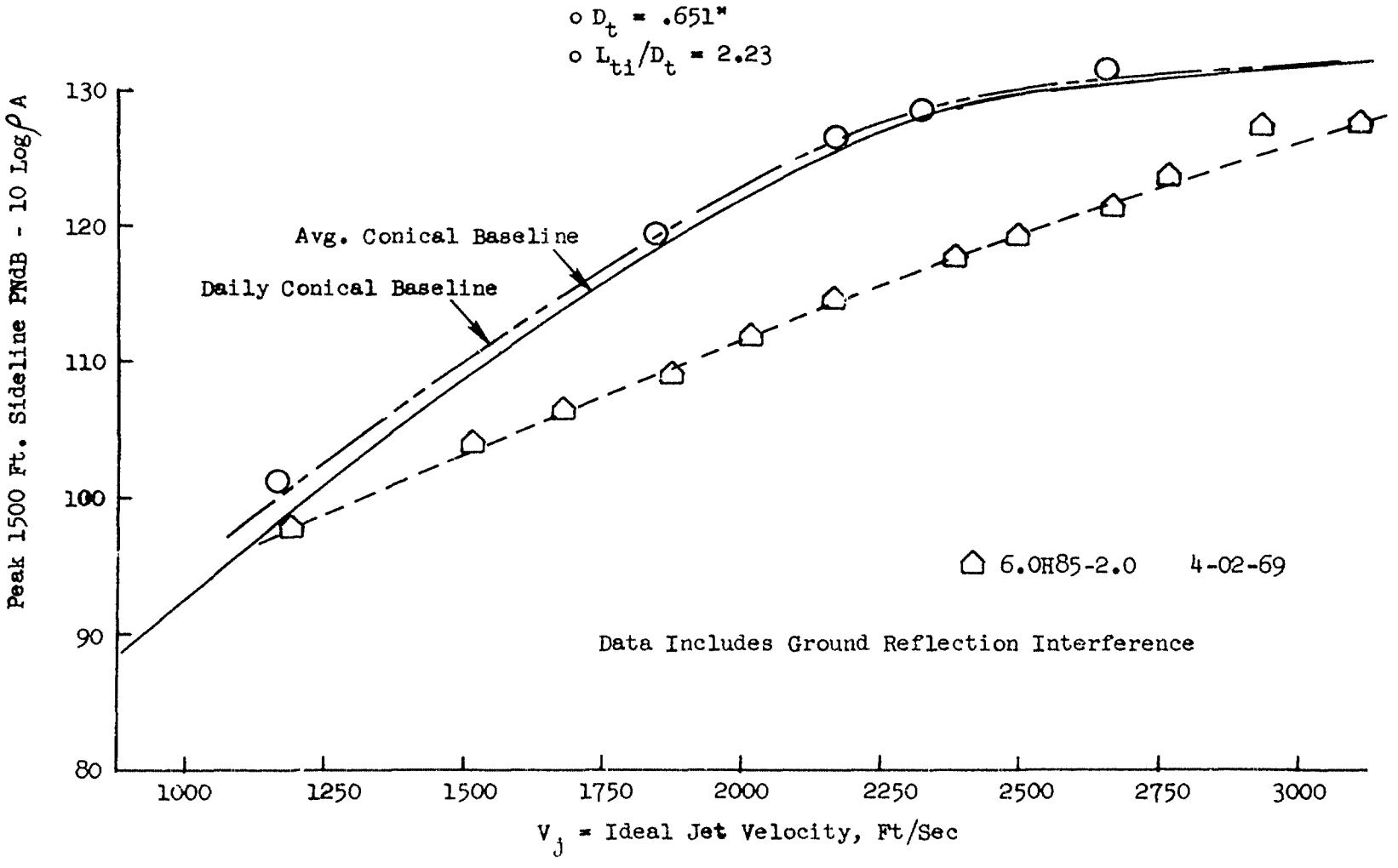

FIGURE V.F.9-7 1500 FT. SIDELINE JET NOISE LEVELS FOR AN 85 HOLE NOZZLE, AR_d = 2.0

TABLE V.F.9-3 TEST SUMMARY

MODEL NO. 6.0 H85-2.0

DESCRIPTION: 85 Hole Plate with Equally Spaced .651" I.D. Holes, AR_d = 2.0

DATE: 6/17/69

SCALE MODEL A_8 = .1965 ft^2

FULL SCALE A_8 = 12.576 ft^2

SCALE FACTOR = 8:1

- o DATA INCLUDES GROUND REFLECTION INTERFERENCE
- o ANGLE REFERENCED TO JET EXHAUST

	TEST CONDITIONS				ACOUSTIC TEST RESULTS						
			IDEAL			320' ARC		300' SIDELINE		1500' SIDELINE	
RDG. No.	P_{T8}/P_o	T_{T8} (°R)	V_j (ft/sec)	W_8 (PPS)	10 log ρA	PEAK PNdB	PEAK ANGLE	PEAK PNdB	PEAK ANGLE	PEAK PNdB	PEAK ANGLE
1	1.401	557	787	11.48	-0.2	105.6	50	104.2	80	86.8	80
2	1.858	557	1050	15.21	-0.1	109.8	80	110.3	80	92.9	80
3	2.288	557	1200	18.67	0.4	113.4	60	113.0	80	95.5	80
4	2.729	557	1308	22.19	0.8	115.3	50	114.9	80	97.5	80
5	3.113	557	1381	25.23	1.1	116.2	50	115.4	80	98.0	80
6	3.492	2687	3164	12.92	-5.4	140.5	50	138.4	50	122.8	50
7	3.333	2613	3069	12.48	-5.4	138.9	50	136.8	50	121.3	50
8	3.320	2418	2948	12.95	-5.1	137.6	50	135.5	50	120.0	50
9	3.210	2224	2793	12.94	-4.8	135.4	50	133.2	50	117.9	50
10	2.990	2099	2641	12.39	-4.8	133.0	50	130.7	50	115.3	50
11	2.793	1780	2363	12.80	-4.2	130.0	30	126.2	50	110.7	50
12	2.592	2124	2496	10.74	-5.2	131.5	40	127.5	40	112.2	40
13	2.534	1651	2177	12.14	-4.1	128.0	30	124.7	50	108.0	50
14	2.364	1573	2052	11.53	-4.1	125.8	30	122.4	50	106.0	50
15	2.074	1506	1862	10.25	-4.1	122.5	50	120.4	70	103.4	70
16	1.811	1520	1701	8.94	-4.3	119.7	50	117.4	50	100.3	50
17	1.665	1234	1427	9.27	-3.4	114.8	50	113.4	80	96.1	80
18	1.586	1525	1513	7.85	-4.4	116.6	60	115.7	60	98.5	60
19	1.435	1164	1177	8.26	-3.2	111.0	60	110.1	60	92.9	60

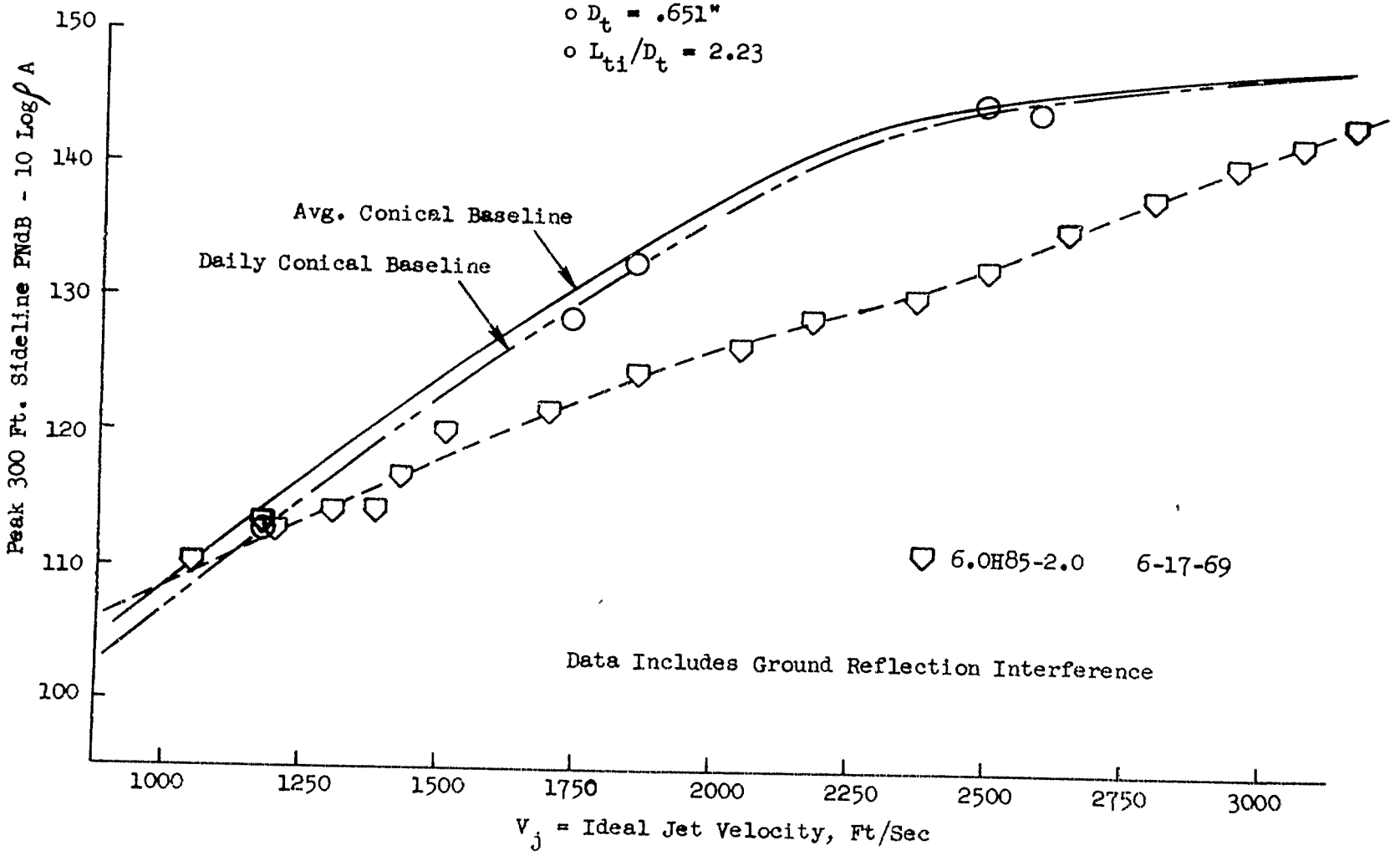

FIGURE V.F.9-8 300 FT. SIDELINE JET NOISE LEVELS FOR AN 85 HOLE NOZZLE, AR_d = 2.0

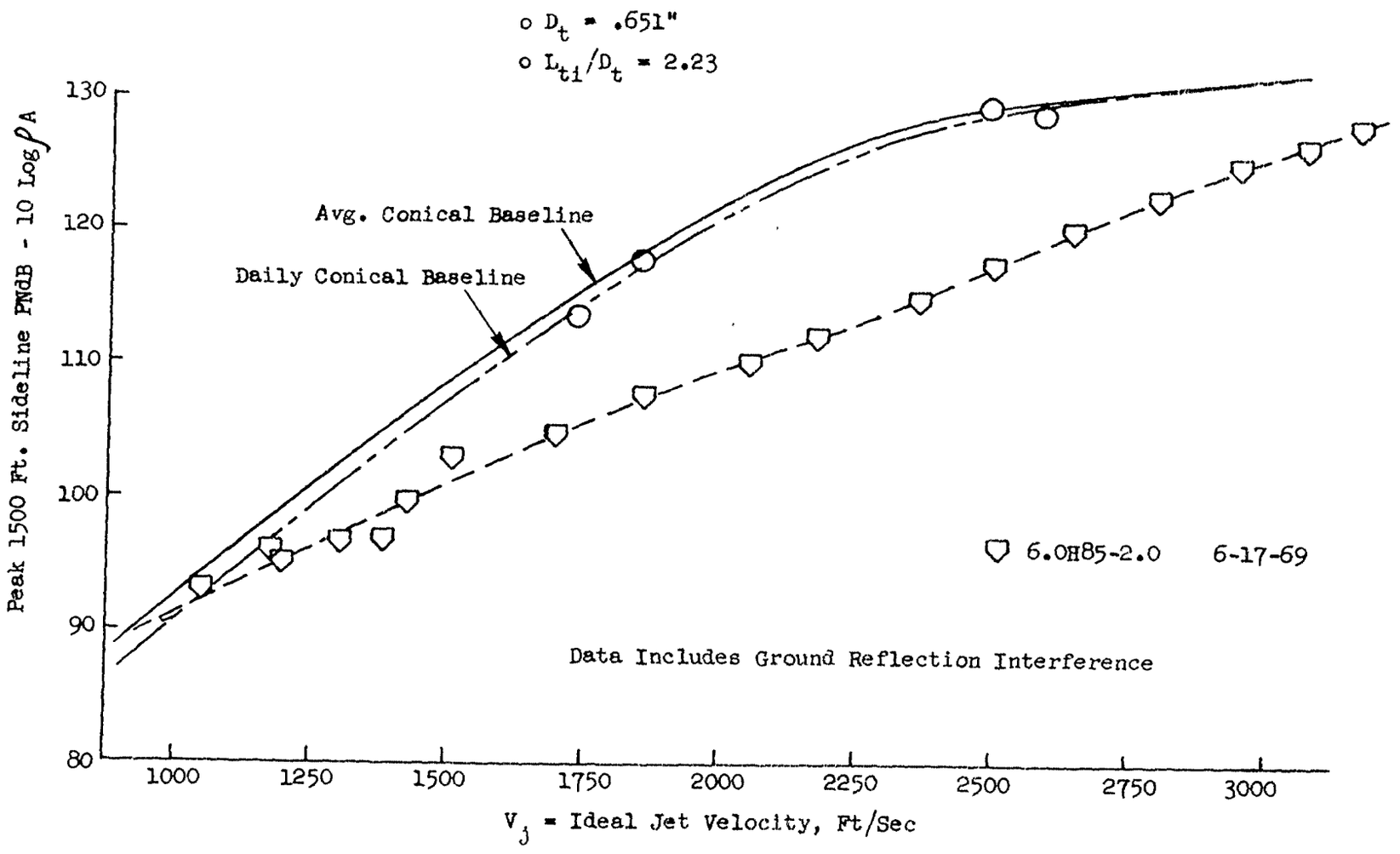

FIGURE V.F.9-9 1500 FT. SIDELINE JET NOISE LEVELS FOR AN 85 HOLE NOZZLE, AR_d = 2.0

TABLE V.F.9-4 TEST SUMMARY

MODEL NO. 6.0 H85-2.3

DESCRIPTION: 85 Hole Plate with Equally Spaced .651" I.D. Holes, AR_d = 2.3

DATE: 3/18/69

SCALE MODEL A_8 = .1965 ft^2

FULL SCALE A_8 = 12.576 ft^2

SCALE FACTOR = 8:1

- o DATA INCLUDES GROUND REFLECTION INTERFERENCE
- o ANGLE REFERENCED TO JET EXHAUST

	TEST CONDITIONS				ACOUSTIC TEST RESULTS						
			IDEAL			320' ARC		300' SIDELINE		1500' SIDELINE	
RDG. No.	P_{T8}/P_o	T_{T8} (°R)	V_j (ft/sec)	W_8 (PPS)	10 log ρA	PEAK PNdB	PEAK ANGLE	PEAK PNdB	PEAK ANGLE	PEAK PNdB	PEAK ANGLE
1	1.422	1161	1161	8.09	-3.4	112.7	50	112.3	70	94.7	70
2	1.593	1521	1518	7.74	-4.5	117.2	40	116.0	70	98.5	70
3	1.654	1240	1422	6.92	-3.5	116.5	70	116.5	70	98.8	70
4	1.818	1506	1698	8.83	-4.3	120.8	40	119.9	70	102.3	70
5	2.066	1527	1871	9.99	-4.2	124.5	40	122.1	70	104.7	70
6	2.324	1552	2020	11.15	-4.0	127.0	40	123.9	50	106.6	50
7	2.540	1636	2170	11.74	-4.1	129.1	40	126.3	50	109.4	40
8	2.590	2130	2500	10.29	-5.2	132.1	40	128.1	40	112.7	40
9	2.795	1804	2379	12.17	-4.3	131.6	40	127.8	50	111.5	50
10	3.006	2130	2665	11.88	-4.8	134.0	40	130.0	40	114.7	40
11	3.230	2222	2797	12.45	-4.8	135.3	40	131.3	40	116.1	40
12	3.325	2397	2937	12.33	-5.1	135.9	40	132.8	50	117.2	50
13	3.323	2593	3054	12.27	-5.4	137.3	40	133.4	40	118.3	40
14	3.512	2648	3147	12.48	-5.3	137.4	40	135.2	50	119.7	50

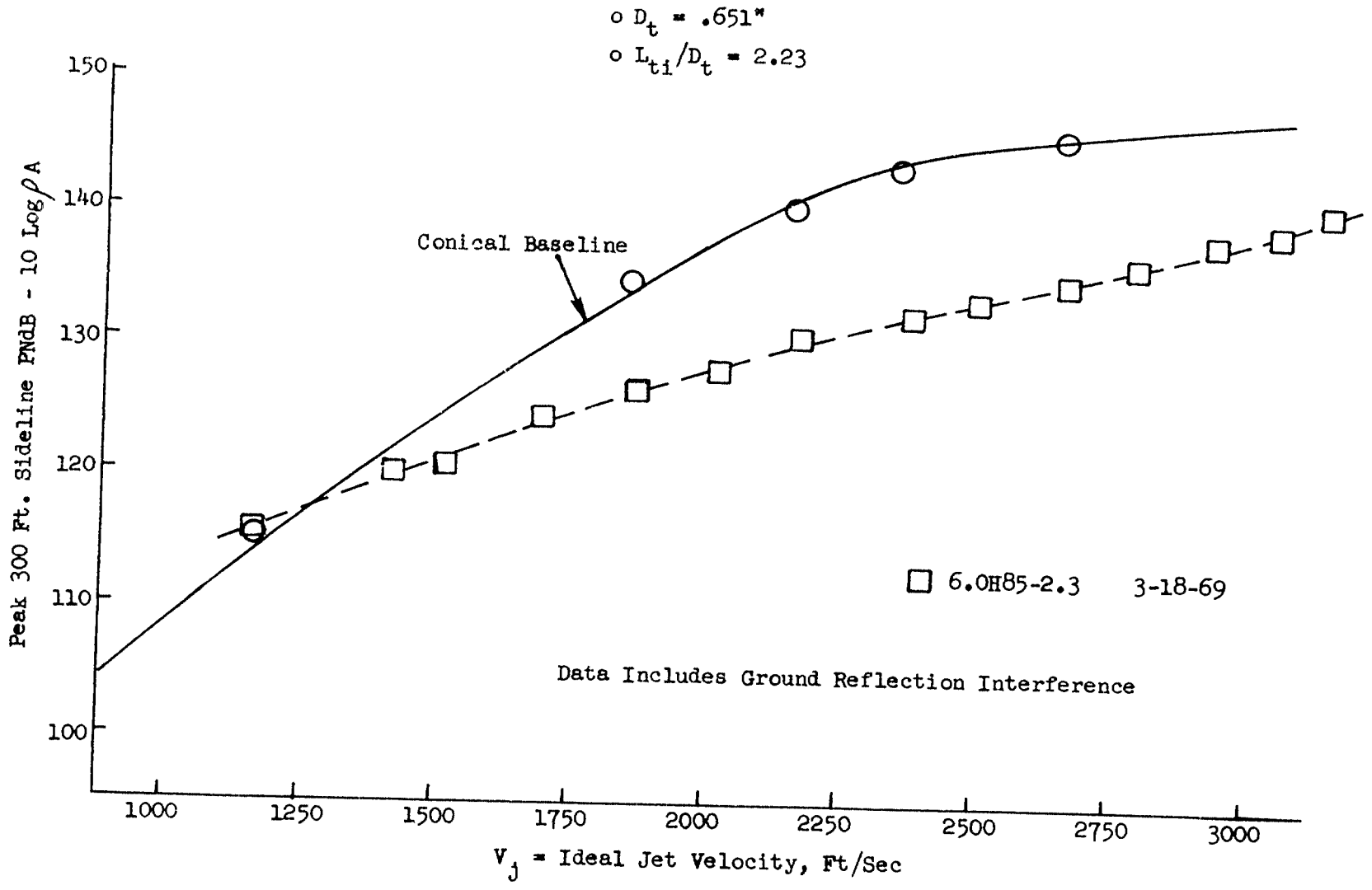

FIGURE V.F.9-10 300 FT. SIDELINE JET NOISE LEVELS FOR AN 85 HOLE NOZZLE, AR_d = 2.3

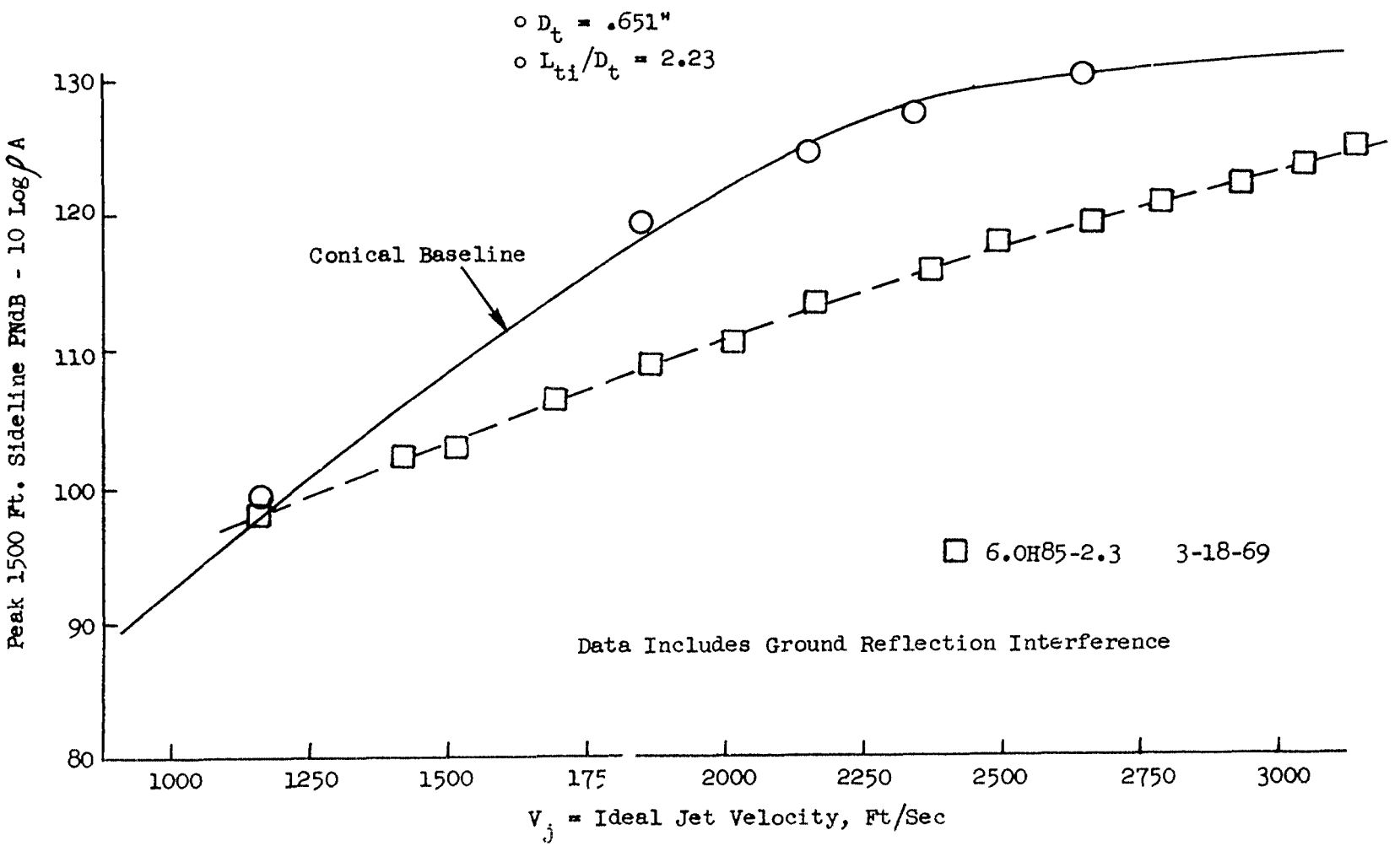

FIGURE V.F.9-11 1500 FT. SIDELINE JET NOISE LEVELS FOR AN 85 HOLE NOZZLE, AR_d = 2.3

TABLE V.F.9-5 TEST SUMMARY

MODEL NO. 6.0 H85-2.7

DESCRIPTION: 85 Hole Plate with Equally Spaced .651" I.D. Holes AR_d = 2.7

DATE: 3/06/69

SCALE MODEL A_8 = .1965 ft^2

FULL SCALE A_8 = 12.576 ft^2

SCALE FACTOR = 8:1

- o DATA INCLUDES GROUND REFLECTION INTERFERENCE
- o ANGLE REFERENCED TO JET EXHAUST

	TEST CONDITIONS				ACOUSTIC TEST RESULTS						
			IDEAL			320' ARC		300' SIDELINE		1500' SIDELINE	
RDG No.	P_{T8}/P_o	T_{T8} (°R)	V_j (ft/sec)	W_8 (PPS)	10 log ρA	PEAK PNdB	PEAK ANGLE	PEAK PNdB	PEAK ANGLE	PEAK PNdB	PEAK ANGLE
1	1.42	1150	1155	8.07	-3.1	114.6	50	114.2	70	96.4	70
2	1.58	1530	1510	7.74	-4.4	120.0	50	119.5	70	101.8	70
3	1.65	1248	1423	9.08	-3.6	119.0	50	118.4	70	100.6	70
4	1.80	1525	1697	8.84	-4.4	122.7	50	122.2	70	104.5	70
5	2.06	1523	1862	10.16	-4.2	125.4	50	123.7	70	106.0	70
6	2.36	1567	2047	11.49	-4.1	128.6	40	125.8	70	108.2	70
7	2.52	1656	2176	11.99	-4.8	129.4	40	126.7	60	109.2	60
8	2.59	2109	2486	10.60	-5.8	131.4	50	129.1	50	111.8	50
9	2.81	1698	2313	12.79	-4.6	130.3	40	127.9	50	110.6	50
10	3.00	2109	2651	12.29	-5.4	132.9	50	130.6	50	114.2	50
11	3.32	2393	2933	12.75	-5.1	135.0	50	132.8	50	117.2	50
12	3.50	2655	3147	12.88	-5.4	135.9	50	133.7	50	118.1	50

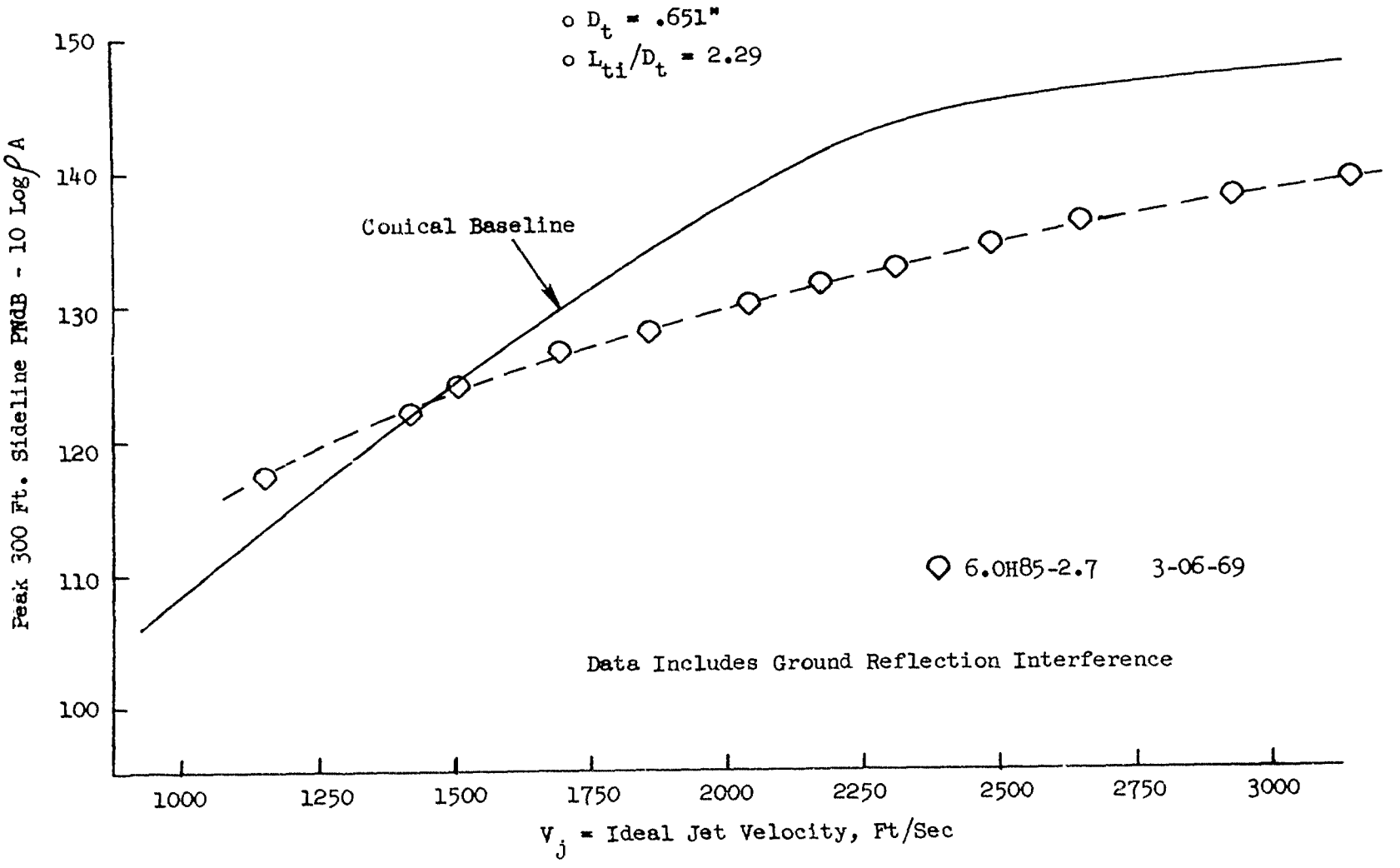

FIGURE V.F.9-12 300 FT. SIDELINE JET NOISE LEVELS FOR AN 85 HOLE NOZZLE, AR_d = 2.7

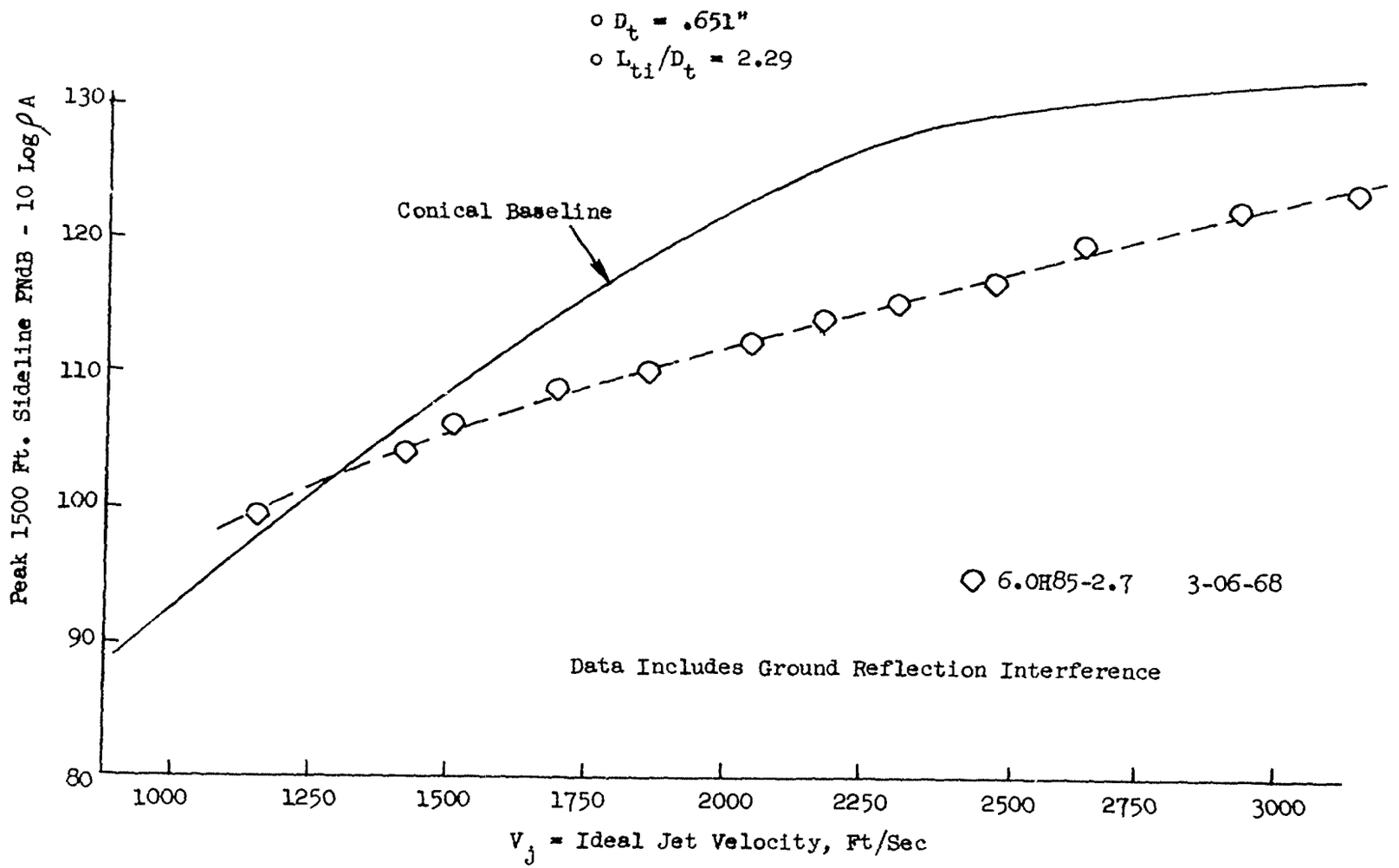

FIGURE V.F.9-13 1500 FT. SIDELINE JET NOISE LEVELS FOR AN 85 HOLE NOZZLE, AR_d = 2.7

TABLE V.F.9-6 TEST SUMMARY

NOTE NO. 6.0 H85-3.1

DESCRIPTION: 85 Holc Plate with Equally Spaced .651" ID Holes, AR_d = 3.1

DATE: 3/19/69

SCALE MODEL A_8 = .1965 ft^2

FULL SCALE A_8 = 12.576 ft^2

SCALE FACTOR = 8:1

- o DATA INCLUDES GROUND REFLECTION INTERFERENCE
- o ANGLE REFERENCED TO JET EXHAUST

RDG. No.	TEST CONDITIONS				ACOUSTIC TEST RESULTS						
			IDEAL			320' ARC		300' SIDELINE		1500' SIDELINE	
	P_{T8}/P_o	T_{T8} (°R)	V_j (ft/sec)	W_8 (PPS)	10 log ρA	PEAK PNdB	PEAK ANGLE	PEAK PNdB	PEAK ANGLE	PEAK PNdB	PEAK ANGLE
3	1.65	1228	1423	9.16	-3.5	117.3	70	117.3	70	99.8	70
4	1.78	1491	1660	8.70	-4.3	116.1	80	117.1	80	99.6	80
5	2.08	1513	1868	10.24	-4.1	123.0	60	122.7	70	105.2	70
6	2.32	1561	2025	11.21	-4.1	124.9	40	124.4	70	106.9	70
7	2.56	1683	2210	12.05	-4.2	127.8	30	125.7	70	108.4	70
8	2.59	2100	2482	10.64	-5.1	129.1	50	127.3	60	110.2	60
9	2.81	1753	2349	12.80	-4.1	128.5	30	127.5	80	110.1	80
10	3.02	2118	2661	12.23	-4.8	130.7	50	128.4	50	111.9	50
11	3.22	2219	2794	12.86	-4.8	132.0	40	129.0	50	113.3	50
12	3.31	2414	2943	12.74	-5.1	132.8	40	130.1	50	114.5	50
13	3.30	2603	3054	12.34	-5.4	133.3	40	131.0	50	115.5	50
14	3.50	2667	3155	13.06	-5.4	134.4	50	132.2	50	116.7	50

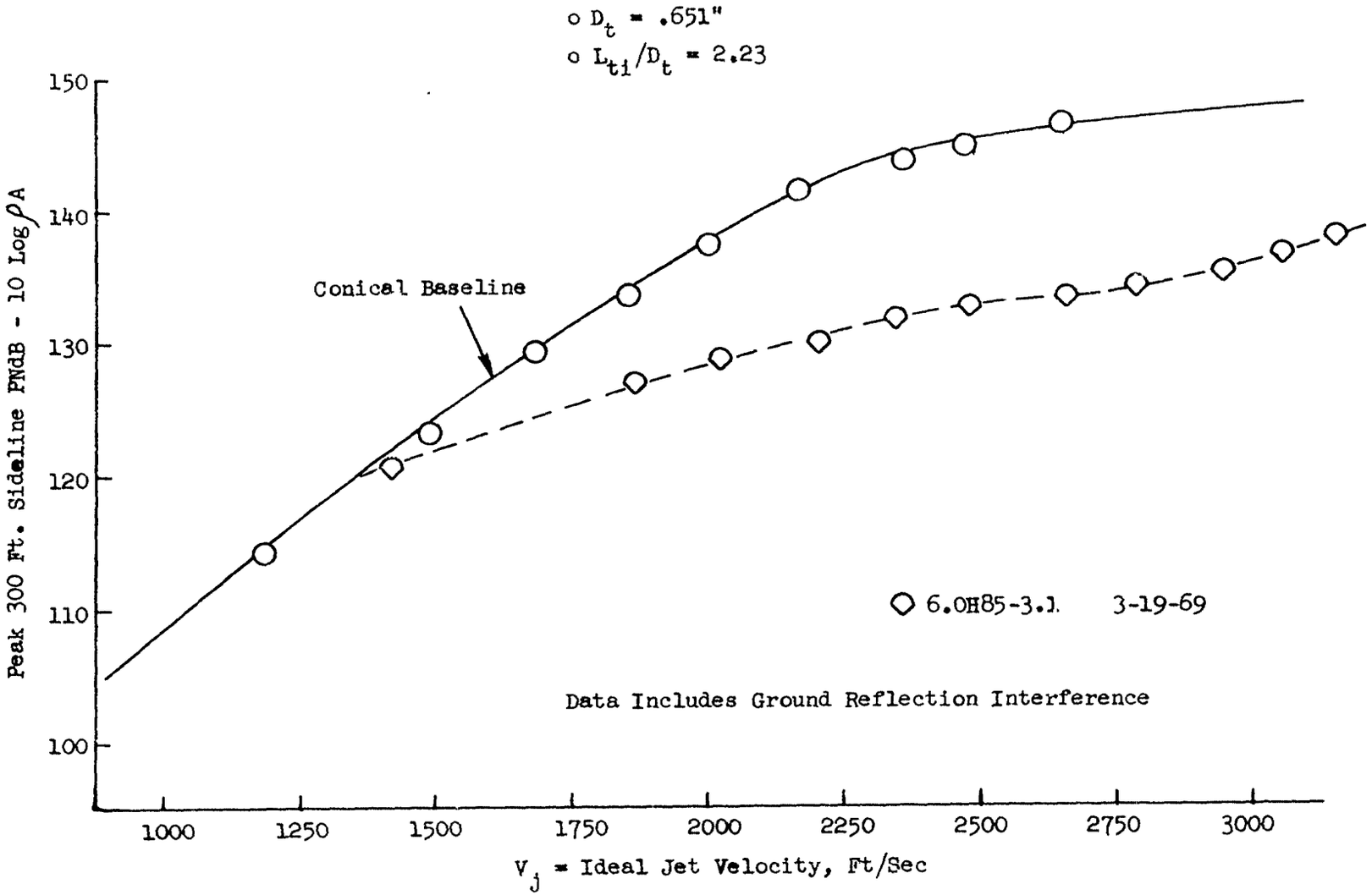

FIGURE V.F.9-14 300 FT. SIDELINE JET NOISE LEVELS FOR AN 85 HOLE NOZZLE, AR_d = 3.1

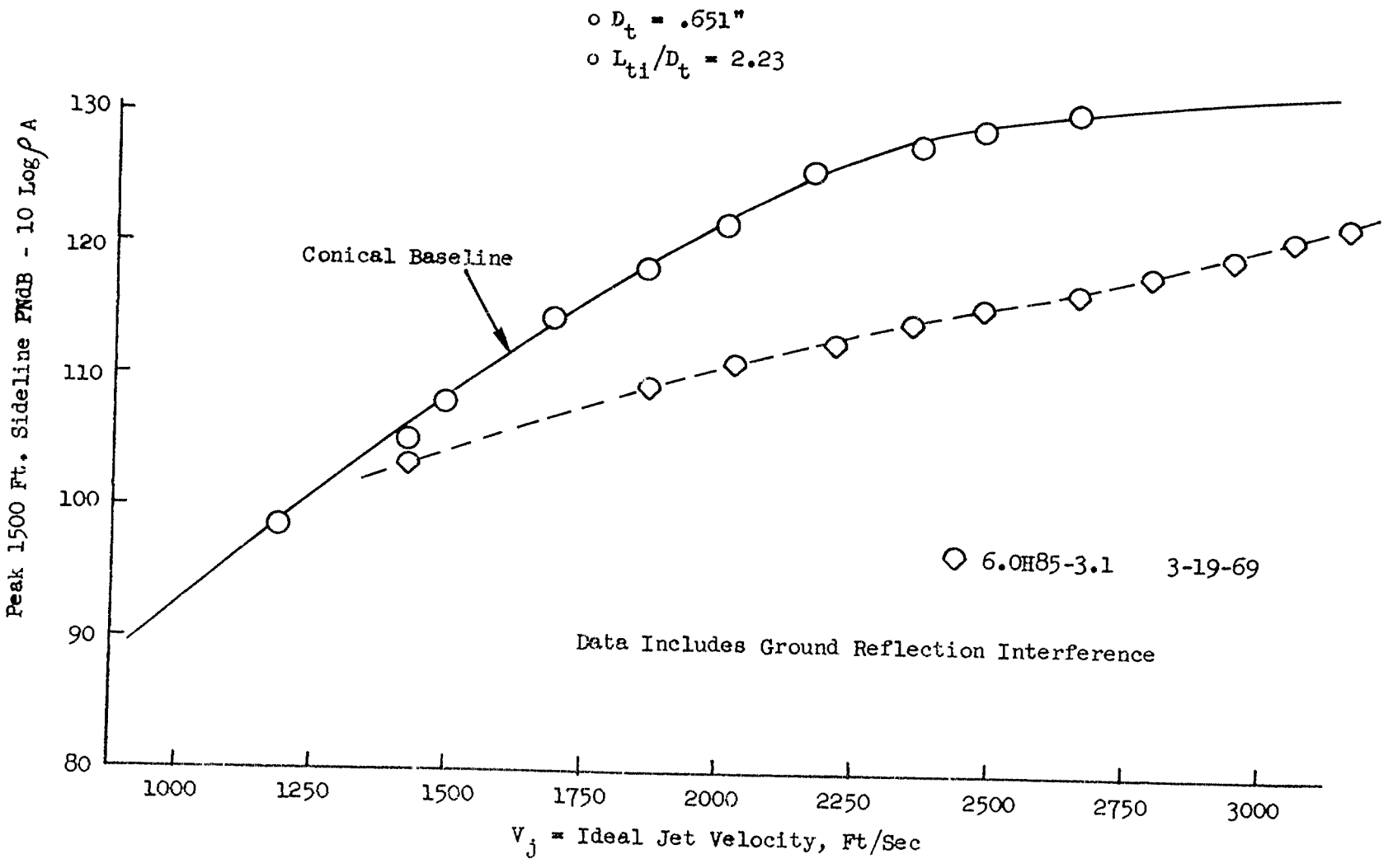

FIGURE V.F.9-15 1500 FT. SIDELINE JET NOISE LEVELS FOR AN 85 HOLE NOZZLE, AR_d = 3.1

TABLE V.F.9-7 TEST SUMMARY

MODEL NO. 6.0 H85- 4.0

DESCRIPTION: 85 Hole Plate with Equally Spaced .651" I.D. Holes AR_d = 4.0

DATE: 4/03/69

SCALE MODEL A_8 = .1965 ft^2

FULL SCALE A_8 = 12.576 ft^2

SCALE FACTOR = 8:1

- o DATA INCLUDES GROUND REFLECTION INTERFERENCE
- o ANGLE REFERENCED TO JET EXHAUST

	TEST CONDITIONS				ACOUSTIC TEST RESULTS						
			IDEAL			320' ARC		300' SIDELINE		1500' SIDELINE	
RDG No.	P_{T8}/P_0	T_{T8} (°R)	V_j (ft/sec)	W_8 (PPS)	10 log ρA	PEAK PNdB	PEAK ANGLE	PEAK PNdB	PEAK ANGLE	PEAK PNdB	PEAK ANGLE
1	1.42	1174	1166	8.25	-3.1	116.5	50	114.7	60	97.2	60
2	1.60	1510	1516	8.02	-4.3	120.4	50	119.3	60	101.7	60
3	1.66	1250	1434	9.22	-3.5	120.1	50	118.9	60	101.3	60
4	1.80	1520	1696	8.90	-4.3	122.9	50	121.7	70	104.1	70
5	2.07	1518	1866	10.29	-4.1	125.2	50	124.3	80	106.8	80
6	2.30	1552	2009	11.07	-4.0	126.3	50	125.5	80	107.9	80
7	2.53	1665	2185	11.93	-4.1	127.3	40	126.4	70	108.9	70
8	2.59	2105	2482	10.71	-5.1	129.1	50	127.8	70	110.4	70
9	2.79	1764	2350	12.74	-4.2	129.1	50	127.3	80	109.9	80
10	3.00	2110	2649	12.40	-4.7	130.6	60	128.6	70/80	111.3	70
11	3.21	2213	2785	12.87	-4.8	131.7	50	129.8	60	112.6	60
12	3.30	2426	2946	12.75	-5.1	132.5	50	130.2	50	113.1	50
13	3.32	2617	3066	12.28	-5.4	133.0	50	131.0	60	113.9	60
14	3.49	2667	3153	12.78	-5.3	133.6	50	131.3	50	114.8	50

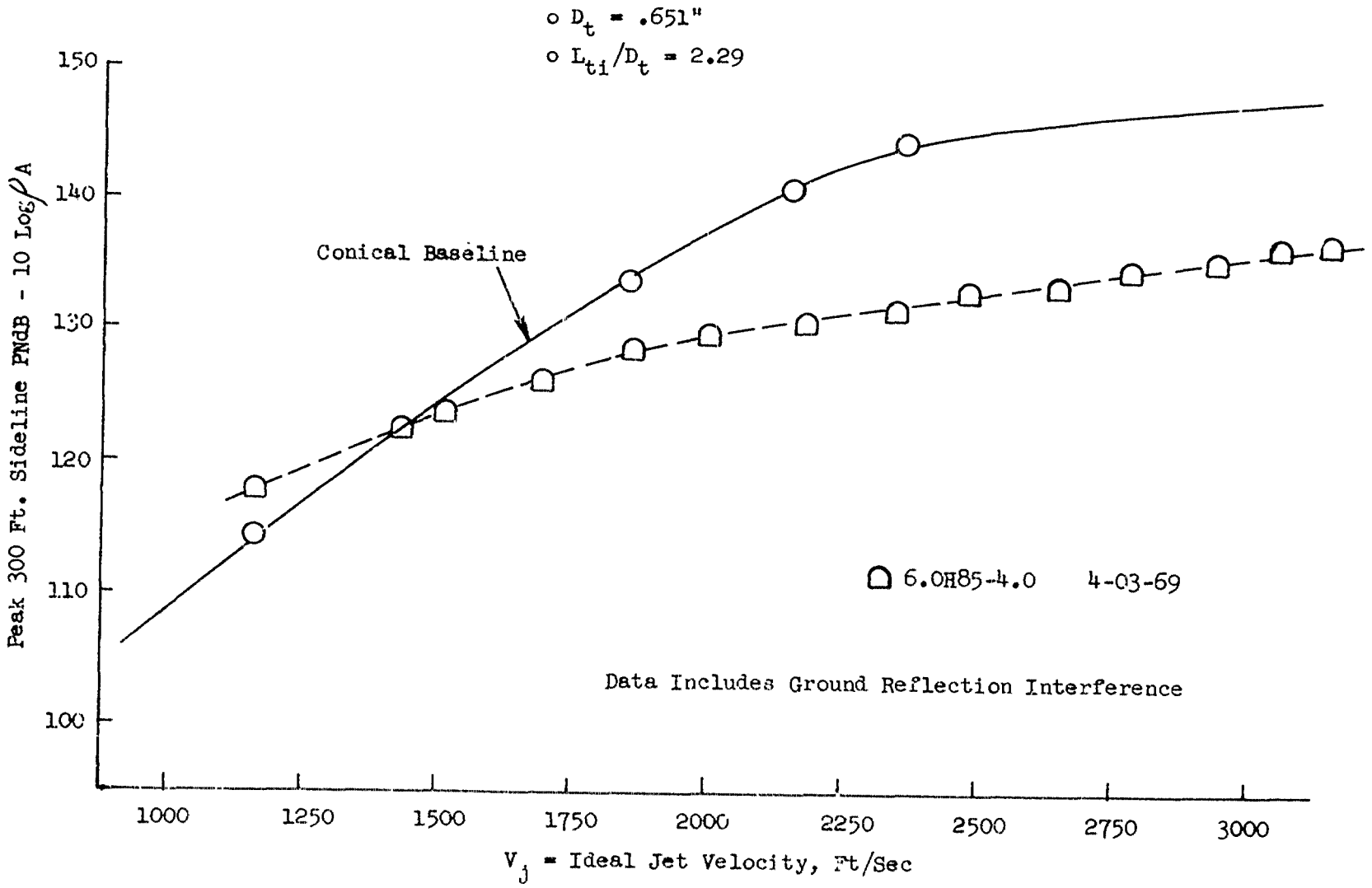

FIGURE V.F.9-16 300 FT. SIDELINE JET NOISE LEVELS FOR AN 85 HOLE NOZZLE, AR_d = 4.0

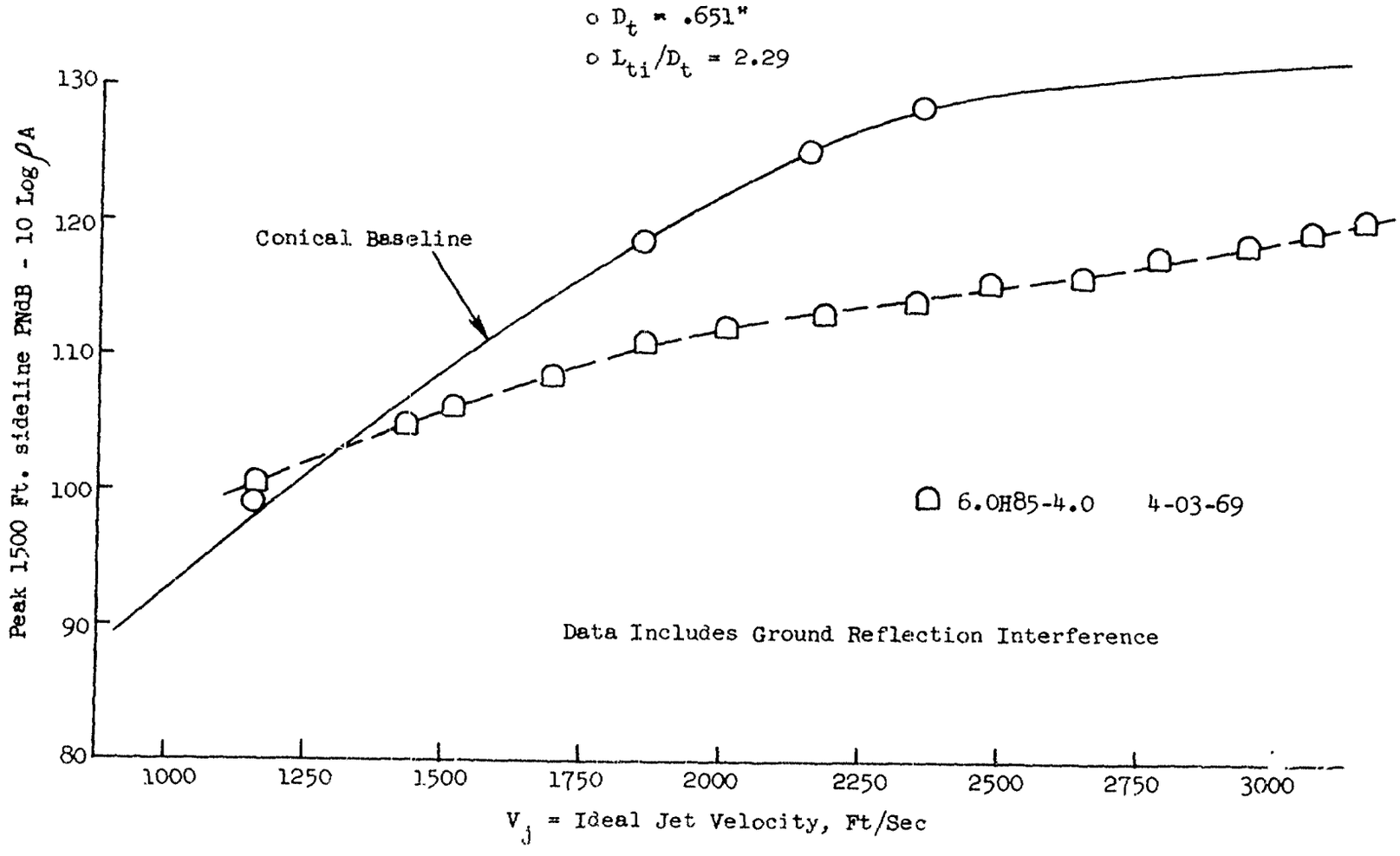

FIGURE V.F.9-17 1500 FT. SIDELINE JET NOISE LEVELS FOR AN 85 HOLE NOZZLE, AR_d = 4.0

TABLE V.F.9-8 TEST SUMMARY

NOZZLE NO. 6.0 H85-4.0

DESCRIPTION: 85 Hole Plate with Equally Spaced .651" ID Holes, AR_d = 4.0

DATE: 5/14/69

SCALE MODEL A_8 = .1965 ft^2

FULL SCALE A_8 = 12.576 ft^2

SCALE FACTOR = 8:1

- o DATA INCLUDES GROUND REFLECTION INTERFERENCE
- o ANGLE REFERENCED TO JET EXHAUST

	TEST CONDITIONS				ACOUSTIC TEST RESULTS						
			IDEAL			320' ARC		300' SIDELINE		1500' SIDELINE	
RDG No.	P_{T8}/P_0	T_{T8} (°R)	V_j (ft/sec)	W_8 (PPS)	10 log ρA	PEAK PNdB	PEAK ANGLE	PEAK PNdB	PEAK ANGLE	PEAK PNdB	PEAK ANGLE
1	1.396	530	764	11.39	0.3	110.5	50	109.0	80	91.6	80
2	1.861	530	1026	15.38	0.3	118.3	50	116.1	80	98.6	80
3	2.276	530	1167	18.60	0.6	121.6	50	120.1	80	102.6	80
5	3.131	530	1351	25.37	0.4	124.1	50	122.2	80	104.6	80
6	3.520	530	1409	28.42	1.7	124.5	50	123.2	80	105.5	80
7	3.210	2189	2771	12.86	-4.7	132.4	50	130.0	80	112.7	50
8	2.800	1751	2346	12.63	-4.1	129.6	50	127.8	80	110.3	70/80
9	3.013	2098	2647	12.27	-4.7	131.6	40	130.3	80	112.9	80
10	3.139	2405	2940	12.69	-5.0	133.0	40/50	130.6	50/80	113.4	50
11	3.304	2598	3051	12.27	-5.4	134.1	40	131.7	80	114.4	80
12	3.507	2659	3152	12.87	-5.3	134.5	50	132.5	80	115.3	80
13	2.594	2098	2481	10.58	-5.1	130.0	40	128.8	80	111.3	80
14	2.551	1623	2165	11.91	-4.0	128.8	50	127.5	80	110.0	80
15	2.366	1545	2034	11.26	-4.0	127.4	50	126.6	80	109.1	80
16	2.070	1502	1858	10.16	-4.1	125.6	50	125.0	80	107.5	80
17	1.809	1499	1688	8.90	-4.2	123.5	50	123.3	80	105.7	80
18	1.659	1219	1413	9.06	-3.4	120.9	50	119.6	60	101.9	60
19	1.596	1499	1509	7.82	-4.3	121.3	50	120.3	60	102.7	60

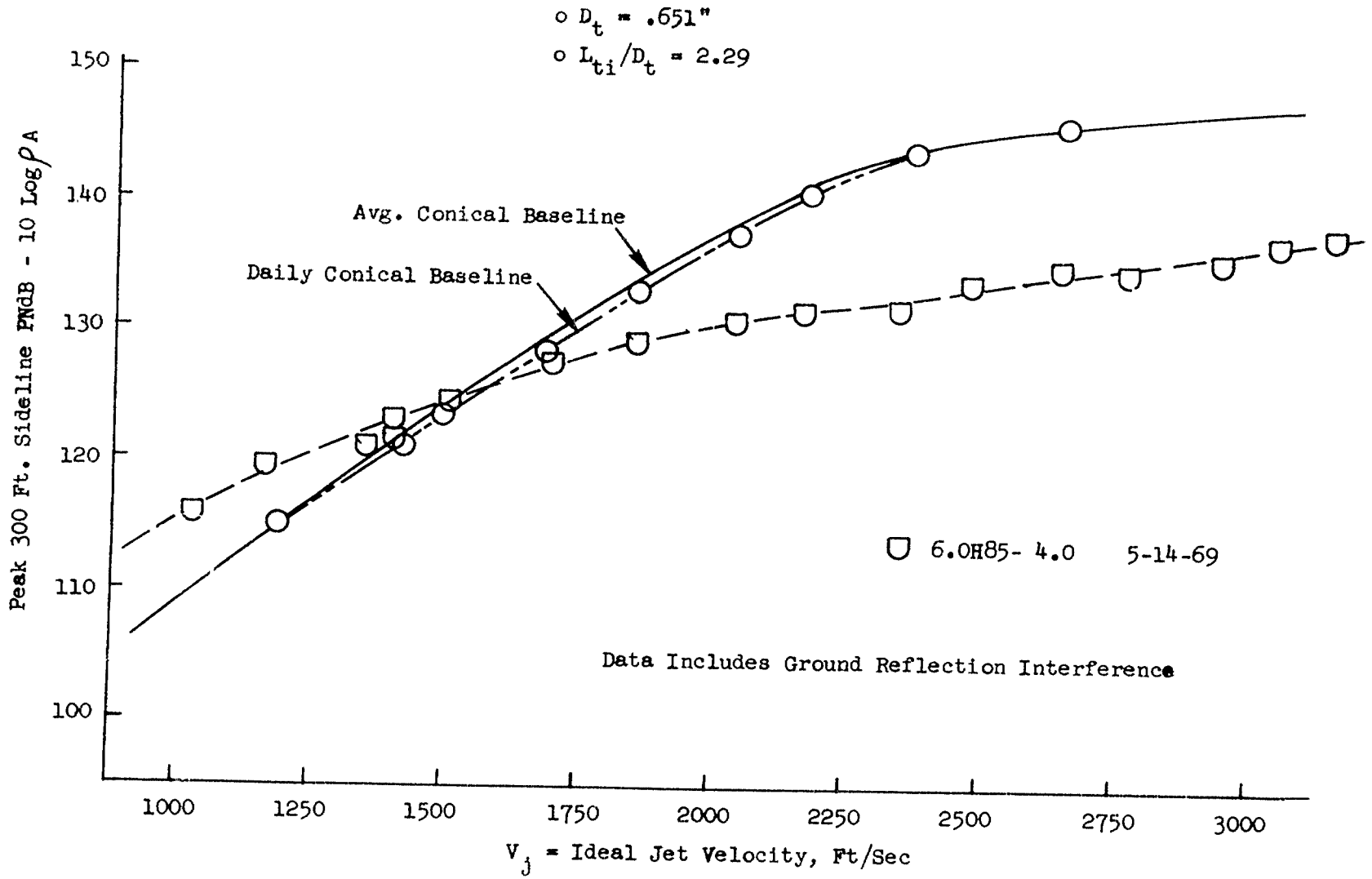

FIGURE V.F.9-18 300 FT. SIDELINE JET NOISE LEVELS FOR AN 85 HOLE NOZZLE, AR_d = 4.0

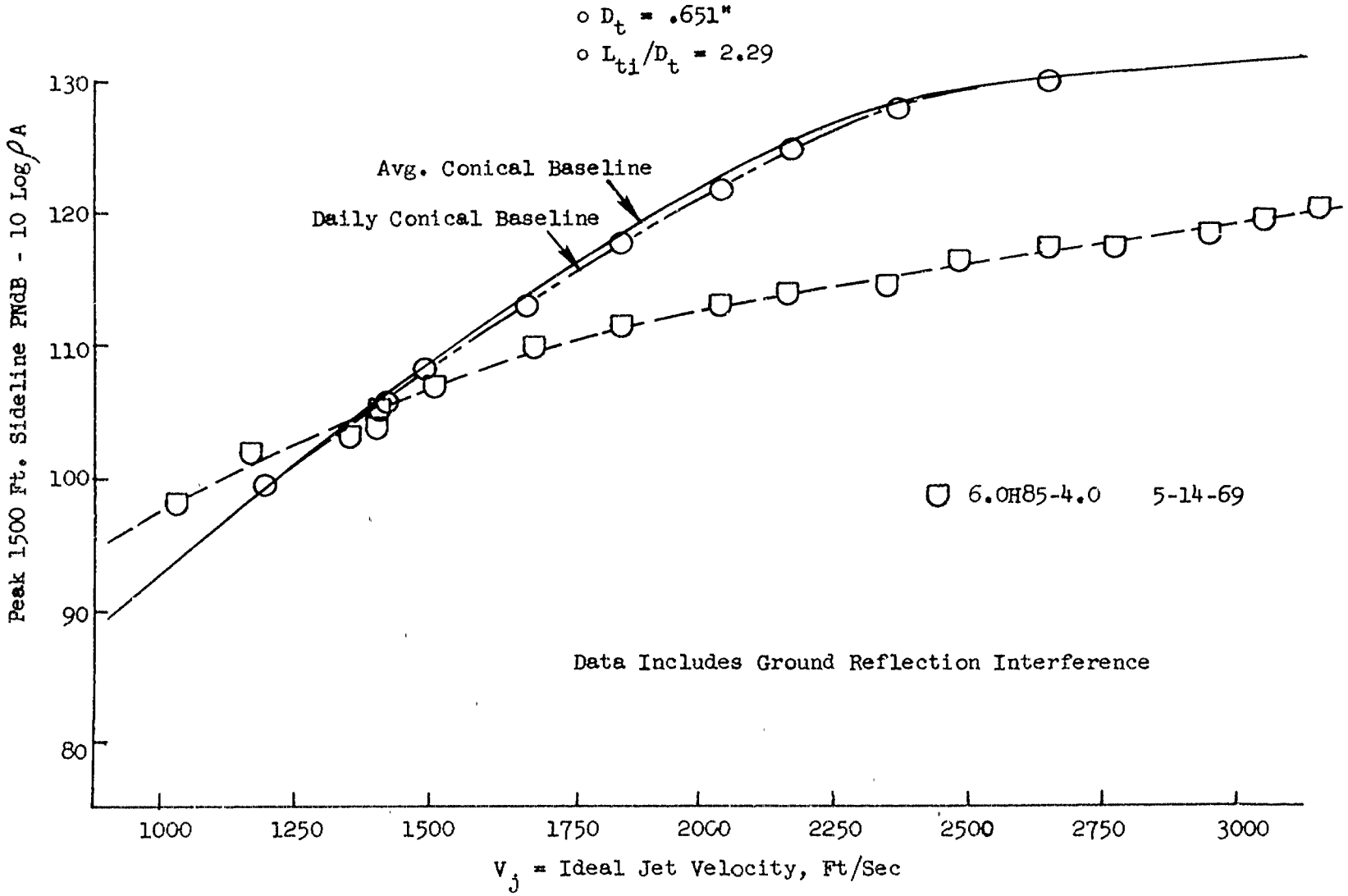

FIGURE V.F.9-19 1500 FT. SIDELINE JET NOISE LEVELS FOR AN 85 HOLE NOZZLE, AR_d = 4.0

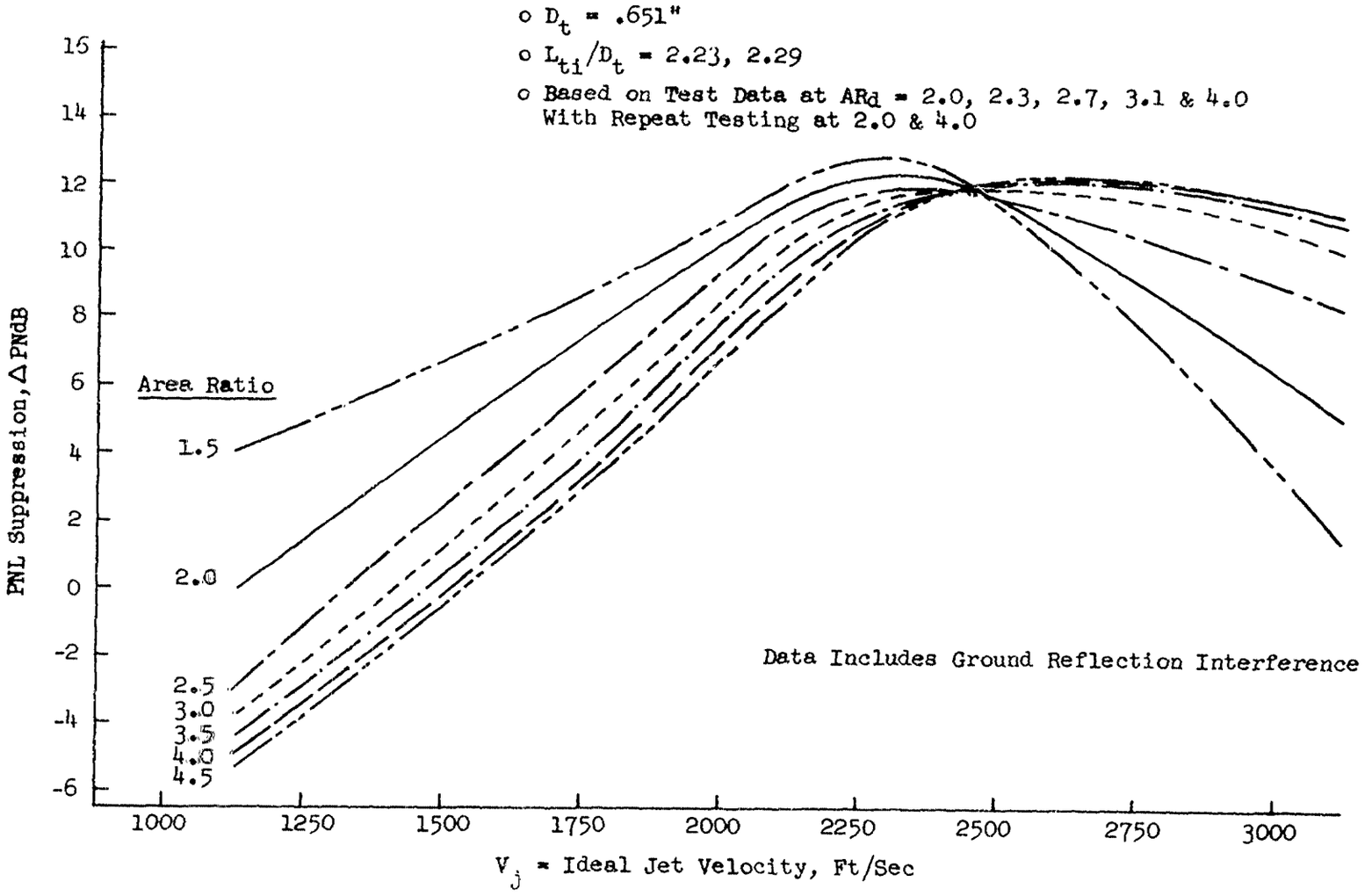

FIGURE V.F.9-20 EFFECT OF AREA RATIO ON 300 FT. SIDELINE PNL SUPPRESSIONS FOR 85 HOLE NOZZLES

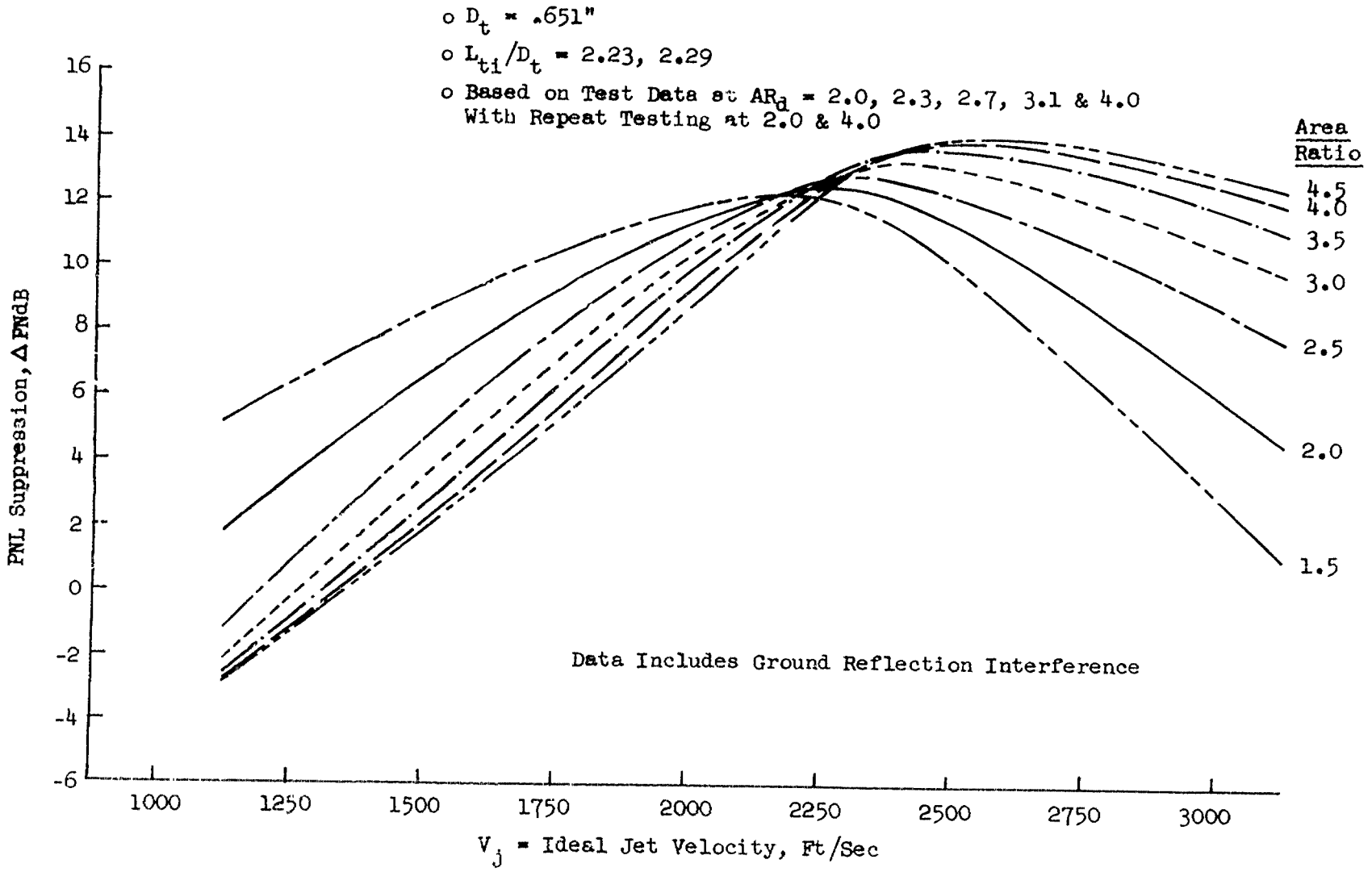

FIGURE V.F.9-21 EFFECT OF AREA RATIO ON 1500 FT. SIDLINE PNL SUPPRESSIONS FOR 85 HOLE NOZZLES

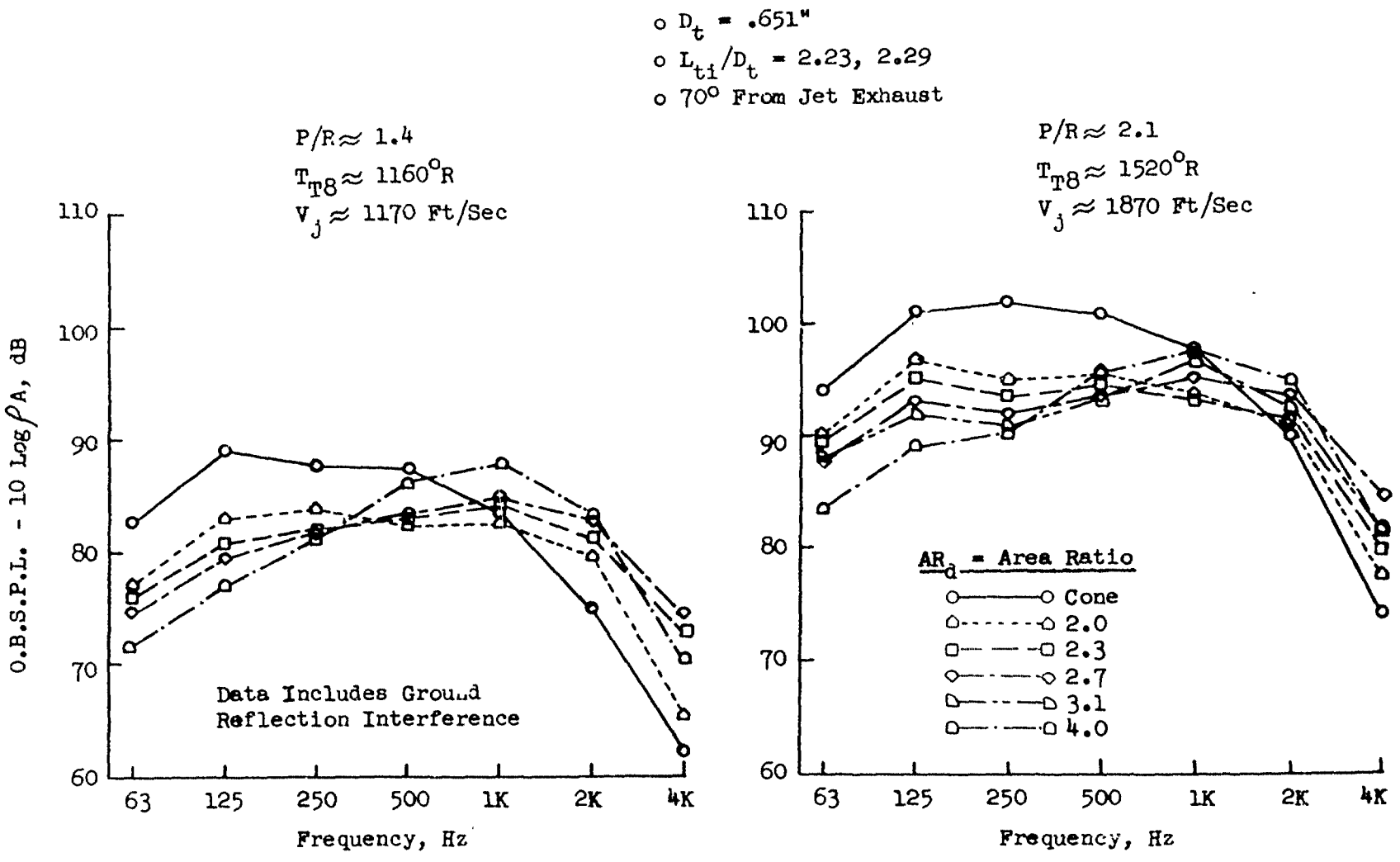

FIGURE V.F.9-22A EFFECT OF AREA RATIO ON 1500 FT. SIDELINE SPECTRA FOR 85 HOLE NOZZLES

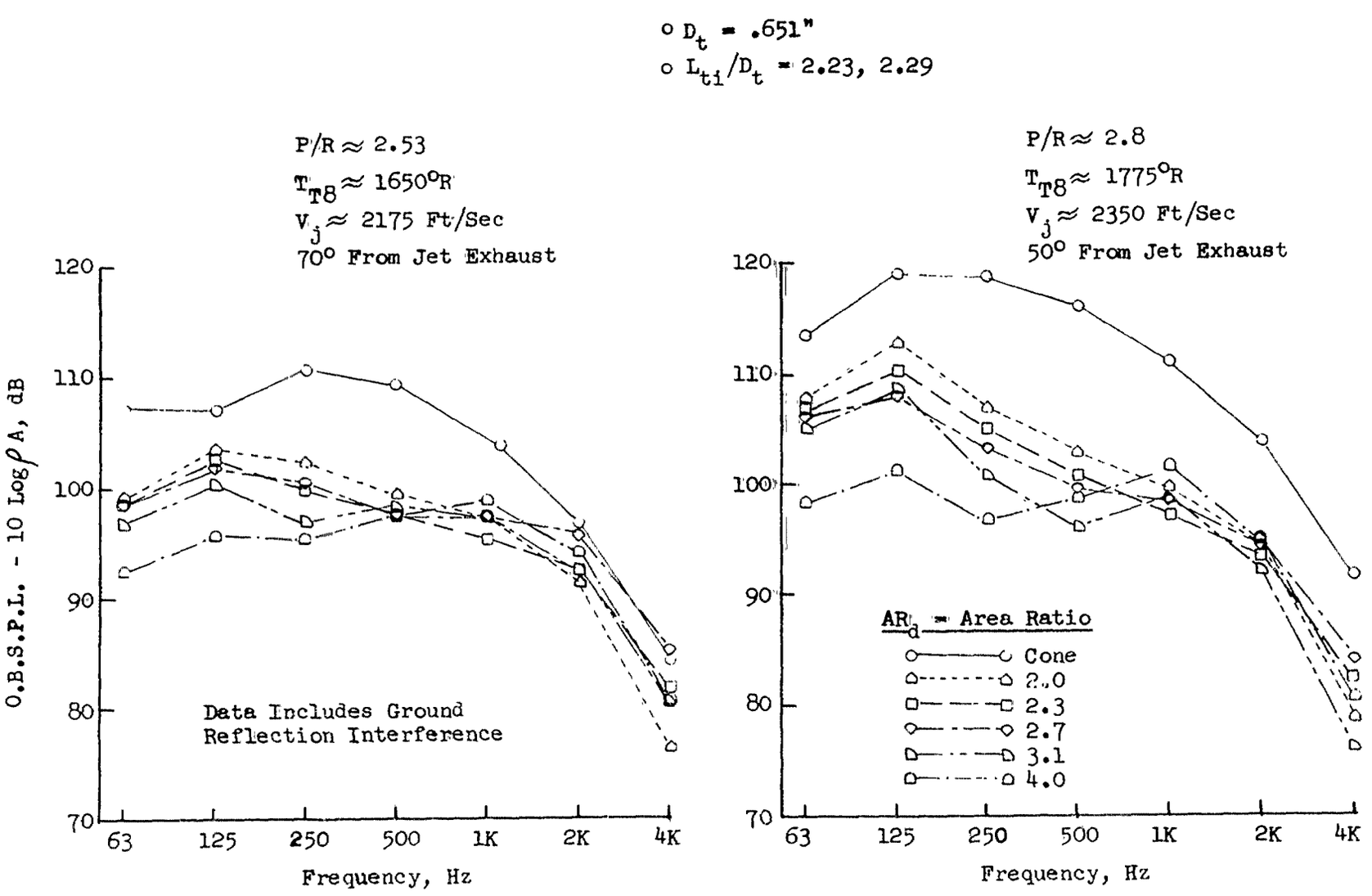

FIGURE V.F.9-22B EFFECT OF AREA RATIO ON 1500 FT. SIDELINE SPECTRA FOR 85 HOLE NOZZLES

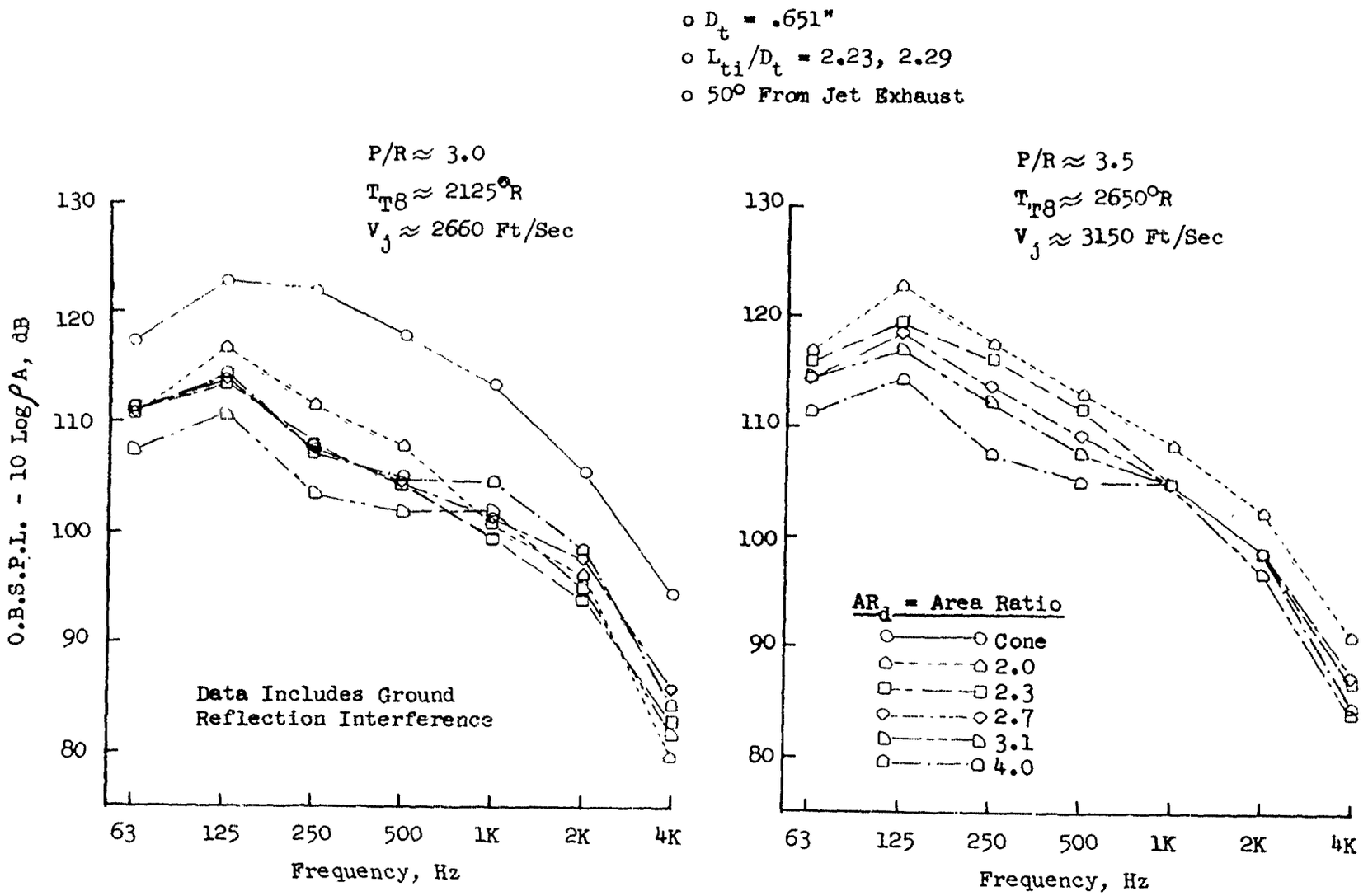

FIGURE V.F.9-22C EFFECT OF AREA RATIO ON 1500 FT. SIDELINE SPECTRA FOR 85 HOLE NOZZLES

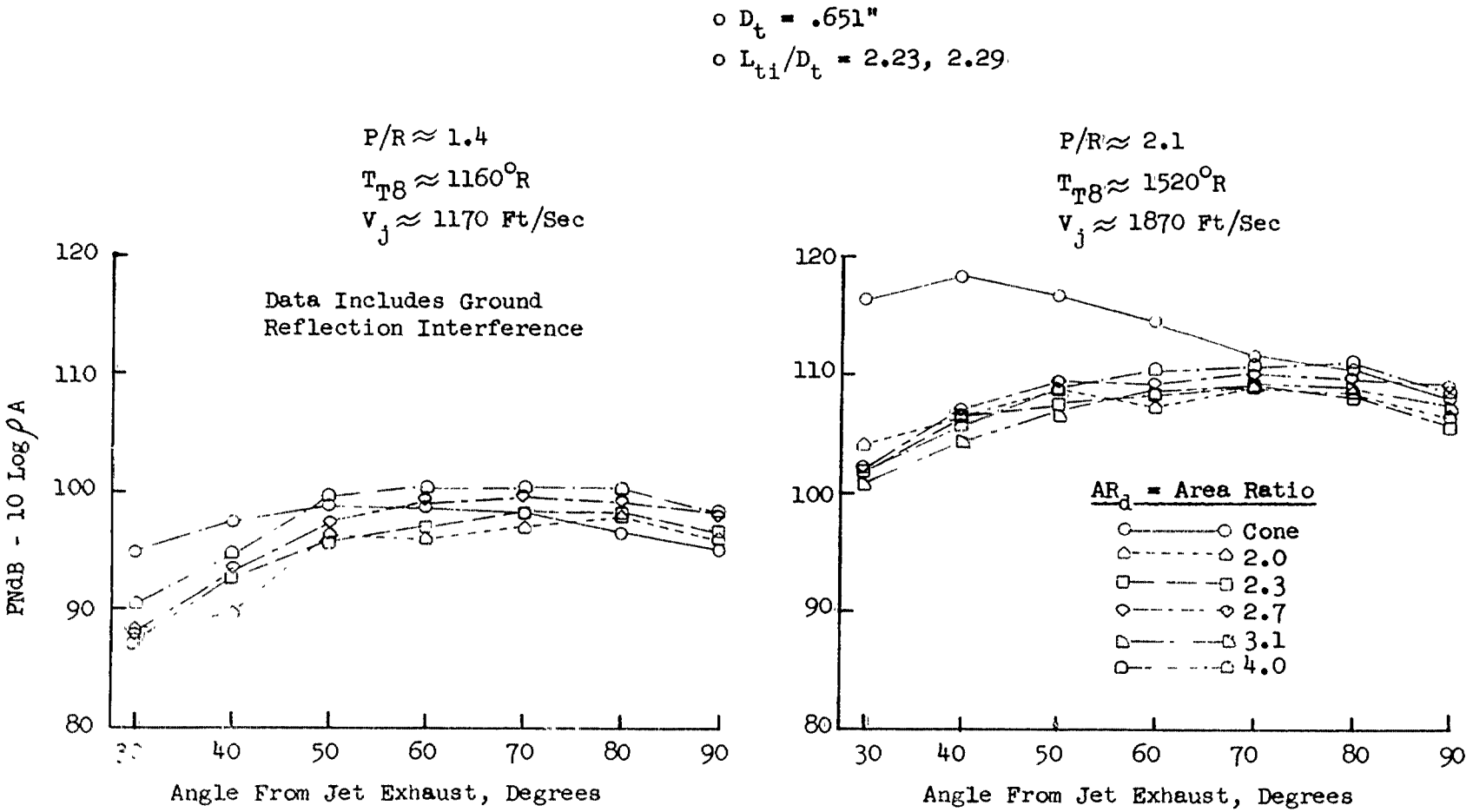

FIGURE V.F.9-23A EFFECT OF AREA RATIO ON 1500 FT. SIDELINE DIRECTIVITY FOR 85 HOLE NOZZLES

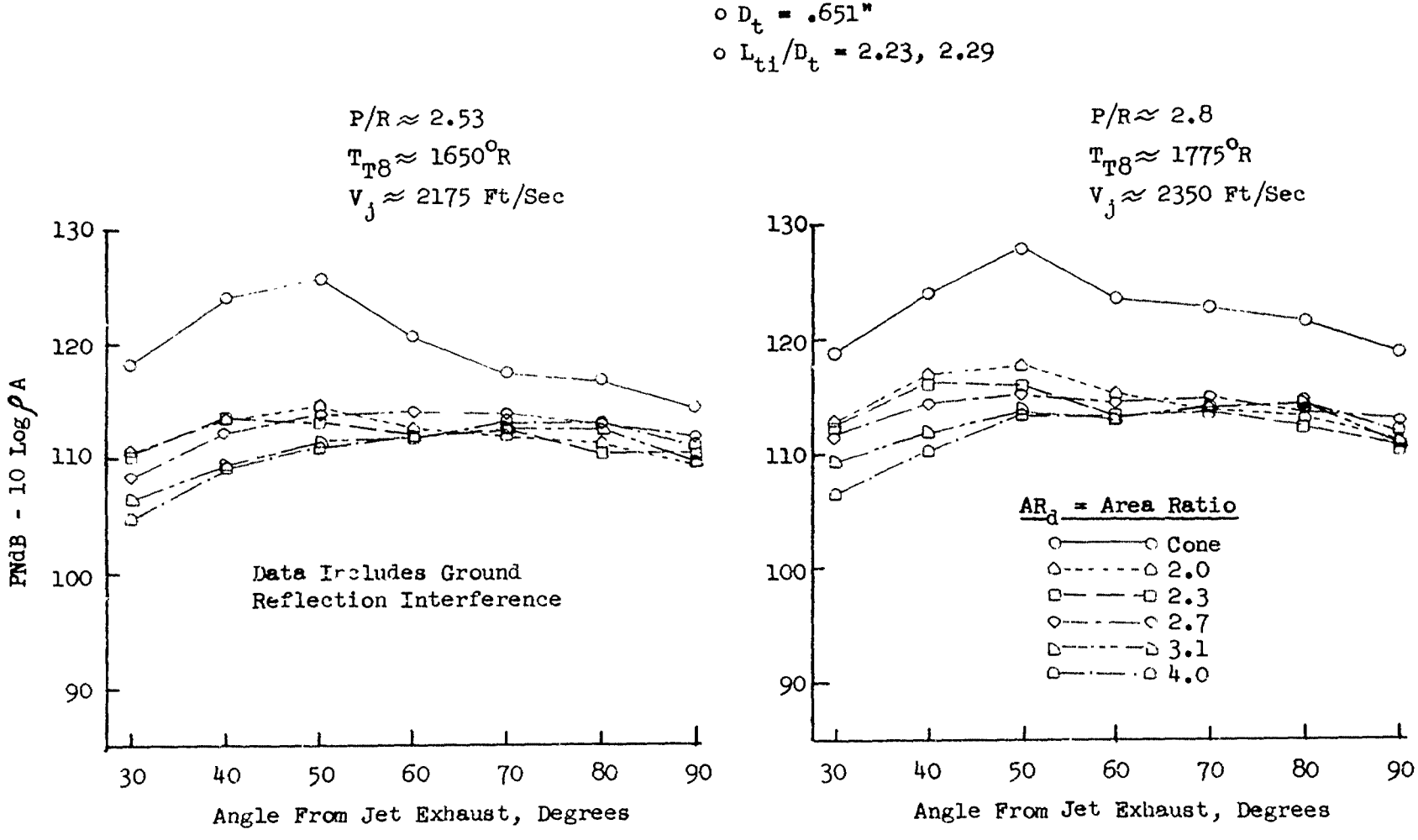

FIGURE V.F.9-23B EFFECT OF AREA RATIO ON 1500 FT. SIDELINE DIRECTIVITY FOR 85 HOLE NOZZLES

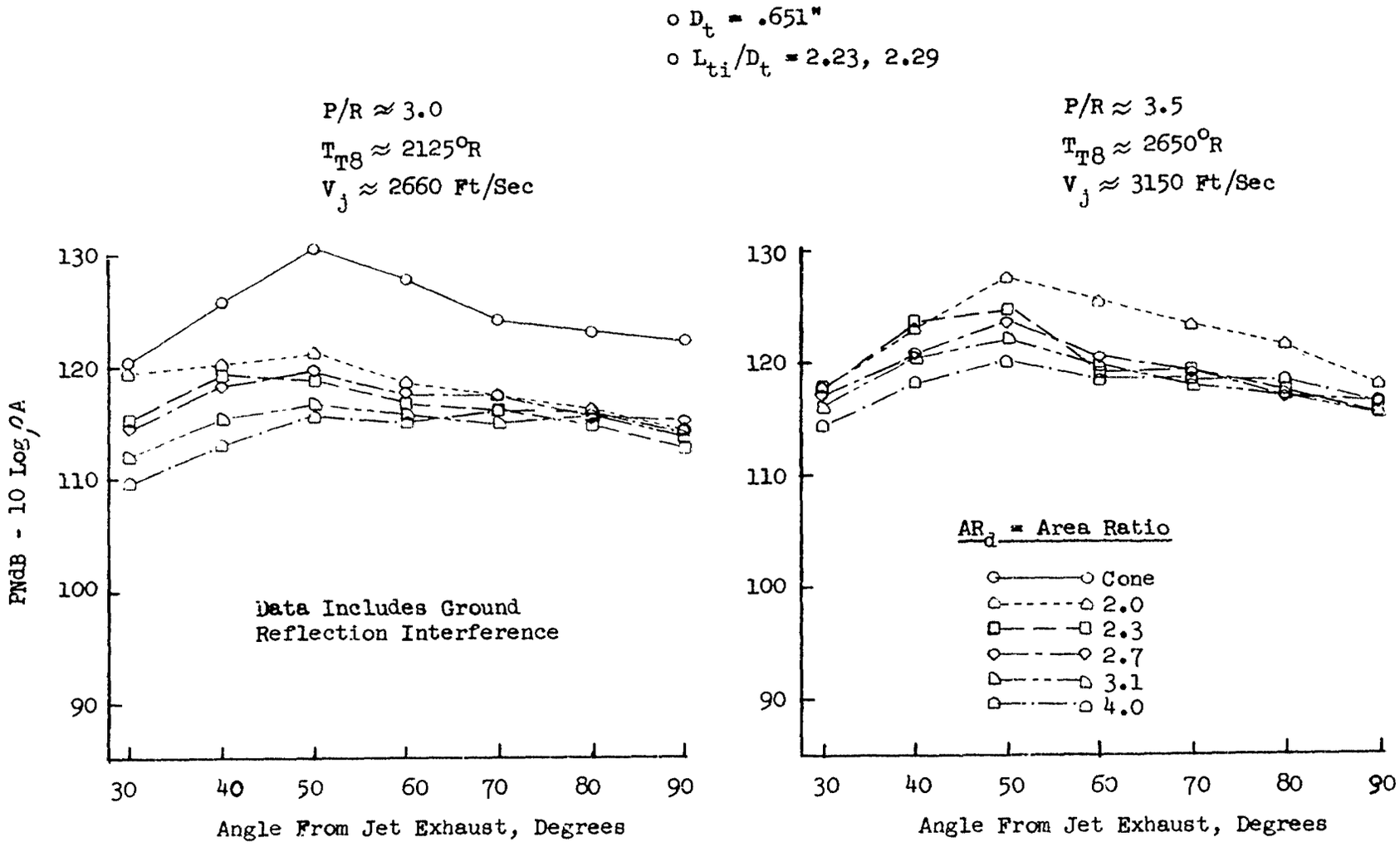

FIGURE V.F.9-23C EFFECT OF AREA RATIO ON 1500 FT. SIDELINE DIRECTIVITY FOR 85 HOLE NOZZLES

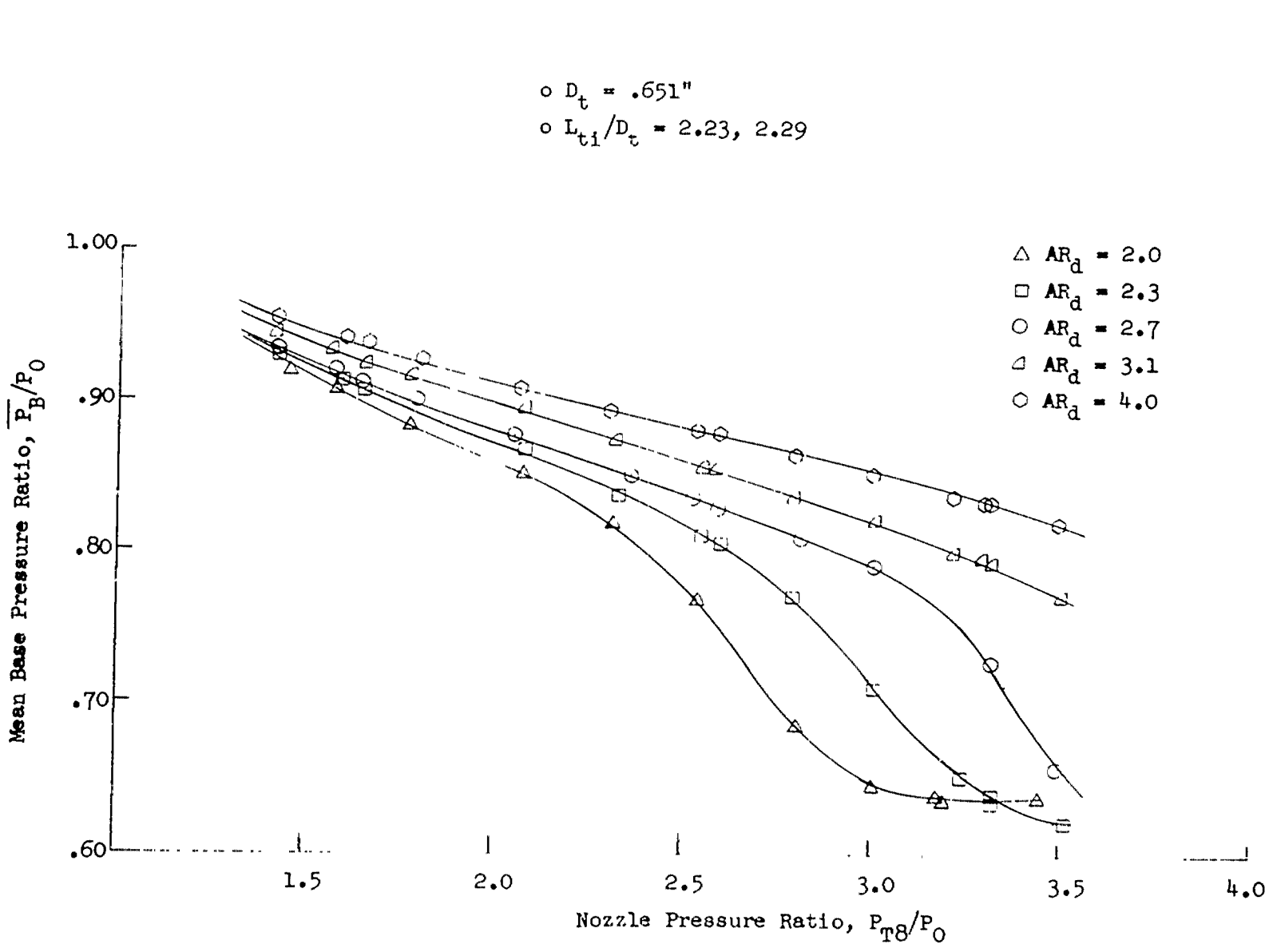

FIGURE V.F.9-24 EFFECT OF AREA RATIO ON MEAN BASEPLATE PRESSURE RATIO FOR 85 HOLE NOZZLES

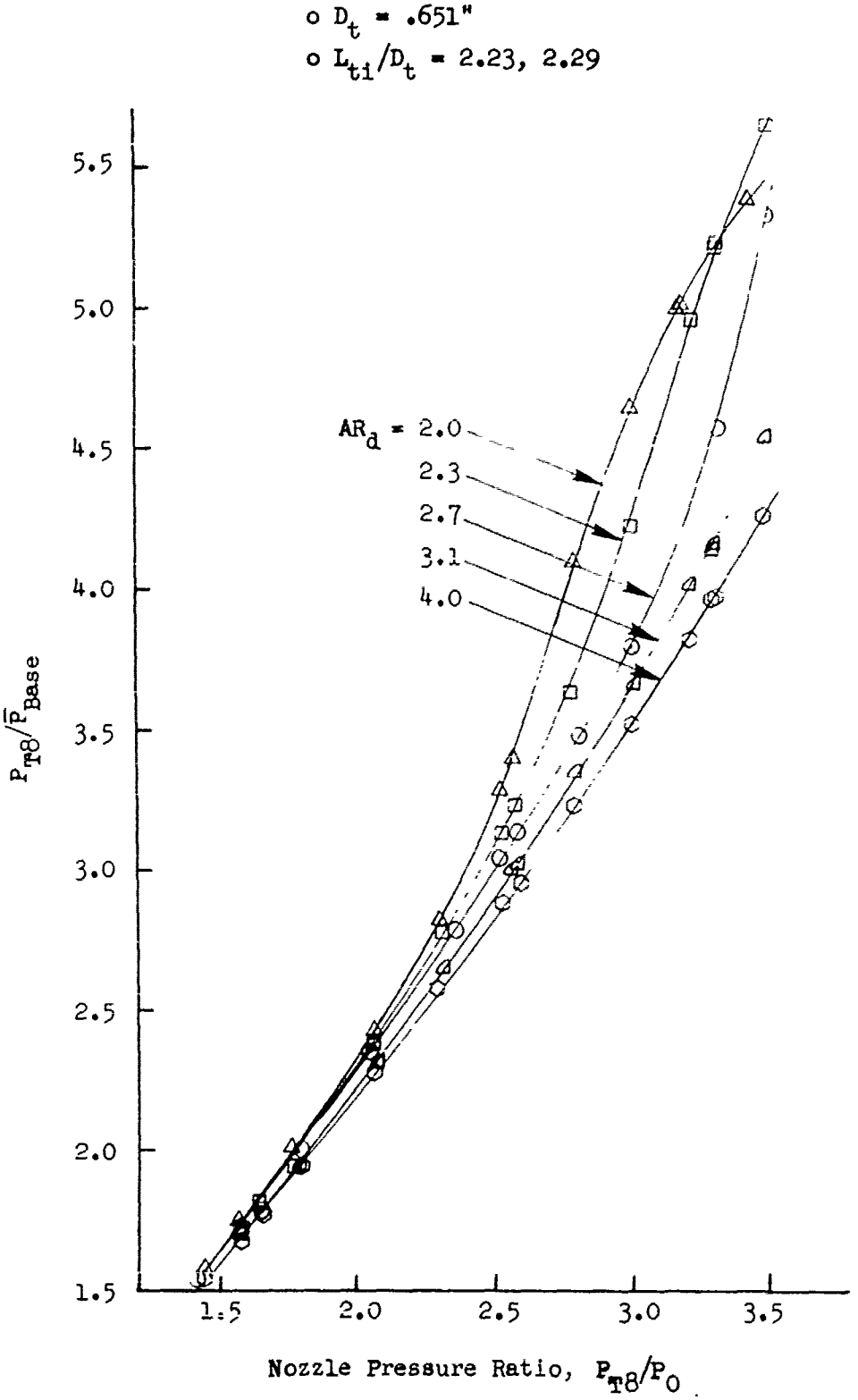

FIGURE V.F.9-25 EFFECT OF AREA RATIO ON NOZZLE EXIT TO MEAN BASEPLATE PRESSURE RATIO FOR 85 HOLE NOZZLES

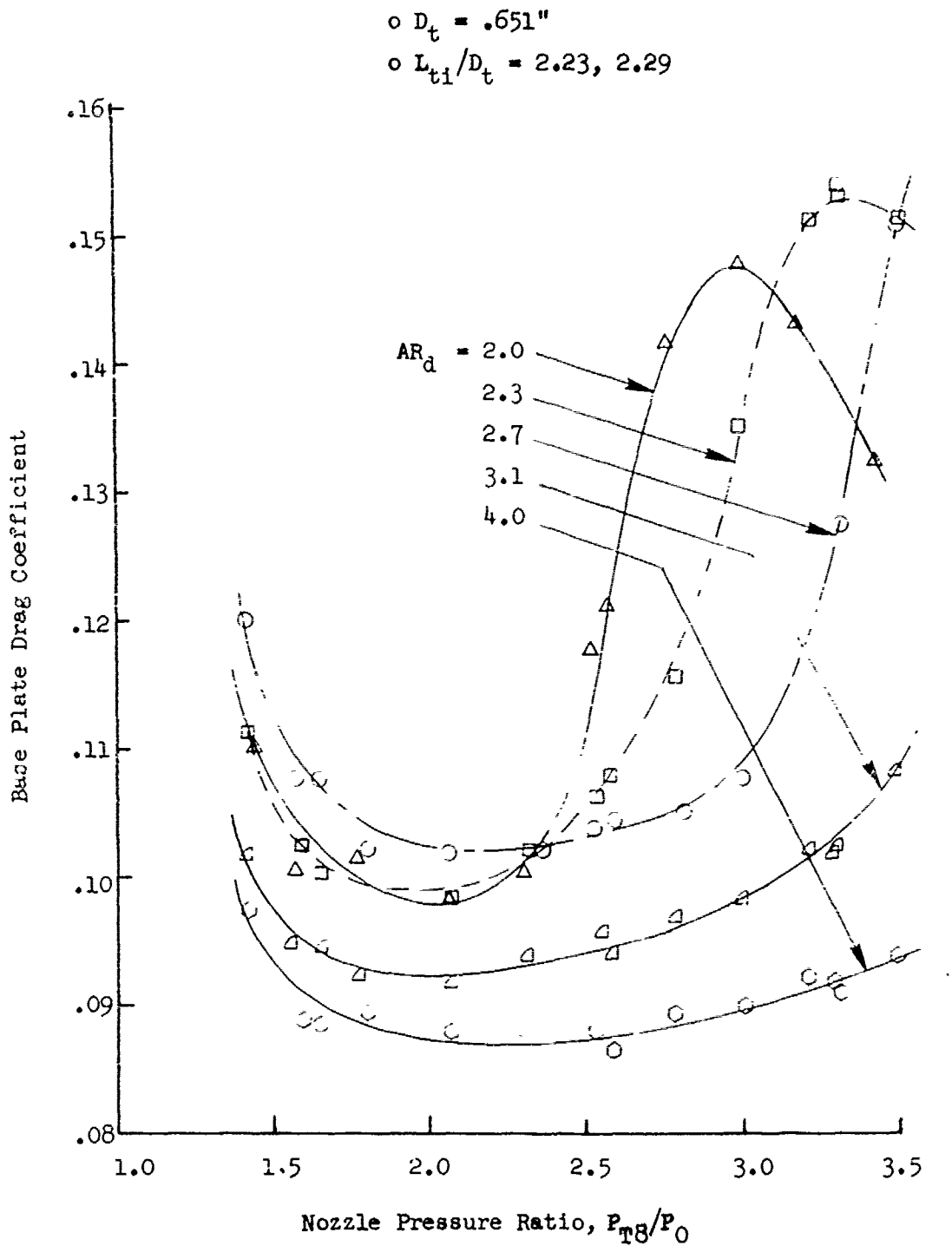

FIGURE V.F.9-26 EFFECT OF AREA RATIO ON BASEPLATE DRAG COEFFICIENT FOR 85 HOLE NOZZLE

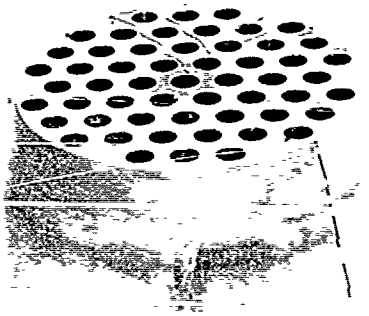

55 Holes

AR_d = 2.7

(Model No. 6.0H55-2.7)

85 Holes

AR_d = 2.7

(Model No. 6.0H85-2.7)

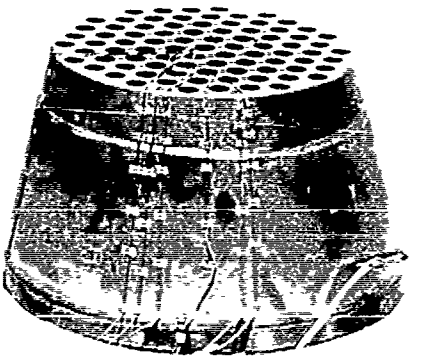

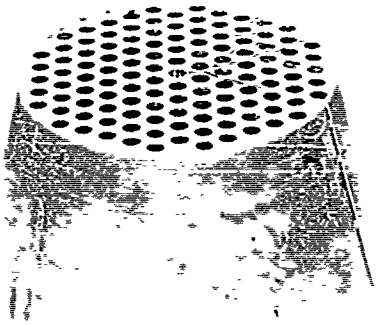

121 Holes

AR_d = 2.7

(Model No. 6.0H121-2.7)

FIGURE V.F.9-27 MULTI-HOLE NOZZLE HARDWARE USED IN PARAMETRIC INVESTIGATION OF HOLE NUMBER

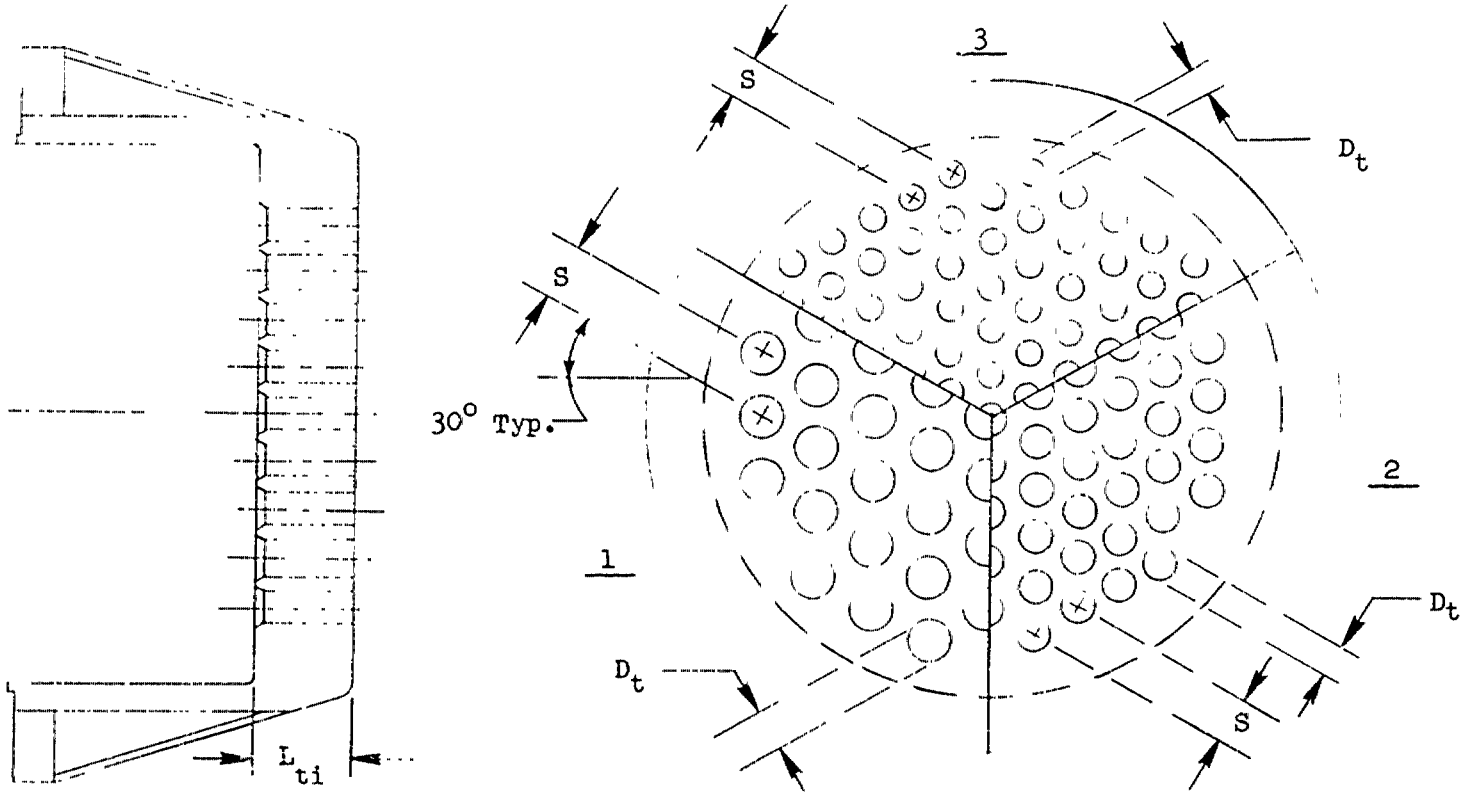

*Repeat Run on 6-26-69

	Number of Holes	Model No.	Test Date	Area Ratio	S	D_t	L_{ti}	L_{ti}/D_t
1	55	6.0H55-2.7	4-07-69*	2.7	1.087"	.809"	1.49"	1.84
2	85	6.0H85-2.7	3-06-69	2.7	.870"	.651"	1.49"	2.29
3	121	6.0H121-2.7	4-08-69	2.7	.725"	.546"	1.49"	2.73

FIGURE V.F.9-28 SCHEMATIC OF 55,85, AND 121 HOLE NOZZLES FOR PARAMETRIC INVESTIGATION OF HOLE NUMBER AT CONSTANT AREA RATIO, AR_d = 2.7

TABLE V.F.9-9 TEST SUMMARY

MODEL NO. 6.0 H55-2.7

DESCRIPTION: 55 Hole Plate with Equally Spaced .809" ID Holes AR_d = 2.7

DATE: 4/7/69

SCALE MODEL A_8 = .1963 ft^2

FULL SCALE A_8 = 12.563 ft^2

SCALE FACTOR = 8:1

- o DATA INCLUDES GROUND REFLECTION INTERFERENCE
- o ANGLE REFERENCED TO JET EXHAUST

	TEST CONDITIONS				ACOUSTIC TEST RESULTS					
			IDEAL			320' ARC		300' SIDELINE		1500' SIDELINE
Rdg No.	P_{T8}/P_o	T_{T8} (°R)	V_j (ft/sec)	W_8 (PPS)	10 log oA	PEAK PNdB	PEAK ANGLE	PEAK PNdB	PEAK ANGLE	PEAK PNdB	PEAK ANGLE
1	1.43	1130	1165	8.27	-3.1	113.2	60	112.5	80	95.3	80
2	1.58	1535	1513	7.81	-4.4	117.3	60/70	117.5	80	100.2	80
3	1.68	1249	1445	9.24	-3.5	117.1	50	116.9	80	99.5	80
4	1.81	1505	1693	8.99	-4.3	120.9	50	120.9	80	103.4	80
5	2.07	1521	1871	10.13	-4.1	124.0	50	122.9	80	105.6	70
6	2.32	1562	2024	11.35	-4.0	126.1	50	124.7	70	107.3	70
7	2.55	1653	2185	12.11	-4.3	128.2	50	125.8	50	108.6	50
8	2.60	2159	2521	10.50	-5.2	130.6	50	128.3	50	111.2	50
9	2.86	1741	2360	12.80	-4.0	130.6	40	128.0	50	111.0	50
10	3.02	2098	2651	12.50	-4.7	132.4	50	130.1	50	114.3	50
11	3.23	2199	2784	12.40	-4.7	133.9	40	131.6	50	116.0	50
12	3.24	2400	2910	12.50	-5.1	134.9	50	132.8	50	117.3	50
13	3.33	2596	3057	12.00	-5.4	134.6	40/50	132.5	50	117.2	50
14	3.35	2659	3103	12.60	-5.4	136.4	50	134.3	50	118.9	50

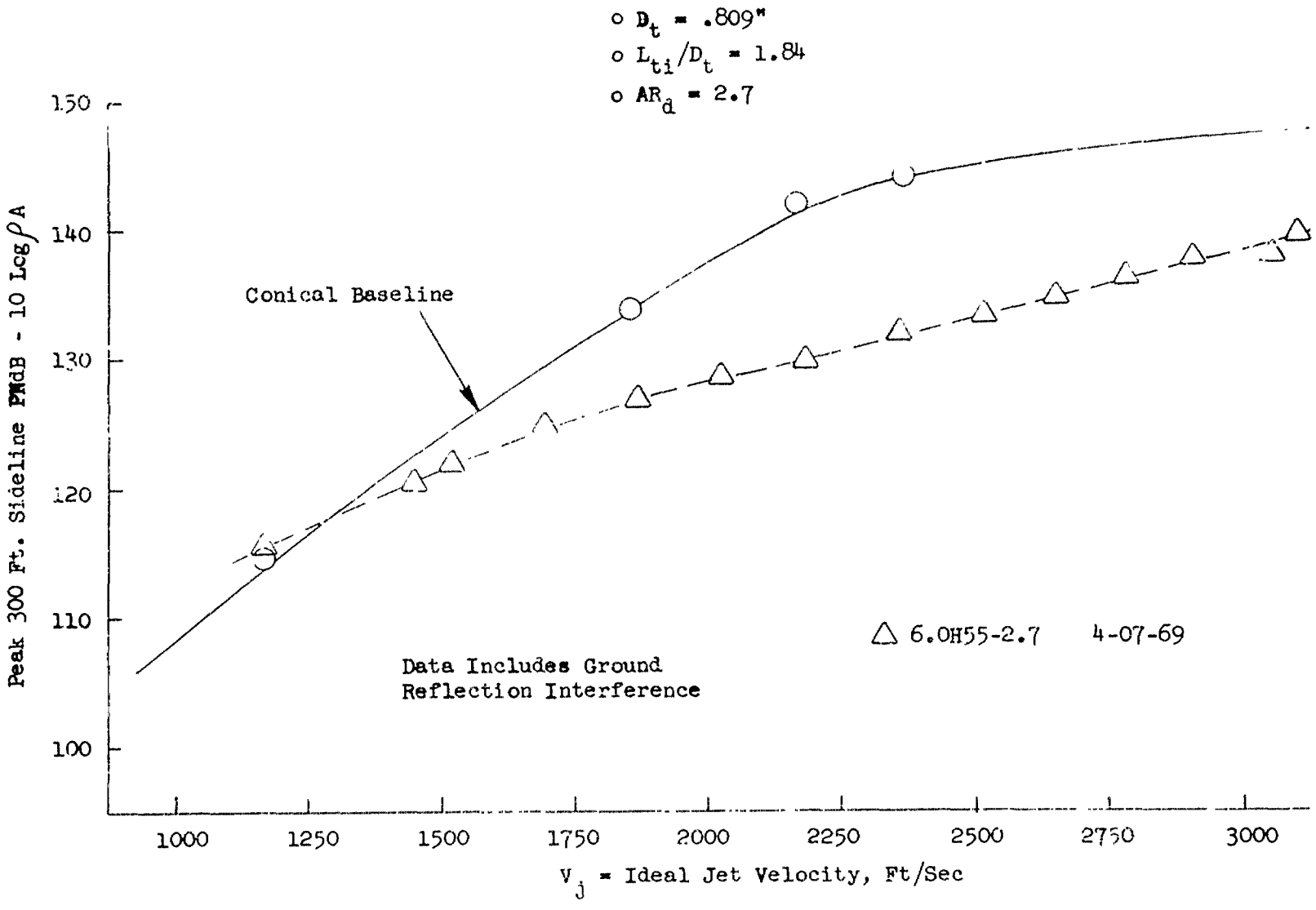

FIGURE V.F.9-29 300 FT. SIDELINE JET NOISE LEVELS FOR 55 HOLE NOZZLE

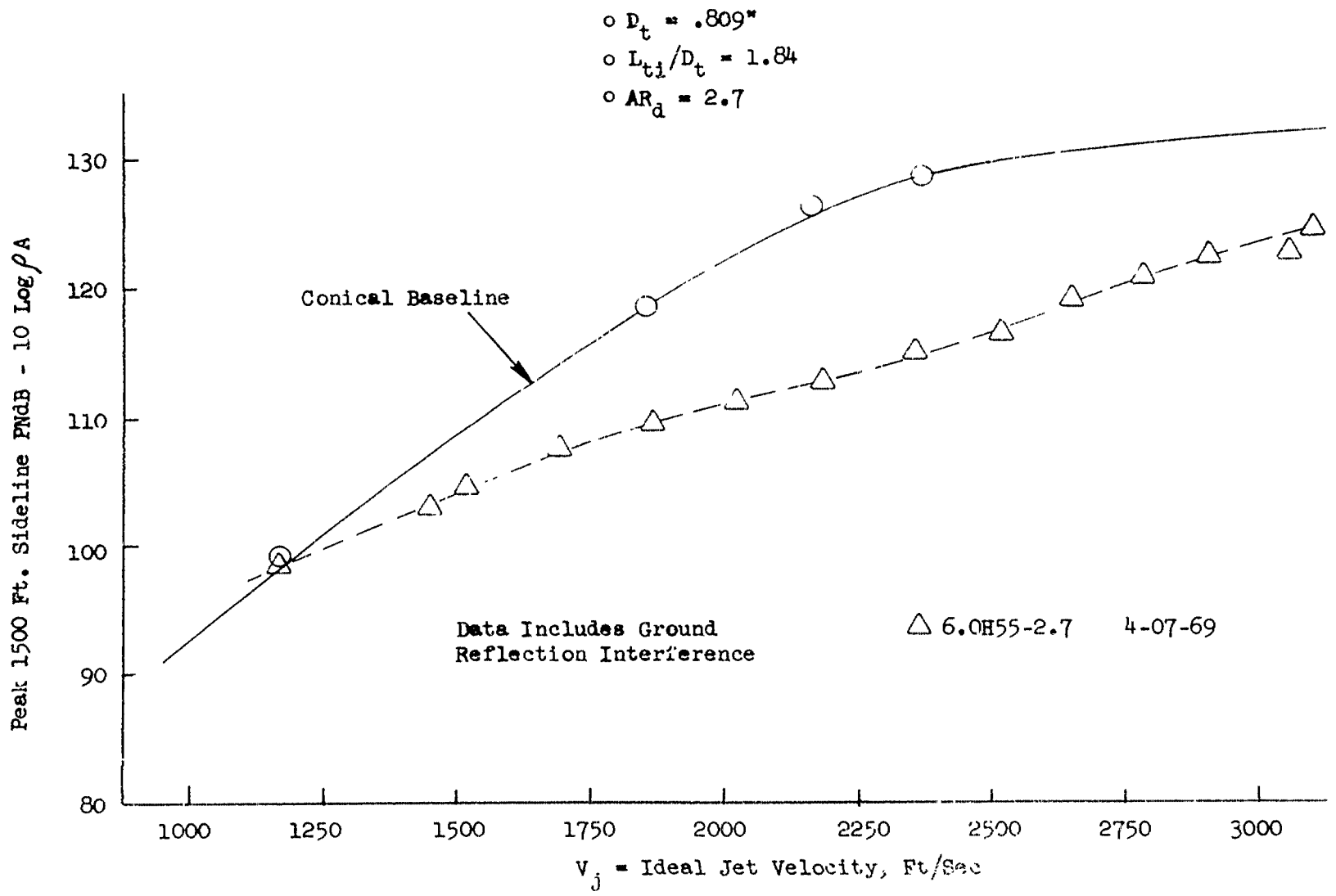

FIGURE V.F.9-30 1500 FT. SIDELINE JET NOISE LEVELS FOR 55 HOLE NOZZLE

TABLE V.F.9-10 TEST SUMMARY

MODEL NO. 6.0 H55-2.7

DESCRIPTION: 55 Hole Plate with Equally Spaced .809" ID Holes, AR_d = 2.7

DATE: 6/26/69

SCALE MODEL A_8 = .1963 ft^2

FULL SCALE A_8 = 12.563 ft^2

SCALE FACTOR = 8:1

- o DATA INCLUDES GROUND REFLECTION INTERFERENCE
- o ANGLE REFERENCED TO JET EXHAUST

RDG No.	TEST CONDITIONS				ACOUSTIC TEST RESULTS						
			IDEAL			320' ARC		300' SIDELINE		1500' SIDELINE	
	P_{T8}/P_o	T_{T8} (°R)	V_j (ft/sec)	W_8 (PPS)	10 log ΔA	PEAK PNdB	PEAK ANGLE	PEAK PNdB	PEAK ANGLE	PEAK PNdB	PEAK ANGLE
2	1.44	1151	1177	8.38	-3.1	116.3	60	115.4	60	97.9	60
3	1.60	1513	1525	7.96	-4.4	120.1	50	118.6	70	101.1	70
4	1.69	1238	1446	9.37	-3.5	119.7	60	119.6	70	102.2	70
5	2.08	1515	1873	10.32	-4.1	126.1	50	125.2	70	107.6	70
6	1.82	1511	1702	9.06	-4.3	123.0	50	122.3	70	104.8	70
7	2.38	1517	2023	11.77	-3.9	129.1	50	126.7	50	109.1	50/60
8	2.55	1648	2181	11.99	-4.1	130.5	50	128.1	50	110.6	50
9	2.82	1778	2370	12.81	-4.2	132.0	50	129.7	50	112.3	50
10	3.33	2418	2951	12.84	-5.1	136.3	50	134.0	50	118.1	50
11	3.52	2695	3178	12.90	-5.4	137.9	50	135.6	50	120.1	50
12	3.32	2591	3051	12.42	-5.4	136.9	50	134.6	50	118.5	50
13	3.24	2225	2802	12.95	-4.8	135.3	50	133.9	60	113.0	60
14	3.10	2129	2697	12.66	-4.7	135.3	50	133.0	50	116.0	50
15	2.61	2117	2499	10.78	-5.1	132.7	50	130.4	50	113.1	50

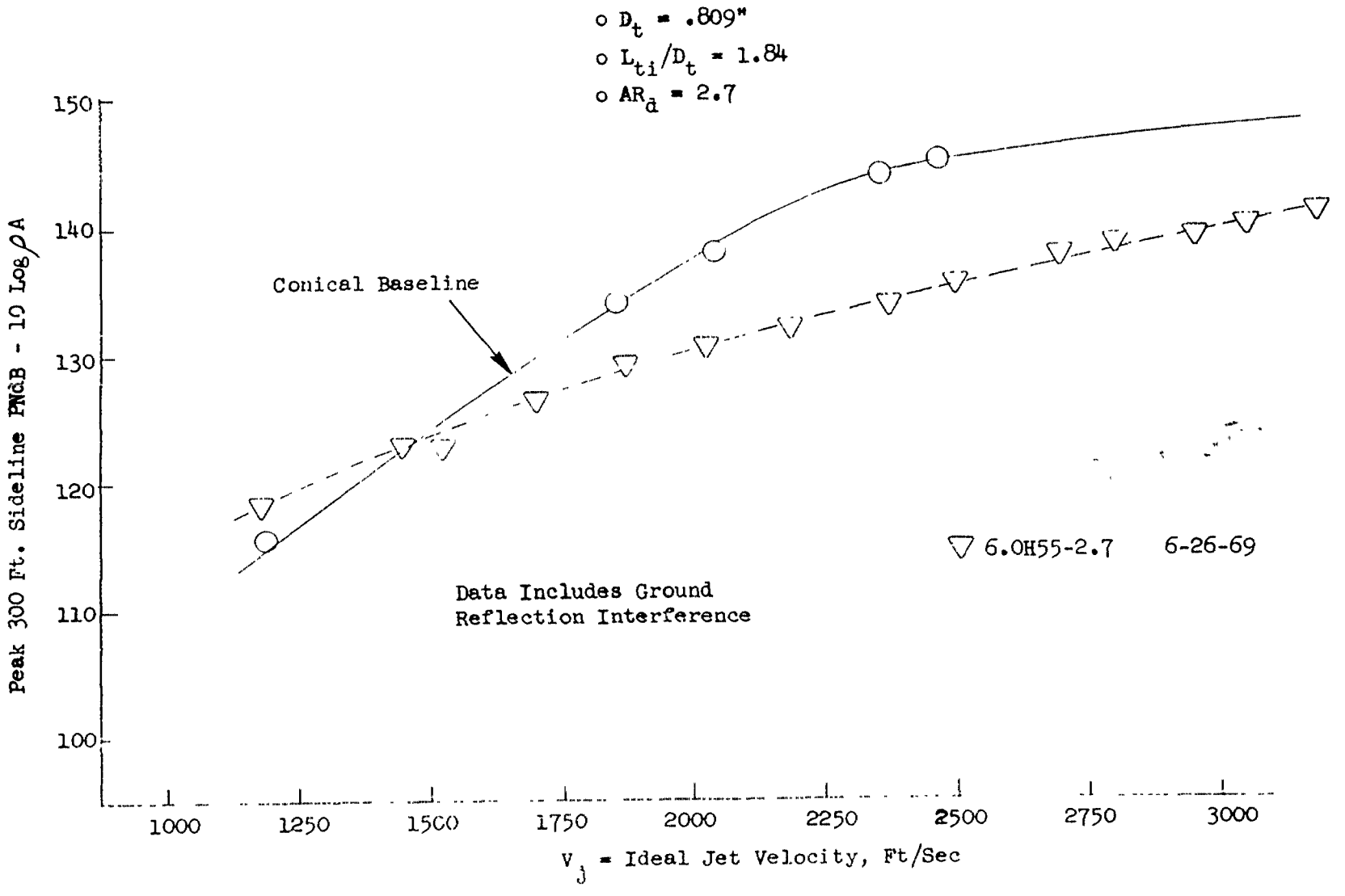

FIGURE V.F.9-31 300 FT. SIDELINE JET NOISE LEVELS FOR 55 HOLE NOZZLE

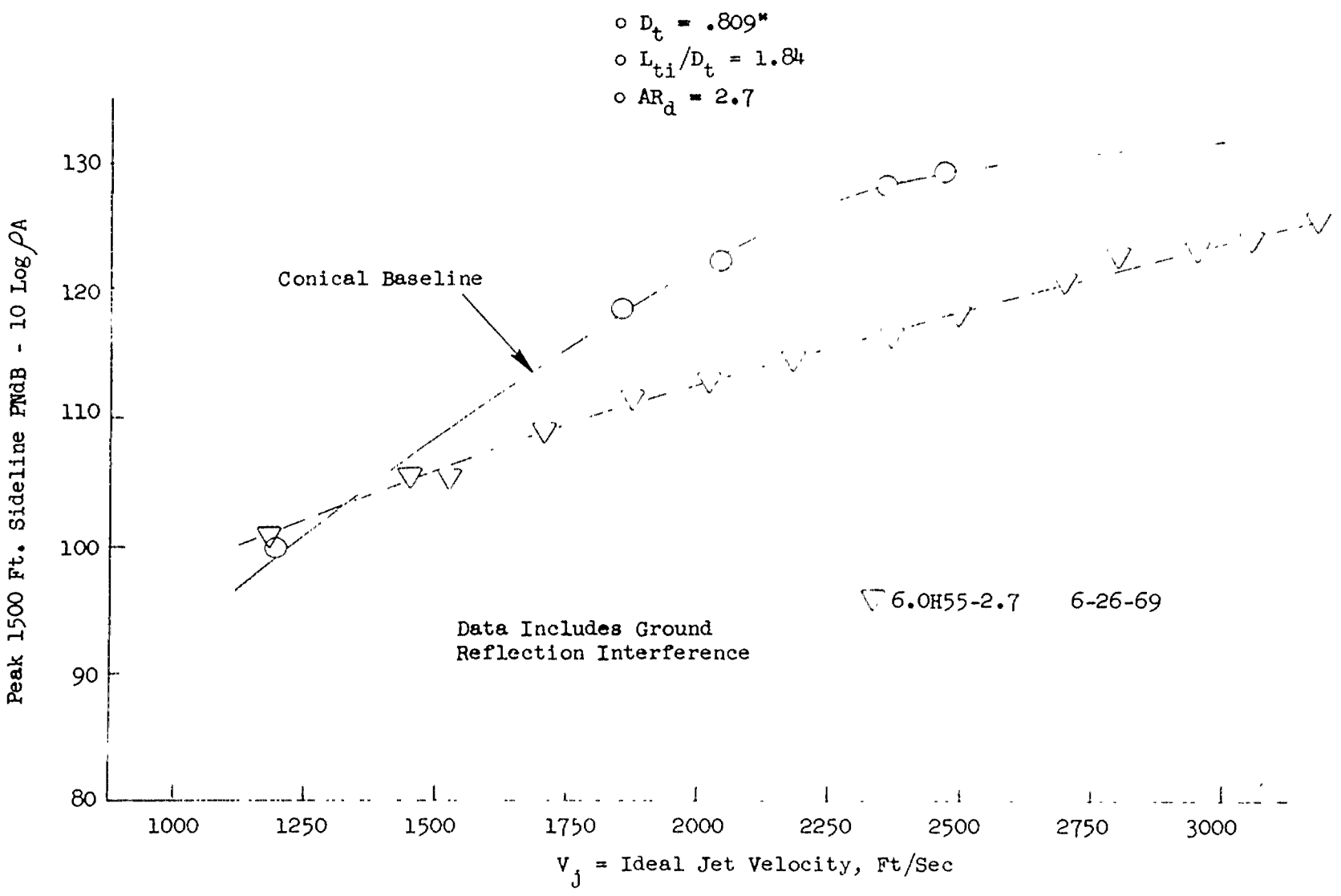

FIGURE V.F.9-32 1500 FT. SIDELINE JET NOISE LEVELS FOR 55 HOLE NOZZLE

TABLE V.F.9-11 TEST SUMMARY

MODEL NO. 6.0 H 121-2.7

DESCRIPTION: 121 Hole Plate with Equally Spaced .546" ID Holes, AR_d = 2.7

DATE: 4/8/69

SCALE MODEL A_8 = .1967 ft^2

FULL SCALE A_8 = 12.589 ft^2

SCALE FACTOR = 8:1

- o DATA INCLUDES GROUND REFLECTION INTERFERENCE
- o ANGLE REFERENCED TO JET EXHAUST

	TEST CONDITIONS				ACOUSTIC TEST RESULTS						
			IDEAL			320' ARC		300' SIDELINE		1500' SIDELINE	
RDG. No.	P_{T8}/P_o	T_{T8} (°R)	V_j (ft/sec)	W_8 (PPS)	10 log pA	PEAK PNdB	PEAK ANGLE	PEAK PNdB	PEAK ANGLE	PEAK PNdB	PEAK ANGLE
1	1.43	1154	1167	8.44	-3.1	112.1	60	112.8	90	93.9	60
2	1.57	1509	1492	8.07	-4.3	116.3	60	115.4	60	98.1	60
3	1.67	1248	1440	9.35	-3.5	115.6	50/60	114.7	70/80	97.3	70/80
4	1.82	1518	1706	9.22	-4.3	119.9	50	118.5	80	101.1	80
5	2.06	1526	1865	10.40	-4.2	122.6	50	126.5	80	103.0	80
6	2.29	1577	2022	11.40	-4.1	124.4	40	122.0	80	104.6	80
7	2.52	1661	2179	12.28	-4.1	126.4	30	123.3	50	106.2	50
8	2.59	2126	2498	10.84	-5.1	128.	30	125.7	50	109.6	50
9	2.81	1772	2363	13.05	-4.2	128.3	30	125.7	50	109.0	50
10	3.00	2133	2665	12.53	-4.8	131.5	40	127.6	40/50	112.2	40
11	3.21	2233	2799	13.07	-4.8	132.1	40	128.1	40/50	112.9	40
12	3.31	2420	2945	12.99	-5.1	132.6	40	128.7	40	113.5	40
13	3.32	2622	3072	12.57	-5.4	133.2	40	129.2	40/50	114.1	40
14	3.49	2697	3169	13.11	-5.4	134.5	40	130.5	40	115.5	40

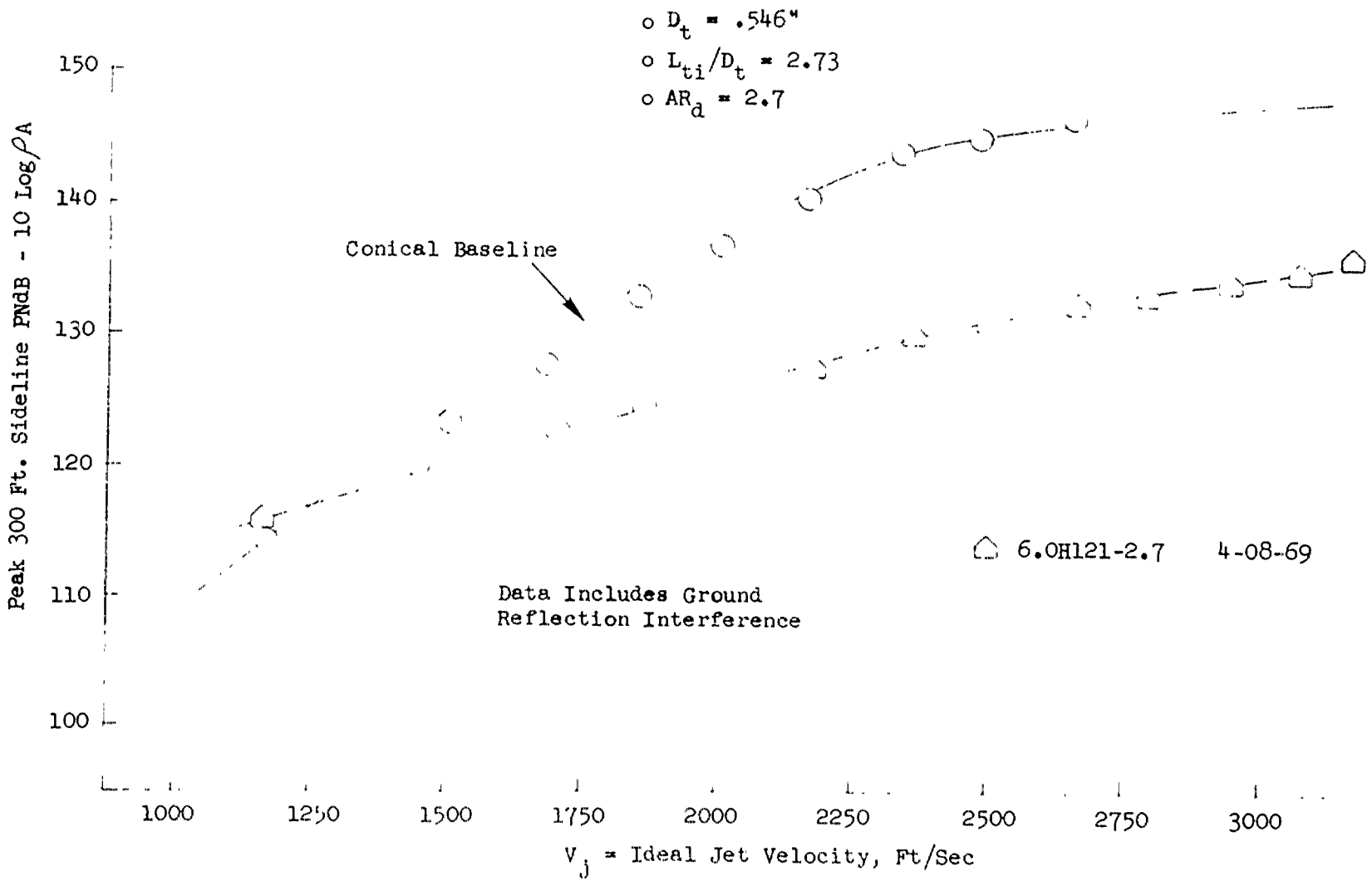

FIGURE V.F.9-33 300 FT. SIDELINE JET NOISE LEVELS FOR 121 HOLE NOZZLE

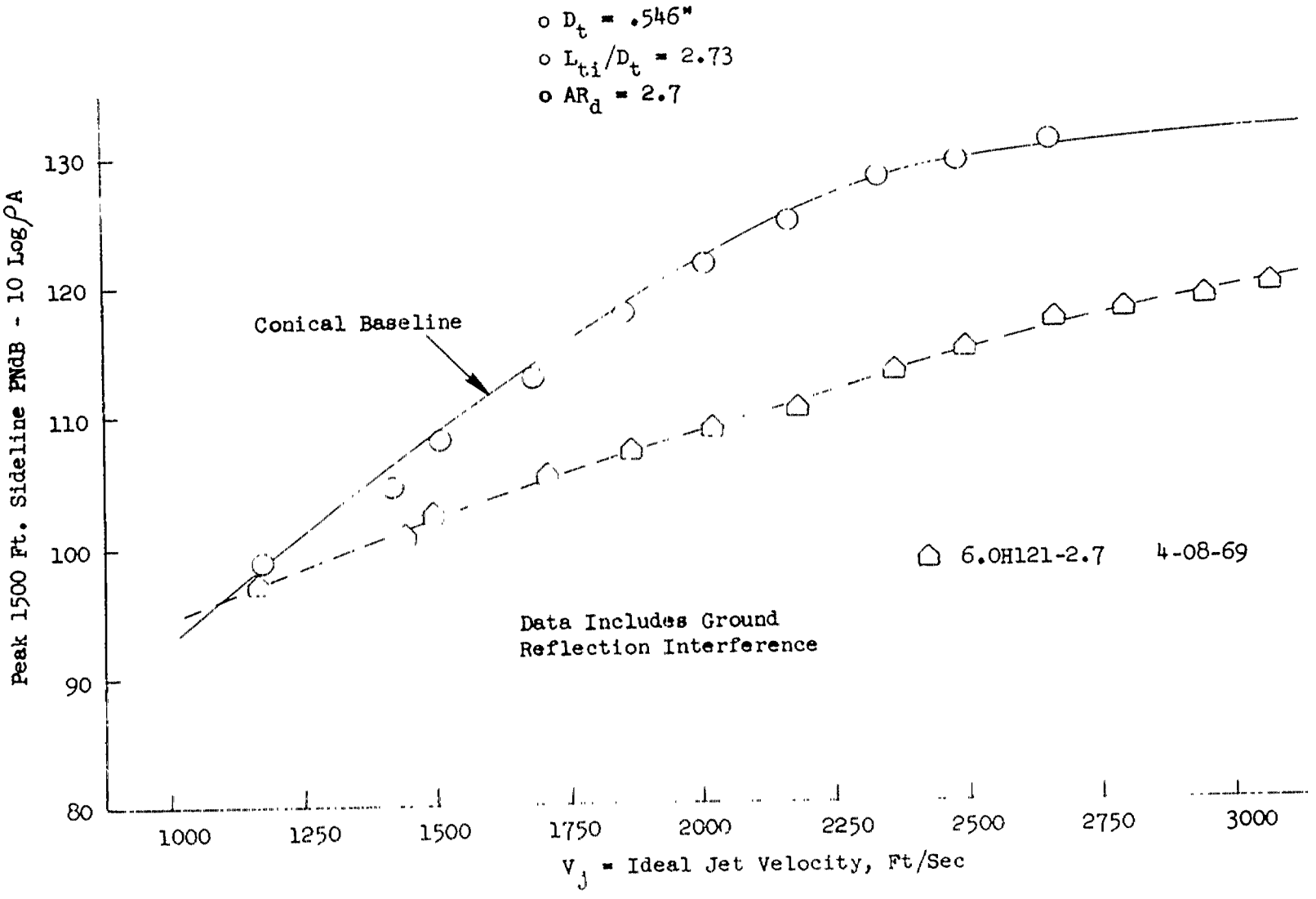

FIGURE V.F.9-34 1500 FT. SIDELINE JET NOISE LEVELS FOR 121 HOLE NOZZLE

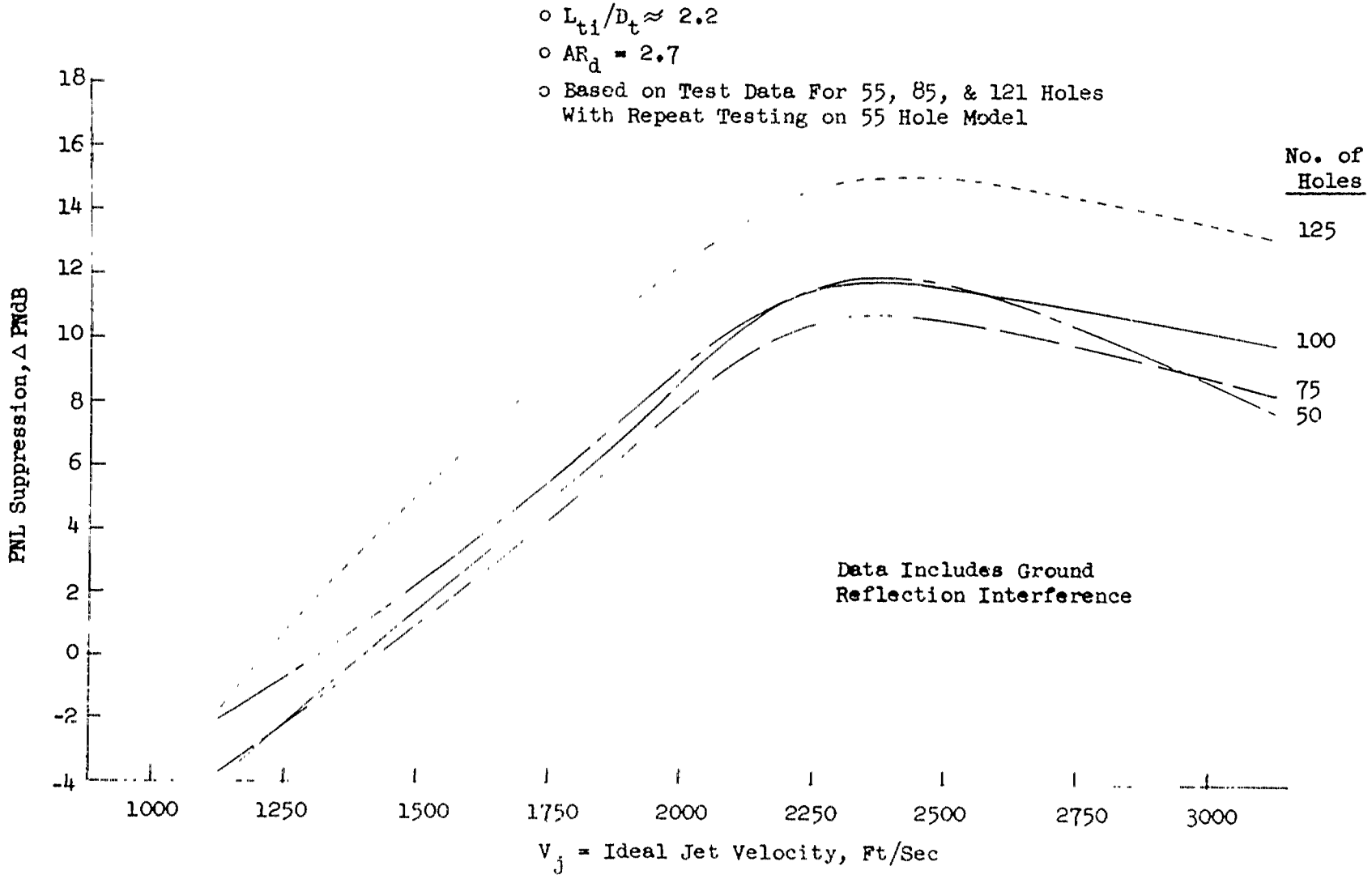

FIGURE V.F.9-35 EFFECT OF HOLE NUMBER ON 300 FT. SIDELINE PNL SUPPRESSIONS FOR MULTI-HOLE NOZZLES

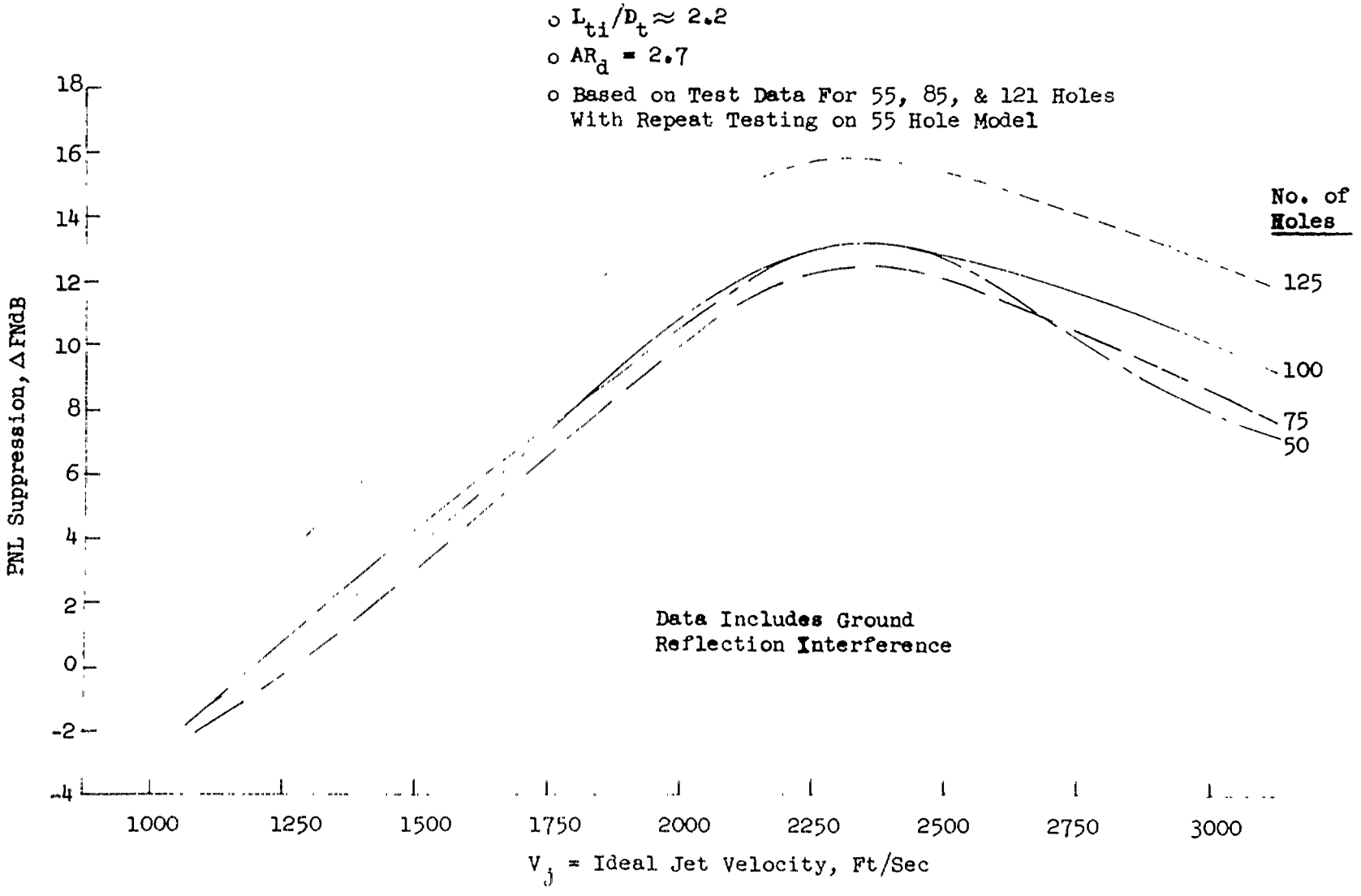

FIGURE V.F.9-36 EFFECT OF HOLE NUMBER ON 1500 FT. SIDELINE PNL SUPPRESSIONS FOR MULTI-HOLE NOZZLES

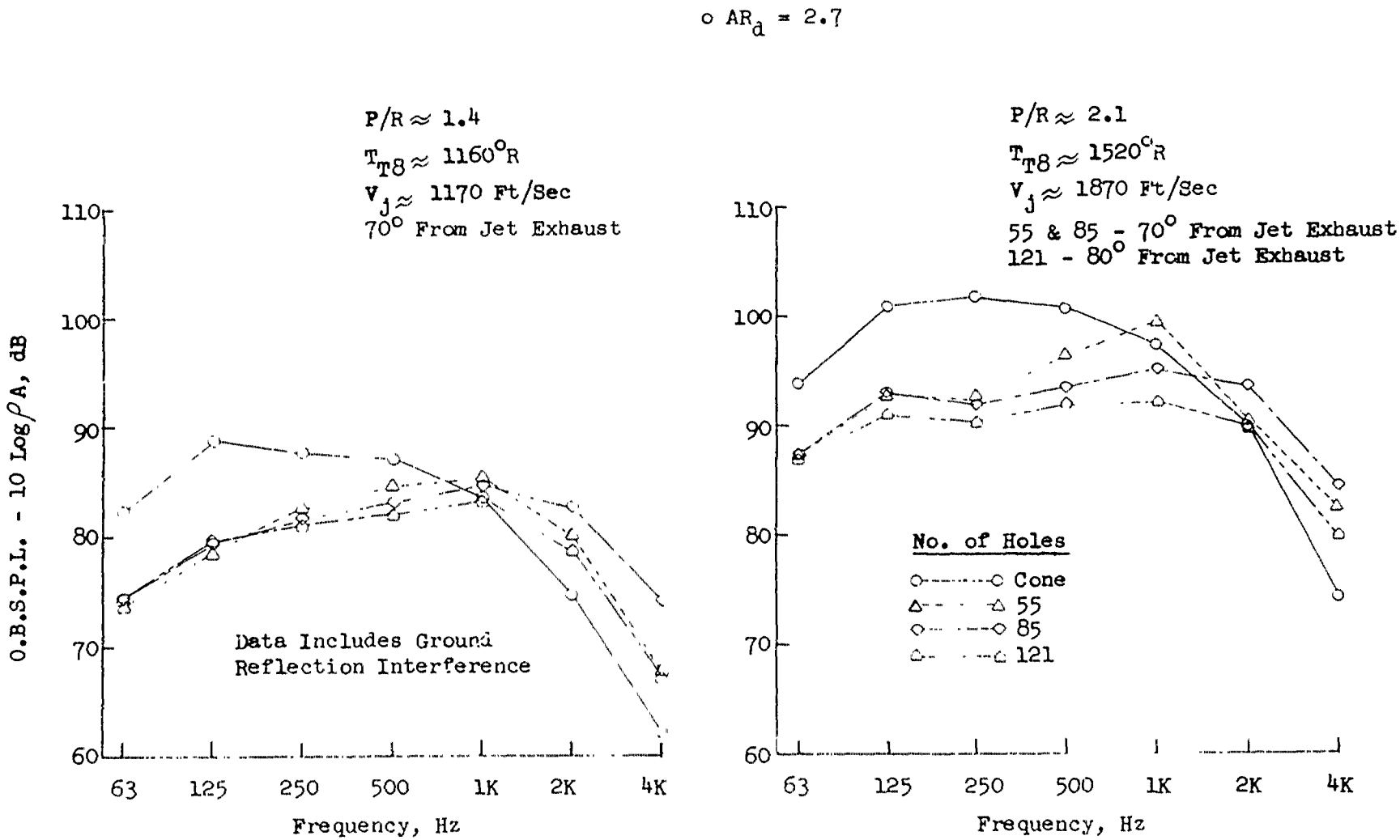

FIGURE V.F.9-37A EFFECT OF HOLE NUMBER ON 1500 FT. SIDELINE SPECTRA WITH 55, 85 AND 121 HOLE NOZZLES

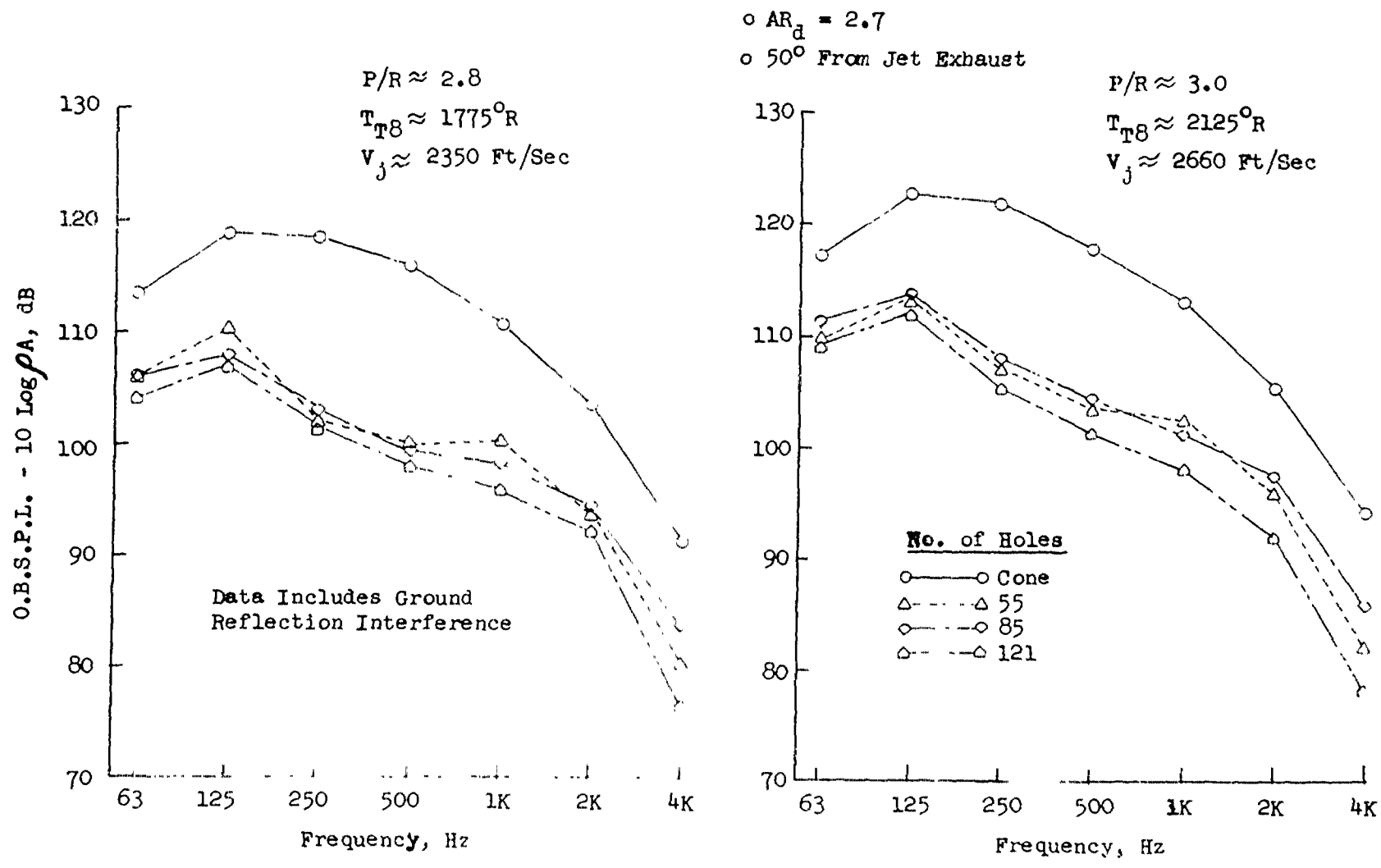

FIGURE V.F.9-37B EFFECT OF HOLE NUMBER ON 1500 FT. SIDELINE SPECTRA WITH 55, 85 AND 121 HOLE NOZZLES

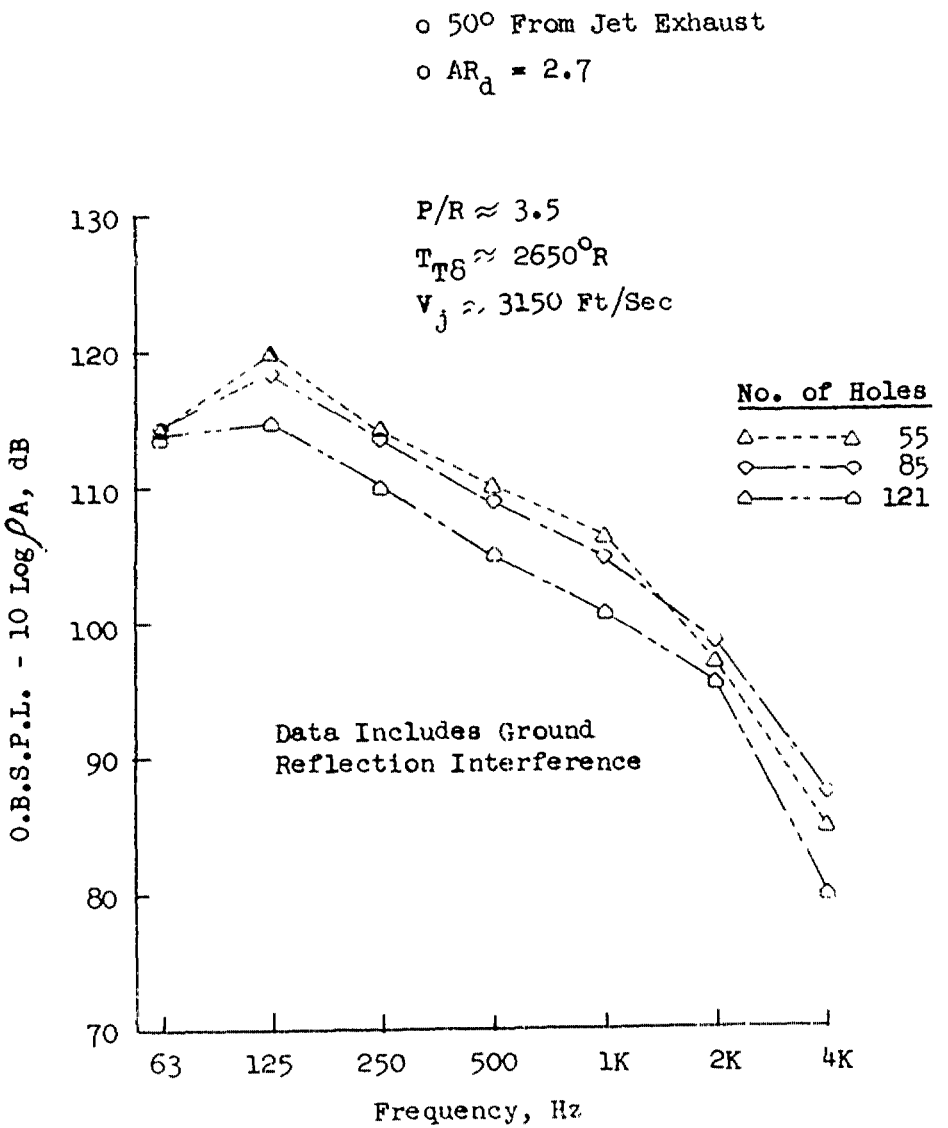

FIGURE V.F.9-37C EFFECT OF HOLE NUMBER ON 1500 FT. SIDELINE SPECTRA WITH 55, 85 AND 121 HOLE NOZZLES

o AR_d = 2.7

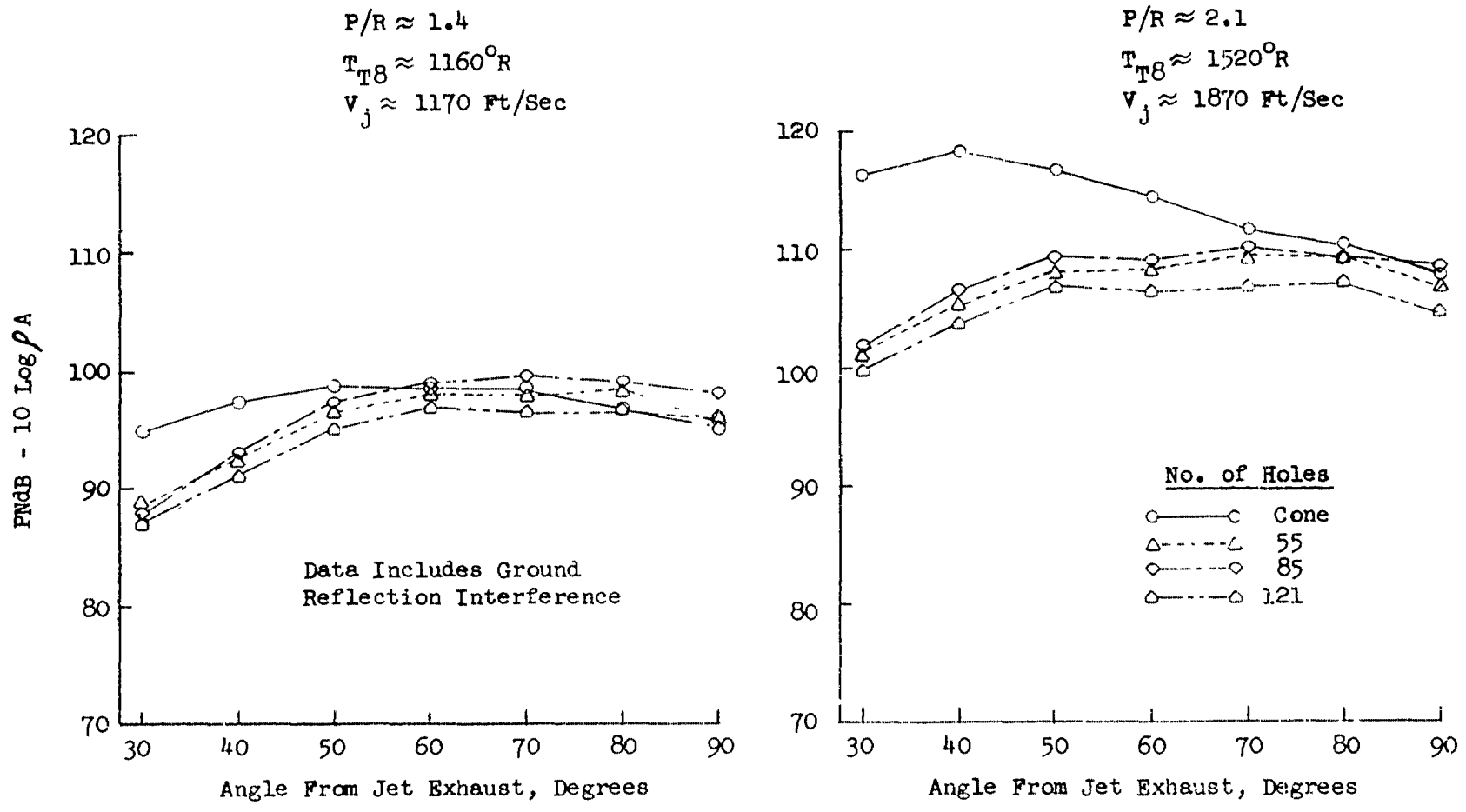

FIGURE V.F.9-38A EFFECT OF HOLE NUMBER ON 1500 FT. SIDELINE DIRECTIVITY WITH 55, 85 AND 121 HOLE NOZZLES

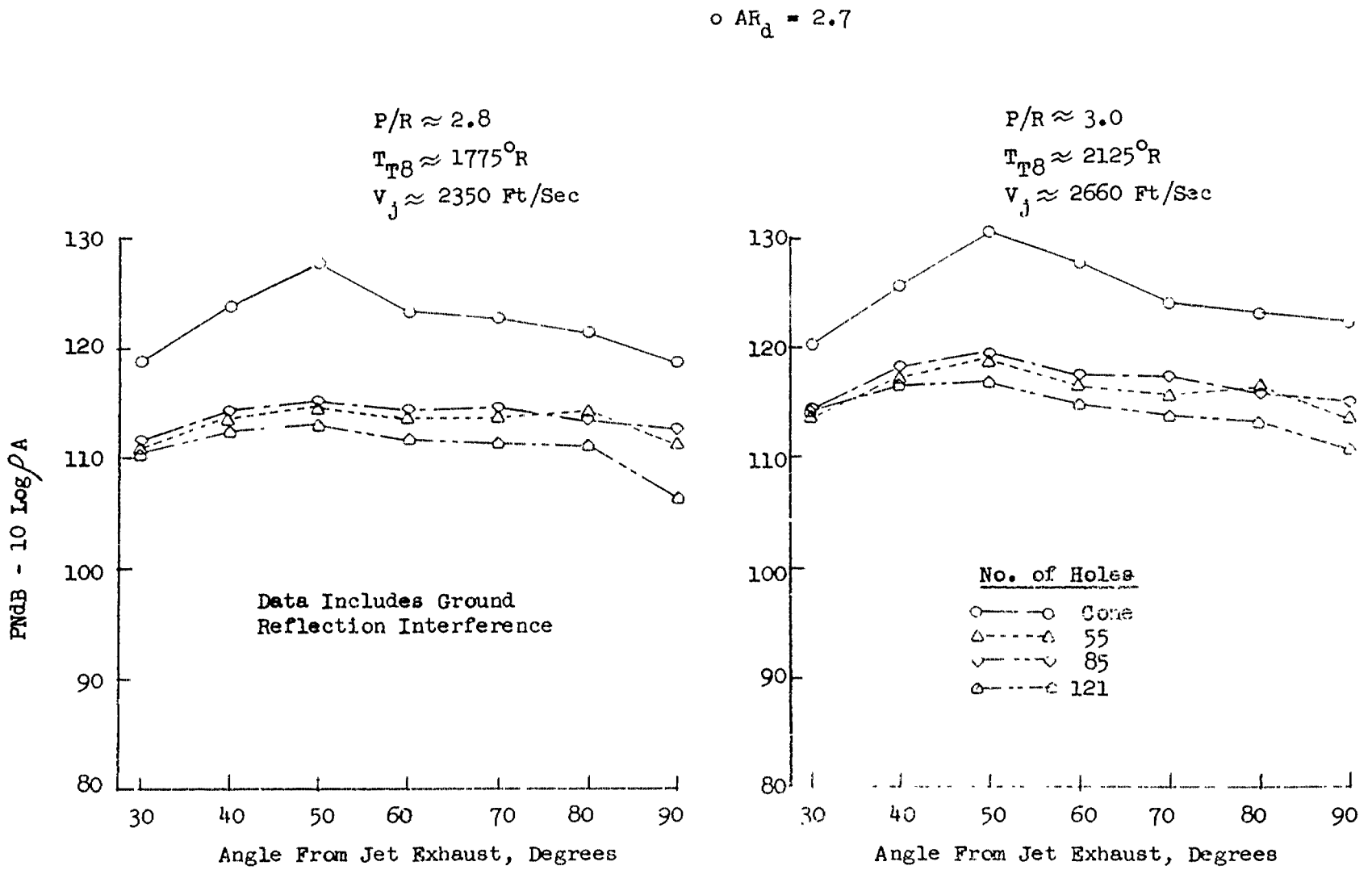

FIGURE V.F.9-38B EFFECT OF HOLE NUMBER ON 1500 FT. SIDELINE DIRECTIVITY WITH 55, 85 AND 121 HOLE NOZZLES

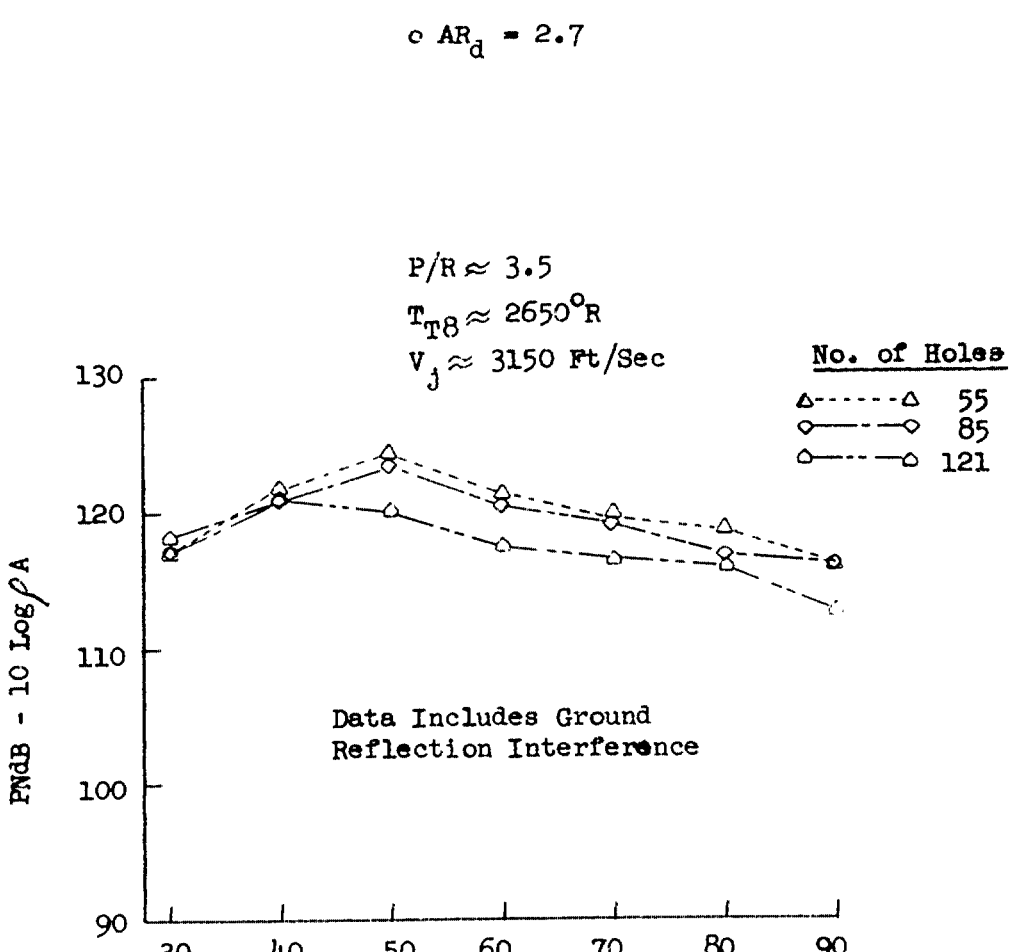

FIGURE V.F.9-38C EFFECT OF HOLE NUMBER ON 1500 FT. SIDELINE DIRECTIVITY WITH 55, 85 AND 121 HOLE NOZZLES

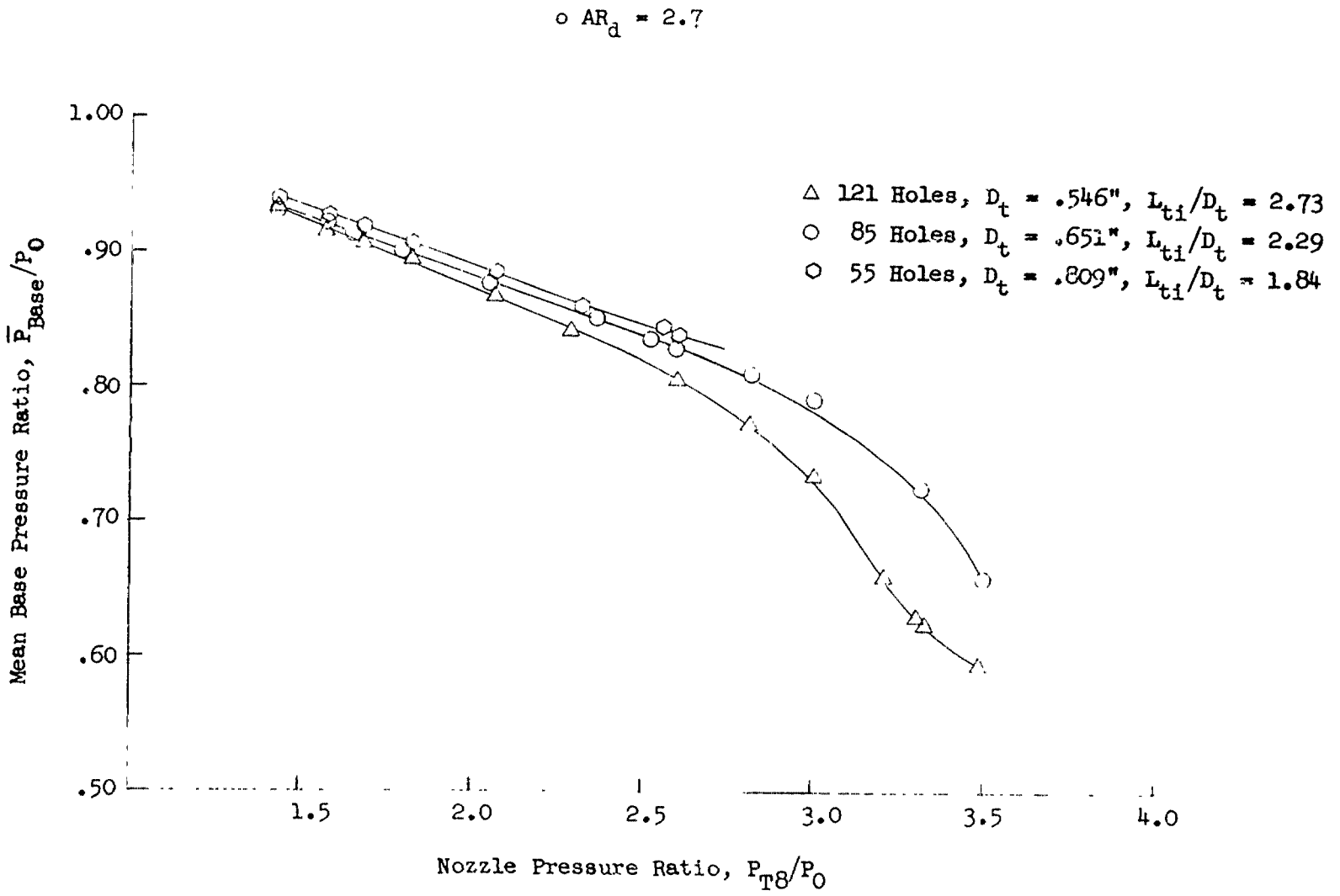

FIGURE V.F.9-39 EFFECT OF HOLE NUMBER ON MEAN BASEPLATE PRESSURE RATIO

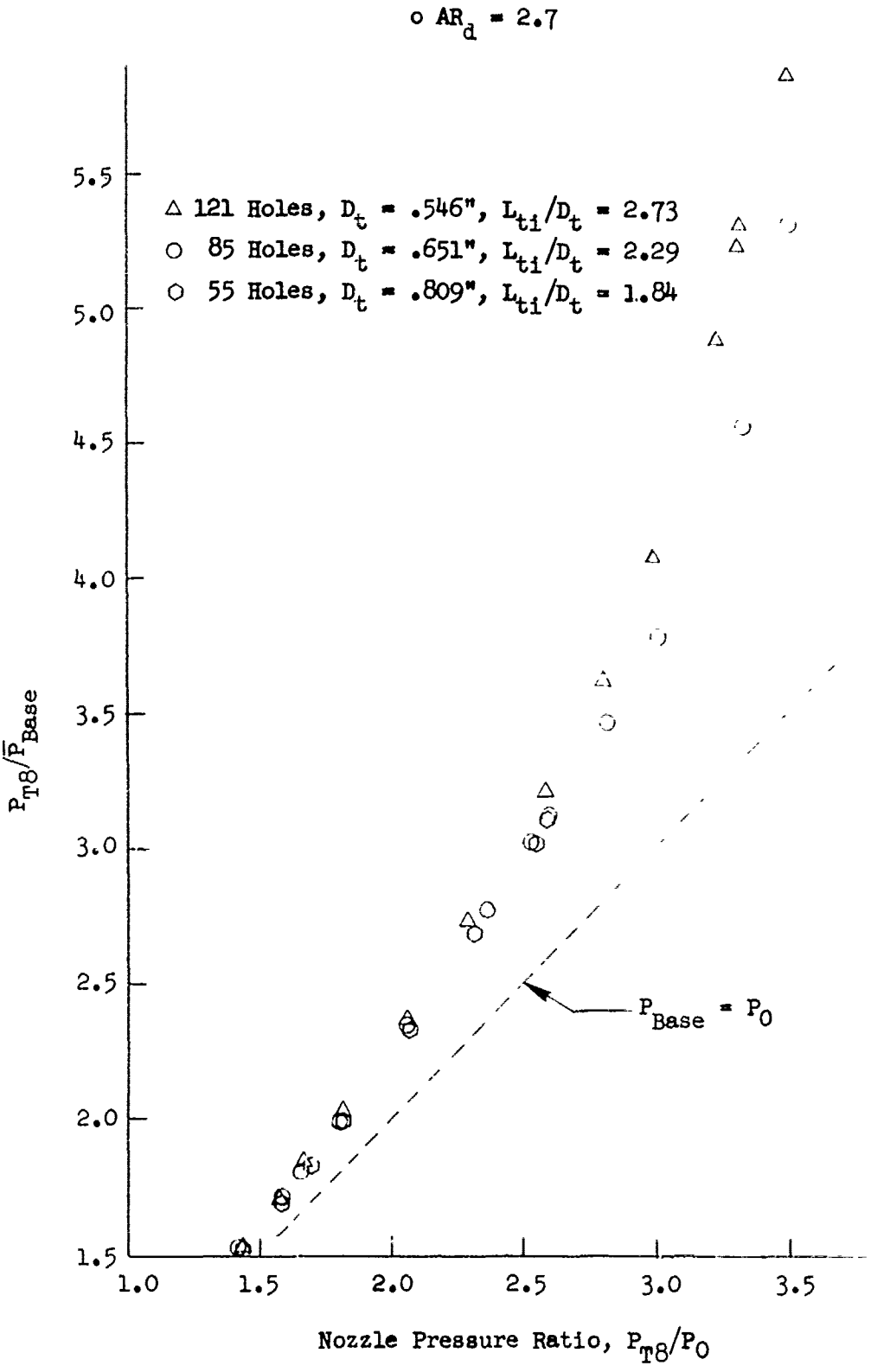

FIGURE V.F.9-40 EFFECT OF HOLE NUMBER ON NOZZLE EXIT TO MEAN BASEPLATE PRESSURE RATIO

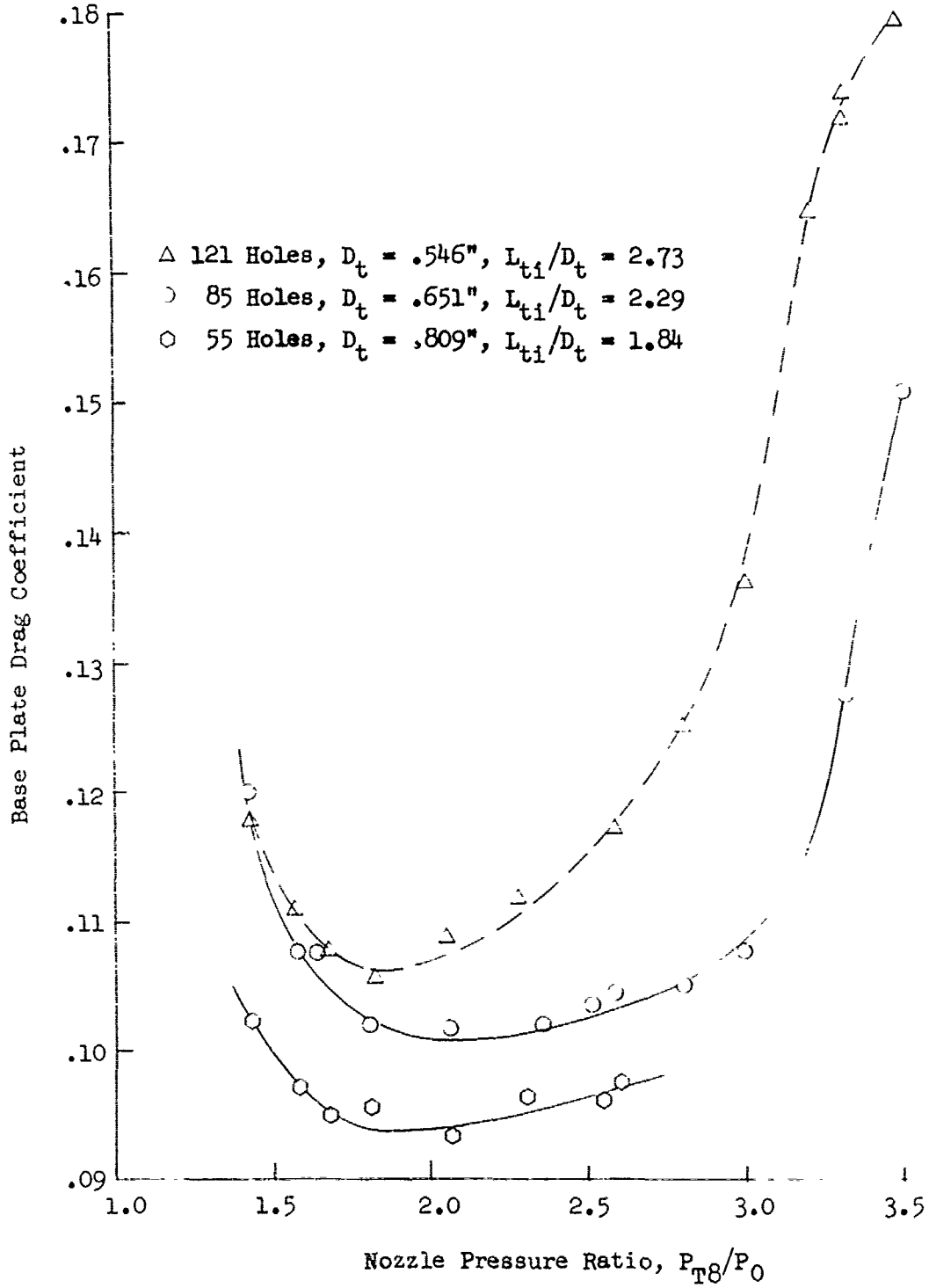

FIGURE V.F.9-41 EFFECT OF HOLE NUMBER ON BASEPLATE DRAG COEFFICIENT

D_S/D_{Td} = 1.05

X_S = 1.73"

(Model No. 6.0H85-2.7-CS1-1)

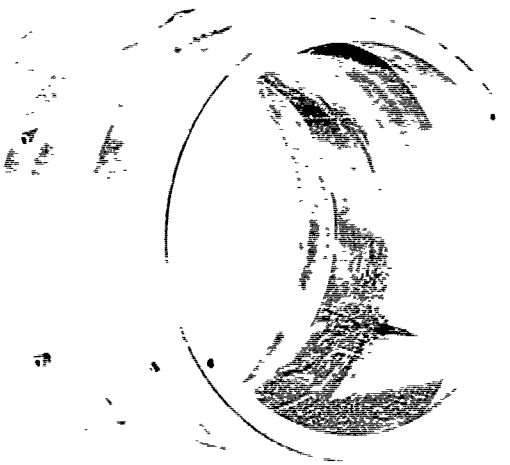

D_S/D_{Td} = 1.10

X_S = 1.73"

(Model No. 6.0H85-2.7-CS2-1)

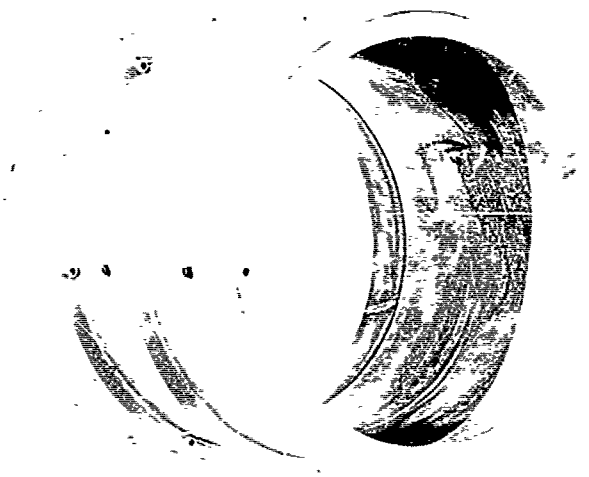

D_S/D_{Td} = 1.15

X_S = 1.73"

(Model No. 6.0H85-2.7-CS3)

FIGURE V.F.9-42 SECONDARY SHROUD HARDWARE USED WITH AN 85 HOLE NOZZLE FOR PARAMETRIC INVESTIGATION OF D_S/D_{Td} RATIO

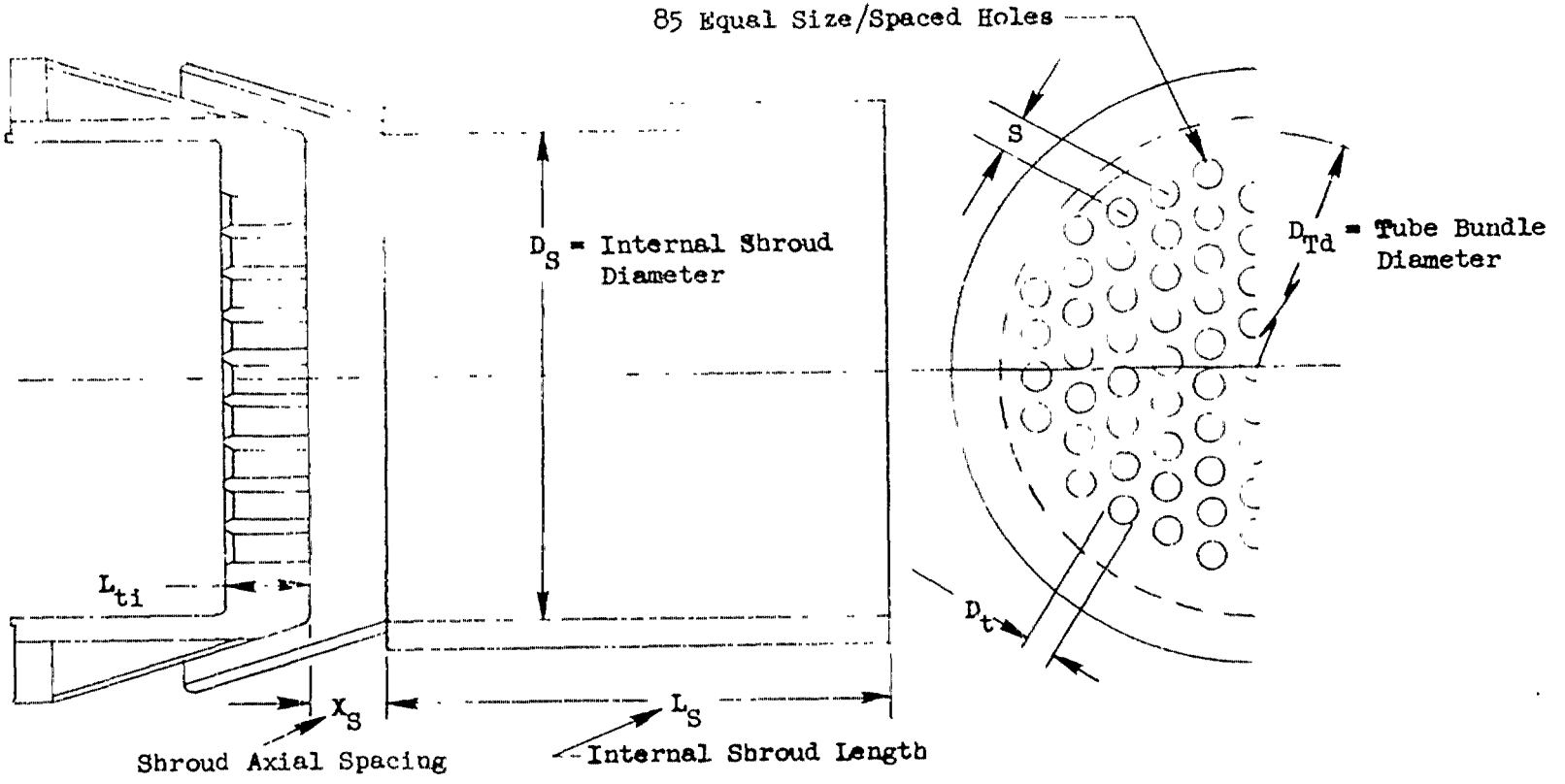

Model No.	Test Date	Primary						Secondary				
		No. Holes	Area Ratio	S	D_t	L_{ti}	L_{ti}/D_t	X_S	L_S	D_S	L_S/D_S	D_S/D_{Td}
6.0H85-2.7-CS1-1	5-05-69	85	2.7	.870"	.651"	1.49"	2.29	1.73"	10.352"	10.352"	1.0	1.05
6.0H85-2.7-CS2-1	5-05-69	85	2.7	.870"	.651"	1.49"	2.29	1.73"	10.845"	10.845"	1.0	1.10
6.0H85-2.7-CS3	3-31-69	85	2.7	.870"	.651"	1.49"	2.29	1.73"	11.338"	11.338"	1.0	1.15

FIGURE V.F.9-43 SCHEMATIC OF SHROUDED 85 HOLE NOZZLE FOR PARAMETRIC INVESTIGATION OF D_S/D_{Td} RATIO

TABLE V.F.9-12 TEST SUMMARY

MODEL NO. 6.0 H85-2.7-CS1-1

DESCRIPTION: 85 Hole Plate with Equally Spaced .651" ID Holes, AR_d = 2.7
X_s = 1.73, D_s/D_{Td} = 1.05

DATE: 5/5/69

SCALE MODEL A_s = .1965 ft^2

FULL SCALE A_s = 12.576 ft^2

SCALE FACTOR = 8:1

- o DATA INCLUDES GROUND REFLECTION INTERFERENCE
- o ANGLE REFERENCED TO JET EXHAUST

	TEST CONDITIONS				ACOUSTIC TEST RESULTS						
			IDEAL			320' ARC		300' SIDELINE		1500' SIDELINE	
RDG. No.	P_{T8}/P_o	T_{TS} (°R)	V_j (ft/sec)	W_8 (PPS)	10 log oA	PEAK PNdB	PEAK ANGLE	PEAK PNdB	PEAK ANGLE	PEAK PNdB	PEAK ANGLE
1	1.44	1149	1174	8.48	-3.1	114.7	60	113.8	60	96.5	60
2	1.61	1529	1538	7.89	-4.4	118.7	70	118.8	70	101.5	70
3	2.08	1240	1698	11.41	-3.3	122.2	60	121.7	70	104.3	70
4	1.81	1523	1700	8.93	-4.3	121.8	70	121.8	70	104.4	70
5	2.08	1513	1869	10.14	-4.1	123.9	60	123.9	70	105.7	70
6	2.36	1569	2045	11.47	-4.1	124.7	60	124.1	70	106.8	70
7	2.54	1645	2177	12.09	-4.1	124.8	60	123.9	60/70	106.6	70
8	2.66	2125	2500	10.62	-5.2	124.9	60	125.3	80	108.1	80
9	2.84	1746	2357	12.46	-4.1	123.9	70	124.1	80	106.8	80
10	3.05	2101	2662	12.19	-4.7	122.8	60	124.7	80	107.4	80
11	3.27	2202	2798	12.53	-4.7	125.0	70	125.0	70/80	107.9	70
12	3.39	2415	2969	12.50	-5.0	125.2	80	125.7	80	108.7	80
13	3.39	2600	3080	12.09	-5.3	125.7	80	126.3	80	109.2	80
14	3.56	2660	3169	12.67	-5.3	128.2	40	126.5	80	109.5	80

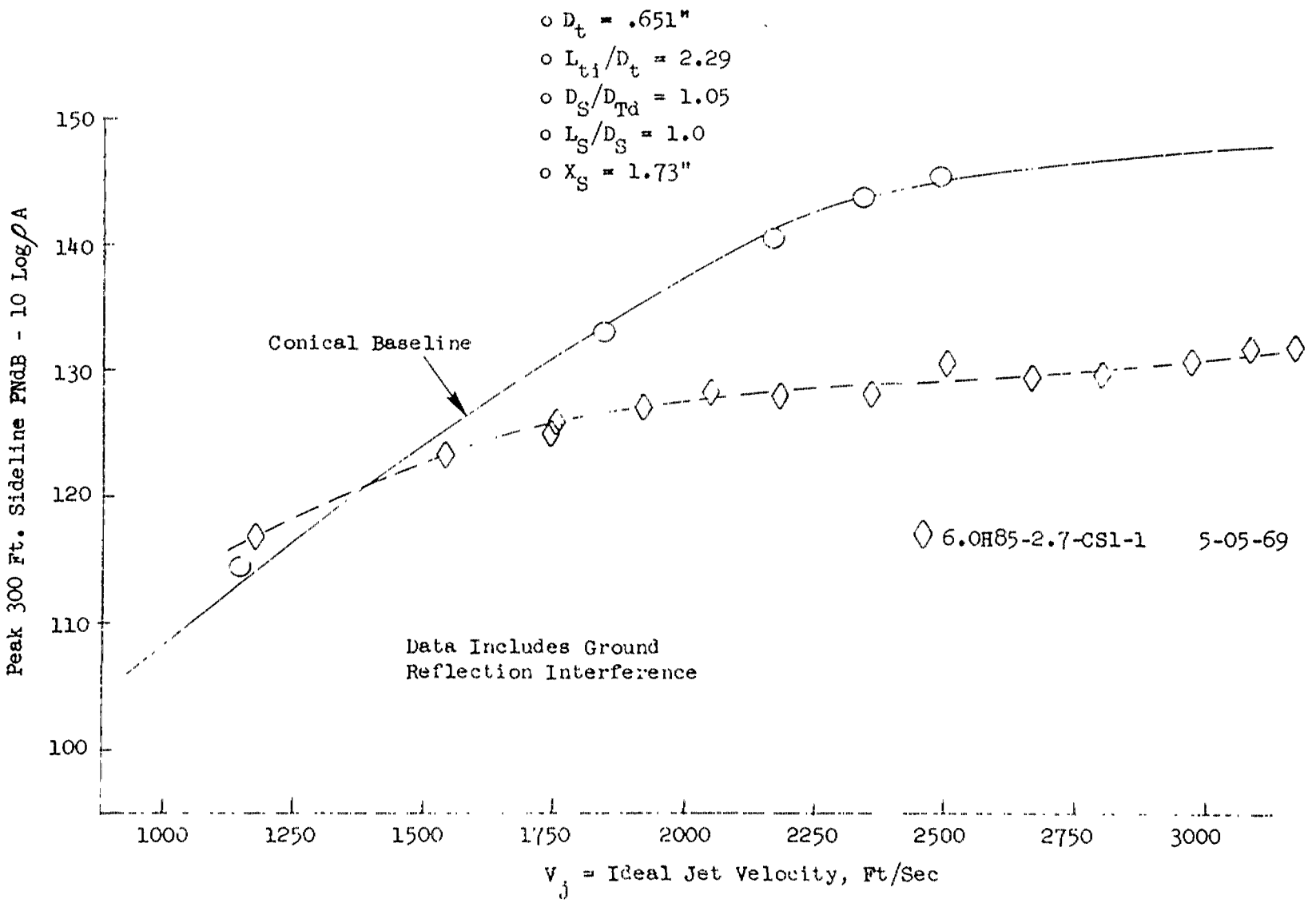

FIGURE V.F.9-44 300 FT. SIDELINE JET NOISE LEVELS FOR SHROUDED 85 HOLE NOZZLE, D_S/D_{Td} = 1.05

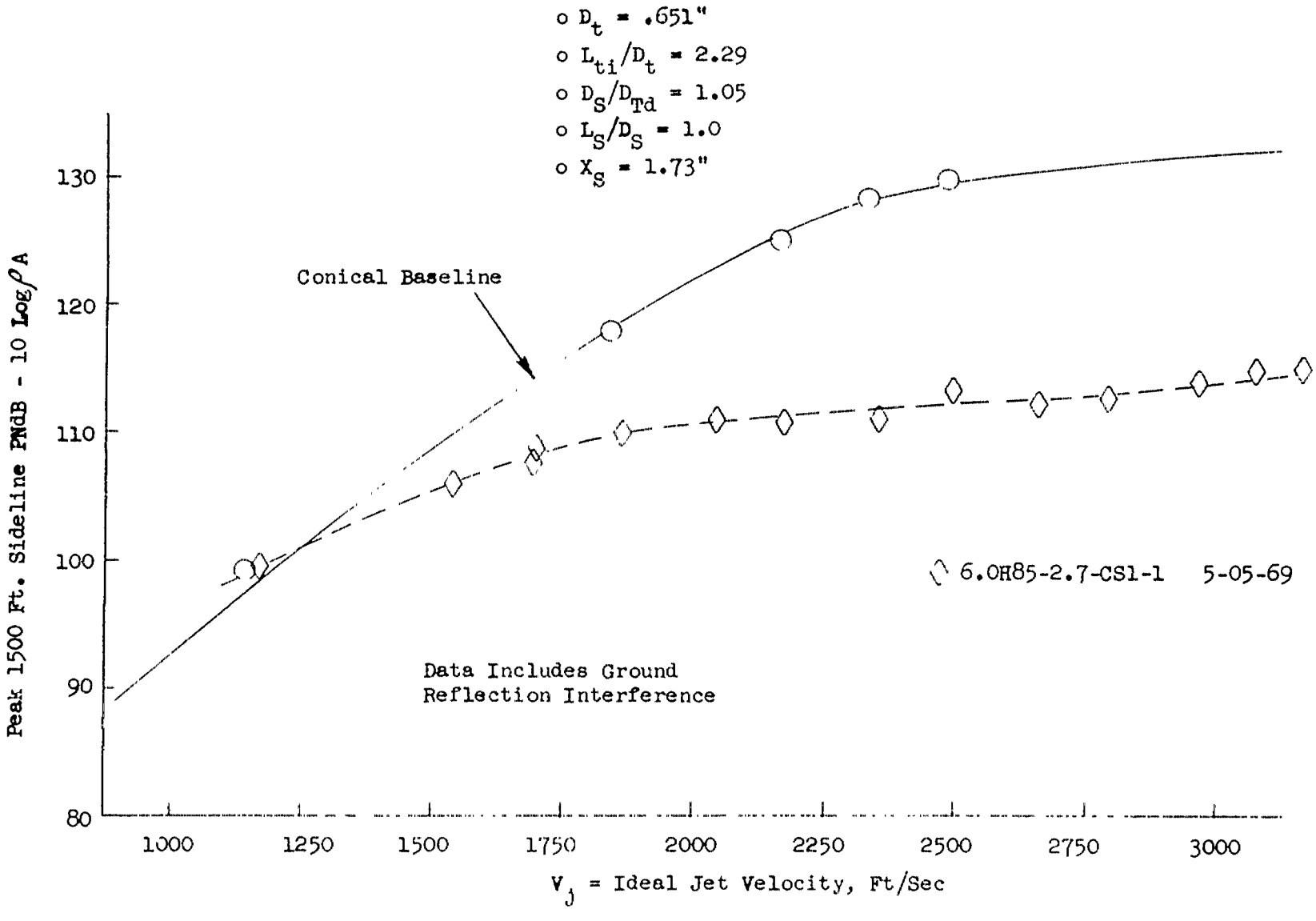

FIGURE V.F.9-45 1500 FT. SIDELINE JET NOISE LEVELS FOR SHROUDED 85 HOLE NOZZLE, D_S/D_{Td} = 1.05

TABLE V.F.9-13 TEST SUMMARY

MODEL NO. 6.0 H85-2.7-CS2-1

DESCRIPTION: 85 Hole Plate with Equally Spaced .651" I.D. AR_d = 2.7
X_s = 1.73, D_s/D_{Td} = 1.10

DATE: 5/5/69

SCALE MODEL A_8 = .1965 ft^2

FULL SCALE A_8 = 12.576 ft^2

SCALE FACTOR = 8:1

- o DATA INCLUDES GROUND REFLECTION INTERFERENCE
- o ANGLE REFERENCED TO JET EXHAUST

	TEST CONDITIONS				ACOUSTIC TEST RESULTS						
			IDEAL			320' ARC		800' SIDELINE		1500' SIDELINE	
RDG. No.	P_{T8}/P_0	T_{T8} (°R)	V_j (ft/sec)	W_8 (PPS)	10 log ΣA	PEAK PNdB	PEAK ANGLE	PEAK PNdB	PEAK ANGLE	PEAK PNdB	PEAK ANGLE
1	1.44	1147	1173	8.42	-3.1	114.0	60	113.1	60	95.9	80
2	1.60	1529	1529	7.89	-4.4	118.4	60	118.2	80	101.0	80
3	1.67	1239	1436	9.35	-3.5	118.5	80	119.0	80	101.7	80
4	1.82	1525	1710	8.99	-4.3	121.0	60	120.6	70	103.3	70
5	2.09	1500	1869	10.26	-4.1	122.8	60	122.8	70	105.4	70
6	2.36	1573	2049	11.37	-4.1	123.9	60	124.2	80	106.9	80
7	2.55	1649	2182	12.05	-4.1	124.7	60	124.3	70/80	107.2	70
8	2.60	2128	2500	11.23	-5.2	125.5	70/80	126.1	80	109.0	80
9	2.81	1788	2374	12.71	-4.2	125.1	70	125.1	70	108.0	70
10	3.02	2100	2650	12.29	-4.7	125.5	60	125.2	80	108.1	80
11	3.23	2224	2800	12.90	-4.8	127.3	70	127.3	70	110.1	70
12	3.33	2432	2959	12.80	-5.1	126.8	70	126.8	70	109.8	70
13	3.33	2593	3056	12.46	-5.4	127.8	70	127.8	70	110.8	70
14	3.50	2650	3144	12.85	-5.3	128.3	30/40	127.7	80	110.9	60

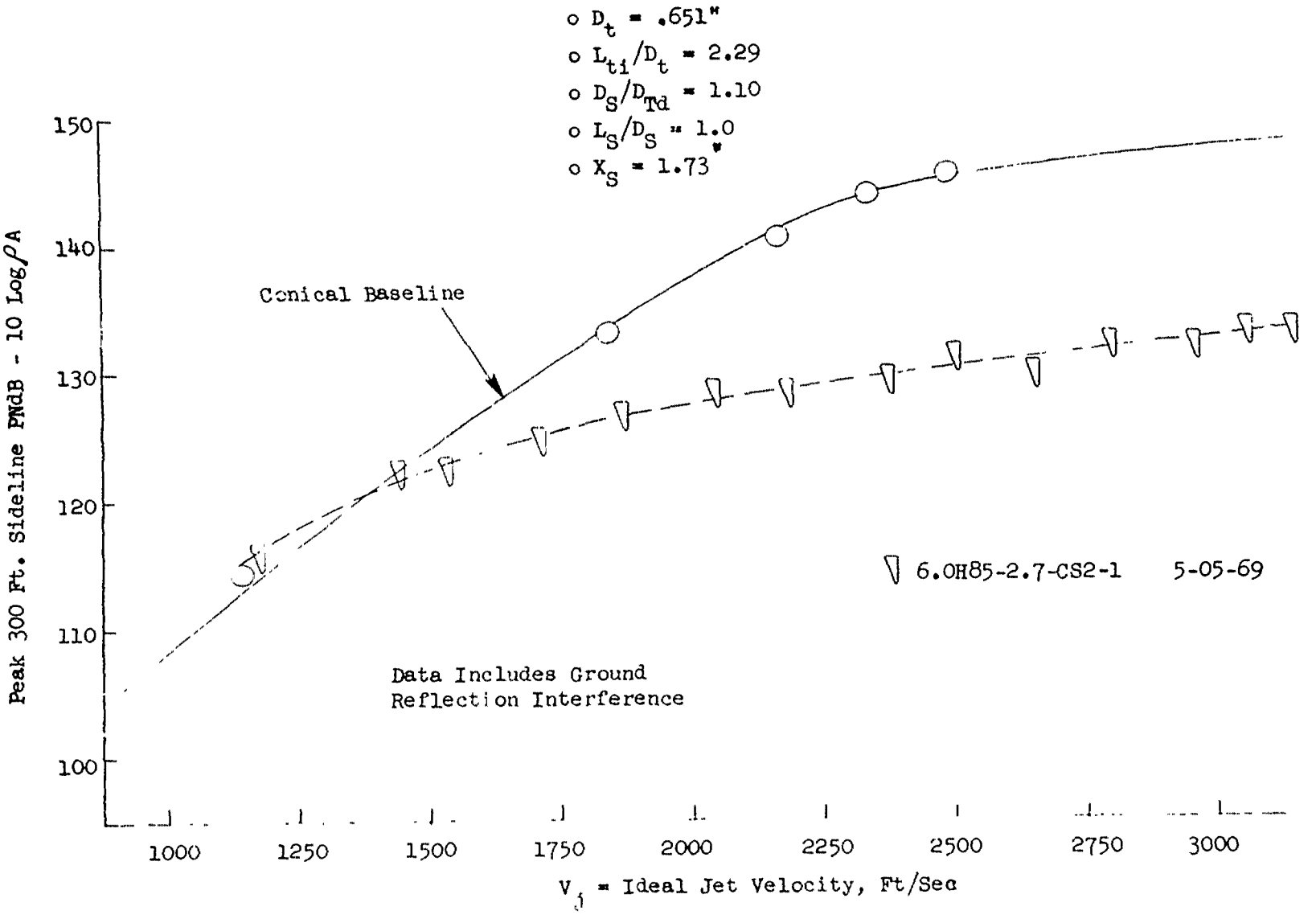

FIGURE V.F.9-46 300 FT. SIDELINE JET NOISE LEVELS FOR SHROUDED 85 HOLE NOZZLE, D_S/D_{Td} = 1.10

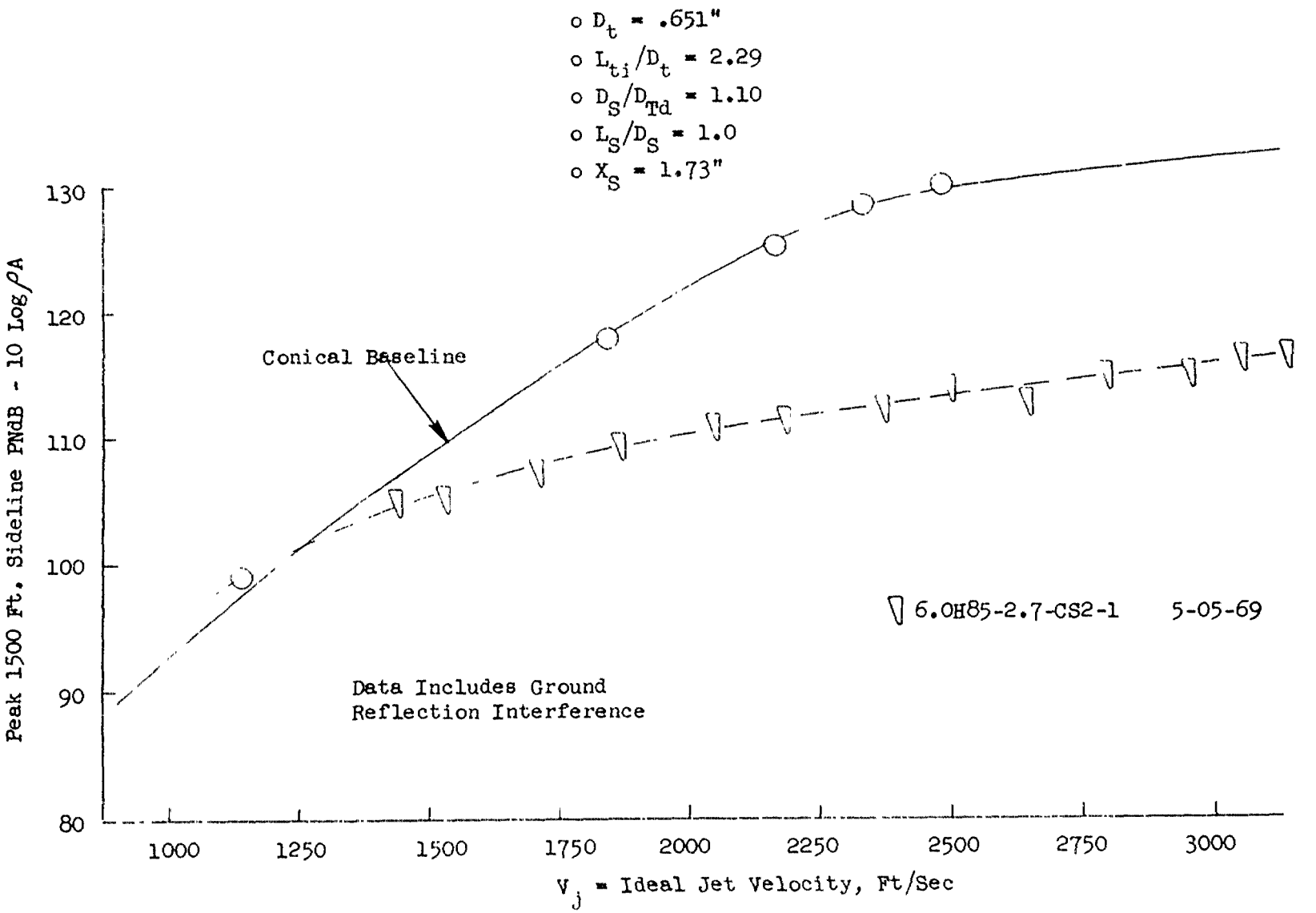

FIGURE V.F.9-47 1500 FT. SIDELINE JET NOISE LEVELS FOR SHROUDED 85 HOLE NOZZLE, D_S/D_{Td} = 1.10

TABLE V.F.9-14 TEST SUMMARY

MODEL NO. 6.0 H85-2.7-CS3

DESCRIPTION: 85 Hole Plate with Equally Spaced .651" ID Holes, AR_d = 2.7, X_s = 1.73, D_s/D_{Td} = 1.15

DATE: 3/31/69

SCALE MODEL A_8 = .1965 ft^2

FULL SCALE A_8 = 12.576 ft^2

SCALE FACTOR = 8:1

- o DATA INCLUDES GROUND REFLECTION INTERFERENCE
- o ANGLE REFERENCED TO JET EXHAUST

	TEST CONDITIONS				ACOUSTIC TEST RESULTS						
			IDEAL			320' ARC		300' SIDELINE		1500' SIDELINE	
RDG No.	P_{T8}/P_o	T_{T8} (°R)	V_j (ft/sec)	W_8 (PPS)	10 log ρA	PEAK PNdB	PEAK ANGLE	PEAK PNdB	PEAK ANGLE	PEAK PNdB	PEAK ANGLE
1	1.40	1141	1127	8.30	-3.2	118.0	50	116.7	60	99.0	60
2	1.56	1511	1485	8.10	-4.4	121.9	60	121.6	80	103.8	80
3	1.62	1247	1397	9.20	-3.5	121.5	60	121.0	80	103.3	80
4	1.78	1504	1672	9.28	-4.2	125.5	60	124.6	60	106.8	80
5	2.02	1516	1836	10.35	-4.1	127.5	60	126.6	60	108.8	60
6	2.22	1557	1970	11.54	-4.1	128.0	60	127.9	80	110.1	80
7	2.49	1628	2144	11.98	-4.0	129.3	50	127.9	80	110.3	70
8	2.54	2122	2472	10.75	-5.1	130.3	60	129.4	60/70	111.9	60/70
9	2.75	1762	2335	12.89	-4.1	129.6	50	128.4	70	110.8	70
10	2.96	2129	2647	12.61	-4.8	130.2	70	130.2	70	112.8	70
11	3.18	2193	2764	13.30	-4.7	130.0	60	129.9	80	112.4	80
12	3.27	2395	2917	13.13	-5.0	130.3	50	129.8	70	112.4	70
13	3.28	2581	3033	12.56	-5.3	131.3	60	130.4	60	113.1	60
14	3.49	2644	3137	13.02	-5.3	131.5	50	130.8	80	113.4	80

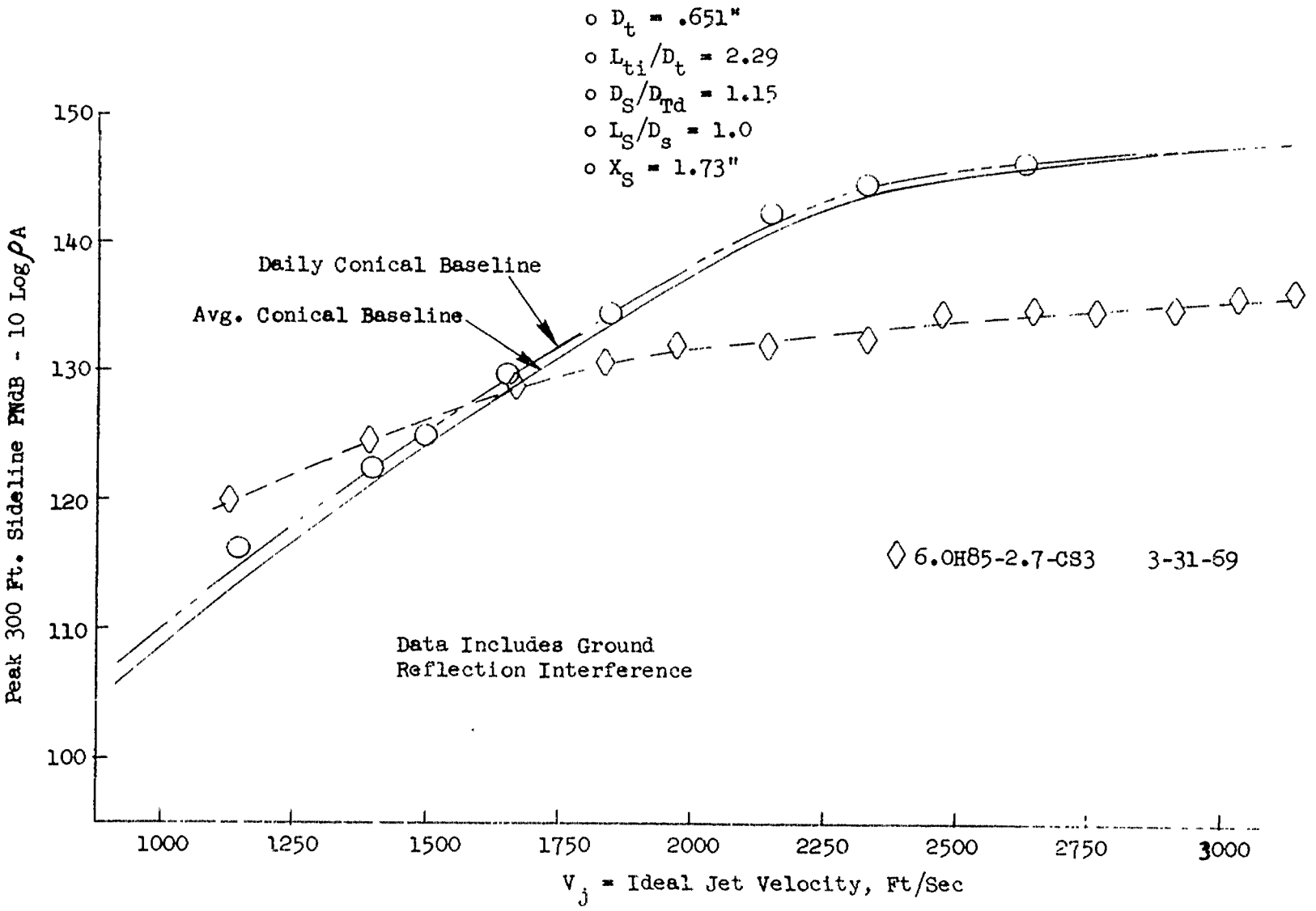

FIGURE V.F.9-48 300 FT. SIDELINE JET NOISE LEVELS FOR SHROUDED 85 HOLE NOZZLE, D_S/D_{Td} = 1.15

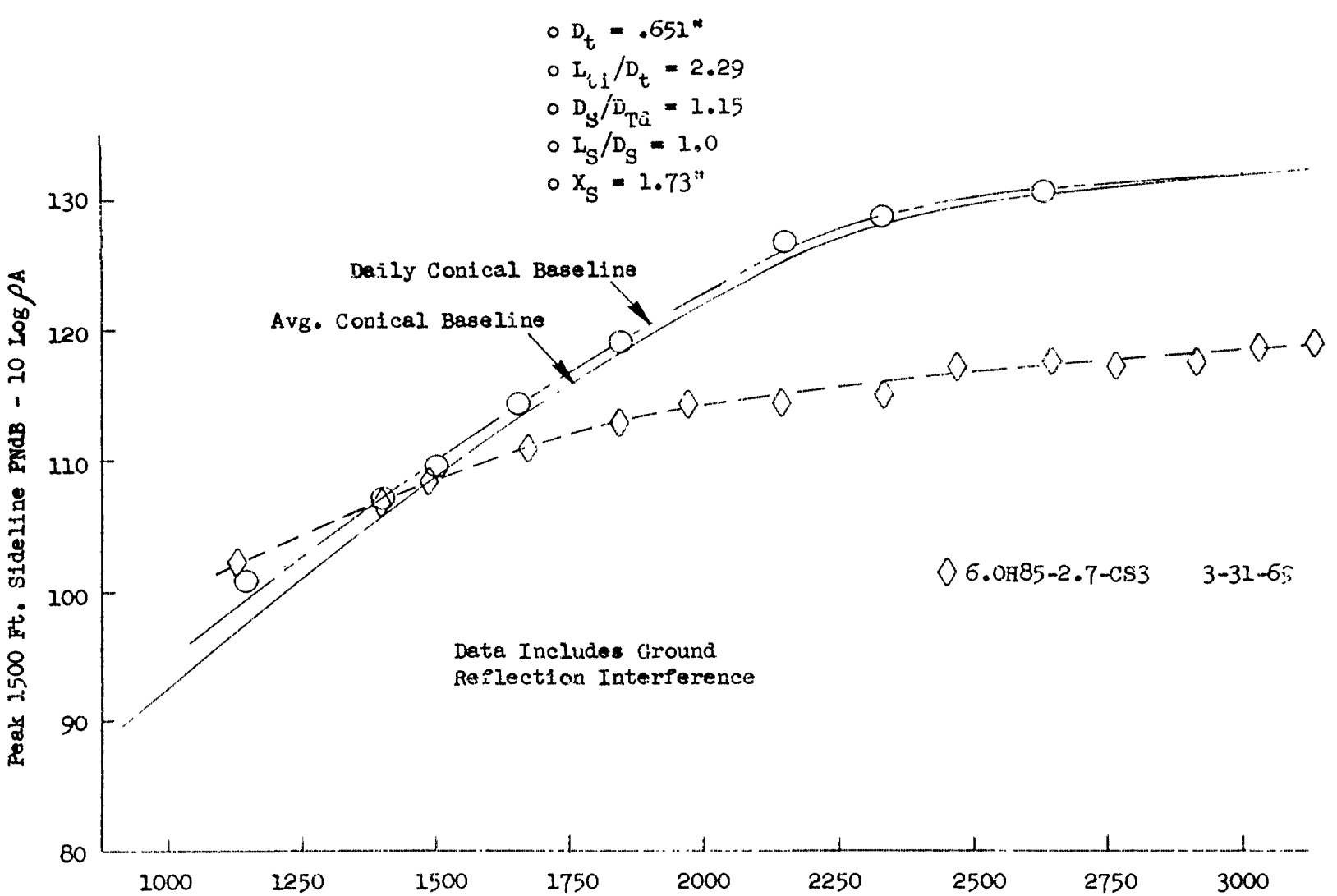

FIGURE V.F.9-49 1500 FT. SIDELINE JET NOISE LEVELS FOR SHROUDED 85 HOLE NOZZLE, D_S/D_{Td} = 1.15

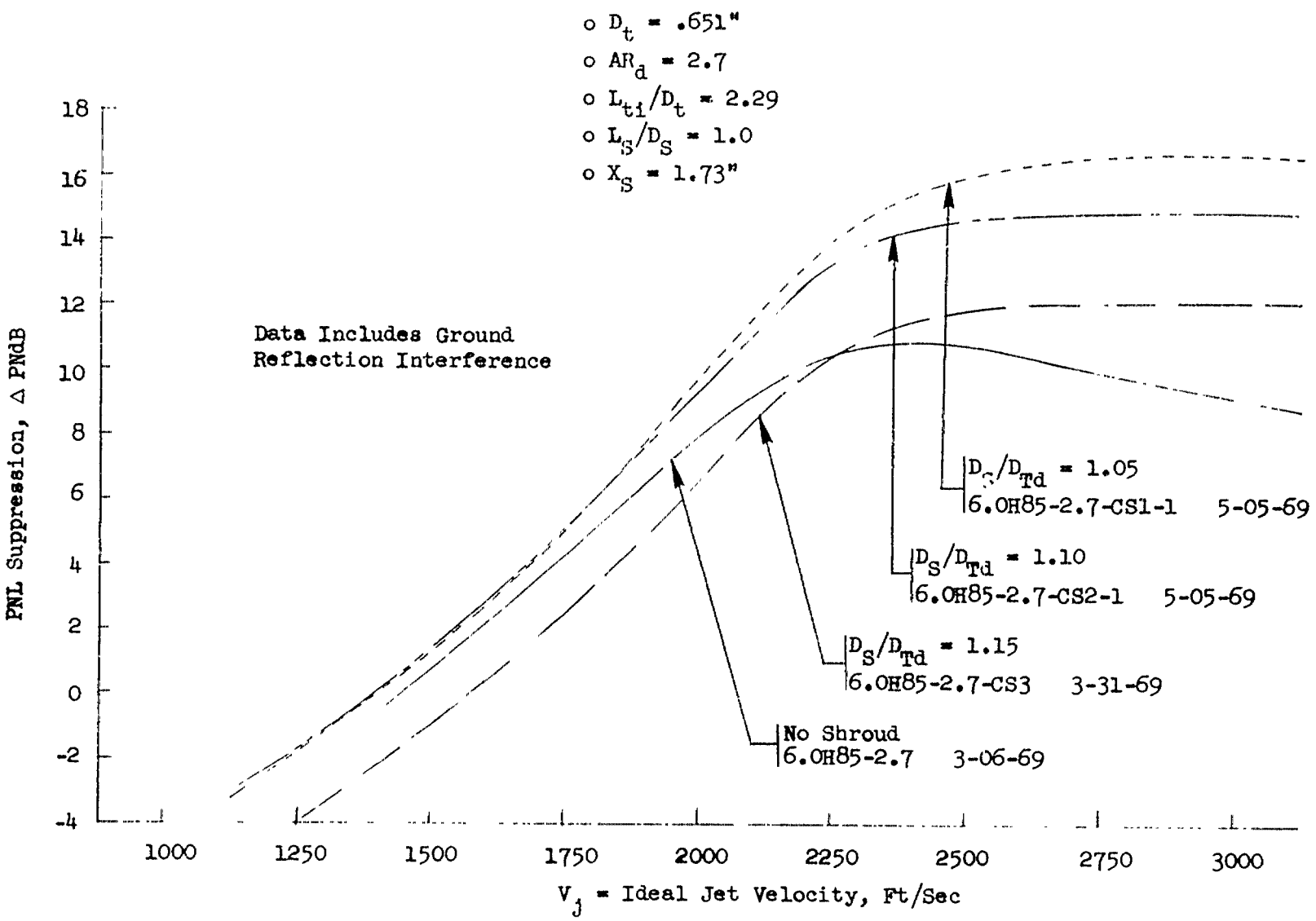

FIGURE V.F.9-50 EFFECT OF D_S/D_{Td} RATIO ON 300 FT. SIDELINE PNL SUPPRESSIONS FOR SHROUDED 85 HOLE NOZZLE

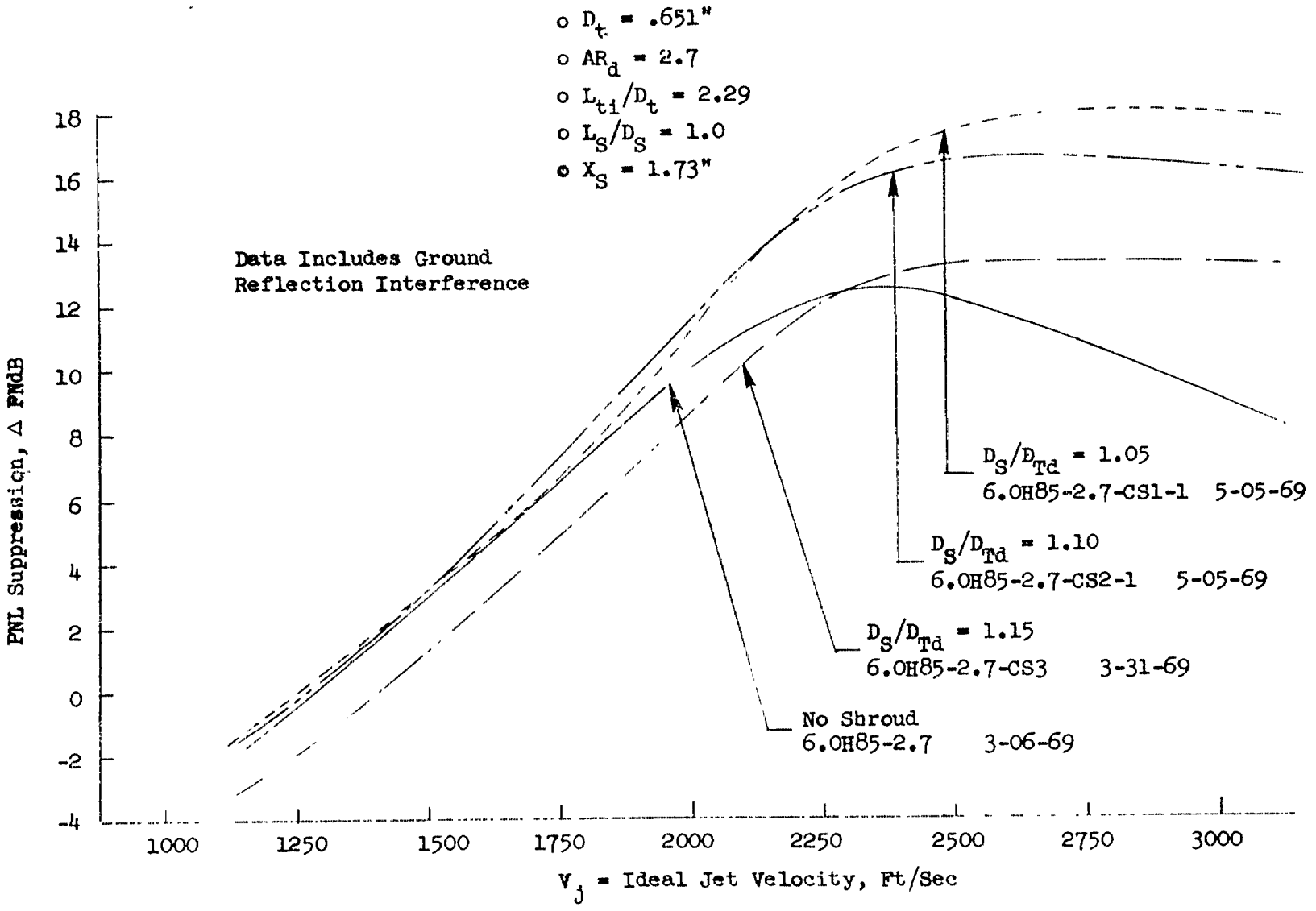

FIGURE V.F.9-51 EFFECT OF D_S/D_{Td} RATIO ON 1500 FT. SIDELINE PNL SUPPRESSIONS FOR SHROUDED 85 HOLE NOZZLE

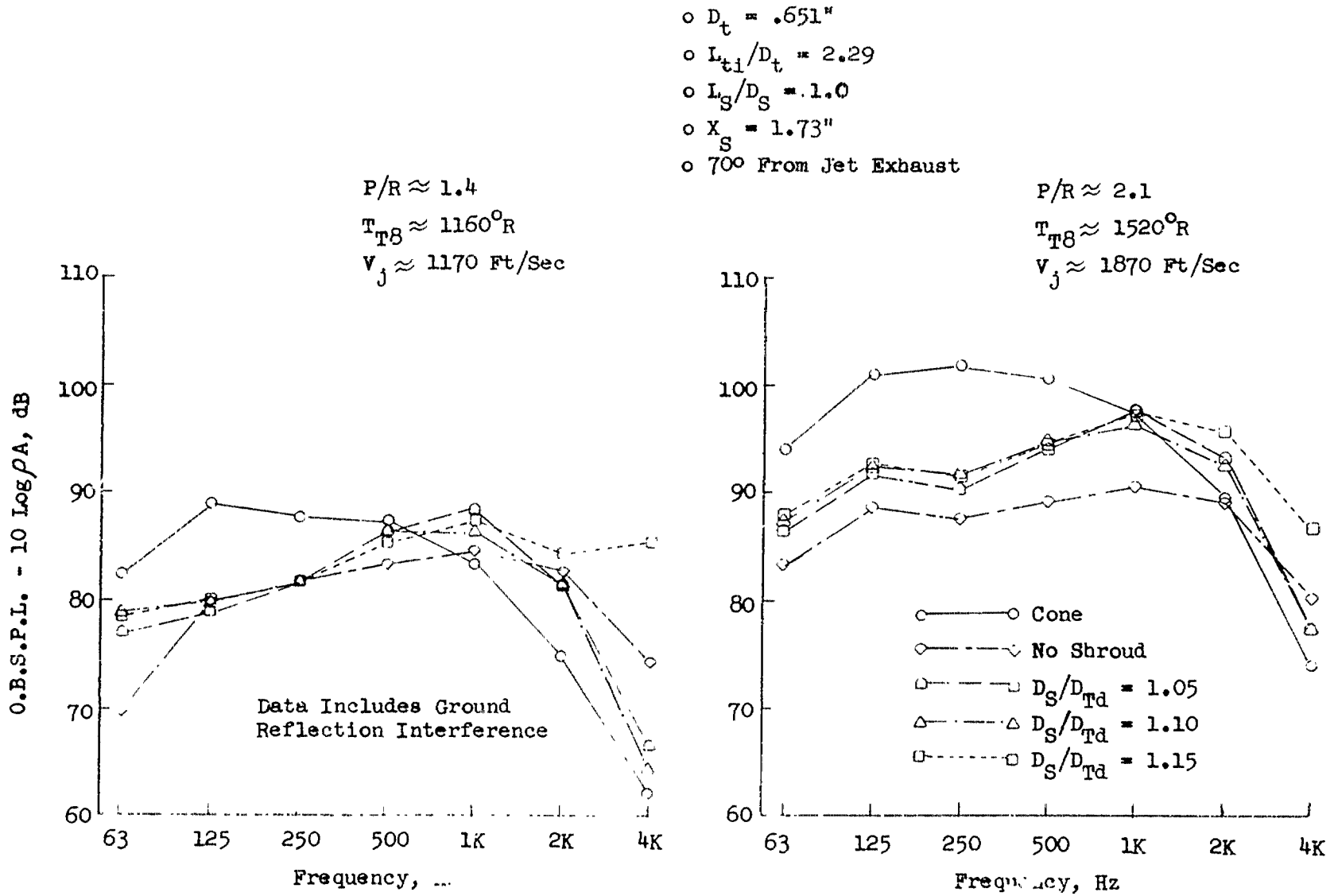

FIGURE V.F.9-52A EFFECT OF D_S/D_{Td} RATIO ON 1500 FT. SIDELINE SPECTRA FOR S .OUDED 85 HOLE NOZZLE

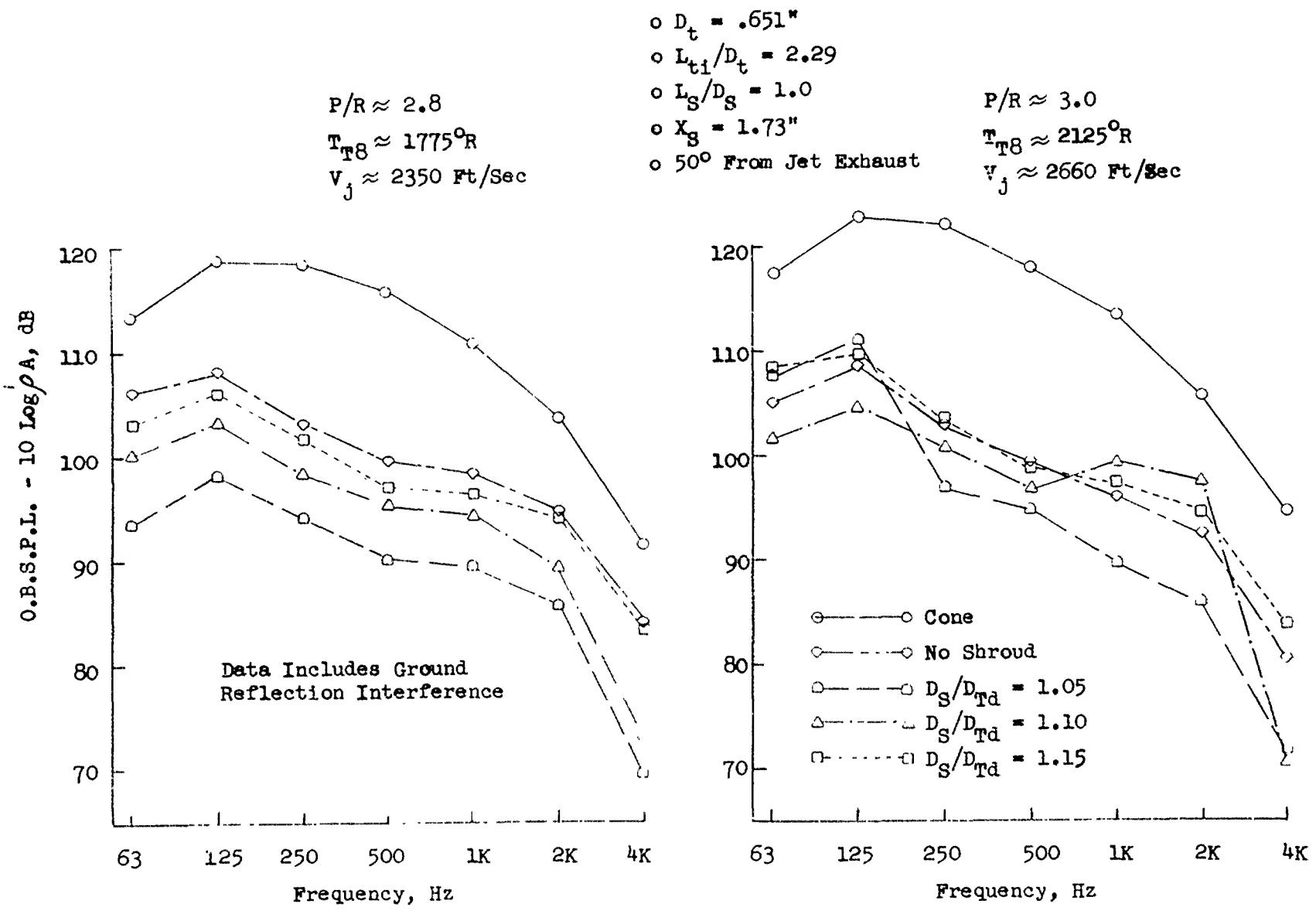

FIGURE V.F.9-52B EFFECT OF D_S/D_{Td} RATIO ON 1500 FT. SIDELINE SPECTRA FOR SHROUDED 85 HOLE NOZZLE

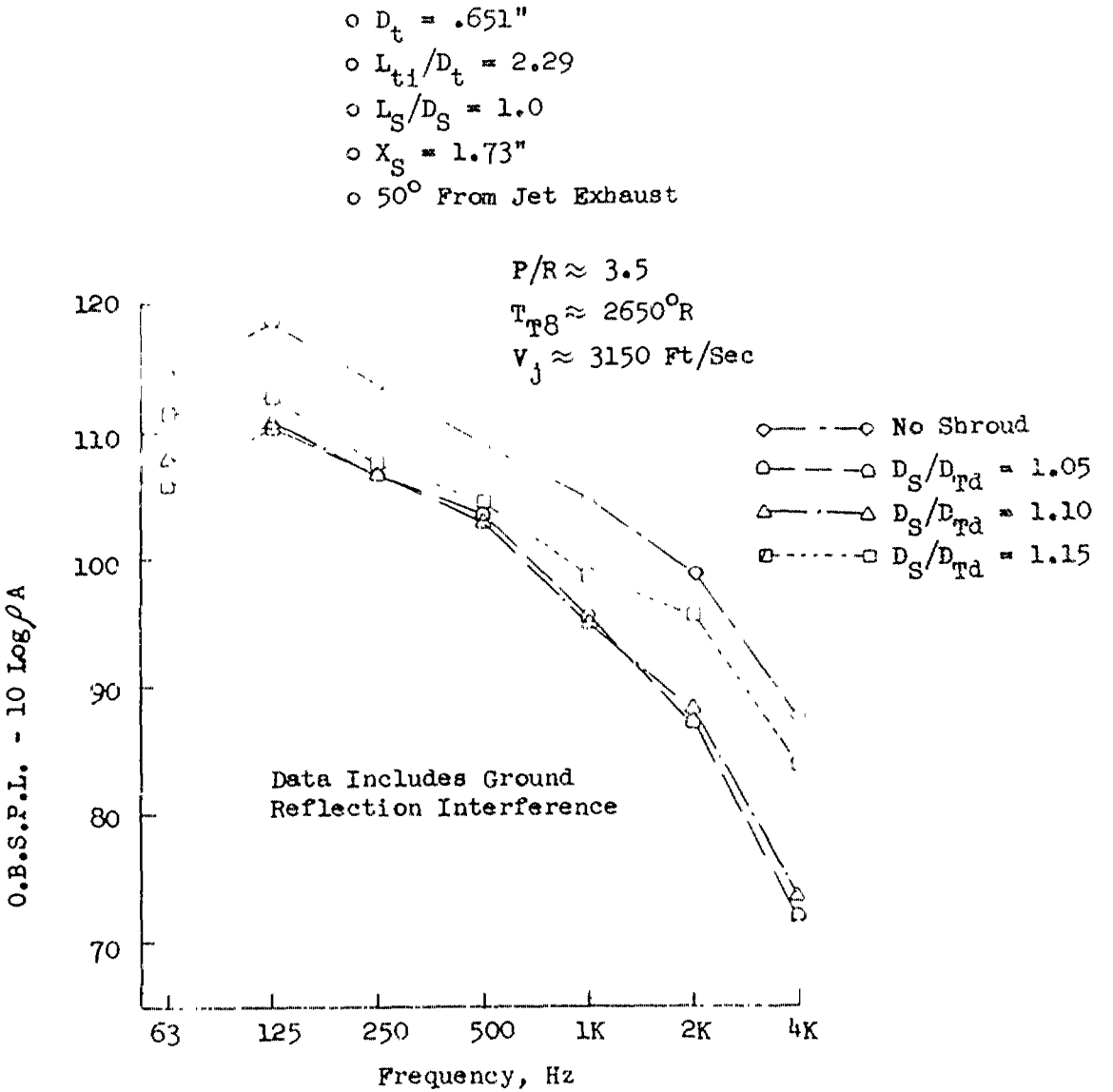

FIGURE V.F.9-52C EFFECT OF D_S/D_{Td} RATIO ON 1500 FT. SIDELINE SPECTRA FOR SHROUDED 85 HOLE NOZZLE

- D_t = .651"
- L_{ti}/D_t = 2.29
- L_S/D_S = 1.0
- X_S = 1.73"

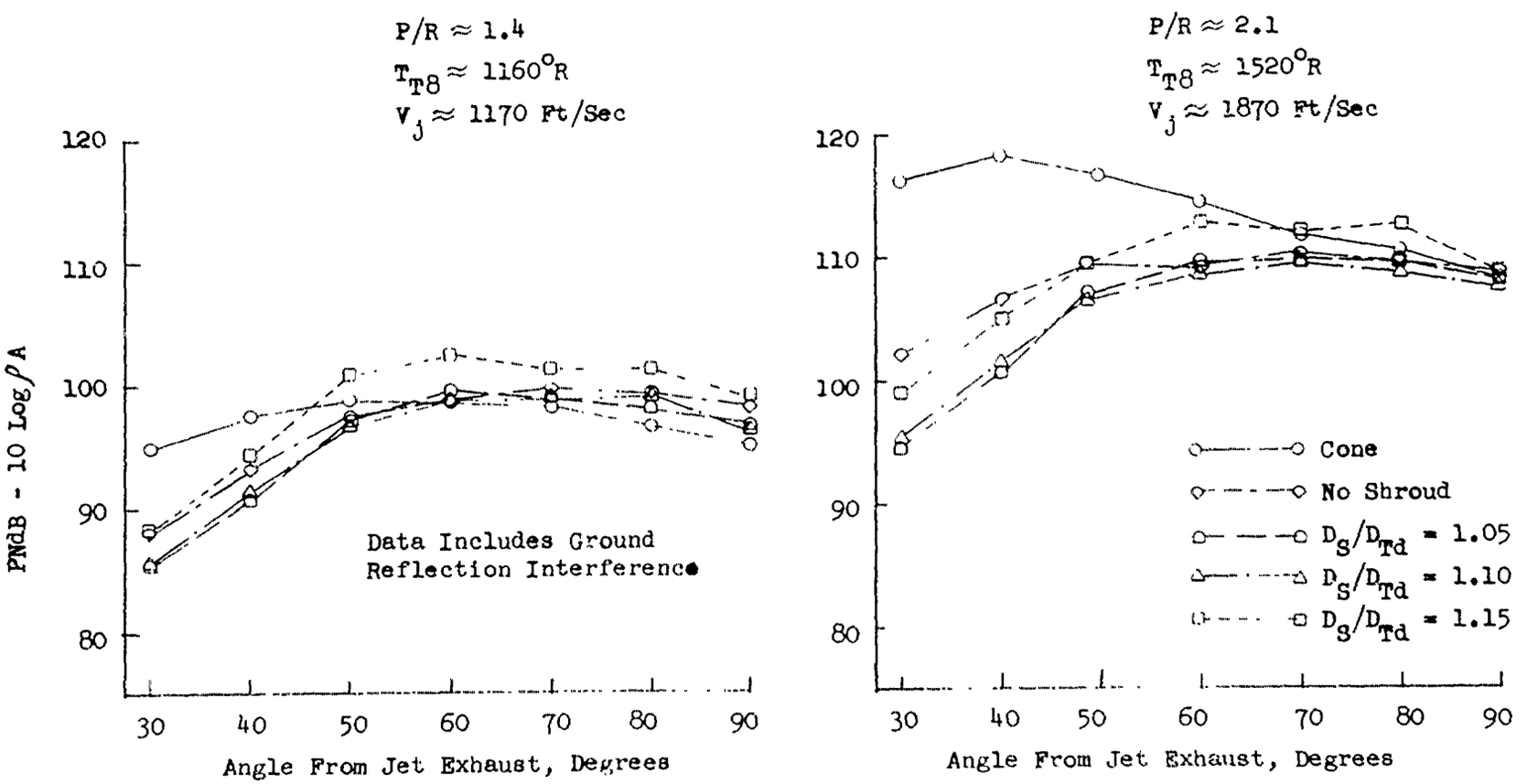

FIGURE V.F.9-53A EFFECT OF D_S/D_{Td} RATIO ON 1500 FT. SIDELINE DIRECTIVITY FOR SHROUDED 85 HOLE NOZZLE

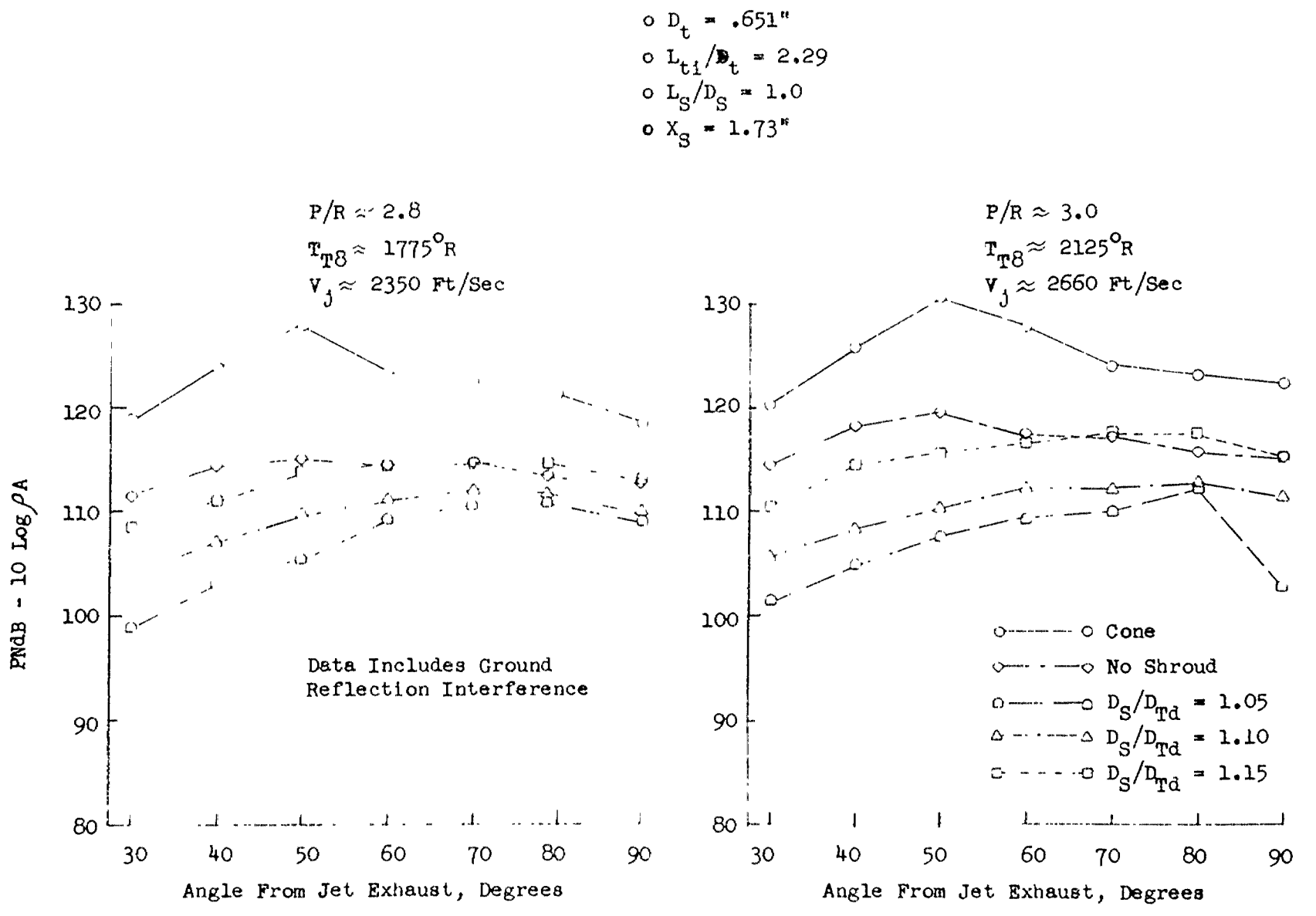

FIGURE V.F.9-53B EFFECT OF D_S/D_{Td} RATIO ON 1500 FT. SIDELINE DIRECTIVITY FOR SHROUDED 85 HOLE NOZZLE

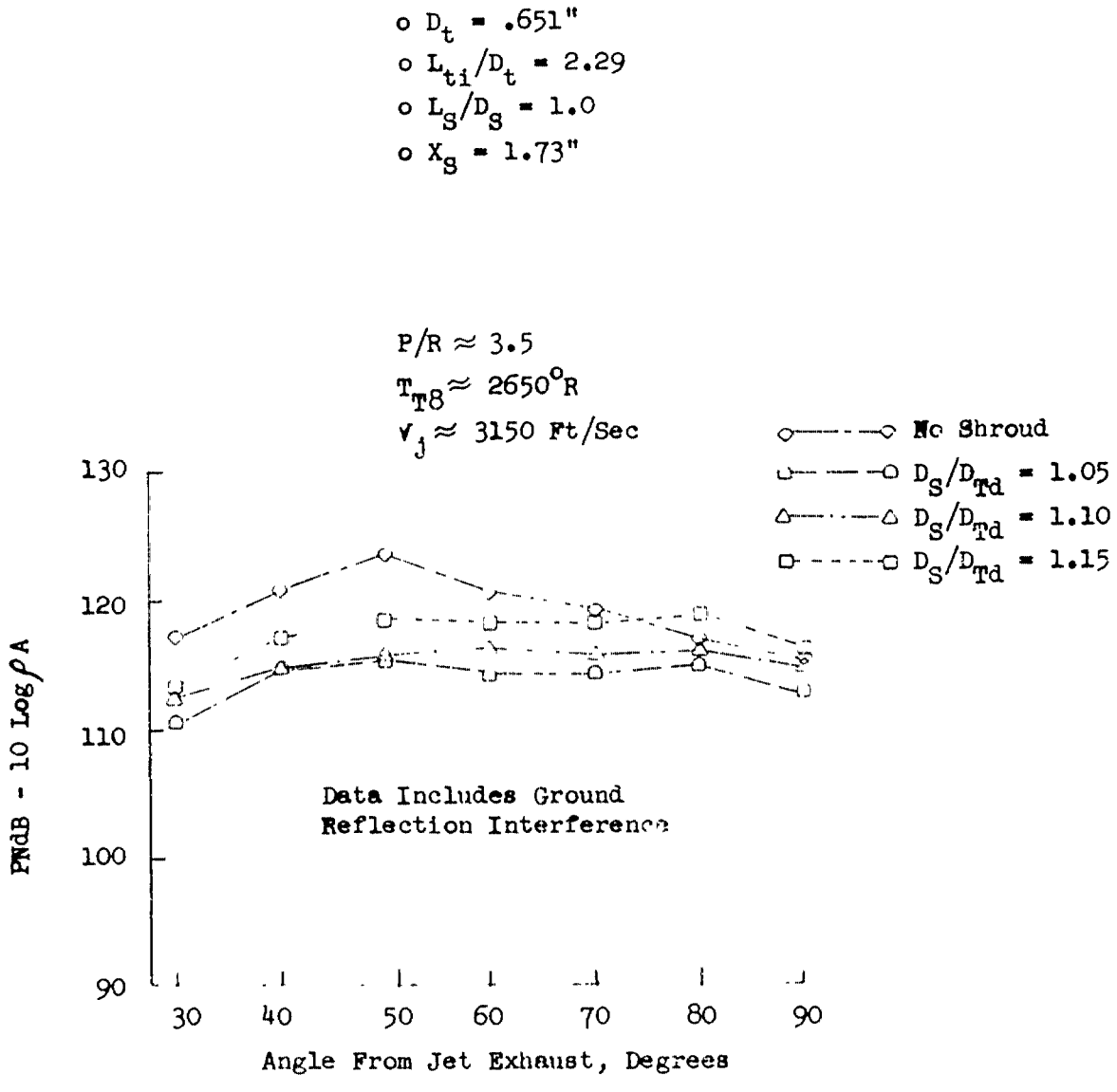

FIGURE V.F.9-53C EFFECT OF D_S/D_{Td} RATIO ON 1500 FT. SIDELINE DIRECTIVITY FOR SHROUDED 85 HOLE NOZZLE

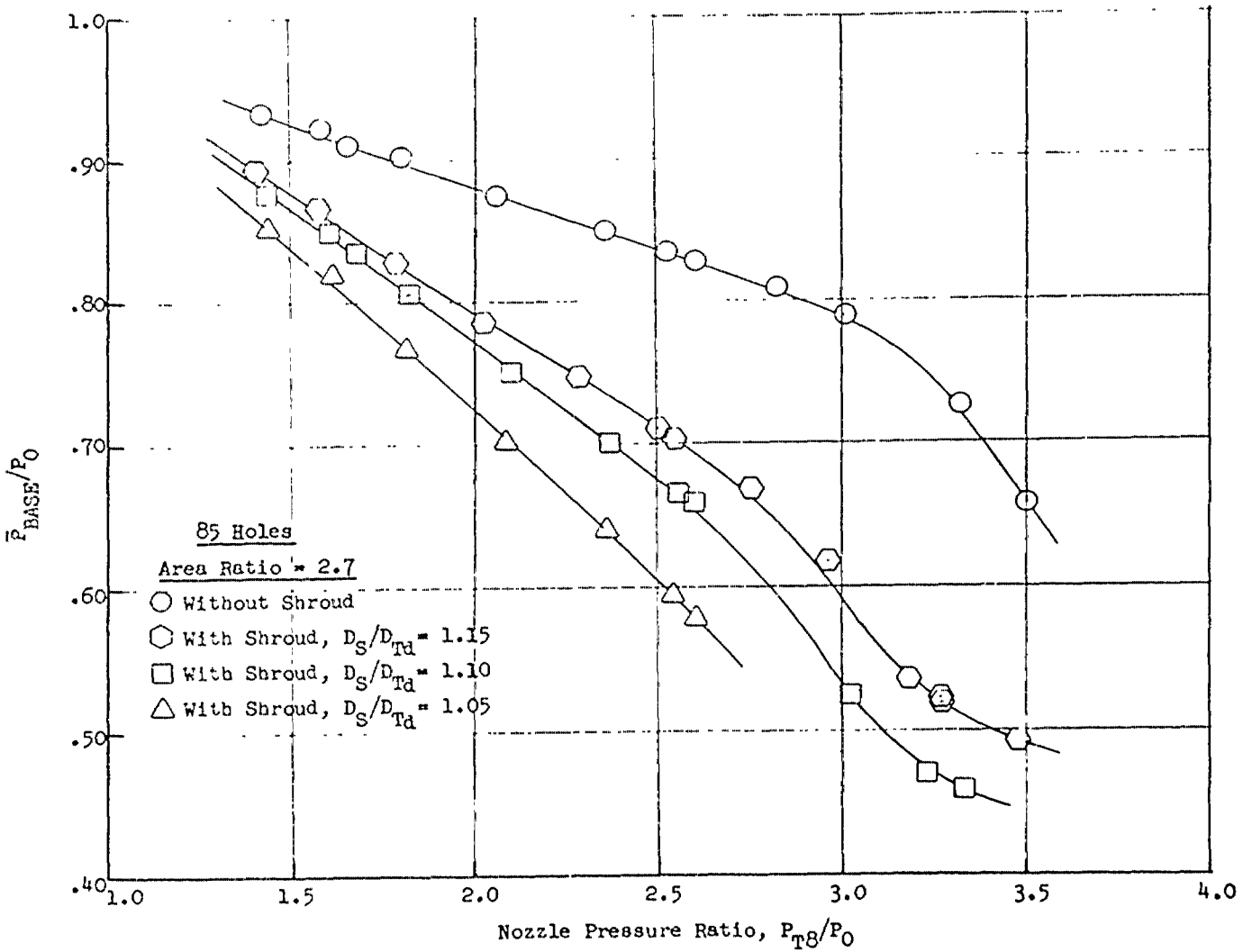

FIGURE V.F.9-54 EFFECT OF D_S/D_{Td} RATIO ON MEAN BASEPLATE PRESSURE RATIO

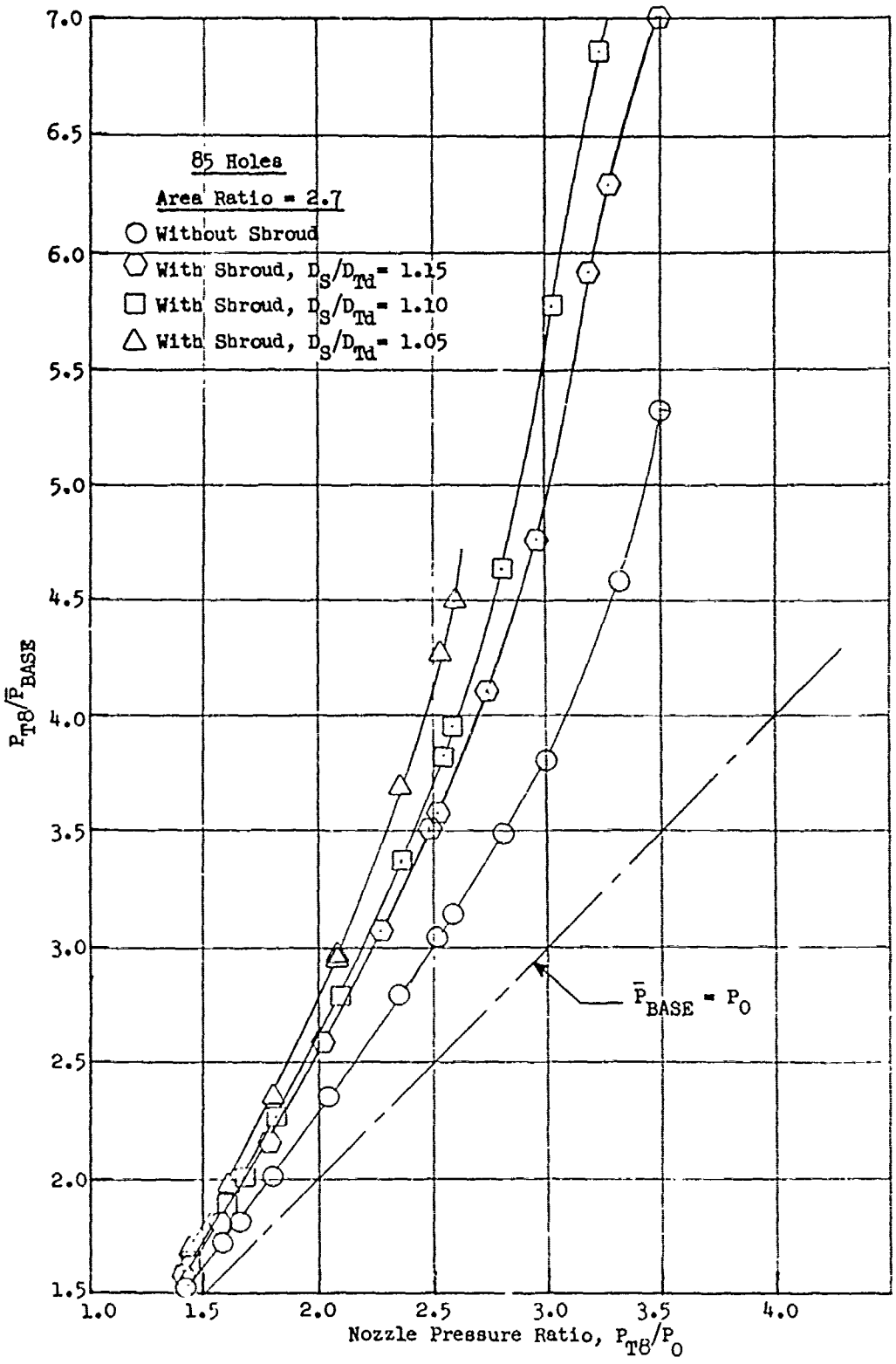

FIGURE V.F.9-55 EFFECT OF D_S/D_{Td} RATIO ON NOZZLE EXIT TO MEAN BASEPLATE PRESSURE RATIO

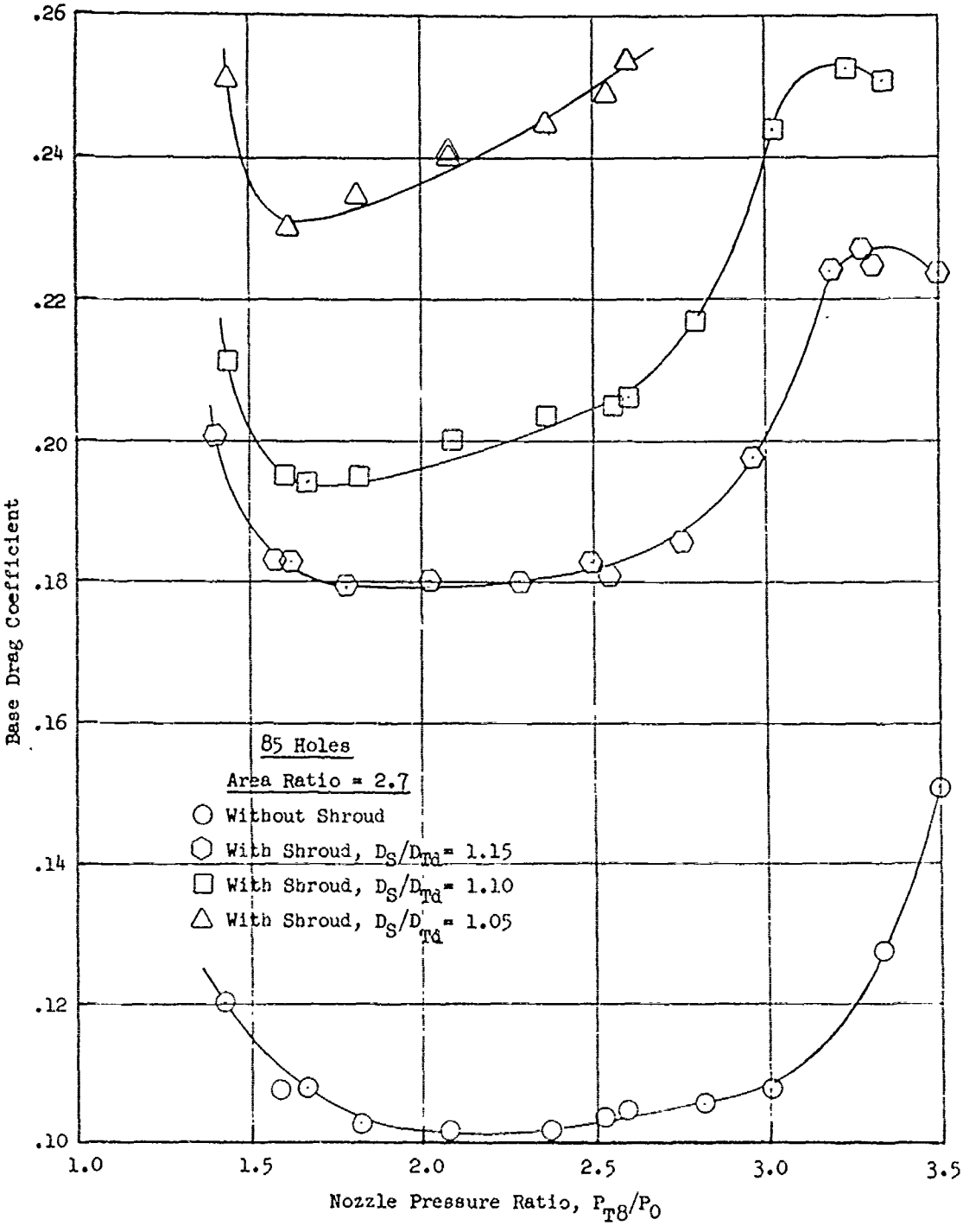

FIGURE V.F.9-56 EFFECT OF D_S/D_{Td} RATIO ON BASEPLATE DRAG COEFFICIENT

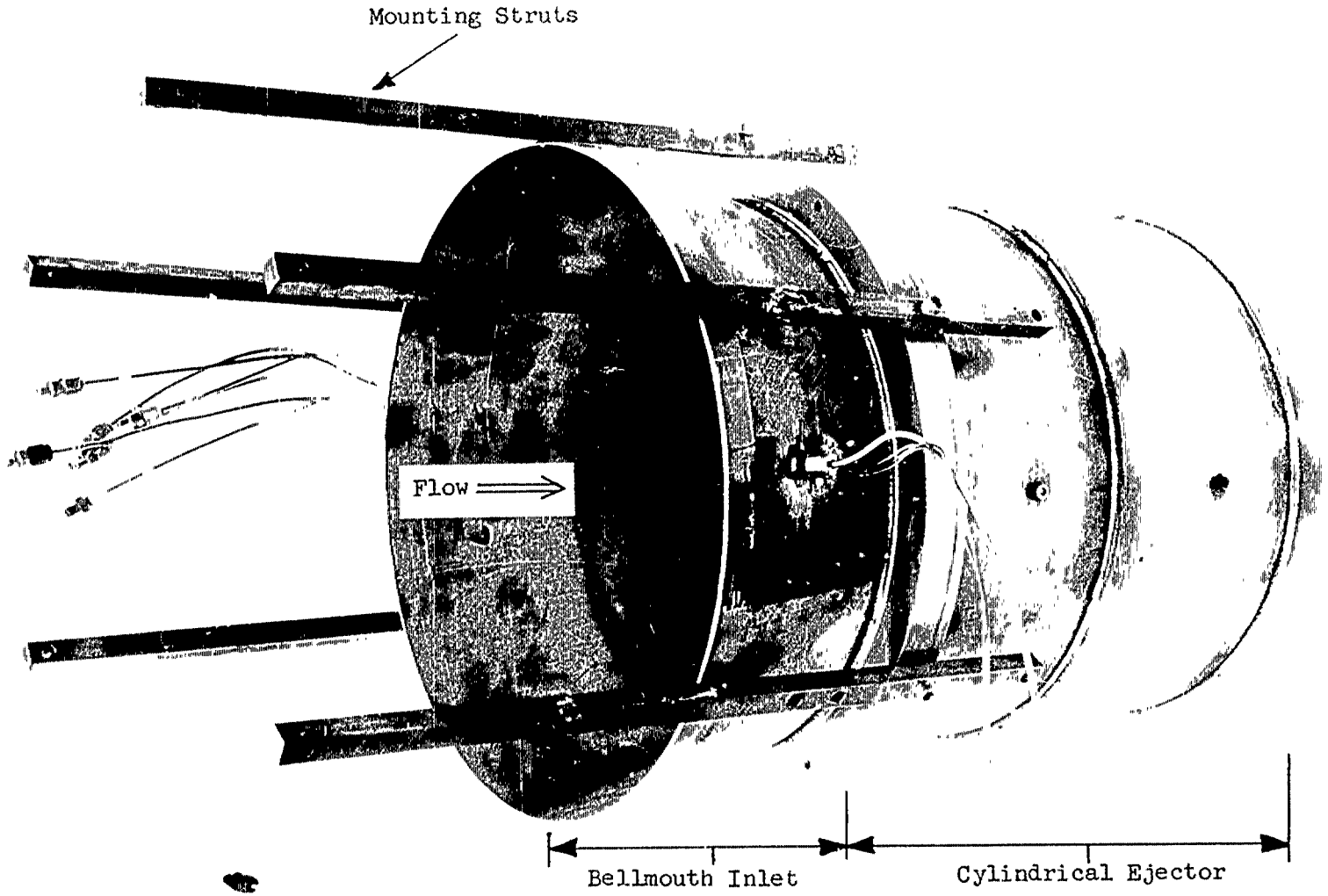

FIGURE V.F.9-57 SHROUD HARDWARE CONFIGURATION USED IN SHROUD AXIAL SPACING VARIATIONS WITH AN 85 HOLE NOZZLE

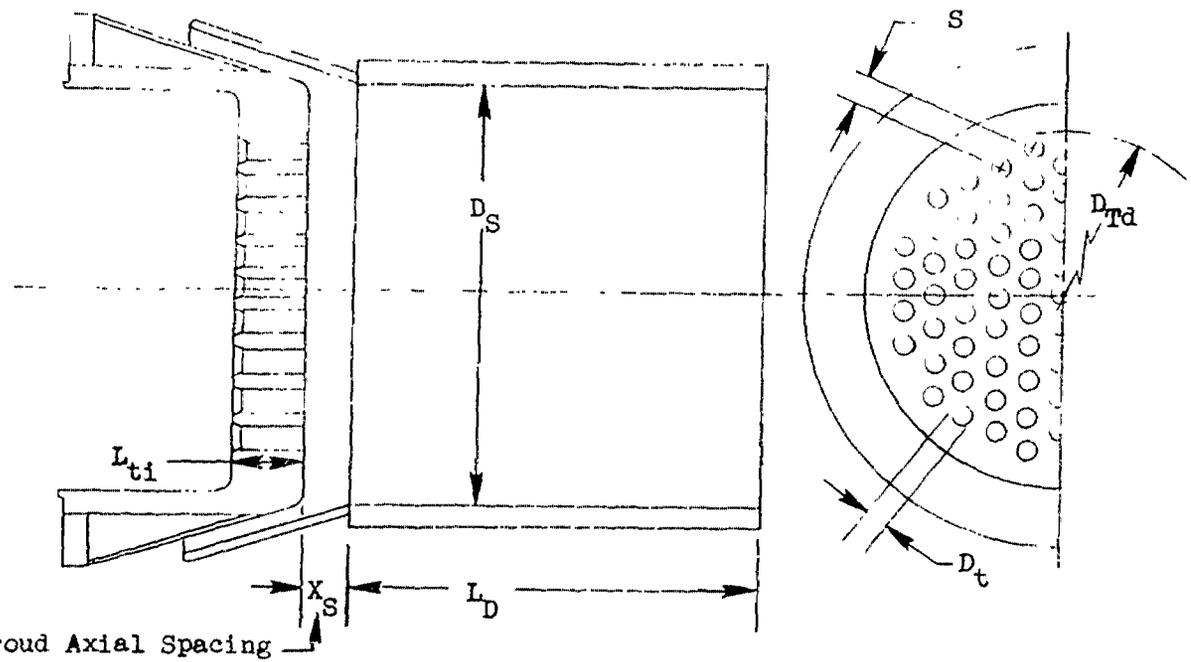

Model No.	Test Date	Primary						Secondary				
		No. Holes	Area Ratio	S	D_t	L_{ti}	L_{ti}/D_t	X_S	L_3	D_S	L_S/D_S	D_S/D_{Td}
6.0H85-2.7-CS2-1	5-05-69	85	2.7	.870"	.651"	1.49"	2.29	1.73"	10.845"	10.845"	1.0	1.10
6.0H85-2.7-CS2-3	7-11-69	85	2.7	.870"	.651"	1.49"	2.29	4.73"	10.845"	10.845"	1.0	1.10
6.0H85-2.7-CS2	3-27-69	85	2.7	.870"	.651"	1.49"	2.29	7.47"	10.845"	10.845"	1.0	1.10

FIGURE V.F.9-58 SCHEMATIC OF SHROUDED 85 HOLE NOZZLE FOR PARAMETRIC INVESTIGATION OF SHROUD AXIAL SPACING

TABLE V.F.9-15 TEST SUMMARY

MODEL NO. 6.0 H85-2.7-CS2-3

DESCRIPTION: 85 Hole Plate with Equally Spaced .651" ID Holes AR_d = 2.7
X_s = 4.73, D_s/D_{Td} = 1.10

DATE: 7/11/69

SCALE MODEL A_8 = .1965 $ft.^2$

FULL SCALE A_8 = 12.576 ft^2

SCALE FACTOR = 8:1

- o DATA INCLUDES GROUND REFLECTION INTERFERENCE
- o ANGLE REFERENCED TO JET EXHAUST

	TEST CONDITIONS				ACOUSTIC TEST RESULTS						
		IDEAL				320' ARC		300' SIDELINE		1500' SIDELINE	
RDG. No.	P_{T8}/P_o	T_{T8} (°R)	V_j (ft/sec)	W_8 (PPS)	10 log ρA	PEAK PNdB	PEAK ANGLE	PEAK PNdB	PEAK ANGLE	PEAK PNdB	PEAK ANGLE
1	2.08	1517	1873	10.40	-4.1	121.5	70	121.5	70	104.2	70
2	3.50	2677	3160	12.88	-5.4	130.1	50	128.0	50	112.7	50
3	3.32	2434	2958	12.78	-5.1	127.6	40	128.0	90	110.8	90
4	3.01	2104	2649	12.54	-4.8	126.3	40	125.6	70	108.5	70
5	2.80	1779	2364	12.69	-4.2	125.3	50	125.1	70	107.9	70
6	2.54	1637	2172	12.13	-4.1	125.6	90	126.3	90	106.8	90
7	1.79	1524	1691	8.90	-4.4	119.8	70	119.8	70	102.6	70
8	1.65	1241	1420	9.15	-3.5	117.0	60	116.8	70	99.7	70

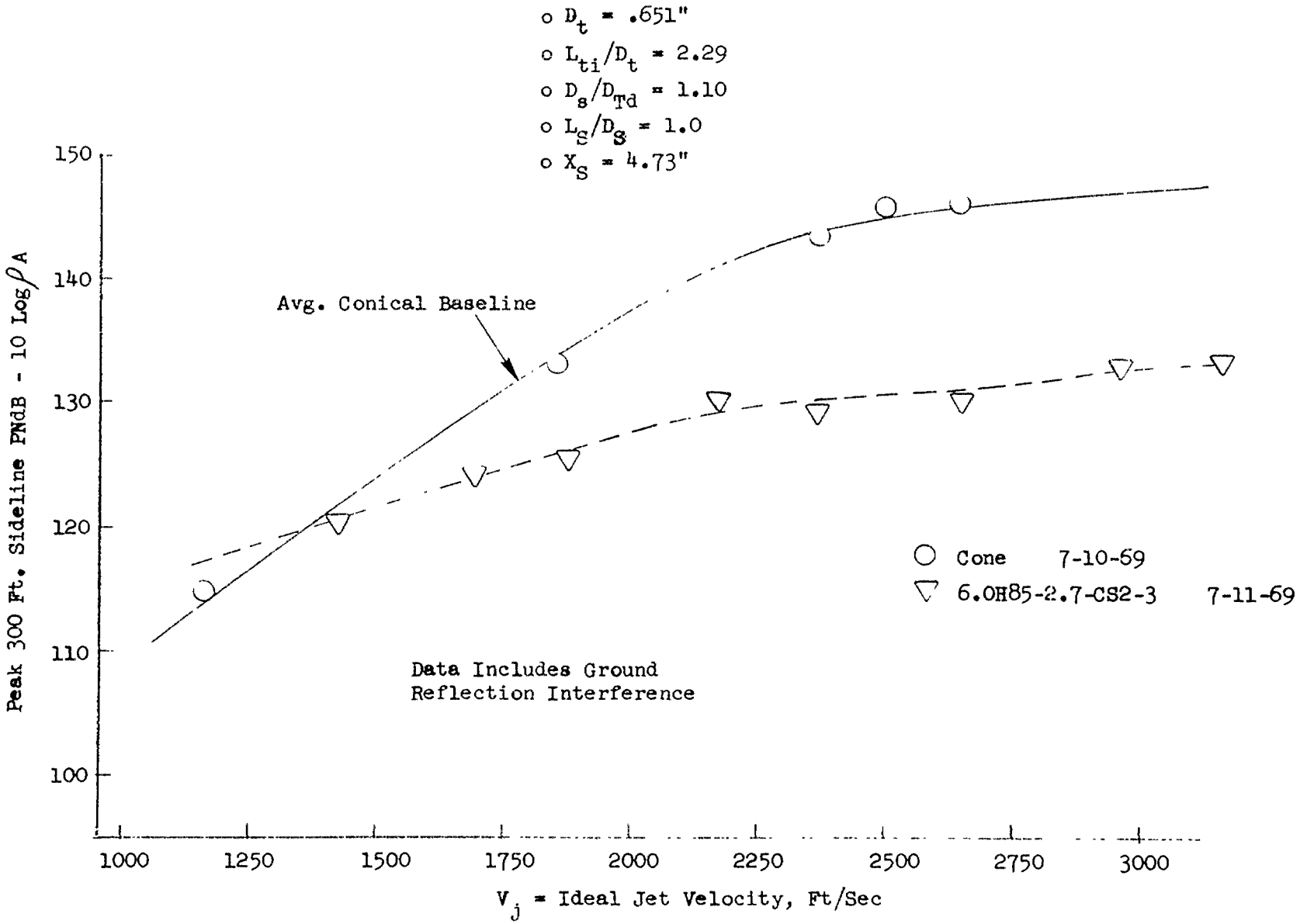

FIGURE V.F.9-59 300 FT. SIDELINE JET NOISE LEVELS FOR SHROUDED 85 HOLE NOZZLE WITH SHROUD AXIAL SPACING, X_S = 4.73"

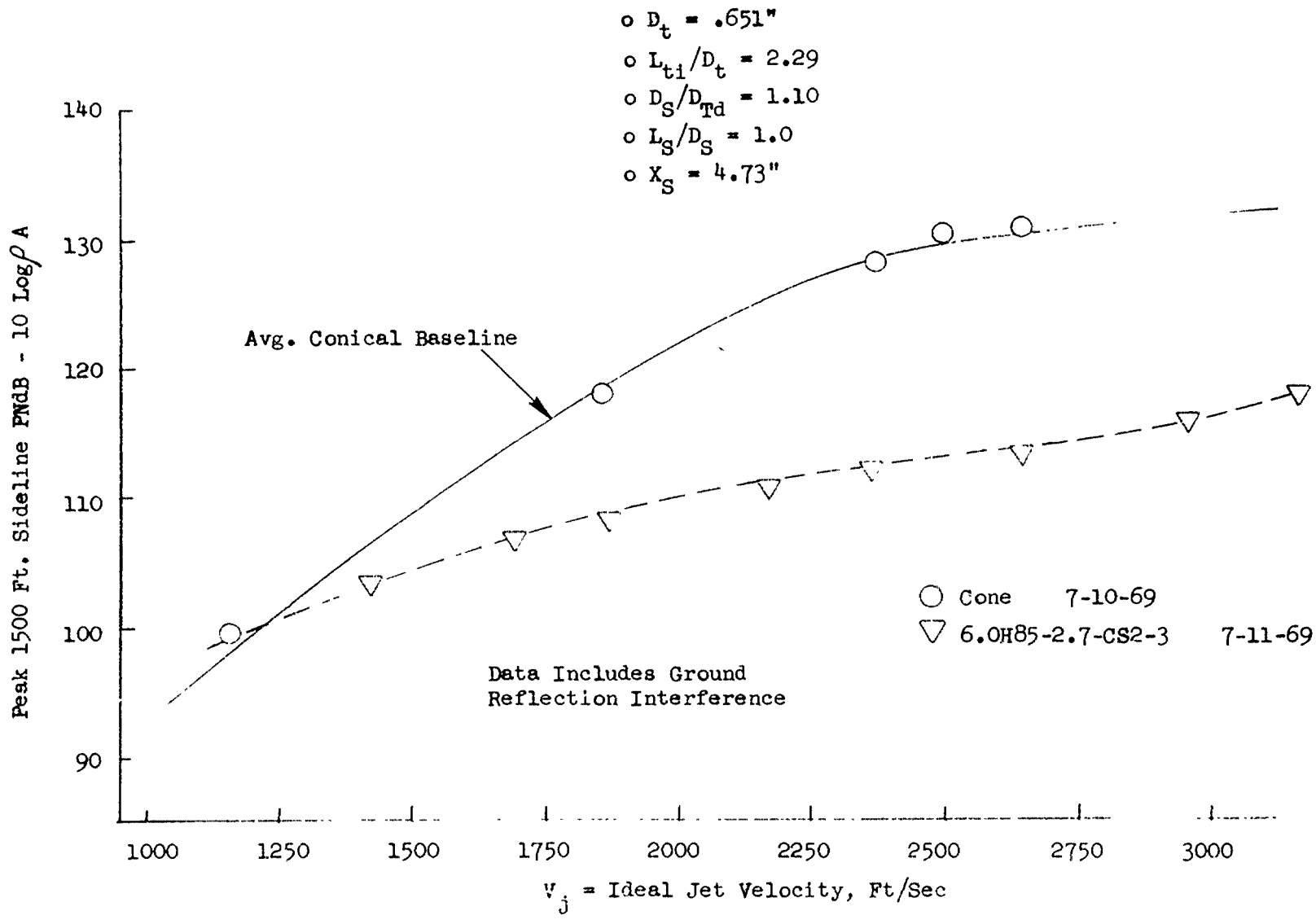

FIGURE V.F.9-60 1500 FT. SIDELINE JET NOISE LEVELS FOR SHROUDED 85 HOLE NOZZLE WITH SHROUD AXIAL SPACING, X_S = 4.73"

TABLE V.F.9-16 TEST SUMMARY

MODEL NO. 6.0-H85-2.7-CS2

DESCRIPTION: 85 Hole Plate with Equally Spaced .651" ID Holes, AR_d = 2.7

X_s = 7.47, D_s/D_{Td} = 1.10

DATE: 3/27/69

SCALE MODEL A_8 = .1965 ft^2

FULL SCALE A_8 = 12.376 ft^2

SCALE FACTOR = 8:1

- o DATA INCLUDES GROUND REFLECTION INTERFERENCE
- o ANGLE REFERENCED TO JET EXHAUST

	TEST CONDITIONS				ACOUSTIC TEST RESULTS						
			IDEAL			320' ARC		300' SIDELINE		1500' SIDELINE	
RDG. No.	P_{T8}/P_o	T_{T8} (°R)	V_j (ft/sec)	W_8 (PPS)	10 log ρA	PEAK PNdB	PEAK ANGLE	PEAK PNdB	PEAK ANGLE	PEAK PNdB	PEAK ANGLE
1	1.42	1153	1149	8.18	-3.4	112.3	60	111.8	70	94.2	70/80
2	1.59	1520	1515	7.99	-4.4	118.0	80	118.6	80	101.0	80
3	1.67	1244	1437	9.33	-3.5	116.7	80	117.3	80	99.7	80
4	1.81	1499	1688	9.15	-4.3	121.1	70	121.4	80	103.7	80
5	2.07	1534	1878	10.34	-4.2	123.4	80	123.9	80	106.3	80
6	2.32	1541	2010	11.41	-4.0	125.1	80	125.6	80	107.9	80
7	2.53	1669	2187	11.90	-4.2	126.5	70	127.0	80	109.4	80
8	2.59	2095	2480	10.79	-5.1	127.4	80	128.0	80	110.5	80
9	2.81	1786	2373	12.68	-4.2	127.3	70	127.7	80	110.1	80
10	3.00	2109	2650	12.40	-4.8	129.6	40	127.2	60/70	111.1	50
11	3.22	2219	2793	13.07	-4.8	131.0	50	129.0	80	113.4	50
12	3.32	2401	2938	12.67	-5.0	131.9	90	132.8	90	113.9	50
13	3.31	2629	3070	12.44	-5.5	133.4	50	131.2	50	115.9	50
14	3.50	2682	3163	13.08	-5.4	132.9	50	130.9	80	115.4	50

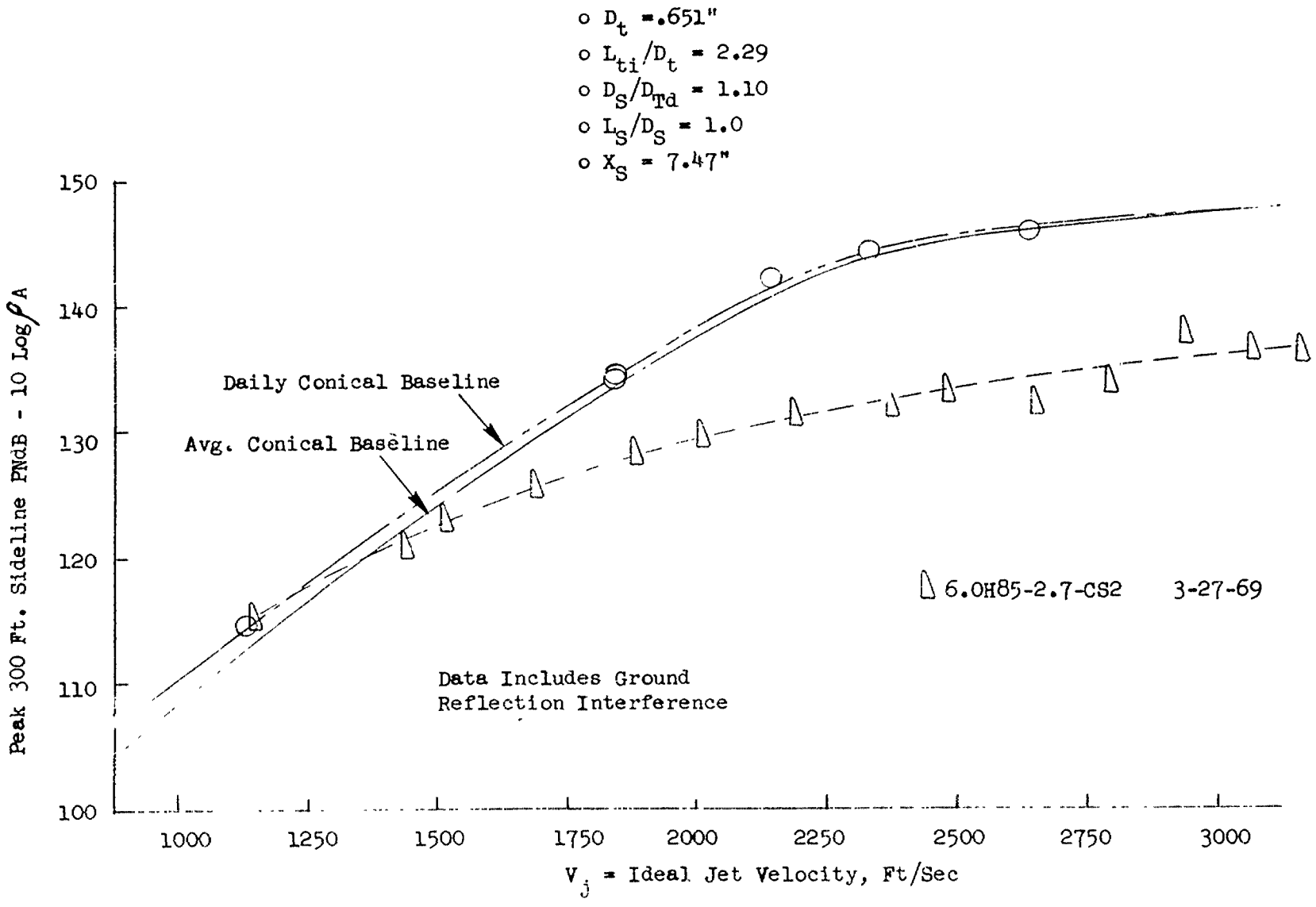

FIGURE V.S.9-61 300 FT. SIDELINE JET NOISE LEVELS FOR SHROUDED 85 HOLE NOZZLE WITH SHROUD AXIAL SPACING, X_S = 7.47"

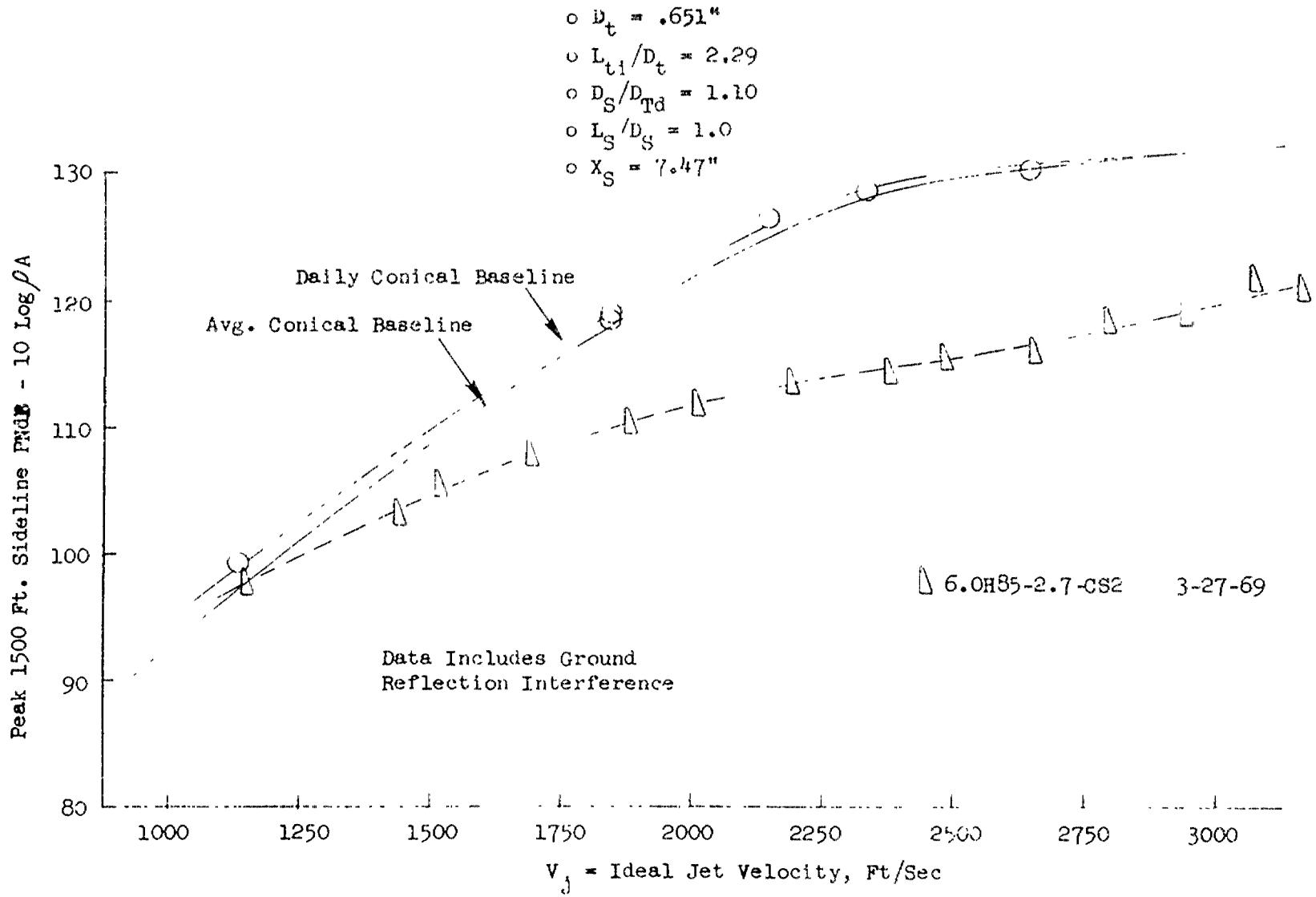

FIGURE V.F.9-62 1500 FT. SIDELINE JET NOISE LEVELS FOR SHROUDED 85 HOLE NOZZLE WITH SHROUD AXIAL SPACING, X_S = 7.47"

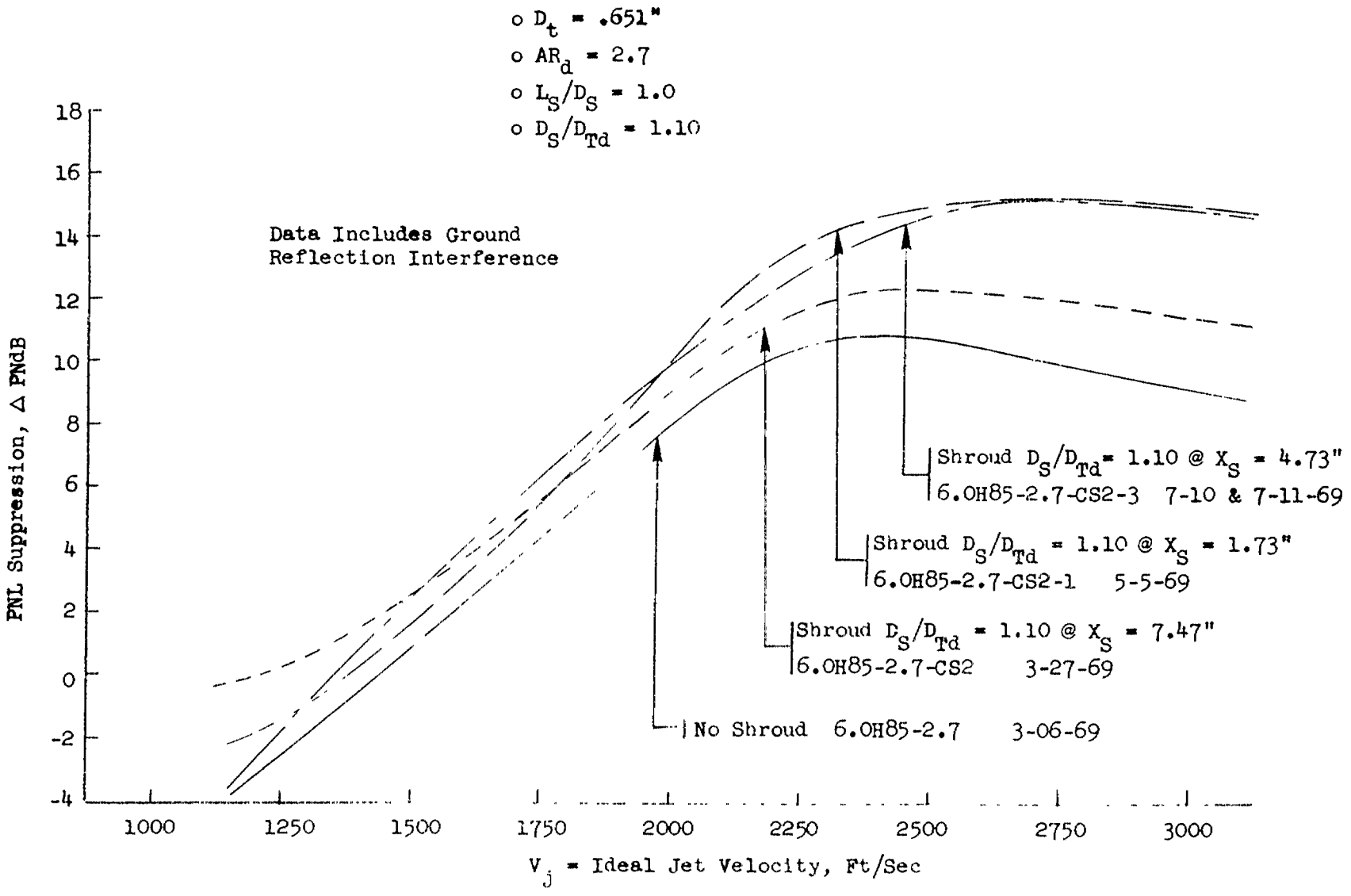

FIGURE V.F.9-63 EFFECT OF SHROUD AXIAL SPACING ON 300 FT. SIDELINE PNL SUPPRESSIONS FOR SHROUDED 85 HOLE NOZZLE

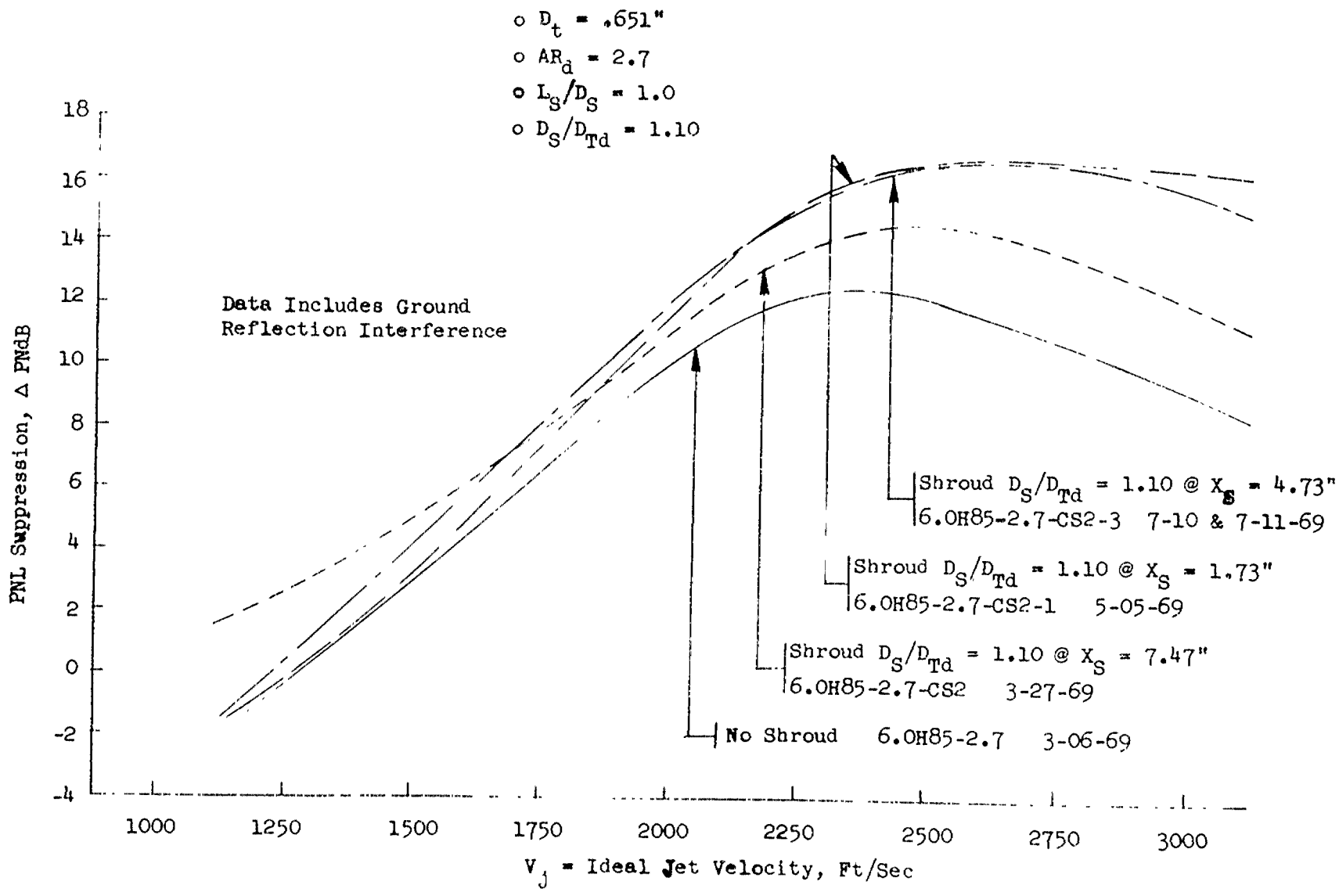

FIGURE V.F.9-64 EFFECT OF SHROUD AXIAL SPACING ON 1500 FT. SIDELINE PNL SUPPRESSIONS FOR SHROUDED 85 HOLE NOZZLE

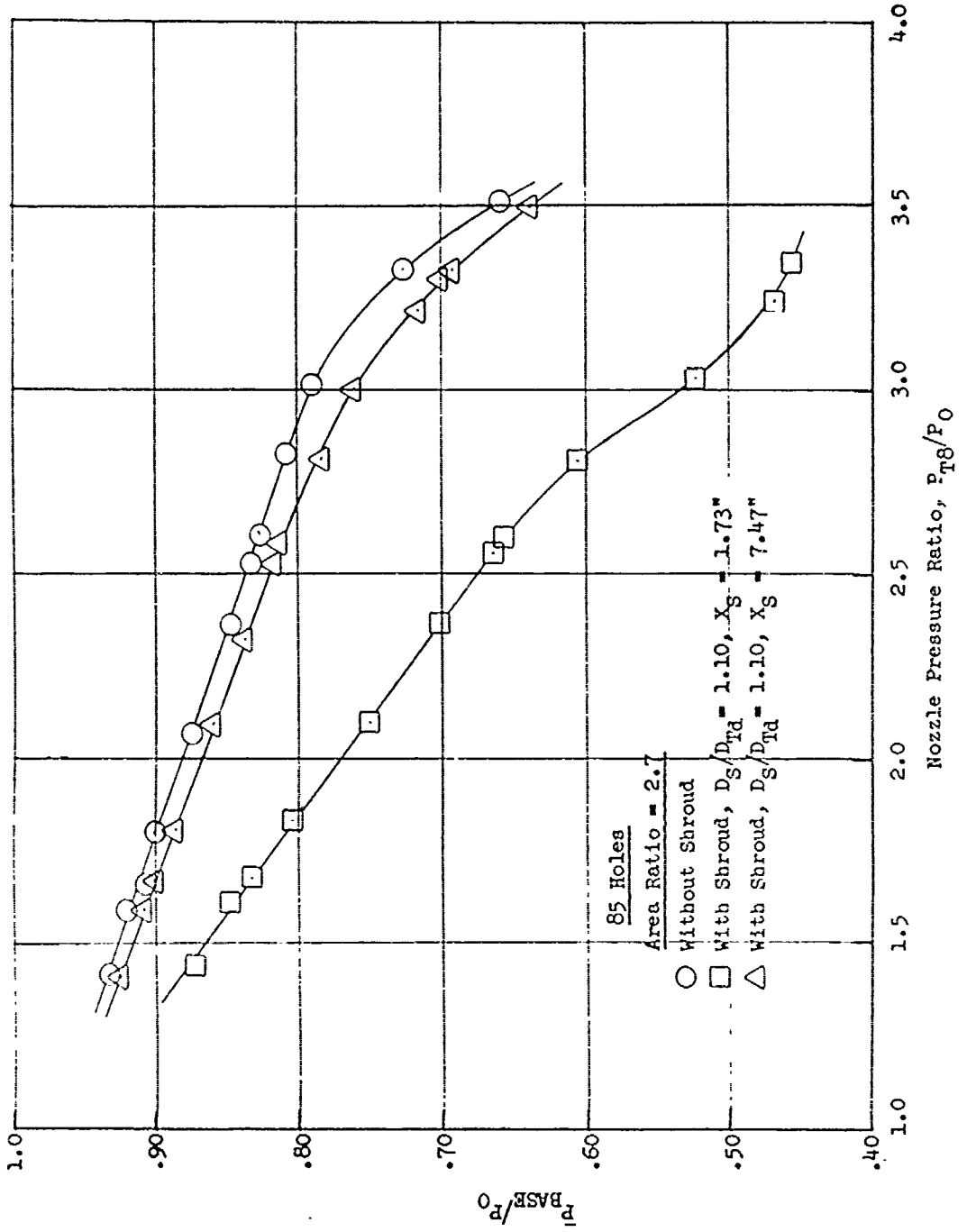

FIGURE V.F.9-65 EFFECT OF SHROUD AXIAL SPACING ON MEAN BASEPLATE PRESSURE RATIO

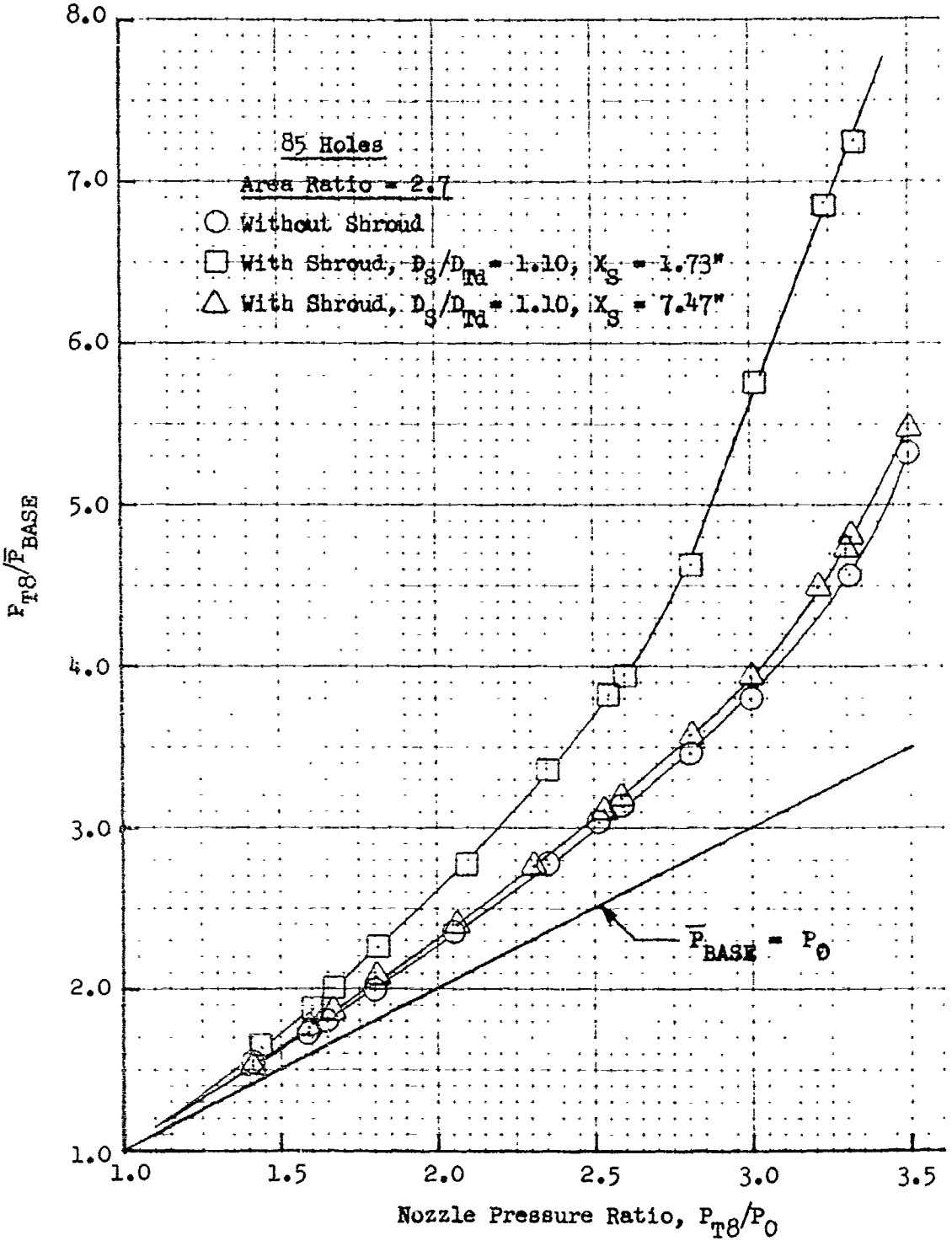

FIGURE V.F.9-66 EFFECT OF SHROUD AXIAL SPACING ON NOZZLE EXIT TO MEAN BASEPLATE PRESSURE RATIO

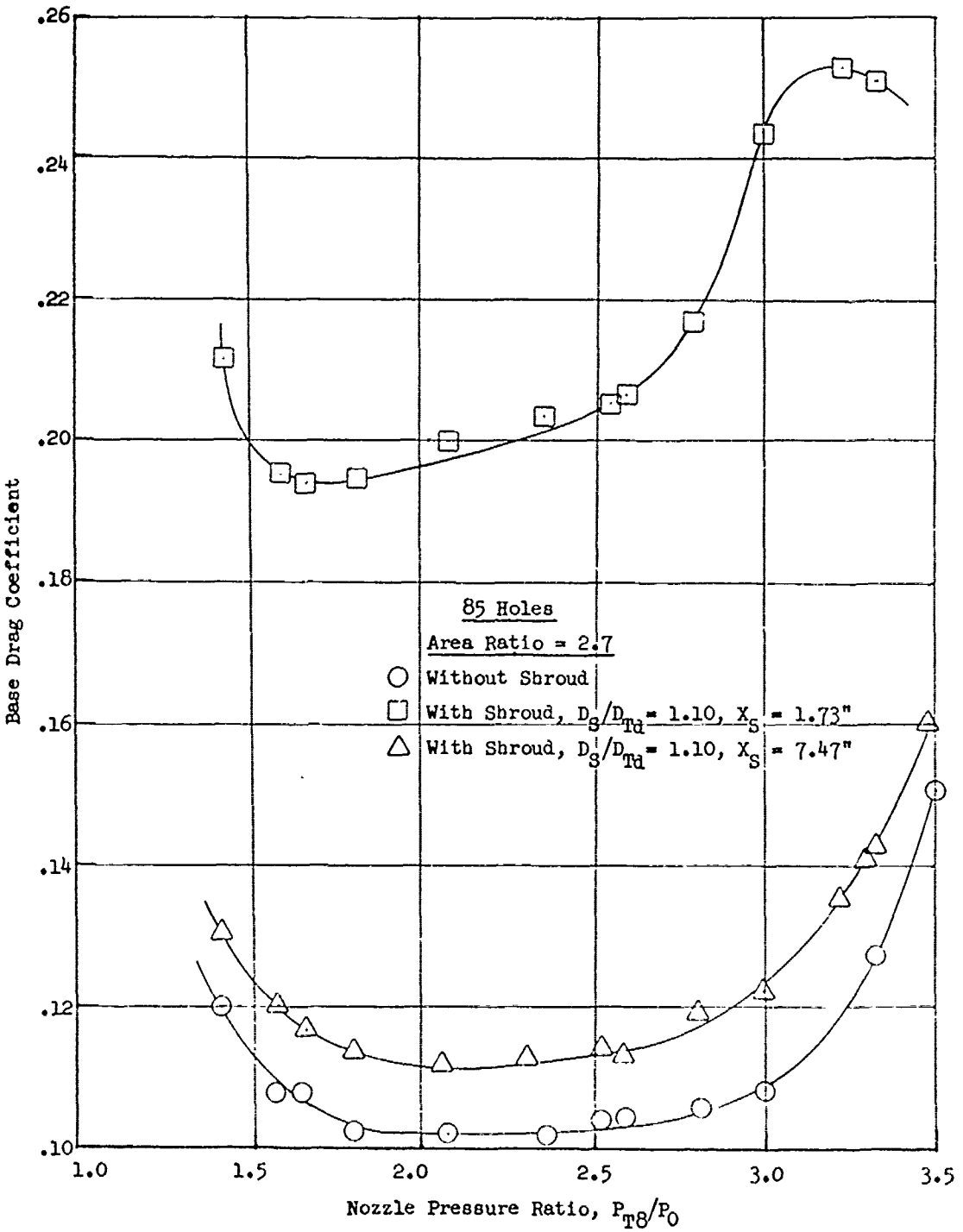

FIGURE V.F.9-67 EFFECT OF SHROUD AXIAL SPACING ON BASEPLATE DRAG COEFFICIENT

V.F.10 MULTI-TUBE PRELIMINARY DESIGN NUMBER 3 (PD-3)

V.F.10 MULTI-TUBE PRELIMINARY DESIGN NO. 3 (PD-3)

Objectives of Test Series

In early 1969 analysis of available suppression nozzle performance data had indicated that a primary nozzle consisting of multi-tubes with convoluted (Greatrex) ends was the most promising candidate to meet the Boeing/GE thrust and suppression level objectives of the GE4/J6C, 633 lbs/sec engine/airframe studies. The main objectives were to attain at least 11 PNdB suppression at the simulated climbout condition with a static takeoff gross thrust coefficient, C_{fg}, of 0.89. The Preliminary Design No. 3 (PD-3) multi-tube suppressor was therefore designed utilizing suggested guidelines of all previous multi-element trade studies. For a viable system the tube number should be between 70 and 100. For practical tube length, tube internal length to internal diameter ratio should approximate 3.0. Equal spacing and hole diameter should be constant as this is one of the more potent suppression parameters. Area ratio (AR_d = ratio of total tube bundle enclosed area to physical tube exit area) should be as large as the engine/aircraft envelope will permit for the high velocity design point of the GE4/J6C. Shroud length and diameter should also be in the range permissible by the engine/aircraft envelope. Greatrex end tubes (partially or fully convoluted) showed an additional suppression of near 4 PNdB. From the analysis an 84 tube nozzle of AR_d = 3 was chosen. An eight-lobed Greatrex tube exit was designed at a 50% lobe penetration into the jet while maintaining the same physical flow area as a non-convoluted tube. Plain (straight) end tube models were also planned to check the suppression gain by Greatrex ends. All tubes were equal flow size and uniformly spaced. Figures V.F.10-1 and -2 schematically show the multi-tube/ejector systems and Figure V.F.10-3 details the tube designs. The auxiliary airflow scheme of the contoured ejector, necessary to supply the exhaust system with sufficient auxiliary flow during the suppressed mode, was changed from the conventional TSEN tertiary door inlet to a "bomb-bay" door type design.

The specific objectives of the planned test series were to determine the aerodynamic and acoustic performance of:

PRECEDING PAGE BLANK-NOT FILMED

- o Greatrex and plain (straight) end tube bundles
- o Staggered and coplanar tube exits
- o Addition of contoured ejector

The aerodynamic tests were performed at the FluiDyne Engineering Corporation, and determined the static gross thrust coefficients, C_{fg}, and primary flow discharge coefficients, C_{D_8}, over a primary nozzle pressure ratio range of $1.4 \leq P_{T8}/P_o \leq 3.5$. For acoustic testing at the JENOTS facility, the nozzles were subjected to a simulated engine cycle running line with exhaust nozzle conditions varying from pressure ratios of 1.5 to 3.5, exit temperatures from 1150 to 2660°R, and ideal jet velocity of 1200 to 3150 ft/sec. Acoustic measurements were taken in octave band form to 31.5KHz at a 40 ft. radius and scaled by a factor of 8:1 to the full scale engine size. Therefore, all data presented are of simulated engine size and frequency range.

Test Configurations

Figure V.F.10-1 schematically shows the eight cold flow aerodynamic test models including two plain tube nozzles (coplanar and staggered exit planes, two Greatrex tube nozzles (coplanar and staggered exit planes) and each of the four primary nozzles with a cylindrical ejector. Each model had 84 tubes plus a center hole and was designed for $AR_d = 3.0$.

The 84 tube pattern was designed to be actuated into the jet stream on six pie-shaped flaps, the center hole forming between the deployed flaps. The aerodynamic cold flow models had a series of small holes drilled to simulate flap leakage in the sealing areas between deployed flaps.

Four of the aerodynamic test configurations were duplicated in high temperature hardware for hot flow acoustic testing at the GE, Evendale, JENOTS facility. These configurations, Models 1, 3, 4 and 5, are schematically shown in Figure V.F.10-2. Plain and Greatrex end tube designs for both cold and hot flow models are shown in Figure F.F.10-3. Photographs of some of the aerodynamic and acoustic models are shown in Figures V.F.10-4 through V.F.10-7.

The models with extended outer row tubes forming coplanar exit planes were made by sleeving and re-brazing the staggered tubes, as seen in Figures V.F.10-4B, V.F.10-5A, and V.F 10-7A and -7B.

A 5.7 inch D_8 conical convergent nozzle was used to establish the acoustic baseline for this test series and all suppressions are referenced to this baseline unless otherwise noted.

Presentation of Test Results

Summaries of aerodynamic nozzle test conditions and acoustic measurement results are presented for the acoustic models as follows:

- Table V.F.10-1; Model 1; Plain Tube - Staggered Exit
- Table V.F.10-2, Model 3; Plain Tube - Coplanar Exit
- Table V.F.10-3, Model 4; Plain Tube - Coplanar Exit plus Ejector
- Table V.F.10-4, Model 5; Greatrex Tube - Staggered Exit

Acoustic test results in the form of 300 ft. and 1500 ft. sidelines normalized peak PNL values are plotted against ideal jet velocity per the following:

- Figure V.F.10-8 & 9; Model 1; Plain Tube - Staggered Exit
- Figure V.F.10-10 & 11; Model 3; Plain Tube - Coplanar Exit
- Figure V.F.10-12 & 13; Model 4; Plain Tube - Coplanar Exit plus Ejector
- Figure V.F.10-14 & 15; Model 5; Greatrex Tube - Staggered Exit

Each figure also has the average baseline conical nozzle line to which the suppressed nozzle is referenced for suppression.

Comparisons of peak PNL suppression versus ideal jet velocity for the four acoustic models are shown at the 300 ft. sideline in Figure V.F.10-16 and at the 1500 ft. sideline in Figure V.F.10-17. Examination shows the Greatrex tubes performed well, as anticipated, up to about 2200 to 2400 ft/sec jet velocity. They completely lost their better suppression margin above V_j of 2500 ft/sec. This was not anticipated as all previous Greatrex tube model tests were performed with temperature limited hardware and tested below 2500 ft/sec. This result, in addition to the lower aerodynamic performance (shown later) at all P_{T8}/P_o values, made the Greatrex tube design unattractive for the GE4/J6C goals.

Extension of the plain tubes to a coplanar exit for better ventilation gained about 3 PNdB suppression at high V_j of 3150 ft/sec in addition to a 3% increase in thrust coefficient (as seen later).

Addition of the secondary shroud to the coplanar plain tube model had minor effects on suppression, except at low and high jet velocities where 1.5 and 2 PNdB gains are seen.

The plain tube staggered exit model performed as anticipated from predictions based on previous parametric studies.

To gauge the changes in octave band spectra and PNL directivity between the three non-shrouded acoustic models and the unsuppressed baseline, Figures V.F.10-18 and V.F.10-19 are presented. Figures V.F.10-18A through -18E are spectral comparisons at the 300 ft. sideline. Of particular interest is the plain tube - coplanar exit model at mid and high jet velocity. The PNL suppression curves of Figures V.F.10-16 and -17 showed the coplanar model to gain about 3 PNdB suppression. The spectra plots show accompanying spectral change to which the increased suppression is attributable. The coplanar tube exit model did not retain the predominant low frequency noise as did the staggered exit model. Figures V.F.10-19A through -19E are the PNL directivity comparisons at the 300 ft. sideline again showing the predominant change of the plain tube coplanar exit model, particularly at mid and high jet velocities and in the region of peak jet noise.

To show the change in noise generation attributable to the Greatrex tube ends when referenced to the plain tube ends, Figures V.F.10-20 through -22 are presented. Figures V.F.10-20A to -20C show the individual OBSPL suppressions. Figure V.F.10-21 shows the OASPL and PNL changes as a function of jet velocity. Figure V.F.10-22 composites the OBSPL changes. At low jet velocity the maximum suppression due to the Greatrex ends is seen in the 500 Hz and 1K Hz bands. At high velocity the 1K, 2K and 4K Hz bands are nearly equally suppressed. These bands are full scale frequency-scaled by 8:1 from model measurements. The OASPL levels are suppressed only in the range of $1000 \leq V_j \leq 2300$ ft/sec. Above that range the changes are mainly in the high frequency bands and do not alter the OASPL. The PNL suppression gain varies from 1 to 4 PNdB in the low to mid V_j range and then drops to negative suppression, or increased noise above the plain end tubes, at high V_j.

To compare the magnitude of spectral change due to addition of Greatrex ends to previous results, Figures V.F.10-23 and -24 are included. Figure V.F.10-23 compares the PD-3 8-lobe 50% penetration Greatrex design to the previously tested 12-lobe (approximately) 80% penetration Greatrex design used in the 37 tube nozzle series at AR_a = 3 and 4. See Section V.F.4 and Figure V.F.4-27. Trendwise the results are quite similar, the only major differences being at higher velocity where the 12-lobe 80% penetration design would possibly anticipate a continued suppression increase due to the curve trends.

Aerodynamic performance results in terms of primary nozzle flow discharge coefficient, C_{D8}, and static gross thrust coefficient, C_{fg}, are presented against primary nozzle pressure ratio in Figures V.F.10-25 and -26; -25 primary nozzles alone and -26 with ejector. Refer to Figure V.F.10-1 for cold flow aerodynamic model schematics.

The following observations can be made:

- For the unshrouded primary nozzle tests, the effect of increasing tube length (coplanar exits) was to increase the thrust coefficient by 3% for both plain and Greatrex tube exits.
- The flow coefficient (C_{D8}) of the coplanar exit Greatrex tube suppressor decreased by 4% while that of the coplanar exit plain tube model remained essentially constant. This indicated that higher internal losses occur in the Greatrex exit suppressor.
- With the secondary shroud installed, the performance gain due to increasing the tube length was only .02% for the Greatrex ends and 1% for the plain end tubes.

As a gauge of the magnitude of problem areas contributing to the total thrust loss of the multi-tube nozzles, a breakdown of losses for the four primary nozzles is shown in Figure V.F.10-27. It becomes obvious that base drag is the single highest contributing factor to low performance. The increased pumping capability of the Greatrex tubes caused the base drag to be quite high; therefore, the low Greatrex performance can be attributed to a tube ventilation problem. With the tube lengths increased in the coplanar models, the base pressure decrement was particularly relieved and performance levels were increased for both the plain and Greatrex coplanar models.

Summary and Conclusions

The PD-3 multi-tube series culminated the parametric tube design studies into a viable engine suppressor system. Conclusions of the aerc-acoustic test series were:

- Greatrex tubes performed well acoustically, gaining 1 to 4 PNL suppression over the plain end tubes, until about 2500 ft/sec, where the better suppression margin was lost. The Greatrex tubes suppressed OASPL levels only in the range of $1000 \leq V_j \leq 2300$ ft/sec. At low V_j the 500 and 1K Hz octave bands are suppressed well by the Greatrex ends, maximum suppression shifting to the 1K, 2K and 4K Hz bands at high V_j. Aerodynamically the Greatrex tubes performed from 5 to 8% lower on C_{fg} than their equivalent models in plain tube ends, eliminating them from practical consideration within the GE4/J6C suppressor system.

- The PD-3 program objectives were met with the plain tube coplanar exit plus ejector model attaining 14.5 PNL suppression at 3150 ft/sec and .90 C_{fg} at $P_{T8}/P_o = 3.5$ against the goals of 11 PNL suppression and .89 C_{fg}. However, the longer tubes at the outer tube bundle created a storage problem with the suppressor retracted.

- Extension of the plain tubes to a coplanar exit without the ejector gained suppression at high V_j in addition to a 3% increase in thrust coefficient. The coplanar tube exit model was the only one which did not retain the low frequency noise dominance at the higher jet velocities. Extension of the Greatrex tubes from staggered to coplanar without the ejector also gained about 3% increase in C_{fg}.

- The addition of the secondary ejector to the coplanar plain tube model had minor effects in suppression, except at low and high V_j, where 1.5 to 2 PNL suppression gains were seen. With the secondary ejector installed, the performance gain due to increasing the tube length from staggered to coplanar was only .02% for the Greatrex ends and 1% for the plain end tubes.

- A breakdown of the thrust losses for the primary nozzles shows base drag to be the highest contributing factor to low performance, the loss being attributed to a tube ventilation problem.

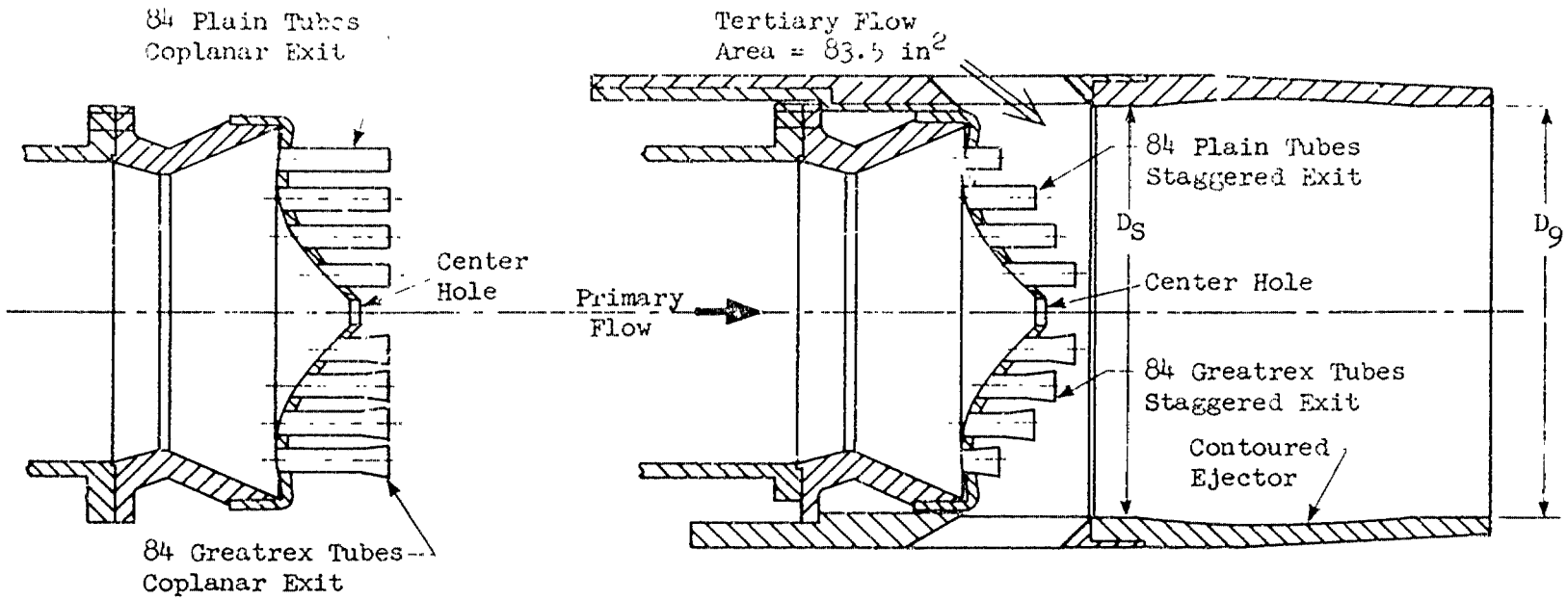

- All Models $AR_d \approx 3.0$
- $D_S = D_9 = 11.808$ In.

MODEL NO.	PRIMARY	SECONDARY	A_8 (in^2)
1	Plain Tubes - Staggered Exit	None	30.33
2	Plain Tubes - Staggered Exit	Contoured Ejector	30.33
3	Plain Tubes - Coplanar Exit	None	30.20
4	Plain Tubes - Coplanar Exit	Contoured Ejector	30.20
5	Greatrex Tubes - Staggered Exit	None	30.31
6	Greatrex Tubes - Staggered Exit	Contoured Ejector	30.31
7	Greatrex Tubes - Coplanar Exit	None	30.25
8	Greatrex Tubes - Coplanar Exit	Contoured Ejector	30.25

FIGURE V.F.10-1 SCHEMATIC OF PD-3 AERODYNAMIC COLD FLOW NOZZLES

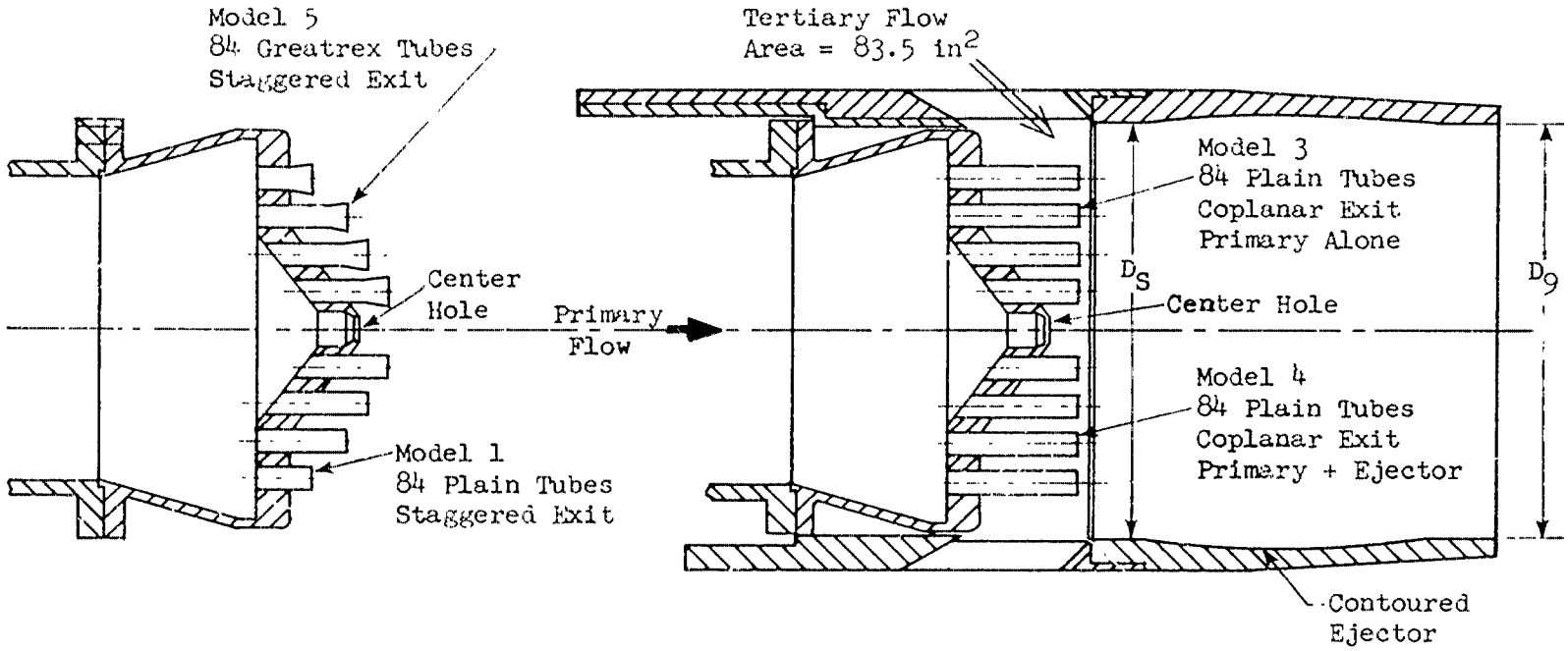

- All Models $AR_d \approx 3.0$
- $D_S = D_9 = 11.808$ In.

MODEL NO.	PRIMARY	SECONDARY	A_8 (in²)	TEST DATES
1	Plain Tubes - Staggered Exit	None	28.51	1-5, 1-6, & 1-12-70
3	Plain Tubes - Coplanar Exit	None	28.51	2-6, 2-11, & 2-16-70
4	Plain Tubes - Coplanar Exit	Contoured Ejector	28.51	3-5 & 3-9-70
5	Greatrex Tubes - Staggered Exit	None	30.79	12-19 & 12-22-69

FIGURE V.F.10-2 SCHEMATIC OF PD-3 ACOUSTIC HOT FLOW NOZZLES

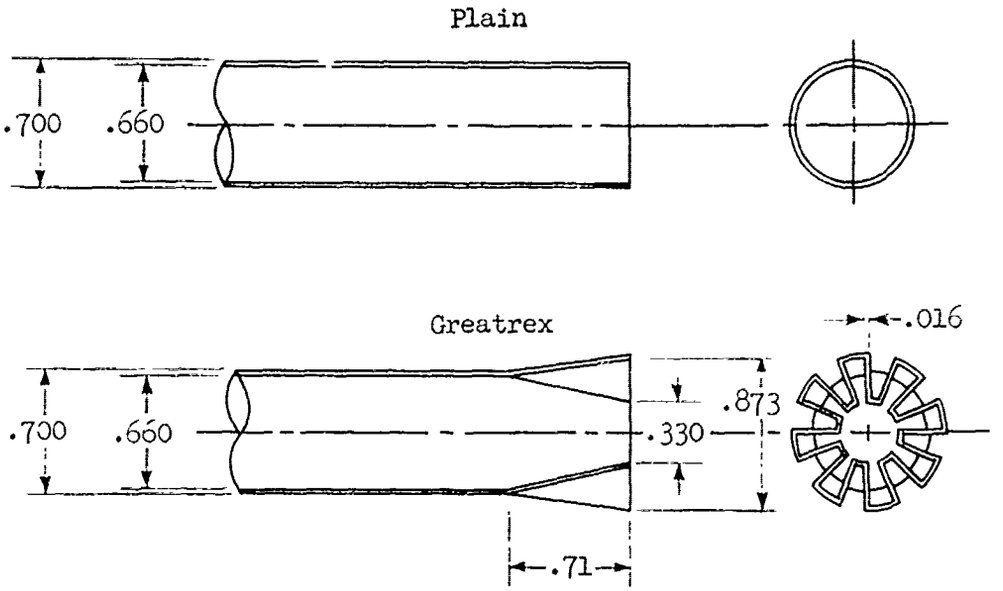

a) Tube Design for Cold Flow Aerodynamic Models

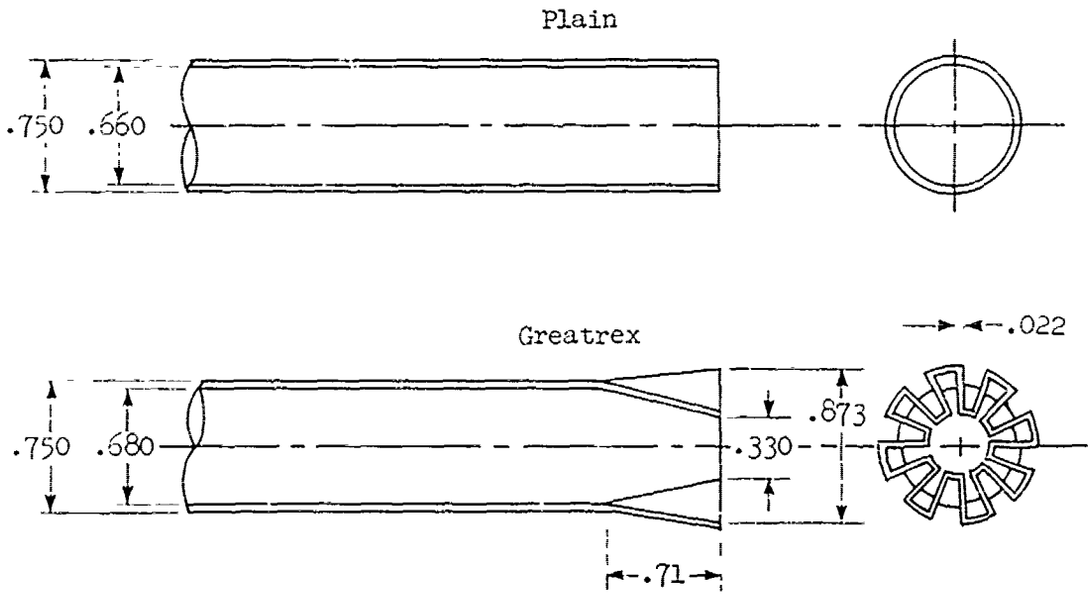

b) Tube Design for Hot Flow Acoustic Models

FIGURE V.F.10-3 PD-3 PLAIN AND GREATREX TUBE DESIGNS FOR COLD FLOW AERODYNAMIC AND HOT FLOW ACOUSTIC MODELS

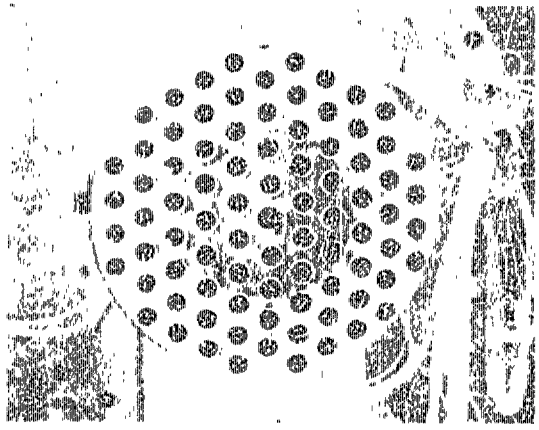

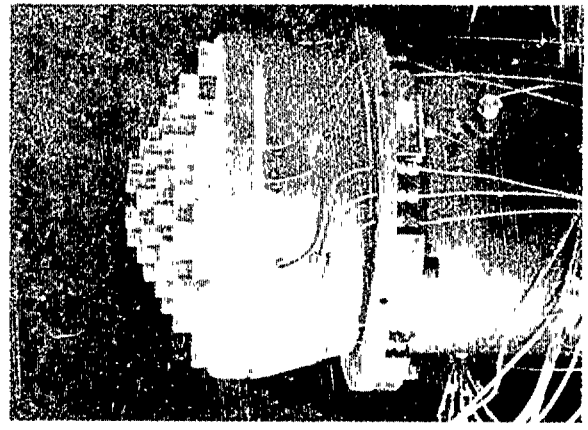

a) Model 1, 84 Plain Tubes - Staggered Exit - Hot Flow Acoustic Hardware

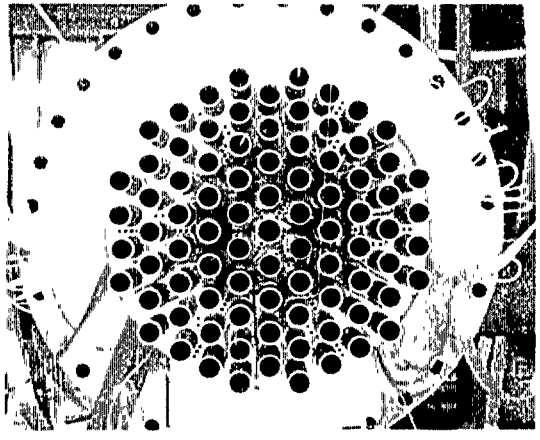

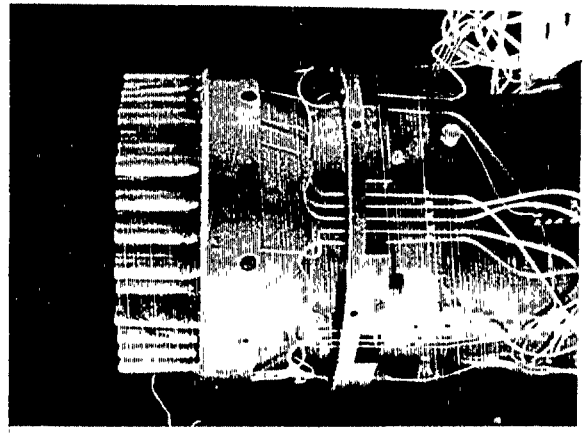

b) Model 3, 84 Plain Tubes - Coplanar Exit - Cold Flow Aerodynamic Hardware

FIGURE V.F.10-4 PD 3 ACOUSTIC AND AERODYNAMIC HARDWARE - MODELS 1 & 3

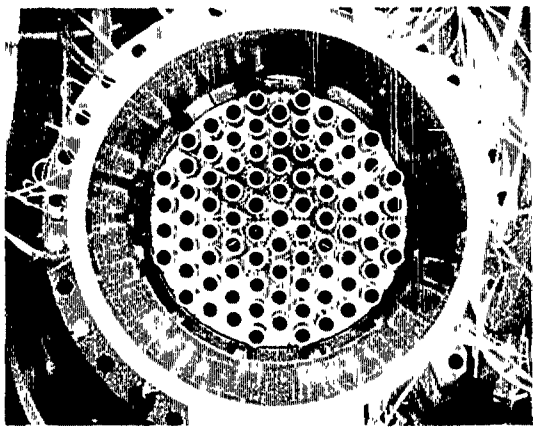

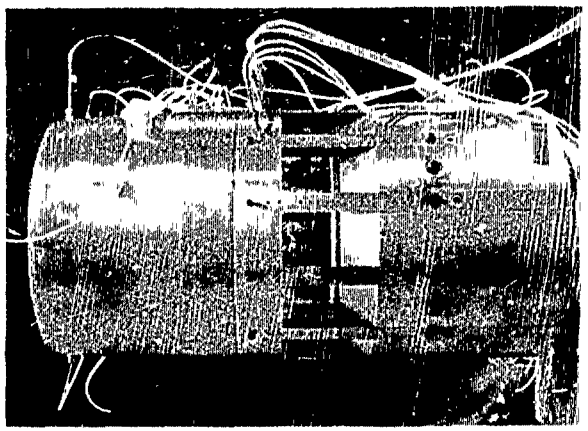

a) Model 4, 84 Plain Tubes - Coplanar Exit - Plus Ejector - Cold Flow Aerodynamic Hardware

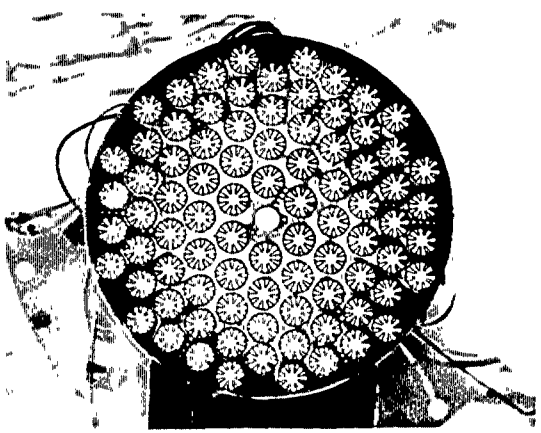

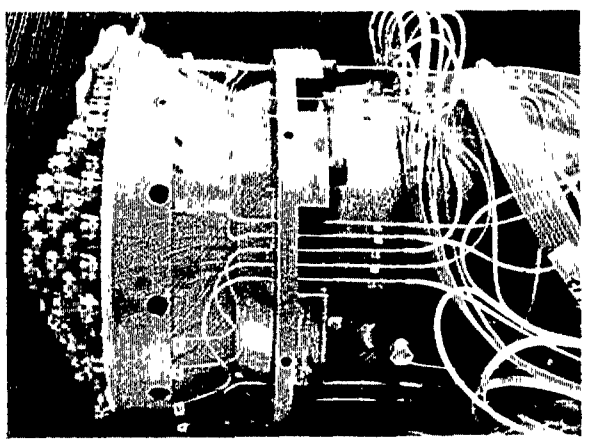

b) Model 5, 84 GREATREX Tubes - Staggered Exit - Cold Flow Aerodynamic Hardware

FIGURE V.F.10-5 PD-3 AERODYNAMIC HARDWARE - MODELS 4 & 5

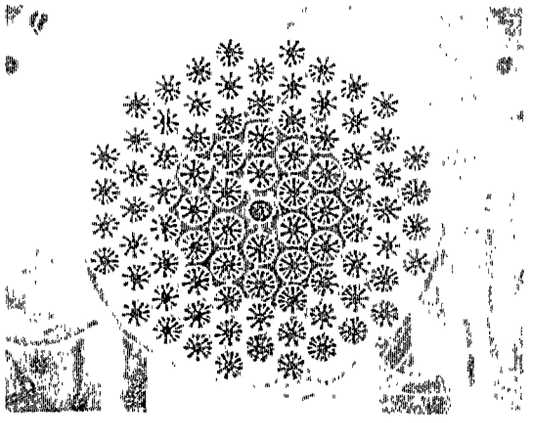

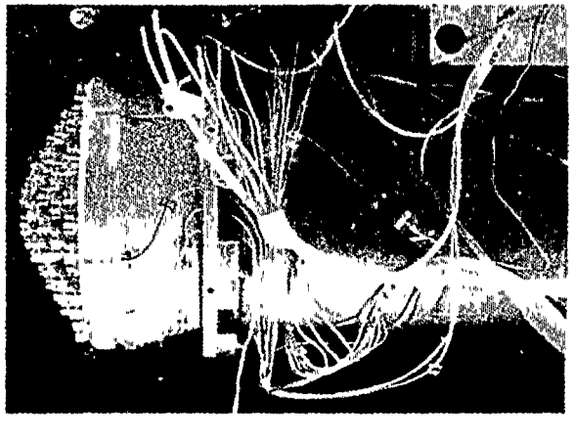

a) Model 5, 84 GREATREX Tubes - Staggered Exit - Hot Flow Acoustic Hardware

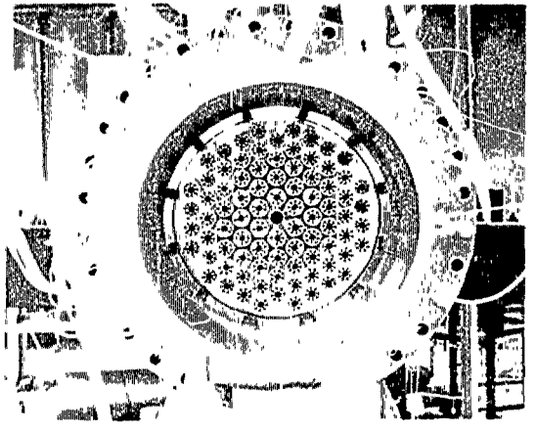

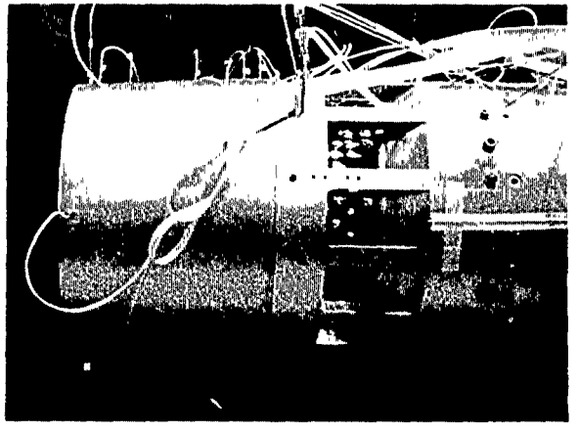

b) Model 6, 84 GREATREX Tubes - Staggered Exit - Plus Ejector - Cold Flow Aerodynamic Hardware

FIGURE V.F.10-6 PD-3 ACOUSTIC AND AERODYNAMIC HARDWARE - MODELS 5 & 6

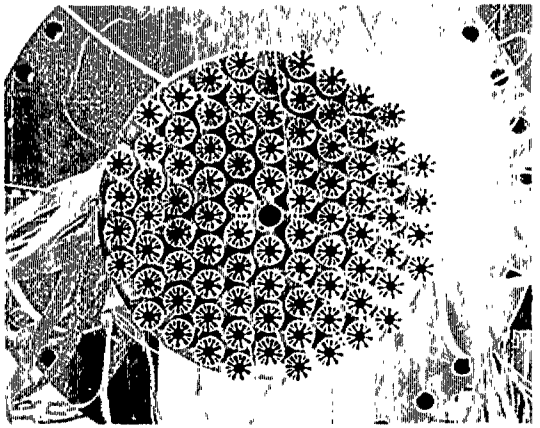

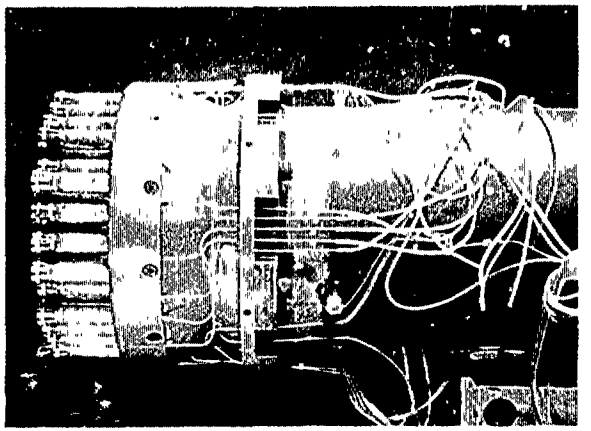

a) Model 7, 84 GREATREX Tubes - Coplanar Exit - Cold Flow Aerodynamic Hardware

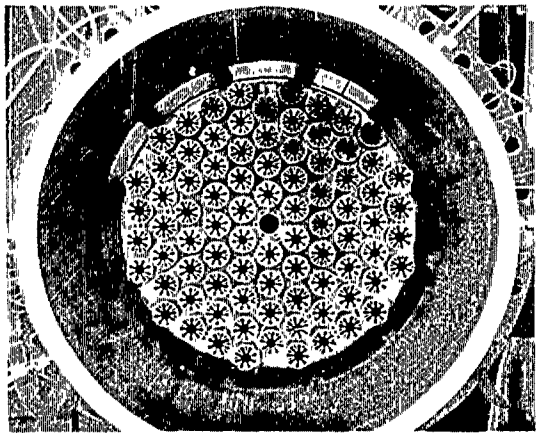

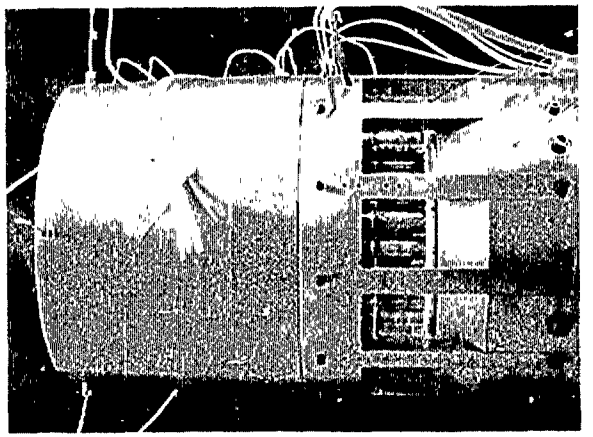

b) Model 8, 84 GREATREX Tubes - Coplanar Exit - Plus Ejector - Cold Flow Aerodynamic Hardware

FIGURE V.F.10-7 PD-3 AERODYNAMIC HARDWARE - MODELS 7 & 8

TABLE V.F.10-1 TEST SUMMARY

MODEL NO. 1

DESCRIPTION: Plain End Tubes, Staggered Exit

DATE: 1/5/70; 1/6/70; 1/12/70

SCALE MODEL A_8 = .1978 ft^2

FULL SCALE A_8 = 12.662 ft^2

SCALE FACTOR = 8:1

- o DATA INCLUDES GROUND REFLECTION INTERFERENCE
- o ANGLE REFERENCED TO JET EXHAUST

RDG NO.	TEST CONDITIONS				ACOUSTIC TEST RESULTS						
			IDEAL			320' ARC		300' SIDELINE		1500' SIDELINE	
	P_{TS}/P_o	T_{TS} (°R)	V_j (ft/sec)	W_8 (PPS)	10 log ρA	PEAK PNdB	PEAK ANGLE	PEAK PNdB	PEAK ANGLE	PEAK PNdB	PEAK ANGLE
1/5/70											
1	1.50	1155	1240	8.49	-3.10	115.1	60	114.2	60	96.8	60
2	1.59	1517	1510	7.96	-4.31	119.7	60	118.8	60	101.3	60
3	1.67	1239	1432	9.34	-3.42	120.0	60	119.0	60	101.5	60
4	1.79	1511	1681	9.24	-4.24	122.3	60	121.4	60	103.9	60
5	2.06	1508	1856	10.49	-4.06	123.8	60	122.9	60	105.5	60
1/6/70											
1	2.24	1509	1953	11.43	-3.93	126.2	50	125.2	60	107.7	60/70
2	2.37	1577	2058	11.93	-4.01	127.2	50	126.2	60	108.5	70
3	2.55	1620	2163	12.53	-3.97	128.2	50	127.0	60	109.5	60
4	2.60	2070	2467	11.19	-4.99	131.8	50	129.5	50	110.9	60
5	3.33	2609	3067	12.95	-5.36	132.9	40	132.2	50	116.6	50
6	3.50	2659	3150	13.20	-5.30	136.1	40	133.3	50	117.7	50
1/12/70											
1	2.80	1787	2371	13.35	-4.17	129.5	50	128.2	60	110.9	60
2	3.00	2117	2656	12.69	-4.73	132.3	50	130.0	50	113.4	50
3	3.00	2239	2800	13.27	-4.80	133.6	40	130.4	50	114.5	50
4	3.33	2439	2964	13.14	-5.07	134.4	40	131.8	50	116.2	50

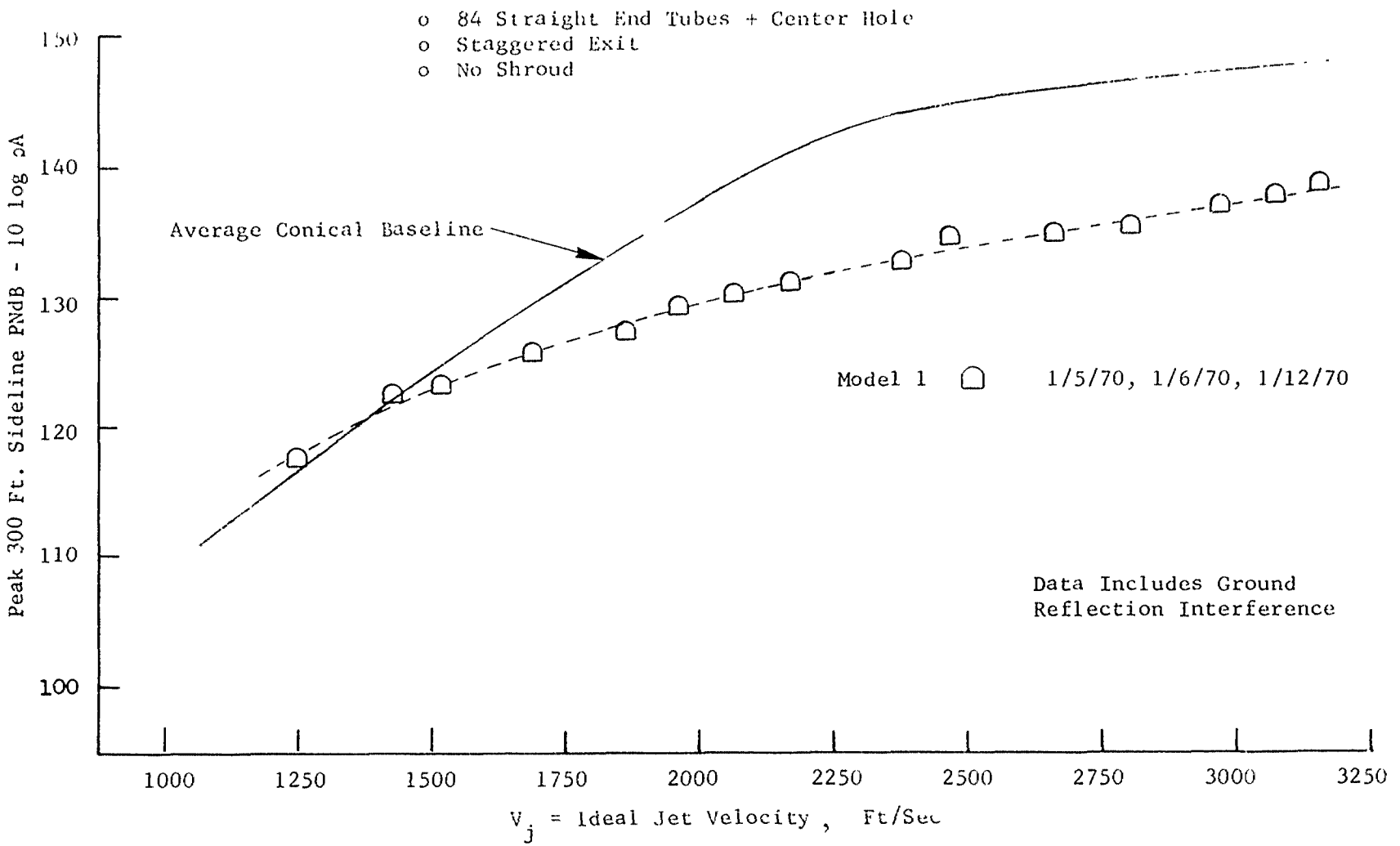

FIGURE V.F.10-8 300 FT. SIDELINE JET NOISE LEVELS FOR PD-3 MODEL 1

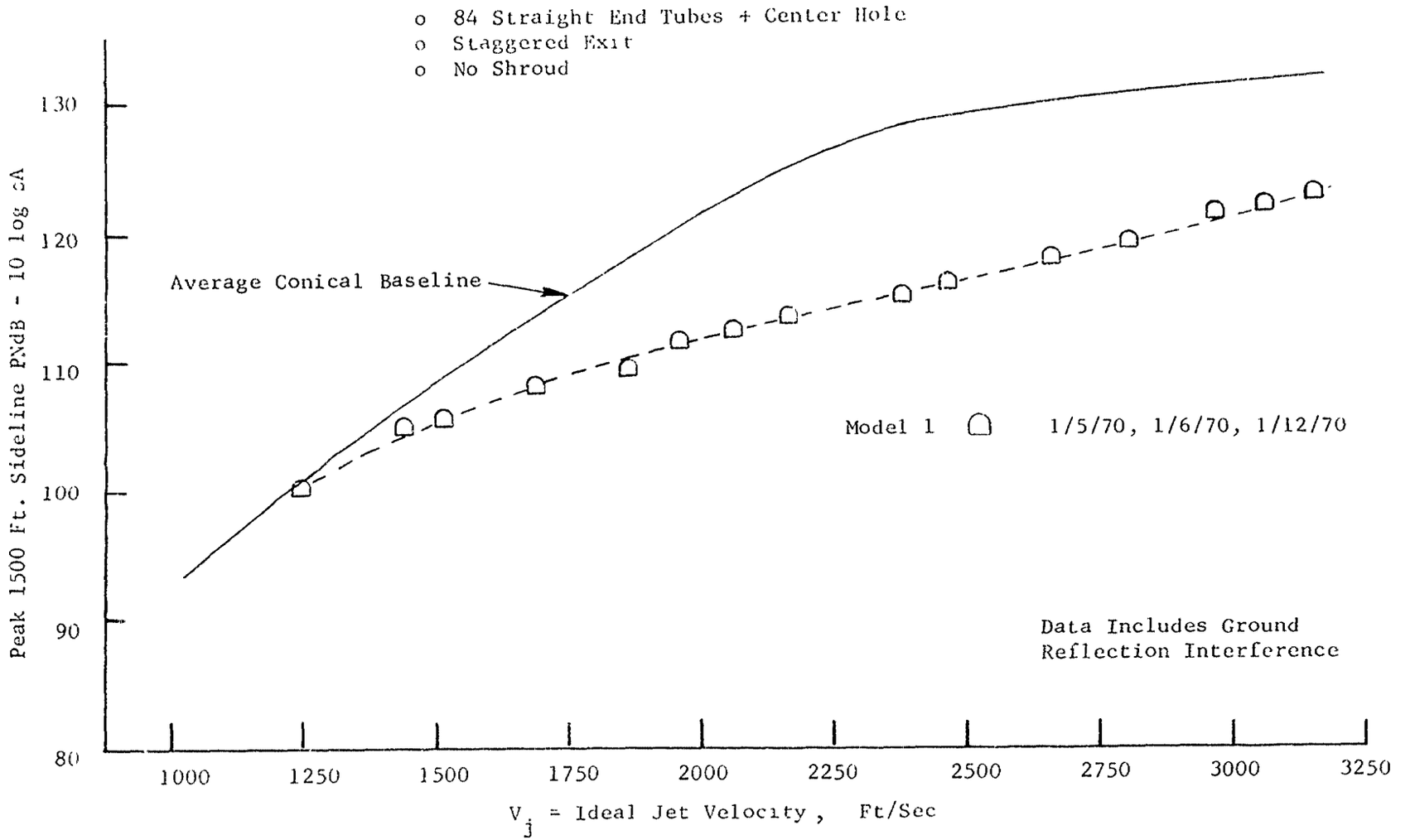

FIGURE V.F.10-9 1500 FT. SIDELINE JET NOISE LEVELS FOR PD-3 MODEL 1

TABLE V.F.10-2 TEST SUMMARY

NOZZLE NO. 3

CONFIGURATION: Plain End Tubes, Coplanar Exit

TEST: 2/6/70; 2/11/70; 2/16/70

SCALE MODEL A_8 = .1978 ft^2

FULL SCALE A_8 = 12.662 ft^2

SCALE FACTOR = 8:1

- DATA INCLUDES GROUND REFLECTION INTERFERENCE
- ANGLE REFERENCED TO JET EXHAUST

RDG NO.	TEST CONDITIONS				ACOUSTIC TEST RESULTS						
			IDEAL			320' ARC		300' SIDELINE		1500' SIDELINE	
	P_{T8}/P_o	T_{T8} (°R)	V_j (ft/sec)	W_8 (PPS)	10 log ρA	PEAK PNdB	PEAK ANGLE	PEAK PNdB	PEAK ANGLE	PEAK PNdB	PEAK ANGLE
2/6/70											
1	3.48	2686	3159	13.01	-5.30	-	-	129.7	70	114.1	40
2	3.31	2629	3072	12.49	-5.34	-	-	129.2	70	113.5	50
3	3.30	2435	2953	12.89	-5.02	-	-	128.9	70	112.1	70
4	3.19	2219	2782	13.06	-4.72	-	-	128.2	70	111.1	70
5	3.00	2120	2657	12.62	-4.68	-	-	127.7	70	110.6	70
6	2.79	1786	2364	12.94	-4.13	-	-	126.4	70	109.2	70
7	2.53	2147	2462	10.65	-5.15	-	-	126.4	70	109.2	70
8	2.53	1662	2182	12.09	-4.04	-	-	124.8	70	107.5	70
9	2.36	1551	2037	11.75	-3.89	-	-	124.1	70	106.7	70
2/11/70											
1	1.47	1136	1198	8.34	-3.05	113.8	70	113.8	70	96.4	70
2	1.60	1509	1519	7.89	-4.32	117.5	70	117.7	80	100.3	70/80
2/16/70											
1	3.51	2666	3157	13.40	-5.28	134.2	30	130.7	50	114.6	50
2	3.03	2126	2669	12.96	-4.70	130.2	50	127.9	50	110.6	50
3	2.38	1562	2053	12.07	-3.93	126.0	50	124.5	70	107.0	70
4	2.25	1526	1965	11.45	-3.95	125.0	50	124.5	70	107.0	70
5	2.08	1527	1879	10.51	-4.09	123.9	50	123.2	70	105.7	70
6	1.83	1526	1716	9.23	-4.26	121.3	50	120.9	70	103.4	70
7	1.68	1527	1601	8.44	-4.32	119.5	50	118.3	80	100.7	60

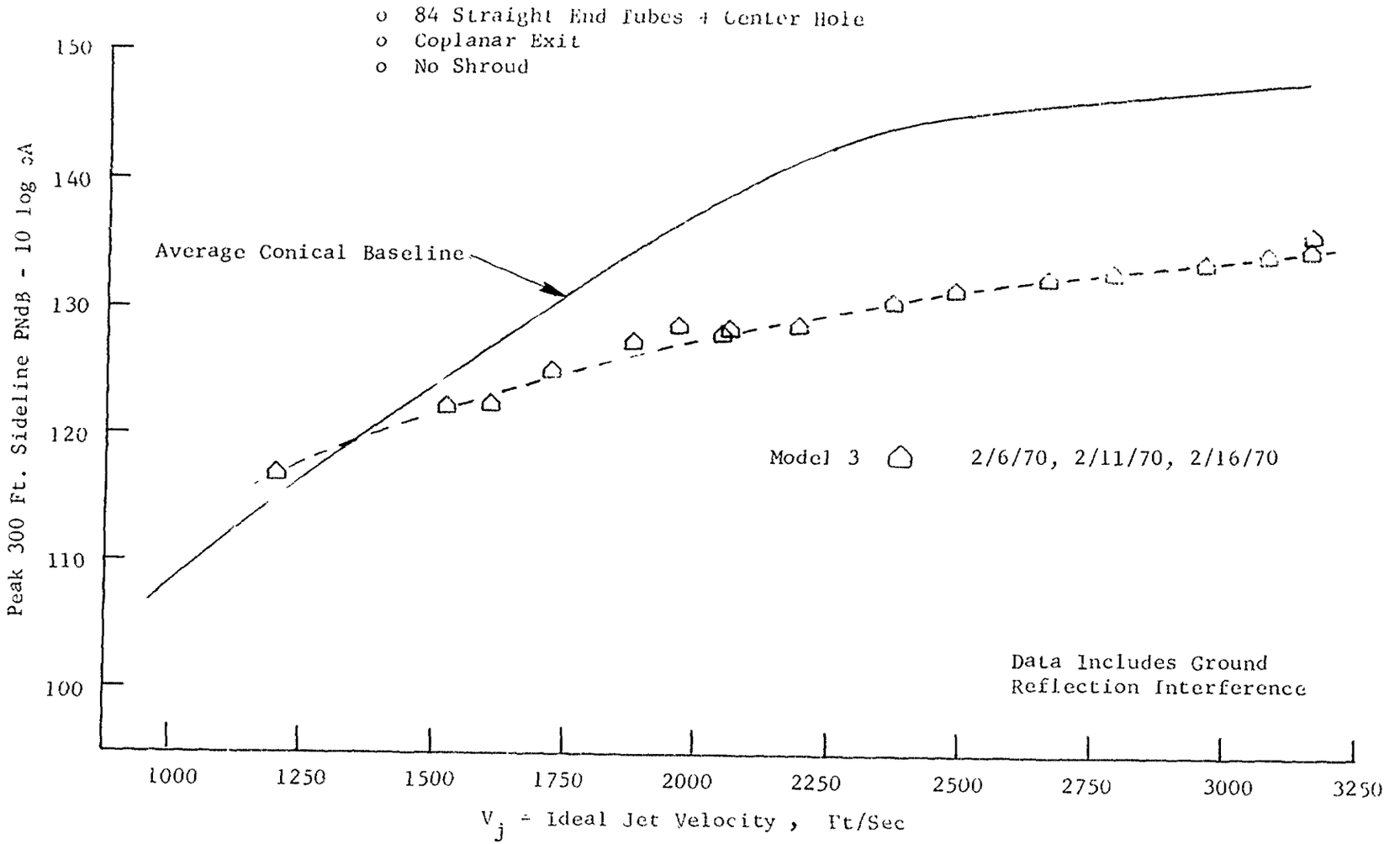

FIGURE V.F.10-10 300 FT. SIDELINE JET NOISE LEVELS FOR PD-3 MODEL 3

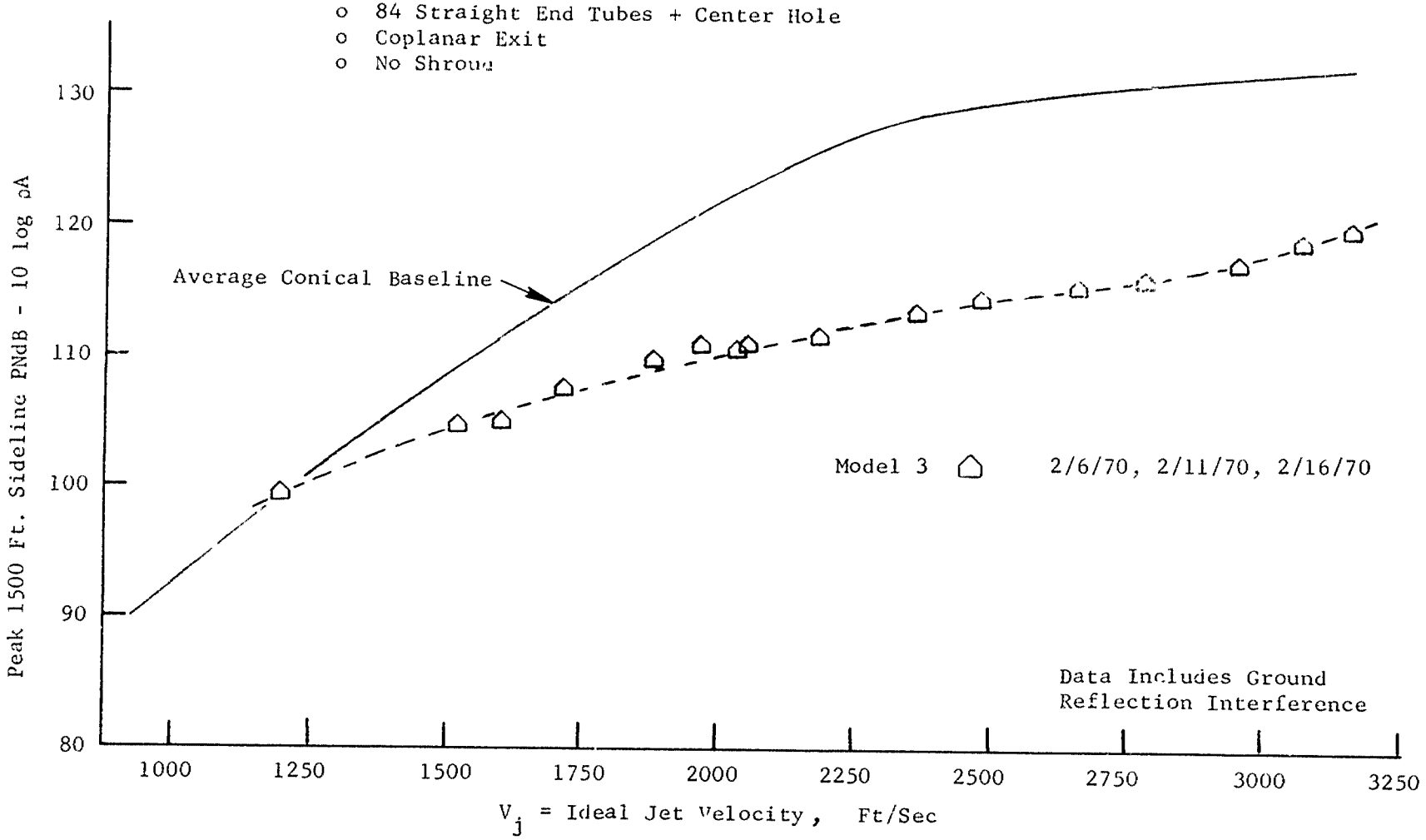

FIGURE V.F.10-11 1500 FT. SIDELINE JET NOISE LEVELS FOR PD-3 MODEL 3

TABLE V.F.10-3 TEST SUMMARY

MODEL NO. 4

DESCRIPTION: Plain End Tubes, Coplanar Exit, Secondary Shroud

DATE: 3/5/70; 3/9/70

SCALE MODEL A_8 = .1978 ft^2

FULL SCALE A_8 = 12.662 ft^2

SCALE FACTOR = 8:1

- DATA INCLUDES GROUND REFLECTION INTERFERENCE
- ANGLE REFERENCED TO JET EXHAUST

	TEST CONDITIONS				ACOUSTIC TEST RESULTS						
			IDEAL			320' ARC		300' SIDELINE		1500' SIDELINE	
RDG NO.	P_{T8}/P_o	T_{T8} (°R)	V_j (ft/sec)	W_8 (PPS)	10 log ρA	PEAK PNdB	PEAK ANGLE	PEAK PNdB	PEAK ANGLE	PEAK PNdB	PEAK ANGLE
3/5/70											
1	1.48	1147	1215	8.39	-3.1	112.1	50	110.8	70	94.3	60
2	1.59	1521	1516	7.86	-4.3	117.0	70	117.0	70	99.7	70
3	1.68	1532	1604	8.52	-4.4	119.2	60	118.8	70	101.5	70
4	1.80	1536	1700	8.86	-4.3	119.5	60	119.2	70	101.9	70
5	2.08	1527	1879	10.34	-4.1	123.6	70	123.6	70	106.2	70
6	2.24	1545	1976	11.12	-4.0	123.1	80	123.7	80	106.2	80
3/9/70											
1	2.37	1567	2049	11.75	-4.0	124.1	50	124.5	90	107.2	90
2	2.54	1658	2186	12.31	-4.1	126.9	60	126.0	60	108.7	60
3	2.66	2151	2545	11.18	-5.1	126.4	70/80	126.9	80	109.6	80
4	2.80	1809	2384	13.04	-4.3	127.1	70	127.1	70	109.7	70
5	3.04	2158	2694	12.75	-4.8	128.7	70	128.8	70	111.5	70
6	3.20	2270	2818	12.93	-4.9	127.3	90	128.0	90	110.6	80/90
7	3.49	2696	3169	13.17	-5.4	129.5	50	129.0	70	112.0	70

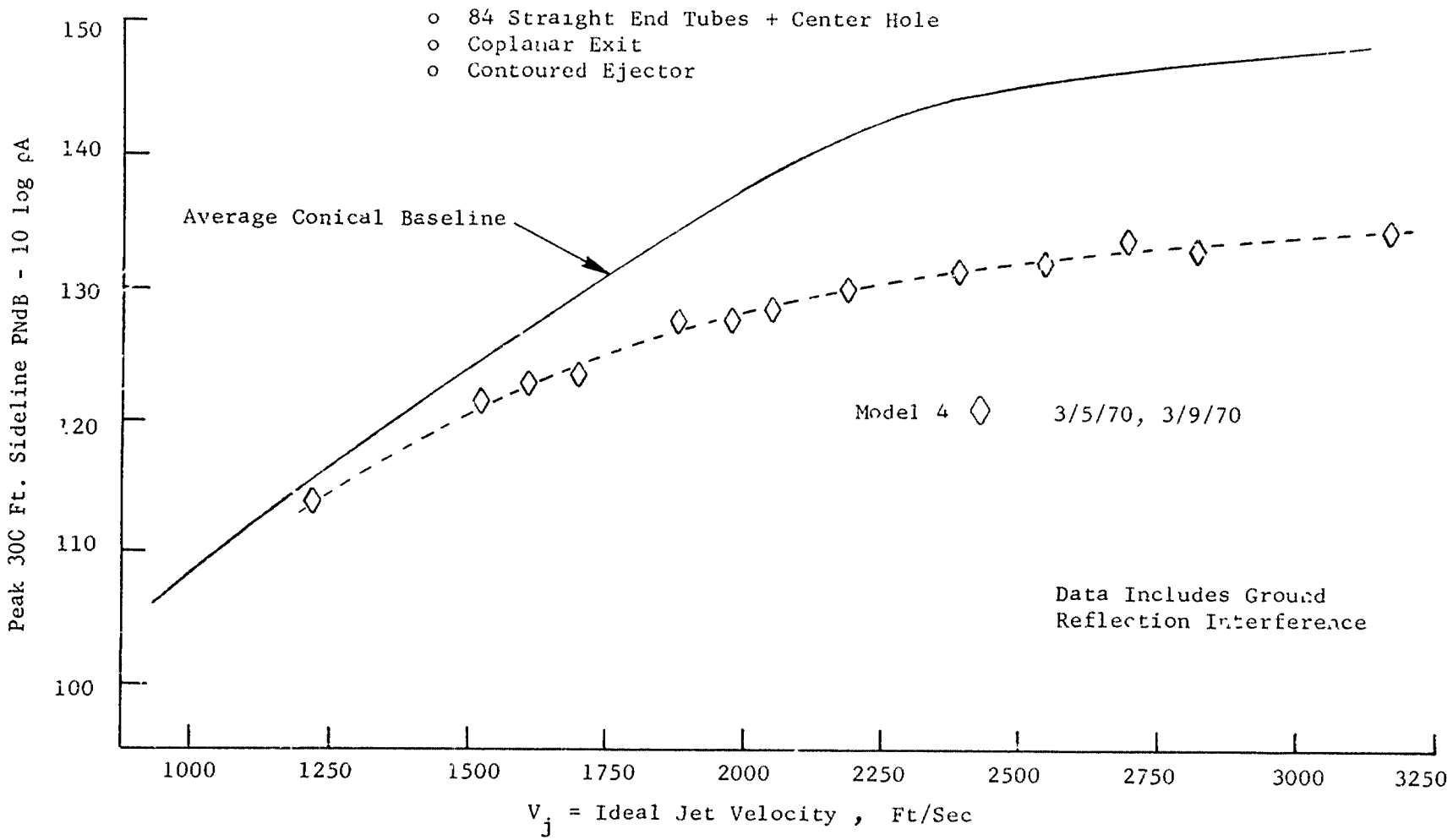

FIGURE V.F.10-12 300 FT. SIDELINE JET NOISE LEVELS FOR PD-3 MODEL 4

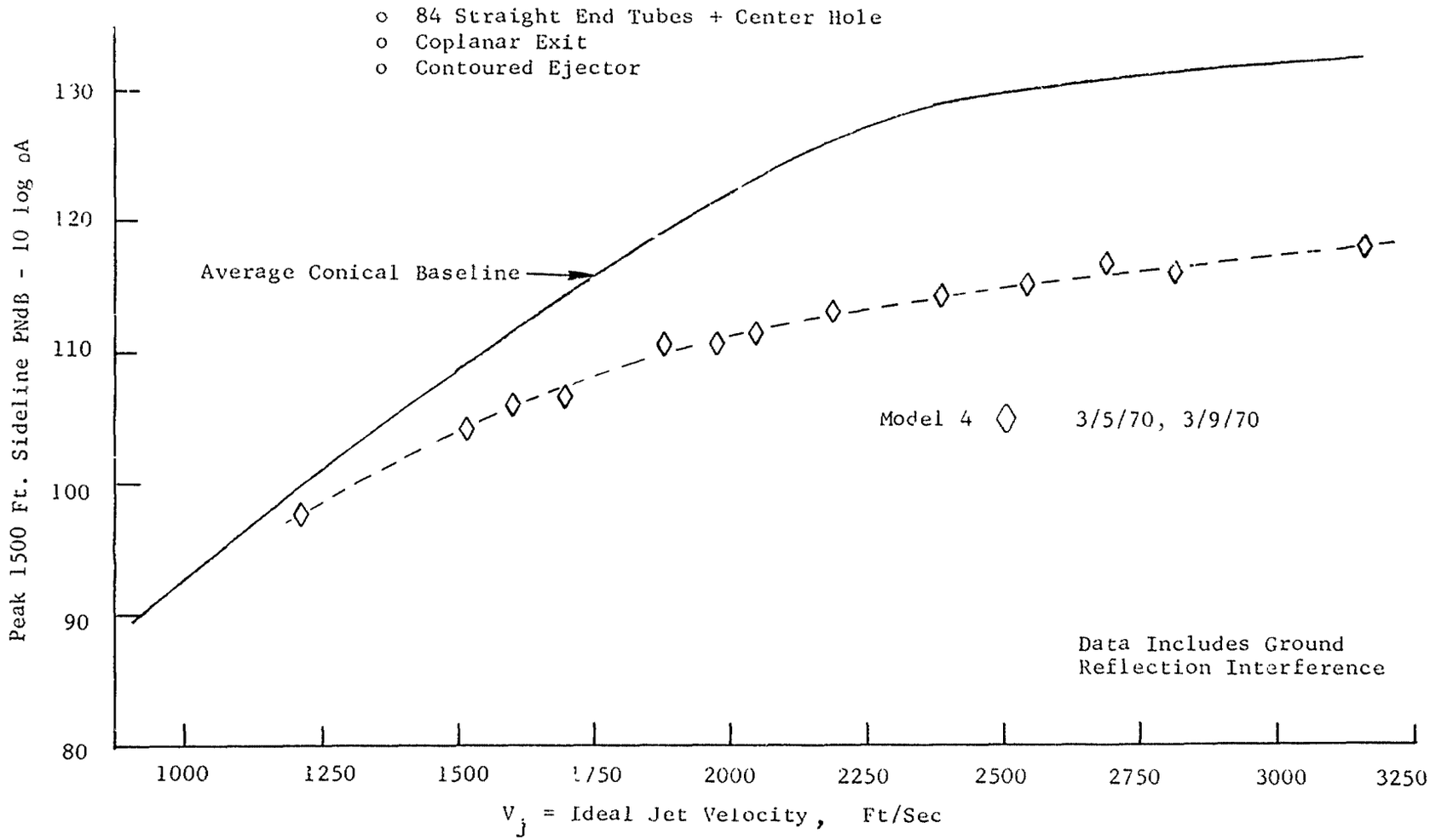

FIGURE V.F.10-13 1500 FT. SIDELINE JET NOISE LEVELS FOR PD-3 MODEL 4

TABLE V.F.10-4 TEST SUMMARY

MODEL NO. 5

DESCRIPTION: Greatrex End Tubes, Staggered Exit

DATE: 12/19/69; 12/22/69

SCALE MODEL A_8 = .2137 ft^2

FULL SCALE A_8 = 13.676 ft^2

SCALE FACTOR = 8:1

- DATA INCLUDES GROUND REFLECTION INTERFERENCE
- ANGLE REFERENCED TO JET EXHAUST

RPG NO.	TEST CONDITIONS				ACOUSTIC TEST RESULTS						
			IDEAL			320' ARC		300' SIDELINE		1500' SIDELINE	
	P_{T8}/P_o	T_{T8} (°R)	V_j (ft/sec)	W_8 (PPS)	10 log ρA	PEAK PNdB	PEAK ANGLE	PEAK PNdB	PEAK ANGLE	PEAK PNdB	PEAK ANGLE
12/19/69											
1	1.46	1159	1198	8.48	-3.1	117.0	40	112.5	60	94.7	60
2	1.61	1521	1538	8.49	-4.3	118.1	50	116.0	60	97.4	60
3	1.66	1235	1427	9.74	-3.4	117.8	50	115.2	50	96.8	60
4	1.82	1512	1700	9.52	-4.2	120.9	50	118.4	50	100.7	50
12/22/69											
1	2.25	1521	1963	11.70	-4.8	121.9	60	121.0	60	103.3	60
2	2.37	1555	2042	12.22	-3.8	123.4	50	122.2	60	104.6	60
3	2.56	1657	2189	12.88	-3.9	125.2	50	123.1	60	106.3	50
4	2.60	2131	2505	11.49	-4.3	129.3	30	125.6	50	109.9	50
5	2.88	1783	2372	13.65	-4.0	129.4	30	125.0	50	109.2	50
6	3.01	2122	2659	13.07	-4.6	132.8	40	128.8	40	113.6	40
7	3.22	2212	2789	13.65	-4.6	134.5	40	131.4	50	.0	50
8	3.33	2403	2942	13.63	-4.8	135.8	40	133.2	50	117.8	50
9	3.32	2593	3054	13.21	-5.2	136.3	50	134.2	50	118.8	50
10	3.52	2656	3153	13.76	-5.2	136.6	50	134.5	50	119.1	50

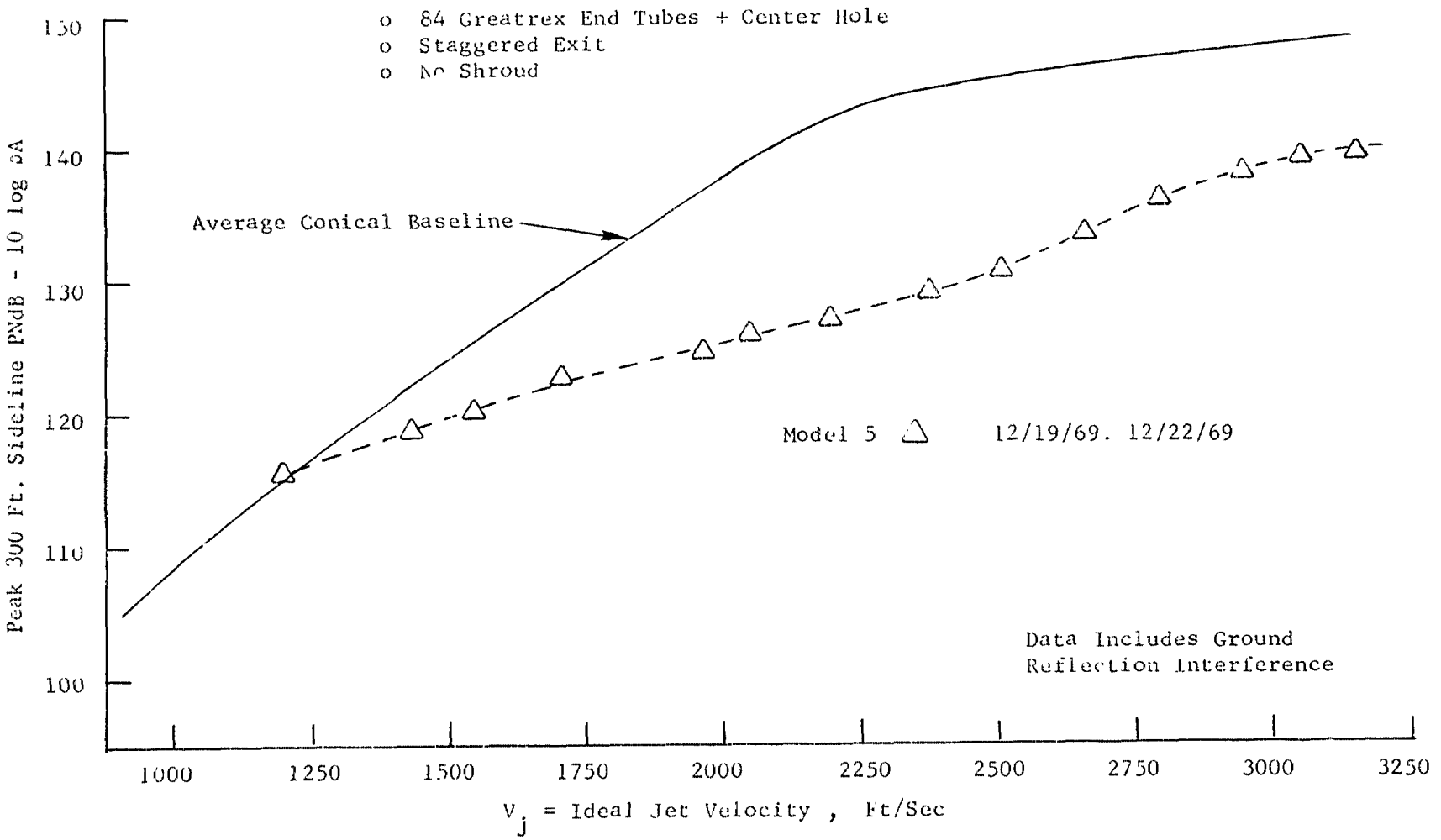

FIGURE V.F.10-14 300 FT. SIDELINE JET NOISE LEVELS FOR PD-3 MODEL 5

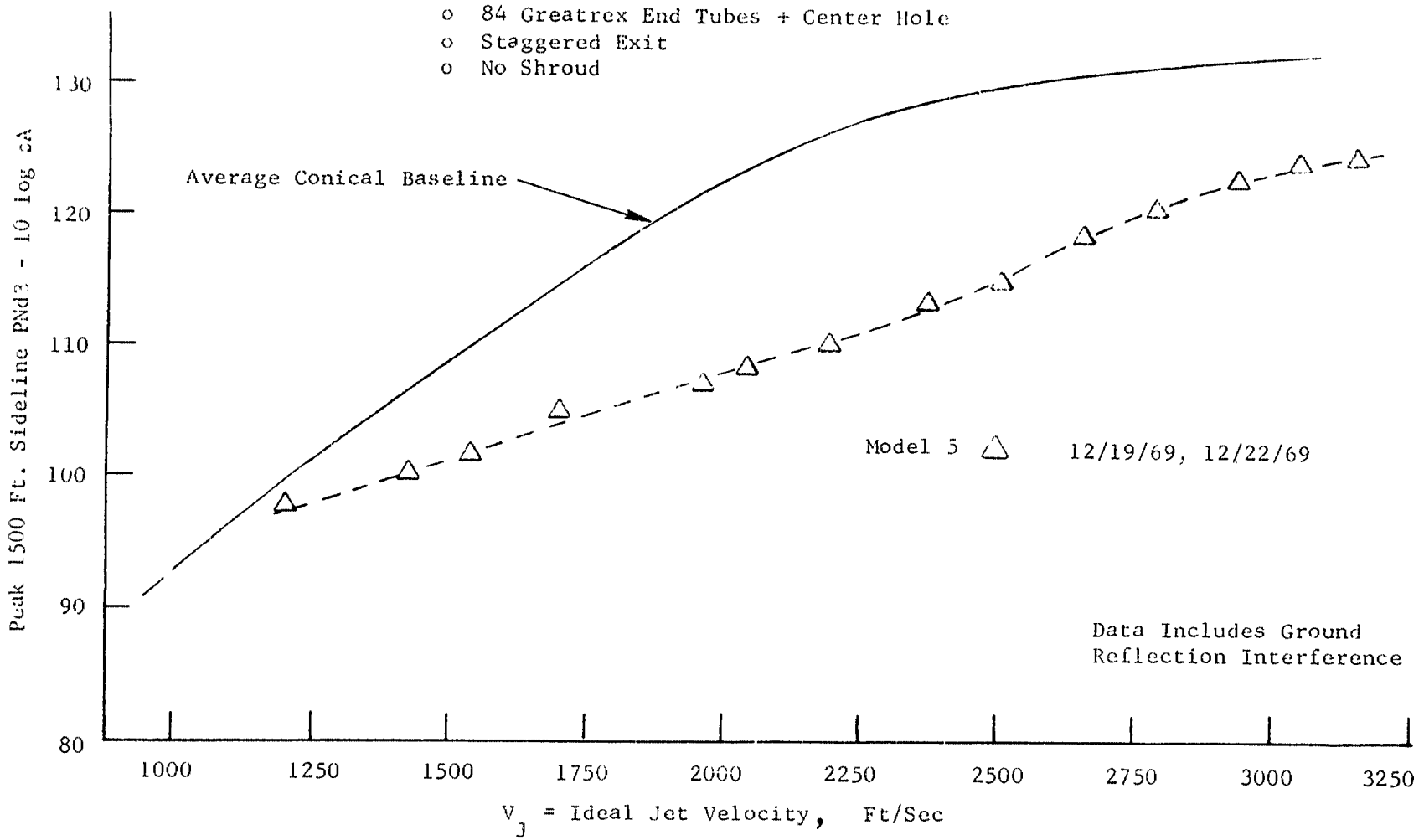

FIGURE V.F.10-15 150C FT. SIDELINE JET NOISE LEVELS FOR PD-3 MODEL 5

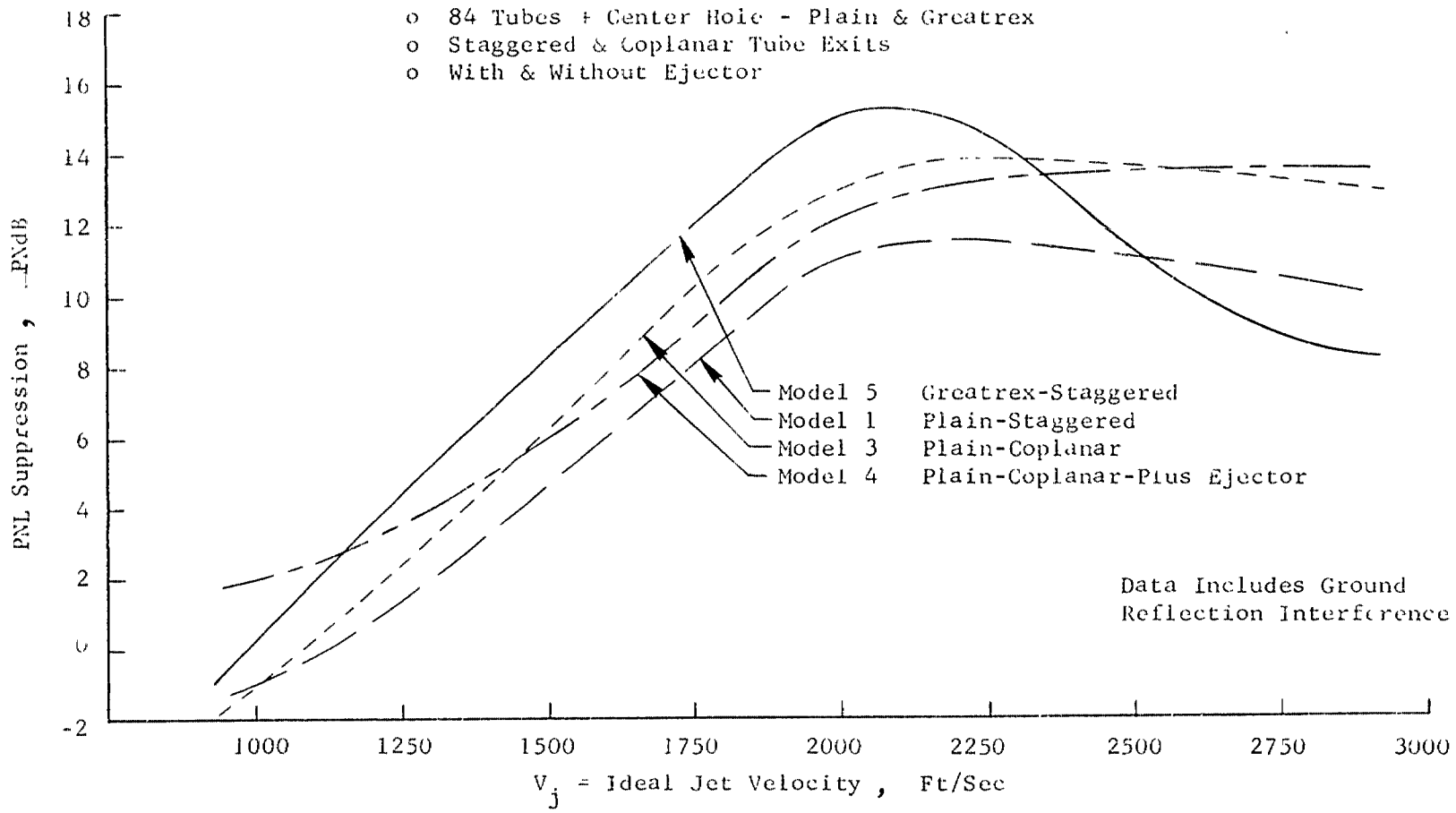

FIGURE V.F.10-16 COMPARISON OF 300 FT. SIDELINE PEAK PNL SUPPRESSION FOR PD-3 MODELS 1, 3, 4 & 5

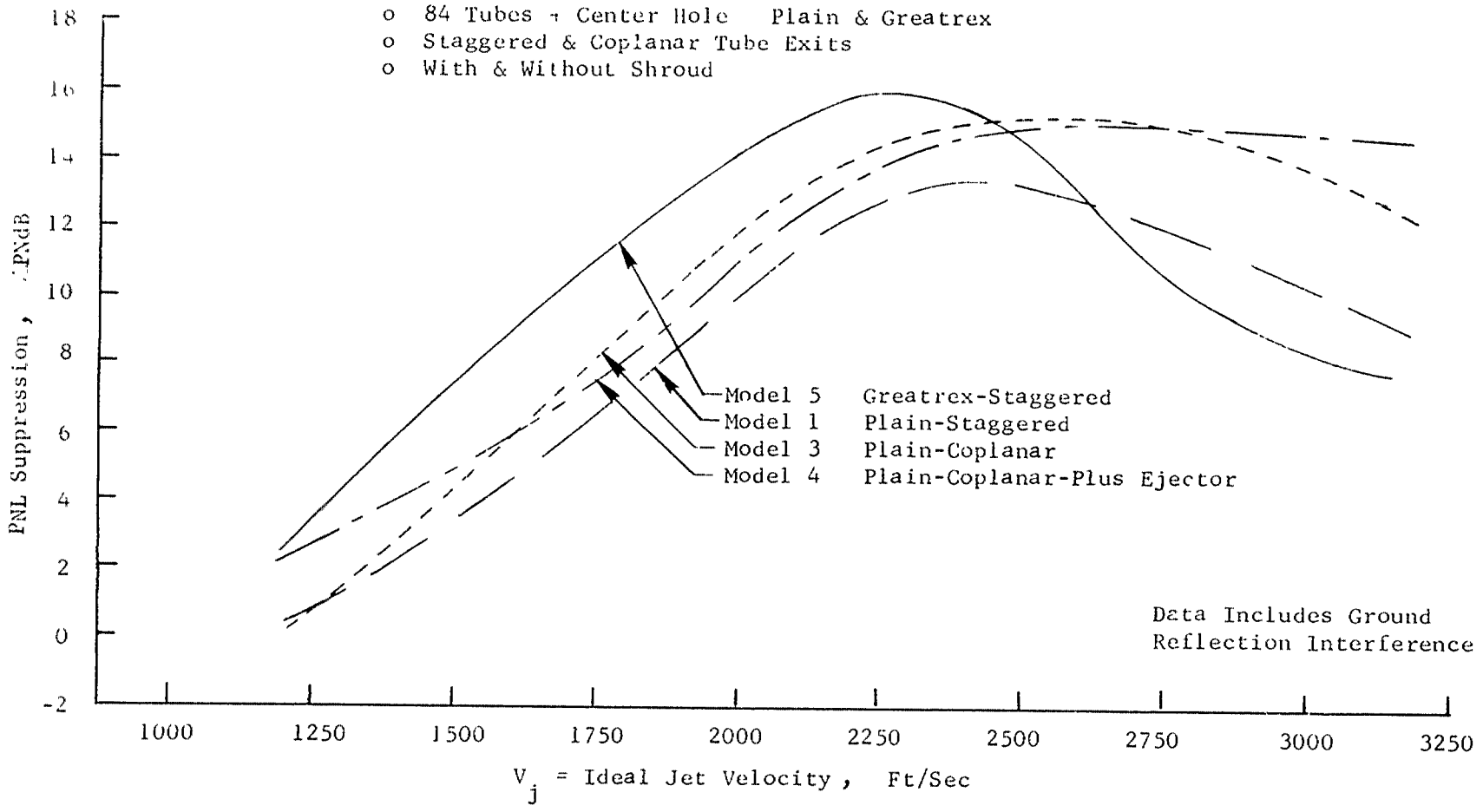

FIGURE V.F.10-17 COMPARISON OF 1500 FT. SIDELINE PEAK PNL SUPPRESSION FOR PD-3 MODELS 1, 3, 4 & 5

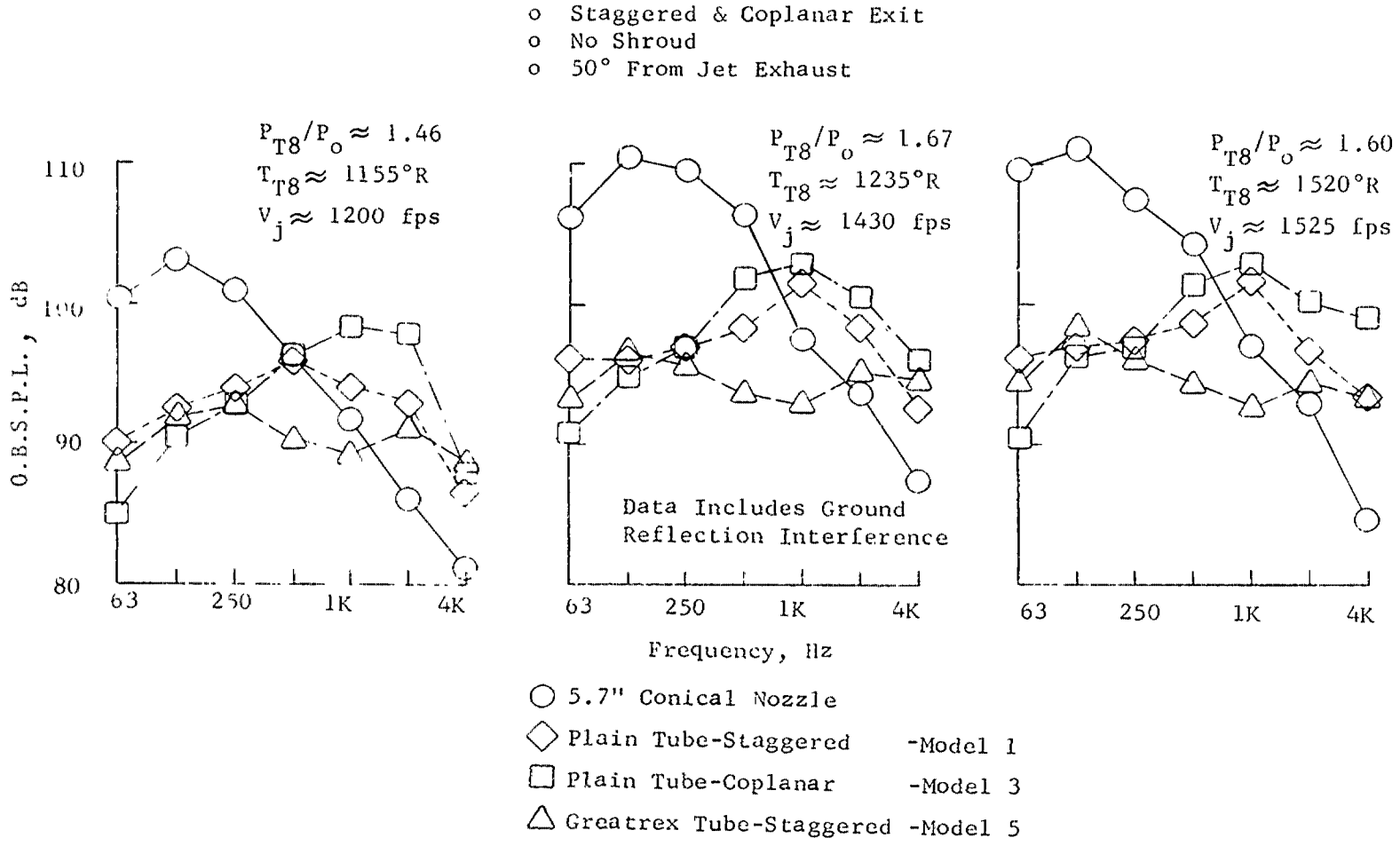

FIGURE V.F.10-18A EFFECT OF PD-3 TUBE END VARIATIONS ON 300 FT. SIDELINE SPECTRA

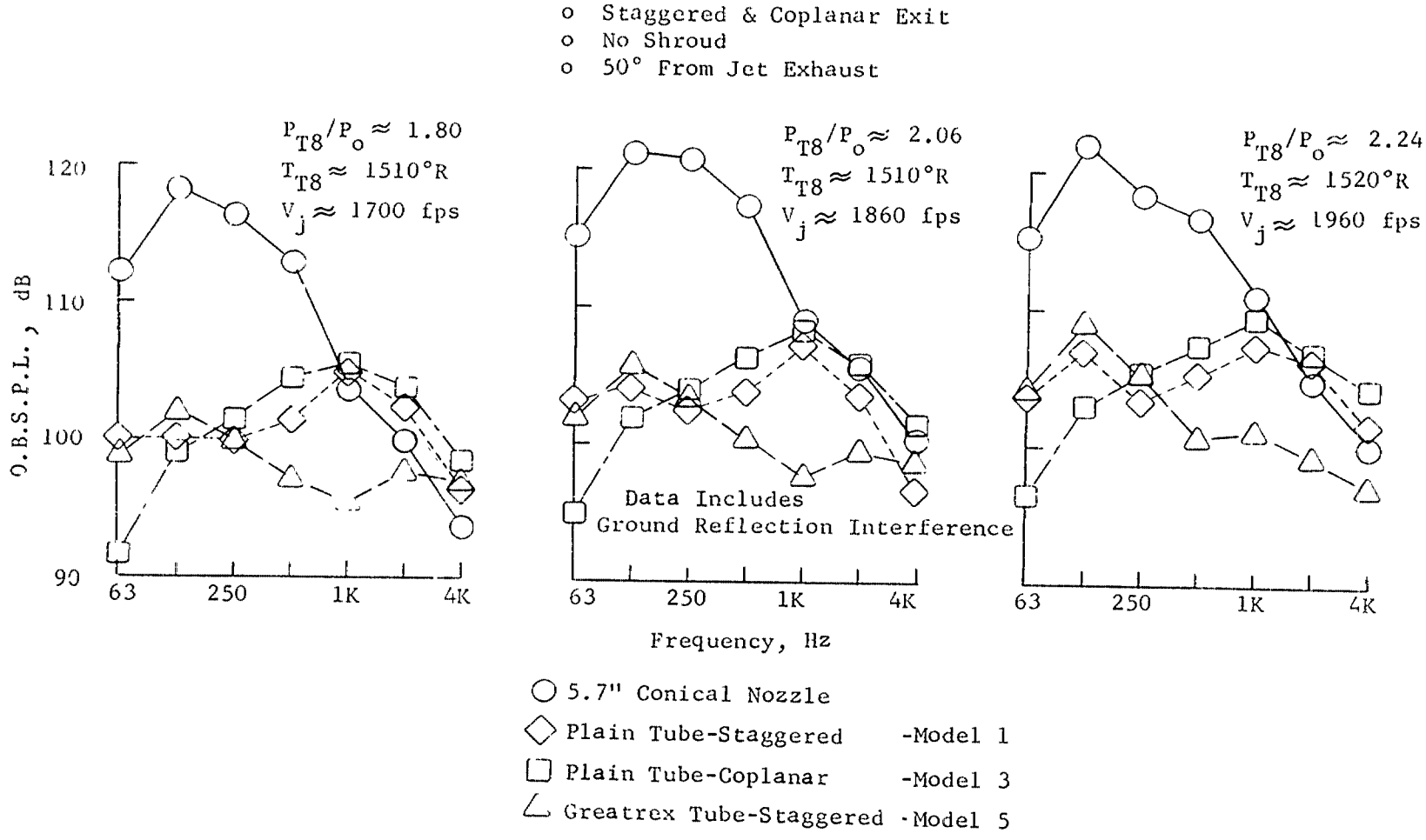

FIGURE V.F.10-18B EFFECT OF PD-3 TUBE END VARIATIONS ON 300 FT. SIDELINE SPECTRA

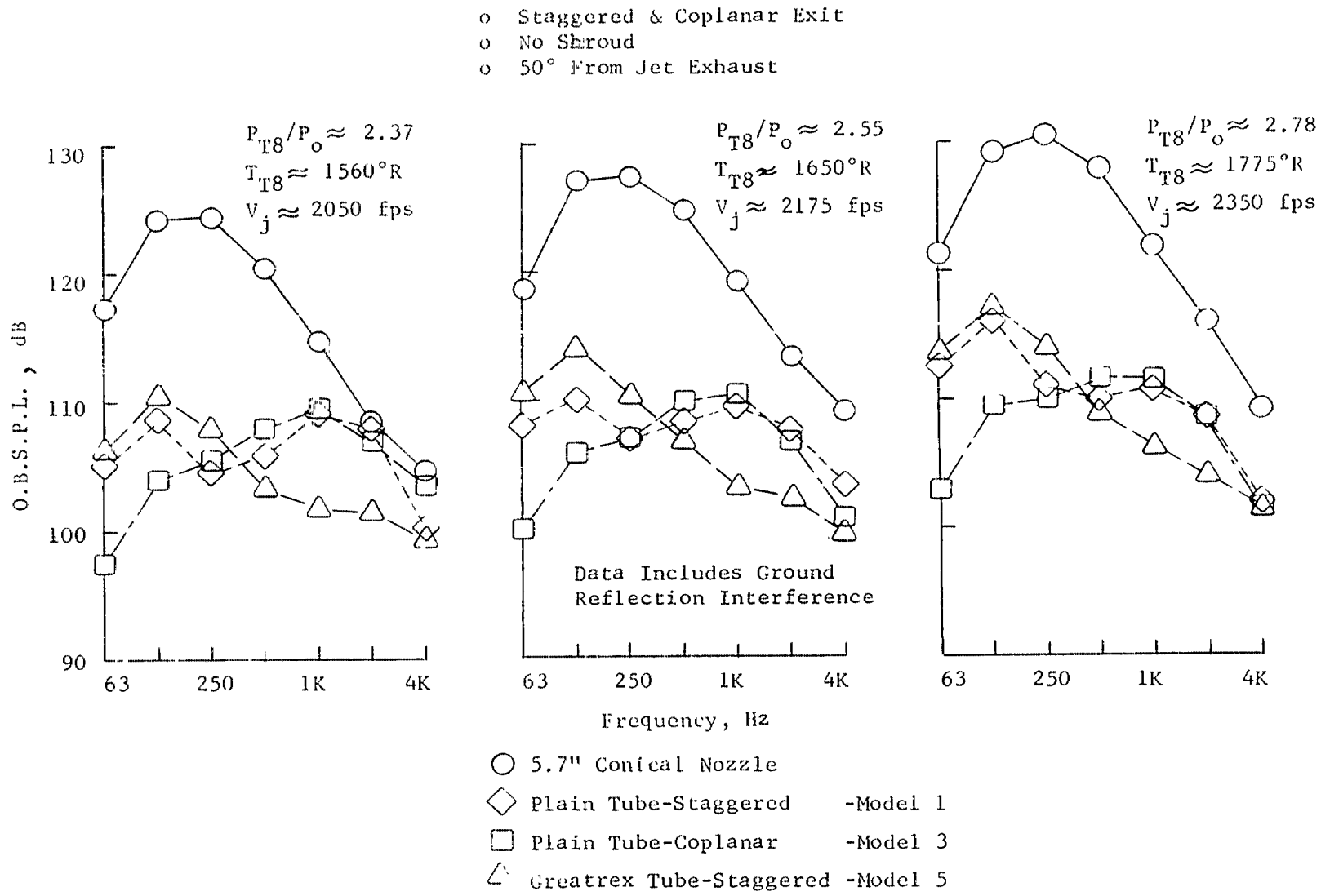

FIGURE V.F.10-18c EFFECT OF PD-3 TUBE END VARIATIONS ON 300 FT. SIDELINE SPECTRA

o Staggered & Coplanar Exit
o No Shroud
o 50° From Jet Exhaust

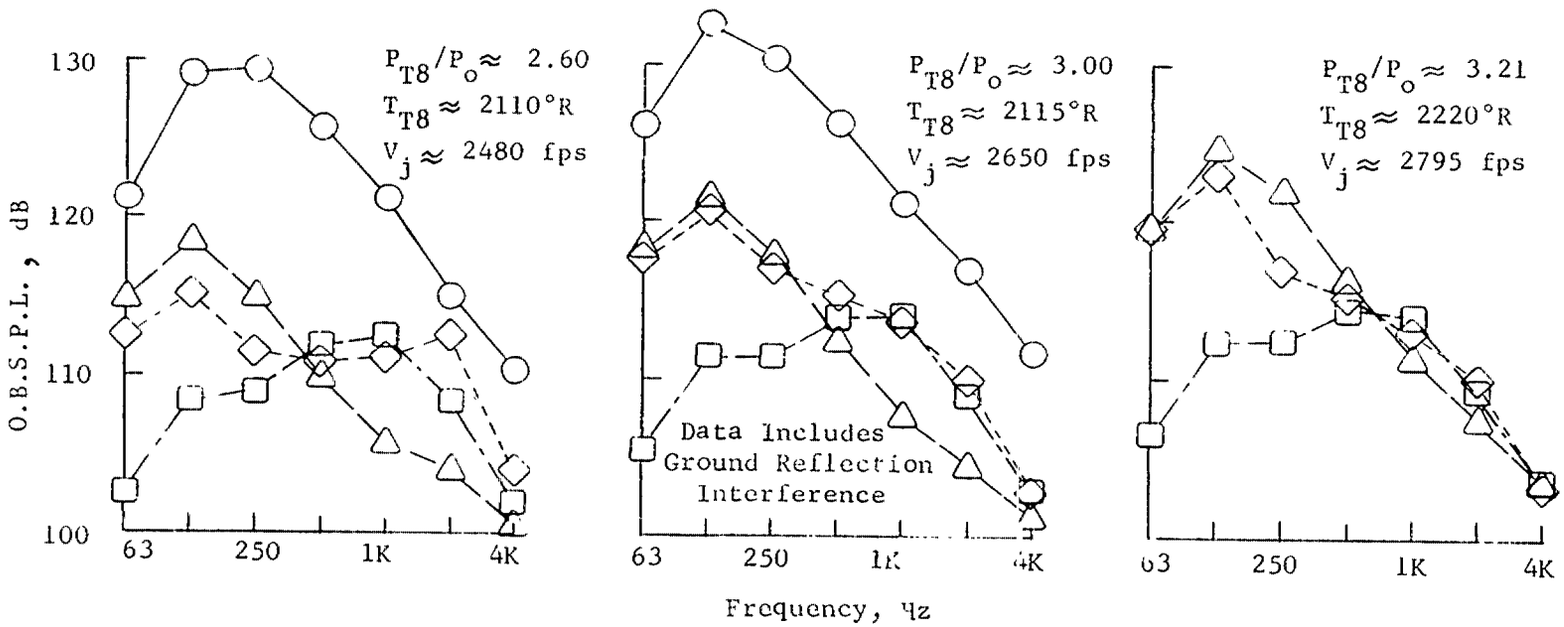

○ 5.7" Conical Nozzle
◇ Plain Tube-Staggered -Model 1
□ Plain Tube-Coplanar -Model 3
△ Greatrex Tube-Staggered -Model 5

FIGURE V.F.10-18D EFFECT OF PD-3 TUBE END VARIATIONS ON 300 FT. SIDELINE SPECTRA

- o Staggered & Coplanar Exit
- o No Shroud
- o 50° From Jet Exhaust

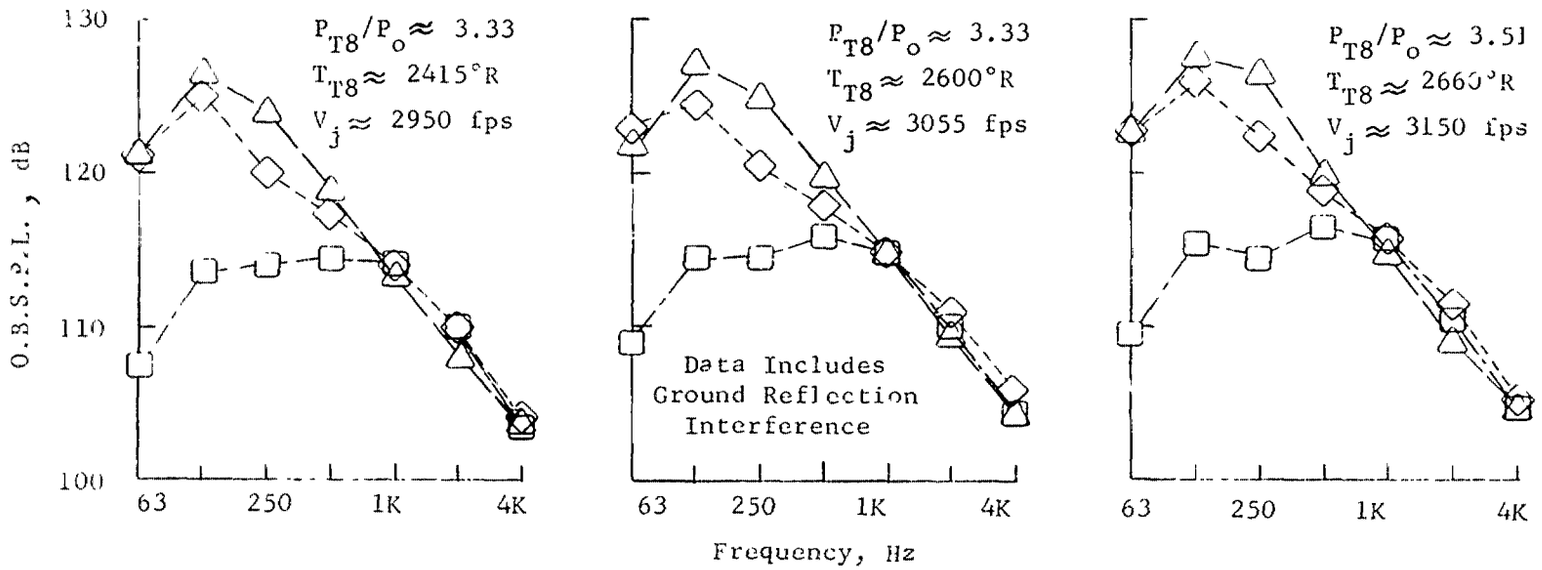

- ◇ Plain Tube-Staggered -Model 1
- □ Plain Tube-Coplanar -Model 3
- △ Greatrex Tube-Staggered -Model 5

FIGURE V.F.10-18E EFFECT OF TUBE END VARIATIONS ON 300 FT. SIDELINE SPECTRA

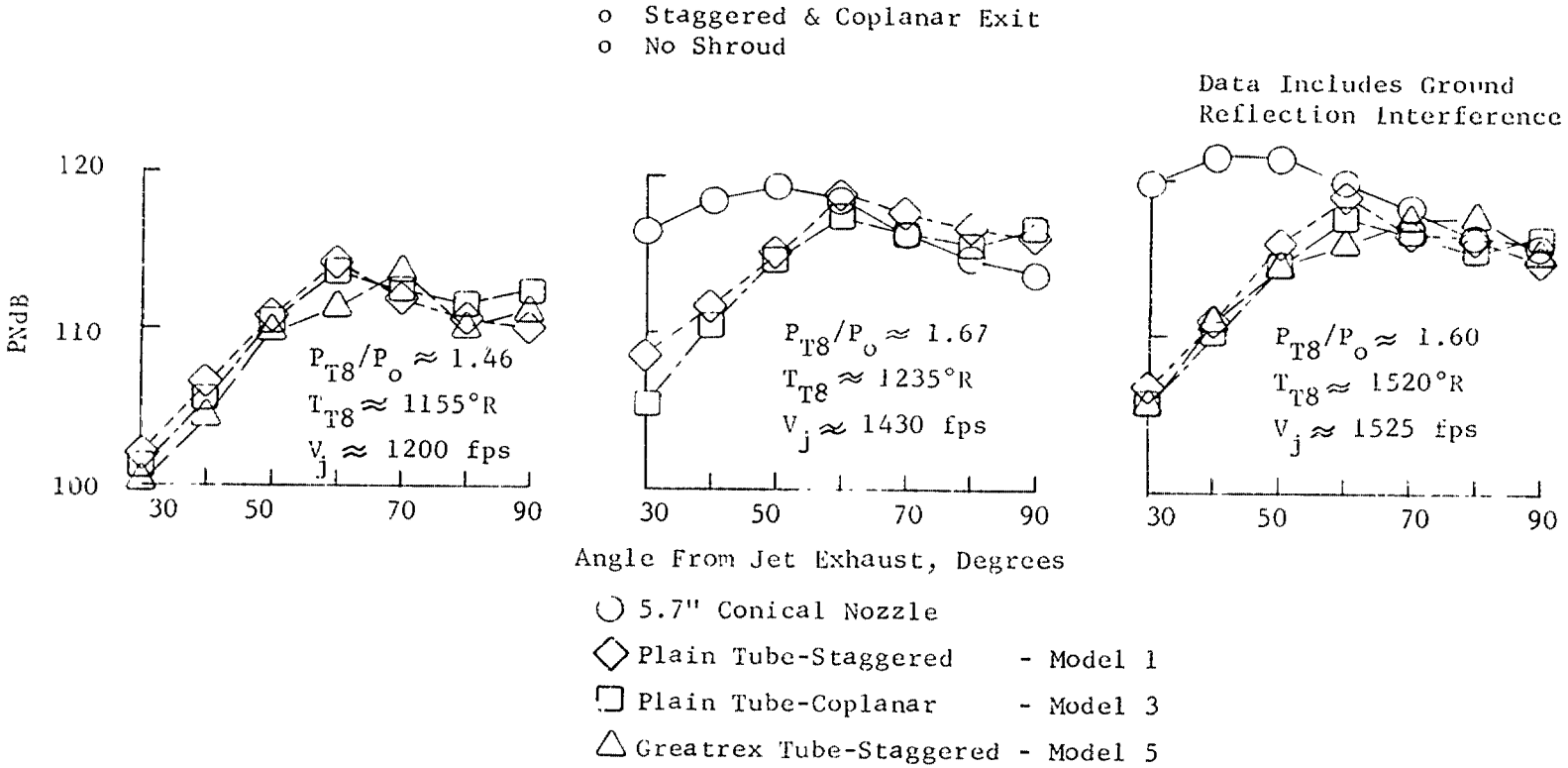

FIGURE V.F.10-19A EFFECT OF PD-3 TUBE END VARIATIONS ON 300 FT. SIDELINE DIRECTIVITY

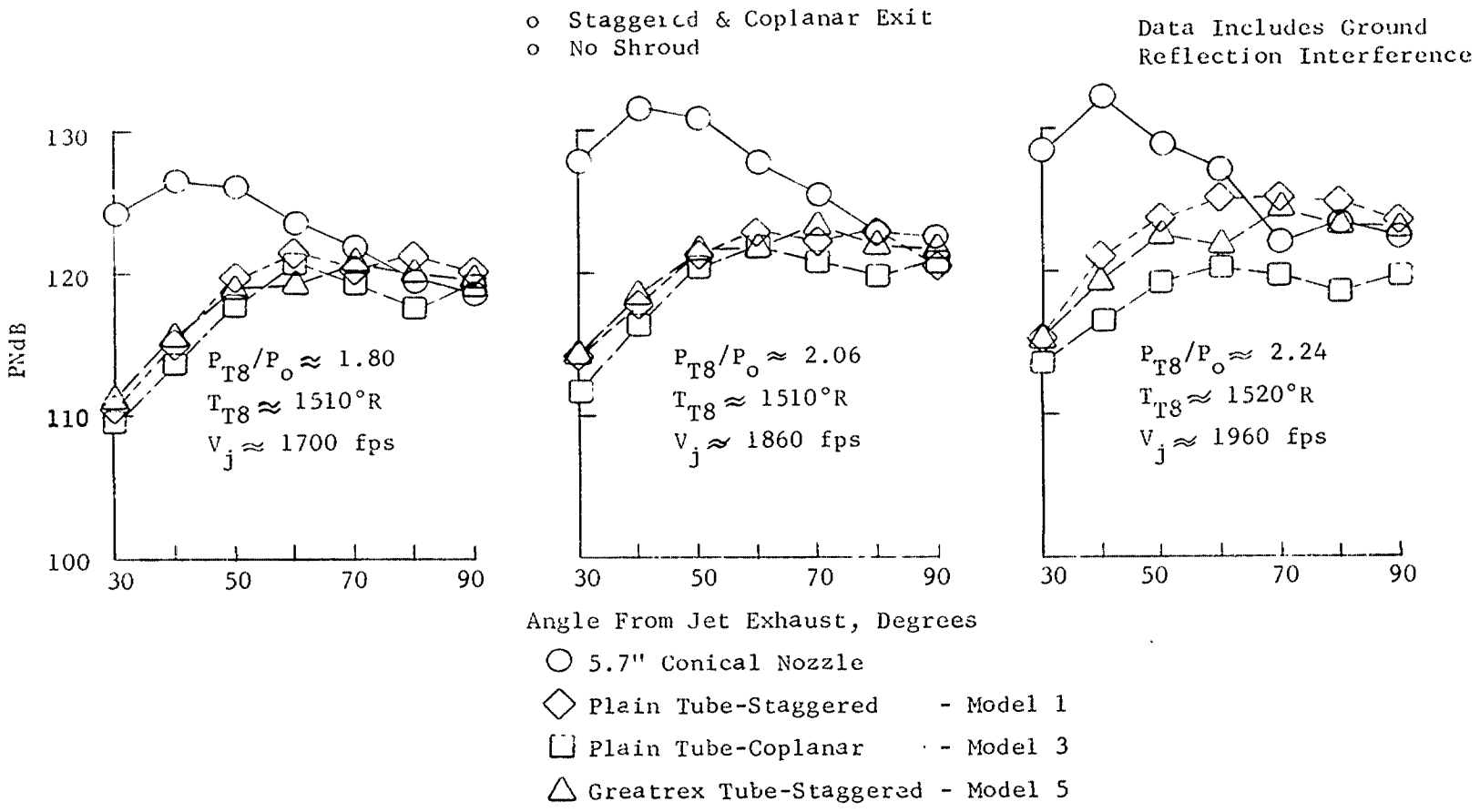

FIGURE V.F.10-19B EFFECT OF PD-3 TUBE END VARIATIONS ON 300 FT. SIDELINE DIRECTIVITY

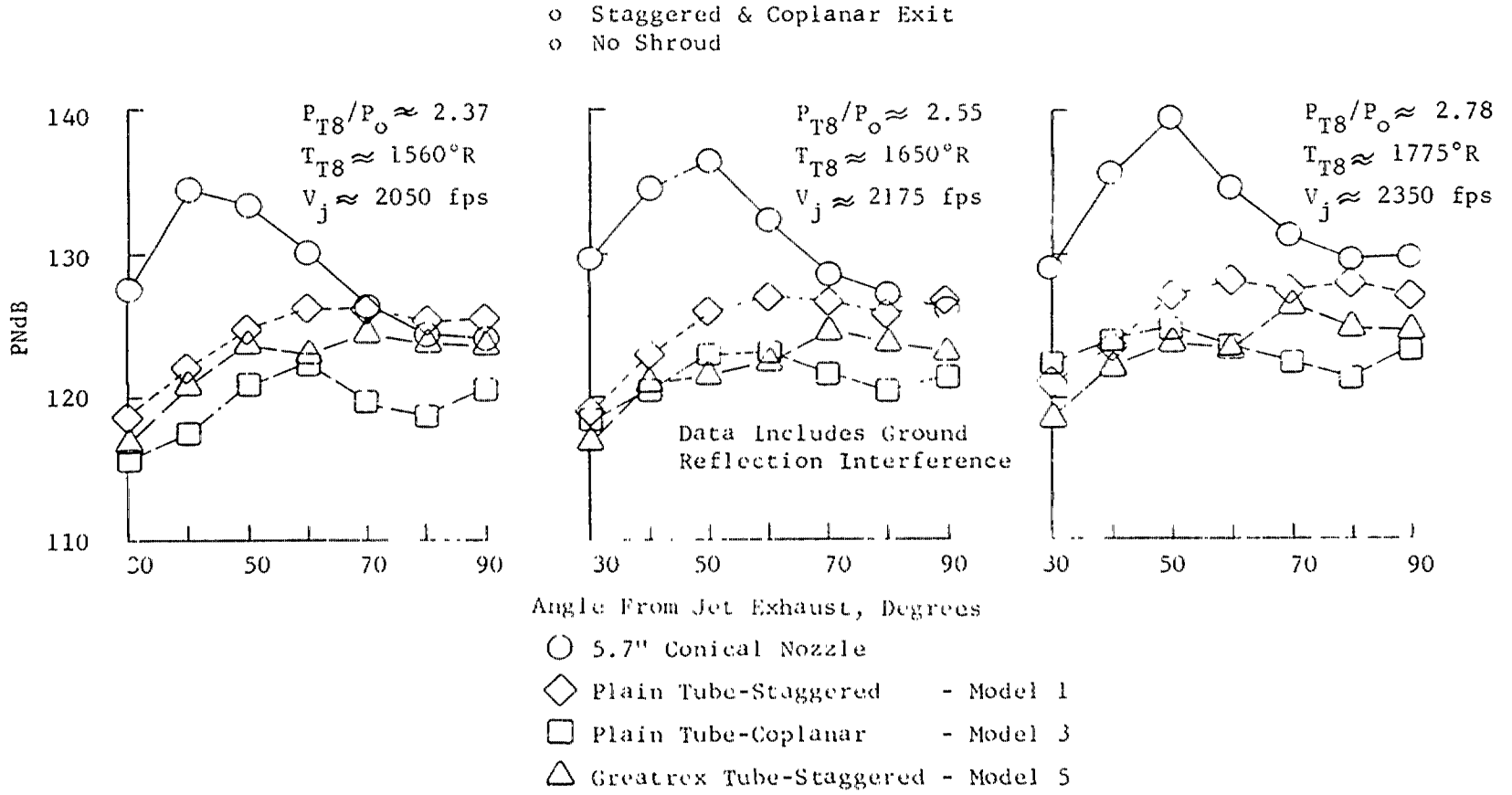

FIGURE V.F.10-19C EFFECT OF PD-3 TUBE END VARIATIONS ON 300 FT. SIDELINE DIRECTIVITY

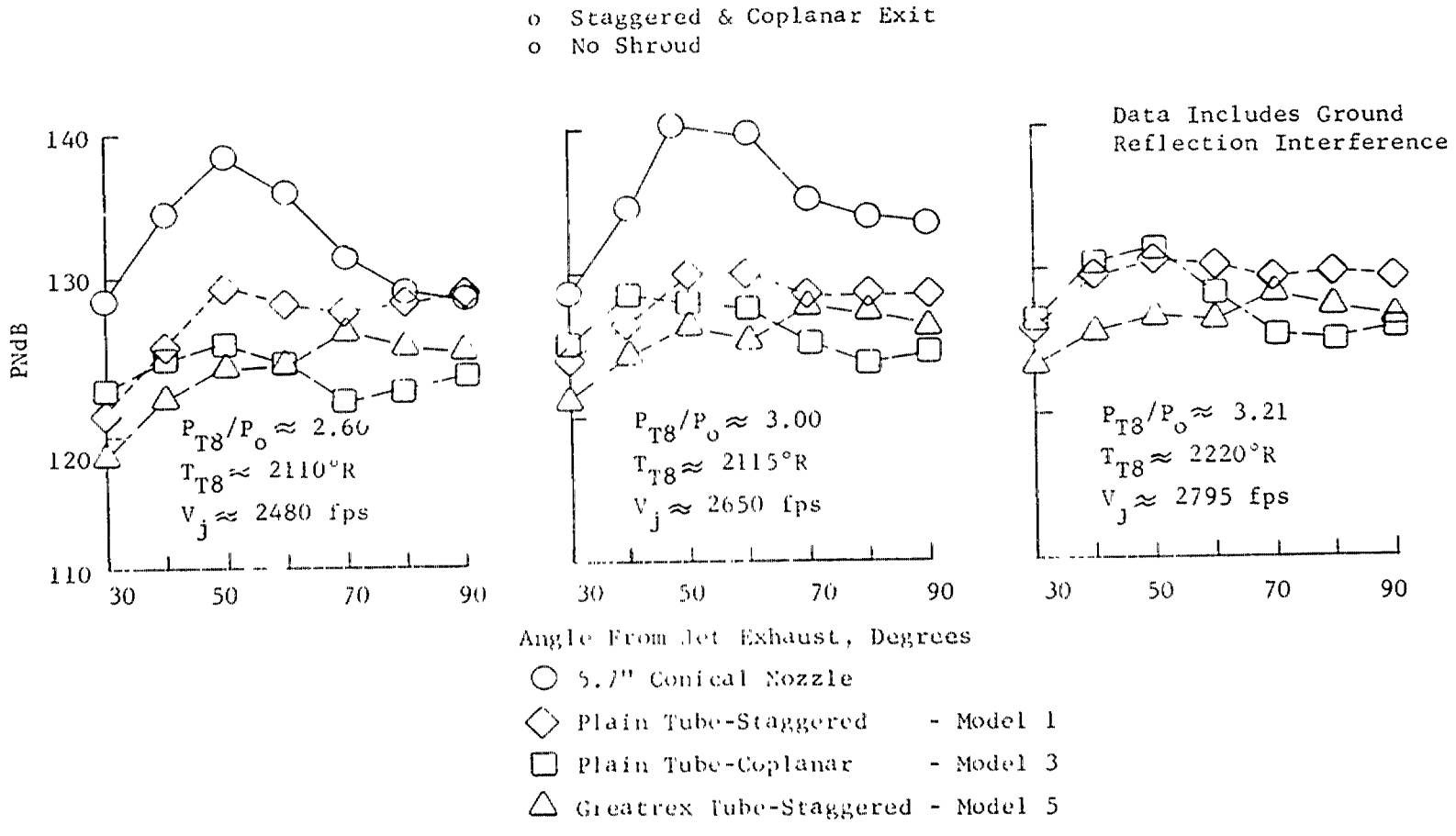

FIGURE V.F.10-19D EFFECT OF PD-3 TUBE END VAPIATIONS ON 300 FT. SIDELINE DIRECTIVITY

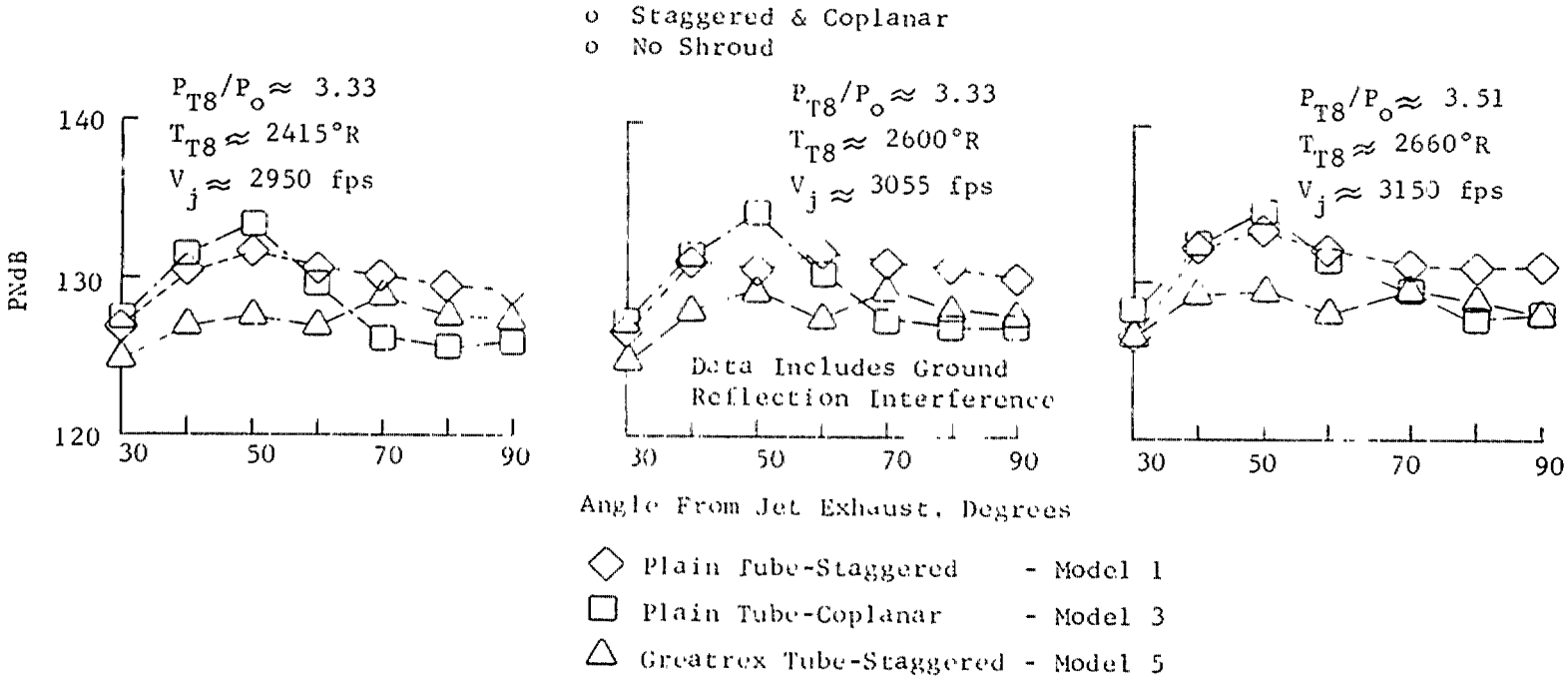

FIGURE V.F.10-19E EFFECT OF PD-3 TUBE END VARIATIONS ON 300 FT. SIDELINE DIRECTIVITY

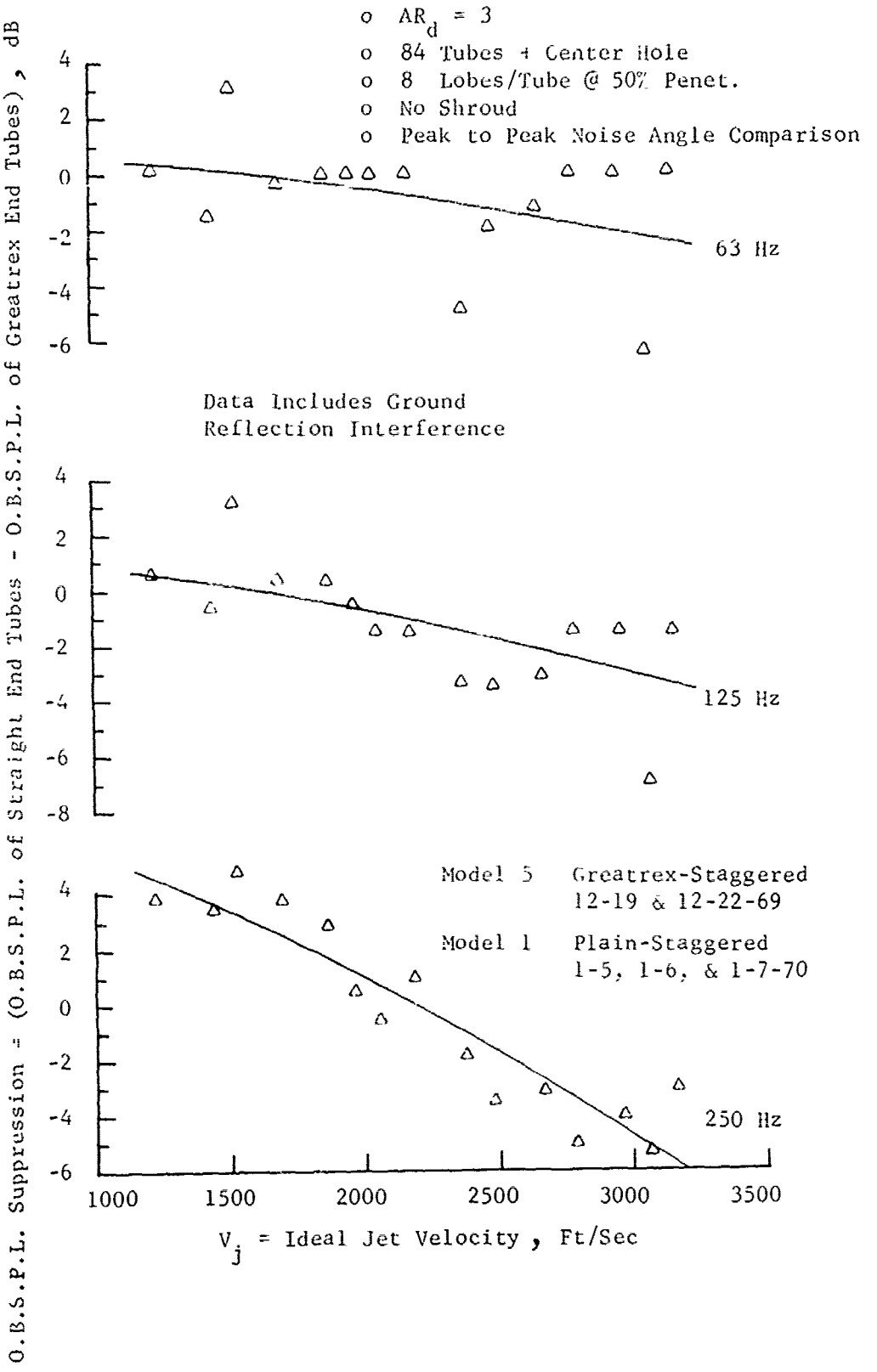

FIGURE V.F.10-20A OCTAVE BAND SPECTRAL SUPPRESSION ATTRIBUTABLE TO ADDITION OF PD-3 GREATREX TUBE ENDS

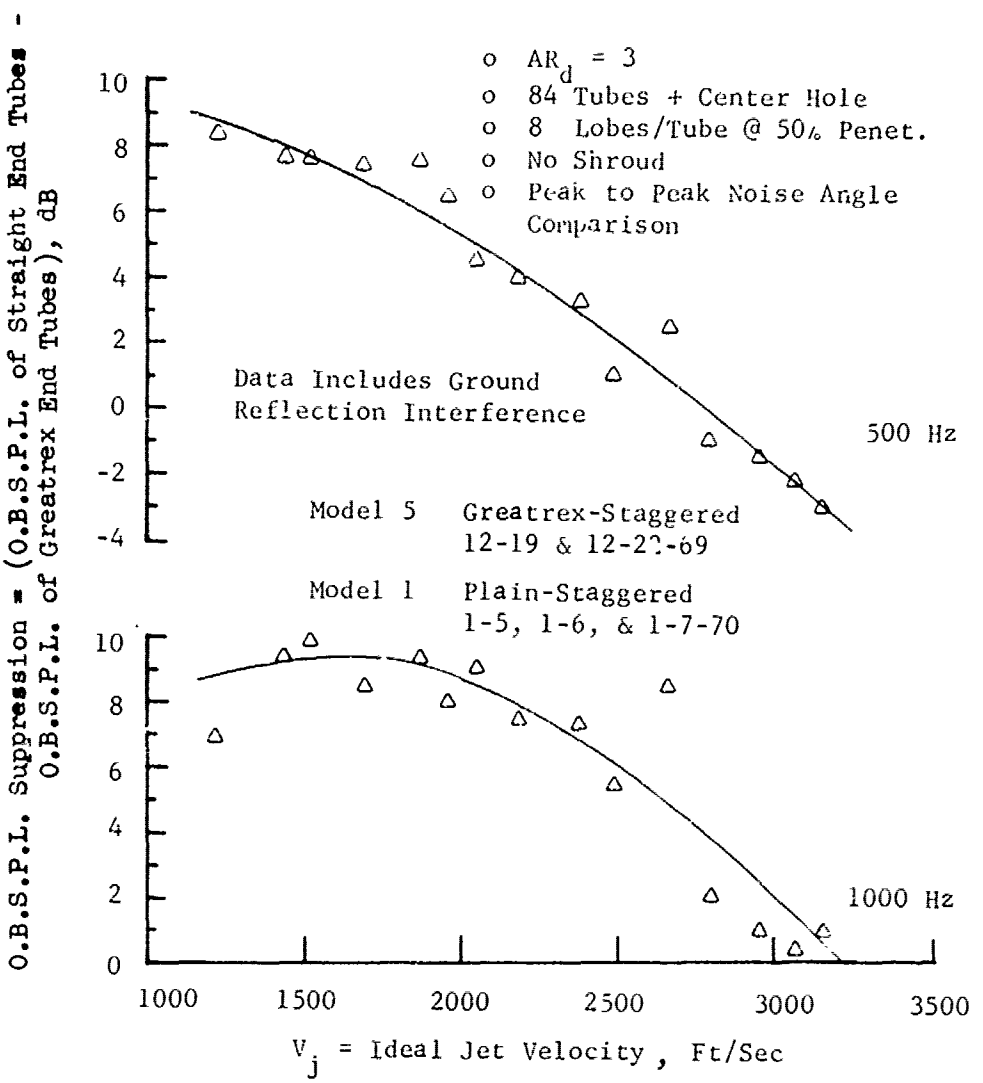

FIGURE V.F.10-20B OCTAVE BAND SPECTRAL SUPPRESSION ATTRIBUTABLE TO ADDITION OF PD-3 GREATREX TUBE ENDS

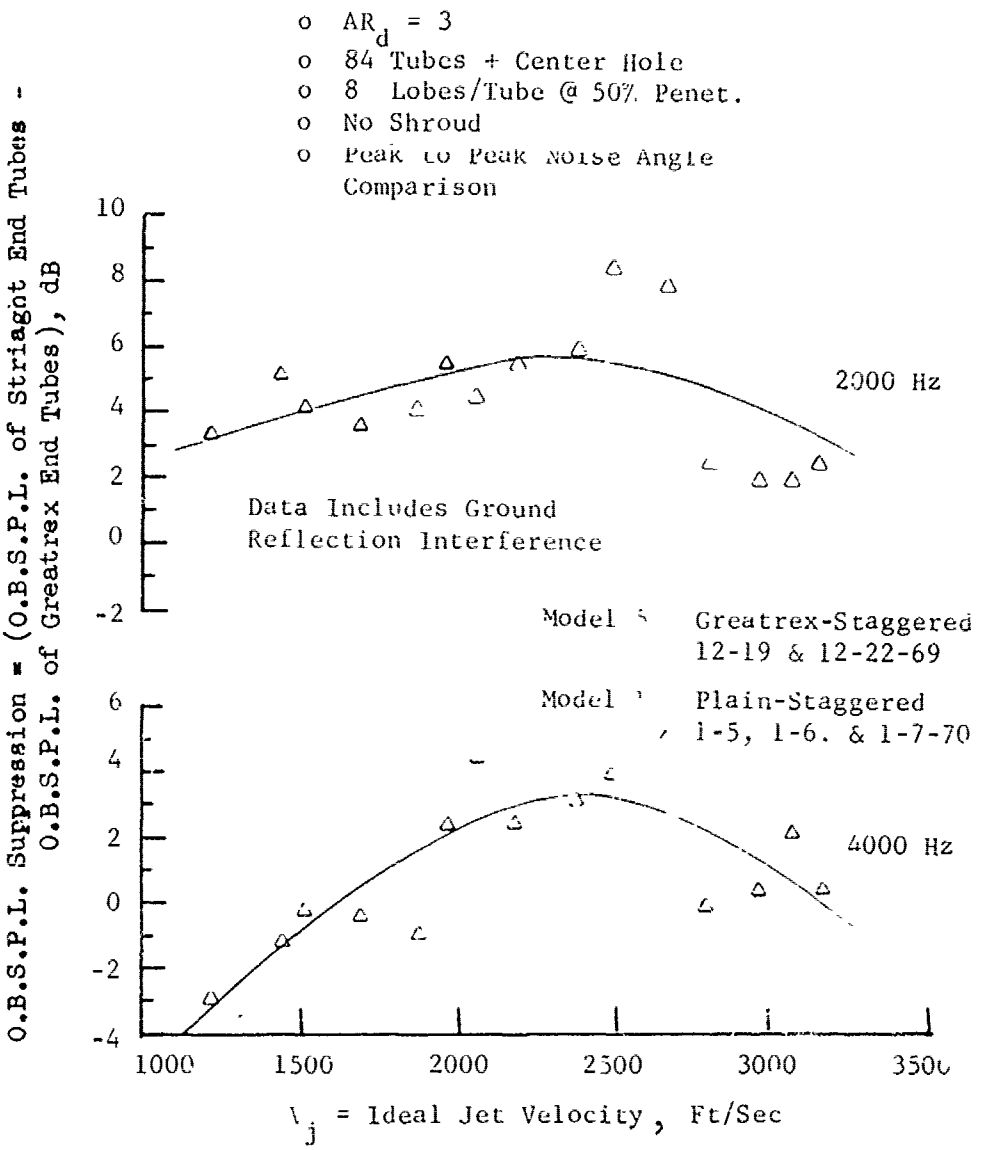

FIGURE V.F.10-20C OCTAVE BAND SPECTRAL SUPPRESSION ATTRIBUTABLE TO ADDITION OF PD-3 GREATREX TUBE ENDS

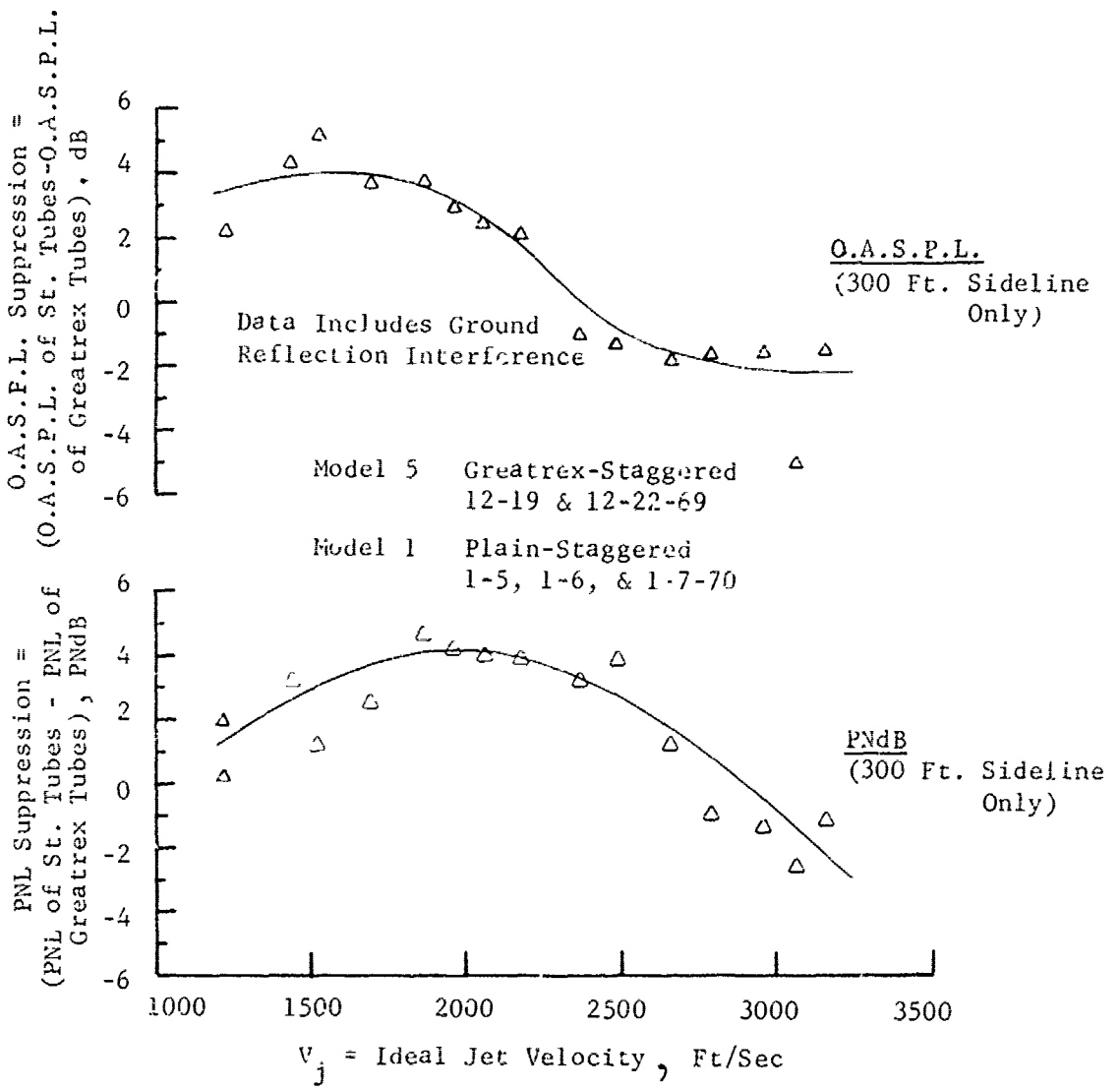

FIGURE V.F.10-21 O.A.S.P.L. AND PNL SUPPRESSION ATTRIBUTABLE TO ADDITION OF PD-3 GREATREX TUBE ENDS

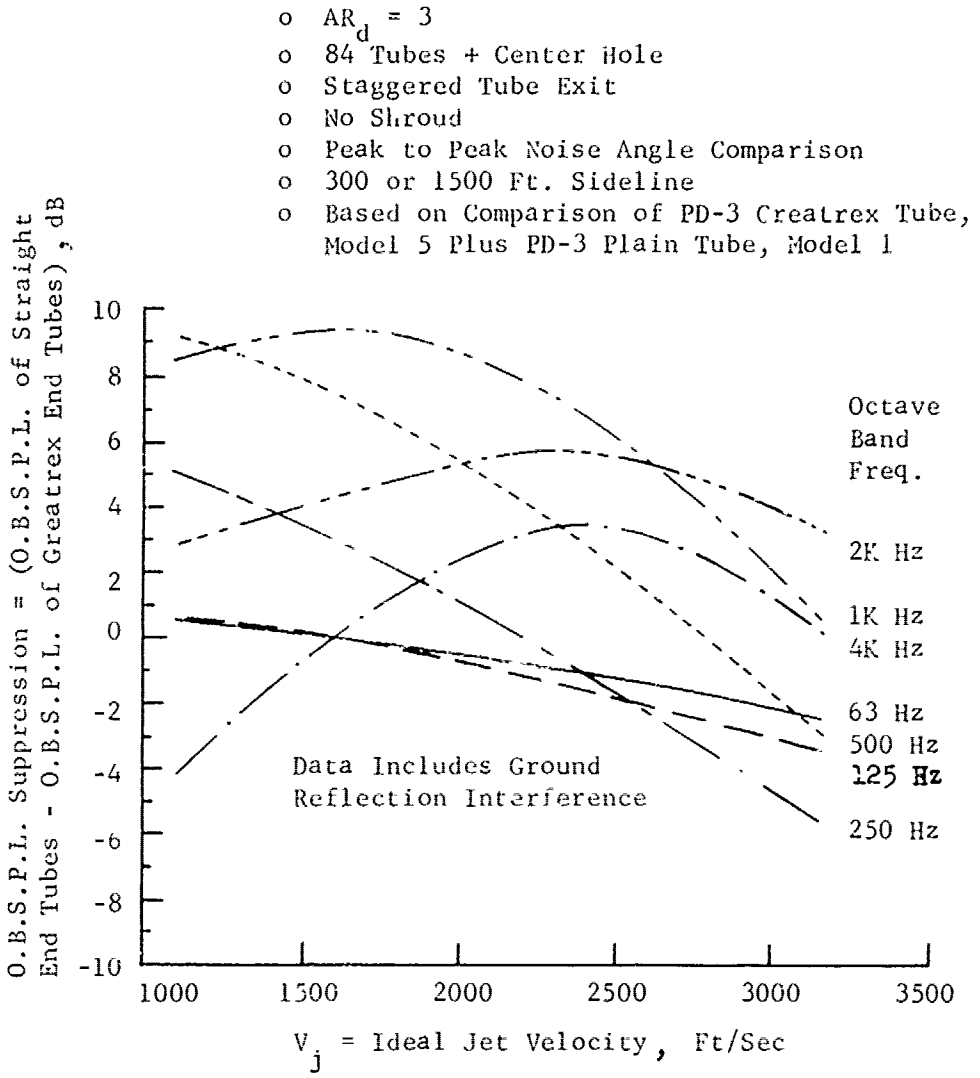

FIGURE V.F.10-22 SUMMARY OF OCTAVE BAND SPECTRAL SUPPRESSION ATTRIBUTABLE TO ADDITION OF PD-3 GREATREX TUBE ENDS

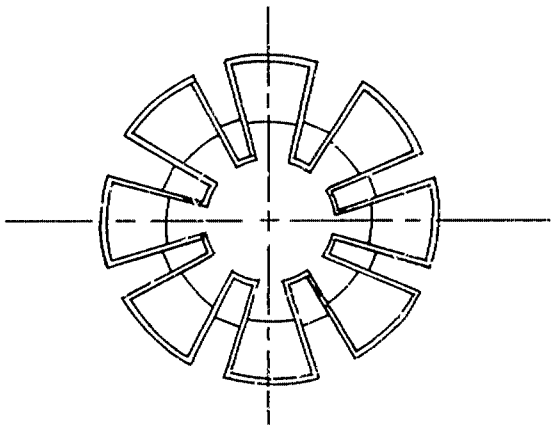

PD-3 Greatrex Tube

- 8 Lobe
- ≈50% Penetration

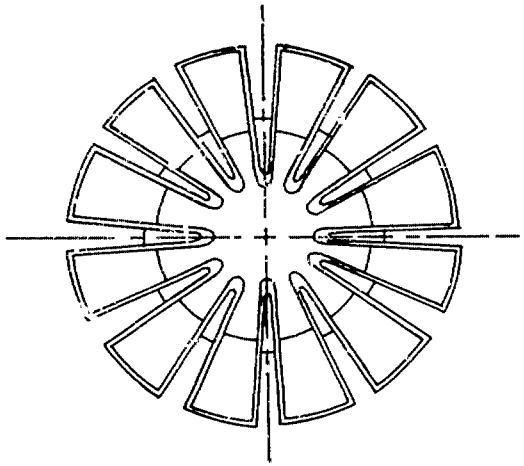

Greatrex Tube For 37-Tube Models

- 12 Lobe
- ≈80% Penetration

FIGURE V.F.10-23 COMPARISON OF GREATREX TUBE END DESIGNS FOR PD-3 AND 37 TUBE MODELS

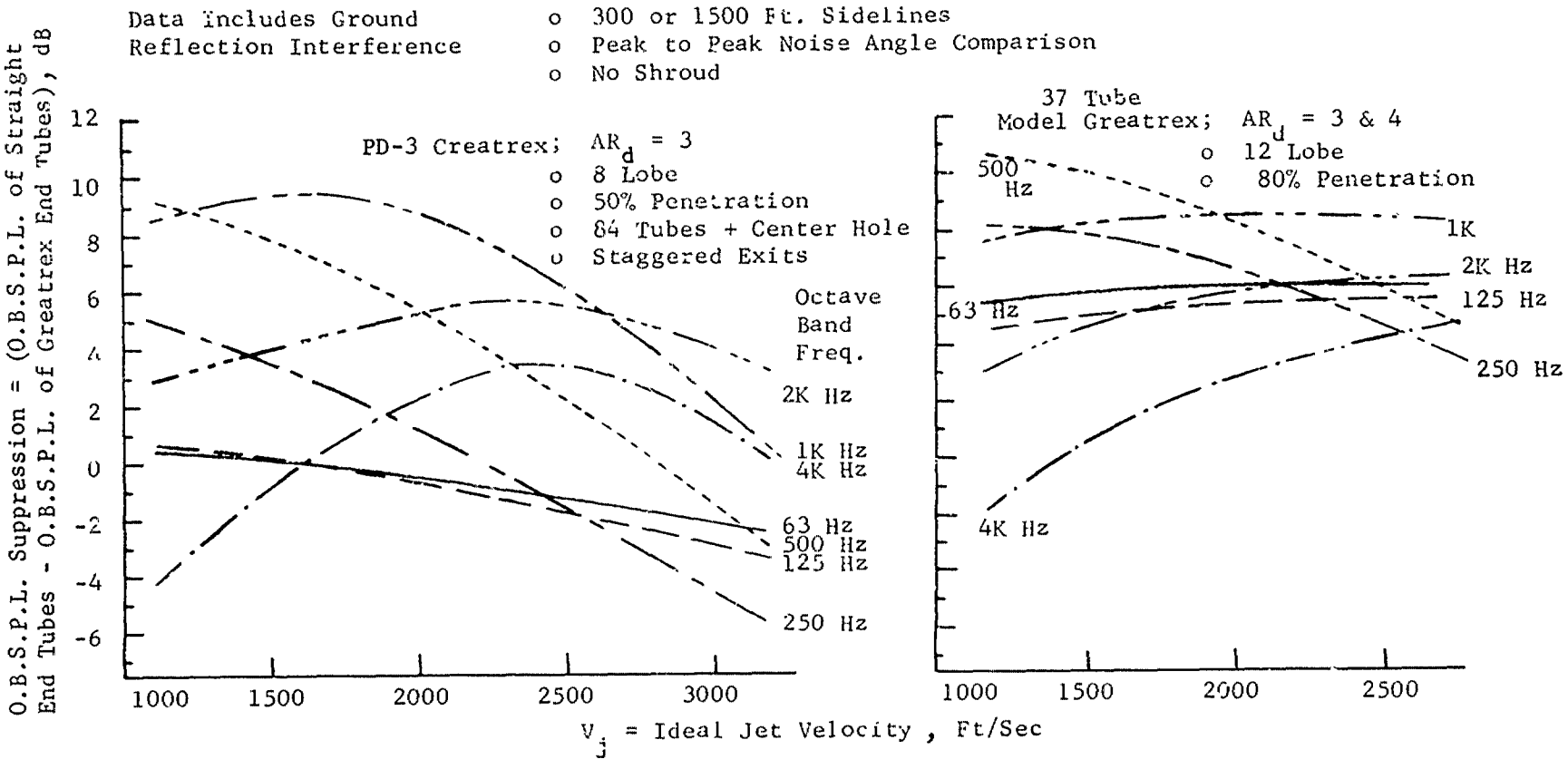

FIGURE V.F.10-24 COMPARISON OF OCTAVE BAND SPECTRAL SUPPRESSION ATTRIBUTABLE TO GREATREX TUBE ENLS ON PD-3 AND 37 TUBE MODELS

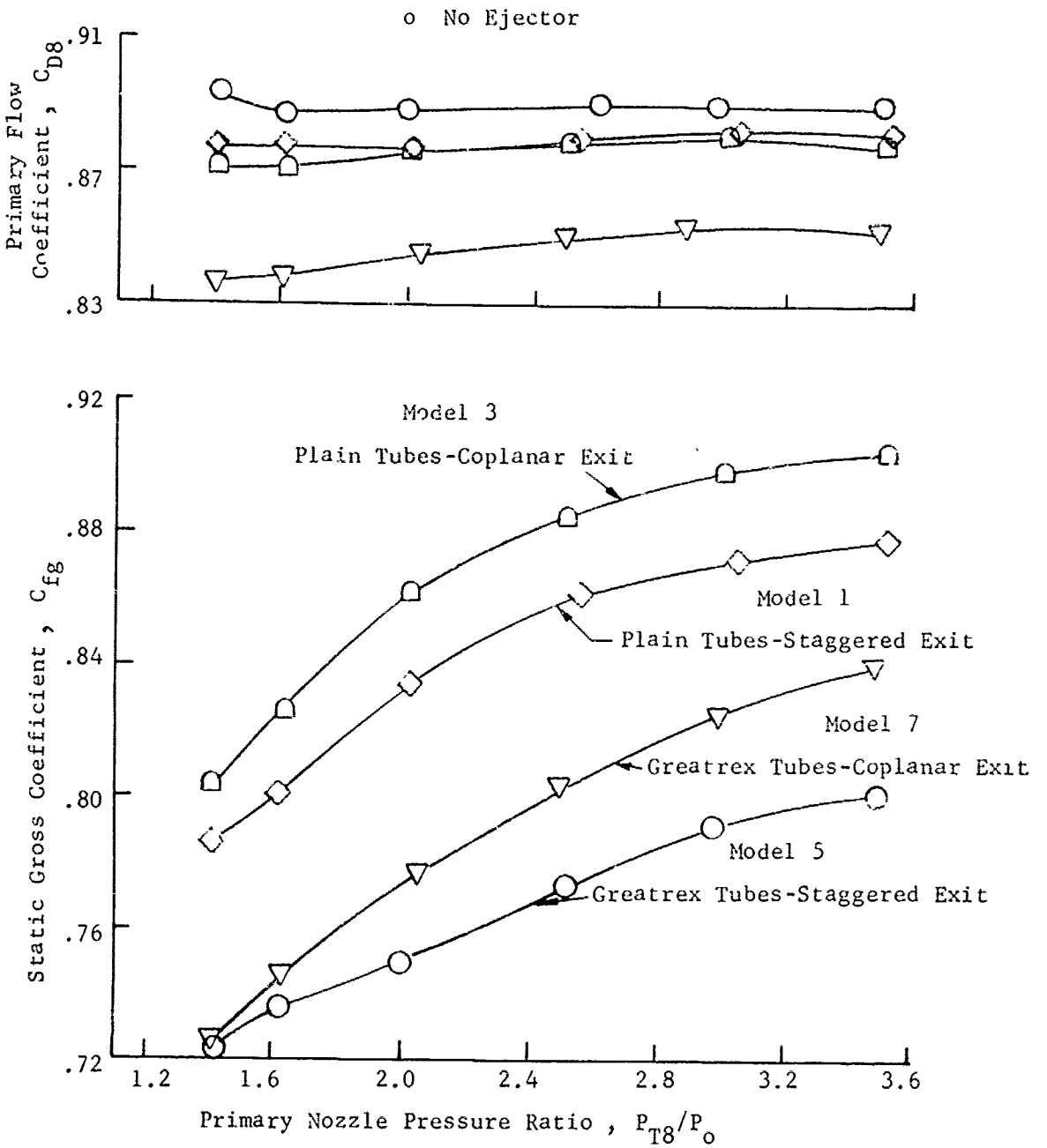

FIGURE V.F.10-25 AERODYNAMIC PERFORMANCE (C_{D8} AND C_{fg}) FOR PD-3 MODELS 1, 3, 5 & 7 WITHOUT EJECTOR, COMPARING GREATREX AND PLAIN TUBES, STAGGERED AND COPLANAR EXITS

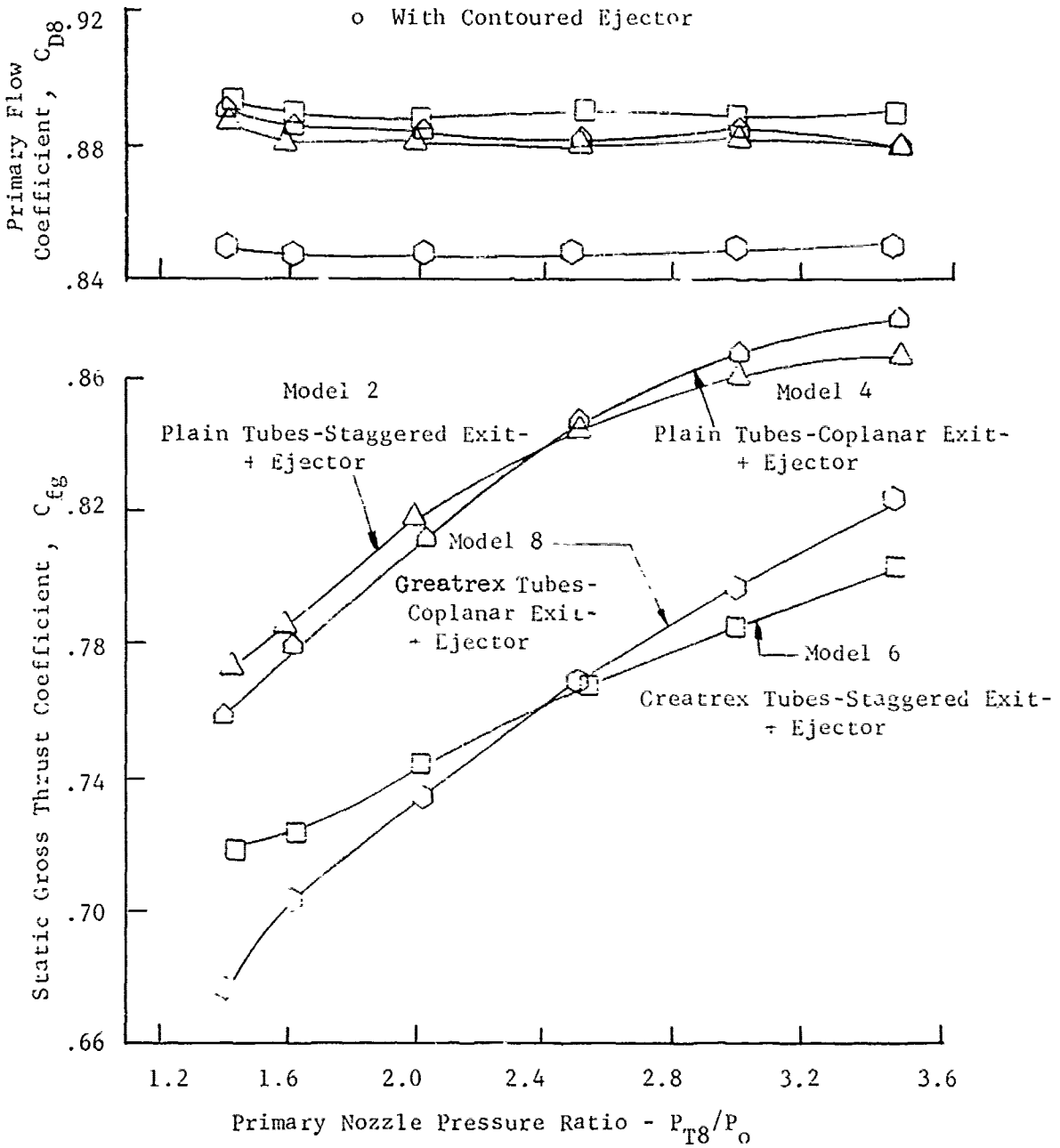

FIGURE V.F.10-26 AERODYNAMIC PERFORMANCE (C_{D8} AND C_{fg}) FOR PD-3 MODELS 2, 4, 6 & 8 WITH EJECTOR, COMPARING GREATREX AND PLAIN TUBES, STAGGERED AND COPLANAR EXITS

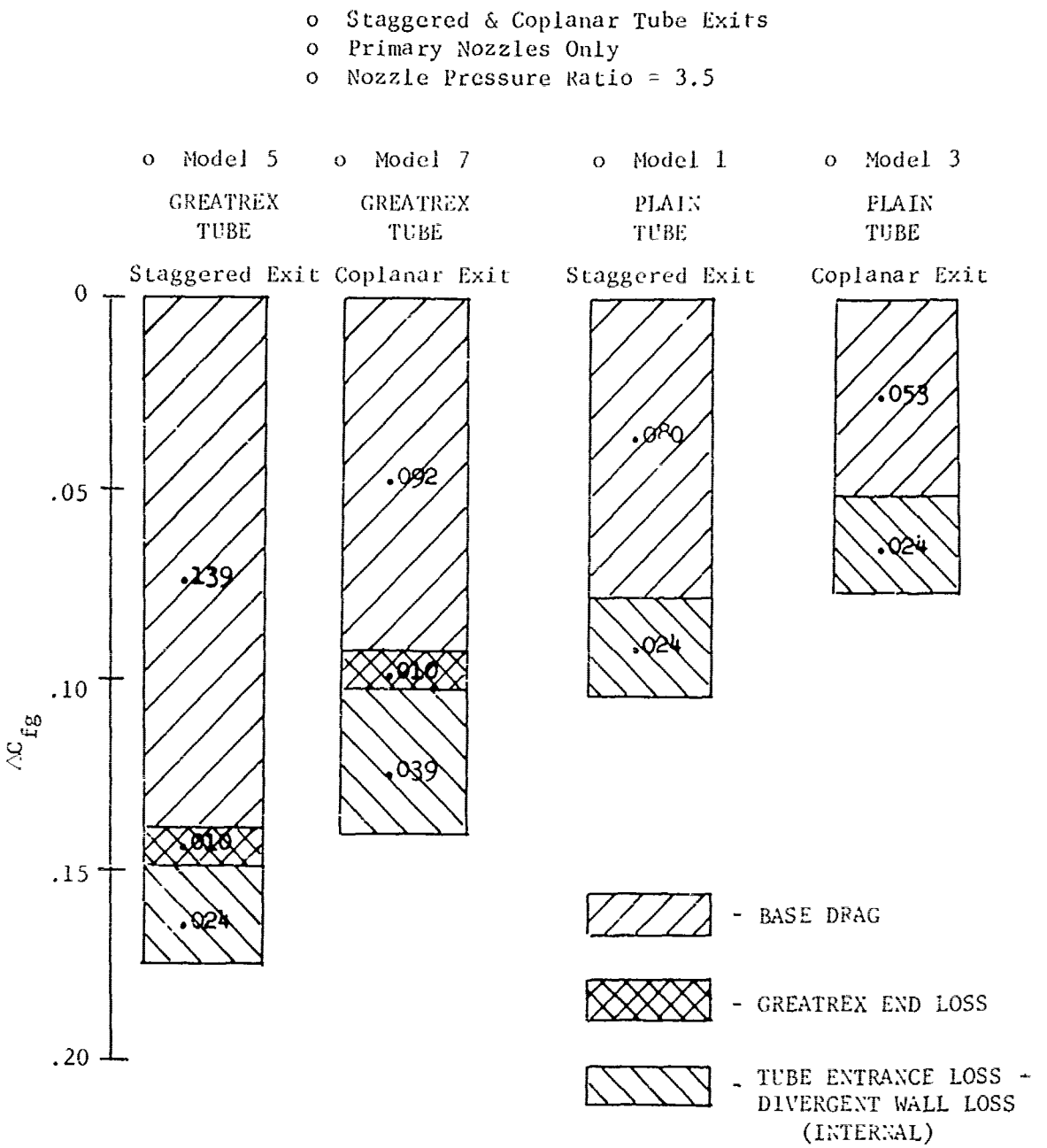

FIGURE V.F.10-27 THRUST LOSS BREAKDOWN FOR PD-3 PLAIN AND GREATREX TUBE COLD FLOW AERODYNAMIC MODELS

APPENDIX A. NOMENCLATURE

Symbol		Units
A, A_8	Physical flow area at nozzle plane 8	(in^2),$(ft.^2)$
AR_d,A/R	Area Ratio: ratio of total circumscribed tube bunde area to physical flow area (tube nozzles)	
A/R	Area Ratio: ratio of total annulus area to physical flow area (annular plug nozzles)	
C/A	Chromel - Alumel wires used in thermocouples	
C_{D8}	Nozzle discharge coefficient: ratio of actual flow rate to ideal flow rate	
C_{fg}	Nozzle gross thrust coefficient, static and installed	
dB	Decible, re: 0.0002 dynes/cm^2	
D_S	a) Throat diameter of TSEN (Two stage ejector nozzle) b) initial minimum internal diameter of cylindrical ejector (shroud)	(in)
D_t	Tube internal diameter	(in)
D_{Td}	Circumscribed tube bundle diameter	(in)
D_8	Internal diameter of conical primary nozzle at primary exit, plane 8	(in)
D_9	Internal diameter of secondary ejector at secondary exit, plane 9	(in)
EPNL	Effective percieved noise level	(EPNdB),(dB)
F_g	Measured gross thrust	(lb_f)
F_N	Net thrust	(lb_f)
$\frac{fD}{V}$	Strouhal number; a calculated function of frequency (f), nozzle diameter (D), and ideal jet velocity (V)	

APPENDIX A. NOMENCLATURE (Continued)

Symbol		Units
k	Ratio of specific heat	
L	Axial reference location of variable position inlet centerbody	(in)
L_S	Shroud internal length	(in)
L_t	Tube external length	(in)
L_{ti}	Tube internal length	(in)
M, M_o	Mach number	
% N_c	Percent corrected speed	(rpm)
OASPL	Overall sound pressure level; calculated by summation of sound pressure levels of each octave or 1/3 octave band	(dB)
OASPL-10 log ρA	Normalized OASPL	(dB)
PNL	Perceived noise level; a calculated annoyance weighted sound level	(PNdB),(dB)
PNdB	Contraction of PNL, dB	(PNdB),(dB)
PNdB-10 log $\rho^2 A$	Normalized PNL	(PNdB)
PNdB-10 log ρA	Normalized PNL	(PNdB)
P_o	Ambient pressure	(psia)
$\bar{P}_{Base}$	Mean baseplate static pressure	(psia)
P_L	Local wall static pressure	(psia)
P_{T8}	Nozzle exhaust total pressure	(psia)
Peak PNL	Highest perceived noise level generated; usually referenced to a specific angle and distance from the source	(PNdB),(dB)
Peak OASPL	Highest overall sound pressure level generated; usually referenced to a specific angle and distance from the source	(dB)
% RH	Percent atmospheric relative humidity	

APPENDIX A. NOMENCLATURE (Concluded)

Symbol		Units
S	Distance between centerlines of tube/hole rows	(in)
SPL	Sound pressure level; a level of sound pressure that occurs in a specified frequency range at any specified interval of time.	(db)
T_{T8}	Nozzle exhaust total temperature	(°R),(°F)
V_j, V_J	Fully developed ideal jet velocity	(ft/sec)
W_B	Bleed weight flow (air or water)	(lb/sec)
W_8	Engine nozzle weight flow	(lb/sec)
W_T	Total primary and secondary flow	(lb/sec)
$\dot{W}$	Flow rate	(lb/sec)
X_S	Axial spacing from exit plane of primary nozzle to: a) throat (D_S) of TSEN (Two stage ejector nozzle) or b) initial minimum internal diameter of cylindrical ejector (shroud)	(in)
α	Tab angle	(deg)
β	Orifice coefficient	
θ	Angle between a straight line from source to microphone, and engine or nozzle centerline; referenced to inlet or exhaust	(deg)
ρ	Density of jet stream	(lb_m/ft^3)